Abstract Volume
16th Swiss Geoscience Meeting

Bern, 3oth November – 1st December 2018

A Habitable Planet

UNIVERSITÄT
BERN

sc | nat

Swiss Academy of Sciences
Akademie der Naturwissenschaften
Accademia di scienze naturali
Académie des sciences naturelles

Aletsch Glacier

The Aletsch Glacier in Switzerland with a length of 23 km and a surface area of ca. 80 km^2 is the largest glacier in Europe. Originating at the upper slopes of the Eiger, Mönch and Jungfrau in the Bernese Oberland, the glacier flows down into the Valais. Like most glaciers worldwide the Aletsch Glacier is retreating in response to global warming, having lost well over 3 km of its length since 1870. The retreat of the glacier causes major slope instabilities.

On the southeastern slopes of the Aletsch Glacier near Moosfluh a huge rock mass (c. 150 million m^3) is actively moving downslope towards the glacier. In the fall of 2016 the rock mass at Moosfluh moved at a velocity of up to 80 cm/day and cracks of several hundred meters in length and up to tens of meters in depth opened on the upper parts of the slope. Pre-existing tectonic structures, such as Alpine shear zones and exfoliation joints in the gneisses making up the slopes at Moosfluh, contribute to the slope instabilities.

The mass movement at Moosfluh is the subject of several ongoing field-based studies and is being permanently monitored by stationary time-lapse cameras, satellite synthetic aperture radar interferometry, differential GPS, airborne digital photogrammetry, and a local seismic network.

Photo credit: Guido Schreurs

Earthrise

Fifty years ago, in December of 1968, the Apollo 8 crew flew from the Earth to the Moon and back again. Frank Borman, James Lovell, and William Anders were launched atop a Saturn V rocket on December 21, circled the Moon ten times in their command module, and returned to Earth on December 27.

The Apollo 8 mission's impressive list of firsts includes: the first humans to journey to the Earth's Moon, the first to fly using the Saturn V rocket, and the first to photograph the Earth from deep space. As the Apollo 8 command module rounded the farside of the Moon, the crew could look toward the lunar horizon and see the Earth appear to rise, due to their spacecraft's orbital motion.

Their famous picture of a distant blue Earth above the Moon's limb was a marvelous gift to the world.

Photo credit: Apollo 8, NASA

16th Swiss Geoscience Meeting, Bern 2018

Table of contents

http://www.geoscience-meeting.ch

Organisation

Host Institution

Institute of Geography & Institute of Geological Sciences of the University of Bern

Patronnage

Platform Geosciences of the Swiss Academy of Sciences SCNAT

Local Organizing Committee

Sébastien Boillat
Stefan Brönnimann
Regula Gesemann
Jörg Hermann
Martina Catharina Kauzlaric
Adrien Mestrot
Klaus Mezger
Daniela Rubatto
Guido Schreurs (President SGM2018)
Md Sarwar Hossain Sohel
Chinwe Ifejika Speranza
Tobias Sprafke
Heinz Veit
Hendrik Vogel

Coordination

Pierre Dèzes

Sponsors

Swiss Geological Survey, swisstopo
CHGEOL
Geobrugg AG
Geographica Bernensia
Geotechnisches Institut
Gloor Instruments
Institute of Geography & Institute of Geological Sciences of the University of Bern
International Union of Geodesy and Geophysics (IUGG)
International Union of Geological Sciences (IUGS)
nagra
Swiss Academy of Sciences (SCNAT)
Swiss Drilling
Swiss Gemmological Institute (SSEF)
ThermoFisher Scientific
Zeiss
University of Bern

Participating Societies and Organisations

Georesources Switzerland Group

International Union of Geodesy and Geophysics, Swiss Committee (IUGG)

International Union of Geological Sciences, Swiss Committee (IUGS)

Kommission der Schweizerischen Paläontologischen Abhandlungen (KSPA)

Swiss Association of Energy Geoscientists (SASEG)

Swiss Association of Geographers (ASG)

Swiss Association for Geographic Education (VGDch)

Swiss Commission for Remote Sensing (SCRS)

Swiss Commission of Oceanography and Limnology

Swiss Commission on Atmospheric Chemistry and Physics (ACP)

Swiss Committee for Stratigraphy (Platform Geosciences/SCNAT)

SWISS DRILLING

Swiss Geodetic Commission (SGC)

Swiss Geological Society (SGG/SGS)

Swiss Geological Survey (swisstopo)

Swiss Gemmological Society (SGG)

Swiss Geomorphological Society (SGGm/SSGm)

Swiss Geophysical Commission (SGPK)

Swiss Geothermal Society

Swiss Hydrogeological Society (SGH)

Swiss Hydrological Commission (CHy)

Swiss Paleontological Society (SPG/SPS, Swiss Geological Society)

Swiss Snow, Ice and Permafrost Society (SIP)

Swiss Society for Hydrology and Limnology (SGHL/SSHL)

Swiss Society for Quaternary Research (CH-QUAT)

Swiss Society of Mineralogy and Petrology (SMPG/SSMP, Swiss Geological Society)

Swiss Tectonics Studies Group (Swiss Geological Society)

0. Plenary Session

1. The Rare Earth Elements: Demand, Global Resources, and Challenges for Resourcing Future generations

Kathryn Goodenough

British Geological Survey, Edinburgh

Decarbonisation of the global economy is now seen as a priority for our habitable planet. A key part of this is the switch away from fossil fuels, towards renewable energy sources and electric cars. These new, 'green' technologies are manufactured using a wide range of raw materials, including critical metals such as the rare earth elements (REE), lithium, niobium and tantalum. Of these, the REE have attracted particular attention, because of the dominance of China in their production. This talk will summarise new research, carried out as part of the EURARE, SoS RARE, and HiTech AlkCarb projects, on global geological resources of the REE. Despite the name, the rare earth elements are not rare in the Earth's crust; REE enrichments are particularly associated with alkaline igneous rocks and carbonatites, but can also be found in a range of other geological environments, from volcaniclastic sediments to weathered granites. Our ongoing research aims to improve understanding of how these REE deposits form, and how they can be effectively mined, which will underpin the availability of these resources for years to come.

2. On the origin and early evolution of the atmosphere

Bernard Marty

Ecole Nationale Supérieure de Géologie, Université de Lorraine, Nancy, France

Recent advances in space missions (e.g., the European Space Agency Rosetta mission) and in the geochemistry of ancient rocks permit to have insights into the origin of atmospheric/oceanic volatiles such as water, nitrogen, noble gases, and into the composition of the atmosphere during the first half of Earth's history. In particular, the ROSINA instrument (PI, K. Altwegg, Univ. Bern) on board of the Rosetta spacecraft has analysed noble gases, among other elements and species. The isotopic composition of the heaviest stable noble gas, xenon, suggests strongly that comets have contributed volatile elements to the ancient atmosphere, up to ~20 % for Xe, but less than 1 % for water. Most of major volatiles such as water, carbon and nitrogen species were probably contributed by small bodies formed in the inner solar system during the major episodes of Earth's accretion.

Our group in Nancy, France, has also studied direct samples of the ancient atmosphere through the analysis of fluid inclusions in Archean hydrothermal quartz. These fluids are a mixture of hydrothermal components and presumably Archean seawater containing dissolved paleo-atmospheric gases. The partial pressure of atmospheric nitrogen was comparable to, or even lower than, the present-day P_{N2}, leaving the possibility of a higher P_{CO2} 3.5 Ga ago. The isotopic composition of paleo-atmospheric nitrogen was similar to the modern one, suggesting that N_2 did not escape to space and that there existed already a sufficiently robust terrestrial magnetic field. In contrast, the isotopic composition of paleo-atmospheric Xe evolved with time through isotope fractionation, as a result of preferential escape of xenon to space, likely related to its low first ionization potential and to the higher far UV flux of the young Sun. The salinity (Cl) of the Archean oceans was comparable to the modern one, but the seawater K content was about 30 % lower than Modern, in possible relation to a limited continental crust volume at that time.

3. Causes for 20th century glacier retreat and implications for future sea-level rise

Ben Marzeion

Institute of Geography and MARUM - Center for Marine Environmental Science, University of Bremen, Germany

Melting glaciers have become icons of anthropogenic climate change. Their strong mass loss, most likely the biggest contributor to sea-level rise during the 20th century, and often documented in impressive picture comparisons, seems to unequivocally demonstrate the human interference with the climate system. However, glaciers respond to climate change with a lag. Observed glacier change is therefore often the result of climate change preceding the time of observation many decades, or even centuries.

Using formal detection and attribution methods, we show that only about 30 % of the global glacier mass loss since 1850 is attributable to anthropogenic forcing. However, this anthropogenic fraction increased almost linearly within the 20th century, reaching about 70 % in the past two decades.

The imbalance of glacier mass with concurrent climate conditions implies a strong commitment to further mass loss in the future. Different lines of evidence show that even without any additional warming, glaciers would eventually lose about one third of their present day mass. They will thus remain an important contributor to sea-level rise in the 21st century. Any additional emission will increase the committed glacier mass loss at a rate of roughly 15 kg of ice per kg of CO_2 emitted
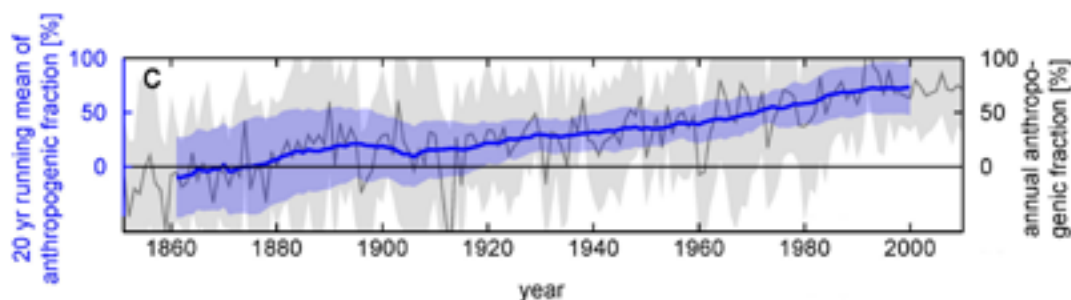

Figure: Annual and 20 yr running mean of the anthropogenic fraction of global glacier mass loss. Shading indicates 1 standard deviation of ensemble.

4. Identifying social-ecological adaptation pathways to a habitable planet

Lindsay Stringer

Sustainability Research Institute, School of Earth and Environment, University of Leeds

Planet Earth is currently undergoing rapid transformations that affect its habitability, both now and into the future. Global temperatures are rising to the extent that there are uncertainties over whether we can achieve the Paris Agreement climate mitigation goal of keeping rises below 1.5-2 °C. At the same time, recent reports by the Intergovernmental science-policy Platform on Biodiversity and Ecosystem Services (IPBES) indicate that globally, biodiversity losses are at accelerated rates similar to the 'big five' mass extinctions in the fossil record. These kinds of challenges call into question the future habitability of some parts of the planet due to changes in temperature, sea level, seasonality shifts and extreme weather events, and the Earth's ability to continually provide the ecosystem services that humans demand from it. We are already seeing movement of people away from desertified dryland areas where land is no longer productive, access to water is insufficient to meet human demands, and populations lack options to support their wellbeing and development. Even in other (non-dryland) areas that currently enjoy sufficient water, human activities are degrading the land to the extent that ecosystem services are lost and poverty is being exacerbated. Restoration of degraded ecosystems is not always viable. Restoration is a slow process, the economic costs can be prohibitive, and future climate projections mean restoration to a desired previous state may not even be possible.

In this presentation, I argue that the kinds of challenges we see in relation to land degradation and desertification, our understanding of the drivers of change, and the human responses and adaptations being undertaken at present, offer important, useful insights into present and near-term future challenges and how we can manage them. However, it is important to recognise that current human adaptation research focuses on goal-oriented, short-term scenarios, and considers present-day economic, political, legal and social structures and human values, yet, the scale of environmental changes we are looking at extends beyond these time horizons.

Sustainability science commonly considers multiple time frames and advocates transdisciplinary approaches to understanding coupled human-environment systems. Often this involves looking forward, analysing the trade-offs associated with different decision options and identifying the 'winners' and 'losers' under different future scenarios. It is nevertheless vital that we look backward sufficiently as well. Past conditions evidenced in the fossil and palaeoclimate records reflect those projected for the post-2100s. By delving much further back into the past and understanding the climate and biodiversity conditions of the deep past, it could help us to identify how and where people can live in a radically changed future Earth. This would enable us to layer social and technological scenarios over deep past conditions, identifying future social-ecological adaptation pathways that can be directly applied in research, policy and practice to help keep our planet habitable.

01. Structural Geology, Tectonics and Geodynamics

Guido Schreurs, Neil Mancktelow, Paul Tackley, Daniel Egli

Swiss Society of Mineralogy and Petrology (SSMP)

TALKS:

1.1   Akker I.V., Zwingmann H., Todd A., Berger A., Herwegh M.: The role of sheet-silicates in the formation of spaced cleavages under changing physico-chemical conditions

1.2   Bastias J., Spikings R., Ulianov A., Grunow A., Chiaradia M., Riley T., Burton-Johnson A.: The Gondwanan margin in West Antarctica: insights from the Triassic metamorphic basement of the Antarctic Peninsula

1.3   Beaussier S.J., Gerya T., Burg J.-P.: Effects of extensional inheritance on passive margin collapse

1.4   Behr W.M., Becker T.W.: Sediment Control on Subduction Plate Speeds

1.5   Bergemann C.A., Gnos E., Whitehouse M.J.: Dating retrograde tectonic activity in the Mont Blanc and Aiguilles Rouges massifs dated through ion probe analysis of hydrothermal cleft monazite

1.6   Brett A.C., Diamond L.W., Weber S., Gilgen S.: Rock-matrix versus fracture-controlled fluid pathways in the upper oceanic crust

1.7   Candioti L.G., Schmalholz S.M., Duretz T., Picazo S.: The Alpine cycle: Modelling orogenic wedge formation from generation of hyper-extended passive margins and forced subduction to continent-continent collision

1.8   Delunel R., Schlunegger F., Valla P.G., Dixon J., Glotzbach C., Kober F., Norton K.P., Salcher B., Wittmann H., Christl M.: Review of Alpine denudation rates from detrital ^{10}Be concentrations

1.9   Giorgetti C., Tesei T., Scuderi M.M., Collettini C.: Reactivation of Gouge-bearing Faults: an Experimental Insight

1.10   Kiss D., Candioti L.G., Podladchikov Y., Duretz T., Schmalholz S.M.: Thermal softening induced strain localization: from first order features to high resolution lithospheric scale numerical models

1.11   Lu G., Fellin G., Winkler W., Willett S.D., Guillong M.: Fast exhumation in early Oligocene and syn-collisional volcanism as revealed by combined FT and U-Pb analysis of detrital zircons in the Central Alps

1.12   Mock S., Herwegh M., Schlunegger F., von Hagke Ch., Dunkl I.: New Thermochronological Constraints on Thrust Activity in the Subalpine Molasse: Implications for the Late Miocene Evolution of the Central Alps

1.13   Ricchi E., Gnos E., Berger A., Rubatto D., Bergemann C.: Constraining deformation phases in the Aar Massif and the Gotthard Nappe (Switzerland) using Th-Pb crystallization ages of fissure monazite-(Ce)

1.14   Spitz R., Schmalholz S.: 3D finite strain quantification and numerical modelling of the transition between viscous folding and thrusting.

1.15   Sternai P., Sue C., Husson L., Serpelloni E., Becker T., Willett S., Faccenna C., Walpersdorf A., Castelltort S.: Present-day uplift of the European Alps: mechanisms and relative contributions

1.16   Yan J., Ballmer M.D., Tackley P.J.: The Evolution and Distribution of Chemical Heterogeneity in the Earth's Mantle

POSTERS:

P 1.1   Bessat A., Pilet S., Duretz T., Schmalholz S.M.: Numerical modelling of lithospheric flexure at subduction zones: investigation of forces involved in the flexure and in melt extraction from the LVZ.

P 1.2   Borderie S., Mosar J., Maillot B.: Stress in the Alpine foreland – a kinematic and mechanical approach

P 1.3   Borderie S., Vendeville B.C., Graveleau F., Witt C., Dubois P., Baby P., Calderon Y.: The Chazuta Thrust, a large-transport thrust in an evaporites-floored basin (Huallaga Basin, Peru): insights from analogue modelling.

P 1.4   Bouscary C., King G., Herman F., Biswas R., Chanard K., Lavé J., Hetényi G.: Luminescence dating and landscape evolution of the Himalaya, Nepal

P 1.5   Colavitti L., Hetényi G. and AlpArray Working Group: A new technique to construct crustal 3-D Vs models: Implementation of Ray Tracing, Model Parameterization and Inversion

P 1.6   Diehl T., Kissling E., Lee T., Nibourel L., Schmid S.: Linking seismicity with faults: Insights from a new high-resolution earthquake catalog of Switzerland

P 1.7   Dorostkar O., Carmeliet J.: Effect of grain friction on characteristics of seismic cycles in a sheared granular fault gouge

P 1.8   Fabbri S.C., Allenbach R., Herwegh M., Krastel S., Lebas E., Lindhorst K., Madritsch H., Wessels M., Wielandt-Schuster U., Anselmetti F.S.: Bedrock structure, postglacial infill and neotectonic fault structures in Lake Constance

P 1.9   Gilgannon J., Berger A., Poulet T., Regenauer-Lieb K., Veveakis M., Barnhoorn A., Herwegh M.: Upscalling microstructural analysis: A new approach applied to experimentally deformed calcite aggregates

P 1.10   Haddad A., Ganas A., Kassaras I., Lupi M.: Seismicity in Western Peloponnese and Ionian Islands: A new investigation with a local network

P 1.11   Hässig, M., Moritz, R., Popkhadze, N., Ulianov, A., Chiaradia, M., Galoyan, G.: Reconstruction of the geodynamic and magmatic evolution of the Somkheto-Karabah and Pontides Arcs from the Mesozoic to Early Cenozoic across Armenia, Georgia and NE Turkey

P 1.12   Hetényi G., Epard J.-L., Colavitti L., Hirzel A.H., Kiss D., Petri B., Scarponi M., Schmalholz S.M., Subedi S.: Spatial relation of surface faults and crustal seismicity: a first comparison in the region of Switzerland

P 1.13   Jiwani-Brown E.A., Lupi M., Pacheco J.F., Planes T. , Mora M.: A seismological study to investigate the volcanic behaviour of the Irazú-Turrialba complex

P 1.14   Kaveh Firouz A., Khodaverdian A., Danciu L.: Present-day crustal deformation of the Turkish-Iranian Plateau: insights from kinematic modelling

P 1.15   Kiss D., Duretz T., Schmalholz S.M.: High-resolution thermo-mechanical numerical simulations of basement-cover deformation with application to the Helvetic nappe system

P 1.16   Lee T., Diehl T., Kissling E., Wiemer S.: High-resolution earthquake catalogue and seismic velocity models to image the structure of seismogenic faults zones in the Valais (Switzerland)

P 1.17   Madella A. , Ehlers T.A.: Understanding seaward-concave subduction zones: insights from critical taper theory and forearc seismicity

P 1.18   Madonna C., Podladchikov Y., Burg J.-P.: Laboratory evidence of viscous heating-induced strain localization

P 1.19   Mair D., Lechmann A., Herwegh M., Nibourel L., Schlunegger F.: Understanding variations in the Alpine deformation imprint on the Aar massif's basement-cover-contact – the case of the Jungfrau-Eiger Mountains (Central Alps, Switzerland)

P 1.20   Malatesta L.C., Bruhat L., Finnegan N.J.: Co-location of the downdip end of seismic locking and the continental shelf break.

P 1.21   Mock S., Herwegh M., Diehl T., Möri A., Kissling E.: Approach for a new seismotectonic model of Switzerland

P 1.22   Nibourel L., Rahn M., Berger A., Herman F., Dunkl I., Herwegh M.: Neogene exhumation of the Aar Massif controlled by crustal thickening and paleogeography

P 1.23   Nosenzo F., Balestro G., Groppo C., Festa A.: Geological-structural and metamorphic study of the Southern Dora-Maira Massif in Valmala (Varaita Valley, Western Alps)

P 1.24   Scarponi M., Hetényi G., Plomerová J., Solarino S., Berthet T., Baron L.: High-resolution imaging of the Ivrea Geophysical Body: A joint seismic and gravity approach

P 1.25   Schenker F.L., Ambrosi C., Scapozza C., Czerski D., Maino M., Castelletti C., Gouffon Y.: Structural and metamorphic data in the nappes of the Lepontine Dome (Central Alps)

P 1.26   Tackley P.J., Jain C., Rozel A.B., Lourenco D., Gerya T.V.: Archean tectonics and the generation of continental TTG crust in global mantle convection models

P 1.27   Ueda K., Gerya T., Willett S., May D.: Break-up of continental lithosphere interacting with upper mantle and surface processes

P 1.28   Vaughan-Hammon J.D., Moulas E., Schmalholz S.M.: Numerical two-wedge model applied to the Alpine orogeny

P 1.29   Vaughan-Hammon J.D., Luisier C., Schmalholz S.M.: Strain partitioning linked to high-pressure metamorphism in the Monte Rosa metagranitoids

P 1.30   Verbeken B., Schmitt N., Foubert A., Mosar J.: Microstructures in damage zones of limestone strike-slip fault in Eclépens.

P 1.31   Winterberg S., Picotti V., Willett S.: Uplift and exhumation history questions Messinian fluvial unconformities within the Alps

P 1.32   Zwaan F., Corti G., Keir D., Sani F.: The Western Afar Margin, Ethiopia: A new and detailed structural interpretation of a developing passive margin

P 1.33   Zwaan F., Schreurs G., Buiter S.J.H.: A direct comparison of experimental set-ups for simulating extensional tectonics

1.1
The role of sheet-silicates in the formation of spaced cleavages under changing physico-chemical conditions

Ismay Vénice Akker [1], Horst Zwingmann [2], Andrew Todd [3], Alfons Berger [1], Marco Herwegh [1]

[1] *Institute of Geological Sciences, University of Bern, Baltzerstrasse 1+3, CH-3012 Bern, Switzerland (ismay.akker@geo.unibe.ch)*

[2] *Division of Earth and Planetary Sciences, Graduate School of Science, Kyoto University, Sakyo-ku, Kyoto, 606-8502, Japan*

[3] *Commonwealth Scientific and Industrial Research Organisation (CSIRO) Earth Science and Resource Engineering, P.O. Box 1130, Bentley, Western Australia 6102, Australia*

In this study, we investigate the microstructures and geochemistry of slate samples from the Infrahelvetic Flysch units in the Glarus Alps (Switzerland). Samples within this paleo-accretionary wedge show metamorphic peak temperatures from 200 to 320 °C, with increasing metamorphism from the North Helvetic Flysch units, close to the village Weesen towards the Ultrahelvetic Flysch units around Segnesspass, the latter in the close vicinity of the Glarus thrust. Along this metamorphic gradient substantial dehydration takes place, which is linked to specific physico-chemical changes in sheet-silicates resulting in the formation of a spaced cleavage. Different stages in the evolution of the spaced cleavage are now imaged with high-resolution SEM imaging and quantified with Auto-Correlation Function (ACF). The ACF shows that: (1) the microlithon size; (2) the elongation of the microlithons; as well as (3) the far field correlations (overall schistosity) are increasing with metamorphic grade. At the grain scale, the macroscopic cleavage is defined by SPO (shape preferred orientation) of sheet silicates combined by shape changes of large minerals (mainly calcite and quartz) due to pressure solution or viscous deformation processes (diffusion and dissolution-precipitation creep). Phase segmentation of the high-resolution SEM images shows: (1) mica aggregates (about 30 μm) are often deformed; (2) relatively large sheet-silicates (sizes of the long axis of about 20-30 μm) are aligned bedding parallel and (3) relatively small sheet-silicates (long axis of 0.8-2 μm) are also aligned bedding parallel and form an interconnected network. The physical conditions of local fluid-mineral equilibria are unravelled by quantitative mineral chemistry of sheet-silicates (i.e. white mica, chlorite). K-Ar measurements of different grainsize fractions from such rocks yield apparent ages, because of inheritance of detrital grains and their incomplete recrystallization even in the small grain size fractions. Interestingly, however, the apparent ages of fine-grain size fractions are younger compared to coarser ones indicating a volumetrically less advanced resetting progress in the course grains in comparison to the fine grains. Hence the combination of quantitative microstructural and geochemical analyses provides new and important insights into the maturation process of slates. Different tools to quantify the amount of resetting (isotopes, mineral chemistry) show a low amount of detrital input in the fine fraction as well as some resetting in the course grain size fractions.

1.2

The Gondwanan margin in West Antarctica: insights from the Triassic metamorphic basement of the Antarctic Peninsula

Joaquin Bastias [1], Richard Spikings [1], Alexey Ulianov [2], Anne Grunow [3], Massimo Chiaradia [1], Teal Riley [4], Alex Burton-Johnson [4]

[1] *Earth Science Department, University of Geneva, rue de Maraîchers 13, 1205 Geneva, Switzerland (joaquin.bastias@unige.ch)*
[2] *Institute of Earth Sciences, University of Lausanne, Géopolis, 1015 Lausanne, Switerland*
[3] *Byrd Polar and Climate Research Center, The Ohio State University, 108 Scot Hall, 1090 Carmack Road, Columbus, OH 43210, USA*
[5] *British Antarctic Survey Cambridge, CB3 OET, UK.*

We present a study of seven orthogneisses from the Triassic metamorphic basement of the Antarctic Peninsula that combines zircon U-Pb LA-ICP-MS data with isotopic tracing (Hf in zircon and Sr-Nd-Pb in bulk rock) and whole rock geochemistry. Our results address the current debate regarding the allochthonous vs in-situ origin of the Antarctic Peninsula crust, and the configuration of various lithospheric fragments during the disassembly of southern Gondwana and the subsequent assembly of West Antarctica. The rocks analyzed are part of the metamorphic basement, which precludes the collisional event, constituting useful material to study the pre-accretional history of Antarctic Peninsula. In addition, we compare these data from the Peninsula with other domains of West Antarctica such as Thurston Island and in South America, including Patagonia.

West Antarctica is composed of five former fragments of Gondwana, and the Antarctic Peninsula is currently proximal to Patagonia. Prior to Mesozoic break-up, these blocks were located along an active continental margin that was consuming proto-Pacific oceanic lithosphere (e.g. Storey, 1988). Rifting of Gondwana drove block translation and rotations that eventually lead to the assembly of West Antarctica (e.g. Grunow et al. 1987), although the details of these processes are poorly constrained.

The Antarctic Peninsula hosts a Mesozoic-Cenozoic arc that intrudes early Mesozoic and late Paleozoic sedimentary and metamorphic rocks. Early interpretations utilised litho-stratigraphical correlations between Patagonia and the Antarctic Peninsula to suggest that both formed part of the Mesozoic Andean margin (e.g. Suarez, 1976). Later, Vaughan and Storey (2000), mapped a regionally extensive shear zone in Palmer Land, and proposed that the Antarctic Peninsula formed by the collision of an allochthonous arc (Central Domain) with a former Gondwanan block (Eastern Domain). Burton-Johnson and Riley (2015) question the collisional model on reviewing the basis of sedimentary provenance and the isotopic composition of the igneous units.

Zircons of orthogneisses of the metamorphic basement are complex and yield Triassic rims and Paleozoic cores (zircon U-Pb dates; Flowerdew et al., 2006, Riley et al., 2012). Our LA-ICP-MS analyses of zircon rims in the Central Domain yield U-Pb concordia ages spanning between 207.5 ±5.2 and 216.6 ± 2 Ma, and 203.3 ± 0.6 and 223.4 ± 1.8 Ma in the Eastern Domain, which overlap. However, the ages of the inherited cores are considerably different. The Central Domain records continuous activity until the Late Silurian, with an exceptional age in the Middle Proterozoic. In contrast, the Eastern Domain reveals magmatism during the Triassic, Early Devonian and Late and Early Proterozoic. Evidencing a possible magmatic gap during the Permian-Devonian in the Eastern Domain, that it is present in the Central Domain, suggesting possible different sources for these inherited cores. Furthermore, a comparison of the ages of inherited cores of the orthogneisses with U-Pb provenance studies of the Antarctic Peninsula and Patagonia show that: i) the detritus of Eastern Domain and Patagonia have significant activity gaps while magmatism was occurring in the Central Domain (during the Devonian and Carboniferous); ii) the Eastern Domain show remarkably similarities on the pattern of the inherited cores of its orthogneisses and the detritus of its Triassic sedimentary rocks, suggesting that probably both were nearby prior the Triassic.

Major oxides and trace elements reveal subalkaline, dominantly peraluminous, supra-subduction zone rocks (Pearce et al., 1984), although one orthogneiss of the Central Domain with a concordia zircon U-Pb age of 216.6 ± 2 Ma is metaluminous. The rocks yielded trace element compositions with enriched LILE/HFSE, negative Nb, P and Ti anomalies, flat REE that are characteristic of convergent margins (Pearce et al., 1984).The geochemical data suggest that the protolith of the Triassic metamorphic basement of the Antarctic Peninsula formed in an arc.

Concordant U-Pb data of zircons were used to obtain Hf isotopic compositions were it was conducted the LA-ICP-MS geochronological data. The Eastern Domain yields εHfi values of -14.1 to -7.4, while values from the Central Domain span between -13.8 and -3.8. These values are consistent with crustal recycling, showing that from the Proterozoic through the Paleozoic and Triassic the source of the magmas remained consistently crustal.

The Late Triassic ages recorded in the rims of the zircons shows that this metamorphism affected a large section of the Antarctic Peninsula, and that the Central and Eastern domains formed part of the Gondwanan margin. However, these ages acquired from Paleozoic cores suggest that, prior to the Late Triassic, relative to older rocks to the east, and that it was located either further south or north. Paleogeographic reconstructions argue against the possibility of the Central Domain being connected with Patagonia, rendering it more plausible that it was located towards the south.

REFERENCES

Burton-Johnson and Riley. 2015. JGS 172 (6), 822-835.

Dalziel and Wilson. 2017. AGU Fall Meeting Abstracts. T22D-01

Flowerdew et al. 2006. GSAM 119 (3-4), 275-288.

Grunow et al. 1987. EPSL 88 (1), 16-26.

Millar et al. 2002. JGS 159 (2), 145-157.

Pearce et al. 1984. JGS 16, 77-94.

Riley et al. 2012. JGS 169 (4), 381-393.

Storey. 1988. Techtonophysiscs 155, 381-390.

Suarez. 1976. Geology 4 (4), 211-214.

Vaughan and Storey. 2000. JGS 157 (6), 1243-1256.

1.3
Effects of extensional inheritance on passive margin collapse

Stéphane Jon Beaussier [1], Taras Gerya [2], Jean-Pierre Burg [1]

[1] Geologisch Institut, ETH Zürich, Sonnegstrasse 5, CH-8092 Zürich (stephane.beaussier@erdw.ethz.ch)
[2] Geophysical Institute, ETH Zürich, Sonnegstrasse 5, CH-8092 Zürich

The Wilson Cycle, describing the repeated opening and closing of ocean basins, implies a conversion of passive into active continental margins. However, the buoyancy of the oceanic lithosphere by itself is insufficient to overcome the high strength of the continental margin lithosphere. To lower this bulk strength, the existence of weak zones below the margin has often been speculated. Yet, the conditions of formation of these weak zones have been rarely studied.

Using a high-resolution 3D thermomechanical model – I3ELVIS (Gerya and Yuen, 2003) - of the Wilson Cycle we investigate the formation of the weak zones and their effects on the initiation of subduction at passive margin. For this we use the recent grain-damage rheology (Bercovici and Ricard, 2012) to have a self-consistent model of grain-size evolution in the mantle lithosphere and formation of the related weak-zones.

Results shows that stress concentration in the lithospheric mantle during rifting can induce localized grain-size reduction, which prompts the formation of long-lived weak zones above the lithosphere-asthenosphere boundary. Because this boundary is deflected by the asthenosphere upwelling during rifting, the damage-zones systematically dip away from the ocean. The reactivation of the damaged-zones as reverse zones during convergence allows for subduction initiation at the passive margin. Results show that this subduction mechanism is controlled by the continental Moho temperature. With a high Moho temperature (700° C) the weak zones partially heal through grain coarsening during seafloor-spreading. The resulting ductile strength of the margin is then too high to allow subduction initiation through passive margin collapse. These results show that the thermomechanical conditions of the continental lithosphere at the time of rifting exert a major control on the strength of the passive margin lithosphere and therefore the likeliness to have subduction initiation.

REFERENCES
Bercovici, D., Ricard, Y., 2012. Mechanisms for the generation of plate tectonics by two-phase grain-damage and pinning. Phys. Earth Planet. Inter. 202–203, 27–55. doi:10.1016/j.pepi.2012.05.003
Gerya, T. V., Yuen, D. a., 2003. Characteristics-based marker-in-cell method with conservative finite-differences schemes for modeling geological flows with strongly variable transport properties. Phys. Earth Planet. Inter. 140, 293–318. doi:10.1016/j.pepi.2003.09.006

1.4
Sediment Control on Subduction Plate Speeds

Whitney M. Behr, Thorsten W. Becker

Geologisch Institut, ETH Zürich, Sonnegstrasse 5, CH-8092 Zürich

Tectonic plate velocities predominantly result from a balance between the potential energy change of the subducting slab and viscous dissipation in the mantle, bending lithosphere, and slab-upper plate interface. A range of observations suggest that slabs may be weak, implying a more prominent role for plate interface dissipation than previously thought. The shallow thrust interface is commonly assumed to be weak due to an abundance of fluids and near-lithostatic pore fluid pressures, but little attention has been paid to the influence of the deeper, viscous interface. Here we show that the deep interface viscosity in subduction zones is strongly affected by the relative proportions of sedimentary to mafic rocks that are subducted to depth. Where sediments on the down-going plate are sparse, the deep interface is dominated by mafic lithologies that metamorphose to eclogites, which exhibit viscosities 5-50 times the asthenospheric mantle, and reduce subduction plate speeds. In contrast, where sediments are abundant and subducted to depth, the deep interface viscosity is 1-2 orders of magnitude lower than the asthenospheric mantle, thus allowing significantly faster plate velocities. This correlation between subduction plate speed and deep sediment subduction may help explain dramatic accelerations and decelerations in convergence rates, such as those documented for India-Asia convergence over the Cenozoic.

1.5

Dating retrograde tectonic activity in the Mont Blanc and Aiguilles Rouges massifs dated through ion probe analysis of hydrothermal cleft monazite

Christian A. Bergemann [1,2], Edwin Gnos [2] and Martin J. Whitehouse [3]

[1] Earth and Environmental Sciences, University of Geneva, Rue des Maraîchers 13, 1205 Geneva, Switzerland
[2] Natural History Museum of Geneva, route de Malagnou 1, 1208 Geneva, Switzerland
[3] Swedish Museum of Natural History, Box 50007, SE104-05 Stockholm, Sweden

Millimeter-sized hydrothermal monazites from open fissures (clefts) associated with different cleft generations in the Mont Blanc and Aiguilles Rouges massifs have been investigated by ion microprobe (SIMS). The interaction of hydrothermal fluids with the wall rock causes partial dissolution and alteration of the rock. Disequilibration of the fluid-rock syste within the cleft through tectonic activity led to mineral crystallization within the cleft and subsequent stepwise crystal growth. High precision isotope dating yields monazite crystallization ages. Unlike ^{238}U-^{206}Pb ages, ^{232}Th-^{208}Pb hydrothermal monazite ages are not affected by excess Pb and yield a higher precision than ages obtained through the U system.

Of the two cleft generations sub-horizontal clefts formed in a compressive phase, while the sub-vertical clefts formed during younger, strike-slip movements along boundaries on both sides of the Mont Blanc massif and Permocarboniferous deposits of the Aiguilles Rouges massif.

The studied crystals show three main growth phases at ca. 11.5 to 10.5 Ma, 9 Ma and 8 to 7 Ma, with relics of an older crystallization phase. This age pattern is interpreted as signifying (re-)crystallization during the start of dextral strike-slip deformation and later phases of activity along the strike-slip fault system.

All of the crystals are porous and complexly-zoned, an indication of dissolution-reprecipitation processes. Comparison of monazite crystallization ages with thermochronometers indicates that the network of vertical shear zones with down-dip lineation in the Mont Blanc massif became strongly overprinted at around 11.5 Ma. The identified deformation phases indicate the external massifs of the Western Alps to not only share a comparable tectonic position within the Alpine arc having also undergone a similar tectonic evolution.

1.6
Rock-matrix versus fracture-controlled fluid pathways in the upper oceanic crust

Alannah C. Brett [1], Larryn W. Diamond [1], Samuel Weber [1], Samuel Gilgen

[1] Institute of Geological Sciences, University of Bern, Baltzerstrasse 3, CH-3012 Bern (alannah.brett@geo.unibe.ch)

Permeable pathways in the upper oceanic crust control the geometry of mid-ocean ridge (MOR) hydrothermal circulation cells and the resulting chemical exchanges between the crust and seawater. Knowledge of the rock-matrix permeability and the fracture permeability along these pathways is required to enable realistic reactive-transport modelling of mass and heat transfers, such as those involved in forming volcanogenic massive sulphide (VMS) deposits at seafloor discharge sites.

To address this issue, we have examined the permeability distributions in the sheeted dike complex (SDC) and overlying lavas of the Semail ophiolite, Oman, as an example of MOR-type upper crust formed by fast spreading. We have distinguished alteration in recharge zones, where precursor basalts have been altered to "spilites" containing chlorite + albite + actinolite, from alteration in discharge zones, characterized by "epidosites" comprised of epidote + quartz + titanite ±Fe-oxides (Gilgen et al., 2016). For each alteration type we have determined the matrix permeabilities of altered lavas and dikes by standard laboratory measurements. We have also mapped fracture networks in each alteration zone and as a function of distance from seafloor faults. For these zones we estimated fracture permeability distributions by stochastic fracture modelling of discrete fracture networks (DFN).

Our results show that pillow stacks have bulk matrix permeabilities of $\sim 2 \times 10^{-16}$ m^2 where spilitised and $\sim 5 \times 10^{-16}$ m^2 where epidotised, whereas sheeted dikes have average matrix permeabilities of $\sim 2 \times 10^{-19}$ m^2 where spilitised and $\sim 3 \times 10^{-17}$ m^2 where epidotised. Fracture permeability is most prominent along normal faults, which are spaced at kilometre-scale in most of the ophiolite. The faults are bordered on each side by damage zones ~ 100 m wide, with fracture frequencies of ~ 0.001 m^{-3} and fractures lengths ≤ 50 m (Fig. 1). Within these fault-proximal zones, connected fracture networks make an appreciable contribution to the bulk permeability. Outside of the damage zones fractures frequency decreases to ~ 0.0002 m^{-3} and fractures are shorter (0.5–20 m). Thus, fractures in the fault-distal zones are rarely connected and hence they do not constitute a permeable network. The distal zones are nevertheless pervasively altered, demonstrating that matrix permeability is the dominant fluid pathway in these zones. At the outcrop-scale, flow leading to either pervasive spilitisation or epidotisation follows rock-matrix pathways that are largely inherited from precursor igneous textures.

Spilitisation reduces the porosity and permeability of precursor basalts, whereas epidotisation enhances porosity and permeability. In the cores and rims of pillow lavas, epidotisation increases the connected porosity by 9–17 vol.% and increases permeability by up to 3 orders of magnitude (reaching 3×10^{-15} m^2). In the SDC, porosity increases by 9–14 vol.% and permeability increases by up to 2.5 orders of magnitude (reaching 4×10^{-15} m^2). Therefore, as well as creating a significantly permeable pathway, epidotisation enables self-propagation of fluid flow without the need for fracture networks. Although epidosites represent segments of fluid upflow zones, in the Semail ophiolite they do not occur preferentially along faults that focus flow towards the known VMS deposits. Instead, discharge of the fluid that forms epidosites may occur diffusely over large areas of the seafloor at some distance from black-smoker-type vents.
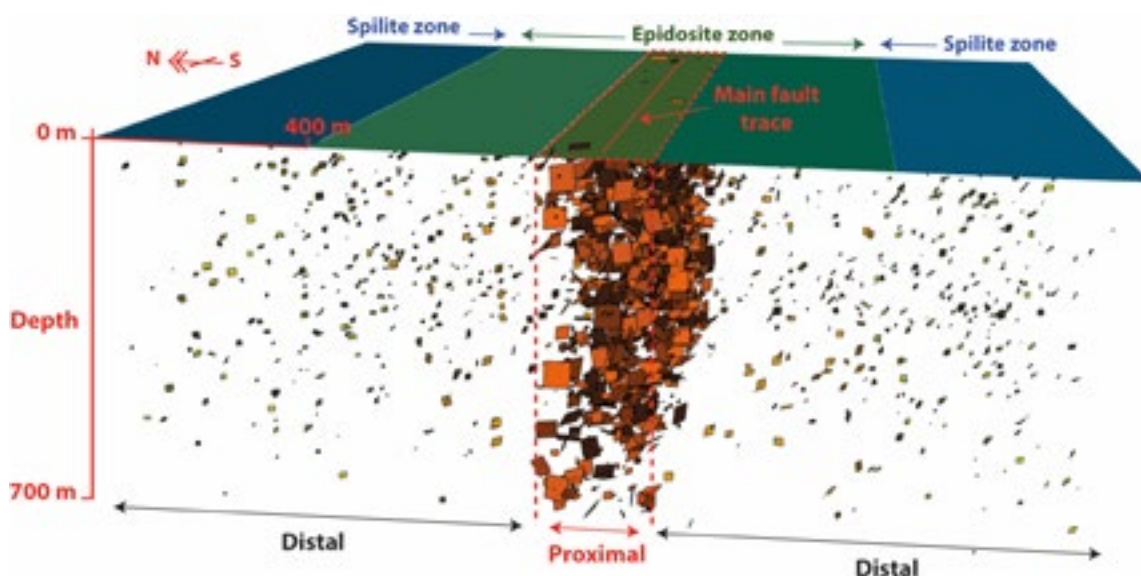
Figure 1. Discrete fracture network models surrounding a major seafloor fault, show distinct proximal and distal connectivities (DFN's pertain to three zones; proximal epidosite, distal epidosite and distal spilite). Only fractures that connect to at least one other fracture are displayed, which in the distal zones is a negliable fraction of the total individual fractures (average DFN contains 84000).

REFERENCES

Gilgen, S., Diamond L.W., & Mercolli, I., 2016: Sub-seafloor epidosite alteration: Timing, depth and stratigraphic distribution in the Semail ophiolite, Oman, Lithos, 260, 191–210.

1.7
The Alpine cycle: Modelling orogenic wedge formation from generation of hyper-extended passive margins and forced subduction to continent-continent collision

Lorenzo G. Candioti [1], Stefan M. Schmalholz [2], Thibault Duretz [3], Suzanne Picazo [4]

[1] *Institut des sciences de la Terre (ISTE), Université de Lausanne, Quartier Mouline, CH-1015 (Lorenzo.Candioti@unil.ch)*
[2] *Institut des sciences de la Terre (ISTE), Université de Lausanne, Quartier Mouline, CH-1015*
[3] *Univ. Rennes 1, UMR CNRS 6118, France*
[4] *University of Leicester*

The concept of orogenic wedges has been applied to explain the geodynamic evolution of many orogens worldwide. Recent numerical modelling studies have investigated orogenic wedge formation in a shortening lithosphere which was initially homogeneous, that is, having initially a constant crustal thickness. However, many orogens, such as the Western Alps, are characterised by the collision of hyper-extended passive margins which exhibited a significant variation of crustal thickness from the onset of subduction. Also, the pre-Alpine Liguria-Piemonte basin likely lacked a significant amount of newly formed oceanic lithosphere and consisted mainly of inherited and impregnated subcontinental mantle exhumed to the seafloor until embryonic ocean formation.

We perform high resolution 2D thermo-mechanical lithospheric scale numerical simulations to study the dynamics of the Alpine cycle. Modelling of this cycle is subdivided into the following stages: (I) in a slow spreading rift system, a ~400 km wide basin which contains exhumed lithospheric mantle and is bounded by regions of hyper-extended continental crust is generated. (II) the self-consistently modelled hyper-extended passive margin system is thermally relaxed. During this stage, the lithosphere is neither compressed nor extended. No spontaneous subduction initiation due to the densification of the cooling exhumed mantle occurs in the models. After thermal relaxation, (III) the evolved system is shortened and a one-sided, forced subduction is initiated within the proximal part of the passive margin without prescribing any weak zone. (IV) the basin is closed and an orogenic wedge forms during continent-continent collision.

First, we quantify the impact of the initial geometric configuration from the onset of rifting by varying the mechanical strength of the crust, being either an alternating sequence of horizontal mechanically strong and weak layers, or a non-layered, homogeneous strong crust. Second, we vary the duration of the thermal relaxation period to investigate the effect of distinct thermal structures of the basin from the onset of convergence on subduction initiation and orogenic wedge formation. Third, we examine the control of the lithospheric mantle strength on the evolution of the full Alpine cycle by using either dry or wet olivine flow law parameters for the mantle lithosphere and asthenosphere. In cases of low viscosities in the mantle, small density contrasts along the lithosphere-asthenosphere boundary might induce Rayleigh-Taylor instabilities. To ensure that the algorithm accurately resolves such instabilities, we first perform a benchmark simulation for large scale thermal convection. Fourth, we use a parameterisation for serpentinisation of the exhumed mantle lithosphere by replacing the olivine rheology of the top 7 km in the evolved basin by an antigorite rheology at the end of the cooling period. Fifth, we focus on the dynamics within the evolving orogenic wedge investigating the flow field of the crustal material and pressure variations within the wedge.

Potential applications of the model results to the Western Alpine orogeny are discussed.

1.8
Review of Alpine denudation rates from detrital [10]Be concentrations

Romain Delunel [1], Fritz Schlunegger [1], Pierre G. Valla [1], Jean Dixon [2], Christoph Glotzbach [3], Florian Kober [4], Kevin P. Norton [5], Bernhard Salcher [6], Hella Wittmann [7], Markus Christl [8]

[1] *University of Bern, Switzerland (romain.delunel@geo.unibe.ch),*
[2] *Montana State University, USA*
[3] *University of Tübingen, Germany*
[4] *Nagra, Switzerland*
[5] *University of Wellington, New-Zealand*
[6] *University of Salzburg, Austria*
[7] *GFZ Potsdam, Germany*
[8] *ETH Zürich, Switzerland*

Within the past decade, many studies have reported catchment-wide denudation rates for the European Alps based on *in situ* [10]Be concentrations measured in river sediments. One of these pioneering contributions was conducted along a north-south traverse through the Central Alps of Switzerland (Wittmann et al., 2007) and revealed an apparent correlation between [10]Be-inferred denudation and surface uplift rates. Here we report a compilation of >350 denudation rate data that now allows discussing how denudation rates vary from west to east across the European Alps.

The reported compilation yields a dense and original picture of the denudation rates for Alpine watersheds covering tens-to-thousands square kilometers and integrating the last 0.1-10 ka. We use this compilation to assess how [10]Be-inferred denudation rates distribute with respect to landscape properties (*i.e.* topographic metrics), environmental conditions (*i.e.* climate or hydrology) and geodetic settings (*i.e.* surface uplift) across the entire orogen, with the aim to identify the respective contributions of internal (tectonic) *vs.* external (climatic) drivers to the recent erosion history of the European Alps.

Our results show that although [10]Be-inferred denudation rates are scattered at small scale (especially in the Central Alps), consistent patterns are emerging when considering the Alps as a whole. In general, [10]Be-inferred denudation rates scale with topographic metrics such as basins' mean-elevation, slope gradient and relief; but interestingly they are independent of both intensity and distribution of precipitation and/or water runoff (proxies for modern climate). Because the rates of denudation in the Alps do correlate with metrics extracted from the Alpine topography, we infer a partial control related to the late-Pleistocene climatic and erosive conditions (landscape memory). In addition, we find a close relationship between denudation rates and surface uplift in our dataset, confirming previous observations at smaller-scale. We finally re-evaluate the isostatic response to recent erosional unloading along a west-east traverse across the Alps. While millennial denudation and instrumental surface uplift balance each other through isostatic compensation in both the Western and Eastern Alps, excess uplift can be observed in the Central Alps. These observations, in agreement with independent geophysical/geomorphological evidence in the Alps, further suggest that deep-crustal mechanisms (*e.g.* related to the geometry of the subducted European slab) also contribute as internal forces to the processes of denudation and rock uplift operating at the surface.

REFERENCES
Wittmann, H. et al. (2007). Relation between rock uplift and denudation from cosmogenic nuclides in river sediment in the Central Alps of Switzerland. Journal of Geophysical Research: Earth Surface, 112(F4).

1.9
Reactivation of Gouge-bearing Faults: an Experimental Insight

Carolina Giorgetti [1], Telemaco Tesei [2], Marco M. Scuderi [3], Cristiano Collettini [1,2]

[1] LEMR, ENAC, EPFL, Station 18, CH-1015 Lausanne, Switzerland (carolina.giorgetti@epfl.ch)
[2] Rock Mechanics Laboratory, Department of Earth Sciences, Durham University, Elvet Hill, Durham DH1 3LE, UK
[3] Department of Earth Sciences, Sapienza University, Piazzale A. Moro 5, 00185 Rome, Italy
[4] HP-HT Laboratory, National Institute of Geophysics and Volcanology, Via di Vigna Murata 605, 00143 Rome, Italy

Fault zones in the brittle crust constitute pre-existing weakness zones which can be reactivated depending on their friction, their orientation within the stress field and the stress field magnitude. Analytical approaches to evaluate the potential for fault reactivation are generally based on the assumption that faults are zero-thickness ideal planes characterized by constant friction. However, natural faults are complex structures which typically can host cataclastic fault zones of finite thickness. Here we experimentally investigate the reactivation of gouge-bearing faults at different orientations to the maximum principal stress and compare it with theoretical predictions based on analytical models. We simulate pre-existing faults by conducting triaxial experiments on sandstone cylinders containing a saw-cut, filled with a clay-rich gouge and located at various orientations to the maximum principal stress, ranging from 30° to 80°. The pre-existing faults were axially loaded at strain rates of $3.5*10^{-6}$ s^{-1}, under a constant confining pressure of 10 MPa. Our results show the reactivation of pre-existing faults when oriented at 30°, 40° and 50° to the maximum principal stress and the formation of a new fracture for fault orientations higher than 50°. Although these observations are in agreement with the fault lock-up predicted by analytical models, the differential stress required for reactivation strongly differs from theoretical predictions. In particular, unfavorable oriented faults appear systematically weaker, especially when a thick gouge layer is present. We infer that the observed weakness relates to the rotation of the stress field within the gouge layer during distributed deformation which precedes unstable fault reactivation, as suggested by microstructural observations. Thus, the assumption of zero-thickness planar fault provides only an upper bound to the stress required for reactivation of misoriented faults, which may result in misleading predictions of fault reactivation.

1.10

Thermal softening induced strain localization: from first order features to high resolution lithospheric scale numerical models

Dániel Kiss [1], Lorenzo G. Candioti [1], Yury Podladchikov [1], Thibault Duretz [1,2], Stefan M. Schmalholz [1]

[1] Institute of Earth Sciences, University of Lausanne, CH-1015 Lausanne (daniel.kiss@unil.ch)
[2] Géosciences Rennes, Univ. Rennes 1, UMR CNRS 6118, France

Localization of strain plays a major role during geodynamic processes, such as mountain building, and in particular during the formation of shear zones on all geological scales. In the uppermost part of the lithosphere, that is characterized by low confining pressures, strain localization is controlled by brittle-frictional mechanisms. Strain localization is possible at higher confining pressures too, where brittle fracture is unlikely. At these high confining pressures, strain localization in quasi-homogenous domains requires a softening mechanism and we consider here thermal softening (i.e. shear heating), which may be the controlling mechanism of lithospheric scale shear zone formation and subduction initiation.

Thermal softening is a result of the conversion of mechanical work into heat (i.e. shear heating) and of the temperature dependence of rock viscosities. Previous studies have shown that thermal softening can cause strain localization and the formation of large-offset shear zones in ductile materials whose deformation behavior is described with creep flow laws (e.g. dislocation creep). Also, it has been shown that thermal softening induced shear localization can result in significant stress drops of a few hundred MPa.

To quantify shear zone formation by thermal softening we apply three approaches of different complexity, namely (1) dimensional analysis and analytical solutions, (2) numerical simulations with simple flow laws and model configurations but in turn for 1D, 2D and 3D deformations, and (3) high-resolution 2D thermo-mechanical simulations of lithosphere-asthenosphere deformation. Fundamental features of the modelled shear zones are that (i) they are constantly widening due to heat conduction and (ii) that their finite strain variation across the shear zone is smaller (almost an order of magnitude) than the associated temperature variation. We show the general applicability of these features, which have been studied with 1D simple-shear models, by comparing the 1D simple-shear results with results of 2D and 3D shear zone development under pure shear. Finally, we compare the results of the 1D simple shear zone model with results of high-resolution 2D numerical simulations of lithospheric shortening and subduction. In these simulations, we first model the formation of hyper-extended passive margins and mantle exhumation by extending a continental lithosphere. After a period of thermal relaxation, we start to compress the extended configuration, which leads to subduction initiation by thermal softening; in agreement with results of the 1D, 2D and 3D models performed for simpler rheologies and configurations.

1.11
Fast exhumation in early Oligocene and syn-collisional volcanism as revealed by combined FT and U-Pb analysis of detrital zircons in the Central Alps

Gang Lu [1], Giuditta Fellin [2], Wilfried Winkler [1], Sean D. Willett [1], Marcel Guillong [2]

[1] Geological Institute, ETH Zurich, Sonneggstrasse 5, 8092 Zurich, Switzerland, (gang.lu@erdw.ethz.ch)
[2] Institute for Geochemistry and Petrology, ETH Zurich, Clausiusstrasse 25, 8092 Zurich, Switzerland

Detrital zircon fission-track analysis (DZFT) from syn-orogenic sediments provide a powerful tool to examine the exhumation history of orogenic belts. In addition, U-Pb age dating (LA-ICP-MS) of detrital zircon is helpful in provenance analysis, especially for documenting syn-sedimentary volcaniclastic influx. Both methods are used together to determine the short-term collisional evolution of the Central Alpine orogenic belt as reconstructing the Early Oligocene exhumation and understanding the syn-collisional Periadriatic magmatism. Three samples show similar detrital ZFT age populations, with three different peaks: 33-40 Ma (P1, 20%); 72-91 Ma (P2, 30-40%); and 180-203 Ma (P3, 40-50%). However, there are several grains with similar ZFT ages and U-Pb ages in the P1 (undivided), which supposed to be of volcanic origin. Then, the P1 is divided into: 8-14% of volcanic grains (P1-Voclanic), and 6-13% of basement grains (P1-Basement). The data show that the contribution of volcanogenic input from the Periadriatic magmatic complex is significant in the syn-tectonic sediments, which were ignored in previous studies. These volcanic zircons (P1-Voclanic) must be excluded from the exhumation rate evaluation of the basement. The lag times (P1-Basement) show an increasing trend of 8-15 Myr from Middle to Late Eocene in the foreland basin. This average lag time can be translated into a short-term average exhumation rate from 0.4 to 0.7 km/Myr. Compared with undivided P1 peak which indicates a subcritical wedge state, the basement P1 peak shows a transition at 30 Ma from subcritical to supercritical wedge state. The reasons for decreasing exhumation rate may be the declining of Periadriatic fault movement and volcanic activity (major period: 32-30 Ma). The results provide evidence for a short pulse of fast exhumation in the Central Alps during 32 and 30 Ma. This period is seen as a result of rapid surface uplift and syn-collisional volcanism in the Central Alps, which were caused by European slab break-off and mantle upwelling, as well as the amplified activity of Periadriatic fault system.

REFERENCES
Bernet, M., Brandon, M.T., Garver, J.I., Balestrieri, M.L., Ventura, B., and Zattin, M., 2009, Exhuming the Alps through time: Clues from detrital zircon fission-track ages: Basin Research, v. 21, p. 781–798.
Carrapa, B., 2009, Tracing exhumation and orogenic wedge dynamics in the European Alps with detrital thermochronology: Geology, v. 37, p. 1127–1130.
Jourdan, S., Bernet, M., Tricart, P., Hardwick, E., Paquette, J. L., Guillot, S., ... & Schwartz, S. (2013). Short-lived, fast erosional exhumation of the internal western Alps during the late early Oligocene: Constraints from geothermochronology of pro-and retro-side foreland basin sediments. Lithosphere, 5(2), 211-225.

1.12

New Thermochronological Constraints on Thrust Activity in the Subalpine Molasse: Implications for the Late Miocene Evolution of the Central Alps

Samuel Mock [1], Marco Herwegh [1], Fritz Schlunegger [1], Christoph von Hagke [2], István Dunkl [3]

[1] Institute of Geological Sciences, University of Bern, Baltzerstrasse 1+3, CH-3012 Bern (samuel.mock@geo.unibe.ch)

[2] RWTH Aachen University, Institute of Structural Geology, Tectonics and Geomechanics, Lochnerstraße 4-20, D-52056 Aachen

[3] University of Göttingen, Geoscience Center, Sedimentology and Environmental Geology, Goldschmidtstr. 3, D-37077 Göttingen

The sedimentary archives and the tectonic history of foreland basins can be used to resolve the influence of deep-seated processes on mountain building. Due to its well-established history, the northern Molasse Basin of the European Alps is especially suited to constrain the geodynamic evolution of a collisional orogen. Age constraints on the basin's exhumation history provide a substantial contribution to the understanding of the orogen's geodynamic development. In this study, we present new thermochronological data from the Subalpine Molasse in the Lake Thun area (Switzerland), which we compare to published data from along the Alps in order to investigate the young exhumation history of the North Alpine foreland.

Based on low-temperature apatite (U-Th-Sm)/He thermochronology, we constrain break-back thrusting in the Subalpine Molasse between 12 Ma and 5 Ma, thus occurring coeval to the main deformation phase in the adjacent Jura fold-and-thrust belt and to the main NW-directed thrusting phase in the Aar Massif. A comparison to similar studies from the Subalpine Molasse of eastern Switzerland and Bavaria (e.g. Ortner et al. 2015; von Hagke et al. 2012) show that this pattern of tectonic activity is, however, not unique to areas which are bordered by External Crystalline Massifs (ECMs; e.g. Aar Massif), but is consistent along the entire front of the Central Alps. This means that regardless of the hinterland's architecture, which is highly non-cylindrical along the Alpine chain, the foreland experiences major thrusting in the late Miocene and that thrusting in the Subalpine Molasse is through going, i.e. not necessarily spatially and kinematically linked to the extrusion of ECMs. The orogen-scale occurrence of this late Miocene thrusting event though suggests a driving force acting on a large wavelength, i.e. at the crustal scale. The recently promoted rollback model for the Alps (Kissling and Schlunegger 2018; Schlunegger and Kissling 2015) and new findings on the Aar Massif's uplift and exhumation history (Herwegh et al. 2017) may be used to explain the observations of our study

REFERENCES

Herwegh, M., Berger, A., Baumberger, R., Wehrens, P., & Kissling, E. (2017). Large-Scale Crustal-Block-Extrusion During Late Alpine Collision. *Scientific Reports*, *7*, 413. doi:10.1038/s41598-017-00440-0

Kissling, E., & Schlunegger, F. (2018). Rollback Orogeny Model for the Evolution of the Swiss Alps. *Tectonics*, *37*(4), 1097–1115. doi:10.1002/2017TC004762

Ortner, H., Aichholzer, S., Zerlauth, M., Pilser, R., & Fügenschuh, B. (2015). Geometry, amount, and sequence of thrusting in the Subalpine Molasse of western Austria and southern Germany, European Alps. *Tectonics*, *34*(1), 1–30. doi:10.1002/2014TC003550

Schlunegger, F., & Kissling, E. (2015). Slab rollback orogeny in the Alps and evolution of the Swiss Molasse basin. *Nature Communications*, *6*, 8605. doi:10.1038/ncomms9605

von Hagke, C., Cederbom, C. E., Oncken, O., Stöckli, D. F., Rahn, M. K., & Schlunegger, F. (2012). Linking the northern Alps with their foreland: The latest exhumation history resolved by low-temperature thermochronology. *Tectonics*, *31*(5), TC5010. doi:10.1029/2011TC003078

1.13
Constraining deformation phases in the Aar Massif and the Gotthard Nappe (Switzerland) using Th-Pb crystallization ages of fissure monazite-(Ce)

Emmanuelle Ricchi [1], Edwin Gnos [2], Alfons Berger [3], Daniela Rubatto [3], Christian Bergemann [1]

[1] Earth and Environmental Sciences, University of Geneva, Rue des Maraîchers 13, 1205 Geneva, Switzerland (emmanuelle.ricchi@unige.ch)
[2] Natural History Museum of Geneva, Route de Malagnou 1, 1208 Geneva, Switzerland
[3] Institut für Geologie, University of Bern, Baltzerstrasse 1+3, 3012 Bern, Switzerland

Hydrothermal monazite-(Ce), (LREE,Th)PO4, is found in alpine fissures and clefts that formed during tectonic movements under peak to retrograde metamorphic conditions. Subsequent tectonic movements lead to a stepwise growth of minerals on the cleft walls (e.g., Mullis, 1996). The age of this growth stages can be estimed by dating growth domains in monazite-(Ce). In the Tauern window, Austria, it was found that cleft monazite-(Ce) crystallized in a temperature range of ~200-300°C (Gnos et al., 2015).

Crystallization ages of fissure monazite-(Ce) were measured using the Th-Pb isotopic system with the great advantage that this isotopic system is not affected by diffusion under cleft conditions (Cherniak et al., 2004) and that monazite-(Ce) is very resistant to radiation damage (e.g. Meldrum et al., 1998). In presence of hydrous fluid, chemical disequilibrium can trigger crystallization or dissolution/reprecipitation of monazite and reset the isotopic system (e.g. Grand'Homme et al., 2016; Seydoux-Guillaume et al., 2002, 2012). Therefore, hydrothermal monazite-(Ce) is able to record several deformation events through multiple growth and dissolution episodes (e.g. Bergemann et al., 2017; Berger et al., 2013).

Th-Pb data of growth domains of monazite-(Ce) grains from the Aar Massif (AM) and the Gotthard Nappe (GN) were aquired at the SwissSIMS facility. Comparison of Th-Pb fissure monazite-(Ce) crystallization ages to existing crystallization and cooling ages (zircon/apatite fission tracks, muscovite/illite ages from fault gouges, ((U-Th)/He ages) showed that early monazite-(Ce) crystallization occurred slightly above or below the zircon fission track closure temperature and the youngest crystallization overlaps with the apatite fission track closing temperature. Monazite-(Ce) also grows at temperatures of muscovite/illite crystallization in fault gauges. Spot ages show that the earliest stage of crystallization recorded by fissure monazite-(Ce) occurred around 20.2 Ma in the GN and about 3 Ma later in the AM, and the latest crystallization event was recorded at 5.1 Ma in the AM. Under monazite crystallization conditions, protracted deformation was recorded over 14 Ma and distinct phases of monazite-(Ce) growth can be linked with deformation events in the AM and GN area. In the GN, two growth domain age ranges comprised between 16-15 Ma and 14-13 Ma were identified to correspond to the Chièra and post-Chièra deformation phases. In this area only horizontal clefts are found whereas in the AM, both horizontal and vertical clefts orientation is present. In the AM, four growth domain age ranges of 15-14 Ma, 12-9.5 Ma, 12-10 Ma and 9-6 Ma respectively, correspond to the Handegg, Oberaar, Pfaffenchopf and Rhone-Simplon deformation phases.

REFERENCES

Bergemann, C., Gnos, E., Berger, A., Whitehouse, M., Mullis, J., Wehrens, P., Pettke, T., Janots, E., 2017. Th-Pb ion probe dating of zoned hydrothermal monazite and its implications for repeated shear zone activity: An example from the central alps, Switzerland. Tectonics 36, 671–689. https://doi.org/10.1002/2016TC004407

Berger, A., Gnos, E., Janots, E., Whitehouse, M., Soom, M., Frei, R., Waight, T.E., 2013. Dating brittle tectonic movements with cleft monazite: Fluid-rock interaction and formation of REE minerals. Tectonics 32, 1176–1189. https://doi.org/10.1002/tect.20071

Berger, A., Mercolli, I., Herwegh, M., Gnos, E., 2017. Geological Map of the Aar Massif and the Tavetsch and Gotthard Nappes. Federal Office of Topography Swisstopo, Wabern.

Cherniak, D.J., Watson, E.B., Grove, M., Harrison, T.M., 2004. Pb diffusion in monazite: A combined RBS/SIMS study. Geochim. Cosmochim. Acta 68, 829–840. https://doi.org/10.1016/j.gca.2003.07.012

Gnos, E., Janots, E., Berger, A., Whitehouse, M., Walter, F., Pettke, T., Bergemann, C., 2015. Age of cleft monazites in the eastern Tauern Window: constraints on crystallization conditions of hydrothermal monazite. Swiss J. Geosci. 108, 55–74. https://doi.org/10.1007/s00015-015-0178-z

Grand'Homme, A., Janots, E., Seydoux-Guillaume, A.M., Guillaume, D., Bosse, V., Magnin, V., 2016. Partial resetting of the U-Th-Pb systems in experimentally altered monazite: Nanoscale evidence of incomplete replacement. Geology 44, 431–434. https://doi.org/10.1130/G37770.1

Meldrum, A., Boatner, L.A., Weber, W.J., Ewing, R.C., 1998. Radiation damage in zircon and monazite. Geochim. Cosmochim. Acta 62, 2509–2520. https://doi.org/10.1016/S0016-7037(98)00174-4

Mullis, J., 1996. P-T-t path of quartz formation in extensional veins of the Central Alps P-T-t path of quartz formation in

extensional veins of the Central Alps *. Schweiz. Miner. petrogr. mitt. 76, 159–164. https://doi.org/10.5169/seals-57694

Seydoux-Guillaume, A.M., Montel, J.M., Bingen, B., Bosse, V., de Parseval, P., Paquette, J.L., Janots, E., Wirth, R., 2012. Low-temperature alteration of monazite: Fluid mediated coupled dissolution-precipitation, irradiation damage, and disturbance of the U-Pb and Th-Pb chronometers. Chem. Geol. 330–331, 140–158. https://doi.org/10.1016/j.chemgeo.2012.07.031

Seydoux-Guillaume, A.M., Paquette, J.L., Wiedenbeck, M., Montel, J.M., Heinrich, W., 2002. Experimental resetting of the U-Th-Pb systems in monazite. Chem. Geol. 191, 165–181. https://doi.org/10.1016/S0009-2541(02)00155-9

1.14
3D finite strain quantification and numerical modelling of the transition between viscous folding and thrusting.

Richard Spitz [1], Stefan M. Schmalholz [1]

[1] Institute of Earth Sciences, University of Lausanne, Bâtiment Géopolis, CH-1015 Lausanne (richard.spitz@unil.ch)

Field observations (Pfiffner, 1993) in the Swiss Alps and 2D numerical studies (Jaquet et al. 2014) have shown that folding and thrusting is strongly controlled by the mechanical stratigraphy of the geological units. The mechanical stratigraphy is defined by the thickness ratio between competent and incompetent units, where incompetent units constitute frequently detachment horizons. Depending on this ratio either thrusting or folding can be initiated during bulk shortening.

To investigate the control of the lateral variation of this mechanical stratigraphy on the transition between thrusting and folding during bulk shortening, we employ a three-dimensional numerical model with a non-linear viscous rheology. Our 3D configuration consists of a stiff viscous layer that is embedded in a weaker viscous matrix. The layer has a pre-existing weak zone to initiate the folding and thrusting on each side of the model domain. We utilize several initial geometries with varying detachment horizon thickness and different angular orientation of the weak zone.

We focus here on the quantification of the 3D deformation and compute the finite strain ellipsoid for different domains of the model. We calculate the Nadai strain, which quantifies the overall accumulated strain, and the Lode's ratio, which quantifies the strain symmetry such as constriction or flattening. Nadai strain and Lode's ratio are utilized to construct so-called Hsu-diagrams (Hsu, 1966) in order to illustrate the three-dimensional finite strain state.

Our results demonstrate that the Nadai strain does not vary significantly between the folding and thrusting domain, however, the thrusting domain shows systematically higher values. The strain symmetry varies significantly between the different configurations. However, the thrusting domain shows more constrictional strain, whereas folding exhibits more flattening strain. Furthermore, the lateral transition between folding and thrusting generates locally a simple shear, or strike-slip, deformation although the bulk deformation of the model domain corresponds to pure shear. Moreover, we present several visualization methods for 3D finite strain calculated in numerical models.

REFERENCES

Pfiffner, O. A. (1993). The structure of the Helvetic nappes and its relation to the mechanical stratigraphy. Journal of structural Geology, 15, 511-511.

Jaquet, Y., Bauville, A., & Schmalholz, S. M. (2014). Viscous overthrusting versus folding: 2-D quantitative modeling and its application to the Helvetic and Jura fold and thrust belts. Journal of Structural Geology, 62, 25-37.

Hsu, T. C. (1966). The characteristics of coaxial and non-coaxial strain paths. Journal of Strain Analysis, 1(3), 216-222.

1.15

Present-day uplift of the European Alps: mechanisms and relative contributions

Pietro Sternai [1], Christian Sue [2], Laurent Husson [3], Enrico Serpelloni [4], Claudio Faccenna [5], Thorsten Becker [6], Andrea Walpersdorf [3]

[1] *Département de Sciences de la Terre, Université de Genève, Geneva, Switzerland*
[2] *Chrono-Environnement, CNRS, Université de Bourgogne Franche-Comté, Besançon, France*
[3] *ISTerre, Université de Grenoble Alpes, CNRS, Grenoble, France*
[4] *Istituto Nazionale di Geofisica e Vulcanologia, Centro Nazionale Terremoti, Bologna, Italy*
[5] *Dipartimento di Scienze, Università di Roma III, Rome, Italy*
[6] *Institute for Geophysics, Jackson School of Geosciences, University Texas at Austin, Austin, Texas, USA*

Recent measurements of surface vertical displacements of the European Alps show widespread uplift at rates of up to ~2.5 mm/a in the north-western and central Alps and ~1 mm/a across a continuous region from the eastern to the south-western Alps. Such a rock uplift rate pattern is at odds with the horizontal strain rate field, characterized by shortening and crustal thickening in the eastern Alps and very limited deformation in the central and western Alps. Proposed mechanisms of rock uplift rate include isostatic response to the last deglaciation, long-term erosion, detachment of the western Alpine slab, as well as lithospheric and surface deflection due to sub-Alpine asthenospheric convection. Here, we assess prior work and present new estimates of the contributions from such proposed mechanisms. Lithospheric adjustment to deglaciation and erosion may account for the great majority of the observed surface uplift rates in the eastern Alps, which, if correct, suggests that topography due to plate tectonic related horizontal shortening and crustal thickening is reduced by other mechanisms. In the central and western Alps, the lithospheric adjustment to deglaciation and erosion likely accounts for roughly half of the rock uplift rates, which points to a noticeable contribution by mantle-related processes such as detachment of the European slab and/or asthenospheric upwelling. While it is difficult to independently constrain the patterns and magnitude of mantle contributions to ongoing Alpine vertical displacements at present, future AlpArray-related data should provide additional insights to better constrain these processes. Regardless, it is increasingly clear that interactions between tectonics *s.l.* and surface unloading processes, rather than individual forcings, are required to explain the current Alpine topographic change.

1.16

The Evolution and Distribution of Chemical Heterogeneity in the Earth's Mantle

Jun Yan [1], Maxim D. Ballmer [1], and Paul J. Tackley [1]

[1] Institute of Geophysics, ETH Zurich, Zurich, Switzerland (jun.yan@erdw.ethz.ch)

A better understanding of the compositional structure of the Earth's mantle is needed to place the geochemical record of surface rocks into the context of Earth accretion and evolution. Cosmochemical constraints imply that lower-mantle rocks may be enriched in silicon relative to upper-mantle pyrolite, whereas geophysical observations tend to support whole-mantle convection and mixing. To resolve this discrepancy, it has been suggested that subducted mid-ocean ridge basalts (MORBs) segregate from harzburgites to be accumulated in the mantle transition zone (MTZ) and/or lower mantle. However, the key parameters that control MORB segregation and accumulation remain poorly constrained. Here, we use global-scale 2D thermochemical convection models to investigate the influences of plate and mantle rheology on the evolution and distribution of chemical heterogeneity. In particular, we focus on the accumulation of subducted MORB within a reservoir in the MTZ. Our results show that deep-rooted plumes as well as stagnant slabs deliver MORB to the MTZ to establish a MORB-reservoir. Relatively low viscosities in the MTZ tend to facilitate the segregation of MORB from harzburgite, and accumulation of MORB in the MTZ. In turn, relatively high viscosities in the lower-mantle tend to suppress the accumulation of MORB at the core-mantle boundary, while promoting the entrainment of MORB by plumes and related delivery to the MTZ. Finally, relatively high plate yield stresses tend to sustain the formation of large MORB piles in the deep mantle, but with little or no effect on MORB-enrichment in the MTZ reservoir. For a wide range of parameters, we find a moderate enhancement of MORB in the MTZ (~15% MORB plus ~85% pyrolite) after 4.5 Gyrs model time, a prediction that can be tested using seismic observations. Our results suggest that the MTZ may play an important role in regulating heat and material fluxes through the mantle.

P 1.1

Numerical modelling of lithospheric flexure at subduction zones: investigation of forces involved in the flexure and in melt extraction from the LVZ.

Annelore Bessat [1], Sébastien Pilet [1], Thibault Duretz [2], Stefan Markus Schmalholz [1]

[1] Institute of Earth Sciences, University of Lausanne, Géopolis, CH-1015 Lausanne (annelore.bessat@unil.ch)
[2] Geosciences Rennes, University of Rennes 1, F-35042 Rennes

Petit-spot volcanoes were found fifteen years ago by Japanese researchers at the top of the subducting plate in Japan (Hirano 2006). This discovery is of great significance as it highlights the importance of tectonic processes for the initiation of intraplate volcanism. The location of these small lava flows is unusual and seems to be related to the plate flexure, which may facilitate the extraction of low degree melts from the base of the lithosphere,

The presence of melts (0.1 to 2%) at the base of the lithosphere has been hypothesized previously to explain changes in electric and seismic properties at 70-90 km depth, i.e. within the low velocity zone (LVZ) (Sifré et al., 2014). A critical question is related to the process associated with the extraction of theses low degree melts from the LVZ to produce the petit-spot volcanoes observed on the sea floor.

First models suggested that extension associated to plate bending allows large cracks to propagate across the lithosphere promoting the extraction of melts from the base of the lithosphere (Hirano 2006 & Yamamoto 2014). However, the study of petit-spot mantle xenoliths from Japan (Pilet 2016) has demonstrated that low degree melts are not directly extracted to the sea floor but percolate, interact and metasomatize the oceanic lithosphere.

In order to understand the melt extraction process in the region of plate bending, we performed 2D thermo-mechanical numerical simulations of subduction based on the general plate geometry observed in Japan. The aim of the numerical modelling is to determine the distribution of deformation mechanisms and to quantify differential stresses within a bending lithosphere. The numerical model considers viscoelastoplastic deformation, a combination of laboratory-derived flow laws (e.g. diffusion creep, dislocation creep and Peierls creep) and heat transfer. The models are applied to quantify the distribution of stress, strain rate, and viscosity in and around the flexed lithosphere since these quantities likely control the percolation of melt initially stocked at the base of the lithosphere. We considered two subduction end-members, namely forced- and free- subduction scenarios in order to determine their main differences. Furthermore, we quantified the spacial variations of the gravitational potential energy (GPE) during subduction to measure the forces driving subduction.

Initial results show that plate flexure changes the distribution of the deformation mechanism in the flexure zone, between 40 km to 80 km depth. A change of the dominant deformation mechanism in the subducting lithospheric slab was observed about 200 to 300 km away from the trench. The main deformation mechanism evolves from diffusion creep to dislocation creep and then to Peierls creep. These changes are linked to the augmentation of the stresses in the flexure zone. At the base of the lithosphere, diffusion creep is observed within a thin layer (20 km), which becomes even thinner (10 km) as subduction progresses.

The model allows also to calculate the horizontal deviatoric stress which allow to determine regions in compression or in extension. The results show that the horizontal deviatoric stresses at the lithosphere-asthenosphere-boundary vary as function of the subductions scenarios. Further work will be necessary to prove whether or not the associated stress distribution is compatible with the development of porosity waves, a critical process to extract melts in low porosity media.

REFERENCES

Hirano, N., Takahashi, E., Yamamoto, J. et al. 2006: Volcanism in Response to Plate Flexure. Science, 313, 1426-1428
Pilet, S., Abe, N., Rochat, L. et al. 2016: Pre-subduction metasomatic enrichment of the oceanic lithosphere induced by plate flexure. Nature Geoscience, 9, 898-904
Sifré, D., Gardés, E., Massuyeau, M. et al. 2014: Electrical conductivity during incipient melting in the oceanic low-velocity zone. Nature, 509, 81-87
Yamamoto, J., Korenaga, J., Hirano, N., and Kagi, H. 2014: Melt-rich lithosphere-asthenosphere boundary inferred from petit-spot volcanoes. Geology, 42, 967-970

P 1.2

Stress in the Alpine foreland – a kinematic and mechanical approach

Sandra Borderie [1], Jon Mosar [1], Bertrand Maillot [2]

[1] Unit of Earth Sciences, Geosciences Department, University of Fribourg, Chemin du Musée 6, CH-1700 Fribourg
(sandra.borderie@unifr.ch)
[2] Laboratoire GEC, Maison Internationale de la Recherche, Université de Cery-Pontoise, 1 rue Descartes,
F-95000 Neuville-sur-Oise

The Alpine foreland comprises the wedge-top Molasse Basin and the Jura fold-and-thrust belt. The sedimentary cover is deformed due to the outward propagation of the Alpine orogenic wedge. Deformation roots into a major Triassic evaporitic *décollement*. In these two areas, a part of the deformation in the sedimentary cover is characterized by conjugate tear faults. Recent studies indicate that some faults could be close to failure. However, few data are available to fully constrain the state of stress of this foreland. The goal of this project is to better understand the present deformation of the Alpine foreland. To do this, we populate the current model of the studied area with mechanical parameters. We use the Optum G2 and SLAMTec softwares that apply the principles of the Limit Analysis. Optum G2 computes the stress and the velocity fields at the initiation of the deformation. SLAMTec models 2D mechanical evolutions of thrust sequences. Combining these static and kinematic approaches enables to generate models of various mechanical scenarios. Based on existing cross-sections, structural map and 3D models in the foreland, we will test various parameters such as the influence of the position and thickness of the *décollement*, the influence of basement-inherited structures, or the geometry of the known fault systems. We expect that the results will allow explaining the structural state of the Alpine foreland and will give direct information about the current stress field. These data could then be used to assess the risk linked to exploration and exploitation of natural resources.

P 1.3

The Chazuta Thrust, a large-transport thrust in an evaporites-floored basin (Huallaga Basin, Peru): insights from analogue modelling.

Sandra Borderie [1], Bruno C. Vendeville [2], Fabien Graveleau [2], César Witt [2], Pierre Dubois [3], Patrice Baby [4],
Ysabel Calderon [5]

[1] Unit of Earth Sciences, Department of Geosciences, University of Fribourg, Chemin du Musée 6, CH-1700 Fribourg
(sandra.borderie@unifr.ch)
[2] Univ. Lille, CNRS, Univ. Littoral Côte d'Opale, UMR CNRS 8187, LOG, Laboratoire d'Océanologie et de Géosciences,
F-59 000 Lille
[3] Perenco – Oil and Gas, 8 Hanover Square, London W1S 1HQ, England
[4] Géosciences Environnement Toulouse (GET), Université de Toulouse,
CNRS UMR 5563 / UR 234 IRD / UPS Toulouse / CNES, 14 Avenue Edouard Belin, F-31400 Toulouse.
[5] PERUPETRO S.A., Avenida Luis Aldana n°320, San Borja, Lima 41, Peru.

The Huallaga Basin in the Sub-Andean (North Peru) is a foreland basin where deformation involves an evaporites-related *décollement*. The basin comprises several syntectonic depocenters, one of which is the Biabo Syncline located at the back of the Chazuta Thrust. This thrust is a flat-floored thrust that has accommodated more than 40 km of horizontal displacement. Despite such a large displacement, the hangingwall has remained remarkably intact with little or no internal deformation and has incorporated a large volume of evaporites at its base.

In order to unravel the formation and evolution of the Chazuta Thrust, we conducted a series of analogue physical experiments that tested the role of various parameters (overburden thickness and geometry, occurrence of early folds, erosion of the foldbelt front). The main goal is to investigate a system in which most of the deformation is accommodated in the frontal part of the chain (Chazuta Thrust), whereas deformation of the thrust sheet itself remains minor.

Results from our experimental investigations suggest that the three key parameters that have allowed for such a long-lived, large-slip frontal thrust to operate are (1) the wedge-shaped syntectonic sediments sourced from the hinterland, (2) the presence of the Biabo Syncline that acted as a bulldozer pushing the evaporites forward, forcing distal inflation and (3) the erosion at the front that favoured a farther advance of the frontal thrust, dragging passively large volumes of evaporites with it.

P 1.4

Luminescence dating and landscape evolution of the Himalaya, Nepal

Chloé Bouscary [1], Georgina E. King [2], Frédéric Herman [2], Rabiul H. Biswas [2], Kristel Chanard [3], Jérôme Lavé [4], György Hetényi [5]

[1] Institute of Geological Sciences & Oeschger Centre for Climate Change Research, University of Bern, Switzerland
  (chloe.bouscary@geo.unibe.ch)
[2] Institute of Earth Surface Dynamics, University of Lausanne, Switzerland
[3] IGN France, Université Paris Diderot - LAREG, France
[4] CRPG, UMR 7358 CNRS - Université de Loraine, Nancy, France
[5] Institute of Earth Sciences, University of Lausanne, Switzerland

The 2015 Mw 7.8 Gorkha earthquake in Nepal, which caused widespread devastation and loss of life, reveals some gaps in our understanding of the deformation of the Himalaya. Here we aim to constrain recent - Quaternary - changes in deformation in Nepal, through quantifying exhumation rates using luminescence thermochronometry.

Optically Stimulated Luminescence (OSL)-thermochronometry [Guralnik B. et al., 2015; King G.E. et al., 2016] is a recently developed very-low-temperature thermochronometer, sensitive to temperatures of 30-100°C, based on luminescence dating of quartz and feldspar minerals. It offers the potential for precise constraint of cooling histories over recent timescales, and provides high-resolution cooling histories beyond the range of other thermochronometric systems. Applying this new technique to feldspar extracts of a set of samples from the Nepalese-Himalaya provides insights into the cooling and thus exhumation/erosion history of the Himalayan fold-and-thrust belt, giving a better understanding of the Quaternary dynamics of the Himalayas.

The Himalaya mountain belt is the result of compressional orogeny due to the continental collision between the Indian and the Eurasian tectonic plates. Different shear zones and north-dipping crustal-scale thrusts accommodate this convergence. In this project, the objective is to analyse samples collected across some of the most tectonically significant structures in the Himalayan orogen. This allows us to better define the location of the main faults, which is still debated [Searle M. et al., 2008; Parsons A.J. et al., 2016], and by quantifying exhumation rates on each side of the faults, to assess the long-term deformation across the major thrusts.

Preliminary results from five samples along the Marshyangdi River give a better idea of the location of the Main Central Thrust (MCT), and indicate variations in exhumation rates between the different tectonic structures. Whilst potentially relating to local surface process and/or climatic differences (i.e. fluvial incision rates, glacial erosion), these data could also indicate recent tectonic deformation, potentially implying Quaternary fault reactivation within this region.

REFERENCES

Guralnik B. et al. 2015: Radiation-induced growth and isothermal decay of infrared-stimulated luminescence from feldspar. Radiation Measurements 81, 224-231

King G.E. et al. 2016: Multi-OSL-thermochronometry of feldspar. Quaternary Geochronology 33, 76-87

Martin A.J. 2017: A review of definitions of the Himalayan Main Central Thrust. International Journal of Earth Sciences (Geol. Rundsch.) 106, 2131-2145

Parsons A.J. et al. 2016: Geology of the Dhaulagiri-Annapurna-Manaslu Himalaya, Western Region, Nepal, 1 :200,000. Journal of Maps 12(1), 100-110

Searle M. et al. 2008: Defining the Himalayan Main Central Thrust in Nepal. Journal of the Geological Society 165, London, 523-534

P 1.5
A new technique to construct crustal 3-D Vs models: Implementation of Ray Tracing, Model Parameterization and Inversion

Leonardo Colavitti [1], György Hetényi [1] & the AlpArray Working Group

[1] Institut des sciences de la Terre, University of Lausanne, Quartier UNIL-Mouline, Bâtiment Géopolis, CH-1015 Lausanne
 (leonardo.colavitti@unil.ch)

We develop a new tool in which we use P-to-S converted waves to construct a fully 3-D shear-wave velocity model of the crust. This technique requires a dense seismological network to map the less-studied S-wave velocities.

We implement an accurate ray-propagator which respects Snell's law in 3-D at any interface geometry. First, we employ an existing ray-shooting tool (Knapmeyer 2004) to calculate P-ray geometry in a global velocity model (iasp91) to arrive at the station. Then, starting from the piercing point at the local Moho, we shoot an S-wave to the surface, which is several km away from the station. We therefore adjust the ray parameter to make the corresponding crustal S-waves arrive at the station.

A synthetic precision test with flat Moho and constant crustal velocity shows that the converted waves reach the station within 10 m. Using local velocity structure and complex Moho geometry, the mean distance is about 150 m (median ~ 40 m) from the station.

We parameterize the model grid using square cells in X and Y directions and define its based on the ray coverage map of actual data. For a 20-year dataset at more than 180 stations recording about 300 000 traces, the mesh size is typically 25x25 km. For each layer, we define an S-wave velocity at the top and at the bottom: this allows to accommodate both velocity gradients within and velocity jumps between layers.

The individual velocity profile along each trace is etracted from the 3-D initial model and the velocity model is continously updated during the inversion process.

We envisage to manage the inversion by the stochastic Neighbourhood Algorithm (Sambridge 1999a), looking at the ensemble of models that sample the good data-fitting regions of a multidimensional parameter space. We plan to test our approach first a 1-layer Vs model and then introduce intra-crustal discontinuities (e.g. Conrad).

Our first focus region is the Central Alps, where a well-defined Moho map (Spada et al. 2013) and a high-resolution P-wave velocity model (Diehl et al. 2009) are available. We plan to extend our study to the entire Alpine domain in frame of the AlpArray project (Hetényi et al. 2018).
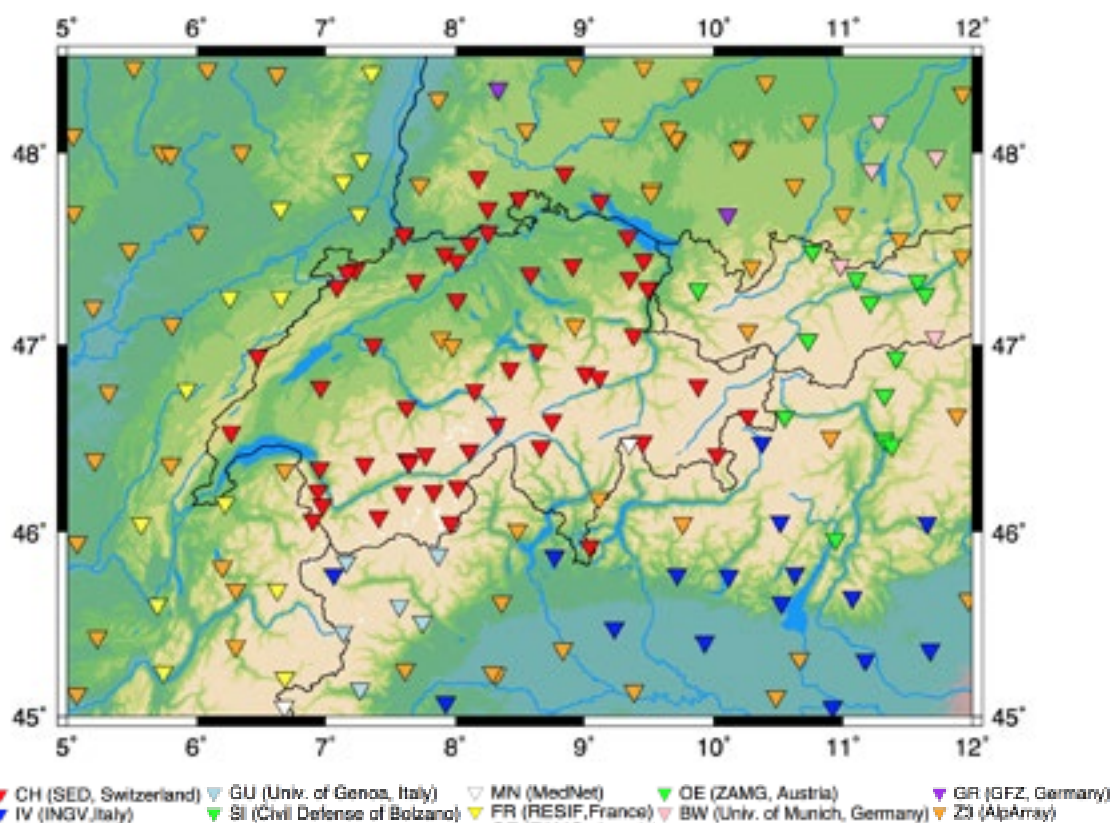

Figure 1. Seismic stations used in the Central Alps.

REFERENCES

Diehl, T., Husen, S., Kissling, E. and Deichmann, N. 2009: High resolution 3-D P-wave model of the Alpine crust, Geophys. J. Int. 179, 1133-1147.

Hetényi, G., Molinari, I., Clinton, J., Bokelmann, G., Bondár, I., Crawford, W. C., Dessa, J-X., Doubre, C., Friederich, W., Fuchs, F., Giardini, D., Gráczer, Z., Handy, M. R., Herak, M., Jia, Y., Kissling, E., Kopp, H., Korn, M., Margheriti, L., Meier, T., Mucciarelli, M., Paul, A., Pesaresi, D., Piromallo, C., Plenefisch, T., Plomerová, J., Ritter, J., Rümpker, G., Šipka, V., Spallarossa, D., Thomas, C., Tilmann, F., Wassermann, J., Weber, M., Wéber, Z., Wesztergom, V., Živčić, M., AlpArray Seismic Network Team, AlpArray OBS Cruise Crew, AlpArray Working Group. 2018: The AlpArray Seismic Network – a large-scale European to image the Alpine orogen. Surv. Geophys 39, 1009-1033.

Knapmeyer, M. 2004: TTBox: A MatLab toolbox for the computation of 1D teleseismic travel times, Seismol. Res. Lett. 75(6), 726-733.

Sambridge, M., 1999a. Geophysical inversion with a neighbourhood algorithm. I – Searching a parameter space. Geophys. J. Int. 138, 479-494.

Spada, M., Bianchi, I., Kissling, E., Piana Agostinetti, N. and Wiemer, S. 2013: Combining controlled-source seismology and receiver function information to derive 3-D Moho topography for Italy, Geophys. J. Int. 194(2), 1050-1068.

P 1.6
Linking seismicity with faults: Insights from a new high-resolution earthquake catalog of Switzerland

Tobias Diehl [1], Edi Kissling [2], Timothy Lee [1], Lukas Nibourel [3], Stefan Schmid [2]

[1] Swiss Seismological Service, ETH Zurich, 8092, Switzerland (tobias.diehl@sed.ethz.ch)
[2] Institute of Geophysics, ETH Zurich, 8092, Switzerland
[3] Institute of Geological Sciences, University of Bern, Switzerland

The connection of seismicity with geologically or geophysically mapped faults is a prerequisite for a seismotectonic interpretation but crucially depends on the accuracy and precision of hypocentre solutions reported in earthquake catalogues. In most cases, changes in the network configuration, analysis techniques (e.g. seismic phase picking) and location procedures (e.g. seismic velocity models) introduce significant inconsistencies to earthquake catalogues and therefore hamper high-resolution seismotectonic interpretations. A consistent and realistic estimate of location uncertainties is often missing in many catalogues.

To overcome such limitations in the instrumental earthquake catalogue of the Swiss Seismological Service (SED), we applied an iterative relocation procedure to improve seismic velocity models and hypocentre locations in Switzerland. The proposed procedure involves tomographic inversions of P and S waves of about 3700 local earthquakes to solve the coupled hypocentre – velocity structure problem in 1D and 3D. Nonlinear location algorithms are used to derive consistent uncertainty estimates for the entire catalogue. Finally, we apply relative relocation techniques, combined with waveform cross-correlation to resolve the fine structure of seismicity and to resolve the geometry of active faults in the Alps and its foreland. In addition, the comparison of focal depths with the 3D velocity structure derived from the tomographic inversion will help to constrain host lithologies of upper-crustal seismicity.

We focus on the source region of the ML 4.6 Urnerboden earthquake of 2017, located in the Helvetic nappes immediately adjacent to the northernmost outcrops of the crystalline Aar massif because this region is particularly suited for linking seismicity with geologically and geophysically mapped faults. The seismotectonic interpretation considers absolute locations, 3D velocity structure, high-precision relative relocations, focal mechanisms, geological profiles, structural and geomorphological analysis. Our results document a rare but striking agreement in the seismicity pattern observed within the Aar crystalline massif near its basement-cover contact with faults outcropping at the earth's surface in the Helvetic nappes due to neotectonic activity along subvertically oriented strike slip faults. Such agreement suggests that the entire upper crustal section down to the uppermost portion of the Aar massif presently deforms as a block, with the deformation in the sediments of the Helvetic nappes not being decoupled from deformation within the underlying *parautochthoneous* wedge of the Aar crystalline massif any more. This implies a change from thrusting mode active during the latest stages of Alpine orogeny active during the Miocene towards neotectonic activity dominated by strike-slip mode in the analysed region.

P 1.7

Effect of grain friction on characteristics of seismic cycles in a sheared granular fault gouge

Omid Dorostkar [1,2] & Jan Carmeliet [2]

[1] Department of Civil, Environmental and Geomatic Engineering, Swiss Federal Institute of Technology Zurich (ETH Zurich), Stefano-Franscini-Platz 5, CH-8093 Zurich (domid@ethz.ch)

[2] Department of Mechanical and Process Engineering, Swiss Federal Institute of Technology Zurich (ETH Zurich), Leonhardstrasse 21, CH-8092 Zurich

The stability of mature faults is shown to depend on properties of fault gouge material. The granular fault gouge is created due to frictional processes that take place in fault damage zone, and a direct result of wear and communition. Grain shape, surface roughness and particle size distibution of gouge material control the dynamics of fault system and can affect the characteristics of seismic cycles. Here we study the effect of micro-scale grain roughness approximated by the inter-particle friction coefficient on the characteristics of seismic cycles using 3-D DEM numerical simulations. We simulate stick-slip dynamics and systematically vary the inter-particle friction coefficient recording hundreds of slip events to perform statistical analyses. We show that the fault gouge stick-slip frictional capacity (macroscopic friction coefficient), dilation and their variability nonlinearly increase with the particle roughness (inter-particle friction coefficient), but then saturates to a plateau value. Our results show that the average recurrence time and its variability decreases with increasing particle roughness. A rougher fault gouge with higher inter-parrticle friction coefficient shows a more complex nucleation phase during the stick period. The energy budget analysis of system reveals that a fault system with higher grain roughness is capable of storing higher potential energy but releases the stored energy more frequent compared to a smoother fault. Our results in this study are consistent with numerical and experimental works and complete them by a focus on micromechanics of fault damage zone, showing how numerical models and in particular discrete element simulations can help boost our understanding from fault mechanics.

P 1.8
Bedrock structure, postglacial infill and neotectonic fault structures in Lake Constance

Stefano C. Fabbri [1], Robin Allenbach [2], Marco Herwegh [3], Sebastian Krastel [4], Elodie Lebas [4], Katja Lindhorst [4], Herfried Madritsch [5], Martin Wessels [6], Ulrike Wielandt-Schuster [7], Flavio S. Anselmetti [1]

[1] Institute of Geological Sciences and Oeschger Centre for Climate Change Research, University of Bern, Baltzerstr. 1+3, CH-3012 Bern (stefano.fabbri@geo.unibe.ch)
[2] Bundesamt für Landestopografie swisstopo, Seftigenstrasse 264, CH-3084 Wabern
[3] Institute of Geological Sciences, University of Bern, Baltzerstr. 1+3, CH-3012 Bern
[4] Institute of Geosciences, Christian-Albrechts-Universität zu Kiel, Otto-Hahn-Platz 1, D-24118 Kiel
[5] Nagra, Nationale Genossenschaft für die Lagerung radioaktiver Abfälle, Hardstrasse 73, CH-5430 Wettingen
[6] Landesanstalt für Umwelt Baden-Württemberg, Institut für Seenforschung, Argenweg 50/1, D-88085 Langenargen
[7] Landesamt für Geologie, Rohstoffe und Bergbau, Albertstr. 5, D-79104 Freiburg im Breisgau

In November 2017, a consortium between Swiss and German research and governmental institutions carried out a 2D multichannel reflection seismic survey on perialpine Lake Constance. The survey revealed new insights into the diverse geometry of the lake basins, their sedimentary infill, the underlying bedrock structure and paleo- and neotectonic fault features. The lines were shot complementary to a reconnaissance survey that was conducted along the main basin (Upper Lake Constance) and Lake Überlingen in 2016 and were extended to the shallower basins of Lower Lake Constance in the east.

The seismic data aims to close gaps between existing onshore seismic data vintages from Switzerland and Germany, to identify and characterize fault structures in Cenozoic and Mesozoic bedrock and to unravel the sedimentary evolution of the overdeepened lake basin, shaped by multiple glaciations. Of special interest are various fault zones across the eastern basins, such as the Hegau-Lake Constance Graben, the Randen, Mindelsee, Schienerberg Fault Zones (Egli et al., 2016), as well as the Roggwil, St. Gallen and Rhine Valley Fault Zone across the main basin (Heuberger et al., 2016). Considering the present off-fault paleoseismic evidence in the peri-alpine region, primary on-fault evidence should be present as well (Kremer et al., 2017; Diehl et al. 2018). However, seismogenic fault structures with clear surface ruptures are scarcely found in Switzerland (Ustaszewski and Pfiffner., 2008).

The seismic investigation of Lake Constance revealed a new N-S striking fault structure, that is robustly imaged on four individual seismic sections in the main lake basin. It offsets Molasse bedrock reflections, extends upwards into overlying glacial- and glacio-lacustrine deposits up to Holocene layers and even displaces the lake floor by approximately 1 m. This displacement is also confirmed by the bathymetric lake map. The new lake seismic dataset will improve our comprehension concerning the activity of complex fault patterns rooting in Molassic and Mesozoic strata in the North Alpine Foreland basin. In addition, the dataset will substantially contribute to our understanding of the glacial overdeepenings and their possible relationship with deep-rooted fault structures.

REFERENCES

Diehl, T., Clinton, J., Deichmann, N., Cauzzi, C., Kastli, P., Kraft, T., Molinari, I., Bose, M., Michel, C., Hobiger, M., Haslinger, F., Fah, D., and Wiemer, S., (2018) Earthquakes in Switzerland and surrounding regions during 2015 and 2016. Swiss Journal of Geosciences, 111(1-2), p. 221-244.

Egli, D., Mosar, J., Ibele, T., Madritsch, H., 2016, The role of precursory structures on Tertiary deformation in the Black Forest—Hegau region. International Journal of Earth Science: doi:10.1007/s00531-016-1427-8.

Heuberger, Roth P., Zingg O., Naef H., and Meier B. P., 2016, The St. Gallen Fault Zone: a long-lived, multiphase structure in the North Alpine Foreland Basin revealed by 3D seismic data. Swiss Journal of Geosciences, 1–20.

Kremer, K., Wirth, S.B., Reusch, A., Faeh, D., Bellwald. B., Anselmetti, F.S., Giardclos, S., and Strasser, M., 2017: Lake-sediment based paleoseismology: limitations and perspectives from the Swiss Alp. Quaternary Science Reviews 168, 1-18.

Ustaszewski, M., Pfiffner, O.A., 2008. Neotectonic faulting, uplift and seismicity in the central and western Swiss Alps. Geol. Soc. Lond. Spec. Publ. 298, 231-249.

P 1.9

Upscalling microstructural analysis: A new approach applied to experimentally deformed calcite aggregates

James Gilgannon [1], Alfons Berger [1], Thomas Poulet [2], Klaus Regenauer-Lieb [2], Manolis Veveakis [2], Auke Barnhoorn [3] and Marco Herwegh [1]

[1] *Institute of Geological Sciences, University of Bern, Baltzerstrasse 1+3, CH-3012 Bern, Switzerland (james.gilgannon@geo.unibe.ch)*
[2] *School of Petroleum Engineering, The University of New South Wales, Kensington NSW 2033, Australia*
[3] *Faculty of Civil Engineering and Geosciences, TU Delft, Stevinweg 1, Delft, The Netherlands*

When a rock is deformed the energy of deformation must either be stored or dissipated and both the storage and dissipation are achieved through micro-scale adjustments in the rock. Examples of these adjustments would be twinning, crystal defect production, chemical reactions and dynamic recrystallisation. In general microstructural and petrologic studies focus on documenting these small-scale adjustments and relating them to larger scales through continuum assumptions, e.g. thermodynamics and continuum mechanics. Many of the techniques used to capture evidence of the aforementioned microstructural adjustments require an imaging resolution of at least below 1 micron. This is restrictive and therefore evidence of microstructural change is often limited to neighbourhoods of investigation that range from a few hundred microns, up to a few millimetres. This can produce a picture that is filled with lots of small heterogeneities while in fact the rock is deforming in a very homogeneous way at the larger length scale.

Here we revisit an experimental run on Carrara marble by Barnhoorn et al. (2004) to explore the heterogeneities in the rock. The deformation was shown to be diffused at the sample scale but underwent significant microstructral changes during large-strain torsion experiments (Barnhoorn et al., 2004). Here we apply a combination of scanning electron microscopy techniques, spatial statistics and wavelet analysis to understand how and where microstructural adjustments happen. Ultimately we demonstrate that significant microstructural adjustment occurred and that it is systematic throughout the entire sample. The systematic locations of the microstructural changes probably relate to domains where the most work is imposed on the sample. Therefore, despite grain-scale heterogeneities in the starting material the bulk material properties dominate the rocks response to deformation. Furthermore, once deformation induced more local heterogeneities, like grain size differences, this did not effect the larger scale. Our evidence highlights the care that must be taken when relating local microstructural differences to larger scales of interpretation.

REFERENCES

Barnhoorn, A., Bystricky, M., Burlini, L. & Kunze, K. 2004: The role of recrystallisation on the deformation behaviour of calcite rocks: large strain torsion experiments on Carrara marble, Journal of Structural Geology, 26, 885-903.

P 1.10
Seismicity in Western Peloponnese and Ionian Islands: A new investigation with a local network

Haddad Antoine [1], Planes Thomas [1], Ganas Athanassios [2], Kassaras Ioannis [3] & Lupi Matteo [1]

[1] *Crustal Deformation and Fluid Flow Group, University of Geneva (antoine.haddad@unige.ch)*
[2] *National Observatory of Athens*
[3] *University of Athens – Department of Geophysics and Geothermy*

From July 2016 to May 2017, we investigated the seismicity in Western Peloponnese and the Ionian Islands to study the crustal deformation of the region. We deployed a network composed of 15 temporary stations (Short Period Lennartz 1s) and 9 permanent seismic stations of the Hellenic Unified Seismological Network (HUSN).

We contructed the catalogue using STA/LTA method and auto-picking using PhasePApy python package (Chen and Holland 2016). Next, we applied the matlab tool PSPicker (Baillard et al. 2014) to refine P- and S-wave arrivals detecting 1515 local earthquakes. In order to constrain the 1D optimum local velocity model using the location error minimizatiin technique, we divided the area into 4 regions corresponding to 4 refined 1D velocity models. The relocated events show a complex crustal architecture with seismicity from 2 to 30 km depth. To highlight the kinematics deformation of the region we calculated moment tensor solutions for the major events (i.e. M>3). By combining the focal mechanisms and the (micro)seismic activity we were able to identify key seismogenic structures.
Finally, we present the preliminary results of an ambient noise tomography pointing out the shallow velocities anomalies beneath the Greek Ionian sea.

REFERENCES
Baillard, C., Crawford, W. C., Ballu, V., Hibert, C., & Mangeney, A. (2014). An automatic Kurtosis-Based P and S phase picker designed for local seismic networks. Bulletin of the Seismological Society of America, 104(1), 395-409. http://doi.org/10.1785/0120120347
Chen, C., & Holland, A. A. (2016). PhasePApy: A Robust Pure Python Package for Automatic Identification of Seismic Phases. Seismological Research Letters, 87(6), 1384–1396. http://doi.org/10.1785/0220160019

P 1.11

Reconstruction of the geodynamic and magmatic evolution of the Somkheto-Karabagh and Pontides Arcs from the Mesozoic to Early Cenozoic across Armenia, Georgia and NE Turkey

Marc Hässig [1], Robert Moritz [1], Nino Popkhadze [2], Alexey Ulianov [3], Massimo Chiaradia [1], Ghazar Galoyan [4]

[1] Department of Earth Sciences, University of Geneva, 13 rue des Maraîchers, 1205 Geneva, Switzerland (marc.haessig@unige.ch)

[2] Al. Jalenidze Institute of Geology, I. Javakhishvili Tbilisi State University, 1 Chavchavadze Avenue, 0179 Tbilisi, Georgia

[3] Institute of Earth Sciences, University of Lausanne, Quartier UNIL-Mouline, Bâtiment Géopolis, 1015 Lausanne, Switzerland

[4] Institute of Geological Sciences, National Academy of Sciences of Armenia, 24A Marshall Baghramian Avenue, 0019 Yerevan, Armenia

During the Mesozoic and early Cenozoic the southern margin of the Eurasian continent recorded the closure of the northern Neotethys oceanic domain. The Somketo-Karabagh and Pontides magmatic arcs in current day Armenia, Georgia and NE Turkey attest for subduction, obduction, and micro-plate accretion events ending with Eurasia-Arabia collision and complete closure of Neotethys oceans.

Three main domains are distinguished in the Lesser Caucasus and NE Anatolia (Figure 1), including from South to North: (1) the South Armenian Block and the Tauride-Anatolide Platform (SAB-TAP), Gondwanian-derived continental terranes; (2) the Sevan-Akera and Ankara-Erzincan suture zones (AESAS) distinguished by the northern limit of ophiolite bodies which were thrusted onto the SAB-TAP; and (3) the Eurasian margin, represented by the Eastern Pontides and the Somkheto-Karabagh magmatic arcs. These two belts are in continuation with one another along the Eurasian margin. Their formation is due to the north-dipping Tethyan subduction under the southern Eurasian margin followed by collision. The onset of the north-dipping subduction is not well constrained. However, studies conducted in the Caucasus, Georgia and the Pontides reveal coeval calc-alkaline magmatic activity since the Early or Middle Jurassic. Yet, Cenomanian to Santonian ages have been proposed as well.

New observations, radiometric dating, geochemical and isotopic data of magmatic rocks of the Alaverdi district in NE Armenia and the Bolnisi district in SE Georgia (Lesser Caucasus region) complete a comprehensive dataset pertaining to the Eurasian margin from W Azerbaijan, Armenia, Georgia and into NE Turkey. Results obtained range from calc-alkaline to high-k magmatic arc activity during Late Jurassic times (158-148 Ma) in the Alaverdi district and calc-alkaline to shoshonitic magmatic arc activity during Campanian times (83-81 Ma) in the Bolnisi district. This additional insight is key for the unravelling of the evolution of the magmatism occurring there, and subsequently the evolution of subduction dynamics. In light of the implications of their geochemical characteristics, we can constrain the source and petrogenesis of the subduction-related magmatic rocks. Considering the complexity of the regional, structural and magmatic evolution along the southern Eurasian margin, our multi-disciplinary approach allows us to constrain the plate tectonic and geodynamic evolution of the Pontides-Lesser Caucasus segment of the Tethyan belt.

REFERENCES

Gamkrelidze, I.P., Pruidze, M.P., Gamkrelidze, M.I., & Loladze, M.I. 2013. Tectonic Map of Georgia (scale 1: 500 000). Meridiani, Tbilisi.

Hässig, M., Rolland, Y., Sosson, M., Galoyan, G., Sahakyan, L., Topuz, G., Çelik, Ö.F., Avagyan, A., & Müller, C. 2013. Linking the NE Anatolian and Lesser Caucasus ophiolites: evidence for large-scale obduction of oceanic crust and implications for the formation of the Lesser Caucasus-Pontides Arc. Geodinamica Acta, 26, 311-330.

Sosson, M., Stephenson, R., Sheremet, Y., Rolland, Y., Adamia, S., Melkonian, R., Kangarli, T., Yegorova, T., Avagyan, A., Galoyan, G., Danelian, T., Hässig, M. Meijers, M., Müller, C., Sahakyan, L., Sadradze, N., Alania, V., Enukidze, O., Mosar, J. 2016. The eastern Black Sea-Caucasus region during the Cretaceous: New evidence to constrain its tectonic evolution. Comptes Rendus Geoscience, 348, 23-32.
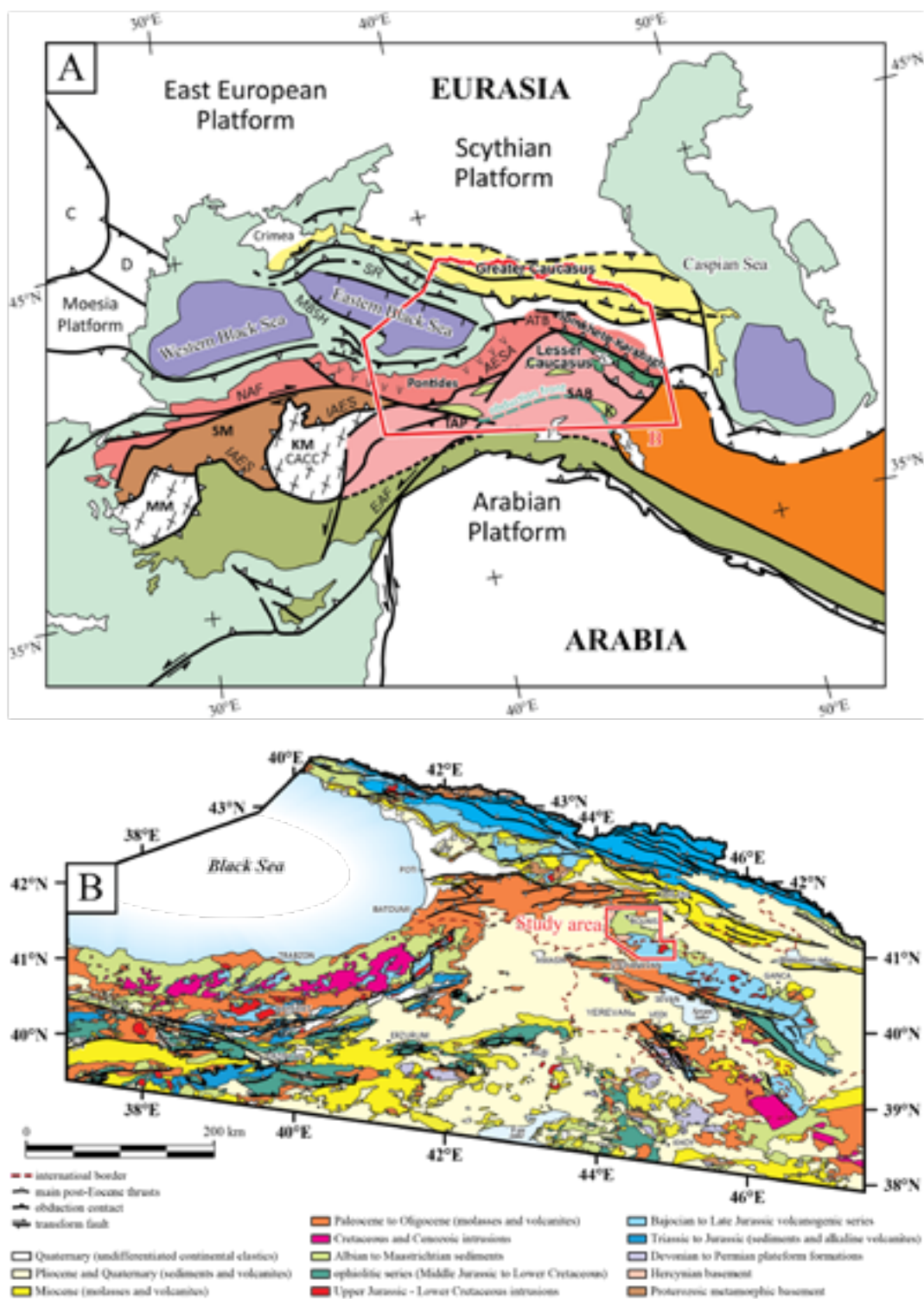
Figure 1. A, sketch structural map of the Middle East and Lesser Caucasus regions, after Sosson et al. (2016), modified. Position of map B is indicated. B, structural map of the Eastern Pontides, Lesser Caucasus and Greater Caucasus, after Hässig et al. (2013) and Gamkrelidze et al. (2013), modified.

P 1.12

Spatial relation of surface faults and crustal seismicity: a first comparison in the region of Switzerland

György Hetényi [1], Jean-Luc Epard [1], Leonardo Colavitti [1], Alexandre H. Hirzel [2], Dániel Kiss [1], Benoît Petri [1], Matteo Scarponi [1], Stefan M. Schmalholz [1], Shiba Subedi [1]

[1] *Institute of Earth Sciences, University of Lausanne, UNIL-Mouline Géopolis, CH-1015 Lausanne, Switzerland (gyorgy.hetenyi@unil.ch)*
[2] *IT Services, University of Lausanne, UNIL-Sorge Amphimax, CH-1015 Lausanne, Switzerland*

The deformation pattern in active orogens is in general diffuse and distributed, and is expressed by spatially scattered seismicity and fault network. We select two relating datasets in the region encompassing Switzerland and analyse how they compare with each other. The datasets are not complete but are the best datasets currently available which fully cover the investigated area at a uniform scale. The distribution of distances from each earthquake to the nearest fault suggests that about two-thirds of the seismicity occurs near faults, yet about 10% occurs far from known faults. These numbers are stable for various selections of earthquakes and even when considering location uncertainties. Earthquake magnitudes in the catalogue are smaller than what could be expected from faults lengths. This suggests that the deep fracture pattern is more segmented than the superficial one, or mostly partial rupture during earthquakes, and (partly) the impropriety of the scaling law. Statistics on the distances from each fault to the nearest earthquake reveal that all supposedly-active faults in Switzerland have experienced a typically felt (magnitude 2.5 or larger) event, and only one out of six has not done so in the past four decades. Future applications of the presented approach to more complete or comprehensive fault databases may result in revised numbers regarding the connection between deep and superficial fracture patterns, representative of the regional stress regime.

The public and educational message: (1) in the region of Switzerland, earthquakes can happen in areas without known or mapped faults; (2) not all faults produce earthquakes within a human lifetime, but they seem to do so over long times.
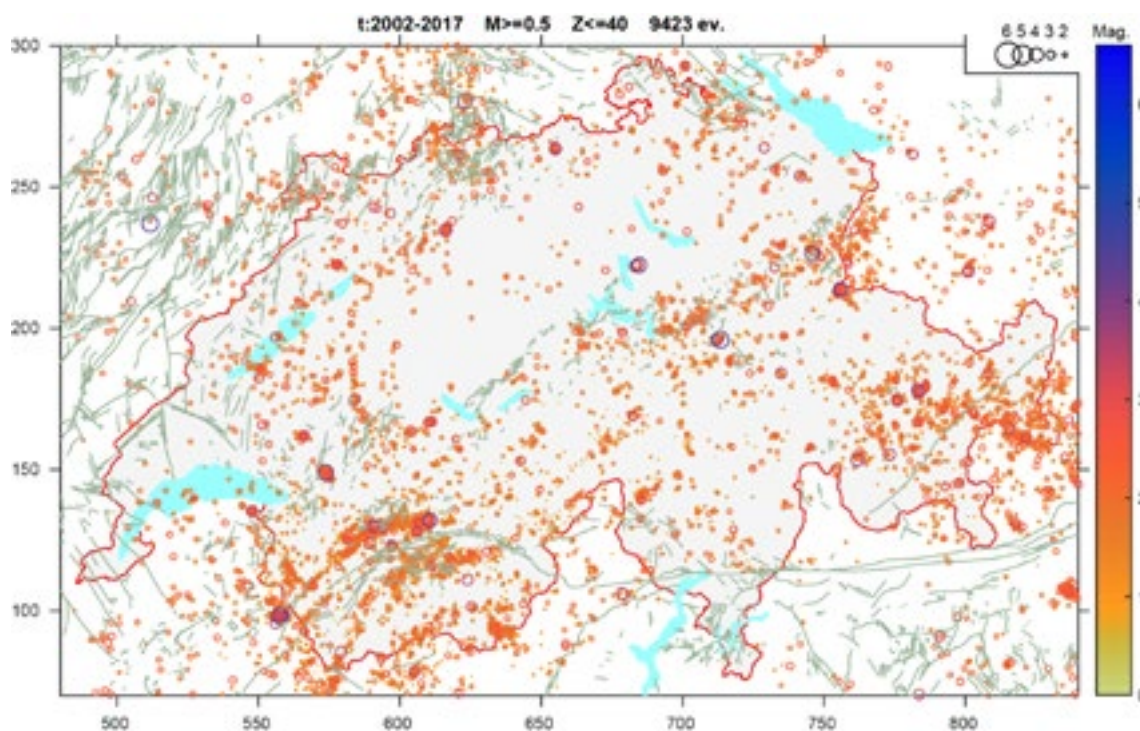

Figure 1. Map view of M≥0.5 events in the time window 2002-2017 in the entire study area, with respect to supposedly-active faults (in pale green). Co-ordinates are shown in the Swiss grid in km.

REFERENCES

Hetényi, G., Epard, J.-L., Colavitti, L., Hirzel, A. H., Kiss, D., Petri, B., Scarponi, M., Schmalholz, S. M. & Subedi, S. 2018: Spatial relation of surface faults and crustal seismicity: a first comparison in the region of Switzerland, Acta Geodaetica et Geophysica, in press. doi:10.1007/s40328-018-0229-9

P 1.13

A seismological study to investigate the volcanic behaviour of the Irazú-Turrialba complex

Elliot Amir Jiwani-Brown [1], Matteo Lupi [1], Javier F. Pacheco [2], Thomas Planes [1], Mauricio Mora [3]

[1] Département des Sciences de la Terre et de Géophysique, Université de Genève, Rue des Maraîchers 13, CH-1205 Genève, Switzerland (elliot.jiwani-brown@unige.ch)
[2] Observatorio Vulcanológico y Sismológico de Costa Rica (OVSICORI), Universidad Nacional Costa Rica, 2386-3000 Heredia, Costa Rica
[3] Red Sismológica Nacional (RSN), Escuela Centroamericana de Geología, Universidad de Costa Rica, Calle Masis, San José Province, Mercedes, Costa Rica

The analysis of unique seismic signals in geothermal and hydrothermal systems presents a valuable insight into the characteristic evolution of volcanic processes, event triggering (volcanic or seismic) and sensitivity to local and regional influences.

The Irazú and Turrialba Volcanic Complex (ITVC) marks the end of a 10-volcano sequence in Costa Rica, distinguishable by an abrupt variation in the lineament of this volcanic arc. The ITVC presents a location of two differing physical states, the closed system of Irazú and actively venting open conduit system of Turrialba. This presents a diverse volcanic setting ideal to deploy a temporary 20 station seismic network. Complemented by the permanent network, a detailed study of this hydrothermal region is undertaken, with influences from the tectonic setting analysed. Seismic data are being used to provide an insight into the temporal variations of this volcanic complex.

Specific seismic identifiers attributed to volcanic processes provide important information pertaining to the geometric and dynamic features of the ITVC. The most common and distinguishable volcano seismic signals are Long Period signals, volcano tectonic events and tremors. A classification of these signals is made to distinguish the temporal evolution of fluid migration and possible permeability changes in this active system. We use a cross-correlation approach followed by a differential travel-time grid search associated with back projections, to stack and normalize the seismic signal allowing us to locate emerging signals. From the results, a spatial and temporal analysis of these signals can reveal patterns of magma migration, locations of conduit systems, contact points between volcanic reservoirs and even fluid driven fracturing events (Chouet 1996; Woods et al., 2017).

Volcano seismic signals generated by the Irazú Turrialba Volcanic Complex and recorded by this network establish a temporal and spatial interpretation of the underlying magmatic plumbing system.

REFERENCES

Chouet, B. A. (1996). Long-period volcano seismicity: its source and use in eruption forecasting. Nature, 380(6572), 309.
Woods, J., Donaldson, C., White, R. S., Caudron, C., Brandsdóttir, B., Hudson, T. S., & Ágústsdóttir, T. (2018). Long-period seismicity reveals magma pathways above a laterally propagating dyke during the 2014–15 Bárðarbunga rifting event, Iceland. Earth and Planetary Science Letters, 490, 216-229.

P 1.14

Present-day crustal deformation of the Turkish-Iranian Plateau: insights from kinematic modelling

Amaneh Kaveh Firouz [1], Alireza Khodaverdian [2], Laurentiu Danciu [2]

[1] Geological Institute, ETH Zurich, Sonneggstrasse 5, CH -8092 Zurich, Switzerland (amaneh.kaveh@erdw.ethz.ch)
[2] Swiss Seismological Service (SED), ETH Zurich, Sonneggstrasse 5, CH -8092 Zurich, Switzerland

Convergence between the Arabian and Eurasian Plates causes crustal deformation that is partly accommodated within the Turkish-Iranian Plateau and Caucasus mountain belts. The Neo-tectonics of the region is a complex combination of active faults, tectonic uplift, Neogene-Quaternary volcanism, sea-level fluctuations and offset drainage networks. The dominant faults are the NW-SE striking eastern segment of the North Anatolian Fault (NAF) and North Tabriz Fault (NTF), both with shallow and diffuse seismicity and dextral strike slip component. Seismic activity is concentrated along these active faults and is often considered, together with fault properties (location, geometry and slip-rates), a proxy to the crustal deformation. To quantitatively evaluate the spatial distribution of ongoing crustal deformation in the study region, we developed a regional kinematic model, built upon geological information (tectonic plate boundary, fault traces and slip-rates), geodetic measurements (GPS measurements), and principal stress directions.

In this contribution, we present the results of the kinematic model for the E-Turkish-NW Iranian Plateau and surrounding areas. Firstly, the slip rates for all mapped faults are estimated and secondly, the regional strain rate fields are evaluated. Inherent uncertainties are associated to both geodetic and geologic measurements and quantitatively accounted for in our kinematic model. The kinematic slip rates of the faults in the region indicate a high active shortening (~11 mm/yr) across the Alborz-Talesh, Bitlis and Greater Caucasus Mountain ranges. High strain rate fields (Log ε=-14.4 to -15.4 s-1) are concentrated in narrow zones along the eastern segment of NAF to NTF in the Turkish-Iranian Plateau, which might be in relative agreement with morphotectonic studies clarifying active faulting in the region as well as the observed seismicity. However, there are various regions of high strain fields that are not located along fault systems, which might indicate unknown or unmapped active faults. Low strain rate fields are observed in the plateau and valley, away from active features as indicated by low seismicity.

P 1.15

High-resolution thermo-mechanical numerical simulations of basement-cover deformation with application to the Helvetic nappe system

Dániel Kiss [1], Thibault Duretz [1,2], Stefan M. Schmalholz [1]

[1] Institute of Earth Sciences, University of Lausanne, CH-1015 Lausanne (daniel.kiss@unil.ch)
[2] Géosciences Rennes, Univ. Rennes 1, UMR CNRS 6118, France

Nappe systems are typical of many orogenic belts. A well-known example is the Helvetic nappe system in the Swiss Alps, which consist of sedimentary units that have been sheared and thrusted over the crystalline basement of the European passive margin during the Alpine orogeny. These sedimentary units form, for example, the parautochtonous Morcles nappe of the infrahelvetic complex, which is situated below the Helvetic Wildhorn super-nappe.

Although nappes were recognized a century ago and have been studied since then, the mechanisms responsible for nappe generation and nappe stacking are still debated. We present 2D high-resolution thermo-mechanical numerical simulations of the shearing of basement-cover system with half-graben representing the upper crust of the European passive margin. The scope of the numerical simulations is to evaluate the impact of the (1) geometry of the basement-cover interface, (2) presence of mechanical layering resembling the alternation of shale-rich and carbonate-rich sedimentary units, and (4) the rotation of the basement during shearing due to the flexure of the lithosphere in the foreland. The final aim of the simulations is to reconstruct the overthrusting of the Helvetic nappes over the nappes of the infrahelvetic complex.

P 1.16

High-resolution earthquake catalogue and seismic velocity models to image the structure of seismogenic faults zones in the Valais (Switzerland)

Timothy Lee [1], Tobias Diehl [1], Edi Kissling [2], Stefan Wiemer [1]

[1] *Swiss Seismological Service, ETH Zurich, 8092, Switzerland (timothy.lee@sed.ethz.ch)*
[2] *Institute of Geophysics, ETH Zurich, 8092, Switzerland*

The seismicity in the Valais (southwest Switzerland) mainly distributed north and south of the Rhone-Simplon line (RSL). The seismicity north of the RSL concentrating at Rawil formed an E-W lineament, sub-parallel to the RSL, but offset by 5-10 km to the north. The RSL forms the tectonic boundary between the Penninic and the Helvetic nappes and is characterized by dextral deformation, which continued at least until 3 Ma. The apparent offset between seismicity and the RSL raises the question where current deformation is localized along the EW striking section of the RSL. Focal depths within this lineament, on the other hand, will provide insights to what degree the underlying basement is involved in the brittle deformation.

To study the fault geometries and the long-term spatio-temporal behavior of such seismogenic zones at high-resolution in the Valais, it is crucial to have accurate and precise earthquake locations with consistent uncertainty estimates. However, the current bulletin of the Swiss Seismological Service (SED), spanning 35 years of data, is biased by changing station network geometries over time. This causes varying hypocentre location quality and completeness of earthquake catalogues. Moreover, changing procedures and algorithms used for earthquake location can introduce systematic errors when combined into one single catalogue. Such catalogues are largely inconsistent in terms of location accuracy. Therefore, we establish a high-quality earthquake catalogue by relocating absolute hypocentre locations of the last 35 years with the minimum 1-D model approach for the Valais region. This catalogue is complete and consistent in terms of accuracy. To further increase the precision of hypocentres, the 1-D models and hypocentres are then used as initial value for a regional relative relocation with waveform cross-correlation to resolve the fine-structure of seismicity.

The new catalogue will provide new insights into the seismotectonics of the Valais and allow the detailed comparison of seismicity and geologically mapped faults. From the preliminary results, we find out the focal depth of seismicity lineament at Rawil range from very shallow (~0 km) to 15 km. Regarding the depth of crystalline basement (~10 km), this may suggest part of the basement is involved in the current deformation. However, most likely only limit to the uppermost basement. We also constrain the Vp/Vs ratio through high-quality S phases. The inversion reveals a high Vp/Vs within the first 2.5 km depth, which may indicate the carbonate sedimentary layer. Furthermore, we compare our results to previous studies of the 2014-2017 St-Leonard and 2011 Sierre seismic sequences.

P 1.17

Understanding seaward-concave subduction zones: insights from critical taper theory and forearc seismicity

Andrea Madella [1], Todd A. Ehlers [1]

[1] Department of Geosciences, University of Tübingen, Wilhelmstraße 56, DE-72070 Tübingen
(andrea.madella@ifg.uni-tuebingen.de)

Seaward-concave forearcs are characterized by along-strike differences in surface uplift and exhumation, however, the causes and style of such variations are still a matter of debate. Although forearc uplift is generally considered to be linked to plate interface processes, in fact it is unclear which mechanism effectively produces long-term (Ma) vertical displacement and emergence of coasts. In this study we use the Coulomb-wedge model (e.g. Wang & Hu., 2006) to study the proximal forearc of the Peru-Chile and northern Japan subduction zones, two seaward-concave margins characterized by relative subsidence at the curvature hinge, flanked by actively uplifting limbs. The Coulomb-wedge theory postulates that a wedge's taper angle is the function of the frictional strength of the wedge material and of the basal detachment. Accordingly, along-strike variations of long-term forearc uplift may reflect changes of (i) slab dip angle, (ii) wedge material strength and/or (iii) plate interface friction. Here, we further explore the latter hypothesis by comparing the spatial distribution of interplate friction (inferred from the measured taper) and the pattern of background forearc seismicity (obtained from the ISC global earthquake catalog). We anticipate that high interplate friction would spatially correlate with larger amounts of seismic moment released in the adjacent forearc. Preliminary results for Peru-Chile show a positive correlation of seismic moment and interplate strength, indicating a wedge in equilibrium. Conversely, in northern Japan a complex relationship between long-term deformation and plate-interface processes is deduced. In both margins, however, low values of interplate friction are needed in order to explain the observed geometry.

REFERENCES

Wang, K. and Hu, Y. 2006: Accretionary Prisms in Subduction Earthquake Cycles: The Theory of Dynamic Coulomb Wedge: Dynamic Coulomb Wedge, Journal of Geophysical Research: Solid Earth 111, B06410,1-16.

P 1.18

Laboratory evidence of viscous heating-induced strain localization

Claudio Madonna [1], Yury Podladchikov [2], Jean-Pierre Burg [1]

[1] Geological Institute, ETH Zurich, Sonneggstrasse 5, CH-9092 Zurich
(claudio.madonna@erdw.ethz.ch)
[2] Institute of Earth Sciences, University of Lausanne, CH-1015 Lausanne

In this study we aim to investigate the dynamics of thermally activated strain localization of homogenous and isotropic materials with a strongly temperature-dependent rheology. We present results on coupled thermo-mechanical uniaxial compression experiments on glassy polymer samples with prismatic shape at room temperature and at different strain rates.

With an infrared camera we have captured the spatial and temporal superficial temperature variation. Experimental results are validated with a thermo-mechanical numerical model. The experimental results show a localized strong temperature increase due to viscous heating along planar zones that ultimately become fracture planes. This results are then extrapolated for geological relevant conditions where viscous heating can control large scale shear zones.

P 1.19

Understanding variations in the Alpine deformation imprint on the Aar massif's basement-cover-contact - the case of the Jungfrau-Eiger Mountains (Central Alps, Switzerland)

David Mair [1], Alessandro Lechmann [1], Marco Herwegh [1], Lukas Nibourel [1], Fritz Schlunegger [1]

[1] Institute of Geological Sciences, University of Bern, Baltzerstrasse 1+3, CH-3012 (david.mair@geo.unibe.ch)

The NW rim of the external Aar Massif was exhumed from ~10 km depth to its present position at 4 km elevation above sea level during several Alpine deformation stages. Different models have been proposed for the timing and nature of these exhumation stages over the last decades (e.g. Burkhard, 1988; Herwegh *et al.*, 2017). One key observation is that although field data allows to locally distinguish multiple deformation stages, before and during the Aar Massif's exhumation, all related structures formed under similar P, T conditions at the NW rim (Mair *et al.*, 2018). This deformation's peak temperatures ranged between 250 °C and 330 °C and allowed for the tectonic incorporation of brittlely deformed basement gneisses into the Mesozoic sedimentary cover rocks, which reacted in a ductile manner. The incorporated basement wedges had already been recognized early in the 20th century, but so far, their spatial distribution and their significance has not been systematically studied. However, these gneiss wedges are of great importance since they represent fault zone markers and can be used as proxies for the displacement along the faults.

We use them along with stratigraphic data to link the different structural fabrics in the basement and the Mesozoic cover. We do so by updating pre-existing maps, collecting structural data, and producing a 3D model of the basement-cover-contact. Further we retro-deform tectonic cross-sections within a framework suitable for both basement and cover.

This allows us to differentiate 3 phases of deformation at the NW rim: While the first one mainly affected the sedimentary cover rocks (thin skinned tectonics), the latter two deformed basement rocks of the Aar massif as well (thick skinned tectonics). We find, that along the SW-NE strike of the basement-cover-contact, especially the last phase left a localized and heterogeneous deformation imprint. These deformation stages resulted in the exhumation of the rocks in the Jungfrau-Eiger mountains and together with surface erosion, they are credited for today's spectacular morphological expression.

REFERENCES

Burkhard, M. 1988: L'Helvétique de la bordure occidentale du massif de l'Aar (évolution tectonique et métamorphique), Eclogae Geologicae Helvetiae, 81, 63–114.

Herwegh, M., Berger, A., Baumberger, R., Wehrens, P. and Kissling, E. 2017: Large-Scale Crustal-Block-Extrusion During Late Alpine Collision, Scientific Reports, 7, 413.

Mair, D., Lechmann, A., Herwegh, M., Nibourel, L. and Schlunegger, F. 2018: Linking Alpine deformation in the Aar Massif basement and its cover units – the case of the Jungfrau-Eiger Mountains (Central Alps, Switzerland), Solid Earth Discussions, accepted for publication; doi: 10.5194/se-2018-49.

P 1.20
Co-location of the downdip end of seismic locking and the continental shelf break.

Luca C. Malatesta [1], Lucile Bruhat [2], Noah J. Finnegan [3]

[1] Institute of Earth Surface Dynamics, University of Lausanne, CH-1015 Lausanne (lcmalate@ucsc.edu)
[2] Laboratoire de Géologie, École Normale Supérieure, 75231 Paris
[3] Earth and Planetary Sciences Department, University of California Santa Cruz, Santa Cruz, CA 95064, USA

In subduction zones, onshore geodesy provides the main data used to map seismic locking on the plate interface. Based on observations at the Cascadia subduction, we propose a new offshore control by establishing a rationale for the co-location of the locking depth and the shelf break, not the coastline as previously proposed. The erosive shelf of a subduction margin results from the combination of continuous uplift and active wave erosion. The long-term uplift is driven by 1) the non-recoverable fraction of interseismic deformation that mimics the pattern of elastic deformation and 2) continental uplift (e.g. isostasy). We combine a wave erosion model with an elastic deformation model to show how the hinge line that marks the transition from interseismic subsidence to uplift pins the location of the shelf break. The width of the shelf is then set by the amount of coastal retreat under wave erosion. A global compilation of subduction zones with well-resolved locking depths confirms our model with shelf breaks lying much closer to the locking depth than coastlines (mean distances landward of the locking depth of 4.7 and 43.1 km respectively). The morphology of a subduction margin integrates thus hundreds of seismic cycles and it can inform seismic coupling stability through time.
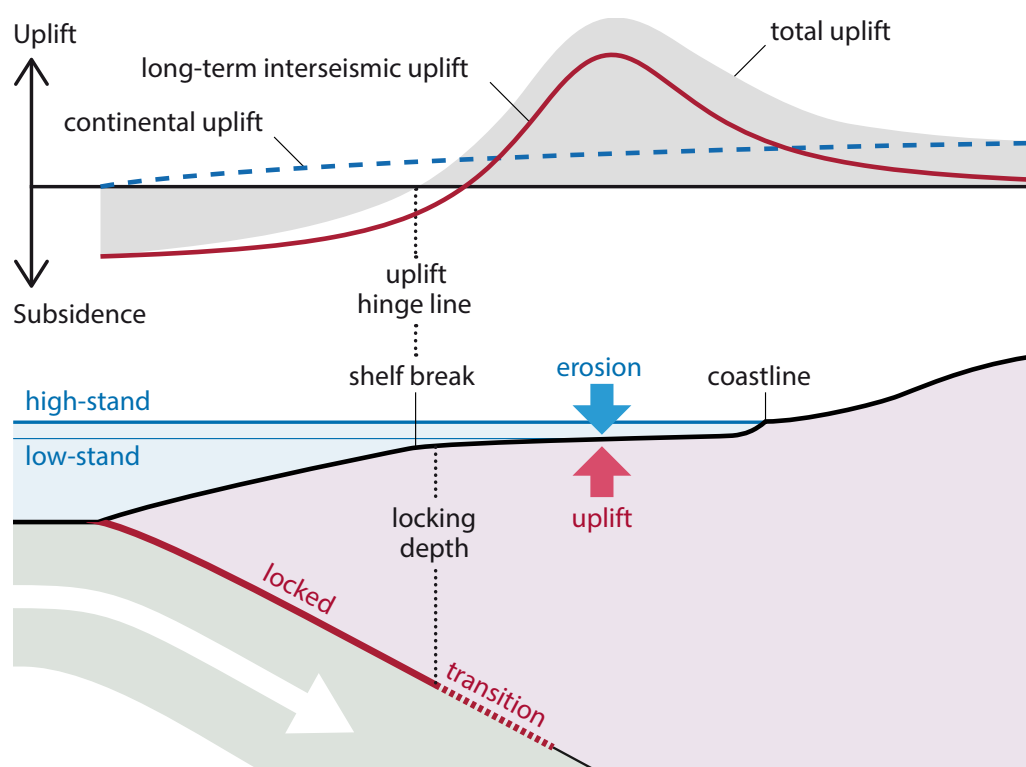
Figure 1. An erosive continental shelf requires wave-base erosion and rock uplift. These conditions are met landward of the uplift hinge line set by the combined patterns of interseismic and continental uplift (top). The shelf break is anchored at the hinge line, and the shelf can grow landward by coastal retreat (bottom). The interseismic deformation is controlled by the pattern of locked, transitional, and creeping segments of the megathrust.

P 1.21
Approach for a new seismotectonic model of Switzerland

Samuel Mock [1], Marco Herwegh [1], Tobias Diehl [2], Andreas Möri [3], Edi Kissling [4]

[1] Institute of Geological Sciences, University of Bern, Baltzerstrasse 1+3, CH-3012 Bern (samuel.mock@geo.unibe.ch)
[2] Swiss Seismological Service, ETH Zurich, Sonneggstrasse 5, CH-8092 Zurich
[3] Federal Office of Topography swisstopo, Seftigenstrasse 264, CH-3084 Wabern
[4] Institute of Geophysics, ETH Zurich, Sonneggstrasse 5, CH-8092 Zurich

In the year 1997, the Swiss Geophysical Commission (SGPK) launched the project "Seismotectonic Atlas of Switzerland" with the goal of a first nationwide inventory of seismotectonic relevant data. In the course of the project, the contribution of the Swiss Seismological Service (SED) focused on the calculation of earthquake focal mechanisms, the identification of stress regimes from stress inversions and possible ways to present the information on digital maps. Another goal of the project was the compilation of a map of active faults within the Swiss Alps from geological field data. The latter task, however, turned out to be challanging due to a lack of field-based evidence for recent fault activity and therefore only a handful of clearly active (i.e. neotectonic) faults could be mapped. Hence, large uncertainties regarding the seismotectonic interpretation remained.

With the advances in earthquake monitoring and processing (e.g. improved data quality, significant densification of the seismic network, improved seismic velocity models, and relative relocation techniques), accuracy and precision of hypocenters improved significantly, so that today, location uncertainties can be narrowed down to the subkilometer scale (e.g. Diehl et al. 2017). In addition, recent re-processed and re-interpreted 2D and new high-resolution 2D and 3D reflection seismic data as well as geological 3D models provide new insights into the subsurface structural setting of the Swiss Molasse Basin (e.g. Allenbach et al. 2017; Heuberger et al. 2016; Sommaruga et al. 2012). Furthermore, with swisstopo's harmonization of geological vector data (GeoCover) a more complete structural dataset becomes available. Insofar, the interplay between seismicity and faults can now be investigated in much more detail. Finally, the Global Navigation Satellite System (GNSS) in Switzerland provides increasing data volumes, leading to steady improvements of surface deformation estimates in the Alps and its foreland.

In the light of these new developments, the SGPK has launched a follow-up project called "Seismotectonic Model of Switzerland". In the corresponding pilot study presented here, we try to highlight different aspects and possibilities of seismotectonic interpretation, but also the pitfalls associated with it. Furthermore, we try to establish a strategic roadmap for the development of a future seismotectonic model of Switzerland.

REFERENCES

Allenbach, R. P., Baumberger, R., Kurmann, E., Michael, C. S., & Reynolds, L. (2017). GeoMol: Geologisches 3D-Modell des Schweizer Molassebeckens - Schlussbericht. *Berichte der Landesgeologie*, *10*, 128 pp.

Diehl, T., Kraft, T., Kissling, E., & Wiemer, S. (2017). The induced earthquake sequence related to the St. Gallen deep geothermal project (Switzerland): Fault reactivation and fluid interactions imaged by microseismicity. *Journal of Geophysical Research: Solid Earth*, *122*(9), 7272–7290. doi:10.1002/2017JB014473

Heuberger, S., Roth, P., Zingg, O., Naef, H., & Meier, B. P. (2016). The St. Gallen Fault Zone: a long-lived, multiphase structure in the North Alpine Foreland Basin revealed by 3D seismic data. *Swiss Journal of Geosciences*, *109*(1), 83–102. doi:10.1007/s00015-016-0208-5

Sommaruga, A., Eichenberger, U., & Marillier, F. (2012). Seismic Atlas of the Swiss Molasse Basin. *Matériaux pour la Géologie de la Suisse - Géophysique*, (44).

P 1.22

Neogene exhumation of the Aar Massif controlled by crustal thickening and paleogeography

Lukas Nibourel [1], Meinert Rahn [2], Alfons Berger [1], Frédéric Herman [3], István Dunkl [4], Marco Herwegh [1]

[1] Institute of Geological Sciences, University of Bern, Baltzerstrasse 1+3, CH-3012 Bern (lukas.nibourel@geo.unibe.ch)
[2] Institute of Earth and Environmental Sciences, University of Freiburg, Freiburg, Germany
[3] Institute of Earth Sciences, University of Lausanne, CH-1015Lausanne, Switzerland
[4] Department Sedimentology / Environmental Geology, Geoscience Center, Georg-August-Universität Göttingen,
    D-37077 Göttingen, Germany

We examine the tectonic contribution to the Neogene cooling and exhumation history of the Aar Massif, Swiss Alps. 89 new and 634 published (U–Th–Sm)/He data on zircon, apatite and zircon fission track ages (AFT, ZFT) are shown in map view as well as on massif-perpendicular and massif-parallel sections, illustrating significant changes in the along-strike thermal overprint and cooling age pattern. Although structural relief and exposed metamorphic grade are highest in the central Aar Massif, youngest cooling ages of all studied thermochronology systems are situated in the eastern- and westernmost surface outcrops (Chur and Brig areas), while ages gently increase toward the center of the massif. Elevation normalized AFT, ZHe and ZFT cooling ages in the central Aar Massif (Reuss Valley) are constant, also in massif-perpendicular direction, and do not reflect the significant structural relief recorded at the top basement marker horizon of the Aar Massif. This is in large contrast to the easternmost cross-section (Chur area), where we observe a bell-shaped AFT age distribution with an age minimum that coincides with the hinge of the Aar Massif culmination. Results of a linear inversion method (Fox et al., 2014, Herman and Brandon, 2015) based on all available thermochronoly data highlight that maximum exhumation rates initially occurred at the central Aar Massif, then laterally migrated to the east and west between ca. 12 and 6 Ma, and possibly thereafter. This along-strike evolution is best explained by collisional shortening and thickening starting at the southernmost edge of a European continental margin with a convex shape. Such a scenario is in agreement with the observed transition from compressional- to strike-slip-dominated tectonics in the central southern Aar Massif at ca. 12-15 Ma (Rolland et al., 2009) and with the coeval activation of north-vergent crustal ramps at the external massif front (Herwegh et al., 2017).

The youngest AFZ, ZHe and ZFT cooling ages in the Chur and Brig areas correlate with domains of highest recent surface uplift (Schlatter, 2014), suggesting that exhumation in these regions has accelerated since at least 6-8 Ma. Although glacial erosion, deglaciation and ongoing isostatic compensation might explain the overall increase of exhumation rates since ca. 2 Ma, differential exhumation along and across the strike the Aar Massif extends far into pre-glacial times. Our results indicate that compressional tectonics represent the key driving force for the past exhumation and recent surface uplift patterns, while glacial erosion and likely also other climatic effects are of secondary importance.

REFERENCES

Fox, M., Herman, F., Willett, S.D., & May, D. A. 2014: A linear inversion method to infer exhumation rates in space and time from thermonchronometric data, Earth Surf. Dyn., 2,47–65, https://doi.org/10.5194/esurf-2-47-2014.

Herman, F., & Brandon, M. 2015: Mid-latitude glacial erosion hotspot related to equatorial shifts in southern Westerlies, Geology, 43(11), 987-990, https://doi.org/10.1130/G37008.1.

Herwegh, M., Berger, A., Baumberger, R., Wehrens, P., & Kissling, E. 2017: Large-scale crustal-block- extrusion during late alpine collision: Scientic Reports, 7, 413, https://doi.org/10.1038 /s41598-017-00440-0.

Rolland, Y., Cox, S. F. & Corsini, M. 2009: Constraining deformation stages in brittle-ductile shear zones from combined field mapping and $^{40}Ar/^{39}Ar$ dating: The structural evolution of the Grimsel Pass area (Aar Massif, Swiss Alps). Journal of Structural Geology 31, 1377–1394, https://doi.org/10.1016/j.jsg.2009.08.003.

Schlatter, A., 2014: Kinematische Gesamtausgleic- hung der Schweizer Landesnivellementlinien 2013 und Detaildarstellung der rezenten verti- kalen Ober ächenbewegungen in der Zentralschweiz: Nagra Arbeitsbericht NAB 14–38.

P 1.23
Geological-structural and metamorphic study of the Southern Dora-Maira Massif in Valmala (Varaita Valley, Western Alps)

Francesco Nosenzo [1], Gianni Balestro [1], Chiara Groppo [1], Andrea Festa [1]

[1] Dipartimento di Scienze della Terra, Università degli Studi di Torino, Via Vaperga Caluso 35, IT-10125 Torino

This study presents new field, structural and petrographic data for a portion of the southern Dora-Maira Massif (western Alps), with the aim of reconstructing its tectono-stratigraphic and tectono-metamorphic architecture.

The southern Dora-Maira Massif is a (ultra)-high pressure ((U)HP) tectonic nappe stack consisting of different continental crust units which underwent (U)HP metamorphism during the Alpine orogenesis. The study area is located immediately south of the world-famous UHP Brossasco-Isasca Unit and exposes, from the lower to the upper structural level, a quartz-eclogitic unit (i.e the Rocca Solei Unit: RSU) and a blueschists-facies unit (i.e. the Dronero-Sampeyre Unit: DSU), relatively poorly known in terms of lithostratigraphy and metamorphic conditions. Such a geological setting, in which a blueshists-facies metamorphic unit overlays eclogitic metamorphic units, is a unique feature in the Internal Cristalline Massifs and the geodynamic processes responsible for its formation are still debated. Moreover, lithologies apparently related to an oceanic setting (already reported by Carraro et al., 1971 and Henry, 1990) are tectonically interposed between the RSU and the DSU, and their origin has not been interpreted yet.

The detailed field, structural and petrographic study, supported by a geological map at 1:10,000 scale with related GIS-database, was carried out in the Valmala area (a right tributary of the Varaita Valley). Here a lithologically heterogeneous unit named as "Valmala Shear Zone" (VSZ) is tectonically sandwitched between the RSU and the DSU.

The VSZ, which is several kilometers long and about 500 meters thick, shows a "block in matrix" structure. In its lower portion, blocks of metabasics, meta-ultrabasics and calchschists, lenticular in shape and up to hundreds of meters in size, are embedded in a matrix dominated by micaschists, locally rich in carbonates. On the contrary, in the upper portion of the VSZ blocks of micro-augen gneisses and minor impure marbles, lenticular to tabular in shape and up to tens of meters wide, are embedded in a matrix of micaschists and paragneisses.

In the DSU, a metasedimentary Polymetamorphic Complex has been recognised basing on the occurrence of relict pre-Alpine porfiroblastic garnet, and distinguished from a Monometamorphic Complex mostly consisting of metavolcanics. Our finindings show that the structural setting of the studied sector is the result of five deformational stages (from D1 to D5). The D2 is the most pervasive one, responsible for the development of the regional foliation S2 and for the activation of the tectonic contacts separating the three tectonic units. Both the VSZ and the DSU preserve relicts of the peak metamorphic assemblage compatible with the blueschist-facies (Gln + Grt ± Zo in the metabasics; Ctd + Grt ± Gln ± Lws in the micaschists). Preliminary petrologic data on the metapelites from the DSU constrained peak P-T conditions of ca. 470°C, 19 kbar, in the lawsonite-blueschist facies.

REFERENCES

Carraro, F., Bonsignore, G., Gregnanina, A., Malaroda, R., Schiavanato, G. 1971: Carta geologica d'Italia, Argentera-Dronero, 78-79.

Henry C. 1990: L'unité a coesite du massif Dora-Maira (Alpes Occidentales) dans son cadre petrologique et structural. PhD's thesis. Univeristè Paris 6.

P 1.24

High-resolution imaging of the Ivrea Geophysical Body: A joint seismic and gravity approach

Matteo Scarponi [1], György Hetényi [1], Jaroslava Plomerová [2], Stefano Solarino [3], Théo Berthet [4], Ludovic Baron [1], AlpArray-Ivrea Working Group

[1] *Institute of Earth Sciences, University of Lausanne, Switzerland*
[2] *Institute of Geophysics, Czech Academy of Sciences, Prague, Czech Republic*
[3] *Istituto Nazionale di Geofisica e Vulcanologia INGV, c/o DICCA University of Genova, Italy*
[4] *Department of Earth Sciences, Uppsala University, Sweden*

The Ivrea geophysical body (IGB) is a piece of Adriatic plate lower lithosphere, detached during the European-African continental collision. Consequently located at upper crustal depths along the inner arc of Western Alps (Italy), its northeastern portion exposes middle to lower-crustal rocks at the surface in the so-called Ivrea-Verbano Zone. This body is characterised by two main geophysical anomalies: high density and high seismic velocity.

We here aim at refining the IGB structural image, combining high quality seismic and gravity data, together with rock density analyses and geological mapping of the area. The most recent results on IGB structure come from local earthquake tomography, providing no higher resolution than 15 km (Solarino et al., 2018, Diehl et al., 2009). To achieve a higher resolution image, we deployed ten broadband seismic stations along a 50 km linear West-East profile crossing the Insubric Line, the Ivrea-Verbano Zone at the level of the Sesia Valley, and two lakes. Teleseismic earthquakes are used to image sharp and broad discontinuities by means of P-to-S receiver function (RF), performing data stacking and migration. First results already begin to delineate the IGB structure and highlight shallow seismic interfaces, presenting eastward deepening and being well located above the Moho discontinuity.

We also collected 180 new gravity measurements, approaching the target 2-D coverage of 1 point every 4 to 9 km^2. Together with the existing data, these gravity surveys provide constraints on the IGB density distribution. The surface geological map of the area allows us to compute and refine the Bouguer anomaly map, accounting for rock densities observed on the field, which deviate from the typically used value 2.67 g/cm^3. We ultimately aim at developping a 3-D gravity model over the whole Ivrea-Verbano area.

Combining high quality data from different datasets allows us to obtain a newly detailed image of the IGB structure and geophysical Moho itself. Seismic and gravity data will be combined to study 1) contour features in terms of velocity and density contrasts and 2) bulk properties in terms of density distribution. The results will also contribute to the development of further projects in the area, such as the deep drilling project DIVE (https://doi.org/10.5194/sd-23-47-2017).

REFERENCES
Diehl T, Husen S, Kissling E, Deichmann N (2009) High-resolution 3-D P-wave model of the Alpine crust. *Geophys J Int* 179(2): 1133-1147. doi:10.1111/j.1365-246X.2009.04331.x
Solarino S, Malusà MG, Eva E, Guillot S, Paul A, Schwartz S, Zhao L, Aubert C, Dumont T, Pondrelli S, Salimbeni S, Wang Q, Xu X, Zheng T Zhu R (2018) Mantle wedge exhumation beneath the Dora-Maira (U) HP dome unravelled by local earthquake tomography (Western Alps). *Lithos*, *296*: 623-636. doi: 10.1016/j.lithos.2017.11.035

P 1.25
Structural and metamorphic data in the nappes of the Lepontine Dome (Central Alps)

Filippo Luca Schenker [1], Christian Ambrosi [1], Cristian Scapozza [1], Dorota Czerski [1], Matteo Maino [2], Claudio Castelletti [1,4], Yves Gouffon [3]

[1] Institute of Earth Sciences, University of Applied Sciences and Arts of Southern Switzerland (SUPSI), Via Trevano, CH-6952 Canobbio (filippo.schenker@supsi.ch)
[2] Dipartimento di Scienze della Terra e dell'Ambiente, University of Pavia, via Ferrata 1, 27100 Pavia, Italy
[3] Swiss Geological Survey, Federal Office of Topography swisstopo, Seftigenstrasse 264, CH-3084 Wabern
[4] now at CSD Ingegneri SA, Via P.Lucchini 12, 6901 Lugano, Svizzera

New structural and published petrological data on the new geological map and cross sections (1:10'000) of the Osogna sheet (Geological Atlas of Switzerland no. 1293, 1:25'000) are critically discussed. The area includes most nappes of the Lepontine Dome, from bottom to top: the lower penninic units of the Leventina, Simano, Adula/Cima-Lunga and Maggia. These nappes derive from the same post-Variscan gneissic crust, this complicates their lithological distinction within the nappe pile.

All lithologies show a sub-horizontal penetrative foliation that dips gently W to the NW and E to the SE due to doming at the megascale and which intensity varies between rock-types. Close to the Insubric Line to the S, the main foliation plunges with a steep angle to the S. On the foliation plane the mineral and stretching lineation dips NW or SE depending on the plane dip direction. Lineation direction averages at 134°±15° and dips at 14°±9°. The kinematic analysis indicates a top-to-the-NW shearing.

The geological map shows lithological boundaries that are locally incongruent with the tectonic contacts of the published maps. In the southern part of the Lepontine dome the boundary between the Leventina and the Simano gneisses is interpreted as a moderately deformed magmatic contact that limits the allochthonous character of the Simano unit. Folding and re-activation of the magmatic contact occurred at peak metamorphic conditions between 570 and 620 °C and < 0.6 GPa.

The boundary between the Simano and the Adula/Cima-Lunga units is unclear because of internal and lateral lithological variations occurring at different scales. However, the shear zone is visible through a strain gradient recognizable with a bottom to top closing up of folds (from close to isoclinal folds) and a parallelization of the lithological and structural elements.

The boundary between the Adula/Cima Lunga and the Maggia units follows a folded surface at the base of a granodioritic gneissic body (Cocco gneiss) which in the literature is diagnostic for the Maggia nappe. Along this shear zone, syn- to post-mylonitic leucosomes attest partial melting during deformation.

The High Pressure (HP) metamorphism is limited to minor rock volumes of the Adula/Cima Lunga unit and in one eclogite in the Simano unit and PT conditions peak around ~750°C and 2.5 GPa. The later Barrovian metamorphism is associated with incipient partial melting in the lower units and shows PT conditions ranging from ~600 °C and 0.5 GPa in the Leventina unit to ~650°C and 0.7 GPa in the Adula/Cima Lunga unit.

The correlation of these results is fundamental to better understand the thermobarometric evolution patterns of the Lepontine Dome and the formation of tectonic nappes in general.

P 1.26

Archean tectonics and the generation of continental TTG crust in global mantle convection models

Paul J. Tackley [1], Charitra Jain [1], Charitra Jain [1], Antoine B. Rozel, Diogo Lourenco [2], Taras V. Gerya [1]

[1] Institut für Geophysik, Departement Erdwissenschaften, ETH Zürich, CH-8092 (ptackley@ethz.ch)
[2] Department of Earth and Planetary Sciences, University of California, Davis, USA

The tectonic mode in the Archean, and when and how continents formed, are two key unresolved questions. Here we investigate these issues using global simulations of Earth evolution from post magma ocean to the present day, including self-consistently calculated production of basaltic oceanic crust and TTG continental crust. We use the code StagYY in a 2D spherical annulus geometry. The mantle starts with a uniform pyrolytic composition and has an initially hot core. Basaltic crust is formed by partial melting of pyrolytic material, while TTG is formed by partial melting of basalt in certain (P,T) windows [Moyen, 2011] in the presence of water. Produced magma is erupted at the surface and intruded into the crust with a ratio that is specified a priori. After an early overturn of post-magma-ocean-formed crust, we find that the tectonic mode was likely neither modern-day plate tectonics nor a rigid lid, but rather, one characterized by abundant mostly intrusive magmatism resulting in a hot, weak, deformable lithosphere – a "Plutonic Squishy lid" (PSL) [Lourenco, 2017]. In this mode, a thick basaltic crust is recycled at its base by eclogite drips plus episodic delamination of depleted lithosphere [Sizova, 2015]. Abundant TTG crust is produced, with a production rate far exceeding typical continental crustal growth curves [Rozel 2017; Jain 2018]. At the same time it can also be destroyed by entrainment in downwellings. These models thus indicate that (i) subduction was not necessary for the production of early continental crust, (ii) intrusive magmatism was dominant during the Archean (as opposed to "heat pipe" extrusive magmatism), and (iii) Archean tectonics was characterised by a weak, hot deformable lithosphere undergoing extensive delamination as well as significant horizontal motion.

REFERENCES

Moyen, J.-F. 2011: The composite Archaean grey gneisses: Petrological significance, and evidence for a non-unique tectonic setting for Archaean crustal growth Lithos 123, 21-36.

Lourenço, D. J. 2017: The influence of melting on the thermo-chemical evolution of rocky planets' interiors, Doctoral thesis, ETH Zurich, DOI:10.3929/ethz-b-000228308

Sizova, E., T. Gerya, K. Stüwe & M. Brown 2015: Generation of felsic crust in the Archean: A geodynamic modeling perspective, Precamb. Res, 271, 198-224.

Rozel, A. B., G. J. Golabek, C. Jain, P. J. Tackley & T. Gerya 2017: Continental crust formation on early Earth controlled by intrusive magmatism, Nature 545, 332-335.

Jain, C. 2018: Self-Consistent Generation of Continents and Their Influence on Global Mantle Dynamics, Doctoral Thesis, ETH Zurich, DOI:10.3929/ethz-b-000276316.

P 1.27
Break-up of continental lithosphere interacting with upper mantle and surface processes

Kosuke Ueda [1], Taras Gerya [1], Sean Willett [1], Dave May [2]

[1] Department of Earth Sciences, ETH Zürich, Sonneggstrasse 5, Zürich, Switzerland (kosuke.ueda@erdw.ethz.ch)
[2] Department of Earth Sciences, University of Oxford, South Parks Road, Oxford, OX1 3AN, United Kingdom

Lithospheric deformation during rifting involves complex interactions between mantle, crust and surface processes. We investigate the interactions of both upper mantle and lithosphere, and of lithosphere and surface processes,using three-dimensional numerical models. We employ a thermomechanical, visco-plastic code that we couple to a surface process model. The latter evolves the surface by linear diffusion and coupling is accomplished through horizontal advection of topography. This model is used to investigate the effects of erosional efficiency and the impact of mantle plume generation. We investigate the use of integrated work metrics as a measure of rift progression.

In the simplest case, extension along one direction and not including plumes, two factors are found to control rift initiation. The timing of rift initiation is primarily determined by the Moho temperature and thus the integrated rheological strength, but surface process efficiency also plays a significant role. Under fixed thermomechanical conditions, timing of initiation of rifting varies by up to 15%, or ca. 1 Myr, depending on surface process efficiency (i.e. diffusivity). Plume impingement localizes extension and strongly accelerates rift initiation, with earlier initiation for larger plumes. Despite the efficient rift localization by plumes, an impact of mass redistribution by surface diffusion on the timing is also observed. Triaxial far-field forcing (slow horizontal convergence in the direction normal to extension) delays relative rift initiation. In this case, spreading of plume material can facilitate secondary delamination around the tips of the propagating central rift zone.

Analysis of the mechanical work in the entire model over time, measured as energy conversion due to viscous deformation (shear heating, or viscous dissipation; including plastic deformation, which is incorporated through an effective viscosity), depicts the long-term differences in model evolution. Output of total work over time follows a common pattern. Plumes and surface-process variations offset these curves relative to each other, and reflect the effect both have on rifting, even if differences are not apparent from model structures alone.

P 1.28
Numerical two-wedge model applied to the Alpine orogeny

Joshua D. Vaughan-Hammon [1], Evangelos Moulas [1], Stefan M. Schmalholz [1]

[1] Institute of Earth Sciences, University of Lausanne, Lausanne 1015, Switzerland (joshua.vaughan-hammon@unil.ch)

Two prominent phases of deformation characterize the structure and current geometry of the western-central Alps: 1) nappe emplacement and stacking associated with single-vergent, NW-directed thrusting, and 2) backfolding associated with doubly-vergent, SE-directed movement. For the Monte Rosa region, early subduction and delamination of crustal units has been proposed to explain the nappe stack sequences that emplace ophiolite units onto continental crustal units, associated with areas of high-pressure metamorphism. However, the reasons for switching to late-stage backfolding associated with major uplift at lower grade metamorphic conditions is still ambiguous. This change in deformation style of the Alpine orogeny could potentially be explained by the relative weakening of the orogenic, wedge-shaped, lid with respect to the lower wedge in which nappe stacking took place.

We present simple two-dimensional numerical simulations of two-wedge corner flow, which aim to understand the mechanisms that control the large-scale geometries of the Alpine orogeny. The model consists of a lower wedge situated above the subducting European plate and an upper wedge, which represents the orogenic lid. The model is based on incompressible power-law viscous flow. We aim to quantify: 1) the differences between numerical solutions and analytical solutions valid for simple geometries and linear viscous flow, 2) the impact of variable viscosity contrasts between the two wedges, 3) the impact of an evolving deformable interface between the two wedges, and 4) the impact of linear and power-law viscous flow on the results. Moreover, we compare our model results with the current geometry and tectono-metamorphic history of the Monte Rosa region in the Western Alps.

P 1.29
Strain partitioning linked to high-pressure metamorphism in the Monte Rosa metagranitoids

Joshua D. Vaughan-Hammon[1], Cindy Luisier[1], Stefan M. Schmalholz[1]

[1] Institute of Earth Sciences, University of Lausanne, Lausanne 1015, Switzerland
  (joshua.vaughan-hammon@unil.ch)

The Monte Rose nappe consists of pre-Variscan paragneisses, which were intruded by Permian granitic bodies. The current position of the basement complex resides within the collisional Austroalpine-Penninic wedge, and derives originally from the northern European crust. During the Alpine orogeny, the Monte Rosa incurred a high-P imprint interpreted as the subduction of continental material below the overriding Austroalpine units. Within the metagranites this high-P imprint manifests as 10- 50 m wide "whiteschist" bodies consisting of chloritoid, talc, phengite and quartz $\pm$ kyanite or garnet. These whiteschist bodies represent pre-Alpine hydrothermally altered areas which consequently underwent high-pressure Alpine metamorphism. Structurally, the metagranites show strong heterogeneity exhibiting various degrees of strain intensity. However, to this date no deformation associated with Alpine high-pressure metamorphism has been observed as all shear zones are characterized by a greenschist-facies overprint.

We present detailed structural maps of strain intensity within the Monte Rosa metgagranites of the Verra glacial cirque, upper Ayas valley, North Italy. We aim to investigate the strain intensity and relative timing of deformation surrounding the high-pressure whiteschists, and bordering the contact with the surrounding basement paragneisses. Our results show that the metagranite exhibits strong strain partitioning. A large area of the metagranites are undeformed and show pristine magmatic textures, even preserving original intrusive contacts with country rock paragneisses. The highest strain intensities are present 1) near the intrusion-county rock contact, and 2) surrounding the high-pressure whiteschist lenses.

P 1.30
Microstructures in damage zones of limestone strike-slip fault in Eclépens.

Benjamin Verbeken; Nicole Schmitt; Anneleen Foubert; Jon Mosar

Departement de Géosciences – Sciences de la Terre, Université de Fribourg, Chemin du Musée 6, CH-1700 Fribourg

The La Sarraz fault system is composed of hectometre-scale subvertical striking NW-SE faults on a branch of the Pontarlier fault system N-S crosscutting Jura Fold-and-Thrust Belt. The Mormont Anticline is present at the southeastern termination of the La Sarraz-Mormont fault northern branch and absent on the southwestern side of the fault zone. The Eclépens quarry is located between two major branches of the La Sarraz-Mormont fault zone.

The La Sarraz-Mormont fault plane measures 150 meters long and half of the fault's damage zone has a width of 8 meters. The damage zone of the fault consists of fractured host rock, non-foliated cataclasite, foliated cataclasite, and fault gouge. Herein we present a preliminary study of the micro deformation observed in nine samples from the damage zone of the fault. One sample from fault plane, two samples from core zone, one sample from foliated cataclasite and one sample from fractured host rock. Thin sections obtained from oriented hand samples and analysed with cathodoluminescence allowed us to develop a hypotheses of the relative chronological sequence of micro deformation processes present.

The luminescence of the minerals surrounding ooids show a circular bright intensity corresponding to an early cementation. Frequently, between the ooids a darker luminescence is present, most probably originating from a posterior reducing environment corresponding to a secondary cementation. Thereafter, frequent pressure dissolution between ooids is detected. The soluble minerals, with the same intensity as the ooids, is not observed in the vicinity of the ooids but rather in the veins. Veins observed in these thin sections are mostly mineral precipitation on mode I openings. This assumption is confirmed by the observation of half-ooids conserved on both side of the veins. The mineral composition of the studied veins, however, show a darker luminescence than the ooids. The darker intensity observed in the veins might be linked to a late overpressure discharge of reduced fluids. Pressure dissolution took place between the matrix and the veins, this is indicated by the stylolites peaks (brighter luminescence) penetrating the veins (darker luminescence).

The observation of the micro tectonic indicators present in these thin sections allowed us to build the relative chronology of an early cementation, followed by crack and seal processes concurrent to a compression, dissolution and re-precipitation of minerals.

P 1.31

Uplift and exhumation history questions Messinian fluvial unconformities within the Alps

Sascha Winterberg [1], Vincenzo Picotti [1], Sean Willett [1]

[1] Geological Institute, ETH Zürich, Sonneggstrasse 5, 8092 Zürich, Switzerland

Erosion, uplift and exhumation of the Alps are the most important forces shaping the orogen. Glacial overprint left a major signature on the geomorphology of the valleys. A period of dramatic incision conditions occurred during the dessication of the Mediterranean in the Messinian stage when the sea level was lowered by tousands of meters. Canyons incised deep into the bedrock around the Mediterranean. The Messinian unconformity is seen in many seismic profiles of the Po Plain, the Rhône Valley and the Southern Alps. This led to the conclusion that the unconformities of the overdeepened valleys are Messinian in age (Bini et al. 1978). This view prevails today, and even in the center of the Alps the incision below today's sea level has been attributed to Messinian river incision (e.g. Bargossi et al. 2010).

We re-evaluated the incision with paleo-geographic maps and estimates of rock uplift that are extracted from exhumation derived from thermochronometric data (Fox et al. 2016) and sediment budget calculations (Kuhlemann 2007). The study is also constrained by borehole data and seismic profiling in Sinnich in the Adige valley and other published valley fill data. From this, we reconstructed the paleo elevation of the Messinian river profiles in the Alps. Rock uplift regionally estimated must be subtracted from the modern position of the "Messinian" unconformity in order to determine its paleo-elevation in the Messinian. Post-Messinian uplift is supported by observations of Pliocene sediments that are warped up at the southern foothills of the Alps and eroded within the Alps.

We found that the restored profiles in the center of the Alps were at a paleo-elevation at or below the minimum estimated Messinian salinity crisis (MSC) sea level. A Messinian age of the unconformities within the Alps can therefore be excluded, unless the estimate of the sea level or rock uplift is not regionally valid. The alternative interpretation for the inner Southern Alpine valleys is that they are glacial in origin. We predict that a longitudinal seismic section would reveil swells that caused lacustrine sedimentation after ice retreat.
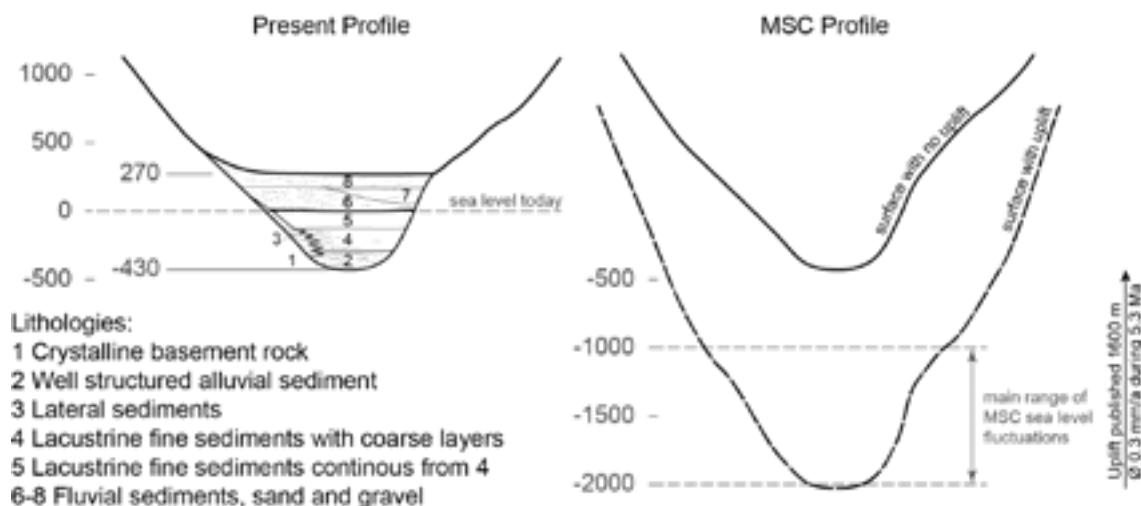

Figure 1. Present day profile from drilling and seismic interpretation. Messinian Salinity Crisis (MSC) profile with and without uplift correction.

REFERENCES

Bargossi, G., Bove, G., Cucato, M., Gregnanin, A., Morelli, C., Moretti, A., Poli, S., Zanchetta, S., Zanchi, A., Ambrosi, S., 2010: NOTE ILLUSTRATIVE della CARTA GEOLOGICA D'ITALIA alla scala 1: 50.000. Foglio 013 MERANO.

Bini, A., Cita, M.B., Gaetani, M., 1978: Southern Alpine lakes—Hypothesis of an erosional origin related to the Messinian entrenchment. Marine Geology 27, 271-288.

Fox, M., Herman, F., Willett, S.D., Schmid, S.M., 2016: The Exhumation history of the European Alps inferred from linear inversion of thermochronometric data. American Journal of Science 316, 505-541.

Kuhlemann, J., 2007: Paleogeographic and paleotopographic evolution of the Swiss and Eastern Alps since the Oligocene. Global and Planetary Change 58, 224-236.

P 1.32

The Western Afar Margin, Ethiopia: A new and detailed structural interpretation of a developing passive margin

Frank Zwaan [1], Giacomo Corti [2], Derek Keir [1,3], Federico Sani [1]

[1] Dept. of Earth Sciences, University of Florence, Italy (frank.zwaan@unibe.ch)
[2] National Research Council of Italy, Florence, Italy
[2] Dept. of Ocean and Earth Science, University of Southampton, United Kingdom

The Afar Rift in Ethiopia forms the northernmost segment of the East African Rift System (EARS) and represents one of the rare locations where active continental break-up and the formation of a young passive margin can be examined. A key element in the system is the poorly studied Western Afar Margin (WAM) along the western edge of the Afar, which marks a sharp decrease in topography from the Ethiopian Plateau into Afar (Fig. 1). This developing passive margin is marked by a series of marginal grabens associated with dominant antithetic faulting, as well as ongoing seismicity that pose severe risks to the local population (Fig. 1). How the WAM and its marginal grabens were formed, as well as why it is still actively deforming when deformation should have shifted to the rift axes in the Afar remains unclear. In this study we aim to establish the first detailed structural map of the whole margin, which may serve as a base for further efforts to better understand the evolution and associated tectonic mechanisms in the area.

We apply various methods to chart the structures in the study area. Using satellite imagery and digital elevation models (DEM) we have drafted a detailed fault map of the whole WAM (Fig. 1). We observe how the NNW-SSE oriented marginal grabens are bounded by large faults and are arranged in a right-stepping fashion, separated by transfer zones with a high fault density. Faults have generally the same NNW-SSE strike, except for the southernmost part of the WAM (Fig. 1) By examining slope breaks, hanging wall structures, basin geometry and comparing our interpretation with published data, we can also assess the fault vergence and the quality of our interpretation.

Seismicity analysis of two datasets retrieved between 2007-2009 and 2011-2013 provides further insights (Fig. 1). The main rift axes in the Afar are clearly visible, as well as the seismicity along the WAM. Focal mechanisms from e.g. the GCMT project indicate general normal faulting, which is in accordance with the extensional nature of Afar. By plotting earthquakes and focal mechanisms in section, we obtain an impression of fault activity and fault vergence. Section B-B' shows various aligned earthquakes, indicating dominantly westward dipping faults, one of which may be the eastern boundary fault of the marginal graben (see topography profile). Note however, that our seismicity datasets have a short timespan and may not register all active faults in the area, thus caution is advised when interpreting.

Further efforts will involve fieldwork to verify our interpretation of the major faults in the area. This work will also form the basis for a series of analogue models to test various scenarios for WAM formation and to reveal the dynamic evolution of the study area.
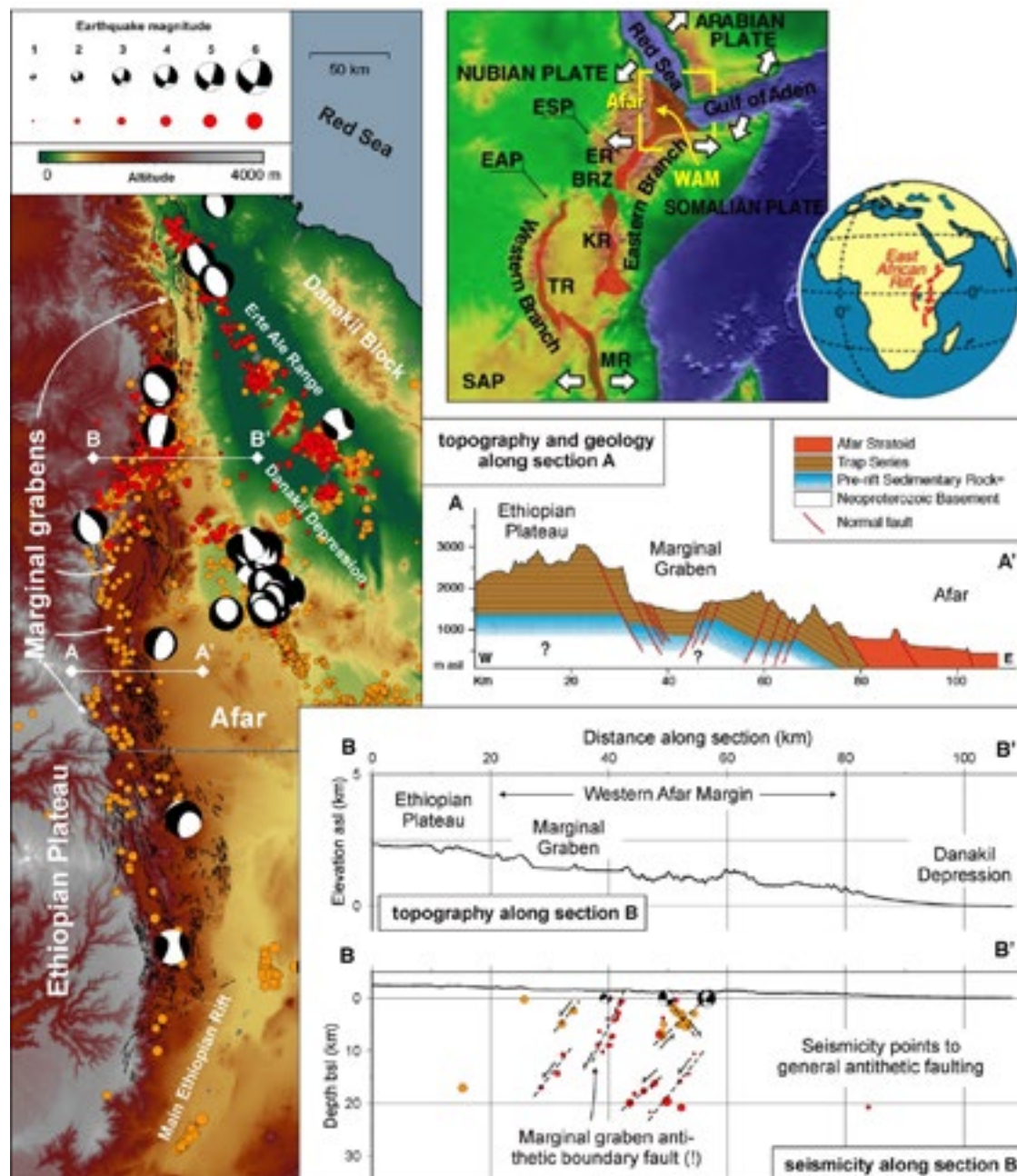
Figure 1. Western Afar Margin (WAM) with fault interpretation (black lines), earthquake location (2 datasets: red and orange dots) and earthquake focal mechanisms (GCMT). Location of the Afar in the East African Rift System. BRZ: Broadly Rifted Zone; EAP: East African Plateau; Southern African Plateau; ER: Ethiopian Rift; ESP: Ethiopian–Somalian plateaus; KR: Kenya Rift; MR: Malawi Rift; SAP: Southern African Plateau; TR: Tanganyika Rift. A-A' shows the general topography and structure of the WAM. B-B' depicts topography, locations and focal mechanisms of earthquakes and interpreted faults geometries. Modified after Corti (2009) and Beyene & Abdelsalam (2005).

REFERENCES

Beyene, A., Abdelsalam, M.G. 2005. Tectonics of the Afar Depression: A reviw and synthesis. Journal of African Earth Sciences, 41, 41-59.

Corti, G. 2009. Continental rift evolution: From rift initiation to incipient break-up in the Main Ethiopian Rift, East Africa. Earth-Science Reviews, 96, 1-53.

P 1.33
A direct comparison of experimental set-ups for simulating extensional tectonics

Frank Zwaan [1,2], Guido Schreurs [2], Susanne Buiter [3,4]

[1] *Dept. of Earth Sciences, University of Florence, Italy (frank.zwaan@geo.unibe.ch)*
[2] *Institute of Geological Sciences, University of Bern, Switzerland*
[3] *Team for Solid Earth Geology, Geological Survey of Norway, Trondheim, Norway*
[4] *The Centre for Earth Evolution and Dynamics, University of Oslo, Norway*

Analogue modellers have historically used different experimental machines and materials to investigate a wide variety of tectonic settings. These methods have yielded valuable insights in tectonic processes, but it is often challenging to compare results from different studies directly. We here present a systematic comparsion of different experimental methods simulating continental extension.

We use either a rubber base, a foam base, rigid basal plates or conveyor-type basal sheets to deform overlying experimental materials. The rubber and foam base induce distributed deformation, whereas the plate/sheets bases create sharp velocity discontinuities. For each set-up we test brittle-only (sand) and brittle-viscous (sand and silicone) material layering to simulate the brittle upper and ductile lower crust. These different configurations represent specific tectonic settings. In selected set-ups, we add a structural weakness (a so-called "seed") to further localize faulting. We also vary the extension velocity and viscous layer thickness for a specific experimental sub-set. X-ray CT allows for a detailed 3D analysis of internal and external evolution of the experiments.

A strong difference in faulting style develops between brittle-only experiments with a basal plate or sheet compared with foam or rubber base set-ups (Fig. 1). Foam/rubber base experiments develop distributed faulting. In the case of a rubber base strong boundary effects (conjugate strike-slip faults) occur due to lateral contraction of the rubber sheet (Fig. 1e, f). Pre-defined viscous weaknes-ses generate central grabens, but do not prevent pervasive faulting (Fig. 1a, b, e, f). Basal plate/conveyor plate experiments strongly localize faulting above the velocity discontinuity with little boundary effects at the sidewalls (Fig. 1i, j).

Brittle-viscous experiments have weak brittle-viscous coupling and show mainly deformation along the sidewalls. In our reference experiments, rifts only develop when seeds are used (Fig. 1c, d, g, h, k, l). In contrast to their brittle-only equivalents, our brittle-viscous basal plate/conveyor plate experiments without a seed do, therefore, not localize de-formation (Fig. k, l). Yet at high extension rates, coupling between the brittle and viscous layers increases and downbending occurs along the central axis of the experiment (Fig. 1n). Additional experiments with high brittle-to-viscous thickness ratios lead to the formation of a dual rift structure (Fig. 1p). By contrast, high coupling due to fast exension in foam and rubber base models causes wide rifting (Fig. 1m).

Our results clearly illustrate the strong influence of set-ups on analogue experiments, highlighting the importance of 1) selecting the right set-up for a specific tectonic setting and 2) including detailed information on experimental boundary conditions to allow proper comparison with results from other studies.
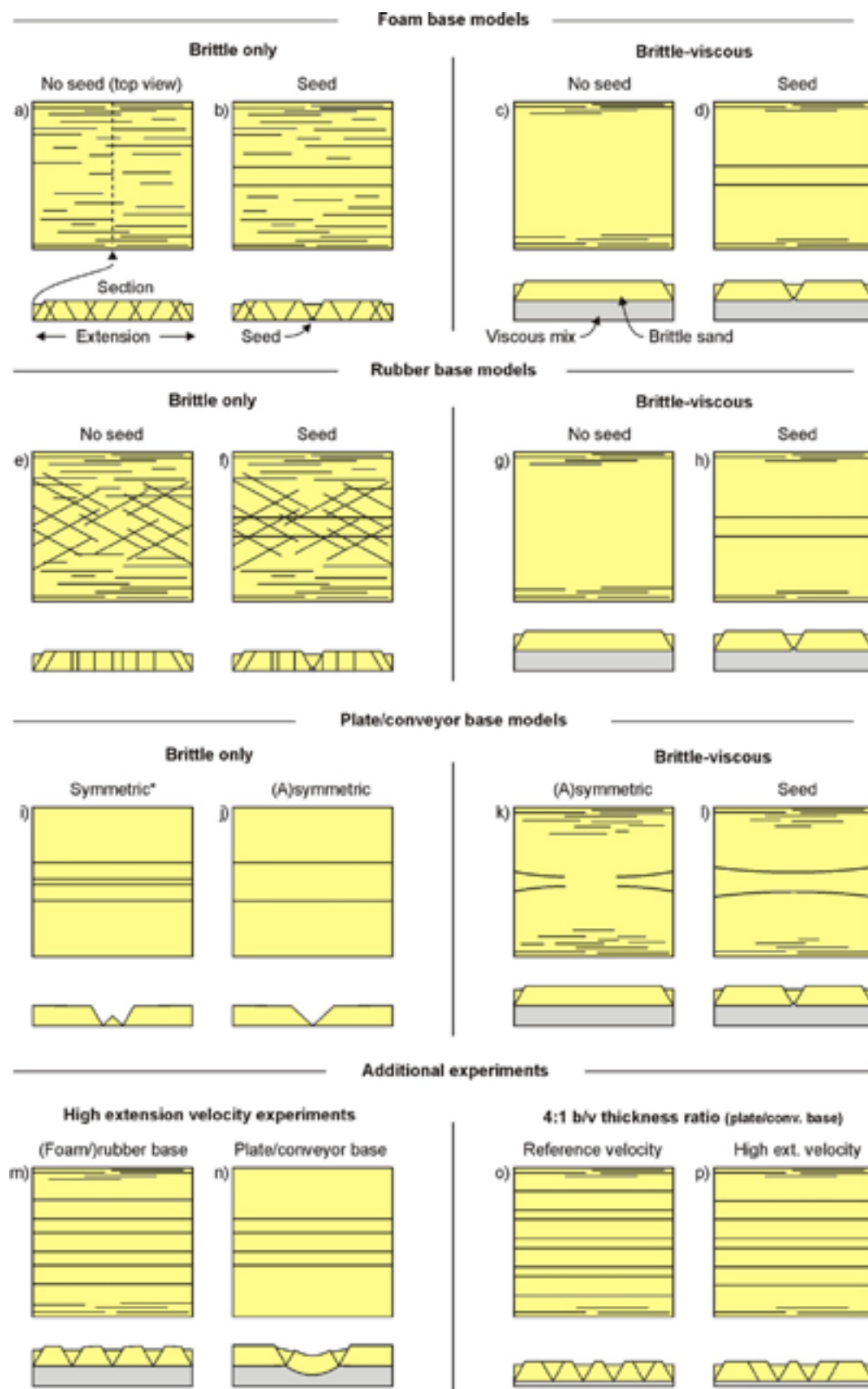
Figure 1. Schematic summary of experimental results (top views and sections). (a-l) Experiments with reference brittle-to-viscous ratios and reference extension rates (* = plate base only). (m-p) Additional brittle-viscous tests with high extension velocities and/or high brittle-to-viscous ratios.

02. **Mineralogy, Petrology, Geochemistry**

Sébastien Pilet, Bernard Grobéty, Eric Reusser

Swiss Society of Mineralogy and Petrology (SSMP)

TALKS:

2.1 Belgrano T.M., Diamond L.W., Vogt Y., Biedermann A., Gilgen S.A., Al-Tobi K.: A new map of the Oman ophiolite extrusives: insights into protoarc crust composition, boninite distribution and sulphide deposit prospectivity

2.2 Blattmann T., Wang S.-L., Lupker M., Märki L., Haghipour N., Wacker L., Chung L., Bernasconi S., Plötze M., Eglinton T.: Sulphuric acid-mediated weathering on Taiwan buffers geological sinks of atmospheric carbon

2.3 Bouvier A.-S, Baumgartner L.P., Rose-Koga E.F., Schiano P.: What can we learn from $\delta^{18}O$ in olivine-hosted melt inclusions?

2.4 Bovay T., Rubatto D., Lanari P., Baumgartner L.: Garnet as a key mineral to trace the origin of fluid-rock interactions in high grade metamorphic rocks (Western Alps, Switzerland)

2.5 Bulle F., Rubatto D., Ruggieri G., Luisier C., Bouvier A.S.: Oxygen isotopes in white mica from the Larderello geothermal field – a tool to trace fluid flow in a complex magmatic – hydrothermal system

2.6 Ewing T.A., Rubatto D., Hermann J.: Formation of felsic lower continental crust: insights from U–Pb geochronology of detrital zircon from lower crustal granulites

2.7 Georgatou A., Chiaradia M.: Magmatic sulphide saturation in subduction and postsubduction magmas

2.8 Gianola O., Bartoli O., Ferri F., Cesare B., Galli A., Ferrero S., Capizzi L.: Melt inclusions and crustal anatexis at ultra-high temperature conditions

2.9 Hämmerli J*., Kemp T., Whitehouse M. (*Recipient Paul Niggli Medal): Invited talk: Metamorphic resetting explains the Hf and Nd paradox in Eoarchean rocks

2.10 Jollands M, Kempf E, Hermann J, Müntener O.: Fast H loss from hydroxylated Si vacancies in experimentally dehydrated olivine

2.11 Klimentyeva D., Heinrich C., Von Quadt A.: Formation of massive sulfide orebodies at Bor (Serbia)

2.12 Maltese A., Mezger K., Upadhyay D.: A new perspective on Earth's differentiation history from single zircon Hf isotope analysis

2.13 Nitsche C., Radimilahy C., Schreurs G., Serneels V.: Petrology and Medieval Indian Ocean Trade: Studying Amphibole-bearing Softstone Vessels and Quarries in North Eastern Madagascar

2.14 Popov D., Spikings R: Diffusion of Ar in alkali feldspar from Shap granite (UK): fracturing of crystals and non-linear Arrhenius trajectories

2.15 Ravindran A., Mezger K., Balakrishnan S., Kooijman E., Schmitt M., Raith M.M.: Apatite and barite preserve initial $^{87}Sr/^{86}Sr$ isotope ratios: implications for Mesoarchean crust-mantle evolution

2.16 Reynes J., Hermann J.: Water retention in garnets from subducted crust, Zermatt, Switzerland

2.17 Roman Alday M.C., Kouzmanov K., Harlaux M., Stefanova E.: Comparative study of XRF and portable XRF analysis and application in hydrothermal alteration geochemistry: The Elatsite porphyry Cu-Au-PGE deposit, Bulgaria

2.18   Vho A., Lanari P., Rubatto D., Giuntoli F.: Fluid-rock interaction in subduction zones: an integrated thermodynamic and $\delta^{18}O$ fractionation modelling approach

2.19   Wotzlaw J.F., Guillong M., Bastian L., Forni F., Balashova A., Mattsson H., Bachmann O.: In-situ garnet ^{238}U-^{230}Th geochronology of Holocene silica-undersaturated volcanic tuffs at millennial-scale precision

POSTERS:

P 2.1   Andrew M., Graham S.: Advances in geological microanalysis: Correlation and Machine Learning

P 2.2   Bejaoui J., Sellamiand A., Braham A.: Mineralization and fluid inclusion investigations of the Miocene sandstone hosted fluorite ore deposits, Northeastern Tunisia

P 2.3   Benz J.-M., Klimentyeva D., von Quadt A., Heinrich C.A.: Sr isotope geochemistry of the Bor Cu-Au system: Is Late Cretaceous seawater involved in magmatic- hydrothermal ore formation?

P 2.4   Brunner M., Müller L., Von Quadt A., Peytcheva I., Ivascanu P.: U/Pb zircon dating of Miocene magmatism in the Apuseni Mountains (Romania) and time relationship of intrusive events at the Certej Deposit

P 2.5   Calder M.F., Arribas A., Chang Z., Hedenquist J.W.: Porphyry-style alteration and vein types of the Far Southeast porphyry Cu-Au deposit, Mankanyan District, Philippines

P 2.6   Caricchi L., Sheldrake T.E., Pioli L., Simpson G., Bali E.: Holuhraun-Bardarbunga 2014-2015 (Iceland) eruption: reconstructing deep magma dynamics with cluster analysis

P 2.7   Curry A., Caricchi L., Lipman P.: Rapid, distinct magma generation preceding four caldera-forming eruptions in the Southern Rocky Mountain Volcanic Field

P 2.8   Davies J.H.F.L., Greber N.D., Schaltegger U.: Do U-Pb zircon dates from residual melts in mafic magmatic systems record protracted crystallization?

P 2.9   Demers-Roberge A., Jollands M., Tollan P., Müntener O.: Water in orthopyroxene: orientation and thickness calibration using FTIR: from the lab to natural samples

P 2.10   Domínguez-Carretero D., Kouzmanov K., Dini A.: Architecture of a distal skarn system: Calamita Fe-skarn deposit, Elba Island, Italy

P 2.11   El Korh A., Boiron M.-C., Cathelineau M., Deloule E., Luais B.: Tracing Sn and W pre-concentrations in the Limousin ophiolite and Variscan granites

P 2.12   Golay T., Moritz R., Popkhadze N., Natsvlishvili M.: The Sakdrisi Au-Cu deposit, Bolnisi mining district, Georgia: providing a genetic model based on petrographic, geochemical, structural and alteration studies.

P 2.13   Grosjean M., Moritz R., Rezeau H., Melkonyan R., Hovakimyan S., Ulianov A.: Temporal and geochemical characterization of the Tejsar magmatic complex, northern Armenia, Lesser Caucasus

P 2.14   Hantsche A., Kouzmanov K., Vassileva R.: Pyroxene geochemical evolution in a distal Pb-Zn skarn body, Madan, Bulgaria

P 2.15   Higgins O., Caricchi L., Blundy J., Melekhova L.: A geochemical and petrological study to constrain the magmatic history of St Kitts and Nevis (Lesser Antilles)

P 2.16   Hovakimyan S., Moritz R., Tayan R., Harutunyan M., Rezeau H., Melkonyan R., Hovhannisyan A.: Tectonic setting of the Cenozoic Kadjaran porphyry Cu-Mo – epithermal system, Armenia, Lesser Caucasus

P 2.17   Kempf E., Hermann J.: Prograde metamorphism in the Bergell contact Aureole: A field and experimental study

P 2.18   Leuthold J.: High temperature crystal-melt reactions in mafic igneous complexes

P 2.19   Manzotti P., Ballèvre M., Baumgartner L., Müntener O., Pitra P., Robyr M., Ruffet G.: Sodic amphibole and sodic clinopyroxene in the Dent Blanche (Western Alps): new constraints for an old question

P 2.20   Marxer F., Ulmer P.: Polybaric fractional crystallisation of arc magmas – an experimental study

P 2.21   Monsef R., Monsef I., Esmaili R.: Cenozoic magmatism in northwestern of Central Iran Block: Roll back, mantle upwelling and extension

P 2.22   Moulas E., Schmalholz S., Podladchikov Y., Tajčmanová L., Kostopoulos D., Baumgartner L.: Relation between mean stress, thermodynamic and lithostatic pressure

P 2.23   Müller L., von Quadt A., Peytcheva I., Ruff R., Halga S.: Geochronology and geochemistry of zircons from the Rovina Valley Project and the Stanija Prospect – Apuseni Mountains (Romania): constraints from LA-ICP-MS/ TIMS dating, trace and REE geochemistry of zircons and whole rock

P 2.24   Müller I.A., Waajen I., Frieling J., Bijl P., Ziegler M.: Carbonate clumped isotope climate reconstructions on fossil coral samples of the Early Eocene

P 2.25   Myint Myat Phyo, Guillong M., Berger A., Balmer W., Franz L., Hao A.O. Wang, Krzemnicki M.S.: A geochronological study of zircon and zirconolite observed in ruby and spinel gemstones and in marble host rock from Mogok, Myanmar

P 2.26   Naumenko-Dèzes M., Rolland Y., Gallet S., Lanari P., Villa I.M.: High precision Ar/Ar age traverses reveal intragrain inhomogeneities of pristine magmatic micas

P 2.27   Nformidah S., Tollan P., Hermann J., Tchouankoue J.P.: Spinel lherzolite xenoliths from the Cameroon Volcanic Line (CVL): Implications for mantle processes and equilibrium conditions

P 2.28   Pein S.F., Diamond L.W., Belgrano T.M.: Characterisation of hydrothermal recharge alteration of seafloor basalts in the Oman ophiolite

P 2.29   Pistone M., Petri B., Müntener O., Almqvist B.S.G., Zanetti A., Hetényi G., Zappone A.S., Baumgartner L.P.: Unravelling magma emplacement mechanism in the lower crust: A forensic investigation of the Mafic Complex, Ivrea-Verbano Zone (Italy)

P 2.30   Pohlner J.E., Schmitt A.K., Chamberlain K.R., Austermann G., Hildenbrand A.: U-Pb baddeleyite geochronology: two case studies from the western Avalon Peninsula, Newfoundland

P 2.31   Richter L., Diamond L.W.: Epidosite formation in the oceanic crust: Composition and P–T properties of the metasomatizing fluid

P 2.32   Roman Alday M.C., Kouzmanov K., Harlaux M., Stefanova E.: Comparative study of XRF and portable XRF analysis and application in hydrothermal alteration geochemistry: The Elatsite porphyry Cu-Au-PGE deposit, Bulgaria

P 2.33   Schaltegger U., Ovtcharova M., Davies J.H.F.L., Greber N.D., Farina F., Widmann P., Lena L.: How to achieve 100 ppm precision on a U-Pb zircon age: recent developments and their limitation

P 2.34   Schenker F.L., Scapozza C.: Soapstones: fields and production laboratories between Ticino and Moesano

P 2.35   Schmitt J., Seth B., Köhler P., Willenbring J., Fischer H.: On CF_4 – a trace gas in granites and in the past atmosphere

P 2.36   Tollan P., Ellis B., Troch J., Neukampf J., Bachmann O., Hermann J.: A method for determining magmatic volatile records by FTIR analysis of unexposed melt inclusions and their minerals hosts

P 2.37   Weber G., Simpson G., Caricchi L.: Thermal perspectives on the diversity and temporal evolution of magma chemistry

P 2.38   Weber S., Diamond L.W., Alt-Epping P.: Insights into formation of epidosites in oceanic crust from reactive-transport modeling

P 2.39   Zuluaga N., Belgrano T., Diamond L.W.: Hydrothermal alteration associated with volcanogenic massive sulfide (VMS) deposits in the Semail Ophiolite, Oman

P 2.40   Zurbriggen R.: Relationships of banded amphibolites and Ordovician orthogneisses in pre-Variscan basements of the Alps

2.1

A new map of the Oman ophiolite extrusives: insights into protoarc crust composition, boninite distribution and sulphide deposit prospectivity

Thomas M. Belgrano*, Larryn W. Diamond*, Yves Vogt*, Andrea R. Biedermann*,**, Samuel A. Gilgen*, Khalid Al-Tobi[3]

[1] *Institute of Geological Sciences, University of Bern, Baltzerstrasse 1+3, CH-3012 Bern, Switzerland*
[2] *Institute for Rock Magnetism, University of Minnesota, 100 Union St SE, 55455 Minneapolis, USA*
[3] *National Earth Secrets, P.O. Box 1242, PC 130 Athaibah, Muscat, Sultanate of Oman*

Studies of Western Pacific arc basement indicates that vast swathes of 'protoarc' oceanic crust 100s of km wide and 1000s of km long form during subduction initiation events prior to the establishment of steady intra-oceanic subduction. A similar tectonic setting for the formation of the Tethyan ophiolite chain has been inferred from their remarkable structural, geochemical and geochronological similarities with the West Pacific protoarc record.

The petrogenesis of the characteristic volcanic rock types of these settings—forearc basalts and boninites—are reasonably well understood, however, very little is known about their abundance and distribution in poorly preserved protoarc crust . With this in mind, the Semail ophiolite (Oman–U.A.E.)—the world's largest and most complete subaerial exposure of oceanic crust—provides a prime opportunity for a quantitative consideration of the different volcanic rock types in protoarc crust. Uplift and erosion of the ophiolite has exposed a 300 km long strip, or ~500 km2, of volcanics in a gently east-dipping cross section along the northeastern margin of the Hajar mountains. This simple structure, the lack of vegetation, and the abundance of previous petrogenetic studies on the extrusive sequence means that the spatial distribution of each volcanic episode is well-testable in map-view.

We have collated geochemical analyses and maps from the literature and collected and analysed a further 200 samples from the ophiolite to better define the field, geochemical and magnetic characteristics of its volcanic units. These characteristics were then used during field and aeromagnetic mapping of the lava units both in outcrop and under sedimentary cover throughout the northern ophiolite. The resulting map provides a new framework for research in the ophiolite extrusives, it sets the first constraints on the relative abundance of boninites in Oman, and it provides a new tool for targeting Au-enriched volcanogenic massive sulphide deposits hosted in these boninites.

2.2

Sulphuric acid-mediated weathering on Taiwan buffers geological sinks of atmospheric carbon

Thomas Blattmann [1], Shing-Lin Wang [2,3], Maarten Lupker [1], Lena Märki [1], Negar Haghipour [1], Lukas Wacker [4], Ling-Ho Chung [5], Stefano Bernasconi [1], Michael Plötze [6] & Timothy Eglinton [1]

[1] *Geological Institute, ETH Zurich, Sonneggstrasse 5, 8092 Zurich, Switzerland (thomas.blattmann@erdw.ethz.ch)*
[2] *Department of Geosciences, National Taiwan University, No. 1, Sec. 4, Roosevelt Rd., Taipei 10617, Taiwan*
[3] *Department of Oceanography, National Sun Yat-sen University, 70 Lienhai Rd., Kaohsiung 80424, Taiwan*
[4] *Ion Beam Physics, ETH Zurich, Otto-Stern-Weg 5, 8093 Zurich, Switzerland*
[5] *National Museum of Natural Science, No. 1, Guanqian Rd., Taichung 40453, Taiwan*
[6] *Institute for Geotechnical Engineering, ETH Zurich, Stefano-Franscini-Platz 3, 8093 Zurich, Switzerland*

The chemical composition of the Gaoping River in Taiwan reflects the weathering of both silicate and carbonate rocks found in its metasedimentary catchment. Major dissolved ion chemistry and radiocarbon signatures of dissolved inorganic carbon (DIC) reveal the importance of pyrite-derived sulphuric acid weathering on silicates and carbonates. Two-thirds of the dissolved load of the Gaoping River derives from sulphuric acid-mediated weathering of rocks within its catchment. This is reflected by low DI^{14}C signatures, with rock-derived carbonate constituting a ^{14}C-free DIC source. Using an inverse modelling approach, we provide quantitative constraints of mineral weathering pathways and calculate atmospheric CO_2 fluxes resulting from the erosion of the Taiwan orogeny over geological timescales.

2.3
What can we learn from δ^{18}O in olivine-hosted melt inclusions?

Anne-Sophie Bouvier [1], Lukas Baumgartner [1], Estelle Rose-Koga [2], Pierre Schiano [2]

[1] Institut des sciences de la Terre, University of Lausanne, batiment Geopolis, CH-1015 Lausanne
 (anne-sphie.bouvier@unil.ch)

[2] Laboratoire Magmas et Volcans, University of Clermont-Auvergne, Campus universitaire des Cezeaux, 6 Avenue
 Blaise Pascal, 63170 Aubière, France

Melt inclusions are small droplets of melt trapped during crystal growth. They are often used to trace primary magmatic processes possibly lost in whole rocks, especially when trapped in olivine (e.g., Kent, 2008). The majority of the data from olivine-hosted melt inclusions (OHMIs) consists of major, volatile and trace elements. OHMIs usually show large chemical variability, which can result in term of post-entrapment processes (element diffusion, host crystal crystallization, bubble growth), crystallization process (e.g., boundary layer) or source process (e.g., fluid contributions, melting rates…). A few studies reports stable isotopes in OHMIs (e.g., Hauri et al., 2002; Rose et al., 2001;). The large range of compositions measured for different stable isotopes were interpreted in term of fluid input(s) into the mantle wedge (arc settings) or magma mixing and crustal assimilation (Iceland) (e.g., Bouvier et al., 2008; Hartley et al., 2013).

A recent study of δ^{18}O in OHMIs from 2 MORBs samples show an individual range of isotopic variations up to 2.5‰ (Manzini et al., submitted), whereas the average bulk rock δ^{18}O for fresh unaltered MORB is 5.5 ± 0.3‰. Oxygen isotopes variation in OHMIs from the 2 different samples is not correlated with any trace element ratios nor volatiles, suggesting that the variability is not linked to a source process. For each sample, only ~40% of OHMIs are in isotopic equilibrium with their host. This population of OHMIs show rather small variation, suggesting limited (<1‰) source heterogeneity. The current dataset suggest that the measured varibility is mostly due to pre to syn-entrapment O diffusion, but the exact physical processsus responsibe for the disequilibrium remains unclear.

For arc samples, larger δ^{18}O variations are expected, because fluids are involved in the magma genesis of most arc magmas. For example, OHMIs in samples from 5 different arcs only show a maximum of 2.7‰ variation within a sample (Bouvier et al., submitted), similar to the isotopic range measured in the MORB samples. Also, in one arc sample for which δ^{18}O was measured in the host olivine, ~40% of OHMIs seems to be in isotopic equilibrium with their host, a proportion similar to that found in the MORB samples. This suggests that the process generating olivine-MI isotopic disequilibrium (lower and higher partitioning values) is not MORB specific. A better understanding of the processes generating the oxygen isotopic disequilibrium between MI and their host olivine from various samples may bring new information about MI entrapment processes, crystal growth and/or magma transport.

REFERENCES

Bouvier, A.-S., Métrich, N., Deloule, E. 2008 : Slab-Derived Fluids in the Magma Sources of St. Vincent (Lesser Antilles Arc): Volatile and Light Element Imprints. J. Petrol. 49, 1427–1448. https://doi.org/10.1093/petrology/egn031

Bouvier, A.-S., Manzini, M., Rose-Koga, E.F., Nichols, A.R.L., Baumgartner, L. submitted: Tracing of Cl input into the sub-arc mantle through the combined analysis of B, O and 1 Cl isotopes in melt inclusions, submitted to EPSL.

Hartley, M.E., Thordarson, T., Fitton, J.G. 2013: Oxygen isotopes in melt inclusions and glasses from the Askja volcanic system, North Iceland. Geochim. Cosmochim. Acta 123, 55–73. https://doi.org/10.1016/j.gca.2013.09.008

Hauri, E., 2002. SIMS analysis of volatiles in silicate glasses, 2: isotopes and abundances in Hawaiian melt inclusions. Chem. Geol. 183, 115–141.Kent, A.J.R. 2008: Melt Inclusions in Basaltic and Related Volcanic Rocks. Rev. Mineral. Geochemistry 69, 273–331. https://doi.org/10.2138/rmg.2008.69.8

Manzini, M., Bouvier, A.-S., Baumgartner, L.P., Rose-Koga, E.F., Schiano, P., Shimizu, N. submitted: Localized small scale process recorded by large oxygen isotope variations in olivine-hosted melt inclusions from two MORB samples, submitted to EPSL.

Rose, E.F., Shimizu, N., Layne, G.D., Grove, T.L., 2001. Melt production beneath Mt. Shasta from boron data in primitive melt inclusions. Science 293, 281–3. https://doi.org/10.1126/science.1059663

2.4
Garnet as a key mineral to trace the origin of fluid-rock interactions in high grade metamorphic rocks (Western Alps, Switzerland)

Thomas Bovay [1], Daniela Rubatto [1,2], Pierre Lanari [1], Lukas Baumgartner [2]

[1] Institut für Geologie, University of Bern, Baltzerstrasse 3, CH-3012 Bern
(thomas.bovay@unibe.ch)
[2] Institut des sciences de la Terre, University of Lausanne, Bâtiment Geopolis, UNIL-Mouline, CH-1015 Lausanne

Fluids are known to play key roles in subduction interface processes. Water-rock interaction at the ocean floor hydrates the mafic crusts and the underlying mantle. During subduction, mineral dehydration reactions in the different rock types constituting the slab produce fluids that interact with nearby rocks and can lead to the formation of metasomatic reaction zones. The Theodul Gletscher tectonic Unit outcrops within the Zermatt Saas ophiolite (Western Alps) consists of an association of micaschists and mafic boudins resting on serpentinites that underwent eclogitic facies metamorphism during Alpine subduction (2.4±0.1 GPa and 550±50 °C). Schists located close to a mafic boudins systematically display textural evidences for fluid-rock interaction suggesting heterogeneous fluid activity and permeability at the outcrop scale.

The bulk rock chemistry of the mafic rocks displays high CaO concentration ranging from 15.9 to 22.4wt% and low Na_2O and MgO concentration ranging from 0.3 to 0.5 wt% and from 4.3 to 11.3 wt% respectively. These major chemical variations are typical for alteration process occurring at the seafloor by interaction with seawater prior to subduction. Rare earth element (REE) patterns show strong enrichment in light-REE.

Garnet was targeted in order to characterise the fluid rock interaction along the P-T evolution. This metamorphic mineral is present in every lithology of the tectonic unit and can preserve prograde to peak metamorphic zoning for major elements. After investigation under BSE imaging and EPMA mapping garnets show evidence of a multi-stage evolution. At the contact zones between the schists and the high-grade boudins, euhedral garnet porphyroblasts are observed within the schists. The size (ranging from tens of μm to several cm in diameter) and abundance of garnet increase towards the contact. In the schists, the largest garnet grains are composed of a Fe-Ca-rich core (of possible pre-Alpine origin), a Fe-Mg-rich mantle and a Ca-rich rim. The textural relationships between the garnet compositions suggest a replacement of the core by the second generation and fracture filling occurring together with rim-core replacement during rim growth of the last generation. Garnets in the mafic rocks show both normal growth zoning and replacement textures with an increase in grossular content from core to rim.

In situ oxygen isotope analyses of garnet porphyroblasts from the schists show a marked change in $\delta^{18}O$ signatures from 12‰ in the core to 4‰ in the rim. This decrease is coherent with chemical zoning observed for major elements. Garnet from the mafic boudins has $\delta^{18}O$ values from 0.5 to 2‰. The strong variations in oxygen isotopic composition are evidence for open system behaviour. This petrological, micro-textural and geochemical investigation highlights multiple stages of fluid exchanges and possibly diverse fluid sources and pathways from seafloor alteration to peak metamorphism.

2.5

Oxygen isotopes in white mica from the Larderello geothermal field – a tool to trace fluid flow in a complex magmatic – hydrothermal system

Florian Bulle [1], Daniela Rubatto [1/3], Giovanni Ruggieri [2], Cindy Luisier [3], Anne-Sophie Bouvier [3]

[1] *Institut für Geologie, Universität Bern, Baltzerstrasse 1+3, CH-3012 Bern (florian.bulle@geo.unibe.ch)*
[2] *CNR-Instituto di Geoscienza e Georisorse, Via La Pira 4, I-50121 Firenze*
[3] *Institut des Sciences de la Terre, University of Lausanne, Géopolis, CH-1015 Lausanne*

White mica is present in all major stratigraphic units in the Larderello geo-thermal field (LGF) including the metasedimentary units that form the "upper reservoir" (UR) as well as the granite intrusions and the contact metamorphic basement that constitutes the actively exploited "lower reservoir" (LR). Texturally and chemically distinct generations of white mica record stages of magmatic crystallization, thermometamorphic/hydrothermal replacement and fluid/rock interaction in the dynamic environment of the LGF. The chemical and $^{18}O/^{16}O$ composition of white mica varies at the intra- and inter-grain scale. The majority of the analysed white mica can be classified as muscovite (K: 0.93±.03, 1σ, Si: 3.1±.1, ^{VI}Al: 1.8±.1; apfu, per 11 oxygens). The compositional variability is the result of three dominant cation exchanges, 1) paragonite-muscovite [K—Na], 2) Tschermak [Si+(Mg^{2+}, Fe^{2+})—2Al] and 3) pyrophyllite [(K, Na)— $_1$]. The shift in $\delta^{18}O$ reflects varying degrees of fluid/ mineral interaction with either dominantly low-$\delta^{18}O$ (meteoric) or high-$\delta^{18}O$ (magmatic) fluids. Granite and contact metamorphic lithologies (micaschist and gneiss of the crystalline basement) contain white mica with overlapping crystal chemistry (mostly due to exchange 1 and 2), whereas the metasedimentary white mica show the highest variation via exchange 1 and 3. *In-situ* Secondary Ion Mass Spectrometry (SIMS) $^{18}O/^{16}O$ analysis of white mica resolve the fluid/mineral interaction on microscale and identifies a dramatic spread of $\delta^{18}O$ values between ~1–14‰. Metasediments (phyllite and quartzite) from the UR inherit this large spread in $\delta^{18}O$, with texturally and chemically distinct white mica populations (Fig.1) ranging from late hydrothermal (~1–6‰; low Na, mid Mg apfu), over partially altered ($\delta^{18}O$=~8–9‰; low Na, low to mid Mg) to detrital ($\delta^{18}O$=~14‰; high Na, low Mg). The $\delta^{18}O$ values of the detrital white mica resembles that of bulk unaltered micaschist from the Northern Appeninnes (Gianelli and Ruggieri, 2002), whereas the late hydrothermal white mica has similar $\delta^{18}O$ values to other secondary minerals and the meteoric-dominated fluid circulating in the late hydrothermal stage (present day temperatures up to 450°C; Petrucci et al., 1994). Downhole towards the LR, white mica from two contact metamorphic micaschist samples shows either 1) homogeneous $\delta^{18}O$ values of ~9‰ that were likely re-homogenized during the early hydrothermal stage, or 2) large spread in $\delta^{18}O$ from 2 to 12‰ in grains of variable texture and chemistry. The later micaschist sample is cross-cut by a thin high-temperature hydrothermal vein with texturally different white mica than the host rock, but both populations display the same spread in $\delta^{18}O$ values. Two granite samples from Carboli contain chemically variable white mica with a homogeneous primary magmatic $\delta^{18}O$ of ~10‰, whereas two older granite samples from Radicondoli have instead heterogeneous magmatic to hydrothermal white mica with variations in $\delta^{18}O$ of ~4–10‰. The pronounced intra-grain $\delta^{18}O$ variability of up to 6‰ in this white mica occurs in domains with higher Fe and Mg around chlorite inclusions, as a result of interaction with low-$\delta^{18}O$ fluids that perculated downwards to depths of 3–5 km through extensional shear zones (Bellani et al., 2004).

The new microscale $\delta^{18}O$ data of white mica at the LGF reveal that 1) $^{18}O/^{16}O$ exchange is not necessarily coupled with major element exchange and white mica recrystallization, 2) $^{18}O/^{16}O$ variability occurs and persists at the μm-scale in an active geothermal field and 3) localized infiltration of low-$\delta^{18}O$ fluids occurs with little fluid/rock interaction along faults, fractures and cleavages down to ~4.6 km.

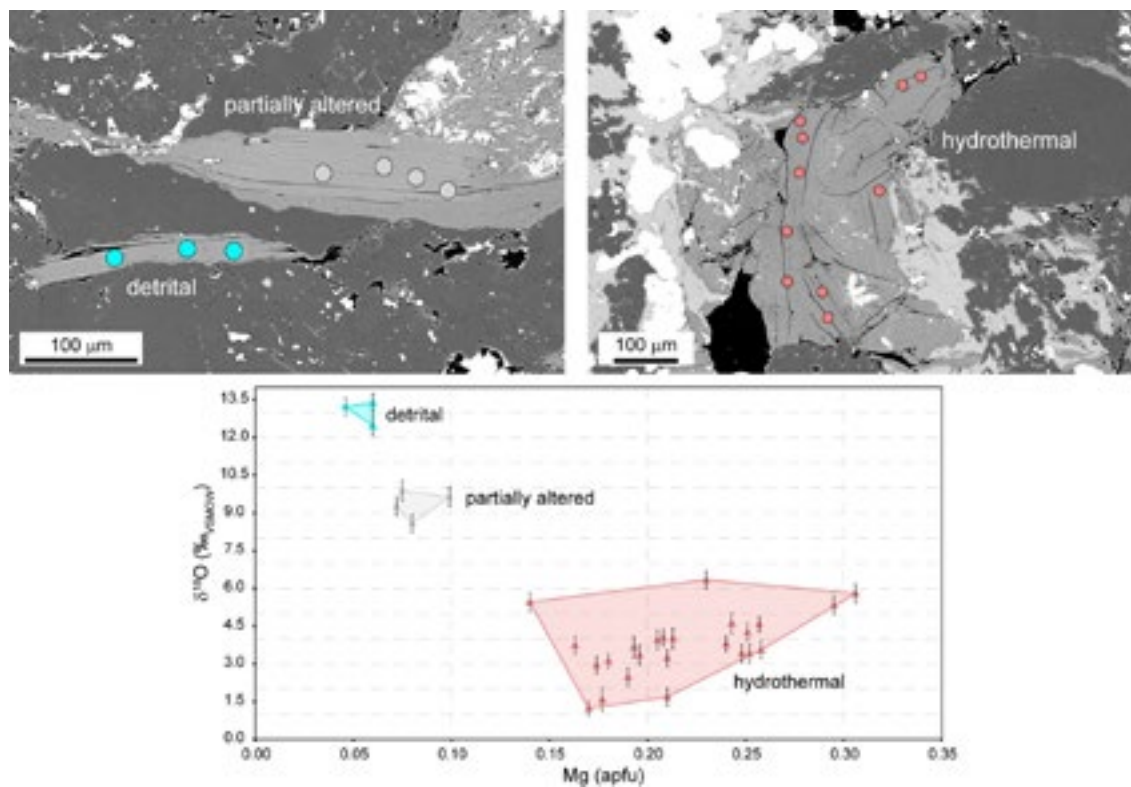Figure 1. Back-scattered electron (BSE) images of muscovite populations in quartzite from the UR with corresponding δ^{18}O values versus Mg content.

REFERENCES

Bellani, S., Brogi, A., Lazzarotto, A., Liotta, D., Ranalli, G., 2004. Heat flow, deep temperatures and extensional structures in the Larderello Geothermal Field (Italy): constraints on geothermal fluid flow. J. Volcanol. Geoth. Res. 132, 15–29.

Gianelli, G., Ruggieri, G., 2002: Evidence of a contact metamorphic aureole with high-temperature metasomatism in the deepest part of the active geothermal field of Larderello, Italy. Geothermics 31, 443–474.

Petrucci, E., Gianelli, G., Puxeddu, M., Iacumin, P., 1994: An oxygen isotope study of silicates at Larderello, Italy. Geothermics 23, 327–337.

2.6

Formation of felsic lower continental crust: insights from U–Pb geochronology of detrital zircon from lower crustal granulites

Tanya Ewing [1], Daniela Rubatto [1&2], Jörg Hermann [1]

[1] Institute of Geological Sciences, University of Bern, Balzerstrasse 1+3, CH-3012 Bern (tanya.ewing@geo.unibe.ch)
[2] Institute of Earth Sciences, University of Lausanne, UNIL-Mouline, CH-1015 Lausanne

The European Alps and the wider European area preserve numerous fragments of Variscan lower continental crust that have been widely studied to document the Permian extension, Jurassic continental rifting and Tertiary Alpine orogeny that reworked and ultimately exhumed these fragments of lower crust. Relatively little attention has been paid to the nature and formation of this lower continental crust prior to its Carboniferous–Permian evolution. Of particular interest is the widespread occurrence of felsic lithologies in these lower crustal relics, including in the classic example of the Ivrea Zone (Italy). High seismic velocities and the common occurrence of mafic lower crustal xenoliths have lead to the lower continental crust traditionally being interpreted as dominantly mafic in composition (e.g. Rudnick and Gao, 2003). This view has recently been challenged, with the suggestion that a considerable proportion of the lower crust could be felsic and metasedimentary (Hacker et al., 2011). The composition of the lower continental crust has fundamental implications for the thermal, rheological and seismic velocity characteristics of the crust, as well as for models of crustal differentiation and reworking. Constraining the nature and formation of felsic lower crust from the European Alps has the potential to inform this debate.

In this study we use detrital zircon cores preserved in Permian granulite facies metapelites from the Malenco Unit (Eastern Alps, Italy) to characterise felsic lower crust from a crust–mantle transition zone. U–Pb geochronology of zircon cores that show clear textural evidence for a detrital origin gave an age spectrum recording the major orogenies known to have affected Gondwana, in particular the Pan-African (650–500 Ma) and Caledonian (450–400 Ma), with subordinate Precambrian detritus with ages up to ~2.5 Ga. Th/U ratios >0.2 for the detrital cores suggest that detritus was dominantly derived from eroded magmatic sources. The presence of a significant population of 450–400 Ma detrital zircons indicates that deposition of the sedimentary protolith occurred after 400 Ma, and thus after the Caledonian orogeny. Exclusively Permian ages for metamorphic zircon rims in the same samples record granulite facies conditions associated with gabbroic underplating during extension following the Variscan orogeny. Our results demonstrate that uplift and erosion of igneous source rocks, deposition of the sedimentary protolith, and transport of the protolith from the surface to lower crustal conditions all occurred within a single orogenic cycle. The absence of a significant population of either detrital or metamorphic zircon with Carboniferous ages indicates that the Malenco lower crust did not experience significant partial melting during the Variscan orogeny. This contrasts with lower crustal relics from the Bohemian Massif, which document widespread anatexis at (U)HP–UHT conditions during Variscan continental subduction (e.g. Bröcker et al., 2009; Walczak et al. 2017). The new geochronological constraints for the Malenco granulites will be integrated with zircon trace element analysis and Ti-in-zircon thermometry, as well as petrological constraints for the host granulites, to explore implications for the timescales and mechanisms of formation of felsic lower continental crust.

REFERENCES

Bröcker, M., Klemd, R., Cosca, M., Brock, W., Larionov, A.N. & Rodionov, N. 2009: The timing of eclogite facies metamorphism and migmatization
in the Orlica–Śnieżnik complex, Bohemian Massif: constraints from a multimethod geochronological study, Journal of Metamorphic Geology, 27, 385–403.
Hacker, B.R., Kelemen, P.B. & Behn, M.D. 2011: Differentiation of the continental crust by relamination, Earth and Planetary Science Letters, 307, 501-516.
Rudnick, R., & Gao, S. 2003: Composition of the Continental Crust, In: Holland, H.D., Turekian, K.K. (Eds.), The Crust. Elsevier–Pergamon, Oxford, pp.1–64.
Walczak, K., Anczkiewicz, R., Szczepański, J., Rubatto, D. & Košler, J.: Combined garnet and zircon geochronology of the ultra-high temperature metamorphism: Constraints on the rise of the Orlica-Śnieżnik Dome, NE Bohemian Massif, SW Poland, Lithos, 292-293, 388–400.

2.7
Magmatic sulphide saturation in subduction and post-subduction magmas

Ariadni Georgatou [1], Massimo Chiaradia [1]

[1] Department of Earth Sciences, University of Geneva, Rue des Maraîchers 13, 1205 Geneva, Switzerland
(ariadni.georgatou@unige.ch)

Porphyry deposits are associated with both subduction and post-subduction settings. In both geodynamic settings the fertility of the magma is thought to be controlled mainly by an incompatible behaviour of economic chalcophile metals during magmatic evolution as well as their partitioning into an exsolving fluid phase before they become sequestered by magmatic sulphides.

The main aim of this project is to constrain the physicochemical conditions under which magmatic sulphide saturation occurs and investigate its possible role for the processes of ore genesis during magmatic evolution in two different geodynamic settings above by studying magmatic sulphide inclusions (MSI) in volcanic complexes and in their enclaves. The geological areas investigated are: (a) the Quaternary Ecuadorian volcanic arc, hosting, among others, the Llurimagua Cu-Mo and Cascabel Cu-Au Miocene porphyry deposits (subduction setting), (b) the Miocene volcano-plutonic complexes of Konya (hosting the Doganbey Cu-Mo-W porphyry and Inlice Au-epithermal) and Usak (hosting the Kisladag 5.5 Moz Au porphyry), in Western Turkey (post-subduction settings), (c) the Kula Plio-Quaternry volcano, in the Usak basin, in Turkey (intraplate OIB-like signature volcano in post-subduction setting), and (d) the active volcanic center of Nisyros in Eastern Greece with no direct porphyry deposit association (subduction setting).

In most investigated areas (except the Kula volcano most mafic rocks with OIB signatutes) Cu behaves as a compatible element, showing a decreasing trend with magmatic evolution, indicating that Cu is lost/stored on the way to the surface within the continental crust (Chiaradia, 2014).

The following preliminary results on petrography and mineral chemistry include only the areas of Ecuador, Konya and Kula (data from Usak and Nisyros are in the process of acquisition).

From petrographical observations MSI were found in different amounts in all investigated rocks covering a wide compositional range (SiO_2=47-67 wt.% and MgO=6.5-1 wt.%), indicating that in both subduction and post-subduction settings, sulphide saturation occurs throughout magmatic evolution. In all study areas MSI display similar texture and host mineral (mostly globular, up to 40 μm in size and hosted by magnetite crystals, see Georgatou et al., 2018 for details) with the exception of Kula volcano. Kula presents larger MSI (up to 200 μm) hosted mainly by pyroxene (and amphibole) and found also in the groundmass as oxide-sulphide aggregates.

From microprobe analyses MSI from Kula (whole rock Cu mean=29 ppm) are unusually Cu-poor and Ni-rich with maximum contents of 32.5 and 25.9 wt%, respectively, compared to those of Konya (whole rock Cu mean=12.5 ppm) and Ecuador (whole rock Cu mean=27.5 ppm), which are mostly hosted by magnetite and have maximum Cu and Ni contents of 73 and 9 wt%, and 65.7 and 10 wt%, respectively. This immplies that Cu is getting more efficiently sequestrated in Konya compared to other investigated magmatic provinces.

A general observation resulting from petroghraphy and mineral chemistry is that the Cu-poorest MSI are hosted by olivine (and less by amphibole) phenocrysts and show usually globular shapes whereas the Cu-richest MSI are found in magnetite crystals and are usually smaller and rectangular, indicating that the sulphide phase was entrapped as a melt and crystallized along the crystallographic planes of the mineral (Georgatou et al., 2018). This may indicate a two stage magmatic sulphide saturation process: an early stage crystallizing Cu-poor MSI (composed of both mss/iss) and a later stage producing only Cu-rich MSI (also seen by others, e.g. Agangi & Reddy, 2016).

Preliminary results indicate that enclaves (and especially the ones rich in amphibole and pyroxene) carry in all study areas a greater amount of MSI compared to the host rock. In addition both Ecuador and Konya enclaves carry MSI which are Cu-poorer compared to the ones found in the host rock, whereas Kula MSI found both inside and outside of the enclaves seem to have similar composition.

Further mineral analysis (also by LA-ICP-MS), thermobarometry and Qemscan analysis on enclaves are needed to investigate the timing/P-T conditions of sulphide saturation (early vs late) in the crust.

REFERENCES

Agangi, A., Reddy, S.M., 2016: Open-system behaviour of magmatic fluid phase and transport of copper in arc magmas at Krakatau and Batur volcanoes, Indonesia, Journal of Volcanology and Geothermal Research 327, 669–686.

Chiaradia, M. 2014: Copper enrichment in arc magmas controlled by overriding plate thickness, Nature Geoscience, v. 7, p. 43-46.

Georgatou A., Chiaradia M., Rezeau H. & Wälle M. 2018: Magmatic sulphides in Quaternary Ecuadorian arc magmas, Lithos 296-299, 580-599.

Jenner, F.E., O'Neill, H.S.C., Arculus, R.J. & Mavrogenes, J. 2010: The magnetite crisis in the evolution of the arc-related magmas and the initial concentration of Au, Ag and Cu, Journal of Petrology 51, 2445–2464.

Matjuschkin, V., Blundy, J.D. & Brooker, R.A. 2016: The effect of pressure on sulphur speciation in mid- to deep-crustal arc magmas and implications for the formation of porphyry copper deposits, Contributions to Mineralogy and Petrology 171, 66.

2.8
Melt inclusions and crustal anatexis at ultra-high temperature conditions

Omar Gianola [1], Omar Bartoli [1], Fabio Ferri [1], Bernardo Cesare [1], Andrea Galli [2], Silvio Ferrero [3], Luca Capizzi [4]

[1] Dipartimento di Geoscienze, Università degli Studi di Padova, Via G. Gradenigo 6, 35131 Padua, Italy.
(omar.gianola@unipd.it)
[2] Institute of Geochemistry and Petrology, ETH Zurich, Clausiusstrasse 25, 8092 Zurich, Switzerland
[3] Universität Potsdam, Institut für Erd- und Umweltwissenschaften, 14476 Potsdam, Germany
[4] Department of Earth Sciences, University of Milan, Via Botticelli 23, 20133 Milan, Italy.

Deep levels of the continental crust can attain, on a regional scale, extreme thermal regimes, such as ultra-high temperature (UHT) metamorphism.

At these conditions, in which temperature exceed 900 °C, rocks buffer the increased thermal gradient undergoing partial melting, a process that is believed to control the geochemical differentiation, reworking and rheology of the lower crust. The Gruf Complex in the European Central Alps is a 12 x 10 km migmatitic body embedded between the Penninic units of the Alpine nappe stack and some Tertiary intrusions. The main rock types outcropping in the Gruf Complex consist of migmatitic orthogneisses, paragneisses and micaschists, leucogranites and charnockites. Migmatitic orthogneisses and charnockites are characterized by the presence of UHT granulites, which occur as schlieren and massive enclaves and that represent residual rocks after anatectic crustal melting. The granulitic enclaves are mostly composed of prismatic sapphirine, up to 2 cm large garnet porphyroblasts, Al-rich orthopyroxene, sillimanite and cordierite. Porphyroblastic garnets contain numerous trapped melt inclusions (MI), which are preserved as both hydrous glass coexisting with CO_2 bubbles and crystallized nanogranitoids. These MI have variable sizes, ranging from 5 to 100 μm in diameter. Larger MI are irregular in shape and display offshoots, while tiny inclusions are more isometric. Commonly, crystallized MI contain biotite and/or muscovite, quartz, feldspars, apatite and minor oxides. Rare polycrystalline inclusions also occur within sapphirine. These inclusions often display a negative crystal shape and typically are less than 20 μm in size.

Preliminary experiments with a piston cylinder apparatus show that nanogranitoid inclusions can be rehomogenized at temperature between 850-900 °C and thus allow to constrain the original composition of the melt.

Melt inclusions in the Gruf granulites are interpreted to represent early anatectic melts produced during incongruent, fluid-absent melting reactions and have therefore the potential to shed light on the crustal reworking processes associated with UHT metamorphism.

2.9
Metamorphic resetting explains the Hf and Nd paradox in Eoarchean rocks

Johannes Hammerli [1], Tony Kemp [1], & Martin Whitehouse [2]

[1] Centre for Exploration Targeting, School of Earth Sciences, The University of Western Australia, Perth, Australia
  (johannes.hammerli@my.jcu.edu.au)
[2] Department of Geosciences, Swedish Museum of Natural History, Stockholm, Sweden

Recent models argue for extensive early differentiation of the silicate Earth and formation of voluminous, stabilised continental crust by 3.5 Ga. Consequently, the most ancient samples of continental crust have attracted significant attention, in order to determine the scale and mechanism of early continental growth and mantle-crust differentiation. Eoarchean crustal rocks are therefore key to gain unique insights into the evolution of the Earth's mantle and crust. Interestingly, some rocks representing this ancient continental crust show complicated, decoupled Nd and Hf isotope signatures. While Hf isotopes point to a chondritic source, Nd isotopes have a superchondritic signature, which is inconsistent with a common origin. Explaining and understanding this inconsistency is critical in order to gain insights into Eoarchean crust-mantle differentiation processes at the beginning of crust stabilization on our planet. However, thus far no general agreement has been reached to explain this conflict of isotope signatures. Moreover, some current models invoke speculative processes to explain the Hf and Nd isotope fractionation, such as the presence of magma oceans and Eoarchean subduction zones.

In this study, we investigate which minerals control the Sm-Nd isotope system in Eoarchean meta-igneous rocks that show apparent Hf and Nd isotope decoupling. Our results demonstrate that isotopic resetting during post-emplacement metamorphic processes play a key role in "decoupling" Hf and Nd isotopes. Metamorphic disturbance of the Sm-Nd isotope system is capable of shifting the Nd isotope signature to both more and less radiogenic values, creating apparent Hf and Nd isotope inconsistencies and challenging other models for explaining the Hf-Nd paradox.

2.10
Fast H loss from hydroxylated Si vacancies in experimentally dehydrated olivine

Michael C. Jollands [1], Elias Kempf [2], Jörg Hermann [2], Othmar Müntener [1]

[1] Institute of Earth Sciences, University of Lausanne, 1015 Lausanne, Switzerland
  (anna.karenina@unibas.ch)
[2] Institute of Earth Sciences, University of Bern, 3012 Bern, Switzerland

Knowing the diffusivity of hydrogen in olivine is crucial not only for geospeedometry (diffusion chronometry) applications, but also for constraining the potential for olivine-hosted water to enter the deep mantle. Experiments in pure forsterite ($+Ti^{4+}$) (Padron-Navarta et al., 2014) and observations in the natural assemblage (olivine+antigorite+chlorite+magnetite) from subducted olivine-bearing serpentinites [2] suggest that H associated with the tetrahedral site, i.e. $4xH^+$ charge-compensating a Si^{4+} vacancy is extremely retentive in olivine. We extended the study from synthetic forsterite to natural Fe-bearing olivine (Mg#≈0.95=$(X_{Mg}/(X_{Mg}+X_{Fe}))$), by dehydrating natural olivine-bearing rocks (same assemblage as above) from Zermatt, Switzerland (Kempf and Hermann, 2018) where all H^+ in olivine is associated with the tetrahedral site. Rock pieces were annealed at 1 bar, oxygen fugacity of ~QFM to QFM-5, 875 °C, for one hour, then samples were doubly polished to 100-150μm, and analysed by Focal Plane Array (64x64 bit detector) Transmission Fourier Transform Infrared Spectroscopy to map the resulting OH distribution. We find that 1) serpentine breakdown occurs in a matter of seconds, forming enstatite, thus considerably modifying the silica activity of the system 2) a series of new OH stretching bands grow during dehydration and 3) H loss is considerably (several orders of magnitude) faster than the previous experimental determination in pure forsterite. However, this does not mean that these previously determined Ds (Padron-Navarta et al., 2014) are incorrect, rather that the physical process may be different. Natural olivine has the capacity (likely via Fe^{2+} oxidation, even at Mg#=0.95) to allow H to leave the tetrahedral site (hence new OH bands), move onto a different site where faster diffusion is enabled, then rapidly exit the crystal (hence apparently fast diffusion). Numerical modelling of a combined diffusion plus reaction / inter-site redistribution process supports this suggestion. This may be the explanation for some recent studies of relative peak-specific diffusivities in natural samples, which do not match the relative diffusivities obtained experimentally. This clearly complicates the use of H diffusion for geospeedometry – suggestions of how to recognise simple diffusion, versus diffusion plus reaction in natural samples, and how to proceed in the latter case, will be discussed.

REFERENCES
Kempf, E., and Hermann, J. (2018). Geology 46: 571-574.
Padron-Navarta, J. A., et al. (2014). Earth Plan. Sci. Lett. 392: 100-112.

2.11
Formation of massive sulfide orebodies at Bor (Serbia)

Dina Klimentyeva [1], Christoph Heinrich [1] & Albrecht Von Quadt [1]

[1] Institute of Geochemistry and Petrology, ETH Zurich, Clausiusstrasse 25, 8092 Zurich
(dina.klimentyeva@erdw.ethz.ch)

The Bor metallogenic zone contains world-class porphyry copper, high- and low-sulphidation epithermal deposits of Bor, Veliki Krivelj and a recently discovered Cukaru Peki with over 20 million tons of Cu and 1000 tons of Au (Jelenković et al., 2016). In addition to the porphyry and epithermal style veins, massive high-grade sulfide lenses are present at Bor. The massive sulfide lenses are located within the zones of advanced argillic alteration and vuggy silica. Pyrite + chalcopyrite assemblage dominating the lower part of the orebody, pyrite + digenite + chalcocite + covellite represent the main association in the central part, and enargite veinlets cross-cutting the massive sulfide ore occur predominantly in the upper part of the T orebody and at the margins.

We performed leaching experiments to figure out which elements are truly immobile, and what elements are depleted and enriched in parallel to the massive suflide formation process. The distinct change of enrichment patterns occur at the transition from the massive sulfide with residual quartz to true massive sulfide, with Au and Cu being greatly enriched in the massive sulfide sample.
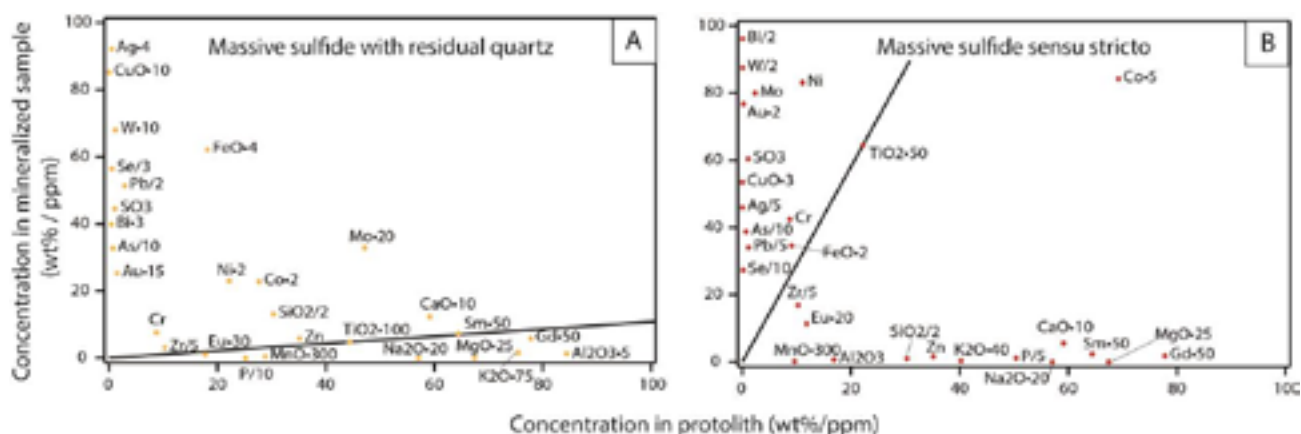

Figure 1. Isocon diagrams with element concentration of mineralized samples plotted against the barren protolith (sample 67-258). Oxides are expressed in wt%, trace elements in ppm. Elements plotting above the isocon line represent gains, elements plotting below the isocon lines are losses. A. Sample BB3-23, massive sulfide with appreciable amount of residual quartz (pyrite, quartz, chalcocite, covellite and minor colusite). F. Sample BB4-48, massive sulfide (pyrite, chalcocite, covellite, minor quartz, rutile and kaolinite).
Presence of vapour inclusions in the Cu- and Au-poor core of the pyrite from the epithemal veins could indicate that vapour played significant role in the formation of earlier pyrite, but was not present in the late Cu- and Au-rich stage. One of the possible explanations for the extreme last-stage enrichment of Cu and Au is condensation of low-density Cu- and Au-enriched vapour into the aqueous fluid (Heinrich, 2005), possibly supersaturated with Cu and Au.

REFERENCES

Heinrich, C. A., 2005. The physical and chemical evolution of low-salinity magmatic fluids at the porphyry to epithermal transition: a thermodynamic study. Mineralium Deposita, 39(8): 864-889

Jelenković, R., Milovanović, D., Koželj, D., and Banješević, M., 2016. The Mineral Resources of the Bor Metallogenic Zone: A Review. Geologia Croatica, 69(1): 143-155

2.12

A new perspective on Earth's differentiation history from single zircon Hf isotope analysis

Alessandro Maltese [1], Klaus Mezger [1] & Dewashish Upadhyay [2]

[1] Institut für Geologie, Universität Bern, Baltzerstrasse 1+3, CH-3012 Bern (alessandro.maltese@geo.unibe.ch)
[2] Department of Geology and Geophysics, Indian Institute of Technology, 721302 Kharagpur, India

The evolution of Earth's crust-mantle system through geologic time has been investigated for many decades using various radio-isotope systems (e.g., DePaolo & Wasserburg, 1976). These studies are somewhat limited by the fact that only about 10 % of globally exposed rocks are of Archean age and most of them are difficult to access. A serious complication is that these rocks were typically affected by multiple episodes of metamorphic overprinting which makes it difficult to retrieve robust initial isotope compositions using *bulk* rock samples (e.g., Moorbath et al., 1997). These initial isotope ratios provide key constraints on the extent of mantle depletion and concomitant formation of granitic continental crust. In order to circumvent the problem of open-system modification of ancient rocks, many geochemical investigations conduct *in-situ* analysis of individual growth zones in the robust mineral zircon. That way it is possible to obtain U-Pb ages in combination with Hf isotope ratios measured on the same spot or at least same grain. Thus, the timing of rock formation and information about the differentiation of the silicate Earth can be more reliably constrained. However, all *in-situ* methods can only produce Hf data of modest precision, although with high spatial resolution (e.g., Fisher et al., 2011).

An alternative approach is to select individual zircon crystals without complex age zoning and determine their Hf-isotope composition by MC-ICP-MS after chemical purification of Hf. This approach enables high precision Hf isotope measurements of single crystals with uncertainties of better than 0.3 ε-units. In addition, the scatter of data is significantly less than that observed for *in-situ* data from individual zircon grains from the same sample. The higher resolution possible with this method is particularly relevant for early Archean samples where the differences in Hf- isotopes between the depleted mantle and crust are still very small and difficult to resolve.

This *bulk* method was applied to (single) zircon grains from the Archean Bastar Craton, India. The data are accompanied by previously acquired U-Pb data (LA-ICP-MS) for the temporal framework. The most primitive sample with an age of 3.59 Ga yields ε_{Hf} = +1.55 ±0.22. Younger samples progressively yield more negative initial values down to ε_{Hf} = -3.06 ±0.18 following a linear relationship. This data set provides firm constraints on Archean crust-mantle dynamics. While the formation of continental crust may have started early in Earth's history, only a minor amount of enriched felsic continental crust had formed by ca. 3.6 Ga. Globally, the widespread occurrence of Archean crustal fragments with ages from 3.6-3.2 Ga may indicate the initiation of rapid and extensive growth of continental crust.

REFERENCES

DePaolo, D.J. & Wasserburg, G.J. 1976: Inferences about magma sources and mantle structure from variations of $^{143}Nd/^{144}Nd$. Geophys. Res. Lett. 3, 743-746.

Moorbath, S., Whitehouse, M.J. & Kamber, B.S. 1997: Extreme Nd-isotope heterogeneity in the early Archaean — fact or fiction? Case histories from northern Canada and West Greenland. Chem. Geol. 135, 213-231.

Fisher, C.M., Hanchar, J.M., Samson, S.D., Dhuime, B., Blichert-Toft, J., Vervoort, J.D. & Lam, R. 2011: Synthetic zircon doped with hafnium and rare earth elements: A reference material for in situ hafnium isotope analysis. Chem. Geol. 286, 32-47.

2.13
Petrology and Medieval Indian Ocean Trade:
Studying Amphibole-bearing Softstone Vessels and Quarries in North Eastern Madagascar

Christoph Nitsche [1], Chantal Radimilahy [2], Guido Schreurs [3], Vincent Serneels [1]

[1] *Department of Geosciences, University of Fribourg, Fribourg, Switzerland*
[2] *University of Antananarivo, Antananarivo, Madagascar*
[3] *Institute of Geological Sciences, University of Bern, Bern, Switzerland*

During the Medieval Period, the North Eastern Coast of Madagascar was settled by the Islamised Rasikajy Population, who established several small towns along the coast. The archaeological record of this period yields abundant findings of local and imported ceramics, iron smelting slags and turned softstone pots, many of which were discovered in the famous cemetery site of Vohémar.

Extraction and first brute shaping of these pots was carried out in quarries in the hinterland, while the finishing most likely took place in coastal manufacturing centres. Up to now, around 20 of these quarries are known for Northern Madagascar and are being sampled systematically for this study. The aim of this study is a petrographic and geochemical characterisation of the quarries to allow subsequent provenance applications.

In the literature, the raw material used for the vessel production in Madagascar is referred to as chloriteschist, an ambiguous term considering its mineralogy and general lack of deformation. It is a mafic to ultramafic meta-cumulate, that was metasomatically metamorphosed under greenschist to amphibolite conditions and should be called Talc-Chlorite-Amphibole-Granofels by modern petrographic standards. It crops out in small 10 to 100 m scale lenses throughout the northern part of the island, seemingly independent of the respective geological units.

This rock type can be compared to an occurrence in Southern Germany, where it was first mentioned, described and named *Hoesbachite* after its location in the Spessart Mountains. Likewise, the softstone used in Madagascar comprises a complex assemblage of up to three generations of amphibole in a matrix of chlorite+talc+magnetite±anthophyllite±ilmenite±rutile. Due to the textural complexity and heterogeneous nature of this rock, we use a combined approach of texturally controlled microanalytics, bulk rock chemistry and optical parameters for the characterisation of the quarried localities.

Establishing a petrographical and taxonomical database of quarries and artefacts will allow the tracing of shipping routes both in Madagascar and along the Indian Ocean Trade network, as the occurrence of amphibole distinguishes this material from conventional soapstones described e.g. in Egypt and Southern Iran.

2.14

Diffusion of Ar in alkali feldspar from Shap granite (UK): fracturing of crystals and non-linear Arrhenius trajectories

Daniil Popov [1], Richard Spikings

[1] *Department of Earth Sciences, University of Geneva, Rue des Maraîchers 13, CH-1205 Geneva*
  (Daniil.Popov@unige.ch; d.vs.popov@gmail.com)

We investigate the mechanisms that drive redistribution and loss of radiogenic Ar from alkali feldspar. Several authors suggest that thermally activated volume diffusion is predominantly responsible, and that $^{40}Ar/^{39}Ar$ data obtained from this mineral by step-heating can be used to constrain the thermal histories of rocks (e.g. using multi-diffusion domain (MDD) theory; Lovera et al., 1989). Inversion of $^{40}Ar/^{39}Ar$ data to a time-temperature path is made under several assumptions, one of which is that boundaries that define diffusion domains in nature are also preserved during in vacuo step-heating. However, some researchers argue that heating of alkali feldspars results in significant textural modification, thus questioning the stability of the boundaries of diffusion domains during laboratory treatment (e.g. Parsons et al. 2010; Fitz Gerald et al., 2006). Here we attempt to identify the boundaries of diffusion domains and assess their stability by correlating Arrhenius trajectories with modifications of feldspar texture that occur in response to heating and cooling.

The problem was explored by combining two types of experiments. In vacuo repetitive step-heating experiments were used to obtain Arrhenius trajectories from fragments of alkali feldspar megacrysts from Shap granite (UK), with shortest dimension lengths of ~0.4, ~1 and ~2.2 mm. A non-linear Arrhenius trajectory from fragments with a shortest dimension length of ~0.4 mm is typical of alkali feldspars used for MDD modelling, i.e. initial (low temperature) heating steps yield higher *log(D/r²)* values than repeated isothermal steps. Non-linear Arrhenius trajectories from fragments with shortest dimension lengths of ~1 and ~2.2 mm are not suitable for MDD modelling because the initial heating steps have lower *log(D/r²)* values than repeated steps. These data suggest that at repeated isothermal steps, larger crystals yield either (i) higher diffusivities, or (ii) shorter diffusion lengths. The latter seems more feasible, given the results of heating experiments in air, which are described below.

Heating experiments in a muffle furnace in air were used to investigate modifications of feldspar texture that occur in response to heating and cooling over laboratory time scales. In addition to previously documented modification of texture, such as homogenisation of exsolution lamellae, or partial re-equilibration of K-feldspar and albite in patch perthite veins (Parsons et al. 2010; Fitz Gerald et al., 2006), we observed numerous cracks that are mostly parallel to the cleavage planes. These cracks are present both in rapidly quenched and slowly-cooled grains. They form an interconnected network and their occurence does not always correlate with other microtextures: although mostly fracturing is more intensive around patch perthite veins, in some cases areas around them are poor in cracks.

Our results indicate that boundaries which define diffusion domains during laboratory step-heating may form during step-heating, possibly by grain fracturing. In smaller (~0.4 mm) feldspar fragments this occurred during the first heating step, while in the larger (~1 and ~2.2 mm) fragments, boundary formation occurred during several consecutive initial heating steps. Heating of feldspar crystals in air resulted in their fracturing. During step-heating of larger grains, fracturing may continue over several heating-cooling cycles. Cracks form an interconnected network, and their occurence does not always correlate with other microtextures. These results indicate the importance of understanding of the structural transformations of feldspar crystals during step-heating before using $^{40}Ar/^{39}Ar$ data for thermochronology.

REFERENCES

Lovera, O.M., Richter, F.M., & Harrison, T.M. 1989: The $^{40}Ar/^{39}Ar$ thermochronometry for slowly cooled samples having a distribution of diffusion domain sizes, Journal of Geophysical Research: Solid Earth, 94(B12), 17917-17935.

Parsons, I., Fitz Gerald, J.D., Lee, J. K., & Ivanic, T. 2010: Time–temperature evolution of microtextures and contained fluids in a plutonic alkali feldspar during heating, Contributions to Mineralogy and Petrology, 160(2), 155-180.

Fitz Gerald, J.D., Parsons, I., & Cayzer, N. 2006: Nanotunnels and pull-aparts: Defects of exsolution lamellae in alkali feldspars, American Mineralogist, 91(5-6), 772-783.

2.15
Apatite and barite preserve initial ^{87}Sr/^{86}Sr isotope ratios: implications for Mesoarchean crust-mantle evolution

Arathy Ravindran [1], Klaus Mezger [1], S. Balakrishnan [2], Ellen Kooijman [3], Melanie Schmitt [3], Michael M. Raith [4]

[1] *Institut für Geologie, Universität Bern, Baltzerstrasse 1+3, 3012 Bern, Switzerland*
[2] *Department of Earth Sciences, Pondicherry University, Puducherry-605014, India*
[3] *Department of Geosciences, Swedish Museum of Natural History, Frescativägen 40, SE-11418 Stockholm, Sweden*
[4] *Steinmann Institut, Universität Bonn, Poppelsdorfer Schloss, D-53115 Bonn, Germany*

Determining the initial ^{87}Sr/^{86}Sr ratios of Archean rocks is quite challenging due to the high Rb/Sr ratios of most rocks that require large corrections for in-situ produced ^{87}Sr. Added to this is the high susceptibility of Rb-Sr system to alteration. However, the minerals barite (sediments, hydrothermal deposits) and apatite (igneous rocks) generally have near zero Rb/Sr and thus corrections for the decay of ^{87}Rb are minimal, allowing for the direct determination of the initial ^{87}Sr/^{86}Sr from individual mineral grains. Barite, formed in some Archaean marine settings, is less susceptible to later alteration than carbonates and thus is more reliable in reconstructing the isotope composition of Archaean seawater. Due to its long residence times and redox insensitivity in the oceans, Sr isotopes can be used to link the Sr-seawater trend with crustal evolution (e.g. Satkoski et al., 2017). Stratiform barites were deposited simultaneously with chromiferous chert in the ~3.3 Ga Ghattihosahalli Schist Belt, Western Dharwar Craton, India (Jayananda et al., 2008). Strong spatial heterogeneities have been preserved in Sr isotopes and major elements despite pervasive ductile deformation and regional amphibolite facies metamorphism over long time-scales. Barite grains with Rb/Sr ratios <0.003 preserve a least radiogenic ^{87}Sr/^{86}Sr ratio of 0.701328±17 (2σ) that most likely records the isotope ratio at the time of formation. This low ^{87}Sr/^{86}Sr for seawater implies a gradual rise in ^{87}Sr/^{86}Sr over time rather than a steep evolution as proposed by Satkoski et al. (2016).

The initial isotopic composition of crustal igneous rocks is preserved in the accessory mineral apatite (e.g. Tsuboi and Suzuki, 2003). In situ Sr isotope measurements of single apatite grains from granitoids and metasedimentary units deposited over a time span from 3.4-2.5 Ga in the western Dharwar Craton give clear insights into the development of Archaean crust in that area. This could bring together a correlation between Sr-seawater evolution and magmatic initial Sr evolution. Rocks with igneous textures preserve pristine initial ratios in their lowest values; the more radiogenic ratios in others record recrystallization and fluid interaction. The low ^{87}Sr/^{86}Sr ratios in barite and some igneous apatites exclude the presence of significantly older evolved crust in the area at 3.4 Ga. This questions the nature of the crust and high net rates of continental growth during that time (Dhuime et al., 2015).

REFERENCES

Dhuime, B., et al. 2015: Emergence of modern continental crust about 3 billion years ago, Nature, 8, 552-555

Jayananda, M., et al. 2008: 3.35 Ga komatiite volcanism in the western Dharwar Craton, southern India: constraints from Nd isotopes and whole-rock geochemistry, Precambrian Research, 162, 160-179

Satkoski, A. M., et al. 2016: A high continental weathering flux into Paleoarchean seawater revealed by strontium isotope analysis of 3.26 Ga barite, Earth and Planetary Science Letters, 454, 28-35

Satkoski, A. M., et al. 2017: Initiation of modern-style plate tectonics recorded in Mesoarchaean marine chemical sediments, Geochimica et Cosmochimica Acta, 209, 216-232

Tsuboi, M. & Suzuki, K. 2003: Heterogeneity of initial ^{87}Sr/^{86}Sr ratios within a single pluton: evidence from apatite strontium isotopic study, Chemical Geology, 199, 189-197

2.16
Water retention in garnets from subducted crust, Zermatt, Switzerland

Julien Reynes [1] & Jörg Hermann [1]

[1] Institute of Geological Sciences, University of Bern, Baltzerstrasse 3, Bern, Switzerland (julien.reynes@geo.unibe.ch)

Garnet is a common mineral in high-pressure metamorphic rocks, formed during prograde dehydration reactions at great depth (>30 km). Garnet is a nominally anhydrous mineral but it can incorporate significant amounts of water in the form of OH groups, with H substituting for cations (1-10 000 ppm H_2O; (Aines and Rossman 1984a).

The Saas-Zermatt ophiolite contains large slices of subducted high-pressure oceanic crust (2.3±0.1 Gpa, 540±20°C; (Angiboust et al. 2009). We investigated water contents in garnet from various rock types using Fourier transform infrared spectroscopy (FTIR). Samples include ultramafic rocks (Uvarovite-Andradite veins in serpentinites), mafic rocks (Meta-rodingites), and various metasediments (Garnet schists and Mn-rich metasediments). Determined water contents range from <1 for almandine garnets from metasediments to 2000 ppm H_2O for uvarovites. We set up a novel approach consisting in correlating high resolution FTIR maps with element distribution maps obtained by electron microprobe (EPMA). This method allows to determine if water incorporation and/or retention is enhanced by an element, and if H diffusion patterns are visible.

The FTIR spectra display different bands according to the composition of the garnet, showing that H incorporated in garnet is strongly influenced by nearest neighbours. Correlation of FTIR and EPMA maps reveal high correlation between chemical zoning and water zoning. Some garnet compositions are thus more likely to retain/incorporate water: Ca^{2+} - Cr^{3+}/Fe^{3+} garnets > Ca^{2+}-Al^{3+} garnets> Mn^{2+}-Al^{3+} garnets >>> Fe^{2+}-Mg^{2+}-Al^{3+} garnets. Most of the garnets preserve water zoning acquired during prograde growth and show little evidences of H diffusional loss during their exhumation back to the surface.

Rock types containing garnet with high water contents represent a small volume in the oceanic crust, and therefore represent a minor contribution to the water budget in subduction zones. Nonetheless, due to the large P-T stability field of garnet, any water incorporated in the crystal structure might be transported to deeper parts of the mantle, after the breakdown of hydrous phases.

REFERENCES
Aines RD, Rossman GR (1984a) The hydrous component in garnets: pyralspites American Mineralogist 69:1116-1126
Angiboust S, Agard P, Jolivet L, Beyssac O (2009) The Zermatt-Saas ophiolite: the largest (60-km wide) and deepest (c. 70–80 km) continuous slice of oceanic lithosphere detached from a subduction zone? Terra Nova 21:171-180

2.17
Comparative study of XRF and portable XRF analysis and application in hydrothermal alteration geochemistry: The Elatsite porphyry Cu-Au-PGE deposit, Bulgaria

Roman Alday, M.C.[1], Kouzmanov, K.[1], Harlaux, M.[1], Stefanova E.[2]

[1] Department of Earth Sciences, University of Geneva, Rue de Maraîchers 13, 1205 Geneva, Switzerland;
   Maria.Roman@etu.unige.ch
[2] Geological Institute, Bulgarian Academy of Sciences, Acad. G. Bonchev Str. 24, 1113 Sofia, Bulgaria

X-ray fluorescence (XRF) spectrometry is a non-destructive analytical technique widely used in Earth and Environmental Sciences to determine the elemental composition of rocks, ores, soils and plants. Portable XRF analysers (pXRF) are increasingly being used in mineral exploration and mining, allowing acquiring rapidly and inexpensively large geochemical data sets in the field. In this contribution, we present the results of a comparative study of 15 samples of hydrothermally altered magmatic and metamorphic rocks from the Elatsite porphyry Cu-Au-PGE deposit in Bulgaria, using both a lab-based WD-XRF (PANalytical Axios^{mAX}) and a pXRF (Thermo Niton XL3t) device.

For analyses performed with the pXRF, the samples were crushed to a fine-grained powder (<80 μm) and mounted in a plastic cup covered by a thin polypropylene film (4 μm-thick) to be analysed on a test stand. Two techniques for sample preparation were used, resulting in slight difference in compaction of the sample measured: the first one consists of analysis of non-pressed powder in the cup (referred to as "powder" in Fig. 1), and in the second case the powder is slightly compressed with an agate pestle (referred to as "pressed powder" in Fig.1). A total of 34 elements were measured using the "Soils & Minerals" protocol within the "Mining Cu/Zn" mode of the pXRF. Measurements were 120s each consisting of two 60s cycles using four different energy filters. For some elements (Al, V, Mn, Mo, Ba) pressed-powder samples show systematically slightly higher values (as high as 10%; Fig. 1C).

Lab-based WD-XRF results were used to perform an empirical calibration of the elemental concentrations obtained by pXRF, following the procedure proposed by Mauriohooho et al. (2016) (Fig. 1A-B). Linear regression analysis of the data allows calculating the correction factor to be applied (corresponding to the slope of the regression line) for each element determined by pXRF. For each filter, the correction factor decreases progressively with the increase of the atomic number of the measured element (Fig. 1D).

Comparing the results obtained using the two sample preparation techniques for the pXRF analyses, we demonstrate that generally both of them provide accurate data comparable with WD-XRF (Fig. 1B), resulting in correlation coefficients >0.9. However for some elements (ex. Al, Sr, Zn), pressed-powder preparation resulted in better correlation between WD-XRF and pXRF analyses.
Unfortunately, due to its low atomic number, Na cannot be quantified by pXRF, and Mg is usually measured with a low level of confidence.

Our results demonstrate that large data sets obtained with a pXRF device can be used after correction based on lab-XRF analyses on selected representative samples for geochemical interpretation on suites of hydrothermally altered samples (mass balance and alteration index calculations).
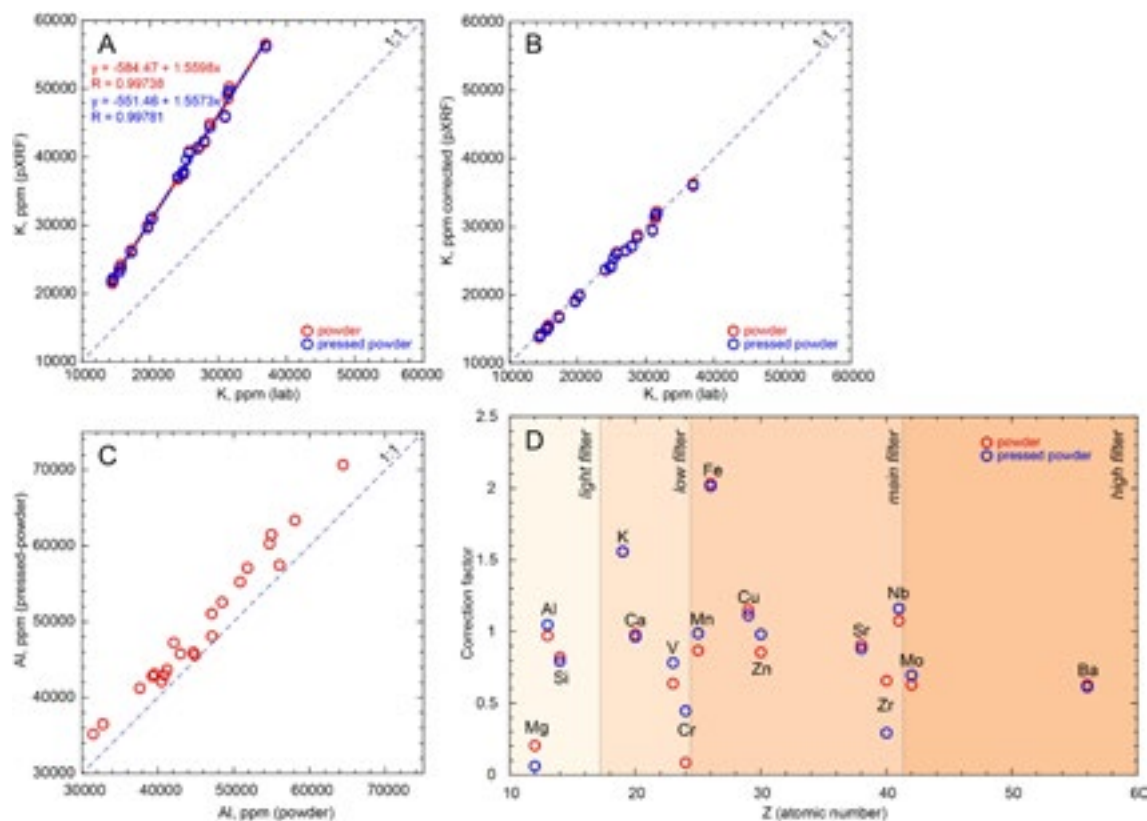
Figure 1. Comparison between lab-based WD-XRF and pXRF analyses of hydrothermally altered rock samples: A) K concentrations of powder and pressed-powder samples vs. lab-XRF analyses; calculated slops from regression analysis are used as correction coefficients; B) Corrected values of K concentrations from pXRF analyses vs. lab-XRF data; C) Powder vs. pressed-powder sample preparation for pXRF analyses (Al concentrations); D) Correction factor as a function of Z (atomic number) of the elements for the four different filters used (light, low, main, high).

REFERENCES

Mauriohooho, K., Barker, S., Rae, A. 2016: Mapping lithology and hydrothermal alteration in geothermal systems using portabke X-ray flourescence (p XRF): A case study from the Tauhara geotheral system, Taupo Volcanic Zone. Geothermics 64 (2016) 125-134

2.18
Fluid-rock interaction in subduction zones: an integrated thermodynamic and δ^{18}O fractionation modelling approach

Alice Vho [1], Pierre Lanari [1], Daniela Rubatto [1,2] & Francesco Giuntoli [3]

[1] Institut für Geologie, University of Bern, CH-3012 Bern (alice.vho@geo.unibe.ch)
[2] Institut de Sciences de la Terre, University of Lausanne, CH-1015 Lausanne
[3] Institut de minéralogie, de physique des matériaux et de cosmochimie, Sorbonne Université, Paris, France

Oxygen stable isotopes are important tools for a wide range of applications in Earth sciences as the oxygen isotopic signature of minerals records the physical and chemical conditions of equilibration. Oxygen isotope fractionation between minerals has been widely used for thermometry, but also to investigate samples that experienced fluid-rock interactions. The petrological interpretation of oxygen isotope data requires the knowledge of the fractionation behaviour between two phases and its evolution with temperature. A few well-documented compilations of fractionation factors are available in the literature, but they are either restricted to small chemical systems or based on different methods, making the data not consistent with each other. In this study, we report the first internally consistent database for oxygen fractionation that includes fractionation factors for most major and accessory phases and a pure H_2O fluid phase. This database has been derived simultaneously using a least square regression technique based on a large dataset of published experimental, theoretical and natural data. All the constraints for a given phase contributed to the refinement of its fractionation properties, making the final database internally consistent.

This database can be applied in a general thermodynamic framework to model the evolution of δ^{18}O in minerals through their metamorphic history. For a given bulk rock composition, the evolution of the mineral assemblages, modes and compositions can be predicted along any P-T path using Gibbs free energy minimization. If the δ^{18}O of one phase is known, it is possible to recalculate the δ^{18}O of the other phases in equilibrium as well as the bulk δ^{18}O. If the bulk δ^{18}O is known, the δ^{18}O values of each phase at any given P-T can be predicted and compared with natural data from mineral and mineral zone analyses. This modelling strategy enhances our ability to investigate samples that experienced complex thermal histories and/or fluid-rock interactions. It also provides a strong theoretical basis for evaluating to what extend a rock has evolved either as an open system with respect to oxygen isotopes, or as a closed system fully or partially re-equilibrated. This approach was applied to investigate the metamorphic and metasomatic evolution of high-pressure (HP) rocks from the Sesia Zone in the Western Alps. These accreted continental fragments consist of poly-metamorphic and mono-metamorphic lithotypes such as metagranitoids, metasediments, and mafic boudins that recorded different pre-Alpine histories and different P-T-t paths during the Alpine orogenic cycle. Several lines of evidence support the presence of fluids at HP conditions. In situ δ^{18}O analysis allows the isotopic composition of mineral zones to be resolved and related to mineral textures reconcilable with growth zoning, but also resorption and replacement processes. The δ^{18}O values of different garnet zones, in combination with petrological modelling, can assist in identifying episodes of external versus internal fluid fluxes. Relics of pre-Alpine garnet in different metasediments from the Eclogitic Micaschist Complex show systematically higher δ^{18}O values with respect to Alpine rims, suggesting a significant input of external fluids between the Permian high-temperature stage and the HP Alpine metamorphism. The oxygen isotope fractionation modelling is critical to reconstruct fluid sources and pathways through the crust during subduction.
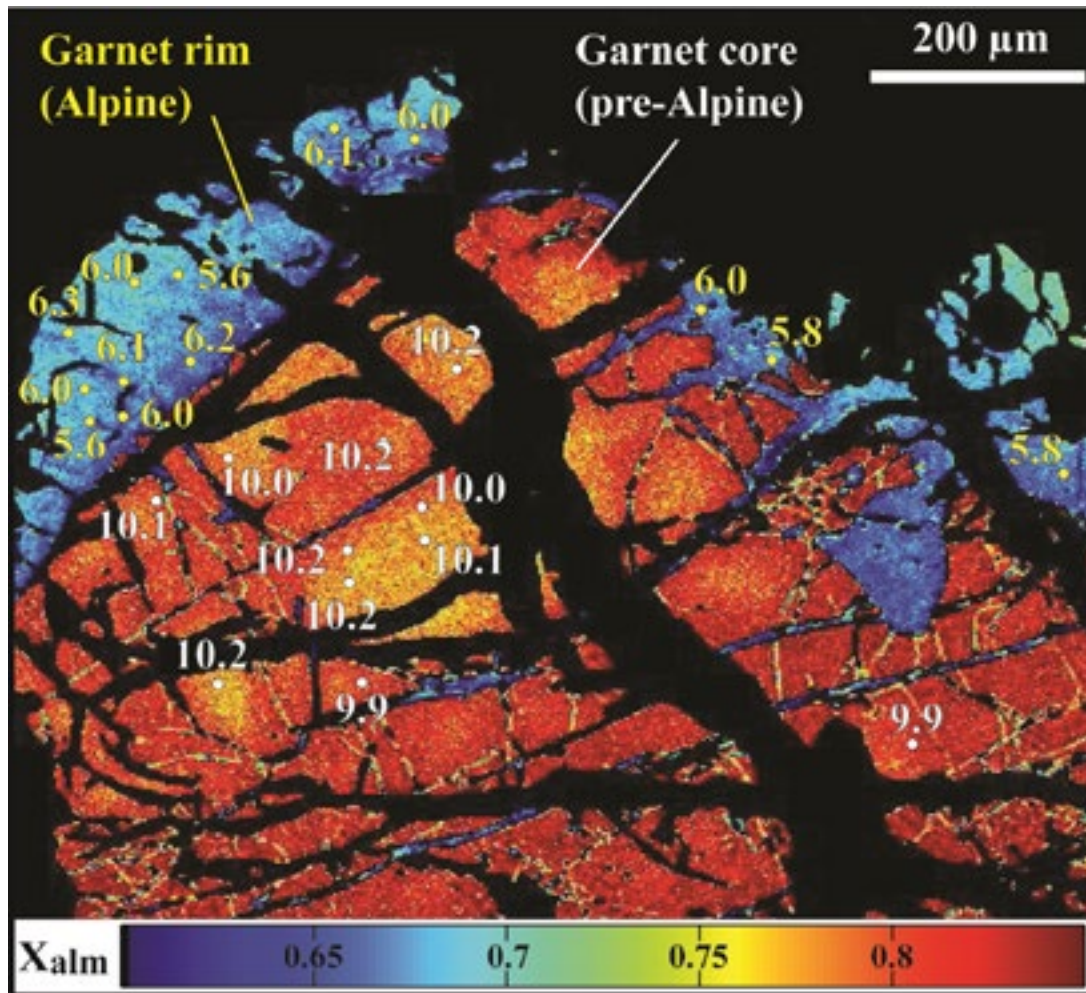
Figure 1. Representative garnet grain from the Eclogitic Micaschist Complex. Pre-Alpine core and Alpine rim are visible in the chemical map. The location of the SIMS analysis (circles) and the corresponding $\delta^{18}O$ value in ‰ are reported. Core and rim $\delta^{18}O$ compositions differ of ~4 ‰.

2.19
In-situ garnet ^{238}U-^{230}Th geochronology of Holocene silica-undersaturated volcanic tuffs at millennial-scale precision

Jörn-Frederik Wotzlaw [1], Marcel Guillong [1], Lena Bastian [1], Francesca Forni [2], Anna Balashova [1], István Dunkl [3], Hannes Mattson [4] & Olivier Bachmann [1]

[1] Institute of Geochemistry and Petrology, ETH Zurich (joern.wotzlaw@erdw.ethz.ch)
[2] Earth Observatory of Singapore, Nanyang Technological University
[3] Sedimentology and Environmental Geology, University of Göttingen
[4] Department of Earth Sciences, Uppsala University

Accurate geochronology of Quaternary silica-undersaturated alkaline volcanic rocks is notoriously difficult. This is because K-rich minerals from these type of rocks commonly contain significant amounts of excess-^{40}Ar, rendering ^{40}Ar/^{39}Ar dates unreliable. This significantly limits our ability to assess the frequency of eruptions in alkaline volcanic provinces, evaluate related volcanic risk and date associated archaeological sites. Here, we present a new approach to dating alkaline volcanic rocks employing ^{238}U-^{230}Th disequilibrium dating of Ca-rich garnet phenocrysts by laser ablation inductively coupled plasma mass spectrometry (LA-ICPMS). We document analytical protocols and apply this technique to date magmatic garnets from historic eruptions of the Somma-Vesuvius volcanic complex (Southern Italy) and from the Engare Sero Footprint Tuff, a volcaniclastic unit attributed to Oldoinyo Lengai (Northern Tanzania) that contains abundant Hominin footprints (Balashova et al., 2016; Liutkus-Pierce et al., 2017). Garnet phenocrysts from historic eruptions of Vesuvius yield well-defined U-Th isochrons with crystallization ages indistinguishable from known eruption ages suggesting that garnet crystallized close to eruption with short pre-eruption residence times. Garnets from the Engare Sero Footprint Tuff yield a U-Th isochron with an age of 4.91 ± 0.58 ka. This date is compatible with ^{14}C and ^{40}Ar/^{39}Ar dates that bracket tuff deposition to between ~5 and ~19 ka (Liutkus-Pierce et al., 2017) but confidently constrains the age of the Engare Sero Footprint Tuff to the mid-Holocene. These examples demonstrate the potential of this new approach for dating Late Pleistocene to Holocene silica undersaturated volcanic rocks at millennial-scale precision and for investigating magma chamber processes beneath active alkaline volcanoes.

REFERENCES

Balashova, A., Mattsson, H.B., Hirt, A.M., Almqvist, B.S.G., 2016: The Lake Natron Footprint Tuff (northern Tanzania): volcanic source, depositional processes and age constraints from field relations, Journal of Quaternary Science, 31, 526–537.

Liutkus-Pierce, C.M., Zimmer, B.W., Carmichael, S.K., McIntosh, W., Deino, A., Hewitt, S.M., McGinnis, K.J., Hartney, T., Brett, J., Mana, S., Deocampo, D., Richmond, B.G., Hatala, K., Harcourt-Smith, W., Pobiner, B., Metallo, A., Rossi, V., 2016: Radioisotopic age, formation, and preservation of Late Pleistocene human footprints at Engare Sero, Tanzania, Palaeogeography, Palaeoclimatology, Palaeoecology, 463, 68–82.

P 2.1
Advances in geological microanalysis:
Correlation and Machine Learning

Matthew Andrew [1], Shaun Graham [2], Dirk Schumann [3], Sebastian Fuchs [4]

[1] Carl Zeiss X-ray Microscopy, Pleasanton, CA, USA (matthew.andrew@zeiss.com)
[2] Carl Zeiss Microscopy, Cambridge, UK
[3] FIBICS, Ottawa, Canada
[4] GEOMAR Helmholtz Centre for Ocean Research, Kiel, Germany

Techniques such as Light Microscopy (LM), Scanning Electron Microscopy (SEM), Automated Mineralogy (AM) and Laser-Ablation Inductively Coupled Plasma Mass Spectroscopy (LA-ICP-MS) (are often viewed in isolation; there has been limited functional development on the correlation and integration of these techniques to advance geological microanalysis. This is required, as geological structures are highly heterogeneous, and so the resolution required to image fundamental microstructures frequently comes at the expense of a field of view representative of that heterogeneity. Even more critically, no single tool gives complete information about the sample, and frequently analyses are complementary. In this paper we will show how these techniques can be integrated together using machine learning and advanced data science to generate unique insights into the geological processes in question, with specific application to multiscale characterization of shales and understaning mineralogical characterization of hydrothermal vents.

Unconventional reservoirs have transformed the energy industry, but a detailed understanding of their structure and flow behavior at the micro and nano scale remains a challenge. Reservoir rocks exhibit strong structural heterogeneities spanning length scales ranging from the km down to the nm or even sub-nm scale (Ringrose, Martinius and Alvestad, 2008). An understanding of mineralogy is critical to understand reservoir flow behavior and geomechanical response (Oliver *et al.*, 2016)2015; Ashton et al., 2013; Ganguly and Cipolla, 2012. Recent developments in high throughput automated digital petrography digitization allow for entire thin sections to be fully digitized in a matter of minutes. Local microfacies can then be identified using machine learning based image classification. These locations can then be used as the targets for high resolution Automated Mineralogy analyses through a common (sample centric) control system. By maintaining the relationship between local microstructure and macroscopic heterogeneity, data can directly upscaled to the pore to core scale.
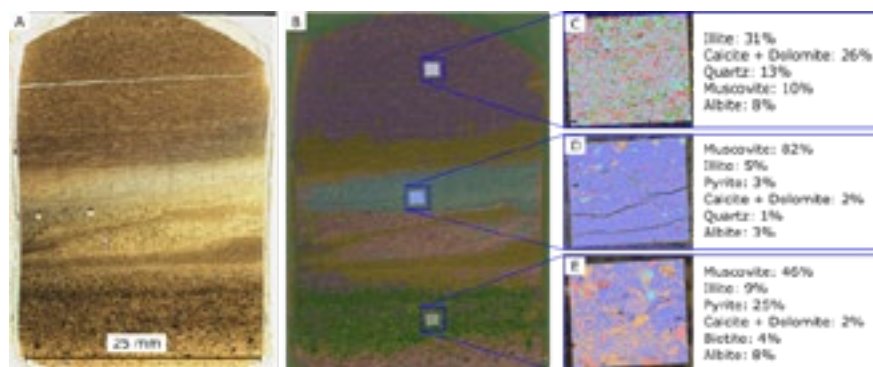

Figure 1: Multiscale analyses of shale rock, with high throughput automated light microscopy (A), classified into local microfacies using machine learning (B). This multimodal classification is then used to define locations for high resolution analyses (C).

One of the principal challenges associated with detailed microanalysis is that of data scale and analysis. With the advent of high throughput, automated mapping technologies, we need equally powerful analytical tools to allow for the interpretation of the resulting data. The last 10 years have seen a transformation in a broad group of technologies frequently grouped together as "machine learning". By integrating and spatially registering disparate datasets acquired on different tools, and feeding the resulting data into a machine learning algorithm (Breiman, 2001), it is possible to automatically classify mineralogical variations over extremely large areas at high resolution extremely rapidly (figure 2).
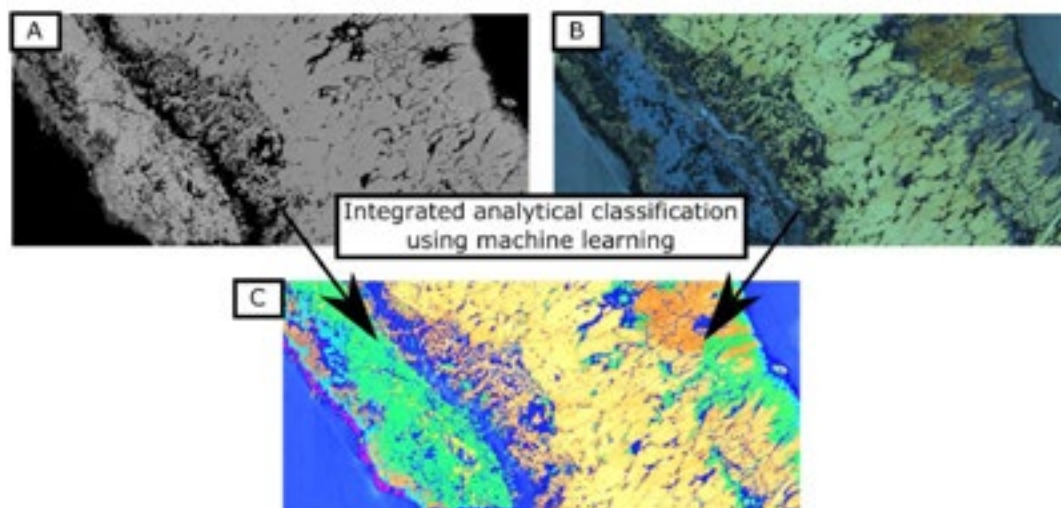
Figure 2. Automated mineralogy overlay of type 1 and type 2 magnetite, imaged using high throughput automated digital petrography, then used to locate regions for LA-ICP-MS analyses.

When applied to subsurface hydrothermal vent samples, this analysis reveals the spatial variation of Chalcopyrite-Bornite alteration, governed by the variation of (and heterogeneity in) fluid flow fields within the vent. This is true both in the center of the central vent flow pathway, where flow and alteration is concentrated, but also within the vent matrix, where flow appears to be strongly concentrated in targeted banded regions.

REFERENCES

Breiman, L. (2001) 'Random forests', *Machine Learning*, 45(1), pp. 5–32. doi: 10.1023/A:1010933404324.

Oliver, G. *et al.* (2016) 'Advanced cuttings analysis provides improved completion design, efficiency and well production', *First Break*, 34(2), pp. 69–76.

Ringrose, P. S., Martinius, a. W. and Alvestad, J. (2008) 'Multiscale geological reservoir modelling in practice', *Geological Society, London, Special Publications*, 309(1), pp. 123–134. doi: 10.1144/SP309.9.

P 2.2

Mineralization and fluid inclusion investigations of the Miocene sandstone hosted fluorite ore deposits, Northeastern Tunisia

Bejaoui Jaloul [1], Ahmed Sellami [2] and Ahmed Braham [2]

[1] UR-MDTN National Center of Nuclear Sciences and Technologies, Tunisia (*bjaoui_geo@yahoo.fr*)
[2] *Office National des Mines, Tunis, Tunisie*

The fluorite-bearing Miocene mineralizations of the Oued M' Tak (Northeastern Tunisia) (Fig.1) are hosted in either glauconitic sandstone units of the Mahmoud Formation (Miocene: Upper Langhian) and the lower part and bioclastic limestone of Aïn Grab Formation (Miocene: Middle Langhian).

Field studies show clearly the same depositing mechanism for mineralization outcropping in the different areas in Oued M'Tak.

Mineralization shows different textures: massive, geodic and disseminate. The fluorite is locally accompanied with sphalerite, quartz, and calcite. Cavities are filled by idiomorphic, cubic, zoned fluorite crystals, minor idiomorphic calcite scalenoedrons and extremely rare crystals of sphalerite.

Fluid inclusions in fluorite are characterised by homogenization temperature (Th) between 110°C and 160°C and salinities values ranging from 14 wt % equiv. NaCl to 20 wt % equiv. NaCl.

The gaseous fluid inclusions show ice-melting temperature (Tmi (gas) <-56.6 to -60°C) that reveals the presence pure CO_2 with a small quantity of CH_4.

This mineralization is similar to that of the main Tunisian fluorite deposits.

Mineralogy and microthermoetry studies indicate that the mineralization results from a mixture of two aqueous fluids characterized by differents temperatures and differents salinities. The fluorite deposits are plausibly post Miocene in age and classified in the MVT-Type-class.
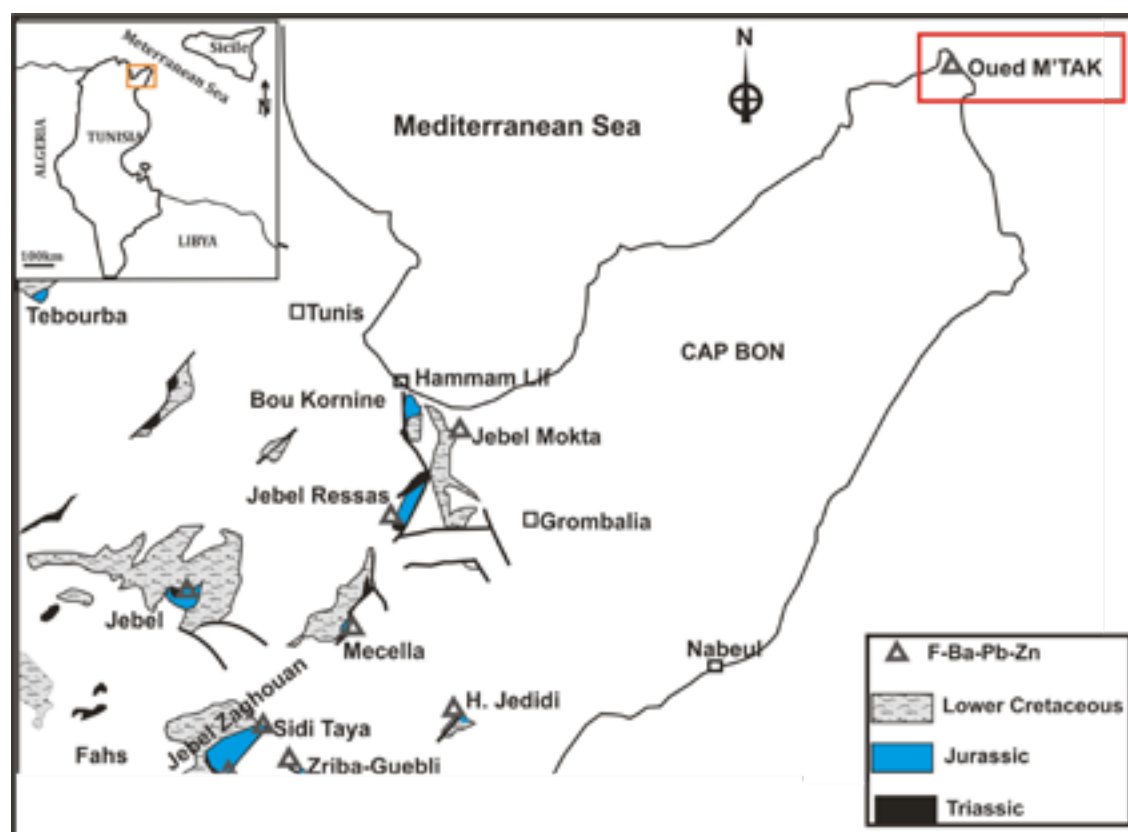

Figure 1. Map showing the Oued M'Tak fluorite deposit, in north-eastern Tunisia (Bejaoui et al., 2013).

REFERENCES

Bejaoui, J, Bouhlel, S, Sellami,A, & Brahem A. 2013: Geology, Mineralogy and Fluid inclusions investigation of the Fluorite deposit at Jebel Kohol, northeastern Tunisia, Periodico di Mineralogia 82(2):217-237.

P 2.3
Sr isotope geochemistry of the Bor Cu-Au system: Is Late Cretaceous seawater involved in magmatic-hydrothermal ore formation?

Jean-Marc Benz [1] Dina Klimentyeva [2], Albrecht von Quadt [2] and Christoph A. Heinrich [2]

[1] Departement of Geography, University of Zurich, Winterthurerstrasse 190, CH-8057 Zurich (jbenz@student.ethz.ch)
[2] Institute of Geochemistry and Petrology, ETH Zurich

Bor is a mine site in Eastern Serbia located in the Late Cretaceous subduction-related andesitic Timok Magmatic Complex (TMC). The Bor Cu-Au deposit hosts economically important amounts of copper and gold, disseminated in several ore bodies with unequal ore grades. In this study two genetically linked ore bodies have been selected, Borska reka, a porphyry ore body and T ore body, a high-sulfidation epithermal ore body, for the extraction of anhydrite from veins. A Rb-Sr isotope dilution approach was used to determine the fluid sources by comparing the $^{87}Sr/^{86}Sr$ ratios of anhydrite on different levels with magmatic whole rock samples, Late Cretaceous seawater and basement whole rock samples. The findings are indicating a close genetic relation of the porphyry part (0.702850 – 0.705889) to primitive magmatic rocks of the TMC (0.703493 – 0.705284) and therefore to magmatic fluids. The range of scatter displays homogeneous to inhomogeneous assimilation of andesitic host rock and minor contamination in a late stage of formation in the upper transitional part of the porphyry system. The scattering of the Sr isotope data of the porphyry part is probably primary. The high-sulfidation epithermal part of the system (0.705331 – 0.706123) shows an overall trend to lay slightly above the primitive magmatic rocks and the scatter cannot be explained by simply inhomogeneous assimilation of andesitic host rock. The scattering in the epithermal part is mainly secondary and caused by mixing of fluids derived from magmatic water and fluids derived from an additional source. Vein cross profiles indicate a coherent trend, without greater perturbation, of increasing $^{87}Sr/^{86}Sr$ ratios towards the internal part of the veins and towards the top part of the deposit. This trend could indicate that the contribution of the contaminating fluid was more evolved in the shallow part of the porphyry-high-sulfidation epithermal system. From the findings influence of seawater to the porphyry-high-sulfidation epithermal system in a late stage of formation is a likely scenario.

P 2.4

U/Pb zircon dating of Miocene magmatism in the Apuseni Mountains (Romania) and time relationship of intrusive events at the Certej Deposit

Manuel Brunner [1], Lukas Müller [1], Albrecht von Quadt [1], Irena Peytcheva [2], Ivăşcanu Paul [3]

[1] Institute of Geochemistry and Petrology, Department of Earth Science, ETH Zürich, Clausiusstrasse 25, CH-8092 Zürich (mbrunner@student.ethz.ch)
[2] Geological Institute, Bulgarian Academy of Science, Sofia, Bulgaria
[3] Eldorado Gold Corporation, Strada Principala 89, Certej, Hunedoara County, Romania

The Southern Apuseni Mountains (SAM) in the Inner Carpathians of Romania are hosting some of Europe's biggest porphyry Cu-Au and epithermal Au-Ag deposits. The source magmas of these deposits are Miocene in age and calc-alkaline in composition. Most of the magmatic rocks in the SAM crop out along two graben-like structures that are oriented NW-SE. Based on the K/Ar method, their emplacement was dated to between 14.7 and 7.4 Ma (Roşu et al., 2004). Being situated about 200 km away from the East Carpathian volcanic arc, active subduction in the Miocene can be excluded. Harris et al. (2013) therefore suggest decompression melting of a previous metasomatized mantle and later asthenosphere upwelling to be the reason for the found magmatic suite.

The Certej project is an epithermal Au-Ag deposit and is situated in the South of the SAM inside the NW-SE orientated Brad-Zlatna basin. The mineralization occurred along the contact of three porphyritic andesite intrusions and the Cretaceous and Neogene basin sediments.

Four sample positions of Roşu et al. (2004) have been redated using the LA-ICP-MS U/Pb dating method on zircons. Drill-core sections of several intrusive bodies at the Certej project were analized with the same method. To narrow down the magmatic activity at the mine site, three main intrusions were dated with ID-TIMS and revealed a lifetime of approximately 75'000 years.

Zircon chemistry (REE, Eu/Eu* and $_{\varepsilon}$Hf) in additon to bulk rock XRF data of eight regional samples and literature data show a trend towards an increasing mantle influence over time in the SAM. It is therfore proposed, that the heterogeneous magma sources could be the product of mixing processes of crustal contaminated early melts with later lithospheric derived melts.

REFERENCES

Harris, C.R., Pettke, T., Heinrich, C.A., Roşu, E., Woodland, S., Fry, B., 2013. Tethyan mantle metasomatism creates subduction geochemical signature in non-arc Cu-Au-Te mineralizing magmas, Apuseni Mountains (Romania). Earth and Planetary Science Letters, v. 366, p. 122-136.

Roşu, E., Seghedi, I., Downes, H., Alderton, D.H.M., Szakács, A., Pécskay, Z., Panaiotu, C., Panaiotu, C.E., Nedelcu, L., 2004. Extension-related Miocene calc-alkaline magmatism in the Apuseni Mountains, Romania: Origin of magmas. Schweizerische Mineralogische und Petrographische Mitteilungen 84, p. 153-172.

P 2.5
Porphyry-style alteration and vein types of the Far Southeast porphyry Cu-Au deposit, Mankanyan District, Philippines

Calder M.F.[1,1], Arribas A.[1], Chang Z.[1,2] and Hedenquist J.W.[1]

[1] EGRU (Economic Geology Research Centre) and Academic Group of Geosciences, James Cook University, Townsville, Queensland 4811, Australia. Email: michael.f.calder@gmail.com
[2] Department of Geology and Geological Engineering, Colorado School of Mines, Golden, CO 80005, USA

Ninety-six underground diamond holes (~102 km) drilled by Far Southeast Gold Resources at the Far Southeast Cu-Au porphyry deposit provides a 3-dimensional exposure of the deposit between 700 and -750m elevations; surface at ~1400m elevation. Drill holes intersect the base of advanced argillic-silicic alteration that hosts the supra-adjacent Lepanto high-sulfidation mineralization, the top of the porphyry deposit as defined by stockwork veins, the main ore body and an underlying subeconomic zone. The 1% Cu equivalent ore shell is mainly located at 500 to -300m elevation.

Alteration assemblages were determined by drill core logging, SWIR (Short Wavelength Infra-Red) spectral analysis, and a petrographic study. Alteration is zoned around veins, or pervasive where zoned assemblages coalesce. Mineral sequence includes early granular grey/white quartz-rich veins with potassic alteration (biotite-magnetite-K-feldspar), followed by euhedral lavender quartz-rich veins (color resulting from the presence of hematite daughter minerals in fluid inclusions) with SCA alteration (sericite-chlorite-albite) – associated with the bulk of Cu deposition as chalcopyrite and bornite – and late anhydrite-rich veins with phyllic alteration (illite-muscovite-pyrite). Thin Cu-sulfide rich veins ('paint' veins) are associated with SCA alteration. Timing between veins is recorded by crosscutting and reopening textures whereas timing of alteration is recorded in overprinting of assemblages, and a change in mineral composition (e.g., albitization of plagioclase affected by SCA alteration).

Shallow advanced argillic mineral assemblages (pyrophyllite-diaspore-alunite-kaolinite) overlie SCA alteration and deep potassic alteration. It is also found at depth, mainly along structures. Illite crystallinity variations recorded by SWIR implies higher temperature of formation with decreasing distance to high grade zones.

Variations in alteration mineralogy are a consequence of a change in temperature and fluid composition of the hydrothermal fluids. Cross-cutting relations that contradict general observations of timing are the result of multiple pulses of hydrothermal fluid that overprinted one another.

P 2.6
Holuhraun-Bardarbunga 2014-2015 (Iceland) eruption: reconstructing deep magma dynamics with cluster analysis

Luca Caricchi [1], Tom E. Sheldrake [1], Laura Pioli [1], Guy Simpson [1], Eniko Bali [2]

[1] Department of Earth Sciences, University of Geneva, rue des Maraîchers 13, 1205 Geneva, Switzerland (luca.caricchi@unige.ch)
[2] Faculty of Earth Sciences, University of Iceland, Askja building, Sæmundargötu 2, 101 Reykjavík, Iceland

Petrography and geochemistry of eruptive products are commonly used to reconstruct magmatic processes occurring at depth and preceding volcanic eruptions. While this approach is central to our understanding of processes occurring at inaccessible depths, analyses and sample preparation are time consuming, which limits the number of samples that can be analysed. This, in turn, hinders the possibility to rank the relative importance of processes on a statistically significant way. We collected samples of the Holuhraun-Bardarbunga eruption, emitted from September 2014 to February 2015 and collected 60 core-to-rim profiles electron microprobe profiles of chemically zoned clinopyroxenes. The analyses were treated using dimensionality reduction and clustering algorithms. This approach allowed us to identify clusters of clinopyroxene zone chemistry, quantify their relative abundances and establish the relative sequence of their appearance in the clinopyroxene profiles (i.e. relative temporal sequence).

The results show that two different magmas were injected at the base of the crust in different proportions (83 vs 7%). Most of these magmas mixed at depth before being transferred at shallow depth and erupted (95%), while the remaining 5% bypassed any intermediate reservoir, were transported at shallow depth and erupted. Variations to this general picture were observed during the eruption that we are currently linking to geophysical observations collected during the eruption (Sigmundsson et al., 2014; Gudmundsson et al., 2016).

Our findings are in line with recently published melt inclusion studies (Bali et al., 2018, Hartley et al., 2018), allow for quantitative assessment of the relative importance of magmatic processes at depth and suggest our approach can provide a frame and be used to target high precision geochemical studies.

REFERENCES

Bali, E. (2018). Melt inclusion constraints on volatile systematics and degassing history of the 2014–2015 Holuhraun eruption, Iceland. Contribution to Mineralogy and Petrology, *173*(9). http://doi.org/10.1007/s00410-017-1434-1.

Gudmundsson, M. T., Jonsdottir, K., Hooper, A., Holohan, E. P., Halldorsson, S. Ofeigsson, B. G., et al. (2016). Gradual caldera collapse at Bardarbunga volcano, Iceland, regulated by lateral magma outflow. Science, 353(6296), http://doi.org/10.1126/science.aaf8988

Hartley, M. E., Bali, E., Maclennan, J., Neave, D. A., & Halldórsson, S. A. (2018). Melt inclusion constraints on petrogenesis of the 2014-2015 Holuhraun eruption, Iceland. Contribution to Mineralogy and Petrology, 173(2). http://doi.org/10.1007/s00410-017-1435-0

Sigmundsson, F., Hooper, A., Hreinsdóttir, S., Vogfjörd, K.S., Ófeigsson, B.G., Heimisson, E.R., et al. (2014). Segmented lateral dyke growth in a rifting event at Bárðarbunga volcanic system, Iceland. Nature, 517(7533), 191–195. http://doi.org/10.1038/nature14111

P 2.7
Rapid, distinct magma generation preceding four caldera-forming eruptions in the Southern Rocky Mountain Volcanic Field

Adam Curry [1], Luca Caricchi [1], and Peter Lipman [2]

[1] Department of Earth Sciences, University of Geneva, Rue des Maraîchers 13, CH-1205 Geneva (adam.curry@unige.ch)
[2] U.S. Geological Survey, 345 Middlefield Road, Menlo Park, California 94025, USA

The Southern Rocky Mountain Volcanic Field (SRMVF) is an exceptional expression of the widespread mid-Cenozoic ignimbrite flare-up in western North America. Within the SRMVF, which is over 1000 km inland of the western edge of North America, the nine caldera-forming eruptions of the central caldera cluster in the San Juan Mountains produced over 8000 km^3 of explosive volcanic rock in less than two million years (28.7 - 26.87 Ma). The last 40 k.y. of this central caldera cycle produced over 1400 km^3 of material during four caldera-forming eruptions, the Rat Creek Tuff (RCT), Cebolla Creek Tuff (CCT), Nelson Mountain Tuff (NMT), and Snowshoe Mountain Tuff (SMT), from oldest to youngest. The RCT and NMT are zoned in composition (dacite to rhyolite) and crystallinity (~5-35 vol%), and the CCT and SMT are crystal-rich (20-35 vol%) and unzoned (dacite). These rapid, sequential eruptions make this an excellent natural laboratory for studying extremely productive magmatic systems. We present petrographic thin section analyses in addition to whole-rock, glass, and mineral major and trace element data to determine 1) genetic links, if any exist, between these eruptions and 2) magmatic reservoir conditions preceding these eruptions. Whole-rock major and trace element patterns imply a common magma generation process in a subduction setting for all four eruptions. Petrography and geochemical data suggest that whereas the zoned and unzoned ignimbrites share some similarities, the pre-eruptive evolution and storage conditions are specific to each eruption. Our results confirm that the thermal, chemical, and physical architecture of large magma reservoirs is complex, leading to the release of magmas with distinct properties in a short period. Such complex magmatic systems call for a revision of models regarding the triggering of large eruptions and a reassessment of the interpretation of geophysical signs of unrest in large, active volcanic systems.

P 2.8

Do U-Pb zircon dates from residual melts in mafic magmatic systems record protracted crystallization?

Joshua H.F.L. Davies [1], Nicolas D. Greber [1], Urs Schaltegger [1]

[1] *Department of Earth Sciences, University of Geneva, Rue des Maraîchers 13, 1205 Geneva (joshua.davies@unige.ch)*

Zircon is found rather commonly in mafic rocks from large igneous provinces (LIP) despite their high crystallization temperatures and low zirconium contents, which apparently contradicts zircon saturation conditions. However, zircon grains in these rocks occur as tiny crystals in pockets of highly evolved melt that crystallize at much lower temperatures than the bulk of the magma and that contains high concentrations of incompatible elements. Consequently, such zircon contains variable and high trace element concentrations. As a consequence, zircon U-Pb ages from mafic rocks are expected to record uniform ages at around the ± 0.02% uncertainty level (once the effects of Pb loss have been removed) and have been instrumental in determining precise and accurate ages for many of the Phanerozic large igneous provinces.

Here we report zircon U-Pb ages from 2 samples from the North Mountain basalt (Bay of Fundy, Canada), one of the earliest eruptions from the Central Atlantic magmatic province (CAMP) that range in age from ~204 Ma to ~201.5 Ma. This age range is significantly longer than what we would expect from typical LIP zircon. CL images of a large suite of these zircon crystals do not contain evidence for xenocrystic cores, also Hf isotope data do not suggest crustal contamination. Simple mass balance calculations suggest that only tiny xenocrystic cores of ~600 Ma (the age mode of zircon from the sediments through which the North Mountain basalt is emplaced) would be required to explain the oldest ages, although these have not been discovered in the CL imaging. Alternatively, the old ages could reflect early magmatic activity associated with the CAMP, which implies (i) that this presumably mafic early magmatism would have to produce zircon with low U, which is a characteristic of the >201.5 Ma grains, and (ii) that these grains would then have to survive transport in a zircon under-saturated mafic melt to the surface, which seems rather unlikely.

In any case, this study highlights the fact that zircon U-Pb data from LIP magmas can be as complicated to interpret as those from more felsic systems.

P 2.9
Water in orthopyroxene: orientation and thickness calibration using FTIR: from the lab to natural samples

Alexandra Demers-Roberge [1], Michael Jollands [1], Peter Tollan [1], Othmar Müntener [1]

[1](ISTE, Université de Lausanne, 1015, Lausanne)
[2](Institut für Geologie, Universität Bern, Baltzerstrasse 1, Bern)

Hydroxyl (colloquially referred to as water) located in crystalline defects of Nominally Anhydrous Minerals (NAMs) can represent a few to hundreds of parts per million (ppm) H_2O. This is enough to affect the phase equilibria and rheological properties of the mantle, and makes NAMs a significant contributor to the total mantle water budget. Fourier Transform Infrared Spectroscopy (FTIR) absorption peak locations in the OH stretching region are related to the local crystallographic environment of the OH chemical bonds in the mineral and can be used to calculate water content. Orthopyroxene, being the second most important phase of the upper mantle, has a greater water storage capacity compared to olivine, making it the dominant host of water in the upper mantle. However, even if many studies have quantified the water content in orthopyroxenes, the hydrogen incorporation and diffusion mechanisms are still not very well constrained. Orthopyroxene is an anisotropic, orthorhombic mineral with two perfect cleavages. In natural samples, the orientation of the crystals may be unknown and the thickness may slightly vary between crystals, which affects FTIR measurements, and thus, water concentration calculations and potentially hydrogen diffusion profiles. This study presents a way of minimizing these uncertainties on orthopyroxenes using calibration coefficients to correct for thickness and orientation using only the information measured by FTIR without any external measurements required.

This is done using the Si-O overtones, located between wavenumbers 1530 and 2250 cm-1 (figure 1). For the thickness correction, a series FTIR measurements were made on 12 orthopyroxene grains, where 30 to 50 microns were removed at each step. A linear regression (forced through the origin) was calculated for three distinct populations and shows that the thickness correction coefficient is orientation dependent (figure 1). Therefore, an orientation determination is calculated using the method of Asimow et al. (2006) adapted for orthopyroxene, allowing the dominant orientation to be determined, and its influence on the Si-O overtones and the water contents. The orientation correction is calculated using the polarization vector of the unoriented sample and by comparing it to the three main axis spectra (a, b and c). These corrections are applied on orthopyroxene from natural backarc-peridotite samples derived from several localities in Southern Patagonia.
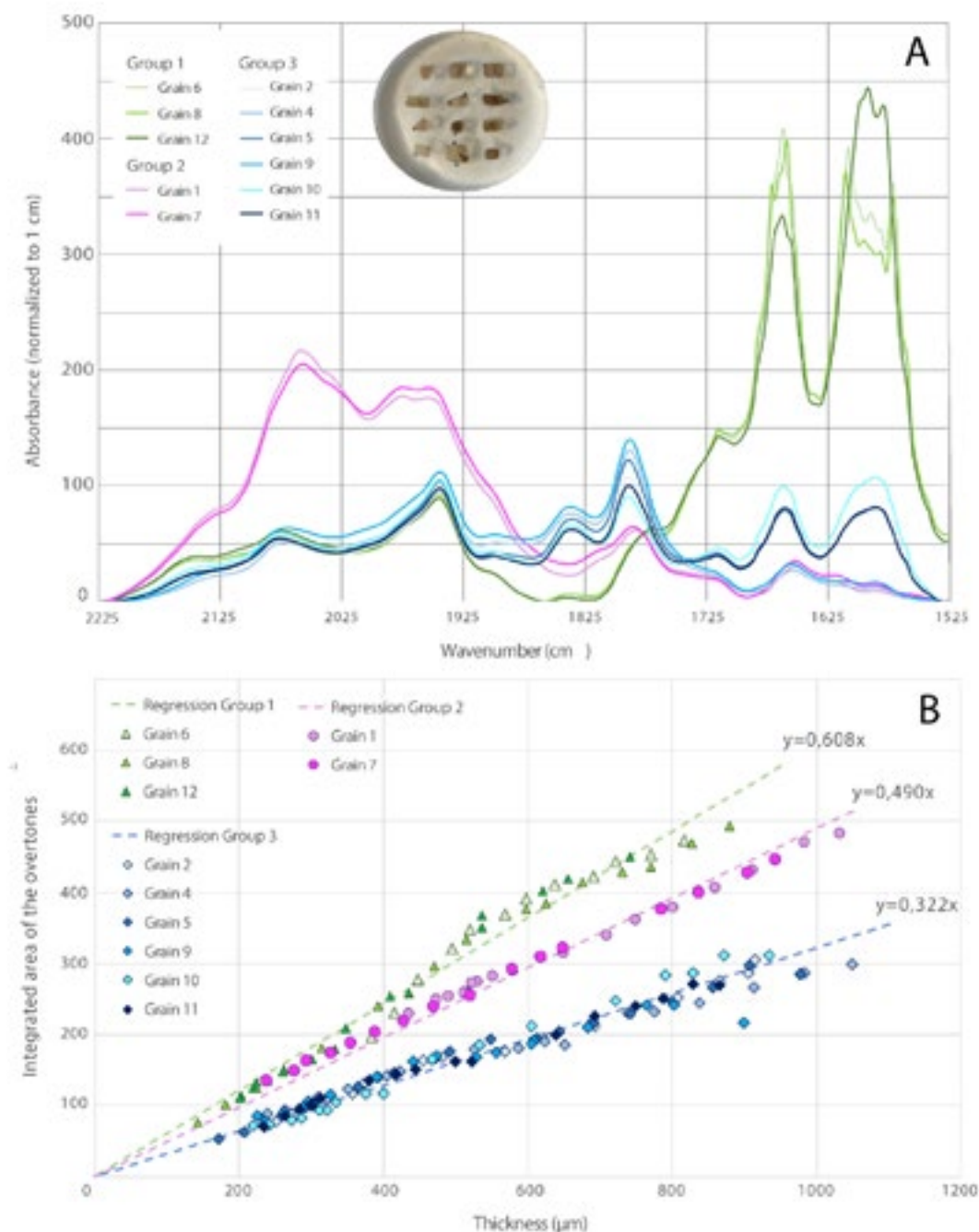
Figure 1 : A) Close-up of the Si-O overtones unpolarized FTIR measurements, showing 3 main groups with different orientations. B) The integrated area of the Si-O overtones plotted against different thicknesses show the 3 groups with the 3 different linea fitting equations, showing the orientation-dependance of the results.

REFERENCE

Asimow et al. (2006): Quantitative polarized infrared analysis of trace OH in populations of randomly oriented mineral grains, American Mineralogist 91, 2778-284.

P 2.10
Architecture of a distal skarn system: Calamita Fe-skarn deposit, Elba Island, Italy

Diego Domínguez-Carretero [1], Kalin Kouzmanov [1], Andrea Dini [2]

[1] Department of Earth Sciences, University of Geneva, Rue des Maraîchers 13, CH-1205, Genève
 (Diego.Dominguez@etu.unige.ch).
[2] Istituto di Geoscienze e Georisorse - CNR, Via Giuseppe Moruzzi 1, IT-56124, Pisa.

The Messinian Fe-ore deposits of the Elba Island (Italy) form a narrow N-S belt along the eastern coast of the Island and have been exploited since the 1st Millenium BC until the 1980's (Tanelli et al., 2001; Dünkel, 2002). Most of them are spatially and genetically associated with distal skarn bodies showing no direct relationship with causative intrusions.

The collapse of the Apenninic orogen, took place during the Oligocene-Miocene and generated the opening of the Tyrrhenian Basin (Keller & Pialli, 1990). As a consequence of the extension, felsic peraluminous magmas were emplaced at shallow crustal levels. This magmatism created the Tuscan Magmatic Province, which affected the central-west part of Italy, including the Elba Island as well (Dini et al., 2002). The granitoids on Elba are emplaced within previously metamorphosed lithologies, dominated by schists, gneisses and marbles. Skarn bodies hosting the Fe-ores on Elba are distal to the large granitic intrusions and the genetic connection with the intrusive magmatism is still debated.

The Calamita Fe-skarn is located in the southernmost part of the mineralized belt. The deposit displays a remarkable N-S zonation and consists of partially interconnected, multi-layered skarn bodies variably associated with magnetite-hematite ores, hosted by dominantly carbonate formations overlaying an extensional fault zone that separates them from the underlying micashishts of the Mt. Calamita Complex. The northern sector of the deposit consists of a garnet (andradite)-dominated skarn, with minor hedenbergite, ilvaite and sulphides (pyrite and chalcopyrite) to the west and a hedenbergite-ilvaite zone to the east. The two zones display a complex gradual contact most probably inheriting former lithological boundaries. The central sector of the deposit is dominated by a hedenbergite-ilvaite skarn, with minor lense-like bodies of garnet-hedenbergite skarn. The southern sector, close to the coast line, consists of a hedenbergite-ilvaite skarn only, with ilvaite being the major mineral in the southernmost outcrops. The lower contact of the skarn with the host Calamita micaschists is extensively epidotized and frequently displays pyrite disseminations and abundant tiny adularia-epidote-amphibole veins. Due to erosion, the host rocks at the upper contact of the deposit have never been observed.

The major skarn silicates at Calamita – hedenbergite, ilvaite and garnet – commonly form massive textuers (typical for the garnet zone), complex intergrowth (garnet-hedenbergite, hedenbergite-ilvaite) textures, indicative of co-precipitation, or banded strongly folded textures with prominent zonation (ex., hedenbergite-ilvaite), reflecting selective replacement along foliation planes of the marble precursor and/or cyclic changes of physical and chemical parameters of the skarn-forming fluids. Textural, AMS, mineral chemistry (major and trace elements) and fluid inclusion analyses of skarn silicates are in progress in order to study the skarn-forming processes at Calamita and eventually to establish geochemical and mineral vectors towards causative magmatic bodies.

REFERENCES

Dini, A., Innocenti, F., Rocchi, S., Tonarini, S. & Westerman, D.S. 2002: The magmatic evolution of the late Miocene laccolith-pluton-dyke granitic complex of Elba Island, Italy. Geological Magazine, 139, 257-279.

Dünkel, I. 2002: The genesis of east Elba iron ore deposits and their interralation with Messinian tectonics. PhD (Tübinger Geowissenschaftliche Arbeiten), 143.

Keller, J. & Pialli, G. 1990: Tectonics of the Island of Elba: A reappraisal. Bolletino della Società Geologica Italiana, 109, 413-425.

Tanelli, G., Benvenuti, M., Costagliola, P., Dini, A., Lattanzi, P., Maineri, C., Mascaro, I. & Ruggieri, G. 2001: The iron mineral deposits of Elba Island: State of the art. Ofioliti, 26 (2a), 239-248.

P 2.11

Tracing Sn and W pre-concentrations in the Limousin ophiolite and Variscan granites

Afifé El Korh [1], Marie-Christine Boiron [2], Michel Cathelineau [2], Etienne Deloule [3] & Béatrice Luais [3]

[1] Unit of Earth Sciences, Department of Geosciences, University of Fribourg, Chemin du Musée 6, CH-1700 Fribourg, Switzerland (afife.elkorh@unifr.ch)

[2] GeoRessources, Université de Lorraine, CNRS, UMR 7359, Boulevard des Aiguillettes, BP 70239, F-54506 Vandœuvre-lès-Nancy, France

[3] Centre de Recherches Pétrographiques et Géochimiques (CRPG), UMR 7358 CNRS-Université de Lorraine, 15 rue Notre Dame des Pauvres, BP 20, F-54501 Vandœuvre-lès-Nancy Cedex, France

The French Massif Central (FMC) is part of the West European Variscan belt, which was formed during the Devonian continent-continent collision between the Gondwana and Baltica, following the closure of oceanic domains opened during the Cambrian-Ordovician and collision of Gondwana-derived continental fragments (Eo-Variscan stage; Silurian-Devonian) (e.g. von Raumer et al., 2015). The FMC is composed of a series of nappes that were piled during the Meso-Variscan period (Devonian-Early Carboniferous; c. 350–360 Ma) (Ledru et al., 1994). The Neo-Variscan stage (Late Carboniferous-Early Permian) corresponds to extensive granitic magmatism and formation of major crustal-scale shear zones. The FMC hosts numerous Variscan ore deposits, some of them being known since the gallo-roman times (e.g. Au). In particular, the FMC contains economic to sub-economic deposits of W and Sn, which were formed during the late stage of uplift (320–290 Ma) (e.g. Marignac and Cuney, 1999; Alexandrov et al., 2000). Most of the W-Sn deposits are hosted by metasediments, while minor W-Sn deposits hosted by rare metal peraluminous granites (RMG) are found in the Northern Limousin (Marignac and Cuney 1999; Vallance et al., 2001). Mineralised structures in the Limousin are vein-hosted and arise from percolation of different hydrothermal fluids related to: 1) the delamination of the lower lithosphere during exhumation of the Variscan belt and, 2) granulite-facies metamorphism at the basis of the lower crust (Vallance et al., 2001; Harlaux et al., 2017). Frequently, metal associations are complex and reflect different source rocks: Au (As, Bi, Sb, Te) W-Sn (Nb, Ta, REE).

We have analysed compatible and incompatible metallic trace elements in the mineral assemblage of a series of rocks from the Limousin ophiolite (serpentinites, amphibolite facies metagabbros and basic dykes) and felsic magmatic series (granites as well as gneisses) (Vaulry W-Sn district; St Yrieix, Cheni and Lauriéras Au districts; St-Sylvestre and La Marche U districts). Determination of the trace element concentrations in non-mineralised rocks is expected to trace the source of Sn and W transported by fluids involved in the formation of Variscan ore deposits.

In the Limousin ophiolite, serpentinites and amphibolites have Sn concentration below the determination limit (<0.25 ppm) and low abundances of W (0.3–1.8 ppm), which differs from the high abundances measured for compatible transition metals (i.e. Sc, V, Cr, Co, Ni, Zn, Cu). In serpentinites, minerals (serpentine, olivine, amphibole, chlorite and spinel) generally display low contents of Sn and W (0.2–5.8 and 0.2–7.6 ppm, respectively). In amphibolites, amphibole has low Sn and W contents (Sn: 0.2–1.2 ppm; W: below detection limit), while higher concentrations are measured in accessory titanite (Sn: 4.7–5.6 ppm, W: 16–18 ppm). W and Sn concentrations are generally below detection limit (<1.2 ppm) in plagioclase. By contrast, high concentrations of Sn and W (0.51 and 14 ppm, respectively) are measured in an ultra high-pressure zoisite-eclogite (Berger et al., 2010) cropping out in contact with the ophiolite massifs. Main host minerals for Sn and W are zoisite (2.8–20 and 10–16 ppm), rutile (13–17 and 111–164 ppm), and retrograde amphibole (1.1–2.3 and 8.6–10 ppm), while garnet, omphacite and retrograde ilmenite have lower Sn and W abundances (Sn: <3.8 ppm, W: <17 ppm).

In granite and gneisses, the metallic trace elements are mainly hosted by biotite (bt) and muscovite (ms), which display significant Sn and W contents. Quartz and feldspars only show minor amounts of Sn (0.59–2.4 ppm), while W is below detection limit (<0.4 ppm). Variations in Sn and W in micas allow tracing the pre-mineralisation concentrations in the granitic massifs: there is a clear geographical correlation between the Sn and W composition of micas and the importance of the W–Sn ore deposits, arguing for a local source of pre-concentrations. Biotite and muscovite from the leucogranites hosting the Vaulry W–Sn ore deposit display the highest Sn and W concentrations (Sn: 200–610 ppm in bt, 196–425 ppm in ms; W: 8.7–77 ppm in bt, 128–193 ppm in ms). W and Sn abundances decrease in the leucogranites from La Marche and St-Sylvestre U districts, which host minor W–Sn deposits, while micas from orthogneiss and granites hosting Au deposits (St Yrieix, Cheni, Lauriéras) show the lowest Sn and W concentrations (Sn: 11–100 ppm in bt, 11–160 ppm in ms; W: 1.9–15 ppm in bt, 2.0–126 ppm in ms).

Our results argue for a local source of W and Sn pre-concentrations, in agreement with Vallance et al. (2001), who has considered the Blond granite as the main source for mineralisation in the Vaulry major W–Sn district. There is no evidence of Sn and W mobilisation from the surrounding rocks. Subsequent percolation of hot pseudo-metamorphic fluids is thought to have leached W and Sn from the granite, and triggered precipitation of W- and Sn-rich minerals (wolframite, scheelite,

cassiterite) in hydrothermal veins (Vallance et al., 2001). By analogy, the St Sylvestre and La Marche leucogranites may be the local source for the minor W–Sn deposits hosted in the two districts while specific element association may be derived locally from some basic lithologies.

REFERENCES

Alexandrov, P., Cheilletz, A., Deloule, E. & Cuney, M., 2000: Comptes Rendus de l'Académie des Sciences, Paris 330, 1-7.

Berger, J., Féménias, O., Ohnenstetter, D., Bruguier, O., Plissart, G., Mercier, J.-C.C. & Demaiffe, D., 2010: Lithos 118, 365-382.

Harlaux, M., Romer, R.L., Mercadier, J., Morlot, C., Marignac, C. & Cuney, M., 2018: Mineralogical Deposita 53, 21-51.

Ledru, P., Autran, A., Santallier, D., 1994: In: Keppie, J.D. (Ed), Pre-mesozoic geology in France and related areas. Springer-Verlag, Berlin Heidelberg, 276-288.

Marignac, C. & Cuney, M., 1999: Mineralium Deposita 34, 472–504.

Von Raumer, J., Stampfli, G.M., Arenas, R. & Martínez, S.S., 2015: International Journal of Earth Sciences 104, 1107-1121.

Vallance, J., Cathelineau, M., Marignac, C., Boiron, M.-C., Fourcade, S., Martineau, F. & Fabre, C., 2001: Tectonophysics 336, 43-61.

P 2.12

The Sakdrisi Au-Cu deposit, Bolnisi mining district, Georgia: providing a genetic model based on petrographic, geochemical, structural, and alteration studies.

Titouan Golay [1], Robert Moritz [1], Nino Popkhadze [2], Malkhaz Natsvlishvili [3]

[1] Department of Earth Sciences, University of Geneva, Rue des Maraîchers 13, CH-1205 Geneva, Switzerland
[2] Ivane Javakhishvili Tbilisi State University, 1 Chavchavdze Avenue, 0179 Tbilisi, Georgia
[3] Rich Metals Group, 1 M. Aleksidze str., 0160 Tbilisi, Georgia

The Late Cretaceous Sakdrisi epithermal Au(-Cu) deposit is located in southern Georgia, 50 km southwest from the capital Tbilisi, in the Bolnisi mining district. The area is located at the transition between the Eastern Pontides to the West and the Lesser Caucasus to the East, both resulting from the convergence of the African-Arabian plates and the European margin, during the N-NE verging subduction and closure of the northern branch of the Neotethys. The mineralization is hosted by a Late Cretaceous bimodal sequence of volcanic and volcano-sedimentary rocks. The deposit is poorly constrained, and the aim of this work is to perform a comprehensive geological, petrographic, alteration and geochemical study to provide a new genetic model. Our preliminary working model is presented in Figure 1.

Sakdrisi consists of a 2-km long cluster of five mineralized centers aligned along a NE-oriented fault zone. The western part of the fault is covered by a barren ignimbrite, crosscut by andesitic and basaltic dikes, while the eastern side mainly consists of andesitic to dacitic volcanic rocks and tuff. Two distinct types of ore are currently exploited in this mine: 1) auriferous quartz-barite and quartz-chalcedony veins surrounded by illite-siderite alteration haloes, in the brecciated silicified and oxidized volcaniclastic rocks of Sakdrisi's lithocap; and 2) a more reduced zone hosting a stockwork of subvertical chalcopyrite-rich quartz-amethyst and quartz-carbonate veins. The latter most certainly represents the deeper parts of the system, and is directly overlain by the lithocap, which has undergone supergene enrichment, suggested by the occurrence of minerals like chalcocite. At the bottom of open pit V (May 2018), gold grade is estimated @1ppm, at a cutoff grade of 0.2 ppm. At the Sakdrisi open pit IV, the grade is 1.6 ppm. Copper is a by-product, and the average grades are 0.12 wt.% at Sakdrisi IV and 0.5 wt.% at Sakdrisi V.

The mineralized host rocks of open pit IV have been overthrusted by a barren ignimbrite, preserving the ore from erosion. A set of NW oriented secondary faults could explain why a supergene enrichment zone was preserved in open pit V, but was eroded in the remaining uplifted blocks. Silification of the host rocks was reported down to a depth of 100-150m below the surface, while epidote and sericite have been described down to 200m below surface in previous studies. Argillic (illite-montmorillonite) and carbonate (ankerite) alterations are very common.

Transmitted and reflected light petrographic studies, together with Raman, XRD and XRF analyses will be performed, in order to define the chronology of mineralizing events and related hydrothermal alteration. U-Pb dating on dike-like structures crosscutting the ore bodies will allow us to constrain the timing of mineralization, as well as ^{40}Ar/^{39}Ar dating on adularia, if present. Spatial (vertical) and temporal physico-chemical evolution of the mineralizing fluids (T°, composition) will be constrained by fluid inclusion petrography and microthermometry analyses on idiomorphic quartz crystals collected at different levels of the open pits. The origin of these fluids will be investigated by stable isotope geochemistry on micas and clay minerals (δ^{18}O, δD) and on sulfides and sulfates, including barite (δ^{34}S). The dataset will be combined with ore grade distribution provided by the mine staff in order to propose a synthetic genetic and exploration model for Sakdrisi.

Possible sequence of geological events at Sakdrisi during Late Cretaceous

Lithocap with gold
in shallow part

Deep silica-hematite bodies ?

Supergene alteration and surface alteration ?
Brecciation and silification of lithocap?

Supergene alteration and enrichment ?

Brecciation and silification ?

Supergene alteration and enrichment ?

Brecciation and silification ?

Quartz-chalcopyrite-sphalerite veins +– Au?

Extension

Erosion, destruction of lithocap?

NS to NW-SE-oriented thrusting

Thrust fault

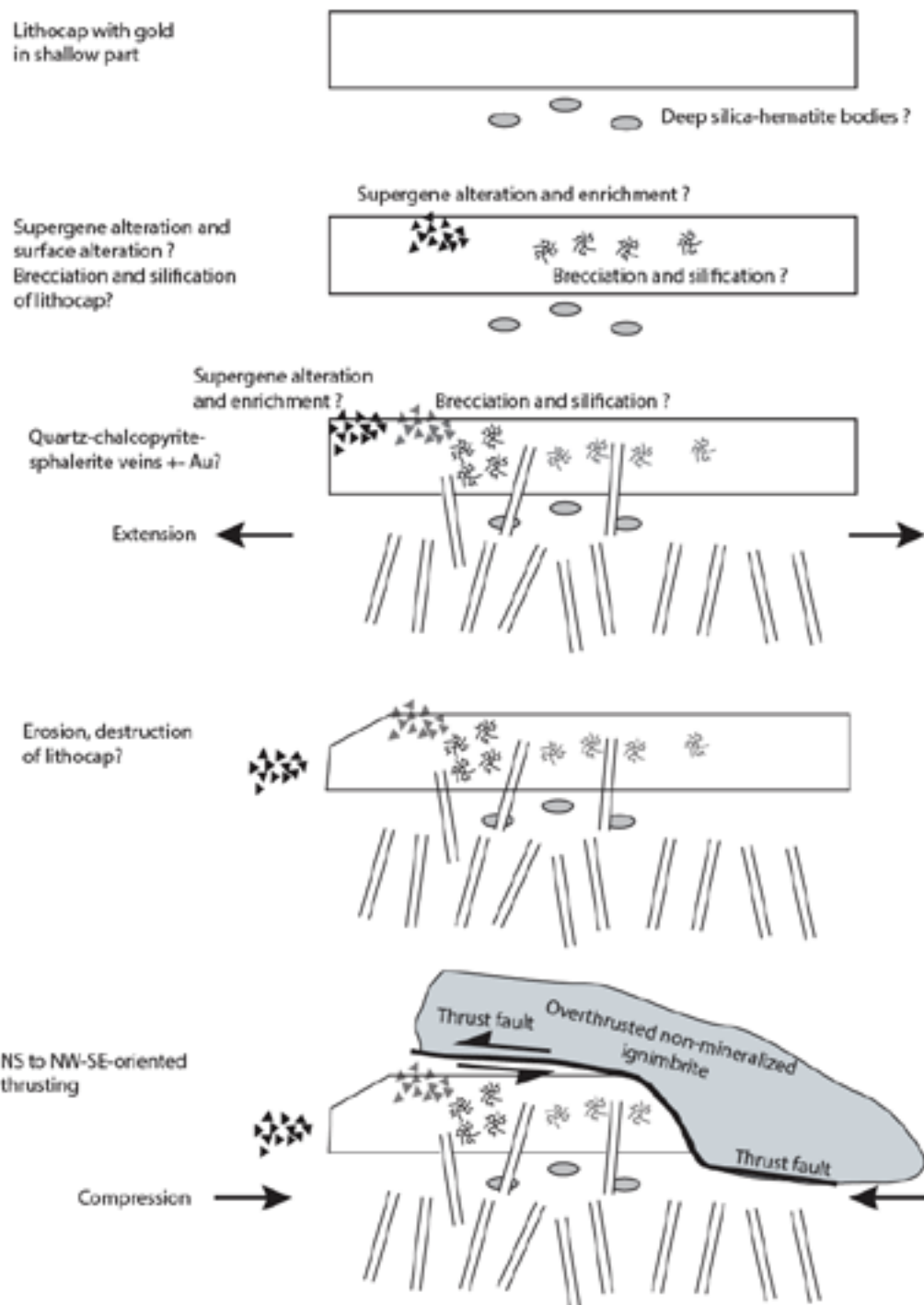Overthrusted non-mineralized ignimbrite

Thrust fault

Compression

Figure 1 – Preliminary genetic model for the Sakdrisi epithermal deposit with a sequence of events from oldest at the top to youngest at the bottom.
¨

P 2.13

Temporal and geochemical characterization of the Tejsar magmatic complex, northern Armenia, Lesser Caucasus

Marion Grosjean [1], Robert Moritz [1], Hervé Rezeau [1,°], Rafael Melkonyan [2], Samvel Hovakimyan [1,2] & Alexey Ulianov [3]

[1] *Department of Earth Sciences, University of Geneva, Switzerland*
[2] *Institute of Geological Sciences, National Academy of Sciences, Yerevan, Armenia*
[3] *Institute of Earth Sciences, University of Lausanne, Lausanne, Switzerland*
[°] *Present address: Department of Earth, Atmospheric, and Planetary Sciences, MIT, Cambridge, USA*

The Tejsar magmatic complex is located in the Lesser Caucasus and belong to the northern part of the South Armenian block along the Amasia-Sevan-Akera suture zone. It consists of a wide range of Cenozoic magmatic rocks emplaced during the convergence of the Arabian plate toward the Eurasian margin, as the result of the Neotethys ocean closure. Dextral strike-slip tectonics along the South Armenian Block result from the oblique plate convergence, which in turn controlled both the magma ascent in the upper crust and the emplacement of associated ore deposits (Hovakimyan et al., in review). The geologic evolution of the Lesser Caucasus remains unclear, therefore constraining the petrography, geochemistry and geochronology of the Tejsar complex will provide new insights in the understanding of the regional geodynamic evolution. The study area includes a large set of magmatic rocks varying from mafic intrusions and lavas to more differentiated rocks (e.g.nepheline syenite). Although the different magmatic rocks have a distinct mineralogy and geochemistry, their ages and isotopic compositions broadly overlap. Zircons crystallized in various intrusions display LA-ICP-MS U-Pb ages ranging from ca.43.2 to ca.38.8 Ma, together with median initial εHf values ranging from +9.1 to +10.0. The latter indicates a dominant mantle-derived origin for these magmas. Complementary radiogenic isotope whole rock data will provide more details about the magmatic source of all these magmatic rocks. Such multi-disciplinary approach aims at understanding the genetic link between the different magmatic pulses of various composition. The question remains whether this geological setting results from various magmatic source processes, crustal differentiation processes or a combination of both?

From an ore deposit point of view, magmatic rocks of the Tejsar area host a low-sulfidation epithermal Au deposit dated at ca. 41.5 Ma. The presence of the deposit highlights the existence of a hydrothermal system at Tejsar, which is also evidenced by different features affecting the nepheline syenite. However, the temporal relationship between the magmatism and the hydrothermal event remains unconstrained and therefore the genetic link is unclear. In addition, a younger magmatic pulse, dated at 28.4 Ma by zircon U-Pb, is also recognized in the area and characterized by a high-K calc-alkaline adakitic-like composition. The granite intrusion is crosscut by quartz veins hosting molybenite mineralization. Despite a 10 m.y.-long gap in the magmatic history, this younger intrusion is also characterized by a mantle-derived origin with a median εHf of +9.4.

Further south in the South Armenian Block, the Amulsar, Bargushat and Meghri-Ordubad regions are three other study areas hosting Cenozoic mantle-derived magmatism associated with epithermal Au and porphyry Cu-Mo deposits (Moritz et al. 2016; Rezeau et al., 2016). All together, combined with our recent results on the Tejsar magmatic complex will certainly provide new insights into the understanding of the regional geodynamic evolution of the Lesser Caucasus and associated petrological processes leading to fertile magmatism. Moreover, the Tejsar area is located at the transition between the Turkish Eastern Pontides and the Lesser Caucasus, and therefore it represents a key location to understand the broad regional geodynamic context shaping the central part of the Tethyan orogenic and metallogenic belt.
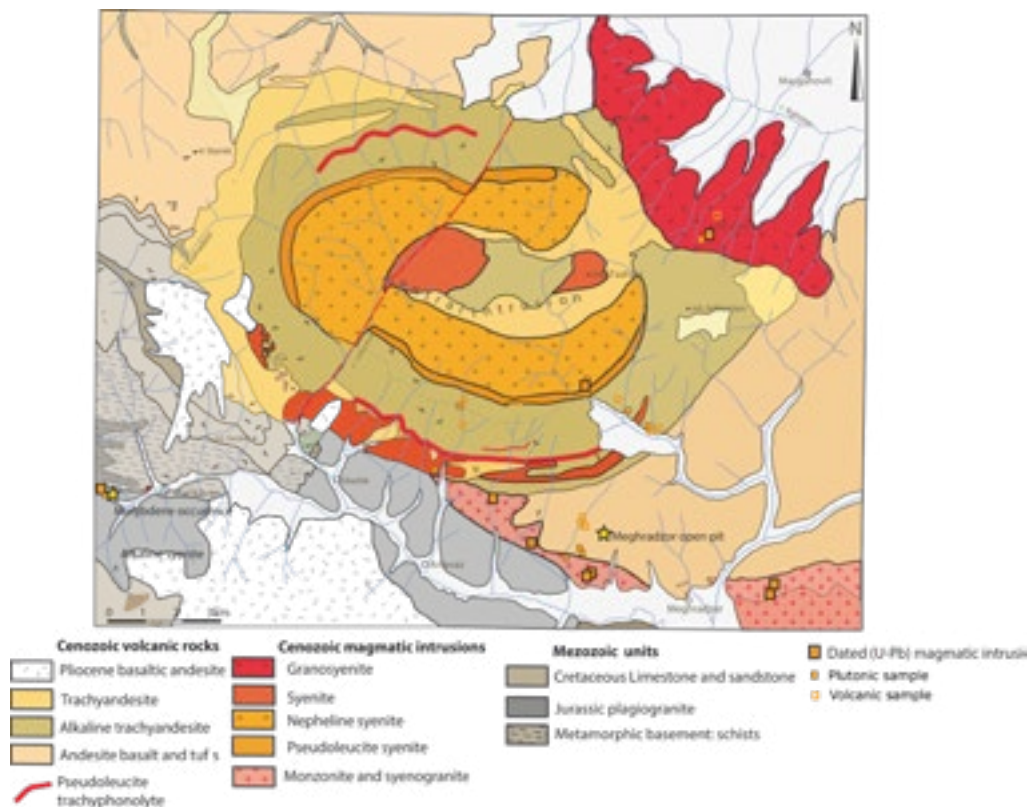
Figure 1. Geological map of the Tejsar magmatic complex located on the northern part of the South Armenian Block (SAB). The SAB is the southern structural unit of the Lesser Caucasus. Maps modified after Bagdasaryan et al., 1969 and Moritz et al.,2016.

REFERENCES

Bagdasaryan, G.P., Ghukasian, R.K., Karamyan, K.A., 1969. Absolute dating of Armenian ore formations. International Geology Review 11, 1166–1172.

Hovakimyan, S., Moritz, R., Tayan, R., Melkonyan, R., Harutyunyan, M., in review. Cenozoic strike-slip tectonics and structural controls of porphyry Cu-Mo and epithermal deposits during geodynamic evolution of the southernmost Lesser Caucasus, Tethyan metallogenic belt. Econ. Geol.

Moritz, R., Melkonyan, R., Selby, D., Popkhadze, N., Gugushvili, V., Tayan, R., Ramazanov, V., 2016b. Metallogeny of the Lesser Caucasus: From Arc Construction to Postcollision Evolution. Soc. Econ. Geol. Special Publication 19, 157–192.

Rezeau, H., Moritz, R., Wotzlaw, J.-F., Tayan, R., Melkonyan, R., Ulianov, A., Selby, D., d'Abzac, F.-X., Stern, R.A., 2016. Temporal and genetic link between incremental pluton assembly and pulsed porphyry Cu-Mo formation in accretionary orogens. Geology 44, 627-630.

P 2.14

Pyroxene geochemical evolution in a distal Pb-Zn skarn body, Madan, Bulgaria

Aaron Hantsche [1], Kalin Kouzmanov [1], Rossitsa Vassileva [2]

[1] Department of Earth and Enviromental Sciences, University of Geneva, Rue des Maraîchers 13, CH-1205 Geneva (arron.hantsche@unge.ch)
[2] Bulgarian Academy of Sciences, Acad. G. Bonchev St. 24, 1113 Sofia, Bulgaria

The metalogeny of the Madan ore field has been associated with the onset of early Oligocene extension-related magmatism in the Central Rhodopes of southern Bulgaria (Marchev et al., 2005). Pb-Zn distal skarn deposits were formed between 29.95-31.22 Ma (Kaiser-Rohrmeier et al., 2013, Hantsche et al., 2017], but little is known about the chemical evolution of the skarn system.

The prograde mineral assemblage in these skarns is dominated by Mn-rich pyroxene, which form spheroidal aggregates, replacing carbonate lenses within the metamorphic basement rocks. At the Petrovitsa deposit near Madan, the relationship between a skarn body and a mineralized vein has been characterized to study the geochemical evolution of a distal skarn system. Sections of preserved prograde skarn were sampled for petrography, bulk rock chemical analysis, and pyroxene geochemistry to better understand chemical evolution that occurs during formation of distal skarn systems.

Concentric growth bands in the pyroxene aggregates are observed at the hand sample and microscopic scale, and occur as variations in grain size and chemistry. Geochemical data from Electron Probe Micro Analysis (EPMA) and X-Ray Fluoresence (XRF) are presented to show variations in major element silicate geochemistry both at the thin-section and outcrop scale away from the vein. Pyroxene compositons, measured by EPMA, indicate hedenbergite [$CaFeSi_2O_6$]-johansennite [$CaMnSi_2O_6$] solid solution. Preliminary results show that alternating chemical compositions cycle between Fe-rich pyroxenes, which are typically fine grained (~1mm), and coarser, Mn-rich pyroxenes (~0.5 to 5 cm) (Figure 1).

Calcium data from the EPMA has been used as an internal standard for LA-ICP-MS trace element analysis. At the coutcrop scale, whole rock geochemistry shows general decrease in Fe, Mg, Sr concentration away from the vein, with increase in Mn, Al, and Na compositions. Ongoing trace elemental analyses of pyroxene will be presented here for the first time.
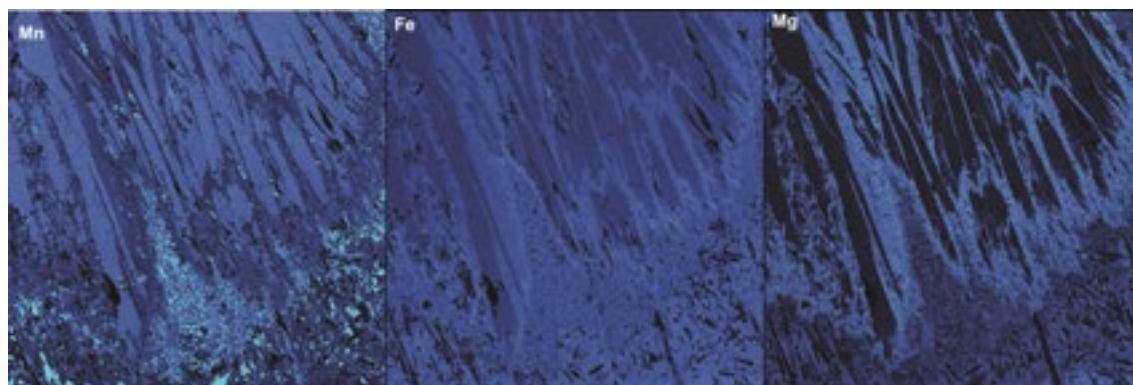

Figure 1. Mn – Fe- Mg Elemental map from JEOL 8200 Superprobe at the University of Geneva.

REFERENCES

Hantsche A.L., Kouzmanov K., Dini A., Vassileva R., Guillong M., von Quadt A. 2017: New U-Pb Age Constraints on Tertiary Magmatism and Pb-Zn Skarn Formation in the Madan District, Central Rhodopes, Bulgaria: Goldschmidt Abstracts, 1533.

Kaiser-Rohrmeier,von Quadt, A., Driesner, T., Heinrich, C., Handler, R., Ovtcharova, M., Ivanov, Z., Petrov, P., Sarov, S., Peytcheva, I., 2013: Post-Orogenic Extension and Hydrothermal Ore Formation: High-Precision Geochronology of the Central Rhodopian Metamorphic Core Complex (Bulgaria-Greece), Economic Geology, 108, 691-718.

Marchev, P., Kaiser-Rohrmeier, M., Heinrich, C., Ovtcharova, M., von Quadt, A., Raicheva, R., 2005: 2: Hydrothermal ore deposits related to post-orogenic extensional magmatism and core complex formation: The Rhodope Massif of Bulgaria and Greece. Ore Geology Reviews, 27, 53-89.

P 2.15

A geochemical and petrological study to constrain the magmatic history of St Kitts and Nevis (Lesser Antilles)

Oliver Higgins [1], Luca Caricchi [1], Jon Blundy [2], Lena Melekhova [2]

[1] Départment de Minéralogie, University of Geneva, Rue de Maraîchaire 13, CH-1205 Genève (Oliver.Higgins@unige.ch)
[2] Department of Earth Sciences, University of Bristol, Wills Memorial Building, Queens Road, Bristol BS8 1RL, UK

Volcanic activity of St Kitts (Nothern Lesser Antilles Volcanic Arc) is represented by a sequence of small volume volcanic domes and lava flows erupted over a timescale of 2 million years. The acitvity of the island is closed by explosive activity (1.8 kA; Harkness et al., 1994). St Kitts is a case study of a system that is active over a long period of of time whilst erupting relatively limited amounts of magma. We intend to analyse samples spanning the entire eruptive history of the island to constrain the temporal evolution of magma geochemistry and the rate of magma supply in the plumbing system. These data will allow us to estimate extrusive intrusive ratios and characterise the processes responsible for the transition from mainly effusive to explosive activity.

We will present preliminary petrographic analysis of the rocks of St Kitts island as well as whole rock geochemical and trace element data. Preliminary zircon trace element data and U/Th model ages may be available, with the aim of using the statistical analysis of zircon age populations to constrain the magma flux (Caricchi et al., 2014). Cluster analysis of chemical zoning in minerals will be applied to obtain constraints on the chemical and physical architecture of the magmatic system over time. The same approach will also be applied to samples of St Martin and Nevis islands (Lesser Antilles).

This project is part of a wider study focusing on our understanding of the physical processes controlling the distribution of frequency and magnitude of volcanic eruptions we observe at a regional and global scale.

REFERENCES

Caricchi, L., Simpson, G., & Schaltegger, U. (2014). Zircons reveal magma fluxes in the Earth's crust. Nature, 511(7510), 24.

Harkness, D. D., Roobol, M. J., Smith, A. L., Stipp, J. J., & Baker, P. E. (1994). Radiocarbon redating of contaminated samples from a tropical volcano: the Mansion 'Series' of St Kitts, West Indies. Bulletin of volcanology, 56(5), 326-334.

Melekhova, E., Blundy, J., Martin, R., Arculus, R., & Pichavant, M. (2017). Petrological and experimental evidence for differentiation of water-rich magmas beneath St. Kitts, Lesser Antilles. Contributions to Mineralogy and Petrology, 172(11-12), 98.

P 2.16
Tectonic setting of the Cenozoic Kadjaran porphyry Cu-Mo – epithermal system, Armenia, Lesser Caucasus

Samvel Hovakimyan [1,2], Robert Moritz [1], Rodrik Tayan [2], Marianna Harutunyan [2], Hervé Rezeau [1,°], Rafael Melkonyan [2] & Arshavir Hovhannisyan [2]

[1] Department of Earth Sciences, University of Geneva, rue des Maraîchers 13, CH-1205 Genève, Switzerland
  (samvel.hovakimyan@unige.ch)
[2] Institute of Geological Sciences of the Armenian National Academy of Sciences, 0019 Yerevan, Republic of Armenia
° Present address: Department of Earth, Atmospheric, and Planetary Sciences, MIT, Cambridge, USA

Recent structural investigations of the major porphyry Cu-Mo and epithermal systems of the southernmost Lesser Caucasus emphasize the fundamental role of regional strike-slip tectonics controlling these deposits and the associated magmatism during the Cenozoic geodynamic evolution of the Central Tethyan belt (Hovakimyan et al., submitted). In this study, we develop a tectonic model for the Oligo- Miocene evolution of the giant Kadjaran porphyry Cu-Mo system in southern Armenia. It is based on detailed district and deposit-scale structural mapping of the orientation and crosscutting relationships of dikes and mineralized veins, including kinematics along the major structures.

Paleostress reconstructions indicate three main tectonic events in the Kadjaran mining district (Fig.1). They are consistent with progressive anticlockwise rotation of paleostress orientations from the middle - late Oligocene to early Miocene, which was linked to the re-organization of the tectonic plates during Arabia-Eurasia collision. NNE-oriented compression and WNW-oriented extension during the middle to late Oligocene resulted in the activation of NS- and NE-oriented structures under dextral strike-slip tectonics. This regime is compatible with the emplacement of N- to NE-oriented early dikes reported by Tayan et al. (2002). The geometry and dominant NE- and NS-orientation of porphyry veinlets and veins dated from 27.3 to 26.4 Ma (Moritz et al., 2016; Rezeau et al., 2016) indicate that porphyry ore formation at Kadjaran occurred under a dextral strike-slip tectonic regime along NS- and NE-oriented structures. It is consistent with paleostress orientations reconstructed for the late Oligocene. During the late Oligocene, principal stress axes record a NS-oriented compression and EW-oriented extension, which reactivated ~NS-oriented structures and controlled the emplacement of fine-grained porphyritic granodioritic and lamprophyre dikes dated between 26.6 and 24.5 Ma (Rezeau et al. 2016), and crosscutting early NE-oriented dikes. During the early Miocene event, WNW-oriented compression and NNE-oriented extension resulted in reactivation of pre-existing structures in a sinistral strike-slip tectonic regime. This setting controlled the emplacement of ~EW-oriented coarse-grained porphyritic granogioritic dikes ranging from 22.2 to 21.2 Ma (Rezeau et al., 2016), which crosscut older dike generations and represent the youngest dike generation in the district (Tayan et al., 2002). An epithermal overprint affected the ore deposit during this event between 20.5 Ma and <22.2 Ma (Molybdenite Re-Os dating; Rezeau et al., 2016). Epithermal veins were mainly emplaced along ~EW-oriented fractures zones, but also along reactivated NS-oriented structures.
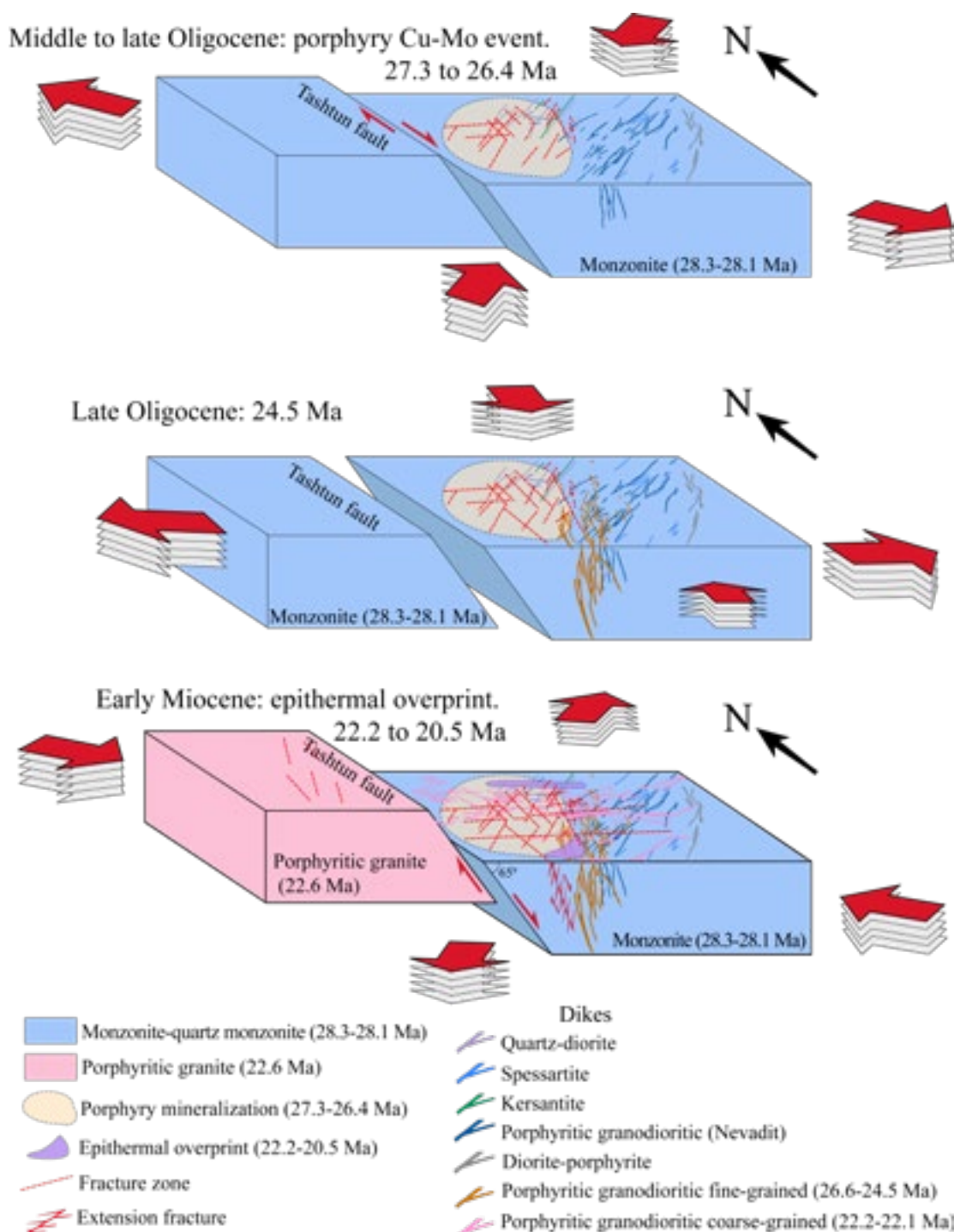
Figure 1. Tectonic evolution of the Kadjaran mining district and formation of the giant porphyry-epithermal system. Ages for magmatism and mineralization are from Moritz et al. (2016) and Rezeau et al. (2016). Dikes are based on a map by Tayan et al. (2002).

REFERENCES

Hovakimyan, S. et al., submitted:. Econ. Geol.
Moritz, R. et al. 2016: Gondwana Research, 37, 465-503.
Rezeau, H. et al. 2016: Geology, 44, 627-630.
Tayan, R. et al. 2002: Proceedings of the Scientific Session of the 90th anniversary Movsesyan S.A., Yerevan, p. 32-44.

P 2.17

Prograde metamorphism in the Bergell contact Aureole: A field and experimental study

Elias Kempf [1], Jörg Hermann [1]

[1] Institut für Geologie, University of Bern, Baltzerstrasse 3, CH-3012 Bern
(elias.kempf@geo.unibe.ch, joerg.hermann@geo.unibe.ch)

The Bergell intrusion, located between Switzerland and Italy, consists of a tonalite and a granodiorite body, which intruded at 32 Ma and 30 Ma respectively. In the upper Val Sissone, a several 100 m thick hornblende-gabbro has been newly found. The intrusion produced a well known contact aureole best studied in the eastern part of the intrusion, in the previously regionally metamorphosed serpentinites that underwent greenschist facies metamorphism (Trommsdorff and Connolly, 1996). With increasing metamorphic conditions, a sequence of reactions can be observed in Val Sissone that can be modelled in the CaO-MgO-Al_2O_3-SiO_2-H_2O (CMASH) system, representing lherzolitic protoliths (Stucki and Trommsdorff, 2001). At 400°C, 3 kbar reaction (**1**) antigorite + brucite = olivine + chlorite + water and the stable assemblage antigorite + olivine + chlorite + water + diopside is expected between 400 - 480 °C, representing regional greenschist facies conditions. Roughly 1.5 km from the contact reaction (**2**) antigorite + diopside = tremolite + chlorite + olivine + water produces the assemblage antigorite + olivine + chlorite + tremolite + water, stable between 480 - 520 °C. 750 m from the contact reaction (**3**) antigorite = olivine + talc + chlorite + water leads to the assemblage olivine + talc + chlorite + tremolite + water that is stable between 520 - 600 °C. 300 m from the contact Reaction (**4**) olivine + talc = anthophyllite + water forms the assemblage olivine + anthophyllite + chlorite + tremolite + water for an expected temperature range of 600 - 700 °C. This assemblage was previously identified to represent peak metamorphic conditions. However, at 100 m from the contact the reaction (**5**) olivine + anthophyllite = enstatite + water, with the assemblage olivine + enstatite + chlorite + tremolite/ hornblende + water is stable corresponding to temperatures of 700 - 730 °C. Moreover, in the first 40 m from the contact reaction (**6**) chlorite = olivine + spinel + enstatite + water and the assemblage olivine + spinel + enstatite + tremolite/ hornblende + water is stable, with a stability field extending between 730 - 820 °C. Reaction (**7**) olivine + tremolite = enstatite + diopside is not observed in the contact aureole. Furthermore, assemblage **5** shows inclusions of anthophyllite, olivine, chlorite and spinel in newly formed enstatite implying the coincidence of the two univariant curves anthophyllite-out and chlorite-out. Our study shows that in Val Sissone the contact metamorphic temperatures were underestimated by 150 - 200 °C at the contact of the intrusion to the serpentinite. While the general sequence of reactions can be well modelled in the simple system, many field observations such as the occurrence of hornblende, the transition from Cr- to Al-spinel and the width of the antophyllite field are inconsistent with existing experiments in simple systems that do not contain Fe, Cr, and Na.

To fill this gap we also performed new experiments using natural serpentinite powders that constitute the system FMCrASH (harzburgite) and NCFMCrASH (lherzolites) in cold seal experiments at 2 kbar from 625 to 725°C. From 625 - 675 °C, olivine, talc, chlorite, magnetite is the stable assemblage in the FMCrASH and additionally tremolite in the NCFMCrASH. At 700 °C olivine, talc, chlorite, Al-spinel and enstatite are stable in the FMCrASH as well as tremolite in the NCFMCrASH. Furthermore, at 725 °C olivine, enstatite, cordierite and Al-spinel occur in the FMCrASH and additionally hornblende in the NCFMCrASH. The hornblende-in reaction is observed at the chlorite-out reaction **5** indicating a continuous reaction between chlorite and tremolite increasing the tschermak and edenite component in the amphibole with temperature. Hence a new stability field consisting of olivine, enstatite, spinel and hornblende is proposed.

REFERENCES

Trommsdorff, V., and Connolly, J. A., 1996, The ultramafic contact aureole about the Bregaglia (Bergell) tonalite: isograds and a thermal model: Schweizerische mineralogische und petrographische Mitteilungen, v. 76, p. 537-547.

Stucki, Andreas, & Supervisor: Trommsdorff, Volkmar. (2001). High Grade Mesozoic Ophiolites of the Southern Steep Belt, Central Alps.

P 2.18
High temperature crystal-melt reactions in mafic igneous complexes

Julien Leuthold [1]

[1] Institute of Geochemistry and Petrology, ETH Zürich, Clausiusstrasse 25, 8092 Zürich (julien.leuthold@erdw.ethz.ch)

Magma chambers are built up incrementally, by repeated injections of hot melt, intruding as sills and dykes into pre-existing crystal mush and cumulate. Magma intrusion is not instantaneous but is a continuous flux over weeks, months or more. The total volume of intruded magma is difficult to estimate, as intrusive contacts are blurred by local reequilibration and segregation of interstitial melt and magma is drained back into the source after emplacement. In consequence, important heat input is neglected in our present perception of magma chamber dynamic. At high recharge rate or long-term magma flux (e.g. fast-spreading ridges, LIPs, arcs), high temperature crystals react with compositionally and thermally distinct intrusive melts (e.g. Leuthold et al., 2014, 2018). Here, I quantify the effect of gabbro cumulate melting and assimilation using 1-atm gas-mixing experimental petrology and compare with natural observations of 'dry' oceanic gabbro.

In gabbro protolith melting experiments ($T_{solidus}$ = 1140°C), hydrated cracked olivine and interstitial pigeonite melt to a dacitic liquid (F<0.01; 1150-1165°C) (Figure 1). The liquid changes to andesitic (F<0.02; 1180°C) and basaltic (F = 0.2; 1200°C) composition with increasing melt fraction and dissolution of clinopyroxene and plagioclase.

In hybrid picrite-gabbro equilibrium experiments, the clinopyroxene and plagioclase stability and the crystallization rate are increased (Leuthold et al., 2015). Cr-spinel abundance in picrite, gabbro and hybrid experiments is <0.5 vol%, unless under oxidizing conditions (≥NNO). The glass SiO_2 and Mg# are increased, the olivine Mg# is increased and the clinopyroxene Mg# is increased and Al-content is decreased. The clinopyroxene REE concentration is decreased, despite a lower D_{REE}.

In picrite-gabbro kinetic experiments reacted for 60 min at conditions where olivine, plagioclase and clinopyroxene are stable in gabbro but only olivine is stable in high-MgO basalt melt (1210°C, NNO-2), gabbro olivine and clinopyroxene are anhedral and plagioclase is euhedral. In the reaction rim, clinopyroxene is absent, olivine anhedral grains are small and Cr-spinel abundance strongly increased (to 1.8 vol%). With extended reaction duration, the reaction rim thickness is increased. Gabbro clinopyroxene grains are overgrown by high Mg# and Cr-rich rim, except in the direct proximity of spinel-rich layer.

As consequences:
1) High Mg# clinopyroxene in spreading ridges are frequently interpreted as crystals crystallized at high pressure or from primitive melt, but may alternatively result from mafic rock assimilation. Rocks microtextural and geochemical observations help to discriminate between processes.
2) Plagioclase reaction is frequently incomplete during partial melting, preventing achievement of global equilibrium, as previously demonstrated by Wolff et al. (2013) in hydrous oceanic gabbro experiments. I thus question whether troctolite cumulate and anorthosite result from gabbro partial melting.
3) Ore-bearing chromitite may crystallize from a hybrid melt, produced by gabbro assimilation by hot high-MgO basalt.
4) The partial melt and hybrid melt chemistry is distinct from the one produced by simple crystallization along the liquid line of descent of a mantle-derived melt. Reaction products are distinct from 'defractionation' process.
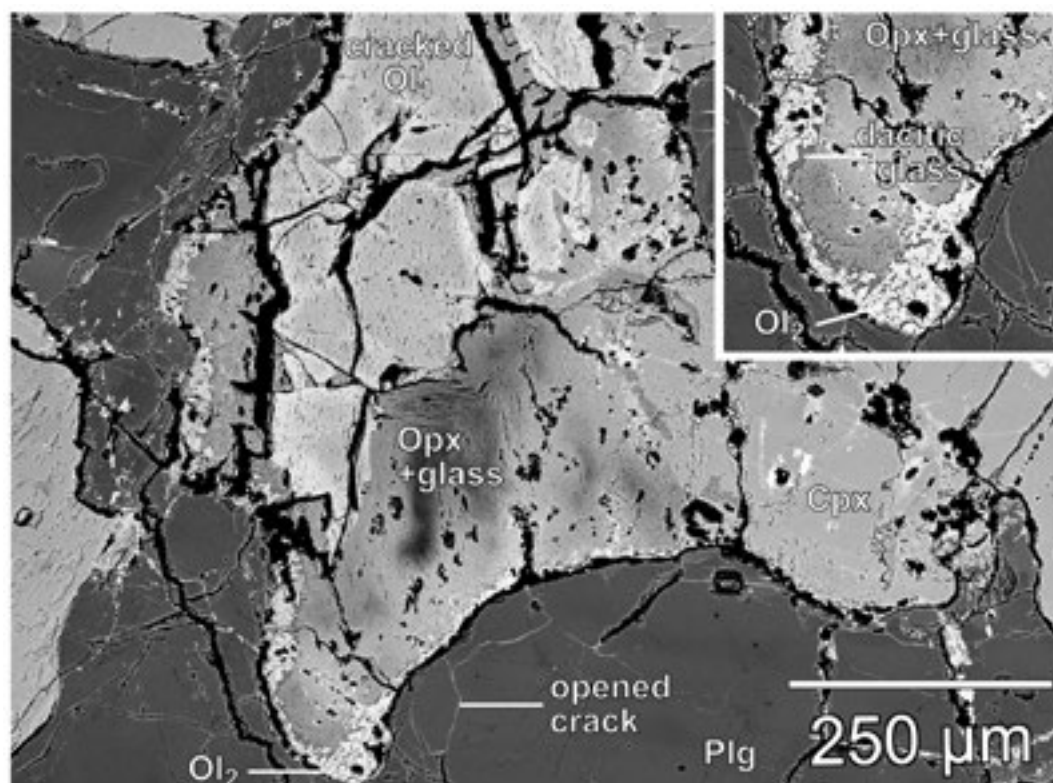
Figure 1. Gabbro partial melting (1-atm, NNO-2, 1165°C, 5h). Destabilization of interstitial Opx along grain boundaries and of hydrated cracked Ol. Generation of a dacitic melt (<1vol%). Eutectic Cpx and Plg are stable.

REFERENCES

Leuthold J., Blundy J.D., Brooker R. 2015: Experimental petrology constraints on the recycling of mafic cumulates: A focus on Cr-spinel from the Rum Layered Intrusion, Scotland, Contributions to Mineralogy and Petrology 170: 12.

Leuthold J., Blundy J.D., Holness M.B., Sides R. 2014: Quantification of successive reactive melt flow episodes in a layered intrusion (Unit 9, Rum Eastern Series, Scotland), Contributions to Mineralogy and Petrology, 167: 1021.

Leuthold J., Lissenberg J. C., O'Driscoll B., Karakas O., Falloon T., Klimentyeva D.N., Ulmer P. 2018. Partial melting of the lower oceanic crust at spreading ridges. Frontiers in Earth Sciences: Petrology: 6(15): 20p.

Wolff P.E., Koepke, J., Feig, S.T. 2013: The reaction mechanism of fluid-induced partial melting of gabbro in the oceanic crust, European Journal of Mineralogy 25: 279-298.

P 2.19
Sodic amphibole and sodic clinopyroxene in the Dent Blanche (Western Alps): new constraints for an old question

Paola Manzotti [1], Michel Ballèvre [2], Lukas Baumgartner [1], Othmar Müntener [1], Pavel Pitra [2], Martin Robyr [1] & Gilles Ruffet [2]

[1] Institute of Earth Sciences, University of Lausanne, Géopolis, Quartier Mouline, Lausanne 1015, Switzerland
   (paola.manzotti@gmail.com)
[2] Géosciences Rennes, UMR CNRS 6118, Université Rennes1, Campus de Beaulieu, Rennes Cedex 35042, France

Determining the P-T conditions of Alpine metamorphism in the Dent Blanche Tectonic System (DBTS) is a difficult task because sensitive bulk-rock compositions are rare (hence the diagnostic mineral assemblages are lacking), and chemical equilibrium has rarely been achieved. Alpine greenschist facies metamorphism is dominant. However, few occurrences of sodic amphibole and sodic clinopyroxene may indicate early, blueschist-facies, metamorphism (first mention Stutz, 1940). We report new field and laboratory results to better document the inferred high pressure history of the Dent Blanche.

Despite systematic search, we have been unable to find blue amphibole in mafic rocks (e.g. in the Permian metagabbros or in the pre-Alpine amphibolites). However, sodic amphibole and sodic clinopyroxene are found in different lithologies from several tectonic units of the DBTS (Mont Gelé and Regondi Units of the Arolla Series; Lower Unit of the Mont Mary). Field, petrographic and geochemical data indicate that these minerals form in different rock types, some approaching isochemical systems, the other requiring significant metasomatism. Three main occurences have been found.

(i) Sodic amphibole forms coronas around magmatic calcic amphibole in undeformed pods of ultramafic cumulates (hornblendites).

(ii) In metasomatized granitic orthogneiss and leucotonalite, sodic amphibole mainly defines rosettes or sheaves, generally without a shape preferred orientation. Only locally they form needles aligned parallel to a mylonitic foliation and a stretching lineation. Pale green, patchy zoned aegirine augite is dispersed in an albite-quartz matrix or forms layers of fine-grained fibrous aggregates. Blue amphibole is slightly zoned with a darker blue core (mostly magnesioriebeckite) and a lighter blue rim (winchite).

(iii) In the Lower Unit of the Mont Mary, sodic amphibole and muscovite define an earlier foliation in fine-grained gneiss and are partially re-oriented parallel to a second schistosity. In these rocks, blue amphiboles display magnesioriebeckite cores surrounded by glaucophane rims.

Bulk rock chemistry of the different lithologies indicates a high Fe^{3+}/Fe_{total} ratio (0.45-0.82). Thermodynamic modelling performed for different rock types (taking into account the measured Fe_2O_3 content) reveals that magnesioriebeckite and aegirine-augite are stable at 6-8 kbar and 400-450 °C.
In addition, preliminary geochronological results on the age of the Alpine metamorphism in the blue amphibole-bearing rocks will be presented.

These data provide better constraints on the Alpine metamorphic evolution of the DBTS, highlight the role of the Fe_2O_3 on stabilizing sodic amphibole and sodic clinopyroxene, and suggest significantly lower pressures for the DBTS than proposed previously.

REFERENCES
Stutz, A.H. 1940: Die Gesteine der Arollaserie im Valpelline (Provinz Aosta, Oberitalien). Schweizerische mineralogische und petrographische Mitteilungen 20, 117-245.

P 2.20

Polybaric fractional crystallisation of arc magmas - an experimental study

Felix Marxer [1], Peter Ulmer [1]

[1] Institute of Geochemistry and Petrology, ETH Zürich, Clausiusstrasse 25, CH-8092 Zürich (felix.marxer@erdw.ethz.ch)

Despite a still ongoing debate, differentiation of primary calc-alkaline liquids by fractional crystallisation is now generally accepted as one of the main driving mechanism controlling the compositional evolution of arc magmas. However, previous experimental studies failed to reproduce the predominantly metaluminous natural rock record by lower crustal crystal fractionation. At high pressures, experimental liquids rather evolve towards peraluminous compositions. The absence of abundant cumulates in the upper crust does not support the alternative scenario of major differentiation at low pressure conditions. Therefore, we propose an alternative process, namely polybaric fractional crystallisation, inferring that arc magmas differentiate progressively by crystal fractionation upon ascent through the crust. This hypothesis is tested through a series of experiments along several P-T ascent trajectories with continuously decreasing temperatures and pressures. Phase equilibria data, chemical compositions of stable mineral phases, liquid lines of descent as well as the evolution of crystal/melt ratios will provide crucial information to improve our understanding of the evolution of the calc-alkaline magmatic series and clarify if fractional crystallisation can be considered as a major process in the differentiation of mantle derived magmas at convergent plate boundaries. Our first experimental results support theoretical considerations on the effect of decreasing crystallisation pressure on mineral phase equilibria: the olivine-clinopyroxene cotectic curve is shifted towards more Cpx-rich compositions (equivalent to a destabilisation of clinopyroxene) rendering residual melts more metaluminous and, therefore, circumventing a rapid evolution of liquid lines of descent towards and into the peraluminous compositional field.

P 2.21
Cenozoic magmatism in northwestern of Central Iran Block: Roll back, mantle upwelling and extension

Reza Monsef [1], Iman Monsef [2] & Rasoul Esmaili [3]

[1] *Department of Geology,Shiraz branch, Islamic Azad University,Shiraz,Iran (zaos13000@yahoo.com)*
[2] *Department of Earth Sciences, Institute for Advanced Studies in Basic Sciences (IASBS),Zanjan, 45137- 66731,Iran*
[3] *University of Chinese Academy of Sciences,Beijing 100049,China*

The cenozoic Uromieh-Dokhtar Magmatic Arc (UDMA) OF Central Iranian block comprises magmatic rocks, which are generally regarded as having been derived from the southern active margin of Eurasian plate (Fig. 1).The successions of lavas, pyroclastic deposits and intrusions of various thikness are alongated in NW-SE direction which are exposed within the UDMA.This study presents zircon U-Pb data analyses of intrusive rocks assotiated with geochemical data from the UDMA, central Iran.Eocene magmatic activities initiated from Ardestan (51-53) and Kashan (50-52) to Saveh (37-40),These volcanic succession largly comprise calc-alkaline rocks occuring as lava flows, pyroclastic layers,intrusives,tuffs and ignimbrites.

Post-collisional magmatic activities were started in Burdigalian (18-20 Ma.) in the Aleh dome (e.g. Qom region) and langian (15-18 Ma.) in Khastak crater (e.g. Salafchegan region) and continued to Quaternary flood basalt (e. g. Ahar region) or along the later eruption in the Sahand (4.2-6.5 Ma.) and Sabalan (0.38 Ma.) volcanoes (Table 1).Geochronology observation show that not only the UDMA magmatism most active and widespread during Eocene and Oligocene (25-52 Ma.), but also continued to Neogene and Quaternary in post –collision setting,where trans-tensional basin system were working due to mantle diapirism and subduction rollback process.Such magmatism maybe generate from the convectively upwelling asthenosphere and/or thermally activated lithospheric mantle during local extension.These geochronological data together with geochemical data suggest that the late Paleocene-Eocene to Neogene to Quaternary magmatic flare-up was most active event in central Iran Block.

No.	Location / Rock name	Age (Ma.)	References
1	Ardestan(East of Esfahan)/Granodiorite	51-53	Sarjoghian & kananian,2017
2	Kashan/ Monzodiorite	50-52	Honarmand et al.,2013
3	Saveh/Granodiorite	37-40	Noun Sandiani et al., 2018
4	Sahand/Ignembrite	4.2-6.5	Chiu et al.,2017
5	Sabalan/Andesite	0.38	Lin et al., 2011
6	Salafchegan/Quartz-monzodiorite	15-18	Monsef,current study
7	Qom/ Granodiorite	18-20.3	Monsef,current study

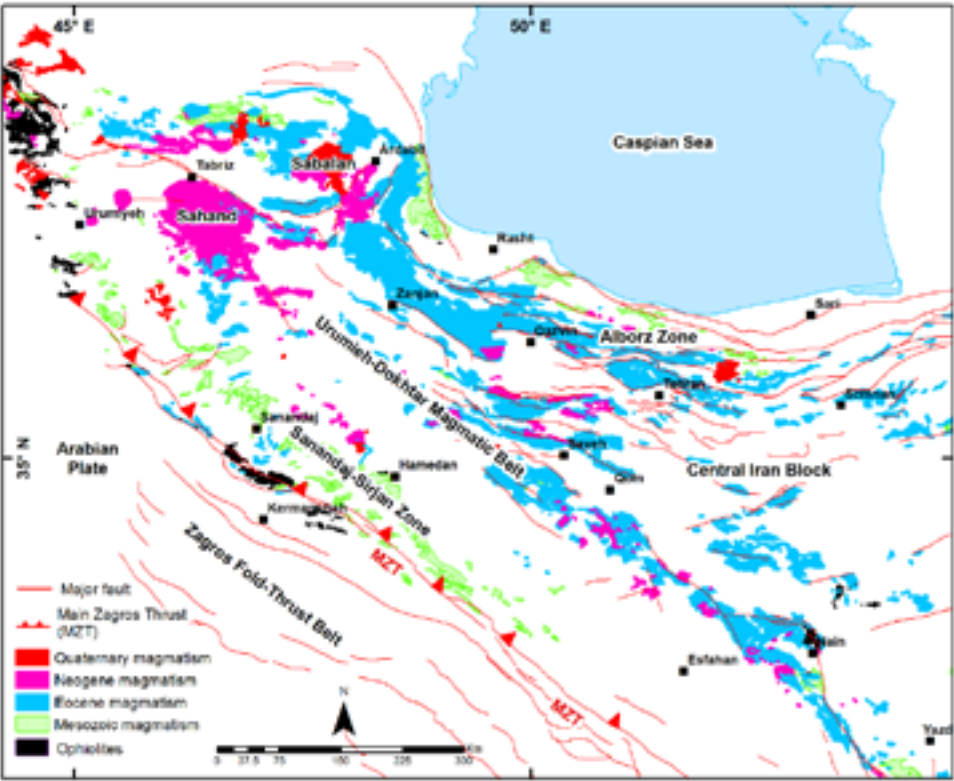Table 1: Zircon U-Pb data results from northwestern Uromieh-Dokhtar magmatic arc

Figure 1: The distribution of cenozoic magmatism in northwesterrn Uromieh-Dokhtar magmatic arc (UDMA) in the central Iran block

REFRENCES:

Chiu, H., Chung, S., Zarrinkob, M., Melkonyan, R., Pang, K., Lee, H., Wang, K., Mohamadi, S. & Khatib, M. 2017: Zircon Hf isotopic constraints on magmatic and tectonic evolution in iran: implication for crustal growth in tethian orogenic belt,Journal of Asian Earth Sciences,145,659-669.

Honarmand, M., Rashidnejad Omran, N., Corfu, M., Emami M. H. & Nabatian,G. 2013:Geochronology and magmatic history of calc-alkaline plutonic complex in the Uromieh-Dokhtar magmatic belt central Iran: Zircon ages as evidence for two major plutonic episodes,Neues Jahrbuch für mineralogie-Abhandlungen,190(1):67-77.

Lin,Y. C., Chung, S. L., Karakhanian, A., Jrbashyan, R., Navasardyan, G., Galoyan, G., Chiu, H. Y., Lin, I. J., Chu, C. H. & Lee, H. Y. 2011: Geochemical and Sr Nd isotopic constraints on the petrogenesis of pre- to post- collisional volcanic rocks in Armenia.EGU general assembly 2011,Geophisical research abstracts,Vol 13, EGU2011-5422.

Nouri Sandiani, F., Azizi, H., Stern, B., Asahara, Y., Khodaparast, S., Madanipour, S. & Yamamoto, K. 2018: Zircon U-Pb dating, geochemistry and evolution of the late eocene Saveh magmativ complex central Iran: partial melts of sub-continental lithospheric mantle and magmatic differentiation,Lithos.

Sarjoghian, F. & Kananian A. 2017: Zircon U-Pb geochronology and emplacement history of intrusive rocks in the Ardestan section,central Iran, Geologica Acta,Vol 15,N 1,15-36,I-X.

Verdel, C., Wernicke, B., P.,Hasanzadeh, J. & Guest, B. 2011: A paleogene extensional arc flare-up in Iran,Tctonics 30,TC 3008.

P 2.22
Relation between mean stress, thermodynamic and lithostatic pressure

Evangelos Moulas [1], Stefan M. Schmalholz [1], Yury Podladchikov [1], Lucie Tajčmanová [2], Dimitrios Kostopoulos [3] & Lukas Baumgartner [1]

[1] University of Lausanne, Institute of Earth Science (ISTE), Lausanne, Switzerland (evangelos.moulas@unil.ch)
[2] ETH Zurich, Department of Earth Science, Zurich, Switzerland
[3] National & Kapodistrian University of Athens, Faculty of Geology & Geoenvironment, Athens, Greece

Pressure is one of the most important parameters to be quantified in geological problems. However, in metamorphic systems the pressure is usually calculated with two different approaches. One pressure calculation is based on petrologic phase equilibria and this pressure is often termed thermodynamic pressure. The other calculation is based on continuum mechanics, which provides a mean stress that is commonly used to estimate the thermodynamic pressure. Both thermodynamic pressure calculations can be justified by the accuracy and applicability of the results. Here, we consider systems with low differential stress (<1 kbar) and no irreversible volumetric deformation, and refer to them as conventional systems. We investigate the relationship between mean stress and thermodynamic pressure. We discuss the meaning of thermodynamic pressure and its calculation for irreversible processes such as viscous deformation and heat conduction, which exhibit entropy production. Moreover, we demonstrate that the mean stress for incompressible viscous deformation is essentially equal to the mean stress for the corresponding viscous deformation with elastic compressibility, if the characteristic time of deformation is 5 times longer than the Maxwell viscoelastic relaxation time that is equal to the ratio of shear viscosity to bulk modulus. For typical lithospheric rocks this Maxwell time is smaller than approximately ten thousand years. Therefore, numerical simulations of long-term (>10 kyrs) geodynamic processes, employing incompressible deformation, provide mean stress values that are close to the mean stress value associated with elastic compressibility. Finally, we show that for conventional systems the mean stress is essentially equal to the thermodynamic pressure. However, mean stress and, hence, thermodynamic pressure can be significantly different from the lithostatic pressure.

P 2.23

Geochronology and geochemistry of zircons from the Rovina Valley Project and the Stanija Prospect – Apuseni Mountains (Romania): constraints from LA-ICP-MS/TIMS dating, trace and REE geochemistry of zircons and whole rock

Lukas Müller [1], Albrecht von Quadt [1], Irena Peytcheva [2], Randall Ruff [3], Sorin Halga [3]

[1] Institute of Geochemistry and Petrology, Department of Earth Science, ETH Zurich, Clausiusstrasse 25, CH-8092 Zurich (muellelu@student.ethz.ch)
[2] Geological Institute, Bulgarian Academy of Science, Sofia, Bulgaria
[3] SAMAX Romania, Subsidiary Euro Sun Mining, Romania

Most of the calc-alkaline and alkaline magmatic rocks in the South Apuseni Mountains were emplaced between 7.4 and 14.7 Ma (based on K-Ar dating) along NW-SE oriented graben structures, and as clusters of magmatic bodies (Rosu et al., 2004). Even though some of the magmas show an adakite-like character typical for subduction zones, they are the result of decompression melting of a previously metasomatized mantle, followed by asthenospere upwelling. The reason for this decompression and the easier ascent of the magma through the continental crust is thought to be the consequnce of rotational tectonics that created pathways with the horst and graben structures (Rosu et al., 2004; Neubauer et al., 2005; Harris et al., 2013).

Associated with this Miocene magmatism are several Cu-Au porphyry and epithermal deposits, which gave the region the name 'Golden Quadrilateral'. Euro Sun Mining Inc. has the license for exploration and mining of four of these porphyry deposits, which are situated in the Rovina Valley Project and Stanija Prospect, respectively. To better understand the relationship between the different intrusions and their mineralization potential we performed U-Pb age dating on zircons by LA-ICP-MS and ID-TIMS on several drill core and outcrop samples. Furthermore trace element compositions, rare earth elements and Hf isotopes were analyzed to characterize differences in the magma composition and thereby unravel heterogeneities in the magma source region.

First results show that three of the sampled deposits are similar in age (around 12.4 Ma), and formed at a time that was very favorable for the formation of porphyry deposits in terms of the tectonic regime as well as the generation of fertile magmas. The fourth deposit is significantly younger (around 11.3 Ma) and is connected to a later magmatic phase that was different in terms of magma evolution. Heterogeneity between the magma source regions is also visible in the Hf isotope ratios. The results of ID-TIMS point out that the youngest porphyry deposit was formed within a very short time span of only a few 10'000 years, what is consistent with recent results on Cu porphyry deposits (Buret et al., 2016).

REFERENCES

Buret, Y., von Quadt, A., Heinrich, C., Selby, D., Wälle, M., Peytcheva, I. 2016: From a long-lived upper-crustal magma chamber to rapid porphyry emplacement: Reading the geochemistry of zircon crystals at Bajo de la Alumbrera (NW Argentina), Earth and Planetary Science Letters, 450, 120-131.

Harris, C.P., Pettke, T., Heinrich, C.A., Rosu, E., Woodland, S., Fry, B. 2013: Tethyan mantle metasomatism creates subduction geochemical signature in non-arc Cu-Au-Te mineralizing magmas, Apuseni Mountains (Romania), Earth and Planetary Science Letters, 366, 122-136.

Neubauer, F., Lips, A., Kouzmanov, K., Lexa, J., Ivascanu, P. 2005: Subduction, slab detachment and mineralization: The Neogene in the Apuseni Mountains and Carpathians, Ore Geology Reviews, 27, 13-44.

Rosu, E., Seghedi, I., Downes, H., Alderton, D.H.M., Szakacs, A., Pecskay, Z., Panaiotu, C., Panaiotu, C.E., Nedelcu, L. 2004: Extension-related Miocene calc-alkaline magmatism in the Apuseni Mountains, Romania: Origin of magmas, Schweizerische Mineralogische und Petrographische Mitteilungen, 84, 153-172.

P 2.24

Carbonate clumped isotope climate reconstructions on fossil coral samples of the Early Eocene

Inigo A. Müller, Irene Waajen, Joost Frieling, Peter Bijl and Martin Ziegler

i.a.muller@uu.nl

The climate of the Early Eocene is often refert to as potential climate analog we are currently heading to. The atmosphere during the Early Eocene contained extremely elevated concentrations of the greenhouse gas CO_2 and published studies on this period found no evidence of Polar ice caps. The lack of Polar ice caps and the elevated pCO_2 lead to a much warmer climate conditions that were completely different to our modern time.

Climate reconstructions from localities close to the Polar circle revealed temperatures between 20 to 30 °C and tropical flora/fauna was widely found in this area. In general most of this data revealed smaller meridional temperature gradient between the Equatorial and Polar regions, which current climate models struggle to reproduce.

In our study we applied carbonate clumped isotope thermometry on fossil coral samples recovered from the Southern coast of Australia, which had an Early Eocene latitude of more than 60 ° South. Our Early Eocene climate reconstructions on the fossil corals that probably grow in the mixed layer close to the surface offer new temperature data from this period that are probably more annual temperatures and thus are a bit colder than other published climate proxies in this area.

P 2.25

A geochronological study of zircon and zirconolite observed in ruby and spinel gemstones and in marble host rock from Mogok, Myanmar

Myint Myat Phyo [1], Marcel Guillong [2], Alfons Berger [3], Walter Balmer [4], Leander Franz [1], Hao A.O. Wang [4], and Michael S. Krzemnicki [4]

[1] Institute of Mineralogy and Petrography, University of Basel, Switzerland (myintmyat.phyo@unibas.ch)
[2] Institute of Geochemistry and Petrology, ETH Zurich, **Switzerland**
[3] Institute of Geological Sciences, University of Bern, Switzerland
[4] Swiss Gemmological Institute SSEF, Aeschengraben 26, 4051 Basel, Switzerland

The Mogok area within the Mogok Metamorphic Belt (MMB) in Myanmar is famous worldwide for its high quality ruby and spinel deposits. Although MMB has been studied extensively in terms of petrography, geochronology and tectonics, only very limited data so far have been reported on U-Pb ages of zircon specifically from the Mogok area, which is a significant segment of the MMB. Our research focuses on U-Pb age dating of zircon and zirconolite inclusions from gem-quality ruby and spinel as well as from marble host rock from the Mogok area to better understand the complex metamorphic events leading to their formation.

Samples were collected in the Mogok area during a field trip in 2016. In the course of gemmological and petrologic studies, zircon inclusions were identified and imaged by Raman spectrometry and scanning electron microscopy. Zoning in zircon was observed using CL-images of a scanning electron microscope equipped with a variable pressure secondary electron detector (VPSE). Zircon and zirconolite inclusions in gemstones and marbles were analysed with LA-ICP-Time-Of-Flight (TOF)-MS and LA-ICP-Sector-Field (SF)-MS using a crater size of 35 μm in TOF-MS and a crater size of 20 μm and 13 μm for SF-MS on small grains and strongly zoned grains. The age dating results by these two methods are well in accordance with each other. Besides geochronology, trace element composition of zircon and zirconolite were analyzed with TOF-MS, which can measure the full mass spectrum from Li to U simultaneously.

The zircon inclusions from gem-quality ruby and spinel mostly show distinct circular zoning in the core, with thick to thin-zoned rims. Some zircons in ruby from Mansin (Eastern Mogok) contain aggregated zircon grains with irregular overgrowth structures at their rims (Fig. 1a). Zirconolites from gem quality ruby are present as subhedral grains whereas zirconolites in marble host rock occur as inclusions within zircons or as rims of zircon (Fig. 1b). They are homogeneous and without zoning in CL-images.
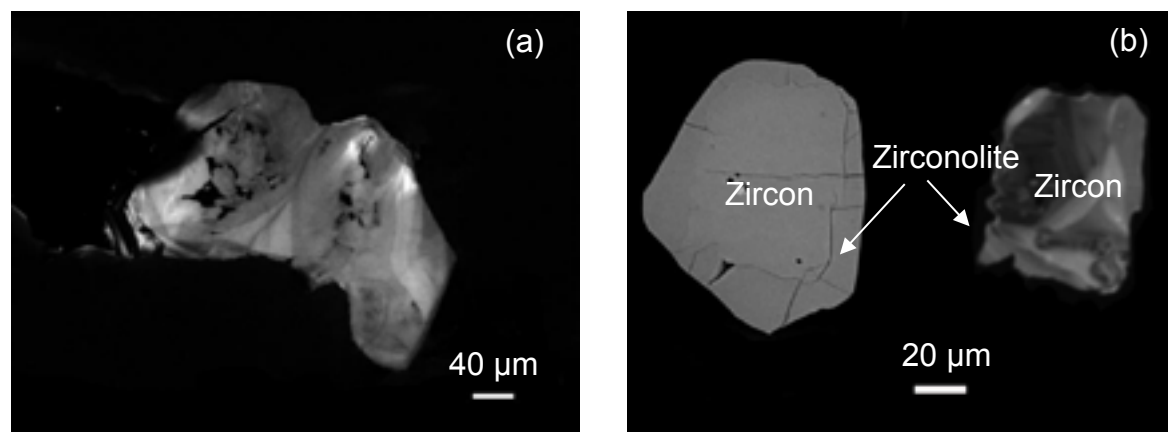

Figure 1. CL- images of (a) aggregated zircon inclusions in ruby from Mansin (eastern Mogok) and (b) zirconolite without zoning (right) and found as rim of a zircon grain (left) from Bawlongyi marble (Western Mogok)

The U-Pb ages of zircon inclusions in gem-quality ruby and spinel revealed two age groups: (1) late Cretaceous (~75 Ma), and (2) late Oligocene (~25 Ma). Zircons from ruby- and spinel-bearing marble from Bawlongyi (western Mogok) yielded a wide range of similar ages 75-25 Ma. In addition, zirconolites from gemstones and ruby- and spinel- bearing marbles yielded ~21 Ma. Our results are well in accordance with Cretaceous to Miocene ages of intrusive igneous rocks, i.e. diorite, granite and granite dykes by Andrew Mitchell et al (2012). The wide range of U-Pb ages indicates several metamorphic events that took place in the Mogok area with the latest event in Early Miocene. Our investigations show that the formation of gem-quality ruby and spinel in the Mogok area most probably took place during the latest metamorphic event.

REFERENCES

Mitchell, A., Chung, S.L., Thura, Oo, Lin, & T. H., Hung, C. H. 2012: Zircon U-Pb ages in Myanmar: Magmatic-metamorphic events and the closure of a neo-Tethys ocean? *Journal of Asian Earth Sciences*, 56, 1-23.

P 2.26
High precision Ar/Ar age traverses reveal intragrain inhomogeneities of pristine magmatic micas

Maria Naumenko-Dèzes [1], Yann Rolland [1], Sylvain Gallet [1], Pierre Lanari [2], Igor M. Villa [2,3]

[1] *Geoazur, Université Nice Sophia Antipolis, France (marie@geosphere.ch)*
[2] *Geologisches Institut, Universität Bern, Switzerland*
[3] *Centro Universitario Datazioni e Archeometria, Università di Milano Bicocca, Italy*

Micas are among widely used minerals for interpretation of the age and duration of magmatic and metamorphic processes. Such interpretations are based on the assumptions that micas were either closed since crystallization/re-equilibration, in which case they yield a flat step-heating age spectrum, or underwent a partial re-opening of the system that is reflected by a discordant age spectrum.

To assess the validity of such assumptions we studied two pristine-looking magmatic museum-grade mica megacrysts, whose Rb-Sr age coincides with the U-Pb age of co-existing minerals.

The first sample, consisting of five phlogopite sheets, 0.2-0.8 cm large, comes from the Phalaborwa carbonatite (NE Transvaal, South Africa), layered intracratonic alkali complex composed mainly of clinopyroxenites with minor carbonatites and phoscorites that intruded an Archean terrain (Eriksson, 1984). All layers of the intrusion have been dated by U-Pb (baddeleyite, zircon) at 2060 ± 3 Ma (Wu et al., 2011), the phlogopite used for this study has been previously dated with Rb-Sr method at 2059 ± 5 Ma (Naumenko-Dèzes et al., 2018).

The second sample, consisting of two 0.8-1.0 cm large muscovite sheets, comes from the Rubikon pegmatite body (Namibia) dated with U-Pb at 505Ma (Melcher et al., 2015). Each grain was cut with a metal blade to create age profiles, each individual piece (ca. 100x1000µm in size) of such profiles was separately irradiated and measured either with a ArgusVI (Nice) and/or a Noblesse (Milano) multicollector mass-spectrometer, step heating by laser (Nice), respectively furnace (Milano).

In all cases we obtained a plateau. Despite this apparent proof of ideality, each piece has a different age (up to 5 %) from its neighbors, without any core-rim relationship (Fig 1a). Such age inhomogeneity also corresponds to compositional inhomogeneity that can be traced for some samples by Ca/K vs age positive correlation. Indeed, quantitate microprobe data for Phalaborwa phlogopite showed alteration bands (3-30µm) along cleavage planes that are marked by a decrease of Ti, Fe, Al and an increase of Mg and Si. Quantitative microprobe data for Rubikon muscovite showed compositional changes (Al, K and Mn) parallel to cleavage planes as well as zones of different composition perpendicular to the cleavage planes (Fig.1b). Patchy intra-grain zonations are diagnostic of altered minerals (Villa & Hanchar, 2017) and support the interpretation that late post-magmatic fluid circulation disturbed both the magmatic chemical zonation and the K-Ar system. In summary, we observe that even museum-grade magmatic micas may show a patchy disturbance of both the K-Ar system and major element composition.
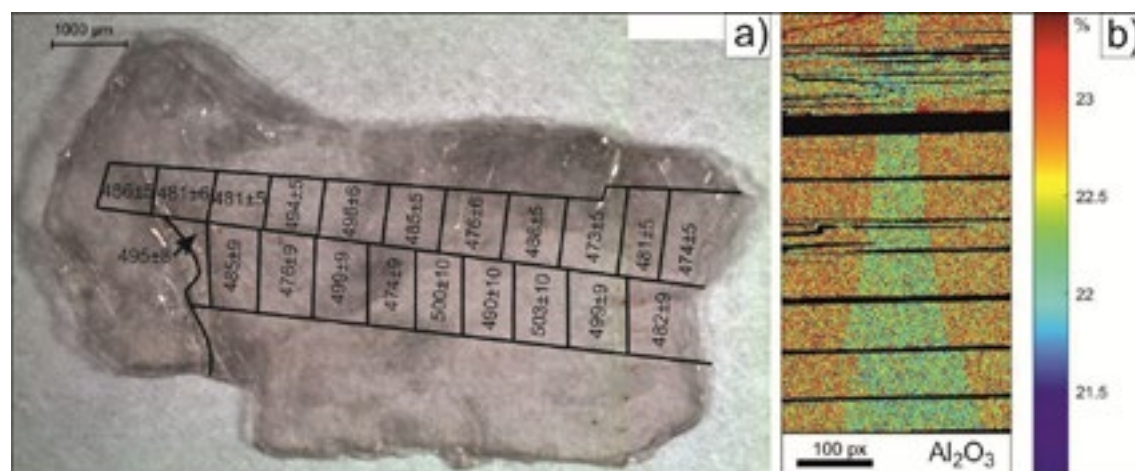

Fig. 1. (a) Ar/Ar age variation within a muscovite grain; (b) Al_2O_3 variation in a muscovite sample, perpendicular to the cleavage mount.

Variations in Ti, Mg and Al concentrations for phlogopites as well as Mn, K and Al for muscovites correspond to more than 5% Ar/Ar age variations inbetween subgrains, even though each individual subgrain gives an "age plateau". The data of this detailed case-study require that correlated intra-grain compositional and age variations be ascribed to hydrothermal events postdating the major phase of magmatic crystallization, and not to a simple temperature-driven diffusion history.

REFERENCES

Eriksson, S.C., 1984. Age of carbonatite and phoscorite magmatism of the Phalaborwa Complex (South Africa). Chemical Geology 46, 291-299.

Wu, F.-Y., Yang, Y.-H., Li, Q.-L., Mitchell, R.H., Dawson, J.B., Brandl, G., Yuhara, M., 2011. In situ determination of U-Pb ages and S-Nd-Hf isotopic constraints on the petrogenesis of the Phalaborwa carbonatite Complex, South Africa. Lithos 127, 309-322.

Naumenko-Dèzes M.O., Nägler Th.F., Mezger K., Villa I.M., 2018. Constraining the ^{40}K decay constant with ^{87}Rb-^{87}Sr – ^{40}K-^{40}Ca chronometer intercomparison. Geochimica et Cosmochimica Acta 202, 235-247.

Villa I.M., Hanchar J.M., 2017. Age discordance and mineralogy. American Mineralogist, 102, 2422–2439.

P 2.27

Spinel lherzolite xenoliths from the Cameroon Volcanic Line (CVL): Implications for mantle processes and equilibrium conditions

Siggy Nformidah [1], Peter Tollan [1], Joerg Hermann [1], Jean Pierre Tchouankoue [2]

[1] Institute of Geological Sciences, University of Bern, Baltzerstrasse 1+3 CH-3012 Bern (ndah.nformidah@geo.unibe.ch)
[2] Department of Geological Sciences, University of Yaounde I

Spinel-bearing xenoliths recovered from Cenozoic alkaline basalt flows of the Wum volcano, located in the central part of the Cameroon Volcanic Line (CVL), at N06°24' and E10°04' have been examined to characterise the petrography, mineral major and trace element composition, water contents and conditions of equilibration of the mantle below the region. Investigated xenoliths are spinel lherzolites showing well equilibrated protogranular textures. One Wum sample contains amphibole, which has not been previously reported in this locality. Two-pyroxene thermometry based on major element exchange yields temperatures of about 930 ± 110 °C assuming a pressure of 15 Kbar, consistent with the spinel stability field. Temperatures estimated from Ca (980 °C), Al (955 °C) and Cr (995°C) thermometers in olivine show a good correlation between the three methods but are higher than the two-pyroxene thermometers. Calculated temperatures based on REE partitioning between clinopyroxene and orthopyroxene are around 1050 °C and are generally higher than the temperatures determined from trace elements in olivine. The water contents of olivines and pyroxenes were determined by FTIR spectroscopy using unpolarised light on unoriented crystals. Olivine typically contains <1 ppm H_2O, whereas orthopyroxene and clinopyroxene have water contents of 17-35 ppm and 85-170 ppm at their cores respectively. Calculated inter-mineral partition coefficients indicate that H distribution is not at equilibrium, typical for mantle samples which have experienced diffusive water loss during ascent, supported by a decrease in water content from core to rim in orthopyroxene. Patterns of rare earth element normalised to primitive mantle values (Palme and O'Neill,2013) of clinopyroxene show different groups: the first group with a depletion in LREE, the second with an enrichment in the LREE and a third group that shows no enrichment or depletion. These patterns reflect different stages of partial melting and metasomatism. Our new data indicate that the xenoliths came from a shallow part of the lithospheric mantle having imprints of several depletion and enrichment events. The high equilibration temperatures suggest extension in the lithospheric mantle related to heating prior to the entrapment of the xenoliths in the alkaline lavas. Moreover, the fact that clinopyroxene with different trace element patterns are present indicates that at least one metasomatic event must have occurred during this extension. Further work will exploit the relationships between melt production in the mantle, metasomatism and crustal evolution in the specific tectonic setting of the CVL.

REFERENCES
Palme, H. and O'Neill, H.S.C. 2004. <http://www.Earthref.org/ ERR/2750 (accessed in June 2013).

P 2.28

Characterisation of hydrothermal recharge alteration of seafloor basalts in the Oman ophiolite

Sarah F. Pein [1], Larryn W. Diamond [1], Thomas M. Belgrano [1]

[1] Institute of Geological Sciences, University of Bern, Baltzerstrasse 1+3, CH-3012 Bern, Switzerland

Convection of seawater through the hot oceanic crust has vast geochemical consequences: it modifies the composition of the crust via hydrothermal reactions, it forms valuable ore deposits, it buffers the composition of the oceans and, via subduction, it influences the composition of arc magmas and the mantle. Current knowledge of alteration in oceanic crust is strongly influenced by ocean drilling studies. However, ophiolites provide more representative insights into lateral variations in alteration. For example, the volcanic sequence of the Semail Ophiolite –the world's largest sub-aerial exposure of oceanic crust– is pervasively altered. The basalts in recharge zones are converted to spilite (chlorite–albite–quartz) assemblages while in discharge zones they are transformed to epidosite (epidote–quartz) assemblages. Massive sulphide deposits, which are common in the ophiolite, are thought to be the final venting sites for these hydrothermal systems.

In order to quantify the extent and impacts of the recharge alteration, we are characterising the geochemistry and mineralogy through a complete section of spilitised upper crust in the Semail ophiolite. We have sampled along transects from the sheeted dyke complex (SDC) to the top of the volcanic pile. The samples have been characterised by petrography and analysed by X-ray diffraction (XRD), X-ray fluorescence (XRF), carbon-nitrogen-sulphur (CNS) analysis, and ICP-MS. Our results confirm an increasing metamorphic grade with stratigraphic depth from brownstone facies (clay-dominated) to zeolite facies (zeolites, celadonite) to greenschist facies (chlorite, actinolite). This 'peak' grade, however is partially overprinted by late low-temperature alteration. Unravelling this overprinted sequence by paragenetic arguments is key to knowing when particular mineral reactions took place during the maturation of this crust and has important implications for the availability of metals for VMS formation.

P 2.29

Unravelling magma emplacement mechanism in the lower crust: A forensic investigation of the Mafic Complex, Ivrea-Verbano Zone (Italy)

Mattia Pistone [1], Benoît Petri [1], Othmar Müntener [1], Bjarne S. G. Almqvist [2], Alberto Zanetti [3], György Hetényi [1], Alba S. Zappone [4], Lukas P. Baumgartner [1]

[1] Institute of Earth Sciences, University of Lausanne (UNIL), Bâtement Géopolis, Quartier UNIL-Mouline, CH-1015, Lausanne, Switzerland
[2] Department of Earth Sciences, Uppsala University, Uppsala, Sweden
[3] Istituto di Geoscienze e Georisorse, Consiglio Nazionale delle Ricerche (CNR), Pavia, Via Ferrata, 1, I-27100 Pavia, Italy
[4] Department of Earth Sciences, ETH-Zurich, Sonneggstrasse 5, CH-8092, Zurich, Switzerland

The Ivrea-Verbano Zone (Southern Alps, Italy) is a unique target for assembling data on magma emplacement mechanism in the Earth's lower crust. In its southern portion cross-cut by the Mastallone (north), Sesia (central), and Sessera river (south), the 13-km thick Permian Mafic Complex consists of hornblende-gabbro (lower part), gabbro-norite (intermediate part) and diorite (upper part), emplaced into a pre-Permian metasedimentary sequence, and represents the deep roots of the Permian Sesia Magmatic System. New field data (foliation and lineation measurements), three-dimensional analysis of oriented rock microstructures by X-ray tomography (50-μm spatial resolution), and calculations of physical properties (rock density, P- and S-wave velocity) based upon mineral chemistry and modal proportions indicate a magma body constructed by the repetitive emplacement of sills. We observe from bottom to top: a) a 2-km thick, cumulate region with an upward increase of pyroxene/amphibole (up to 75%) and oxide content (up to 6%); b) a 10-km main region preserving two 1- to 2-km thick pyroxenite intrusions interlayered with two 4-km thick plagioclase-dominated (up to 80%) zones in the body core, with its northern margin also characterised by presence of garnet (up to 77%); c) a 1.5-km portion composed of a hornblendite embedded in a biotite- (up to 20%) and plagioclase-dominated (up to 60%) region. Respective ~20% and 13% rock density and seismic velocity variations between plagioclase-rich regions and pyroxenite intrusions suggest an internal stratification of physically distinct portions. Indeed, P- to S-wave velocity ratios (V_P/V_S) show a body constructed by mafic pulses (V_P/V_S = 1.75-1.79), denser than the basal cumulate region, overlain by less dense regions (V_P/V_S = 1.84-1.87), which are able to intermingle with and assimilate metapelite septa of the pre-existing crust and, potentially, evolve into a K-rich hydrous body at the roof portion. The Mafic Complex architecture is therefore not the result of a catastrophic gravitational collapse of the pluton during crustal thinning, as previously proposed upon observation of upwardly concave layering and foliation in ophiolitic gabbros, but rather an incremental emplacement of pulses adapted to the geometry of the pre-existing crust.

P 2.30
U-Pb baddeleyite geochronology: two case studies from the western Avalon Peninsula, Newfoundland

Johannes E. Pohlner [1,2], Axel K. Schmitt [1], Kevin R. Chamberlain [3], Gregor Austermann [1] & Anne Hildenbrand [1]

[1] Institut für Geowissenschaften, Universität Heidelberg, Im Neuenheimer Feld 234-236, 69120 Heidelberg, Germany (johannes.pohlner@web.de)
[2] Unit of Earth Sciences, Department of Geosciences, University of Fribourg, Chemin du Musée 6, CH-1700 Fribourg, Switzerland
[3] Department of Geology and Geophysics, University of Wyoming, 1000 E. University Ave., Laramie, WY 82071-2000, USA

Baddeleyite ZrO_2 is one of the most commonly used geochronometers for mafic rocks. Compared to zircon, baddeleyite is more robust to Pb loss, but small degrees of discordance are common and cannot be eliminated by chemical abrasion techniques. The mechanisms responsible for this discordance are not well understood, but crucial for accurate age interpretation. Aiming for an improved understanding of natural baddeleyite U-Pb systematics, we performed a case study on early Paleozoic dikes and sills of the Spread Eagle Intrusive Complex (SEIC) and Cape St. Mary's sills (CSMS) of the Avalon Zone of Newfoundland (Canada). We combine detailed microtextural observations with U-Pb geochronology by secondary ionization mass spectrometry (SIMS) and thermal ionization mass spectrometry (TIMS).

Stratigraphically constrained intrusion ages are ca. 495-510 Ma (SEIC) and 400-500 Ma (CSMS). Low grade metamorphism took place during the Acadian Orogeny (ca. 360-420 Ma). Baddeleyite is often intergrown with zircon in four texturally different assemblages: (1) baddeleyite with younger metamorphic zircon rims, (2) baddeleyite with coeval igneous zircon, (3) baddeleyite with older xenocrystic zircon inclusions (one SEIC sample), and (4) altered igneous zircon with secondary baddeleyite inclusions (one CSMS sample). SIMS analysis (e.g., Schmitt et al. 2010) was performed either in thin section (in situ) or on crystal separates (grain mounts), to further distinguish and constrain the petrologic significance of these textural types. Selected crystals from grain mounts were subsequently used for single crystal TIMS analyses.

SIMS in situ results are, within error limits, concordant and in good agreement with the stratigraphic estimates, even in samples with baddeleyite crystal diameters <10 µm. However, some grain mount samples yielded reversely discordant data, resulting in overestimated $^{206}Pb/^{238}U$ ages, although this problem did not occur in secondary reference baddeleyite analyzed in the same sessions. TIMS data agree with SIMS in situ results and stratigraphic estimates, but are always normally discordant. Replicate TIMS analyses indicate variable discordance in SEIC baddeleyite, whereas CSMS baddeleyite analyses cluster at moderate discordance (Figure 1).

Reverse discordance in SIMS analyses is probably due to bias in the U/Pb relative sensitivity calibration. This could be due to beam overlap onto zircon intergrown with baddeleyite, but microtextural inspection suggests that other yet unidentified factors play a role. $^{207}Pb/^{206}Pb$ ages are insensitive to the calibration, but precision is often compromised by high common Pb. For SIMS analysis, surface contamination and/or contributions from adjacent phases are possible sources of common Pb. However, steady common Pb intensities even for some analyses with spots entirely on baddeleyite suggest that some common Pb is intrinsic to these crystals, as it is known from metamict zircon.

The complex pattern of SEIC analyses requires mixing between at least three age components, micropetrographically identified as: (1) magmatic baddeleyite crystallization, (2) metamorphic zircon formation, and (3) Pb loss in zircon. Ideally, baddeleyite and zircon domains should have been separated chemically prior to TIMS analysis using the step dissolution method of Rioux et al. (2010), but small crystal size of and/or radiation damage in zircon may have defied complete separation. The SEIC TIMS results allow only to broadly confine the intrusion age (>485 Ma), which is better approximated by the SIMS $^{207}Pb/^{206}Pb$ date (497 ± 7 Ma). Due to the spatial resolution of ca. 10 µm, intergrown zircon domains can be avoided more easily by SIMS. Secondary zircon domains are much more rare in CSMS baddeleyite than in SEIC, so another process must be responsible for the discordance observed in both methods. Previously hypothesized mechanisms for baddeleyite discordance (e.g., alpha recoil, radon loss, or protactinium excess) have different consequences for U-Pb systematics, resulting in permissible ages from 430.8 ± 0.4 Ma to at least 438.7 ± 2.4 Ma (2σ) for the CSMS sample. This study shows that baddeleyite geochronology can yield accurate ages in favorable circumstances, but also that U-Pb systematics for baddeleyite from mafic rocks affected by typical low-grade metamorphism are not simple. Further studies are necessary to identify the dominant processes responsible for baddeleyite discordance. To enhance baddeleyite geochronology, multi-method approaches with a focus on microtextures are useful.
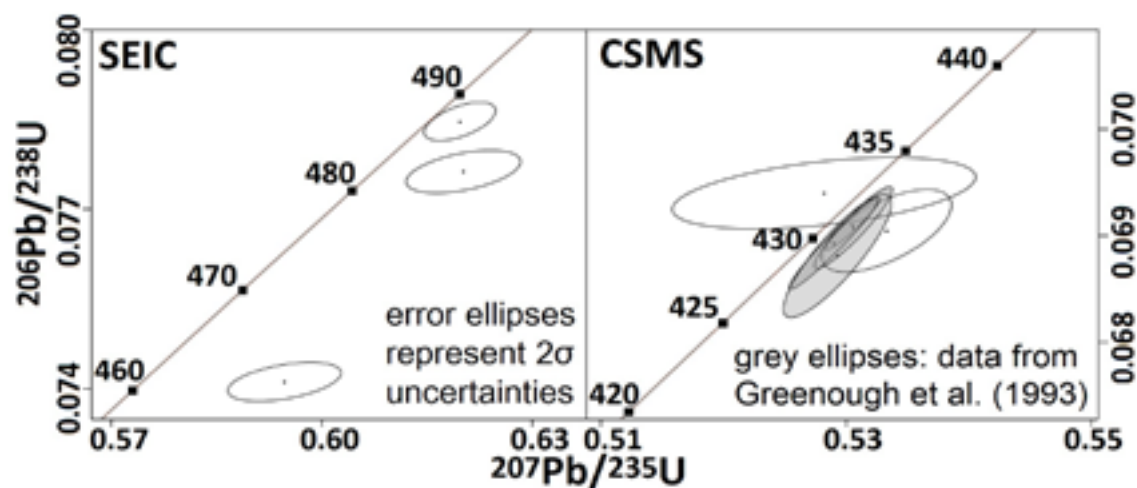
Figure 1. Concordia plot of the TIMS results for SEIC and CSMS samples.

REFERENCES

Greenough, J. D., Kamo, S. L. & Krogh, T. E. 1993: A Silurian U-Pb age for the Cape St. Mary's sills, Avalon Peninsula, Newfoundland, Canada: implications for Silurian orogenesis in the Avalon Zone, Canadian Journal of Earth Sciences, 30, 1607-1612.

Rioux, M., Bowring, S., Dudás, F. & Hanson, R. 2010: Characterizing the U–Pb systematics of baddeleyite through chemical abrasion: application of multi-step digestion methods to baddeleyite geochronology, Contributions to Mineralogy and Petrology, 160, 777-801.

Schmitt, A. K., Chamberlain, K. R., Swapp, S. M. & Harrison, T. M. 2010: In situ U–Pb dating of micro-baddeleyite by secondary ion mass spectrometry, Chemical Geology, 269, 386-395.

P 2.31
Epidosite formation in the oceanic crust: Composition and P–T properties of the metasomatizing fluid

Lisa Richter [1] & Larryn W. Diamond [1]

[1] Institute of Geological Sciences, University of Bern, Baltzerstrasse 3, CH-3012 Bern (lisa.richter@geo.unibe.ch)

Epidosites are former igneous rocks (dikes, lavas, trondhjemite intrusions) that have been hydrothermally altered to epidote + quartz + titanite + Fe-oxides. They have been proposed as markers of deep upflow in sub-seafloor hydrothermal convection cells, and as sources of metals in seafloor black-smoker sulphide deposits. In order to test these proposals by geochemical modelling, the composition of the metasomatizing fluid and the P–T conditions of alteration must be identified. Fluid inclusion studies have reported evidence from diabase dikes that epidosites formed from aqueous solutions with seawater salinity (e.g. Nehlig and Juteau,1988). In apparent contradiction, other studies have provided fluid inclusion evidence from altered trondhjemites that epidotization was caused by hypersaline brines (e.g. Cowan & Cann, 1988; Juteau et al., 2000).

We have collected epidosites from the sites of the original studies in the Semail (Oman) and Troodos (Cyprus) ophiolites and reexamined their fluid inclusions. Our analyses of primary inclusions in epidote and coeval quartz confirm that epidotization of basaltic dikes and lavas was due to solutions with seawater salinity (~ 4.0 wt.% TDS). In the epidosites overprinting trondhjemites we also discovered primary aqueous inclusions with the same salinity, in contrast to the earlier studies. The primary hypersaline inclusions in these rocks, reported by previous workers, are confined to paragenetically earlier hydrothermal–magmatic quartz and hence they are unrelated to epidotization. Since these brines coexist with inclusions of water vapour, they represent phase separation of either magmatic water or early infiltrations of seawater.

Temperature and pressure reconstructions from the fluid inclusion data reveal that epidotization occurred over a range of conditions, from 240 to 440 °C at hydrostatic pressures of 25–50 MPa. Thus, both the P–T conditions and the Ca-enriched, Mg-depleted fluid composition are consistent with epidosites representing upflow zones of deeply convected seawater.

REFERENCES

Cowan J. & Cann J. 1988: Supercritical two-phase separation of hydrothermal fluids in the Troodos ophiolite. Nature, 333, 259–261.

Juteau, T., Manac'h G., Moreau, O., Lecuyer, C. & Ramboz, C. 2000: The high temperature reaction zone of the Oman ophiolite: new field data, microthermometry of fluid inclusions, PIXE analyses and oxygen isotopic ratios. Marine Geophys Res, 21, 351–385.

Nehlig, P., & Juteau, T. 1988: Flow porosities, permeabilities, and preliminary data on fluid inclusions and fossil geothermal gradients in the crustal sequence of the Sumail ophiolite, Oman. Tectonophysics, 151, 199–21.

P 2.32

Comparative study of XRF and portable XRF analysis and application in hydrothermal alteration geochemistry: The Elatsite porphyry Cu-Au-PGE deposit, Bulgaria

Roman Alday, M.C.[1], Kouzmanov, K.[1], Harlaux, M.[1], Stefanova E.[2]

[1] Department of Earth Sciences, University of Geneva, Rue de Maraîchers 13, 1205 Geneva, Switzerland; (Maria.Roman@etu.unige.ch)
[2] Geological Institute, Bulgarian Academy of Sciences, Acad. G. Bonchev Str. 24, 1113 Sofia, Bulgaria

X-ray fluorescence (XRF) spectrometry is a non-destructive analytical technique widely used in Earth and Environmental Sciences to determine the elemental composition of rocks, ores, soils and plants. Portable XRF analysers (pXRF) are increasingly being used in mineral exploration and mining, allowing acquiring rapidly and inexpensively large geochemical data sets in the field. In this contribution, we present the results of a comparative study of 15 samples of hydrothermally altered magmatic and metamorphic rocks from the Elatsite porphyry Cu-Au-PGE deposit in Bulgaria, using both a lab-based WD-XRF (PANalytical Axios^{mAX}) and a pXRF (Thermo Niton XL3t) device.

For analyses performed with the pXRF, the samples were crushed to a fine-grained powder (<80 μm) and mounted in a plastic cup covered by a thin polypropylene film (4 μm-thick) to be analysed on a test stand. Two techniques for sample preparation were used, resulting in slight difference in compaction of the sample measured: the first one consists of analysis of non-pressed powder in the cup (referred to as "powder" in Fig. 1), and in the second case the powder is slightly compressed with an agate pestle (referred to as "pressed powder" in Fig.1). A total of 34 elements were measured using the "Soils & Minerals" protocol within the "Mining Cu/Zn" mode of the pXRF. Measurements were 120s each consisting of two 60s cycles using four different energy filters. For some elements (Al, V, Mn, Mo, Ba) pressed-powder samples show systematically slightly higher values (as high as 10%; Fig. 1C).

Lab-based WD-XRF results were used to perform an empirical calibration of the elemental concentrations obtained by pXRF, following the procedure proposed by Mauriohooho et al. (2016) (Fig. 1A-B). Linear regression analysis of the data allows calculating the correction factor to be applied (corresponding to the slope of the regression line) for each element determined by pXRF. For each filter, the correction factor decreases progressively with the increase of the atomic number of the measured element (Fig. 1D).

Comparing the results obtained using the two sample preparation techniques for the pXRF analyses, we demonstrate that generally both of them provide accurate data comparable with WD-XRF (Fig. 1B), resulting in correlation coefficients >0.9. However for some elements (ex. Al, Sr, Zn), pressed-powder preparation resulted in better correlation between WD-XRF and pXRF analyses.
Unfortunately, due to its low atomic number, Na cannot be quantified by pXRF, and Mg is usually measured with a low level of confidence.

Our results demonstrate that large data sets obtained with a pXRF device can be used after correction based on lab-XRF analyses on selected representative samples for geochemical interpretation on suites of hydrothermally altered samples (mass balance and alteration index calculations).
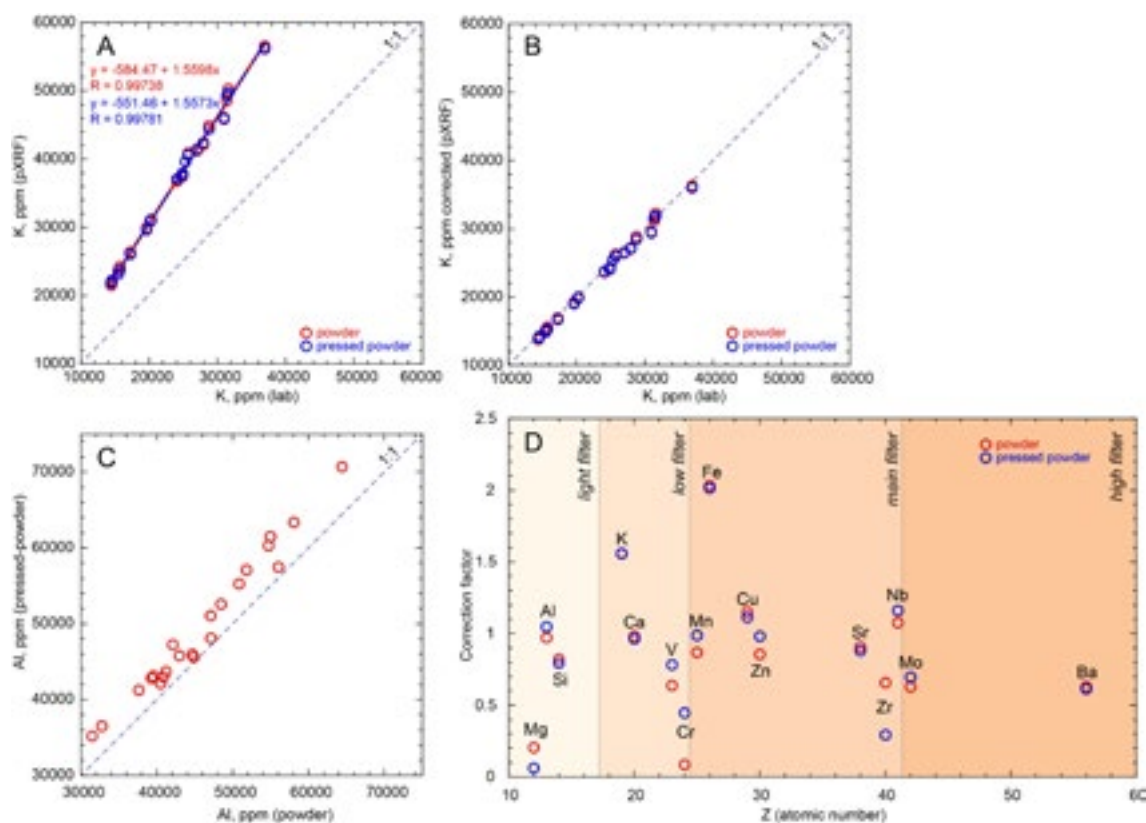
Figure 1. Comparison between lab-based WD-XRF and pXRF analyses of hydrothermally altered rock samples: A) K concentrations of powder and pressed-powder samples vs. lab-XRF analyses; calculated slops from regression analysis are used as correction coefficients; B) Corrected values of K concentrations from pXRF analyses vs. lab-XRF data; C) Powder vs. pressed-powder sample preparation for pXRF analyses (Al concentrations); D) Correction factor as a function of Z (atomic number) of the elements for the four different filters used (light, low, main, high).

REFERENCES

Mauriohooho, K., Barker, S., Rae, A. 2016: Mapping lithology and hydrothermal alteration in geothermal systems using portabke X-ray flourescence (p XRF): A case study from the Tauhara geotheral system, Taupo Volcanic Zone. Geothermics 64 (2016) 125-134

P 2.33

How to achieve 100 ppm precision on a U-Pb zircon age: recent developments and their limitation

Urs Schaltegger [1], Maria Ovtcharova [1], Joshua H.F.L. Davies [1], Nicolas D. Greber [1], Federico Farina [1], Philipp Widmann [1], Luís Lena [1]

[1] Department of Earth Sciences, University of Geneva, Rue des Maraîchers 13, 1205 Geneva (joshua.davies@unige.ch)

U-Pb geochronology has seen unprecedented developments during the last few years. The run for higher and higher precision of dates from ever lower volumes of material (especially zircon) has required a series of innovations: chemical pre-conditioning of sample material, micro-sampling, highly precise and reproducible micro-chemical procedures, and innovations in low-level mass spectrometry. At the same time the needed volume of zircon for isotope-dilution TIMS dating became equivalent or dropped below that sampled by laser-ablation ICP-MS, but is still largely higher than that ablated by secondary ion beam mass spectrometry techniques. This talk will give an outline of the main developments that were necessary to achieve our presently best precision of 0.01-0.02% for an ID-TIMS $^{206}Pb/^{238}U$ age of a geological sample, from improvements in low-volume microchemistry, to mass spectrometry techniques.

Achieving long-term, intra-sample, and intra-laboratory reproducibility at the 0.01-0.02% level is by far more challenging than it is for precision. We will show data that document (i) our continuous efforts to assess accuracy; (ii) our tests of system reproducibility with natural reference materials or synthetic reference solutions; and (iii) our results of intercalibrating our two TIMS platforms (a 15 years old and recently upgraded Triton from Thermo Scientific vs. a recent Phoenix from IsotopX) at the same level of precision

Examples how improved temporal resolution can offer new insights into fundamental questions of planetary dynamics comprise synchrony of large igneous provinces, dramatic change of the Carbon cycle and associated mass extinctions, the role of internal vs. external forcing in climate change, or the role of large-scale continental glaciations for major evolutionary discontinuities in the biosphere recorded in the geological past.

P 2.34
Soapstones: fields and production laboratories between Ticino and Moesano

Filippo Luca Schenker [1] & Cristian Scapozza [1]

[1] Institute of Earth Sciences, University of Applied Sciences and Arts of Southern Switzerland (SUPSI), Via Trevano, CH-6952 Canobbio (filippo.schenker@supsi.ch)

The soapstone fields known along the Alpine mountain range in the territory of France, Italy and Switzerland are about ~400 of which 120 are located in Southern Switzerland (Ticino and Moesano) together with 14 production laboratories. The extraction, the use and the function of soapstone manufactories have influenced the historical and economical evolution of Alpine etnographic contexts since the Iron Age, with a peak of production of pots ("laveggi") between the last centuries of the Roman Empire and the Late Middle Ages. From the XII century the soapstone was also used for stoves and in architecture as documented in the romanic S. Nicolao church in Giornico.

The recovery of this historical identity is based on the study of archeological artifacts and on the reconstruction of historical commercial networks. For this purpose, tracing back the extraction site of an archeological artifact becomes fundamental to reconstruct the ancient commercial roads across the Alps. The mineralogical content of soapstone artifacts has sucessfully been used to distinguish the provenance of artifacts coming from the Valtellina or from the Val d'Aosta. However, the petrographic method shows some limits because several types of soapstone can be found in more than one Alpine region. Here, we present (i) a database of soapstone fields and production laboratories updated after Pfeifer and Serneels (1986) and Mannoni et al. (1987) that includes new findings and (ii) new bulk-rock geochemical analyses to support the petrographic characterization of soapstones. The small differences in mineral and in major- and trace-elements compositions should help to localize the fields.

Eight types of soapstone can be distinguished in southern Switzerland; some of them are characteristic of a specific area. The preliminary geochemical results show that the chemical composition can be significantly different even between the same type of soapstone and that H_2O and CO_2 (LOI), U and Cr can be tentatively linked to the metamorphic grade and the mineralogy of the soapstone, permitting to better reconstruct the geological framework of the rock and therefore also the location from which it has been extracted.

Even though the geochemical implications need further analyses to be verified, this preliminary study shows that the geochemical characterization is an added value to the study of the archeological artifacts of soapstone.

Figure 1. Soapstone pots of Roman Period and of Modern Epoch, coming from archeological sites in Ticino (©Ufficio dei beni culturali, Bellinzona).

REFERENCES

Mannoni, T., Pfeifer, H. R., & Serneels, V. 1987: Giacimenti e cave di pietra ollare nelle Alpi. Archeologia dell'Italia Settentrionale, 5, 7-46.

Pfeifer, H. R., & Serneels, V. 1986: Inventaire des gisements de pierre ollaire au Tessin et dans les régions voisines: aspects minéralogiques et miniers. In: 2000 anni di pietra ollare, Quaderni d'informazione del dipartimento dell'ambiente del Canton Ticino, 11, 147-235.

P 2.35
On CF$_4$ – a trace gas in granites and in the past atmosphere

Jochen Schmitt [1], Barbara Seth [1], Peter Köhler [2], Jane Willenbring [3], Hubertus Fischer [1]

[1] Climate and Environmental Physics, Physics Institute, and Oeschger Centre for Climate Change Research, University of Bern, CH-3012 Bern, Switzerland (schmitt@climate.unibe.ch)
[2] Alfred-Wegener-Institut Helmholtz-Zentrum für Polar- und Meeresforschung (AWI), Bremerhaven, Germany
[3] Geosciences Research Division, Scripps Institution of Oceanography, University of California, San Diego, USA

In 1966, pioneering geochemical trace gas analyses of fluid inclusions revealed that natural fluorite contains significant amounts of polyfluorinated organic compounds (Kranz, 1966). It turned out much later that one of these compounds, tetrafluoromethane (CF$_4$), can be found as well in the preindustrial atmosphere at a concentration of around 36 ppt (parts per trillion), a mass of around half a million tonnes (Harnisch et al., 1996). Further analyses revealed that CF$_4$ is not only present in fluorite samples, but also in granites and gneisses (Harnisch et al., 2000). It is assumed that CF$_4$ is produced and enclosed in the accessory fluorite crystals that are present in some granites. Several pathways were suggested that involve e.g. F$_2$ produced at lattice defects within the CaF$_2$ crystal that reacts with CO$_2$ or organic carbon within the fluid inclusions to form CF$_4$. In addition to CF$_4$, a suite of other fluorinated compounds have been identified, like SF$_6$ and NF$_3$, suggesting that a reservoir of F$_2$ reacts with any impurities available in the CaF$_2$ crystal. The CF$_4$ content of granites shows a large spread that may reflect different mineralogical composition or cooling history.

The release of CF$_4$ into the atmosphere due to processes that allow CF$_4$ to escape from the fluid inclusions (e.g. weathering or tectonic processes) leads to a built-up of CF$_4$ in the atmosphere (Harnisch et al., 2000; Deeds et al., 2015). CF$_4$ is a chemically very stable gas and natural destruction processes are only possible above an altitude of around 50 km in the mesosphere and thermosphere. Therefore, already small emission fluxes in the range of several tonnes CF$_4$ per year are required to generate this natural CF$_4$ background. The observed atmospheric CF$_4$ concentration at any time in the past is therefore a function of the global emission flux (e.g. from weathering of granites) and the atmospheric sink flux. Experimental studies and chemical transport models estimate the lifetime of CF$_4$ to be around 100,000 years. This extreme lifetime results from the fact that the entire volume of the troposphere and stratosphere has to be transported into the mesosphere and above.

In this presentation we show our 800,000 year long record of atmospheric CF$_4$ using air trapped in Antarctic ice core samples. This record documents systematic changes of the past atmospheric CF$_4$ concentration that are related to major changes in global climate. The main feature of our CF$_4$ record are changes that parallel the glacial/interglacial cycles with pronounced and rapid CF$_4$ increases during the deglaciations at the end of each glacial cycle. We interpret these deglacial CF$_4$ rises as pulses from increased weathering of granitic source material. Warmer climate, increased rainfall and runoff generally favour chemical weathering rates, thus are consistent with CF$_4$ rises during the deglacial phases. Additionally, the large North American and Fennoscandian ice sheets generated large amounts of moraine material that was transported towards the southern edges of these ice sheets. With the disintegration of the large ice sheets during the deglaciation, vast previously glaciated areas and forelands were left behind covered with fresh material. As fluorite is rather soluble in water, CF$_4$ could be released from the granites already at an early weathering phase at the start of the interglacial.

The second feature of our record is a long-term increase of CF$_4$ starting at around 420 kyr that is superimposed on the glacial/interglacial cyclicity. The onset of this long-term rise occurs at a distinct point in time as this period marks the Mid-Brunhes event (MB). Interglacial warm phases occurring after the Mid-Brunhes event are typically more intense (e.g. higher CO$_2$ and sea level) than the interglacials before. During these so called lukewarm interglacials the sea level did not reach the current Holocene values, implying that some ice sheets in Canada or Scandinavia survived the deglacial retreat.

External climate forcings, like orbital parameters, are not systematically different for the intervals before and after the MB, thus cannot explain this regime shift. Therefore, internal changes, like the gradual removal of the deep regolith layer that once covered the Canadian shield throughout the Pliocene and Mid-Pleistocene may have caused this change in ice sheet response. Since large igneous provinces with outcropping granites (CF$_4$-bearing source rock) overlap with regions covered by the North American and Fennoscandian ice sheets, the CF$_4$ rise may point to changes in these regions. For example, the regolith or saprolite layer covering the granite has likely lost all the CF$_4$ that was originally present in the granite. Once this layer has been scraped off, glacial erosion reaches the unweathered granite below and thus provides material for an additional source of CF$_4$. Overall, our CF$_4$ record measured on Antarctic ice core samples shows that a fancy organic gas located in trace amounts in granitic rocks provides clues on the temporal evolution of large-scale changes in weathering or other landscape processes. However, our knowledge on the processes determining the amount of CF$_4$ produced in granites and other fluorite-bearing rocks is very limited. Therefore, more measurements of CF$_4$ in rock samples are highly needed to further explore this new parameter.

REFERENCES

Deeds, D. A., Kulongoski, J. T., Mühle, J., and Weiss, R. F. 2015: Tectonic activity as a significant source of crustal tetrafluoromethane emissions to the atmosphere: Observations in groundwaters along the San Andreas Fault, Earth and Planetary Science Letters, 412, 163-172.

Harnisch, J., Borchers, R., Fabian, P., Gäggeler, H. W., and Schotterer, U. 1996: Effect of natural tetrafluoromethane, Nature, 384, 32-32.

Harnisch, J., Frische, M., Borchers, R., Eisenhauer, A., and Jordan, A. 2000: Natural fluorinated organics in fluorite and rocks, Geophysical Research Letters, 27, 1883-1886.

Kranz, R. 1966: Organische Fluor-Verbindungen in den Gaseinschlüssen der Wölsendorfer Flussspäte, Naturwissenschaften, 53, 593-600.

P 2.36

A method for determining magmatic volatile records by FTIR analysis of unexposed melt inclusions and their minerals hosts

Peter Tollan [1], Ben Ellis [2], Juliana Troch [2], Julia Neukampf [2], Olivier Bachmann [2], Jörg Hermann [1]

[1] Intitut für Geologie, Universität Bern, Baltzerstrasse 1, CH-3012 Bern (peter.tollan@geo.unibe.ch)
[2] Departement Erdwissenschaften, ETH Zürich, Sonneggstrasse 5, CH-8092 Zürich

Melt inclusions provide one of the few opportunities to directly measure magmatic volatile concentrations. Transmission Fourier transform infrared spectroscopy (FTIR) is an accurate, precise and cost-effective method of achieving this. However, sample preparation is highly challenging, requiring that crystals are individually polished such that melt inclusions are double-exposed at both top and bottom surfaces and then their thickness precisely determined. This is not only time-consuming and difficult, but results in the destruction of almost the entire crystal and the remaining volatile record contained within. Here we show that the attenuation of the infrared absorption band relating to the Si-O structure of the quartz at 2136 cm^{-1} can be used to determine the thickness of melt inclusions in quartz crystals several hundred microns thick without the need to double-expose. This thickness estimate can then be used in combination with O-H related absorption at 5230 cm^{-1}, 4520 cm^{-1} and C-O related absorption at 2350 cm^{-1} to calculate water concentration, water speciation and CO_2 concentration. Principle advantages of this method are much quicker and easier sample preparation, the ability to measure many melt inclusions per crystal and to assess variations of volatile contents in inclusions trapped in the core and the rim of the host. Additionally there is the possibility to combine this with complementary measurements of OH within the host mineral itself to assess volatile equilibrium.

We demonstrate the effectiveness of this method by reporting H_2O and CO_2 for 38 melt inclusions trapped within 11 quartz crystals from the 1.3 Ma Mesa Falls Tuff, Yellowstone Volcanic Field. H_2O and CO_2 concentrations average 3.1± 0.3 wt.% and 129 ± 46 ppm respectively, with CO_2 showing a much greater spread in concentration over relatively invariant H_2O. In general there are no significant differences between volatile concentrations of fully encapsulated melt inclusions at the crystal cores and rims indicating limited influence of post-entrapment degassing. Melt embayments which are open to the external environment however have significantly lower water concentrations (0.9-2.4 wt.%), although their CO_2 concentrations are indistinguishable from melt inclusions at the crystal cores. Quartz crystals themselves contain 17 ± 4 ppm water, with the infrared spectra revealing charge balance of H^+ by Al^{3+}. Concentration maps show that H_2O is strongly zoned, with progressively less water towards the crystal rim, in contrast to the melt inclusion record. Laser ablation profiles show that Al has a similar concentration distribution, indicating that the H_2O profiles are mainly controlled by the availability of Al in quartz, rather than due to diffusive loss, explaining why the melt inclusions show such limited core-rim variation. Further work will combine these directly measured volatile concentrations with estimates from rhyolite-MELTS modelling and mineral hygrometry, establishing a uniquely detailed view of volatile evolution for the Yellowstone magmatic system.

P 2.37

Thermal perspectives on the diversity and temporal evolution of magma chemistry

Gregor Weber, Guy Simpson & Luca Caricchi

Department of Earth Sciences, University of Geneva, Rue des Maraîchers 13, CH-1205 Geneva (gregor.weber@unige.ch)

Detailed chemical analyses of single volcanic and plutonic complexes has revealed that some magmatic systems are prone to produce a wide range of compositions, while others sample rather monotonous chemistry through time. It has been suggested that these differences are related to barriers in magma properties like density and viscosity. The reason why such filters would act with large differences in efficiency between neighboring volcanoes remains, however, enigmatic.

We designed a combined thermal and petrological model to explore how magma injection rates are linked to the chemical variablity and long-term temporal evolution of mid to lower crustal magma reservoirs. To quantify the possibility of finding magma of a specific chemistry through time, we calculated a weighted average mobile magma composition, which we defined as magma with less than 50% crystals and all the interstitial melt. We find that the average mobile magma chemistry generally evolves in a reversed sense of igneous differentiation from silicic towards more mafic in time. Similar trends are sometimes observed in the plutonic and volcanic rock record, which indicates that they are linked to the incremental assembly of magmatic bodies. Our analysis also shows that the long-term geochemical variability relates to the frequency-size distributions of injections and the thermal state of the crust. High frequency pulses of small batches of magma into relativley hot or deep crustal settings produce tighter chemical variability compared to less frequent but larger recharge events into colder or more shallow environments. Our combined numerical and petrological model provides a framework to link the temporal evolution of magma chemistry in the volcanic and plutonic record to magma fluxes and the thermal architecture of magmatic systems.

P 2.38

Insights into formation of epidosites in oceanic crust from reactive-transport modeling

Samuel Weber [1], Larryn W. Diamond [1], Peter Alt-Epping [1]

[1] Institute of Geological Sciences, University of Bern, Baltzerstrasse 3, CH-3012 Bern (weber@geo.unibe.ch)

Basaltic oceanic crust is subject to extensive fluid-rock interaction soon after its formation. Driven by hot, shallow intrusives, infiltrating seawater is heated and chemically modified by chemical reactions with basaltic wall-rocks. The rocks in turn are pervasively altered to «spilites» consisting of chlorite + albite + quartz + hematite + titanite ± actinolite, commonly with relict augite. Along the discharge path of these convective systems, the fluid is thought to alter pre-existing spilites to «epidosites», i.e. rocks consisting of epidote + quartz + Fe-oxides + titanite. When the fluid reaches the seafloor at focused vents, it may form black smokers, eventually producing volcanogenic massive sulfide (VMS) deposits.

Epidosites have been studied from various ophiolites as well as from recent oceanic settings. They are usually reported from the sheeted dyke complex, but large epidosites also occur in the pillow lavas in the Semail Ophiolite in Oman.

In this study we have used thermodynamic calculations at subseafloor pressures and temperatures to constrain the range in fluid compositions that can produce massive epidosites via metasomatism. Mineral parageneses found at epidosite reaction fronts in combination with reactive-transport modeling further constrained essential fluid parameters such as Ca and Na activities and the pH of the fluid. Additionally, water–rock ratios required for the formation of epidosites could be calculated using the reactive-transport code Flotran. The model ratios are far greater than those proposed in the literature based on isotopic tracers, but they are comparable to those based on hydrothermal experiments. Overall, the modelled results reproduce the changes in mineralogy, whole-rock composition and rock porosity observed in the Semail Ophiolite.

P 2.39

Hydrothermal alteration associated with volcanogenic massive sulfide (VMS) deposits in the Semail Ophiolite, Oman

Nicolas Zuluaga [1], Thomas Belgrano [1] and Larryn W. Diamond [1]

[1] Institute of Geological Sciences, University of Bern, Baltzerstrasse 1+3, CH-3012 Bern, Switzerland
  (nicolas.zuluagavelasquez@students.unibe.ch)

High geothermal gradients during the formation of oceanic crust drive deep circulation of seawater and chemical exchange with the rocks along its fluid pathways. If this modified fluid discharges on the seafloor through focused vents, it forms black smokers that may develop into volcanogenic massive sulfides (VMS) deposits. Alteration around the underlying stockwork zone of these deposits is characterized by replacement of the precursor basalt to assemblages of pyrite + quartz + chlorite. Interestingly, the Fe content of this chlorite tends to increase towards the main upflow zone beneath these deposits (Zierenberg et al., [1988]). This gradient may shed light on the composition of the upwelling fluid and mixing between this fluid and Mg-rich unmodified seawater. Moreover, understanding this gradient may lead to improved exploration vectoring. One way to map this gradient is via short-wave infrared (SWIR) spectrometry, as the Mg-Fe(OH) SWIR absorption features of chlorite vary dependently with Mg# (Lypaczewski and Rivard, [2018]; Neal et al., [2017]).

The Semail Ophiolite hosts numerous VMS deposits in its mafic extrusive sequence (Gilgen et al., [2014]), and thus represents an excellent opportunity to test for alteration patterns. However, little is known about the structure and footwall alteration of these deposits. To address this, we mapped the lithologies and alteration styles in the pits of previously-mined VMS deposits and sampled the altered footwall basalts. Thereafter we measured SWIR spectra of the chloritised samples using a Portable Infrared Mineral Analyzer (PIMA). We applied a Savitzky-Golay filter ([1964]) to smooth the SWIR spectra and to obtain precise spectral positions for the Mg-Fe(OH) vibration peak. These positions are then compared to chlorite compositions analysed by election microprobe to test previously published spectral proxies for composition.

Preliminary results show that two distinct alteration styles exist around the deposits: a proximal alteration with Fe-rich chlorite associated with minor quartz and sulfides, and an overprinting regional alteration with Mg-rich chlorite and albite. The Mg# of these chlorites varies from 0.45 to 0.75 and the corresponding SWIR spectra are shifted by at least 30 nm between the two compositions. Further work will aim to describe the gradient between these composition and fingerprint VMS-related from overprinting chlorite.

REFERENCES

Gilgen, et al., 2014: Sub-seafloor epidosite alteration: Timing, depth and stratigraphic distribution in the Semail ophiolite, Oman. Lithos 260: 191-210.

Lypaczewski, P. & Rivard, B. 2018: Estimating the Mg# and AlVI content of biotite and chlorite from shortwave infrared reflectance spectroscopy: Predictive equations and recommendations for their use. Applied Earth Observation and Geoinformation 68: 116-126.

Neal, L., Wilkinson, J.J., Mason, P.J. & Chang, Z. 2017: Spectral characteristics of propylitic alteration minerals as a vectoring tool for porphyry copper deposits. Journal of Geochemical Exploration 184: 179-198.

Savitsky, A. & Golay, M.J.E. 1964: Smoothing and differentiation of data by simplified least squares procedures. Analytical Chemistry 36: 1627-1639.

Zierenberg, R.A., Shanks III, W.C., Seyfried, W.E., Koski, R.A. & Strickler, M.D. 1988: Mineralization, alteration, and hydrothermal metamorphism of the ophiolite-hosted Tuner-Albright sulfide deposit, Southwestern Oregon. Journal of Geophysical Research 93: B5: 4657-4674.

P 2.40
Relationships of banded amphibolites and Ordovician orthogneisses in pre-Variscan basements of the Alps

Roger Zurbriggen

Feldmatt 10, CH-6206 Neuenkirch (roger-zurbriggen@bluewin.ch)

Despite of the individual character of each of the pre-Variscan basement units of the Alps, they show analogous formations (paragneisses, migmatites, peraluminous orthogneisses, and amphibolites) and structures indicating similar genetic processes. There is consensus regarding the protoliths of the gneisses and migmatites. But the protoliths of the amphibolites are under discussion because their age is largely unknown and original structures often are overprinted by Variscan and Alpine tectonics. However, the amphibolites (i) are typically banded from millimeter to meter-scale (in all units; e.g., Fig. 1a), (ii) are intercalated with para- and orthogneisses on a map-scale (especially in the Aar massif and Silvretta nappe), (iii) can vary in percentage from 3 area% (Strona-Ceneri zone) to 22 area% (Silvretta nappe), (iv) are associated with metagabbros, meta-ultramafics and (meta-) eclogites (in all units), (v) can be migmatic and occur within migmatite formations (Aar massif).

Most studies interpret the banded amphibolites as members of an ophiolite sequence (due to their MORB signature and association with eclogites and ultramafic rocks) or bimodal metavolcanics (due to their compositional banding). Both tectonic settings are supported by case studies. But from a general perspective of subduction-accretion tectonics of the Ordovician orogeny (Fig. 1b and Zurbriggen 2017) they cannot serve as main setting due to following reasons: A clear ubiquitous ophiolite stratigraphy is lacking and obduction is the exception rather than the rule in accretionary complexes. Furthermore, a rhythmic alteration of acidic and basic layers of volcanic rocks might occur as local phenomenon but is unlikely to explain banded amphibolite formations over geographically large distances.

New field observations from Sassella (Silvretta nappe), Lötschental, Betten, Gletsch (Aar massif), Val Piora (Gotthard nappe), and Molinetto (Strona-Ceneri zone) indicate that the banding of the amphibolites results from a tectono-metamorphic overprint of (i) sets of mafic dykes, (ii) multiple intrusions and intermingling of acidic, intermediate and mafic magmas, (iii) migmatites, and (iv) tectonic mélanges of sediments, mafic and ultramafic rocks.

This large variety of protoliths of banded amphibolites (Fig. 1c) reflects the dynamics in a subduction channel, the overlying mantle wedge and the base of a subduction-accretion complex (Fig. 1d). The mantle underneath large subduction-accretion complexes can be of lithospheric and asthenospheric type and its melting can be induced by fluids and decompression, respectively. As a result, large amounts of basaltic melts intrude the accreted sediments and induce their melting. This produced a similar amount of peraluminous magmas, the cause for widespread acidic Ordovician magmatism in these basement units.

It is proposed that the production of banded amphibolite formations occurs in two major steps. The first step is related to magma interaction processes in the "zone of intermingling" (c. 5-10 km thick) at the base of a subduction-accretion complex (Fig. 1b). There, basaltic melts (and slices of mélange diapirs containing ultramafics and eclogites) intrude the metagreywackes causing their melting. The solidus of a basaltic melt (c. 900°C; drawn in Fig. 1b) is near to the liquidus of greywacke. Therefore, homogeneous mixing of the two major magmas is unlikely as can be observed in the compositional gap in chemical diagrams. Thus, dyke intrusion and intermingling are major processes, which significantly increase the interface area and resulting heat exchange between crystallizing basaltic melts and cooler metagreywackes and their peraluminous melts (Fig. 1d).

The second step is related to thrusting within the accretionary complex. Similarly as the peraluminous magmas, which intrude syntectonically along steep thrust zones to form sheets of orthogneisses, the intermingled and interlayered mafics are sheared into steep thrust zones and get mylonitized under amphibolite facies conditions. The products are banded amphibolites in all variations. Their spatial association with metagabbros, meta-ultramafics and (meta-) eclogites is due to the intersection of the steep thrust zones with the "zone of intermingling" (Fig. 1b) containing these lithologies as described above (see first production step).
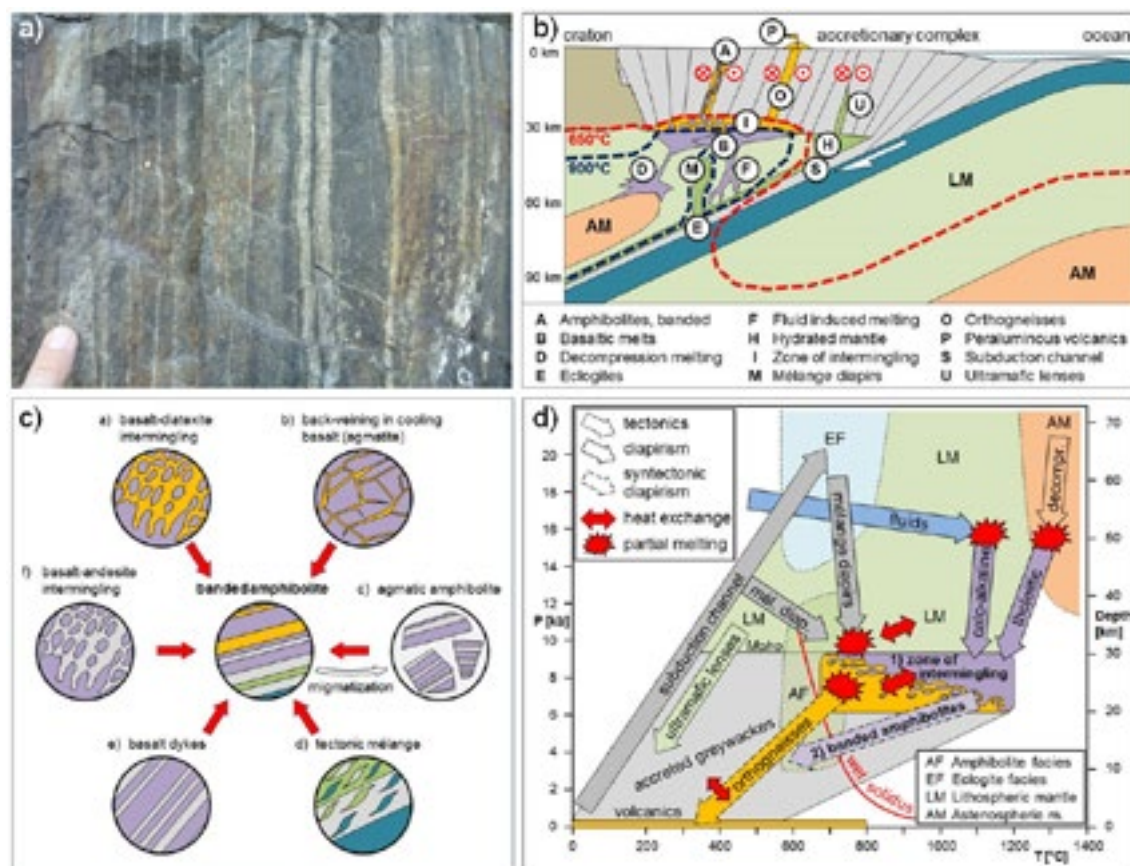
Figure 1. (a) Banded amphibolite from Molinetto (Strona-Ceneri zone; finger for scale). (b) Tectonic setting of an early Paleozoic subduction-accretion complex (Zurbriggen 2017). (c) Scheme of possible protoliths (a-f), which are metamorphosed and mylonitized (red arrows) to result in banded amphibolite. (d) P-T diagram illustrating the two-step production of banded amphibolites in a subduction-accretion complex with peraluminous magmatism.

REFERENCES
Zurbriggen, R. 2017: The Cenerian orogeny (early Paleozoic) from the perspective of the Alpine region. IJES, 106, 517–529.

03. Non-traditional stable isotope geochemistry: development and applications

Afifé El Korh, Andres Rüggeberg

TALKS:

3.1 Greber N.D. (Recipient Paul Niggli Medal)   Invited talk: The U and Mo isotopic compositions of Archean granitoids

3.2 Grosjean M., André-Mayer A.S., Deloule E., Turlin F., Eglinger A., Muchez P., Debruyne D., Voudouris P., Rouxel O.: SIMS Cu-isotopes study: Cu-sulfides standard elaboration and application on the Copperbelt (RDC, Zambia)

3.3 Looser N., Guillong M., Laurent O., Fernandez A., Samankassou E., Moscariello A., Bernasconi S.M.: Tracking temperature and $\delta^{18}O_{fluid}$ evolution during burial with combined carbonate clumped isotopes and in-situ (LA-ICP-MS) U-Pb dating – A case study in the Swiss Jura Mountains

3.4 Nägler, T F., Pierret M.-C., Voegelin A.R., Pettke T., Aschwanden L., Villa I.M.: Small catchment scale Mo isotope balance and its implications for global Mo isotope cycling

3.5 O'Sullivan E., Nägler T., Wille M., Kamber B.: Ocean redox state at the dawn of the Boring Billion: Mo isotopic constraints from a 1.85 Ga black shale

3.6 Pathak D., Mezger K.: A non-traditional stable isotope method to understand Sn isotope fractionation in geochemical and cosmochemical processes

3.7 Rickli J., Janssen D., Elwood M., Hassler Ch., Jaccard S.: Southern Ocean dissolved chromium isotope compositions

3.8 Wolf M., Romer R.L., Glodny J.: Isotopic fractionation (Li, B, Sr, Nd, and Pb) during partial melting

3.1
The U and Mo isotopic compositions of Archean granitoids

Nicolas D. Greber [1]

[1] Départment de Science de la Terre, Université de Genève, Rue de Maraîchaire 13, CH-1205 Genève,
   nicolas.greber@unige.ch

Molybdenum and U isotopic compositions of marine sedimentary rocks are increasingly used to reconstruct changing redox conditions of the ocean and the atmosphere as far back as around 3.0 billion years. The interpretation of the sedimentary record relies on established U and Mo isotope and element cycles of the modern oceans. An important aspect of these oceanic cycles are the U and Mo input signatures. It is generally assumed that weathering of emerged landmasses is one of the major sources of Mo and U to the oceans. To date, these continental contributions are estimated using U and Mo compositions of modern igneous rocks. Consequently, the interpretation of the Archean sedimentary record relies on the assumption that the U and Mo isotopic composition of the emerged continental crust stayed constant over time. This, however, has never been tested. Here, U and Mo isotopic compositions and concentrations of 2.8 to 3.1 billion year old TTGs from the northern Kaapvaal Craton and Southern Marginal Zone of the Limpopo Belt are presented. All TTGs have significantly lower U and Mo concentrations than their modern counterparts, in agreement with previously published values. The Mo isotopic compositions of the TTGs vary significantly, but in average they show a positive offset compared to the bulk silicate Earth (BSE). This isotopic pattern agrees with that of modern granites and granodiorites, which are also around 0.3‰ heavier than the BSE (Yang et al., 2017). The U isotopic compositions of the TTGs range from -0.05‰ to -0.25‰ and thus overlap with the signature of modern granites and granodiorites (Tissot and Dauphas 2015). However, they average at a heavier value (-0.19 ± 0.04 ‰) than that of modern felsic rocks and the estimate of the continental crust (around -0.30 ‰). Even though the low spatial resolution of the data set prevents from estimating a global average U and Mo isotopic composition of the Archean continents, these preliminary results call for a more rigorous assessment of the isotopic composition of Archean igneous rocks.

REFERENCES

Yang, J., Barling, J., Siebert, C., Fietzke, J., Stephens, E., & Halliday, A. N. (2017). The molybdenum isotopic compositions of I-, S-and A-type granitic suites. Geochimica et Cosmochimica Acta, 205, 168-186.

Tissot, F. L., and Dauphas, N. (2015). Uranium isotopic compositions of the crust and ocean: Age corrections, U budget and global extent of modern anoxia. Geochimica et Cosmochimica Acta, 167, 113-143.

3.2
SIMS Cu-isotopes study: Cu-sulfides standard elaboration and application on the Copperbelt (RDC, Zambia)

Marion Grosjean [1], Anne-Sylvie André-Mayer [2], Etienne Deloule [3], François Turlin [2],[°], Aurélien Eglinger [2], Philippe Muchez [4], David Debruyne [4], Panagiotis Voudouris [5] and Olivier Rouxel [6]

[1] Department of Earth Sciences, University of Geneva, Switzerland
[2] GeoRessources, Université de Lorraine, CNRS, CREGU, France
[3] CRPG, CNRS, Université de Lorraine, France
[4] KU Leuven, Geodynamics and Geofluids Research Group, Department of Earth and Environmental Sciences,
   Celestijnenlaan 200E, 3001 Leuven, Belgium
[5] National and Kapodistrian University of Athens, Faculty of Geology & Geoenvironment,
   Dept. of Mineralogy and Petrology, Athens, Greece
[6] IFREMER, Laboratoire Cycles Géochimiques et ressources, Brest, France
[°] Now at: Université du Québec à Montréal, Département des Sciences de la Terre et de l'Atmosphère, Montréal, Canada

Cu isotopes have rarely been studied via in situ method. This study constitutes one of the first SIMS Cu-isotope analyses. They have been carried out in the CRPG laboratory (Nancy, France) on a Cameca IMS 1270 - 1280HR2. The elaboration of a Cu standard was necessary to obtain accurate results and to quantify the matrix effect. A chalcopyrite standard (Plm ccp standard) from the Stanos shear zone (Paliomylos transect, Greece) was first calibrated via conventional methods, on the Thermo-Neptune MC-ICP-MS of the IFREMER institute (Brest, France). Its true value was determined at $\delta^{65}Cu=0.445‰$. This standard was used to define two secondary reference materials, another chalcopyrite standard (Lmw ccp standard) and a bornite standard (Lmw bn standard) from the Lumwana Cu deposit (Western Zambian Copperbelt). Cu isotopes signatures from chalcopyrites of the Central African Copperbelt (CAC) were measured and normalized to the different standards (Figure 1). The CAC presents two generations of Cu-sulfide stocks (Selley et al. 2005, Muchez et al., 2015, Turlin et al., 2016). In the Congolese and Eastern Zambian Copperbelt, the first generation consists of diagenetic mineralization which is followed by a second orogenic Cu-sulfide stock, during the compressive stage of the Pan African orogeny (Muchez et al., 2015; Selley et al., 2005). This study has been led to provide constrain on the source of the different generations of sulphides hosted by the kyanite-micaschists of the Lumwana deposit (Western Zambian part of the CAC). It is still unclear whether the syn-orogenic Cu-sulfide stock is a reworking of a diagenetic mineralization (Figure 1) or if they have different sources (Turlin et al., 2016).

Cu isotopes signatures of the Lumwana diagenetic mineralization have been compared to (i) the Cu isotope signatures of the syn- and post-orogenic mineralization of the Lumwana deposit and to (ii) the Cu isotope signatures of several generations of sulphides in the Congolese and Eastern Zambian Copperbelt. Chalcopyrite from the whole Copperbelt (Congolese, Eastern Zambian and Western Zambian) display Cu isotope signatures ranging between -2.42±0.07‰ and +1.56±0.04‰ (Figure 1).

In the Western Zambian Copperbelt, signatures of the Lumwana diagenetic sulfide stock are similar to those of the late-Lufilian stock. No clear comparison can be established with mineralization of the Congolese and Eastern Zambian Copperbelt. The average $\delta^{65}Cu$ of several deposits tends to show an enrichment in ^{65}Cu with increasing $P\text{-}T$ conditions. However, this observation is not systematic and the origin of the fractionation needs to be better understood. Future $\delta^{65}Cu$ signatures on bornite will provide complementary data to constrain the comparison of the different sulfide stock signatures. The present study gives a first database of the Cu isotopes signatures for Cu-sulfides of the deposits from all metamorphic facies of the Copperbelt and represents a unique database to discuss Cu-isotopes fractionation during the mineralization process(es).
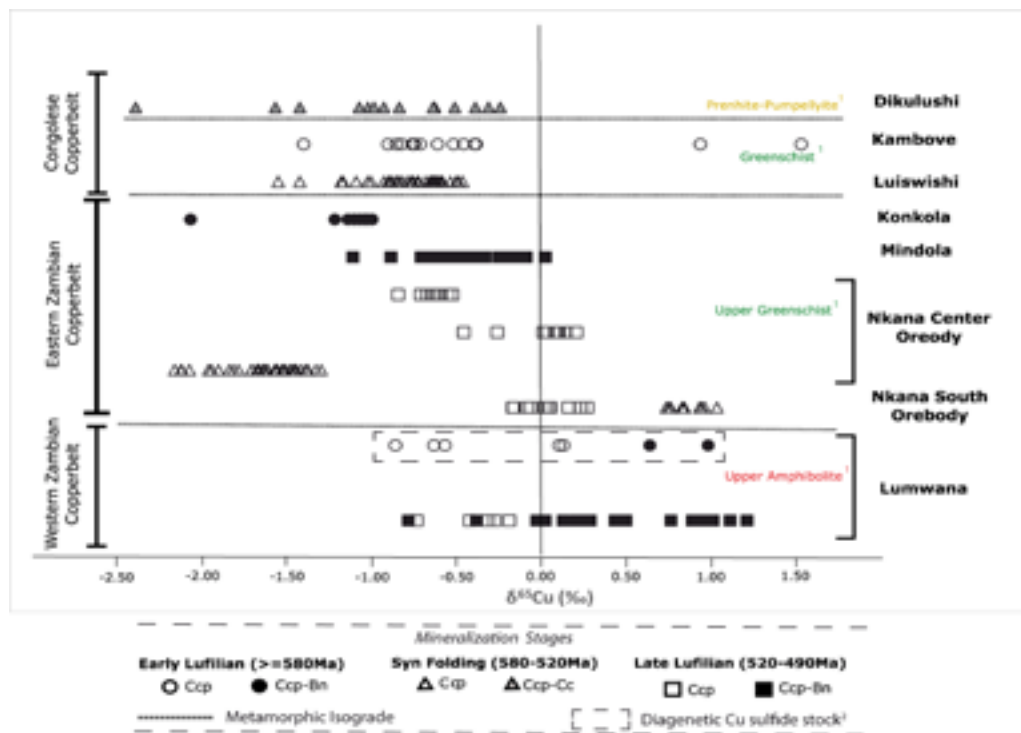
Figure 1. Synthesis diagram of the geological data related to chalcopyrite Cu-isotopes signatures in the CAC Copperbelt. Ages of the different mineralization stages are from Haest et al. (2010), Muchez et al. (2015), Selley et al. (2005) and Turlin et al. (2016). Other references: 1 = Selley et al. (2005); 2 = Turlin et al. (2016). Abbreviations: Bn = bornite; Cc = chalcocite; Ccp = chalcopyrite;.

REFERENCES

Haest, M., Schneider, J., Cloquet, C., Latruwe, K., Vanhaecke, F., Muchez, P., 2010. Pb isotopic constraints on the formation of the Dikulushi Cu–Pb–Zn–Ag mineralisation, Kundelungu Plateau (Democratic Republic of Congo). Miner. Deposita 45, 393–410.

Muchez, P., André-Mayer, A.-S., El Desouky, H.A., Reisberg, L., 2015. Diagenetic origin of the stratiform Cu–Co deposit at Kamoto in the Central African Copperbelt. Miner. Deposita 50, 437–447.

Selley, D., Broughton, D., Scott, R., Hitzman, M., Bull, S., Large, R., McGoldrick, P., Croaker, M., Pollington, N., Barra, F., 2005. A new look at the Geology of the Zambian Copperbelt. Soc. Econ. Geol. 100th Anniversary Volume, 965–1000.

Turlin, F., Eglinger, A., Vanderhaeghe, O., André-Mayer, A.-S., Poujol, M., Mercadier, J., Bartlett, R., 2016. Synmetamorphic Cu remobilization during the Pan-African orogeny: Microstructural, petrological and geochronological data on the kyanite-micaschists hosting the Cu(–U) Lumwana deposit in the Western Zambian Copperbelt of the Lufilian belt. Ore Geol. Rev. 75, 52–75.

3.3

Tracking temperature and $\delta^{18}O_{fluid}$ evolution during burial with combined carbonate clumped isotopes and in-situ (LA-ICP-MS) U-Pb dating – A case study in the Swiss Jura Mountains

Nathan Looser [1], Marcel Guillong [1], Oscar Laurent [1], Alvaro Fernandez [1], Elias Samankassou [2], Andrea Moscariello [2] & Stefano M. Bernasconi

[1] Department of Earth Sciences, ETH Zurich, Sonnegstrasse 5, CH-8092 Zurich (nathan.looser@erdw.ethz.ch)
[2] Department of Earth Sciences, University of Geneva, Rue de Maraîchaire 13, CH-1205 Geneva

Carbonate clumped isotopes allow to reconstruct the temperature of carbonate mineral formation as well as the $\delta^{18}O$ of the precipitating fluids in the temperature range between ambient temperatures and 200–300 °C (Eiler 2011). When different diagenetic carbonate phases are identified, the ambient burial temperatures and the $\delta^{18}O_{fluid}$ compositions at the corresponding stages of the diagenetic and thermal history can be determined without the need for any assumptions about the fluids involved as it is the case when using conventional oxygen isotopes. Thanks to the recently developed in-situ laser ablation-inductively coupled plasma-mass spectrometry (LA-ICP-MS) U-Pb dating of carbonates (Li et al. 2014) it is now possible to date carbonate cements and veins on sub-mm scales, allowing to set absolute time frames for diagenetic and tectonic events.

In this study, we apply this new tool of combined carbonate clumped isotopes and in-situ U-Pb dating (Δ_{47}/U-Pb thermochronology) to constrain the diagenetic and thermal history of Late Triassic and Early Jurassic formations in the Swiss Tabular Jura Mountains. Thereby, we also compare our findings with an existing basin evolution model (Mazurek et al. 2006). Analyzed calcite and dolomite phases include various diagenetic cements, different generations of veins, mineralogically preserved and recrystallized fossils, nodules, and matrix. The temperatures acquired in the analyzed diagenetic carbonates range between ambient and approx. 140 °C and the calculated $\delta^{18}O_{fluid}$ compositions show variations of more than 20 ‰ over the last 200 Ma.

REFERENCES

Eiler, J. M. 2011: Paleoclimate reconstruction using carbonate clumped isotope thermometry. Quaternary Science Reviews, 30, 3575–3588.

Li, Q., Parrish, R. R., Horstwood, M. S. A., and Mc Arthur, J. M. 2014: U-Pb dating of cements in Mesozoic ammonites. Chemical Geology, 376, 76–83.

Mazurek, M., Hurford, A. J., and Leu, W. 2006: Unravelling the multi-stage burial history of the Swiss Molasse Basin: integration of apatite fission track, vitrinite reflectance and biomarker isomerisation analysis. Basin Research, 18, 27–50.

3.4
Small catchment scale Mo isotope balance and its implications for global Mo isotope cycling

Thomas F. Nägler [1], Marie-Claire Pierret, Andrea R. Voegelin [1], Thomas Pettke [1], Lukas Aschwanden [1], Igor M. Villa [1] [3]

[1] Institut für Geologie, Universität Bern, Baltzerstrasse 1+3, CH-3012 Bern (naegler@geo.unibe.ch)

[2] Laboratoire d'Hydrologie et de Géochimie de Strasbourg, EOST, Université de Strasbourg/CNRS, 1 rue Blessig, F-67084 Strasbourg

[3] Centro Universitario Datazioni e Archeometria, Università di Milano Bicocca, I-20126 Milano

The mass balance of molybdenum (Mo) was studied in the Strengbach catchment (eastern France, 440 km of the nearest coast). Monitoring of rainfall, vegetation, and soil characteristics in this 0.8 km2 catchment was started decades ago. We present Mo concentrations and isotope compositions of about 60 samples including bedrock types, perennial springs, soil profiles, and the roots and leaves of two tree species, and finally the outflowing brook. Both stream waters and bedrocks show Mo concentrations at least one order of magnitude lower than global averages. The Mo isotope composition of topsoils and organic matter (foliage, litter, and roots) is rather homogeneous. Net biological fractionation is thus subordinate to the differences in the Mo sources. The efficient Mo recycling from organic litter to plants keeps Mo bioavailable. The Mo data, supplemented with new and literature Sr isotope data, are used to identify the source(s) of Mo and Sr and their (transient) storage within the catchment. The resulting best model identifies rock weathering and seawater derived aerosol as the principal Mo sources, indicating a 23 % to 44 % Mo fraction of seawater origin in the dissolved load. Moreover, soil in the Strengbach catchment has reached steady state for Mo (the time constant to achieve soil steady state is calculated to be in in the order of 50 years) i.e. the Mo isotope composition of fluxes to and from the catchments soil are identical. To date, all global Mo isotope cycling models have assumed a continental runoff value based on inferred average continental crust signatures and/or river water averages, where the latter are taken as representing a weathering product of the former. Our finding of a prominent fraction of the Mo in surface waters of the Strengbach catchment being derived from marine aerosols -even hundreds of km away from the seashore- implies that future Mo isotope global cycling models need to take into account the recoupling of airborne Mo. The exact mass balance of contributing Mo sources to the bulk airborne load, are unknown at present. Additional possible contributions to the aerosol input (volcanic exhalations, fixation of aerosols onto atmospheric dust particles, and anthropogenic sources) are possible but not evident in case of the Strengbach catchment.

3.5
Ocean redox state at the dawn of the Boring Billion: Mo isotopic constraints from a 1.85 Ga black shale

Edel O'Sullivan [1], Thomas Nägler [1], Martin Wille [1] and Balz Kamber [2]

[1] *Institut für Geologie, Universität Bern, Baltzerstrasse 1+3, 3012 Bern (edel.osullivan@geo.unibe.ch)*
[2] *Faculty of Science and Engineering, Queensland University of Technology, Brisbane*

The stepwise oxygenation of the Earth's atmosphere has long been a topic of debate. The use of Mo abundance and isotopic signatures in marine shales and carbonates as a paleoredox indicator has facilitated the reconstruction and refinement of the Great Oxidation Event (ca. 2.45-2.32 Ga) and the subsequent period of quiescence known as the Boring Billion (ca. 1.8 – 0.8 Ga). However, as the number of Mo isotopic case studies grow, it has emerged that the GOE may not have occurred as a single event, but rather as a gradual and variable increase beginning as far back as 2.9 Ga (e.g. Ohmoto et al. 2006). This brings to question whether the current accepted oxygen curve through the Archaean-Proterozoic boundary is an artefact of sample preservation and therefore an incomplete dataset, particularly during the Boring Billion. Here we complement the existing Mo abundance and isotope record with a 1.85 Ga black shale deposited in the wake of the GOE, directly at the beginning of the Boring Billion.

The authigenic enrichment of Mo in marine sediments is in itself an indicator of sufficiently oxidising conditions, which enable mobility of Mo in its highest oxidation state, necessary to build up a dissolved marine Mo reservoir. Its isotopic composition is dependent on the oxic to anoxic/euxinic Mo sedimentation ratio and can provide an indication of the extent of oxic environments in the ocean through time. This ocean signature can be recorded in euxinic sediments, where quantitative removal of Mo by efficient adsorption onto organic particles in the presence of H_2S occurs without fractionation. The Mo isotopic composition of true euxinic black shales is therefore interpreted as reflecting that of the contemporary ocean water.

We have chosen to analyse the Mo isotopic composition of a black shale from the unique post-impact "basin fill" sediments of the 1.85 Ga Sudbury impact crater, Ontario, Canada. The impact is interpreted as having struck a shallow ocean in the active foreland basin of the Penokean Orogenic belt, creating a large crater filled with water within which post-impact volcanism prevailed for up to 200,000 years (Ames et al. 2006). As impact-related processes ceased, the carbonaceous shales of the Onwatin Formation, the focus of this study, were deposited in the resulting depression on the ocean floor. Molybdenum and Uranium enrichment factors of the Onwatin Formation suggest that the samples were deposited in an anoxic deepwater basin in an open ocean setting (O'Sullivan et al. 2016). This, along with high total organic carbon, ranging from ca. 2 to $13_{wt}\%C_{org}$, and the presence of authigenic pyrite, indicates that total scavenging of Mo was likely and thus little or no fractionation of Mo isotopes occurred. It is therefore assumed that the heaviest Mo isotopic value provides a minimum value for the 1.85 Ga global ocean.

REFERENCES

Ames D. E., Jonasson I. R., Gibson H. L. and Pope K. O. 2006: Impact generated hydrothermal system—constraints from the large paleoproterozoic Sudbury Crater, Canada. In Biological Processes Associated with Impact Events (eds. C. Cockell, I. Gilmour and C. Koeberl). Springer, Berlin Heidelberg, pp. 55– 100.

Emerson, S.R., Huested, S.S., 1991. Ocean anoxia and the concentrations of molybdenum and vanadium in seawater. Marine Chemistry 34 (3–4), 177–196.

Ohmoto, H., Watanabe, Y., Ikemi, H., Poulson, S.R., Taylor, B.E., 2006: Sulphur isotope evidence for an oxic Archean atmosphere. Nature 442 (24), 908–911.

O'Sullivan, E. M., Goodhue, R., Ames, D. E. and Kamber, B. S. 2016: Chemostratigraphy of the Sudbury impact basin fill: volatile metal loss and post-impact evolution of a submarine impact basin. Geochimica et Cosmochimica Acta, v. 183, 198–233.

3.6
A non-traditional stable isotope method to understand Sn isotope fractionation in geochemical and cosmochemical processes

Dipankar Pathak [1] & Klaus Mezger [1]

[1] Institut für Geologie, Universität Bern, Baltzerstrasse 1+3, 3012 Bern, Switzerland (dipankar.pathak@geo.unibe.ch)

Tin is a moderately volatile, chalcophile, and siderophile element, and with the highest number of 10 stable isotopes amongst all chemical elements, it provides a great scope to understand metal stable isotope fractionation in different natural processes. It is only now, that due to continuous development of MC-ICP-MS technology, efficient ionisation and thus high precision measurement of Sn isotopes are possible (Laeter & Jeffery, 1965; Laeter & Jeffery, 1967; Loss et al., 1990; McNaughton & Rosman, 1990). We present a robust technique, developed to measure mass-dependent and mass-independent isotope variability of Sn in a range of natural materials containing ~20-1000s of ng Sn, with high precision. One of the most challenging steps in measuring Sn isotope ratios, is sample preparation, and careful attention is required to avoid loss of Sn during sample processing, which can lead to significant isotope fractionation that can obscure the natural signal. Considering the volatile nature of some Sn compounds, a systematic low temperature (≤ 70 ºC) sample processing, together with an organic matter removal method is applied, to address these hindrances in precise and accurate Sn isotope ratio measurements. A multi-staged ion chromatographic technique was developed to isolate Sn from other matrix and interfering elements, capable of achieving ~100% recovery of Sn, even from samples containing as little as ~20 ng of Sn. A double-spike technique is also implemented to correct for fractionation of Sn isotopes during sample processing and analysis. We used a NIST SRM 3161a Sn standard, and several other commercially available Sn standard solutions, to test the viability of this method, amongst which the NIST Sn standard provides the best long-term external reproducibility. With this method, is now possible to measure natural fractionation of Sn isotope ratios with a precision of 2SD = 0.035 ‰ for $\delta^{122/116}Sn$ and 2SD = 0.046 ‰ for $\delta^{122/118}Sn$ (internally correcting instrumental bias, without using double spike), and apply the method to study different chemical fractionation processes during Earth's differentiation and evolution.

REFERENCES

De Laeter, J. R., & Jeffery, P. M. (1965). The isotopic composition of terrestrial and meteoritic tin. Journal of Geophysical Research, 70(12), 2895-2903.

De Laeter, J. R., & Jeffery, P. M. (1967). Tin: its isotopic and elemental abundance. Geochimica et Cosmochimica Acta, 31(6), 969-985.

Loss, R. D., Rosman, K. J. R., & De Laeter, J. R. (1990). The isotopic composition of zinc, palladium, silver, cadmium, tin, and tellurium in acid-etched residues of the Allende meteorite. Geochimica et Cosmochimica Acta, 54(12), 3525-3536.

McNaughton, N. J., & Rosman, K. J. R. (1991). Tin isotope fractionation in terrestrial cassiterites. Geochimica et Cosmochimica Acta, 55(2), 499-504.

3.7
Southern Ocean dissolved chromium isotope compositions

Jörg Rickli [1], David Janssen [1], Michael Elwood [2], Christel Hassler [3] & Samuel Jaccard [1]

[1] Institute of Geological Sciences and Oeschger Centre for Climate Change Research, University of Bern
[2] Australian National University, College of Science, Canberra
[3] University of Geneva, Department F.-A. Forel for environmental and aquatic sciences

Variations in the Cr isotope composition of seawater - expressed as $\delta^{53}Cr$ - may serve as a useful tool for understanding biological and physical processes in the modern and past oceans. Specifically, the relatively short seawater residence time of Cr of a few thousand years and its redox sensitivity may imply that records of past seawater Cr isotope compositions can yield information on shorter time scale changes in seawater redox conditions and biological carbon export. At present, there is, however, only little data available that allows constraining the processes, which govern the spatial $\delta^{53}Cr$ distribution in the modern ocean.

We present dissolved $\delta^{53}Cr$ for several water column profiles from the Subtropical to the Polar Front of the Southern Ocean, collected during the Antarctic Circumnavigation Expedition (ACE). On a site-by-site basis, the profiles are relatively homogenous in terms of Cr concentrations and isotope compositions, with only modest surface ocean Cr depletion and subtle changes towards heavier $\delta^{53}Cr$ values. On a regional scale, there is, however, a relatively strong correlation between $\delta^{53}Cr$ and nitrate concentrations, where nitrate steadily increases southwards while $\delta^{53}Cr$ values decrease. This suggests that the $\delta^{53}Cr$ distribution is linked to nutrient cycling in the Southern Ocean. The Cr data confirms and isotopic fraction of $\varepsilon \cong -0.8$ during Cr uptake, consistent with earlier findings (Scheiderich et al., 2015).

REFERENCES

Scheiderich K., Amini M., Holmden C. and Francois R. 2015: Global variability of chromium isotopes in seawater demonstrated by Pacific, Atlantic, and Arctic Ocean samples, Earth Planet. Sci. Lett. 423, 87-97.

3.8
Isotopic fractionation (Li, B, Sr, Nd, and Pb) during partial melting

Mathias Wolf [1], Rolf L. Romer [1] & Johannes Glodny [1]

[1] German Research Centre for Geoscience GFZ, Telegrafenberg, D–14473 Potsdam (mwolf@gfz-potsdam.de)

Radiogenic isotope signatures of magmatic rocks are widely used to constrain the sources and/or contributions of different magma reservoirs based on mass balance calculations. These applications assume isotopic equilibration between the melt and its source. Observations from migmatic rocks show that this assumption may be incorrect and that isotopic fractionation may occur at magmatic temperatures. In these cases, the isotopic signatures do not reflect the sources and mass balance gives incorrect relative contributions.

The Sr, Nd, and Pb isotopic signatures of a partial melt depend on three factors: (i) parent (P) to daughter (D) ratio of the minerals in the protolith, (ii) time between protolith formation and partial melting, and (iii) character of the partial melting reaction. Contrasting P/D ratios (e.g. Rb/Sr, Sm/Nd, and Th,U/Pb) for different mineral phases will with time lead to distinct isotopic signatures that may persist up to conditions of partial melting. The chemical and isotopic contributions to the melt are defined by the nature of the melting reaction and by the phases that participate in partial melting. As the various isotopic systems are controlled by different minerals, melt and restite may show contrasting isotopic signatures. Extraction of early melts modifies the isotopic composition of the restite and changes the nature of the melting reaction, which may lead to contrasting isotopic fingerprints in later melt batches.

As the whole rock Rb and Sr budget is controlled by rock forming minerals, the Sr isotopic signature is controlled by the character of the melting reaction. In contrast, Sm and Nd budgets are largely controlled by accessory phases (e.g. apatite, monazite, allanite, and xenotime). In contrast to common rock forming minerals, their stability is mainly controlled by their solubility in the melt and, therefore, by the composition of the melt and temperature. The behavior of Pb depends on both, rock forming minerals (e.g. feldspar, contributes to common Pb) and accessory phases (e.g. zircon, contributing to radiogenic Pb). As long as the same melting reaction takes place, the Sr and Nd isotopic signature of the melt is buffered by rock forming minerals and the solubility of accessory phases, respectively. In contrast, the restites domains may have highly variable isotopic signatures as the modal abundance of major and minor minerals in these domains varies. Remelting of such isotopically modified restites leads to distinct isotopic signatures in later melt batches that may therefore be misinterpreted to reflect contributions from different reservoirs.

Isotopic fractionation of Li and B results from the contrasting coordination of these elements in different phases and depends on temperature. Fractionation may be particularly strong during low temperature processes. In high-grade metamorphic and magmatic rocks, Li and B isotopic fractionation is commonly assumed to be insignificant. This assumption is in conflict with observed Li and B isotope variations in high-temperature migmatites. Data from a cm-scale melt-restite profile show a step-like change in δ^7Li (7 δ^7Li-units) over the contact, whereas $\delta^{11}B$ shows less variation. These findings suggest that (i) Li and B isotopic compositions of melt and restite are mineralogically controlled and (ii) fractionation by other processes (i.e. diffusive isotope fractionation) is irrelevant at magmatic conditions.

04. Gemmology

Michael S. Krzemnicki, Laurent E. Cartier

Swiss Gemmological Society (SGG)
Swiss Society of Mineralogy and Petrology (SSMP)

TALKS:

4.1   Balmer W.A., Hauzenberger C.A., Fritz H., Sutthirat C.: Marble-hosted ruby deposits of the Morogoro Region, Tanzania

4.2   Krzemnicki M.S.: Colour instability of Padparadscha-like Sapphires

4.3   Myint Myat Phyo, Bieler E., Franz L., Balmer W., Krzemnicki M.S.: A new suite of inclusions in spinel from Mogok (Myanmar) – a study using Raman microspectroscopy and scanning electron microscopy

4.4   Xu W., Link K., Liu C., Kiefert L.: Age determination of zircon inclusions in sapphire from Kashmir and characterization with Raman spectroscopy

4.1
Marble-hosted ruby deposits of the Morogoro Region, Tanzania

Balmer W.A.[1], Hauzenberger C.A., Fritz H., Sutthirat C.

[1] *Department of Geology, Faculty of Science, Chulalongkorn University, Bangkok, Thailand*

The ruby deposits of the Uluguru and Mahenge Mts, Morogoro Region, are related to marbles which represent the cover sequence of the Eastern Granulites in Tanzania. In both localities the cover sequences define a tectonic unit which is present as a nappe structure thrusted onto the gneissic basement in a north-western direction. Based on structural geological observations the ruby deposits are bound to mica-rich boudins in fold hinges where fluids interacted with the marble-host rock in zones of higher permeability. Petrographic observations revealed that the Uluguru Mts deposits occur within calcite-dominated marbles whereas deposits in the Mahenge Mts are found in dolomite-dominated marbles. The mineral assemblage describing the marble-hosted ruby deposit in the Uluguru Mts is characterised by corundum-dolomite-phlogopite ± spinel, calcite, pargasite, scapolite, plagioclase, margarite, chlorite, tourmaline whereas the assemblage corundum-calcite-plagioclase-phlogopite ± dolomite, pargasite, sapphirine, titanite, tourmaline is present in samples from the Mahenge Mts. Although slightly different in mineral assemblage it was possible to draw a similar ruby formation history for both localities. Two ruby forming events were distinguished by textural differences, which could also be modeled by thermodynamic T–XCO_2 calculations using non-ideal mixing models of essential minerals. A first formation of ruby appears to have taken place during the prograde path (M1) either by the breakdown of diaspore which was present in the original sedimentary precursor rock or by the breakdown of margarite to corundum and plagioclase. The conditions for M1 metamorphism was estimated at ~750 °C at 10 kbar, which represents granulite facies conditions. A change in fluid composition towards a CO_2 dominated fluid triggered a second ruby generation to form. Subsequently, the examined units underwent a late greenschist facies overprint. In the framework of the East African Orogen we assume that the prograde ruby formation occurred at the commonly observed metamorphic event around 620 Ma. At the peak or during beginning of retrogression the fluid composition changed triggering a second ruby generation. The late stage greenschist facies overprint could have occurred at the waning stage of this metamorphic episode which is in the range of ~580 Ma.

4.2
Colour instability of Padparadscha-like Sapphires

Michael S. Krzemnicki [1]

[1] Swiss Gemmological Institute SSEF, Aeschengraben 26, CH-4051 Basel (michael.krzemnicki@ssef.ch)

Padparadscha is a sought-after variety of corundum showing subtle pinkish orange to orangey pink colour. Originally known from alluvial deposits in Sri Lanka, similar stones today are also known from southern Tanzania and Madagascar. The colour of padparadscha is mainly related to the presence of traces of Cr^{3+}, Fe^{3+}, and/or colour centers. These colour centers, however, are not all stable when exposed to sunlight, but generally can be reactivated by a short (few minutes) exposure to ultraviolet light. Similar reversible photochromism (or tenebrescence) has already been reported for near colourless corundum and yellow sapphires (Nassau & Valente, 1987; Gaievskyi et al., 2014; Hughes, 2017).

The present study presents spectroscopic data and colour measurements (RGB) of 34 corundum samples with padparadscha-like colour originating from classic deposits in Sri Lanka and from more recent discoveries in Madagascar (Ilakaka and Ambatondrazaka). Interestingly, the specimens from Ambatondrazaka (central Madagascar) show a tendency to change their colour in the course of weeks (or hours by using a fading test) by shifting from pinkish orange (colour centre active) to pure pink (after fading). The instable orange colour can be restored in a few minutes by UV light (Figure 1).

before testing   after 5 minutes LWUV   after fading test

Figure 1. Fancy sapphire from Ambatondrazaka (Madagascar) of 9.1 ct showing pink colour (actually the chromium-related stable colour of this stone), which shifts to pinkish orange after activation of an orange colour centre, and subsequently returns to pure pink after fading (back to stable colour).

Our study reveals that in terms of consumer protection, it is mandatory for any gem testing laboratory to carry out a colour stability test for any padparadscha sapphire, as only stones with a stable colour should be attributed the variety name padparadscha.

REFERENCES

Gaievskyi, I., Iemelianov, I., & Belichenko, E. 2014: Unusual optical effect in blue sapphire, Gems & Gemology, 50, 2, 161-162.

Hughes, R.W. 2017. Ruby & Sapphire: a gemologist's guide. RWH Publishing, Thailand, 816 pp.

Nassau, K., & Valente, G.K. 1987. The seven types of yellow sapphire and their stability to light. Gems & Gemology, 23, 4, 222-231.

4.3
A new suite of inclusions in spinel from Mogok (Myanmar) - a study using Raman microspectroscopy and scanning electron microscopy

Myint Myat Phyo [1], Eva Bieler [2], Leander Franz [1], Walter Balmer [3] and Michael S. Krzemnicki [3]

[1] Institute of Mineralogy and Petrography, University Basel, Switzerland (myintmyat.phyo@unibas.ch)
[2] Swiss Nano Imaging Lab, Swiss Nanoscience Institute, University Basel, Switzerland
[3] Swiss Gemmological Institute SSEF, Aeschengraben 26, 4051 Basel, Switzerland

This is the first detailed study of spinel inclusions from different marble-type gem localities within the Mogok area, Myanmar, using optical microscopy, Raman microspectroscopy and scanning electron microscopy (SEM) equipped with an energy dispersive spectroscopy EDS. For this study we analysed 100 gem-quality spinels of pink to red, orangey, and purplish grey colour, which were collected from six different localities of the Mogok area. 87 alluvial samples were collected by the first author directly from mining sites (Yadanar Kadae Kadar, Bawlongyi, Kyauksin, Kyauksaung, Pyaungpyin and Mansin) and 13 samples were collected from local markets.
Initially, the surfaces of all gem-quality spinel crystals were polished to get an overview on their inclusions. Afterwards, all mineral inclusions were investigated with the polarization microscope and with the Raman spectrometer. Problematic and particularly interesting mineral inclusions were brought to sample surfaces by polishing and finally these mineral inclusions were identified with SEM using secondary electron images (SE), back-scattered electron images (BSE) and energy dispersive spectroscopy (EDS).

The following 17 new minerals were identified for the first time as inclusions in spinel from Mogok (in alphabetical order): amphibole (pargasite), anatase, baddeleyite, boehmite, brucite, chlorite, clinohumite, clinopyroxene, diaspore, goethite, geikielite, gypsum, halite, marcasite, molybdenite, periclase and pyrrhotite. Furthermore, we found anhydrite, apatite, carbonate (calcite, dolomite and magnesite), graphite, chondrodite, phlogopite and zircon, which were already known as mineral inclusions in spinel from Mogok. Particularly interesting is the first discovery of geikielite ($MgTiO_3$) in spinel from the Mogok area. It forms tiny, colourless flakes of maximum 20 µm diameter oriented along the (111) crystallographic direction of spinel. Their regular orientation - presumably as epigenetic precipitates – is related to the spinel structure. This inclusion is similar to geikielite-rich ilmenite exsolution lamellae described from chromite-chrome spinel from metacarbonates of the Oetztal-Stubai complex in Austria (Mogessie et al. 1988). Furthermore, exsolutions of dolomite in calcite inclusions were identified by SEM- BSE and detected with EDS. Numerous solid inclusions consisted of different mineral phases (e.g. calcite intergrown or aggregated with various primary and secondary mineral phases such as dolomite, apatite, anhydrite, gypsum). These intergrowths, however, were beyond the resolution of the Raman microspectroscopy and could only be detected by SEM microscopy.

In conclusion, we found that spinels of gem quality from the six sampled localities within the Mogok area have significantly different populations of mineral inclusions, which are shown in Figure 1. The findings of the present study sheds light on the formation of spinel in the Mogok area and possibly will enable gemmologists to better separate Mogok spinels from those originating from other marble-related spinel deposits worldwide.

Figure 1. The population of inclusions found in spinel in different localities of spinel mines and the gem market in Mogok, Myanmar.

REFERENCES
Mogessie, A., F., Purtscheller, F., & Tessadri, R. 1988: Chromite and chrome spinel occurrences from metacarbonates of the Oetztal-Stubai Complex (northern Tyrol, Austria) *Mineralogical Magazine*, 52, 229-236.

4.4
Age determination of zircon inclusions in sapphire from Kashmir and characterization with Raman spectroscopy

Wenxing Xu [1], Klemens Link [1], Chuanzhou Liu [2] and Lore Kiefert [1]

[1] Gübelin Gem Lab, Maihofstrasse 102 CH-6006 Luzern (wenxing.xu@gubelingemlab.com)
[2] Institute of Geology and Geophysics, Chinese Academy of Sciences, Beijing, 100029, China

Zircon inclusions in selected sapphire samples from Kashmir origin were studied by HR SIMS and Laser-Ablation-ICPMS for U-Pb age determination, as well as Raman spectrometry. The U-Pb age dating results show that Kashmir sapphires are of 24.97 ± 0.22 Ma, which matches within their Alpine-Himalayan orogeny origins. It was also detected that Kashmir zircon inclusion contain significant higher REE and U concentration than zircon from other origins. Furthermore Raman features of zircon inclusions in the Kashmir sapphire showed a similarity of frequency of zircon v1 and v3 band and FWHM, which are related to their trace element content, age, metamictization degree, and pressures within sapphire. Comparing the sapphire from Madagascar, the Raman features provide a non-destructive methodic possibility to distinguish sapphire origins based on their zircon inclusions.
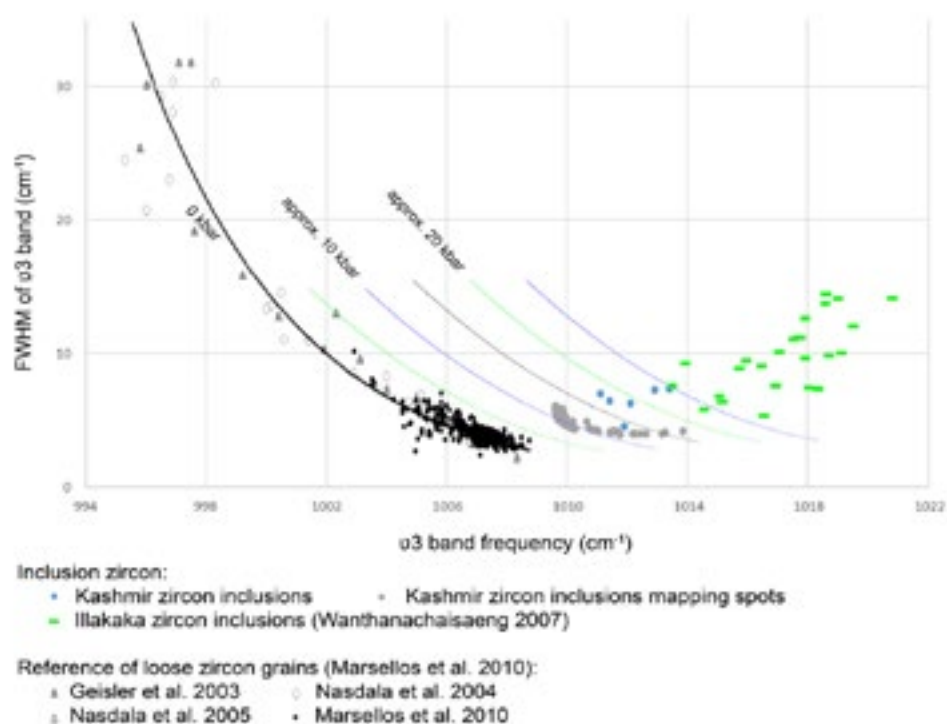
Figure 1. Plotting υ3 band frequency versus FWHM, comparing zircon inclusions in Kashmir sapphire of this study with Ilakaka sapphire and loose zircon from different origins

REFERENCES

Marsellos, A.E., & Garver, J.I., 2010: Radiation damage and uranium concentration in zircon as assessed by Raman spectroscopy and neutron irradiation, American Mineralogist, Volume 95, 1192-1201.

Wang, W., & Scarratt, K., & Emmett J.L., & Breeding C.M., & Douthit T.R., 2006: The effects of heat treatment on zircon inclusions in Madagascar sapphires. Gems and Gemology, 42 (2), 134-150.

Wanthanachaisaeng, B., 2007: The influence of heat treatment on the phase relations in mineral growth systems, PhD Thesis, Johannes Gutenberg University of Mainz. https://publications.ub.uni-mainz.de/theses/volltexte/2007/1463/pdf/1463.pdf

05. Palaeontology

Christian Klug, Torsten Scheyer, Lionel Cavin

*Schweizerische Paläontologische Gesellschaft,
Kommission des Schweizerischen Paläontologischen Abhandlungen (KSPA)*

TALKS:

5.1   Anquetin J., Billet G.: Peer Community in Paleontology (PCI Paleo): a community-driven, transparent, free and open peer-review platform for Paleontology

5.2   Antcliffe J.B.: Anoxia can increase the rate of decay for cnidarian tissue: Using *Actnia equina* to understand the early fossil record

5.3   Burek I., Anquetin J.: New material from the Banné Marls (Kimmeridgian) in Glovelier (JU) reveals novel insights on plesiochelyid turtle morphology

5.4   Daley A.C., Antcliffe J.B., Drage H.B., Pates S.: The early fossil record of Euarthropoda and the Cambrian Explosion

5.5   Ferrante C., Cavin L., Furrer H., Martini R.: Coelacanths from the Middle Triassic of Switzerland show unusual morphology

5.6   Friesenhagen T., Knappertsbusch M.: Test-Size Evolution of the Planktonic Foraminifer *Globorotalia menardii* in the Tropical Atlantic Since the Upper Miocene

5.7   Galasso F., Pereira P., Fernandes P., Spina A., Marques J.: Permian–Triassic palynology of the Karoo Supergroup from the N'Condédzi region, Tete Province,Mozambique

5.8   Gueriau P.: Besides phase-contrast tomography, synchrotron imaging also rhymes with chemical mapping: new advances in 2D synchrotron imaging of fossils

5.9   Klug C., Samankassou E., Pohle A., Zapalski M., Korn D..: Couscous ai frutti di mare – the spectacular Moroccan mudmound locality Hamar Laghdad and its palaeoecology

5.10   Laibl L.: Early post-embryonic stages of Cambrian trilobites: morphological and ecological disparity

5.11   Maridet O., Balme C., Lapauze O., Legal S., Lu X., Mennecart B., Tissier J., Vasilyan D., Costeur L.: The locality of Murs (Southeastern France): Rediscovery of a forgotten Early Oligocene fauna

5.12   Rollot Y., Joyce W.G.: New insights into the cranial circulation and innervation of baenid turtles

5.13   Scheyer T.M., Klein N.: Bone Histology of *Cyamodus hildegardis* (Placodontia: Cyamodontoidea) from the Besano Formation of Monte San Giorgio, Switzerland: inferences for Ecology and Lifestyle

5.14   Tissier J., Antoine P.O., Becker D.: Oligocene-Miocene Rhinocerotidae from Europe: systematics, phylogeny and diversification

5.15   Vasilyan D., Sakahyan L., Hovakimyan H., Lazarev S., Maul L., Caves J.K.: New data on the upper Miocene continental record of Armenia

5.16   Weinkauf M.F.G., Hoffmann R., Wiedenroth K., Goeddertz P., De Baets K.: Morphological disparity and ontogeny of the endemic heteromorph ammonite genus *Aegocrioceras*

5.17   Zahner M., Brinkmann W.: The first theropod skeleton from Switzerland and what it tell us about the early evolution of neotheropod dinosaurs

POSTERS:

P 5.1   Schläfli P., Gobet E., Tinner W., Schlunegger F.: Biostratigraphic dating and reconstruction of vegetation
responses to Quaternary climate change in the Swiss North Alpine foreland

P 5.2   Sharma N., Adatte T., Sordet V., Vennemann T., Keller G., Schoene B., Khadri S.: Paleonvironmental
implications of Deccan volcanism relative to the KTB extinction: evidences from the red bole record

5.1

Peer Community in Paleontology (PCI Paleo): a community-driven, transparent, free and open peer-review platform for Paleontology

Jérémy Anquetin [1,2], Guillaume Billet [3]

[1] *Jurassica Museum, Route de Fontenais 21, CH-2900 Porrentruy (jeremy.anquetin@jurassica.ch)*
[2] *Department of Geosciences, University of Fribourg, Chemin du musée 6, CH-1700 Fribourg*
[3] *CR2P, UMR CNRS 7207, MNHN, Sorbonne Université, 8 rue Buffon, FR-75005 Paris*

Academic publishing is becoming increasingly costly for institutions, users, and ultimately the taxpayer. This system is undergoing major changes, but the current transition from subscription journals towards an author-pays model (Gold Open Access or Hybrid) is unlikely to significantly reduce the overall cost of publishing.

A faster, more transparent, completely open access, and free publishing system is now possible thanks to modern technologies. This system can be based on preprints, which have successfully been in use for more than 25 years in physics, mathematics, astronomy and computer sciences. Preprints provide a way to freely and rapidly share research results and to promote early feedback from a wider audience, but remain fundamentally non-peer-reviewed.

The Peer Community In (PCI) project calls for the creation of non-profit communities of researchers to peer-review articles available as preprints outside of conventional journals. The first community (PCI Evolutionary Biology) now counts more than 375 scientists after two years of activity. Launched in early 2018, Peer Community in Paleontology (PCI Paleo) is backed up by an international Managing Board and a growing group of recommenders (= editors).

PCI Paleo is completely free and transparent. Submitted preprints are evaluated by an editor and at least two external referees. If the paper is finally accepted, a final version is uploaded online and permanently linked to a recommendation text (written by the editor) and the peer-review reports, which are published by PCI Paleo (Fig. 1). Papers recommended by PCI Paleo are therefore transparently peer-reviewed, fully citable (DOI) and Open Access, obviating the need to publish them in conventional journals and significantly reducing the cost of academic publishing.
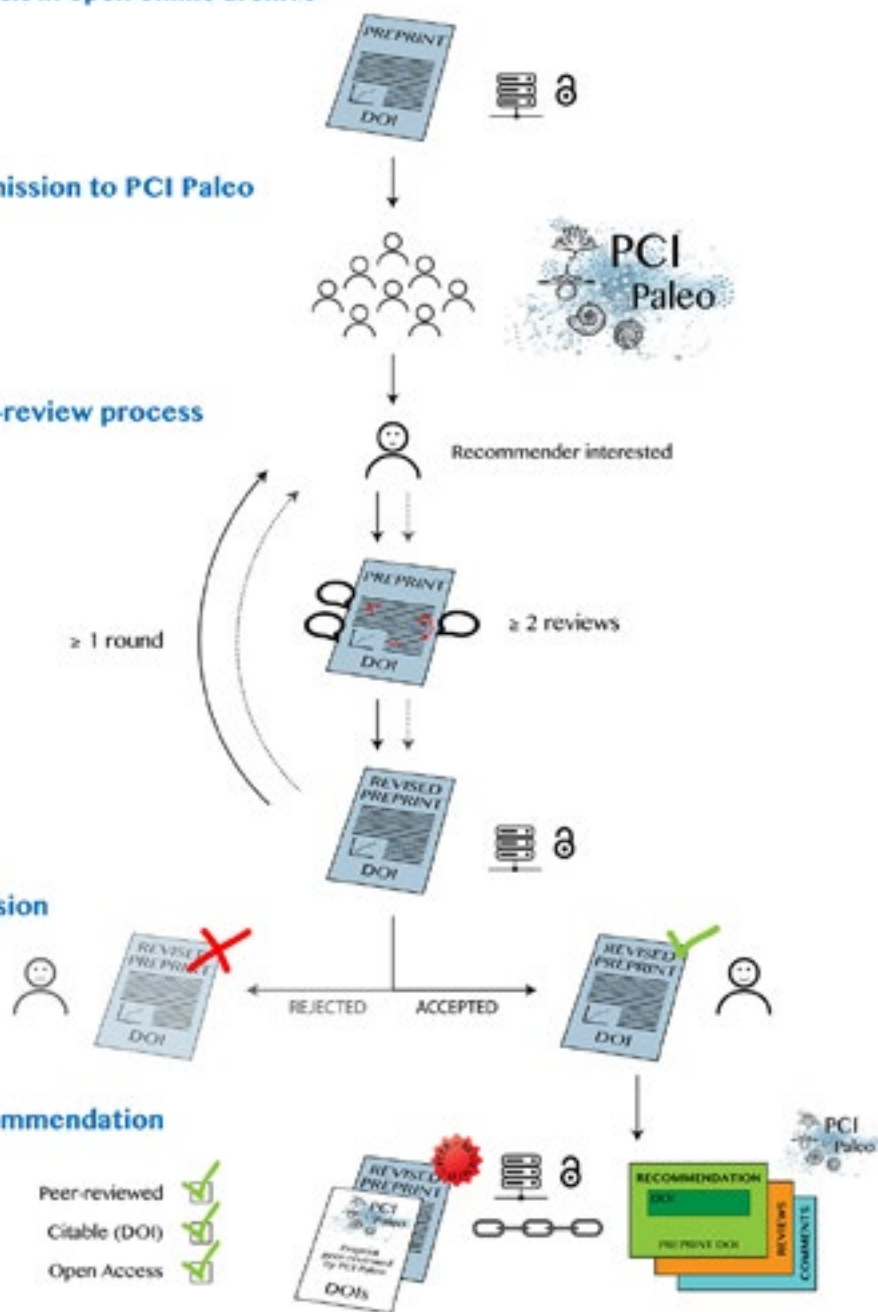
Figure 1. The PCI Paleo workflow is very similar to that of conventional peer-reviewed journals, except that the evaluation process is transparent since the peer-review reports are published alongside the final version of the paper.

5.2
Anoxia can increase the rate of decay for cnidarian tissue: Using *Actnia equina* to understand the early fossil record

Jonathan B. Antcliffe [1]

[1] Institute of Earth Sciences, University of Lausanne, 1015 Lausanne, Switzerland. (Jonathan.Antcliffe@unil.ch)

An experimental methodology is developed on a cnidarian model organism to serve as a comparison to previous such studies on bilaterians. We examine whether there is inherent bias against the fossilization of cnidarian tissue and their diagnostic characters and under what conditions these occur and in what way. These experiments show that cnidarian decay begins with a primary rupturing of the epidermis, followed by rapid loss of recognizable internal morphological characters. It also suggests that unlike in bilaterian taxa, diploblastic tissue is not universally decayed more slowly under anoxic or reducing conditions and some cnidarian characters even decay more quickly under anoxic conditions than they do under oxic conditions. This suggests the decay pathways acting may be different to those affecting bilaterian tissue. Further, fossil Lagerstätten that rely on anoxia for soft tissue preservation such as the Burgess Shale Type deposits may be uniquely bad windows for diploblastic preservation. Such experiments are providing crucial insights in to how soft tissue is preserved in Konservat-Lagerstätten and how we can best understand the exquisite fossils they contain.

5.3

New material from the Banné Marls (Kimmeridgian) in Glovelier (JU) reveals novel insights on plesiochelyid turtle morphology

Irena Burek [1,2] & Jérémy Anquetin [1,2]

[1] JURASSICA Museum, Route de Fontenais 21, CH-2900 Porrentruy (irena.burek@hotmail.com)
[2] Department of Geosciences, University of Fribourg, Chemin du musée 6, CH-1700 Fribourg

Plesiochelyidae are relatively large coastal marine turtles known exclusively from the Late Jurassic of Western Europe (Germany, Switzerland, United Kingdom, France, Spain and Portugal). The Jura Mountains have historically been a hotspot for the study of this group, mostly thanks to the famous locality of Solothurn (Rütimeyer, 1873; Bräm, 1965). Between 2000 and 2011, numerous plesiochelyids remains have been collected from Kimmeridgian deposits (Lower *Virgula* Marls and Banné Marls) in the area of Porrentruy (JU) during the construction of the A16 Transjurane highway. This material notably led to the recent description of the new species *Plesiochelys bigleri* (Püntener et al., 2017). In 2014, new fragmentary turtle material was collected from the Banné Marls (Reuchenette Formation, lower Kimmeridgian) along a forest track in Glovelier (JU). Two years later, a complete turtle shell was discovered at exactly the same spot. This shell missed an anterior peripheral that turned out to be part of the material found in 2014, which confirms the close association of the elements collected two years apart. The available material consists of the complete shell, some additional shell elements, a few bones from the appendicular and vertebral skeleton, and a fragmentary basicranium. This material belongs to at least two individuals. The new material from Glovelier can be confidently assigned to the species *P. bigleri*. It confirms the presence of this species in the Banné Marls (only two other incomplete shells from this layer were previously referred to this species) and slightly extends its spatial distribution. More importantly, the new material confirms the differences with the closely related species *P. etalloni* and provides new insights into the cranial and shell morphology of *P. bigleri*. In the context of this study, skulls of *P. bigleri* and *P. etalloni* were CT-scanned in order to further explore the internal cranial anatomy of these species and reveal new morphological characters. Among others, the position of the cerebral and palatine carotid canals relative to each other, is a new character that clearly distinguishes the two species.

Figure 1. MJSN CBE-0003, dorsal view on carpace of *Plesiochelys bigleri* (lower Kimmeridgian, Glovelier, Switzerland).

REFERENCES

Bräm H. 1965. Die Schildkröten aus dem oberen Jura (Malm) der Gegend von Solothurn. Schweizerische Paläontologische Abhandlungen 83:1–190.

Püntener C., Anquetin J., Billon-Bruyat J-P. 2017a. The comparative osteology of Plesiochelys bigleri n. sp., a new coastal marine turtle from the Late Jurassic of Porrentruy (Switzerland). PeerJ 5:e3482. DOI: 10.7717/peerj.3482.

Rütimeyer L. 1873. Die fossilen Schildkröten von Solothurn und der übrigen Juraformation. Neue Denkschrift der allgemeinen schweizerischen naturforschenden Gesellschaft 25:1–185.

5.4
The early fossil record of Euarthropoda and the Cambrian Explosion

Allison C. Daley [1], Jonathan B. Antcliffe [1], Harriet B. Drage [2,3], and Stephen Pates [2]

[1] Institute of Earth Sciences, University of Lausanne, Géopolis, CH-1015 Lausanne (allison.daley@unil.ch)
[2] Department of Zoology, University of Oxford, The Tinbergen Building, South Parks Road, Oxford, OX1 3PS, UK.
[3] Oxford University Museum of Natural History, Parks Road, Oxford, OX1 3PW, UK.

As the most abundant and diverse animal phylum, Euarthropoda have been major components of animal ecosystems for over 500 million years. Euarthropod fossils have also been key for examining the dynamics of the rapid early radiation of animals during the Cambrian Explosion. This event is documented by the Cambrian fossil record, however Precambrian ancestors to the Metazoa have long been sought. Here we use the early fossil record of euarthropods as a model to explore the quality of fossil data as it relates to the Cambrian Explosion. Numerous types of fossil preservation, including soft-bodied macrofossils from Burgess Shale Type (BST) localities, biomineralised exoskeletons, microfossils, and trace fossils are compared and contrasted across the Ediacaran-Cambrian boundary to constrain when euarthropods first evolved.

BSTs provide the most complete metazoan example of phylum-level anatomical construction in the euarthropod stem lineage during the Cambrian from 518 million years ago (Ma). The stem lineage includes non-biomineralized groups such as Radiodonta (e.g. *Anomalocaris*) that provide insight into the step-by-step construction of euarthropod morphology, including the exoskeleton, biramous limbs, segmentation, and cephalic structures (Daley et al. 2009). Trilobites are crown group euarthropods that appear in the fossil record at 521 Ma, before the stem lineage fossils, implying a ghost lineage that needs to be constrained. These constraints come from the trace fossil record, which show the first evidence for total group Euarthropoda (*Cruziana*, *Rusophycus*, *etc.*) at around 537 Ma (Wolfe et al. 2016). A deep Precambrian root to the euarthropod evolutionary lineage is disproven by a comparison of Ediacaran and Cambrian lagerstätten (Brasier et al. 2011). BSTs from the latest Ediacaran Period (e.g. Miaohe Biota, 550 Ma) are abundantly fossiliferous with algae but completely lack animals, which are also missing from other Ediacaran windows, such as phosphate deposits (e.g. Doushantuo, 560 Ma). This constrains the appearance of the euarthropod stem lineage to no older than 550 Ma. While each of the major types of fossil evidence (BSTs, trace fossils, and biomineralised preservation) have their limitations and are incomplete in different ways, when taken together they allow a coherent picture to emerge. In congruence with analyses from molecular paleobiology (e.g. Rota Stabelli et al. 2013), our comprehensive fossil data set suggests an entirely Cambrian origin and subsequent radiation for total group Euarthropoda.
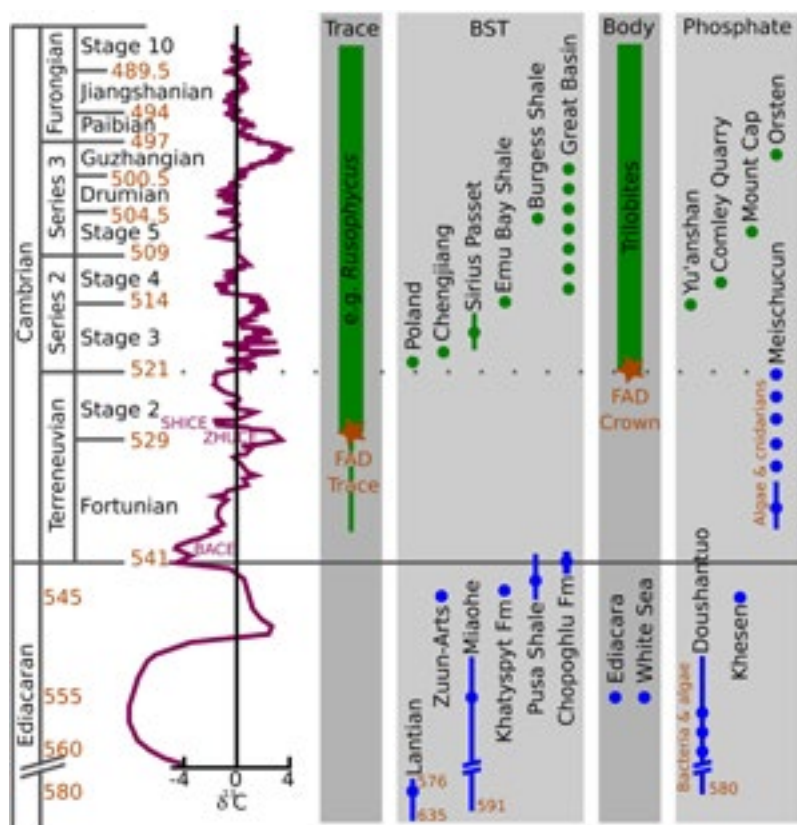

Figure 1. Timescale of Cambrian fossil evidence of euarthropods. Age of localities show in columns for trace fossils, BSTs, body fossils, and phosphatic microfossils. Localities in green show evidence of euarthropods, localities in blue do not. Orange stars indicate the FAD of total group Euarthropoda (FAD Trace) and crown group euarthropods (FAD Crown). Data from Antcliffe et al. (2014).

REFERENCES

Antcliffe, J.B., Callow, R.H.T. & Brasier, M.D. 2014: Giving the early fossil record of sponges a squeeze. Biological Reviews, 89, 972–1004.

Brasier, M.D., Antcliffe, J.B. & Callow, R. 2011: Evolutionary trends in remarkable fossil preservation across the Ediacaran-Cambrian transition and the impact of metazoan mixing. In: Taphonomy: Bias and Process Through Time (Ed. By Allison, P.A. & Bottjer, D.). Springer, Amsterdam, 519–567.

Daley, A.C., Budd, G.E., Caron, J.B., Edgecombe, G.D. & Collins, D. 2009: The Burgess Shale anomalocaridid *Hurdia* and its significance for early euarthropod evolution. Science, 323, 1597–1600.

Rota-Stabelli, O., Daley, A.C. & Pisani, D. 2013: Molecular timetrees reveal a Cambrian colonization of land and a new scenario for ecdysozoan evolution. Current Biology, 23, 392–398.

Wolfe, J.M., Daley, A.C., Legg, D.A. & Edgecombe, G.D. 2016: Fossil calibrations for the arthropod Tree of Life. Earth Sciences Reviews, 160, 43–110.

5.5
Coelacanths from the Middle Triassic of Switzerland show unusual morphology

Christophe Ferrante [1,2], Lionel Cavin [2], Heinz Furrer [3] & Rossana Martini [1]

[1] Department of Earth Sciences, University of Geneva, Rue des Maraîchers 13, 1205 Genève
  (christophe.ferrante@ville-ge.ch)
[2] Department of Geology and Palaeontology, Natural History Museum of Geneva, CP 6434, 1211 Genève 8
[3] Palaeontological Institute and Museum, University of Zurich, Karl Schmid-Strasse 4, 8006 Zurich

The iconic example of "living fossil" is represented by the extant coelacanth *Latimeria*, which belongs to a lineage with a monotonous morphology since the oldest representative in the Devonian. In most studies this very conservative anatomy is explained by a relatively slow evolving morphologic rate. However, somes coelacanths presenting unusual morphologies are reported from the Paleozoic (Middle – Late Devonian and Early Carboniferous) and from the Mesozoic (Early – Middle Triassic). Alongside a high morphological disparity of coelacanths, the Triassic also witnessed a peak of diversity of the clade making even more interesting this time interval (Cavin et al., 2013).

In Switzerland, three coelacanth taxa, with more or less pronounced unusual anatomical features, are known from the Middle Triassic Besano Formation of Monte San Giorgio, Canton Ticino, and from the Prosanto Formation of the Ducan and Landwasser area, Canton Graubünden. This two sites show similar vertebrate assemblages. Based on U-Pb datation, the middle part of the Besano Formation (latest Anisian) is considered to be a time equivalent of the middle part of the Prosanto Formation whereas the upper part is correlated to the uppermost Besano Formation and the Lower Meride Limestone (Furrer et al., 2008).

Ticinepomis peyeri has been described from a complete specimen of the Besano Formation (Rieppel, 1980). In the Prosanto Formation an isolated caudal fin and a subcomplete specimen have been refered to *T. peyeri* (Cavin et al., 2013). Another coelacanth, *Foreyia maxkuhni*, has been recently described (Cavin et al., 2017) from the upper Prosanto Formation on the basis of one complete and one sub-complete specimens. A third taxon, based on an incomplete specimen from the Besano Formation, was referred with caution to *Holophagus picenus* (Rieppel, 1985).

An ongoing study (Ferrante et al., 2017) has pointed out that this third taxon is represented by a large collection of more than 50 specimens housed in the Palaeontological Institute and Museum, University of Zurich. First analyses suggest that this material probably belongs rather to a new genus of a coelacanth with unusual morphological caracters among actinistians.

The skull roof of the new taxon is divided into two parts which are separated by an intracranial joint. They consists of the usual bones composing the actinistian skull. This taxon differs from the common condition of actinistians by the shape and proportion of the bones. Most "conservative" actinistian skulls have the anterior portion circa 1.5 to 2 times longer than the posterior part. In the new taxon, the anterior part of the skull is almost as long as the posterior portion. This unusal ratio is observed in a few Paleozoic genera, such as *Caridosuctor* and *Rhabdoderma*. In *F. maxkuhni* the anterior part of the skull roof is shorter than the posterior part, as in the the Palaeozoic *Miguashaia* and *Sassenia*, while *T. peyeri* presents the usual actinistian condition (Cavin et al., 2017).

The new taxon has massive cheek ossifications with some fused bones and two proportionally very large opercles, which is not the normal condition in actinistians. *F. maxkuhni* presents a fusion of the lachrymojugal and the squamosal bones (Cavin et al., 2017). At the opposite, in *T. peyeri* the lachrymojugal is long and thin as other actinistians but has an unusual high postorbital limb (Rieppel, 1980).

Dermal bones of the new taxon are strongly ornamented with densely packed large pointed tubercles quite similar to *F. maxkuhni*. In *T. peyeri* some bones are also ornamentated but only with few distinct rounded tubercles (Rieppel, 1980). Scales of the new taxon are ornamented with many elongate sharp spines caudally oriented.

Although having derived caracters, several features of *Foreyia maxkuhni* and the new taxon evoke basal coelacanths from the Palaeozoic. In a recent cladistic analysis (Cavin et al., 2017), *F. maxkuhni* and *T. peyeri* are placed as sister-genera despite their important morphological differences, and both are nested within the latimeriid family. Our research will propose a new cladistic analyses in order to resolve the phylogenetic position of the new taxon relatively to the contemporaneous *F. maxkuhni* and *T. peyeri*, and more generally within actinistans.

REFERENCES

Cavin, L., Furrer, H. & Obrist, C. 2013: New coelacanth material from the Middle Triassic of eastern Switzerland, and comments on the taxic diversity of actinistans. Swiss Journal of Geosciences 106, 161-177.

Cavin, L., Mennecart, B., Obrist, C., Costeur, L. & Furrer, H. 2017: Heterochronic evolution explains novel body shape in a Triassic coelacanth from Switzerland. Scientific Reports, 1-7.

Ferrante, C., Martini, R., Furrer, H. & Cavin, L. 2017: Coelacanths from the Middle Triassic of Switzerland and the pace of actinistian evolution. Research & Knowledge, vol. 3, (2), 59-62.

Furrer, H., Schaltegger, U., Ovtcharova, M. & Meister, P. 2008: U-Pb zircon age of volcanic layers in Middle Triassic platform carbonates of the Austroalpine Silvretta Nappe (Switzerland). Swiss Journal of Geosciences 101, 595-603.

Rieppel, O., 1980: A new coelacanth from the Middle Triassic of Monte San Giorgio, Switzerland. Eclogae Geologicae Helvetiae 73/3, 921-939.

Rieppel, O., 1985: A second actinistian from the Middle Triassic of Monte San Giorgio, Kt. Tessin, Switzerland. Eclogae Geologicae Helvetiae 78, 707-713.

5.6
Test-Size Evolution of the Planktonic Foraminifer *Globorotalia menardii* in the Tropical Atlantic Since the Upper Miocene

Thore Friesenhagen [1,2], Michael Knappertsbusch [1]

[1] *Natural History Museum Basel, Augustinergasse 2, CH-4001 Basel, Switzerland*
[2] *Department Umweltwissenschaften, University of Basel, Bernoullistrasse 32, CH-4056 Basel*
  (thore.friesenhagen@unibas.ch)

In previous studies, Knappertsbusch analyzed the trend of the test size of the planktonic foraminifer *Globorotalia menardii* and its related forms, which are suitable model species for the investigation of evolutionary processes, on both sides of the Panamanian Isthmus. It was revealed that the test size of *G. menardii* seems to gradually increase in the Pacific over the last 8Ma; however, in the western Atlantic Ocean a rapid decrease in test size is observed after the closure of the Panamanian Isthmus and the climate minimum in the Gelasian (2.588 – 1.806Ma). An extreme increase occurred at 2Ma and has lasted until present.

Two hypotheses have been suggested to explain this extreme increase in test size: it was triggered by either (1) a punctuated evolutionary event or (2) the dispersal of specimens from the Indian Ocean via the Agulhas leakage.
This study addresses the question whether the difference of the morphological trends in *G. menardii* tests between the Atlantic and Pacific can be explained by the dispersal of specimens from the Indian Ocean into the Atlantic.

Therefore, samples from ODP 108 Site 667A, the most distal area influenced by Agulhas, in the eastern Atlantic were investigated and several morphometric parameters (spiral height, axial length, keel angles, convexity, etc.) of *G. menardii* tests were measured. Two other sites, one in the south-eastern Atlantic and one along the tropical eastern border of Africa are planned for investigation. If greater sized specimens dispersed from the Indian Ocean, a similar variation trend of test size of *G. menardii* in both the Indian and Atlantic Oceans is expected for the last ca. 2Ma.

The results from Site 667 show a very similar morphological test size trend in comparison to the western Atlantic sites ODP 925B and DSDP 502. A test size minimum is observed in the early Gelasian (maximum axial length of 600µm at 2.3Ma), followed by a doubling of the test size (1200µm in axial length) within 0.3Ma. This indicates a common evolutionary history of the test size of G. menardii between the eastern and the western tropical Atlantic.

The similar trends in the Atlantic sites, as well as a slightly earlier beginning of the test size increase at the east Atlantic Site 667 (2.058Ma) in comparison to the west Atlantic Sites 925B and 502 (1.95Ma and 1.7Ma, respectively), favour the hypothesis of a dispersal from the Indian Ocean into the Atlantic via the Agulhas leakage.

5.7
Permian–Triassic palynology of the Karoo Supergroup from the N'Condédzi region, Tete Province,Mozambique

Francesca Galasso [1], Zélia Pereira [2], Paulo Fernandes [3], Amalia Spina [4], João Marques [5]

[1] Paläontologisches Institut und Museum, Universität Zürich ,Karl-Schmid-Strasse 4, CH-8006 Zürich, Switzerland. (francesca.galasso@pim.uzh.ch)

[2] Laboratório Nacional de Energia e Geologia (LNEG), Rua da Amieira, Apartado 1089, 4466-901 S. Mamede Infesta, Portugal.

[3] Centro de Investigação Marinha e Ambiental (CIMA), Universidade do Algarve, Campus de Gambelas, 8005-139 Faro, Portugal.

[4] Department of Physics and Geology, University of Perugia.Via Pascoli, 06123 Perugia, Italy.

[5] Gondwana Empreendimentos e Consultorias, Limitada, Rua B, no. 233, Bairro da COOP, Caixa Postal 832, Maputo, Mozambique.

Sediments of the Karoo Supergroup are well represented in Mozambique in various sedimentary basins. These basins are located along the Zambezi River valley in Tete Province, Central-West Mozambique. The Moatize-Minjova Basin is one of these basins which sedimentary succession is regarded as the key stratigraphic section for the Lower Karoo Supergroup in Mozambique, including from base to the top: the Vúzi (glaciogenic), the Moatize (coal bearing) and the Matinde formations. In this work we present palynological data obtained from three cores drilled for coal exploration by Coal India in the N'Condédzi region.

Core A1TM-058 encompasses a ca. 1000 m thick succession, consisting of interbedded shales, carbonaceous shales, coals seams and sandstones. Close to the base of the borehole, the Mesoproterozoic basement rocks (gabbros and anorthosites) of the Tete Suite were penetrated. CITM-014 (ca. 500 m depth) and A1TM-039 (ca. 600 m depth) boreholes have similar lithologies mainly composed of red sandstones interbedded with brown siltstones and red to grey mudstones. The three cores analzyed based on palynological studies make a composed stratigraphic section with ca. 2000 m thick. We described six palynoassemblages and established three discrete Palynobiozones based on these assemblages. Three biozones were established of Lopingian age (Galasso et al., in preparation) dominated mainly by taeniate pollen grain, such as *Guttulapollenites hannonicus*, *Lueckisporites virkkiae* and *Weylandites lucifer* in sample of core. The other three biozones were established in the Triassic (from Lower to Upper Triassic) (Galasso et al., in preparation). These palynoassemblages are characterized by bisaccate pollen grains such as *Alisporites* spp., *Protohaploxypinus* spp., *Striatopodocarpites* spp., and *Falcisporites* spp. (*F. stabilis*) and common *Gnetaceaepollenites sinuosus*, *Lunatisporites pellucidus*, *Platysaccus queenslandi* and *Weylandites lucifer*, and spores as *Aratrisporites* sp., *Densoisporites nejburgii*, *D. playfordii*, *Densoisporites* sp., *Lundbladispora brevicula* and *Playfordiaspora crenulata*.

Biozones of distinct Middle Triassic were not recognized probably due to a major hiatus. This may be related to a period of non-deposition and tectonism with uplift and erosion. The presence of reworked Permian palynomorphs encountered in the boreholes CITM-014 and A1TM-039 considered Upper Triassic character due to the presence of spores such as *Anapiculatisporites spiniger/Carnisporites anteriscus*, *Dictyophyllidites* sp. *Lophotriletes novicus*, *Nevesisporites fossulatus*, *Retitriletes* sp., *Stiattella seebergensis*, *Uvaesporites* sp. and *Zebrasporites* sp. and the pollen grains as *Cycadopites* sp., *E. vigens* and *Samaropollenites speciosus* assigned to the *Enzonalasporites vigens* biozone, (Galasso et al., in preparation) and strongly suggests that, the erosional event have occurred in the Middle Triassic.

REFERENCES
Galasso, F., Fernandes, P., Pereira, Z., Spina, A., Marques, J., Permian-Triassic palynology of N'Condédzi sub-basin, Moatize-Minjova Coal Basin, Mozambique (in preparation).

5.8
Besides phase-contrast tomography, synchrotron imaging also rhymes with chemical mapping: new advances in 2D synchrotron imaging of fossils

Pierre Gueriau [1]

[1] Institute of Earth Sciences, University of Lausanne, Géopolis, CH-1015 Lausanne, Switzerland (pierre.gueriau@unil.ch)

For most palaeontologists, "synchrotron imaging" is only seen as a more effective variant of laboratory-based X-ray micro-computed tomography (µCT), allowing to access the internal morphology of fossils with an unprecedented level of detail and contrast, with no, or only limited, sample preparation. However, other synchrotron imaging techniques are used in palaeontology, mainly to study flat fossils, for which µCT largely fails because of the strong difference in X-ray absorbance along its flat and long dimensions. Among them, synchrotron X-ray fluorescence (XRF) major-to-trace elemental mapping is now used on a very regular basis. This technique, which produces 2D distributions of major-to-trace elements over decimetre-scale objects with a micrometric lateral resolution or even better, not only provides new morphological information in revealing hidden anatomies (Bergmann et al. 2010; Gueriau et al. 2014, 2018), but also offers unexpectedly detailed palaeobiological (e.g., Wogelius et al. 2011), palaeoenvironmental and taphonomic information (e.g., Gueriau et al. 2015) through the characterization of the organic and elemental compositions of the fossils. Here, I will review the new advances in synchrotron XRF, demonstrated against a wide range of fossils, from different ages and depositional environments. New developments towards synchrotron X-ray diffraction (XRD) mineralogical mapping will also be presented. Insights into minerals identification and distribution, as well as crystals structure, size and orientation show great promise for fossil anatomical and taphonomic studies, as well as other poorly understood mineralization processes.

REFERENCES

Bergmann, U., Morton, R. W., Manning, P. L., Sellers, W. I., Farrar, S., Huntley, K. G., Wogelius, R. A., & Larson, P. L. 2010: *Archaeopteryx* feathers and bone chemistry fully revealed via synchrotron imaging, Proceedings of the National Academy of Sciences, USA, 107, 9060-9065.

Gueriau P., Mocuta C., Dutheil D.B., Cohen S.X., Thiaudière D., the OT1 Consortium, Charbonnier S., Clément G., & Bertrand L. 2014: Trace elemental imaging of rare earth elements discriminates tissues at microscale in flat fossils, PLoS One, 9, e86946.

Gueriau P., Mocuta C., & Bertrand, L. 2015: Cerium anomaly at microscale in fossils, Analytical Chemistry, 87, 8827-8836.

Gueriau P., Jauvion C., & Mocuta C. 2018: Show me your yttrium, and I will tell you who you are: implications for fossil imaging, Palaeontology. Published online 12 June 2018, DOI: 10.1111/pala.12377.

Wogelius, R. A., Manning, P. L., Barden, H. E., Edwards, N. P., Webb, S. M., Sellers, W. I., Taylor, K. G., Larson, P. L., Dodson, P., You, H., Da-Qing, L., & Bergmann, U. 2011: Trace metals as biomarkers for eumelanin pigment in the fossil record, Science, 333, 1622-1626.

5.9

Couscous ai frutti di mare – the spectacular Moroccan mudmound locality Hamar Laghdad and its palaeoecology

Christian Klug [1], Elias Samankassou [2], Alexander Pohle [1], Mikolaj Zapalski [3] & Dieter Korn [4]

[1] *Paläontologisches Institut und Museum, Universität Zürich, Karl Schmid-Strasse 4, CH-8006 Zürich, Switzerland (chklug@pim.uzh.ch)*
[2] *Département des Sciences de la Terre, Université de Genève, CH-1205 Genève*
[3] *University of Warsaw, Faculty of Geology, Żwirki i Wigury 93, 02-089 Warszawa, Poland.*
[4] *Museum für Naturkunde, Leibniz-Institut für Evolutions- und Biodiversitätsforschung, Invalidenstraße 43, 10115 Berlin*

Hamar Laghdad is a locality situated in the Moroccan eastern Anti-Atlas. It is remarkable in many respects; from a geoscientists view, it is primarily the tens of more or less perfectly exhumed carbonate mudmounds of Early Devonian age. While geologists might admire the exposed succession of Early Palaeozoic sediments followed by Lochkovian volcanics that underlie the mound-carbonates, palaeontologists rather appreciate the wealth of different habitats and thus fossil diversity that is preserved in and around the mound sediments. For this work, we sampled several assemblages in order to better understand ecological changes around the time of mudmound-growth and how the peculiar palaeo-topography might have fostered this local palaeobiodiversity-hotspot (Klug et al. 2018

REFERENCES
Klug, C. Samankassou, E., Pohle, A., De Baets, K., Franchi, F. & Korn, D. 2018: Oases of biodiversity: Early Devonian palaeoecology at Hamar Laghdad, Morocco. – In: Klug, C. & Korn, D. (eds.): Palaeontology of the Devonian of Hamar Laghdad (Tafilalt, Morocco). Special volume honouring JOBST WENDT. – Neues Jahrbuch für Geologie und Paläontologie, Abhandlungen: 30 pp.

5.10
Early post-embryonic stages of Cambrian trilobites: morphological and ecological disparity

Lukáš Laibl [1]

[1] Institute of Earth Sciences, University of Lausanne, Bâtiment Géopolis, CH-1015 Lausanne (lukas.laibl@unil.ch)

Early post-embryonic stages of Cambrian trilobites show unexpectedly wide variety of morphologies and were adapted to different modes of life. Numerous examples of basal trilobites shows that the ancestral type of development in this group was direct, with comparatively small post-embryonic stages. The indirect development, characterised by presence of a metamorphosis, originated several times independently in Eodiscida, Corynexochina, Illaenina, Solenopleuridae, Conocoryphidae and Shumardiidae, probably as a response to various selective pressures. Size increase of early post-embryonic stages together with other morphological and developmental modifications is characteristic for some members of Paradoxididae and Conocoryphidae. Such modifications are likely related to lecithotrophic development. Some early stages of Olenellidae, Estaingiidae and Paradoxididae show modification of their cephalic and/or thoracic spines, that might be related to predator deterrence and/or to stability on the sea bottom. Such morphological and ecological modifications show that trilobite early developmental stages were well adapted to various environments already few milion years after the origin of the group. These modifications also show that even early trilobites were effectively reacting to selective pressures by exploring new habitats or by avoiding predation.
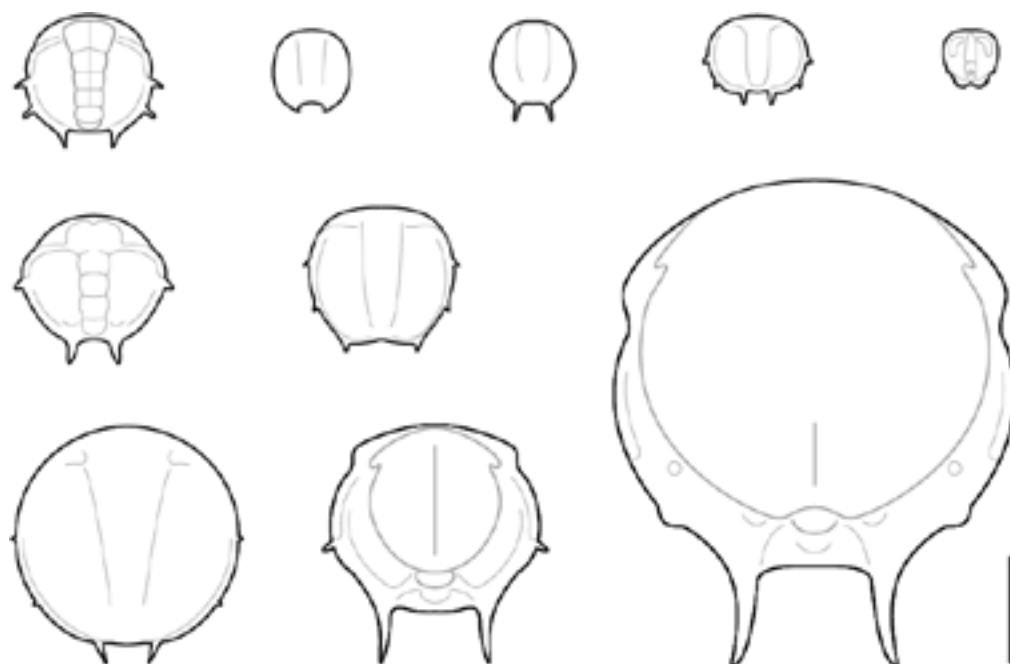

Figure 1. Examples of early post-embryonic stages of Cambrian trilobites. Scale bar = 0.5 mm. Modified from Laibl et al. (2014, 2017, in press) and Laibl (2017).

REFERENCES

Laibl, L., Fatka O., Crônier C., & Budil P. 2014: Early ontogeny of the Cambrian trilobite *Sao hirsuta* from the Skryje-Týřovice Basin, Barrandian area, Czech Republic, Bulletin of Geosciences, 89, 293–309.

Laibl, L. 2017: Patterns in Palaeontology: The development of trilobites, Palaeontology Online, 7/10, 1–9.

Laibl, L., Esteve, J., & Fatka, O. 2017: Giant postembryonic stages of *Hydrocephalus* and *Eccaparadoxides* and the origin of lecithotrophy in Cambrian trilobites, Palaeogeography, Palaeoclimatology, Palaeoecology, 470, 109–115.

Laibl, L., Cederström, P., & Ahlberg, P. in press: Early post-embryonic development in *Ellipsostrenua* (Trilobita, Cambrian, Sweden) and the developmental patterns in Ellipsocephaloidea, Journal of Paleontology, online early access.

5.11

The locality of Murs (Southeastern France): Rediscovery of a forgotten Early Oligocene fauna

Olivier Maridet [1,2], Christine Balme [3], Océane Lapauze [1,2], Stéphane Legal [3], Xiaoyu Lu [1,2], Bastien Mennecart [4], Jérémy Tissier [1,2], Davit Vasilyan [1,2] & Loïc Costeur [4]

[1] *Jurassica Museum, Rte de Fontenais 21, CH-2900 Porrentruy (olivier.maridet@jurassica.ch)*
[2] *Department of Geosciences, University of Fribourg, Chemin du Musée 6, CH-1700 Fribourg*
[3] *Parc naturel régional du Luberon, 60 place Jean-Jaurès, BP 122, F-84404 Apt Cedex*
[4] *Naturhistorisches Museum Basel, Augustinergasse 2, CH-4051 Basel*

The locality of Murs, dated to ca. 31Ma (MP23), is located in the Early Oligocene Apt-Forcalquier Basin in Southeastern France. It is known since the 1920's when H.G. Stehlin, curator of the Natural History Museum Basel, went in the region for palaeontological prospections. The scientific interest in this locality remained limited until the 1960's when a mandible of rodent from Murs was described and illustrated for the first time (Thaler 1966). This mandible was later included in a new species of Theridomyidae, *blainvillimys helmeri*, by Vianey-Liaud (1972) and allowed to precise the age of the locality: Early Oligocene, correlated to the terrestrial biochronological level MP23 (Biochrom'97). But most importantly, Rémy (2000) provided for the first time a description of several specimens of large mammals, including a preliminary faunal list of the locality. The latter publication described a new species of Perissodactyla, *Plagiolophus huerzeleri*, based on nicely preserved skulls on a block as well as on other bones. *Plagiolophus huerzeleri* from Murs is the largest species and one of the most recent record of the genus before its extinction.

The presence of this sediment block rich in fossils and historical data found in the archives of the Museum in Basel as well as of numerous well-preserved and unstudied specimens raised our interest and we organised a new excavation of the site in October 2017. After finding the probable location of one of the original sites again, we discovered about 100 fossils including two other exquisitely preserved skulls (e.g. Figure 1), postcranial bones and some teeth of *Plagiolophus*. To date, including the recent discoveries, the fauna is composed of at least 3 perissodactyls (one *Plagiolophus*, two rhinocerotids), 4 artiodactyls (a cainothere, an anthracothere, a ruminant and possibly an entelodontid), a carnivore, one rodent (a theridomyidae), 3 different families of turtles (Testudinae, Geoemydidae, Trionychidae), one crocodile and one fish (Perciformes). The list of material, including the historical collection from Basel and newly excavated specimens hosted at the "Parc naturel régional du Luberon"(PNRL), comprises now a total of nearly 200 specimens. New excavations will be carried out with the hope of increasing the fossil sample and precising the biogeographic and biodiversity context of the Early Oligocene of Southern France.
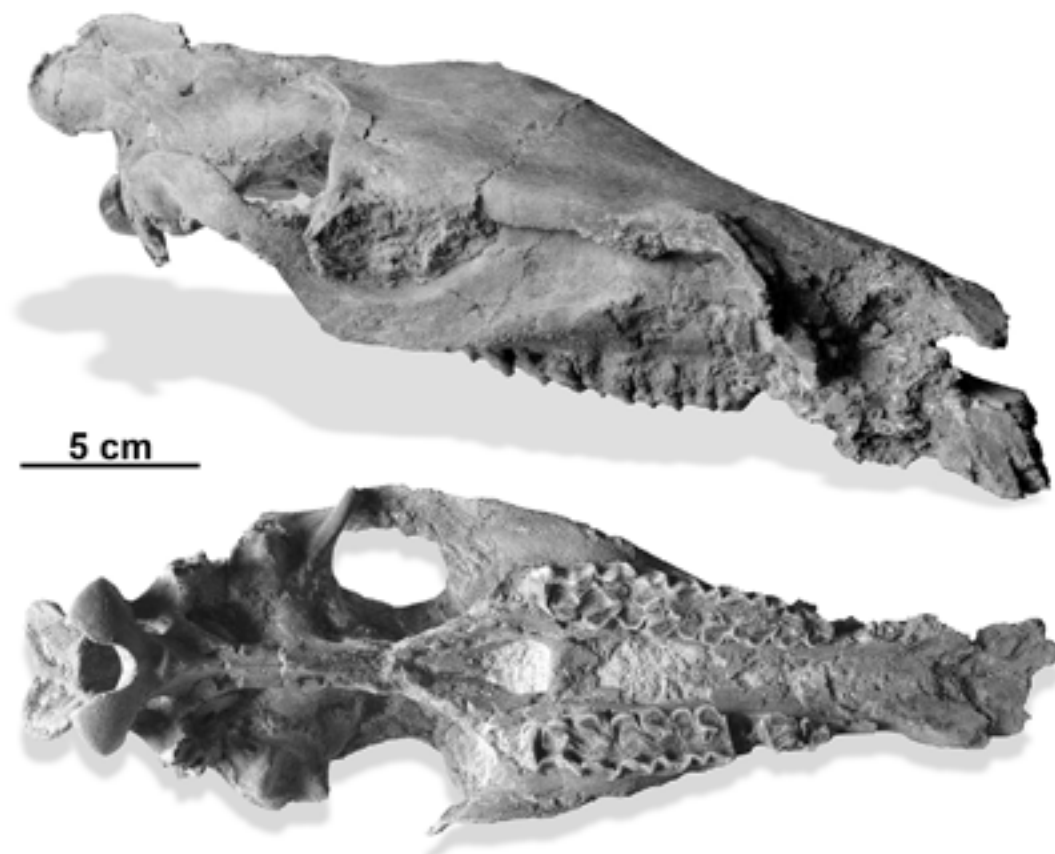
Figure 1. New skull of *Plagiolophus huerzeleri* (PNRL_2100) discovered in 2017 during the excavation in Murs (Early Oligocene).

REFERENCES

BiochroM'97, 1997: Synthèse et tableaux de corrélations, in: Aguilar, J.-P., Legendre, S. & Michaux, J. (Eds.), Actes de Congrès BiochroM'97, Memoires et travaux de l'institut de Montpellier de l'Ecole Pratique des Hautes Etudes, 21, 769–805.

Rémy, J.A. 2000: *Plagiolophus huerzeleri*, une nouvelle espèce de Palaeotheriidae (Perissodactyla, Mammalia) de l'Oligocène inférieur (Rupélien, MP 23), à murs (Vaucluse, France), Geobios, 33, 489–503.

Thaler, L. 1966: Les rongeurs fossiles du Bas-Languedoc. Rapport avec l'histoire des faunes et la stratigraphie du Tertiaire d'Europe, Mémoires du Muséum National d'Histoire naturelle, serie C, Sciences de la Terre, NS 17, 295p.

Vianey-Liaud, M. 1972: L'évolution du genre *Theridomys* à l'Oligocène moyen. Intérêt biostratigraphique, Bulletin du Muséum National d'Histoire Naturelle, Sciences de la Terre, 3ème série, 98, 296–370.

5.12

New insights into the cranial circulation and innervation of baenid turtles

Yann Rollot [1], Walter G. Joyce [1]

[1] *Department of Geosciences, University of Fribourg, Chemin du Musée 6, CH-1700 Fribourg (yann.rollot@unifr.ch)*

Variation to the internal carotid and cranial innervation system has played an important role in the systematics of fossil and living turtles. Baenidae, for instance, a clade of freshwater turtles that persisted from the Early Cretaceous to the Eocene, is diagnosed as a member of Paracryptodira, one of the primary clades of crown turtles, by the location of the foramen posterius canalis carotici interni halfway along the suture between the pterygoid and basisphenoid. Numerous foramina are highlighted in descriptions of baenid skulls, but the exact path of the canals they highlight is typically obscured within the skull making it difficult to assess their true homology. CT scanning and 3D modeling of the internal carotid, lateral head vein, and facial nerve (VII) of a well preserved skull of *Eubaena cephalica* from the Hell Creek Formation of North Dakota revealed that the second bifurcation along the path of the internal carotid canal corresponds to the split with the vidian nerve (VII) and not the palatine branch of the carotid artery. This contradicts previous ideas about the circulation system of baenid turtles, as the palatine branch of the carotid artery was persistently discussed as being present in paracryptodires. As the absence of the palatal branch questions the monophyly of paracryptodires and may have significance to the systematics of turtles, future work will need to clarify the distribution of this pattern across turtles.

5.13
Bone Histology of *Cyamodus hildegardis* (Placodontia: Cyamodontoidea) from the Besano Formation of Monte San Giorgio, Switzerland: inferences for Ecology and Lifestyle

Torsten M. Scheyer [1] & Nicole Klein [2]

[1] *Universität Zürich, Paläontologisches Institut und Museum, Karl Schmid-Strasse 4, CH-8006 Zurich (tscheyer@pim.uzh.ch)*
[2] *Universität Bonn, Steinmann-Institut für Geologie, Mineralogie und Paläontologie, Nußallee 8, D-53115 Bonn, Germany (nklein@posteo.de)*

Cyamodus hildegardis (Peyer, 1931) is one of the best-documented placodonts from the Middle Triassic of Europe (e.g., Pinna 1992; Scheyer 2010). The species belongs to Cyamodontoidea, the clade of well-armoured, crushing-toothed placodonts that carry turtle-like carapaces (and often also a hip shield in European taxa) over their trunk. Although several specimens of the *C. hildegardis* are present in Swiss and Italian collections (e.g., PIMUZ - Paläontologisches Institut und Museum der Universität Zürich; Museo Civico di Storia Naturale di Milano) much of the animal's anatomy and especially its ecology are not well understood. This is to a large degree due to the preservation of the fossils as crushed and flattened specimens in the compacted black shale deposits at Monte San Giorgio. Here we report on new palaeohistological data of the armour plates and endoskeletal elements of the species to elucidate its lifestyle.

For the present study, several small fragments of the postcranium of the holotype specimen of *C. hildegardis* (PIMUZ T 4763, upper Late Anisian Besano Formation, Val Porina, Meride, Canton Ticino, Switzerland) were available, because these were stored separately for several decades in the collections apart from the exhibited holotype specimen at PIMUZ. The fragments, whose position on the body could not be confidently reconstructed, include two keeled armour plates, as well as three other bone fragments from either the appendicular or the axial skeleton.

The armour elements of *C. hildegardis* have an irregular meshwork of longitudinally and transversely oriented structural fibres at their core, surrounded by a peripheral cortex of parallel-fibred tissue that has been cyclically deposited. The vascularisation of the tissue is overall low, consisting of small, scattered primary vascular canals and few larger vascular spaces located in the deeper cortex. Histologically, these armour plates are thus similar to the hexagonal/polygonal plates of other European cyamodontoids, such as *Psephoderma alpinum*. The endoskeletal bone sample of *C. hildegardis* shares with previously sampled *Paraplacodus broilii* and *Psephoderma alpinum* the presence of lamellar-zonal bone tissue and an overall low level of vascularisation. For this reason, the taxa from the Alpine Triassic are likely to have also shared similar ecology/lifestyle traits (Klein et al. 2015a), namely that of slow-swimming bottom walkers inhabiting lagoonal to shallow shelf environments. *C. hildegardis* thus differs from the other species of *Cyamodus* that inhabited the Germanic Basin of the Muschelkalk Sea and which exhibit faster deposited fibrolamellar tissue in their long bones (Klein et al. 2015a, b), indicative of a more active lifestyle.

REFERENCES

Klein, N., Houssaye, A., Neenan, J. M., & Scheyer, T. M. 2015: Long bone histology and microanatomy of Placodontia (Diapsida: Sauropterygia). Contrib. Zool. 84, 59-84.
Klein, N., Neenan, J. M., Scheyer, T. M. & Griebeler E. M. 2015: Growth patterns and life history strategies in Placodontia (Diapsida: Sauropterygia). Royal Soc. Open Sci. 2, 140440.
Pinna, G. 1992: *Cyamodus hildegardis* Peyer, 1931 (Reptilia, Placodontia). Memorie della Società Italiana di Scienze Naturali e del Museo Civico di Storia Naturale di Milano 26, 1-21.
Peyer, B. 1931: Die Triasfauna der Tessiner Kalkalpen III. Placodontia. Abh. Schweiz. Paläontol. Ges. 51, 1-25.
Scheyer, T. M. 2010: New interpretation of the postcranial skeleton and overall body shape of the placodont *Cyamodus hildegardis* Peyer, 1931 (Reptilia, Sauropterygia). Palaeontologia Electronica 13(2), 15A:15p.

5.14

Oligocene-Miocene Rhinocerotidae from Europe: systematics, phylogeny and diversification

Jérémy Tissier [1, 2], Pierre-Olivier Antoine [3], Damien Becker [1, 2]

[1] JURASSICA Museum, Route de Fontenais 21, CH-2900 Porrentruy (jeremy.tissier@jurassica.ch)
[2] *Department of Geosciences, University of Fribourg, Chemin du Musée 6, CH-1700 Fribourg*
[3] Institut des Sciences de l'Évolution de Montpellier, UMR 5554 CNRS/IRD/UM/EPHE, University of Montpellier, Place Eugène Bataillon, F-34095 Montpellier cedex 05, France

The earliest alleged Rhinocerotidae (Mammalia, Perissodactyla) appear in the fossil record in the latest Middle Eocene of North America (*Teletaceras radinskyi*). This family was completely absent from Europe until the earliest Oligocene. Their first appearance in Western Europe, along with the origination and the extinction of other groups, defines the Grande Coupure event, a major faunal turnover. After this event, Rhinocerotidae have become a conspicuous faunal element in Europe, until the disappearance of the last European woolly rhinoceros during the latest Pleistocene.

Their systematics still remains poorly resolved, especially during the first stages of their diversification, at the Eocene–Oligocene transition. One genus in particular, *Ronzotherium*, supposed to be a forecomer of the Grande Coupure immigrations to Europe, is problematic. Indeed, only two authors have yet proposed a systematic study of this genus (which may include up to seven species), and their results are radically different: Heissig (1969) proposed a "bushy" evolution of this genus, whereas Brunet (1979) hypothesized a clear anagenetic evolution. These contrasting results are challenging for the comprehension of the genus history, but also for the complete understanding of rhinocerotid evolution, due to the alleged early offshoot position of this genus within the family. It is also a key for the study of the mechanisms of the Grande Coupure event. We propose here a complete revision of *Ronzotherium*, based on phylogenetic methods and including new unpublished material from Swiss localities. In addition to the revision of this particular genus, we also revise Rhinocerotidae from the Oligocene up to the Miocene, based on new unpublished specimens. In total, seven Swiss, two French and one Bosnian localities are revised or studied, and two new species are described, contributing to the revision of *Diaceratherium*, another common European Oligocene-Miocene genus.

These extensive revisions allow us to propose new interpretations of the early history of rhinocerotids and new palaeobiogeographic hypotheses. A new phylogeny is proposed, providing novel data for the study of the Grande Coupure event. Finally, we will present preliminary estimates of the extinction and speciation rates through time of the family, based on a new method relying on the fossil record (Didier et al. 2012; 2017).
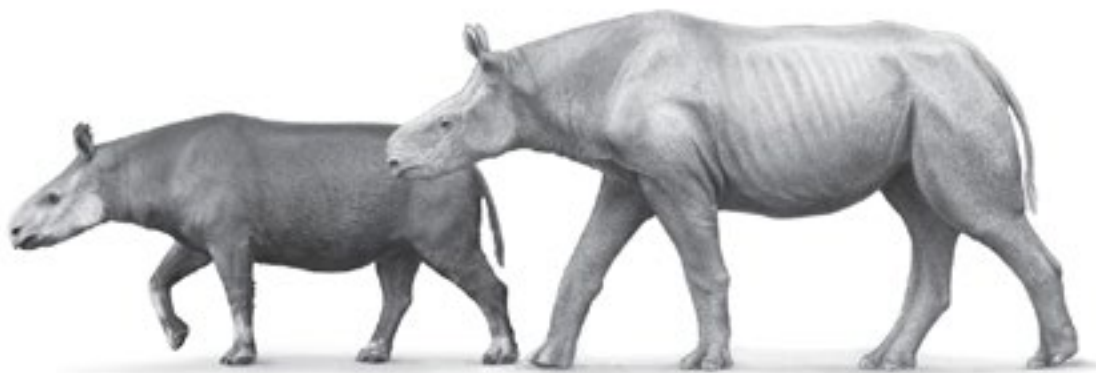

Figure 1. Reconstructions of *Molassitherium* (left) and *Ronzotherium* (right) by Patrick Röschli.

REFERENCES

Brunet, M. 1979. Les grands mammifères chefs de file de l'immigration oligocène et le problème de la limite Eocène-Oligocène en Europe, Paris: Fondation Singer-Polignac (ed.).

Didier, G., Royer-Carenzi, M. & Laurin, M. 2012: The reconstructed evolutionary process with the fossil record. Journal of Theoretical Biology, 315, 26-37.

Didier, G., Fau, M., & Laurin, M. (2017). Likelihood of tree topologies with fossils and diversification rate estimation. Systematic biology, 66, 964-987.

Heissig, K. 1969: Die Rhinocerotidae (Mammalia) aus der oberoligozänen Spaltenfüllung von Gaimersheim bei Ingolstadt in Bayern und ihre phylogenetische Stellung, Abhandlungen der Bayerischen Akademie der Wissenschaften, Mathematisch-Naturwissenschaftliche Klasse, 138, 1-133.

5.15
New data on the upper Miocene continental record of Armenia

Davit Vasilyan [1], Lilit Sahakyan [2], Hayk Hovakimyan [2], Sergei Lazarev [3], Lutz Maul [4], Jeremy Kesner Caves Rugenstein [5]

[1] JURASSICA Museum, Route de Fontaines 21, CH-2900 Porrentruy
[2] Institute of Geological Sciences, National Academy of Science of Armenia, 24A, Marshall Baghramian Avenue, 0019 Yerevan, Republic of Armenia
[3] Palaeomagnetic laboratory "Fort Hoofddijk", University of Utrecht, Budapestlaan 17, 3584 CD, Utrecht, The Netherlands
[4] Research Station of Quaternary Palaeontology Weimar, Senckenberg Research Institute, Am Jakobskirchhof 4, D-99423 Weimar
[5] Department of Earth Sciences, ETH, Sonneggstrasse 5; CH-8092 Zürich

The late Miocene represents an important time period which characterises the rise of modern ecosystems. The upper Miocene continental record in Southern Caucasus is extremely poor. Here we present the first late Miocene age locality from Armenia which reflects dynamic environmental changes in the section, from aquatic (freshwater lake) to terrestrial environments. The studied section Jradzor is located in Central Armenia on the Eranos Mountainous Chain (1940 m a.s.l.), southwest from the Gegham mountains that are of volcanic origin. The base of the section is represented by volcanic breccia, which is overlain by a seven to eight meter thick diatomite package showing fine lamination. The diatomite contains an abundant fossil fauna of fishes, amphibians and a small mammal. Upwards in the section, the package provides sedimentological and palaeontological evidences of intensification of the terrestrial input into the lake and its gradual shallowing. This diatomite package is covered by a lens of lithified volcanic ash of high-K calc alkaline series. The lacustrine environment re-established and the second package of 3 m of diatomite was deposited on top of the lower package. The top of the second diatomite package is overlain with an erosional contact by 40 cm thick volcanic breccia, indicating full regression of the lake. The section follows by an about six meter thick series of terrigenous sediments (sandstones, clay-loess) intercalated by volcanic ash of high-K calc alkaline series. At the base of this package as well as below the (second) volcanic ash a rich amphibian, reptile and small and large mammal fauna has been recorded. The small mammal fauna can be correlated with the MN13 mammal zone, suggesting a late Miocene age of the sediments. The section continues with the second 7 m thick continental loess (mixtures of loess, sand and cobble) dominated package. In its base the package contains at least two fossiliferous horizons with vertebrates (small mammals (MN13 zone) and reptiles). The upper 2-2.5 m of the section are represented by a palaeosol horizon containing evidence of bioturbation. A lens of scoria (of 20-80 cm) in this layer is the last evidence of volcanic activity in the area. For comprehensive understanding of the environment, faunal, and vegetation evolution of the late Miocene of the area, further analyses (e.g. stable and radiogenic isotopes, phytolith, and pollen) on the Jradzor section will be provided.

5.16

Morphological disparity and ontogeny of the endemic heteromorph ammonite genus *Aegocrioceras*

Manuel F. G. Weinkauf [1], René Hoffmann [2], Kurt Wiedenroth [3], Peter Goeddertz [4] & Kenneth De Baets [5]

[1] *Département des sciences de la Terre, University of Geneva, Rue des Maraîchers 13, CH-1205 Genève (Manuel.Weinkauf@unige.ch)*

[2] *Institut für Geologie, Mineralogie und Geophysik, Ruhr-University Bochum (RUB), Universitätsstraße 150, D-44801 Bochum*

[3] *Am Hohen Holze, D-30823 Garbsen*

[4] *Steinmann-Institut für Geologie, Mineralogie und Paläontologie, Rhenian Friedrich-Wilhelm University Bonn, Nussallee 8, D-53115 Bonn*

[5] *GeoZentrum Nordbayern, Friedrich–Alexander University Erlangen–Nuremberg, Schlossgarten 5, D-91054 Erlangen*

Intraspecific variation based on heritable traits is considered an important motor for evolution (Hunt 2007) but is seldomly studied in palaeontology, and despite the fact that heteromorph ammonites often show a large range of intra-specific variation, that variation has rarely been quantified. This is unfortunate, since especially loosely coiled forms suffer from severe taxonomic over-splitting due to their large degree of morphological variation (De Baets et al. 2013). To that end, we herein quantify the intraspecific variation and ontogeny of 85 newly collected specimens of the Hauterivian endemic ammonite genus *Aegocrioceras*. All specimens have been collected from concretions in the newly exposed bed 82 in the clay pit Resse in NW Germany (Lower Saxony Basin, Mutterlose & Wiedenroth 2009). Data for the conch morphology (diameter, whorl height, whorl interspace, rib spacing) have been collected in 45° steps using the new software CONCH©. All ammonites have been *a priori* identified as *Aegocrioceras bicarinatum* or *Aegocrioceras semicinctum* following Rawson (1975). Morphological disparity and the development over the ontogeny have been quantified using univariate and multivariate analyses (Fig. 1), and an automated species delimitation algorithm (Ezard et al. 2010) was applied. An assessment of the intra- and inter-specific variation and ontogeny of this population demonstrates the presence of just one species, viz. *A. bicarinatum*. Comparison with the type material of *A. bicarinatum* and *A. semicinctum* reveals large morphological overlap of different shell parameters and does not support a separation of both forms as independent species. The analysed population of *A. bicarinatum* has a high variation in shell morphology including whorl interspace, umbilical width, and whorl expansion. Further, the changes in intraspecific variation through ontogeny have been quantified and we postulate that the two "species" are probably males and females of the same species, showing sexual dimorphism.
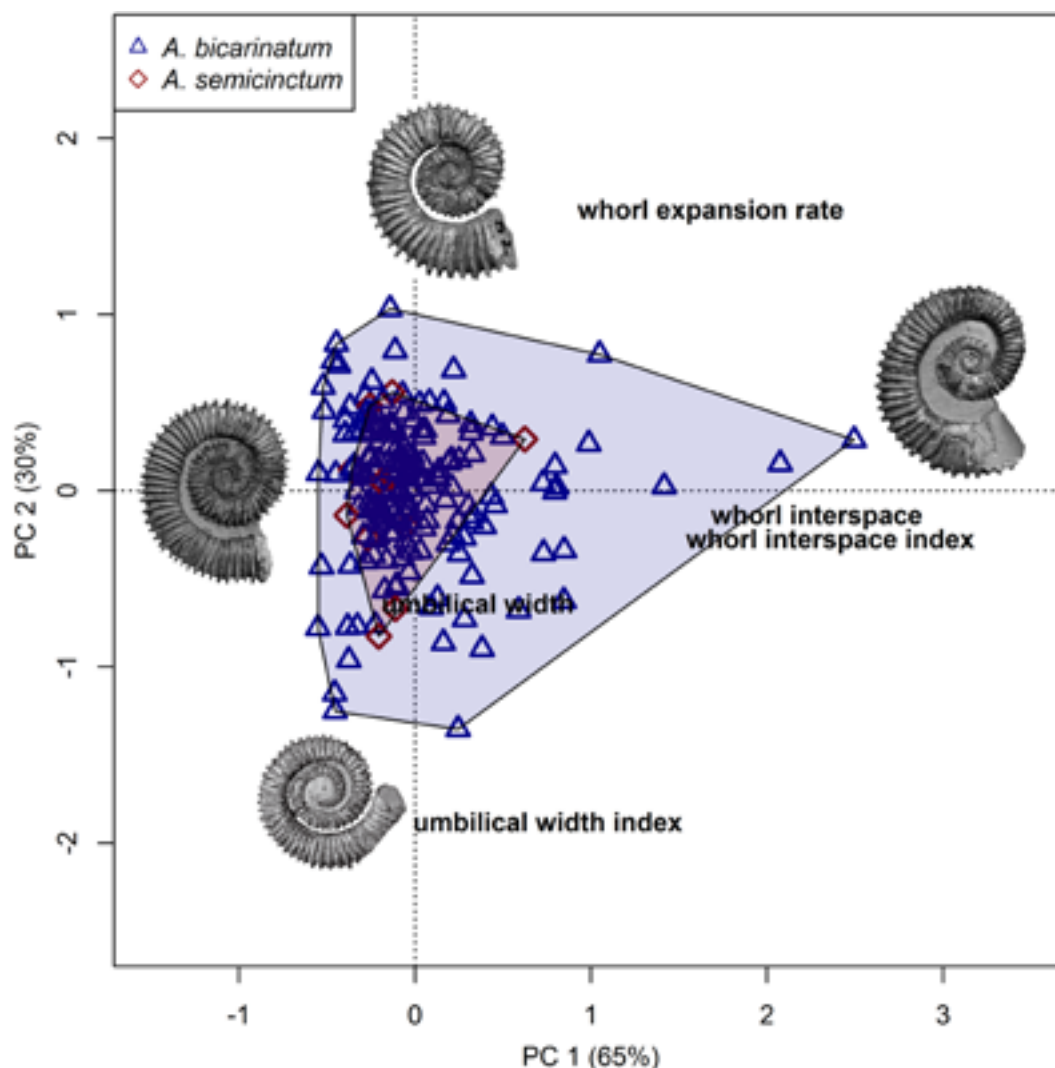
Figure 1. Principal component analysis (PCA) of *A. bicarinatum/A. semicinctum* from the clay pit Resse. Convex hulls encompassing all specimens of the respective species. Representative examples of the morphologies across the PCA space are shown.

REFERENCES

De Baets, K., Klug, C. & Monnet, C. 2013: Intraspecific variability through ontogeny in early ammonoids. Paleobiology 39, 75–94.

Ezard, T. H. G., Pearson, P. N. & Purvis, A. 2010: Algorithmic approaches to aid species' delimitation in multidimensional morphospace. BMC Evolutionary Biology 10, Article 175.

Hunt, G. 2007: The relative importance of directional change, random walks, and stasis in the evolution of fossil lineages. Proceedings of the National Academy of Sciences of the United States of America 104, 18404–18408.

Mutterlose, J. & Wiedenroth, K. 2009: Neue Tagesaufschlüsse der Unter-Kreide (Hauterive–Unter-Apt) im Großraum Hannover–Braunschweig: Stratigraphie und Faunenführung. Berliner paläobiologische Abhandlungen 10, 257–288.

Rawson, P. 1975: Lower Cretaceous ammonites from North-East England: The Hauterivian heteromorph *Aegocrioceras*. Bulletin of the British Museum of Natural History and Geology 26, 131–159.

5.17

The first theropod skeleton from Switzerland and what it tells us about the early evolution of neotheropod dinosaurs

Marion Zahner [1], Winand Brinkmann [1]

[1] Paläontologisches Institut und Museum, University of Zurich, Karl-Schmidstrasse 4, CH-8006 Zurich
(marion.zahner@pim.uzh.ch)

The Gruhalde clay pit in Frick (Canton Aargau, Switzerland) is the most proliferous European locality for Late Triassic saurischian dinosaurs. Since 1961 it is well-known for its abundant, articulated *Plateosaurus* material (Sauropodomorpha, Saurischia), which is derived from the Norian Gruhalde Member of the Klettgau Formation (Upper Keuper). Thousands of isolated and often fragmentary bones are found within this geological unit but the articulated material is concentrated in three distinct layers (Fig. 1). In 2006 and 2009 a spectacular discovery was made in the upper most dinosaur layer of Frick, immediately below the Triassic-Jurassic boundary. Then the first theropod skeleton of Switzerland (SMF 06-1 and 09-2) was excavetad. The impressively well preserved material of the Swiss theropod belongs to a subadult individual of a new genus and species. It comprises parts of the postcranium, an almost complete skull and stomach contents whereof remains of the rhynchocephalian *Clevosaurus* have been identified. While the Late Triassic and Early Jurassic theropod record has greatly improved over the last two decades by a number of new specimens, many taxa are represented by only a few bones that are often hardly diagnostic and especially specimens from Europe are usually very fragmentary. Obviously the Swiss specimen is of special scientific interest due to its old age and its excellent conservation. Additionally it shows a combination of distinctive morphological features that are typically found in either of two considered subgroups within Coelophysoidea: the coelophysids and the dilophosaurids. Traditionally the Coelophysoidea merges most predatory dinosaurs that are more basal than tetanurans but its monophyly is still an open question. In a comprehensive cladistic analysis focusing on taxa that are usually assigned to the Coelophysidae and Dilophosauridae as well as some averostrans the phylogenetic relationships of the new Swiss theropod taxon were tested. As expected, it is recovered within Coelophysoidea *sensu lato*. Therein, the Swiss taxon represents one of the basal most members of neotheropoda other than Coelophysidae. In short the Swiss theropod considerably increases the poor fossil record of Late Triassic European theropods and its unique combination of characteristic traits gives new insights concerning the early diversification and evolution of theropod dinosaurs. Furthermore, the preserved stomach contents provide a contribution to the reconstruction of ancient food chains.
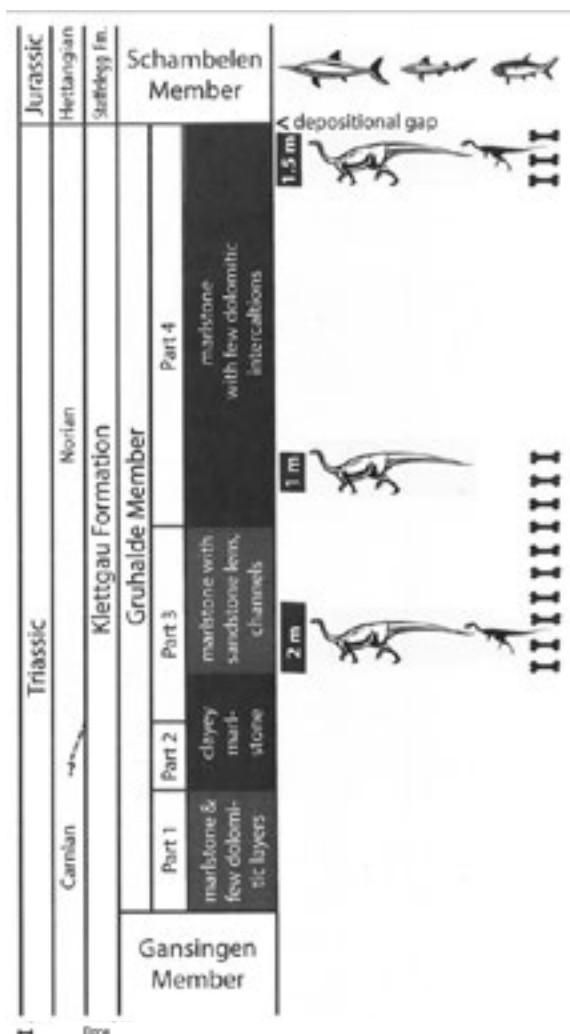
Figure 1. Geological profile of the Gruhalde clay pit in Frick, Switzerland. On the right the three dinosaur layers and the available specimens are shown. The stratigrafical classification is based on Jordan et al. 2016.

REFERENCES

Jordan, P., Pietsch, J. S., Bläsi, H., Furrer, H., Kündig, N., Looser, N., Wetzel, A. & Deplazes, G. 2016: The middle to late Triassic Bänkerjoch and Klettgau formations of northern Switzerland, Swiss J. Geosci. 109, 257-284.

P 5.1
Biostratigraphic dating and reconstruction of vegetation responses to Quaternary climate change in the Swiss North Alpine foreland

Patrick Schläfli [1,2] Erika Gobet [2], Willy Tinner [2] & Fritz Schlunegger [1]

[1] Institute of Geological Sciences, University of Bern, Baltzerstrasse 1+3, CH-3012 Bern (patrick.schlaefli@geo.unibe.ch)
[2] Institute of Plant Sciences and Oeschger Centre for Climate Change Research, University of Bern, Altenbergrain 21, CH-3013 Bern

The last interglacial (Eemian) has been a major focus of recent research efforts because its warmer-than-today conditions offer unique possibilities to assess faunal and vegetational responses to a warmer climate in the future. Nevertheless, the biostratigraphic position and the plant succession during the Eemian in the North Alpine foreland have not been fully deciphered and characterized yet. In fact, despite of several palynologically investigated Eemian sequences (e.g. Dürnten, Kienersrüti, Huriflue, Jaberg, Thalgut, Wässeriflue, Alte Schlyffi, Hunzikenbrücke, Thungschneit; Welten 1982, 1988), only the section at Beerenmösli has been independently dated through U/Th to 115.7±4.8 ka BP (Wegmüller, 1992). It is the major scope of this project to improve the characterization and the temporal calibration of Eemian biostratigraphic records. This will form the basis to correlate the North Alpine Eemian biostratigraphy with NW European Stages and the Marine Isotope Stages (MIS). We address this scope through a high-resolution investigation of new palynonological records and through dating with various chronometers. In particular, lacustrine sediments with Eemian fossiliferous material have been identified at Spiezberg (Zwahlen et al. *pers. communication*), located at the SW margin of Lake Thun (Switzerland). At this site, three fine-grained sand samples have been collected and will be analyzed for IRSL dating purposes in order to get independent ages. Previous palynological and sedimentological investigations at Spiezberg have revealed hiatuses at the top and at the bottom of the Eemian lake deposits. Therefore we will additionally explore further Eemian material, which we expect to encounter in new drillings through Quaternary infillings of overdeepend valleys in the Bern area.

The biostratigraphic dating of Quaternary sediment sequences within overdeepend valleys will contribute to the understanding of the timing of Pleistocene glacial advances and the mechanisms of overdeepening formation. In addition, the planned analyses would represent a major scientific advance in Quaternary biostratigraphy, as they would for the first time since the pioneering work at Beerenmösli generate new physically dated Eemian pollen records from the Swiss North Alpine foreland. Reproducing, refining and chronologically constraining the Eemian biostratigraphies with state-of-the-art approaches would allow better foundations for biostratigraphic comparisons of European pollen archives. Further, the novel records will allow unravelling interglacial vegetation dynamics and processes.

REFERENCES
Welten, M. 1982: Pollenanalytische Untersuchungen im jüngeren Quartär des nördlichen Alpenvorlandes der Schweiz. Beiträge zur Geologischen Karte der Schweiz, N.F. 156. Schweizerische Geologische Kommission, Zürich.
Welten, M. 1988: Neue pollenanalytische Untersuchungen über das Jüngere Quartär des nördlichen Alpenvorlandes der Schweiz, Mittel- und Jungpleistozän. Beiträge zur Geologischen Karte der Schweiz, N.F. 162. Schweizerische Geologische Kommission, Zürich.
Wegmüller, S. 1992: Vegetationsgeschichtliche und stratigraphische Untersuchungen an Schieferkohlen des nördlichen Alpenvorlandes. Denkschriften der Schweizer Akademie der Naturwissenschaften 102, Birkhäuser Verlag, Basel.
Zwahlen, P., Tinner, W. & Vescovi, E. (*pers. communication*): Ein neues Eem-zeitliches Umweltarchiv am Spiezberg (Schweizer Alpen) im Kontext der mittel- und spätpleistozänen Landschaftsentwicklung.

P 5.2
Paleonvironmental implications of Deccan volcanism relative to the KTB extinction: evidences from the red bole record

Nikhil Sharma [1], Thierry Adatte [1], Valentin Sordet [1], Torsten Vennemann [2], Gerta Keller [3], Blair Schoene [3] & Syed Khadri [4]

[1] Institute of Earth Sciences, ISTE, University of Lausanne, 1015 Lausanne, Switzerland (nikhil.sharma@unil.ch)
[2] Institute of Earth Surface Dynamics, IDYST, University of Lausanne, 1015 Lausanne, Switzerland
[3] Department of Geosciences, Princeton University, Guyot Hall, Princeton, NJ 08544, USA
[4] P.G. Department of Geology, Amravati University, Amravati, 444602, India

Recent studies indicate that the bulk (80%) of Deccan trap eruptions occurred over a relatively short time interval in magnetic polarity C29r. U-Pb zircon geochronology shows that the main phase-2 began 250 ky before the Cretaceous-Paleogene (K-Pg) mass extinction and continued into the early Danian suggesting a cause-and-effect relationship [Schoene et al., 2015]. Closer to the eruption center, intra-volcanic red weathered horizons known as red boles can be observed and mark quiescent periods between basalt flows. A typical red bole begins with the fresh underlying basalt and evolves into weathered basalt, then, a layer of basalt in a rounded shape called 'bole' surrounded by clays at the top, which is overlain by the next lava flow. Red boles have increasingly attracted the attention of researchers to understand the climatic and paleoenvironmental impact of Continental Flood Basalts (CFB). Recent advances in U-Pb dating of Deccan lava flows, studies of weathering patterns and paleoclimatic information gained from multiproxy analyses of red bole beds (e.g., lithology, mineralogy, geochemistry) yield crucial evidence of environmental changes triggered by volcanic activity. Red boles consist mainly of red silty clays and represent a comparatively early stage in weathering; characterized by concentrations of immobile elements such as Al and Fe^{3+} ions that are typical of paleo-laterites, which probably developed during the short periods of weathering between eruptions. Clay minerals consist mostly of smectite suggesting semi-arid monsoonal conditions. At least 30 thick red bole layers are present in C29r below the K-Pg boundary between lava flows of phase-2 that erupted over a time span of about 250 ky. The short duration exposures of these red boles are reflected in the mineralogical and geochemical data that indicate rapid weathering (high CIA) linked to increasing acid rains. δD and $\delta^{18}O$ values measured on smectite clays from the red boles lie along the smectite line and approximate the meteoric water composition that prevailed during the Deccan eruptions. Recent isotopic data from analysis of red boles deposited through the main phase-2 suggest significant and rapid changes in rainfall intensity and/or altitude linked to the accumulation of a 3100m thick basalt pile that erupted over a short period of time. These results suggest an increasing paleoclimatic instability beginning at the top of the Bushe formation corresponding to an acceleration in the rate of volcanic emissions 70Ky before the KPg boundary. Finally, the role of mercury as a proximal proxy of Deccan volcanism is analysed. An increase in the mercury content is recorded as we move further away from the eruption center.

06. Stratigraphy

Alain Morard, Reto Burkhalter, Oliver Kempf & Ursula Menkveld-Gfeller

Swiss Commitee for Stratigraphy (SKS/CSS),
Swiss Palaeontological Society (SPG/SPS),

TALKS:

6.1   Castelltort S., Nowak A., Hunger T., Laeuchli C., Honegger L., Spangerberg J., Adatte T., Puigdefabregas C., Fildani A., Chanvry E., Foreman B., Poyatos-More M., Clark J.: Sediment-supply forced deltaic regression during early Eocene hyperthermals in the South-Pyrenean foreland basin, Roda de Isabena, Spain

6.2   Feist-Burkhardt S., Bläsi H., Deplazes G., Hostettler B., Wohlwend S.: High resolution dinoflagellate cyst palynostratigraphy of the Middle Jurassic in northern Switzerland

6.3   Fleischmann S., Picotti V., Bernasconi S., Caves J.K.: Isotope stratigraphy of a Tethyan platform and slope across the Pliensbachian-Toarcian. The impact of the precursor of the Toarcian-OAE on carbonate productivity and climate

6.4   Hilbert-Wolf H., Roberts E., Stevens N., O'Connor P., Lawrence L., Orr T.: Explosive volcanism and the preservation of vertebrates at the close of the Paleogene in the western branch of the East African Rift

6.5   Honegger L., Adatte T., Poyatos-Moré M., Chanvry E., Puigdefabregas C., Clark J., Castelltort S.: Identification and expression of hyperthermal events in continental settings: an example from the early Eocene Pyrenean foreland basin, Spain

6.6   Lauper B., Vogel H., Deplazes G., Jaeggi D., Ariztegui D., Foubert A.: Geochemical characterization of the Opalinus Clay/Passwang Formation boundary

6.7   Lena L., López-Martínez R., Lescano M., Aguirre-Urreta B., Concheyro A., Vennari V., Naipauer M., Samankassou E., Pimentel M., Ramos V.A., Schaltegger U.: The importance of radio-isotopic dating of the stratigraphic record – an example from the Jurassic/Cretaceous boundary

6.8   Pictet A., Kürsteiner P., Tschanz K., Tajika A.: Ammonite biostratigraphy of the Tierwis and Schrattenkalk formations in the Alpstein Massif, northeastern Switzerland

6.9   Widmann P., Bucher H., Leu M., Schneebeli-Hermann E., Goudemand N., Bagherpour B., Schaltegger U.: The timing of the largest Early Triassic extinction: implications for lethally hot vs. lethally cold climate

POSTERS:

P 6.1   Blattmann F.R., Wohlwend S., Becker J.K., Deplazes G.: Tracing facies variability in the Middle Jurassic Passwang-Formation (Frickberg, AG)

P 6.2   Garefalakis P., Schlunegger F.: Stratigraphic architecture of the Upper Marine Molasse implies incipient westward tilt of the foreland plate

P 6.3   Strasky S., Schaltegger U., Ovtcharova M., Hofmann B., Kälin D.: Age determination and correlation of the Wolhusen Bentonite (Upper Freshwater Molasse, Middle Miocene, Napf alluvial fan, Switzerland)

6.1
Sediment-Supply Forced Deltaic Regression During Early-Eocene Hyperthermals in the South-Pyrenean Foreland Basin, Roda De Isabena, Spain

S. Castelltort [1], A. Nowak [1], T. Hunger [1], C. Laeuchli [1], L. Honegger [1], J. Spangerberg [2], T. Adatte [2], C. Puigdefabregas [3], A. Fildani [4], E. Chanvry [5], B. Foreman [6], M. Poyatos-More [7], J. Clark [4]

[1] Département des Sciences de la Terre, Université de Genève, Rue des Maraichers 13, 1205 Genève, Suisse (sebastien.castelltort@unige.ch)
[2] Géopolis, Université de Lausanne, 1015 Lausanne, Suisse
[3] Universitat de Barcelona, Dept. de Geodinàmica i Geofísica, C/ Martí i Franquès,, 08028 Barcelona, Spain
[4] Equinor Research Center, 6300 Bridge Point Parkway, Building 2, Suite 100, Austin, Texas, 78730 USA
[5] TOTAL, Research & Development, avenue Larribau, 64018 Pau cedex, France
[6] Department of Geology, Western Washington University, Bellingham, Washington 98225, USA
[7] Department of Geosciences, University of Oslo, Sem Sælands vei 1, 0371 Oslo, Norway

The Early Eocene Roda Sandstone is a shallow marine deltaic depositional system composed of mixed siliciclastic and carbonate sediments deposited in the NE margin of the Tremp-Graus Basin, Southern Pyrenees, Spain. The sequence stratigraphic architecture of this formation shows several episodes of deltaic progradation followed by carbonate accumulation that have been classically ascribed to sea-level changes or hinterland tectonic pulses. However, the Early Eocene was punctuated by significant climatic variations and carbon cycle perturbations now interpreted as so-called "hyperthermal" events because of their association with important episodes of global warming. We here present the link between these prominent early Eocene climatic signals and the stratigraphic evolution of the Roda formation in order to explore landscape response to hyperthermals. We generated carbon and oxygen stable isotope profiles as well as major and trace elements. Thanks to existing magnetostratigraphic constraints, the obtained isotopic profiles can be correlated with target curves from ODP site 1258, which allows identifying the presence of five hyperthermals correlatable to the I1, I2, J, ETM 3 and L events. Deltaic progradation is systematically correlated with these hyperthermals, while carbonate deposition systematically occurs at the end of hyperthermals or in between. These results suggest that deltaic progradation of the Roda formation could be related to increased sediment transport and continental weathering due to enhanced hydrology during hyperthermals. Conversely, carbonate deposition could result from sediment "starvation" after hyperthermal "clearing events". If this is correct, unlike classical sequence stratigraphic models, our results imply that deltaic progradation is primarily driven by climate-controlled sediment supply in a background of rising and high sea-level, while carbonate deposition represents maximum flooding because of a lack of available clastic material in generally lower sea-level stands.

6.2

High resolution dinoflagellate cyst palynostratigraphy of the Middle Jurassic in northern Switzerland

Susanne Feist-Burkhardt [1,2], Hansruedi Bläsi [3], Gaudenz Deplazes [4], Bernhard Hostettler [5], Stephan Wohlwend [6]

[1] Département des Sciences de la Terre, Université de Genève, Rue des Maraichers 13, CH-1205 Genève
  (feistburkhardt@gmail.com)
[2] SFB Geological Consulting & Services, Odenwaldstrasse 18, D-64372 Ober-Ramstadt
[3] H.R. Bläsi Geo-Consulting, Steinackerstrasse 2, CH-3184 Wünnwil
[4] Nagra, Hardstrasse 73, CH-5430 Wettingen
[5] Naturhistorisches Museum Bern, Bernastrasse 15, CH-3005 Bern
[6] Geologisches Institut, ETH Zürich, Sonneggstrasse 5, CH-8092 Zürich

Dinoflagellate cysts are the group of choice for palynostratigraphical age dating of Middle Jurassic marine sediments. Rapid evolution and wide distribution in marine sediments provide the means for palynostratigraphical age dating at an ultra high resolution level.

In recent years a large series of core and outcrop sections have been studied for the National Cooperative for the Disposal of Radioactive Waste (Nagra), for establishing a sound database on palynostratigraphical data for the Middle Jurassic Dogger in northern Switzerland. These studies created one of the largest and comprehensive palynostratigraphical data set for the Middle Jurassic in Central Europe. Dinoflagellate cyst first and last appearance events provide markers for age dating the sediments at ultra high resolution down to ammonite zone levels, in some parts of the succession even to subzone levels.

The palynostratigraphical research undertaken uses professional methods and software known from their application in the oil industry such as Graphic Correlation. Dinoflagellate cyst first and last appearance datums (FAD's and LAD's) have been used to create a Composite Standard for the region. Dates in the Composite Standard are correlated to ammonite biostratigraphy and calibrated to the newest Geologic Time Scale GTS 2016 (Ogg et al. 2016). As the GTS provides numerical age dates this allows for the interpretation of data in form of depth/age plots. Depth/age plots provide sedimentation rates, illustrate shallowing upward cycles of different magnitudes and allow for an interpretation of the succession in terms of sequence stratigraphy.

For fine-tuning of the Composite Standard in selected parts of the succession several outcrop sections have been studied with direct ammonite age control (e.g. Feist-Burkhardt & Götz 2016).

In the talk we will explain the method of Graphic Correlation and illustrate the power of dinoflagellate cyst palynostratigraphy in the Middle Jurassic of Switzerland.
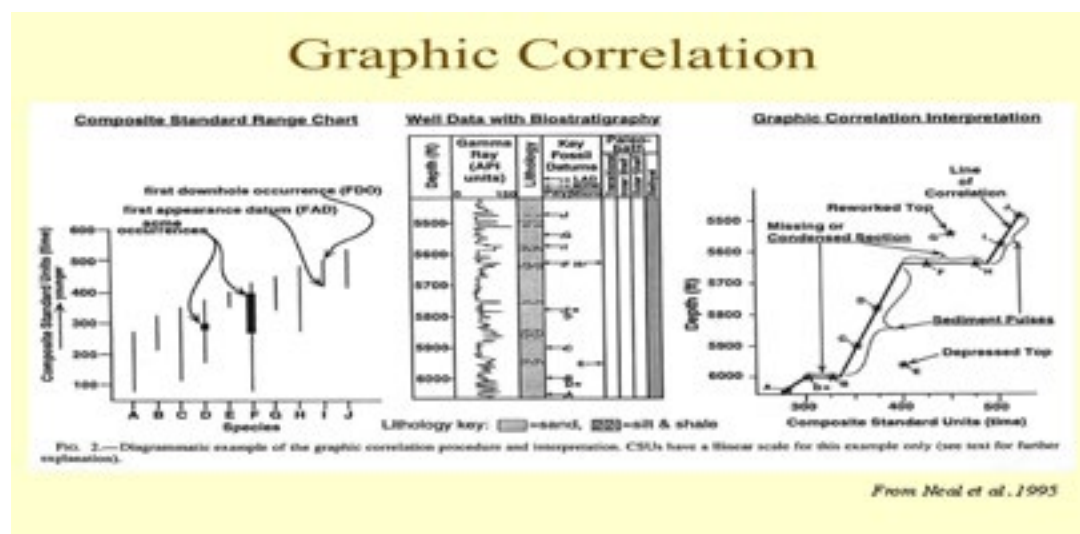

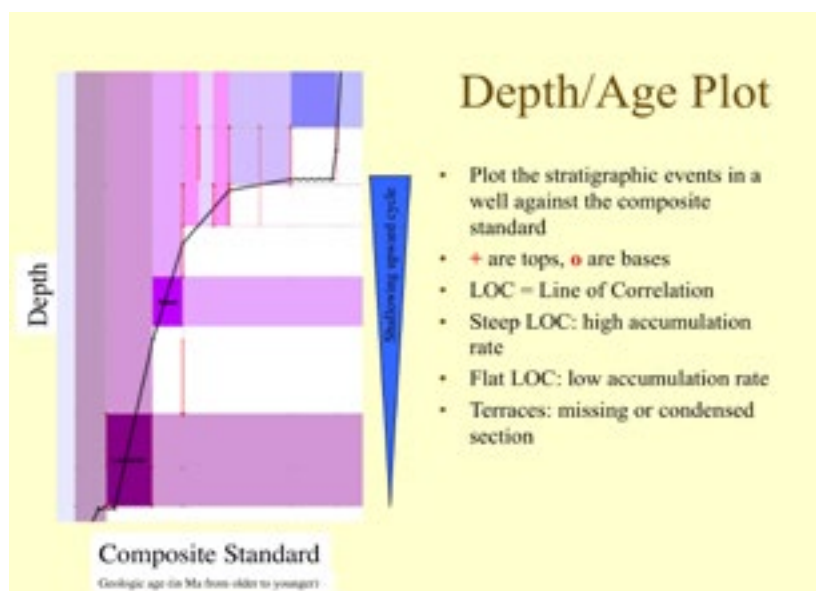Figure 1. Diagrammatic example of the graphic correlation procedure and interpretation (From Neal et al. 1995).

Figure 2. Depth/age plot. Example from the Bajocian, Middle Jurassic, of the Weiach well showing a shallowing upward cycle.

REFERENCES

Feist-Burkhardt, S. & Götz, A.E. 2016: Ultra high resolution palynostratigraphy of the Early Bajocian Sauzei and Humphriesianum zones (Middle Jurassic) from outcrop sections in the Upper Rhine area, southwest Germany. Stratigraphy & Timescales, 1, 325-392.

Neal, J.E., Stein, J.A. & Gamber, J.H. 1995: Integration of the graphic correlation methodology in a sequence stratigraphic study: examples from North Sea Paleogene sections. In: Mann, K.O. & Lane, H.R.: Graphic Correlation. SEPM Special Publications, 53, 95-113.

Ogg, J.G., Ogg, G. & Gradstein, F.M. 2016: The Concise Geologic Time Scale. Cambridge University Press. 184 pp.

6.3

Isotope stratigraphy of a Tethyan platform and slope across the Pliensbachian-Toarcian. The impact of the precursor of the Toarcian-OAE on carbonate productivity and climate

Sarah Fleischmann [1], Vincenzo Picotti [1], Stefano Bernasconi [1] & Jermy Kesner Caves Rugenstein [1]

[1] Institute of Geology, Department of Earth Sciences, ETH Zürich, Sonneggstrasse 5, CH-8092 Zürich
 (flsarah@student.ethz.ch)

The Toarcian Oceanic Anoxic Event (T-OAE) (at ca. 183 Ma) of the Early Jurassic is characterized by a major perturbation of the global carbon cycle, documented by a 5-8‰ shift in negative carbon isotopes followed by a positive carbon isotope excursion (CIE) (Jenkyns, 2010). Some hundreds of thousands of years earlier, at the Pliensbachian-Toarcian (P-To) boundary, a similar pattern of a minor (~1-2‰) negative CIE, followed by a positive shift can be observed in carbonates, organic matter and fossil wood (e.g. Hesselbo et al., 2007; Jenkyns et al., 2002). This precursor of the T-OAE has not been well analyzed so far, possibly due to the wide occurrence of gaps and condensations across the P-To boundary (e.g. Pittet et al., 2014).

Chemostratigraphic and biostratigraphic correlations ($\delta^{13}C_{carb}$) of a well-dated and complete slope-succession with the adjacent carbonate platform sediments, spanning the uppermost Pliensbachian to the lower Toarcian OAE in Northern Italy, allowed the development of a detailed stratigraphy to test the response of the carbonate factory to the P-To event and the T-OAE. Numerical modelling of the negative CIEs of the P-To event and the T-OAE gave new insights on the duration of these perturbations and the amount and source of carbon causing these shifts.

Starting from the latest Pliensbachian (h*awskerense* Subzone), a negative inorganic CIE of around -1.5‰, which was assigned to the P-To event, was found in the slope and platform margin successions. Sligthly preceeding that one, the carbonate platform records a crisis, which was caused by a drop of eustatic sea-level and the emersion of the platform, likely associated with a icehouse climate. The negative CIE of the subsequent T-OAE is recorded in well-bedded, pelagic limestones of the platform margin and inner platform, which document a maximum transgression at the onset of the *serpentinus.* Modelling results suggest the negative CIEs at the P-To transition and the T-OAE had a duration of 250'000 yrs and 400'000 yrs, respectively, and mostly derive from volcanic sources. An increased proportion of isotopically light methane carbon during the T-OAE with respect to the P-To is believed to have been the decisive factor to cause the greater perturbation of the T-OAE, which had a much greater impact on the environment than the P-To event. The best fitting models for the P-To event and the T-OAE propose that these negative CIEs can be generated by an input of 0.12 Gt C/yr and 0.13 Gt C/yr, respectively, which is around 75 times less than today's yearly global carbon emissions from fossil fuel (at least 9.8 Gt C) (McGee, , https://www.co2.earth).

REFERENCES

Hesselbo, S. P., Jenkyns, H. C., Duarte, L. V., & Oliveira, L. C. (2007). Carbon-isotope record of the Early Jurassic (Toarcian) Oceanic Anoxic Event from fossil wood and marine carbonate (Lusitanian Basin, Portugal). Earth and Planetary Science Letters, 253(3), 455-470.

Jenkyns, H. C. (2010). Geochemistry of oceanic anoxic events. Geochemistry, Geophysics, Geosystems, 11(3).

Jenkyns, H. C., Jones, C. E., Gröcke, D. R., Hesselbo, S. P., & Parkinson, D. N. (2002). Chemostratigraphy of the Jurassic System: applications, limitations and implications for palaeoceanography. Journal of the Geological Society, 159(4), 351-378.

McGee, M. (20.09.2015). Global carbon emissions. Retrieved from https://www.co2.earth/global-co2-emissions

Pittet, B., Suan, G., Lenoir, F., Duarte, L. V., & Mattioli, E. (2014). Carbon isotope evidence for sedimentary discontinuities in the lower Toarcian of the Lusitanian Basin (Portugal): Sea level change at the onset of the Oceanic Anoxic Event. Sedimentary Geology, 303, 1-14.

6.4
Explosive volcanism and the preservation of vertebrates at the close of the Paleogene in the western branch of the East African Rift

Hannah Hilbert-Wolf [1], Eric Roberts [1], Nancy Stevens [2], Pat O'Connor [2], Leigh Lawrence [1], & Theresa Orr [1]

[1] Geology Department, James Cook University, Townsville, QLD, Australia (hannah.hilbertwolf@my.jcu.edu.au)
[2] Department of Biomedical Sciences, Ohio University, Athens, OH, USA

The Nsungwe Formation, preserved in the Rukwa Rift Basin of the western branch of the East African Rift System in Tanzania, records one of the most important late Paleogene fossil bearing units in Africa. This formation is particularly important because it provides a rare snapshot into continental African ecosystems just prior to the Paleogene – Neogene transition, when a combination of faunal interchange from Asia and major tectonic and environmental changes drastically affected the East African landscape, climate, and biotas. Many of the most evolutionarily significant specimens from this deposit, such as the earliest Old World monkey and ape fossils (Stevens et al., 2013), the oldest venomous elapsid snake from mainland Africa (McCartney et al., 2014), the earliest evidence of the endemic frog family Ptychadenidae (Blackburn et al., 2015), and a new hyaenodont (Borths and Stevens, 2017) among many other important faunal discoveries, come from a single, taphonomically unique fossil locality known as Nsungwe 2B. We have undertaken a detailed taphonomic and geologic investigation of this key fossil locality.

The Nsungwe 2B locality is found in the lower part of the Songwe Member of Nsungwe Formation, bracketed by two carbonatite ash beds, which have been precisely dated via U-Pb CA-ID-TIMS to between 25.237 ± 0.098 and 25.214 ± 0.021 Ma (Stevens et al., 2013). The lower Songwe Member is characterized by repeating, upward fining successions that display cyclical development of small ephemeral fluvial channel systems that grade upward into volcanic ash rich, semi-arid lakes and wetlands. The Nsungwe 2B locality is located near the base of one of these depositional cycles in the fluvial channel facies. However, this particular channel complex is situated in the most ash-rich part of the stratigraphy and is sedimentologically distinctive. The fossil-bearing channel facies is characterized by a bentonitic, matrix supported sandstone in which the sand-sized fraction is composed of >40% heavy minerals (by weight) that are dominated by euhedral grains of phlogopite, titanite, andradite garnet, and rare pyrochlore. Fossils in this unit are more concentrated than in any other bed throughout the formation, and are typified by disarticulated bone fragments up to 20 cm in length (typically <6 cm in length), and small coprolites up to 2 cm in diameter by 4 cm long. We interpret the deposit as a volcanically influenced hyperconcentrated flow, or lahar. Sedimentologic and paleontologic evidence suggests that this lahar or hyperconcentrated flow moved across the landscape (north eastern rift flank) and into an ephemeral channel belt with standing billabong-like ponds, where it likely concentrated the attritional remains of both aquatic and terrestrial animals into a single bed. The lack of articulated remains suggests that although the deposit is quite unique, it was probably not a catastrophic event. Elevated fossil preservation, particularly of coprolites, is the likely result of a combination of high phosphate from the carbonatitic volcanic ashes, and the swelling nature of the bentonitic clays derived secondarily from the carbonatite ash. These clays likely protected the fossils in this unit from later destruction by acidic groundwater. This and other fossil localities in the Nsungwe Formation were deposited during the initial onset of East African rifting in the western branch, and this unique fossil locality is no doubt linked to the onset of explosive alkaline volcanism.

REFERENCES

Blackburn, D.C., Roberts, E.M., & Stevens, N.J. 2015: The earliest record of the endemic African frog family Ptychadenidae from the Oligocene Nsungwe Formation of Tanzania, Journal of Vertebrate Paleontology, 35:2.

Borths, M.R. & Stevens, N.J. 2017: The first hyaenodont from the late Oligocene Nsungwe Formation of Tanzania: Paleoecological insights into the Paleogene-Neogene carnivore transition, PLoS ONE, 12 (10).

McCartney, J., Stevens, N.J., & O'Connor, P.M. 2014: The Earliest Colubroid-Dominated Snake Fauna from Africa: Perspectives from the Late Oligocene Nsungwe Formation of Southwestern Tanzania, PLoS ONE, 9 (3).

Stevens, N.J., Seiffert, E.R., O'Connor, P.M., Roberts, E.M., Schmitz, M.D., Krause, C., Gorscak, E, Ngasala, S., Hieronymus, T.L., & Temu, J. 2013: Palaeontological evidence for an Oligocene divergence between Old World monkeys and apes, Naure, 497, 611-614.

6.5

Identification and expression of hyperthermal events in continental settings: an example from the early Eocene Pyrenean foreland basin, Spain

Louis Honegger [1], Thierry Adatte [2], Miquel Poyatos-Moré [3], Emmanuelle Chanvry [4], Cai Puigdefabregas [5], Julian Clark [6], Sébastien Castelltort [1]

[1] *Département des Sciences de la Terre, Université de Genève, Rue des Maraichers 13, 1205 Genève*
[2] *Institut des Sciences de la Terre, Géopolis, Université de Lausanne, 1015 Lausanne*
[3] *Department of Geosciences, University of Oslo*
[4] *IC2MP, Université de Poitiers & CNRS, INC, 86000 Poitiers*
[5] *Universitat de Barcelona, Departament de Geodinàmica i Geofísica, C/ Martí i Franquès, s/n, 08028 Barcelona*
[6] *Equinor Research Center, 6300 Bridge Point Parkway, Building 2, Suite 100, Austin, Texas*

Superimposed on a globally warm world, hyperthermals are pronounced global warming events of relatively short duration (< 50 kyrs) observed during the late Palaeocene and early to middle Eocene epochs (Sexton et al., 2011). Between 57.5 and 46.5 Ma, a total of 38 hyperthermals, recorded by important negative carbon isotopic excursions as well as peaks in iron content, have been recognized in marine cores (Westerhold et al., 2018). The most prominent and best known hyperthermal, both in amplitude and duration, is the extensively-studied Palaeocene-Eocene Thermal Maximum (PETM aka ETM1) at 55.93 Ma, which triggered a substantial increase in continental runoff and an important turnover in mammalian fossil assemblage (Slotnick et al. 2012). The analogy between past hyperthermal events and today's anthropogenic climate change has brought a lot of attention towards their study in the recent years. In particular, understanding Earth surface response to such abrupt and extreme warming events is important to assess its potential future response to the current perturbation.

However, while the study of hyperthermal records in marine successions is well established, the question of their preservation potential, and hence record, in continental succession is a matter of debate (Foreman & Straub, 2017). Thus, there is currently a significant lack of data on hyperthermal events in continental successions, despite their importance for the prediction of Earth›s fluvial landscape response to climate change.

In this study, we take advantage of the well exposed fluviatile sedimentary succession of the early Eocene Castissent Formation in the South Central Pyrenees, to generate a new isotopic record of early Eocene hyperthermals. Stable $\delta^{13}C$ profiles from pedogenetic carbonate nodules reveal the hyperthermal event "U" at *ca* 50 Ma and a robust correlation with global $\delta^{13}C$ profile. These data document a stepped $\delta^{13}C$ negative excursion and a relative enrichment in immobile elements (Zr, Ti, Al) in red beds, suggesting more intense weathering and/or longer exposed soils that we associate with landscape stability during a short-lived climatic peaks (Sheldon & Tabor, 2009).

These results give an insight on a larger recognition of hyperthermal events in continental successions as well as the preservation potential of such continental deposits.

REFERENCES

Foreman, B.Z., and Straub, K.M., 2017, Autogenic geomorphic processes determine the resolution and fidelity of terrestrial paleoclimate records: Science Advances, v. 3, p. 1–12, doi: 10.1126/sciadv.1700683.

Sexton, P.F., Norris, R.D., Wilson, P.A., Pälike, H., Westerhold, T., Röhl, U., Bolton, C.T., and Gibbs, S., 2011, Eocene global warming events driven by ventilation of oceanic dissolved organic carbon: Nature, v. 471, p. 349–352, doi: 10.1038/nature09826.

Slotnick, B.S., Dickens, G.R., Nicolo, M.J., Hollis, C.J., Crampton, J.S., Zachos, J.C., and Sluijs, A., 2012, Large-Amplitude Variations in Carbon Cycling and Terrestrial Weathering during the Latest Paleocene and Earliest Eocene: The Record at Mead Stream, New Zealand: The Journal of Geology, v. 120, p. 487–505, doi: 10.1086/666743.

Sheldon, N.D., and Tabor, N.J., 2009, Quantitative paleoenvironmental and paleoclimatic reconstruction using paleosols: Earth-Science Reviews, v. 95, p. 1–52, doi: 10.1016/j.earscirev.2009.03.004.

Westerhold, T., Röhl, U., Donner, B., Zacho, and C., Z.J., 2018, Global Extent of Early Eocene Hyperthermal Events – a new Pacific Benthic Foraminiferal Isotope Record from Shatsky Rise (ODP Site 1209): Paleoceanography and Paleoclimatology, v. 0, p. 626–642, doi: 10.1029/2017PA003306.

6.6
Geochemical characterization of the Opalinus Clay/Passwang Formation boundary

Bruno Lauper [1], Hendrik Vogel [2], Gaudenz Deplazes [3], David Jaeggi [4], Daniel Ariztegui [5] & Anneleen Foubert [1]

[1] Department of Geosciences, University of Fribourg, Chemin du Musée 6, CH-1700 Fribourg (bruno.lauper@unifr.ch)
[2] Institute of Geological Sciences and Oeschger Centre for Climate Change, University of Bern, Baltzerstrasse 1+3, CH-3012 Bern
[3] Nagra, Hardstrasse 73, CH-5430 Wettingen
[4] Federal Office of Topography swisstopo, Seftigenstrasse 264, CH-3084 Wabern
[5] Department of Earth Sciences, University of Geneva, Rue des Maraîchers 13, CH-1205 Geneva

The Opalinus Clay (OPA) is a mudstone formation particularly known in Switzerland as being the selected host rock for deep geological disposal of radioactive waste. In the northern Swiss Jura, the Opalinus Clay is overlain by the Passwang Formation (PF). This alloformation is characterized by parasequences of sandy bioclastic marls and limestones, separated by iron-oolitic beds (Burkhalter 1996). Both formations were interpreted as being deposited in a shallow epicontinental sea covering central Europe during the late Toarcian to Early Bajocian (Ziegler 1990). The basal ooidal ironstone of the PF is often used as a marker delimitating the OPA/PF formational boundary. This lithological transition is however diachronous and shows a high lateral variability.

To unravel the different depositional and diagenetic processes controlling the heterogeneity of this transition, petrographic data are combined with geochemical analyses (µXRF, XRF core scanning) on core material from different locations across northern Switzerland.

Preliminary results evidence the strength of recording high-resolution, continuous elemental variations at high spatial resolution along core sections for stratigraphical purposes. The µXRF and XRF core scanning data show coherent correlations with the lithology. The data allow to reconstruct paleoenvironmental and depositional conditions, and to disentangle diagenetic pathways. The use of non-destructive geochemical methods provides the means to understand lateral heterogeneity in complex transition zones. Moreover, extensive high-resolution datasets over several core sections allow enhanced statistical analyses extending the fields of application.

REFERENCES
Burkhalter, R. M. 1996: Die Passwang-Alloformation (unteres Aalénien bis unteres Bajocien) im zentralen und nördlichen Schweizer Jura, Eclogae Geologicae Helvetiae, 89, 875-934.
Ziegler, P. A. 1990: Geological atlas of western and central Europe (2nd ed.), Shell Internationale Petroleum Mij. B.V. and Geological Society, London.

6.7
The importance of radio-isotopic dating of the stratigraphic record - an example from the Jurassic/Cretaceous boundary

Luis Lena [1], Rafael López-Martínez [2], Marina Lescano [3], Beatriz Aguirre-Urrreta [3], Andrea Concheyro [3], Verónica Vennari [3], Maximiliano Naipauer [3], Elias Samankassou [1], Marcio Pimentel [4], Victor A. Ramos [3] & Urs Schaltegger [1]

[1] Department of Earth Sciences, University of Geneva, 1205 Geneva, Switzerland
[2] Instituto de Geología, Universidad Nacional Autónoma de Mexico, Ciudad de Mexico, 02376, Mexico
[3] Instituto de Estudios Andinos Don Pablo Groeber (UBA-CONICET), Universidad de Buenos Aires, Buenos Aires, 1428, Argentina
[4] Instituto de Geociências, Universidade de Brasilia, Brasilia, DF, 70910-900, Brasil

The emergence of high-precision U-Pb geochronology made the quantification of rates of geological, sedimentary and environmental processes possible. Presently best precisions allow resolution of processes at better than 100ka for the entire Phaerozoic. With such resolution we can address questions concerning the rates of magmatic and ore forming processes in the crust, calibrate precisely geological boundaries, and mass extinction events. The latter, is specifically important because important environmental and faunal information is recoded in sediments. Unravelling the rates of environmental and faunal chage in Earth's history thus identify possible cause-effect relationships between volcanic activity and mass extinctions through the demonstration of contemporaneity.

Here we show U-Pb geochronological data from the Jurassic/Cretaceous transition from two independent stratigraphic sections, one in Argentina (Neuquén Basin) and one from Mexico (Eastern Sierra Madre Province). We identify a few pitfalls when trying to correlate seemignly contemporaneous basin deposits over thousand kilometers. For instance, similar faunal assemblages are diachronous, i.e., a Tithonian fauna assemblage in one section has the same age as Berriasian fauna assembledge in the other. The diachroneity of FAD/LAD of key taxa creates assemblages that can emerge over a protracted period of times, rather than being global and time-equivalent phenomena. This is especially important to keeep in mind when defining stage boundaries, correlating disparate and presumably contemporaneous sedimentary sections, or correlating biological markers to global geochemical cycles (e.g., of carbon), or to magnetic reversals. I closing, an accurate geological time scale requires, in any case, an independent and quantitative geochronological calibration.

6.8
Ammonite biostratigraphy of the Tierwis and Schrattenkalk formations in the Alpstein Massif, northeastern Switzerland

Antoine Pictet [1], Peter Kürsteiner [2], Karl Tschanz [3] Amane Tajika [4]

[1] Musée cantonal de géologie, BFSH-2, 1015 Lausanne, Switzerland (antoine.pictet@unil.ch)
[2] Naturmuseum St. Gallen, Rorschacherstrasse 263, CH-9016 St. Gallen, Switzerland
[3] Schneeglöggliweg 37, CH-8048 Zürich, Switzerland
[4] American Museum of Natural History, Central Park West at 79th Street, New York, 10024-5192, USA

In the Alpstein massif (cantons of Appenzell Auserrhoden, Appenzell Innerrhoden and St. Gallen, Switzerland), a complete succession of uppermost Hauterivian to lower upper Barremian condensed hemipelagic series known as Tierwis Formation crops out. The Tierwis Formation, which records several periods of major palaeoenvironmental change, comprises several key surfaces with glauconite- or phosphate-rich beds associated to numerous ammonites. New discoveries of a large number of ammonites from these levels allow for a precise biostratigraphic dating of these key surfaces and of their associated palaeoenvironmental and palaeoecological events (Pictet, 2017). The Altmann Member is linked to the onset of a glauconite-rich sedimentation and coincides with the Faraoni oceanic anoxic event (Cecca et al., 1994), and with a prominent faunal radiation, and consecutive turnover (< 90%, Compagny et al., 2005). A remarkably increasing diversity and abundance of epipelagic ammonites like the genera *Crioceratites* and *Pseudothurmannia* is found at the base of the Altmann member. These ammonites are replaced by the Barremian genera *Emericiceras* and *Barremites* which are dominant in the middle and upper part of the Altmann Member. The transition between the Altmann and Drusberg members is marked by a polyzonal phosphatic conglomerate or/and by the onset of a marly limestone sedimentation which coincides with the mid-Barremian event (Coccioni et al., 2003) and with a prominent faunal turnover (e.g. Vermeulen, 2005). The above mentioned Barremian ammonites are replaced by diversified Ancyloceratidae, Desmoceratidae, Holcodiscidae and Pulchellinae. The marly limestone alternation of Drusberg Member, which is in direct sedimentary continuation, is intercalated with some poorly known condensed levels comprising ammonites as Desmoceratidae, Ancyloceratidae, Hemihoplitidae and Pulchellinae. The Schattenkalk carbonate platform, which overlies the Tierwis Formation, shows a diachronous late Barremian onset following a SE-ward progradation. Despite its very shallow facies, rare *ex situ* ammonites (Ancyloceratidae) from the outer and deeper parts of the platform were revised and indicate a latest Barremian age.
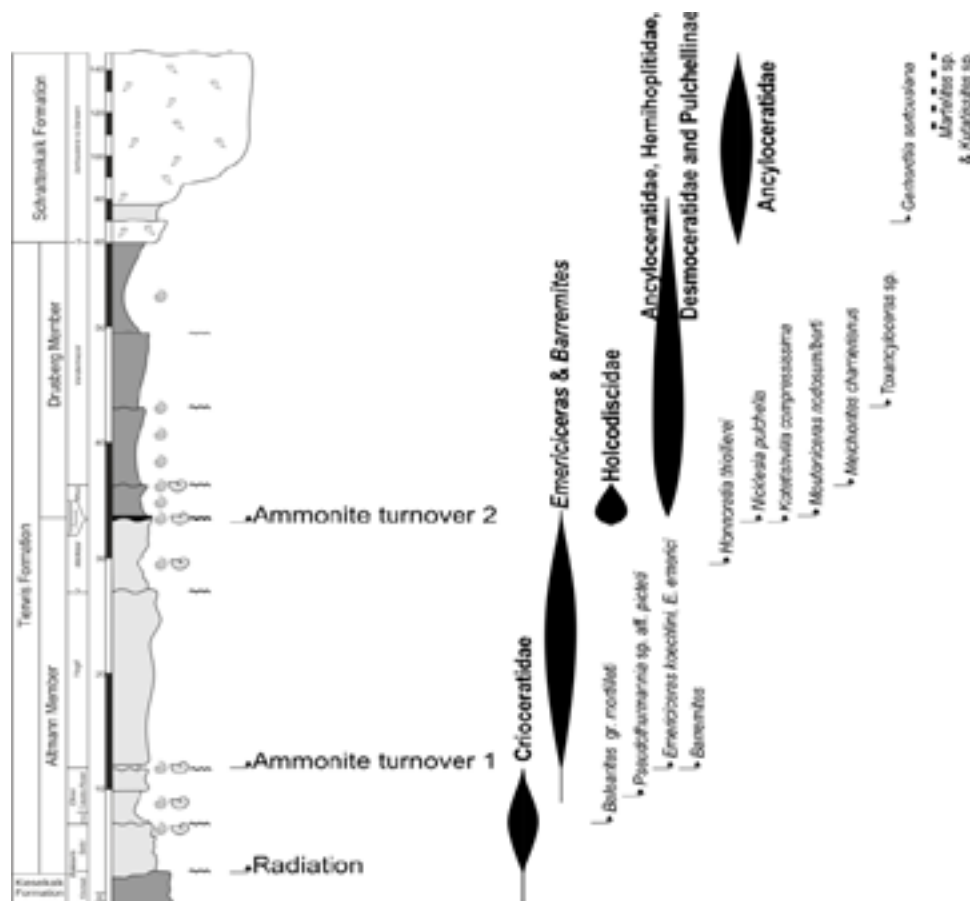
Figure 1. Biostratigraphy of ammonites and aqmes of the Tierwis and Schrattenkalk formations.

REFERENCES

Cecca, F., Marini, A., Pallini, G., Baudin, F., & Begouen, V. 1994: A guide-level of the uppermost Hauterivian (Lower Cretaceous) in the pelagic succession of Umbria–Marche Apennines (Central Italy): the Faraoni Level, Rivista Italiana di Paleontologia e Stratigrafia, 99, 551-568.

Coccioni, R., Galeotti, S., & Sprovieri, M. 2003: The Mid-Barremian Event (MBE): the prelude to the OAE1a, American Geophysical Union Fall Meeting, abstract #PP41B-0835.

Company, M., Aguado, R., Sandoval, J., Tavera, J.M., Jiménez de Cisneros, C., & Vera, J.A. 2005: Biotic changes linked to a minor anoxic event (Faraoni level, latest Hauterivian, early Cretaceous), Palaeogeography, Palaeoclimatology, Palaeoecology, 224, 186-199.

Pictet, A. 2017. Preluds of the Oceanic Anoxic Event 1a along the northern Tethyan margin : a progressive climatic destabilization from the latest Hauterivian (Early Cretaceous) onward, Berichte der Geologischen Bundesanstalt, 120, p. 212, abstract ISSN 107-8880.

Vermeulen, J. 2005: Boudaries, ammonite fauna and main subdivisions of the stratotype of the Barremian, In: Adatte, T., Arnaud-Vanneau, A., Arnaud, H., Blanc-Aletru, M.-C., Bodin, S., Carrio-Schaffauser, E., Föllmi, K., Godet, A., Raddadi, M.C., Vermeulen, J. 2005: The Hauterivian lower Aptian sequence stratigraphy from Jura platform to Vocontian basin: a multidisciplinary approach, Field-trip of the 7th International symposium on the Cretaceous (September 1–4, 2005). Géologie Alpine, Colloques et excursions 7, 181 pp.

6.9

The timing the largest Early Triassic extinction: implications for lethally hot vs. lethally cold climate

Philipp Widmann [1], Hugo Bucher [2], Marc Leu [2], Elke Schneebeli-Hermann [2], Nicolas Goudemand [3], Borhan Bagherpour [2] & Urs Schaltegger [1]

[1] Department of Earth Sciences, University of Geneva, rue des Maraîchers 13, CH-1205 Geneva, Switzerland (Philipp.widmann@unige.ch)

[2] Paleontological Institute and Museum, University of Zurich, Karl Schmid-Strasse 4, CH-8006 Zurich, Switzerland

[3] Univ Lyon, ENS de Lyon, CNRS, Univ. Claude Bernard Lyon 1, IGFL, UMR 5242, 46 Allée d'Italie, F-69364 Lyon Cedex 07, France

Following the Permian-Triassic boundary mass extinction (PTBME), the Early Triassic is characterized by large and recurrent perturbations of the global carbon cycle that are associated with radiation and extinction pulses of marine nektonic organisms and deep ecological turnovers of terrestrial plants. The most drastic setback of the taxonomic diversity of ammonoids and conodonts occurred during the late Smithian, possibly reaching into the base of the early Spathian. A gradual and protracted global positive CIE spanned the entire late Smithian and culminated in the basal early Spathian. The precise radio-isotopic age calibration of the successive biotic events that led to the extinction climax during latest Smithian, the carbon budget, and other environmental proxies are established here for the first time.

Only the oxygen isotope record previously measured from condonts led to infer that the late Smithian was "lethally" hot and supposedly accompanied by an equatorial eclipse of marine vertebrate, as well as by an alleged global peak of anoxia. However, there is mounting evidence that marine and terrestrial biochronological, paleoecological, stratigraphical and geochemical data consitently converge toward a swap between greenhouse and icehouses states during the early late Smithian. A reliable U-Pb age calibration of the extinction phases and of the environmetal proxies is pivotal for sorting out the underlying mechanisms and hence, the respective merits of the two scenarios.

We present here new high precision, chemical abrasion, isotope dilution, thermal ionization mass spectrometry (CA-ID-TIMS) U-Pb ages from single zircon crystals at the <100ka precision level. These were recovered from closely spaced volcanic ash layers distributed from the midlle Smithian to the early Spathian in four sections of the Luolou Formation in the Nanpanjiang Basin (South China). These new sections also benefit from a new robust biochronological scheme based on conodont Unitary Asociations coupled to preliminary ammonoid Unitary Association zones. The new U-Pb ages are integrated into a Bayesian age-depth model that allows precise and reproducible interpolation of the age of the Smithian-Spathian boundary, the duration of the positive CIE, and other events. The age model also allows assessing the duration of the gap at the substage boundary in the Luolou Fm., thus confirming the worldwide distribution of this remarkable hiatus indicative of a global sea-level fall.

P 6.1

Tracing facies variability in the Middle Jurassic Passwang-Formation (Frickberg, AG)

Franziska R. Blattmann [1], Stephan Wohlwend [2], Jens Karl Becker [1] & Gaudenz Deplazes [1]

[1] *National Cooperative for the Disposal of Radioactive Waste (Nagra), Hardstrasse 73, 5430 Wettingen*
[2] *Earth Science Department, ETH Zürich, Sonneggstrasse 5, 8092 Zurich*

Nuclear waste has been a major challenge since the mid-20th century. In Switzerland, the National Cooperative for the Disposal of Radioactive Waste (Nagra) plans to build a long-term nuclear waste repository within the Opalinus Clay. Therefore, a detailed geological investigation of this formation and its confining units is of great importance. The Opalinus Clay is an Early to Middle Jurassic mudstone, which is followed by the Passwang Fm, a parasequence consisting of sandy bioclastic marls, limestone and iron-oolitic beds (Burkhalter 1996).

This study is focused on investigating the continuity of beds within the Passwang Fm and its transition from the underlying Opalinus Clay in the Frickberg outcrop (Wohlwend et al. 2018). This was done by mapping and correlating beds in drone images as well as measuring a spectral gamma-ray (SGR) signal on the outcrop itself with a GT-40S manufactured by GeoRadis. The mapping shows that within the Brüggli Mb (upper Passwang Fm) a variation in thickness and facies of the beds can be recognized. Towards the east of the outcrop discontinuous, wavy sublayers as well as soft sediment deformation can be observed, which is not present in the western part. The SGR measurements reflect the lithologies, particularly the dose rate signal. A correlation between the Th/K ratio and the occurrence of iron ooids can also be observed.

Based on the mapped drone images one can conclude that the variation seen in the Brüggli Mb is the result of sediments being reworked by currents and possibly influenced by a paleotopography. This conclusion coincides with the findings of Bläsi et al. (2012) who investigated these sediments at a larger scale. It is also possible that synsedimentary tectonics played a minor role (Burkhalter 1996, Wetzel et al. 2003). Furthermore this case study shows that the Th/K ratio could potential be an indicator for iron oolithes.

REFERENCES

Bläsi, H.R., Deplazes, G., Schnellmann, M. & Traber, D. 2013: Sedimentologie und Stratigraphie das «Braunen Doggers» und seiner westlichen Äquivalente. Nagra Arbeitsber. NAB 12-051.

Burkhalter, R.M. 1996: Die Passwang-Alloformation (unteres Aalenien bis unteres Bajocien) im zentralen und nördlichen Schweizer Jura. Eclogae Geologicae Helvetiae. 89/3, 875–934.

Wetzel, A., Allenbach, R. & Allia, V. 2003: Reactivated basement strutures affecting the sedimentary facies in a tectonically "quiescent" epicontinental basin: an example from NW Switzerland. Sedimentary Geology 157, 153-172.

Wohlwend, S., Bläsi, H.R., Feist-Burkhardt, S., Hostettler, B., Menkveld-Gfeller, U., Dietze, V. & Deplazes, G. 2018: Die Passwang-Formation im östlichen Falten- und Tafeljura. Nagra Arbeitsber. NAB 18-011.

P 6.2
Stratigraphic architecture of the Upper Marine Molasse implies incipient westward tilt of the foreland plate

Philippos Garefalakis [1], Fritz Schlunegger [1]

[1] University of Bern, Institute of Geological Sciences, Baltzerstrasse 1+3, 3012 Bern, Switzerland
(philippos.garefalakis@geo.unibe.ch)

The sedimentary architecture in foreland basins can be used to reconstruct the basin's geometry and its evolution. Altough the development of the north Alpine foreland basin has been well examined (e.g. Allen et al., 1985), the controls on the 20 ma-old Burdigalian transgression are not fully understood yet. Marine transgressions can occur either through tectonic, eustatic or surface controlled mechanisms. Here, we explain through a stratigraphic approach the link between changes of the foreland plate underlying the Swiss Molasse and the raise of the Aar-massif in the adjacent Alps, where delamination started c. 20 Ma ago (Herwegh et al., 2017). We focus on the deposition of the Upper Marine Molasse (OMM) at both proximal and distal sites. We applied sedimentological techniques to obtain information about the (i) palaeodepositional environment and (ii) palaeoflow direction, and to infer (iii) geometrical shifts of the foreland plate underlying the Molasse deposits.

Examinations at the eastern proximal basin margin revealed that the c. 19.9 Ma-old OMM starts with a 350 m-thick sequence made up of parallel-laminated sandstones and cross-bedded sandstone-interbeds with basal scours and pebbly lags. Based on these observations, we infer a near-coast, wave-dominated sedimentary environment. Discharge directions derived from wave-ripple marks, cross-beds and transcurrent-laminations show a radial pattern with a dominant NE-directed tendency. The overlying c. 19.3 Ma-old deposists consist of m-thick sandstone cross-beds, where individual foresets are covered by current ripple-marks and mudrapes. This suggests a distinct change in the depositional environment towards a tidal-dominated setting, where strong tidal currents in a lower shoreface- to offshore-environment were the dominate sediment transport mechanims. Paleoflow directions suggest a W – E-directed transport, which then changed to a radial pattern with a NW – NE-direction. The 900 m-thick sequence terminates with c. 18.3 Ma-old palaeosoils.

The sedimentary architecture of the western proximal basin margin differs from that in the east. In the west, the c. 350 m-thick and 19.7 to 18.6 Ma-old suite starts with multiple stacks of 2 – 3 m high sigmoidal delta-clinoforms containing a pebbly lag at their base. The overlying sandstones are cross-bedded and contain muddrapes. We interpret this stratigraphic archive as deposits within an estuarine-environment with tidal influence. Similar to the east, discharge directions revealed a NE-directed sediment transport, at least at the base of the section. The overlying c. 19.3 Ma-old suite comprises 5 m-thick sandstone cross-beds superimposed by flow ripples and muddrapes. We interpret these deposits as sandwaves within an offshore, tidal-dominated environment. Discharge directions show a W – E-striking sediment transport. However, compared to the situation in the east, a NE-directed tendency is noticeable. The palaeoflow direction then changes to a N-directed orientation at the top of the section, just before it ends with c. 18.9 Ma-old tidal sediments.

In the distal basin margin, seismostratigraphic investigations show that sedimentation started approximately at 19.3 Ma and thus 0.5 myrs later than at the proximal sites. Also in the distal basin, sedimentation was characterized by the occurrence of 5 – 10 m-high fossiliferous cross-beds, which were deposited in an offshore environment. Discharge directions suggest a SW-oriented sediment transport in the distal eastern part and a NE-oriented flow in the distal western part of the Molasse basin.

In summary, the stratigraphic archives allow us to reconstruct changes in the depositional setting from a wave-dominated- and estuarine-environment to a tidal-dominated-setting. At the proximal basin border, sediment flux predominantly occurred towards the NE prior to 19.3 Ma. Sediment transport changed after c. 19.3 Ma to an axial orientation, and finally to a northward transport at c. 18 Ma. At more distal sites, sedimentation started later. In addition, the distal eastern sites show a NW-dominant transport, while distal western sites point towards the NE, both leading to a possible depocenter situated in the front of the Aar-massif (Allen et al., 1985).

The sedimentological data implies that the Burdigalian transgression, which occurred at c. 20 – 19.3 Ma, was characterized by a deepening and widening of the basin. Palaeoflow discharge directions suggest an incipient tilt of the basin axis from the NE to the N, and then to the SW when the basin became filled. These changes in the depositional environment, the palaeoflow and the basin's geometry are considered to be linked with the 20 Ma-old delamination of the Aar-massif in the adjacent Alps.

REFERENCES

Allen, P.A., Mange-Rajetzky, M., Matter A. & Homewood, P. 1985: Dynamic palaeogeography of the open Burdigalian seaway, Swiss Molasse basin, Eclogae Geologicae Helvetiae, 78, 351-381.

Herwegh, M., Berger, A., Baumberger, R., Wehrens, P. & Kissling, E. 2017: Large-scale crustal-block-extrusion during Late Alpine collision, Scientific Reports, 7, 413, 10 p.

P 6.3

Age determination and correlation of the Wolhusen Bentonite (Upper Freshwater Molasse, Middle Miocene, Napf alluvial fan, Switzerland)

Strasky, Stefan [1], Schaltegger, Urs [2], Ovtcharova, Maria [2], Hofmann, Beda [3], Kälin, Daniel [1]

[1] *Federal office of Topography, Seftigenstrasse 264, CH-3084 Wabern, Switzerland*
  (stefan.strasky@swisstopo.ch)
[2] *Department of Earth Sciences, University of Geneva, rue des Maraîchers 13, CH-1205 Geneva, Switzerland*
[3] *Natural History Museum, Bernastrasse 15, CH-3005 Berne, Switzerland*

Volcanic ash horizons (bentonites) have proven to be very useful marker beds (Rocholl et al. 2017) and chronostratigraphic tie points within the mainly clastic sedimentation of the Middle Miocene Upper Freshwater Molasse. Four stratigraphically distinct bentonite horizons are known from the sedimentary realm of the Hörnli alluvial fan of eastern Switzerland (Pavoni & Schindler 1981), covering the time period of approximately 15.5 Ma to 14.2 Ma. (Urdorf, Küsnacht, Aeugstertal and Leimbach).

In contrast, only one bentonite occurrence is known from the large Napf alluvial fan in western Switzerland. The so-called Wohlhusen bentonite is located on the eastern flank of the Napf alluvial fan. M. Freimoser discovered the bentonite horizon in two drill cores while drilling south of the village Wolhusen in 1978. Heavy minerals were extracted by F. Hofmann and stored at the Natural History Museum of Berne. These mineral separates were used for age determinations on zircon using CA-ID-TIMS U-Pb techniques.

Carefully selected zircon crystals were treated by chemical abrasion prior to dissolution. Single zircon grains were spiked with an internationally calibrated Earthtime ^{202}Pb-^{205}Pb-^{233}U-^{235}U tracer solution, dissolved in HF-HNO$_3$, and Pb and U isolated through anion exchange chromatography. Isotopic analysis was carried out on a Triton thermal ionisation mass spectrometer (Thermo Scientific) at University of Geneva, using a secondary electron multiplier in ion counting mode for Pb and Faraday multicollection using high-resistance amplifiers for U. The dates were corrected for common Pb blank, isotope fractionation during analysis, and initial ^{230}Th disequilibrium. Accuracy and external reproducibility were controlled by means of repeated analysis of a synthetic Earthtime solution and of natural reference zircons. Analytical techniques follow closely those outlined in detail in Davies et al. (2017).

We suggest an age of 15.37 ± 0.01 Ma for the deposition of this bentonite, based on the youngest zircon. For this reason we correlate the Wolhusen bentonite with the Urdorf bentonite of the Hörnli alluvial fan of eastern Switzerland (15.31 Ma ± 0.05 in Gubler 2009).

REFERENCES

Davies, J.H.F.L., Marzoli, A., Bertrand, A., Youbi, H., Ernesto, N. & Schaltegger, U. 2017: End-Triassic mass extinction started by intrusive CAMP activity. − Nature Communications 8, 15596.
Gubler, T. 2009: Blatt 1111 Albis (mit Beitrag von P. Nagy). – Geol. Atlas Schweiz 1:25000, Erläut. 134.
Pavoni, N. & Schindler, C. 1981: Bentonitvorkommen in der Oberen Süsswassermolasse und damit zusammenhängende Probleme. − Eclogae geol. Helv. 74/1, 53−64.
Rocholl, A., Schaltegger, U., Gilg, H.A., Wijbrans, J. & Böhme, M. 2017: The age of volcanic tuffs from the Upper Freshwater Molasse (North Alpine Foreland Basin) and their possible use for tephrostratigraphic correlations across Europe for the Middle Miocene. – Int. J. Earth Sci. (Geol. Rundsch.) https://doi.org/10.1007/s00531-017-1499-0.

07. Seismic Hazard and Risk in Switzerland: From Science to Mitigation

Donat Fäh, Katrin Beyer, Blaise Duvernay

TALKS:

7.1 Bodenmann L., Galans P., Broccardo M., Stojadinovic B.: Measuring the Benefit of Seismic Retrofitting in Reducing the Risk of Direct Earthquake Losses

7.2 Inamasu H., Siani N-G., Roger L.R., Elkady A., Kohrangi M., Lignos D.G.: Seismic Risk Assessment of Existing Steel Frame Buildings in Switzerland

7.3 Hobiger M., Fäh D., Zimmermann E., Michel C., Clinton J., Cauzzi C., Weber F., Duvernay B.: The renewal project of the Swiss strong motion network (SSMNet)

7.4 Hohensinn R., Geiger A.: Stand-alone GNSS Receivers as Velocity Seismometers: Geohazard Monitoring and Earthquake Detection

7.5 Roth P., Danciu L., Duvernay B., Fäh D., Kästli P., Lestuzzi P., Wiemer S.: ERM – Towards the first Swiss seismic risk model

7.6 Bergamo P., Perron V., Panzera F., Hammer C., Fäh D.: Ongoing development of the site response module in the Earthquake Risk Model Switzerland project

7.7 Diana L., Lestuzzi P.: Improving capacity curves and displacement demand prediction for accurate seismic vulnerability assessment at urban scale using mechanical methods

7.8 Michel C.: Earthquake loss scenarios: What, Why, How?

7.9 Kremer K., Anselmetti F.S., Boes R.M., Evers F.E., Fäh D., Fuchs H., Hilbe M., Kopf A., Lontsi A., Nigg V., Razmi M.A., Shynkarenko A., Stegmann S., Strupler M., Vetsch D.F., Wiemer S.: Lake Tsunamis in Switzerland: From causes to hazard

7.10 Shynkarenko A., Kremer K., Stegmann S., Lontsi A.M., Bergamo P., Hobiger M., Hammerschmidt S., Kopf A., Fäh D.: Geotechnical and Seismological Studies to Assess Slope Stability in Lake Lucerne

7.11 Lontsi A.M., García-Jerez A., Molina Villegas J.C., Sánchez-Sesma F.J., Ohrnberger M., Krüger F., Hobiger M.T., Molkenthin C., Shynkarenko A., Fäh D.: A generalized theory for full microtremor H/V (z, f) spectral ratio interpretation in offshore and onshore environments

7.12 Häusler M., Fäh D.: Monitoring the slope instability at Brienz / Brinzauls using ambient vibrations and earthquake recordings

POSTERS:

P 7.1   Bora S., Imperatori W., Bergamo P., Fäh D.: Challenges in earthquake ground-motion prediction for Switzerland

P 7.1   Grolimund R., Boesch E., Fäh D.: Seismicity in Switzerland in the early instrumental period Re-assessment of the period 1911-1963 from a heterogeneous dataset

P 7.3   Chieppa D., Hobiger M., Fäh D.: Investigation of the Swiss Molasse basin with passive seismic methods

P 7.4   Nigg V., Girardclos S., Kremer K., Anselmetti F.S.: Identification and characterization of lake-tsunami deposits in Switzerland

P 7.5   Schweizer N., Fabbri S., Wirth S.B., Anselmetti F.S., Gilli A., Kremer K.: Traces of the Ralligen Rockfall in Lake Thun

P 7.6   Strupler M., Kremer K., Anselmetti F.S., Razmi A., Wiemer S.: A first step towards an extensive estimation of the tsunami hazard in Swiss lakes

P 7.7   Evers F.M., Fuchs F., Razmi A.M., Vetsch D.F., Boes R.M.: Subaqueous Mass Failure: Hydraulic Lab Experiments

P 7.8   Noël C., Pimienta L., Violay M.: Time-dependent deformations of sandstone during fluid pressure oscillations: implications for natural and induced seismicity

P 7.9   Cornelio C., Spagnuolo S., Passelègue F., Nielsen S., Di Toro G., Violay M.: The different effect of fluid viscosity in earthquake nucleation and propagation.

P 7.10   Violay M., Giorgetti C., Cornelio C., Di Stefano G., Wiemer S., Burg J.-P.: A New State-of-the-art Apparatus to Study Earthquake Nucleation and Propagation: HighSTEPS

P 7.11   Antunes V., Planès T., Carrier A., Obermann A., Mazzini A., Ricci T., Sciarra A., Moretti M., Lupi M.: A back-projection location method based on the cross-correlation envelope of signals at different station pairs

P 7.12   Alvizuri C., Hetényi G.: Full moment tensors for exotic seismic sources including induced events, landslides, and nuclear tests

P 7.13   Acosta M., Passelègue F.X., Schubnel A., Gibert B., Violay M.: Influence of fluid pressure level on the nucleation of laboratory earthquakes.

7.1
Measuring the Benefit of Seismic Retrofitting in Reducing the Risk of Direct Earthquake Losses

Lukas Bodenmann [1], Panagiotis Galans [2], Marco Broccardo [3] & Bozidar Stojadinovic [4]

[1] Graduate Student, Chair of Structural Dynamics and Earthquake Engineering, ETH Zurich, Switzerland, CH-8093
[2] Research Associate, ETH Risk Centre, Zurich, Switzerland, CH-8092 (galanis@ibk.baug.ethz.ch)
[3] Research Associate, Chair of Structural Dynamics and Earthquake Engineering, ETH Zurich, Switzerland, CH-8093
[4] Professor, Chair of Structural Dynamics and Earthquake Engineering, ETH Zurich, Switzerland, CH-8093

"To retrofit or not to retrofit" for earthquakes is, often, the question engineers need to answer when working on existing building structures in Switzerland. Even though the seismic hazard in Switzerland is low-to-moderate, earthquakes that cause significant direct (repair costs) and indirect (e.g. business interruption) losses, a number of injuries and, perhaps even some fatalities, may occur. A seismic retrofit decision-making method based mainly on considering the risk of fatalities is implemented in SIA 269/8.

Herein we present a method to measure the benefit of seismic retrofitting a single building structure in terms of reducing the risk of excessive direct losses (Bodenmann, 2017). The hazard component of the method uses seismic hazard curves from open-source databases as provided by EFEHR. Given the geographic coordinates and the soil conditions at the site, the 5% damped elastic pseudo-acceleration spectrum $S_{ae}(T)$ is extracted for different frequencies of occurrence. In this study, the locations of Zurich, Lisbon, Seattle, Reggio Calabria and Los Angeles are considered. The severity component focuses on the assessment of the seismic loss probability distribution for a given single event (called severity distribution). The necessary demand fragility curves are derived, using SPO2IDA (Vavatsikos and Cornell, 2006), as applied in by Iervolino et al., 2016. The dynamic behaviour of a building is described using an elasto-plastic idealization of its static pushover curve, resulting in three parameters: yielding acceleration a_y, fundamental period of vibration T and structural ductility capacity m_c. Combining the fragility curves with damage functions, as in Dolce et al. 2006, we estimate the severity distribution. Compounding severity with the earthquake frequency of occurrence results in exceedance probability curves for seismic loss, or loss distributions.

Risk measures quantify the risk associated with a single building structure exposed to one or more sources of hazard for a given time horizon. A risk measure input is a loss distribution and output is a quantity that summarizes the risk exposure. The risk measures $\rho(x)$ examined in this study are:
- Expected Loss ($EL(x)$): represents the mean seismic loss in the considered time horizon t.
- Expected Shortfall ($ES\alpha(x)$): focuses only on losses above a certain threshold (confidence level α) and refers to the average expected losses given that the losses exceed the α-quantile.

To assess the effect of seismic upgrading we introduce the Degree of Seismic Upgrading, DSU (Bodenmann, 2017). An existing building lacking any seismic design features and having a small lateral strength corresponds to $DSU=0$. Conversely, a fully upgraded building, designed to meet the current seismic building codes, corresponds to $DSU=1$. A risk measure $\rho(DSU)$ is used to define the Normalized Retrofit Benefit ($NRB\rho$) as:

$$NRB_\rho(DSU) = \frac{\rho(0) - \rho(DSU)}{\rho(0) - \rho(1)}$$

The principal feature of the computed $NRB_{EL}(DSU)$ and $NRB_{ES\alpha}(DSU)$ curves shown in Figure 1 is their concavity, indicating that a partial seismic upgrade has a higher-than-proportional return in terms of direct loss risk reduction. For example, an upgrade of 30% allows for a reduction of 52% (Zurich) to 75% (Los Angeles) in the expected loss compared to that achievable with a full seismic upgrade. However, using the Expected Shortfall risk measure reveals that considering high quantiles (effectively, long hazard return periods and high-intensity earthquake events) changes the shape of $NRB_{ES\alpha}(DSU)$ curves to convex, indicating that a partial seismic upgrade yields smaller-than-proportional returns and justifying a full seismic upgrade.
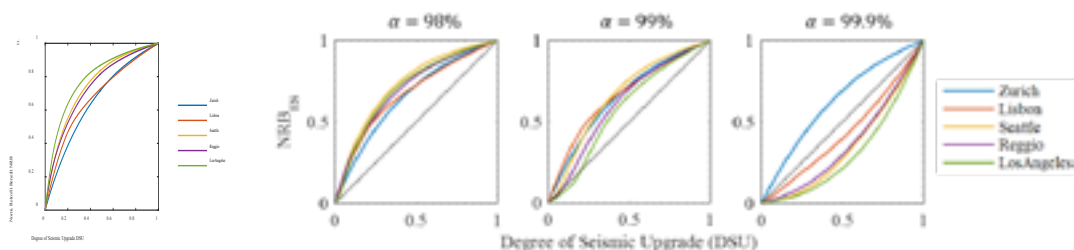
Figure 1. NRB_{EL} and $NRB_{ES\alpha}$ curves for different hazard environments

The proposed direct loss risk-based seismic upgrade evaluation method can be used to inform the building owners on how to most effectively mitigate their exposure to direct seismic losses.

REFERENCES

Bodenmann L. (2017): Application and Comparison of Financial Risk Measures in Earthquake Engineering, Master Thesis, ETH Zurich, Switzerland.

Dolce M, Kappos A, Masi A, Vona M. (2006): Vulnerability Assessment and Earthquake Damage Scenarios of the building stock of Potenza (southern Italy) using Italian and Greek methodologies, Engineering Structures, vol. 28, pp. 357-371.

EFEHR (2017) European Facility for Earthquake Hazard and Risk: www.efehr.org

Iervolino I, Baltzopoulos G, Vamvatsikos D, Baraschino R. (2016) SPO2FRAG V1.0: Software for Pushover-Based Derivation of Seismic Fragility Curves, VII European Congress on Computational Methods in Applied Sciences and Engineering, Crete Island, Greece.

Vamvatsikos D. and Cornell A. (2006) Direct Estimation of the seismic demand and capacity of oscillators with multi-linear static pushovers through IDA: Earthquake Engineering & Structural Dynamics, vol. 35, pp. 1097-1117.

7.2
Seismic Risk Assessment of Existing Steel Frame Buildings in Switzerland

Hiroyuki Inamasu [1], Nebua Ginette Siani [1], Laffely Sacha Roger [1], Ahmed Elkady [1] Mohsen Kohrangi [2] & Dimitrios Lignos [3]

[1] RESSLab, ENAC, École polytechnique fédérale de Lausanne, Bâtiment GC Station 18, CH-1015 Lausanne
[2] Scuola Universitaria Superiore IUSS Pavia, Pavia, Italy
[3] RESSLab, ENAC, École polytechnique fédérale de Lausanne, Bâtiment GC Station 18, CH-1015 Lausanne
  (dimitrios.lignos@epfl.ch)

New and existing steel frame buildings designed in low to moderately seismic regions are typically designed with no capacity design considerations (i.e., no pre-specified energy-dissipative elements). Consequently, such buildings are prone to the formation of undesirable weak-story mechanisms that can trigger structural collapse in the aftermath of earthquakes [1]. To this end, it is important to identify potential structural deficiencies in such buildings and investigate their potential influence on the overall system stability and earthquake-induced collapse risk.

This paper investigates the behavior of an existing 3-story steel building with concentrically braced frames (CBFs). The building is designed in the 1970s in Switzerland. First, structural details that may be detrimental to the seismic response and stability have been identified. In particular, Figure 1 shows an eccentric gusset plate (GP) brace connection with two potential folding lines. This detail can reduce the strength and deformation capacity of the CBF [2,3,4]. Early plastification in the undersized non code-conforming beams/columns could also induce unexpected failure during seismic excitations [3,4].
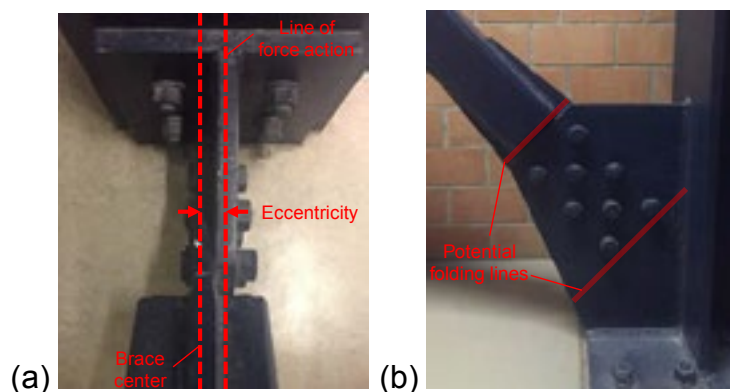

Figure 1. (a) eccentricty in the brace gusste plate-to-column connection; and (b) potential two-hinge mechanism at folding lines

In order to evaluate the effect of such deficiencies on the CBF's seismic performance, a rigourous numerical model was developed in an open source structural analysis software [5,6], as illustrated in Figure 2. The model employs material models that capture complex cyclic deterioration modes in strength and stiffness in beams and columns as well as potential fracture in steel braces and their connections. The seismic risk assessment of the CBF is evaluated through rigorous nonlinear response history analyses using ground motion sets selected based on site-specific probabilistic seismic hazard analysis.

The simulation results suggest that the building experiences a poor seismic performance depending on the design site. In particular, an undesirable two-hinge mechanism developed in each GP, which prevents brace yielding/buckling and potentially lead to the formation of soft-stories. Damage concentration at the connections eventually lead to premature fracture thereby causing building functionality disruption. Potential retrofit schemes are also discussed.
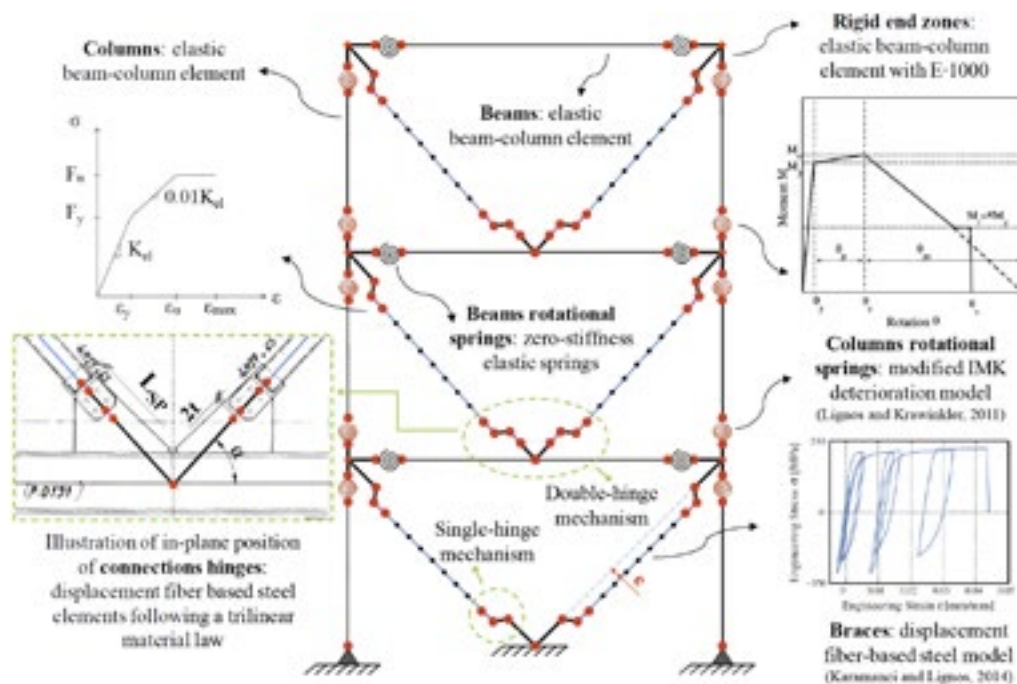
Figure 2. Numerical model specifics of the idealized CBF

REFERENCES

[1] Okazaki, T., Lignos, D. G., Midorikawa, M., Ricles, J. M. & Love, J. 2013: Damage to steel buildings observed after the 2011 Tohoku-Oki earthquake, Earthquake Spectra, 29.S1, S219-S243.

[2] Davaran, A., Gélinas, A. & Tremblay, R. 2015: Inelastic buckling analysis of steel X-bracing with bolted single shear lap connections, Journal of Structural Engineering, 141.8, 04014204.

[3] Simpson, B. G. & Mahin, S. 2018: Experimental and numerical evaluation of older chevron concentrically braced frames with hollow and concrete-filled barces, Journal of Structural Engineering, 144.3, 04018007.

[4] Sen, A. D., Sloat, D., Ballard, R., Johnson, M. M., Roeder, C. W., Lehman, D. E. & Berman, J. W. 2016: Experimental evaluation of the seismic vulnerability of braces and connections in older concentrically braced frames, Journal of Structural Engineering, 142.9, 04016052.

[5] Lignos, D. G. & krawinkler, H. 2011: Deterioration modeling of steel components in support of collapse prediction of steel moment frames under earthquake loading, Journal of Structural Engineering, 137.11, 1291-1302.

[6] Karamanchi, E. & Lignos, D. G. 2014: Computational approach for collapse assessment of concentrically braced frames in seismic regions, Journal of Structural Engineering, 140.8, A4014019.

7.3
The renewal project of the Swiss strong motion network (SSMNet)

Manuel Hobiger [1], Donat Fäh [1], Eric Zimmermann [1], Clotaire Michel [1], John Clinton [1], Carlo Cauzzi [1], Franz Weber [1], Blaise Duvernay [2]

[1] Schweizerischer Erdbebendienst, ETH Zürich, Sonneggstrasse 5, 8092 Zürich (manuel.hobiger@sed.ethz.ch)
[2] Fachbereich Erdbebenvorsorge, Bundesamt für Umwelt, Worblentalstrasse 68, 3063 Ittigen

Since 2009, the Swiss Seismological Service renews and expands its strong motion network (SSMNet). The goals of the project are a densification of the seismic network in areas of elevated earthquake hazard and risk, and a better coverage of the geological and structural variability found in Switzerland. The work is also focused on site effects, and the precise measurement and interpretation of seismic amplification effects. Stations are mainly installed in agglomerations, important industrial areas, and regions of touristic importance. Outdated dial-up stations of the old strong motion network are also replaced within the project.

In the first phase of the project, 30 new stations have been installed between 2009 and 2013 (Michel et al., 2014). The second phase, which is currently ongoing, includes 70 new stations to be installed by 2020 (Hobiger et al., 2017). At the time of writing (30 August 2018), 46 stations of phase 2 are installed (Fig. 1). All new stations are free-field stations and are mainly installed in densely populated urban areas of high seismic risk, but also in more rural areas where relevant earthquakes happened in the past. Four of the 100 stations are planned to be borehole stations with seismic sensors at the surface, in a depth of about 20 m and at about 100 m depth, and additional pore-pressure sensors at different depths. These borehole stations are planned in areas with a potential for liquefaction.
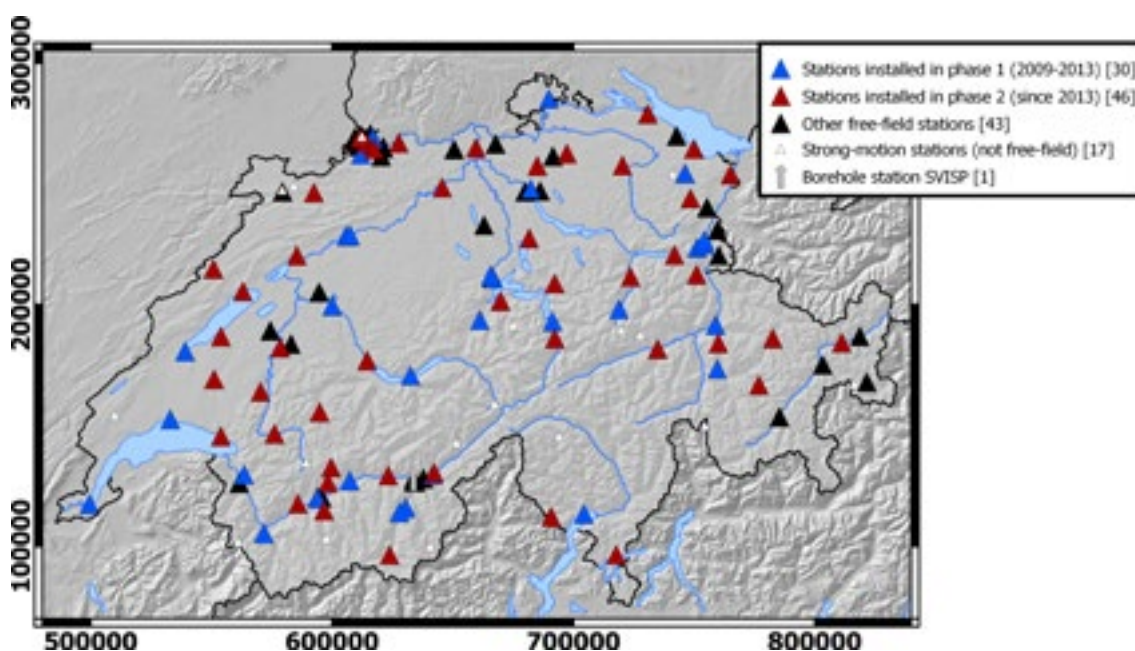

Figure 1. The map shows the free-field strong-motion network on 30 August 2018. It includes 30 stations installed in the first phase of the renewal project, the 46 stations so far installed in the second phase, as well as further strong-motion installations. The coordinates correspond to the Swiss coordinate system CH1903.

The site selection includes an investigation of the areas of interest with seismic and geological means. Suitable public areas of elevated risk, such as hospitals, schools or fire departments are further investigated by installing test stations for several days to measure the local noise level. All the gathered information are taken into account for chosing the final station location.

Once the station is installed, the site is characterized using passive and active seismic methods. Dispersion curves for Love and Rayleigh waves are measured, as well as the ellipticity of the Rayleigh wave particle motion. An inversion of these data yields the shear-wave velocity profile of the station site. Based on these data, we can model the amplification of the structure and compare it with the empirical amplification observed by the new station during earthquakes. At sites with expected non-linear site response or a potential for liquefaction, CPT measurements are also performed, which help in estimating these effects.

We will give an overview of the renewal project and show the different steps from the site selection until the final site characterization.

REFERENCES

Michel, C., Edwards, B., Poggi, V., Burjánek, J., Roten, D., Cauzzi, C., Fäh, D. 2014: Assessment of site effects in alpine regions through systematic site characterization of seismic stations, Bull. Seismol. Soc. Am., 104(6), 2809–2826.

Hobiger, M., Fäh, D., Scherrer, C., Michel, C., Duvernay, B., Clinton, J., Cauzzi, C., Weber, F. 2017: The renewal project of the Swiss Strong Motion Network (SSMNet). Proceedings of the 16th World Conference on Earthquake Engineering (16WCEE), Santiago de Chile, Chile, January 9-13, 2017.

7.4
Stand-alone GNSS Receivers as Velocity Seismometers: Geohazard Monitoring and Earthquake Detection

Roland Hohensinn and Alain Geiger

Institute of Geodesy and Photogrammetry, ETH Zürich
e-mail: rolandh@ethz.ch

Based on time derivatives of carrier phase measurements, the instantaneous velocity of a stand-alone (single) receiver is estimated with a high precision of a few mm/s; it is feasible to even obtain the level of tenths of mm/s. The advantage of single GNSS receiver observations is that only the data from the satellite navigation message is needed, thus discarding any data from a reference network. A field of this method's application is the detection of hazardous movements by GNSS. Examples are the monitoring of hazardous slope movements, like landslides and mudflows. Another interesting field of application is the detection and pre-analysis of large earthquakes. This capability is demonstrated for the 6.5Mw earthquake of October 30, 2016 near the city of Norcia (Italy) and for the 9.0Mw earthquake of March 11, 2011 in Japan (Tohoku-Oki). Based on the findings presented, it can be concluded that estimates of the instantaneous GNSS receiver velocity can contribute to geodetic or geotechnical real-time early warning systems.

7.5
ERM – Towards the first Swiss seismic risk model

Philippe Roth [1], Laurentiu Danciu [1], Blaise Duvernay [2], Donat Fäh [1], Philipp Kästli [1], Pierino Lestuzzi [3] & Stefan Wiemer [1]

[1] Swiss Seismological Service, ETH Zürich, Sonneggstrasse 5, CH-8092 Zürich (philippe.roth@sed.ethz.ch)
[2] Bundesamt für Umwelt, CH-3003 Bern
[3] EPFL ENAC IIC IMAC, GC G1 557 (Bâtiment GC), Station 18,CH-1015 Lausanne

Today, only a patchy answer can be given to the important question of what damage earthquakes can cause in Switzerland. Thanks to the Swiss seismic hazard model developed by the Swiss Seismological Service (SED) at ETH Zurich, we know where and how often certain types of earthquake can be expected and how strong the tremors they cause will be at a given location. Yet, it remains largely unclear what damage earthquakes could cause to buildings and consequently how large the financial losses could be. Commissioned by the Federal Council, the SED, in cooperation with the Federal Office for the Environment (FOEN) and the Federal Office for Civil Protection (FOCP), is now plugging this gap and is devising a seismic risk model, the ERM, to be delivered by 2022.

By combining the seismic hazard, the influence of the local subsurface, the vulnerability and the values of buildings, the model will enable cantonal and national authorities to draw up improved risk overviews and use them to optimise their planning. It will further allow to compile detailed scenarios for different types of earthquakes, and to carry out cost-benefit analyses for earthquake damage mitigation. Besides prevention, the model will serve to quickly and automatically assess where and how much damage can be expected in the occurrence of an event.

7.6
Ongoing development of the site response module in the Earthquake Risk Model Switzerland project

Paolo Bergamo [1], Vincent Perron [1], Francesco Panzera [1], Conny Hammer [1] & Donat Fäh [1]

[1] Schweizerischer Erdbebendienst (SED), ETH Zürich, Sonneggstrasse 5, CH-8092 Zürich (paolo.bergamo@sed.ethz.ch)

The site response module of the project "Earthquake Risk Model Switzerland" aims at providing the site amplification layer to be integrated in the wider work of seismic risk assessment for Switzerland. The module is articulated into three scales of analysis, attaining an increasing degree of resolution: a national level (national scale zonation for an updated classification of seismic response), and a regional and local level (encompassing standard microzonation and site-specific studies) for selected areas (e.g. Rhone valley, Basel area). The present work documents the ongoing development of the project module.

National scale. At the national scale, the final objective is updating the existing macroseismic amplification map, delivering several frequency-dependent seismic response layers, inclusive of aleatory and epistemic uncertainties. This will be achieved resorting to spatial proxies, i.e. indirect site condition indicators covering all (or a significant part of) the Swiss territory. The collections of site proxies will constitute the input layer for a neural/bayesian network structure predicting the site response at – virtually – any given location of Switzerland. The neural/bayesian network will be trained and tested at the sites of 175 SED seismic stations, where the seismic response is measured and known. Our work is presently focusing on the compilation of the site proxies database, privileging datasets of local information with extended spatial coverage (e.g. the ~6000 SED single-station noise measurements for resonance frequency estimation), and layers of diffuse information relating to geology (lithology, subsurface structures, pedo-lithogenic process, rock genesis, see Figure 1) or terrain configuration (digital elevation models).
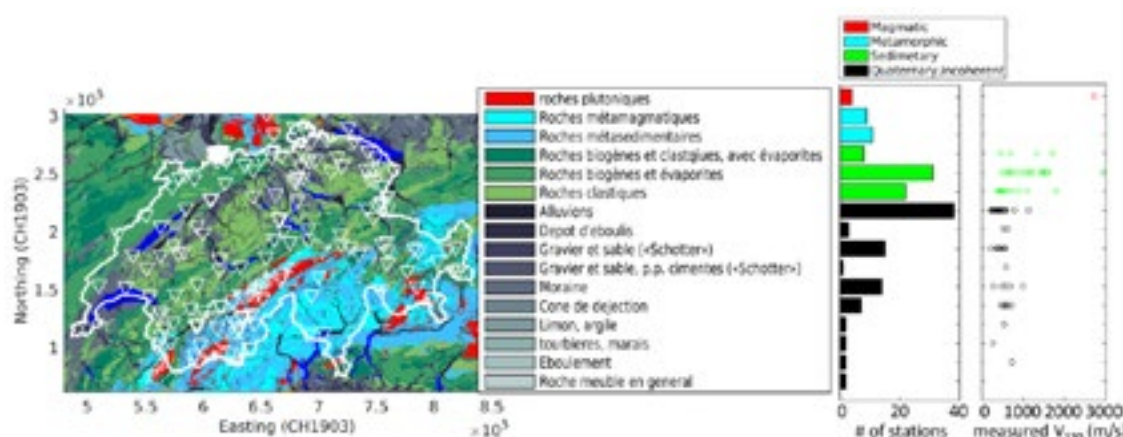

Figure 1 – Left: map of rock genesis (according to Swisstopo, 2005) and locations of SED stations (white triangles). Right: Distribution of SED stations sites according to rock genesis and their measured Vs30 values.

Regional scale. A more detailed analysis of seismic response is to be dedicated to specific regions of interests. In this initial part of the module work, the Rhone valley in Canton Valais has been selected as target. A network of 12 semi-permanent stations has been installed in June 2018 to quantify the amplification (from earthquake recordings) at sites of interest for their geological/topographical configuration and relevant from the risk point of view. In this preliminary stage of the seismic response assessment, we used the horizontal-to-vertical spectral ratio (HVSR) approach (Nakamura 1989) to determine the fundamental resonance frequency of the sites. The HVSR approach consists of computing the spectral ratios between the horizontal mean component and the vertical component of the ambient seismic wavefields recorded simultaneously at one single station. Figure 2 shows an example of sensor installation and HVSR result at site VET03 (Vétroz, VS). A sharp peak on the HVSR curve gives a clear estimates of f_0 ~ 0.5 Hz for this site.

Figure 2. Sensor installation at site VET03, measured HVSR curve and deduced fundamental resonance frequency (f_0) for the site.

Local scale. At the local scale, the focus is on limited areas where modeling and verification of seismic response is to be achieved with higher resolution and detail. The starting point has been a set of 3D geophysical models (Basel, Sion, Visp, Luzern areas) produced in the past by SED and mainly derived from microtremor recording surveys. These models are to be integrated with the geological information from the GeoQuat project of Swisstopo (Wehrens et al., 2017 for the Visp region) and refined, if needed, with further seismic measurement campaigns. The next survey to be carried out is a systematic HVSR microzonation campaign in the area of Sion (VS).

REFERENCES

Bundesamt für Landestopografie (Swisstopo) 2005: GK500, Geologische Karte der Schweiz 1:500000.

Nakamura, Y. 1989: A method for dynamic characteristics estimation of subsurface using microtremor on the ground surface, Railway Technical Research Institute, Quarterly Reports 30.

Wehrens P., Volken S., Preisig G., Gaehwiler M., & Möri A. 2017: GeoQuat project: Benefits of standardization and automation for analyzing and modelling data from Quaternary deposits. Expanded abstract, 2017 Swiss Geoscience Meeting.

7.7

Improving capacity curves and displacement demand prediction for accurate seismic vulnerability assessment at urban scale using mechanical methods

Lorenzo Diana [1] and Pierino Lestuzzi [1]

[1] IMAC (Applied Computing and Mechanics Lab) – IIC – ENAC – Ecole Polytechnique Fédérale de Lausanne (EPFL),
Batiment GC, Station 18, CH-1015 Lausanne Switzerland, (lorenzo.diana@epfl.ch; pierino.lestuzzi@epfl.ch)

The evaluation of seismic vulnerability at urban scale using mechanical methods is influenced by several factors: the definition of an adequate damage scale; the definition of an appropriate building typology classification; the determination of the displacement demand; the knowledge of the detailed seismic hazard.
In the present work, the involvement of refined capacity curves corresponding to especially developed specific typology instead of standard capacity curves and an accurate displacement demand determination are introduced for reliable building damage predictions.

The effects of these two factors are evaluated on the seismic damage distributions calculated for two typical Swiss cities (Sion and Martigny). Both cities are situated in the main seismic zone of Switzerland and microzones are defined for each city with appropriate response spectra. Usually seismic vulnerability assessments at urban scale in Europe are performed in accordance with Risk-UE project: an empirical approach (LM1 method) and a mechanical approach (LM2 method).

The mechanical LM2 method is based on standard capacity curves of traditional building types developed for seismic prone regions (Southern Europe). Existing building types have not been adapted for northern European cities and in general for regions with moderate seismicity. New refined typological curves have been developed for Switzerland for better describing the behaviour of existing standard Swiss buildings with stiff floors under seismic loads (Lestuzzi et al. 2017).

The computation of displacement-demand for existing building, respecting EC8, is usually based in Europe on the N2 method (Fajfar 2000). The N2 method is one of the most widespread methods in Europe for displacement demand determination. It combines pushover analysis of a multi-degree-of-freedom model with response spectrum analysis of an equivalent single-degree-of-freedom system. The inaccuracy of the N2 method has been studied by several researchers (Michel et al. 2014). Modifications to the N2 method have been proposed to improve the accuracy of displacement-demand determination (Diana et al. 2018).

In this study, the impact of typological capacity curves and modified N2 method are investigated independently. The results on the two case studies shows that both refinements contribute to enhance the seismic vulnerability assessment at urban scale. The influence of the two factors relies on the distribution of Swiss types in the general building stocks and on the different seismic hazard of Sion and Martigny.

REFERENCES

Diana, L., Manno, A., Lestuzzi, P., Podestà, S. & Luchini, C. 2018: Impact of displacement demand reliability for seismic vulnerability assessment at an urban scale, Soil Dynamics and Earthquake Engineering, 112, 35-52.

Fajfar, P. 2000: A nonlinear analysis method for performance based seismic design, Earthquake Spectra, 16(3), 573-592.

Lagomarsino, S. & Giovinazzi, S. 2006: Macroseismic and mechanical models for the vulnerability and damage assessment of current buildings, Bulletin of Earthquake Engineering, 4, 415-443.

Lestuzzi, P., Podestà, S., Luchini, C., Garofano, A., Kazantzidou-Firtinidou, D. & Bozzano, C. 2017: Validation and improvement of Risk-UE LM2 capacity curves for URM buildings with stiff floors and RC shear walls buildings, Bulletin of Earthquake Engineering, 15(3), 1111-1134.

Michel, C., Lestuzzi, P. & Lacave, C. 2014: Simplified non-linear seismic displacement demand prediction for low period structures, Bulletin of Earhquake Engineering, 12/4, 1563-1581.

7.8
Earthquake loss scenarios: What, Why, How?

Clotaire Michel [1,2]

[1] *Risk&Safety AG, Bahnhofstrasse 92, CH-5001 Aarau (michel@risksafety.ch)*
[2] *Schweizerischer Erdbebendienst (SED), Eidgenösische Technische Hochschule Zürich (ETHZ), Sonneggstrasse 5,
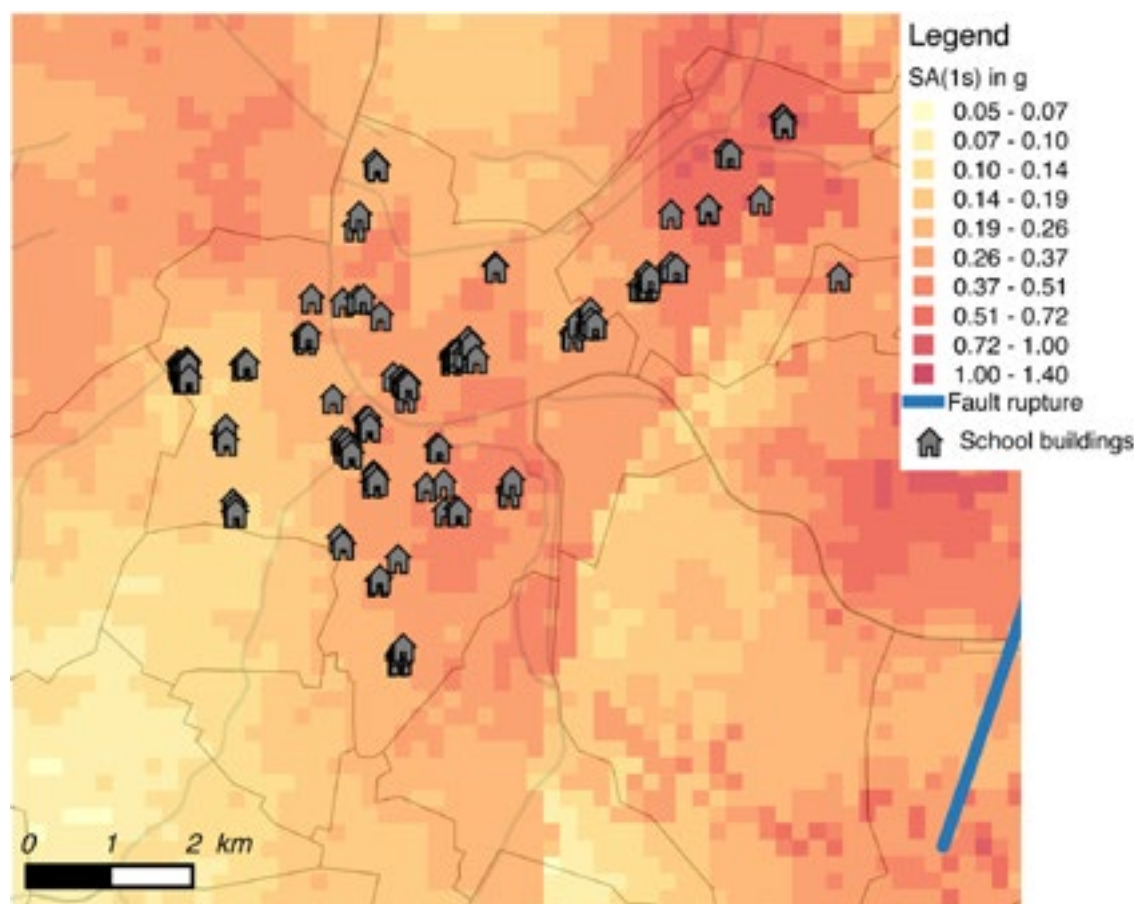CH-8092 Zürich*

Figure 1. Example earthquake scenario for the Basel school buildings (Michel et al., 2017)

Earthquake loss scenarios are conditional probabilistic seismic risk computations. Conditional means here that source characteristics (magnitude, location…) are fixed. Losses are very dependent from these characteristics so that such scenario modelling does not allow to quantify seismic risk. However, earthquake scenarios are useful for earthquake preparedness. They allow to test and adjust emergency planning, particularly to check redundancies and to prepare local populations. They are also useful to check the plausibility of models with respect to past events. The same models can be used for rapid loss assessment just after an event.
This contribution aims at summarizing the good practice of earthquake scenario modelling using recent applications in Switzerland (e.g. Michel et al., 2017, 2018, see Fig. 1).

In particular, scenarios should be based on probabilistic models, which means that uncertainties are accounted for in the models and conscientiously combined. Those are critical to avoid overconfidence in the models and keep the right level of precision. Uncertainties have to be coherently evaluated for all used models and none should dominate the computation (principle of consistent crudeness). Therefore, the level of precision in scenario modelling is driven by the available data and drives the choice of the models.
The roughest computations are performed using so-called empirical or macroseismic methods. In order to adjust for the amplification effects of local geology and account for the seismic vulnerability of the local building stock in an appropriate way, the current trend is using mechanical approaches that allow quantified observations (e.g. measurement of site properties, structural plan…) to be included in the models. However, it can be shown that they can be biased and should be used with care (Michel et al., 2018). As a conclusion, I argue that, contrarily to the recent trend, mechanical approaches cannot be generically formulated and necessarily need fine tuning using appropriate local hazard and vulnerability data.

REFERENCES

Michel, C., Crowley, H., Hannewald P., Lestuzzi P., & Fäh D. 2018: Deriving fragility functions from bilinearized capacity curves for earthquake scenario modelling using the conditional spectrum, Bulletin of Earthquake Engineering, in press.

Michel, C., Hannewald, P., Lestuzzi, P., Fäh, D., & Husen S. 2017: Probabilistic mechanics-based loss scenarios for school buildings in Basel (Switzerland), Bulletin of Earthquake Engineering, 15(4), 1471-1496.

7.9
Lake Tsunamis in Switzerland: From causes to hazard

Katrina Kremer [1], Flavio S. Anselmetti [2], Robert M. Boes [3], Frederic M. Evers [3], Donat Fäh [1], Helge Fuchs [3], Michael Hilbe [2], Achim Kopf [4], Agostiny Lontsi [1], Valentin Nigg [2], Mehdi A. Razmi [3], Anastasiia Shynkarenko [1], Sylvia Stegmann [4], Michael Strupler [1], David F. Vetsch [3] & Stefan Wiemer [1]

[1] Swiss Seismological Service, ETH Zürich, Sonneggstrasse 5, 8092 Zurich
[2] Insitute of Geological Sciences and Oeschger Centre for Climate Change Research, Univ. of Bern, Bern
[3] Laboratory of Hydraulics, Hydrology and Glaciology (VAW), ETH Zurich, Hönggerbergring 26, 8093 Zürich
[4] MARUM, University of Bremen, Leobener Strasse 8, 28359 Bremen

Marine tsunamis have been increasingly discussed in the context of ocean-wide natural hazards since the 2004 Sumatra and the 2011 Tohoku earthquake tsunamis. While ocean tsunamis are usually caused by earthquake-related plate displacements, tsunamis in lakes can have a seismic or aseismic cause. The wave-causing mechanisms are usually related to mass-movement processes that displace large amounts of water causing devastating waves.

Historical evidences in Switzerland has shown that tsunamis occurred in many lakes (e.g. 563 AD in Lake Geneva, 1601 and 1687 AD in Lake Lucerne etc.) causing large damage and also casualties. The causes of these tsunamis were diverse and varying between the different lake basins and events. An interdisciplinary Sinergia project, funded by the Swiss National Science Foundation, uses the outstanding field laboratory of Switzerland's lakes to understand better lake tsunamis by investigating their trigger mechanisms, wave propagation, inundation, sedimentation processes and their related hazard. In this contribution, we will present the project and highlight the main objectives.

7.10
Geotechnical and Seismological Studies to Assess Slope Stability in Lake Lucerne

Anastasiia Shynkarenko [1], Katrina Kremer [1], Sylvia Stegmann [2], Agostiny Marrios Lontsi [1], Paolo Bergamo [1], Manuel Hobiger [1], Steffen Hammerschmidt [2], Achim Kopf [2], Donat Fäh [1]

[1] Swiss Seismological Service, ETH Zurich, Sonneggstrasse 5, CH-8092 Zurich, Switzerland (a.shynkarenko@sed.ethz.ch)
[2] MARUM - Center for Marine Environmental Sciences, University of Bremen, Leobener Strasse 8, 28359 Bremen, Germany

Tsunamis do not only occur in oceans but also in lakes. In lake realm they are usually caused by sublacustrine massmovements or rock falls and despite the smaller spatial scale they might have devastating effects on coastal infrastructure and population. Conducting geophysical and geotechnical studies for the assessment of the subaqueous slope stability is an important step for tsunami hazard assessment and mitigation.

Historical and scientific documents attest the occurrence of several tsunami events in Switzerland in the past centuries, which were related to different triggering mechanisms. In 1601, a tsunami of around 4 m wave height in Lake Lucerne was caused by earthquake-triggered rock fall and sublacustrine mass movements. Another tsunami occurred in 1687 and was caused by a spontaneous delta collapse of the Muota delta in Lake Lucerne.

In this study, we use Lake Lucerne as a natural laboratory to study the pre-conditions and trigger mechanisms of slope failures in different geomorphological settings. This study is part of an SNSF funded Sinergia project.

Based on available geophysical and sedimentological data (reflection seismic profiles, bathymetry data and sediment coring etc.), we can identify locations where slope failures have occurred in the past and areas potentially prone to failure in the future. These sites were investigated in different measurement campaings, for which we present preliminary results:

(1) A geotechnical campaign using dynamic CPTu (Cone Penetration Testing) system (FF-CPTu) that allows a rapid estimation of sediment-mechanical properties (shear strength, pore pressure, etc.) on 150 CPTu profiles at 11 locations. These data allow us to characterize the pre-conditions and potential of failure of the upper part of the slope sediments;

(2) A coring campaign (combined with CPTu campaign) where 20 sediment cores (up to 1.5 m length) have been recovered using a gravity coring system to analyse the sediment-mechanical properties of sediments in the laboratory (shear strength, density, compressional wave velocity, etc.);

(3) Several ocean bottom seismometer (OBS) campaigns providing ambient vibration data recorded at 4 locations using single station and a sensor array configuration. These datasets allow characterizing the subsurface structure, including sediment volumes and seismic velocities.

The combination of these data (fig.1) will allow us to assess slope stability, sediment volumes potentially prone to failure as well as to characterize the behaviour of different slopes under seismic or aseismic loading.

Figure 1. Map of measured CPTu profiles (dark blue circles), retrieved sediment cores (green circles), OBS single station (blue triangles) and OBS array (yellow circles) measurements.

7.11

A generalized theory for full microtremor H/V (z, f) spectral ratio interpretation in offshore and onshore environments

Agostiny Marrios Lontsi [1], Antonio García-Jerez [2,7], Juan Camilo Molina Villegas [3,8], Francisco José Sánchez-Sesma [4] , Matthias Ohrnberger [5], Frank Krüger [5], Manuel Thomas Hobiger [1], Christian Molkenthin [6], Anastasiia Shynkarenko [1], Donat Fäh [1]

[1] Swiss Seismological Service, ETH Zurich, Sonneggstrasse 5, CH-8092 Zurich, Switzerland (agostiny.lontsi@sed.ethz.ch)

[2] Departamento de Química y Física, Universidad de Almeria, La Cañada de San Urbano, 04120 Almería, España,

[3] Facultad de Ingenierías, Universidad de Medellín, Colombia,

[4] Instituto de Ingeniería, Universidad Nacional Autónoma de México, Ciudad Universitaria, CP 04510, México D.F. Delegación Coyoacán, México,

[5] Institut für Erd- und Umweltwissenschaften, Universität Potsdam, Karl-Liebknecht-Str. 24-25, 14476 Potsdam-Golm, Deutschland,

[6] Institut für Mathematik, Universität Potsdam, Karl-Liebknecht-Str. 24, 14476 Potsdam-Golm, Deutschland,

[7] Instituto Andaluz de Geofísica, Universidad de Granada, Calle Profesor Clavera, 12, 18071 Granada, España,

[8] Departamento de ingeniería civil, Facultad de Minas, Universidad Nacional de Colombia – Sede Medellín, Av. 80 ##65 - 223, Medellín, Colombia.

Advances in the field of seismic interferometry have provided a basic theoretical interpretation to the full spectrum of the microtremor horizontal-to-vertical spectral ratio (H/V (f)). The interpretation now applies to ambient seismic noise data recorded both at the surface and at depth. The ambient noise wavefield contains information on the underlying subsurface structure due to multiple scattering and therefore can be used for imaging. The new algorithm, based on the diffuse wavefield assumption, has been used in inversion schemes to estimate seismic wave velocity profiles that are useful input information for engineering and exploration seismology both for earthquake hazard estimation and to characterize surficial sediments layers. However, until now, the developed algorithms are only suitable for on land environments with no offshore consideration. Here, the microtremor H/V (z, f) modeling is extended for applications to marine sedimentary environments for a 1D layered media. The layer propagator matrix formulation is used for the estimation of the Green's functions.

Therefore, in the presence of a water layer on top, the properties of the propagator matrix for the surface layer are modified to account for the properties of the water column. As application example for the proposed algorithm we analyze eight simple canonical layered earth models. Frequencies ranging from 0.2 to 50 Hz are considered as they cover a broad wavelength interval and aid in practice to investigate subsurface structures in the depth range from a few meters to a few hundreds of meters. The modeled H/V (z, f) results indicate that the theoretical formulation is suitable for the interpretation of the full spectrum of the microtremor H/V (z, f) estimated from three-component (3C) ambient noise data recorded in marine environment as well as for on land records. Results show a marginal variation of 5% at most for the fundamental frequency when a water layer is present. The main changes in the modeled H/V spectral ratio are observed in the amplitude. The water layer lead to reductions in H/V peak amplitude of up to 50% atop the solid layers.

7.12
Monitoring the slope instability at Brienz / Brinzauls using ambient vibrations and earthquake recordings

Mauro Häusler [1], Donat Fäh [1]

[1] Swiss Seismological Service, ETH Zurich, Sonneggstrasse 5, CH-8092 Zurich (mauro.haeusler@sed.ethz.ch)

Earthquake-triggered landslides and rockfall form two of the most destructive coseismic phenomena and pose a severe risk to settlements and infrastructure (Keefer, 1984). As an alpine country with moderate seismicity, Switzerland is affected by these secondary seismic effects as well. For example, the aftershock of the M_w 5.8 Sierre earthquake in 1946, the most recent strong earthquake in Switzerland, triggered a large rockfall of several million cubic meters in volume at the Rawilhorn, Valais (Fritsche and Fäh, 2009). Recent developments allow to estimate the likelihood for earthquake-induced mass movements by combining geospatial susceptibility proxies (e.g., slope gradient) with modelled peak ground acceleration, which allows to incorporate coseismic mass movements in a large scale hazard analysis (Cauzzi et al, 2018). However, to asses the actual hazard emanating from a specific slope, detailed in-situ investigations on individual slopes are required.

The final collapse of a slope instability is the result of many interacting influences, such as weathering, geological preconditions and seismic exposure (past earthquakes), which already weakened the inner structure of the slope. Therefore, existing slope instabilities have naturally a higher susceptibility to strong ground shaking and should be investigated with respect to their dynamic response to vibrations. Burjánek et al. (2010) showed that unstable slopes exhibit strong wavefield amplification of factors beyond 8 and that the wavefield polarizes perpendicular to open fractures. As a result of these findings, a variety of processing techniques was developed to measure and characterize the dynamic response of unstable slopes (summarized, e.g., by Kleinbrod, 2018).

We investigate the unstable slope above the village Brienz / Brinzauls (Grisons, Switzerland), which is threatening parts of the village. The settlement itself is situated on a large-scale slump (Flysch, overlaid by Allgäuschiefer slate) with a displacement rate of several dozens of centimeters per year, resulting in structural damages on some of the buildings (Krähenbühl and Nänni, 2017). Consequently, the village and its surrounding were assigned to a "red zone" for natural hazards in 2017, prohibiting any further construction activities. These movements in the foot of the slope also destabilize the uphill rock mass, leading to large deformations and sporadic rock fall activities with volumes up to 150'000 m^3.

We deployed temporary seismic arrays in the village Brienz and on the unstable areas in the rockfall source zone in June 2018 to obtain shear wave velocity profiles and to characterize the seismic wavefield in terms of amplification, resonance frequencies, and polarization. We demonstrate the site-to-reference-spectral-ratio method as a useful technique to quickly outline the unstable area and compare the results to previous seismic studies performed on the same site. The comparison reveals significant changes in both the polarization and the amplification characteristics. To better monitor temporal changes in the seismic response and to investigate the dynamic behavior during earthquakes, we installed an autonomous, semi-permanent seismic station (BRIZ2) on top of the instability in Mai 2018. Since its installation, the station recorded a number of small regional earthquakes, for example, the magnitude 2.9 Zernez event on 16.08.2018 with an epicentral distance of about 40 km. The proximity to another seismic station in the village of Brienz and the use of empirical amplification functions (Edwards et al., 2013) allows for estimating the absolute seismic amplification factors in the unstable area with respect to a reference bedrock (Figure 1). These factors are large and exceed the factor of 10 during an earthquake.

Figure 1. Absolute amplification spectrum of the station BRIZ2, installed on the rock slope instability Brienz / Brinzauls. The input data is the M_{Lh} 2.9 earthquake in Zernez (40 km epicentral distance).

REFERENCES

Cauzzi, C., D. Fäh, D. J. Wald, J. Clinton, S. Losey, and S. Wiemer. 2018, ShakeMap-based prediction of earthquake-induced mass movements in Switzerland calibrated on historical observations. Natural Hazards, 92, no. 2

Burjánek, J., G. Gassner-Stamm, V. Poggi, J. R. Moore, and D. Fäh. 2010, Ambient vibration analysis of an unstable mountain slope. Geophysical Journal International, 180, no. 2,820-828. doi: 10.1111/j.1365-246X.2009.04451.x.

Edwards, B., C. Michel, V. Poggi, and D. Fäh. 2013, Determination of Site Amplification from Regional Seismicity: Application to the Swiss National Seismic Networks. Seismological Research Letters, 84, no. 4

Fritsche, S. and D. Fäh. 2009, The 1946 magnitude 6.1 earthquake in the Valais: site-effects as contributor to the damage. Swiss Journal of Geosciences, 102, no. 3,423. doi: 10.1007/s00015-009-1340-2

Keefer, D. K. 1984, Landslides caused by earthquakes. GSA Bulletin, 95, no. 4,406-421. doi: 10.1130/0016-7606(1984)95

Kleinbrod, U. 2018, Characterization of unstable rock slopes through passive seismic measurements, PhD thesis, ETH Zurich.

Krähenbühl R. and C. Nänni. 2017, Ist das Dorf Brienz-Brinzauls Bergsturz gefähred? Swiss Bull. angew. Geol. 22, no. 2, 33-47

P 7.1
Challenges in earthquake ground-motion prediction for Switzerland

Sanjay Bora [1], Walter Imperatori [1], Paolo Bergamo [1], Donat Fäh [1]

[1] *Swiss Seismological Service (SED), Sonneggstrasse 5, CH-8092 Zurich (sanjay.bora@sed.ethz.ch)*

In the framework of the project "Earthquake research for Swiss nuclear facilities" founded by ENSI, the engineering seismology group of the Swiss Seismological Service (SED) contribute to the development of ground motion models and earthquake scaling and the modeling of wave propagation in complex, non-linear media.

In particular, we focus on improving source scaling, attenuation models and to develop methods for prediction of strong ground motion in Switzerland both at the surface as well as at depth. Two main approaches are investigated: ground-motion prediction equations (GMPEs) and stochastic simulation models (Edwards and Fäh, 2013). Both approaches require adaptions to the local seismicity and careful consideration of their calibration to Swiss conditions. The Fourier spectral and stochastic models correspond to the current state of research and have some advantages over the empirical attenuation relationships, as it is possible to adjust the model to specific local site conditions. The complete understanding in terms of physical parameterization of such models is crucial in order to decouple different effects, which allow building robust predictive models that scale appropriately to large magnitude events. In this regard, variability in source parameter such as stress drop is crucial. Similarly, variability in site-related attenuation parameter kappa is also needed to be understood.

Currently we are involved in investigating different measures of ground motion duration to investigate site effects mainly basin/topographic effects. In addition to the ground motion duration that is based upon time-interval between certain levels of Arias intensity, we explore an additional measure of ground motion. It is derived from the phase of the Fourier spectrum of ground motion, which is essentially referred as group-delay.

Recently, Bora et al. (2015) have developed a new technique for predicting response spectra ordinates, which utilizes two separate empirical models for FAS (Fourier Amplitude Spectrum) and duration of ground motion. This approach is presently calibrated on European (Bora et al., 2015) and NGA-West2 databases. We plan to develop an empirical frequency dependent duration model and an empirical FAS model calibrated upon Japanese dataset.

High-frequency deterministic numerical simulations of wave propagation accounting for realistic sources and complex media have great potential in seismic hazard studies, as they can provide synthetic time-series that may be potentially used to integrate GMPEs in areas where the latter are not well constrained. At the same time, they are key to a better understanding of ground motion variability in the near-source region, where observations are still scarce, and to shed some light on not-well understood topics, like the contribution of scattering and intrinsic absorption to parameter kappa. By exploiting advanced numerical techniques and high-performance computing infrastructures, our investigations indicate that the combined effects of highly heterogeneous media and rough topography may result in peak ground velocity (PGV) variability comparable with that derived from dynamic rupture simulations already at 10-20km from the source. Recently, Vyas et al. (2018) found that the amplitude of Mach waves excited by super-shear rupture speed at the source is sensibly reduced by medium heterogeneities, and not only by variability in the rupture process itself.

At the same time, high-frequency simulations require also accurate modeling of wave propagation through soft soils near the surface. Observation of strong ground motion recordings suggests that water-rich, sandy soils could experience high-frequency amplitude bursts and possibly liquefaction because of pore-water pressure build-up during strong earthquakes. We are developing a procedure to calibrate existing non-linear rheological models, relying on a large number of parameters, based on cone penetration test (CPT) measurements. This, in turn, should help us to explore more reliably the limits of ground motion.

REFERENCES

Bora, S.S., Scherbaum, F., Kuehn, N., Stafford, P. & Edwards, B. 2015: development of a response spectral ground-motion prediction equation (GMPE) for seismic hazard analysis from empirical Fourier spectral and duration model. Bulletin of the Seismological Society of America, 105(4), 2192-2218.

Edwards, B. & Fäh, D. 2013: a stochastic ground-motion model for Switzerland. Bulletin of the Seismological Society of America, 103(1), 78-98.

Vyas, J. C., Mai, P. M., Galis, M., Dunham, E. M. & Imperatori, W. 2018: Mach wave properties in the presence of source and medium heterogeneity, Geophysical Journal International, 214, 2035-2052.

P 7.2

Seismicity in Switzerland in the early instrumental period Re-assessment of the period 1911-1963 from a heterogeneous dataset

Grolimund R., Boesch E., Fäh D.

Swiss Seismological Service, ETH Zurich, Sonneggstrasse 15, 8092 Zürich

The next logical step in the process of improving historical earthquake information for Switzerland after the compilation of the Swiss Earthquake Catalogue ECOS-09 is the historical-critical revision of the Swiss earthquake catalogue for the period from 1878 to 1974. A special focus is set on intermediate-size events of epicentral intensities in the range IV–VI (EMS-98). The revision of this period is presently carried out in an interdisciplinary project funded by the Swiss National Science Foundation (2015–2019). The period in question covers the pre-instrumental [1878–1912] and early-instrumental period [1913–1974] of systematic scientific earthquake observation in Switzerland. Due to their relatively high frequency of occurrence and the increased production of scientific data in this period, the examined event class provides a broad dataset to improve our understanding of seismicity and source-depth distributions as an important element for future seismic hazard and risk assessments.

The re-assessment of the pre- and early instrumental period of scientific earthquake observation in Switzerland involves a multi-tiered analysis of a broad variety of sources containing both qualitative and quantitative data: descriptive as well as parameterized macroseismic information on the one side and historical seismograms and instrumental parameters on the other. The macroseismic re-assessment of events in question according to the European Macroseismic Scale EMS-98 is based on descriptive primary information documented in scientific and non-scientific sources. This data is completed by the integration of original intensity parameters that had been assessed by earlier generations of scientists, generally in the Rossi-Forel scale in the form of tables and macroseismic maps. The maps have been preserved in an unpublished historical "Macroseismic Atlas" covering the whole period of examination. Because the Swiss seismologists adhered to the Rossi-Forel scale from the 1880s to the 1960s, this set of data consists of one of the longest lasting relatively homogeneous set of macroseismic data. The examination of the historical practice of data production and the comparison of this historical macroseismic dataset with macroseismic re-assessment in the modern EMS-98 scale can provide valuable insights for an empirical scale conversion. This may enable us to use the historical assessments in Rossi-Forel (for most of which the primary data have been lost and cannot be reproduced in EMS-98) in the ongoing catalogue revision process.

In addition to the macroseismic method, the historical seismograms recorded by the Swiss network of mechanical seismographs are analyzed as a complementary source of information for the characterization of 20th century seismicity. In 1911, the first instrumental earthquake observatory was installed and in the 1920s a network of sensitive mechanical instruments designed at the SED was set up, that was kept in place for more than 40 years. The three (later four) very similar devices were equipped with inert masses of up to 21 tons that gave them a particularly large sensitivity allowing not only the study of global events as it was common at that time, but also weak and intermediate local and regional earthquakes. The very large repository of historical seismograms recorded by the Swiss seismograph network held by ETH library is being classified and made accessible in a common project with the ETH-library archives, and all available recordings of events that have potentially been felt in Switzerland have been scanned in high resolution. The macroseismic method can therefore be supplemented by an instrumental approach in a next step.

P 7.3
Investigation of the Swiss Molasse basin with passive seismic methods

Dario Chieppa [1], Manuel Hobiger [1] & Donat Fäh [1]

[1] Swiss Seismological Service (SED), Sonneggstrasse 5, Zurich (dario.chieppa@sed.ethz.ch)

Passive ambient vibration measurements are well established to investigate the uppermost shear-wave velocity structures (up to few hundred meters) while the tomographic methods, mostly based on earthquake recordings, are widely used for the study of the deeper crust, at depths of the order of several kilometers. We want to fill the gap between these depth ranges using passive array measurements.

The study area is the Swiss foreland, which is composed, from a geological point of view, of Quaternary deposits, Molasse and Mesozoic deposits of variable thickness (1 to 5 km) and the crystalline basement. The goals of this study are the identification of the main impedance contrasts in the subsurface, their comparison with a-priori information where available and the reconstruction of local shear-wave velocity profiles.

We will present the results of array measurements performed at two different sites located within the Swiss foreland: Schafisheim (AG) and Herdern (TG). In order to investigate different depth ranges, different type of sensors and different array configurations of increasing size were deployed using interstation distances included between a minimum of 8 meters and a maximum of 20 kilometers. At the first site, three arrays of increasing size have been deployed while at the second location only two array configurations were set up. The recorded data were processed using single-station (H/V and ellipticity curves) and array techniques (three-component high-resolution FK, SPAC and Wavefield Decomposition). The obtained measurement results were jointly inverted and combined with other available data to reconstruct a unique shear-wave velocity profile representing both the shallow and the deep structures of the subsurface.

The two resulting shear-wave profiles are compared with available geological profiles to identify the main impedance contrasts and to retrieve the sedimentary thickness variation of the Swiss Molasse basin from north to south.

P 7.4

Identification and characterization of lake-tsunami deposits in Switzerland

Valentin Nigg [1], Stéphanie Girardclos [2], Katrina Kremer [3] & Flavio S. Anselmetti [1],

[1] Institute of Geological Sciences and Oeschger Centre for Climate Change Research, Univerity of Bern, Baltzerstrasse 1+3,
    CH-3012 Bern
[2] Department of Earth Sciences and Institute for Environmental Sciences, University of Geneva, Rue des Maraîchers 13,
    CH-1205 Geneva
[3] Swiss Seismological Service, ETH Zürich, Sonneggstrasse 5,CH- 8092 Zurich

Near- and onshore sedimentary units deposited during tsunami inundation and/or backwash are termed 'tsunami deposits' or 'tsunamiites'. They are characterized by a wide range of petrophysical and lithological signatures, depending mainly on coastal morphology and tsunami-wave energy. In marine settings, tsunami deposits are often used to determine the magnitude and frequency of prehistoric tsunami events.

Based on historical reports, multibeam bathymetric datasets, seismic reflection surveys and numerical wave modelling, previous studies have shown that tsunamis also occurred in perialpine lakes in Switzerland. However, even though historical reports document this underrated natural hazard accurately, a tsunami chronology in Swiss lakes has not been established yet. Within the larger objective of the SNF Sinergia project "Lake Tsunamis: causes, controls and hazard", this study identifies and characterizes lake-tsunami deposits based on sedimentary evidences in the near- and onshore lake setting. We use sediment cores along coastal cross sections and conduct petrophysical sediment analysis encompassing density, magnetic, X-ray imaging scans, lithological analysis as well as geochemical element measurements using an ITRAX XRF core-scanner. For dating purposes, we perform radiocarbon measurements on terrestrial plant remains. Eventually, these results will be correlated with major mass-transport deposits observed in various lake basins and compared with results from numerical models within the SNF-Sinergia project.

P 7.5
Traces of the Ralligen Rockfall in Lake Thun

Nora Schweizer [1], Stefano Fabbri [2], Stefanie B. Wirth [3], Flavio S. Anselmetti [2], Adrian Gilli [1] & Katrina Kremer [4]

[1] Geological Institute, ETH Zurich, Sonneggstrasse, CH-8092 Zürich (norasch@student.ethz.ch)
[2] Insitute of Geological Sciences and Oeschger Centre for Climate Change Research, Univ. of Bern, Bern
[3] Centre for Hydrogeology and Geothermics (CHYN), University of Neuchâtel, Emile-Argand 11, CH-2000 Neuchâtel
[4] Swiss Seismological Service, ETH Zürich, Sonneggstrasse 5, CH-8092 Zurich

Following a historical report, a rockfall occurred in the village Ralligen located at the northern shore of Lake Thun in 598/599. This document also mentions 'dead fish washed ashore' and a 'cooking lake' (Fredegarius, 1888) suggesting the occurrence of an impact wave due to the rockfall.

Lake sediments are excellent natural archives that can record the traces of such rockfalls.
In Lake Thun, single channel (3.5 kHz) and multi-channel (500 Hz) reflection seismic data have been acquired during several field campaigns. These datasets reveal a chaotic to transparent seismic facies with a thickening towards the northern shore of Lake Thun. This seismic unit can be interpreted most probably as the deposit and deformed sediments related to the above mentioned Ralligen Rockfall. Long sediment cores have been retrieved with a Kullenberg gravity corer to date the sediment.

In this contribution, we will present the data related to this rockfall that have collected so far. The main objectives are to determine (1) the volume of the rockfall that would control the height of an impact wave and (2) to test the hypothesis of a seismic trigger as cause for the rockfall.

REFERENCE
Fredegarius (1888) Chronicarum quae dicuntur Fredegarii Scholastici, Liber IV. In : Momenta Germaniae Historica (MGH) (Ed. B. Krusch), Script, Rev. Mer. 128pp.

P 7.6

A first step towards an extensive estimation of the tsunami hazard in Swiss lakes

Michael Strupler [1], Katrina Kremer [1], Flavio S. Anselmetti [2], Amir Razmi [3], Stefan Wiemer [1]

[1] *Swiss Seismological Service, ETH Zurich, Sonneggstrasse 5, CH-8092 Zürich (michael.strupler@sed.ethz.ch)*
[2] *Institute of Geological Sciences and Oeschger Centre for Climate Change Research, University of Bern, Bern, Switzerland*
[3] *Laboratory of Hydraulics, Hydrology and Glaciology (VAW), ETH Zurich, Zürich, Switzerland*

Tsunamis that occur on lakes constitute very rare, yet potentially serious peril.
The occurrence of historical tsunamis in Swiss Lakes has been documented by various studies, e.g. 563 AD and 1584 AD in Lake Geneva (Montadon, 1925; Kremer et al. 2012; Fritsche et al. 2012), 1601 AD and 1687 AD in Lake Lucerne (Schnellmann et al. 2002; Siegenthaler et al. 1987, Hilbe & Anselmetti, 2014). However, to the present day, fundamental information and workflows to characterise quantitatively the tsunami hazard are missing.

The project TSUNAMI-CH, in close collaboration with an interdisciplinary Swiss National Foundation Sinergia project on lake tsunamis, aims at addressing these shortcomings by (I) elaborating a classification scheme for a first-order estimation of the tsunami hazard on Swiss lakes, (II) designing methodological workflows and creating a toolkit for the evaluation of the tsunami hazard, and (III) creating first intensity maps and distributions of warning times for relevant return periods. Here we present some first ideas of a classification scheme, that evaluates the first-order tsunami hazard (with focus on sublacustrine and subaerial landslides and rockslides), based on a set of geophysical and geotechnical parameters. Such parameters include the lake-surface area, water depth, underwater slope gradients, and the type and thickness of the lake-bottom sediments.

An extendable, georeferenced lake database that contains information on the available sets of information for each lake will constitute a central element in the workflow, containing information for the rapid screening of the tsunami hazard on Swiss lakes. We differentiate between i) lakes that are limnogeologically well-investigated (i.e. high-resolution bathymetric, sedimentological, geophysical and geotechnical datasets are available), for which a slope-stability assessment will be conducted, and ii) lakes with incomplete datasets, for which potential landslide areas will be estimated from the above mentioned parameters. The expected results of the extensive characterisation of the tsunami hazard in Swiss lakes should ultimately contribute to a pratice-oriented risk management.

REFERENCES

Fritsche et al. 2012: Historical intensity VIII earthquakes along the Rhone valley (Valais, Switzerland): primary and secondary effects. Swiss Journal of Geosciences 105, 1-18.

Hilbe & Anselmetti, 2014: Signatures of slope failures and river-delta collapses in a perialpine lake (Lake Lucerne, Switzerland). Sedimentology 61,1883-1907.

Kremer et al. 2012: Giant Lake Geneva tsunami in AD 563. Nat. Geosci 5, 756-757.

Montandon, F., 1925: Les éboulements de la Dent du Midi et du Grammont (Examen critique de la question du Tauredunum). Extrait des Mémoires du Globe, tome 64, Genève.

Schnellmann et al. 2002: Prehistoric earthquake history revealed by lacustrine slump deposits. Geology 30, 1131-1134.

Siegenthaler et al. 1987: Earthquake and seiche deposits in Lake Lucerne, Switzerland. Eclogae Geologicae Helvetiae 80, 241-260.

P 7.7
Subaqueous Mass Failure: Hydraulic Lab Experiments

Frederic M. Evers [1], Helge Fuchs [1], Amir M. Razmi [1], David F. Vetsch [1] & Robert M. Boes [1]

[1] Laboratory of Hydraulics, Hydrology and Glaciology (VAW), ETH Zurich, CH-8093 Zürich (evers@vaw.baug.ethz.ch)

Subaqueous or Submarine Mass Failures (SMF) are a potential source of hazardous tsunamis (Figure 1). While the link between seismic events and the magnitude of tsunami waves has been extensively studied and corresponding approaches are included in numerical tsunami warning models, the basic implementation of SMF generated waves is subject to ongoing research. In this context, laboratory experiments are essential for the validation of numerical schemes. Most experimental studies apply rigid slide models whereas only few include granular slides. The objective of this study is to gain a better insight into the hydraulic processes related to wave generation by submarine granular slides based on experiments (Figure 2) as well as establishing a comprehensive data set for the validation of numerical models.
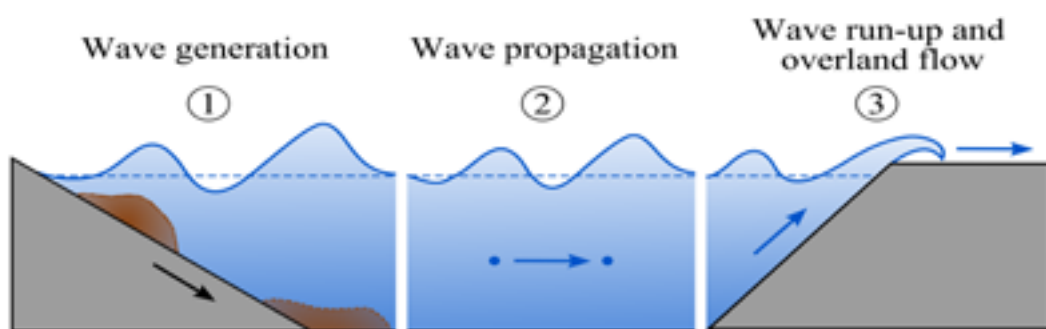
Figure 1. SMF event with (1) wave generation, (2) wave propagation, and (3) wave runup and overland flow.
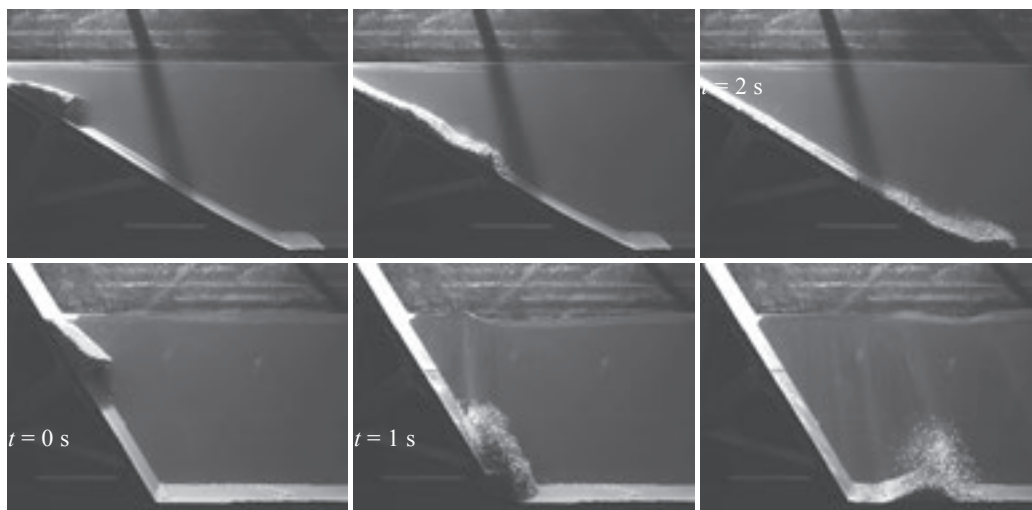

Figure 2. SMF laboratory experiments for $\alpha = 30°$ (top) and 60° (bottom) with m_s = 10 kg, d_g = 8 mm, h = 0.7 m, $d_s \approx$ 0.13 m.

P 7.8

Time-dependent deformations of sandstone during fluid pressure oscillations: implications for natural and induced seismicity

Corentin Noël [1], Lucas Pimienta [1], Marie Violay [1]

[1] Laboratory of Experimental Rock Mechanics, Ecole Polytechnique Fédérale de Lausanne, Lausanne, Switzerland

Fluid pressure is acknowledged as a key parameter affecting stability and rupture phenomena in the upper crust (e.g. earthquake or landslide). Moreover, rock-fluid interactions result in stress corrosion and/or rock alteration (time-dependant mechanisms), enabling rocks to fail at stresses below their short-term failure strength. Because fluid pressures are prone to fluctuate over time and space (e.g. oceanic tides, seasonal hydrology, cyclic fluid injection in reservoirs), hydraulic fatigue could add another time-dependant deformations mechanisms.

Here, we present 10 brittle creep laboratory triaxial experiments that bring new constraints on fluid-rock interactions during cyclic pore fluid variations. The experiments were performed on Fontainebleau sandstone with applying either constant or cyclic (sinusoidal oscillations) pore fluid pressures. During deformation, the rock mechanical properties and the high-frequency acoustic emission signals were monitored to investigate the physics underlying the rupture processes.
Our experimental results show that, under macroscopically drained conditions, rather than its amplitude, the period of the oscillations strongly affects the rock sample strength, time to failure and dilatancy behaviour. Moreover, even for small variation of pore fluid amplitude, and at all pore fluid period, pore pressure oscillations control the acoustic event rate, with an increase of AE rate at maximum pore fluid pressure. Correlation between oscillations and AE rate increased with (i) increasing the differential stress applied to the sample, i.e. getting closer to sample rupture; and (ii) increasing the pore fluid oscillation amplitude and period. In agreement with creep numerical model and wing crack theory, our experiments demonstrate that pore fluid pressure oscillations may strongly affect rocks mechanical behaviour and associated seismic activity.

P 7.9
The different effect of fluid viscosity in earthquake nucleation and propagation.

Chiara Cornelio [1], Elena Spagnuolo [2], Francois Passelègue [1], Stefan Nielsen [3], Giulio Di Toro [4], and Marie Violay [1]

[1] EPFL, Laboratory of Experimental Rock Mechanics, Lausanne, Switzerland (chiara.cornelio@epfl.ch)
[2] Sezione di Sismologia e Tettonofisica, INGV, Rome, Italy
[3] Department of Earth Sciences, Durham University
[4] Department of Geoscience, University of Padua, Padua, Italy

Fluids play an important role in fault zone and in earthquakes generation (Terakawa et al., 2010). The mechanical effect of fluid pressure is to reduce the normal effective stress, lowering the frictional strength of the fault, potentially triggering earthquake ruptures. Fluid injection induced earthquakes, such as in geothermal reservoir, are direct evidence of the effect of fluid pressure on the fault strength (Ellsworth, 2013). However, the frictional fault strength may also vary due to the chemical and physical characteristics of the fluid. Here we investigate the role of fluid viscosity during both earthquake nucleation and propagation. Here we present more than 30 friction experiments performed with the rotary shear apparatus SHIVA (INGV, Rome) (Di Toro et al, 2010) in order to investigate the role of fluid viscosity during a simulated seismic cycle (i.e. from the slow accumulation of strain energy to the nucleation of a seismic slip), at normal effective stress up to 10 MPa. Four different fluid viscosities are tested: distilled water ($\eta \sim 1$ mPa s) and three mixtures of water with glycerol concentrations of 60%wt., 15%wt. and 0.1%wt. (η=10.8, s109.2 and 1226.6 mPa s, respectively) at pore pressure Pf of 2.7 MPa and under drained conditions (Violay et al. 2013). In particular, in order to simulate the seismic cycle we perform creep tests consisting in incrementing stepwise the shear stress on the fault and allowing the slip and the slip-rate to adjust spontaneously (Figure 1.a) until the onset of seismic slip (e.g. earthquake nucleation). In order to study the earthquake propagation phase, we perform standard velocity controlled experiments imposing slip-rate ranging between 10 µm/s and 1 m/s and allowing the shear stress to adjust spontaneously (Figure 1.b). Mechanical data show that fluid viscosity does not influence the reactivation of the fault, which occurs at a friction coefficient of ~0.6 in all the condition and in agreement with the Byerlee's law. The experiments performed under room-humidity conditions show a phase of precursory activity before rupture propagation that is absent in presence of a fluid. On contrary, during earthquake propagation the role of fluid viscosity is important. The dynamic friction coefficient decreases with viscosity, and it depends on the dimensionless Sommerfeld number ($S=6\eta VL/(H2\sigma eff)$), where η is the fluid dynamic viscosity, V is the imposed slip-rate, L is the characteristic length over which the fluid pressure changes, H is the initial height of the asperities and σeff is the effective normal stress as theorized by the elastohydrodynamic lubrication theory (EHD) (Brodsky and Kanamori, 2010).

Extrapolation of our results to crustal conditions suggests that EHD is an effective weakening mechanism during earthquakes. However, at seismic slip-rates, the slip weakening distance (Dc) increases markedly for the fluid viscosities expected in the Earth, potentially favoring slow slip rather than seismic propagation for small to moderate seismic events. Therefore, in the presence of high viscosity fluids, transition from slow nucleation to seismic propagation could not occur until rupture indicatively reaches kilometric lengths.
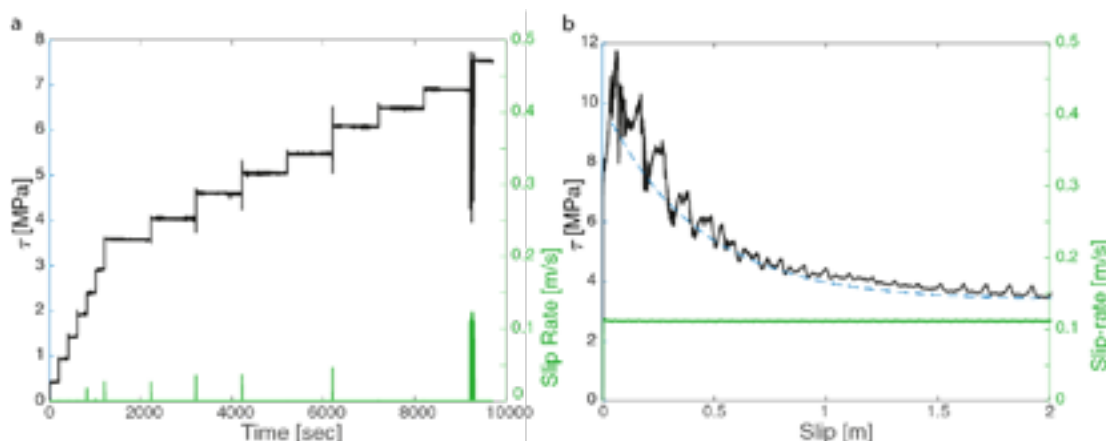

Figure 1. Experimental curve showing a) the evolution of shear stress (black solid line) and slip rate (green solid line) versus time in an creep test performed under by increasing stepwise the shear stress to investigate the stage of the earthquake nucleation; b) the evolution of shear stress and slip rate versus slip in a standard experiment performed under velocity control mode to investigate earthquake propagation. Experiments were performed in the presence of mixture 40% water 60% glyc. (η=10.8 mPa s) under an effective normal load of 10 MPa.

REFERENCES

Terakawa T., Zoporowski, A., Galvan, B., Miller S.A., (2010), High-pressure fluid at hypocentral depths in the L'Aquila region inferred from earthquake focal mechanisms. Geology, 38, 995-998.

Ellsworth, W.L., (2013). Injection-Induced Earthquakes. Science, 341, 6142.

Di Toro, G., Niemeijer, A., Tripoli, A., Nielsen, S., Di Felice, F., Scarlato, P., G. Spada, G., Alessandroni, R., Romeo, G., Di Stefano G., Smith S., Spagnuolo, E., Mariano, S. (2010). From field geology to earthquake simulation: A new state-of-The-art tool to investigate rock friction during the seismic cycle (SHIVA). Rendiconti Lincei, 21, pp.95–114.

Violay, M., Nielsen, S., Spagnuolo, E., Cinti, D., Di Toro, G., Di Stefano, G., (2013). Pore fluid in experimental calcite-bearing faults: Abrupt weakening and geochemical signature of co-seismic processes. Earth and Planetary Science Letters, 361, pp.74–84.

Brodsky, E.E., Kanamory H., (2001). Elastohydrodynamic lubrication of fault. Journal of Geophysical Research. 106, 16, 357 – 374.

P 7.10

A New State-of-the-art Apparatus to Study Earthquake Nucleation and Propagation: HighSTEPS

Marie Violay [1], Carolina Giorgetti [1], Chiara Cornelio [1], Giuseppe Di Stefano [2], Stefan Wiemer [3] and Jean-Pierre Burg [4]

[1] LEMR, ENAC, EPFL, Station 18, CH-1015 Lausanne, Switzerland (carolina.giorgetti@epfl.ch)
[2] National Institute of Geophysics and Volcanology, Via di Vigna Murata 605, 00143 Rome, Italy
[3] Swiss Seismological Service, ETH Zurich, Sonneggstrasse 5, CH-8092 Zurich, Switzerland
[4] Urbana, IL, United States

The mechanics of rupture nucleation and propagation have long been investigated via seismological observations on active faults, geological observations on exhumed faults and rock deformation experiments on laboratory faults. However, the integration of these multidisciplinary observations collected at different scales is still challenging. Particularly, friction experiments are often limited in boundary conditions. Here, we present a state-of-the-art biaxial apparatus able to study both rupture nucleation and propagation at boundary conditions typical of seismogenic faults. The HighSTEPS, High Strain Temperature Pressure Speed, apparatus simulates fault deformation in a wide range of velocities, i.e., from 10 µm/s to 0.2 m/s. Within this velocity range, it is possible to study both the rate-and-state friction and the dynamic weakening, under unique boundary conditions, i.e., normal stress up to 100 MPa, confining pressure up to 100 MPa, pore fluid pressure up to 100 MPa and temperature up to 100 °C. The apparatus consists of a hydraulic system integrated with four linear motors. The hydraulic system allows for the application of normal stress, confining pressure and pore fluid pressure. The normal stress is applied by a horizontal piston. The confining pressure is applied through an oil-confining medium by an intensifier connected to a vessel implemented within the biaxial frame. The pore fluid pressure is applied by two pore fluid intensifiers connected to the sample, which also allow for permeability measurements. In addition, the vessel is implemented with two heating plates for temperature increase and feedthroughs for acoustic sensors and strain gauges. The main peculiarity of this apparatus is the system of four linear motors that are mounted in series in order to apply shearing velocities up to 0.2 mm/s, accelerations up to 10 m/s^2 and shear stresses up to 200 MPa. Moreover, both experiments in sliding velocity control or shear stress control on the experimental faults are possible. Preliminary experiments are coherent with the previous literature. The investigation of fault friction under a wide range of velocities, normal stresses, confining pressures and pore fluid pressures will provide insights into the mechanics of earthquakes and reduce the gap between natural and laboratory observations.

P 7.11

A back-projection location method based on the cross-correlation envelope of signals at different station pairs

Verónica Antunes [1], Thomas Planès [1], Aurore Carrier [1], Anne Obermann [2], Adriano Mazzini [3], Tullio Ricci [4], Alessandra Sciarra [4], Milena Moretti [4], and Matteo Lupi [1]

[1] Department of Earth Sciences, University of Geneva, Geneva, Switzerland,
[2] ETH Zürich,Erdbebendienst (SED), Zurich, Switzerland,
[3] Centre for Earth Evolution and Dynamics (CEED), University of Oslo, Norway,
[4] Istituto Nazionale di Geofisica e Vulcanologia (INGV), Rome, Italy

Locating seismic sources is normally performed on the basis of impulsive arrival pickings which usually cannot be applied when a signal has an emergent onset, especially in a high noisy environment. We developed a python algorithm using a back-projection method based on the cross-correlation envelope of signals recorded at different station pairs. The algorithm works in 7 steps: (1) pre-signal process to remove mean, trend and instrument response, filters and normalizes each trace using a weight factor (2) creates of a 2D grid where the coordinates of the seismic stations are converted and inserted, (3) computes the cross-correlation envelope for each station pair, (4) determines the theoretical differential time from each point of the grid to each station pair, (5) uses the differential time at each point of the grid to get the envelope value to obtain the back-projection for each station pair, (6) stacks all back-projections into one solution and normalizes (7) plots a 2D colored map showing the final solution. The code assumes the mean as homogeneous.

We used the algorithm on data from a seismic network in Central Italy to investigate drumbeat signals generated at the Nirano Mud Volcano. The results show good agreement in location between the drumbeat signal and two major mud cones.

P 7.12
Full moment tensors for exotic seismic sources including induced events, landslides, and nuclear tests

Celso Alvizuri & György Hetényi

Institute of Earth Sciences, University of Lausanne, 1015 Lausanne, Switzerland (celso.alvizuri@unil.ch)

Seismic sources can originate from various phenomena, from mining and induced events to nuclear explosions, to natural processes such as earthquakes, volcanic activity, and landslides. A seismic moment tensor is a 3 × 3 symmetric matrix that characterizes the far-field seismic radiation from a source, and together with its uncertainties can be used to discriminate among sources. Here we present moment tensor estimates for an earthquake in South Korea possibly related to geothermal energy production, for landslides in Greenland and Switzerland on 2017, and for nuclear tests in North Korea. We estimate the moment tensor with a grid search over its six-dimensional space by generating synthetic waveforms at each grid point and then evaluating a misfit function between the observed and synthetic waveforms. The moment tensor uncertainty is described in terms of the variation in waveform misfit on the eigenvalue lune, a probability density function for moment tensor source type, and a confidence curve for the probability that the true moment tensor lies within the neighborhood of the best-fitting moment tensor. We use three-component seismic waveforms from all available regional broadband seismic stations, and compute Green's functions for a layered wavespeed model of the source region. Our moment tensor solutions show clear separation among source types, such as nuclear tests in the positive isotropic region of the eigenvalue lune, collapses in the negative isotropic region, and earthquakes near the double-couple. The optimal moment tensor solutions for the landslides are towards negative isotropic, their probability density functions are localized, and their moment magnitudes range between Mw 4.5 − 5. We find that the landslide in Switzerland requires a source duration in the order of 10s of seconds, and the Greenland event can be analyzed as multiple episodes, with a moment tensor for each episode.

P 7.13

Influence of fluid pressure level on the nucleation of laboratory earthquakes.

Authors: M. Acosta[°1], F.X. Passelègue[1], A. Schubnel[2], B. Gibert[3], M. Violay[1]

[1] *EPFL, LEMR, Lausanne, Switzerland*
[2] *Laboratoire de Géologie, CNRS, UMR, ENS, Paris, FR.*
[3] *Géosciences Montpellier, Université de Montpellier, Montpellier, FR.*
[°]*mateo.acosta@epfl.ch.*

Recent seismological observations highlighted that both aseismic silent slip or foreshock sequences can precede large earthquake ruptures (Tohoku-Oki, 2011, Mw 9.0; Iquique, 2014, Mw 8.1; Illapel, 2015, Mw 8.3). However, the influence of pore fluid pressure level on the earthquake nucleation behaviour remains poorly understood. Here, we report for the first time, experimental results regarding the nucleation of stick-slip instabilities (laboratory proxies for earthquakes) conducted on Westerly Granite saw-cut samples. Experiments were conducted under stress conditions representative of the upper continental crust, i.e confining pressures from 50 to 125 MPa; fluid pressures (water and argon) ranging from 0 to 45 MPa; and temperatures ranging from 25 to 500˚C.

In dry conditions tested, we observe that slip evolves exponentially up to the main instabilities and is escorted by an exponential increase of acoustic emissions. With pressurized fluids, precursory slip evolves first exponentially then switches to a power law of time. There, precursory slip remains silent, independently of the fluid pressure level. The amount of precursory slip (u_{prec}) depends on both fluid pressure and initial shear stress. While increasing the initial shear stress leads to larger precursory slip, increasing the fluid pressure seems to reduce the amount of precursory slip leading to instabilities. Independently of the fluid pressure level, we demonstrate that the amount of precursory energy density ($\tau^* u_{prec}$) released prior to the mainshock (the energy dissipated during the precursory stage) scales linearly with the fracture energy of the main instability (($\tau_0 - \Delta\tau)^* u_{cos}$). These results suggest that the intensity of the precursory stage is a function of the strength of the asperity which is eventually going to rupture.

Our experimental observations imply that the initial background stress and the pore fluid pressure level control the intensity and the nucleation behaviour of the fault. Such observation indicates that (i) that the presence of foreshock sequences is not systematic during earthquake nucleation and seems attenuated in presence of water, (ii) large ambient pore fluid pressure could reduce the intensity and the duration of the precursory stage.

09. Shale-Gas, CO_2 Storage and Deep Geothermal Energy

Lyesse Laloui, Larryn Diamond, Paul Bossart

Swiss Geothermal Society,
Swiss Association of Energy Geoscientists (SASEG)

TALKS:

9.1   Boulicault L., Reynolds L., Allenbach R., Minnig C., Baumberger R.: Latest Results of the GeoTherm and GeoMol Projects for Deep Geothermal Energy

9.2   Diamond L.W., Wanner C., Waber H.N.: Penetration depth of meteoric water and maximum temperatures in orogenic geothermal systems

9.3   Fryer B., Siddiqi G., Laloui L.: Reservoir stimulation and its effect on depletion-induced seismicity

9.4   Grab M., Obermann A., Rinaldi A., Madonna C., Nussbaum C., Jaeggi D., Manukyan E., Maurer H.R., Zappone A.: Geophysical instrumentation for monitoring CO_2-brine injected into the main fault in Mont Terri

9.5   Grimm-Lima M.M., Vogler D., Schädle P., Saar M.O., Xiang-Zhao Kong: Impact of effective normal stress on CO_2 injection into a brine-saturated single fracture with rough surfaces

9.6   Krietsch H., Villiger L., Doetsch J., Gischig V., Amann F.: Complex interplay between fracture opening and shearing during in-situ stimulation experiments

9.7   Ma J., Querci L., Hattendorf B., Saar M., Kong X.Z.: Dissolution of dolomite cement in sandstones when subjected to CO_2-enriched brine

9.8   Makhloufi Y., Samankassou E., Meyer M.: Early dolomitization and dedolomitization of the Late Jurassic limestones in the Geneva Basin (Switzerland and France)

9.9   Minardi A., Laloui L.: Experimental investigation on the sealing capacity of Opalinus Clay to CO_2 injection

9.10   Moscariello A., Clerc N., Pierdona L., De Haller A.: Exploring the interface between shallow and deep geothermal systems: new insights from the Mesozoic-Cenozoic transition.

9.11   Nawratil de Bono C. and GEo-01 team: GEo-01: The first GEothermie 2020 P&D well in the Canton of Geneva – Preliminary results

9.12   Nussbaum C., Guglielmi Y., de Barros L., Cappa F., Birkholzer J., Bossart P.: Aseismic and seismic reactivation of a velocity-strengthening clay-rich fault zone: the Mont Terri Main Fault FS experiment

9.13   Omodeo-Salé S., Eruteya O.E., Guglielmetti A., Moscariello A.: New insights into the thermal and petroleum system of the St Gallen area: Implication for geothermal exploration

9.14   Schmitt N., Jansen G., Miller S., Valley B., Mosar J.: Fracture network stability analysis for coupled EGS prospection project in Eclépens.

9.15   Schneeberger R., Egli D., Lanyon B., Mäder U.K., Berger A., Kober F., Blechschmidt I., Herwegh M.: Large-scale structures governing water flow in crystalline bedrock at Grimsel Test Site (Switzerland).

9.16   Wenning Q.C., Madonna C., Pini R., Kurotori T., Petrini C., Hosseinzadeh Hejazi S.A.: Computerized tomography imaging of fracture aperture distribution and tracer transport within sheared fractures

POSTERS:

P 9.1   Ahkami M., Roesgen T., Saar M.O., Xiang-Zhao Kong: High-resolution temporo-ensemble PIV to resolve pore-scale flow in 3D-printed fractured porous media

P 9.2   Alt-Epping P., Diamond L.W., Wanner C.: Simulations of fluid flow and chemical reactions in the deep orogenic hydrothermal system at Grimsel Pass, Switzerland

P 9.3   Antunes V., Planès T., Carrier A., Martin F., Meyer M., Lupi M.: Detecting microseismicity in the Geneva Basin and surrounding areas using coherence of signals at different stations

P 9.4   Aschwanden L., Diamond L.W., Mazurek M., Davis D.: Creation of secondary porosity in dolostones by upwelling basement water in the foreland of the Alpine Orogen

P 9.5   Carrier A., Lupi M., Fishanger F., Collignon M.: Brand new deep electrical resistivity tomography (ERT) methodology for middle-enthalpy geothermal exploration in the Geneva Basin, Switzerland.

P 9.6   Caspari E., Greenwood A., Baron L., Egli D., Toschini E., Holliger K.: Geophysical characterization of a fracture network surrounding a hydrothermally active shear zone: a case study from the Grimsel pass

P 9.7   Collignon M., Klemetsdal Ø., Møyner O., Alcanié M., Carrier A., Nilsen H., Rinaldi A., Lupi M.: Heat storage in the Canton of Geneva basin: a numerical modelling study

P 9.8   Dutler, N.: Fracture geometry and fracture growth of an in-situ hydraulic fracturing (HF) experiment

P 9.9   Jaeggi D., Hesser J., Nussbaum C., Bossart P.: A new mine-by experiment at the Mont Terri rock laboratory to assess hydromechanical behavior of the sandy facies of Opalinus Clay

P 9.10   Kong X.-Z., Parmigian A, Di Palma P., Leclair S., Saar M.O.: Dynamics of phase exsolution in porous media

P 9.11   Omodeo-Salé S., Do Couto D., Corrado S., Carraro D., Ziegler L., Moscariello A.: Thermal modelling to prevent risks in geothermal exploration: the Geneva Basin case study (Western Switzerland)

P 9.12   van den Heuvel D.B, Mock S., Egli D., Diamond L.W., Herwegh M.: Compilation of data relevant for geothermal exploration – a first step towards a Geothermal Play Fairway Analy-sis of the Rhône Valley, Switzerland

P 9.13   van den Heuvel D.B, Wanner C., Mäder U., Diamond L.W.: Investigating mineral reactions during high-temperature aquifer thermal energy storage (HT-ATES) in the Swiss Molasse Basin

9.1
Latest Results of the GeoTherm and GeoMol Projects for Deep Geothermal Energy

L.Boulicault [1], L. Reynolds [1], R. Allenbach [1], C.Minnig [1], R.Baumberger [1]

[1] Federal Office of Topography swisstopo, Swiss Geological Survey, Seftigenstrasse 264, CH-3084 Wabern
 (lise.boulicault@swisstopo.ch)

In the context of the Energy Strategy 2050, the Swiss Federal Office of Energy (SFOE) and the Swiss Geological Survey at the Federal Office of Topography (swisstopo) launched the GeoTherm project (2016 – 2018). GeoTherm is the first public federal information system for data relevant to deep geothermal energies. It established an infrastructure for the collection, harmonization, storage and web-publication of the data on the public federal website https://map.geo.admin.ch. GeoTherm adds value and provides a long-term access to non-confidential geological data (raw, processed and interpreted). GeoMol is the first public geological 3D model of the Swiss Molasse Basin, jointly developed by swisstopo, seven Swiss cantons and five Swiss universities (https://viewer.geomol.ch). The model data is available at swisstopo free of charge.

In a first part, this presentation gives an updated view of the GeoTherm results after 3 years of project duration. In a second part, results of the expansion of the GeoMol base model to include temperature attributes are presented. These will be in the form of new products, such as a 3D-temperature model as well as several temperature maps (at different depths, horizons, isotherms) of the Swiss Molasse Basin.

Finally, in order to ensure the continued success of the GeoTherm information system and to provide the latest data for planners of geothermal energy projects in Switzerland, the importance of the ongoing, close and transparent collaboration between the federation and all the involved stakeholders is encouraged.

REFERENCES:

Allenbach R., Baumberger R., Kurmann E., Michael C. S., Reynolds L., 2017: GeoMol: Geologisches 3D-Modell des Schweizer Molassebeckens – Schlussbericht. 128 S., 3 Tafeln, Datenträger, 2017. Pages: 128

Brodhag, S. & Oesterling, N., 2014: Datenmodell Bohrdaten. Beschreibung des Kernmodells mit Objetkatalog und UML – Modell. Version 2.0. Bundesamt für Landestopografie swisstopo

Strasky S., Morard A., Möri A., 2016: Harmonising the lithostratigraphic nomenclature: towards a uniform geological dataset of Switzerland. Swiss Journal of Geosciences 109:123–136

9.2
Penetration depth of meteoric water and maximum temperatures in orogenic geothermal systems

Larryn W. Diamond [1], Christoph Wanner [1] & H. Niklaus Waber [1]

[1] Institute of Geological Sciences, University of Bern, Baltzerstrasse 3, CH-3012 Bern (diamond@geo.unibe.ch)

Warm springs emanating from deep-reaching faults in orogenic belts with high topography and orographic precipitation attest to circulation of meteoric water through crystalline bedrock. The depth to which this circulation occurs is unclear, yet it is important for the cooling history of exhuming orogens, for the exploitation potential of orogenic geothermal systems, and for the seismicity of regional faults.

The orogenic geothermal system at Grimsel Pass, Swiss Alps (Hofmann et al., 2004; Belgrano et al., 2016), is manifested by warm springs with a clear isotopic fingerprint of high-altitude meteoric recharge. Their water chemistry and their occurrence within a 3 Ma fossil upflow zone render them particularly favorable to estimate the temperature along the deep flow path via geochemical modeling. As the background geotherm has remained stable at 25 °C/km and as other heat sources are unavailable, the penetration depth can be derived from the deep water temperature. We thus estimate the base of the Grimsel system to be at 230–250 °C and 9–10 km depth.

We propose that deep temperatures in such systems, particularly those with normal background geotherms (< 30 °C/km), have been systematically underestimated. Consequently, far more enthalpy may be accessible for geothermal energy exploitation around the upflow zones than previously thought. Further, the prevalence of recent earthquake foci at Grimsel at ≤ 10 km demonstrates that meteoric water is involved in seismicity of the host faults. Our results therefore call for reappraisal of the heat budget and of the role of meteoric water in seismogenesis in uplifting orogens.

Figure 1. Regional view to NNW of Grimsel area showing topography and conceptual present-day flow path of meteoric water along subvertical strike-slip fault.

REFERENCES
Hofman, M., Helfer, M., Diamond, L.W., Villa, I.M., Frei, R. & Eikenberg, J. 2004: Topography-driven hydrothermal breccia mineralization of Pliocene age at Grimsel Pass, Aar massif, Central Swiss Alps, Schweizerische Mineralogische und Petrographische Mitteilungen, 84, 271–302.

Belgrano, T., Herwegh, M. & Berger, A. 2016: Inherited structural controls on fault geometry, architecture and hydrothermal activity: an example from Grimsel Pass, Switzerland, Swiss Journal of Geosciences, 109, 345–364.

9.3
Reservoir stimulation and its effect on depletion-induced seismicity

Barnaby Fryer [1], Gunter Siddiqi [2] & Lyesse Laloui [1]

[1] Soil Mechanics Laboratory – Chair "Gaz Naturel" Petrosvibri, Station 18, Swiss Federal Institute of Technology in Lausanne, Route Cantonale, 1015 Lausanne, Switzerland (barnaby.fryer@epfl.ch)
[2] Swiss Federal Office of Energy, 3003 Bern, Switzerland

Production from subsurface reservoirs causes stress changes that can lead to induced seismicity (Segall 1989). In the fully coupled theory of poroelasticity, these stress changes are caused by the gradient of pore pressure which acts as an internal force in the momentum balance equation. This implies that, if a smaller pore pressure gradient is required to produce the fluid, smaller stresses will be induced, likely leading to a lower seismicity rate.

According to Darcy's Law the gradient of pore pressure required to achieve a certain fluid production rate is inversely proportional to the permeability. The larger the permeability, the smaller the pore pressure gradient required. Therefore, it is possible that reservoir stimulation techniques may be significant in terms of induced seismicity because, during the reservoir production phase, they will decrease the pore pressure gradient required to produce a certain amount of fluid. For this reason, in this work, a hydraulic fracture's effect on induced seismicity is investigated.

Pore pressure and stress changes are modelled using a fully coupled Finite Volume flow and Finite Element mechanical model. A pseudo hydraulic fracture and the resulting near wellbore permeability increase are modelled using typical parameter values reported in the literature for hydraulic fracturing. Calculated pore pressure and stress changes are then used in a seismicity model based on the model introduced by Dietereich 1994 and extended by Segall & Lu 2015. Seismicity rates are compared for the case when the pseudo hydraulic fracture permeability increase is included to the the case without a stimulated wellbore inflow zone.

The numerical experiment suggests that the near-wellbore permeability increase associated with hydraulic fracturing results in decreasing the stress changes associated with an imposed fluid production rate and thereby indirectly decreases the seismicity rate. These results imply that stimulated wellbore are useful for managing fluid production from reservoirs where production-induced seismicity is an issue.
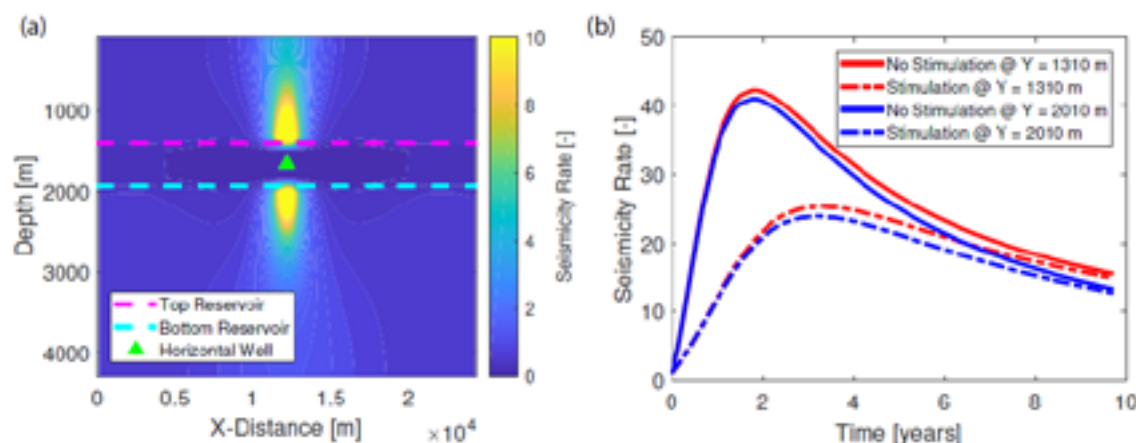

Figure 1. Calculation of (a) the seismicity rate induced by fluid production in an unstimulated reservoir subject to a reverse faulting stress regime after ten years of production and (b) the resulting seismicity rates for a stimulated and non-stimulated production well. The seismicity rates are taken at various depths (Y) vertically in-line with the producing well. The numerical simulation is plain strain with injection occurring via a horizontal well.

REFERENCES
Dietereich, J. 1994: A constitutive law for rate of earthquake production and its application to earthquake clustering, Journal of Geophysical Research, 99, 2601-2618.
Segall, P. 1989: Earthquakes triggered by fluid extraction, Geology, 17, 942-946.
Segall, P. & Lu, S. 2015: Injection-induced seismicity: Poroelastic and earthquake nucleation effects, Journal of Geophysical Research: Solid Earth, 120, 5082-5103.

9.4
Geophysical instrumentation for monitoring CO_2-brine injected into the main fault in Mont Terri

Melchior Grab [1], Anne Obermann [1], Antonio Rinaldi [1], Claudio Madonna [2], Christophe Nussbaum [4], David Jaeggi [4], Edgar Manukyan [1], Hansruedi Maurer [1] & Alba Zappone [2,3]

[1] Institute for Geophysics, ETH Zurich, Sonneggstrasse 5, 8092 Zürich
[2] Geological Institute, ETH Zurich, Sonneggstrasse 5, 8092 Zürich
[3] Institute of Process Engineering, ETH Zurich, Sonneggstrasse 3, 8092 Zürich
[4] Federal Office of Topography Swisstopo, Seftigenstr. 264, 3084 Wabern
 Contact: melchior.grab@erdw.ethz.ch

Confirming the permanent containment is a key challenge for the storage of CO_2 in deep underground reservoirs. Faults in the cap rock of such reservoirs are considered to be a potential path for the CO_2 to escape. The CS-D experiment in Mont Terri aims to better understand mechanisms of CO_2 leakage, and to develop strategies to detect and monitor CO_2 propagation through faults. In the framework of this experiment, a comprehensive geophysical instrumentation is currently being installed in four boreholes. It will complement the hydraulic and geotechnical monitoring and is offering a good opportunity to examine the ability of geophysical techniques to monitor CO_2 propagation at intermediate scales.
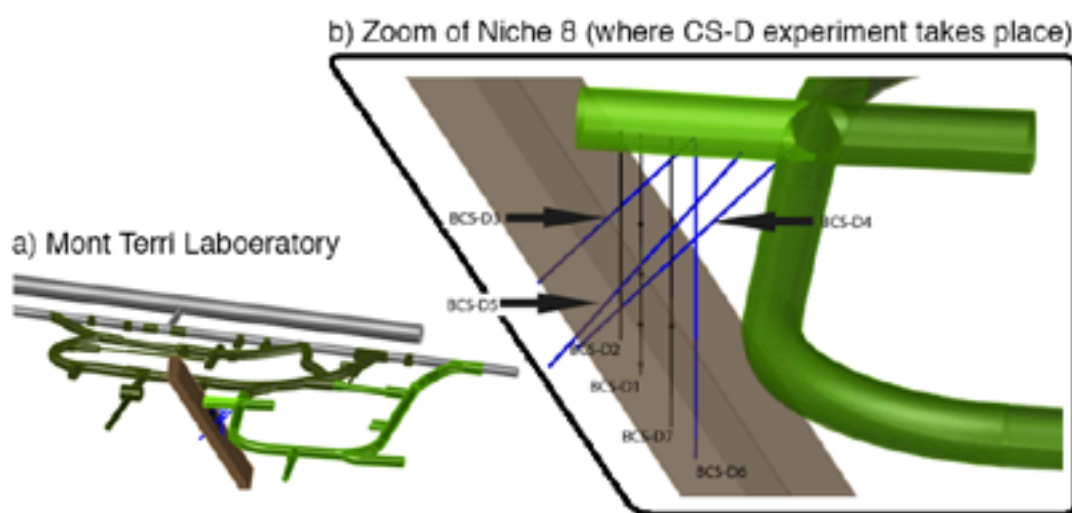

Figure 1 a) The Mont Terri laboratory with niche 8 in light green and the fault zone in brown. b) Position of the boreholes for geophysical monitoring (BCS-D3-6) in blue and in black for the injection and fluid monitoring (BCS-D1,2,7)

The borehole setup of the CS-D experiment (Fig. 1) comprises three vertical boreholes BCS-D1, BCS-D2 and BCS-D7 for fluid injection, pressure monitoring, displacement monitoring, and fluid sampling. For the geophysical monitoring, boreholes BCS-D3 and D4 will be drilled inclined in order to enable the tomographic planes being parallel to the symmetry axis of the anisotropy (normal to the bedding). The boreholes BCS-D5 and -D6 are drilled with different inclinations and at the opposite site of the boreholes -D3 and -D4, such that sensors can be placed in a way to properly locate microseismic events in 3-D.

As shown in Fig. 2, borehole BCS-D3 will be equipped with a cemented 3-component geophone array, similar to the one that has been used for the GM-A experiment (Manukyan et al., 2012). Outside the casing of the boreholes BCS-D3 and D4, ring-shaped electrodes will be implemented for obtaining electrical resistivity tomograms. The casings of the boreholes BCS-D4, -D5 and -D6 will remain empty, such that they can be equipped with mobile S- and P-wave sparker sources for active seismic experiments or with the GmuG system (e.g. Amman et al., 2018), which comprises high-sensitivity piezo-sensors for passive seismic monitoring. The setup is complemented with single 3-component geophone stations cemented at the bottom of boreholes BCS-D4, -D5 and -D6, with a geophone array installed at the gallery wall, and with additional piezo-sensors and accelerometers of the GmuG systems also clamped to the gallery wall.
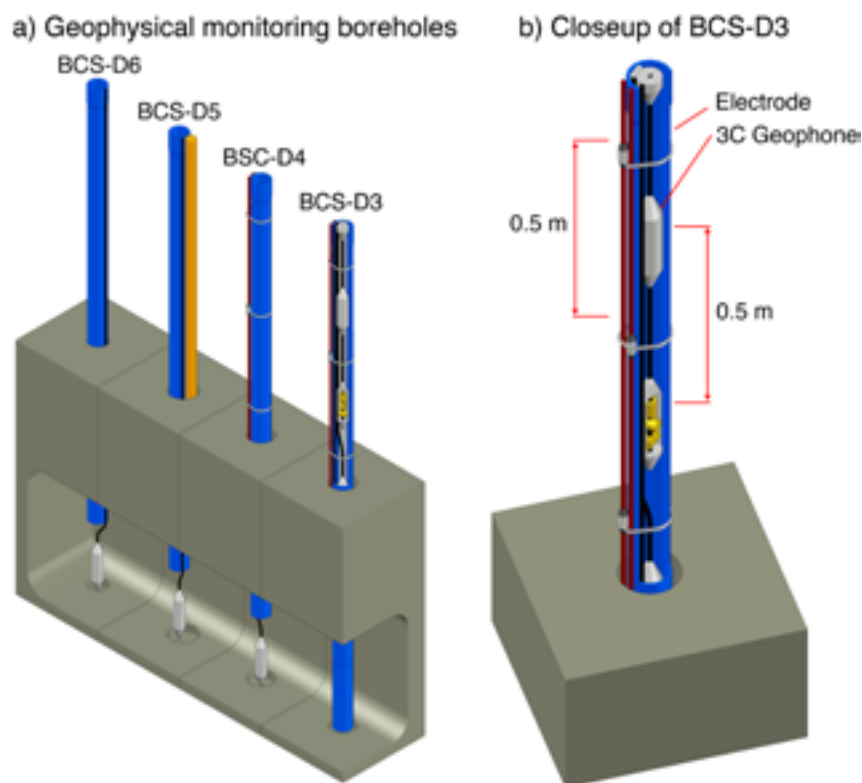
Figure 2 a) Permanent instrumentation of the geophysical monitoring boreholes b) Closeup of borehole BCS-D3 with the geophone and electrode array.

Currently (at the time of the abstract submission) the boreholes of the CS-D experiments are drilled and the permanent geophysical instrumentation is being installed. In the course of the instrumentation, first test data will be recorded, followed by the baseline measurements, once the drilling and instrumentation of all boreholes are completed. We will present the details of the comprehensive geophysical instrumentation of the CS-D experiment and are confident to give a first overview of the geophysical data and performance of our instrumentation.

REFERENCES

F. Amann, et al. (2018). The seismo-hydro-mechanical behavior during deep geothermal reservoir stimulations: open question tackled in a decameter-scale in-situ stimulation experiment, Solid Earth, 9, 115-137. doi: 10.5194/se-9-115-2018.

E. Manukyan, et al. (2012). Seismic monitoring of radioactive waste repositories, Geophysics, 77, EN73-EN83. doi:10.1190/geo2011-0420.1.

9.5
Impact of effective normal stress on CO_2 injection into a brine-saturated single fracture with rough surfaces

Marina M. G. Lima [1], Daniel Vogler, Philipp Schädle, Martin O. Saar, Xiang-Zhao Kong+

Geothermal Energy and Geofluids Group, Institute of Geophysics, ETH Zürich, Sonneggstrasse 5, 8092 Zürich, Switzerland (Emails: [1]marina.lima@erdw.ethz.ch and +xkong@ethz.ch)

Fractures are highly abundant structural features in reservoirs and are crucial for mass and energy transport during reservoir applications such as geological CO_2 storage, Enhanced Geothermal Systems (EGS), nuclear waste disposal, and oil and gas production. Previous studies have shown that fractures dominate fluid and solute transport in the subsurface, with fracture flow often concentrating in flow channels (Brown et al. 1998). Fracture opening and corresponding transport properties are tightly coupled to the effective normal stress on the fracture. However, fracture aperture fields are commonly determined under zero-stress conditions, and therefore do not account for stress effects on the fracture aperture distribution (Pyrak-Nolte et al. 1987).

In this study, we use the fracture geometries of naturally-fractured granite cores from the Grimsel Test Site (GTS) in Switzerland, and numerically model CO_2 injection into these fractures under different effective normal stress conditions. The fracture surfaces of two granite cores of 2.5 x 3.0 cm are first mapped using photogrammetric scans, and the fracture surfaces are subsequently matched to obtain the aperture fields for zero stress conditions (Vogler et al. 2018). Next, we use a Fast Fourier Transform (FFT)-based convolution numerical method (Kling et al. 2018, available in the web application http://contact.engineering/) to generate aperture distributions under different effective normal stresses (0.25 to 10 MPa). Finally, we perform two-phase flow simulations of brine displacement with CO_2 injection within the aforementioned aperture fields, using an in-house application based on the MOOSE framework (Gaston et al. 2009). Analyses on the resulting CO_2 injection patterns enable investigation of the relationships coupling effective normal stress, multiphase flow channeling and fracture transmissivity. The obtained results aid the design of laboratory experiments and reservoir applications focusing on enhanced geothermal systems using CO_2 and geological CO_2 sequestration in fractured reservoirs.
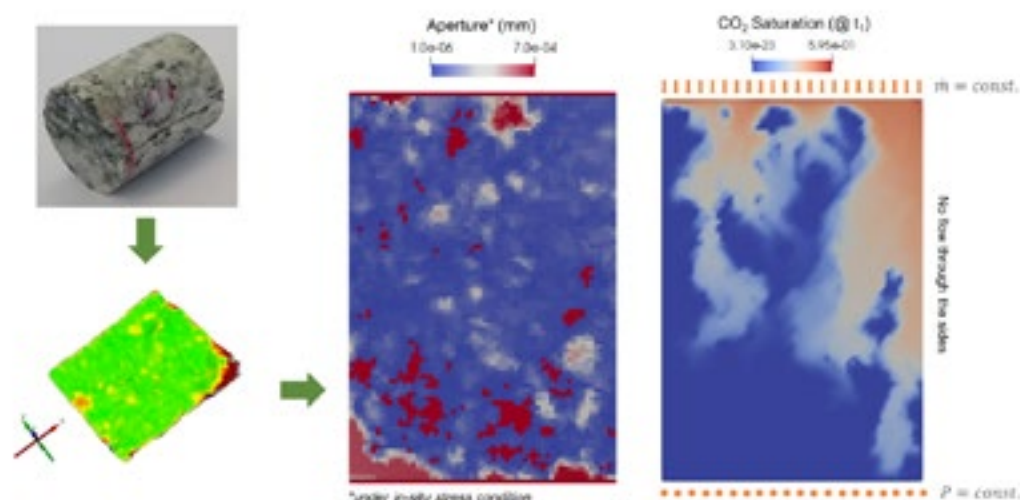

Figure 1. Simulated CO_2 injection into a brine-saturated granite fracture under 0.25 MPa effective normal stress. Simulations are performed at 100°C and with a constant pore fluid pressure at the outlet of 15MPa.

REFERENCES

Brown, S., A. Caprihan and Hardy, R. 1998: Experimental observation of fluid flow channels in a single fracture. Journal of Geophysical Research: Solid Earth, 103(B3), 5125-5132.

Gaston, D., Newman, C., Hansen, G., Lebrun-Grandié, D. 2009: MOOSE: A parallel computational framework for coupled systems of nonlinear equations, Nuclear Engineering and Design, 239(10).

Kling, T., Vogler, D., Pastewka, L., Amann, F. and Blum, P. 2018: Numerical Simulations and Validation of Contact Mechanics in a Granodiorite Fracture. Rock Mech Rock Eng https://doi.org/10.1007/s00603-018-1498-x

Pyrak-Nolte, L. J., Myer, L. R., Cook, N. G. and Witherspoon, P. A. 1987: Hydraulic and mechanical properties of natural fractures in low permeability rock. In 6th ISRM Congress. International Society for Rock Mechanics.

Vogler, D., Settgast, R. R., Annavarapu, C., Madonna, C., Bayer, P., and Amann, F. 2018: Experiments and Simulations of Fully Hydro-Mechanically coupled Response of Rough Fractures exposed to High Pressure Fluid Injection, Journal of Geophysical Research: Solid Earth, 123. https://doi.org/10.1002/2017JB015057

9.6
Complex interplay between fracture opening and shearing during in-situ stimulation experiments

Hannes Krietsch [1], Linus Villiger [1], Joseph Doetsch [1], Valentin Gischig [1,2] & Florian Amann [3]

[1] SCCER-SoE, ETH Zurich, Sonneggstrasse 5, 8092 Zurich (hannesk@ethz.ch)
[2] CSD Ingenieure AG, Bern
[3] Chair for Engineering Geology, RWTH Aachen, Germany

In the framework of the decameter-scale in-situ stimulation and circulation experiment, six hydraulic shearing tests were carried out in February 2017 at the Grimsel Test Site, Switzerland (Amann et al. 2018). These tests aimed to hydraulically reactivate previously mapped and characterized fractures and shear zones. All tests consisted of four injection cycles, with a shut-in and venting phase between each cycle. Both hydroshearing (HS) and hydrofracturing (HF) can be considered as endmember deformation mechanisms that may occur concomitantly during large scale hydraulic stimulations in the context of deep geothermal reservoir engineering. We here report complex interplay between both mechanisms observed during our experiments.

Dynamic deformations were monitored in three boreholes (so-called FBS boreholes) using a total of 60 Fiber-Bragg Grating strain sensors with a base length of 1 m and a resolution of 0.1 μ-strain, and one distributed Brillouin strain (DBS) sensing cable loop (Krietsch et al. 2018). An additional DBS loop was monitoring strain in three additional boreholes (so-called PRP boreholes) that were dedicated to pressure monitoring. These three pressure monitoring boreholes contain a total of seven open pressure monitoring intervals. Deformation and pressure sensors were placed across the shear zones that were targeted during our tests. Acoustic emission sensors were distributed along the tunnel walls and in four boreholes. This setup allows a precise location of acoustic emissions inside the test volume.

Here, we show results of one test that indicated a change in propagation direction of the deformation field inside the stimulated shear zone between injection cycles 3 and 4. Additionally, a strong pressure pulse was monitored in borehole PRP2 interval 2 (referred to as PRP2-2) during cycle 3 and in borehole PRP1 interval 2 (PRP1-2) during cycle 4 (see Fig. 1a). This observation was interpreted as a change in preferential flow path. Based on the located acoustic emissions, it was observed that a geological feature inside the targeted shear zone was reactivated between the two pressure monitoring intervals (i.e., PRP1-2 & PRP2-2) in cycle 3. However, the pressure signals obtained during cycle 3 in PRP1-2 and PRP2-2 indicate a heterogeneous hydro-mechanical reactivation of this geological structure. The seismic events during cycle 4 illustrate an ongoing deformation towards PRP1-2.

We assume from the hydro-mechanical-seismic observations made during cycle 3 and 4 that a redirection of hydraulic channelling was taking place during these cycles.

We further reckon that the channel towards PRP2-2 formed elastically (e.g., hydraulic normal opening) during cycle 3, as it seemed to be closed again during cycle 4. Nevertheless, the channel towards PRP1-2 formed permanently through hydraulic shearing (i.e., shear dilation) as it could be identified in post stimulation hydraulic characterization. This deformation started in cycle 3 in which already a moderate pressure increase was observed in interval PRP1-2. The ongoing, increased deformation during cycle 4 in the vicinity of interval PRP1-2 is also highlighted by occurring seismic events. To constrain the observations made during this experiment, we are currently working on a model that calculates the dislocation field within the test volume due to fracturing and shearing along a known fault plane (Okada 1992). This might help to unravel the complex heterogeneous hydro-mechanical reactivation of the targeted shear zone.
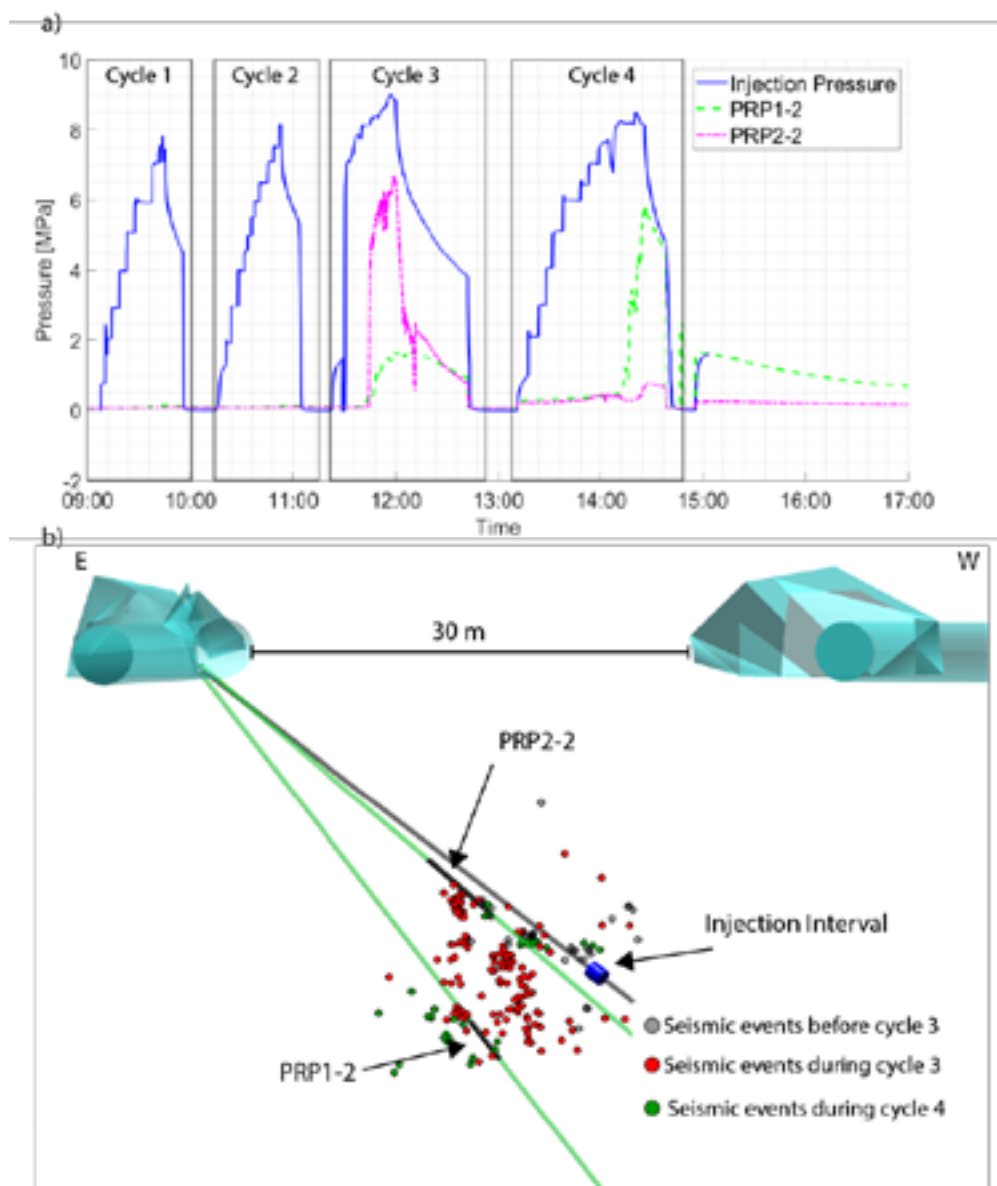
Figure 1. a) Injection protocol with indicated injection cycles and monitored pressure signals. b) Located seismic events plotted inside the test volume with locations of injection and pressure monitoring intervals. It is a view onto the shear zone (i.e., view towards south).

REFERENCES

Amann, F., Gischig ,V., Evans, K.F., et al 2018: The seismo-hydromechanicalbehavior during deep geothermal reservoir stimulations: open questions tackled in a decameter-scale in situ stimulation experiment. Solid Earth 9:115–137. doi: 10.5194/se-9-115-2018

Krietsch, H., Gischig, V., Jalali, M., et al 2018: A comparison of FBG and Brillouin strain sensing in the framework of a decameter scale hydraulic stimulation experiment. American Rock Mechanics Association

Okada, Y. 1992: Internal deformation due to shear and tensile faults in a half-space. Bull Seismol Soc Am 82:1018–1040

9.7
Dissolution of dolomite cement in sandstones when subjected to CO$_2$-enriched brine

Jin Ma [1,°], Lorenzo Querci [2], Bodo Hattendorf [2], Martin O. Saar [1], Xiang-Zhao Kong [1,°°]

[1] *Geothermal Energy and Geofluids Group, Institute of Geophysics, ETH Zürich, Sonneggstrasse 5, 8092 Zürich, Switzerland (°majin@ethz.ch and °°xkong@ethz.ch)*
[2] *Department of Chemistry and Applied Biosciences, ETH Zürich, Vladimir-Prelog-Weg 1-5/10, 8093 Zürich, Switzerland*

Fluid-rock reaction plays a critical role in many natural and engineered geo-systems. Of our particular interest are CO$_2$-based geochemical reactions which are involved in various geological applications related to Carbon Capture, Utilization, and Storage (CCUS) (Xu et al., 2003). These reactions could lead to mineral dissolution and precipitation which may substantially change reservoir's hydraulic, mechanical, thermal, and chemical properties (Tutolo et al., 2014; Luhmann et al., 2017). In this study, we report a reactive flow-through experiment under reservoir conditions on a multi-mineral sandstone from a geothermal reservoir, with the focus on the dissolution reaction of dolomite cement (Ca$_{1.05}$Mg$_{0.75}$Fe$_{0.2}$(CO$_3$)$_2$). We circulate CO$_2$-enriched brine through this sandstone specimen for 137 cycles (~270 hours) to examine the evolution of in-situ hydraulic properties and CO$_2$-based geochemical fluid-rock reactions, where the outflow fluids of a current injection cycle are recycled as the working fluids of its next injection cycle. Based on our effluent chemical analysis, dolomite dissolution is identified to be the major reaction during the experiment. With respect to the release of calcium, we observe a slow release of magnesium at the beginning of the experiment, where the reaction is still far from equilibrium. After that period, calcium, magnesium, and iron are found to be released stoichiometrically. Reactivity of dolomite is determined to be ~2.45 mmol m^{-3} s^{-1} during the first cycle. The corresponding effective surface area of the sample is estimated to be 1.16 10^{-4} m^2/g. An effective coefficient of the reactive surface area for dolomite can then be defined 3.2 10^{-3}, indicating a limited accessibility of the physical surface area. Moreover, we observe a continuous decrease of the effective surface area as the dissolution reaction progresses. This decrease can be qualitatively reproduced using a simple two-dimentional displacement model, where minerals are selectively displaced (dissolved) by fluid based on the pore connectivity and pore size. With this model, we can conclude that for certain dissolution regimes, the effective surface area decreases faster when subjected to a heterogeneous flow than a homogeneous one. Our results provide insights into the understanding of the CO$_2$-based geochemical reactions involved in the aforementioned applications.
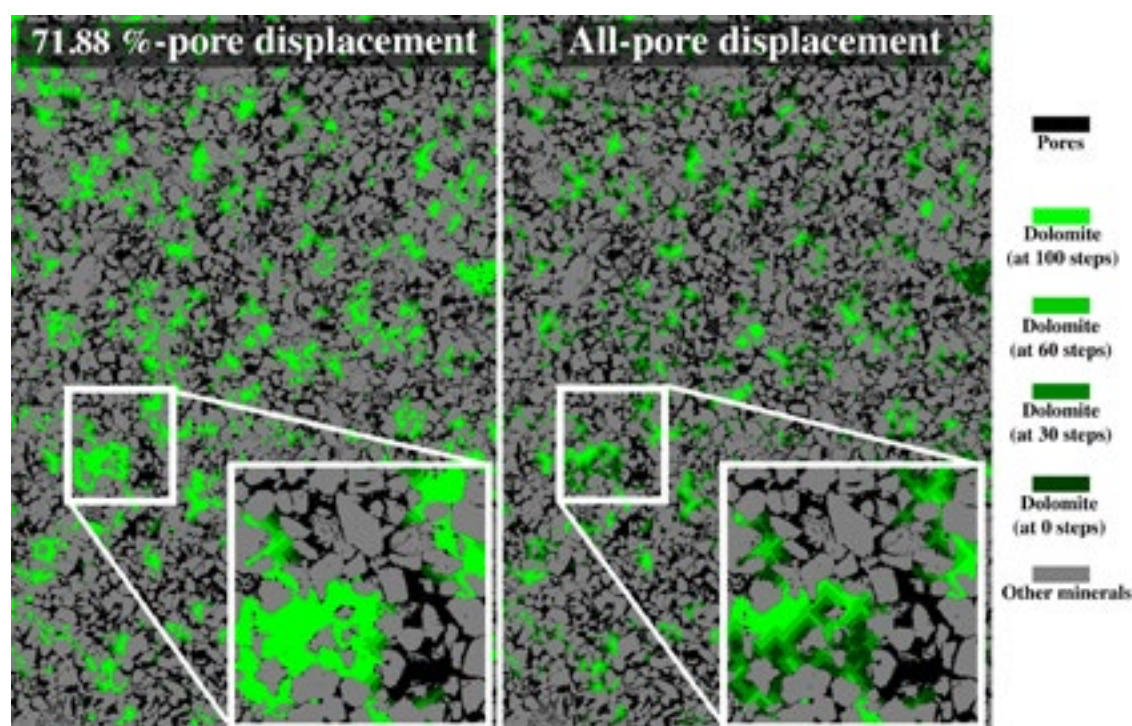

Figure 1. Dolomite dissolution pattern resulting from a simple two-dimentional displacement model: (Left) only 71.88% of the pores (with their sizes larger than 5000 pixel) and (Right) all pores are invloded in the dolomite dissolution reactions.

REFERENCES

Luhmann, A. J.; Tutolo, B. M.; Bagley, B. C. et al. 2017: Permeability, porosity, and mineral surface area changes in basalt cores induced by reactive transport of CO_2-rich brine, Water Resources Research, 53, 1908-1927.

Tutolo, B. M.; Luhmann, A. J.; Kong, X.-Z. et al. 2014: Experimental observation of permeability changes in dolomite at CO_2 sequestration conditions, Environmental science & technology, 48, 2445-2452.

Xu, T.; Apps, J. A.; Pruess, K. 2003: Reactive geochemical transport simulation to study mineral trapping for CO_2 disposal in deep arenaceous formations, Journal of Geophys-ical Research: Solid Earth, 108.

9.8

Early dolomitization and dedolomitization of the Late Jurassic limestones in the Geneva Basin (Switzerland and France)

Yasin Makhloufi [1], Elias Samankassou [1] & Michel Meyer [2]

[1] *Department of Earth Sciences, University of Geneva, Rue des Maraîchers 13, CH-1205 Geneva*
  (yasin.makhloufi@unige.ch)
[2] *Service Industriels de Genève, CP 2777, CH-1211 Geneva*

The Canton of Geneva (Switzerland) is currently exploring the opportunities for geothermal energy exploitation in the Geneva Basin (GB) sub-surface.

Horizons affected by dolomitization, the focus of the present study, are of particular interest because they proved to be productive in time-equivalent deposits currently exploited in Southern Germany and are suitable for geothermal energy production. The Late Jurassic limestones of the GB represent the best potential reservoirs. However, these units exhibit strong heterogeneities in terms of reservoir quality with the occurrence of highly porous sucrosic dolomite intervals as well as dedolomitized intervals exhibiting secondary porosity. The aim of this study is to: (1) assess texture, fabrics, types and distribution of dolomitization, (2) constrain the paragenesis for each stratigraphic and (3) propose potential models of timing and origin of the dolomitization and dedolomitization processes. In this context, an integrated study was led including: detailed outcrop study in the Jura and Salève mountains, thin section analyses (optical microscropy, cathodoluminescence, S.E.M) and the geochemistry of oxygen, carbon and strontium isotopes.

Two types of dolomite were identified: early replacive dolomites (D1) and fabric-destructive sucrosic dolomite (D2), along with two types of corresponding dedolomites. The measured isotopic compositions of D1 dolomites are consistent with a reflux type model of dolomitization induced by high-frequency sea-level changes producing several pulses of dolomitizing brines in a short time span. The D2 sucrosic dolomite represents an advanced level of replacement that obliterated the original fabric leading to high intercrystalline porosity during shallow burial. Dedolomitization is observed at different order of magnitude by either (1) an almost complete dissolution leading to the creation of secondary pore space or (2) a two-step calcitization driven by the infiltration of Ca-rich water leading to dissolution, formation of microvugs and then precipitation of calcite. This dedolomitization would have taken place during long-term emersion events or after the exhumation of the Upper Jurassic limestones.

The study presented here will help to understand the possible mode of dolomitization that occurred in the GB. The results presented here will be implemented in a stochastic model in order to predict the volume and distribution of dolomitic bodies at the basin scale. This step will ultimately help in reservoir modelling which is crucial for further potential exploitation.

9.9
The effect of partial saturation on the mechanical properties of gas shales

Alberto Minardi [1], Lyesse Laloui [1]

[1] Laboratory for Soil Mechanics – Chair "Gaz Naturel" Petrosvibri, Swiss Federal Institute of Technology, EPFL, Lausanne, Switzerland. (alberto.minardi@epfl.ch)

INTRODUCTION

Geomechanical properties of gas shales (such as stiffness and strength) play a fundamental role for an optimised exploitation of shale gas reservoirs. In spite of their relevant importance, laboratory tests are usually performed without considering the water saturation state of the material; specimens are indeed tested either in the as-received state or lab-atmosphere equilibrated state. The water saturation is expected to have a significant impact on the geomechanical properties of gas shales as their mineralogical composition presents large clay content (10-60%). Indeed, there is already significant evidence on the role of water saturation for other clayey geomaterials such as mudstones, claystones, and organic-poor shales (Ewy 2015). This study demonstrates how the geomechanical properties of gas shale cannot be properly evaluated without accounting for the effect of the water saturation. Selected evidence from different tests performed on gas shales samples extracted from different unconvenitonal reservoirs is presented.

MATERIALS AND METHODS

The experimental results presented in the following were performed on a core sample extracted from shale gas reservoirs at a depth of 2700m. The received core sample were partially water saturated, with porosity lower 7%, and clay content between 20% and 30%. The testing set-presented in Ferrari et al. 2018 and Minardi et al. 2018 was adopted to perform the experimental analsyis. The set-up allows performing uniaxial compressive tests with total suction control (Ψ) by using vapour equilibrium technique (typically used also for shales, e.g. Ferrari et al. 2014; Minardi et al. 2016). Different total suction values were imposed to tested sample under constant axial stress to achieve different saturated states. Unloading-reloading paths were carried out after each suction equalization step to evaluate the elastic properties.

RESULTS

The developed testing set-up described in the previous section allows having a comprehensive and precise assessment of the impact of total suction on the elastic properties of gas shales. Figure 1a shows the response of a specimen during three unloading-reloading paths performed at different total suctions (Ψ =150 MPa, Ψ =39 MPa, Ψ =10 MPa), between 15 MPa and 5 MPa of axial stress. In particular, the graph illustrates the unloading phase of the paths, considering the same initial starting point (0% of axial strain and 15 MPa of axial stress) to facilitate the comparison. The impact of total suction on the mechanical response is clearly highlighted. Higher expansion upon unloading is experienced by the specimen as it is equalized to lower values of total suction. This feature leads to a decrease of the elastic modulus (E) measured on the applied stress interval. Figure 1b shows the relationship between the measured elastic stiffness and total suction. The stiffness measured on a second specimen flooded with water (Ψ =0 MPa) before the unloading is also reported. A clear impact of total suction variations on the elastic modulus of the tested gas shale is observed, where a decrease higher than 50% is obtained for the investigated total suction range.
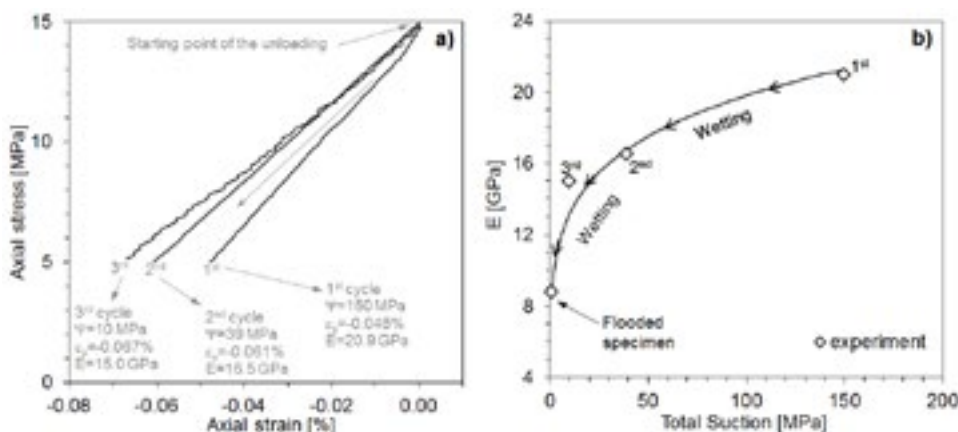

Figure 1. a) Specimen's response during the unloading phase of stress paths performed at different total suctions; b) relationship between elastic stiffness and total suction (Ferrari et al. 2018).

CONCLUSIONS

The presented experimental study highlighted the importance of considering partially saturated conditions for the determination of geomechanical properties of gas shales. Variations higher than 50% for the elastic stiffness have been measured. These outcomes are expected to be of great importance not only to predict the behaviour of these materials in-situ, but also to assess the impact of material preservation and air exposure on core samples used for laboratory testing.

REFERENCES

Ewy R.T. 2015: Shale/claystone response to air and liquid exposure, and implications for handling, sampling and testing. International Journal of Rock Mechanics and Mining Sciences, 80, 388-401

Ferrari A., Favero V., Marschall P., Laloui L. 2014: Experimental analysis of the water retention behaviour of shales. International Journal of Rock Mechanics and Mining Sciences, 72, 61–70

Ferrari A., Minardi A., Ewy R., Laloui L. 2018: Gas shales testing in controlled partially saturated conditions. International Journal of Rock Mechanics and Mining Sciences, 107,110-119.

Minardi A., Crisci E., Ferrari A., Laloui L. 2016: Anisotropic volumetric behaviour of Opalinus Clay shale upon suction variation. Géotechnique Letters, 6(2),144-148.

Minardi A., Ferrari A., Ewy R., Laloui L. 2018: Nonlinear Elastic Response of Partially Saturated Gas Shales in Uniaxial Compression. Rock Mechanics and Rock Engineering, 51(7), 1967-1978.

9.10
Exploring the interface between shallow and deep geothermal systems: new insights from the Mesozoic-Cenozoic transition.

Andrea Moscariello [1], Nicolas Clerc [1,2], Loic Pierdona [1], Antoine De Haller [1]

[1] Department of Earth Sciences, University of Geneva – Rue des Maraichers 13, CH-1205 Geneva
[2] Canton of Geneva, Service de géologie, sols et déchets, Geneva

Little is known about the reservoir characteristics of the Tertiary Molasse succession accumulated in the Geneva foreland basin despite over the last 60 years both academic research and geo-energy exploration projects have been carried out extensively in the Greater Geneva Basin (westernmost part of the North Alpine Molasse Basin). While the general chronostratigraphic framework using biostratigraphic tools and the overall sedimentology is generally known, the internal architecture and tectonostratigraphic significance and the reservoir characteristics of this succession is not yet well described.

In particular, uncertainties exist of the regional distribution of individual stratigraphic units (parasequences) within the Molasse preserved in the Geneva Basin whose knowledge could unravel important element to reconstruct the tectono-stratigraphic evolution of the Molasse foreland in this region. This in turn could allow the development of a better understanding of facies distribution within the succession and improve our prediction of sand/shale distribution and their impact on deep fluid circulation. The Molasse can in fact play an important role in assessing the potential of deep hydrogeological budget as it could provide communication from the shallow ground water flows mostly located within Quaternary deposits and the deep Mesozoic systems, typically charged through pervasive fault systems.

Moreover, the interface between the Oligocene Molasse sandstone and the lower Cretaceous limestones (Urgonian *Auct*.) represented by a 35 mln years unconformity, contains discontinuous lenses of possibly older stratigraphic units (Siderolithic and Gompholite) which can also play a role in controlling the subsurface water flow circulation. The recent observation (N. Clerc in prep) of brittle deformation consisting of low angle inverse faulting in a confined stratigraphic unit including the lower Cretaceous and upper Jurassic might point out to a different geomechanical behavior of different units in response to the compressional stress experienced in this region since Tertiary time. A comprehensive integrated sedimentological, chemostratigraphic and structural study of this interval is under way.

9.11
GEo-01: The first GEothermie 2020 P&D well in the Canton of Geneva - Preliminary results

Carole Nawratil de Bono [1] and GEo-01 team [1]

[1] Services Industriels de Genève, Service de géologie, sols et déchets, Hydrogeol Sarl
   Geneva Geo-Energy Sarl, University of Geneva, Department of Earth Sciences

The GEothermie 2020 program, which consists of three main phases prospection, exploration and exploitation, has recently entered into exploration phase with the drilling of a series of shallow boreholes i.e. ca 600 -1000 m deep below ground level (b.g.l.).

In this framework, the first exploration well GEo-01 has been successfully drilled in 2018 in Satigny, North-West of the city of Geneva. Artesian water flow of 50 l/s and 34°C has been intercepted within the faulted lower Cretaceous carbonate units at various depth intervals ranging between 460 and 670 m b.g.l.. The total well depth was reached at 744 m b.g.l. reaching the Upper Jurassic. The drilling operation in the limestone units has been carried out using water circulation instead of mud-rich fluids. Continuous water flow rate measurement and pressure test were performed at the surface during the entire drilling operations. Large karstic features at 540 m b.g.l., caused a well instability which limited the completion of the logging program as planned throughout the well section. However, thanks to continuous hydraulic tests at surface, the exact depth location of the main source of water flow was identified.

Long-duration hydraulic tests on the artesian flow will be conducted for the next 6 months. During this phase, continuous measurements of temperature, pressure, flow rate, turbidity and hydro-chemical and isotopic analysis will be performed. The second exploration well GEo-02 will be spud in January 2019. The overall goals of this well are similar to the GEo-01 well: test the faulted lower Cretaceous and Upper Jurassic limestones, reach the Kimmeridgian reef complex at 950m as well as improve our knowledge of performing successful geothermal drilling projects. The expected total depth of the well GEo-02 is 1130 m b.g.l..

9.12
Aseismic and seismic reactivation of a velocity-strengthening clay-rich fault zone: the Mont Terri Main Fault FS experiment

Christophe Nussbaum [1], Yves Guglielmi [2], Louis de Barros [3], Frédéric Cappa [3], Jens Birkholzer [2], Paul Bossart [1]

[1] Federal Office of Topography, Swisstopo Fabrique de Chaux CH-2882 St-Ursanne (Switzerland).
[2] Lawrence Berkeley National Laboratory, Energy Geoscience Division, Berkeley, CA, 94720, USA.
[3] University of Côte d'Azur, CNRS, Côte d'Azur Observatory, IRD, Géoazur, 06560 Sophia-Antipolis, France.

In the framework of the FS experiment, we have conducted a series of controlled-injection field-scale experiments in the Mont Terri rock laboratory, reactivating selected parts of the Main Fault intersecting the Opalinus Clay. This very low-permeability claystone is not only studied for its confinement properties as host rock for the disposal of radioactive wastes, but it is also considered as a reference caprock-like formation for CO_2 storage.

The Main Fault corresponds to a second-order structure interpreted as a blind shear fault-bend fold that is detached from the top of the underlying Staffelegg Formation in the hanging wall of the Mont Terri anticline (Nussbaum et al., 2017). Monitored by two 3-component accelerometers, we observed seismic fault slip behavior in a series of 68 events with maximum magnitude M_w=-2.3 associated to mixed normal-shear movement.

The slip propagation was captured between two monitoring points, respectively one injector and one monitoring point set across the fault core, which were continuously probing the three-dimensional movements of the fault zone at high resolution by using the step-rate injection method for in-situ fracture properties (SIMFIP) developed by Guglielmi *et al*. (2013).

We observed an increase with time of the number of plastic displacement transients characterized by displacement rates of 3 to 60 10^{-6} m/s. We can define a succession of three different activation periods: 1) a stress transfer period, 2) a fracture opening period, and 3) a shearing period. The orientation of the displacement vectors showed considerable heterogeneity, which may suggest that the displacement behavior is caused by interactions between multiple second-order fractures in the fault core rather than by slip along a well-defined plane. We discuss the possibility of a structural instability enhanced by aseismic stress transfer and fluid diffusion in a heterogeneous fault core as a potential mechanism of seismic reactivation of a fault.

Recently, a series of laboratory experiments have been conducted to characterize the frictional behavior of gouge material from the same fault (Orellana et al, 2018). Results suggest a velocity-strengthening regime, typical of clay-rich fault materials, indicating that such faults, when reactivated, would slip aseismically.

This discrepancy between lab-scale and field-scale frictional behavior is of great importance when predicting the seismic stability of clay-rich fault zones. It may highlight the existence of other sources of seismicity related to the highly complex structure of a tectonic fault that experiences multiple periods of reactivation and rest.

REFERENCES

Guglielmi Y., Cappa F., Lançon H., Janowczyk J.B., Rutqvist J., Tsang C.F. and Wang J. 2013. Estimation of permeability, elastic and friction properties of fractured rock masses from in situ hydromechanical testing: the High-frequency Pulse Poroelasticity Protocole (HPPP) testing method. Submitted contribution to the ISRM Commission on Testing Methods, *Int J Rock Mech Min Sci and Geomech Abstr special issue.*

Nussbaum, C., Kloppenburg, A., Caër, T., Bossart, P., 2017. Tectonic evolution around the Mont Terri rock laboratory, northwestern Swiss Jura: constraints from kinematic forward modelling. Swiss J. Geosci. 110, 39–66. doi:10.1007/s00015-016-0248-x.

Orellana, L.F., Scuderi, M.M., Collettini, C., Violay, M., 2018. Frictional Properties of Opalinus Clay: Implications for nuclear waste storage. J. Geophys. Res. Solid Earth 123, 157–175. doi:10.1002/2017JB014931.
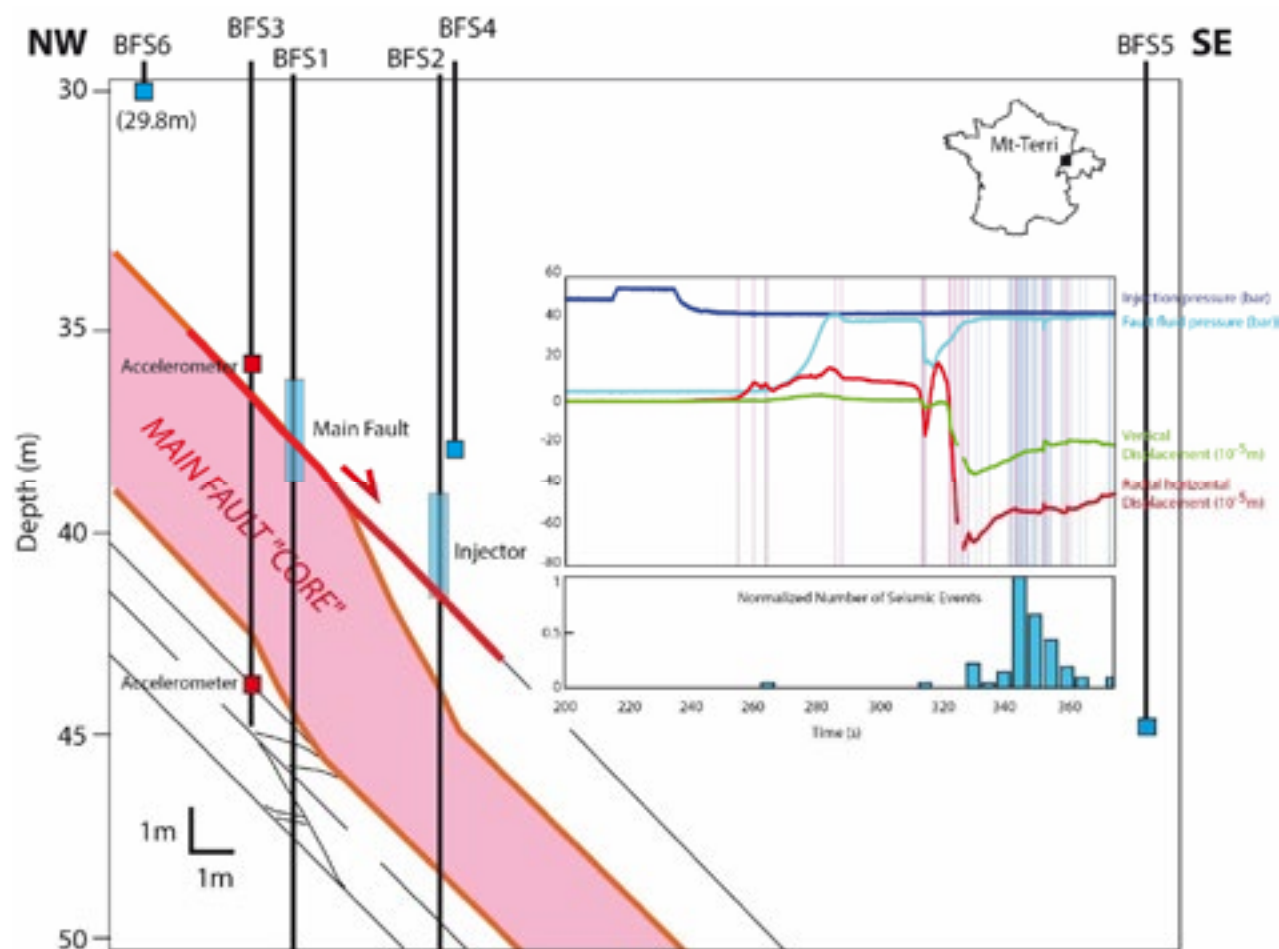
Figure 1: Schematic vertical cross section of the Mont Terri fault-activation experiment (the thick red line indicates the activated section of the fault). Main Fault blue rectangle corresponds to the monitoring interval. Injector blue rectangle is the injection interval. Graphs show the time window when the hydraulic connection propagating from the injector to the Main Fault interval triggers the Main Fault displacement and the seismicity. Vertical magenta lines show the picks of the >3 10^{-6} m/s displacement rate events. Dark blue vertical lines show picks of the seismic events. The lower graph shows the normalized number of seismic events per 5-second time intervals.

9.13
New insights into the thermal and petroleum system of the St Gallen area: Implication for geothermal exploration

Omodeo-Salé, S., Eruteya, O. E., Guglielmetti, A. and Moscariello, A.

[1] Department of Earth Sciences, University of Geneva, rue des Maraichers 13, CH-1205 Geneva
(andrea.moscariello@unige.ch)

Usually, geothermal exploration activities in green fields such as the one in St. Gallen (North-East Switzerland) are confined to limited areas in the surroundings of the well to be drilled, and the chance to move to production operations are strongly dependant on the success of the first exploration well. However, the presence of hydrocarbons in the area are notorious as a potential risk for geothermal exploration. If not properly predicted, the manifestation of overpressured hydrocarbon fluids (oil and gas) can hinder the drilling operations and the whole geothermal project. This was the case of the St Gallen geothermal GT-1 well in 2013. The occurrence of this unexpected event opened several scientific questions, such as: are hydrocarbon hosted in deep reservoir in the area or do local faults network promote the plumbing of fluids? What are the source rocks for these hydrocarbons and their remaining generation potential? What is the realistic estimate of the volume of oil and gas in place in the area?

In this study, we developed a high-resolution 3-D geological and thermal model from the integration of a 3-D seismic reflection survey, well logs and geochemical data. Here, emphaisis was placed on the mapping of the Permo-Carboniferous grabens and the crystalline basement. This interval is of particular importance for our study, since the Permo-Carboniferous unit may host the potential source rocks (coal and carbonaceous shales – based on the Weiach-1 analogue well) that generated the gas found in the St Gallen area. Uncertainties are associated with delineating the depth and geometry of the grabens. In order to simulate the thermal evolution of the basin, the different scenarios reconstructed were used as geological conceptual models. Paleothermal data (vitrinite reflectance and illite cristallinity) were collected to properly reconstruct the thermal maturation timing of the source rocks and hydrocarbons generation and expulsion events.

The findings from this study extend the current understanding of the the petroleum system in the St. Gallen area and may serve as analogue elsewhere in the Swiss Plateau. This work demonstrates how a robust uncertainity-based tectono-stratigraphic interpretation can result into different modelled outcomes on the hydrocarbon volumes estimates. Furthermore, it provides more preciser constrains of potential risk to geothermal exploration.

9.14
Fracture network stability analysis for coupled EGS prospection project in Eclépens.

Nicole Schmitt[1], Gunnar Jansen[2], Stephen Miller[2], Benoît Valley[2], Jon Mosar[1]

[1] Departement de Géosciences – Sciences de la Terre, Université de Fribourg, Chemin du Musée 6, CH-1700 Fribourg
[2] Centre de Hydrogéologie et Géothermie, Université de Neuchâtel, Rue Emile-Argand 11, CH-2000 Neuchâtel

The understanding of fault criticality in foreland basins is of strategic importance for the development of the geothermal resources in Switzerland. Our study is part of a larger joint venture between Swisstopo, the Department of Geosciences of the University of Fribourg and the Centre of Hydrogeology and Geothermics of the University of Neuchâtel. The project is dedicated to the Stress State, Fault Criticality and Fluids; Bearing on resources development in Switzerland. The subproject of Fault anatomy, porosity and pore connectivity: the La Sarraz Fault system, combines different techniques to define porosity and connectivity on faults outcropping in the Eclépens area.

Herein, we present a numerical approach applied to a fault system, exposed in the field, in which we vary: (i) the connectivity of the fractures, (ii) the injection and production wells geographical location and pressure regime, (iii) the local stress on the faults, (iv) the permeability and temperature of the potential aquifers present in the Eclépens area.

We analysed fracture stability within injection and production wells, simulated on four aquifers at depths between 500 and 3000 meters in the Eclépens area. The simulations were modelled in Thermaid (Jansen et al. 2017), an open source for Matlab. Two model fracture networks were used on three geographically different injection and production well locations.

Both networks are based on an observed sub-vertical strike-slip fault system in the area of investigation. A "homogenous" fracture network model simulates identical fracture permeability, porosity, and connectivity within the matrix and faults and governed by a continuous regional stress field acting on all faults. Alternatively, a "heterogeneous" fracture network model, exclusively modelled permeability and porosity within the faults based on values obtained from literature. Furthermore, the local stress field of each studied fault was applied on each individual modelled fault. In contrast with the homogenous fracture network model, the heterogeneous fracture network model considered the optimally oriented faults as being critically stressed, with respect to the local maximum principal stress. In addition, the fluid pressure in the wells was simulated applying three distinct regimes: (a) hydrostatic, (b) critical pore pressure and (c) supra-hydrostatic fluid pressure.

In total 18 simulations were obtained for each aquifer, producing 72 models. The majority of the results (homogeneous and heterogeneous fracture network model) show that the fluid injection critically stressed, not only the targeted fault, but also faults optimally oriented (±22°–32°) in a perimeter of 500 – 1000 m. The production well placed on optimally oriented faults also triggered instability on the faults. However, the production well did not provoke instability on non-optimally oriented faults for hydrostatic and critical pore pressure regimes. The simulations allowed us to explore the stress conditions leading to induced slippage due to fluid pressure variations in injection and production wells on a natural fractured network.

REFERENCES
Jansen G., Miller S., & Valley B. 2017 THERMAID – A matlab package for thermo-hydraulic modeling and fracture stability analysis in fractured reservoirs. SGM 2017, Davos.

9.15
Large-scale structures governing water flow in crystalline bedrock at Grimsel Test Site (Switzerland).

Raphael Schneeberger [1], Daniel Egli [2], Bill Lanyon [3], Urs K. Mäder [2], Alfons Berger [2], Florian Kober [1], Ingo Blechschmidt [1], & Marco Herwegh [3]

[1] Nagra, Hardstrasse 73, 5430 Wettingen (raphael.schneeberger@nagra.ch)
[2] Institute for Geological Sciences, University of Bern, Bern, Switzerland
[3] Fracture Systems Ltd, UK

Crystalline bedrock is often envisaged as the host rock for large engineered projects such as deep geothermal powerplants, deep geological repositories for radioactive waste disposal or groundwater supply. Prediction of groundwater flow paths is therefore of utmost importance for such large projects. Generally, water flow in crystalline bedrock is known to be fracture-dominated.

The Grimsel area in the Swiss Alps exposes crystalline bedrock in a comparably simple geological environment. Moreover, the Grimsel Test Site (GTS) is an underground facility operated by Nagra allowing for an underground study of water-conducting structures in crystalline rocks. The GTS is located within the post- and Late-Variscan granitoids of the Aar massif. Alpine deformation structures such as ductile shear zones and brittle fault zones connect present-day topography with the underground of the GTS. The groundwater encountered in the GTS is of meteoric origin, which is evidence of infiltration from the surface and subsequent percolation through the rock volume above the GTS.

Detailed mapping of deformation structures, such as ductile shear zones, brittle reactivated metabasic dykes, brittle fault zones, and brittle fractures, in conjunction with mapping water inflow points into the underground facility allowed the identification of structural controls on the groundwater flow paths and the definition of a favourability distribution of structures for water conductivity. Water inflow points at the GTS were mapped in winter and summer times as a basis for identification of water-conducting features.

The detected fault structures are steeply dipping southwards and occur as three distinct orientation groups (NE-SW, E-W, and NW-SE trending). Major water-conducting features are brittle reactivated meta-basic dykes, fault or dyke intersections, and brittle reactivated ductile shear zones. Comparison of winter (85 inflow points) and summer (100 inflow points) mappings showed that in winter fewer structures are identified as water conducting due to the reduced air humidity in the tunnel system allowing greater evaporation of water at some infiltration points.

Comparing the orientation of the prevailing structures with the present-day stress field showed that structures preferentially oriented for slip reactivation (high slip-tendency) show a smaller difference in number of water-conducting features between summer and winter compared to features less preferably oriented. This is evidence for a trend of higher conductivity in high slip-tendency features than features with lower slip-tendency.

Generally, it was observed that flow paths are preferentially located at fault intersections and high slip-tendency fault zones. Actual water flow along fault zones is, however, channelized within the fault zone leading to 1D flow channels within the structures rather than 2D water-conducting planes.

9.16

Computerized tomography imaging of fracture aperture distribution and tracer transport within sheared fractures

Quinn C. Wenning [1], Claudio Madonna [1], Ronny Pini [2], Takeshi Kurotori [2], Claudio Petrini [3], Sayed Alireza Hosseinzadeh Hejazi [2]

[1] Geological Institute, ETH Zurich, Sonneggstrasse 5, CH-5092 Zurich (quinn.wenning@erdw.ethz.ch)
[2] Department of Chemical Engineering, Imperial College London, SW7 2AZ, London, United Kingdom
[3] Institute of Geophysics, ETH Zurich, Sonneggstrasse 5, CH-5092 Zurich

Geothermal energy utilization relies on the ability to create a network fractures in the host reservoir with sufficient surface area for heat exchange. The hydromechanical coupling between flow and stress controls the permeability of fractures and faults. While the literature report on studies of stress dependency of fracture aperture and permeability, only few have considered shearing. Even rarer is the ability to image and spatially map fracture aperture changes as a function of shear displacement. In this study, we designed and built a shear-displacement, X-ray transparent core-holder to study the transport of a tracer in fractured rocks that undergo shearing using computerized tomography (CT). The so-called Calibration-Free Missing Attenuation (CFMA) method [Huo et al.., 2016] was applied to quantify and map the distribution of local fracture apertures with a spatial resolution of (0.25 x 0.25) mm^2. Simultaneously, pulse tracer injection experiments were carried out while acquiring X-ray CT scans to obtain time-series images of transport through the rough-walled fracture.

The experiments were performed with Westerly granite and Carrara marble samples (5 cm x 10 cm) to emulate geothermal reservoir rocks at confining pressures of 1.5 MPa with displacement up to 5.75 mm. Solutions of deionized water mixed with KCl (saturating fluid) and KI (tracer fluid) were used due to their similar densities yet contrasting CT numbers. We observe that shearing increases the fracture aperture with displacement, thereby increasing the fracture volume and reducing the surface contact area of the fracture walls that creates flow anisotropy. Larger initial surface roughness causes larger increases in aperture in the Westerly granite as compared to the Carrara marble.

To study the heterogeneous flow properties within the fracture, numerical simulations using the 2-D local-cubic-law approximation coupled with the advection-diffusion equation are performed using the fracture aperture maps as inputs for the fracture permeability field. The numerical models are calibrated by comparing calculated effluent concentration with the measured concentrations from the pulse tracer injection tests The direct imaging of flow through the fracture and numerical simulations are qualitatively similar. The direct imaging of flow through the fracture and numerical simulations are qualitatively similar. Studying aperture changes associated with displacement aids interpretation of hydraulic property changes due to (induced-) seismicity, which can be applied to a range of systems due to the scalability of fractures.

REFERENCES

Huo, D., Pini, R., & Benson, S. M., 2016. A calibration-free approach for measuring fracture aperture distributions using X-ray computed tomography. *Geosphere*, *12*-2, 558-571.

P 9.1
High-resolution temporo-ensemble PIV to resolve pore-scale flow in 3D-printed fractured porous media

Mehrdad Ahkami [1], Thomas Roesgen [2], Martin O. Saar [1], Xiang-Zhao Kong [1]

[1] Geothermal Energy and Geofluids Group, Institute for geophysics, ETH-Zurich, Sonneggstrasse 5, CH-8092, Zurich, Switzerland (xkong@ethz.ch)
[2] Institute of Fluid Dynamics, ETH Zurich, Sonneggstrasse 3, CH-8092, Zurich, Switzerland

Fractures are conduits that allow fast transfer of mass and energy, which are critical to pore-scale physico-chemical processes and their effect on macroscopic flow and transport characteristics. In the present work, we perform fluid flooding experiments using a well-characterized fractured porous medium, manufactured by 3D printing to evaluate the micro-structures of the 2D fluid flow with velocities in the order of sub-millimeter per second. We demonstrate the capability of a temporo-ensemble Particle Image Velocimetry (PIV) method in maximizing the spatial resolution (ultimately at the single-pixel resolution) for such fluid flows using an in-line illumination setup. This method is advantageous in terms of minimizing the pixel counts required for velocity determination, thus resolving high spatial resolution of velocity vectors while capturing a large field of view. Our results indicate log-normal and Gaussian-type distributions of longitudinal and lateral velocities, respectively. It is shown that the velocity in fractures, and the flow interaction between fractures and matrices are controlled by the permeability of background matrix and the orientations of fractures. This study provides a novel experimental and velocimetry framework to extend the physical understanding of flow properties in fractured porous media.

P 9.2
Simulations of fluid flow and chemical reactions in the deep orogenic hydrothermal system at Grimsel Pass, Switzerland

Peter Alt-Epping, Larryn W. Diamond & Christoph Wanner

Institute of Geological Sciences, University of Bern, Baltzerstrasse 3, CH-3012 Bern (alt-epping@geo.unibe.ch)

Thermal waters at temperatures ranging between 17 – 28 °C discharge at a rate of ≤ 10 L/min into a tunnel underneath Grimsel Pass (2164 m) in the Central Alps. Fluid discharge is associated with a fault zone (Grimsel Breccia Fault (GBF)) which is intersected by the tunnel and exposed along a roughly 100 m long tunnel section. The chemical composition of the water sampled in the tunnel suggests that the water is a mixture of old geothermal water and younger cold water. Both components have a meteoric origin. Residence times of the old and young waters have been estimated to be at least 30 ky and about 7 years, respectively (Waber et al., 2017)

The breccia of the GBF formed about 3 Ma years ago. It shows hydrothermal alteration at temperatures of about 165 °C based on oxygen isotope and fluid inclusion data (Hofmann et al., 2004). However, results from Na-K geothermometry on fluid samples suggest that the maximum temperature at depth could be as high as 250 °C. Given the local geothermal gradient this corresponds to a circulation depth of about 10 km.

Hydrothermal circulation is confined to the GBF which constitutes a zone of higher permeability within an otherwise low permeability crystalline rock. The GBF strikes approximately WSW-ENE (Belgrano et al., 2016) and it is thought that recharge of meteoric water into the hydrothermal system occurs in the glaciated mountains WSW of Grimsel pass. These mountains exceed altitudes of 3000 m. It is the difference in elevation head of up to 1000 m between these mountains and Grimsel Pass that is the driving force for hydrothermal circulation within the GBF.

The recharge zone at high altitude, the root or reaction zone at depth and the deeper part of the upflow zone are not accessible to direct observation. Hence we use the massively parallel reactive transport PFLOTRAN to construct a regional scale model of the circulation system in its entirety, constrained by thermal, hydraulic and chemical observations at the discharge site in the tunnel. This model is used to simulate flow and the thermal and chemical evolution of the fluid upon its loop through the system. Although the rock is assumed to be chemically homogeneous, heating and cooling during descent and ascent of the fluid, respectively, lead to local chemical disequilibrium, fluid rock- interaction and mineral dissolution and precipitation reactions. Mineral reactions affect the porosity and permeability of the rock, potentially altering flowpaths and flow velocities. These feedbacks between chemistry and hydraulic conditions are explicitly considered in simulations.

Given the strongly varying topography around Grimpsel Pass and its importance for driving subsurface fluid flow, we use the unstructured grid capability of PFLOTRAN to incorporate the regional topography as upper boundary into the model. The 3D numerical mesh used in this simulation is constructed by meshing a GIS-based surface grid of the local topography and extending the mesh into the third (depth) dimension (Figure 1).
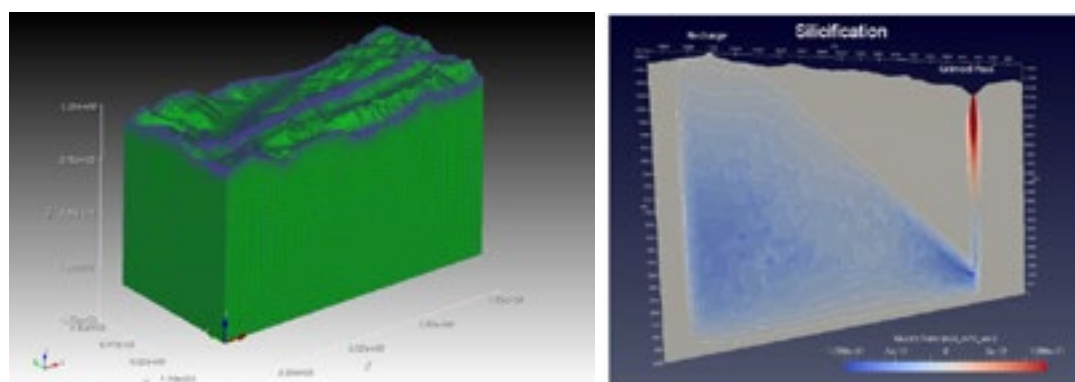

Figure 1. Left panel: 3D model domain and PFLOTRAN mesh with regional topography as upper boundary. Right panel: Quartz dissolution and precipitation rates in the GBF fault plane, showing quartz dissolution in recharge and reaction zones and quartz precipitation in the upper discharge zone.

Simulation results suggest that the flow pattern through the system is primarily controlled by the permeability and its distribution in the rock. For instance, assuming a uniform high permeability distribution throughout the GBF results in convective circulation within the fault plane inhibiting fluid recharge to a depth of 10 km. A high permeability of the rock increases discharge into topographic lows such that there is insufficient water to establish sustained hydrothermal circulation in the fault plane. Only if fluid flow within the GBF plane is focused along (one or several) higher permeability pathways can fluid circulation to a depth of 10 km be sustained. The model predicts the precipitation of quartz in the upflow zone which is consistent with the silicification observed in the GBF at Grimsel Pass (Figure 1).

REFERENCES

Belgrano, T.M., Herwegh, M. & Berger A., 2016: Inherited structural controls on fault geometry, architecture and hydrothermal activity: an example from Grimsel Pass, Switzerland, Swiss J. Geosci., 109, 345-364

Hofmann, B.A., Helfer, M., Diamond, L.W., Villa, I., Frei, R., & Eikenberg, J., 2004: Topography-driven hydrothermal breccia mineralization of Pliocene age a Grimsel Pass, Aar Massif, central Swiss Alps: Schweizerische Mineralogische und Petrographische Mitteilungen, v. 84, No 3, p. 271-302

Waber, H.N., Schneeberger, R., Mäder, U.K., Wanner, C., 2017, Constraints on evolution and residence time of geothermal water in granitic rocks at Grimsel (Switzerland), 15th Water-Rock Interaction Symposium, WRI-15, Procedia Earth and Planetary Science 17, 774-777

P 9.3
Detecting microseismicity in the Geneva Basin and surrounding areas using coherence of signals at different stations

Verónica Antunes [1], Thomas Planès [1], Aurore Carrier [1], François Martin [2], Michel Meyer [2] and Matteo Lupi [1]

[1] Department of Earth Sciences, University of Geneva, Geneva, Switzerland
[2] Services Industriels de Genève - SIG, Geneva, Switzerland

The Canton of Geneva and the Industrial Services of Geneva (SIG) are investigating the potential for geothermal exploitation of the Geneva Basin. Before starting geothermal exploitation it is important to know the location of the local seismicity its rate and its relationship with local tectonic structures. Available data indicate sparse and disperse seismic activity, which can be a consequence of the low number of seismic stations in the area. In order to better estimate the local seismicity, we deployed a dense temporary network composed of 20 broadband stations.

This study introduces the catalogue obtained during the 17 months of the experiment. With the dense temporary network and using an efficient detection method we found new events not listed in the public catalogues. The events epicenters are consistent with local fault structures. The magnitude of completeness of our network was Mc 1.3 using the goodness-of-fit test method. However, this value may be overestimated due the low seismic rate in the area.

We used LASSIE, a new open-source software, capable to efficiently and automatically detect weak seismic events, even in the presence of high background noise (Heimann et al., *in prep*). The detection is done using a grid search to get the maximum value of the coherence of signals at different stations considering the local 1D velocity model. We compare LASSIE performance with standard STA/LTA method and for the month of June 2017 we obtained 124 detections with LASSIE of which 25 local earthquakes, 79 other types of seismic events and 20 false detections. With STA/LTA method we had 2097 detections of which 1993 were false detections.

.

P 9.4

Creation of secondary porosity in dolostones by upwelling basement water in the foreland of the Alpine Orogen

Lukas Aschwanden [1], Larryn W. Diamond [1], Martin Mazurek [1], Donald Davis [2]

[1] Institute of Geological Sciences, University of Bern, Baltzerstrasse 1+3, CH-3012 Bern (lukas.aschwanden@geo.unibe.ch)
[2] Department of Earth Sciences, University of Toronto, 22 Russell Street, M5S 3B1 Toronto, Canada

Creation of secondary dissolution porosity in carbonate rocks during deep burial has the potential to improve reservoir properties for hydrocarbons, gas storage and geothermal applications. However, the occurrence and mechanisms of such porosity enhancement are controversial (Ehrenberg et al., 2012). Here we present compelling evidence for generation of deep burial porosity from the Swiss Molasse Basin, where dissolution of eogenetic anhydrite nodules in dolostones of the Middle Triassic Muschelkalk increased matrix porosity by up to 15 vol.%.

We reconstruct the genesis and evolution of the anhydrite-dissolution porosity based on petrography, porosity determinations, analyses of stable and radiogenic isotopes (δ^2H, δ^{18}O, δ^{13}C, δ^{34}S, ^{87}Sr/^{86}Sr), fluid inclusion studies and laser U–Pb geochronology of secondary calcite.

The results show that modified meteoric waters derived from the Variscan crystalline basement ascended via basement–cover cross-formational faults into the overlying Muschelkalk, where they dissolved the anhydrite nodules throughout an area of at least 55 km^2 at 700–2300 m depth and 40–160 °C. Secondary calcite in anhydrite moulds yields Late Eocene to Middle Miocene U–Pb ages, which coincide with the timing of basement uplift in the foreland bulge of the Swiss Alpine Orogen. This uplift provided the hydraulic gradients to drive meteoric water deep into the adjacent Molasse basin. Similar enhancement of reservoir properties can be expected in dolostones in other foreland basins that are bordered by a foreland bulge in which fractured basement rocks are exhumed.

REFERENCES

Ehrenberg, S.N., Walderhaug, O. & Bjorlykke, K. 2012: Carbonate porosity creation by mesogenetic dissolution: Reality or illusion? AAPG Bulletin, 96, 217–233.

P 9.5

Brand new deep electrical resistivity tomography (ERT) methodology for middle-enthalpy geothermal exploration in the Geneva Basin, Switzerland.

Aurore Carrier [1], Matteo Lupi [1], Federico Fishanger [2], Marine Collignon [1]

[1] Départment des Sciences de la Terre et de Géophysique, University of Geneva, Rue des Maraîchers 13, CH-1205 Genève, Switzerland (aurore.carrier@unige.ch)
[2] Geostudy Astier, via A. Nicolodi, 48, 57121 Livorno, Italy

Sustainable energy development is becoming key in environmental politics. In this framework, the Canton of Geneva is developing the use of hydrothermal energy in the Geneva Basin. The region shares similar geological and petrophysical features with the Paris basin where geothermal energy is used to provide heat since the 70's. Previous geological, petrophysical and geophysical studies have since confirmed the geothermal potential of the Geneva Basin. Geoelectrical methods are the most commonly used methods for water resources prospection. However, the depth of investigation of such methods is limited and remains a key issue.

Here, we elaborate a new methodology based on the use of new Electrical Resistivity Tomography material developed by IRIS Instruments and non-conventional acquisition geometries to investigate regions previously identify as suitable for low to middle enthalpy geothermal exploration. This cableless innovative material avoids the use of km-long and heavy cables and enables great freedom of acquisition and noise removal thanks to continuous signal recording.

Four 4 km long ERT profiles have been realized in the Geneva Basin reaching exploration depths ranging from 800 m to 1000 m. Strong resistivity contrasts are observed between the tertiary molasse sediments and cretaceous limestones. Vertical variations consistent with faults positions inferred on active seismics are also observed. Hence, new information about water content until 800 m depth can be added to active seismic data and will enable to refine static and dynamic fluid flow models for geothermal exploration.

P 9.6
Geophysical characterization of a fracture network surrounding a hydrothermally active shear zone: a case study from the Grimsel pass

Eva Caspari [1], Andrew Greenwood [1], Ludovic Baron [1], Daniel Egli [2], Enea Toschini [1] and Klaus Holliger [1]

[1] *Institute of Earth Sciences, University of Lausanne, UNIL-Mouline, CH-1015 Lausanne (Eva.Caspari@unil.ch)*
[2] *Institute of Geological Sciences, University of Bern, Baltzerstrasse 1+3 CH-3012 Bern*

Hydrothermally active shear zones in crystalline rocks are of interest because of their potential similarities with petrothermal reservoirs and potentially exploitable natural hydrothermal systems. The shear zone investigated in this study is the Grimsel Breccia Fault (GBF), a major WSW-ENE striking sub-vertical ductile shear zone in the Southwestern Aar Granite. The GBF is exhumed from 3-4 km depth, brittlely overprinted and exhibits both fossil and active hydrothermal activity (Belgrano et al., 2016). A shallow borehole was drilled in 2015, which acutely intersects the main breccia fault core and is entirely situated in its surrounding damage zone. Geochemically the rock mass is homogeneous thus the main features are variations of the fabric due to ductile deformation and different degrees of brittle deformation.

A comprehensive suite of geophysical borehole logs, comprising nuclear, sonic and resistivity logs, as well as optical televiewer (OTV) and borehole radar (BHR) data, was collected in 2015, 2016 and 2017. The focus of this study is a detailed characterization of the fracture network in the damage zone of the main fault core from geophysical borehole data. We employ the BHR reflection data to image the damage zone of the GBF and a selection of the borehole logs, to analyse the fine-scale petrophysical variations in response to brittle deformation. To shed light on the characteristics of the hydraulic system, we examine self-potential and fluid resistivity data. To verify the observations and findings from the geophysical data sets we utilize the detailed structural characterization of Egli et al. (2018).

The migrated BHR image reveals a network of intersecting fluid-filled fractures and cataclastic zones in the damage zone surrounding the main fault core (Figure 1a). A comparison of picked reflector dips with fractures dips from the OTV is shown in Figure 1b. Reflectors with dips above 55° from the horizontal with respect to the borehole are well captured in the image and in good agreement with the OTV data. Reflectors can be tracked a few meters into the formation in zones with low signal attenuation, which are indicated by the BHR first-cycle amplitude. A comparison of the well log data to the deforamtion data from the OTV and a simple cluster analysis confirm that the response of the well logs and thus the variations in petrophysical properties are as expected predominantly driven by the brittle deformation. As a result, the petrophysical properties can be categorized by four groups with varying intensity of brittle deformation.The imaged fracture network and high porosity zones associated with brittle deformation are the main flow pathways of the system in its present state. The self-potential data recorded in 2016 and 2017 is remarkable repeatable and contains an abundance of anomalies with varying magnitude. These anomalies can be linked to fractures and are most likely of electrokinetic origin. As such, they are indicative of in- and out flow zones into the borehole. Furthermore, a distinctive layering is observed in the fluid resistivity. These observations may suggest a conduit like hydraulic behavior dominated by the steeply dipping geology and possibly the inflow of water from different sources.
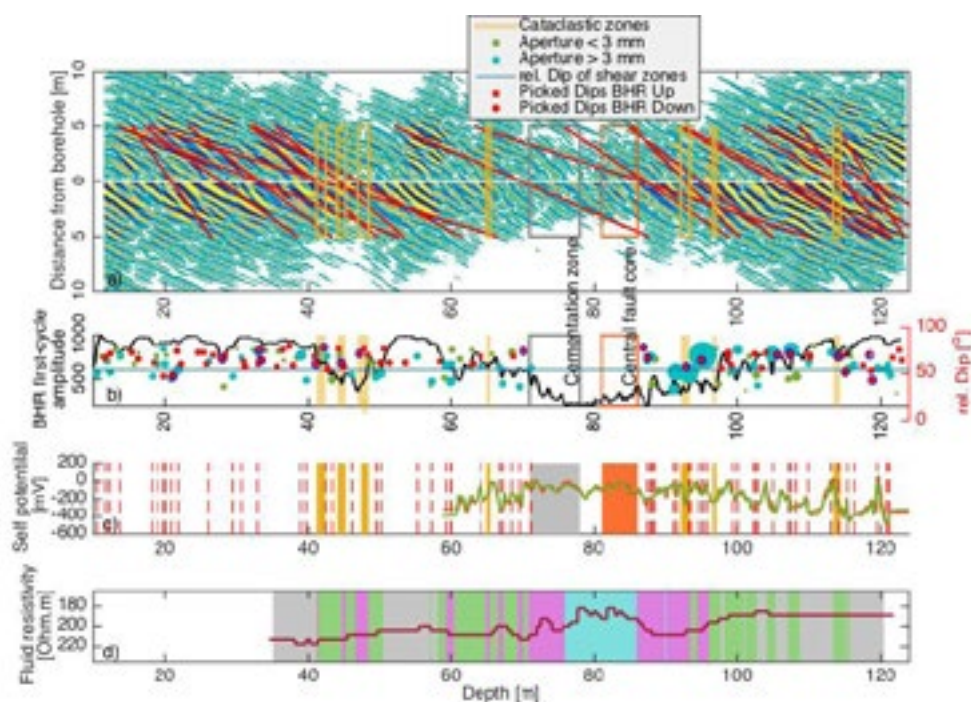
Figure 1. a) Migrated image of the up- and down going reflection data plotted in positive distance from borehole trajectory. Overlain are selected fracture dips picked from the image (red lines). b) BHR first-cycle amplitude, relative dip of fractures from OTV data and picked from the BHR migrated. c) Brittle deformation data from the OTV overlain by corrected self potential data from 2016 and 2017. d) Petrophysicsal groups identified by cluster analysis overlain with fluid resistivity of 2016.

REFERENCES

Belgrano, T. M., M. Herwegh, and Berger, A. 2016: Inherited structural controls on fault geometry, architecture and hydrothermal activity: an example from Grimsel Pass, Switzerland. Swiss Journal of Geosciences, 109(3).

Egli, D., Baumann, R., Küng, S., Berger, A., Baron, L. and Herwegh, M. 2018: Structural characteristics, bulk porosity and evolution of an exhumed long-lived hydrothermal reservoir. Tectonophysics in submission

P 9.7

Investigation of heat storage strategy in the Geneva basin: a numerical study

Marine Collignon [1], Øystein Klemetsdal [2], Olav Møyner [2], Marion Alcanié [1], Aurore Carrier [1] Halvor Nilsen [2], Antonio Rinaldi [3], Matteo Lupi [1].

[1] Department of Earth Sciences, University of Geneva, Rue des Maraichers 13, CH-1205 Geneva (marine.collignon@unige.ch).
[2] Department of Applied Mathematics, SINTEF, Forskningsveien 1, NO-0373 Oslo.
[3] Swiss Seismological Service, ETH Zürich, Sonneggstrasse 5, CH-8092 Zürich

The rapid and worldwide economic development and increasing population of the last fifty years have triggered a constantly rising demand for energy. However, the limited amount of natural resources, as well as the global warming and pollution caused by industrial gas emissions and wastes urge to the development and production of renewable and sustainable energy. In addition to production, energy conservation and storage became equally crucial to make use of excess energy and waste in future times of high energy demand. Seasonal temperature variations induce an imbalance between the energy supply and demand that could be restored by thermal energy storage in aquifers. The principle of an aquifer thermal energy storage system consists in storing, during warm seasons, the excess thermal energy in water by injecting it into an aquifer and extracting it again during cold seasons, when the energy demand is high.

The last two decades, many geological and geophysical studies were conducted in the Geneva Basin to investigate its geothermal potential for energy production. A large data set is now available, including exploration wells, active seismic, gravity and geoelectrical data. The low permeability of the geological units and the low temperature gradient are not promising for electricity production and the shallower horizons (within the first 2 km) are now investigated for seasonal heat storage or direct heat production for modern buildings whose heating systems do not require high temperature (>80 C).

In this study, we use the current and available data set to investigate the possible heat storage strategy in the Geneva basin. For this purpose, we use the Matlab toolbox MRST (Matlab Reservoir Simulation Toolbox) in which we have implemented a geothermal module. This work presents the newly implemented module, synthetic heat storage simulations and finally applied simulations to the Geneva Basin. The geological model has been mostly developed based on gravity and geoelectrical data while the dynamic flow model is constrained by the data from the well, recently drilled in Satigny. Several structural case scenarios and aquifer conditions are tested to investigate the feasibility of heat storage in the Geneva Basin. These simulations will be further constrained by the data of ongoing drilling prospections in the basin.

P 9.8
Fracture geometry and fracture growth of an in-situ hydraulic fracturing (HF) experiment

Dutler Nathan [1°], Valley Benoît [1], Gischig Valentin [2], Villiger Linus [3], Krietsch Hannes [4], Doetsch Joseph [4],
Jalali Mohammadreza [5], Amann Florian [5]

[1] *Centre for Hydrogeology and Geothermics, University of Neuchâtel*
[2] *CSD Engineers, Bern*
[3] *Swiss Seismological Service, ETH Zurich*
[4] *Dep. of Earth Sciences, ETH Zurich*
[5] *Dep. of Engineering Geology and Environmental Management, RWTH Aachen*
° *nathan.dutler@unine.ch*

Six hydraulic fracturing experiments were conducted at the Grimsel Test Site (GTS), Switzerland. The aim was to study the geometry of induced hydraulic fractures (HFs), their interactions with the pre-existing fracture network, and the hydro-mechanical coupled response during hydraulic fracturing. All six tests were performed by targeted injection using a double packer and followed a similar injection protocol to study the response of the rock mass at different injection locations and the influence of injection fluid characteristics (Dutler et al., 2018). For the later, water or a xanthan-salt-water (XSW) mixture were injected. The viscosity of the XSW mixture was 35 times higher than water. Except for HF6, all HFs were initiated in borehole section without pre-existing discontinuities (Jalali et al., 2018).

Several monitoring systems were installed to study transient pressure propagation, deformation within the rock mass and along shear zones, and seismic activities during the injection tests. The geometry of hydraulic fractures was determined by located microseismic events as well as by the deformation and the pressure response at points distributed within the rock mass (more in Amann et al. (2018)). The deformation was measured using two different systems: 1) chains of fiber Bragg grating (FBG) sensors and 2) distributed strain sensing (DSS) optical fibers.

Figure 1 and 2 show selected monitoring results used to evaluate the geometry of the hydraulic fracture during HF2 test. The FBG sensor at 5.4 m in FBS1 (Fig. 1, dark blue) followed a few second later by the sensor at 6.1 m (Fig. 1, black) show abrupt extensions during the propagation cycle of the test HF2. We interpret this as a direct observation of fracture opening due to fluid flow and thus permit to track the propagation of the hydraulic fracture. The study of the microseismicity record and the DSS data suggest that the HF bifurcate and that the flow path toward the FBG sensors is not unique. One need to note also that during this test a flow path developed toward the lower part of the injection well, below the double packer were pressure was also measured (referred as INJBE on Fig. 1 and 2). Pressure started increasing in this interval after the first propagation cycle (C21) and exceeded 3 MPa at this end of the main injection. This allowed developing other links as for example with the FBG deformation sensor at 7.8 m whose response seems to be strongly dictated by the pressure record in the INJBE interval. A small pressure response is also visible in the interval PRP11, suggesting a transient pressure change in the vicinity without any direct flow path to PRP11. Independent information suggest that the PRP11 interval is connected indirectly to our system via the shear zone S11 (not shown in Fig. 2, S11 shear zone is a major structure crossing our experimental volume).

The position of the microseismic events show a strongly asymmetric fracture propagation about the injection point with a propagation direction which is essentially only downward. The events aligns on a plane that agrees well with the assumed stress field from the stress characterization phase. The plane is oriented 190/75°, with a minimum principal stress axis oriented sub-horizontal North.

This contribution gives an overview of the fracture growth from the microseismic events and deformation observations during hydraulic injection during various experiments and injection cycles. It allow to track in-situ hydraulic fracture propagation with a resolution never achieved before. It highlights clearly the complexity of the fracture propagation processes that in the details involves a network of fractures while at large the overall orientation of the propagation plan is consistent with the stress field.
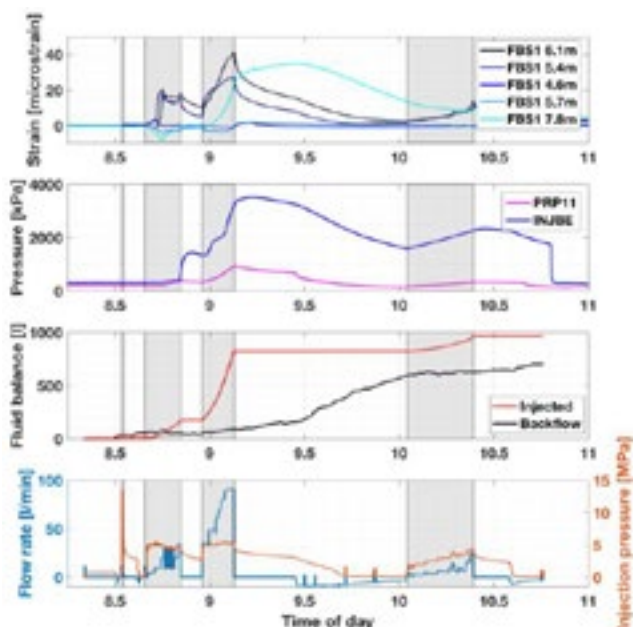
Figure 1: Selected data for the experiment HF2, with FBG sensor data on top, pressure interval observation, fluid balance and injection protocol incl. injection pressure response.
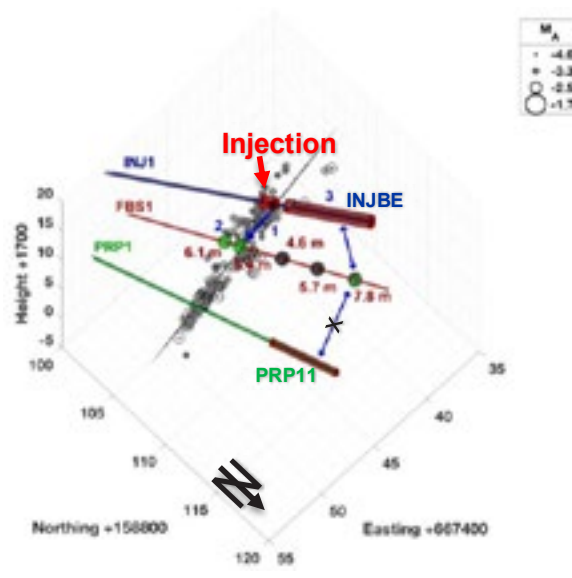

Figure 2: Fracture geometry of experiment HF2.

REFERENCES

Amann, F., Gischig, V., Evans, K., Doetsch, J., Jalali, M. R., Valley, B., … Giardini, D. (2018). The seismo-hydro-mechanical behaviour during deep geothermal reservoir stimulations : open questions tackled in a decameter- scale in-situ stimulation experiment. Solid Earth, 9(August), 115–137. https://doi.org/https://doi.org/10.5194/se-9-115-2018

Dutler, N. O., Valley, B., Gischig, V. S., Jalali, M., Doetsch, J., Krietsch, H., … Amann, F. (2018). Observations of fracture propagation during decameter-scale hydraulic fracturing experiments (pp. ARMA2018-0256). Seattle: American Rock Mechanics Association.

Jalali, M., Klepikova, M., Doetsch, J., Krietsch, H., Brixel, B., Dutler, N. O., … Amann, F. (2018). A Multi-Scale Approach to Identify and Characterize the Preferential Flow Paths of a Fractured Crystalline Rock. In 2nd International DFNE Conference (p. 0734). Seattle.

P 9.9

A new mine-by experiment at the Mont Terri rock laboratory to assess hydromechanical behavior of the sandy facies of Opalinus Clay

David Jaeggi [1], Jürgen Hesser [2], Christophe Nussbaum [1] & Paul Bossart [1]

[1] Bundesamt für Landestopografie, Swisstopo, Seftigenstrasse 264, 3084 Wabern (david.jaeggi@swisstopo.ch)
[2] Bundesanstalt für Geowissenschaften und Rohstoffe, BGR, Stilleweg 2, 30655 Hannover

Since initial excavation of the security gallery of the Mont Terri highway tunnel in 1989, every 10 years or so the Mont Terri Project Partners have excavated new, and extended existing, galleries and niches in the Opalinus Clay. Currently, 700 m of galleries and niches are actively being used for experiments. Besides rock mechanical experiments, the Project Partners have conducted six mine-by experiments with different tunnel orientations, five in the shaly facies and one in the sandy facies. In 2018/19, another 500 m of galleries and niches will be excavated south of the existing rock laboratory, mainly in the stiffer and highly variable sandy facies (Jaeggi & Bossart, 2014). In April 2019, we will carry out a new mine-by test, the MB-A experiment (hydromechanical characterization of the sandy facies before and during excavation), along a 30 m tunnel section oriented parallel to bedding strike. We will explore both the sandy and the carbonate-rich sandy facies that are sandwiched between the shaly facies (Figure 1).
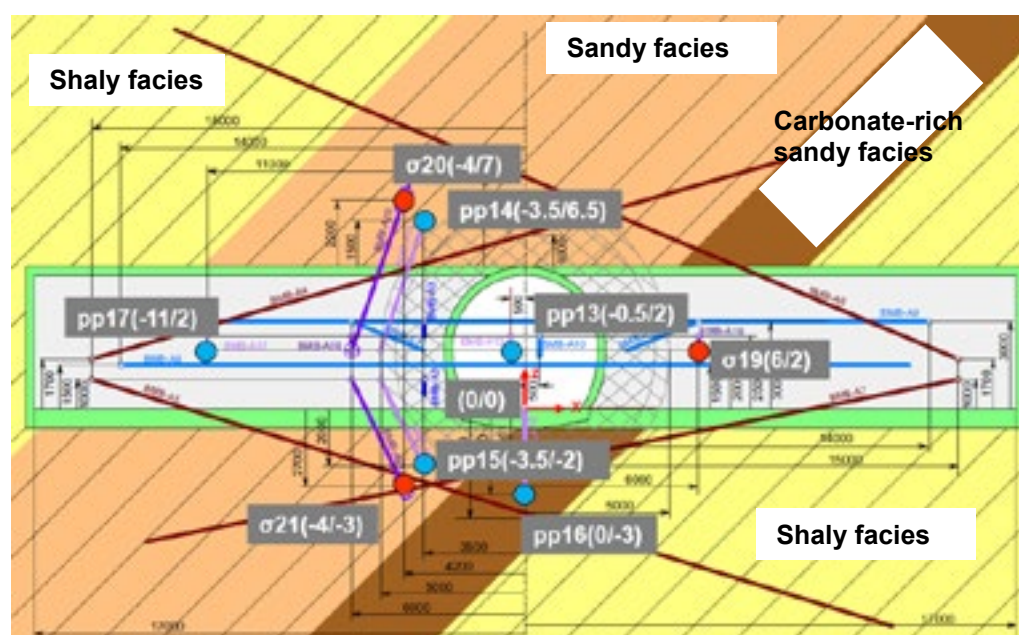

Figure 1. Vertical section through the MB-A experiment. View from the two instrumentation niches 7 and 8 on the left and right-hand side respectively. Positions of sensors for measuring porewater pressure (pp) and stress (σ) are given with x and z local coordinates.

In our talk, we present the concept and layout of this 1:1-scale experiment, the instrumentation scheme, and some selected data from predictive modeling (Parisio, 2016, Jaeggi & Madaschi, 2017, Li, 2018). Knowledge of the hydromechanical (HM) response of the Opalinus Clay is important for tunnel excavation and lining in deep underground infrastructures as well as for caprock characterization before initiation of any CO_2 injection. We carried out the predictive simulations for the heterogeneous, anisotropic, and elastic/plastic case to estimate the HM behavior of the rock mass during excavation. The results of our model predict overpressures along bedding immediately at the initiation of excavation and a pressure decrease vertical to bedding that results in a long-term pressure decrease parallel to bedding. Modeled pressures at instrumented boreholes increase from 2.0 to 2.8 MPa just before excavation and drop to 1.2 MPa after excavation. Deformation within the rock mass at distances >3 m from the tunnel are in the mm-range, which seems to be reasonable for sandy facies.

REFERENCES

Jaeggi, D. & Bossart, P. 2014: Kompilation der lithologischen Variabilität und Eigenschaften des Opalinus-Ton im Felslabor Mont Terri, Expertenbericht swisstopo, Landesgeologie z. Hd. ENSI, Landesgeologie 2014, Bericht 09-08.

Jaeggi, D. & Madaschi, A. (2017): MB-A (Mine-by test in sandy facies) Experiment: Predictive modeling using Code_Aster – model setup and results, Mont Terri Project Technical Note, TN2017-85.

Li, C. (2018): Numerical modelling of tunnel excavation for the MBA experiment, Mont Terri Project Technical Note, TN2018-70.

Parisio, F. (2016): Constitutive and numerical modeling of anisotropic quasi-brittle shales, Thesis EPFL, No 7053.

P 9.10
Dynamics of phase exsolution in porous media

Xiang-Zhao Kong [1,°], Andrea Parmigiani [2], Paolo Di Palma [3], Sébastien Leclaire [4], Martin O. Saar [1]

[1] *Geothermal Energy and Geofluids Group, Institute of Geophysics, ETH-Zurich, Sonneggstrasse 5, 8092 Zurich, Switzerland*
[2] *FlowKit Sàrl, Route d'Oron 2, 1010 Lausanne, Switzerland*
[3] *IRSA-CNR Water Research Institute, Via Salaria km 29.300, Rome, Italy*
[4] *Department of Chemical Engineering, Polytechnique Montréal, Quebec, Canada*
  (°Corresponding author's email: xkong@ethz.ch)

Changes in thermodynamic conditions can drive reservoir fluids becoming over-saturated with their dissolved substance. This eventually can lead to volatile exsolution and/or phase separation with the emergence and growth of a second phase. Examples of these processes include gas formation in sediments, CO_2 exsolution in nature or during geologic CO_2 sequestration in reservoirs, and gas bubble formation in magmas. This conversion from a single-phase to a multiphase fluid system is known to alter the physical properties of reservoir fluids (e.g. their buoyancy, viscosity, and capillarity). In this work, we are interested in investigating, via multiphase numerical modeling, using a lattice-Boltzmann method, the system response to phase exsolution/separation from a solution, where fluid flow is driven by hydraulic gradients and where buoyancy stresses, potentially arising from the emergence of a dispersed phase, can be neglected (i.e. low Bond number). We focus our discussions on two main aspects: 1) the characterization of the evolution of the exsolved non-wetting phase (including size, shape, and mobility of the emergent droplets), and 2) phase separation effects on fluid discharge (i.e. the hydraulic response to the evolving capillary stresses on the emergence of two-phase fluid flow). We explore a wide parameter space of capillary numbers and fluid saturations to characterize droplet evolution, size and shape distribution, and system capillary-clogging patterns. Our results provide insights into the understanding of the phase separation dynamics during the aforementioned processes.
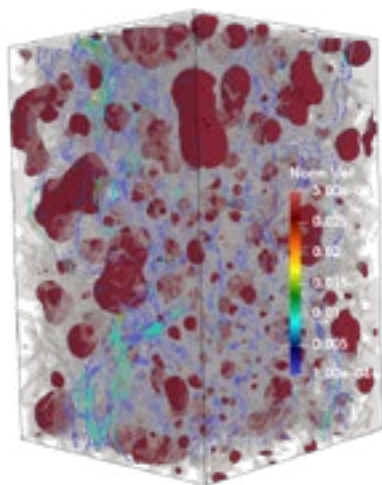

Figure 1. Magnitude of the norm of seepage velocity (solids are rendered transparently in gray) and non-wetting droplets (in red).

P 9.11

Thermal modelling to prevent risks in geothermal exploration: the Geneva Basin case study (Western Switzerland)

Omodeo-Salé, S.[1°], Do Couto, D.[2], Corrado, S.[3], Carraro, D.[1], Ziegler, L.[4] and Moscariello, A.[1]

[1] Department of Earth Sciences, University of Geneva, Geneva (Switzerland);
[2] Institut des sciences de la Terre de Paris (ISTeP) Sorbonne University, Paris (France)
[3] Dipartimento di Scienze della Terra, Università degli Studi di Roma3, Roma (Italy)
[4] Institute of Petroleum and Coal, RWTH, Aachen University (Germany)
°silvia.omodeosale@unige.ch

The geothermal potential of the Geneva Basin (Switzerland) is today under investigation through a variety of exploration activities. In the sedimentary basins geothermal resources are invariably linked to and possibly also coupled to hydrocarbon resources. Both resources can share the same reservoirs and their occurrence is strictly related to the thermal and tectonic histories of the basin.

Currently, the geothermal energy prospection, exploration finding activities is confined to local studies of limited geographical extent – a few 10s km^2 surrounding the area of potential geothermal well to be drilled. However, the presence of oil and gas in the basin can constitute a serious risk for geothermal exploration. During the drilling activity, relevant seismic stimulations can be produced, as a consequence overpressure of gas or oil stored in the rock (e.g., St. Gallen accident, in 2013). Therefore, a regional scale hydrocarbon prospection, of the area where geothermal activity want to be carried out, is mandatory to prevent risks.

The potential for oil and gas generation and accumulation in a sedimentary basin is strictly related to the temperature attained by the basin infill over the time and to the presence of deposits rich in organic matter. The temperatures recorded in the basin deposits are direct consequence of the tectono-sedimentary evolution of the basin. The extension rate of the crust controls the heat flow in the basin area, as a consequence of the asthenosphere upraise, and the sedimentation rate determines the burial depth. Therefore, in order to estimate the amount of hydrocarbons stocked in the subsoil, the integrity of the geological evolution of the basin need to be taken into account.

In this work, by computing 1D modelling, we quantitatively simulate the thermal history of the Geneva Basin. 1D modelling reconstructs temperature variation over the time in a vertical point of the basin, herein chosen at the Humilly-2 well location, the reference stratigraphic section of the basin. In the model, the petrophysical features of the units constituting the considered stratigraphic sequence were integrated, together with the geochemical properties of the potential hydrocarbons source rocks. To validate the modelling results, paleothermal proxies, such as vitrinite reflectance, fluid inclusions and illite crystallinity, were used.

The results performed by this work permit to estimate the thermal maturation state of the potential source rocks of the area and to assess first hypothesis on the hydrocarbons generation, migration timing. Integrating in the future these data in a more complex 3D model, our knowledge on the location of potential oil and gas reservoirs in the region could be considerably improved.

P 9.12

Compilation of data relevant for geothermal exploration – a first step towards a Geothermal Play Fairway Analysis of the Rhône Valley, Switzerland

Daniela B. van den Heuvel, Samuel Mock, Daniel Egli, Larryn W. Diamond, Marco Herwegh

Institute of Geological Sciences, University of Bern, Baltzerstrasse 1+3, CH-3012 Bern (daniela.vandenheuvel@geo.unibe.ch)

In 2013 the Swiss government decided on a step-by-step replacement of nuclear power by renewable energy sources to generate electricity as part of the Energy Strategy 2050. In this context, interest into deep geothermal energy as a potential source of electricity has increased again. The most active geothermal domain in Switzerland is the Rhône Valley. The steep topography and many fault and fracture zones allow water precipitated onto the mountain slopes to percolate to great depths where it is heated by the background geothermal gradient and then driven to the surface where it emerges as hot springs along the traces of major faults within the valley. Several such thermal occurrences are known and some are exploited for spa purposes and district heating such as the 110 °C, 28 L/s system at Lavey-les-Bains. It can be assumed that such fluid-conducting fault zones are much more common and more extensive than the surface observations suggest. Unfortunately, the thick cover of Quaternary sediments deposited within the Rhône Valley obscures these thermal water occurrences, leading most likely to underestimation of the geothermal potential within the region.

In order support future potential studies and guide geothermal exploration, we are conducting a so-called Play Fairway Analysis (PFA) in the Rhône Valley. This approach, adopted from the hydrocarbon exploration industry, spatially correlates data on various properties known to be directly associated with geothermal systems. The two most important data categories are "heat source", i.e. data indicating the presence of hot fluids, and "permeability", i.e. the availability of flow paths for the hot fluids to move. In order to evaluate these categories, we are currently compiling all data available within the Rhône Valley including geological and geophysical surveys, geologic structures, temperature measurements and estimates as well as hydrogeological/-chemical data. The compilation will eventually be made available as a GIS map and an accompanying report and represents the first step of a PFA for the entire Rhône Valley. For a full PFA, the data compiled needs to be extrapolated and turned into regional potential maps for "heat source" and "permeability". By combining these regional maps, an overall "favourability map" can be obtained which will show the areas within the Rhône Valley where future exploration is most likely to be successful.

P 9.13

Investigating mineral reactions during high-temperature aquifer thermal energy storage (HT-ATES) in the Swiss Molasse Basin

Daniela B. van den Heuvel, Christoph Wanner, Urs Mäder, Larryn W. Diamond

Institute of Geological Sciences, University of Bern, Baltzerstrasse 1+3, CH-3012 Bern
(daniela.vandenheuvel@geo.unibe.ch)

As part of the Swiss Energy Strategy 2050, Switzerland aims to substantially reduce its energy consumption over the next few decades. Besides developing new, renewable sources of energy, a more efficient use of the energy currently produced will be crucial in reaching this goal. One option is the increased use of surplus heat from industry (e.g. municipal waste incinerators) for district heating. While heat generation from these industrial sources is more or less constant, the heating demand is characterised by a strong seasonality. In order to overcome this problem of demand and supply, excess thermal energy can be stored in the subsurface during summer and recovered and fed into the district heating network during winter. This so-called aquifer thermal energy storage (ATES) is already in use across Europe but not yet in Switzerland. In order to increase the potential of ATES, the temperature of the injected water should be increased to over 25 °C. A new international project (GEOTHERMICA HEATSTORE) aims at lowering costs, reducing risks, and optimizing the performance of such "high-temperature" aquifer thermal energy storage (HT-ATES) systems. In Switzerland, two pilot projects are currently being developed as part of the EU- and BFE-funded GEOTHERMICA HEATSTORE project: (1) a 200 – 500 m deep ATES system (max. 120 °C) in the OSM sandstones connected to the waste-to-energy and wood fired plants in the outskirts of Bern and (2) a deep ATES system (> 50 ˚C) in Cretaceous porous limestone connected to a waste-to-energy plant close to Geneva.

While more energy can be stored in a HT-ATES, the higher temperatures enhance the interactions between the injected fluid and the reservoir formation. This leads to enhanced mineral dissolution and precipitation reactions during recharging of the reservoir as well as during the storage period. In order to investigate these rock-water interactions, especially reactions in the carbonate system, we are performing laboratory experiments on drill core samples from both pilot sites under the conditions planned. By measuring changes in the fluid composition as a function of time, we can infer the stoichiometry and kinetics of mineral dissolution and precipitation reactions. In addition, we are investigating different conditions (e.g. variations in pH, salinity or p_{CO2}) in order to generate data transferrable to other reservoir formations. Eventually, all our experimental data will be fed into 3D thermochemical models for both sites. These models can be used to inform further development of the two sites as well as help to predict the long-term behaviour of the reservoir formation. In addition, the models can be used as a planning tool to develop more sites inside and outside of Switzerland in the future.

10. Celebrating 50 Years of International Ocean Drilling (1968-2018)

Silvia Spezzaferri, Gretchen Früh-Green, Marc Lever, Judith McKenzie, Helmut Weissert, Andrea Moscariello, Flavio Anselmetti

Swiss Commission of Oceanography and Limnology, SWISS DRILLING

TALKS:

10.1   Bernasconi S.M., Fernandez A., Meja L.M., Stoll H.: Recent advances in carbonate clumped isotope thermometry: towards high resolution paleoclimate reconstructions from marine sediments

10.2   Fentimen R., Früh-Green G.L., Foubert A., Spezzaferri S.: Facies analyses and benthic foraminiferal assemblages from the Atlantis Massif (MAR 30°N)

10.3   Fernandez A., Mejia L.M., Jaroszewicz E., Guitian J., Zhang H., Bernasconi S., Stoll H.: Tropical sea surface temperatures during the Cretaceous Thermal Maximum

10.4   Jaccard S.L., Hayes C.T., Martinez-Garcia A., Hodell D.A., Anderson R.F., Sigman D.M., Haug G.H.: Two Modes of Change in Southern Ocean Productivity Over the Past Million Years

10.5   Kroon D., Leg 208 Scientific Party and Many Others: Windows of climate and carbon cycle variability on orbital time scales from the Late Cretaceous to Quaternary

10.6   Leila M., Moscariello A.: Origin and evolution of the Eonile River unraveled by a deep basin -onshore correlation: the role of the Messinian Salinity Crisis in shaping the modern Egyptian landscape.

10.7   Rüggeberg A., Spezzaferri S., Stainbank S., Coletti G., Kroon D., Lüdmann T., Eberli G., Betzler C.: Paleodepth reconstruction of the Inner Sea based on benthic foraminifera, IODP Exp. 359, Maldives

10.8   Spezzaferri S., Anselmetti F., McKenzie J., Weissert H. and Guests: 50 years of International Ocean Drilling – The early years

10.9   Stainbank S., Rüggeberg A., Spezzaferri S., Kroon D., de Leau E.S., Zhang M., Raddatz J.: Planktonic foraminifera calcification depths in the Indian Ocean: controls and implications

10.10   Stoll H., Guitian J., Hernandez I., Mejia L.M., Tanner T., Zhang H.: New estimations of past atmospheric CO_2 from ancient algae

POSTERS:

P 10.1   Eickenbusch P., Jørgensen B.B., Lever M.A.: Short-chain organic acid concentrations and implications for microbial life in active serpentinite mud volcanoes of the Mariana forearc

P 10.2   Frueh-Green G.L., Orcutt B.N., Rouméjon S., Lilley M.D., Morono Y., IODP Expedition 357 Science Party: In search of life in the subseafloor of serpentinized peridotites: An overview of IODP Expedition 357 (Atlantis Massif, Mid-Atlantic Ridge 30°N)

P 10.3   Guitián J., Phelps S., Polissar P.J., Hernández-Almeida I., Stoll H.M.: Oligocene-Miocene sea surface temperatures from North Atlantic sediments.

P 10.4   Hernández-Almeida I., Diz P., Bernárdez P., Pérez-Arlucea M., Hall I.: Variability in the East Equatorial Pacific paleoproductivity during the Middle and Late Pleistocene

P 10.5   Karpoff A.M., Manatschal G., Pinto V.H., Ulrich M., Sauter D.: Rifted margins revisited: insights from ODP sites off Iberia and field observations in the Alps

P 10.6   Knappertsbusch M., Friesenhagen T.: Morphological evolution of menardiform globorotalids are different in the Atlantic and Pacific oceans

P 10.7   McKenzie J.A., Huebscher C., Aloisi G., Bertoni C., Camerlenghi A., Evans N., Hodell D., Lofi J.: Demise of a salt giant: Dolomite formation at the termination of the Messinian Salinity Crisis in the Ionian Basin of the Central Mediterranean Sea

P 10.8   Mejia L.M., Fernandez A., Guitian J., Zhang H., Bernasconi S., Stoll H.: Unraveling the potential for sea surface temperature reconstructions using coccolith clumped isotopes

P 10.9   Ternieten L., Früh-Green G.L., Bernasconi S.M., Lilley M.D.: Carbon Geochemistry and Mineralogy of Serpentinized Mantle Peridotites at the Atlantis Massif: Results from IODP Expedition 357

P 10.10 Zhang H., Stoll H., Chuanlian Liu: The relationship between inorganic/organic carbon pump and benthic foraminifera carbon isotope in the last 5 Ma: a perspective from tropical ocean

10.1

Recent advances in carbonate clumped isotope thermometry: towards high resolution paleoclimate reconstructions from marine sediments.

Stefano M. Bernasconi [1], Alvaro Fernandez [1], Luz Maria Meja [1] & Heather Stoll [1].

[1] *Geologisches Institut, ETH Zürich, Sonneggstrasse 5, 8092 Zürich (stefano.bernasconi@erdw.ethz.ch)*

Carbonate clumped isotope thermometry, which is based on the measurement of the abundance of ^{13}C-^{18}O bonds in carbonate minerals, is a very promising tool for many applications in geosciences ranging from paleoceanography to the study of diagenesis and tectonics.

The application of this tool in paleoclimatology and paleoceanography, however, has been limited by the large samples sizes required by traditional measurement methods (3-10 mg for a single analysis), the complex analytical methodology, and contrasting published temperature calibrations which add considerable uncertainty in climate reconstructions.

In this contribution we will shortly describe the latest improvements in small sample analysis [Meckler et al. 2015; Müller et al., 2017] and demonstrate that it is now possible to obtain measurements with errors better than ±3°C (at the 95% CI) with only 1.4 mg of carbonate. Moreover we will show that with the introduction of carbonate standard materials differences in calibrations are being resolved. With the combination of these improvements with a novel statistical data analysis we were able to produce the first high-resolution reconstruction of glacial interglacial changes in temperature and oxygen isotope composition of seawater using foraminifera from ODP Site 975 in the western Mediterranean Sea (Rodriguez-Sanz et al., 2017).

The next step is the application of these methods to coccolith calcite as an additional tool to reconstruct absolute seawater temperatures in sediments devoid of sufficient foraminifera or where foraminifera are not well preserved.

The rich archives of ODP and IODP cores and new cores from future IODP cruises can now be studied with this new tool to provide better quantitative information on paleotemperatures and the evolution of seawater oxygen isotope composition through time.

REFERENCES

Meckler A.N., Ziegler M., Millàn M.I., Breitenbach S.F.M. and Bernasconi S.M. (2014) Long-term performance of the Kiel carbonate device with a new correction scheme for clumped isotope measurements. Rapid Communications in Mass spectrometry, 28, 1705-1715

Müller, I.A., Fernandez, A., Radke, J., van Dijk, J., Bowen, D., Schwieters, J., Bernasconi, S.M. (2017) Carbonate clumped isotope analyses with the long-integration dual-inlet (LIDI) workflow: scratching at the lower sample weight boundaries. Rapid Communications in Mass Spectrometry. 31, 1057-106.

Rodríguez-Sanz, L., Bernasconi, S.M., Marino, G., Heslop, D., Müller, I.A., Fernandez, A., Grant, K.M., Rohling, E.J. (2017) Penultimate deglacial warming across the Mediterranean Sea revealed by clumped isotopes in foraminifera. Scientific Reports, 7 (1), art. no. 16528

10.2
Facies analyses and benthic foraminiferal assemblages from the Atlantis Massif (MAR 30°N)

Robin Fentimen [1], Gretchen L. Früh-Green [2], Anneleen Foubert [1] and Silvia Spezzaferri [1]

[1] Département de Géosciences, Université de Fribourg, Chemin du Musée 6, 1700 Fribourg
[2] ETH Zurich, Institute of Geochemistry and Petrology, Clausiusstrasse 25 CH-8092 Zürich

The Atlantis Massif is a dome-like exposure of serpentinized peridotite situated at 30°N and 15 km west of the Mid-Atlantic Ridge axis (Früh-Green et al. 2003). The Atlantis Massif is reknown for hosting the Lost City Hydrothermal Field (LCHF) which desplays numerous active venting structures reaching up to 60 m high (Kelley et al. 2001). The summit of the Atlantis Massif is capped by 1 to 3 m of flat-lying sedimentary breccias overlain by variably lithified fossiliferous pelagic limestone (Kelley et al. 2005). This study focuses on benthic foraminiferal assemblages and facies analyses from the pelagic carbonate sand cap recovered from Site M0069 during IODP Expedition 357 (Früh-Green et al. 2016). Site M0069 is situated at a water depth of 850.90 m at the top of the Atlantis Massif. Hole M0069A was drilled to a depth of 16.44m and recovered 12.29 m of core, with 2.8 m of carbonate sand in the top 6.5m (Früh-Green et al. 2017). Samples have been sieved for foraminiferal counting and scanned with high-resolution X-ray computer tomographic techniques to document foraminiferal preservation and secondary cementation. The non-venting sites such as Site M0069 are recognized to host a wide range of organisms, more particularly cold-water corals (CWC) such as *Lophelia*, gorgonians, and *Desmophyllum* (Kelley et al. 2005). Benthic foraminiferal assemblages from the carbonate cap of the Atlantis Massif show resemblances with other recent CWC environments. Noticeably, *Discanomalina coronata*, a species described as a possible indicator for CWC environments (Margreth et al. 2009), is present in sediments at Site M0069. However, diversity at Site M0069 is lower than in other recent CWC environments. The infaunal species *Cassidulina crassa*, *Globocassidulina subglobosa* and *Ehrenbergina trigona* dominate benthic foraminiferal assemblages at site M0069. Epibenthic foraminifera are rare, contrary to benthic foraminiferal assemblages from CWC environments from the Norwegian Fjords, Porcupine Seabight and Western Mediterranean.

REFERENCES
Früh-Green, G. L, Kelley, D. S, Bernasconi, S. M., Karson, J. A., Ludwig, K. A.

Butterfield, D. A.; Boschi, C., & Proskurowski, G. 2003: 30,000 Years of Hydrothermal Activity at the Lost City Vent Field, Science, 301, 495-498.

Früh-Green, G. L., Orcutt, B. N., Green, S., Cotterill, C., & the Expedition 357 Scientists. 2016: Expedition 357 Preliminary Report: Atlantis Massif Serpentinization and Life. International Ocean Discovery Program.

Früh-Green, G.L., Orcutt, B.N., Green, S.L., Cotterill, C., & the Expedition 357 Scientists. 2017: Proceedings of the International Ocean Discovery Program, 357.

Kelley, D. S., Karson, J. A., Blackman, D. K., Früh-Green, G. L., Butterfield, D. A., Lilley, M. D., Olson, E. J., Schrenk, M. O, Roek, K. K., Lebonk, G. T., Rivizzigno, P., & the AT3-60 Shipboard Party. 2001: An off-axis hydrothermal vent field near the Mid-Atlantic Ridge at 30°N, Nature, 412, 145-149.

Kelley, D. S., Karson, J. A., Früh-Green, G. L, Yoerger, D. R., Shank, T. M., Butterfield, D. A., Hayes, J. M., Schrenk, M. O., Olson, E. J., Proskurowski, G., Jakube, M., Bradley, A., Larson, B., Ludwig, K., Glickson, D., Buckman, K., Bradley, A. S., Brazelton, W. J., Roe, K., Elend, M. J., Delacour, A., Bernasconi, S. M., Lilley, M. D., Baross, J. A., Summons, R. E., & Sylva, S. P. 2005: A Serpentinite-Hosted Ecosystem:The Lost City Hydrothermal Field, Science, 307, 1428-1434.

Margreth, S., Rüggeberg, A., & Spezzaferri, S. 2009: Benthic foraminifera as bioindicators for cold-water coral reef ecosystems along the Irish margin, Deep-Sea Research I, 56, 2216–2234.

10.3
Tropical sea surface temperatures during the Cretaceous Thermal Maximum

Alvaro Fernandez [1], Luz Maria Mejia [1], Elzbieta Jaroszewicz [2], Jose Guitian [1], Hongrui Zhang [1], Stefano Bernasconi [1], Hetaher Stoll [1]

[1] Geological Institute, ETH Zürich, Sonneggstrasse 5, CH-8092, Zürich (alvaro.bremer@erdw.ethz.ch)
[2] Institute of Geological Sciences, Polish Academy of Sciences, Twarda 51/55, 00-818 Warszawa, Poland

The Cretaceous is believed to have been much warmer than the present, with a green-house climate characterized by a lack of large scale continental ice-sheets, and with thermophilic floras and faunas present at high latitudes. Temperature reconstructions from this time are of crucial societal importance because they help us understand how the Earth system behaves under elevated concentrations of atmospheric CO_2. However, new temperature reconstructions are needed because existing data (mostly $\delta^{18}O$ and TEX86 based estimates) suffer from limitations that can result in inaccurate estimates. Moreover, there are large periods of time (tens of millions of years) where our knowledge comes from only a few measurements from a single proxy or where no data are available.

Here, we present clumped isotope temperatures from carefully separated coccolith size fractions from Demera Rise (Ocean Drilling Site 1260). This site was chosen because of its high clay content, and consequently, low diagenetic potential, and because of the availability of previous paleothemperature estimates from the same sediments (Tex86 and $\delta^{18}O$ of well-preserved planktonic foraminifera). Our observations confirm that equatorial Atlantic ocean temperatures during the 'middle' Cretaceous were markedly warmer than the present and were similar to tropical ocean temperatues during the Early Eocene. Our resutlts highlight the potential of clumped isotopes and coccoliths for deep time reconstructions of temperature and the isotopic composition of seawater.

10.4
Two Modes of Changes in Southern Ocean Productivity Over the Past Million Years

Samuel L. Jaccard [1], Christopher T. Hayes [2], Alfredo Martinez-Garcia [3], David A. Hodell [4], Robert F. Anderson [2], Daniel M. Sigman [5] & Gerald Haug [2]

[1] Institut of Geological Sciences and Oeschger Center for Climate Change Research, University of Bern, Bern (samuel.jaccard@geo.unibe.ch)
[2] Lamont-Doherty Earth Observatory, Columbia University, Palisades, NY, USA
[3] Max-Planck Institute for Chemistry, Mainz, Germany
[4] Godwin Laboratory for Paleo- climate Research, Department of Earth Sciences, University of Cambridge, Cambridge, UK
[5] Department of Geosciences, Princeton University, Princeton, NJ, USA

Export of organic carbon from surface waters of the Antarctic Zone of the Southern Ocean decreased during the last ice age, coinciding with declining atmospheric carbon dioxide (CO_2) concentrations, signaling reduced exchange of CO_2 between the ocean interior and the atmosphere. In contrast, in the Subantarctic Zone, export production increased into ice ages coinciding with rising dust fluxes, thus suggesting iron fertilization of subantarctic phytoplankton. Here, a new high-resolution productivity record from the Antarctic Zone is compiled with parallel subantarctic data over the past million years. Together, they fit the view that the combination of these two modes of Southern Ocean change determines the temporal structure of the glacial-interglacial atmospheric CO_2 record, including during the interval of "lukewarm" interglacials between 450 and 800 thousand years ago.

10.5

Windows of Climate and Carbon Cycle Variability on Orbital Time Scales from the Late Cretaceous to Quaternary

Dick Kroon [1], Leg [208] Scientific party and many others

[1] School of GeoSciences, University of Edinburgh, Edinburgh, EH9 3JW, UK

One of the grand challenges of Paleoceanography is the development of an orbital-scale, astronomically-tuned deep-sea benthic C and O isotope stack spanning the length of the Cenozoic (i.e., last 66 myr) and into the Late Cretaceous. As a major step toward this goal, Leg 208 drilled several boreholes along a depth transect to recover complete sequences covering this time interval. I will present an overview of key segments of the geological record informing our understanding of past oceans and climate. These segments, generated with samples (~ 3ky) from pelagic cores recovered during ODP Leg 208 from sites on Walvis Ridge, is the result of more than a decade long coordinated effort of several groups. In addition to over thousands of stable isotope analyses of benthic foraminifera, a parallel effort was undertaken to resolve (by core log and XRF) and tune bedding cycles to orbital curves, an iterative process involving correlation and calibrations to sections with radiometric age constraints. There are several critical climate/extinction events embedded within these segments including the Late Maastrichtian warming event, K/Pg boundary, Paleocene Carbon Isotope Maximum (PCIM), Paleocene-Eocene Thermal Maximum (PETM), and Mid Pleistocene Transition (MPT), the nature of which are now better understood within this high-fidelity long term stable isotope framework. I will conclude that these tuned hi-fidelity isotope records resolve key features of the evolution of climate and the carbon cycle across major intervals, but also that new records along depth transects from different oceans are required to make further progress.

10.6

Origin and evolution of the Eonile River unraveled by a deep basin -onshore correlation: the role of the Messinian Salinity Crisis in shaping the modern Egyptian landscape.

Mahmoud Leila [1], Andrea Moscariello [2]

[1] Department of Earth Sciences University of Mansoura, Egypt
[2] Department of Earth Sciences, University of Geneva – Rue des Maraichers 13, CH-1205 Geneva
 (andrea.moscariello@unige.ch)

The distribution, pattern and architecture of the Messinian facies deposited before, during and after the Messinian salinity crisis (MSC) have been investigated in an onshore location inside the Nile delta region. This allow us to unravel the erosional and infill history of the deep Eonile Canyon. The study is supported by sedimentological and biostratigraphic evidence, integrated with seismic.

In particular provenance study of the main canyon and smaller tributary valleys of the complex Messinian erosional system allow us for the first time to support with mineralogical and geochemical evidence the origin of the present-day Nile catchment. Specifically, we have distinguished the origin of the main Eonile canyon and identified the occurrence of a tributary network of less incised valleys which formed at the border of the steeply dipping continent margin during the MSC sea level fall.

The sedimentary facies sequence infilling the canyon systems also provides evidence of the subaerial erosion by gravity processes (debris flow) occurring within the Nile river canyon and the 2-step processes of the transgressive event at the end of the MSC dramatic sea-level fall. The first transgressive event is recorded within the late Messinian with the establishment of an estuarine system replacing a continental fluvial environment. The transgression continues throughout the end of the Messinian reaching the maximum flooding conditions well within the lower Pliocene.

The tentative correlation between the onshore and offshore stratigraphy allows us to locate chronostratigraphically the formation of the main incision with respect to the deep basin stratigraphy. On the basis of this work we propose that the main erosional process of the Nile Canyon would correspond to the second main evaporitic bed recorded in the deep basin when the effects of sea level fall was enhanced by the synchronous isostatic uplift of the Mediterranean margins.

10.7
Paleodepth reconstruction of the Inner Sea based on benthic foraminifera, IODP Exp. 359, Maldives

Andres Rüggeberg [1], Silvia Spezzaferri [1], Stephanie Stainbank [1], Giovanni Coletti [2], Dick Kroon [3], Thomas Lüdmann [4], Gregor Eberli [5], Christian Betzler [4]

[1] Department of Geosciences, University of Fribourg, Chemin du Museè 6, 1700 Fribourg, Switzerland (andres.rueggeberg@unifr.ch)
[2] Department of Earth and Environmental Sciences, Milano-Bicocca University, Piazza della Scienza 4, 20126 Milano, Italy
[3] School of GeoSciences, Grant Institute, University of Edinburgh, The King's Buildings, James Hutton Road, Edinburgh EH9 3FE, United Kingdom
[4] Institute for Geology, Bundesstrasse 55, 20146 Hamburg, Germany
[5] CSL-Center for Carbonate Research, University of Miami, 4600 Rickenbacker Causeway, Miami, FL 33149, USA

International Ocean Discovery Program (IODP) Expedition 359 was designed to address changes in sea level, circulation and the monsoon evolution in the Indian Ocean. The Maldives archipelago represents an ideal and unique sedimentary archive to reconstruct the onset and intensification of the monsoon-related currents and carbonate platform history from the Oligocene to the Present (Betzler et al. 2016).

Depth below sea level has a significant effect upon the type and amount of sediment deposited on the sea floor. In this study we applied the transfer equation to estimate paleodepths proposed by Hohenegger (2005) and tested on the Erathosthenes Seamount, a carbonate platform in the eastern Mediterranean Sea, by Spezzaferri and Tamburini (2007). The paleodepth estimations are based on frequency distributions of benthic foraminifera species along the reported depth range. Increasing knowledge about the depth range of species stabilizes this estimation which is based on confidence limits to avoid unjustified precision (Hohnegger 2005).

The variations of paleodepth in the sedimentary deposits recovered at IODP Expedition 359 Holes 1468A, 1467B and C drilled in the Maldivian archipelago are used to understand the evolution of the Inner Sea. In addition, seismic and sedimentary data together with the reconstructed paleodepths are used to interpret on-sets of different phases in carbonate platform growth and the establishment of drift deposition in this region from the Oligocene to the Pleistocene.

REFERENCES
Betzler C, et al., 2016. The abrupt onset of the modern South Asian Monsoon winds. Scientific Reports 6:29838, doi:10.1038/srep29838.
Hohenegger J, 2005. Estimation of environmental paleogradient values based on presence/absence data: a case study using benthic foraminifera for paleodepth estimation. Palaeogeography, Palaeoclimatology, Palaeoecology 217: 115–130.
Spezzaferri S, Tamburini F, 2007. Paleodepth variations on the Eratosthenes Seamount (Eastern Mediterranean): sea-level changes or subsidence? eEarth Discuss. 2:115–132.

10.8
50 years of International Ocean Drilling - The early years

Silvia Spezzaferri [1], Flavio Anselmetti [2], Judith McKenzie [3], Helmut Weissert [3] and Guests

[1] Department of Geosciences, Université de Fribourg, 1700 Fribourg (silvia.spezzaferri@unifr.ch)
[2] Geologisches Institut, Universität Bern, Baltzerstrasse 1+3, 3012 Bern
[3] Department of Earth Sciences, ETH.Z, Sonneggstrasse 5, 8092 Zürich

During 2018, the Earth Science community celebrates 50 years of the highly successful drilling accomplishments of the International Ocean Drilling Program. In August 1968, the dedicated research drilling vessel "Glomar Challenger" was launched, and the Deep Sea Drilling Project (DSDP) was started with the purpose to obtain sediment and rock samples to test the seafloor-spreading hypothesis. With the confirmation and the establishment of the theory of plate tectonics in the early 1970ties, the goals of DSDP were directed towards the study of new questions related to the world's oceans and their history. Research targets were developed within the framework of "Earth System Science". Paleoceanography, tectonics and evolution of continental margins and associated oceans, petrology and geochemistry of oceanic sediments and lithosphere were included into new research programs to be studied using the facilities of the "Glomar Challenger".

Swiss scientists participated in the program sailing as shipboard scientists beginning with DSDP Leg 3. Their expertise in stratigraphy, sedimentology and geochemistry was of pivotal importance for the development of new concepts in ocean research. Some of the exciting results in the early phase of the ocean drilling program included the verification of the seafloor-spreading hypothesis, the recognition of Oceanic Anoxic Events, the discovery of the Messinian Salinity Crisis, the understanding of diagenesis of deep-sea sediments, including the formation of chert and the identification of the carbonate ooze-chalk-limestone transition. A fundamental new approach for all of these discoveries was the application of the evolving concept of integrated stratigraphy, which combined bio-, chemo- and magnetostratigraphy as tools to interpret past changes. The success of the original Deep Sea Drilling Program (DSDP 1968-1983) grew into the truly international cooperative Ocean Drilling Program (ODP 1983-2003), which continued to explore the Earth's subseafloor using the facilities of a more advanced ocean research drilling vessel, the "JOIDES Resolution". Switzerland became a contributing partner in this program as a member of a European consortium, and Swiss scientists continue to sail on an annual basis.

In 2003, ocean drilling experienced a major step to extend research capabilities with the introduction of three independent drilling platforms, that is, a renovated "JOIDES Resolution", a riser drill ship "Chikyu" and specialized Mission Specific Platforms. The science plan for the new International Ocean Drilling Program (IODP 2003-2013) added new research themes, such as geobiology and geomicrobiology of the deep sub-seafloor biosphere, to complement and extend the geophysical, geological and geochemical programs. Since 2013, international co-operation with Swiss participation continues via the International Ocean Discovery Program: Exploring the Earth Under the Sea.

50 years of International Ocean Drilling has had a profound impact on the development of Earth Sciences, starting with the establishment of plate tectonics and continuing with the rapidly growing fields of paleoceanography, paleoclimatology, marine geology and tectonics, seafloor geochemistry and petrology and the discovery of the importance of the deep biosphere. Switzerland has been and will be a pivotal member of this community of explorers. Since 2013, scientists at Swiss institutions are united under the www.swissdrilling.ch umbrella, merging scientific ocean and continental drilling under one roof supported by the Swiss National Science Foundation.

10.9

Planktonic foraminifera calcification depths in the Indian Ocean: controls and implications

Stephanie Stainbank [1], Andres Rüggeberg [1], Silvia Spezzaferri [1], Dick Kroon [2], Erica S. de Leau [2], Manlin Zhang [2] & Jacek Raddatz [3]

[1] Department of Geosciences, Université of Fribourg, Chemin du Museè 6, 1700 Fribourg, Switzerland (stephanie.hayman@unifr.ch)

[2] School of GeoSciences, Grant Institute, University of Edinburgh, The King's Buildings, James Hutton Road, Edinburgh EH9 3FE, UK

[3] Institute of Geosciences, Goethe-Universität Frankfurt, Altenhöferallee 1, 60438 Frankfurt am Main, Germany

Planktonic foraminifera live in the upper ~ 500m of the world's oceans (Hemleben et al. 1989) and the geochemical signatures, preserved in their calcitic shells, have been used extensively to reconstruct long-term climate records (e.g. Bunzel et al., 2017). Here, we aim to use foraminiferal habitat preferences to reconstruct the thermocline dynamics over marine isotope stages (MIS) 11 (interglacial) and 12 (glacial) from Site U1467 drilled by the International Ocean Discovery Program (IODP) Expedition 359 in the Maldives. In this region the seasonal reversal in the South Asian Monsoon (SAM) winds and their associated ocean currents are the main climatic controls. We combined geochemical analyses of shells of multiple species to infer temperature and salinity changes for the northern Indian Ocean with reference to SAM dynamics. In total, 14 planktonic and two benthic foraminiferal species were analysed for their stable isotopic signatures ($\delta^{18}O$ and $\delta^{13}C$) and Mg/Ca ratios. Specimens were picked from narrow size fractions to limit isotopic offsets.

Prior to undertaking paleo-reconstructions, understanding the controls on the modern day foraminifera apparent calcification depths (ACD) is important. As the modern thermocline is known for our region, from published local CTD (Conductivity Temperature Depth) data, three methods ($\delta^{18}O$-temperature equations, $\delta^{18}O$ equilibrium values and Mg/Ca-temperature equations) used for calculating foraminiferal ACDs were tested (Birch et al. 2013; Rippert et al. 2016). Through comparison of the three methods, most deviation was seen for surface mixed layer (SML) species dwelling in the top ~ 70 m of the water column. This is due to the homogenous nature of the SML thus small differences between methods can result in large discrepancies in the ACD estimates. Furthermore, user discretion for select variables (e.g. allocated seawater $\delta^{18}O$ value and selection of Mg/Ca calibration equations) can incorporate additional errors. We show all methods were robust and the combined use of two or three served to validate the calculated estimates.

Our ACD's were in good agreement with published records (e.g. Birch et al. 2013; Rippert et al. 2016). However, they highlight the importance of local hydrographic controls which are vital considerations when comparing data from different geographical regions. Similarly to other studies (e.g. Schiebel et al., 2001; Rippert et al. 2016), the majority of our SML and thermocline species are associated with the deep chlorophyll maximum (DCM) which serves as a food source. Finally, the calculated ACDs, assuming the investigated species maintain their depth habitats based on food strategy in the past, are used to reconstruct the thermocline dynamics over MIS11 and 12. Overall, our study confirms the significance of multi-species foraminiferal geochemical studies. It highlights the wealth of information that can be extracted yet, shows the importance in species, method and variable selection when conducting these paleo-climatic and -oceanographic reconstructions.

REFERENCES

Birch, H. S., Coxall, H. K., Pearson, P. N., Kroon, D. & O'Regan, M. 2013: Planktonic foraminifera stable isotopes and water column structure: Disentangling ecological signals. Marine Micropaleontology, 101, 127–145.

Bunzel, D., Schmiedl, G., Lindhorst, S., Mackensen A., Reolid, J., Romahn, S. & Betzler, C. 2017: A multi-proxy analysis of Late Quaternary ocean and climate variability for the Maldives, Inner Sea. Climate of the Past, 13, 1791-1813.

Hemleben, C. H., Spindler, M. & Anderson, O. R. 1989: Modern planktonic foraminifera (363 pp). New York: Springer.

Rippert, N., Nürnberg, D., Raddatz, J., Maier, E., Hathorne, E., Bijma, J. & Tiedemann, R. 2016: Constraining foraminiferal calcification depths in the western Pacific warm pool. Marine Micropaleontology, 128, 14-27.

Schiebel, R., Waniek, J., Bork, M. & Hemleben, C. 2001: Planktonic foraminiferal production stimulated by chlorophyll redistribution and entrainment of nutrients. Deep-Sea Research Part 1: Oceanographic Research Papers, 48, 721–740. doi:10.1016/S0967-0637(00)00065-0.

10.10
New estimations of past atmospheric CO$_2$ from ancient algae

Heather Stoll [1], Jose Guitian [1], Ivan Hernandez [1], LuzMaria Mejia [1], Thomas Tanner [1] & Hongrui Zhang [1]

[1] Geologisch Institut, ETH Zürich, Sonnegstrasse 5, CH-8092 Zurich (heather.stoll@erdw.ethz.ch)

Phytoplankton biomarkers preserved for tens of millions of years in seafloor sediments recovered by the (I)ODP program, have yielded the greatest number and highest temporal resolution pCO$_2$ estimations for the Cenozoic. However, many of these published estimations, especially those from the last 20 Ma, pose paradoxes with regard to evidence for cooling. Recent work exploiting microfossils to contrain secondary influences on the proxy relationships such as cell size and growth rate, as well as careful consideration of the calibrations of the proxy-CO$_2$ relationship during glacial cycles of known CO$_2$ variation and cultures, has led to fundamental new interpretations of past proxy data and significant revisions in estimated pCO$_2$. In this presentation, we review the key records, support for new interpretations, implications of the new CO$_2$ records, and challenges for future pCO$_2$ reconstruction from the phytoplankton record of deep marine sediments.

P 10.1
Short-chain organic acid concentrations and implications for microbial life in active serpentinite mud volcanoes of the Mariana forearc

Philip Eickenbusch [1], Bo Barker Jørgensen [2] & Mark Alexander Lever [1]

[1] Department of Environmental Systems Science, Institute of Biogeochemistry and Pollutant Dynamics, ETH Zurich, Universitätstrasse 16, CH-8092 Zurich (philip.eickenbusch@usys.ethz.ch)
[2] Center for Geomicrobiology, Aarhus University, Ny Munkegade 116, DK-8000 Aarhus

During IODP Expedition 366, the JOIDES Resolution drilled into flanks and summits of three active serpentinite mud volcanoes on the Mariana forearc, which differ in distance to the Mariana trench (55-72 km) and therefore also in their distance to the underlying subducting slab (13-18 km). The volcanoes are characterized by distinct compositions of the upwelling mud and fluids, where high pH values up to 12.5 are one evident challenge for possible microbial life in these systems. We measured concentrations of the short-chain organic acids formate, acetate, propionate, butyrate, pyruvate and lactate by 2-dimensional ion chromatography (Glombitza et al. 2014). Total carbon of short-chain organic acids makes up 10 to 30 per cent of total dissolved organic carbon. We observe elevated formate (up to 118 µM) and acetate (up to 55 µM) concentrations downhole at the summit of Asút Tesoru (Site U1496) when compared to its flank sites and summit and flank sites of Fantangisña and Yinazao. In general, formate and acetate concentrations and ratios in summit sites correlate with distance of the mud volcanoes to the trench, and therefore slab. These short-chain organic acids, which are likely produced during serpentinization and subsequent Fisher-Tropsch-type reactions, are favourable substrates for microbial catabolism in marine sediments. We discuss the potential of microbial life using these short-chain organic acids under the harsh conditions present in the serpentinite mud volcanoes of the Mariana forearc.
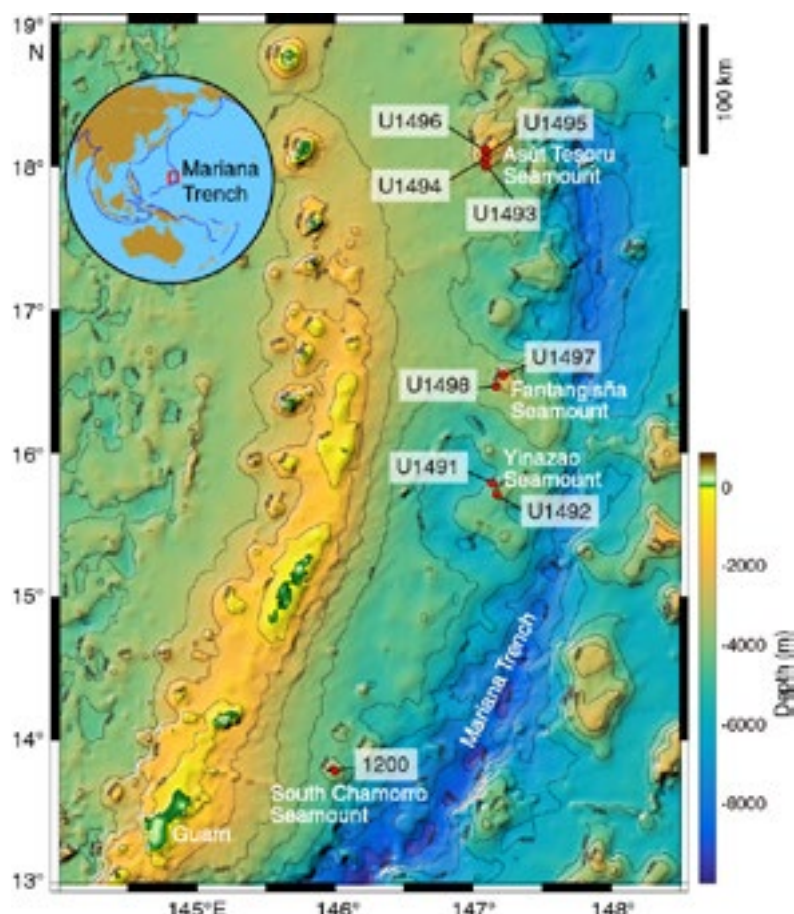

Figure 1. Location map of Sites U1491–U1498 and 1200 on South Chamorro Seamount (Fryer et al. 2018).

REFERENCES

Fryer, P., Wheat, C.G., Williams, T., & the Expedition 366 Scientists 2018: Expedition 366 summary, Proceedings of the International Ocean Discovery Program Volume 366.

Glombitza, C., Pedersen, J., Røy, H. & Jørgensen, B. B. 2014: Direct analysis of volatile fatty acids in marine sediment porewater by two-dimensional ion chromatography-mass spectrometry, Limnology and Oceanography: Methods, 12, 455-468.

P 10.2
In search of life in the subseafloor of serpentinized peridotites:
An overview of IODP Expedition 357 (Atlantis Massif, Mid-Atlantic Ridge 30°N)

Gretchen L. Früh-Green [1], Beth N. Orcutt [2], Stèphane Rouméjon [1], Marvin D. Lilley [3], Yuki Morono [4] and the IODP Expedition [357] Science Party [5]

[1] ETH Zurich, Institute of Geochemistry and Petrology, Clausiusstrasse 25
   CH-8092 Zürich (frueh-green@erdw.ethz.ch)
[2] Bigelow Laboratory for Ocean Sciences, East Boothbay ME, USA
[3] School of Oceanography, University of Washington, Seattle, WA, USA
[4] Japan Agency for Marine-Earth Science and Technology, Kochi Institute for Core Sample Research, Kochi, Japan
[5] http://www.ecord.org/expedition357/participants/

We provide an overview of IODP Expedition 357, which successfully used two seabed rock drills to core 17 shallow holes at 9 sites across Atlantis Massif (Mid-Atlantic Ridge 30°N; Figure 1). A major goal of this expedition is to investigate serpentinization processes and microbial activity in the shallow subsurface of highly altered ultramafic and mafic sequences that have been uplifted to the seafloor along a major detachment fault zone. More than 57 m of core were recovered, with borehole penetration ranging from 1.3 to 16.4 meters below seafloor, and core recovery as high as 75% of total penetration. The cores show highly heterogeneous rock type and alteration associated with changes in bulk rock chemistry that reflect multiple phases of magmatism, fluid-rock interaction and mass transfer within the detachment fault zone (Früh-Green et al., 2017).

Recovered ultramafic rocks are dominated by harzburgite with intervals of dunite and minor pyroxenite veins; gabbroic rocks occur as melt impregnations and veins. Dolerite intrusions and basaltic rocks represent the latest magmatic activity. The proportion of mafic rocks are volumetrically less than the amount of mafic rocks recovered previously by drilling the central dome of Atlantis Massif at IODP Site U1309, suggesting a different mode of melt accumulation in the mantle peridotites at the ridge-transform intersection. The cores revealed a high degree of serpentinization and metasomatic alteration that is dominated by talc-amphibole-chlorite overprinting. Metasomatism is most prevalent at contacts between ultramafic and mafic domains (gabbroic and/or doleritic intrusions) and points to channeled fluid flow and silica mobility during exhumation along the detachment fault. The presence of the mafic lenses within the serpentinites and their alteration to mechanically weak talc, serpentine and chlorite may also be critical in the development of the detachment fault zone and may aid in continued unroofing of the upper mantle peridotite/gabbro sequences.

New technologies were also developed for the seabed drills to enable biogeochemical and microbiological characterization of the environment. An in situ sensor package and water sampling system recorded real-time variations in dissolved methane and hydrogen, oxygen, pH, oxidation reduction potential, temperature and conductivity during drilling and sampled bottom water after drilling. Systematic excursions in these parameters together with elevated hydrogen and methane concentrations in post-drilling fluids provide evidence for active serpentinization at all sites. In addition, chemical tracers were delivered into the drilling fluids for contamination testing, and a borehole plug system was successfully deployed at some sites for future fluid sampling. The plugged boreholes were visited in a follow-up expedition in 2018. A major achievement of Expedition 357 was to obtain microbiological samples along a west–east profile, which will provide a better understanding of how microbial communities evolve as ultramafic rocks are altered and emplaced on the seafloor. The presence of life in this subseafloor environment is confirmed by cell counts, which revealed cell densities on the order of 10 – 10^4 cells per cubic centimetre of rock. Our results indicate that the subsurface of the serpentinite basement of Atlantis Massif provides a potentially important niche for anaerobic hydrogen-, methane- and sulfur-cycling microorganisms.
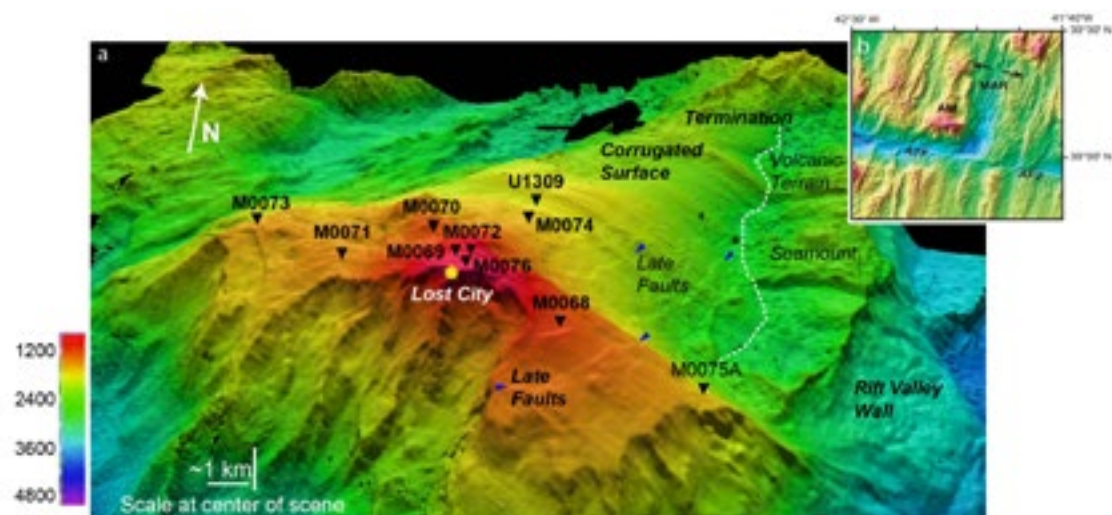
Figure 1. Bathymetry of the Atlantis Massif. (a) 3-D terrain model with a northward view of the detachment fault surface showing striations associated with detachment faulting, cross-cutting tectonic structures, with locations of the Expedition 357 drill sites, the Lost City hydrothermal field (yellow star) and IODP Site U1309. Based on new multibeam bathymetry acquired at 50 m per pixel resolution. b) Inset shows the location of the Atlantis Massif (AM) at the intersection of the Mid-Atlantic Ridge (MAR) and the Atlantis Transform Fault (ATF) and Fracture Zone (AFZ).

REFERENCES

Früh-Green, G. L., et al. (2017), Atlantis Massif Serpentinization and Life, Proceedings of the International Ocean Discovery Program, College Station, TX, http://dx.doi.org/10.14379/iodp.proc.357.2017

P 10.3
Oligocene-Miocene sea surface temperatures from North Atlantic sediments

José Guitián [1], Samuel Phelps [2], Partigya J. Polissar [2], Iván Hernández-Almeida [1] and Heather M. Stoll [1]

[1] Geological Institute, ETH, Zurich, Switzerland (jose.guitian@erdw.ethz.ch)
[2] Lamont-Doherty Earth Observatory, Columbia University, NY, USA

Major changes in the carbon cycle and atmospheric CO_2 along the Cenozoic have been suggested to be a determining cause of the climatic evolution from a ''green-house Earth' to an 'ice Earth', driving the global temperature and limiting the polar ice sheet growth. During the Oligocene-Miocene time interval, pCO_2 atmospheric concentrations are estimated to be higher than pre-industrial levels with a long-term decline. Therefore it is a period of interest for understanding the feedback between greenhouse gases and climate system. However, direct sea surface temperatures estimations for cited period are lacking especially for the west North Atlantic, and the low resolution and uncertainties of the carbon dioxide existing records, make difficult to relate them with the climatic history.

Coccolithophores, unicellular calcifying phytoplankton, are susceptible to atmospheric CO_2 variations. Hence, the organic compounds (long-chain unsaturated alkenones) produced by a specific family of coccolithophores (*Reticulofenestra spp*.) can be used for reconstruct both sea surface temperatures and past atmospheric CO_2 estimations.

In this study, a Sea Surface Temperature record has been produced from the Uk'37 ratio in alkenones present in North Atlantic sediments, site 1406A (IODP Exp. 342, 40°N) for the time interval 30 Ma to 17 Ma with a resolution of ~250Kyr. The record shows temperatures from 24°C to 27°C and exhibits three characteristic intervals potentially correlated with three marked Cenozoic excursions: the late Oligocene warming, Oligocene-Miocene transient cooling of 3.5°C, and temperature increasing heading the middle Miocene warming. Since accurate temperatures are necessary to apply into the alkenone phytoplankton proxy to reconstruct pCO_2, this might be an important contribution in temperature reconstruction for the Cenozoic ocean. In this study we also produce a new record of phytoplankton carbon isotopic fractionation (εp) derived from $\delta^{13}C$ on alkenones and isotopic composition of foraminifera, which allow to generate pCO_2 estimations. First tests, where we have implemented required coccolithophore cell physiological factors (as cell size or growth rate) show three marked decreasing steps along a long drop trend which correlates with previously published research, but differs in amplitude.

P 10.4
Tropical sea surface temperatures during the Cretaceous Thermal Maximum

Alvaro Fernandez [1], Luz Maria Mejia [1], Elzbieta Jaroszewicz [2], Jose Guitian [1], Hongrui Zhang [1], Stefano Bernasconi [1], Heather Stoll [1]

[1] *Geological Institute, ETH Zürich, Sonneggstrasse 5, CH-8092, Zürich (alvaro.bremer@erdw.ethz.ch)*
[2] *Institute of Geological Sciences, Polish Academy of Sciences, Twarda 51/55, 00-818 Warszawa, Poland*

The Cretaceous is believed to have been much warmer than the present, with a green-house climate characterized by a lack of large scale continental ice-sheets, and with thermophilic floras and faunas present at high latitudes. Temperature reconstructions from this time are of crucial societal importance because they help us understand how the Earth system behaves under elevated concentrations of atmospheric CO_2. However, new temperature reconstructions are needed because existing data (mostly $\delta^{18}O$ and TEX86 based estimates) suffer from limitations that can result in inaccurate estimates. Moreover, there are large periods of time (tens of millions of years) where our knowledge comes from only a few measurements from a single proxy or where no data are available.

Here, we present clumped isotope temperatures from carefully separated coccolith size fractions from Demera Rise (Ocean Drilling Site 1260). This site was chosen because of its high clay content, and consequently, low diagenetic potential, and because of the availability of previous paleothemperature estimates from the same sediments (Tex86 and $\delta^{18}O$ of well-preserved planktonic foraminifera). Our observations confirm that equatorial Atlantic ocean temperatures during the 'middle' Cretaceous were markedly warmer than the present and were similar to tropical ocean temperatues during the Early Eocene. Our resutlts highlight the potential of clumped isotopes and coccoliths for deep time reconstructions of temperature and the isotopic composition of seawater.

P 10.5
Rifted margins revisited: insights from ODP sites off Iberia and field observations in the Alps

Anne Marie Karpoff [1], Gianreto Manatschal [1], Victor Hugo Pinto [2], Marc Ulrich [1] & Daniel Sauter [1]

[1] Institut de Physique du Globe de Strasbourg, CNRS-UMR 7516, Université de Strasbourg, 1 rue Blessig, F-67084 Strasbourg (amk@unistra.fr)
[2] Petrobras, Av. Rep. do Chile 330, Rio de Janeiro, RJ 330

Already more than 40 years ago, mantle rocks have been drilled at the distal Galicia margin during ODP Leg 103 (Boillot et al. 1987). The discovery of exhumed mantle rocks, predicted by Italian geologists working in the Apennines (Decandia & Elter 1969), is not only at the origin of a paradigm shift in the interpretation of magma-poor rifted margins but also of the beginning of more than 40 years of intense on- and offshore geological and geophysical surveys including several DSDP, ODP and IODP Legs. These studies investigated the architecture of the Ocean-Continent Transition (OCT) at magma-poor rifted margins and the processes controlling lithospheric breakup and formation of oceans as well as the reactivation and formation of collisional orogens. Our research in Strasbourg was, since the early days of the discovery of exhumation of mantle rocks, focused on this process and of its consequences, recorded in the sedimentary sequences and the related geochemical cycle (e.g. the serpentinization process).

The examples are from the conjugate Newfoundland-Iberia margins, ultra-slow spreading ridges (SWIR) and preserved remnants of fossil OCTs exposed in the Alps and Pyrenees. Our investigations enabled to describe the role of detachment faulting and its control on the tectono-sedimentary and magmatic evolution of OCT. The development of high-resolution seismic imaging techniques allows also to recognize similar structures at other rifted margins. At present it is assumed that more than 50% of the world margins formed at low magmatic budgets, showing evidence for hyperextension and mantle exhumation. Thus, 40 years after the first drilling of exhumed mantle during ODP Leg 103, it is generally accepted that mantle exhumation is a common process occurring at many of the global rifted margins. However, while the existence of exhumed mantle domains is not anymore debated, the effects of widespread mantle serpentinization on global Earth element cycles and the environmental implications remain to be investigated. The main problem in determining the serpentinization impact is the access to rocks (ultramafics and sediments) that registered the mantle exhumation. While present-day OCTs are covered by thick sediments and are at abyssal depth, which makes the access to these domains difficult and only possible by deep sea drilling, remnants of ancient OCTs exposed in orogens are alternative ways for archives with records of the influence of serpentinization linked to lithospheric breakup. At present, samples from such OCTs are accessible from few sites, the most important and best described so far being the Iberia-Newfoundland and the Alpine examples, particularly the Tasna, Totalp and Platta units in the Central Alps (SE-Switzerland).

Here we present a comparative study using dataset from the Alps and the Iberia-Newfoundland conjugate margins in which we describe and try to quantify the importance of serpentinization in the transfer of elements between the Earth's reservoirs during mantle exhumation and magma-poor rifted margins evolution (Pinto et al. 2015, 2016).The intrusion and circulation of seawater in mantle rocks has the potential to change the seawater chemistry and sustain primitive life and to control the depositional environments related to hydrothermal systems. A first-order quantification of serpentinization along the Iberia OCT allowed to quantify the volume of absorbed water in this OCT domain (Pinto et al. 2016). Moreover, we established a mass budget and element transfer during serpentinization by first order mass balance calculations. The water-rock reactions can induce a significant loss of Si, Mg, Fe, Mn, Ca, Ni and Cr, and their transfer along detachment faults towards marine and sedimentary basins in hyperextended domains (Pinto et al. 2015, 2016).

Apart from presenting our ongoing research on the role of serpentinization on global mass fluxes, we also want to show that the combination of oceanic drilling and field observations can provide access to one of the last archives of the Earth history that remain to be investigated and understood, which is that of how continents rupture and new oceans form. The DSDP, ODP and IODP programs are at the origin of many major discoveries in this research domain. Therefore, keeping IODP alive, by submitting innovative and challenging IODP drilling projects is a key for the Margin community in continuing research on how rift systems evolve, and oceanic basins form and develop.

This contribution is dedicated to Yves Lancelot.

REFERENCES

Boillot, G. et al. 1987: i (ODP Leg 103, western Galicia margin, Spain). Tectonophysics, 132, 33-342.

Decandia, F.A. & Elter, P. 1969: Riflessioni sul problema delle ofioliti nell'Appennino settentrionale (nota preliminare). Atti della Società Toscana di Scienze Naturali, 75, 1–9.

Pinto, V.H., Manatschal, G., Karpoff, A.M. & Viana, A.R. 2015: Tracing mantle-reacted fluids in magma-poor rifted margins: The example of Alpine Tethyan rifted margins. Geochem. Geophys. Geosyst. 16, 3271–3308.

Pinto, V.H., Manatschal, G., Karpoff, A.M., Ulrich, M. & Viana, A.R. 2016: Seawater storage and element transfer associated with mantle serpentinization in magma-poor rifted margins: a quantitative approach. Earth Planet. Sci. Lett. 459, 227-237.

P 10.6
Morphological evolution of menardiform globorotalids are different in the Atlantic and Pacific oceans

Michael Knappertsbusch [1] & Thore Friesenhagen [1,2]

[1] Naturhistorisches Museum Basel, Augustinergasse 2, CH-4001 Basel (michael.knappertsbusch@unibas.ch)
[2] Geologisches Institut, University of Basel, Bernoullistrasse 32, CH-4056 Basel (thore.friesenhagen@unibas.ch)

In our research agenda "Evolutionary prospection of calcareous pelagic microfossils" the paleobiogeography of morphological evolution and speciation in planktonic foraminifera is investigated, with special attention to the tropical Neogene plexus of *Globorotalia menardii*. Our investigations cover the past 8 million years from deep-sea cores in the Caribbean Sea (DSDP Sites 502), the tropical Atlantic (ODP Sites 925B and 667A), the tropical Pacific Ocean (DSDP Site 503, eastern Pacific, ODP Site 806, Ontong Java Plateau) and locations in the Indian Ocean. Special attention is given to the possibility of large scale dispersal of menardiform globorotalids from the Indian or Pacific homes via the Agulhas Current around the southern tip of Africa. During glacial to interglacial transitions this current system is known for repeated seeding of tropical plankton faunas from the Indian Ocean into the South-Atlantic since at least the Pleistocene. From sudden size increase patterns of menardiform shells observed at Hole 925A we suspect Agulhas leakage of menardiforms to reach back until about 1.95 Ma (Knappertsbusch 2016). Our new results from ODP Site 667A support this idea as manifested by an Agulhas' influence-peripheral, time-transgressive, transatlantic expansion of large menardiform globorotalids from 2.3 Ma – 2.06 Ma in the east Atlantic to 2.58-1.7 Ma in the west Atlantic/Caribbean Sea (Friesenhagen 2018; Knappertsbusch and Friesenhagen 2018). The documentation of such large scale dispersal is of great interest not only for biostratigraphers but adds to the paleobiogeographic interpretation of morphological signals from fossil plankton shells in the sedimentary record, especially in the case of morphologically closely related forms. In this context and in order to differentiate between processes of morphological evolution from immigration/dispersal, the morphological evolution of menardiform globorotalids is currently investigated at ODP Hole 806C (Ontong-Java Plateau, tropical West Pacific). This area reflects stable and warm environmental conditions back to Pliocene times, and is completely outside of Agulhas' influence. From the 21 investigated samples at Site 806 studied so far a more gradual evolutionary pattern of menardiform shells comes indeed to light in that area. At Site 806 axial length (dX) versus spiral height (dY) measurements show no abrupt size increase between 2.3 Ma and 1.7 Ma at Hole 806C, which is different from those observed in the tropical Atlantic and Caribbean Sea. Overall, the data seem to support our expectations of a more gradual pattern for *G. menardii* evolution in the western Pacific, similar to the menardiform shell evolution pattern observed earlier at Eastern Equatorial Pacific DSDP Site 503, but trends still need further refinement by additional measurements and statistical analysis.
The above observations are based on measurements derived from shell outlines in keel view collected using our automated shell orientation and imaging robot called AMOR. In close collaboration with ingenieurs from the Institute of Automation at FHNW in Brugg a second, following-up device AMOR2 (see Figure 1) was recently realized, which will greatly help us to accelerate collection of the needed large amount of morphometric measurements for our studies about *G. menardii*.

Figure 1. New AMOR 2 (22 August 2018). Left, Motorized 4-axis tilting stage combined with a binocular microscope, digital camera, motorzoom and motorized magnification changer. Microfossils placed in the Plummer cell can be automatically positioned under the microscope and oriented, focused, and imaged. Right side: Box containing motion controllers and electronics. The robot is operated via customized AMOR4 software written in LabView 14. In contrast to the earlier version, AMOR2 has additional functions for microfossil orientation and does no longer need a frame grabber. AMOR2 would not have been possible without the help of Daniel Binggeli (FHNW) and voluntary worker at NMB, Prof. em. Jean Eisenecker (FHNW).

REFERENCES

Friesenhagen, T. 2018: The Evolution of Test Size of the *Globorotalia menardii* in the Atlantic and Indian Oceans since the Upper Miocene. Abstract. FORAMS 2018 Symposium, 17-22 June 2018, Edinburgh, UK., Session VIII, temporary abstracts, 203.

Knappertsbusch, M. and Friesenhagen, T. 2018: Prospecting patterns of morphological evolution in menardiform globorotaliids along Agulhas' trackway: Review and research in progress. Abstract. FORAMS 2018 Symposium, 17-22 June 2018, Edinburgh, UK., Session IX, temporary abstracts, 331.

Knappertsbusch, M. 2016: Evolutionary prospection in the Neogene planktic foraminifer *Globorotalia menardii* and related forms from ODP Hole 925B (Ceara Rise, western tropical Atlantic): evidence for gradual evolution superimposed by long distance dispersal ? Swiss Journal of Palaeontology, 135, 205-248.

Further info:
https://micropal-basel.unibas.ch/Research/EVOLPRO/AGULHAS.html
https://micropal-basel.unibas.ch/

P 10.7

Demise of a salt giant: Dolomite formation at the termination of the Messinian Salinity Crisis in the Ionian Basin of the Central Mediterranean Sea

Judith A. McKenzie [1], Christian Huebscher [2], Giovanni Aloisi [3], Claudia Bertoni [4], Angelo Camerlenghi [5], Nick Evans [6], David Hodell [6], Johanna Lofi [7]

[1] Geological Institute, ETHZ, Sonneggstrasse 5, CH-8092 Zurich (sediment@erdw.ethz.ch)
[2] Geophysics Institute, University of Hamburg, Bundesstrasse 55, D-20146 Hamburg
[3] Universite Pierre et Marie Curie, 4, Place Jussieu, F-75005 Paris
[4] University of Oxford, South Parks Road, UK-OX2 3AN Oxford
[5] Istituto Nazionale di OGS, Borgo Grotta Gigante 42/c, I-34010 Trieste
[6] University of Cambridge, Downing Street UK-CB2 3EQ Cambridge
[7] UMR, Universiy of Montpellier, Place E. Batallon, F-34095 Montpellier

The "Deep Sea Drilling Program" was launched in mid-August 1968 with scientific drilling operations on the research vessel "Glomar Challenger". The project was designed to test the newly evolving plate tectonic/seafloor spreading hypothesis. In fact, this primary goal was amazingly achieved within the first 10 years of ocean drilling, as sediment and rock samples recovered from beneath the seafloor provided the direct proof of the hypothesis. In the same period, this major accomplishment was enhanced by additional discoveries, many of which have continued to impact Earth science research during the following 40 years with scientific ocean drilling programs (DSDP, ODP, and both IODPs).

For example, although seismic reflection profiles had previously revealed the presence of diapiric structures similar to salt domes beneath the Mediterranean seafloor, the areal extent and magnitude of this most recent and largely undeformed salt giant was only revealed in 1970 during DSDP Leg 13 with the drilling of 6 sites along a W-E transect of the deep basins (Ryan, 2009). To explain the existence of this salt giant deposited between 5.96 and 5.33 Ma, a controversial desiccation hypothesis was put forward, whereby an ocean the size of the Mediterranean Sea must have dried up and was subsequently reflooded with marine waters after the deposition of a vast evaporite complex (Hsü et al., 1973). Although later drilling expeditions (DSDP Leg 42A, ODP Legs 107, 160, and 161) have confirmed the presence of extensive evaporite deposits in all of the deep Mediterranean basins, this phenomenon, known as the Messinian Salinity Crisis (MSC), still remains veiled in mystery calling for further exploration in greater detail using more advance ocean drilling techniques. To this end, the COST Action "Uncovering the Mediterranean Salt Giant" (MEDSALT https;//medsalt.eu) was established to develop drilling proposals to study the Messinian salt layer preserved beneath the deep Mediterranean seafloor. As the current projected ship-track for the JOIDES Resolution will bring IODP operations into the North Atlantic during FY2021 through FY2022, we anticipate the possiblitity for renewed drilling in the coming years to study the Messinian salt giant.

One of the MEDSALT goals is a deep biosphere drilling objective to investigate the factors controlling the physical and biogeochemical environment of dolomite vs. gypsum deposition. Deciphering exact mechanisms for the formation of massive dolomite deposits has long been an enigma in sedimentary geology. The recognition that microbes can play a role in dolomite precipitation processes has added a new dimension to the study of the origin of dolomite formations. In 1975 at DSDP Leg 42A, Site 374 in the Ionian Abyssal Plain, a massive dolomite deposit was found directly associated with the underlying Messinian salt giant. A recent seismic survey conducted to map the extent of this dolomite body revealed that it is quite extensive, covering an area approximately equivalent to Sicily (~25'000 km^2). Based on geochemical and sedimentological evidence recorded at Site 374, we propose that modern subsurface dolomite precipitation is ongoing and the site is a "natural laboratory" in which to investigate microbial phenomena in the context of a giant evaporite deposit. Our proposal to drill into the Messinain evaporite complex buried in the deepest region of the Ionian Basin aims to recover biological, pore-water and sediment samples to provide biogeochemical data for formulating an actualistic model for the origin of massive dolomite deposits associated with other salt giants in the rock record.

REFERENCES
Hsü, K.J., Ryan, W.B.F. & Cita, M.B. 1973: Late Miocene dessication of the Mediterranean, Nature, 242, 240-244.
Ryan, W.B.F. 2009: Decoding the Mediterranean salinity crisis, Sedimentology, 56, 95-136.

P 10.8
Unraveling the potential for sea surface temperature reconstructions using coccolith clumped isotopes

[1]Luz Maria Mejia [1], Alvaro Fernandez [1], Jose Guitian [1], Hongrui Zhang [1], Stefano Bernasconi [1], Hetaher Stoll [1]

[1] *ETH Zürich, Sonneggstrasse 5, 8092 Zürich (luz.mejia@erdw.ethz.ch)*

Coccolithophores are geographycally and chronologically ubiquitous climate regulators and key contributors to marine calcium carbonate export to the deep ocean. Despite their relevance to the carbon cycle, very few studies have focused on determining if reliable absolute sea surface temperatures (SST) can be obtained using clumped isotope thermometry in their calcite. Under the current anthropogenic warming, it is urgent to reach a consensus on Earth climate sensitivity, for which accurate SST recontructions during past periods of CO_2 similar to those projected for the future, are required. For this purpose, the application of clumped isotope thermometry to coccolith calcite is promising, as a surface signal is ensured, opposed to foraminieral calcite. However, it is still not clear whether there are vital effects in coccolith clumped isotopes, potentially related to similar mechanisms causing vital effects in carbon isotopes.

We will present preliminary clumped isotope SST reconstructions from ODP Site 982 (North Atlantic) from the last ~16 Ma based on different coccolith size fractions. Since cells of different sizes experience different degrees of carbon limitation, believed to cause vital effects in carbon isotopes, we expect vital effects in coccolith clumped isotopes to be evidenced in the analysis of well-separated discrete size fractions. The record will be compared to SSTs derived from alkenones, assuming no temperature-saturation of this proxy at this latitude and during this time interval.

To determine whether variability in clumped isotopes between size fractions or potential disagreement with alkenone SSTs records are due to carbon limitation, we combine clumped isotopes with data of carbon isotopic fractionation of coccolith calcite (ε_{cocco}) and fractionation during photosynthesis measured in alkenones (ε_p). The later will be used to reconstruct CO_2 trends in the studied site and evaluate the selective pressure of carbon limitation through time in different size fractions.

This study constitutes one of the first approaches to unravel the potential of this technique to reconstruct absolute SSTs in the deep past, when and where other widely-used temperature proxies are not reliable, providing new data to better understand climate sensitivity.

P 10.9

Carbon Geochemistry and Mineralogy of Serpentinized Mantle Peridotites at the Atlantis Massif: Results from IODP Expedition 357

Lotta Ternieten [1], Gretchen L. Früh-Green [1], Stefano M. Bernasconi [1] and Marvin D. Lilley [2]

[1] ETH Zurich, Institute of Geochemistry and Petrology, Clausiusstrasse 25
  CH-8092 Zürich (lotta.ternieten@erdw.ethz.ch)
[2] School of Oceanography, University of Washington, Seattle, WA, USA

Serpentinization is a fundamental process that controls rheology and geophysical properties of the oceanic lithosphere and has major consequences for heat flux, geochemical cycles and microbial activity in a wide variety of environments. International Ocean Discovery Program (IODP) Expedition 357: Atlantis Massif Serpentinization and Life was conducted to better understand the role of serpentinization in driving hydrothermal systems, in sustaining microbiological communities, and in the sequestration of carbon in ultramafic rock (Früh-Green et al., 2017). Our study focuses on a better understanding hydration and carbonation processes in the altered mantle peridotites from the Atlantis Massif and to evaluate how, when and where the formation of abiotic vs biotic carbon compounds is favoured in serpentinizing environments. Petrological and stable isotope studies are used to characterize the speciation and source of carbon, the distribution of carbonates, and the identification of different carbonate veins and organic compounds in the IODP Exp. 357 drill cores.

Samples of serpentinites from all drill sites at the Atlantis Massif have measurable carbon content, sometimes in low concentrations only. Higher carbon concentrations are in general related to a higher concentration of carbonate in the rock. The total organic carbon (TOC) content is in general lower than the total inorganic carbon (TIC) content and varies between 100 ppm and 1000 ppm; however, in some samples the TOC content is higher than the TIC. The isotopic composition of total carbon in the rock matrix and veins varies between +3 ‰ and -30‰. The $\delta^{13}C$ values of carbonate (measured as TIC) range between +3 ‰ and -14 ‰ and $\delta^{13}C$ values of TOC range between -21 ‰ and -29 ‰. Some samples have negative total carbon values of the bulk rock and at the same time $\delta^{13}C$ values close to 0‰ in carbonate veins. $\delta^{13}C$ values less than approximately -15‰ could indicate an organic component or biological input to the system. Calculated precipitation temperatures of carbonates from the rock matrix and veins range from 0 °C to 200 °C.

The samples locally contain dolomite as a high temperature carbonate phase. The carbonates can be divided into two types. Type I has $\delta^{13}C$ values > -2‰, $\delta^{18}O$ > 0‰ and precipitation temperature < 40 °C and represent seawater-derived carbonates. Optical microscope investigations show that carbonate veins of Type I crosscut minerals and other veins, which indicate that they are the latest veining event. Type II carbonates have $\delta^{13}C$ values of less than -2‰, and $\delta^{18}O$ less than -5‰, which correspond to precipitation temperatures from 40°C to 200°C. The more negative $\delta^{13}C$ values point to a non-seawater component and possibly reflect a contribution of carbon from biological methane.

REFERENCES

Früh-Green, G. L., et al. (2017), Atlantis Massif Serpentinization and Life, Proceedings of the International Ocean Discovery Program, College Station, TX, http://dx.doi.org/10.14379/iodp.proc.357.2017

P 10.10

The relationship between inorganic/organic carbon pump and benthic foraminifera carbon isotope in the last 5 Ma: a perspective from tropical ocean

Hongrui Zhang [1,2]; Heather Stoll [1]; Chuanlian Liu [2]

[1] *ETH Zurich, Zurich, Switzerland;*
[2] *Tongji University, Shanghai, China*

The long eccentricity cycle (~405 kyr) has been widely found in the benthic foraminifera carbon isotope records since the Cretaceous, which can be regarded as one of the most stable orbital cycles recording the dynamic of ocean carbon cycle. However, this ~405 kyr cycle signal began to disappear since the Quaternary. Several hypothesis have been suggested to explain the ocean DIC (dissolve inorganic carbon) carbon isotope variations, especially during the last 1.2 Myr. The variation of inorganic/ organic pump ratio and marine primary producer type (coccolithophore/ diatom ratio) were though as important ways controlling the whole ocean DIC δ^{13}C.

In this study, cross spectrum analyses were carried on among the carbon isotope, bulk sediment PIC:POC ratio and several coccolithophoric productivity proxies, including the percentage of *Florispher profunda*, the coccolith abundance and the C37 content from tree different cores, to test the lead or lag of ocean DIC δ^{13}C to different potential driving factors. We found that the C37 content records lag the δ^{13}C in the South China Sea core ODP 1143, while those from Eastern Pacific in face with δ ^{13}C signal in the core ODP 846. The δ^{13}C signal did not show significant relationship with C37 in another Eastern Pacific core. The F. profunda data in the core ODP 1143 showed a strong ~500 kyr cycle, while did not show any correlation with δ^{13}C on ~405 kyr band. Moreover, the bulk sediment PIC:POC ratio only had significant relation with δ ^{13}C on ~40 kyr band, which was the glacial-interglacial cycles before Mid-Pleistocene transition.

Our analyses do not support the hypothesis that the variation of inorganic/organic pump ratio changed the ocean DIC carbon isotope so far, at least not in the South China Sea. The of ocean DIC δ^{13}C seems to vary with coccolithophore productivity on both ~405 kyr and ~100 kyr band, while the response of δ^{13}C to C37 content does not show a uniform pattern. However, more records around the world, including the biogenic opal and more bulk sediment PIC:POC data, should be compared before drawing a credible conclusion in a global perspective.

11. Quaternary environments: landscapes, climate, ecosystems, human activity during the past 2.6 million years

Naki Akçar, Christine Pümpin, Stéphanie Girardclos, Gaudenz Deplazes, Stephanie Wirth, Jean Nicolas Haas, René Löpfe, Loren Eggenschwiler

Swiss Society for Quaternary Research (CH-QUAT)

TALKS:

11.1   Akçar N., Yeşilyurt S., Christl M., Vockenhuber C.: Fluctuations of the Eastern Antarctic Ice Sheet in Queen Maud Land

11.2   Baggenstos D., Häberli M., Schmitt J., Fischer H.: An attempt to reconstruct planetary radiative imbalance over the last 40,000 years

11.3   de Potter Longchamp C., Goyette Pernot J.: Influence of the geology and meteorological conditions on indoor radon concentrations in the Jura mountains: preliminary results of the Interreg project Jurad-bat

11.4   Grischott R., Kober F., Ivy-Ochs S., Hippe K., Lupker M., Christl M., Vockenhuber C., Maden C.: Timing the deposition of Swiss Deckenschotter with cosmogenic isochron burial dating

11.5   Groos A.R., Akçar N., Vockenhuber C., Veit H.: Glacial chronology of the Bale Mountains and its implications for the early human occupation of the southern Ethiopian Highlands

11.6   Hofmann B.A., Akçar N., Valla P.: Twannberg: Meteorite strewn field and glacial transport

11.7   Hofmann F.M., Alexanderson H., Schoeneich P., Mertes J.R., Léanni L., ASTER Team (Aumaître G., Bourlès D.L., Keddadouche K.): [10]Be exposure dating reveals multiple glacier advances and still stands in the southern Écrins massif (French Alps) during the Late Glacial and the Early Holocene

11.8   Kronig O., Ivy-Ochs S., Grazioli S., Luetscher M., Schide K., Gallen S., Vockenhuber C.: Quantifying subglacial erosion beneath the Tsanfleuron glacier, Switzerland

11.9   Lombardo U.: Neotectonics drove landscape evolution in SW Amazonia

11.10   Luetscher M., Moseley G.E., Festi D., Hof F., Spötl C., Edwards R.L.: A new speleothem record of the last interglacial (MIS-5e) from the Sieben Hengste

11.11   Singeisen C., Ivy-Ochs S., Wolter A., Kronig O., Yesilyurt S., Vockenhuber Ch., Akcar N.: New insights into the detachment mechanism, runout and age of the Kandersteg rock avalanche

11.12   Spillmann T., Madritsch H., Deplazes G., Hauvette L., Fiebig B., Keller L., Hölker A.: Seismic analysis of overdeepened Quaternary deposits, northern Switzerland

11.13   Studer A.S., Sigman D.M., Martínez-García A., Thöle L.M., Michel E., Jaccard S.L., Lippold J.A., Mazaud A., Wang X.T., Robinson L.F., Adkins J.F., Haug G.H.: Increased nutrient supply to the Southern Ocean during the Holocene and its implications for the pre-industrial atmospheric CO_2 rise

11.14   Zaki A.S., Schuster M., King G., Herman F., Castelltort S.: How was the amount of precipitation perturbed during the Late Pleistocene in North Africa?

POSTERS:

P 11.1   Affolter S., Häuselmann A. , Fleitmann D., Leuenberger M.: Temperature reconstruction using speleothem fluid inclusions from Milandre cave, Jura Mountains, Switzerland

P 11.2   Amsler H.E., Schmid N., Jaccard S.L., Kuhn G., Ikehara M.: Variations in near-bottom flow of ACC during the past glacial cycle in SW Indian Ocean

P 11.3   Bandou D., Schläfli P., Schwenk M., Douillet G.A., Kissling E., Schlunegger F.: Gravity model of the overdeepenings from the Bern area

P 11.4   Beccari V., Basso D., Almogi-Labin A. , Hyams-Kaphzan O. , Makovski Y. , Spezzaferri S.: Macro- and micro-fauna from cold-seeps in the Palmahim Disturbance Zone (off-shore Israel)

P 11.5   Bolland A., Rey F., Tinner W., Heiri O.: Using chironomids to constrain Late Glacial climate trends in Burgäschisee, Switzerland

P 11.6   Buechi M.W., Deplazes G., Anselmetti F.S.: Sedimentology of the glacial facies within the Deckenschotter of Northern Switzerland

P 11.7   Czerski D., Mosetti L., Cardani Vergani R., Pellegrini M., Federici-Schenardi M., Gillioz M., Scapozza C.: The evolution of the fluvial environments and the history of human settlements during the Late Holocene on the Piano di Magadino (Cantone Ticino, Switzerland): new sedimentological and geoarchaeological data

P 11.8   Dieleman C., Akçar N., Christl M., Vockenhuber C.: Isochron-burial dating of Swiss Deckenschotter

P 11.9   Gegg L., Buechi M.W., Deplazes G., Madritsch H., Mueller D., Preusser F., Anselmetti F.S.: In quest of a pre-LGM (sub-)glacial history: drilling the overdeepened Lower Aare Valley

P 11.10   Råman Vinnå L., Bouffard D., Wüest A., Girardclos S., Dubois N.: Spatial focusing of lake sedimentation by wind driven circulation

P 11.11   Dubois N., Råman Vinnå L., Rabold M., Hilbe M., Anselmetti F.S., Wüest A., Meuriot L., Jeannet A., Girardclos S.: Subaquatic slope instabilities due to river correction and artificial dumps (Lake Biel, Switzerland)

P 11.12   Šegvić B., Girardclos S., Zanoni G., González C.A., Steimer-Herbet T., Besse M.: Fe-Mn nodules in young soils of Grand-Saconnex (Geneva, Switzerland): encrustation hampered by the Late Neolithic soil drainage?

P 11.13   Gribenski N., Valla P., Preusser F., Crouzet C., Buoncristiani J.F.: Constraining the maximum glacial timing of the Lyon Lobe, French Alps, Using OSL dating

P 11.14   Ivy-Ochs S., Viganò A., Rossato S., Martin S., Vockenhuber C., Rigo M., Campedel P.: Reconstructing the sequence of massive rock-slope failures in Valle di Tovel, Trentino (Italy)

P 11.15   Kamleitner S., Ivy-Ochs S., Monegato G., Gianotti F., Salcher B., Reitner J.M.: Tackling North-South differences of the Last Glacial Maximum in the Alps

P 11.16   Lechleitner F.A., Amirnezhad-Mozhdehi S., Columbu A., Comas-Bru L., Labuhn I., Pérez-Mejías C., Rehfeld K.: What do speleothems in Western Europe record? Assessing regional and temporal trends in speleothem $\delta^{18}O$ with the SISAL database

P 11.17   Lehmann A., Paul C., Filippidou S., Ballif L., Dyer S., Junier P., Vennemann T.: Reconstruction of ecological evolution of lakes based on multidisciplinary proxies: the case of Lake Liambezi, Botswana.

P 11.18   Ludwig A.: Evolution of local topography by fluvial and hillslope processes: a GIS-based study in the eastern Jura Mountains and the Wutach valley (southern Germany)

P 11.19   Magrani F., Valla P.: Spatial patterns of glacial erosion in the Alpine foreland: Morphometric analysis of overdeepenings

P 11.20   Mair D., Lechmann A., Yesilyurt S., Tikhomirov D., Vockenhuber C., Akçar N., Schlunegger F.: Erosional dynamics of steep high alpine headwalls revealed by exposure ages (Eiger mountain, Central Swiss Alps)

P 11.21   Makri S., Grosjean M., Rey F., Gobet E.: Long-term high-resolution productivity and meromixis dynamics on the Swiss Plateau (Lake Moossee, Switzerland) inferred from Hyperspectral Imaging

P 11.22   Mohammadi A., Moazzen M., Moazzen M., Kaveh Firouz A.: Investigations on different rock types used in Urartian Gavur castle in Azerbaijan Province, NW Iran

P 11.23   Negga H., Jaramillo-Vogel D., Rime V., Schaegis J.-C., Perrochet L., Wyler P., Filfilu E., Hailu A., Braga J.C., Balemwal A., Tesfaye K., Foubert A.: Palaeo-environmental evolution of the Danakil Depression during the Pleistocene (Northern Afar, Danakil Depression)

P 11.24   Ott R., Gallen S., Ivy-Ochs S., Caves Rugenstein J.K., Willett S., Helman D., Fassoulas C., Vockenhuber C., Christl M., Haghipour N.: Quantification of chemical and mechanical denudation in karst landscapes and mechanisms for steep and high carbonate topography on the island of Crete

P 11.25   Rigoussen D., Diaz N., Van Thuyne J., Verrecchia E.: Occurrence and significance of sepiolite deposits in the Chobe enclave (Northern Kalahari Basin, Botswana)

P 11.26   Schwenk M.A., Bandou D., Schläfli P., Douillet G.A., Schlunegger F.: Origin and preservation of pre-Eemian lacustrine deposits in overdeepenings along the Aare Valley between Thun and Bern

P 11.27   Serra E., Gribenski N., Valla P.G.: Alpine Glacier Fluctuations and Paleoclimatic Reconstructions

P 11.28   Stalder C., El Kateb A., Camozzi O., Spangenberg J., Therzhaz L., Spezzaferri S.: Living benthic foraminifera from cold water coral ecosystems in the Mellilla Mound Field, Alboran Sea, Western Mediterranean

P 11.29   Thöle L., Martinez-Garcia A., Studer A.S., Auderset A., Moretti S., Mazaud A., Michel E., Jaccard S.L.: Reconstruction of sea surface temperature gradients in the Southern Indian Ocean over the last glacial cycle

P 11.30   Luyao Tu, Grosjean M.: High-resolution eutrophication history records and phosphorus retention in Lake Burgaschi (Switzerland) since ~1800 AD

P 11.31   Van Thuyne J., Verrecchia E.P.: Fungus-growing termites as geological agents transforming savanna landscapes

P 11.32   Wartenweiler S.H., Gilli A., Rey F., Bernasconi S.M., Gobet E., Tinner W.: A high-resolution late-glacial lake sediment record of climate changes and associated environmental impacts from Moossee (Switzerland)

P 11.33   Yesilyurt S., Dogan U., Ivy-Ochs S., Vockenhuber C., Akçar N.: Evidence for a local last glacial maximum during the MIS-3 in eastern Turkey

P 11.34   Gallach X., Deline P., Carcaillet J., Ravanel L., Perrette Y., Lafon D., Ogier C.: TCN dating of high-elevated rockfalls in the Mont Blanc massif. A new method of dating rockfalls in the Mont Blanc massif using reflectance spectroscopy

11.1
Fluctuations of the Eastern Antarctic Ice Sheet in Queen Maud Land

Naki Akçar [1], Serdar Yeşilyurt [1], Marcus Christl [2] & Christof Vockenhuber [2]

[1] Institut für Geologie, University of Bern, Baltzerstrasse 1+3, CH-3012 Bern (akcar@geo.unibe.ch)
[2] Laboratory of Ion Beam Physics, ETH Zurich, Otto-Stern-Weg 5, 8093 Zurich

Today, Sør Rondane Mountains in the Queen Maud Land acts as a barrier to the Eastern Antarctic Ice Sheet in Antarctica. This is displayed by the difference in altitude of the ice surface to the south and north of the mountain chain. To the south, ice surface reaches altitudes above 2500 meters above sea level and forms an ice plateau. Lowlands of ice are found at altitudes of around 1500 meters to the north of the mountain chain. Huge glacier tongues, such as Hansen, Gunnestad and Byrd glaciers among others, are actively draining the ice from the plateau to the lowlands. The focus of this study is on the records of deglaciation of the Eastern Antarctic Ice Sheet (EAIS) and subglacial erosion in the Sør Rondane Mountains (Figure 1). Therefore, our goal is to reconstruct the changes in the drainage pattern of the EAIS in time. To do this, we will reconstruct the chronology of deglaciation by surface exposure dating the ice margin records and determine the rates of subglacial erosion by analyzing suite of in-situ produced cosmogenic nuclides (^{10}Be, ^{14}C, ^{26}Al and ^{36}Cl) in the surfaces of glacially molded bedrock.

During the first field campaign in the Sør Rondane Mountains in the Queen Maud Land at the Princess Elisabeth Station within the BELARE 2017-2018 Expedition between January 11 and February 12 2018 under the auspices of Turkish Republic Presidency, supported by the Ministry of Science, Industry and Technology, and coordinated by Istanbul Technical University Polar Research Center, we first visited nunataks south and west of Princess Elisabeth Station: Utsteinen, Perlebandet and Teltet nunataks. Among these, we studied Utsteinen nunatak and the local terminal moraine in detail. Utsteinen is composed of granite and pegmatite. We then identified abandoned valleys. These are located few hundred meters above today's active glaciers and free of ice. Therefore, we focused on: (1) the Dubois Pass in Vikinghøgda; (2) the Dry Valley and the Ketelers Glacier in Widerøe Mountains; and (3) Nunataks on the right-lateral of the Gunnestad Glacier, to the east of the Yuboku Valley in Walnum Mountains (Figure 1). Finally, we completed the reconnaissance study of Mount Nils Larsen. These nunataks are made of Late Proterozoic Amphibolite-facies and lower-grade metamorphic rocks intruded by Paleozoic granites and pegmatites and partially covered by Quaternary tills except for the Dubois Pass, which consists of granulite facies metamorphic rocks.

In order to go back in time with the drainage pattern of the Eastern Antarctic Ice Sheet, we collected 38 surface samples from the erratic boulders left in these valleys by the ice at the time of surface lowering. We analyzed the accumulation of in-situ cosmogenic ^{10}Be, ^{14}C, ^{26}Al and ^{36}Cl in these samples and then determined the timing and amount of the thinning of the ice sheet, as well as the subglacial erosion. First results will be presented.
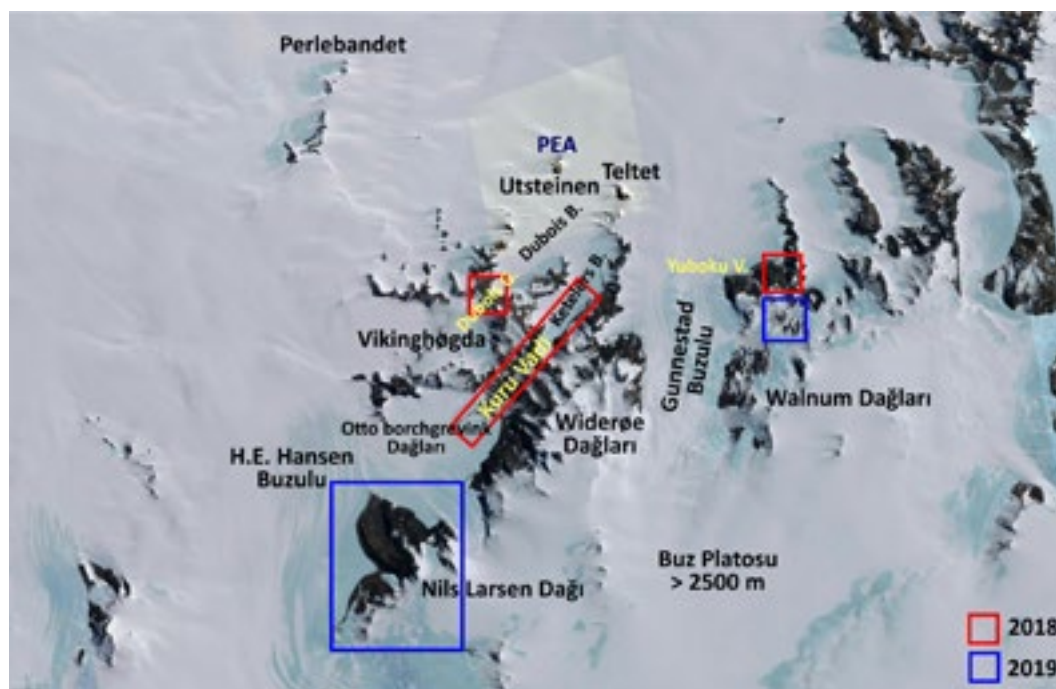

Figure 1. Location of PEA and nunataks in the western Sør Rondane Mountains. Red rectangles indicate the studied nunataks during the BELARE 2017-2018. Blue rectangles show the nunataks proposed for the BELARE 2018-2019.

11.2
An attempt to reconstruct planetary radiative imbalance over the last 40,000 years

Daniel Baggenstos [1], Marcel Häberli [1], Jochen Schmitt [1], Hubertus Fischer [1]

[1] *Physikalisches Institut, Klima- und Umweltphysik, Universität Bern, Sidlerstrasse 5, CH-3012 Bern (baggenstos@climate.unibe.ch)*

Global climate change arises from an energy imbalance at the top of the atmosphere (TOA). The direct measurement of TOA radiative fluxes is difficult even today, such that most assessments of it are based on changes in the total energy content of the Earth system. We apply the same approach to estimate the long term evolution of the planetary radiative imbalance in the past.

The energy budget of the climate system is dominated by the ocean's heat capacity. On Pleistocene timescales the latent heat changes associated with the waxing and waning of the large ice sheets are of similar magnitude as the ocean heat uptake. Ice core noble gas thermometry allows us to estimate changes in ocean heat content, while sea level reconstructions provide a measure for the contribution of the ice sheets from their latent heat release or consumption. The temporal derivation of the sum of these two dominant components should yield the planetary radiative imbalance.

We present measurements of noble gas derived mean ocean temperature from the EDC ice core covering the past 40,000 years. We infer TOA radiative imbalance as described above. As expected from the relatively stationary climates of the last glacial maximum and the Holocene, the radiative imbalance is close to 0.0 W/m^2 in those periods. During the deglaciation a positive imbalance is maintained for ~10,000 years, with two distinct peaks that reach up to 0.4 W/m^2, highlighting the importance of internal variability in the climate system.

11.3

Influence of the geology and meteorological conditions on indoor radon concentrations in the Jura mountains: preliminary results of the Interreg project Jurad-bat

Céline de Potter Longchamp [1], Joëlle Goyette Pernot [1]

[1] *Hight School of Engineering and Architectur, Pérolles 80, CH-1700 Fribourg (celine.depotterlongchamp@hefr.ch)*

Radon is a natural radioactive gas present everywhere in the earth's crust and may cause lung cancer when it decays after inhalation (WHO 2009). In Switzerland, it is the second cause of lung cancer after smoking and after the Federal Office of Public Health (FOPH, https://www.bag.admin.ch): 200-300 deaths per years are linked to radon. As the product of the decay of Uranium, radon is present everywhere and preferentially on igneous rocks. In Switzerland, we find higher radon concentrations in Aples but also in the limestones of Jura. The amount of indoor radon concentrations depends on the underlying rocks but also of the permeability of the soils, routes (faults, folds, sinkholes, …) driving the gas to the surfaces (Pampuri et al., 2018) and on meteorological conditions.The goal of the Interreg (France – Switzerland) project Jurad-bat is to improve knowledge of the indoor radon risk management, to create a database collecting cross-border data on indoor air quality and to develope a WEB plateform. Through this platform, different public (such as building professionals, architects, deputy as well as large public…) will be able to share experiments, ask for questions, search for informations, training and so on.

In order to do so it is of great importance to have a better knowledge of radon dynamic at the interface in between the soil under the house and the indoor air. So we have to caracterise the influence of the geology and meteorological parameters on the fluctuations of the gas inside builings located in the Jura mountains. Figure 1a present the studied area and the results of radon measurements (national database of Swiss FOPH) exceeding the new limit value of 300 Bq/m^3 (Ordonnance sur la radioprotection, ORaP 2017). As first constatation, we can note a huge concentration of building exceeding the new reference value and that a significant amount of these points are located in the proximity of folds and geologic faults. However limestone is not known for it's uranium enrichment which is the mother of radon gas. What do explain this unusual occurrence? Does it have a specific impact on indoor radon concentration?

Considering the geology and tectonic structure of the soil to study the impact of meteorological conditions and the influence of a building on radon concentration variations, two houses were instrumented for one year. Measurements are still going. One building is a 1895 familial house completely renovated and located on Neuchâtel lake's shore. The second one is an old farm ($_\sim$ 1850) partially refurbished and situated at la Brévine that is located at 1000 meters altitude. In these two buildings, we measure the same parameters in analogous conditions. The parameters are radon concentration,

temperature, atmospheric pressure, humidity, indoor and outdoor pressure differential and CO_2 with a timestep of 60 minutes. Measurments are also conducted in the soil around the houses. Meteorological conditions of the two places are coming from the closest meteorological stations from MeteoSwiss. Through these two cases, we noticed the influence of the human behavior and indoor conditions on radon concentration.

In Figure 1b present 10 days measurements of radon concentration and pressure in a non-isolated North-West oriented room . We can see that radon concentrations are inversly correlated with indoor pressure variations. Indeed, high radon concentrations, 1730 Bq/m^3 for the higher, correspond to lowest pressure values, 880 hPa.

To summarize, the indoor radon concentration depends on the nature of the underlying soil and rock, the meteorological conditions but also the type of building and the behavior of the inhabitant.
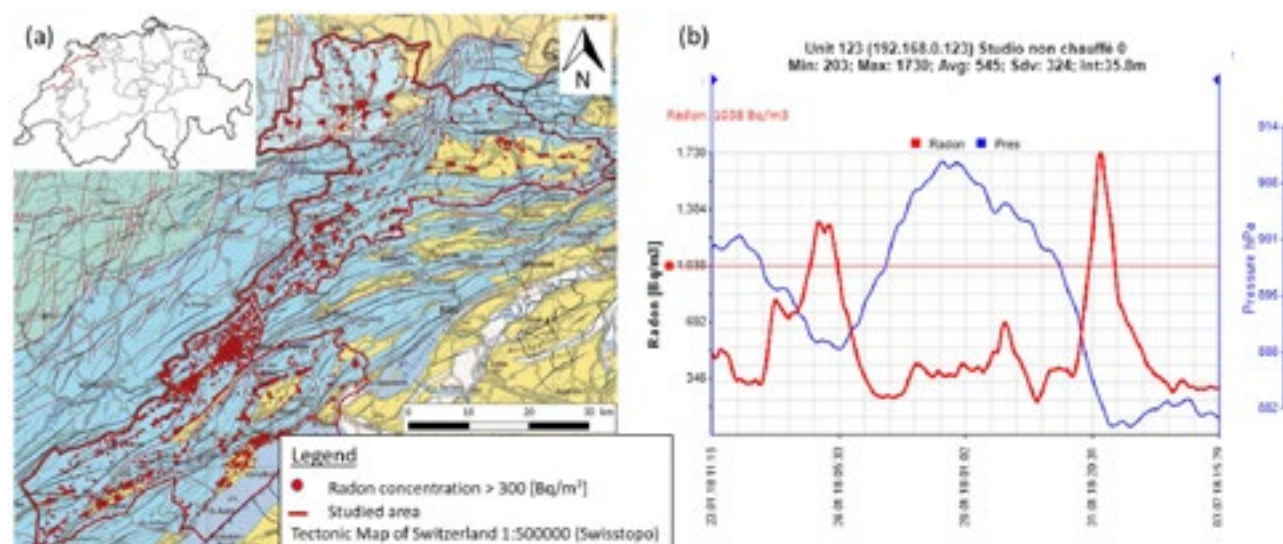
Figure 1. (a) indoor radon concentrations higher than 300 Bq/m³ in the Jura and Neuchâtel cantons; (b) indoor radon concentration during a 10 days period and the pressure.

REFERENCES

Spicher, A.1976: carte tectonique de la Suisse, 1:500000, Commission Géologique Suisse.

World Health Organization (WHO) 2009: WHO handbook on indoor radon: A public health perspective. Hajo Zeeb & Ferid Shannoun (Eds.). IBSN 978-92-4-154767-3/

Ordonnance sur la radioprotection (ORaP), 2018.

Pampuri, L., Caputo, P. & Valsangiacomo, C. 2018 : Effects of buildings' refurbishment on indoo air quality. Result of a wide survey on radon concentrations before and after energy retrofit interventions. Sustainable Cities and Society 42 100-106.

11.4
Timing the deposition of Swiss Deckenschotter with cosmogenic isochron burial dating

Reto Grischott*, F. Kober**, S. Ivy-Ochs*, K. Hippe*, M. Lupker[3], M. Christl*, C. Vockenhuber*, C. Maden[3]

[1] Labor für Ionenstrahlphysik, ETH Zürich, Otto-Stern-Weg 5, CH-8093 Zürich
[2] NAGRA, Hardstrasse 73, 5430 Wettingen
[3] Geologisches Institut, ETH Zürich, Sonneggstrasse 5, CH-8092 Zürich

The landscape in the northern Alpine Foreland is the combined result of numerous glaciations as well as tectonic and climatic processes. Aggradation of glaciofluvial sediments and the subsequent fluvial incision led to the development of terraces. The oldest terraces preserved in the Foreland – the so-called Deckenschotter – are morphostratigraphically divided into the Higher and Lower Deckenschotter units which are separated mostly by a significant altitude difference of ~100-150 m. Both gravel terraces represent spatially extensive paleosurfaces and can form plateaus up to 200-300 m above the modern valley bottom. The Higher and Lower Deckenschotter terraces have originally been defined due to their specific altitude range and a strong incision event must have been occurred between. Knowing the timing of deposition and incision of these terraces is of special interest for modelling the long-term safety of the deep geological repositories for nuclear waste disposal in the northern Alpine Foreland (NAGRA, 2014). Furthermore, absolute ages of former fluvial systems are crucial to establish incision and erosion scenarios, river drainage patterns and related base-level reconstructions.

Dating glaciofluvial gravels which are much older than the age range of radiocarbon methods has been a challenge. However, Balco and Rovey (2008) presented the isochron burial dating approach to determine a depositional age of a sediment unit. The method makes use of the differential decay of an in-situ produced nuclide pair in a mineral target (here: ^{26}Al and ^{10}Be in quartz) and the fact that pebbles in the initial fluvial sediment have different nuclide signatures due to varying erosion. The measured nuclide ratios of ^{26}Al and ^{10}Be enables to reconstruct a regression through the data in the ^{26}Al-^{10}Be-Plot whose slope is indicative for the age. A recent publication proves the applicability of the method but also discusses the problems of measuring ^{26}Al in old glacial sediments (Akçar et al., 2017). The low inheritance of glaciofluvial sediments and a subsequent long burial time result in low ^{26}Al concentrations and therefore a low ^{27}Al background is required because of the ^{26}Al/^{27}Al detection limits. Accordingly, careful cleaning of the samples is needed. Samples with a sufficiently low total Al content were further processed for the analysis of cosmogenic ^{10}Be and ^{26}Al.

In this study, we aim to reconstruct the chronology of the Deckenschotter units along a transect in space and time at three locations: the gravel pit Tromsberg in Kirchdorf (AG) and Feusi in Oberweningen (ZH) which both represent the Higher Deckenschotter (HDS) of the Dürn-Gländ region and a nearby gravel pit at Bärengraben in Würenlingen (AG) representing the Lower Deckenschotter (TDS) of the Iberig region. Previous age estimates for HDS suggest an age range of 1.5 ±0.2 Myr based on isochron burial dating at the nearby site Siglistorf which is farther north of the sampled sites (Akçar et al., 2017) and 1.8 to 2.5 Myr based on mammalian faunal assemblages (MN17) at site Irchel (Bolliger et al. 1996). At all three sites, a combination of pebbles from various lithologies, sand lenses and amalgated vein quarz clasts were sampled at the base of the 10-15 m high outcrops in order to maximize the spread in the data.

Additionally, two sites representing valley fillings during the period of the Hochterrasse (HT) are attempted to date. A gravel pit in Beringen (SH) representative for the Klettgau valley filling was chosen for a cross-calibration with recently established luminescence chronologies (Lowick et al., 2015). The latter question a previously established age estimates based on the interpretation of sedimentary facies and lithostratigraphy (Graf, 2009) making an independent age estimate desirable. Here, sands and pebbles at the base of the active, 40 m deep gravel pit were collected assuming that shielding was nearly complete and postburial production is negligible. The same principle of "true" or simple burial dating was applied to a drillcore from Glatttal valley filling (drill core Bülach, Buechi et al. (2018)). Again, existing luminescence data serve as an opportunity to cross-calibrate the age of the sediment deposition.

We will present some initial field and preliminary analytical data. First age estimates from sites with a solid data base will be presented and discussed in the context of landscape change.

REFERENCES

Akçar, N., Ivy-Ochs, S., Alfimov, V., Schlunegger, F., Claude, A., Reber, R., Christl, M., Vockenhuber, C., Dehnert, A., Rahn, M., and Schlüchter, C., 2017, Isochron-burial dating of glaciofluvial deposits: First results from the Swiss Alps: *Earth Surface Processes and Landforms*, v. 42, no. 14, p. 2414-2425.

Balco, G., and Rovey, C. W., 2008, An Isochron Method for Cosmogenic-Nuclide Dating of Buried Soils and Sediments: *American Journal of Science*, v. 308, no. 10, p. 1083-1114.

Bolliger, T., Fejfar, O., Graf, H. R. & Kälin, D. (1996): Vorläufige Mitteilung über Funde von pliozänen Kleinsäugern aus den höheren Deckenschottern des Irchel (Kt. Zürich). – Eclogae geol. Helv. 89/3, 1043–1048.

Buechi, M. W., Graf, H. R., Haldimann, P., Lowick, S. E., and Anselmetti, F. S., 2018, Multiple Quaternary erosion and infill cycles in overdeepened basins of the northern Alpine foreland: *Swiss Journal of Geosciences*, v. 111, no. 1, p. 133-167.

Graf, H. R., 2009, Stratigraphie von Mittel- und Spätpleistozän in der Nordschweiz, Bern : Landesgeologie, Beiträge zur geologischen Karte der Schweiz. Neue Folge, 198 S. p.:

Lowick, S. E., Buechi, M. W., Gaar, D., Graf, H. R., and Preusser, F., 2015, Luminescence dating of Middle Pleistocene proglacial deposits from northern Switzerland: methodological aspects and stratigraphical conclusions: *Boreas*, v. 44, no. 3, p. 459-482.

Nagra (2014): Sicherheitstechnischer Bericht zu SGT-Etappe 2: Sicherheitstechnischer Vergleich und Vorschlag der in Etappe 3 weiter zu untersuchenden geologischen Standortgebiete. Nagra Technischer Bericht NTB 14-01.

11.5
Glacial chronology of the Bale Mountains and its implications for the early human occupation of the southern Ethiopian Highlands

Alexander Raphael Groos [1], Naki Akçar [2], Christof Vockenhuber [3] & Heinz Veit [1]

[1] Institute of Geography, University of Bern, Hallerstrasse 12, CH-3012 Bern (alexander.groos@giub.unibe.ch)
[2] Institute of Geological Sciences, University of Bern, Baltzerstrasse 1+3, CH-3012 Bern
[3] Institute for Particle Physics and Astrophysics, ETH Zürich, Otto-Stern-Weg 5, CH-8093 Zürich

The Bale Mountains in southern Ethiopia represent the largest afro-alpine environment above 4,000 m on the African continent (Miehe & Miehe 1994). Even though ice caps and outlet glaciers are absent in the southern Ethiopian highlands nowadays, typical landscape features (U-shaped valleys, cirques, moraines, erratic boulders, roche moutonnées etc.) as well as geomophological phenomena (e.g. large sorted patterned grounds) indicate different phases of extensive glacial and periglacial activity in the Bale Mountains during the Pleistocene (Osmaston et al. 2005). Detailed knowledge of the glacial history and palaeo-climate in the region is still lacking, as it is for most of the high African mountains, except for Mt. Kenya, Kilimanjaro and Rwenzori (Mark & Osmaston 2008). Information on the timing and extent of the maximum glaciation in southern Ethiopia are contributing to a better understanding of the palaeo-climate and landscape evolution of the alpine environment. They serve as an important proxy for palaeo-ecologists and archeologists to answer the question whether humans already migrated to the more humid and meltwater-supplying mountains in East Africa during the late Pleistocene – a period when the lowlands were dry and probably uninhabitable. The extent of palaeo-glaciations in southern Ethiopia is determined by extensive mapping of terminal and lateral moraines in the field as well as on high-resolution satellite imagery. Surface exposure dating is applied to 75 boulders from the Bale and Arsi Mountains to constrain the timing of the different glacial stages.

REFERENCES
Mark, B. G. & Osmaston, H. A. 2008: Quaternary glaciation in Africa: key chronologies and climatic implications. Journal of Quaternary Science, 23, 589-608.
Miehe, S. & Miehe, G. 1994: Ericaceous Forests and Heathlands in the Bale Mountains of South Ethiopia - Ecology and Man's Impact. Stiftung Walderhaltung in Afrika, Hamburg.
Osmaston, H. A., Mitchell, W. A. & Osmaston J. A. N. 2005: Quaternary glaciation of the Bale Mountains, Ethiopia. Journal of Quaternary Science, 20, 593-606.

11.6
Twannberg: Meteorite strewn field and glacial transport

Beda A. Hofmann [1] [2], Naki Akçar [2], Pierre Valla [2]

[1] *Naturhistorisches Museum Bern, Bernastrasse 15, CH-3005 Bern (beda.hofmann@geo.unibe.ch)*
[2] *Institut für Geologie, Baltzerstrasse 1+3, CH-3012 Bern*

Since the find of the first 15.9 kg piece of the Twannberg meteorite in 1984, numerous additional specimens have been found, mainly 2015-2018. By end of August 2018, >1130 specimens with a total mass of ~120 kg were known. Twannberg is part of the extremely rare type IIG class of iron meteorites (Hofmann et al. 2009, Wasson & Choe 2009), which allows the easy recognition of new finds as being part of the same fall event. Twannberg meteorites occur in three find areas (Fig. 1): A mass-sorted strewn field relict of 5.7x1 km is present on Mont Sujet (altitude 1000-1370 m), while finds in the Twannberg-Magglingen area are distributed over 3.2x0.9 km (altitude 950-1080 m), show no mass-sorting and are associated with glacial till external of the Last Glacial Maximum (LGM). A series of smaller fragments was found in the Twannbach canyon, where they likely were eroded out from pre-LGM till. The mass-sorted Mont Sujet finds indicate a fall direction from northeast to southwest. Twannberg was a large meteorite with a pre-atmospheric mass of at least 250 t (Smith et al. 2017). The age of the Twannberg fall is 202±33 ka based on $^{41}Ca/^{36}Cl$ (Smith et al. 2017), possibly lower by ~20 ka when using an updated half life for ^{41}Ca (Smith et al. 2018).
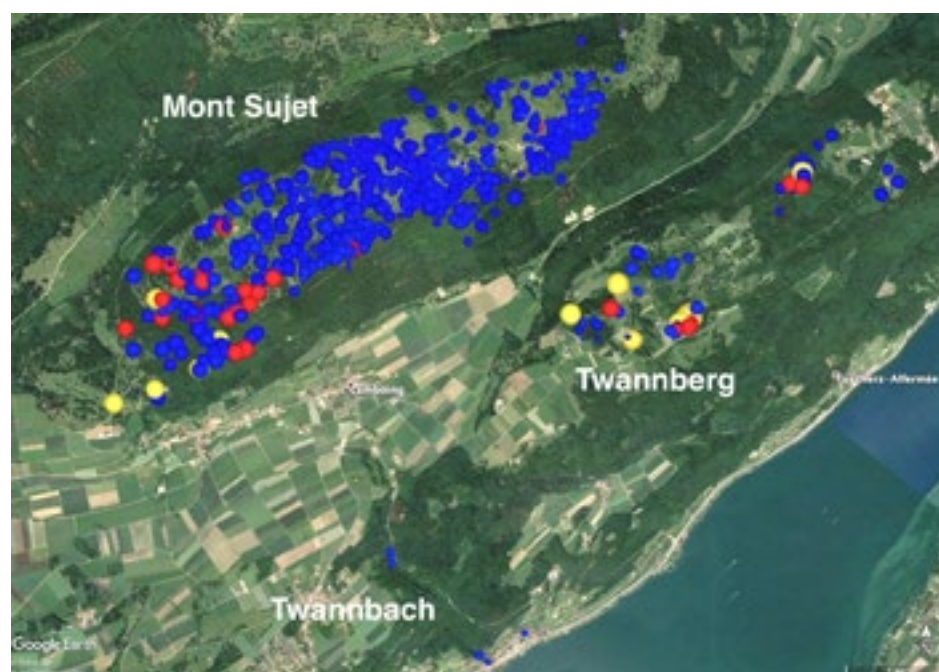
Figure 1. Known distribution of Twannberg meteorite finds as of August 2018. Blue: <0.4 kg, red: 0.4-1 kg, yellow: >1 kg. Lake of Biel is at bottom right. Image: Google Earth.

The terrestrial age is surprisingly high, but consistent with associated glacial sediments of the second last glaciation (Beringen or MIS6). The currently observed distribution of meteorite fragments in the Twannberg-Magglingen area requires glacial transport in direction northeast over a distance of at least 5-10 kilometers shortly after the fall event.
Absence of mechanical wear, as demonstrated by preserved fusion crust on some transported specimens, indicates a transport on the ice, and not at the base of the glacier. The most likely scenario is a fall on the ice, followed by transport over several kilometers. The presence of a part of the undisturbed strewn field on Mont Sujet shows that moving ice did not affect the higher parts of Mont Sujet above ~1200 m altitude at the time of the fall. The distribution of Twannberg meteorite fragments therefore provides information about the minimum extent of the second last glaciation in the Swiss Jura. Attempts to date meteorite-hosting loess-like soils on Mont Sujet and a glacial boulder at ~1300 m altitude in the area are currently underway.

The search for Twannberg meteorite fragments is mainly carried out by a group of meteorite collectors-enthousiasts in close collaboration with the Natural History Museum Bern, the "Abteilung Naturförderung, Amt für Landwirtschaft und Natur (LANAT)" of the Canton of Bern and the Archaeological Survey of the Canton of Bern.

REFERENCES

Hofmann, B.A., Lorenzetti, S., Eugster, O., Krähenbühl, U., Herzog, G., Gnos, E., Eggimann, M., Wasson, J.T. 2009: The Twannberg (Switzerland) IIG iron meteorites: Mineralogy, chemistry and CRE ages, Meteoritics and Planetary Science, 44, 187-199.

Smith, T., Hofmann, B.A., Leya, I., Merchel, S., Pavetich, S., Rugel, G., Scharf, A. 2017: The cosmic-ray exposure history of the Twannberg iron meteorite (IIG), Meteoritics and Planetary Science, 52, 2241-2257.

Smith, T., Hofmann, B.A., Leya, I., Merchel, S., Rugel, G., Pavetich, S., Scharf, A. 2018: The cosmic-ray exposure history of the big iron Twannberg (IIG) meteorite. Annual Meeting of the Geoscience Union (CGU), Beijing, October 2018.

Wasson, J.T., Choe, W.-H. 2009. The IIG iron meteorites: Probable formation in the IIAB core, Geochimica et Cosmochimica Acta, 73, 4879-4890.

11.7

[10]Be exposure dating reveals multiple glacier advances and still stands in the southern Écrins massif (French Alps) during the Late Glacial and the Early Holocene

Felix Martin Hofmann [1], Helena Alexanderson [1], Philippe Schoeneich [2], Jordan R. Mertes [3], Laëtitia Léanni [4] & ASTER Team1[4]

[1] Department of Geology, Lund University, Sölvegatan 12, SE-22362 Lund (fmhofmann9892@gmail.com)
[2] Institut d'urbanisme et de géographie alpine, Université Grenoble-Alpes, 14 – 14 bis, avenue Marie Reynoard, F-38100 Grenoble
[3] Arctic Geology Department, The University Centre in Svalbard (UNIS), P.O. Box 156, N-9171 Longyearbyen
[4] CNRS, IRD, INRA, Coll France, UM 34 CEREGE, Aix-Marseille Université, Technopôle de l'Environnement Arbois-Méditerranée, BP 80, F-13545 Aix-en-Provence

The chronology of post-Last Glacial Maximum (LGM) glacier fluctuations in the French Alps is poorly understood and only few chronological constraints on Late Glacial and Early Holocene glacier variability have hitherto been obtained (e.g. Chenet et al. 2016). This study aims at filling this gap by mapping and dating moraines in two neighbouring valleys in the southern part of the Écrins massif. Some of the pre-Little Ice Age (LIA) moraines in one of the valleys have already been mapped and assigned to the Late Glacial/Early Holocene transitional period (Hofmann 2016). Therefore, these moraines were considered a suitable target to obtain additional chronological benchmarks to enable palaeoclimatic as well as palaeogeographic reconstructions.

As a first step of the study, aerial photographs from the French National Institute of Geographic and Forest Information (IGN) were used for establishing a Digital Surface Model (DSM) and an orthophoto of the study area through the use of the structure-from motion approach. The moraines in the studied area were mapped using a combination of a DSM-based hillshade, field notes and photographs and were numbered based on their relative position in the field to finally establish a morphostratigraphy.

Secondly, the [10]Be concentration in the quartz mineral fraction of 41 boulders from selected moraines was determined to infer the duration of their surface exposure to cosmic rays. The obtained [10]Be exposure ages were then compared with previously published [10]Be exposure ages from moraines at key sites across the Alps, recalculated according to the most recent published production parameters for suitable comparison.

As a third step, the Equilibrium Line Altitude (ELA) depression relative to the end of the LIA during the deposition of all pre-LIA moraines in the study area was reconstructed to allow for stratigraphical correlations of non-sampled moraines with dated moraines. The GlaRe ArcGIS toolbox (Pellitero et al. 2016) was used to establish digital elevation models of the palaeoglaciers during moraine deposition. The application of a second ArcGIS toolbox (Pellitero et al. 2015) enabled their ELAs to be determined, whereby an accumulation area ratio of 0.67 was assumed throughout, as done elsewhere in the Alps (Ivy-Ochs 2015).

A [10]Be exposure age from a large boulder on the distal side of the lowermost sampled moraine indicates that this moraine may have been shaped during a temporary halt in glacier recession or the culmination of a glacial re-advance before the onset of Greenland interstadial 1. Given the location of the moraine at the confluence of two valleys, the moraine was probably deposited at the common margin of the glaciers from both valleys. During this potential event, the ELA of the palaeoglacier from the southern valley was depressed by about 210 m relative to the LIA ELA, whereas the ELA of the formerly confluent two glaciers from the northern valley must have been situated at a 500-600 m lower elevation than at the end of the LIA. The moraine was certainly reached or re-occupied by the palaeoglacier from the southern valley at the onset of Greenland Stadial 1 (GS-1) when the ELA was 220 m lower than at the end of the LIA. The [10]Be exposure ages indicate multiple glacier advances or still stands during GS-1 and potentially during the Early Holocene which were associated with ELA depressions of 120-220 m relative to the end of the LIA.

The review of data from regional and hemispheric palaeoclimatological archives other than glaciers suggest that the lowermost sampled moraine was shaped or re-occupied during a glacial re-advance which was triggered by the hemispheric cooling at the onset of GS-1. The agreement of our new [10]Be exposure ages with recalculated exposure ages from moraines at other sites in the Alps that have been assigned to the Egesen and the Kartell stadials, suggest a common climatic origin of the glacier advances or still stands. Since the reconstructed ELA depressions in the southern Écrins massif during the Late Glacial/Holocene transitional period are in good agreement with the results of previous studies from

[1] Georges Aumaître, Didier L. Bourlès & Karim Keddadouche

the Austrian and Swiss Alps (Ivy-Ochs 2015), it can be inferred that these regions were then subjected to atmospheric circulation patterns similar to those at the end of the LIA. Overall, the new [10]Be exposure ages contribute to a significant refinement of the chronology of post-LGM glacier fluctuations in the Écrins massif.

REFERENCES

Chenet, M., Brunstein, D., Jomelli, V., Roussel, E., Rinterknecht, V., Mokadem, F., Biette, M., Robert, V., Léanni, L. & ASTER Team 2016: [10]Be cosmic-ray exposure dating of moraines and rock avalanches in the Upper Romanche valley (French Alps): Evidence of two glacial advances during the Late Glacial/Holocene transition. Quaternary Science Reviews, 148, 209-221.

Hofmann, F. M. 2016: Les fluctuations glaciaires dans le vallon de Rougnoux. Tables, drawings and photographs.

Ivy-Ochs, S. 2015: Glacier variations in the European Alps at the end of the last glaciation. Cuadernos de investigación geográfica, 41, 295-315.

Pellitero, R., Rea, B. R., Spagnolo, M., Bakke, J., Hughes, P., S. Ivy-Ochs, S., Lukas, S. & Ribolini, A. 2015: A GIS tool for automatic calculation of glacier equilibrium-line altitudes. Computers & Geosciences, 82, 55-62.

Pellitero, R., Rea, B. R., Spagnolo, M., Bakke, J., Ivy-Ochs, S., Frew, C. R., Hughes, P., Ribolini, A., Lukas, S. & Renssen, H. 2016. GlaRe, a

GIS tool to reconstruct the 3D surface of palaeoglaciers. Computers & Geosciences, 94, 77-85.

11.8

Quantifying subglacial erosion beneath the Tsanfleuron glacier, Switzerland

Olivia Kronig [1], Susan Ivy-Ochs [1], Sandra Grazioli [3], Marc Luetscher [2], Katherine Schide [3], Sean Gallen [3], & Christof Vockenhuber [1]

[1] Laboratory of Ion Beam Physics, Otto-Stern-Weg 5, CH-8039 Zürich (okronig@phys.ethz.ch)
[2] Swiss Institute for Speleology and Karst Studies (SISKA), Rue de la Serre 68, CH-2301 La Chaux-de-Fonds
[3] Geological Institute, ETH Zürich, Sonneggstrasse 5, CH-8092 Zürich

Knowledge of subglacial erosion rates is critical for understanding the long-term evolution of the shape of the Alps. In most cases subglacial erosion rates are estimated over the whole glacier footprint by measuring the sediment (entrained and dissolved) load in the outflowing meltwater. As production of cosmogenic nuclides drops-off predictably with depth down into rock, measurement of their concentrations allows quantification of the depth of erosion into bedrock beneath a glacier (Wirsig et al., 2017). Both methodologies, meltwater sediment yield and cosmogenic nuclides, have thus far only been used in crystalline bedrock. Subglacial erosion on a limestone bed has rarely been directly, quantitatively measured before. In contrast to a crystalline bed, the presence of karst plays a decisive role. Therefore our primary scientific question is: To which extent and in which way does the presence of subglacial karst affect the hydrological drainage system and influence glacial erosion rates and patterns across the bed of the Tsanfleuron glacier.

We use a combined approach of detailed geomorphological mapping and cosmogenic nuclide measurements to ascertain how much the Tsanfleuron glacier has eroded its limestone bed over the last several millennia. The Tsanfleuron glacier (ca. 3 km^2 in 2015) is located on a gentle slope near Sanetschpass in the western Swiss Alps. Since the Little Ice Age, ongoing glacier retreat revealed more and more of the polished limestone bed. Furthermore, abundant straight and sinuous subglacial Nye-channels, as well as scallops on the lee-side of roche mountonnées can be observed. Karst features of the glacier forefield include swallow holes and pervasive fault-controlled linear drainage entryways. Study of these features was enabled by high resolution imagery and digital elevation model (8 cm) acquired with a drone (E-Bee; https://www.sensefly.com/drones/ebee.html), which supported field mapping and production of a detailed geomorphological map.

A first set of 14 samples were taken inside and outside of the prominent LIA moraine and analysed for ^{36}Cl concentration. To calculate the subglacial erosion rates the MECED model by Wirsig et al. (2017) was used. The combination of the detailed map and the determined erosion rates give new insights on how karst drainage of subglacial meltwater affects subglacial abrasion by the Tsanfleuron glacier. These preliminary results will be complemented in summer 2018 with additional samples taken very close to the current ice margin. Multi-decimetre drill cores of the limestone will be used to look at the ^{36}Cl production depth profile to provide additional information about erosion patterns in the former glacier bed.

Figure 1. 3D view of the Tsanfleuron glacier, produced with a SWISSIMAGE 1 m and 25 cm resolution on the swissALTI3D (2 m resolution), Geodata © swisstopo.White numbered dots show sample location and number. The glacier is, at its front, approximately 1.7 km wide

REFERENCES
Gremaud, V., Goldscheider, N., Savoy, L., Favre, G. & Masson, H. 2009: Geological structure, recharge processes and underground drainage of a glacierised karst aquifer system, Tsanfleuron-Sanetsch, Swiss Alps, Hydrogeology Journal, 17, 1833-1848.

Wirsig, C., Ivy-Ochs, S., Reitner, J. M., Christl, M., Vockenhuber, C., Bichler, M., & Reindl, M. 2017: Subglacial abrasion rates at Goldbergkees, Hohe Tauern, Austria, determined from cosmogenic 10Be and 36Cl concentrations, Earth Surface Processes and Landforms, 42, 1119-1131.

11.9
Neotectonics drove landscape evolution in SW Amazonia

Umberto Lombardo [1,2]

[1] CASES research group, Universitat Pompeu Fabra, Ramon Trias Fargas 25-27, 08005, Barcelona, Spain
  (umberto.lombardo@@upf.edu)
[2] Institute of Geography, University of Bern, Hallerstrasse 12, CH-3012 Bern, Switzerland

A growing number of studies suggest that the Holocene has been a period of important paleoecological and landscape changes in SW Amazonia. These changes have been triggered by a combination of factors: neotectonics, climate change and river avulsions.We know that the southern movement of South American Summer Monsoon caused an increase in precipitations at about 4 to 3 kyr BP and the southward expansion of the Amazonian rainforest into north-eastern LM at the expense of the savannah; and that large scale river shifts formed fluvial distributary systems that covered most of the Bolivian Amazon. However, despite clear evidence of neotectonic activity during the Holocene, the contribution of this to the shaping of the landscape of SW Amazonia is still unclear. Here, I will present new data, retrived from remote sensing and field work in the Bolivian Amazon, showing how and when neotectonic events controlled both vegetation and river dynamics.
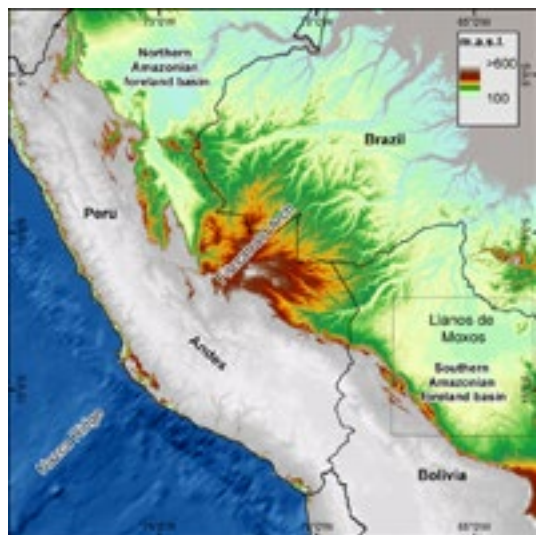
Figure 1. Topographic map of western South America with some important geological features. The south-eastern part of the Fitzcarrald Arch constitutes the LM's north-western border, which, together with the Brazilian Shield, to the north-east of the LM, forms a continuous barrier which impedes the drainage of the LM

REFERENCES
Lombardo, U. 2014: Neotectonics, flooding patterns and landscape evolution in southern Amazonia. Earth Surf. Dynam., 2(2), 493-511.
Lombardo, U., Rodrigues, L., Veit, H. 2018: Alluvial plain dynamics and human occupation in SW Amazonia during the Holocene: a paleosol-based reconstruction. Quaternary Science Review, 180: 30-41

11.10

A new speleothem record of the last interglacial (MIS-5e) from the Sieben Hengste

Marc Luetscher [1,2], Gina E. Moseley [2], Daniela Festi [3], Florian Hof [4], Christoph Spötl [2] & R. Lawrence Edwards [5]

[1] Swiss Institute for Speleology and Karst Studies (SISKA), Serre 68, CH-2300 La Chaux-de-Fonds
  (marc.luetscher@isska.ch)
[2] Institute of Geology, University of Innsbruck, Innrain 52, A-6020 Innsbruck
[3] Institute of Botany, University of Innsbruck, Sternwartestraße 15, A-6020 Innsbruck
[4] Swiss Society for Speleology
[5] Department of Earth Sciences, University of Minnesota

Quantifying the duration and magnitude of past interglacials is of prime importance to understand ecological adaptation to a warmer world. The Swiss Alps are particularly sensitive to even small hydroclimatic changes and thus require reliable records to unravel the complex spatial response. Here, we present a new speleothem record (7H-12) from the Sieben Hengste cave system, Switzerland, encompassing the last interglacial period (MIS-5e). The onset into the interglacial is dated at 129.8± 0.8 ka, consistent within error with other recently published records of Termination II for the European Alps (Häuselmann et al., 2015; Moseley et al., 2015). However, in marked contrast to these speleothem records, 7H-12 shows a rapid increase in $\delta^{18}O$, which reaches a climax at 128.4±0.8 ka and is followed by a gradual depletion until 117.5 ka. This distinct pattern, characterized by low interannual variability, suggests that 7H-12 was little affected by local processes and, thus, may represent a robust archive for the last interglacial at a regional scale. Pollen extraction from the speleothem calcite reveals concentrations of ca. 20 palynomorphs per gramm, with tree pollen assemblages dominated by *Alnus*, *Hedera, Corylus* and *Picea.* Several of these species are presently absent from the cave's hydrological catchment area, clearly indicating warmer conditions consistent with the stalagmite $\delta^{18}O$ record. Overall, this sample offers a unique opportunity to quantify the amplitude of the climate signal and its regional paleoenvironmental response over the entire last interglacial.

REFERENCES

Häuselmann A. et al., 2015. Timing and nature of the penultimate deglaciation in a high alpine stalagmite from Switzerland. Quat. Sci. Rev., 126, 264-275.

Moseley G. et al., 2015. Termination-II interstadial/stadial climate change recorded in two stalagmites from the north European Alps. Quat. Sci. Rev., 127, 229-239.

11.11

New insights into the detachment mechanism, runout and age of the Kandersteg rock avalanche

Corinne Singeisen [1], Susan Ivy-Ochs [2], Andrea Wolter [1], Olivia Kronig [2], Serdar Yesilyurt [3], Christof Vockenhuber [2], Naki Akçar [3]

[1] Geological Institute, Department of Earth Sciences, ETH Zurich, Sonneggstrasse 5, CH - 8001 Zürich
  (c.singeisen@bluewin.ch)
[2] Laboratory of Ion Beam Physics, ETH Zurich, Otto-Stern Weg 5, CH - 8093 Zurich
[3] Geological Institute, University of Bern, Baltzerstrasse 1 + 3, CH – 3012 Bern

In this study, improved understanding of the timing and process of the Kandersteg rock avalanche was achieved through a combination of field and remote mapping, cosmogenic nuclide dating and runout modelling. The Kandersteg rock avalanche is one of the largest rock slope failures in the Alps. Its volume was estimated to about 750 - 900 million m^3 and the landslide deposit stretches over about 10 km^2.

The event has previously been suggested to have occurred 9600 years ago based on dating lacustrine deposits underlying reworked rock avalanche material (Tinner et al. 2005). However, new ages derived from direct dating of the blocky landslide deposit can be presented in this study. This new understanding of the time of failure puts the Kandersteg rock avalanche in a new context.

Structural analysis of the source area shows that the basal sliding plane largely follows bedding. Bedding planes of Oehrlikalk with interbedded marl layers must have acted as a weakness zone crucial for the detachment of the event. Today's prominent lateral scarp of the rock slope failure is marked by a steeply dipping fault oriented NW-SE. This fault can be assigned to a prominent discontinuity set in the study area which is oriented normal to the fold axis of the regional-scale Doldenhorn fold. In the head scarp of the Fisistock release area both bedding planes and a steeply NW dipping discontinuity set are exposed.
It can be concluded that the structural setting of the Kandersteg rock avalanche fulfills the typical criteria for the development of large translational rock slope failures. The Kandersteg rock avalanche can hence be seen as an impressive and classical example for a structurally controlled rock slope failure.

Through field observations, structural analysis and runout modelling using DAN3D one can separate four main phases of rock avalanche emplacement. In a first phase, the rock mass detached from the upper fold limb of the recumbent Doldenhorn nappe along pre-existing discontinuities. The sliding body then fragmented and hit the valley floor and steep valley sides near Kandersteg causing intense crushing of the main landslide body but preserving a characteristic boulder carapace. In a next phase the dry fragmented rock avalanche propagated northward over a substrate of fluvial sediments. The source rock stratigraphy was preserved in the deposit. Tertiary sandstones outcropping high up on the Fisistock were deposited farthest from the source while Kieselkalk boulders are found predominantly in the proximal parts of the deposit overlying the main landslide body composed of Oehrlikalk. Internal tensile deformation of the landslide body led to the formation of hummocky terrain with transverse ridges. In a final phase the landslide became more fluid through entrainment of water and water-rich sediments. Landslide movement continued northwards where it stopped at a distance of around 10 km from the source approximately 8 minutes after initial failure. The results of this study hence provide fundamental information on emplacement processes of long-runout events that evolve into more fluid mass movements due to the entrainment of sediment substrate.

REFERENCES

Tinner et al. (2005) 'Der nacheiszeitliche Bergsturz im Kandertal (Schweiz): Alter und Auswirkungen auf die damalige Umwelt.', *Swiss Journal of Geosciences,* 98, pp. 83-95.

11.12
Seismic analysis of overdeepened Quaternary deposits, northern Switzerland

Thomas Spillmann[1], Herfried Madritsch[1], Gaudenz Deplazes [1], Louis Hauvette [2], Bernd Fiebig [2], Lorenz Keller [3], & Andreas Hölker [4]

[1] Nagra, Hardstrasse 73, CH-5430 Wettingen (thomas.spillmann@nagra.ch)
[2] Geneva Petroleum Consultants International S.A., Geneva
[3] roXplore gmbh, Amlikon
[4] Geophytec GmbH, Jestetten

Quaternary deposits in overdeepended valleys in northern Switzerland provide important data for the site selection of geological repositories for radioactive waste in Switzerland (Nagra, 2014). Specifically, high-level radioactive waste must be placed deep enough not to be critically affected by future glaciation periods and related erosion processes. In order to improve the characterization of Quaternary deposits around Glatt and Thur rivers (Figure 1), Nagra undertook a 2D reflection seismic campaign in the winter of 2016/17. In this article, we outline the survey design, data acquisition, summarize its processing and highlight key interpretation results.

The project design was guided by (1) identification of geologically significant sections across the Glatt and Thur valleys, (2) proximity of borehole information, and (3) feasibility of seismic data acquisition with respect to topographic and cultural obstacles. The seismic survey included 16 seismic lines with a total length of 41.7 km (ca. 5200 shot points; 63% by vibrator and 37% dynamite sources). Individual line lengths varied from 1.5 to 6.6 km. The acquisition density and related field parameters also varied and were chosen with respect to the expected target depths. The seismic data acquisition itself was commissioned to a contractor (DMT, Germany).

The seismic data processing involved geometry setup, static corrections (restricted to the mostly thin weathering layer), signal enhancement, stacking velocity analysis, normal moveout correction, residual statics, stacking and post-stack Kirchoff time migration. A key advance of the time imaging analysis was to limit the static corrections to shallow depths, thereby keeping relatively low velocities in the Quaternary deposits. For this reason, reflections from underlying Tertiary and deeper deposits presented an artificial curvature.

We corrected this artificial curvature by application of a wave-equation post-stack depth migration procedure. This procedure required line-specific velocity fields that were developed using an iterative process combining interpretation and processing techniques. Information from the boreholes, preliminary deposit shapes and geological plausibility criteria were combined with velocity measurements to construct the velocity fields.

The resulting time and depth migrated images were used to provide new insights of the Quaternary deposits by developing geologically plausible shapes of the base Quaternary horizons. Typical truncations of reflectivity were generally recognised in the survey areas, resulting in a new record of the valley flanks. The Quaternary-internal structure was assessed by projecting lithological markers and units from available boreholes onto the seismic lines. Moreover, the linking of lithological units with a certain seismic signature guided the characterisation of the Quaternary infill.

This study provides important new advances into the infill record of the overdeepend valleys. Furthermore, it served as important database for the siting of new Quaternary exploration boreholes. The core material from these boreholes in combination with the results from this study promise new insights into the complete infill record of overdeepend valley-forming processes.

REFERENCES

Nagra (2014): SGT Etappe 2: Vorschlag weiter zu untersuchender geologischer Standortgebiete mit zugehörigen Standortarealen für die Oberflächenanlage: Geologische Grundlagen. Nagra Tech. Rep. NTB 14-02.
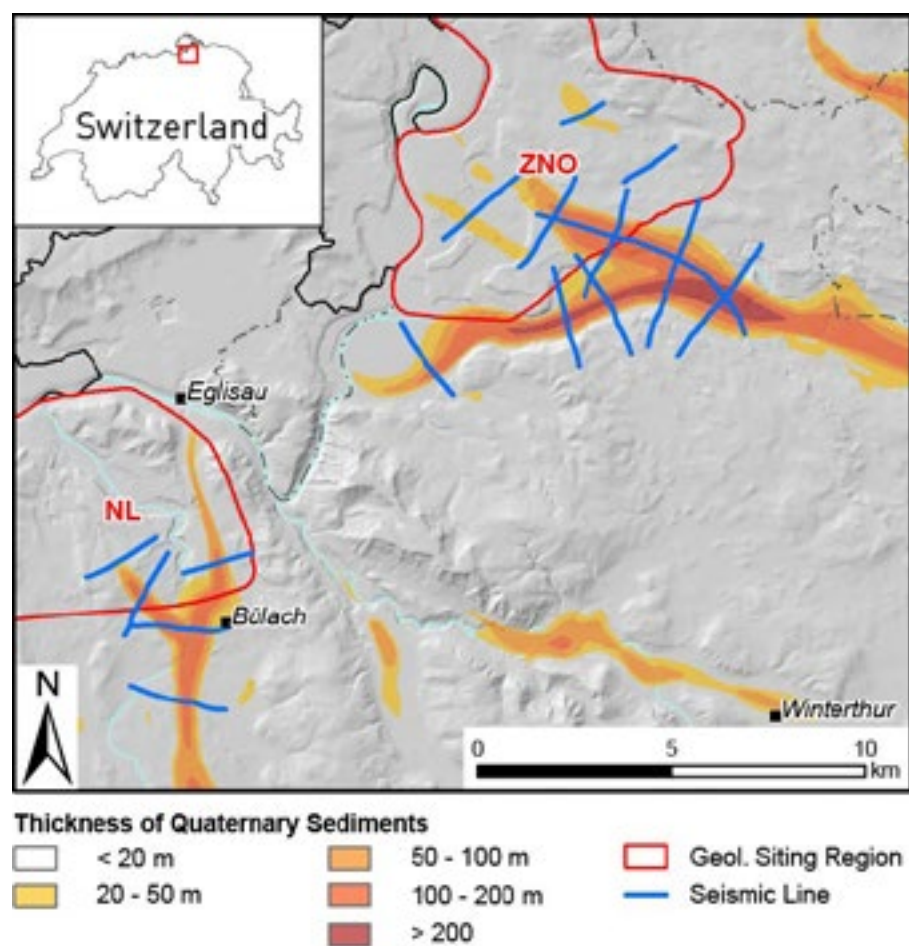
Figure 1. Map showing overdeepend Quaternary deposits in the siting regions for high-level radioactive waste Nördlich Lägern (NL) and Zürich Nordost (ZNO). The seismic line layout is shown in blue.

11.13

Increased nutrient supply to the Southern Ocean during the Holocene and its implications for the pre-industrial atmospheric CO_2 rise

Anja S. Studer [1,2], Daniel M. Sigman [3], Alfredo Martínez-García [2], Lena M. Thöle [4], Elisabeth Michel [5], Samuel L. Jaccard [4], Jörg A. Lippold [6], Alain Mazaud [5], Xingchen T. Wang [3,7], Laura F. Robinson [8], Jess F. Adkins [7] & Gerald H. Haug [2,9]

[1] *Department of Environmental Sciences, University of Basel, Basel, Switzerland (anja.studer@unibas.ch)*
[2] *Max Planck Institute for Chemistry, Climate Geochemistry Department, Mainz, Germany*
[3] *Department of Geosciences, Princeton University, Princeton, NJ, USA*
[4] *Institute of Geological Sciences and Oeschger Center for Climate Change Research, University of Bern, Bern, Switzerland*
[5] *Laboratoire des Sciences du Climat et de l›Environnement (LSCE), Gif-sur-Yvette Cedex, France*
[6] *Institute of Earth Sciences, Heidelberg University, Heidelberg, Germany*
[7] *Division of Geological and Planetary Sciences, California Institute of Technology, Pasadena, CA, USA*
[8] *Bristol Isotope Group, School of Earth Sciences, University of Bristol, Bristol, UK*
[9] *Department of Earth Sciences, ETH Zurich, Zurich, Switzerland*

A rise in the atmospheric CO_2 concentration of ~20 parts per million over the course of the Holocene has long been recognized as exceptional among interglacials and is in need of explanation. Previous hypotheses involved natural or anthropogenic changes in terrestrial biomass, carbonate compensation in response to deglacial outgassing of oceanic CO_2, and enhanced shallow water carbonate deposition. Here, we compile new and previously published fossil-bound nitrogen isotope records from the Southern Ocean that indicate a rise in surface nitrate concentration through the Holocene. When coupled with increasing or constant export production, these data suggest an acceleration of nitrate supply to the Southern Ocean surface from underlying deep water. This change would have weakened the ocean's biological pump that stores CO_2 in the ocean interior, possibly explaining the Holocene atmospheric CO_2 rise. Over the Holocene, the circum-North Atlantic region cooled, and the formation of North Atlantic Deep Water appears to have slowed. Thus, the 'seesaw' in deep ocean ventilation between the North Atlantic and the Southern Ocean that has been invoked for millennial-scale events, deglaciations and the last interglacial period may have also operated, albeit in a more gradual form, over the Holocene.

REFERENCES

Studer, A.S., Sigman, D.M., Martínez-García, A., Thöle, L.M., Michel, E., Jaccard, S.L., Lippold, J.A., Mazaud, A., Wang, X.T., Robinson, L.F., Adkins, J.F. & Haug, G.H. 2018. Increased nutrient supply to the Southern Ocean during the Holocene and its implications for the pre-industrial atmospheric CO_2 rise. *Nature Geoscience*, published online July 30, https://doi.org/10.1038/s41561-018-0191-8

11.14

How was the amount of precipitation perturbed during the Late Pleistocene in North Africa?

Abdallah S. Zaki [1,°], Mathieu Schuster [2], Georgina King [3], Frederic Herman [4], Sebastien Castelltort [1]

[1] Department of Earth Sciences, University of Geneva, Rue des Maraichers 13, 1205 Genève, Switzerland
  °(abdallah.zaki@etu.unige.ch)
[2] Institut de Physique du Globe de Strasbourg, UMR 7516 CNRS-Université de Strasbourg, Strasbourg, France
[3] Institute of Geological Sciences, University of Bern, Bern, 3012, Switzerland
[4] Institute of Earth Surface Dynamics, University of LausanneLausanne, CH-1015 Switzerland

During the Late Pleistocene, several studies have identified climate oscillations in North Africa based on changes of paleodischarge and sediment loads from the Atbara, Blue Nile and White Nile and from cave speleothems in northern Africa and southern Europe (Foucault and Stanley, 1989; Hoffmann et al., 2016). These studies concluded that climate oscillations during the Late Pleistocene were associated with six well-documented wet phases between 65 ka and 10 ka ago.

Independently of the above mentioned studies, several generations of inverted channel segments in the southern part of Egypt and northern part of Sudan have been identified by field and remote sensing studies (Giegengack, 1968; Zaki and Giegengack, 2016; Giegengack and Zaki, 2017). These river channels evidence that much wetter conditions existed in the past in the Sahara Desert. A chronological framework for these geomarkers is necessary to propose a robust paleoclimate reconstruction. Several of these outcrops are now submerged beneath the waters of Lake Nasser, however in this study, we collected samples from other outcrops in the southern part of Egypt in order to explore their potential association with the wet phases of the Late Pleistocene and the implications for landscape response to extreme climate change. The analyses planned involve ^{14}C, Optically-Stimulated Luminescence, and cosmogenic nuclide dating to constrain the ages of these outcrops and the timing of incision and infilling of the preserved channels. In addition, we will present new data on channel geometry, grain size and inferred paleoslopes with the aim of estimating paleodischarge.

REFERENCES

Foucault, A., and Stanley, D.J. (1989). Late Quaternary paleoclimatic oscillations in East Africa recorded by heavy minerals in the Nile delta: Nature, v. 339, p. 44–46, doi:10.1038/339044a0.

Giegengack, R.F., 1968. Late Pleistocene History of the Nile Valley in Egyptian Nubia.Unpublished Ph.D. Thesis, Yale University.

Giegengack, R.F., Zaki, A.S. (2017). Inverted topographic features, now submerged beneath the water of Lake Nasser, document a morphostratigraphic sequence of high-amplitude late-Pleistocene climate oscillation in Egyptian Nubia. Journal of African Earth Sciences 136, 176-187. doi.org/10.1016/j.jafrearsci.2017.06.027

Hoffmann, D. L., Rogerson, M., Spötl, C., Luetscher, M., Vance, D., Osborne, A., Fello, N., Moseley, G. (2016). Timing and causes of North African wet phases during the last glacial period and implications for modern human migration, Sci. Rep.-UK, 6, 36367, https://doi.org/10.1038/srep36367, 2016.

Zaki, A. S., R. Giegengack (2016). Inverted topography in the southeastern part of the Western Desert of Egypt. Journal of African Earth Sciences 121, 56-61. doi: 10.1016/j.jafrearsci.2016.05.020

P 11.1
Temperature reconstruction using speleothem fluid inclusions from Milandre cave, Jura Mountains, Switzerland

Stéphane Affolter [1,2,3], Anamaria Häuselmann [4,2], Dominik Fleitmann [5, 2] and Markus Leuenberger [1,2]

[1] Climate and Environmental Physics, Physics Institute, University of Bern, Switzerland (affolter@climate.unibe.ch)
[2] Oeschger Centre for Climate Change Research, University of Bern, Switzerland
[3] now at: International Foundation High Altitude Research Stations Jungfraujoch and Gornergrat, Bern, Switzerland
[4] Geological Institute, University of Bern, Switzerland
[5] Department of Archaeology and Centre for Past Climate Change, Geography and Environmental Science,
   University of Reading, UK

Apart from the well-known ice core archive in the polar region, speleothems are a great alternative for providing a direct witness of the past water cycle for low to middle latitudes. Among speleothems, stalagmites constitute a well preserved and precisely dated continental climate archive that record past environmental and climate changes namely through carbon ($\delta^{13}C_c$) and oxygen ($\delta^{18}O_c$) isotope composition of the calcite. Furthermore, stalagmites contain fluid inclusions (micrometric voids in the calcite matrix) that are filled with fossil water from past precipitation falling above the cave at the time the inclusions were formed, and thus are able to provide hydrogen (δD) and oxygen ($\delta^{18}O_{fi}$) isotopes of past drip water. All these parameters were measured for the last 14'000 years on two stalagmites coming from Milandre Cave (Jura Mountains, NW Switzerland), an area that have climate conditions representative for Western and Central Europe. Whereas the time resolution is high for calcite measurements (mean resolution of 4 years), block samples used for fluid inclusion measurements shows a ~10-20 years for the last 2000 years and ~50 years resolution beyond.

For the study site, there is a strong isotope-temperature dependency for recent precipitation allowing paleotemperature reconstruction from oxygen and hydrogen isotopes, whereas changes in $\delta^{13}C_c$ are mainly related to changes in soil microbial activity and vegetation type and activity above the cave. Moreover, connecting the fluid inclusion results to the available calcite oxygen isotope data may significantly increase the temporal resolution of past temperature reconstructions.

P 11.2

Variations in near-bottom flow of ACC during the past glacial cycle in SW Indian Ocean

Helen Eri Amsler [1], Nicole Schmid [1], Samuel L. Jaccard [1], Gerhard Kuhn [2] & Minoru Ikehara [3]

[1] *Institute of Geological Sciences and Oeschger Centre for Climate Change Research, University of Bern, Baltzerstrasse 1+3, CH-3012 Bern, Switzerland (helen-eri.amsler@geo.unibe.ch)*
[3] *Alfred-Wegener-Institut Helmholtz-Zentrum für Polar- und Meeresforschung, Am Alten Hafen 26, 27568 Bremerhaven, Germany*
[4] *Center for Advanced Marine Core Research, Kochi University, 200 Monobe-otsu, Nankoku, 783-8502*

The meridional overturning circulation of the ocean plays a key role in global climate variability by storing and redistributing heat, fresh water, carbon and nutrients. In the North Atlantic surface water sinks to the abyss, but a major part of this cycle is the return path from the ocean's interior through upwelling in the Southern Ocean. This upwelling is largely regulated by the latitudinal position of the Southern westerly winds associated with the deep-reaching Antarctic Circumpolar Current (ACC) (Rintoul et al. 2001).

Observations in the last few decades show progressively poleward intensifying winds and climate models suggest a possibly related increase in ACC transport and southward shifting of its mean position and increased upwelling. However, a number of recent numerical studies have shown that the sensitivity of the large-scale circulation in the Southern Ocean may be reduced by eddy-effects (Böning et al 2008).

As there remains significant uncertainty regarding the degree of sensitivity of the Southern Ocean circulation to wind stress and the response of the Antarctic circumpolar transport, our aim is to investigate the temporal and latitudinal evolution of the ACC dynamics over the last glacial cycle.

Previous studies suggested a stronger ACC during glacials in the Indian Ocean (Mazaud et al. 2010), but more recent studies in the Drake Passage and Scotia Sea indicate less throughflow during glacials and lateral differences in current speeds (McCave et al. 2014, Lamy et al. 2012). Here we present the sortable silt mean-size of a series of cores across the ACC in the SW Indian Ocean, the mean-size of the re-deposited silt fraction being proportional to the near-bottom flow velocity. Combining this with the ^{230}Th-data and the assuption that its rain rate is equivalent to its production from the decay of ^{234}U in the overlying water column allows a characterization of lateral sediment redistribution on the sea floor within the ACC flow regime.

REFERENCES
Böning C.W., Dispert A., Visbeck M., Rintoul S. R., Schwarzkopf F. U. (2008) Nature Geoscience, 1, 864-869.
Lamy F., Arz H. W., Kilian R., Lange C. B., Lembke-Jene L., Wengler M., Kaiser J., Baeza-Urrea O., Hall I. R., Harada N., Tiedemann R. (2015) PNAS, 112, 13496–13501.
Mazaud A., Michel E., Dewilde F., Turon J. L. (2010) G3, 11, doi:10.1029/2010GC003033.
McCave I. N., Crowhurst S. J., Kuhn G., Hillenbrand C-D., Meredith M. P. (2014) Nature Geoscience, 7, 113-116.
Rintoul S. R., Hughes C., Olbers D. (2001) in Siedler, G., Church, J., Gould, J. (eds). Ocean Circulation and Climate, Academic Press, 271-302.

P 11.3
Gravity model of the overdeepenings from the Bern area

Dimitri Bandou [1], Patrick Schläfli [1], Michael Schwenk [1], Guilhem A. Douillet [1], Edi Kissling [2] & Fritz Schlunegger [1]

[1] *Institut für Geologie, Universität Bern, Balzerstrasse 1+3, CH-3012 Bern (dimitri.bandou@geo.unibe.ch)*
[2] *Institut für Geophysik, ETH Zürich, Sonnegstrasse 5, CH-8092 Zürich*

The Swiss plateau has been covered by glaciers, which cut valleys several hundreds of meters in depth into its bedrock. These features are called tunnel valleys or overdeepenings (Preusser et al. 2010; Reber et al., 2016) and were possibly formed prior to 200'000-300'000 years before present, as new dating has shown (M. Schwenk, pers. comm. 2018, Preusser et al., 2010). The goal of this work is to understand which mechanisms lead to the formation of these morphological structures through their imaging by a high-precision gravity survey. We plan to measure the density difference between the Quaternary valley fill and the enclosing Tertiary Molasse (Matter et al. 1980). The collected gravity data will be analysed through computing, with the aim to reconstruct probable 3D models of the overdeepenings. We will then use the reconstructed geometry to better understand the origin of these overdeepenings and the mechanisms that formed them. In particular, we plan to test whether these morphologies are relict features of e.g. riverbeds of yet unknown age, inherited architectures that were reactivated by the passage of glaciers or if they represent purely glacigenic features, formed by burst of melt water or by a continuous subglacial flow.

REFERENCES

Matter, A., Homewood, P., Caron, C., Rigassi, D., vanStuijvenberg, J., Weidmann, M. and Winkler, W., 1980 : Flysch and molasse of western and central Switzerland. In: Geology of Switzerland – A Guide Book, Part B: Geological Excursions (R. Trümpy, ed.), pp. 261-292. Wepf, Basel

Preusser, F., Reitner, J.M. and Schlüchter, C., 2010: Distribution, geometry, age and origin of overdeepened valleys and basins in the Alps and their foreland. Swiss Journal of Geoscience, 103, 407-426

Reber, R. & Schlunegger, F. 2016 : Unravelling the moisture sources of the Alpine glaciers using tunnel valleys as constraints, Terra Nova,Vol 28, No. 3, 202-211

P 11.4
Macro- and micro-fauna from cold-seeps in the Palmahim Disturbance Zone (off-shore Israel)

Valentina Beccari [1], Daniela Basso [2], Ahuva Almogi-Labin [3], Orit Hyams-Kaphzan [3], Yizhaq Makovski [4] & Silvia Spezzaferri [1]

[1] University of Fribourg, Department of Geosciences, Chemin du Musée 6, 1700 Fribourg, Switzerland
  (valentina.beccari@unifr.ch)
[2] University of Milano-Bicocca, Department of Earth and Environmental Sciences, Piazza della Scienza 4, 20126 Milano,
[3] Geological Survey of Israel, Jerusalem 9550161, Israel
[4] Dr. Moses Strauss Department of Marine Geosciences, Leon H. Charney School of Marine Sciences (CSMS),
  University of Haifa, Haifa 31905, Israel

Seepage related features sediments were sampled during the EU Eurofleets SEMSEEP Cruise on the RV Aegaeo in 2016 along the Israeli continental slope (Makovsky et al., 2017).
A box corer with a sampling area of 30 x 30 cm and a maximal penetration of 60 cm was used to collect the sediment surface samples and subcores.
Samples for living foraminiferal studies were processed following the protocol of Schönfeld et al. (2012). Samples from subcores were washed with a 32µm mesh sieve.
The most relevant occurrence of seeps offshore Israel is in the Palmahim Disturbance Zone (PDZ), a large-scale (~50x15 km) rotational slide, rooted in the Messinian evaporites on the southern Israeli margin.
In the Eastern Mediterranean evidence of chemosynthetic life has been so far described from mud volcanoes (e.g., Corselli and Basso, 1996) and other localities characterized by cold seeps such as the Alboran Sea and Gela Basin (Taviani, 2014).
A typical and endemic methane seep benthic foraminiferal fauna has not been documented in the PDZ, however, benthic foraminiferal assemblages are characterized by the genera *Bolivina, Bulimina, Uvigerina, Lenticulina, Globobulimina* and *Chilostomella* defined as highly tolerant species of low oxygen environment.
Chemosynthetic macro-faunal assemblages were recovered in the PDZ. They are characterized by loose and articulated shells of mytilids (e.g. *Idas ghisottii*), lucinids (e.g. *Lucinoma kazani, Myrtea spinifera*), thyasirids (e.g. *Thyasira biplicata*), vesicomyids (e.g. *Isorropodon perplexum*) and gastropods (e.g. *Taranis moerchii, Lurifax vitreus).* Fragments of the callianassid decapod *Calliax* sp. are consistently present and abundant in the samples.
The coupling of low oxygen benthic foraminiferal species with chemosynthetic molluscs suggest that the two groups of organisms share the same chemosynthetic environment.

REFERENCES

Corselli, C. and Basso, D. 1996: First evidence of benthic communities based on chemosynthesis on the Napoli Mud Volcano (Eastern Mediterranean). Mar. Geol. 132 (1), 227-239.

Makovsky, Y., Rüggeberg, A., Bialik, O., Foubert, A., Almogi-Labin, A., Alter, Y., Bampas, V., Basso, D., Feenstra, E., Fentimen, R., Friedheim, O., Hall, E., Hazan, O., Herut, B., Kallergis, E., Karageorgis, A., Kolountzakis, A., Manousakis, L., Nikolaidis, M., Pantazoglou, F., Rahav, E., Renieris, P., Schleinkofer, N., Sisma Ventura, G., Stasnios, V., Weissman,A. and the EuroFLEETS2 SEMSEEP Participants, 2017: South East Mediterranean SEEP carbonate, R/V Aegaeo Cruise EuroFLEETS2 SEMSEEP, 1-38.

Schönfeld, J., Alve, E., Geslin, E., Jorissen, F., Korsun, S., Spezzaferri, S. and Members of the FOBIMO Group 2012: The FOBIMO (FOraminiferal BIo-MOnitoring) initiative – Towards a standardised protocol for soft-bottom benthic foraminiferal monitoring studies. Mar. Micropal., 94-95, 1-13, 10.1016/j.marmicro.2012.06.001.

Taviani, M. 2014: Marine Chemosynthesis in the Mediterranean Sea. In Goffredo, S. and Dubinsky Z. (Eds.), The Mediterranean Sea: Its history and present challenges, 69, Springer, Dordrecht DOI 10.1007/978-94-007-6704-1_5.

P 11.5
Using chironomids to constrain Late Glacial climate trends in Burgäschisee, Switzerland

Alexander Bolland [1], Fabian Rey [1], Willy Tinner [2] and Oliver Heiri [1]

[1] Departement Umweltwissenschaften ,Universität Basel, Klingelbergstrasse 27 CH-4056 Basel
(alexanderwilliam.bolland@unibas.ch)
[2] Institute of Plant Sciences, Universität Bern, Altenbergrain 21 CH-3013 Bern

There are very few chironomid based temperature reconstructions for the Late Glacial period prior to 14,700 cal. BP in Switzerland, and none that are temporally well constrained. This represents a significant gap in our understanding of late glacial temperature dynamics prior to reforestation of the Swiss lowlands. Furthermore, this knowledge gap is exemplified by new vegetation reconstructions indicating climatic warming events as early as 16,000 cal. BP (Rey et al. 2017) which do not currently have any local independent temperature proxies with which to compare. Lake sediments have been retrieved from Burgäschisee, a small lake on the Swiss plateau, and have been used to produce the first reliably dated chironomid record between 18,000 - 14,700 cal. BP in Switzerland. The record displays changes in chironomid composition on a centennial scale and will be presented and discussed alongside extracts from the Burgäschisee pollen record (Rey et al. 2017), allowing a comparison of these independent proxies and facilitating a more robust interpretation of early climatic warming in the Swiss Late Glacial.

Initial interpretations of the chironomid record suggest a gradual increase in summer temperatures across the study period. At the earliest part of the record ca. 18,200 cal. BP the chironomid assemblages consist almost entirely of cold stenotherms such as Micropsectra radialis-type and Corynoneura arctica-type. Over time, types associated with warmer temperatures, such as Tanytarsus glabrescens-type and Dictrotendipes nervosus-type, replace many of the cold stenotherms. Sergentia coracina-type, also a cold stenotherm, remains the dominant type for the entire record, which suggests that although temperatures were increasing, cold environments in the lake persisted. Despite persistence of cold water types and gradual chironomid assemblage change, detrended correspondence analysis suggests a distinct separation between assemblage compositions from earlier than and from later than 16,000 cal. BP (Figure 1), corresponding with the early warming event observed in the pollen record (Rey et al. 2017).

Further work is required to evaluate the chironomid assemblage response to climatic change, and determine if the separation at 16,000 cal. BP is a threshold response to gradual warming or indeed a distinct warming event. This will include the development of a chironomid-based temperature reconstruction, which will attempt to quantitatively assess July air temperature change in the Swiss lowlands during the Late Glacial.
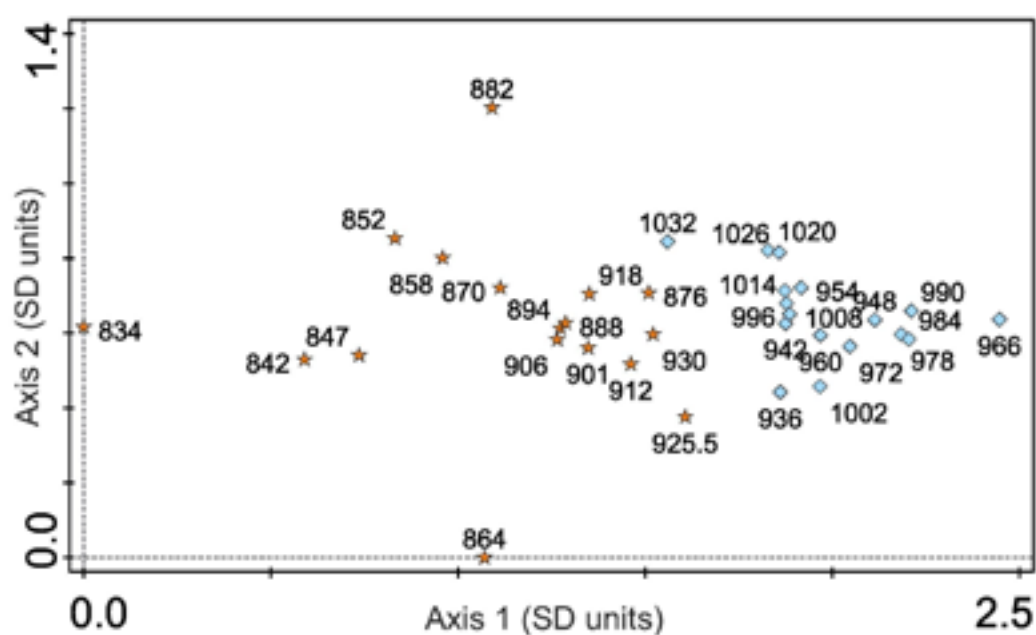
Figure 1. Detrended correspondence analysis of chironomid assemblages in the Burgäschisee sediment core. Axis 1 appears to be representative of temperature change, lower values (to the left) representing assemblages typical of warmer conditions. Blue diamonds are samples from earlier than 16,000 cal. BP and orange stars are from samples later than 16,000 cal. BP. Numbers labeling the aforementioned symbols, represent the depth of the corresponding sample in the Burgäschisee core (cm).

REFERENCES

Rey, F., Gobet, E., van Leeuwen, J.F.N., Gilli, A., van Raden, U.J., Hafner, A., Wey, O., Rhiner, J., Schmocker, D., Zünd, J., and Tinner, W. 2017: Vegetational and agricultural dynamics at Burgäschisee (Swiss Plateau) recorded for 18,700 years by multi-proxy evidence from partly varved sediments. Veg Hist Archaeobot. 26, 571-586. DOI 10.1007/s00334-017-0635-x.

P 11.6
Sedimentology of the glacial facies within the Deckenschotter of Northern Switzerland

Marius W. Buechi [1], Gaudenz Deplazes [2], Flavio S. Anselmetti [1]

[1] *Institute of Geological Sciences & Oeschger Centre for Climate and Climate Change Research, University of Bern, Baltzerstrasse 1+3, CH-3012 Bern (marius.buechi@geo.unibe.ch)*
[2] *National Cooperative for the Disposal of Radioactive Waste (Nagra), Hardstrasse 73, CH-5430 Wettingen*

The Höhere and Tiefere Deckenschotter Groups of Northern Switzerland are dominated by fluvial to fluvio-glacial sediments. In some outcrops, the gravelly facies is associated with diamictons interpreted as glacial tills (e.g. Heim 1891, Frei 1912, Graf 1993). Despite the importance of these presumed glacial deposits as markers of ice-contact during the Early Pleistocene, they remain relatively poorly studied. We present results from an ongoing project to better constrain the depositional environment of these diamicts at selected key sites using detailed macro- to microscale sedimentology, fabric and geotechnical analyses. Our analyses will help to better constrain the extent and characteristics of glacier advances related to the first extensive glaciations of the Alps.

REFERENCES
Heim, A. 1891: Die Geschichte des Zürichsees. Neujahrsblatt der Naturforschenden Gesellschaft Zürich 93, 1-16.
Frei, R. 1912: Monographie des Schweizerischen Deckenschotters. Beiträge zur geologischen Karte der Schweiz 37 (N.F.).
Graf, H. R. 1993: Die Deckenschotter der zentralen Nordschweiz. PhD Thesis, Diss. ETH Nr. 10205.

P 11.7

The evolution of the fluvial environments and the history of human settlements during the Late Holocene on the Piano di Magadino (Cantone Ticino, Switzerland): new sedimentological and geoarchaeological data

Dorota Czerski [1], Luisa Mosetti [2], Rossana Cardani Vergani [2], Michele Pellegrini [2], Maruska Federici-Schenardi [3], Mattia Gillioz [4] & Cristian Scapozza [1]

[1] Institute of Earth Sciences, University of Applied Sciences and Arts of Southern Switzerland (SUPSI), Campus Trevano, 6952 Canobbio, Switzerland (dorota.czerski@supsi.ch)
[2] Section of Archaeology, Ufficio dei Beni Culturali del Cantone Ticino, Viale Stefano Franscini 30a, 6501 Bellinzona, Switzerland
[3] Paese 99, 6541 Santa Maria in Calanca, Switzerland
[4] Via Pedemonte 28a, 6500 Bellinzona

In recent times many sedimentological, geomorphological and geoarchaeological studies were carried out at many locations on the Piano di Magadino, trying to reconstruct the evolution of the paleoenvironmental conditions of the area during the Late Holocene subepoch. The age and stratigraphy of the deposits were determined using the radiocarbon dating method on organic matter debris and on charcoals. This, combined with an accurate sedimentological characterization of the deposit, archaeological observations and dating, allowed interpreting the depositional context for the sedimentary and archaeological sequences found on the Piano di Magadino.

This contribution focuses on new dating and stratigraphy determined in two archaeological sites in Progero (Gudo, RFD 1078; 2'715'900/1'114'530, CH1903+/LV95) and in Gudo (RFD 80; 2'716'720/1'114'800, CH1903+/LV95).

In Progero two main phases of enhanced hydrosedimentary activity shown by coarse alluvial deposits could be observed. The first phase consists in a palaeochannel at the bottom of the lithostratigraphy. The fine sandy to clayey layers overlaying it indicate a calm period which was dated by radiocarbon geochronology on charcoal between 1440 and 1285 BC (Middle Bronze Age). The following second alluvial phase shows many events with coarse material deposits succeeding and crosscutting each other. These deposits are attributed to lateral alluvial fans or debris flows from the valley slope. After this phase, the first records of human settlement in the area are observed, which consist of anthropogenic backfillings containing some ceramic debris of the Bronze Age. Afterwards two events of finer deposits of fluvial origin are present; both are intercalated by remnants of Bronze Age human constructions. These deposits are most probably attributed to a temporary palaeomeander of the Ticino river, which allowed the sudden deposition of very fine material by rapid decantation. The presence of anthropogenic pavements at that time confirms the proximal position to the river (both the stream from the valley slope and the Ticino river) of the human settlements.

The site of Gudo is located northeast compared to the first site, closer to the valley slope and in a higher stratigraphical position. For this site four layers with coarser grain size deposits were observed suggesting four events of major hydrosedimentary activity in the area, which were constrained by radiocarbon dating: 400–370 BC (Early Iron Age), 200–170 BC (Middle Iron Age), 10–340 AD (Roman Period), 540–1000 AD (Early Middle Ages). A wall of Iron Age found between the two first events confirms the dating and suggests a stable human settlement in the area during the Iron Age, as well as the need to build a dam for containing the floods, most likely coming from the Ticino river. The Early Middle Ages increase in hydrosedimentary activity was documented also by historical informations and by new radiocarbon dating in the Ticino river alluvial plain.

The observations and dating carried out in Progero and in Gudo allowed highlighting six phases of hydrosedimentary activity (Figure 1); these can be completed by more recent information from historical sources, adding two others phases of hydrosedimentary activity in 1178 AD and between 1690 and 1868 AD, which means during the last phase of the Little Ice Age. Therefore, the integration of archaeological information in classical geomorphological and historical studies on the evolution of fluvial environments on the Ticino river catchment allowed the definition of eight phases of hydrosedimentary activity since the Early Bronze Age (Figure 1).
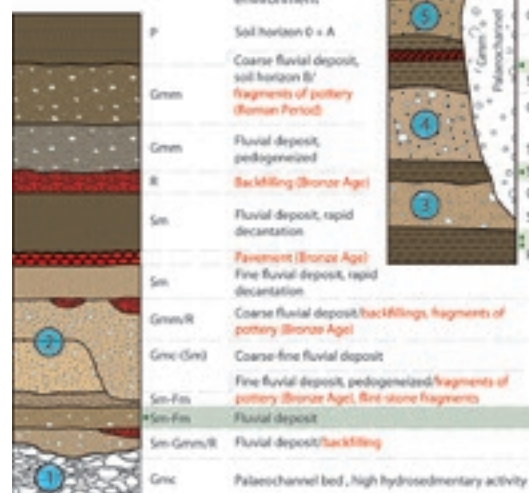
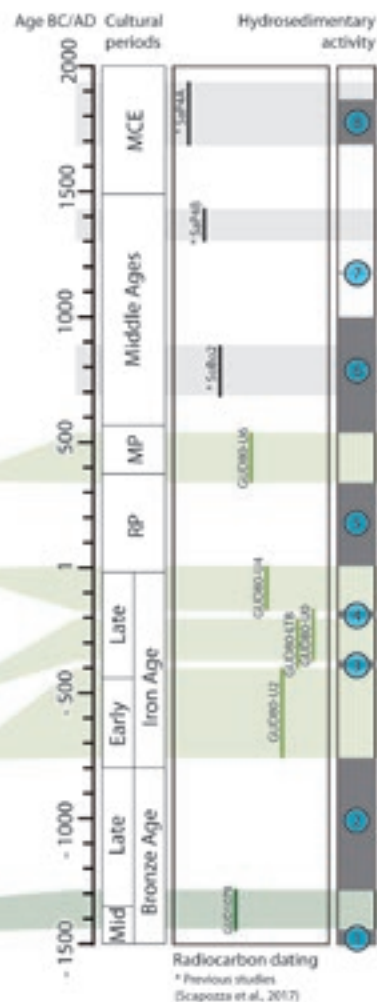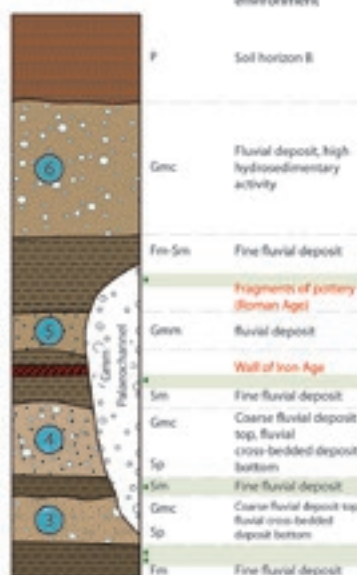Figure 1. Representative stratigraphy of the two studied sites and derived phases of enhanced hydrosedimentary activity.

P 11.8
Isochron-burial dating of Swiss Deckenschotter

Catharina Dieleman [1], Naki Akçar [1], Marcus Christl [2] & Christof Vockenhuber [2]

[1] Institut für Geologie, University of Bern, Baltzerstrasse 1+3, CH-3012 Bern (catharina.dieleman@geo.unibe.ch)
[2] Laboratory of Ion Beam Physics, ETH Zurich, Otto-Stern-Weg 5, 8093 Zurich

During the past 2.6 Ma, at least 13 glaciations have overriden the northern Swiss Alpine Foreland (Schlüchter, 1988). The imprints of these advances can be found in four distinct units, which are divided by their morphostratigraphy and topography (Graf, 1993). They show a reversed stratigraphic relationship. This means that deposits at a higher elevation are considered to be older than deposits at a lower elevation. The four units are from the oldest to the youngest: Higher Deckenschotter (HDS; Höhere Deckenschotter), Lower Deckenschotter (TDS; Tiefere Deckenschotter), Higher Terrace (HT; Hochterrasse) and Lower Terrace (NT; Niederterrasse) (Graf, 1993, 2009). The HDS and TDS deposits represent the oldest Quaternary deposits in Switzerland and are characterised by a succession of glacio-fluvial gravels intercalated with glacial and/or overbank deposits (Graf, 1993). They are separated by a significant phase of incison (Graf and Müller, 1999). Recently, HDS and TDS deposits at several sites were dated to around 2 Ma and to around 1 Ma by depth-profile and isochron-burial dating techniques using the cosmogenic nuclides ^{10}Be and ^{26}Al (Akçar et al., 2014; Claude et al., 2017; Akçar et al., 2017). The recently established chronology is challenging the attributed morphostratigraphy as deposits of around 1 Ma are located at the same elevation as ca. 2 Ma old deposits. Therefore, how far can the approach "*same elevation means same age*" explain the chronology?

The aim of this study is to date HDS and TDS deposits at new sites to disentangle the sequence of events into a more complex model than thought so far as well as to reconstruct the landscape evolution in the northern Alpine Foreland. For this reason, we concentrate on additional sites at Irchel as well as the region around Mandach and Lake Constance as the might represent analogues to the Irchel. For each site sediment analysis will be applied to identify the provenance, the transport meachanism and the depositional envrionment. The chronology will be established by isochron-burial dating using in-situ produced cosmogenic ^{10}Be and ^{26}Al. The combination of the results allows to reconstrcut the landscape evolution. The sampling for this study has taken place at 11 HDS and TDS sites: three HDS sites at Irchel, three HDS and three TDS sites in the Mandach region, as well as one HDS and one TDS site in the region of Lake Constance. For each site, one sediment sample consisting of quartz pebbles and at least nine clasts of various lithologies, shapes and sizes were collected. After the physical separation of quartz, seven samples and the sediment sample will be further processed for the accelerator mass spectrometry measurements of cosmogenic ^{10}Be and ^{26}Al at the ETH Zurich.

REFERENCES

Akçar, N., Ivy-Ochs, S., Alfimov, V., Claude, A., Graf, H.R., Dehnert, A., Kubik, P.W., Rahn, M., Kuhlemann, J., and Schlüchter, C. 2014: The first major incision of the Swiss Deckenschotter landscape: Swiss Journal of Geosciences, v. 107, p. 337–347, doi: 10.1007/s00015-014-0176-6.

Akçar, N., Ivy-Ochs, S., Alfimov, V., Schlunegger, F., Claude, A., Reber, R., Christl, M., Vockenhuber, C., Dehnert, A., Rahn, M., and Schlüchter, C. 2017: Isochron-burial dating of glaciofluvial deposits: First results from the Swiss Alps: Earth Surface Processes and Landforms, v. 42, p. 2414–2425, doi: 10.1002/esp.4201.

Claude, A., Akçar, N., Ivy-Ochs, S.D., Schlunegger, F., Kubik, P.W., Dehnert, A., Kuhlemann, J., Rahn, M., and Schlüchter, C. 2017: Timing of early Quaternary gravel accumulation in the Swiss Alpine Foreland: Geomorphology, v. 276, p. 71–85, doi: 10.1016/j.geomorph.2016.10.016.

Graf, H.R. 1993: Die Deckenschotter der zentralen Nordschweiz: ETH Zurich, 187 p.

Graf, H.R. 2009: Stratigraphie und Morphogenese von frühpleistozänen Ablagerungen zwischen Bodensee und Klettgau: Eiszeitalter und Gegenwart - Quaternary Science Journal, v. 58, p. 12–53.

Graf, H.R., and Müller, B. 1999: Das Quartär: Die Epoche der Eiszeiten., in Bolliger, T. ed., Geologie des Kantons Zürich, Thun: Ott Verlag, p. 71–95.

Schlüchter, C. 1988: The Deglaciation of the Swiss-Alps: A Paleoclimatic Event with Chronological Problems: Bulletin de l'Association française pour l'étude du Quaternaire, v. 2, p. 141–145.

P 11.9
In quest of a pre-LGM (sub-)glacial history: drilling the overdeepened Lower Aare Valley

Lukas Gegg [1], Marius W. Buechi [1], Gaudenz Deplazes [2], Herfried Madritsch [2], Daniela Mueller [3], Frank Preusser [3] & Flavio S. Anselmetti [1]

[1] *Institute of Geological Sciences & Oeschger Centre for Climate and Climate Change Research, University of Bern, Baltzerstrasse 1+3, CH-3012 Bern (lukas.gegg@geo.unibe.ch)*
[2] *National Cooperative for the Disposal of Radioactive Waste (Nagra), Hardstrasse 73, CH-5430 Wettingen*
[3] *Institute of Earth and Environmental Sciences, Albert-Ludwigs-University Freiburg, Albertstr. 23b, D-79104 Freiburg*

During the Pleistocene, extensive and repeated glaciations have carved the foreland of the European Alps and left deeply incised trough structures, overdeepened valleys, behind. Subsequently, these sediment traps were infilled with sub- and proglacial deposits, often related to multiple glaciations. Therefore, overdeepened valleys can serve as excellent archives of pre-LGM glaciations, whose relics were otherwise largely obliterated by the following ice advances.

To gain insights into the pre-LGM glacial and fluvial history of northern Switzerland and to constrain the process of subglacial erosion, we currently investigate the Lower Aare Valley with four scientific drillings targeted at the overdeepened Gebenstorf-Stilli trough and the Rinikerfeld paleochannel. Our study area is situated just beyond the local LGM, at the confluence of the Aare with Reuss and Limmat, where the valley is deeply incised into limestones of the Lägern structure (southeastern margin of the Swiss Jura). The recovered drill cores are evaluated in terms of sedimentology, geotechnical properties and geochronology as well as /and complemented by outcrop studies. We present the current status of the project and include first results from the already completed boreholes.

P 11.10
Spatial focusing of lake sedimentation by wind driven circulation

Love Råman Vinnå [1], Damien Bouffard [1,2], Alfred Wüest [1,2], Stéphanie Girardclos [3] & Nathalie Dubois [4,5]

[1] Physics of Aquatic Systems Laboratory, Margaretha Kamprad Chair, École Polytechnique Fédérale de Lausanne, Institute of Environmental Engineering, CH-1015 Lausanne
[2] Department of Surface Waters - Research and Management, Eawag, Swiss Federal Institute of Aquatic Science and Technology, Seestrasse 79, CH-6047 Kastanienbaum [3] Department of Earth Sciences AND Institute for Environmental Sciences, University of Geneva, Rue des Maraîchers 13, CH-1205 Geneva (stephanie.girardclos@unige.ch)
[4] Department of Surface Waters - Research and Management, Eawag, Swiss Federal Institute of Aquatic Science and Technology, Überlandstrasse 133, CH-8600 Dübendorf
[5] Department of Earth Sciences, ETHZ, Zürich, Soneggstrasse 5, CH-8092 Zürich

Sedimentation patterns in aquatic systems affects the biosphere as well as utilitarian water resources management. We investigate grain size specific sedimentation patterns in the perialpine Lake Biel, greatly influenced by the upstream diversion of the Aare River into the lake. The majority of the river supplied sediment arrived to the lake in short term suspended sediment concentration (SSC) events. These were linked to weather systems originating out over the Atlantic Ocean, resulting in seasonal varying sediment supply. The Atlantic weather systems, besides controlling the temporal frequency of the SSC events in the river, furthermore focused the sedimentation inside the lake. This led to large amounts of sediment being deposited on steep topography, resulting in series of subaqueous slides. Furthermore, the high flow speed in both river inlets and outlets caused selective sedimentation of particle sizes, with increased mass occurrence rate of sand (63 to 2000 µm) in high energetic environments, while smaller sized silt and clay (< 63 µm) clearly dominated in the low energetic deeper parts of the lake.

P 11.11

Subaquatic slope instabilities due to river correction and artificial dumps (Lake Biel, Switzerland)

Nathalie Dubois [1,2], Love Råman Vinnå [3], Marvin Rabold [1], Michael Hilbe [4], Flavio S. Anselmetti [4], Alfred Wüest [3,5], Laetitia Meuriot [1], Alice Jeannet [6,7] & Stéphanie Girardclos [6,7]

[1] *Department of Surface Waters - Research and Management, Eawag, Swiss Federal Institute of Aquatic Science and Technology, Überlandstrasse 133, CH-8600 Dübendorf*
[2] *Department of Earth Sciences, ETHZ, Zürich, Soneggstrasse 5, CH-8092 Zürich*
[3] *Physics of Aquatic Systems Laboratory, Margaretha Kamprad Chair, École Polytechnique Fédérale de Lausanne, Institute of Environmental Engineering, CH-1015 Lausanne*
[4] *Institute of Geological Sciences and Oeschger Centre for Climate Change Research, University of Bern, Baltzerstrasse 1+3, CH-3012 Bern*
[5] *Department of Surface Waters - Research and Management, Eawag, Swiss Federal Institute of Aquatic Science and Technology, Seestrasse 79, CH-6047 Kastanienbaum*
[6] *Department of Earth Sciences, University of Geneva, Rue des Maraîchers 13, CH-1205 Geneva*
[7] *Institute for Environmental Sciences, University of Geneva, idem.*

The "Jura water corrections" was the largest river engineering project ever undertaken in Switzerland. It completely changed the Lake Biel system. Our study documents an effect that is likely the consequence of the deviation of the Aare River into the lake in 1878.

Several mass-transport deposits (MTD) were identified along the lake's shore from bathymetric, high-resolution seismic reflection and sediment core datasets. Individual MTDs were dated from radionuclide activities. MTD's from the 1960s-1970s are attributed to dumping of excavated material, when the channels flowing into and out of Lake Biel were widened and deepened. But two nearby earthquakes in 1964 and 1965 cannot be ruled out as possible triggers. Three additional medium-scale mass movements followed in 1970s-1990s (uncertain dating), 2000 and 2009 and have unknown triggers. Together with the largest - and slightly older - MTD, they form a recent large mass-movement complex, specific of Lake Biel and not observed in other peri-alpine lakes of Switzerland. The cause of these repeated slope failures is likely linked to the large increase of sediment delivered by the Aare River since its deviation into Lake Biel. This enhanced sediment input resulted in sediment overloading, which may have caused large mass movements on the eastern shore along the flow path of the Aare in the lake.

P 11.12
Fe-Mn nodules in young soils of Grand-Saconnex (Geneva, Switzerland): encrustation hampered by the Late Neolithic soil drainage?

Branimir Šegvić [1], Stéphanie Girardclos [2,3], Giovanni Zanoni [1], Carlos Arbiol González [4],Tara Steimer-Herbet [5], Marie Besse [5]

[1] Department of Geosciences, Texas Tech University, Lubbock, TX 79409, USA
[2] Department of Earth Sciences, University of Geneva, Rue des Maraîchers 13, CH-1205 Genève
  (stephanie.girarclos@unige.ch)
[3] Institute for Environmental Sciences, University of Geneva, idem.
[4] Department of Earth Sciences, Memorial University of Newfoundland, St. John's NL A1B 3X9, Canada
[5] Laboratory of Prehistoric Archaeology and Anthropology, Department F.-A. Forel for Environmental and Aquatic
  Sciences, University of Geneva, Boulevard Carl-Vogt 66, CH-1211 Genève.

Perialpine areas have undergone significant changes following the last glaciation and particularly through the Holocene. This study relies on geochronological, mineralogical and geochemical clues to explain the formation and paleoenvironmental significance of Fe-Mn nodules in young soils (~4.5 ka BCE) of Geneva Basin. The nodules, with an average 2 mm in diameter, have an onion-like and quasi-layered internal architecture defined by selective enrichments in Fe and Mn. Fe-rich mica, present in soil matrix, has been proved to serve as a main source of Fe and Mn. Several steps in mica weathering were recognised leading to the formation of nodules – vermiculitization, microcracking, Fe-Mn segregation and re-precipitation. Mineral alterations were boosted by long periods of summer warm climate during Boreal and Atlantic times as suggested by clay content of analysed colluvium. Moreover, archaeological ages and radiocarbon dating of charcoal yielded coherent Fe-Mn encrustation ages (4.8–4.3 ka BCE and 4.5–4.4 ka BCE, respectively) that coincide with the Holocene temperature maximum (~4 ka BCE) in Central Europe. Terrain morphology that led to better water retention formed prior to ~8 ka BCE ago during undefined Late Glacial time. This promoted seasonal changes in redox conditions that facilitated the mobilization, distribution and re-precipitation of Fe and Mn. Established conditions lasted until Late Neolithic (3.4–2.2 ka BCE) when different agricultural practices changed favourable hydromorphic environment effectively putting an end to further nodule formation.

REFERENCE
Šegvić, B., Girardclos, S., Zanoni, G., Arbiol González, C., Steimer-Herbet, T. & Besse, M. 2018: Origin and paleoenvironmental significance of FeMn nodules in the Holocene perialpine sediments of Geneva Basin, western Switzerland, Applied Clay Science, 160, 22-39.

P 11.13

Constraining the maximum glacial timing of the Lyon Lobe, French Alps, Using OSL dating

Natacha Gribenski [1], Pierre Valla [1], Frank Preusser [2], Christian Crouzet [3], Jean François Buoncristiani [4]

[1] Institut of Geological Sciences, University of Bern, Baltzerstrasse 3, 3012 Bern, Switzerland
  (natacha.gribenski@geo.unibe.ch)
[2] Institute of Earth and Environmental Sciences, University of Freiburg, Fahnenbergplatz, 79085 Freiburg, Germany
[3] ISTerre-Institut des Sciences de la Terre, Université Joseph Fourier, CNRS, 38041 Grenoble, France
[3] Centre de Recherches de Climatologie, UMR 6282 Biogéosciences, CNRS/Univ Bourgogne Franche-Comté,
  Dijon, France

Detailed reconstruction of former glacier maxima in the European Alps indicate that large ice expansion occurred on the northern side of the Alps, with wide piedmont lobes spreading over more than 50 km into the Swiss, German, Austrian and French lowlands. Maximum glacial extents are relatively well constrained chronologically in the northern Alps, suggesting a glacial maxima around 22-24 ka (Wirsig et al., 2016), in phase with the global records. However, the timing of the Late Pleistocene glaciation maximum of the Lyon Lobe, French Alps, is controversial due to major discrepancy between geomorphic evidence and modelled glacier extent (Seguinot et al., 2018). A clear and robust chronological constrain of the Lyon Lobe is critical as it would have major implication in term of past atmospheric circulation pattern. Traditional dating techniques such as radiocarbon and cosmogenic nuclides exposure are challenging in this area due to the scarcity of organic material incorporated within glacial deposits and the lack of in-place moraine boulders. In these circumstances, Optically Stimulated Luminescence (OSL) techniques, which allow the dating of buried sedimentary material, offer a promising alternative.

In this study, we investigate the feasibility of using OSL to date the glacial deposits of the Lyon lobe, and present a preliminary timing of its Late Pleistocene maximum extent.

REFERENCES

Wirsig, C., Zasadni, J., Christl, M., Akçar, N., Ivy-Ochs, S. 2016: Dating the onset of LGM ice surface lowering in the High Alps, Quaternary Science Reviews, 143, 37-50.

Seguinot, J., Jouvet, G., Huss, M., Funk, M., Ivy-Ochs, S. & Preusser, F. *in review* 2018: Modelling last glacial cycle ice dynamics in the Alps, The Cryosphere Disc., https://doi.org/10.5194/tc-2018-8.

P 11.14

Reconstructing the sequence of massive rock-slope failures in Valle di Tovel, Trentino (Italy)

Susan Ivy-Ochs [1], Alfio Viganò [3], Sandro Rossato [2], Silvana Martin [2], Christof Vockenhuber [1], Manuel Rigo [2], Paolo Campedel [3]

[1] Laboratory of Ion Beam Physics, ETH-Honggerberg, CH-8093 Zurich (ivy@phys.ethz.ch)
[2] Dipartimento di Geoscienze, Universita di Padova, 35133 I-Padova
[3] Servizio Geologico della Provincia Autonoma di Trento, 38121 I-Trento

Using field mapping, remote imagery interpretation (2 m lidar kindly provided by the Autonomous Province of Trento) and cosmogenic ^{36}Cl exposure dating we reconstruct the origin of the blocky deposits in the upper reaches of the Valle di Tovel in the Adamello Brenta Geopark in the Brenta Dolomites. Blocky deposits cover nearly the whole valley floor for a length of about 10 km from an elevation of 1900 down to 900 m a.s.l. Oetheimer (1992) estimated a total volume of more than 300 Mm^3. Although several independent bodies, sourced in the steep surrounding rock walls which reach up to 2700 m a.s.l., are apparent (Oetheimer 1992, Ferretti and Borsato 2004) detailed reconstruction of the timing and sequence of the catastrophic events is challenging.

Hypotheses for the age and origin of the blocky deposits range from a Lateglacial rock-slope failure onto a glacier (Oetheimer 1992) to mainly 16th century events. At that time, blocking of the outflow led to lake level rise of about 18 m as shown by dendrochronological ages of drowned trees, many of which are still standing on the lake bottom. The lake itself is renowned for the red color due to algal bloom it had during summers up until 1964 (Kulbe et al. 2005).

Interpretation of the evolution of the valley involves disentangling the numerous interfering deposits of megablocks released intermittently from the exceptionally steep valley walls. Although there are distinct differences in the amount of vegetation in the different sectors this is clearly not directly translatable into age, and other factors may play just as important a role. Present permafrost is likely restricted to ridge tops above about 2500 m a.s.l. (Boeckli et al. 2012), nevertheless cooling atypical for the elevation of the blocky deposits due to processes like the 'chimney effect' (Delaloye et al. 2003) over the course of the Holocene cannot be ruled out.

REFERENCES

Boeckli, L., Brenning, A., Gruber, S. & Noetzli, J. 2012: Permafrost distribution in the European Alps: calculation and evaluation of an index map and summary statistics, The Cryosphere 6, p.807-820.

Delaloye R., Reynard E., Lambiel C., Marescot L., & Monnet R. 2003: Thermal anomaly in a cold scree slope (Creux du Van, Switzerland), In: Proceedings of the 8th International Conference on Permafrost 2125. Balkema: Zurich.

Ferretti, P., & A. Borsato. 2006: Geologia e geomorfologia della Valle e del Lago di Tovel, Studi Trentini di Scienze Naturali, Acta Biologica 81, 173–187.

Kulbe, T., Anselmetti, F., Cantonati, M. & Sturm, M., 2005. Environmental history of Lago di Tovel, Trento, Italy, revealed by sediment cores and 3.5 kHz seismic mapping, Journal of Paleolimnology, 34, 325-337.

Oetheimer C. 1992. La foresta sommersa del Lago di Tovel (Trentino): reinterpretazione e datazione dendrocronologica. Studi Trentini di Scienze Naturali 67: 3–23.

P 11.15
Tackling North-South differences of the Last Glacial Maximum in the Alps

Sarah Kamleitner [1], Susan Ivy-Ochs [1], Giovanni Monegato [2], Franco Gianotti [3], Bernhard Salcher [4] & Jürgen M. Reitner [4]

[1] Laboratory of Ion Beam Physics, ETH Zürich, Otto-Stern-Weg 5, CH-8093 Zurich (kamsarah@phys.ethz.ch)
[2] Institute of Geosciences and Earth Resources, CNR, Via G. Gradenigo 6, I-35131 Padua
[3] Department of Earth Sciences, Università degli Studi di Torino, Via Valperga Caluso 35, I-10125 Torino
[4] Department of Geography and Geology, University of Salzburg, Hellbrunnerstrasse 34, A-5020 Salzburg
[5] Geological Survey of Austria, Neulinggasse 38, A-1030 Vienna

During the last glacial cycle, temperatures and precipitation patterns were markedly different from today and shifts in the North Atlantic atmospheric circulation distinctly affected moisture delivery to Europe. Sensitive to climate change, glaciers quickly respond to altered precipitation patterns that manifest as spatial and temporal rates of glacier growth. The timing and extent of glacial maxima in the Alps therefore provide basic information on changing moisture sources throughout the last glaciation. The position of LGM Rhine and Ticino/Toce glacier directly North-South of each other with an existing linkage in their accumulation area, qualifies them to study the main controls of spatial and temporal patterns of glacier growth. However, the lack of detailed chronological information currently restricts their use for paleo-climatic reconstruction. This project aims to overcome these limitations by using geomorphological and sedimentological mapping, remote sensing and surface exposure dating to constrain the timing of LGM, recessional/ re-advance stages and ultimate withdrawal from the forelands for both glacier systems. Precisely dated LGM ice margins will help to understand similarities and differences in glacier timing North and South of the Alps and will have the potential to unravel variations in past moisture distribution. Gained results will further serve as point of comparison for the validation of glacier models in collaboration with the Laboratory of Hydraulics, Hydrology and Glaciology (VAW ETHZ).

P 11.16

What do speleothems in Western Europe record? Assessing regional and temporal trends in speleothem δ^{18}O with the SISAL database

Franziska A. Lechleitner [1], Sahar Amirnezhad-Mozhdehi [2], Andrea Columbu [3], Laia Comas-Bru [2], Inga Labuhn [4], Carlos Pérez-Mejías [5] & Kira Rehfeld [6]

[1] Department of Earth Sciences, University of Oxford, South Parks Road, Oxford OX1 3AN, UK
 (franziska.lechleitner@earth.ox.ac.uk)
[2] UCD School of Earth Sciences, University College Dublin, Dublin 4, Ireland
[3] Department of Biological, Geological and Environmental Sciences, University of Bologna, Via Zamboni 67, 40126
 Bologna, Italy
[4] Institute of Geography, University of Bremen, Germany
[5] Department of Geoenvironmental Processes and Global Change, Pyrenean Insitute of Ecology, Avda.
 Montañana 1005, 50059 Zaragoza, Spain
[6] Institute of Environmental Physics, Ruprecht-Karls-Universität Heidelberg, Im Neuenheimer Feld 229, 69210
 Heidelberg, Germany

Speleothems can provide very high resolution palaeoclimate records with exceptional chronological control, and thus have become powerful archives of past terrestrial climate variability. The stable oxygen isotope ratio (δ^{18}O) in speleothems provides information principally on past changes in temperature, precipitation, and atmospheric circulation, and is increasingly used for the evaluation of isotope-enabled climate models.

Here we make use of the recently published SISAL (Speleothem Isotopes Synthesis and Analysis) database, resulting from the effort of an international PAGES working group (Atsawawanunt et al., 2018). Our objective is to review and assess the potential of available speleothem δ^{18}O records from Western Europe. We investigate how the spatial distribution of the records in the database is representative for climate conditions in Europe, and compare modern speleothem data to precipitation δ^{18}O. Overall, speleothem δ^{18}O mirrors the spatial trends found in precipitation δ^{18}O, highlighting the potential of this archive for palaeo-precipitation and -temperature reconstructions. Coherent regional trends in speleothem δ^{18}O are found over stadial-interstadial transitions of the last glacial, especially in high altitude Alpine records that reflect a dominant temperature signal. Over the Holocene and the last 2000 years, regional trends are more difficult to capture, due to lower signal-to-noise ratios in interglacial climate at mid-latitude sites, as well as issues with chronological uncertainty and resolution in the records. These results highlight the potential of Western Europe for speleothem palaeoclimate reconstruction, and the usefulness of these records for the evaluation of climate model outputs.

REFERENCES

Atsawawanunt, K., Comas-bru, L., Mozhdehi, S.A., Deininger, M., Harrison, S.P., Baker, A., Boyd, M., Kaushal, N., Ahmed, S.M., Ait Brahim, Y., Arienzo, M., Bajo, P., Braun, K., Burstyn, Y., Chawchai, S., Duan, W., Hatvani, I.G., Hu, J., Kern, Z., Labuhn, I., Lachniet, M., Lechleitner, F.A., Lorrey, A., Perez-Mejias, C., Pickering, R., Scroxton, N., Members, S.W.G., 2018. The SISAL database: a global resource to document oxygen and carbon isotope records from speleothems. Earth Syst. Sci. Data Discuss. doi:10.5194/essd-2018-17

P 11.17

Reconstruction of ecological evolution of lakes based on multidisciplinary proxies: the case of Lake Liambezi, Botswana.

Anaël Lehmann [1], Christophe Paul [2], Sevasti Filippidou [2], Léandre Ballif [1], Shannon Dyer [1], Pilar Junier [2], Torsten Vennemann [1].

[1] Institute of Earth Surface Dynamics, University of Lausanne, CH-1015 Lausanne
 (anael.lehmann@unil.ch, torsten.vennemann@unil.ch)
[2] Laboratory of Microbiology, Institute of biology, Rue Émile-Argand 11, CH-2000 Neuchâtel

Lake Liambezi is an ephemeral lake that is seasonally replenished from several distinct sources of water. It is located at the Eastern side of Caprivi Strip, straddling the border between Namibia and Botswana. The drainage basin of the lake is a large, flat wetland, including some woodlands, which contains a typically slow-flowing floodplain river (Seaman et al., 1978; Peel et al., 2015). Seaman et al. (1978) estimated a drainage basin of some 300 km^2, of which 100 km^2 is open water at its full size. The Lake changes its shape, size, and depth seasonally and over the years due to fluctuating contributions of water from its distinct source regions. Its depth averages about 2.5 m (Seaman et al. 1978) but can reach 7 m at its peak (Peel et al. 2015). The lake forms two elongated basins with a South-West to North-West direction joined by a main channel.

The main source of water for Lake Liambezi is the Zambezi River with two different entries during years of flooding. A first entry is through the Chobe River, which can reverse its flow direction and enter the lake from the east of the southern basin. A second entry is via the Bukalo Channel from the Caprivi floodplain of the Zambezi River and it enters the lake from the northeast of the northern basin. Another source of water is the Kwando River that percolates through the wetlands out via the Linyanti Channels. Its waters flow eastward along the Namibia-Botswana border into the lake from the west of the two basins. Rainfall and runoff from the area north of the lake also contributes to the water inputs. Depending on the lake level, an outflow from the lake is permit via the Chobe River (Seaman et al. 1978, and Peel et al. 2015).

The present study is based on two field campaigns: one, a reconnaissance study during the dry season (September 2016), while a second one was conducted at the end of the rainy season during March 2017. Water from multiple sources of ground and surface waters were collected to better understand the drainage and hydrodynamics in this relatively flat area (Dyer, 2017). It was also established that the present climate supports a vegetation representing both the C3 and C4 photosynthetic cycles (Ballif, 2018). While the former is favored in wet/cold environments, the latter is pronounced in dry/warm settings. These two functional types differ profoundly in their physiology, metabolism, water-use efficiency, resource acquisition and growth form. They also discriminate very differently against ^{13}C during photosynthesis, such that the C-isotope composition of organic matter accumulated in soils or sediments may provide valuable information on the local ecosystem. In parallel to these geochemical studies the endospore forming communities have been analysed together with physical (grain size) analyses. During the second field campaign three cores of 40 cm each were sampled. One in the Northern basin a second in the Southern basin and the last one in the northern part of the channel between the two basins. Sediments of the cores were first characterized by scanning electron microscopy that indicated a large fraction of diatoms in the sediments. Subsequent isotope analysis of carbon ($^{13}C/^{12}C$ and ^{14}C), nitrogen, hydrogen and oxygen of the organic matter and also RockEval measurements will evaluate the composition and quality of the organic matter as it is expected to be largely of autochthonous origin within the sediments of the lake. The lithogenic fraction is analysed via X-ray diffraction and fluorescence for the mineralogy and bulk chemical composition. Collectively, these analyses should allow for good estimates of the sedimentation rates, age of the sediment and a paleoecological interpretation that will then be compared to information obtained from endospore forming communities, a novel biological marker proposed in paleoecological reconstructions.

REFERENCES

Ballif, L. 2018: Carbon and nitrogen stable isotope compositions as environmental proxies in savannas of northern Botswana. Unpubl. Master of Science in Biogeosciences, UNIL.

Dyer, S. 2017: Water cycle in the Northern Kalahari. Unpubl. Master of Science in Biogeosciences, UNIL.

Peel, RA., Tweddle, D., Simasiku, EK., Martin, GD., Lubanda, J., Hay, CJ., Weyl, OLF. 2015: Ecology, fish and fishery of Lake Liambezi, a recently refilled floodplain lake in the Zambezi Region, Namibia. African Journal of Aquatic Science 40:4, 417-424.

Seaman, M.T., Scott, W.E., Walmsley, R.D., van der Waal, B.C.W., & Toerien, D.F. 1978: A limnological investigation of Lake Liambezi, Caprivi. Journal of the Limnological Society of Southern Africa 4:2, 129-144.

Figure 1. Southern Basin of Lake Liambezi during the dry season (September 2016). The water level is low during this season. Lehmann A.

Figure 2. SEM image of a core sample showing coal and diatoms. The core samples show diatoms and organic matter as major content.

P 11.18
Evolution of local topography by fluvial and hillslope processes: a GIS-based study in the eastern Jura Mountains and the Wutach valley (southern Germany)

Andreas Ludwig [1]

[1] Nationale Genossenschaft für die Lagerung radioaktiver Abfälle (Nagra), Hardstrasse 73, CH-5430 Wettingen
(andreas.ludwig@nagra.ch)

Landscape erosion is a key aspect in assessing the long-term safety of a deep-geological repository for radioactive waste in Switzerland. Besides large-scale processes, such as the glaciation of the Alpine Foreland or major changes in the Aare-Rhine fluvial system, fluvial incision along local tributaries and hillslope processes directly contribute to erosion on the siting region scale. Here, aspects of these smaller-scale processes are analysed in a comparative study for two lithologically similar regions with different incision history: the Nagra siting region Jura Ost (JO) and parts of the Wutach valley (Southern Germany). Following a prominent drainage reorganization about 18ka ago, where parts of the Danube headwaters ("Donau-Wutach") were deflected towards the Rhine, the Wutach valley experienced Late Pleistocene river downcutting of up to 150m within only 6ka (Einsele & Ricken 1995). In contrast, JO is considered to have seen minor incision during the same period.

To evaluate the processes, I used a GIS-based analysis, including 1) the extraction of tributary stream longitudinal profiles and 2) manual mapping of "hillslope process domains" based on digital terrain models, geological maps and orthophotos. Step 2 provides an area-covering terrain classification, separating "non-hillslopes" from "hillslopes", and within the latter, different degrees of landslide evidence. Results are analysed with respect to potential controlling factors, such as lithology and local relief.

The marked Late Pleistocene base level fall in the Wutach valley is still manifested in the present-day landscape. According to the mapping result, nearly the entire hillslope domain is characterized as landslide morphology.
The corresponding areal proportion in JO, in contrast, is smaller and variable depending on the lithostratigraphic unit; increasingly more landslides are observed in JO from calcareous to marly and finally clay-rich formations. Lithological effects on erodibility are further observed in tributary stream longitudinal profiles in both study areas, where knickpoints spatially coincide with more resistant bedrock. This behaviour reduces the magnitude of fluvial incision in the upstream sections, at least temporarily contributing to the conservation of upland low-relief areas with presumably low erosion rates, i.e. the "Bözbergplateau" in JO and the relict "Donau-Wutach" landscape. The extensive landslide morphology of the Wutach valley below such knickpoints reflects the high geomorphic process rates following the Late Pleistocene incision (see also Einsele & Ricken 1995). The two different study areas, which represent temporally different times in landscape evolution and morphological adjustment, provide valuable insights for describing potential future erosion scenarios on the siting region scale.

REFERENCES
Einsele, G., & Ricken, W. 1995: The Wutach gorge in SW Germany: late Würmian (periglacial) downcutting versus Holocene processes, Zeitschrift für Geomorphologie, N.-F. Supplement-Band, 100, 65-87.

P 11.19

Spatial patterns of glacial erosion in the Alpine foreland: Morphometric analysis of overdeepenings

Fabio Magrani [1], and Pierre Valla [1]

[1] Institut of Geological Sciences and Oeschger Centre for Climate Change Research, University of Bern, Baltzerstrasse 1+3, CH-3012 Bern (fabio.magrani@geo.unibe.ch)

Alpine overdeepenings consist of widespread geomorphic features shaped by glacial erosion, with up to hundreds of meters carving over the Quaternary. The biggest features in Switzerland are located in the Alpine foreland in the form of major lakes (e.g. Léman, Biel or Neuchâtel) or sediment infills (e.g. in the Bern area).

Their occurrence and geometry in the Swiss foreland have been investigated (Dürst-Stucki & Schlunegger 2013), however both their spatial distribution, morphometric characteristics and Quaternary evolution during successive glaciations remain poorly constrained (e.g. Preusser et al. 2010).

This study consists on the morphometric analysis of glacial overdeepenings in the Alpine foreland to get quantitative constrains on their shape characteristics and spatial occurrence. The aim is to understand how much the bedrock resistance, local settings (lithological contrasts, faults, foreland vs mountain) or drainage network control the location and geometry of overdeepenings. To that aim, differences in their spatial trends (area, length, width and thickness) and the potential influence of lithology, faults/folds and hydrological network will be investigated.

A combined bedrock model derived from Mey et al. (2016) and Dürst-Stucki & Schlunegger (2013) models was generated so as to better constrain the Quaternary sedimentary thickness in flatter regions (Alpine foreland) and in the high-relief regions (Swiss Alps).

Besides, cross-section profiles, shape-factor computation, upstream drainage confluence locations and valley symmetry for big overdeepened features (individual features with areas > 2 km^2) are undergoing analysis. This will, ultimately, provide an overview of the main spatial trends and possible controls related to overdeepenings formation and development. This will allow a broader understanding on the erosive processes by glaciers during Quaternary times.

The study of overdeepenings has implications both for human habitability and for targeting potential geo-resources. Further information about subglacial processes and paleoclimatic conditions involved in deep foreland erosion at the km-scale will require numerical ice flow modeling (ie: Egholm et al. 2012). This will further enhance our comprehension on the evolution of these geomorphic features.

REFERENCES

Dürst-Stucki, M., & Schlunegger, F. 2013: Identification of erosional mechanisms during past glaciations based on a bedrock surface model of the Central European Alps. Earth Planet. Sci. Lett, 384, 57.

Egholm, D., Pedersen, V. K., Knudsen, M.F., Larsen, N.K. 2012: Coupling the flow of ice, water, and sediment in a glacial landscape evolution model. Geomorphology,141-142, 47.

Mey, J., Scherler, D., Wickert, A.D., Egholm, D.L., Tesauro, M., Schildgen, T.F., Stecker, M.R. 2016: Glacial isostatic uplift of the European Alps. Nature Communications, 7, 10.

Preusser et al. 2010: Distribution, geometry, age and origin of overdeepened valleys and basins in the Alps and their foreland. Swiss J. Geoscience, 103, 407.

P 11.20
Erosional dynamics of steep high alpine headwalls revealed by exposure ages (Eiger mountain, Central Swiss Alps)

David Mair [1], Alessandro Lechmann [1], Serdar Yesilyurt [1], Dmitry Tikhomirov [1,2], Christof Vockenhuber [3], Naki Akçar [1]
& Fritz Schlunegger [1]

[1] *Institute of Geological Sciences, University of Bern, Baltzerstrasse 1+3, CH-3012 (david.mair@geo.unibe.ch)*
[2] *Department of Geography, University of Zurich, Winterthurerstrasse 190, CH-8057*
[3] *Laboratory of Ion Beam Physics, ETH Zurich, Otto-Stern-Weg 5, CH-8093*

Exposure ages of various landforms, such as moraines, fluvial terraces, fault scarps or previously ice-covered bedrock have been routinely determined by measuring concentrations of in-situ terrestrial cosmogenic nuclides (TCN) over the last decades.

We applied this method to a steep and vertical headwall (the Eiger north face) by measuring ^{36}Cl concentrations on 5 depth profiles within the Eiger limestones. To achieve this, we benefited from the unique situation of a railway tunnel that was drilled through the mountain and that has several connections to the surface. This enabled us to collect depth-profile samples at 2 sites within the north face and at 3 sites in the southern flank (Fig. 1). The mountain itself displays distinctive differences in morphology with a step-like, over-steepened and very rough north face compared to a steep and comparatively smoother southern flank.

Our results show low cosmogenic ^{36}Cl concentrations for the surface samples, translating into young apparent exposure ages of <2 ka. Interestingly, samples at depth yielded concentrations that translate to much older apparent exposure ages. Subsequent depth profile modelling allowed to confirm the robustness of the young surface exposure ages, while constraining the thickness of the eroded rock to <5m and hinting at significant nuclide inheritance. This consistent TCN pattern suggests a complex erosional history governed by small scale (cm to meter sized blocks) episodic rockfall events rather than large scale (tens of meters) landslides or steady state erosion from chemical weathering.
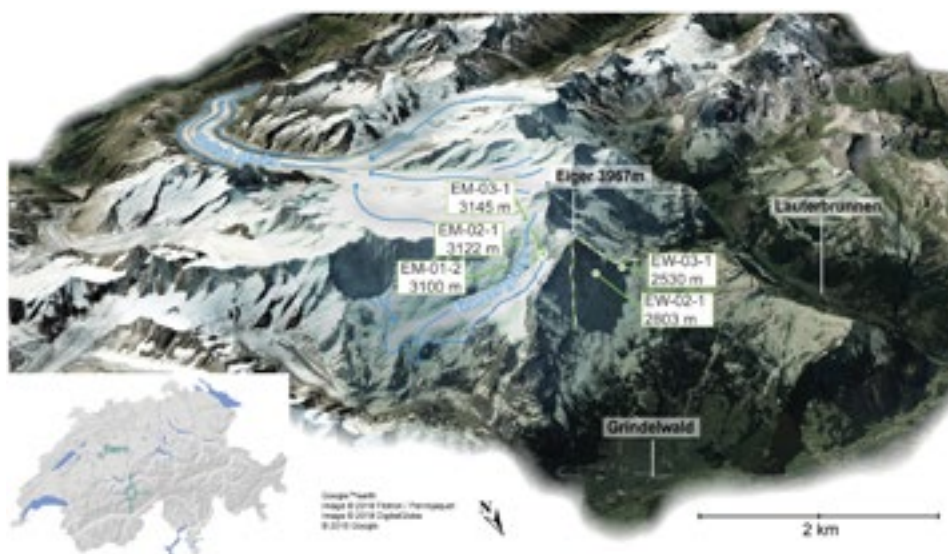

Figure 1. Sample sites for the ^{36}Cl depth profiles around the Eiger mountain.

P 11.21

Long-term high-resolution productivity and meromixis dynamics on the Swiss Plateau (Lake Moossee, Switzerland) inferred from Hyperspectral Imaging

Stamatina Makri [1], Martin Grosjean [1], Fabian Rey [2], Erika Gobet [2]

[1] Institute of Geography & Oeschger Centre for Climate Change Research, University of Bern, Erlachstrasse 9a,
  CH-3012 Bern, Switzerland
[2] Institute of Plant Sciences & Oeschger Centre for Climate Change Research, University of Bern, Altenbergrain 21,
  CH-3013 Bern, Switzerland

The Anthropocene has seen unprecedented environmental change and fundamental ecosystem services are increasingly at stake. Anthropogenically altered biogeochemical cycles, combined with climate change have resulted in adverse ecosystem impacts, increased productivity and anoxia in freshwater systems (Chapman, 1998; Hecky, 2010). However, little is known about lake eutrophication and episodes of hypoxia and meromixis in the past, because this is difficult to measure analytically. Here, we discuss recent developments in novel hyperspectral imaging HSI techniques by our group. The aim is to show how and when meromixis/hypoxia has developed over Holocene time scales and how meromixis has been modulated by anthropogenic impacts (deforestation, erosion, nutrient cycling).

A sound scientific assessment of such changes must rely on a long-term perspective and high-resolution data. Hyperspectral Imaging (HSI) is a novel, fast, non-destructive and cost effective scanning method able to detect diagnostic sedimentary pigments at very high spectral (3 nm) and spatial (40 µm pixel size) resolution .The reflectance spectrum depends on the absorption properties of organic and inorganic substances under the sensor field, and can be used to characterize the sediment composition (e.g. sedimentary pigments). These provide quantitative information about paleoproductivity, past mixing regimes and anoxia in lakes over long (i. e. Holocene) time scales (Butz et al, 2015, 2017).

We are currently focusing on small eutrophic lakes on the Swiss Plateau, Lakes Moossee and Burgäschisee with biogenic varves. Further work is planned in biochemically varved lakes in the Masurian Lakeland, NE Poland (Lakes Żabińskie, Łazduny and Jaczno). We use hyperspectral indices to infer quantitatively Chl a and chlorins as an indicator for aquatic productivity and Bacteriopheophytin a (Bphe a) as an indicator for meromixis (Butz et al, 2016). Bphe a is a diagenetic product of Bacteriochlorophyll a (Bchl a), produced by anoxygenic phototrophic bacteria in the chemocline. Pigment compositions are inferred from sets of spectral indices, such as the Relative Absorption Band Depths (RABD). Indices are calibrated with absolute pigment concentrations of selected samples as measured by HPLC, using linear regression (e.g correlation coefficient of R=0.94, p < 0.001 with a coefficient of determination of $R2 = 0.89$) (Butz et al, 2015).

Lake Moossee contains a complete paleoproductivity and meromixis record at annual resolution (varve years) for the Holocene and Late-Glacial times (past 15,500 years). Hyperspectral imaging data provide evidence for repeated meromixis events in the mid-Holocene. Pollen data suggest that repeated coming and going in meromixis was related to substantial human disturbance in the catchment (Neolithic and Early Bronze Age land use, deforestation and reforestation after land abandonment). In this period, meromixis appears/disappears repeatedly for long periods of ca. 300 years and shows how land use changes affected the biogeochemical cycle in the lake.

REFERENCES

Butz C, Grosjean M, Fischer D, Wudnerle S, Tylmann W, Rein B (2015), Hyperspectral imaging spectroscopy: a promising method for the biogeochemical analysis of lake sediments. J Appl Remote Sens 9:096031

Butz C, Grosjean M, Poraj-Górska A, Enters D, Tylmann W. (2016), Sedimentary Bacteriopheophytin a as an indicator of meromixis in varved lake sediments of Lake Jaczno, north-east Poland, AD 1891–2010, Glob. Planet. Change 144: 109–118.

Chapman, L. J., C. a. Chapman, T. L. Crisman, and F. G. Nordlie (1998), Dissolved oxygen and thermal regimes of a Ugandan crater lake, Hydrobiologia, 385, 201–211.

Hecky, R. E., R. Mugidde, P. S. Ramlal, M. R. Talbot, and G. W. Kling (2010), Multiple stressors cause rapid ecosystem change in Lake Victoria, Freshw. Biol., 55, 19–42.

P 11.22
Investigations on different rock types used in Urartian Gavur castle in Azerbaijan Province, NW Iran

Ali Mohammadi*,[3], Mahsa Moazzen**, Mohssen Moazzen*, Amaneh Kaveh Firouz[3]

[1] Department of Earth Sciences, Faculty of Natural Science, University of Tabriz, 29 Bahman Blvd. 51666, Tabriz, Iran
   (ali.mohammadi@erdw.ethz.ch; mohammadi.a79@gmail.com)
[2] Tabriz Islamic Art University, Faculty of Islamic Arts, Azadi Street, 36931, Tabriz, Iran
[3] Department of Earth Sciences, ETH Zurich, Sonneggstrasse 5, 8092, Zurich, Switzerland

The Azerbaijan area in NW Iran includes more than 80 Urartian historical buildings ruins, belonging to the Iron Age (Kroll, 2011). Limited studies on these buildings ruins are on archeological aspects and there is no published account on their geo-archeological features, including the nature of rock materials used in the construction of these buildings. The Urartian Gavur Castle, located at the south of the Aras Araz River was selected for geo-archeological studies and detecting the possible source of the used materials, due to the variety of lithologies used in the construction of this castle. The results of this study can be used in further investigations on geo-archeological aspects of the Urartian buildings in NW Iran and the adjacent countries. Petrographical and geochemical investigations show more than fifteen different types of the sedimentary and igneous rocks are used in the construction of the Gavur Castle, among which the Upper Cretaceous turbiditic sandstones make more than 90% of the materials used. Andesite and granite are used as rectangular blocks in the castle walls. There is a wide range of sedimentary and mafic, intermediate and felsic igneous rocks as debris resulted from the destroying walls. This debris appears as pebbles with good roundness and sphericity. More likely these rocks are collected from the Pliocene polymict conglomerate at the south-west of the castle.

REFERENCES
Kroll, S., 2011, Urartian cities in Iran. Urartu: transformation in the East. Aktüal Arkeoloji, p.150-169.

P 11.23

Pleistocene palaeo-environmental changes in the Danakil Depression (Northern Afar, Ethiopia)

Haileyesus Negga [1], David Jaramillo-Vogel [1], Valentin Rime [1], Jean-Charles Schaegis [1], Lea Perrochet [1], Patrizia Wyler [1], Ermias Filfilu [2], Addis Hailu [2], Juan Carlos Braga [3], Balemwal Atnafu [2], Tesfaye Kidane [2,4], and Anneleen Foubert [1].

[1] *Department of Geosciences, University of Fribourg, Switzerland*
[2] *School of Earth Sciences, Addis Ababa University, Ethiopia*
[3] *Department of Stratigraphy and Paleontology, University of Granada, Spain*
[4] *Department of Geology, School of Agricultural, Earth and Environmental Sciences, College of Agriculture, Engineering and Sciences, University of Kwazulu-Natal, Westville Campus, Durban, South Africa*

The Danakil Depression, located in the northern apex of the Afar triangle, Ethiopia, is part of an active rifting zone due to the break-up of the Afro-Arabian plateau since Oligocene times. The Danakil Depression is nowadays a dry desert with elevations of 120m below sea level in the central part of the basin. According to seismic data and new core analyses, a 2km thick evaporite sequence alternating with marine marls evidence several episodes of Red Sea incursions followed by desiccation since the Neogene.

The presence of at least two fringing coralgal reef terraces outcropping at the the western margin of the basin, confirms that open marine Red Sea conditions were established during interglacial Marine Isotope Stages (MIS) 5e and 7 (Jaramillo-Vogel et al. 2018). Monospecific bivalves, associated microbialites, aragonitic crusts and coeval spherules, present on top of the coralgal reef units and pre-dating massive gypsum deposits, indicate the intermediate step-wise closure of the connection with the Red Sea and the systematic shift towards more hypersaline environments.

Interestingly, in several outcrops along the margin it is possible to observe lacustrine sediments that are intercalated between the two marine terraces. The occurrence of these unconsolidated carbonaceous sediments, rich in gastropods and charophytes, can be followed along several kilometers. They follow an erosive surface caused by the desiccation of the basin after MIS7. But, the transition to the marine deposits of MIS5e is gradual, implying that no major change in lake level preceeded the marine deposition.

REFERENCES
 Atnafu, B., Kidane, T., Foubert, A., Jaramillo-Vogel, D., Schaegis, J.-C. and Henriet J.-P. 2015: Reading history in Afar. EOS, 96, 12–15.
Jaramillo-Vogel, D., Foubert, A., Braga, J.C., Schaegis, J-C., Atnafu, A., Grobety, B., Kidane, T., 2018: Pleistocene sea-floor fibrous crusts and spherulites in the Danakil Depression (Afar, Ethiopia). Sedimentology.

P 11.24
Quantification of chemical and mechanical denudation in karst landscapes and mechanisms for steep and high carbonate topography on the island of Crete

R. Ott [1], S. Gallen [1], S. Ivy-Ochs [1], J.K. Caves Rugenstein [1], S. Willett [1], David Helman [3], Charalampos Fassoulas [4], C. Vockenhuber [1], M. Christl [1], N. Haghipour [1]

[1] Department of Earth Sciences, ETH Zurich, Zurich, Switzerland
[2] Department of Geosciences, Colorado State University, Fort Collins,
[3] Department of Geography and Environment, Bar Ilan University, Ramat-Gan, Israel
[4] National History Museum of Crete, University of Heraklion, Heraklion, Greece

Quantifying chemical versus mechanical weathering in carbonate catchments has proven problematic due to the difficulties estimating the long-term total or mechanical denudation in carbonates. On Crete —as with many other regions worldwide— carbonate massifs form high mountain ranges whereas topography is lower in areas with clastic-metamorphic rocks. This observation suggests that differences in denudation between more carbonate rich rocks and more quartzofeldspathic units imparts a fundamental control on topographic form. Here we present 16 new cosmogenic ^{10}Be and 8 cosmogenic ^{36}Cl basin-average denudation rate measurements from clastic and carbonate bedrock catchments to quantify substrate erodibility. We compare total denudation rates to dissolution rates calculated from 70 new and published water samples from Crete to quantify the amount of dissolution responsible for long-term denudation. Basin-average denudation rates of clastic-metamorphic units in western Crete are ~ 0.1 mm/a, which is one magnitude lower than coastal uplift rates measured in southwestern Crete. Basin-average denudation rates derived from 36Cl in the 8 carbonate catchments are slightly higher than catchments draining clastic-metamorphic rocks; however, these carbonate catchments have greater relief as they are at the margins of the elevated carbonate plateaus. Average dissolution rates measured from all different water sources in carbonate areas yield a mean dissolution rate of ~ 0.06 mm/a, suggesting that only about half of the mass-loss is attributable to dissolution processes and that mechanical weathering plays an important role at the catchment scale weathering of carbonates. We develop a numerical model for carbonate denudation incorporating mechanical and chemical weathering components to test which parameters besides erodibility are likely to control high and steep carbonate topography. We find that the loss of runoff from surface to groundwater drainage in karst regions is an efficient way to steepen topography and maintain erosion rates that balance the uplift field. We apply this model to Cretan karst landscapes where we calculate water budgets for 4 carbonate catchments and observe losses of up to 90 % of runoff to groundwater. Therefore, we suggest that the loss of runoff in carbonate catchments imposes a first order control on steep and high carbonate topography.

P 11.25

Occurrence and significance of sepiolite deposits in the Chobe enclave (Northern Kalahari Basin, Botswana)

Dimitri Rigoussen [1], Nathalie Diaz [2], John Van Thuyne [1,3] & Eric P. Verrecchia [1]

[1] Institute of Earth Surface Dynamic, Geopolis, University of Lausanne, Lausanne Switzerland
  (dimitri.rigoussen@unil.ch)
[2] Department of Geography, Royal Holloway University, Surrey, Egham, UK
[3] Van Thuyne-Ridge Research Center, Kasane, Botswana

The Chobe Enclave (Northern Botswana) is situated in a present-day semi-arid climate. It is characterized by a flat high plateau undergoing neotectonism, with an active faulting structure, possibly related to a western branch of the East African Rift System (Bufford et al., 2012). Belonging to the large sand Kalahari Basin, the Chobe enclave includes some meter-thick carbonate deposits, which are not yet clearly explained although previously interpreted as Quaternary calcretes (Burrough et al., 2008). Some of these carbonate layers contain sepiolite-rich beds, which were not detected until now. Sepiolite is a trioctahedral Mg-rich clay commonly formed in saline lacustrine-palustrine environments under the influence of groundwater of high Mg+Si/Al ratios (Galan and Singer, 2011). In Botswana, these sepiolitic layers are composed of pure neoformed sepiolite (Fig. 1A, B), associated with Ca-carbonate (as micrite and microsparite) and amorphous silica phases, as well as some detrital quartz grains (Fig. 1C). Consequently, recent data question the calcrete interpretation, pointing to a more complex lacustrine/palustrine origin. Sepiolite needs alkaline waters (8 < pH < 9.5) to precipitate, as well as solutions supersaturated regarding Si and Mg ions (Galan and Singer, 2011): these conditions seriously challenge the source of such solutions in this siliceous basin. In conclusion, as hydrothermal and/or evaporitic environmental settings are frequently invoked to explain the formation of this fibrous clay, sepiolite authigenesis has probably taken place in the Chobe Enclave in a closed lacustrine/palustrine slightly evaporitic basin, with an intermittent input of groundwater influenced by regional hydrothermalism.
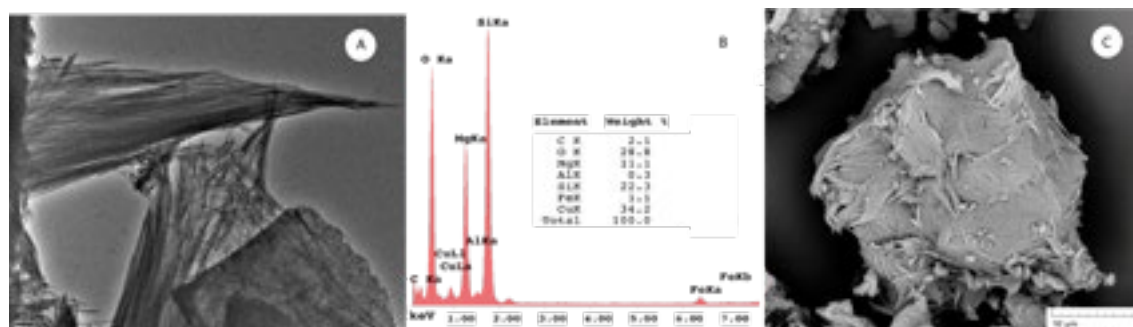

Figure 1: Microscopic aspect, with a representative EDAX analysis, of the sepiolite-rich bed. (A) Transmission Electron Microscope image showing the fibrous nature of the clay; (B) EDAX analysis of sepiolite crystals in (A) with the two major elements, Si and Mg, composing sepiolite. (C) Scanning Electron Microscope image of a quartz grain coated by a mesh of dense sepiolite.

REFERENCES

Bufford, K. M., A. Atekwana, E., G. Abdelsalam, M., Shemang, E., et al. 2012: Geometry and Faults Tectonic Activity of the Okavango Rift Zone, Botswana: Evidence from Magnetotelluric and Electrical Resistivity Tomography Imaging, *Journal of African Earth Sciences*, 65, 61-71.

Burrough, S.L. & Thomas, D.S.G. 2008: Late Quaternary Lake-Level Fluctuations in the Mababe Depression: Middle Kalahari Palaeolakes and the Role of Zambezi Inflows, *Quaternary Research* 69, 388-403.

Galan, E. & Singer, A. (Eds) 2011: Developments in palygorskite-sepiolite research. *Dvpt in Clay Sci.*, 3, 501 pp.

P 11.26

Origin and preservation of pre-Eemian lacustrine deposits in overdeepenings along the Aare Valley between Thun and Bern

Michael A. Schwenk [1], Dimitri Bandou [1], Patrick Schläfli [1], Guilhem A. Douillet [1], Fritz Schlunegger [1]

[1] Institut für Geologie, Universität Bern, Balzerstrasse 1+3, CH-3012 Bern
(michael.schwenk@geo.unibe.ch)

Repeated glacier advances affected the Swiss Plateau during the Quaternary. Deeply carved valleys, where the bedrock surface is located far below the current drainage level, are a prominent feature on the Swiss Plateau. How and when the glaciers lead to the formation of so-called overdeepenings is still a matter of debate.

A detailed model of the bedrock surface is available for the Aare Valley between Thun and Bern (Dürst Stucki, 2010). The model discloses a large, elongated overdeepening along the Aare Valley and a set of adjacent, minor overdeepenings. Furthermore, former investigations showed that a large portion of sediment infill in the overdeepenings could be of pre-Eemian age (Preusser & Schlüchter, 2004; Preusser et al., 2005). However, the three investigate locations along the Aare Valley do not suffice for a credible correlation.

In order to narrow down a probable, minimum age of overdeepening formation in the Aare Valley we will try to resolve its sedimentary framework. Therefore, we will conduct two scientific drilling in the area around Bern. A minor overdeepening is located SW of Bern-Bümpliz. There, lacustrine deposits crop out at the former clay pit REHHAG. Preliminary results of luminescence dating of the lacustrine sediments yield a minimum age of 220 ka. Furthermore, the sediment succession, taken from public drill log data, appears to mirror the one found in the scientific drilling near Meikirch (Preusser et al., 2005). Not only do both locations show a similar sedimentological succession, the thickness and elevation/absolute position of the lacustrine sediments at both locations are about the same.

Therefore, we decided to locate our first drilling at the former clay pit REHHAG to attempt a correlation between the two sites. In the framework of this task, we will include more pre-Eemian lacustrine deposits along the Aare Valley. Therewith, we plan to resolve the depositional conditions of these widespread lacustrine deposits. Eventually, we will correlate these deposits with the glacial and interglacial framework of the formation and filling of the overdeepenings in the Aare Valley.

REFERENCES

Dürst Stucki, M., Reber, R., Schlunegger, F., 2010. Subglacial tunnel valleys in the Alpine foreland: An example from Bern, Switzerland. Swiss J. Geosci. 103, 363–374. https://doi.org/10.1007/s00015-010-0042-0

Preusser, F., Drescher-Schneider, R., Fiebig, M., Schlüchter, C., 2005. Re-interpretation of the Meikirch pollen record, Swiss Alpine Foreland, and implications for Middle Pleistocene chronostratigraphy. J. Quat. Sci. 20, 607–620. https://doi.org/10.1002/jqs.930

Preusser, F., Schlüchter, C., 2004. Dates from an important early Late Pleistocene ice advance in the Aare valley, Switzerland. Eclogae Geol. Helv. 97, 245–253. https://doi.org/10.1007/s00015-004-1119-4

P 11.27
Alpine Glacier Fluctuations and Paleoclimatic Reconstructions

Elena Serra [1,2] Natacha Gribenski [1], Pierre G. Valla [1,2]

[1] *Institute of Geological Sciences, University of Bern, Baltzerstrasse 1+3, CH-3012 Bern, Switzerland*
[2] *Oeschger Centre for Climate Change Research, University of Bern, Falkenplatz 16, CH-3012 Bern, Switzerland*
   (elena.serra@geo.unibe.ch)

Several paleoclimate studies provide evidence for a shift in Alpine atmospheric circulation during the Last Glacial Maximum (LGM), at the onset of Alpine glaciers retreat (Florineth and Schlüchter, 2000; Monegato et al., 2017). Before the LGM, the Alpine precipitation regime was probably dominated by southwesterly advection of atmospheric moisture from the Mediterranean, due to the southward migration of the North Atlantic storm track. After the LGM, the North Atlantic storm track moved northward and present-day atmospheric circulation was established, controlled by northerly atmospheric moisture coming from the Atlantic (Luetscher et al. 2015). However, both the exact timing of this shift in atmospheric circulation and the connected magnitude change in precipitation rates and associated glacier response remain elusive.

The overall aim of this research project is to shed light on Alpine paleoclimatic conditions since the LGM, by using glacier fluctuations in Aosta Valley (Italy) as proxy. Indeed, because glacier mass-balance is highly sensitive to both temperature and precipitation changes, past ice-extent and thickness can be used as quantitative markers of paleoclimatic conditions (e.g. Ivy-Ochs et al., 2008).

The reconstruction of post-LGM ice thickness and extent fluctuations will be achieved using detailed geomorphological mapping together with high-resolution rock surface dating of glacially polished bedrock and erratics (in-situ produced Terrestrial Cosmogenic Nuclides, TCN) and glacio-fluvial and glacio-lacustrine deposits (Optically Stimulated Luminescence,OSL), in different glacial catchments of Aosta Valley with contrasted orographic exposure. The dataset coming from the combination of these two dating techniques will provide high-resolution spatial and temporal reconstructions of paleo-glacier oscillations, during both the Late-glacial and the Holocene times.

Differences in glacier responses between Aosta Valley glacial catchments are expected because of distinct orographic conditions and moisture sources, therefore constraining a shift in paleo-atmospheric circulation.

These time-transgressive paleo-glacier responses will in turn be used as calibration constraints for ice modelling to quantify changes in paleo-precipitation rates and patterns since the LGM and to better understand the glacier response to these changes.

REFERENCES

Florineth, D., & Schlüchter, C., 2000: Alpine evidence for atmospheric circulation patterns in Europe during the Last Glacial Maximum, Quaternary Research, 54(3), 295-308.

Ivy-Ochs, S., Kerschner, H., Reuther, A., Preusser, F., Heine, K., Maisch, M., Kubik, P.W., & Schlüchter, C., 2008: Chronology of the last glacial cycle in the European Alps, Journal of Quaternary Science, 23(6-7), 559-573.

Luetscher, M., Boch, R., Sodemann, H., Spötl, C., Cheng, H., Edwards, R.L., Frisia, S., Hof, F., & Müller, W., 2015: North Atlantic storm track changes during the Last Glacial Maximum recorded by Alpine speleothems, Nature Communications, 6, 6344.

Monegato, G., Scardia, G., Hajdas, I., Rizzini, F., & Piccin, A., 2017: The Alpine LGM in the boreal ice-sheets game, Scientific Reports, 7(1), 2078.

P 11.28
Living benthic foraminifera from cold water coral ecosystems in the Mellilla Mound Field, Alboran Sea, Western Mediterranean

Claudio Stalder [1], Akram El Kateb [1], Osvaldo Camozzi [1], Jorge Spangenberg [2], Loubna Therzhaz [3], Silvia Spezzaferri [1]

[1] Department of Geosciences, University of Fribourg, Chemin du Musée 6, CH–1700 Fribourg, Switzerland (silvia.spezzaferri@unifr.ch).
[2] Institute of Earth Surface Dynamics, University of Lausanne, Building Géopolis, CH–1015 Lausanne, Switzerland.
[3] Group of research ODYSSEE, Materials Nanotechnologies and Environment Laboratory (LMNE), Materials Sciences Research Center.

Quantitative investigation on living (stained) benthic foraminifera, TOC, $\delta^{13}C_{org}$ and $\delta^{15}N_{org}$ from cold-water coral (CWC) surface sediments form 5 box cores recovered on the Melilla Mounds Field (MMF) in the Alboran Sea, western Mediterranean Sea, are presented for the first time.

Benthic foraminiferal assemblages are more diverse on-mound offering more numerous ecological niches than off-mound. The mud layer covering the coral rubbles debris suggests that the MMF is today exposed to sediment siltation.

Geochemical characterization shows that these sediments contain relatively fresh (labile) organic carbon but also reworked refractory components. The $\delta^{15}N$ of the organic fraction suggests that important atmospheric N_2-fixation and degradation processes occur at the MMF and/or that specific hydrographic conditions provide the mound-tops with freshly exported phytodetritus.

P 11.29

Reconstruction of sea surface temperature gradients in the Southern Indian Ocean over the last glacial cycle

Lena M. Thöle [1], Alfredo Martínez-García [2], Anja S. Studer [3], Alexandra Auderset [2], Simone Moretti [2], Alain Mazaud [4], Elisabeth Michel [4], Samuel L. Jaccard [1]

[1] Institute of Geological Sciences, University of Bern and Oeschger Centre for Climate Change Research, University of Bern (lena.thoele@geo.unibe.ch)
[2] Max Planck Institute for Chemistry, Climate Geochemistry Department, Mainz, Germany
[3] Aquatic and Isotope Biogeochemistry, Department of Environmental Sciences, University of Basel
[4] Laboratoire de Sciences et de l'Environnement (LSCE), Gif-sur-Yvette, France

Over glacial-interglacial cycles, the Southern Ocean exerts a major leverage on atmospheric CO_2 concentrations and thus Earth's climate[1]. The Antarctic Circumpolar Current (ACC) plays a crucial role in the global heat and nutrient distribution, Antarctic sea ice dynamics, and the upwelling of CO_2- and nutrient-rich subsurface waters. As micronutrients and light are limiting primary production in this area, nutrients that are brought up to the surface are not completely consumed, engendering a degree of inefficiency in the biological pump thereby allowing for CO_2 to escape to the atmosphere. Due to its dynamical association with the Westerlies, changes in the strength and/or equatorwards shifts of the ACC during glacial periods has been hypothesized. However, paleoceanographic reconstructions are still ambiguous and changes in ACC dynamics on glacial/interglacial timescales remain to be under debate[2,3].

We make use of the strong latitudinal temperature gradients observed over the different zones north and south of the ACC today[4], that act as a main driver of the flow strength. Thus, we reconstructed TEX86-based sea surface temperatures (SSTs) for three cores located in the modern Antarctic Zone (AZ), Polar Frontal Zone (PFZ) and Subantarctic Zone (SAZ), respectively. These data allow us to calculate changes in the temperature gradients since the penultimate glacial period, inferring the dynamics of changing ACC strengths. We argue that larger SST gradients during warm periods accelerated the ACC flow and consequently upwelling intensities, ultimately leading to enhanced CO_2 outgassing. Smaller glacial SST gradients had the opposite effect, thus helping to sequester more CO_2 in the deep ocean.

These results will help to better understand past changes in ACC dynamics, provide a more complete picture of the past Southern Ocean and its relevance for CO_2 sequestration over glacial-interglacial cycles.

REFERENCES

[1] Sigman, D. M., Hain, M. P. & Haug, G. H. 2010: The polar ocean and glacial cycles in atmospheric CO_2 concentrations, Nature, 466 (7302), 47-55, doi:10.1038/nature09149

[2] McCave, I. N., Crowhurst, S. J., Kuhn, G., Hillenbrand, C.-D. & Meredith, M. P. 2014: Minimal change in Antarctic Circumpolar Current flow speed between the last glacial and Holocene, Nature Geosciences, 7, 113–116, doi:10.1038/NGEO2037.

[3] Mazaud, A., Michel, E., Dewilde, F. & Turon, J. L. 2010: Variations of the Antarctic Circumpolar Current intensity during the past 500 ka., Geochemistry, Geophysics, Geosystems, 11, 8, doi:10.1029/2010GC003033.

[4] Armour, K. C., Marshall, J., Scott, J. R., Donohoe, A. & Newsom, E. R. 2016: Southern Ocean warming delayed by circumpolar upwelling and equatorward transport, Nature Geosciences, 9, 549-554, doi:10.1038/NGEO2731.

P 11.30

High-resolution eutrophication history records and phosphorus retention in Lake Burgaschi (Switzerland) since ~1800 AD

Luyao Tu, Martin Grosjean

Oeschger Centre for Climate Change Research and Institute of Geography, University of Bern

Increasing primary productivity in lakes (eutrophication) has been a detrimental environmental problem since the industrial revolution. In most cases, excessive phosphorus (P) inputs are considered as the main contributor to lake eutrophication. It has been widely accepted that internal P loading from lake sediments can also have a profound impact on the trophic state and prevent the lake from recovery (Cao et al. 2016). However, the relevance of different P forms in the sediments for eutrophication process has received little attention so far.

Burgaschi lake is classified as eutrophic to highly eutrophic since 1970s. Although recent eutrophication history in Burgaschi lake is well documented, very little is known about how the trophic status of this lake changed since 20th century even in the further past. Since 1970s, some in-lake restoration techniques have been applied in this lake aiming to mitigate eutrophication and improve the lake status. It is not well known about how the lake sediments have recorded and responded to these treatments.

In the study, we will address critical knowledge gaps for longer eutrophication history reconstruction of Burgaschi lake and develop new insights into the relevance of P fraction of the sediments to eutrophication. We will analyze varved lake sediments from Lake Burgaschi. Green pigments (Chl *a* and chlorins) inferred from high-resolution hyperspectral imaging scanning will be used to reconstruct the productivity history of the lake since ~1800 AD. A sequential P-extraction with five fractions will be performed to uncover P species retention in the sediments (Lukkari et al. 2017).

The current results show that when the primary productivity of the lake was higher, P retention in the sediments was decreased. The work is still under way. More results will be shown in the meeting then.

REFERENCES

Barbieri A, & Simona M. 2001: Trophic evolution of Lake Lugano related to external load reduction: Changes in phosphorus and nitrogen as well as oxygen balance and biological parameters. Lakes Reserv Res Manag, 6(1):37–47.

Cao X., et al., 2016: Phosphorus mobility among sediments, water and cyanobacteria enhanced by cyanobacteria blooms in eutrophic Lake Dianchi. Environmental Pollution, 219: 580-587.

Lukkari K et al. 2017: Fractionation of sediment phosphorus revisited. I: Fractionation steps and their biogeochemical basis. Limnology and Oceanography: Methods 5:433 -444.

P 11.31
Fungus-growing termites as geological agents transforming savanna landscapes

John Van Thuyne [1,2], Eric P. Verrecchia [1]

[1]Institute of Earth Surface Dynamics, University of Lausanne, CH-[1015] Lausanne (john.vanthuyne@unil.ch)
[2]VanThuyne-Ridge Research Centre, Chobe Enclave, Kasane, Botswana.

This research aims at evaluating the biogeochemical, mineralogical, and physical impacts of fungus-growing termites in soils covering savanna landscapes. In 1990, Julia Allen Jones was the first to earmark the concept of "ecosystem engineer" in tropical and sub-tropical savanna ecosystems, referencing to the role of fungus-growing termites. Fungus-growing termites (subfamily Macrotermitinae, Isoptera) share an exosymbiosis with fungi belonging to the Termitomyces genus. In order to maintain the symbiosis possible, Macrotermitinae must maintain specific hydric and thermic conditions. Therefore, fungus-growing termites build large biogenic structures as large epigeal mounds, easily visible in sub-tropical areas of Africa and Asia. By doing so, fungus-growing termites are able to increase by an order of magnitude of 3 to 4 the alkalinity of soils. They also increase their carbonate contents, the C/N ratios and concentrate nutrients such as potassium and phosphorus. Through the process of selection and transportation of sand grains in their bucal cavity and their mixing with saliva, fungus-growing termites modify the chemical compositions and the mineralogical propreties of clays. They also act as accelerating agents of clay alteration and chemical weathering in tropical ecosystems. The activities of fungus-growing termites tend to slightly raise locally the land surface providing some recolonization advantages.They concentrate nutrients, forming a pattern of fertile lands, and enhancing the growth of vegetation by creating islands of fertility.The selection of very fine sands, in order to meet the construction requirement for their mounds, create patches of clayey sands that have the property to retain water for long periods of time, producing scattered pockets of water in semi-arid regions.
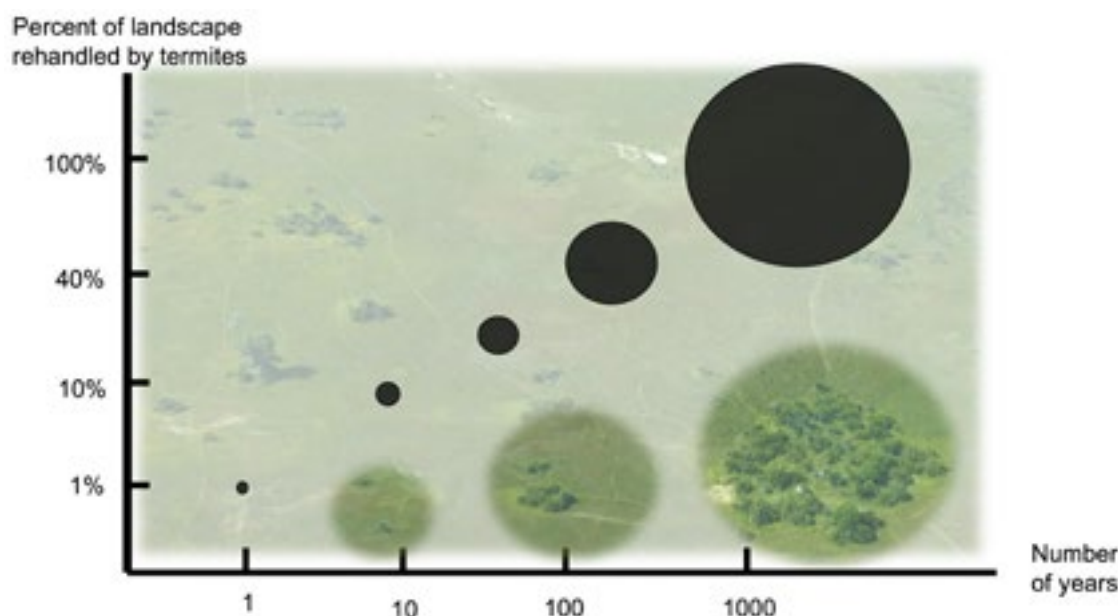

Figure 1. With a density of approximatly 12 mounds per hectare averaging 10 square meters on the ground surface, and knowing that most mounds are occupied for 10 to 20 years Holt et al.(1980), it can be estimated that at this rate, every 100 to 1000 years the entire soil surface of an hectare of semi-arid savanna has been rehandled by fungus-growing termites.

REFERENCES
Allen-Jones J. (1990) Termites, soil fertility and carbon cycling in dry tropical Africa: a hypothesis. J Trop. Ecol., 6, 3: 291-305
Holt et al. (2000) Termites and Soil Properties. Termites: Evolution, Sociality, Symbioses, Ecology. Chapter 18, 389-407.

P 11.32
A high-resolution late-glacial lake sediment record of climate changes and associated environmental impacts from Moossee (Switzerland)

Stephan H. Wartenweiler [1], Adrian Gilli [1], Fabian Rey [2], Stefano M. Bernasconi [1], Erika Gobet [3], Willy Tinner [3]

[1] Department of Earth Sciences, ETH Zurich, Sonneggstrasse 5, CH-8092 Zurich (stephawa@student.ethz.ch)
[2] Department of Environmental Sciences, University of Basel, Klingenbergstrasse 27, CH-4056 Basel
[3] Institute of Plant Sciences, University of Bern, Altenbergrain 21, CH-3013 Bern and Oeschger Centre for Climate Change Research, University of Bern, Falkenplatz 16, CH-3012 Bern

The transition from the last glacial to the current interglacial (i.e. Holocene) comprises several abrupt major and minor climatic excursions. Lake sediments deposited during this time interval represent valuable terrestrial archives, since they have the potential to show past climate changes at high-resolution. In this study, the stable oxygen isotope composition of lacustrine carbonates from Moossee (Switzerland) was analyzed in order to receive a high-resolution climate record for the last glacial termination and the onset of the Holocene (ca 15,000 a BP to 11,000 a BP). Moreover, a precise age-depth model has been established by the correlation of the oxygen isotope record measured on the lacustrine carbonates and oxygen isotope records from Greenland ice-cores (i.e. NGRIP). During the Oldest and Younger Dryas as well as during minor cold oscillations interrupting the Bølling/Allerød interstadial, the comparison of the stable oxygen isotope record and XRF data on the elemental composition of the sediment allowed to resolve leads and lags between the onset of these cold periods (i.e. negative shifts of the oxygen isotope values) and the reaction of the sedimentary system (i.e. elevated detrital input into the lake). The comparison with the lacustrine record from Gerzensee (van Raden et al., 2013) indicates that large-scale climate changes as well as local factors had an influence on the records during the last glacial termination. Finally, the combination of the measured $\delta^{13}C$ and XRF data has been used to show the importance of biological activity in the lake for the stable carbon isotope record.

REFERENCES
Van Raden, U.J., Colombaroli D., Gilli A., Schwander J., Bernasconi S.M., van Leeuwen J.F.N., Leuenberger M., Eicher U. 2013: High-resolution late-glacial chronology for the Gerzensee lake record (Switzerland): $\delta^{18}O$ correlation between a Gerzensee-stack and NGRIP. Palaeogeogr., Palaeoclimatol., Palaeoecol. 391, 13-24.

Symposium 11: Quaternary environments

P 11.33

Evidence for a local last glacial maximum during the MIS-3 in eastern Turkey

Serdar Yeşilyurt [1], Uğur Doğan [2] & Susan Ivy-Ochs [3], Christof Vockenhuber [3] Naki Akçar [1],

[1] Institute of Geological Sciences, University of Bern, Baltzerstrasse 1-3, CH-3012 Bern (serdar_yesilyurt@yahoo.com)
[2] Department of Geography, Ankara University, 06100 Sıhhiye Ankara Turkey
[3] Laboratory of Ion Beam Physics, ETH Zurich, Otto-Stern Weg 5, CH - 8093 Zurich

As Turkey is located in the Alpine-Himalayan mountain belt, it has a mountainous landscape with ranges extending parallel to the coast in the north and south. This landscape causes moist air masses to leave precipitation mostly in the coastal regions. Therefore, the central parts of Turkey have lower precipitation compared to the coast, and the continental climate prevails. This inbalance results in different equilibrium line altitudes (ELA) on the coast and inland. In order to explore, in this study, how this inbalance in the past was and how it was changing in time and space, we focus on the remnants of past glaciations in the eastern Turkish mountains, where significant evidence of past glaciations are present, but poorly constrained. To do so, we studied the glacial geology in the Kavuşşahap Mountains, Mount Bingöl, Munzur Mountains and Tahtalı Mountains in detail and reconstructed the glacial chronology with surface exposure dating.

In the field, we mapped the glacial landforms and erosional features in detail and collected surface samples from erratic boulders on the moraines for cosmogenic ^{36}Cl analysis. Detailed geomorphological mapping indicate that these areas have experienced several glacial advances. For instance, glaciers reached a maximum length of 17 km in the Narlıca Valley in the Kavuşşahap Mountains and descended to an altitude of 2350 m above sea level. The reconstructed chronology in this valley show that the oldest glacial advance, thus the local last glacial maximum extent occurred during the MIS-3 (Marine Isotope Stage 3) in this valley. We found that the ELA was 1150 m lower than today, which point to about 10ºC decrease in average yearly temperature in the region.

P 11.34

TCN dating of high-elevated rockfalls in the Mont Blanc massif. A new method of dating rockfalls in the Mont Blanc massif using reflectance spectroscopy

Xavi GALLACH[1,2], Philip Deline[1], Julien Carcaillet[2], Ludovic Ravanel[1], Yves Perrette[1], Dominique Lafon[3], Christophe Ogier[2]

[1]Laboratoire EDYTEM. Université Savoie Mont Blanc, CNRS. 73000 Chambéry, France
 xavi.gallach@univ-savoie.fr
[2]Laboratoire ISTerre. Université Grenoble Alpes, CNRS. 38000 Grenoble, France
[3]IMT Mines Alès. 30100 Alès, France

Rockfalls and rock avalanches are active processes in the Mont Blanc massif, with infrastructure and alpinists at risk. Thanks to a network of observers (hut keepers, mountain guides, alpinists) set up in 2007 current rockfalls are well surveyed and documented. Rockfall frequency has been studied over the past 150 years by comparison of historical photographs, showing that it strongly increased during the three last decades, likely due to permafrost degradation caused by the climate change. In order to understand the possible relationship between rockfall frequency and the warmest periods of the Lateglacial and the Holocene, we study the morphodynamics of some selected high-elevated (> 3000 m a.s.l.) rockwalls of the massif on a long timescale.

Since rockfall deposits in glacial areas are evacuated by the glaciers, our study focuses on the rockfall scars. ^{10}Be TCN dating of a rockwall surface gives us the rock surface exposure age, interpreted as a rockfall age. Here we present a dating dataset of 80 samples carried out between 2006 and 2016 at six high-elevated rockwalls in the Mont Blanc massif. The resulting ages vary from present (0.04 ± 0.02 ka) to far beyond the Last Glacial Maximum (*c.* 100 ka). Three clusters of exposure ages are correlated to i) two Holocene Warm Periods (7.50 - 5.70 ka), ii) the Bronze Age Optimum (3.35 - 2.80 ka) and iii) the Roman Warm Period (2.35 - 1.75 ka). A fourth age cluster has been detected with ages ranging 4.91 – 4.32 ka. The biggest cluster, ranging 1.09 ka – recent, shows rather small volumes (< 15,000 m^3). This is interpreted as the normal erosion activity corresponding to the current climate.

Furthermore, a relationship between the colour of the Mont Blanc granite and its exposure age has been established: fresh rock surface is light grey (e.g. in recent rockfall scars) whereas weathered rock surface shows a colour in the range grey to orange/red: the redder a rock surface, the older its age. Reflectance spectroscopy is used to quantify the granite surface colour. We explored the spectral data in order to find an index to measure the rock weathering evolution along time, thus allowing to date the rock surface exposure age using reflectance spectroscopy: the GReen Infrared GRanite Index (GRIGRI), based on the Remote Sensing-used GRVI Vegetation Index. GRIGRI uses the ratio between Green (530 nm) and Photographic Infrared (770 nm) reflectance to obtain the index, directly related to the granite exposure age (r= 0.861). The GRIGRI method has been tested for 8 samples where TCN dating failed, and for two samples where ^{10}Be exposure age is considered outlier. The resulting ages, according to the geomorphology of the scars and their surroundings, are plausible.

12. Geomorphology for a habitable planet

Nikolaus Kuhn, Christoph Graf, Isabell Kull, Geraldine Regolini, Isabelle Gärtner-Roer, Margreth Keiler, Christophe Lambiel, Christian Scapozza, Reynald Delaloye, Negar Haghipour

Swiss Geomorphological Society (SGmS)

TALKS:

12.1   Bigler S., Zimmermann M., Keiler M.: Assessment and documentation of a large-scale debris flow in Barsem, Tadjikistan.

12.2   Hirschberg J., McArdell B., Molnar P.: A systematic comparison of rainfall thresholds for debris flows initiation at the Illgraben catchment

12.3   Märki L., Lupker M., Gajurel A., Haghipour N., Schide K., France-Lanord C., Lavé J., Morin G., Gallen S., Eglinton T.: Inter-seismic monsoonal control on organic and inorganic long-term carbon budget of Himalayan erosion

12.4   Sobecka K., Allen J.: Cycles of Discussion, Circulation of Images

12.5   Strozzi T., Wegmüller U., Caduff R., Raezo H.: Sentinel-1 Persistent Scatterer Interferometry – Continuity for precise slope displacement observations over Switzerland

12.6   Vos H.C., Fister W., Kuhn N.J.: Assessing the boundary conditions of dust emission from croplands in the Free State, South Africa

12.7   Zaki A.S., Edgett K.S., Gupta S., Castelltort S.: Inverted fluvial networks in the Sahara as a terrestrial analogue to study the geomorphology, sedimentology, and paleohydrology of similar landforms on Mars

POSTERS:

p 12.1   Giaccone E., Mariéthoz G., Lambiel C.: How geomorphological factors and microclimate influence alpine vegetation? Cases study in the Western Swiss Alps

p 12.2   de Palézieux L., Leith K., Loew S.: Assessing the predictive capacity of hillslope projected channel steepness for rockslope instability in the High Himalaya of Bhutan

p 12.3   Douillet G.A., Kueppers U., Schlunegger F.: Pyroclastic dune bedforms: macroscale structures and lateral variations

p 12.4   Elkadi J., Lehmann B., King G.E., Kronig O., Biswas R., Ivy-Ochs S., Christl M., Herman F.: Constraining paleo-ice extents and post glacier erosion in the Western Alps since the Last Glacial Maximum.

p 12.5   Greenwood P., Baumann P., Pulley S., Kuhn N.: The invasive alien plant, Impatiens glandulifera (Himalayan Balsam), and increased soil erosion: causation or association? Case studies from a river system in Switzerland and the UK

p 12.6   Greenwood P., Bauer J., Kuhn N.: Hillslope sediment transport by tree-throw: a field study in the Jura Mountains, northwest Switzerland

p 12.7   Krenz J., Kuhn B., Kuhn N.: Assessing Badland Sediment Sources Using Unmanned Aerial Vehicles in the Karoo rangelands, South Africa

p 12.8   Schlatter D.D., Hughes H.S.R., Schenkel R., Pasqualini I., Brichet N.S.: An ice-free Northwest Passage: What are the consequences for exploration and exploitation of mineral resources and other raw materials in Greenland and in the Canadian Arctic?

p 12.9   Sprafke T., Veit H.: Biomantles and cover beds – competing concepts for soil formation and landscape evolution?

p 12.10   Walter F., Mangeney A.: Seismic constraints on effective friction of rock-ice avalanches

p 12.11   Bruni E., Gallen S., Picotti V., Willett S.: Origin and Late Quaternary emplacement of the unique fans in the Klados River catchment, Crete, Greece

p 12.12   Salehipour Milani A., Yazdani T.: Modeling behavior and hazards of Popocatépetl Volcano, Mexico

p 12.13   Tonini M., Zanetta F., Amato F., Kanevski M.: Modelling natural hazards using Machine Learning: the case study of landslides in Canton Valais, Switzerland

12.1
Assessment and documentation of a large-scale debris flow in Barsem, Tadjikistan.

Sophie Bigler [1], Markus Zimmermann [1], Margreth Keiler [1]

[1] Institute of Geography, University of Bern, Hallerstrasse 12, 3012 Bern, CH

A large-scale debris flow event occurred in July 2015 in the high mountains of the Tajik Pamir, transporting about 4.2 million m³ of material. The starting zone of the event is located in a periglacial area at 4100 m. asl. from where the material was transported along and additional sediments eroded within the 7km long channel until they reached the fan at 2350 m. asl within the village of Barsem. An in-depth field investigation, interviews with local villagers of Barsem, analysis of digital elevation models (before and after) and an analysis of videos, photos from during the event and satellite imagery (before and after) could reveal new findings concerning the triggering, the sediment budget and the sequence of the 30 to 40 individual surges.

The presentation will focus on following main aspects of the study:

- The analysis of aggregated weather data (TRMM, ERA-interim), observations from local villagers and recordings from the local weather station 40km upstream from Barsem indicates extraordinary meteorological conditions: prior to the event a long and cold spring was followed by a sudden start of a very hot summer. These conditions led to the conclusion that a quick, intensive snow and ice melt increased the amount of water in the starting zone and additionally, aggregated avalanche snow in the channel contributed to the run-off. In the nights before the event thunderstorms were recorded by local witnesses. The TRMM data revealed an unusual amount of precipitation in mid-July.

- The sediment budget is based on twenty-eight cross-sections extracted from a digital elevation model with 0.5m resolution and verified in the field. Furthermore, the situation before the event along the whole flow path was inferred from various sources like a DTM (30 m Terra Aster), few photographs and satellite imagery and a morphological interpretation of the terrain. The analysis showed, that 20% of the eroded sediment originates from the starting zone, but mainly deposited in the upper area; and 60% were eroded in the channel as well as 15% of the transported material was eroded from the old fan deposits in the lowest part of the channel.

The combination to the different detailed analysis in this study allowed a precise reconstruction of the event that lasted from the 16th to the 23rd of July, with peak activities on the 16th and the night from the 17th to the 18th of July. The newly built fan was no longer altered strongly after the 18th, even though several flows still occurred until the 23rd of July. Most probably, the triggering of the event was caused by the collapse or liquefaction of the terminal moraine where melting permafrost must be assumed. A glacial lake outburst flood (GLOF) as a trigger could be excluded by the detailed reconstruction of the event with the high number of surges.

12.2
A systematic comparison of rainfall thresholds for debris flows initiation at the Illgraben catchment

Jacob Hirschberg [1,2], Brian McArdell [1] & Peter Molnar [2]

[1] Swiss Federal Institute for Forest, Snow and Landscape Research WSL
[2] Institute of Environmental Engineering ETH Zürich

Since the 1980's, rainfall intensity-duration (ID) thresholds have been used to define a rainfall threshold for triggering debris flows and other slope failures. ID thresholds can be obtained by applying linear regression to the rainfall duration and mean intensity (or cumulated rainfall) of observed debris flow triggering events. While this procedure is objective, the simplification of the triggering mechanism causes large inaccuracies when used for early warning systems, because rainfall events lying above the threshold do not trigger a debris flow (Figure 1).
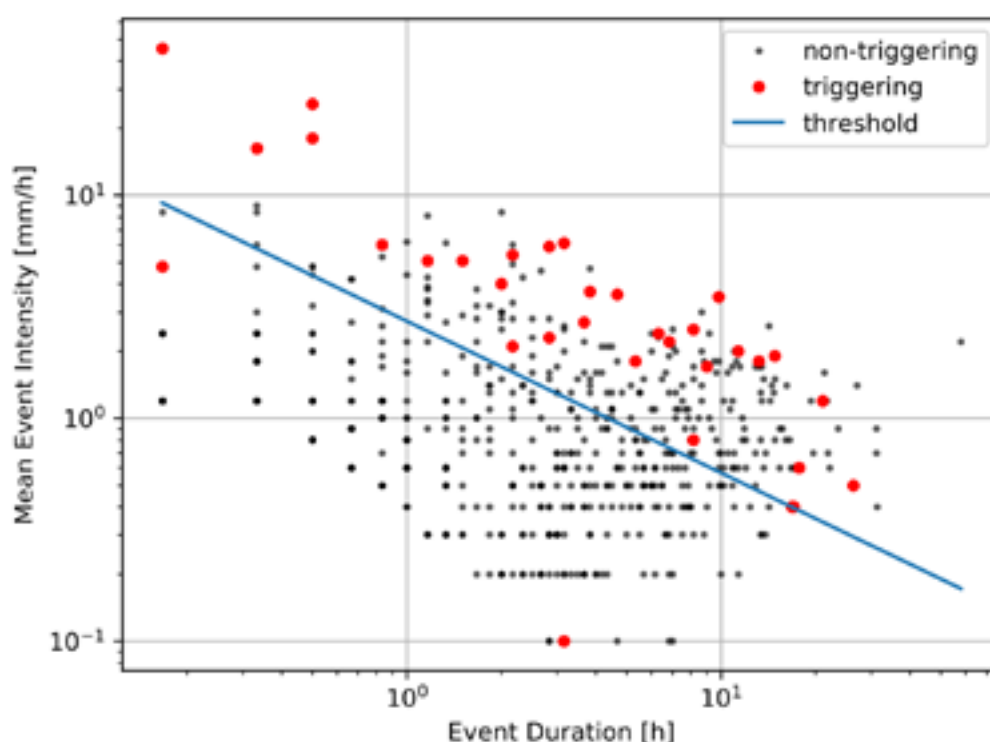
Figure 1. Intensity-duration threshold (blue) obtained by linear regression on the triggering events and shifted to maximize the performance in separating debris flow triggering (red) and non-triggering (black) rainfall events. While the threshold perfroms well in debris flow detection, many black dots are above the threshold, causing large inaccuracies in the prediction. Considering more rainfall properties, such as peak rainfall intensity, leads to a better performance.

The Illgraben debris-flow observation station, operated starting in the year since 2000, has successfully recorded 75 debris flows and debris floods. Rainfall data are available from 2001 from three tipping-bucket rain gauges installed within the catchment at different locations. Thus, the data record enables a thorough analysis of the interaction of rainfall and debris flow initiation.

We apply Receiver Operating Characteristics[1] (ROC) surface to analyze the predictive power of a range of rainfall properties in debris flow forecasting. In a subsequent step, we explore the predicitve potential of statistical learning methods such as Random Forests[2] (RF). The RF method is often used for classification tasks, as it is known for its ability to deal with interacting and correlating predictor variables. Consequently, RF is attractive for the classification into debris flow triggering and non-triggering events based on rainfall properties such as duration, mean intensity, peak intensity and cumulated rainfall. Results indicate that RF is able to increase debris flow detection while lowering false detection rate.

The results support characterization of debris flow triggering with rainfall. However, they do not address other factors such as antecedent wetness of the catchment prior to rainfall or the availability of sediment for debris flow initiation. These factors will be included in a next step in a modelling framework based on the SedCas (Sediment Cascade) model[3] to improve the prediction of debris flow activity.

REFERENCES

[1] Fawcett, T. (2006). An introduction to ROC analysis. *Pattern recognition letters*, *27*(8), 861-874.

[2] Breiman, L. (2001). Random forests. *Machine learning*, *45*(1), 5-32.

[3] Bennett, G. L., Molnar, P., McArdell, B. W., & Burlando, P. (2014). A probabilistic sediment cascade model of sediment transfer in the Illgraben. *Water Resources Research*, *50*(2), 1225-1244.

12.3

Inter-seismic monsoonal control on organic and inorganic long-term carbon budget of Himalayan erosion

Lena Märki [1] , Maarten Lupker [1], Ananta Gajurel [2] , Negar Haghipour [3,1], Katherine Schide [1], Christian France-Lanord [4] , Jérôme Lavé [4], Guillaume Morin [5] , Sean Gallen [6] , Timothy Eglinton [1]

[1] *ETH Zurich, Geological Institute, Zürich, Switzerland*
[2] *Tribhuvan University, Central Department of Geology, Kathmandu, Nepal*
[3] *ETH Zurich, Ion Beam Physics, Departement of Physics, Zürich, Switzerland*
[4] *Centre de Recherche Pétrograpiques et Géochimiques, CNRS – Université de Lorraine,*
 Vandoeuvres-lès-Nancy, France
[5] *UMPC, Laboratoire d'océanographie de Villefranche-sur-mer, France*
[6] *Colorado State University, Department of Geosciences, Fort Collins, USA*

The erosion of mountain ranges plays an important role in the carbon cycle and may influence the global climate on geological timescales. Here, we investigate the controls on the magnitude of the main carbon sinks, namely silicate weathering and subsequent carbonate precipitation as well as the export and burial of organic carbon, in the Central Himalaya. In this contribution we focus on quantifying the impact of the April 2015 Gorkha earthquake (Mw 7.8) on the export of organic carbon and the chemical weathering rates providing a carbon budget of such a rare, high magnitude, event.

We acquired river suspended sediment and water samples during 3 monsoon seasons (2015-2017) from the Narayani River, a large tributary of the Ganges. The Gorkha earthquake triggered a large number of landslides in the steep valleys of the High Himalaya (Roback et al., 2017). The Narayani is one of the major outlets of the Central Himalaya and its eastern part was heavily affected by the Gorkha earthquake providing a broader scale test of the impact of the earthquake on biogeochemical cycles. Daily samples provide high-resolution time-series and a set of samples from the monsoon 2010 gives a pre-earthquake reference point. Combining suspended sediment load data with total organic carbon (TOC) as well as its stable and radiocarbon isotopic compositions, we try to reconstruct the sources of organic carbon in suspended sediments. Analyses of river water chemistry allow us to estimate the chemical weathering-related carbon budget of the catchment before and after the earthquake.

Our preliminary results confirm that carbon drawdown from the burial of organic carbon of the Central Himalaya is about 3 times more important than the silicate weathering carbon sink (France-Lanord & Derry, 1997). We show that the co-seismic landslides of the Gorkha earthquake did not significantly influence sediment loads, carbon export and chemical weathering fluxes at the scale of the studied large catchment. However, the magnitudes of organic carbon export and of silicate weathering fluxes are strongly controlled by river discharge. We therefore suggest that the long-term carbon budget of such a Himalayan catchment is mainly controlled by the monsoon intensity and the hydrological budget during inter-seismic periods and not by rare but intense co-seismic events as has been suggested in other systems.

REFERENCES

France-Landord, C. & Derry, L. 1997: Organic carbon burial forcing of the carbon cycle from Himalayan erosion, Nature, 390, 65-67.

Roback, L. et al., 2017: The size, distribution, and mobility of landslides caused by the 2015 Mw 7.8 Gorkha earthquake, Nepal, Geomorphology, 301, 121-138.

12.4
Cycles of Discussion, Circulation of Images

Karolina Sobecka [1], Jamie Allen [2]

[1] Institute for Aesthetic Practice and Theory, Basel Academy of Art and Design FHNW, Freilager-Platz 1, Basel
(Karolina.Sobecka@fhnw.ch)
[2] Institute of Experimental Design and Media Cultures / Critical Media Lab, Basel Academy of Art and Design, FHNW,
Freilager-Platz 1, Basel (Jamie.Allen@fhnw.ch)

Karolina Sobecka (karolinasobecka.com) and Jamie Allen (jamieallen.com) are collaborating researchers, part of a research group interested in environmental humanities, art, design and science at the *Hochschule für Gestaltung und Kunst FHNW* in Basel, and associated with the media arts production facilities at the Critical Media Lab Basel. We are artist-researchers who often manifest our work as artworks, events and through mediums other than text-based publications, while writing and publications focus on the relationships between aesthetics, knowledge and environment (Allen 2017). Methodologically this work and research often encounters interdisciplinary collectives as a means of evoking, reflecting and understanding communities of practice (Allen *et. al* 2011) and attempts to devise alternative representations of these. Our current project and focus is on exploring the ways that climate science and planetary magnitude technologies are represented, deliberated and thought about in science, engineering on through policy, governance, technology and popular media.

The use of different languages, linguistic metaphors and canonical examples in discussions relating to our common environment of planet earth greatly influence the ways in which we imagine solutions, design decisions, create policy and enact governance. Geoengineers use hopeful, domestic and clarifying phrasings like "resetting the global thermostat", to describe the necessity and effectiveness of, for example, aerosol injection into Earth's atmosphere. The term "greenhouse effect", for example, coined in 1907, forms part of a rhetorical trajectory begun by geologist Thomas Sterry Hunt in 1867 when he wrote of climatological conditions "producing an effect precisely as if we had covered the whole earth with an immense dome of glass, had transformed it into a great Orchid-house" (Hunt 1867). What would be different about our technological and geoengineering landscape were modelled on a somewhat or completely different "as if"?

Research into the ways that discourse can change behaviour is a central part of behavioural research around dilemma of the commons, and how the mobilisation of nomenclature and information is best transferred to embodied or actionable knowledge (Nerlich 2010). Just as with language, but further to and along with it, choice made regarding the formats and contexts of events and discussions, the visualisation of data, the distribution of images and iconography and the rendering of time based media (audio and video), impacts the ways in which we treat ecosystems and imagine their modulation and adjustment. How we imagine the future is predicated on the means and mediums we use to plan for and project into this future (Fløttum, et. al 2014).

For the 16th Swiss Geoscience Meeting in Bern, we propose a brief textual and image based interview and study for three of the workshops that are taking place at the event in Bern on November 30th and December 1st, 2018. We would like to discuss with groups prior to the sessions, via a quick questionaire and gathering of materials, the ways in which they imagine the work they are doing and the presentations they will make in Bern. From these resources, collected over the weeks following the abstract submission deadline of August 31st, 2018 and prior to the event itself, we would develop short reflections for the participating groups, to be presented as part of workshops. These would take the form of a re-narativisation of the thematics, common examples, linguistic tropes, visual concurrences and aesthetics and information design styles emergent in the discussions and materials presented in Bern. (We have made contact with the "Geomorphology for a habitable planet at the Swiss Geoscience Meeting" and the "Sustainable social-ecological systems: from local to global challenges at the Swiss Geoscience Meeting" who have expressed interest in the research)

We would hope that such perspective, as arts and design researchers exploring the way that climate engineering is deliberated and communicated, would be of use to the community of researchers participating in Bern and these materials would for us form the basis for further research outputs to be shared with the groups in attendance.

Figure 1. Recent fieldwork in China, visiting the coal fired power plant carbon capture facilities and discussing with plant engineers.

REFERENCES

Allen, J., 2018. The Overgrounds and Undergrounds of Pure and Applied Science: Cosmic Collisions and Industrial Collusion. Media Theory, 2(1), pp.352-392.

Allen, J., Clarke, R., Galani, A. and Wajda, K., 2011, November. Creative Ecologies in Action: Technology and the Workshop-as-artwork. In Proceedings of the 8th ACM conference on Creativity and cognition (pp. 309-310). ACM.

Fløttum, K., Gjesdal, A.M., Gjerstad, Ø., Koteyko, N. and Salway, A., 2014. Representations of the future in English language blogs on climate change. *Global Environmental Change*, *29*, pp.213-222.

Hunt, T.S., 1867. The chemistry of the primeval Earth. *Geological Magazine*, *4*(40), pp.477-478.

Nerlich, B., Koteyko, N. and Brown, B., 2010. Theory and language of climate change communication. Wiley Interdisciplinary Reviews: Climate Change, 1(1), pp.97-110.

12.5

Sentinel-1 Persistent Scatterer Interferometry – Continuity for precise slope displacement observations over Switzerland

Tazio Strozzi [1], Urs Wegmüller [1], Rafael Caduff [1] & Hugo Raezo [2]

[1] *Gamma Remote Sensing, Worbstrasse 225, CH-3073 Gümligen (strozzi@gamma-rs.ch)*
[2] *Federal Office for the Environment, Hazard Prevention Division, CH-3003 Bern*

The European Space Agency (ESA) has been providing repeated SAR data since the beginning of the 1990's with the ERS-1, ERS-2 and ENVISAT missions launched in 1991, 1995 and 2002, respectively. During these last decades, Persistent Scatterer Interferometry (PSI) has demonstrated to be a powerful tool to measure and monitor surface deformations using large stacks of SAR images (Strozzi et al., 2013, Wegmüller et al., 2013). The Sentinel-1 constellation – ESA follow-on SAR mission specifically designed for SAR interferometric applications and displacement monitoring – is operational since 2014 and has an expected lifetime of 20 years. With both Sentinel□1A and Sentinel-1B satellites, SAR images from the same orbit are acquired every 6 days over Europe and distributed following a free and open data policy. Various nation-wide maps of land deformation were recently released, e.g. in Germany (Haghighi and Motagh, 2017) and the United Kingdom (www.geomaticventures.com/uk-map). Over Switzerland, hazards due to slope instabilities affect about 6% of the territory and there is therefore a high interest on systematic Sentinel-1 PSI deformation maps and time series of surface motion.

Considering the south-east facing slope of Val Lumnezia as an example of one of the most active and large landslides in inhabited areas in Switzerland (Raetzo et al., 2007), we will discuss peculiarities of Sentinel-1 PSI processing over the Alps, where snow-cover and atmospheric stratification cause special challenges. In particular, during winter months interferograms computed with long time intervals are decorrelated and processing has to be limited to summer acquisitions only. In spite of the large number of Sentinel-1 acquisitions available, this has the consequence that an overall observation period of several years is required for a robust processing and only scatterers moving with velocities smaller than a few cm/year can be typically captured. Maps of the average displacement rates and time-series of motion from Sentinel-1 data for the time period 2015-2018 will be discussed in comparison to results from Radarsat-2 data, regularly acquired from 2011 to 2017 over the Swiss Alps and providing a robust PSI solution for recent years, and past maps obtained from the ERS and ENVISAT SAR sensors (Figure 1). The observed deformation rates reach values of up to several cm/year with a relatively high density of PSI-points inside the villages and for the alpine zone. Differential SAR interferograms (InSAR) will be also presented to highlight the complementarity with PSI for the study of the faster moving parts of the landslide. We conclude that for the study of very slow moving Alpine slopes, Sentinel-1 PSI provides an efficient opportunity for repeated monitoring over intervals of a few years.

REFERENCES

Haghighi, M., & Motagh, M. 2017: Sentinel-1 InSAR over Germany: Large-Scale Interferometry, Atmospheric Effects, and Ground Deformation Mapping, zfv 4/2017, digitally available under www.geodaesie.info.

Raetzo, H., Wegmüller, U., Strozzi, T., Marks, F. & Farina, P. 2007: Monitoring of Lumnez Landslide with ERS and ENVISAT SAR data, Proceedings of the 2007 ESA ENVISAT Symposium.

Strozzi, T., Ambrosi, C., & Raetzo, H. 2013: Interpretation of Aerial Photographs and Satellite SAR Interferometry for the Inventory of Landslides, Remote Sensing, 5(5): 2554-2570.

Wegmüller, U., Strozzi, T., & Gruner, U. 2013: Verschiebungsmessungen mittels Satellitenradar im Urner Reusstal oberhalb der Nord-Süd-Verkehrsachse im Zeitraum 1992 – 2010, Swiss Bull. angew. Geol., 18(2): 139-153.
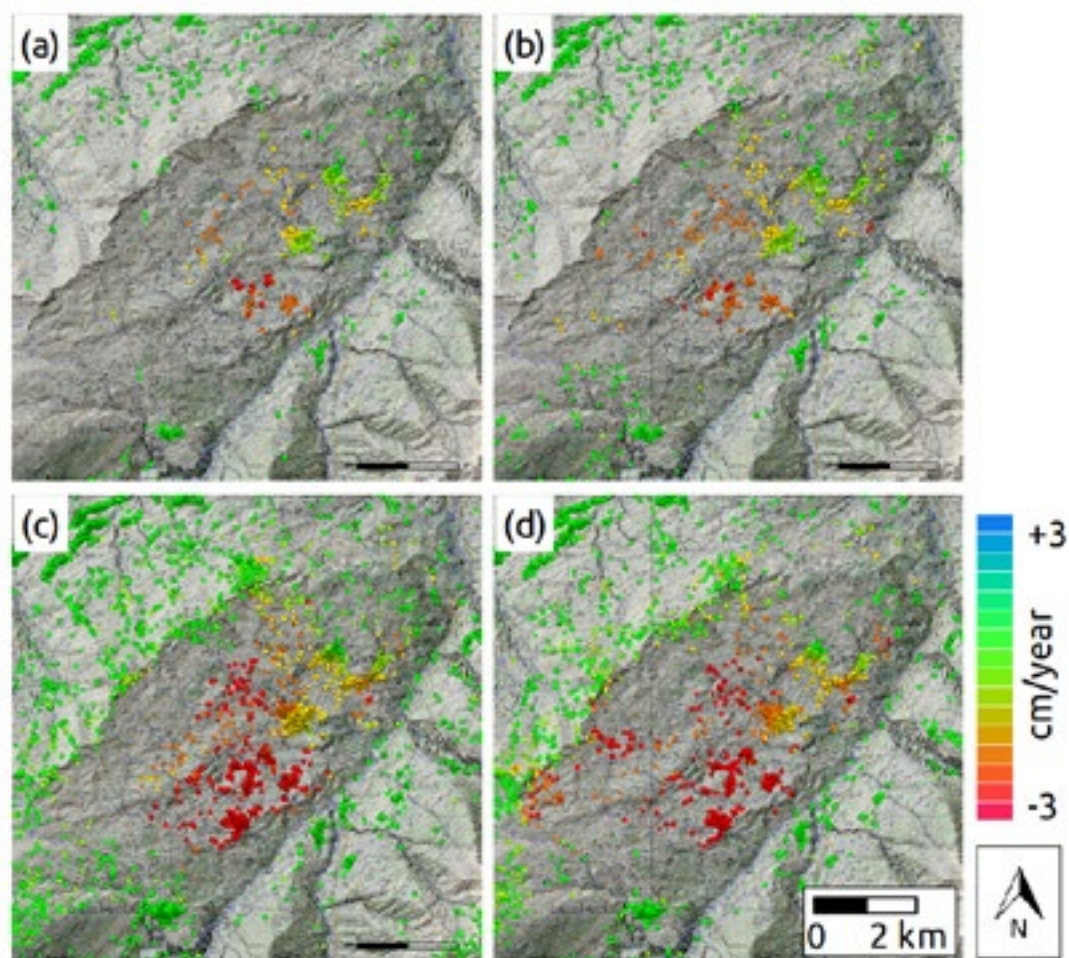
Figure 1. Average displacement rates of persistent scatterers in the satellite LOS direction from (a) ERS SAR data of the time period 1992-2000, (b) ENVISAT ASAR data for the time period 2003-2010, (c) Radarsat-2 data for the time period 2011-2017 and (d) Sentinel-1 data for the time period 2015-2018.

12.6

Assessing the boundary conditions of dust emission from croplands in the Free State, South Africa

Heleen C. Vos [1], Wolfgang Fister [1] & Nikolaus J. Kuhn

[1] Physical Geography and Environmental Change, University of Basel, Klingelbergstrasse 27, CH-4056 Basel
(heleen.vos@unibas.ch)

The Free State Province is one of the regions in South Africa with the highest dust emissions. In contrast to most dust sources in South Africa, which have a solely natural origin, the dust producing areas in the Free State are largely located in intensively cultivated croplands. The dust emissions from the dominating Arenosols and Luvisols are likely to have a severe impact on human health, global climate, and biogeochemical cycles. Beside the regional or even global off-site effects of these dust emissions, there is also the direct soil degradation by the wind erosion at a local scale. The removal of fine, nutrient- and organic-rich particles leads to a reduction of soil fertility and crop production. The dust emissions from these croplands are driven by soil and weather conditions, as well as crop management and local tillage practices. This project, which is funded for four years by the Swiss National Fund and the National Research Foundation of South Africa, aims to address these different drivers. The first work package focuses on locating the points of origin of the dust and the factors that might lead to exposed and bare croplands, such as droughts or agricultural management practice. The second part of this study focusses on measuring and reproducing soil characteristics and the physical boundary conditions for dust emission on these exposed croplands. The third part of this study will address the human health issues associated with these dust plumes in cities nearby, with a focus on the microbiome that is captured with the dust.

The work package of the University of Basel involves experimental measurements with a wind tunnel, a rainfall simulator and a Portable In-Situ Wind ERosion Lab (PI-SWERL). These methods are used to assess dust emission rates from surfaces in this region. The main focus hereby is laid on crust formation and deterioration, since these sandy soils are prone to crusting due to relatively high clay contents. The combination of field and laboratory measurements will generate a better understanding of the processes and site specific conditions that cause the high dust emissions in this agricultural region of South Africa

12.7

Inverted fluvial networks in the Sahara as a terrestrial analogue to study the geomorphology, sedimentology, and paleohydrology of similar landforms on Mars

Abdallah S. Zaki [1], Kenneth S. Edgett [2], Sanjeev Gupta [3], Sebastien Castelltort [1]

[1] *Department of Earth Sciences, University of Geneva, Rue des Maraichers 13, 1205 Genève, Switzerland (abdallah.zaki@etu.unige.ch)*
[2] *Malin Space Science Systems, Inc., P.O. Box 910148, San Diego, CA 92191, USA*
[3] *Department of Earth Sciences and Engineering, Imperial College London, London, SW7 2AZ, UK*

Based on planimetric patterns, more than 200 sites of sinuous ridges have been identified on Mars from spacecraft imagery, including MOC (0.5/12 m/pixel), THEMIS IR (100m/pixel), VIS (18-36 m/pixel), CTX (~6 m/pixel), and HiRISE (~0.3 m/pixel), and the list continues to grow (e.g., Williams, 2007; William et al., 2007; Williams et al., 2011; Davis et al., 2016). These sites are interpreted to be remnants of ancient fluvial activity, but the nature of the fluid, its source and the mechanism of flow at play are a matter of debate (e.g., Williams, 2007; Williams et al., 2007, 2009; Zimbelman and Griffin, 2010). Distinguishing "pathways" for future exploration of planet Mars is the one of the most important challenges for future studies of Mars geology using orbiter data because the amount of landing sites and distances that rovers can explore are limited on the Martian surface. Orbiter instruments have long provided crucial perspectives on the entire planet. However, possible exploration pathways cannot yet be determined only through remotely-sensed data. Terrestrial analogues are highly important as models of the geological processes that may have occurred on Mars. For example, how can we use current observations of inverted channels on Mars to generate hypotheses about 1) ancient fluid flow conditions on this planet, 2) sedimentary facies models for inverted channel networks, 3) sources, sinks and directions of flows and particulate sediment transport, 4) conditions of burial, lithification and exhumation versus induration of the fluvial sediments on the surface. All these questions could find preliminary answers through comparison with terrestrial analogues.

Inverted fluvial networks in the Egyptian Sahara offer a natural laboratory for inverted topographic features that involved some degree of sediment lithification (the channels were buried, lithified in the subsurface, and then exhumed) in the Dakhla Depression and of sole sediment induration (i.e. the channel fills were never deeply buried, and thus also not subsequently exhumed) in the southern part of Egypt. Therefore, in this study, we collected 33 samples from these two sites for petrographic analyses (thin-section), cathodoluminescence to examine their cement materials, and Electron Microbeam microscopy to look at the shape of sand grains in order to decipher the relative importance of aeolian and fluvial processes on sediment transport. Finally, drawing on geometrical similarity, we intend to use current grain size estimates of channel fills in the Antoniadi Crater inverted valley networds in order to provide first-order estimates of palaeohydrology at this location.

REFERENCES

Williams, R. M. E., Chidsey Jr, T. C., Eby, D. E. (2007). Exhumed paleochannels in central Utah – Analogs for raised curvilinear features on Mars, In: G. C. Willis, M. D. Hylland, D. L. Clark, T. C. Chidsey Jr. (editors), Central Utah – Diverse geology of a dynamic landscape, Utah Geological Association Publication 36, 220–235, Salt Lake City, Utah, USA.

Williams, R. M. E., R. P. Irwin III, J. R. Zimbelman (2009). Evaluation of paleohydrologic models for terrestrial inverted channels: Implications for application to Martian sinuous ridges, Geomorphology 107, 300–315. doi:10.1016/j.geomorph.2008.12.015

Williams, R.M.E. (2007). Global spatial distribution of raised curvilinear features on Mars. Lunar Planet. Sci. Conf. 38th, Abstract # 1821.

Williams, R.M.E., R.P. Irwin III, J.R. Zimbelman, T.C. Chidsey Jr., Eby, D.E. (2011). Field guide to exhumed paleochannels near Green River, Utah: Terrestrial analogs for sinuous ridges on Mars, in Analogs for Planetary Exploration, edited by W. B. Garry and J. E. Bleacher, Geological Society of America Special Papers 483, 483–505. doi:10.1130/2011.2483(29)

Zimbelman, J.R., Griffin, L.J. (2010). HiRISE images of yardangs and sinuous ridges in the lower member of the Medusae Fossae Formation, Mars. Icarus, 205, 198-210.

Davis, J.M., Balme, M., Grindrod, P.M., Williams, R.M.E., Gupta, S. (2016). Extensive Noachian fluvial systems in Arabia Terra: Implications for early Martian climate. Geology ; 44 (10): 847–850. doi: https://doi.org/10.1130/G38247.1

P 12.1

How geomorphological factors and microclimate influence alpine vegetation? Cases study in the Western Swiss Alps

Giaccone Elisa [1], Mariéthoz Grégoire [1], Lambiel Christophe [1]

[1] Institute of Earth Surface Dynamics (IDYST), University of Lausanne, CH-1015 Lausanne, Switzerland
 (elisa.giaccone@unil.ch)

In alpine systems, landform movements, earth surface processes and microclimate can have impacts on the microhabitat conditions and modify species richness, composition and distribution patterns of plant communities (Le Roux & Luoto 2014). Considering the high vulnerability of the alpine environments, it becomes very important to analyze and understand the impact and the influence of landforms processes on plant species.

For this purpose, a multi-methodological approach was applied in three focus sites in the Western Swiss Alps (Les Outans, Col des Perris Blancs and Les Martinets; elevation between 2000 and 2500 m; Fig. 1). The sites are characterized by a high geomorphological variability: multi-age moraine deposits, rock glaciers, talus slopes and stabilized area allow the presence of different plant communities (from pioneer species to grassland species).

In these sites, 73 plots were studied. For each plot, vegetation survey was carried out and species cover, species richness and evenness were calculated. Furthermore, ground surface temperature, topographic variables, earth surface processes (ESPs – solifluction, rill erosion, nivation and frost weathering) and landform morphodynamics index were assessed. Mean, maximum and minimum temperatures, freezing degree days (FDD), growing degree days (GDD) and growing season length (GSL) were calculated from the temperature data, obtained from miniature temperature loggers iButton® DS1922L. The relation between plant communities and environmental variables were analyzed with multivariate linear models, non-metric multi-dimensional scaling (NMDS - Oksanen et al., 2007) and multivariate regression techniques (generalized linear model, GLM, and generalized additive model, GAM - e.g. le Roux and Luoto, 2014).

Based on results, species cover and species richness were significantly and positively correlated (Spearman's rank correlation $\rho = 0.82$; p-value < 0.001). ESPs had a significant and positive infuence on species cover and species richness (respectively $\rho = -0.45$; $p < 0.001$; $\rho = -0.37$; $p < 0.001$), negative on evenness ($\rho = 0.35$; $p < 0.01$).

NMDS analysis indicated that GSL, morphodynamics index and GDD were the most explanatory variables of plant community composition (ordination stress = 22%). GSL had the highest values of linear fit ($R^2 = 50\%$, p-value < 0.001), followed by morphodynamics index ($R^2 = 49\%$, p-value < 0.001) and GDD ($R^2 = 43\%$, p-value < 0.001).

Additionally, the regression models for species cover and species richness were significantly improved by the addition of the morphodynamics index. Indeed, in both GLMs and GAMs, the explained deviance of species cover and species richness was augmented. This showed that, to explain alpine plant community distribution, the landform morphodynamics is a key factor.

REFERENCES

Le Roux, P.C. & Luoto, M. 2014: Earth surface processes drive the richness, composition and occurrence of plant species in an arctic-alpine environment. Journal of Vegetation Science 25, 45-54.
Oksanen, J., Kindt, R., Legendre, P., O'Hara, B., Stevens, M.H.H., Oksanen, M.J., et al. 2007: The vegan package. Community ecology package 10, 631-637.
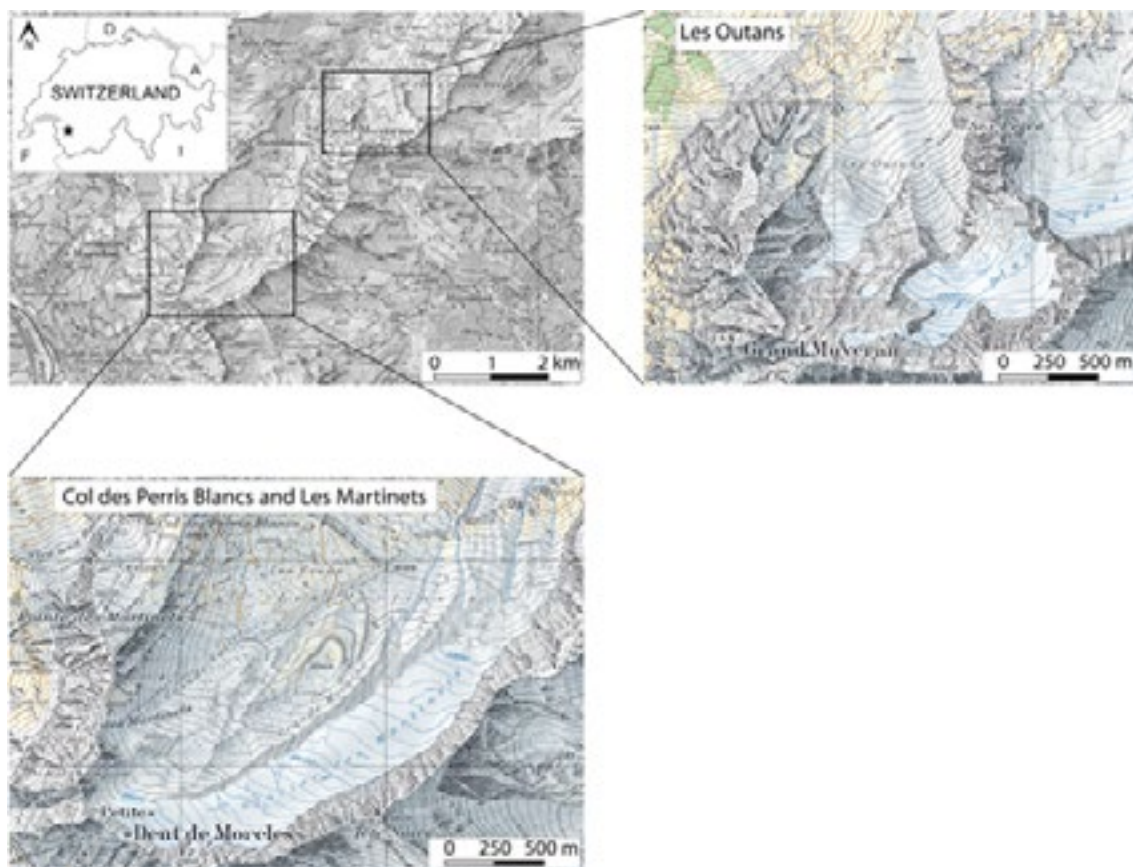
Figure 1. Locations of the three selected sites.

P 12.2

Assessing the predictive capacity of hillslope projected channel steepness for rockslope instability in the High Himalaya of Bhutan

Larissa de Palézieux [1], Kerry Leith [1], Simon Loew [1]

[1] Geological Institute, ETH Zurich, Sonneggstrasse 5, CH-8092 Zurich
 (larissa.depalezieux@erdw.ethz.ch)

With large alluvial planes, narrow gorges, prominent knickpoints, and chains of terraces or cut-off ridges, the deeply-incised valleys below 3000 m a.s.l. in Bhutan record distinct changes in rates of spatial and temporal fluvial incision. In regions with little geological knowledge, excess topography has been shown to be a good predictor for landslide distribution (Blöthe et al., 2015). The authors suggest this indicates a structural control, specifically that topogaphy which exceeds a specific threshold angle will attain static equilibrium via gravitational slope movements. Since 2016 the engineering geology group at ETHZ has been working on cataloguing active and dormant slope instabilities in NW Bhutan using a combination of satellite-based remote sensing, 5m-resolution digital elevation models, and field observations. Here, we compare the predictive capacity of the excessive topography approach to a method in which we relate relative stream energy through the normalized channel steepness index (k_{sn}) to landslide occurrence. Initial observations indicate that regions of excess topography generally coincide with those of increased channel steepness, hinting at a causal relationship. While further work is required, an assessment of enhanced erosional power using hillsope extrapolated k_{sn} values may provide an additional means of characterizing the spatial distribution of landslides in such environments. This supports the notion that slope instabilities are the result of a combination of structural bedrock control and surface erosional activity.

REFERENCES

Blöthe, J. H., Korup, O., & Schwanghart, W. (2015). Large landslides lie low : Excess topography in the Himalaya-Karakoram ranges, 43(6), 523–526. https://doi.org/10.1130/G36527.1

P 12.3
Pyroclastic dune bedforms: macroscale structures and lateral variations

Guilhem Amin Douillet [1], Ulrich Kueppers [2], Fritz Schlunegger [1]

[1] Institut für Geologie, Universität Bern, Baltzerstrasse 1+3, CH-3012 Bern (guilhem.douillet@geo.unibe.ch)
[2] Earth and Environmental Sciences, Ludwig-Maximilians-Universität, Theresienstrasse 41, D-80333 München

Pyroclastic currents are catastrophic flows of gas and particles triggered by explosive volcanic eruptions and belong to particulate density currents. They occasionally deposit dune bedforms with peculiar lamination patterns, from what is thought to represent the dilute, low concentration, and fluid-turbulence supported end member of the pyroclastic currents. Here, we present a high resolution dataset of sediment plates (lacquer peels) with several closely spaced lateral profiles representing sections through single pyroclastic bedforms from the August 2006 eruption of Tungurahua, Ecuador (Douillet et al. 2018a).

Most of the sedimentary features contain backset bedding and preferential stoss-face deposition. From the ripple scale (few cm) to the largest dune bedform scale (several m length), similar patterns of erosive-based backset beds are evidenced. Recurrent trains of sub-vertical truncations on the stoss side of bedforms reshape and steepen the bedforms. In contrast, sporadic coarse-grained lenses and lensoidal lenses flatten structures by filling troughs. The coarsest (clasts up to 10 cm), least sorted and massive bedforms still exhibit lineation patterns that follow the general backset architecture.
Drastic variations in stratal architecture are evidenced between flow-parallel profiles separated by a few tens of centimeters, and further emphasize the local nature of truncations, both in flow-parallel and perpendicular directions.

We infer that the bedforms' sedimentary patterns result from four formation mechanisms: "differential draping", "slope-influenced saltation", "truncative bursts", and "granular-based events". Whereas most of the literature makes a straightforward link between backset bedding and Froude-supercritical regime bedforms, we interpret stoss-depositional laminae as the products of slow and subcritical currents (Douillet et al. 2013). Further, we show that features generally taken as diagnostic of dunes, antidunes, and chute-and-pools can be found on the same horizon and in a single bedform, only laterally separated by short distances (10s of cm), and do not directly inform for a Froude-regime interpretation of a pyroclastic current (Douillet et al. 2018b).

Rather, our data stress the influence of the pulsating and highly turbulent nature of the currents that interact with pre-existing morphology in a very high sedimentation environment of weak and waning currents. The role of coherent flow structures such as Görtler vortices may also be significant in shaping pyroclastic bedforms and influencing the dynamics of pyroclastic currents.

Quantification of near-bed flow velocities are made via comparison with wind tunnel experiments (Douillet et al. 2014). We estimate that shear velocities of ca. 0.30 m.s-1 (equivalent to pure wind velocity of 6 to 8 m.s-1 at 10 cm above the bed) could emplace the constructive bedsets, whereas the truncative phases would result from bursts with impacting wind velocties of at least 30-40 m.s-1.

REFERENCES
Douillet, G. A., Pacheco, D. A., Kueppers, U., Letort, J., Tsang-Hin-Sun, È., Bustillos, J., Hall, M., Ramón, P., and Dingwell, D.B. (2013) Dune bedforms produced by dilute pyroclastic density currents from the August 2006 eruption of Tungurahua volcano, Ecuador, B. Volcanol., 75, 1–20
Douillet, G.A., Rasmussen, K.R., Kueppers, U., Lo Castro, D., Merrison, J., Iversen, J., Dingwell, D.B. (2014) Saltation threshold for pyroclasts at various bedslopes: Wind tunnel measurements. J. Volc. Geotherm. Res. 278-279:14-24
Douillet, G.A., Kueppers, U., Mato, C., Chaffaut, Q., Bouysson, M., Reschetizka, R., Hölscher, I., Witting, P., Hess, K.U., Cerwenka, A., Dingwell, D.B., Bernard, B. (2018) Revisiting the lacquer peels method with pyroclastic deposits: Sediment plates, a precise, fine-scale imaging method and powerful outreach tool. Journal of applied Volcanology. In press
Douillet G.A., Bernard B., Bouysson M., Chaffaut Q., Dingwell D.B., Gegg L., Holscher I., Kueppers U., Mato C., Ritz. V., Schlunegger F., Witting P. (2018b) Pyroclastic dune bedforms: macroscale structures and lateral variations. Examples from the 2006 pyroclastic currents at Tungurahua (Ecuador). Sedimentology. Accepted manuscript, preliminary version available at https://eartharxiv.org/3sxtf/. DOI: 10.31223/osf.io/3sxtf

P 12.4

Constraining paleo-ice extents and post glacier erosion in the Western Alps since the Last Glacial Maximum.

Joanne Elkadi [1], Benjamin Lehmann [1], Georgina E. King [1], Olivia Kronig [2], Rabiul Biswas [1], Susan Ivy-Ochs [2], Marcus Christl [2] & Frédéric Herman [1].

[1] Institute of Earth Surface Dynamics, Faculty of Geosciences and Environment, University of Lausanne, CH-1012 Lausanne (joanne.elkadi@unil.ch)
[2] Laboratory of Ion Beam Physics, ETH Zurich, 8093 Zurich, Switzerland.

With the current climate regime, our ability to assess past conditions is crucial for predictions of future climate scenarios and landscape evolution. The aim of this study is to contribute towards a more detailed understanding of the glacial history and post-glacial erosion across the Central and Western Alps, which encompasses some of the highest topography in Europe. Since glaciers in mountaineous areas are particularly sensitive to climate change, precisely constraining these processes in this region would provide invaluable information on the local, and potentially global, climate at the time. Here we reconstruct the glacial history of the Gorner glacier in Zermatt, Switzerland, since the Last Glacial Maximum (LGM). The method used in this study combines the applications of both cosmogenic ^{10}Be and optically stimulated luminescence (OSL) to surface bedrock exposure dating (e.g. Gosse and Phillips, 2001; Lehmann et al., 2018). Cosmogenic ^{10}Be builds up in quartz through time as a result of cosmic ray penetration within approximately the first 3 m of the rock surface (Lal, 1991). On the other hand, OSL surface exposure dating is based on the measurement of a light sensitive signal that produces a distinctive profile with rock depth (Sohbati et al., 2011). This is due to the the propagation of a bleaching front usually found within the first 1-5 mm. Preliminary Holocene and Lateglacial exposure ages and post glacial erosion rates, from samples collected down a vertical transect in the study area, will be presented.

REFERENCES

Gosse, J.C. & Phillips, F.M. 2001: Terrestrial in situ cosmogenic nuclides: theory and application, Quaternary Science Reviews, 20, 1475-1560.
Lehmann, B., Valla, P.G., King, G.E., Herman, F. 2018: Investigation of OSL surface exposure dating to reconstruct post-LIA glacier flucturations in the French Alps (Mer de Glace, Mont Blanc massif), Quaternary Geochronology, 44, 64-74.
Lal, D. 1991: Cosmic ray labeling of erosion surfaces: in situ nuclide production rates and erosion models. Earth Planet. Sci. Lett. 104, 424-439.
Sohbati, R., Murray, A., Jain, M., Buylaert, J.P., Thomsen, K. 2011: Investigating the resetting of OSl signals in rock surfaces. Geochronometria 38, 249-258.

P 12.5

The invasive alien plant, Impatiens glandulifera (Himalayan Balsam), and increased soil erosion: causation or association? Case studies from a river system in Switzerland and the UK

Philip Greenwood [1], Patrick Baumann [1], Simon Pulley [2], Nikolaus J. Kuhn

[1] Physical Geography & Environmental Change, Department of Environmental Sciences, University of Basel, Klingelbergstr. 27, CH-4056 Basel (philip.greenwood@unibas.ch)
[2] Sustainable Agriculture Sciences, Rothampsted Research, North Wyke, Devon, UK

A monitoring investigation undertaken along the River Ibach, northwest Switzerland over the winter 2012/2013, found that riparian areas recently supporting the invasive plant Himalayan Balsam (HB) recorded significantly higher erosion rates than nearby uninvaded areas. This communication sythesises the latest findings about the influence of HB on sedimentation processes, again, from the Ibach, but also from a second river system in southwest UK. Erosion pins, a micro-profile bridge and a digital caliper were used to measure changes in soil surface profile (SSP) at selected riparian areas supporting HB plants along both rivers. Values were statistically compared against equivalent data recorded from nearby reference areas supporting mixed perennial vegetation. A comparison of source and sediment geochemistry was also undertaken on soil from HB-invaded and uninvaded floodplain areas along the Ibach, to assess the potential for identifying the extent to which either group acts as a sediment source. Erosion pin data indicate that soil loss from HB-colonised areas was significantly greater than soil loss from reference areas in two out of the four periods at the River Ibach site, and in two out of three measurement periods at the River Taw site. Colonisation of new HB sites may initially occur by hydrochorous processes, but HB plants may increase colonisation potential by trapping additional fine sediment and organic matter, including viable HB seeds. Geochemical results from the Ibach suggest that high inputs of suspended sediment originate from sources close to the river channel, but HB-invaded floodplain sources have geochemical properties that are most similar to suspended river sediment. The findings from both rivers led us to rethink our original hypothesis; that HB promotes soil erosion, to an amended hypothesis in which HB may be associated with areas where high erosion is sometimes recorded. Whilst initial colonisation may be due to hydrochorous processes, as HB becomes increasingly established, the displacement of perennial vegetation increases the risk of erosion during the winter period when live HB plants are absent. Preliminary geochemical findings of floodplain soils supporting different vegetation types along the Ibach tentatively suggest that at least some material originating from HB sites may enter the watercourse.

P 12.6
Hillslope sediment transport by tree-throw: a field study in the Jura Mountains, northwest Switzerland

Philip Greenwood [1], Jan Bauer [1], Nikolaus J. Kuhn [1]

[1] *Physical Geography & Environmental Change, Department of Environmental Sciences, University of Basel, Klingelbergstr. 27, CH-4056 Basel (philip.greenwood@unibas.ch)*

A field-based study was undertaken in a small (< 10 km^2) catchment located in the mountainous Jura region of northwest Switzerland, to quantify sediment generation and annual sediment transport rates by tree throw on forested hillslopes. The locations and dimensions of 215 individual tree throws were mapped in 12 separate areas, with a cumulative area equivalent to 5.3 ha, resulting in an average density of 43 tree throws per ha. All tree throws generated 20.1 m^3 of fine sediment (< 2 mm dia.), or the equivalent of 3.8 * 10^{-4} m^3 m^{-2} within surveyed area. Tree throws were originally attributed to two extreme weather events, known as Storms Lothar and Martin, which swept through west and central Europe in late December 1999. Taking the 18-year period since the occurrence of both storms, this represents an annual sediment transport rate of 2.7 x 10^{-5} m^3 m^{-1} yr^{-1}, or the equivalent of 2.8 x 10^{-2} kg m^{-1} yr^{-1}. This estimate is comparable with sediment transport rates reported in forested areas elsewhere. Exploring the relationship with wind on tree throw fall orientation, it was found that 65.5% of all tree throws (143) generally fell in a downslope direction irrespective of hillslope aspect on which they were located. This suggests that Storms Lothar and Martin were not responsible for tree throw, as originally perceived, but instead, implies a failure of the roots to maintain secure anchorage. Given the high density of tree throws and their relative maturity in this particular catchment (av. age 41 years), we hypothesise that once mature trees attain a certain height and mass, their ability to remain stable and upright is compromised, probably by the limited depth of root penetration. This we attribute to the commensurately thin soil profile overlaying often steep hillslopes, and to the presence of bedrock close to the surface; all of which serves to reduce their stability and vulnerable to sudden upheave.

P 12.7
Assessing Badland Sediment Sources Using Unmanned Aerial Vehicles in the Karoo rangelands, South Africa

Juliane Krenz, Brigitte Kuhn & Nikolaus Kuhn

[1] *Physical Geography & Environmental Change, Department of Environmental Sciences, University of Basel, Klingelbergstr. 27, CH-4056 Basel (philip.greenwood@unibas.ch)*

Badlands are areas of intensive erosion, characterized by a strongly dissected and gullied landscape with sparse or absent vegetation unusable for agriculture. Badland erosion is a major sediment source for river systems in drylands. High erosion rates thus not only account for a loss of soil productivity, but ultimately can also lead to reservoir siltation. In South Africa, land degradation is a significant environmental problem throughout the whole country. Erosion frequently leads to the formation of badland features on overgrazed rangelands such as the Karoo highveld. However, it remains unclear how much sediment the heavily eroded sites characterized by badland features contribute to watercourses and reservoirs. Identifying the relevance of the badlands as a sediment source in the Karoo is therefore critical for measures aimed at reducing reservoir siltation and ensuring the country's water supply. Measuring and mapping sediment movement in badlands has so far been challenging because of the varied topography that is not captured by conventional mapping procedures. Unmanned Aerial Vehicles (UAVs) offer an alternative that potentially provides information on the required spatial scale. The aim of this study was to investigate the use of UAVs for generating high-resolution DTMs of badland features and sediment deposits in the Karoo rangelands of South Adfrica. Combining groundtruthing with UAV imagery, we obtained a high-resolution orthomosaic and DTM that enabled us to identify, map and quantify the volume of badland erosion features as well as the key depositional areas downstream. A comparison of eroded and deposited volume showed that while badlands represent a significant source of sediment, areas affected by other forms of erosion were the dominant source. Images acquired by UAVs thus improved our understanding of catchment sediment dynamics, in particular the relevance of badland erosion as source.

P 12.8

An ice-free Northwest Passage: What are the consequences for exploration and exploitation of mineral resources and other raw materials in Greenland and in the Canadian Arctic?

Denis M. Schlatter [1°], Hannah S. R. Hughes [2], Ronald Schenkel [3], Isabella Pasqualini [4] and Nathalia S. Brichet [5]

[1] Helvetica Exploration Services GmbH, Carl-Spitteler-Strasse 100, CH-8053 Zürich
  (° denis.schlatter@helvetica-exploration.ch; http://www.helvetica-exploration.ch)
[2] Camborne School of Mines, University of Exeter, Tremough Campus, Penryn, UK
[3] Sailcoach, Letzistrasse 50, CH-8006 Zürich
[4] École Nationale Supérieure d'Architecture de Versailles, 5, avenue de Sceaux - BP 20674 // 78006 Versailles Cedex
[5] Saxo-Instituttet, Københavns Universitet, Karen Blixens Plads 8, 2300 København S, Denmark

Since the days when the father of plate tectonics, Alfred Wegener carried out his West Greenland expedition and established his station "Eismitte" on the inland-ice in the early 1930s, the effects of climate change has caused the melting of sea-ice and the retreat of glaciers. Glaciers that once extended to the sea are now melting and have retreated for several hundred meters (Fig. 1). The same effects can also be seen along the Northwest Passage that has become ice-free for the first time in recorded history. In contrast, the Northwest Passage was ice-bound during Sir John Franklin's expedition in 1848, which famously ended in the loss of the ships "Erebus" and "Terror" in the vicinity of King William Island located west of Baffin Island in Nunavut, Canada (Fig. 2). In this contribution we show how the opening of the Northwest Passage could represent an efficient Europe - Asia shipping trade route linking the Atlantic Ocean with the Pacific Ocean through the Arctic Ocean.

There are known occurrences of gold, diamonds, copper, zinc, lead, nickel, rare earth minerals, molybdenum, titanium and iron in North and West Greenland as well as the Canadian Arctic, and the opening of the Northwest Passage will signal increased mineral exploration and exploitation for commodities in these areas. Examples of large past and active mineral mines that are located in the Arctic include the Polaris zinc mine, the Nanisivik zinc-lead mine, the Mary River iron mine, the Raglan nickel mine or the Ekati and Diavik diamond mines (Fig. 2). Recent research has also shown that mud and glacial rock flour produced by the Greenland Ice Sheet (GRIS) is highly valued as a cropland additive due to its fertilizing properties for improving arable land quality and the CO_2 capture (Sarkar et al. 2018). Another direct consequence of the melting of the GRIS is the substantial fresh water resources that will be released by the ice melting and that may be captured before this water reaches the salty ocean waters – thus the GRIS melting may present drinking water resources. The GRIS has been losing mass of about 262 Gt/year in recent years and this is explained by recent increase in atmospheric and oceanic temperatures and it is estimated that the melting of the GRIS was larger in recent years, than during any previous period since measurements were made over the last 150 years (van As et al. 2016).

Climate change and the related and expected future consequences to the GRIS and the Arctic ice represent a negative change from a global perspective, yet there are likely to be beneficiaries such as shipping companies that could utilize a sea ice-free Northwest Passage making such routes logistically feasible and profitable. This would open up further exploration for mineral resources and other raw materials in the Arctic, with access via the Northwest Passage and other Arctic sea routes bringing commodities to market and the prospect of wealth to these Arctic areas. But we ask, what are the socioeconomic and environmental factors at play in this scenario and should this be viewed as a positive side-effect of ice loss caused by the global warming?

Figure 1. Quamarvjuk Fjord, West Greenland: in 1930 (left picture, from J. Georgi), and in 2012 (right picture, from D. Schlatter).

Figure 2. Northwest Passage route(s) shown in red, and location of the King William Island where Sir John Franklin's expedition met a tragic ending after becoming trapped in the ice. Shown on the map are also locations of mines. (Map from Wikipedia).

REFERENCES

van As, D., Fausto, R.S., Cappelen, J., van de Wal, R.S.W., Braithwaite, R.J., Machguth, H. & the PROMICE project team. 2016: Placing Greenland ice sheet ablation measurements in a multi-decadal context. Geological Survey of Denmark and Greenland Bulletin 35: 71-74

Sarkar, S.R., Rose, N.M., Hassenkam, T. & Rosing, M. 2018: Glacial rock flour as an agent for soil improvement. Goldschmidt Conference, 2018, Boston. https://goldschmidt.info/2018/abstracts/abstractView?id=2018003280, 1 page

P 12.9
Biomantles and cover beds – competing concepts for soil formation and landscape evolution?

Tobias Sprafke [1], Heinz Veit [1]

[1] Institute of Geography, University of Bern, Hallerstrasse 12, 3012 Bern. (tobias.sprafke@giub.unibe.ch)

Soils are the complex interface of the major geospheres at the earths surface and provide several services for nature and society. Knowledge on the rate of soil formation is essential for various reasons, including sustainable land use and the understanding of surface evolution.

Quantitative measurements and models of weathering, pedogenesis and surface evolution seldom take into account that most soils in the temperate zone formed from Quaternary slope deposits with variable amounts of aeolian dust (Kleber & Terhorst 2013). Ignoring the "Cover Bed" concept leads to overestimations of soil production rates and underestimation of their real value for nature and society.

Researchers have tried to apply the "Cover Bed" concept to the tropics, assuming major phases of colluviation or dust admixture to explain the formation of thick tropical soils. However, the role of soil engineers like termites or ants in producing thick solum from local weathering products is underestimated in such approaches. The "Biomantle" concept (Johnson et al. 2005) can be applied with confidence in regions with very active biota; still past changes in climate and landscape dynamics need to be acknowledged.

In this contribution we provide evidence from literature and from own partly unpublished results that both, the "Cover Bed" and the "Biomantle" concept are not exclusive and have their relevance in both, the temperate and the tropical zone. Neither the effect of paleoecological changes and biological overprinting should be ignored. Spatial and temporal differentation and interdisciplinary approaches are necessary. This task is of main interest for the Cluster "Erosion through time" established at the Geographical Institute of the University of Bern.

REFERENCES

Kleber, A. & Terhorst, B. 2013: Chapter 1 - Introduction. – A. Kleber & B. Terhorst (Eds.): Mid-Latitude Slope Deposits (Cover Beds). – Developments in Sedimentology 66. Elsevier, pp. 1-8.

Johnson, D.L., Domier & J.E.J., Johnson, D.N. 2005: Reflections on the nature of soil and its biomantle. Annals of the Association of American Geographers 95, pp. 11–31

P 12.10
Seismic Constraints on Effective Friction of Rock-Ice Avalanches

Fabian Walter [1] & Anne Mangeney [2]

[1] *Versuchsanstalt für Wasserbau, Hydrologie und Glaziologie VAW, ETH Zürich, CH-8093 Zürich*
  (walter@vaw.baug.ethz.ch)
[2] *Institut de Physique du Globe de Paris, F-75238 Paris cedex 05*

The Earth's surface is prone to nearly continuous erosion of sediments. Rockfalls, sediment transport in rivers, debris flows and avalanches are processes, which shape the Alpine environment, often via catastrophic events. In order to assess the hazard potential of the largest mass movements, in particular, it is important to reliably forecast runout and deposition, which is often done with numerical models describing granular flows.

A standard modeling approach is the assumption of shallow flow, which allows simplification of the full momentum and mass conservation equations. However, in order to accurately model rock, snow or ice avalanches, the effective friction of the shallow granular mass has to be known. On one hand, effective friction can be viewed as a tuning parameter when matching before/after event DEM's. On the other hand, effective friction is a critical unknown when using granular flow models to predict the runout and deposition of future avalanches.

Given ongoing climate change, permafrost decay and other environmental changes, our planet may face changes in disposition and composition of unstable granual material. Therefore, a physical understanding of effective friction in granular flow material is imperative for predictive model runs. Here we focus on using seismic data for constraining effective friction of granular flow models. We first review previous granular flow studies that incorporated information from seismograms and then discuss the potential of this approach in special cases, such as ice-rock masses, pure ice avalanches and submarine landslides. Compared to other model constraints such as release area and deposition geometry, seismic signals are often available in near-real time and capture event dynamics rather than static information before and after the event. Seismic data therefore play an important role in catastrophic mass movement studies.

P 12.11

Origin and Late Quaternary emplacement of the unique fans in the Klados River catchment, Crete, Greece

Elena Bruni [1], Sean Gallen [2], Vincenzo Picotti [1], Sean Willett [1]

[1] Geological Institute, Department of Earth Sciences, ETH Zürich, Sonneggstrasse 5, CH-8001 Zürich
  (brunie@student.ethz.ch)
[2] Department of Geosciences, Colorado State University, Fort Collins, Colorado 80523, USA

This study presents new data on the formation of large Holocene fans and terraces. The focus lies on the ~11.5 km^2 Klados River basin located on the southwestern coastline of Crete, Greece. This catchment is notable for the preservation of large, triangular fan deposits that have accumulated at the river mouth indicating previous large-scale episodic sedimentation events. The seaward facing cliffs of the fan are unique among other alluvial fans on Crete in terms of their large size, step-wise stratigraphy and sedimentology (Figure 1).

A study performed on the fan sequence places the fan formation into the Pleistocene and explains their development with climate changes, tectonic activity and resulting sea level changes (Mouslopoulou et al., 2017)eustasy and tectonics interact to shape the late Quaternary landscape is poorly known. Alluvial fans often provide useful indexes that allow the decoding of information recorded on complex coastal landscapes, such as those of the eastern Mediterranean. In this paper we analyse and date (using infrared stimulated luminescence (IRSL. This interpretation is not satisfying because of suspect geochronology, the lack of explanation for the disproportionate amount of sediment compared to the small size of the catchment, and the missing statement regarding the differences between these fans and other fans on Crete. An alternative explanation for the formation of this unique fan sequence is that it is substantially younger and related to rare catastrophic events that are known to affect the island such as the 365 AD earthquake. In this thesis, radiocarbon dating, mapping, sedimentology, stratigraphy and a landslide runout model are applied to solve the question of the provenance and formation mechanisms of the Domata fans.

The results indicate a Holocene landslide filled the palaeo-topography of the Klados Gorge, and supplied the clastic material for subsequent debris flows during high-intensity precipitation events. The frequency of these events controlled the close succession of the fans with each major terrace corresponding to at least one peak event. The river is still highly susceptible to external perturbations and another large, catastrophic mass-wasting event may occur.

Figure 1 The river mouth at Domata beach is dominated by the dual structure of the escarpments termed Upper Fan and Lower Fan (arrows). Other river systems in the region do not show any similar deposits, which suggests intrinsic factors forced the Klados River into building the disproportionate fans (tripinview, 2017).

REFERENCES

Mouslopoulou, V. *et al.* (2017) 'Distinct phases of eustatic and tectonic forcing for late Quaternary landscape evolution in southwest Crete , Greece', *Earth Surface Dynamics*, 5, pp. 511–527.

tripinview (2017) *Overview of Crete- Chania*. Available at: https://www.tripinview.com/
presentation?id=64851&lang=en&layer=overview.

P 12.12
Modeling behavior and hazards of Popocatépetl Volcano, Mexico

Alireza Salehipour Milani [1], Toktam Yazdani [2]

[1] Department of Physical Geography,Faculty of Earth Science,University of Shahid Beheshti, Velenjak,Tehran ,Iran
  (ar.salehipour@gmail.com)
[2] Department of Physical Geography,Faculty of Earth Science,University of Shahid Beheshti, Velenjak,Tehran ,Iran

Popocatepetl Volcano is on the volcanic front of the central Mexican magmatic arc (Trans-Mexican Volcanic Belt)(Fig.1). This volcano is the third highest active volcano in the Northern Hemisphere. The volcano presents a great hazard to Mexico City and to other nearby cities and towns from a possible major volcanic eruption. Popocatépetl is one of Mexico's most active volcanoes threatening a densely populated area that includes Mexico City with more than 20 million inhabitants. In 1994, volcanic activity at Popocatépetl renewed with the formation of ash-rich plumes up to 7 km high. In April 1996, lava emissions filled the crater and were accompanied by a series of explosions that produced eruptive columns up to 8 km high. Volcanologists are always working to understand how volcanic hazards behave, and what can be done to avoid them. Assessment and management of volcanic risk are important scientific, economic, and political issues, especially in densely populated areas threatened by volcanoes. Volcano Hazards Modeling's are one of the most important tools for managements of volcanic hazards behaviors. We tested VORIS 2.0.1 (Felpeto et al., 2007), a freely available software (http://www.gvb-csic.es) based on a probabilistic model that considers topography as the main parameter controlling the lava flow propagation. Up to this version, VORIS is able to simulate ash fallout, lava flows and pyroclastic density currents. VORIS 2.0.1 also includes tools for the computation of volcanic susceptibility. Ash fallout simulations were based on the advection-diffusion model. Wind data (Speed and direction in atmosphere layer) for the advection model correspond to records from the Phillip Goldston Intl. station in during one of ash fallout in 19 april 2016. Model show Direction of ash fallout in that time to the South East (fig. 2). The lava flow (probabilistic) model applied assumes that topography and flow thickness play major roles in determining lava paths (Felpeto et al., 2007). The simulations were run for all cells in the Aster DEM and the sum of the 10000 iterations provided a map with the probability for any particular cell of being covered by a lava flow. Figure 3 consists of a lava-flow simulation probability map, which shows that there is a high probability that the east ward of caldera will be affected by lava flows. Pyroclastic density currents (PDCs) were simulated using the energy cone mode (Sheridan and Malin, 1983) with input parameters of topography, the collapse equivalent height (Hc) and angle (θ). The latter is obtained by the arctangent of the ratio between Hc and L, where L represents the run-out length (Felpeto et al., 2007; Toyos et al., 2007). The output of the model is the maximum potential extent that can be affected by the flow to eastward of Volcano(Fig.4).

REFERENCES

Alicia Felpeto., Joan Marti & Roman Ortiz. 2007: Automatic GIS-based system for volcanic hazard assessment, Journal of Volcanology and Geothermal Research 166 ,106–116.
Toyos G.P., Cole P.D., Felpeto, A., Martí, J. 2007: A GIS-based methodology for hazard mapping of small pyroclastic density currents. Natural Hazards 41 (1), 99–112.
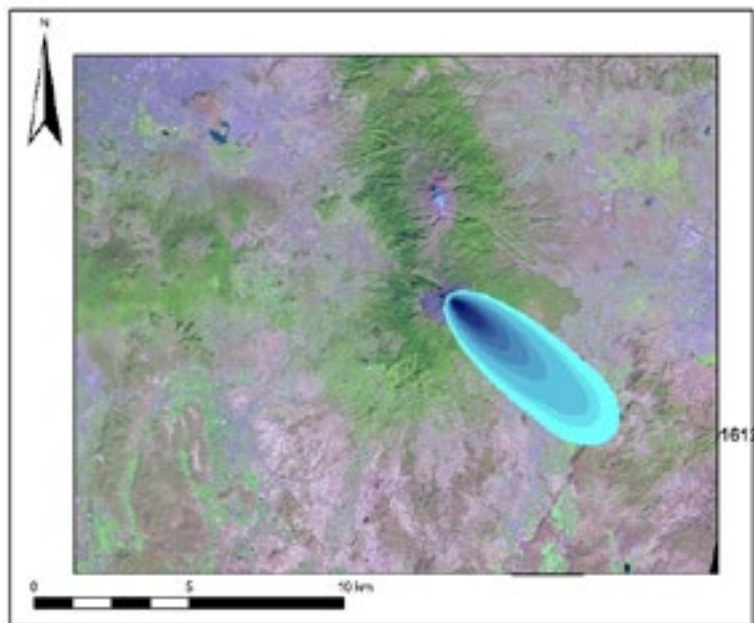
Figure 1. Location of Popocatepetl Volcano

Figure 2. Ash Fallout Direction in Popocatepetl Volcano Eruption in 19 April2016

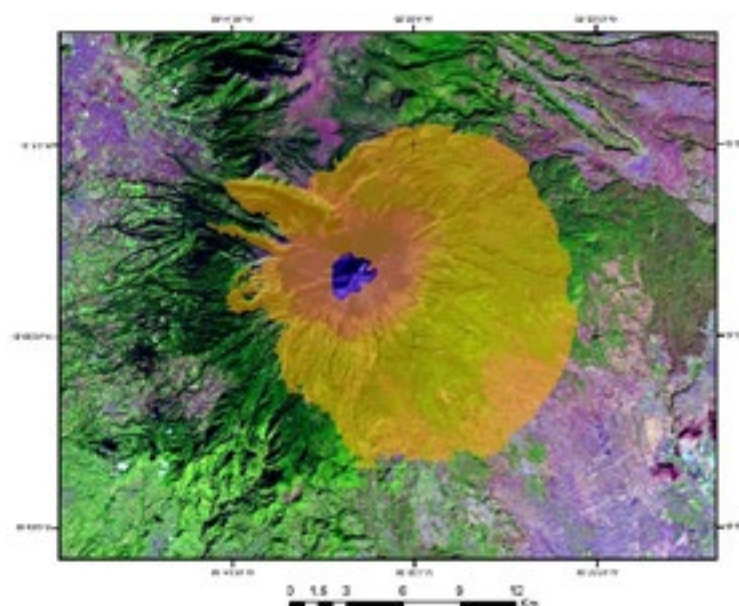Figure 3. Lava Flow Direction modeling in Popocatepetl Volcano

Figure 4. Pyroclastic density currents modeling in Popocatepetl Volcano

P 12.13
Modelling natural hazards using Machine Learning: the case study of landslides in Canton Valais, Switzerland

Marj Tonini, Francesco Zanetta, Federico Amato, Mikhail Kanevski

Institute of Earth Surface Dynamics, Faculty of Geosciences and Environment, University of Lausanne, Switzerland (marj.tonini@unil.ch)

Recently, several approaches have been adopted to analyse spatially distributed natural hazards and ongoing phenomena such as landslides. Numerous studies ultimately aim to evaluate the probability of a landslide to occur in a given area, under the basic assumption that the considered event is more likely to take place in the future in areas with similar conditions to those where it was observed in the past.

The main objective of the present study is to elaborate landslide susceptibility mapping using a machine learning (ML) algoriothm, Random Forest (RF). ML algorithm are statistical-based approaches capable of learning from data and make predictions starting from the acquired knowledge through the modelling of the hidden relationships between a set of input and output variables (i.e. the predisposing factors and the occurrence of the phenomenon). After a training procedure to calibrate the parameters of the model, susceptibility maps can be displayed. The main benefit is that these approaches are data driven. Hence, they do not need a priori knowledge of the process. Moreover, RF directly provides the measurement of the importance of each variable.

The following environmental variables were considered in this study as predisposing factors to construct the input space: slope angle, curvature, profile curvature, plan curvature, lithology, NDVI, river proximity and road proximity. Each factor can be seen as a proxy for local conditions, namely the terrain mechanic and hydrological properties and shear stress conditions. The landslides inventory was elaborated by Pedrazzini et al. (2016) and consist on the footprint of various types of observed gravitational slope deformations, a common geomorphological feature in mountainous areas associated with terrain erosion processes.

The RF algorithm successfully produced a landslides susceptibility map for Canton Valais and was able to define variables importance in predicting landslides occurrence. More generally, the proposed approach proved to be particularly effective to deal with large, high dimensional spatial data, which reflects the great flexibility of ML methods. The investigation of other natural hazards could benefit from this same methodology.

Figure 1. Landslide susceptibility maps of Canton Valais, Switzerland

REFERENCES

Kanevski,M., Pozdnoukhov, A., Timonin V. 2009 : Machine Learning for Spatial Environmental Data: Theory, Applications and Software, Epfl Press, Lausanne

Leuenberger, M., Parente, J., Tonini, M., Pereira, M.G., Kanevski M. 2018: Wildfire susceptibility mapping: Deterministic vs. stochastic approaches, Environmental Modelling & Software, 101, 194-203

Pedrazzini, A., Humair, F., Jaboyedoff, M., Tonini, M. 2016, Characterisation and spatial distribution of gravitational slope deformation in the Upper Rhone catchment (Western Swiss Alps), Landslides, 13:2, 259-277.

13. Cryospheric Sciences

Margit Schwikowski, Martin Heggli, Matthias Huss, Jeannette Nötzli, Daniel Tobler, Andreas Vieli

Swiss Snow, Ice and Permafrost Society

TALKS:

13.1   Brugger S.O., Gobet E., Rohr C., Schanz F.R., Rey F., Schwörer C., Sigl M., Schwikowski M., Tinner W.:
         Millennial ice record reveals industrial footprint in European vegetation

13.2   Caduff R., Strozzi T.: Mapping and monitoring of Arctic lowland active layer permafrost movement with satellite
         SAR interferometry

13.3   Cicoira A., Vieli A., Faillettaz J.: Investigating the influence of temperature and liquid water on variations in
         rockglacier flow

13.4   Ferguson J., Vieli A.: Modelling steady states and the transient response of debris-covered glaciers

13.5   Gräff D., Walter F., Clyne E.: In-situ Measurements of an Active Seismic Fault at the Bed of an Alpine Glacier

13.6   Haeberli M., Baggenstos D., Schmitt J., Kellerhals T., Fischer H.: Long-term change in ocean heat content using
         ice core noble gas thermometry

13.7   Imhof M., Cohen D., Jouvet G., Seguinot J., Funk M.: Comparing shallow and full-Stokes models of the Rhine
         Glacier during the Last Glacial Maximum

13.8   Kronenberg M., Machguth H., Eichler A., Schwikowski M., Hoelzle M.: Changing firn properties on glaciers in
         Central Asia

13.9   Mollaret C., Wagner F., Hilbich C., Hauck C.: Petrophysical joint inversion of electrical and refraction seismic
         datasets in alpine permafrost to image ice, water and air contents

13.10   Paul F., Rastner P., Azzoni R.S., Fugazza D., Le Bris R., Nemec J., Rabatel A., Ramusovic M., Schwaizer G.,
         Smiraglia C.: Glacier shrinkage in the Alps continues unabated as revealed by a new glacier inventory from
         Sentinel 2

13.11   Preiswerk L.E., Walter F.: What does ambient seismic noise tell us about glacial crevassing?

13.12   Steiner L., Meindl M., Geiger A.: Quantification of Snow Water Equivalent Using Buried Low Cost GPS Antennas

13.13   Walter A., Lüthi P.M., Vieli A.: Analysing calving activity of Eqip Sermia, Greenland, using continuous direct
         observations

13.14   Wicky J., Hauck Ch.: Assessing the influence of convection in the active layer of a rock glacier on ground
         temperatures

13.15   Zekollari H., Huss M., Farinotti D.: Modelling the evolution of Alpine glaciers under the EURO-CORDEX RCM
         ensemble

POSTERS:

P 13.1   Church G.J., Bauder A., Maurer H.R.: Seasonal evolution of englacial conduits through repeated ground penetrating radar measurements

P 13.2   Hellmann S., Bauder A., Kerch J., Maurer H.: Crystal orientation fabric analysis on ice core samples from a temperate Alpine glacier

P 13.3   Lindner F., Walter F., Laske G.: Locating and monitoring glaciohydraulic tremors on Glacier de la Plaine Morte, Switzerland

P 13.4   Neyer F., Guillaume S., Limpach P., Geiger A.: Long-term multi-resolution terrestrial photogrammetry at the Moosfluh landslide

P 13.5   Azisov E., Barandun M., Hoelzle M., Kronenberg M., Vorogushyn S., Saks T., Usubaliev R.: A more than 100 years time series of seasonal mass balance for Golubin Glacier, Northern Tien Shan

P 13.6   Ghirlanda A., Kronenberg M., Barandun M., Azisov E., Kayumov A., Kenzehbaev R., Machguth H., Saks T., Tarasov Y., Usubaliev R., Yakovlev A., Hoelzle M.: Mass balance monitoring and capacity building in Central Asia

P 13.7   Grab M., Langhammer L., Bauder A., Rabenstein L., Schmid L., Maurer H.R.: Ice volume estimation in the Swiss Alps from helicopter-borne GPR and glaciological modeling

P 13.8   Groos A.R., Munz L., Bertschinger T.: The potential of low-cost UAVs and open-source photogrammetry software for high-resolution glacier monitoring – A case study from the Kanderfirn (Swiss Alps)

P 13.9   Lüthi M.: Calorimetric determination of the unfrozen water content in glacier ice

P 13.10   Schulthess M., Mölg N., Vieli A.: Inverting debris thickness on glaciers from UAV thermal imagery

P 13.11   Van Dongen E., Walter A., Jouvet G., Farinotti D., Funk M.: Monitoring and modeling a recurrent calving event at Bowdoin Glacier, Greenland

P 13.12   Vieli A.: State and evolution of thermal conditions of a small ice cap on Disko Island, West Greenland

P 13.13   Mölg N., Bolch T., Walter A., Vieli A.: Reconstructing century-long debris-covered glacier history from observation. How are changes in debris cover, surface topography, mass balance, and flow dynamics connected and interacting?

P 13.14   Förster S., Huss M., Funk M.: The effect of volcanic eruptions on the long-term evolution of Alpine glaciers

P 13.15   Lehmann P., Seth B., Schmitt J., Fischer H.: Development of a method for the measurement of $\delta^{15}NH_4$ in ice core samples

P 13.16   Maechler L., Bereiter B., Scheidegger P., Walther R., Tuzson B., Schmitt J., Emmenegger L., Fischer H.: Towards gas measurements in extremely thinned ice with sublimation extraction and mid-IR spectroscopy

P 13.17   Schmidely L., Bock M., Nehrbass-Ahles C., Silva L., Schmitt J., Fischer H., Stocker T.: Calibration of the new wet-extraction system for CH_4 and N_2O, and plans for high-resolution measurements in the EPICA Dome C ice core (EDC)

P 13.18   Silva L., Nehrbass-Ahles C., Schmidely L., Schmitt J., Fischer H., Stocker T.F.: Exploring centennial-scale CO_2 reconstruction in the last interglacial

P 13.19   Amschwand D., Ivy-Ochs S., Frehner M., Kronig O., Christl M.: Combining exposure dating, finite-element modelling, and feature tracking to decipher rockglacier evolution: A case study from the Bleis Marscha rockglacier (Val d'Err, Grisons)

P 13.20   Cohen D., Zwinger T., Person M., Haeberli W., Fischer U.H.: Effects of ice cover and permafrost on groundwater flow during the last glacial cycle in the Swiss lowlands

P 13.21   Haeberli W., Magnin F., Linsbauer A.: Modeling permafrost occurrence, glacier-bed topography and possible future lakes for assessing changing hazard conditions in cold mountain regions

P 13.22   Mollaret C., Pellet C., Hilbich C., Hauck C.: Towards a joint database and statistical analysis of electrical resistivity and refraction seismic tomography datasets in mountain permafrost

P 13.23   Hilbich C., Hauck C., Hählen N.: Establishing a permafrost monitoring network in the Bernese Alps: geophysical characterisation of potential monitoring sites and validation of permafrost distribution models

P 13.24   Bavay M., Egger T., Fierz C.: Interactive snow profile edition with niViz

P 13.25   Capelli A., Reiweger I., Schweizer J.: Prediction of snow failure: mission impossible?

P 13.26   Richter B., van Herwijnen A., Rotach M.W., Schweizer J.: How meteorological input uncertainty affect modeled snow instability

13.1
Millennial ice record reveals industrial footprint in European vegetation

Sandra O. Brugger [1,2], Erika Gobet [1,2], Christian Rohr [2,3], Federica R. Schanz [1], Fabian Rey [1,2], Christoph Schwörer [1,2], Michael Sigl [2,4], Margit Schwikowski [2,4,5] & Willy Tinner [1,2]

[1] *Institute of Plant Sciences, University of Bern*
[2] *Oeschger Center for Climate Change Research, University of Bern*
[3] *Institute of History, University of Bern*
[4] *Paul Scherrer Institute, Villigen*
[5] *Department for Chemistry and Biochemistry, University of Bern*

Wild fires are a disturbance agent across the continents, driving ecosystem dynamics and societal hazards. We conducted ice-core palynology using pollen and spores as proxies for vegetation composition and land use activity, microscopic charcoal for fire activity, and spheroidal carbonaceous particles (SCP) for fossil fuel combustion. The results derive from the highest glacier of Europe (4452 m asl), from Colle Gnifetti. To our knowledge they provide the first long-term and high-resolution palynological record of Europe from an ice-core.

The central position and large microfossil catchment of the Colle Gnifetti allows us to address vegetation and societal responses to climatic change and wildfire disturbance on a subcontinental scale, presumably covering substantial parts of Western, Central, and Southern Europe. The ice core record provides an excellent chronological control for the past millennium, particularly over the most recent 200 years, the period that experienced important climatic changes and an increasing globalization of economy.

We reconstruct large scale impacts such as extreme weather, societal innovations, agricultural crises, and pollution in Europe. Surprisingly, pollution tracers occur in the record as early as 1750 AD. They anticipate industrialization in the Alpine region but coincide with a shift to large-scale maize production in Northern Italy and strongly increased fire activity. Our multiproxy record may allow desentagling the role of climate and humans for vegetation composition and biomass burning.

13.2
Mapping and monitoring of Arctic lowland active layer permafrost movement with satellite SAR interferometry

Rafael Caduff [1], Tazio Strozzi [1]

[1] Gamma Remote Sensing AG, Worbstrasse 225, CH-3073 Gümligen (caduff@gamma-rs.ch)

Active layer in arctic permafrost lowland regions is expected to increase in extent and thickness with increasing mean annual temperatures. Seasonal thawing and freezing of the uppermost soil layer is considered in most cases for building infrastructures, including transportation ways such as roads or airfields, in arctic regions. However, an increase in active layer thickness and in permafrost thaw activity may shift the stability conditions beyond the structural limit of the infrastructures leading to potential failure. Not only local structural issues may be affected by increased permafrost thaw. The knowledge of the state of permafrost thaw activity outside inhabited areas is crucial as well for the monitoring of the development in greenhouse gas emissions (mainly CO_2 and CH_4) from permafrost soils. A wide area monitoring of the permafrost thaw activity in arctic regions in high temporal and spatial resolution is therefore important for understanding and predicting the role of thawing permafrost for global climatic trends.

We propose a remote-sensing approach for the identification of active layer thawing using satellite radar interferometry (Strozzi et al. 2018). We use the ground motion as proxy since freezing and thawing of the soil leads to volume changes and results in heaving and settling in flat terrain. Differential SAR Interferometry (DInSAR) and persistent scatterer interferometry (PSI) are widely used methods, that allow the precise detection and quantification of ground movements from space. With Sentinel-1 acquisitions regularly available every 6 to 12 days over arctic regions, temporal and spatial patterns of permafrost activity can be monitored on a regular basis even in remote areas.

We will illustrate the general workflow on feasibility studies performed in the Qaanaaq (NW-Greenland) and Ilulissat (W-Greenland) areas using Sentinel-1 data. We will introduce an approach to generate permafrost thaw activity maps from ground motion maps and critically discuss our findings. Open questions such as the influence on the InSAR results of superficial (melt)water, soil moisture changes, and the active layer thickness will be addressed. Finally, an outlook will be given on the use of a standardized permafrost soil activity map as tool for planning and construction works in arctic regions.
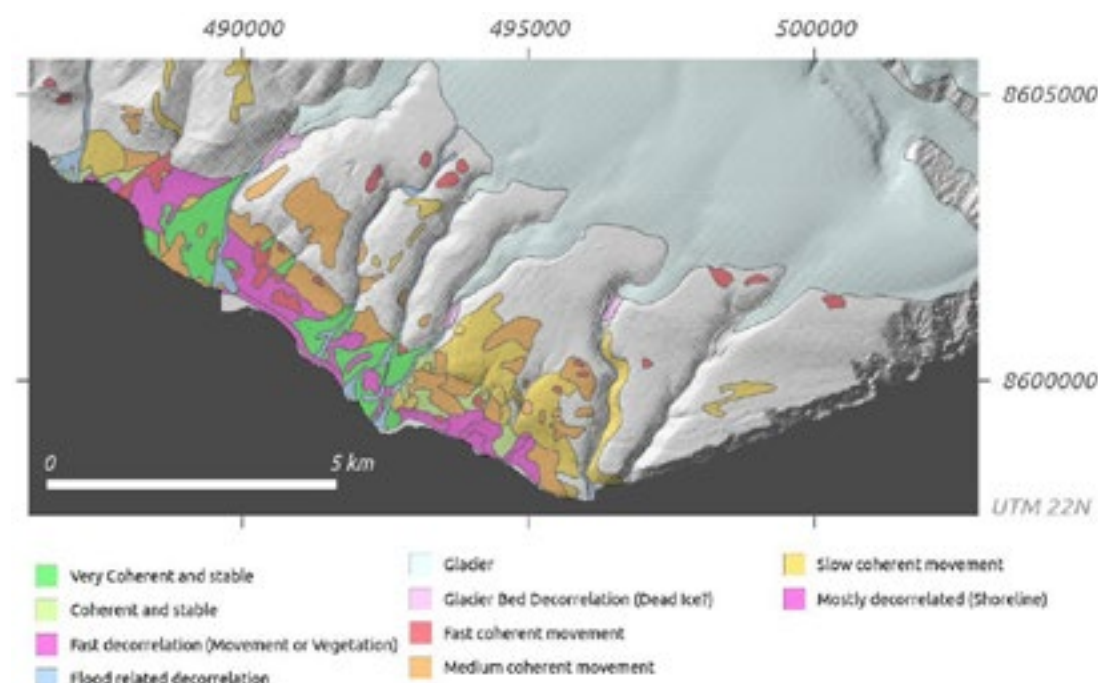

Fig. 1. Map of Sentinel-1 InSAR derived surface movements in the Qaanaaq area (NW-Greenland). Data cover the time between 2015-2018.

REFERENCES

Strozzi, T.; Antonova, S.; Günther, F.; Mätzler, E.; Vieira, G.; Wegmüller, U.; Westermann, S.; Bartsch, A. 2018: Sentinel-1 SAR Interferometry for Surface Deformation Monitoring in Low-Land Permafrost Areas. *Remote Sensing, 10*, 1360.

13.3
Investigating the influence of temperature and liquid water on variations in rockglacier flow

Alessandro Cicoira [1], Andreas Vieli [1] and Jérome Faillettaz [1]

[1] Department of Geography, University of Zurich, Switzerland (alessandro.cicoira@geo.uzh.ch)

In the past decades, seasonal and inter-annual variability in rockglacier velocities have been observed (Wirz et al., 2016). Temperature forcing along with input of liquid water have been proposed as key processes to explain these variations in kinematics (Ikeda et al, 2008). However, the relative influence of these mechanisms have not yet been quantitatively assessed against real-world data (Kääb et al, 2007). We investigate the processes governing variability in rockglacier flow using 1-dimensional numerical models that couple heat conduction to different creep relations and include variations in pore water pressure (Arenson and Springman, 2005). We compare the modelling with borehole temperatures and surface velocity measurements from several sites of the PERMOS and PermaSense monitoring networks. We find that velocity variations cannot be explained from the influence of temperature forcing on rockglacier rheology alone. Coupling variations in water input to a water pressure dependent creep relation, we are able to reproduce velocity variations both in magnitude and temporal pattern over time scales from several months to several years.

REFERENCES

Arenson, L.U., Springman, S.M., (2005). Mathematical descriptions for the behaviour of ice-rich frozen soils at temperatures close to 0 °C. *Canadian Geotechnical Journal* 42(2): 431-442.

Haeberli, W., Hallet, B., Arenson, L.U., Elconin. R., Humlum, O., Kääb, A., Kaufmann, V., Ladanyi, B., Matsuoka, N., Springman, S., Mühll, D.V., 2006. Permafrost creep and rock glacier dynamics. *Permafrost and Periglacial Processes* 17: 189–214.

Ikeda, A., Matsuoka, N., Kääb, A., 2008. Fast deformation of perennially frozen debris in a warm rock glacier in the Swiss Alps: an effect of liquid water. *Journal of Geophysical Research* 113F01021.

Kääb, A., Frauenfelder, R., Roer, I., 2007. On the response of rockglacier creep to surface temperature increase. *Global and Planetary Change* 56: 172–187.

Wirz, V., Geertsema, M., Gruber, S., Purves, R.S., 2016. Temporal variability of diverse mountain permafrost slope movements derived from multi-year daily GPS data, Mattertal, Switzerland. *Landslides* 13:67– 83.

13.4
Modelling steady states and the transient response of debris-covered glaciers

James Ferguson [1], Andreas Vieli [1]

[1] Department of Geography, University of Zurich, Winterthurerstrasse 190, 8057 Zurich, Switzerland
(james.ferguson@geo.uzh.ch)

Debris-covered glaciers are commonly found in alpine landscapes of high relief and increasingly play an important role in a warming climate. When a continuous surface debris layer is thick enough, it reduces the underlying ice ablation rate, which in turn reduces thinning, surface evolution and, therefore, affects the ice dynamics. This results in extended debris-covered glacier tongues with low surface slopes and that are dynamically almost inert. Furthermore, debris-covered glaciers are expected to respond much slower to changes in climate forcing than their debris free counterparts. However, it is not clear whether debris-covered glaciers can have steady states and this affects our ability to better understand the transient response of a debris-covered glacier to climate variations.

In this work, we incorporate a debris source and its transport into a simplified ice flow model. Using both analytical and numerical methods, we explore conditions under which steady states of debris-covered mountain glaciers are possible. We discuss how realistic steady states are by comparing the results to observations and investigate the implications on response times of debris-covered glaciers.

13.5
In-situ Measurements of an Active Seismic Fault at the Bed of an Alpine Glacier

Dominik Gräff [1], Fabian Walter [1], Elisabeth Clyne [2]

[1] Laboratory for Hydraulics, Hydrology and Glaciology (VAW), ETH Zurich, Hönggerbergring 26, CH-8093 Zurich
   (graeff@vaw.baug.ethz.ch)
[2] Department of Geosciences, Pennsylvania State University, University Park, Pennsylvania, USA

Much like for tectonic strike-slip faults in the earth crust, at the bed of glaciers, frictional processes causing seismogenic stick-slip motion exist. While on one hand ice deforms according to a non-linear rheology with a stress dependent viscosity and hence differently from tectonic plates, smooth sliding and stick-slip motion at the interface between glaciers and the underlying bedrock are analogous to creeping and locked sections on tectonic faults.

Until recently, observations of sudden processes at the bed of glaciers were limited to monitoring stick-slip sources form the glacier surface. Here, we show a new approach to study the subglacial environment that was carried out in a field campaign in summer 2018:
By analyzing multi-seasonal recordings from seismometers on the ice in the challenging environment of the ablation zone of four alpine glaciers, the clustering and swarming behavior of basal stick-slip faults was studied in order to determine an optimal site to carry out the first in-situ measurements of an active seismogenic fault at a bi-material interface beneath a glacier. Much like drilling into seismogenic strike-slip faults in crustal studies, enabled by guided fast hot water drilling we target borehole experiments to specific glacier bed regions where spatially limited microseismic stick-slip sliding happens and combine them with the recordings of a high-densitiy network of seismometers at the glacier surface.

From the various measurements we can determine the subglacial water- and thus pore pressure evolution and its effect on the fault stability, while the regular recurrence rate of the microseismic stick-slip events allows to predict both the time and magnitude of the next slip event. Futhermore the in-situ borehole measurements enable us to study material properties such as the till and ice characteristics within the stick-slip asperities and compare them to off-site reference measurements in seimically non-active regions of the glacier bed. Finally from acceleration, ice deformation measurements, and borehole camera videos from the glacier bed, we can estimate the amount of aseismic and co-seismic sliding, which cannot be obtained remotely from the ice surface.

Summed up, with the various in-situ measurements of an seismogenically active strike-slip fault beneath an alpine glacier combined with passive seismic long term monitoring, we open a unique posibility for studying seismogenic stick-slip motion at a bi-material interface in a natural environment.

13.6
Long-term change in ocean heat content using ice core noble gas thermometry

Marcel Haeberli [1], Daniel Baggenstos [1], Jochen Schmitt [1], Thomas Kellerhals [1] & Hubertus Fischer [1]

[1] Physics Institute, Climate and Environmental Physics, University of Bern, Sidlerstrasse 5, CH-3012 Bern
(haeberli@climate.unibe.ch)

The novel method of ice core noble gas thermometry allows us to reconstruct a global mean ocean temperature (GMOT) on the basis of physical principles.
The xenon/krypton or krypton/N_2 ratio in the atmosphere is a direct proxy for GMOT because of the temperature dependence of their solubility coefficients.

The GMOT, which is the most integrative and representative parameter for quantifying long-term changes in the Earth's energy budget, can be estimated using high-precision measurements of noble gas elemental ratios from gases trapped in glacial ice. Using multi-isotopic gas parameters of N_2, Ar, Kr and Xe, we are able to quantify for dynamics in the firn and ice including fractionation effects (gravitational enrichment, thermodiffusion) as well as for possible gas loss happening in the ice.

We are focusing on peak glacial and interglacial conditions over the last 700'000 years, i.e. covering the last eight glacial and interglacial intervals. The only proxies for ocean temperatures during this time period are sediment cores which have a very strong spatial variability of ocean temperatures between and even within individual basins.

We performed Xe/Kr and Kr/N2 analyses on around 100 ice core samples from EDC and EDML over the last 700 ky. The measurements imply warmer ocean temperature during interglacials and a significantly colder temperature during glacial times. The results are in line with the deep ocean temperature reconstructions from sediment cores.
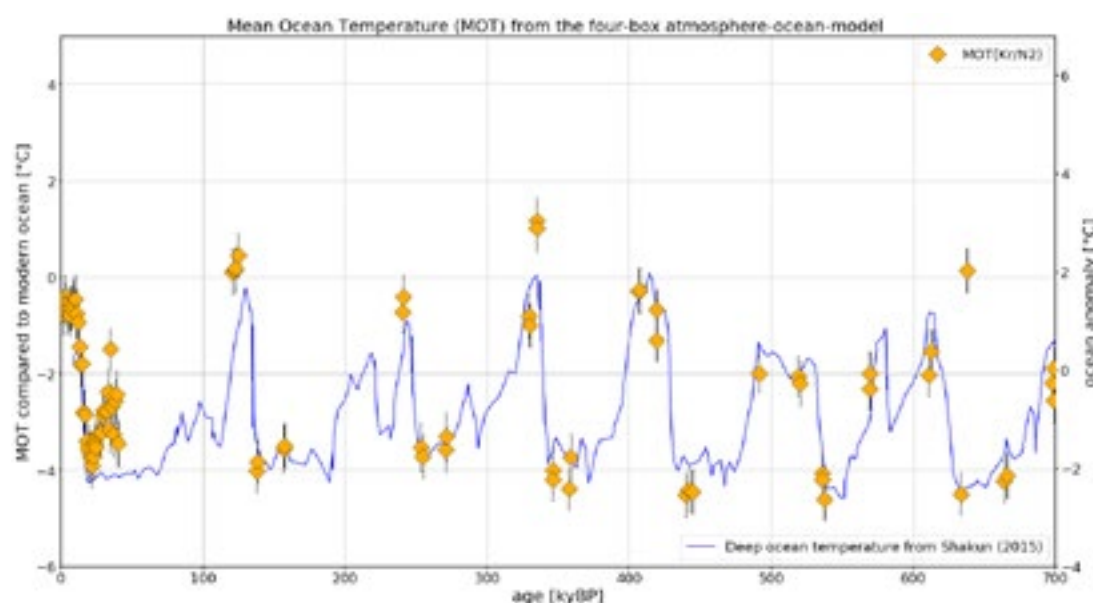
Figure 1. Yellow diamonds are the Global Mean Ocean Temperature (GMOT) records relative to today derived from the atmospheric gas ratio of Kr/N2 using ice core samples from EDC. The blue line is the deep ocean temperature derived from sediment core measurements from Shakun (2015).

REFERENCES

Headley, M. & Severinghaus, J.P. 2007: A method to measure Kr/N2 ratios in air bubbles trapped in ice cores and its application in reconstructing past mean ocean temperature, Journal of Geophysical Research: Atmospheres, 112, D19.
Bereiter, B., Shackleton, S., Baggenstos, D., Kawamura, K., Severinghaus, J.P. 2018: Mean global ocean temperatures during the last glacial transition, Nature 553, 39-44.

13.7
Comparing shallow and full-Stokes models of the Rhine Glacier during the Last Glacial Maximum

Michael Imhof [1], Denis Cohen [2], Guillaume Jouvet [1], Julien Seguinot [1], Martin Funk [1]

[1] VAW, ETH Zürich, Hönggerbergring 26, CH-8049 Zürich (imhof@vaw.baug.ethz.ch)
[2] Department of Earth and Environmental Science, New Mexico Tech, Socorro, NM, 87801, USA

Paleo ice-sheet models often use simplified stress balances to simulate the ice motion on the time scale of a glacial cycle. For instance, the Parallel Ice Sheet Model (PISM, The PISM authors 2015) has shown a good agreement between modelled and geomorphologically reconstructed ice extent of the European Alpine ice sheet at the Last Glacial Maximum (LGM). However, the modelled maximum ice surface elevation was found up to 800 m higher than the reconstructions based on trimlines (Seguinot et al. 2018). The full-Stokes model Elmer/Ice (Gagliardini et al. 2013) was also applied to the Rhine Glacier at the LGM (Cohen et al. 2018). This offers a unique opportunity to determine the limitations of using a mechanically-simplified model such as PISM to reproduce the ice thickness and dynamics of a former ice field over a complex topography.

For that purpose, we perform an analogous simulation to Cohen et al. (2018) using PISM. We find that the two models -- Elmer/Ice and PISM -- agree well with respect to sliding velocities. However, the shear velocities (surface speed minus sliding speed) modelled by PISM with the Shallow Ice Approximation (SIA) are substantially lower than the ones computed with the full-Stokes model. The reason for this is an artificial ice flux limiter in the SIA in PISM that is used in complex terrain. Allowing less flux limitation results in larger shear velocities -- more similar to Elmer/Ice -- but comes along with increased computational costs. This difficulty of PISM to model the deformation velocities -- especially at high elevation in the accumulation area -- might partly explain the discrepancy in ice surface elevation found in previous studies.

REFERENCES

Cohen, D., Gillet-Chaulet, F., Haeberli, W., Machguth, H., and Fischer, U. H.: Numerical reconstructions of the flow and basal conditions of the Rhine glacier, European Central Alps, at the Last Glacial Maximum, The Cryosphere, 12, 2515-2544, https://doi.org/10.5194/tc-12-2515-2018, 2018.

Gagliardini, O., Zwinger, T., Gillet-Chaulet, F., Durand, G., Favier, L., de Fleurian, B., Greve, R., Malinen, M., Martín, C., Råback, P., Ruokolainen, J., Sacchettini, M., Schäfer, M., Seddik, H., and Thies, J.: Capabilities and performance of Elmer/Ice, a new-generation ice sheet model, Geosci. Model Dev., 6, 1299-1318, https://doi.org/10.5194/gmd-6-1299-2013, 2013.

The PISM authors 2015: PISM, a Parallel Ice Sheet Model, URL: http://www.pism-docs.org, 2015.

Seguinot, J., Jouvet, G., Huss, M., Funk, M., Ivy-Ochs, S., and Preusser, F.: Modelling last glacial cycle ice dynamics in the Alps, The Cryosphere Discuss., https://doi.org/10.5194/tc-2018-8, in review, 2018.

13.8
Changing firn properties on glaciers in Central Asia

Marlene Kronenberg [1], Horst Machguth [1], Anja Eichler [2,3], Margit Schwikowski [2,3,4] & Martin Hoelzle [1]

[1] Department of Geosciences, University of Fribourg, Chemin de Musée 4, CH-1700 Fribourg
  (marlene.kronenberg@unifr.ch)
[2] Laboratory of Environmental Chemistry, Paul Scherrer Institute, CH-5232 Villigen
[3] Oeschger Centre for Climate Change Research, University of Bern, CH-3012 Bern
[4] Department of Chemistry and Biochemistry, University of Bern, CH-3012 Bern

It has been shown that glacier mass changes in certain areas of Central Asia and neighbouring regions are less negative than the global average. Balanced or even positive mass changes have been identified for glaciers in the Pamir, Karakoram and western Kunlun (e.g. Brun et al., 2017). The reasons for glaciers in these regions being relatively close to equilibrium, however, remain unresolved. In-situ measurements of mass balance and detailed observations especially from the little studied accumulation zones might be the key to detecting and understanding the processes behind the relatively low glacier mass loss or mass gain in these areas.

Here, we focus on two glaciers located in Kyrgyzstan: Gregoriev Ice cap located in the Inner Tien Shan and Abramov Glacier situated in the Pamir Alay (Fig. 1). Abramov Glacier is located close to the regions of low glacier mass loss while Gregoriev is located in an area of pronounced glacier decline. We use snow pits, firn cores and GPR measurements to derive present-day accumulation characteristics, including annual accumulation rates and snow distribution. Furthermore, we compile past accumulation rates for Abramov Glacier based on the exceptionally detailed glacier mass balance monitoring data (1960s to 1990s) (Pertziger, 1996; WGMS, 2015) as well as from ice cores reaching down to the early 1920s (Kislov, 1982). For Gregoriev Ice cap, we use information derived from repeated cores drilled between the 1960s and 2000s (e.g. Thompson et al., 1993) to derive past accumulation rates. First results indicate contrasting firn changes for the two study sites. Data from recently drilled cores show that the firn ice content for Gregoriev Ice cap has increased during the last decades whereas the stratigraphy of Abramov Glacier firn remains relatively similar to the one observed 40 years ago.

Figure 1. Location map of Abramov Glacier and Gregoriev Ice cap.

REFERENCES

Brun, F., Berthier, E., Wagnon, P., Kääb, A. & Treichler, D. 2017: A spatially resolved estimate of High Mountain Asia glacier mass balances from 2000 to 2016. Nature Geoscience, 10, 668–674.
Kislov, B. V. 1982: Forminrovanie i reshim firnovo-ledyanoy toltshi gornogo lednika (in Russian). Formation and regime of firn

of a mountain glacier (in Russian). PhD Thesis. Sredneasiatskiy regionalnyy nautshno-issledovatelskiy institut. Tashkent.

Pertziger, F. 1996: Abramov Glacier data reference book: climate, runoff, mass balance. Tashkent, Uzbekistan: Central Asian Regional Research Hydrometeorlogical Institute.

Thompson, L. G., Mosley-Thompson, E., Davis, M., Lin, P. N., Yao, T., Dyurgerov, M. & Dai, J. 1993: Recent warming: ice core evidence from tropical ice cores with emphasis on Central Asia. Global and Planetary Change, 7(1–3), 145–156.

WGMS 2015: Global Glacier Change Bulletin No. 1 (2012-2013). Zemp, M., Gärtner-Roer, I., Nussbaumer, S. U., Hüsler, F., Machguth, H., Mölg, N., Paul, F. & Hoelzle, M. (Eds.). Zurich, Switzerland: ICSU(WDS)/IUGG(IACS)/ UNEP/UNESCO/ WMO, World Glacier Monitoring Service, Zurich, Switzerland, publication based on database version: doi:10.5904/wgms-fog-2015-11.

13.9

Petrophysical joint inversion of electrical and refraction seismic datasets in alpine permafrost to image ice, water and air contents

Coline Mollaret [1], Florian Wagner [2], Christin Hilbich [1] & Christian Hauck [1]

[1] Departement of geosciences, University of Fribourg, Chemin du Musée 4, CH-1700 Fribourg (coline.mollaret@unifr.ch)
[2] Department of Geophysics, University of Bonn, Meckenheimer Allee 176, DE-53115 Bonn

Electrical Resistivity Tomography (ERT) is one of the most commonly used geophysical methods for permafrost monitoring (Hauck & Kneisel, 2008). Ice can be indeed well distinguished from liquid water due to its different electrical properties. However, this method has also limitations as it requires to solve an inverse problem which is usually under-determined and has no unique solution. To reduce the uncertainties and improve the interpretability of the inversion model, geophysical methods are usually combined with ground truth measurements or other geophysical methods. Nevertheless, ice and air are both materials characterized by very high electrical resistivity and are consequently hard to distinguish using ERT alone. Ice can, however, be well distinguished from air from their P-wave velocity properties (3500 m/s vs 330 m/s). Hilbich (2010) showed how refraction seismic monitoring alone can successfully characterize ground ice gain and loss. This is why Refraction Seismic Tomography (RST) is an optimal second geophysical method to be combined with ERT to assess ice or liquid water content and their respective spatio-temporal variabilities.

To fully exploit two geophysical datasets to improve the reliability of the results, several possibilities to combine the independent datasets have been successfully achieved. In this contribution, we jointly invert for the liquid water, ice, air and rock saturations using petrophysical relationships in order to reduce the occurrence of inversion artefacts. A petrophysical joint inversion for the liquid water, ice, air and rock saturations is applied using the general framework for joint inversions provided in pyGIMLI (Rücker et al., 2017). The saturation models are constrained between 0 and 1. The rock content is constrained to be close the a priori estimate prescribed prior to the inversion. In the first instance, several porosity models (homogeneous soil and porosity model derived from boreholes information) are considered as a priori knowledge.

For comparison purposes, we use the petrophysical equations employed by Hauck et al. (2011) in the so-called 4-phase model (4PM), which uses individual ERT and RST inversions and petrophysical relationships to estimate ice, water and air contents. The commonly used Archie's law (Archie, 1942) links the electrical resistivity to the water saturation, while a combination of the equations by Wyllie et al. (1956) and Timur (1968) links the P-wave velocities with the water, ice, air and rock contents.

In a first step, we apply the joint inversion scheme to synthetic datasets, representing different soil types (low/high porosity, low/high ice content), to validate the general applicability of our approach. In a second step, the saturations are jointly inverted from field datasets, which span a large range of conditions from ice-rich permafrost (rock glacier) to ice-poor permafrost sites. Finally, the sensitivities of the different parameters are analysed and the calculated water and ice contents are discussed in relation with the active layer thickness and temperature dataset, when available.

Permanently frozen soils are a very sensitive climate indicator in mountain terrains. Commonly, only soil temperatures are monitored in permafrost research. Indirect geophysical methods are applied to cover a 2nd or 3rd dimension. Jointly interpreting two distinct geophysical datasets is a common procedure for a better ground characterization. Here, we jointly invert the ice water and air saturations from two geophysical datasets to reduce the uncertainties and improve the interpretability of the subsurface. We particularly focus on the individual importance of the parameters on the results and potential improvement of the joint inversion results compared with standard individual inversions.

REFERENCES

Archie, G. E., 1942: The electrical resistivity log as an aid in determining some reservoir characteristics. Petrol. Trans. Am. Inst. Min. Metallur. Eng. 146, 54–62.

Hauck, C., & Kneisel, C., 2008: Applied Geophysics in Periglacial Environment. Cambridge: Cambridge University Press.

Hauck, C., Böttcher, M., & Maurer, H., 2011: A new model for estimating subsurface ice content based on combined electrical and seismic datasets. Cryosphere, 5, 453–468.

Hilbich, C., 2010: Time-lapse refraction seismic tomography for the detection of ground ice degradation, The Cryosphere, 4, 243–259.

Rücker, C., Günther, T. & Wagner, F.M., 2017: pyGIMLi: An open-source library for modelling and inversion in geophysics. Computers and Geosciences, 109, 106-123.

Timur, A., 1968: Velocity of compressional waves in porous media at permafrost temperatures. Geophysics 33, 584–595.

Wyllie, M. R., Gregory, A. R., & Gardner, G. H. F., 1956: An experimental investigation of factors affecting elastic wave velocities in porous media, Geophysics, 23(3), 459–493.

13.10
Glacier shrinkage in the Alps continues unabated as revealed by a new glacier inventory from Sentinel 2

Frank Paul [1], Philipp Rastner [1], Roberto Sergio Azzoni [2], Davide Fugazza [3], Raymond Le Bris [1], Johanna Nemec [4], Antoine Rabatel [5], Mélanie Ramusovic [5], Gabriele Schwaizer [4], Claudio Smiraglia [3]

[1] Department of Geography, University of Zurich, Winterthurerstr. 190, CH-8057 Zurich (frank.paul@geo.uzh.ch)
[2] Department of Environmental Science and Policy, University of Milan, Milan, Italy
[3] Department of Heart Sciences "Ardito Desio", University of Milan, Milan, Italy
[4] ENVEO IT GmbH, Innsbruck, Austria
[5] Univ. Grenoble Alpes, CNRS, IRD, Grenoble-INP, Institut des Géosciences de l'Environnement, Grenoble, France

The on-going glacier shrinkage in the Alps requires frequent updates of glacier outlines to have an accurate database for modelling purposes (e.g. determination of run-off, mass balance, or future glacier extent) and other applications. With the launch of the first Sentinel 2 (S2) satellite in 2015, it became possible to create a consistent, alpine-wide glacier inventory with an unprecedented spatial resolution of 10 m. Fortunately, already the first S2 images acquired in August 2015 provided excellent mapping conditions for about 95% of the glacierized regions in the Alps.

We have used this opportunity to compile a new alpine-wide glacier inventory in a collaborative team effort. In all countries, glacier outlines from the latest national inventories had been used as a guide to compile a consistent update. Cloud cover over some glaciers required including selected Landsat scenes from 2015 and 2016. Due to the intense manual editing required for the numerous debris-covered glaciers, uncertainty was determined by a multiple digitizing experiment with all participants.

Overall, we derived a total glacier area of 1792 km^2 when considering 4260 glaciers >0.02 km^2. This is 14.7% less than the 2100 km^2 derived for the last alpine-wide glacier inventory that was derived from Landsat scenes acquired in 2003, and is equivalent to a mean annual area loss rate of -1.2%. The real loss is even somewhat higher, as the better spatial resolution of S2 allowed us to map glaciers that are not considered in the 2003 inventory, i.e. the 2003 sample is slightly smaller.

13.11
What does ambient seismic noise tell us about glacial crevassing?

Lukas E. Preiswerk [1] & Fabian Walter [1]

[1] *Laboratory of Hydraulics, Hydrology and Glaciology, ETH Zürich, Switzerland, preiswerk@vaw.baug.ethz.ch*

Ambient seismic noise on glaciers is mostly composed of surface waves, which carry information about elastic properties of the ice body through which they pass. Here, we apply this concept to study the ice structure in the uppermost part of a glacier, i.e. the density, depth and orientation of near-surface crevasses. We first analyze data from a temporary seismic array of an Alpine avalanching glaciers in Switzerland, i.e. the hanging glacier in the Eiger-Westflanke, with 3 seismometers (corner frequencies: 1 Hz, array aperture: ~30m, installed for 5 months). There exists a prominent influence of near-surface crevasses on the orientation of the seismic wavefield polarization, and specific resonance frequencies depend on crevasse depths.

In a designated experiment on a small lake-calving glacier near Klausenpass, Switzerland, we apply our results using seismometers operational for a few hours at increasing distances from the calving front. We analyze this dataset with methods established in seismic site characterization, such as spectral ratios and wavefield polarization analysis. Using independent measurements from the "plumb-line system" (Mottram and Benn, 2009), we assess the accuracy of our seismic crevasse-depth measurement method.

Our method aims to monitor glacial crevasses as they grow and become deeper before calving events. Such a monitoring tool would not only improve calving models, but also prove useful for hazard assessment of avalanching glaciers.

REFERENCES
Mottram, R. H., & Benn, D. I. (2009). Testing crevasse-depth models: a field study at Breiðamerkurjökull, Iceland. Journal of Glaciology, 55(192), 746–752. https://doi.org/10.3189/002214309789470905

13.12
Quantification of Snow Water Equivalent Using Buried Low Cost GPS Antennas

Ladina Steiner [1], Michael Meindl [1], and Alain Geiger [1]

[1] Institute of Geodesy and Photogrammetry, ETH Zurich, Switzerland   (ladinasteiner@ethz.ch)

Extensive amount of water stored in snow covers has a high impact on flood development during snow melting periods. Early assessment of the snow water equivalent in mountain environments enhance early-warning and thus prevention of major impacts. Sub-snow GNSS techniques are lately suggested to determine liquid water content, snow water equivalent or considered for avalanche rescue. This technique is affordable, flexible, and provides accurate and continuous observations independent on weather conditions.

The potential to quantify snow water equivalent above a GPS antenna placed underneath a snowpack is evaluated using phase based differential GPS processing. Therefore, a measurement network is set-up at the WSL SLF test site "Weissfluhjoch" consisting of a GPS reference station above the snow pack and a low-cost GPS antenna mounted on the ground underneath the snowpack. These measurements are analysed for the winter seasons 2015/16-2017/18. The results are compared to the reference sensors (snow pillow, snow scale, and manual SWE observations) provided by the WSL SLF.

Results of this point-wise estimation of snow water equivalent agree very well with the reference sensors within 5 percent over the three seasons, including the melting periods. Systematic and stochastic effects on the GPS residuals induced by the overlying snowpack could be significantly reduced.

13.13
Analysing calving activity of Eqip Sermia, Greenland, using continuous direct observations

Andrea Walter [1,2], Martin P. Lüthi [1], Andreas Vieli [1]

[1] *Department of Geography, University of Zurich, Winterthurerstr. 190, CH-8057 Zurich*
  (andrea.walter@geo.uzh.ch)
[2] *ETH Zürich, VAW, Hönggerbergring 26, 8093 Zürich*

Recently, many marine-terminating glaciers of the Greenland ice sheet revealed rapid retreat, thinning and flow acceleration. These glaciers lose about half of their mass by calving, a process which can change on short timescales. Despite their importance for global sea level rise, major limitations in understanding the dynamics of these glaciers remain. To overcome such limitations, especially detailed observational data is needed.

We observed an outlet glacier in West-Greenland during an eight-day field campaign in 2018 by using a terrestrial radar interferometer, pressure sensors and a time-lapse camera. A combination of these technologies provides us with displacement and topographical data with a spatial resolution of 5 meters in one minute intervals, water height data with a temporal resolution of 2 seconds and images of the glacier front every 10 seconds. This continuous very detailed dataset enables us to get new insights of the calving process. We use these data to establish detailed calving event statistics which are compared to environmental forcing like tides or weather conditions. By identifying source areas and ice volumes of individual calving events we quantitatively investigate the relationship between calving front geometry, calving rate and potential drivers. Additionally, the comparison between the individual datasets allows us to link the shape of tsunami wave oscillations to different calving types and event volumes. Therefore, we can extend the individual calving event statistics from short timescale to long timescale over 5 years.

13.14

Assessing the influence of convection in the active layer of a rock glacier on ground temperatures

Jonas Wicky [1], Christian Hauck [1]

[1] Alpine Cryosphere and Geomorphology Group, Unit of Geography, Department of Geosciences, University of Fribourg, Chemin du Musée 4, 1700 Fribourg (jonas.wicky@unifr.ch)

In the Swiss Alps permafrost is a widespread phenomenon with a great impact on the landscape particularly regarding natural hazards. Permafrost occurrence is not only influenced by meteorological parameters and the elevation of the site, also landform and subsurface substrate have a significant impact on the ground thermal regime. Mountain permafrost is often covered by coarse blocky material with a high permeability which allows air to circulate within the ground. Thus, convective heat transfer takes place and influences the ground temperatures.

Numerical modelling approaches in mountain permafrost often either neglect or parametrize ground convection (e.g., Pruessner et al. 2018, Luethi et al. 2017, Scherler et al. 2014). Explicit modelling approaches are rare. In a previous study we successfully modelled the influence of convection on the thermal regime of an Alpine talus slope (Wicky & Hauck, 2017). In this study, we present results from numerical experiments on the effect of air circulation within the porous active layer of an Alpine rock glacier. The model solves for air flow coupled with heat transfer on a 2D domain and is setup within COMSOL Multiphysics. We use data for forcing and validation from the Murtèl rock glacier in the Engadin (Eastern Swiss Alps) provided by the Swiss permafrost monitoring network (PERMOS, 2016).

The model results show that convective heat transfer in the active layer has a significant effect on the thermal regime of a rock glacier. Winter temperatures are highly influenced by convective heat transfer due to the unstable thermal stratification of the air which allows a pronounced convective cooling, whereas summer temperatures show almost no sensitivity to convective heat transfer. Wintertime air circulation is characterized by vertical multicellular convection. During summer a gentle down flow of air takes place (Fig. 1). The prevailing air circulation pattern and the efficiency of cooling strongly depend on the thermal gradient between ground and atmosphere temperatures as well as on the material properties. Especially the permeability of the porous active layer plays an important role.

Compared to borehole data, the model performs well but shows some discrepancy at depth, which is maybe due to convection within the rock glacier body (ice core) which is not represented so far and uncertainties in the material properties, especially regarding the permeability. Our results highlight that air convection cannot be neglected in porous permafrost substrate and should be considered in future modelling approaches. Under warming climate conditions and increased permafrost thaw a proper understanding of the ground thermal regime is crucial to model reliable future projections.
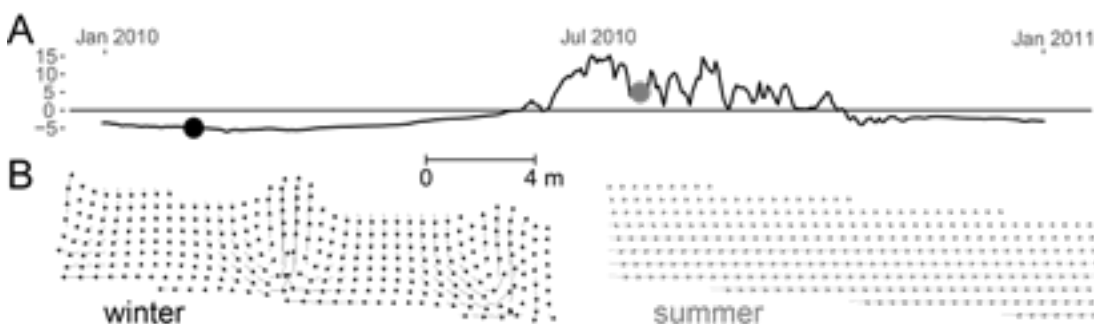

Figure 1. (A) Boundary temperature from the uppermost thermistor at Murtèl borehole COR_0287 (PERMOS, 2016) with a black (grey) dot indicating the time of the circulation snapshot B. (B) Typical circulation patterns within the active layer of a rock glacier. Wintertime multicellular convection (left) and summertime down flow (right).

REFERENCES

Luethi, R., Phillips, M. & Lehning, M. 2017: Estimating Non-Conductive Heat Flow Leading to Intra-Permafrost Talik Formation at the Ritigraben Rock Glacier (Western Swiss Alps). Permafrost and Periglacial Processes 28(1), 183-194.

PERMOS 2016: PERMOS Database. Swiss Permafrost Monitoring Network, Fribourg, Switzerland.

Pruessner, L., Phillips, M., Farinotti, D., Hoelzle, M., & Lehning, M. 2018: Near-surface ventilation as a key for modeling the thermal regime of coarse blocky rock glaciers. Permafrost and Periglacial Processes 29(3), 152-163.

Scherler, M., Schneider, S., Hoelzle, M. & Hauck, C. 2014: A two-sided approach to estimate heat transfer processes within the active layer of the Murtèl–Corvatsch rock glacier. Earth Surface Dynamics 2(1), 141-154.

Wicky, J. & Hauck, C. 2017: Numerical modelling of convective heat transport by air flow in permafrost talus slopes. The Cryosphere 11(3), 1311-1325.

13.15
Modelling the evolution of Alpine glaciers under the EURO-CORDEX RCM ensemble

Harry Zekollari [1,2], Matthias Huss [1,3], Daniel Farinotti [1,2]

[1] Laboratory of Hydraulics, Hydrology and Glaciology (VAW), ETH Zürich, Zürich, Switzerland (zharry@ethz.ch)
[2] Swiss Federal Institute for Forest, Snow and Landscape Research (WSL), Birmensdorf, Switzerland
[3] Department of Geosciences, University of Fribourg, Fribourg, Switzerland

The retreat of the ca. 3500 glaciers in the European Alps has severe implications for the availability of water resources, natural hazards, and the perception of mountains as a recreational environment. To date, studies on the future evolution of glaciers typically rely on parameterizations, in which ice dynamics are not explicitly accounted for. So far, only few studies have explicitly coupled ice flow and surface mass balance processes, and these have mostly focused on individual glaciers, rather than regional scales.

Here, we model the 1990-2100 evolution of all glaciers in the European Alps accounting for both surface mass balance and ice dynamic processes. For doing so, we include an ice flow component into the Global Glacier Evolution Model (GloGEM). Glacier outlines from the Randolph Glacier Inventory are utilized, while an inversion approach is used to estimate the initial glacier thickness. For model validation and calibration, we rely on a vast dataset, including in-situ and geodetic mass balance measurements, glacier length changes, and surface velocity measurements amongst others. This allows for a novel, glacier-specific calibration procedure. The climatic data for the validation and the historical period is drawn from the ENSEMBLES daily gridded observational dataset (E-OBS v.17.0), while for future climatic conditions we rely on EURO-CORDEX Regional Climate Model simulations.

Under a RCP2.6 scenario, the glacier volume loss projected for the end of the century (ca. 60% against a 2003 baseline), is lower than most previous estimates that did not account for ice flow explicitly. Under a RCP8.5 scenario, instead, future glacier evolution is dictated by increased surface melt, reducing the importance of ice dynamics effects. Under such a scenario, Alpine glaciers are projected to largely disappear by the end of the century, with a volume and area loss of 90-95% and around 90%, respectively.

P 13.1

Seasonal evolution of englacial conduits through repeated ground penetrating radar measurements

Gregory Church [1], Andreas Bauder [1], Hansruedi Maurer [2]

[1] Laboratory of Hydraulics, Hydrology and Glaciology (VAW), ETH Zürich, Hönggerbergring 26, CH-8093 Zürich
  (church@vaw.baug.ethz.ch)
[2] Department of Earth Sciences, Institute of Geophysics ETH Zürich, Zürich, Switzerland

Englacial and subglacial meltwater conduits are constantly evolving throughout the season on temperate glaciers, and they strongly influence glacier dynamics and the catchment hydrology. Additionally, it is important to monitor these englacial systems for natural hazard management.

Here, we present a study conducted on Rhone Glacier, Switzerland. This is a temperate glacier located in the central Swiss Alps (Figure 1, left) flowing in a southerly direction from an altitude of 3600 m down to 2200 m. Since 1878 the glacier has retreated 1700 m exposing a granite bedrock and a proglacial lake formed in 2005 due to the excessive retreating.

We have monitored the englacial drainage system in the lower ablation zone throughout the 2018 season using a PulseEkko 25MHz ground-penetrating radar (GPR) system. GPR is highly sensitive to the presence of water and is therefore a suitable tool to monitor englacial conduit evolution.
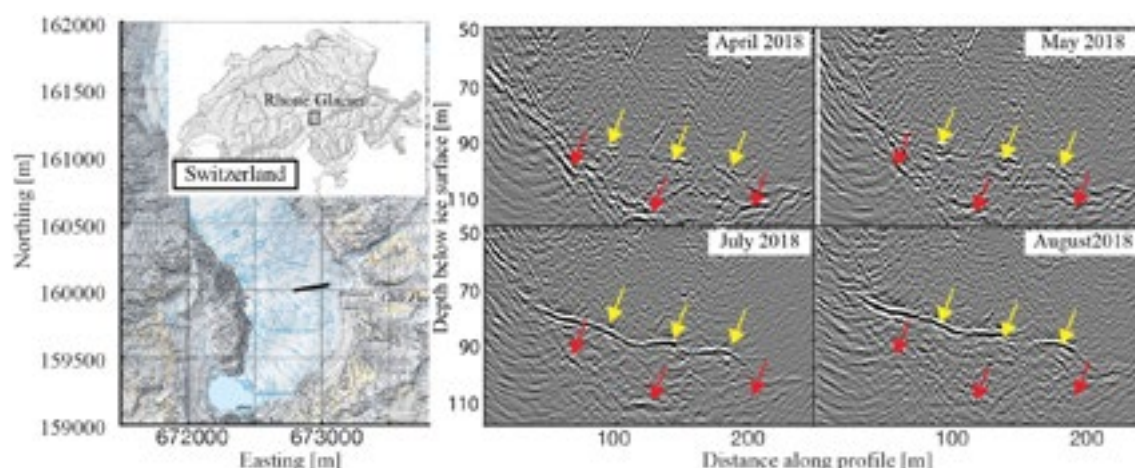
Figure 1. Left: Location map of Rhone glacier and surface-based GPR location shown in black. Right: Ground-penetrating radar sections over an englacial conduit (yellow arrows) and bedrock (red arrows) for different months throughout 2018.

The GPR results (Figure 1, right) show an englacial network developing over a season. Analysis of the englacial GPR reflection strength indicated the hydrological conduit conditions. Weak GPR reflection amplitude at the beginning of the year indicated dry conditions with a small quantity of debris-rich ice. In contrast, strong GPR reflection amplitudes in July and August indicated free water within the englacial conduit. These observations were confirmed by a borehole drilling campaign and the use of a borehole camera in August 2018 to identify the reflection origin. The source of the englacial meltwater conduits is fed from the numerous runoff streams on the eastern moraine. These streams run subglacially alongside the glacier flank and become englacial conduits at 80 m below the ice surface potentially flowing through cracks and crevasses.

Temporal changes that were detected from the repeated GPR surveys indicate that a temperate glacier exhibits strong seasonal changes in hydrological conditions. We have been able to monitor these temporal changes remotely with GPR and with additional in-situ borehole observations.

P 13.2
Crystal orientation fabric analysis on ice core samples from a temperate Alpine glacier

Sebastian Hellmann [1,2], Andreas Bauder [1], Johanna Kerch [3], Hansruedi Maurer [2]

[1] Versuchsanstalt für Wasserbau, Hydrologie und Glaziologie, ETH Zürich, Hönggerbergring 26, CH-8092 Zürich
  (sebastian.hellmann@erdw.ethz.ch)
[2] Institute of Geophysics, ETH Zürich, Sonneggstrasse 5, CH-8092 Zürich
[3] Alfred-Wegener-Institute for Polar and Marine Research, Am alten Hafen 26, D-27568 Bremerhaven

Ice under natural conditions shows a typical hexagonal crystal structure with an optical axis perpendicular to the basal planes often referred to as c-axis (Cuffey&Patterson, 2010). In the direction of the c-axis the crystal is significantly harder under pressure compared to the other directions.
Polar ice cores or cores from cold alpine ice have been analysed extensively in recent years (Montagnat et al., 2014; Weikusat et al., 2017; Kerch et al., 2018) showing a direct relationship between the stress regime and the crystal orientation. Furthermore, cystal orientation fabric (COF) was found to affect geophysical measurements such as acoustics and ground-penetrating radar by introducing an anisotropy effect (Diez et al. 2014).

Our investigations are focussed on the ablation zone of Rhone Glacier. Using geophysical experiments in a ring of 12 boreholes we try to detect crystal anisotropy effects in acoustic waves also for those shallow temperate glaciers. These finding are compared with an 80 m long ice core drilled in the center of the ring in summer 2017. Due to the specific technique (Schwikowski et al., 2014), the orientation of the ice core relative to the direction of glacier flow could be preserved, thereby allowing a direct comparison with the geophysical measurements from different azimuth angles.
The COF of the ice core was analysed for 7 different depths along the ice core using the G50 fabric analyser at Alfred-Wegener-Institute in Bremerhaven, Germany. 9-12 ice core thin sections with a diameter of 6-8 cm in 3 perpendicular directions were prepared due to a relatively large grain size of several centimeters to measure a reasonable amount of crystals in each depth for the statistical evaluation.

Figure 1 shows the detected c-axis orientations along the profile. In the upper part of the glacier a mainly vertically oriented COF could be identified. This pattern changes with increasing depth towards a more horizontal COF. However, the analysis of the ice core data has to be improved. Detailed analyses showed that several small grains were probably formed due to recrystallisation after ice core retrieving or could have been melt water veins that randomly refroze during storage. Those particular crystals may lead to a miss-interpretation. Therefore the grain size needs to be considered when analysing the images of the thin sections.
We present the method and results of our ice core analysis and compare these findings with our acoustic measurements in context of a potential anisotropy effect visible in travel times of elastic waves. Our study contributes to a better understanding of crystal anisotropy in temperate glacier ice and links between glaciological and geophysical methods.
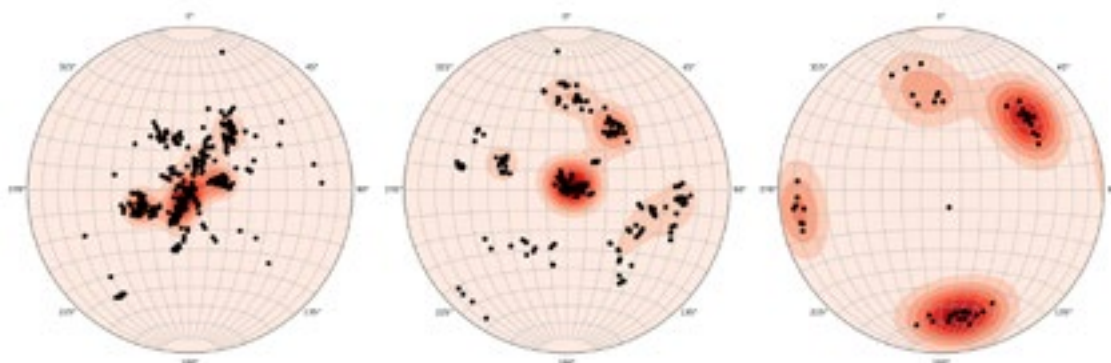

Figure 1. COF analysis in different depths (2 m, 52 m, 79 m below surface) of an ice core from Rhone Glacier, Central Swiss Alps showing an transition from mainly vertically oriented ice crystals towards more horizontal distribution with increasing depth.

REFERENCES

Cuffey, K.M. and Paterson, W.S.B. 2010: The physics of glaciers, 4th ed. Elsevier, Amsterdam.

Diez, A., Eisen, O., Weikusat, I., et al. 2014: Influence of ice crystal anisotropy on seismic velocity analysis. Annals of Glaciology, 55(67), 97–106.

Kerch, J., Diez, A., Weikusat, I. and Eisen, O. 2018: Deriving seismic velocities on the micro-scale from c-axis orientations in ice cores.

Montagnat, M., Azuma, N., Dahl-Jensen, D., et al. 2014: Fabric along the NEEM ice core, Greenland, and its comparison with GRIP and NGRIP ice cores. The Cryosphere, 8(4), 1129–1138.

Schwikowski, M., Jenk, T.M., Stampfli, D. and Stampfli, F. 2014: A new thermal drilling system for high-altitude or temperate glaciers. Annals of Glaciology, 55(68), 131–136.

Weikusat, I., Jansen, D., Binder, T., et al. 2017: Physical analysis of an Antarctic ice core – towards an integration of micro- and macrodynamics of polar ice. Philosophical Transactions of the Royal Society A: Mathematical, Physical and Engineering Sciences, 375(2086), 20150347.

P 13.3
Locating and monitoring glaciohydraulic tremors on Glacier de la Plaine Morte, Switzerland

Fabian Lindner [1], Fabian Walter [1] & Gabi Laske [2]

[1] Laboratory of Hydraulics, Hydrology and Glaciology, ETH Zürich, Hönggerbergring 26, CH-8093 Zürich
 (lindner@vaw.baug.ethz.ch)
[2] Scripps Institution of Oceanography, UC San Diego, USA

In glaciated regions where temperatures allow melting, the resulting surface runoff is routed through and beneath glaciers. In case the water supply overwhelms the capacity of the subglacial conduits, the water pressure at the glacier's base is increased. This pressure increase promotes basal motion, hence, glacial hydraulics influences ice flow. On its passage through and beneath the glacier, the water interacts with the ice walls due to turbulent flow or excitation of resonances in the conduits. These processes act as seismic sources emitting waves which – given the wave generation is sufficiently strong – can be recorded at the glacier's surface as continuous seismic tremors (Bartholomaus et al., 2015; Gimbert et al., 2016; Roeoesli et al., 2016). We attempt to locate such tremors observed on Glacier de la Plaine Morte in summer 2016 and investigate the time evolution of their source locations. Our data include the signal from the drainage of an ice-dammed lake which resulted in a sudden perturbation of the subglacial drainage system. We apply a classic array processing technique to measure the source direction as observed in different parts of the glacier. These measurements are combined with a more holistic approach using the seismic recordings from different parts of the glacier simultaneously. We identify times where tremors are generated in moulins. Furthermore, analysis of the background signal suggests that it is generated in a channel-like structure close to the glacier terminus. These results show that surface seismic measurements allow insights into the subglacial drainage system – an otherwise hard-to-access environment.

REFERENCES

Bartholomaus, T. C., Amundson, J. M., Walter, J. I., O'Neel, S., West, M. E., & Larsen, C. F. (2015). Subglacial discharge at tidewater glaciers revealed by seismic tremor. Geophysical Research Letters, 42(15), 6391-6398.

Gimbert, F., Tsai, V. C., Amundson, J. M., Bartholomaus, T. C., & Walter, J. I. (2016). Subseasonal changes observed in subglacial channel pressure, size, and sediment transport. Geophysical Research Letters, 43(8), 3786-3794.

Roeoesli, C., Walter, F., Ampuero, J. P., & Kissling, E. (2016). Seismic moulin tremor. *Journal of Geophysical Research: Solid Earth*, *121*(8), 5838-5858.

P 13.4

Long-term multi-resolution terrestrial photogrammetry at the Moosfluh landslide

Fabian Neyer[1], Sébastien Guillaume[1], Philippe Limpach[2] & Alain Geiger[1]

[1] *Institute of Geodesy and Photogrammetry, ETH Zurich, 8093 Zurich, Switzerland (fabian.neyer@geod.baug.ethz.ch)*
[2] *BSF Swissphoto, Dorfstrasse 53, CH-8105 Regensdorf-Watt*

Risks and hazard analyses of potential environmental mass movements are typically based on geodetic measurements (GPS, total station, laser, radar, imagery, etc.) or qualitative interpretation by experts. Each methodology has its strengths and weaknesses, whereas the ultimate goal is to combine the various techniques to obtain an undisturbed picture of the scene with high confidence. This work focuses on the combination of high-precision GPS and image-based estimates using permanent multi-resolution online camera systems.

Our monitoring system was installed in the Aletsch area, focusing on the Moosfluh landslide. While permanent GPS stations are within the landslide area, three permanent camera systems are mounted on stable rock on the opposite side of the valley. There are currently two online and real-time GPS stations on the landslide that can be identified in the images. Image coordinates of the GPS antenna centers are linked to their estimated coordinates and thus serve as an absolute references. To increase the network of known coordinates, additional ground control points were measured and assigned in the image spaces using QDeadalus (Guillaume et al., 2016). QDeadalus is a total station equipped with a video camera with a small field of view. About 20 natural landmarks were measured from two different viewpoints at distances between 1.5 and 3.5 kilometers. The additional natural control points could be measured to an accuracy of a few centimeters and were subsequently included in the self-calibrating photogrammetric bundle adjustment of the network. GPS was also used to estimate accurate camera position coordinates. Fixing the station coordinates improves the 3-dimensional reconstruction accuracy significantly (Neyer, 2016), thus camera positions were fixed in the subsequent adjustments.

All cameras are synchronized to the level of a few seconds such that synchronized multi-view time lapse of images results. For each epoch, a set of points (tie points) is determined and matched across the different views. The same tie points are also tracked across the different epochs such that for each feature, a 3-dimensional trajectory can be estimated. Due to the nature of the creep phenomena, some rock boulders experience - despite obvious translations - also large rotations. For a successful match in the image spaces through time, we estimate the parameters of local similarity transformations by the principles of least-squares image matching.

Two of the three permanent camera stations are dual camera systems, i.e., an overview and a zoom camera with a smaller field of view. The latter focuses on an area of interest that is also visible in the overview camera. Features detected in the zoom image are mapped into the coordinate system of the overview camera with a precision of about 0.02 pixels. Apart from logistical advantages, this also allows to use the high resolution images for a more accurate feature selection while not having more station parameters to solve in the adjustment. As a result, object coordinates identified in the zoom images show smaller standard deviations, i.e., they are approximately proportional to the ratio of the different focal lengths between the zoom and the overview cameras.

A network with three camera stations is usually a weak photogrammetric network, i.e., the robustness and reliability are low. While object point accuracies are in the order of 1 to 0.5 pixels (when back-projected), the accurate identification of features across multiple views is currently the limitation of the method. Presently we use SURF descriptors and manual identification for matching across the views. Alternatively, least-squares matching could be performed but it becomes difficulty or inaccurate when features are seen from angular separations larger than about 20 degrees (which the case here). Nevertheless, the proposed processing pipeline delivers direct 3-dimensional rock trajectories at an error level of a few centimeters in the area of interest.

Here we give insights into the applied measuring and processing techniques of this project, illustrate its potentials and limitations, as well as showing results obtained so far.

REFERENCES:

Guillaume S., Clerc J., Leyder C., Ray J., Kistler M. 2016. Contribution of the Image-Assisted Theodolite System QDaedalus to Geodetic Static and Dynamic Deformation Monitoring, 3rd Joint International Symposium on Deformation Monitoring, JISDM2016, Vienna, Austria, March 30 - April 1, 2016

Neyer F. 2016: Monitoring Rock Glaciers by Combining Photogrammetric and GNSS-Based Methods, Doctoral Thesis, ETH Zürich

P 13.5

A more than 100 years time series of seasonal mass balance for Golubin Glacier, Northern Tien Shan

Erlan Azisov [1], Martina Barandun [2], Martin Hoelzle [2], Marlene Kronenberg [2], Tomas Saks [2], Sergiy Vorogushyn [3] & Ryskul Usubaliev [1]

[1] Central Asian Institute for Applied Geosciences, Timur Frunse Street 73/2, KG-720072 Bishkek (e.azisov@caiag.kg)
[2] Department of Geosciences, University of Fribourg, CH-1700 Fribourg
[3] German Research Center for Geosciences, DE-Potsdam

Golubin is a mountain glacier (Figure 1) with an area of 5.5 km^2 (in 2002) and spans an elevation range from 3300 to 4400 m a.s.l. The glacier is located in the Ala-Archa catchment, in the Kyrgyz Ala-Too range, northern Tien Shan. Mass balance of Golubin Glacier was measured by the glaciological method from 1969 to 1994 and regular annual measurements have been reinitiated in 2010. In 2013, an automamtic weather station and an automatic camera for transient snow line observations have been installed in the vicinity of the glacier. Furthermore, precipitation and temperature data are available from Alplager weather station located at 2340 m a.s.l. since 1980. In addition to these insitu data, complimentary information on glacier mass and area changes can be obtained from remote sensing data and reanalysis data can be used to extend the precipitation and temperature time series.

In this study, we combine different data sets and methods to derive a centennial time series of seasonal glacier mass balance of Golubin Glacier. In a first step (i), we calibrate a mass balance model (Huss, 2009) with annual mass balance measured for 2010-17. The model is forced with data from Alplager station. In the following, (ii) we apply the calibrated model to calculate the mass balance back to 1980. (iii) The modelled mass balance is evaluated against historic mass balance measurements. As a next step, (iv) the model is run with Reanalysis data reaching back to 1901 and the model calibration steps were repeated. The therefrom obtained cumulative mass balances are validated against published geodetic mass balances of the glacier (e.g. Bolch 2015) and against secular glacier mass balances derived from length changes following the approach of Hoelzle (2003).

REFERENCES

Bolch T. 2015: Glacier area and mass changes since 1964 in the Ala Archa Valley, Kyrgyz Ala-Too, northern Tien Shan, Ice and Snow, 1(129), 28-39.

Hoelzle, M., Azisov, E., Barandun, M., Huss, M., Farinotti, D., Gafurov, A., Hagg, W. Kenzhebaev, R., Kronenberg, M. Machguth, H., Merkushkin, A., Moldobekov, B., Petrov, M., Saks. T., Salzmann, N., Tarasov, Y., Usubaliev, R., Yakovlev, A. & Zemp, M. 2017: Re-establishing glacier monitoring in Kyrgyzstan and Uzbekistan, Central Asia. Geoscientific Instrumentation, Methods and Data Systems, 6(2).

Hoelzle, M., Haeberli, W., Dischl, M. &Peschke, W. 2003: Secular glacier mass balances derived from cumulative glacier length changes, Global Planet. Change, 36, 295–306.

Huss, M., Bauder, A. & Funk, M. 2009: Homogenization of long-term mass-balance time series, Ann. Glaciol., 50, 198–206.
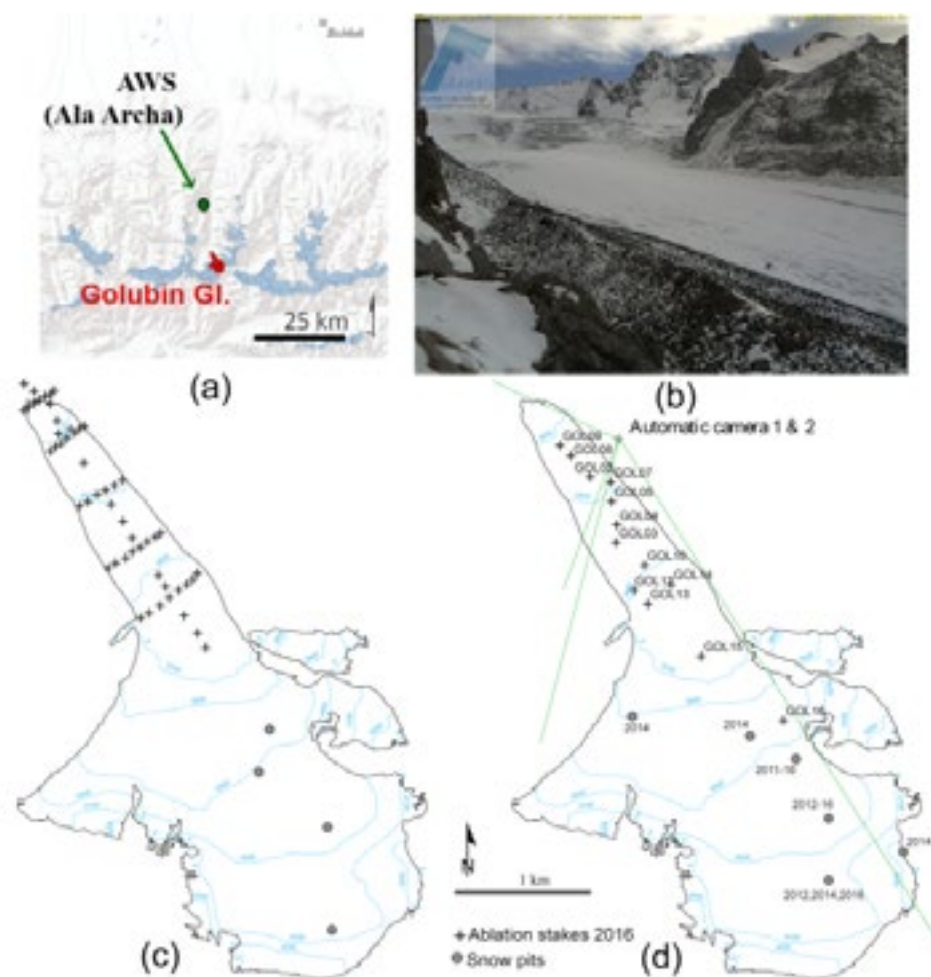
Figure 1. From Hoelzle et al. (2017). Historical (c) and new (d) mass balance network on the Golubin Glacier (Kyrgyzstan) with corresponding (overview) map (a) and snow line camera picture (b).

P 13.6
Mass balance monitoring and capacity building in Central Asia

Alyssa Ghirlanda [1], Marlene Kronenberg [1], Martina Barandun [1], Erlan Azisov [2], Abdulhamid Kayumov [3], Ruslan Kenzehbaev [2], Horst Machguth [1], Tomas Saks [1], Yura Tarasov [4], Ryskul Usubaliev [2], Andrey Yakovlev [5], Martin Hoelzle [1]

[1] Department of Geosciences, University of Fribourg, Switzerland (alyssa.ghirlanda@unifr.ch)
[2] Central Asian Institute for Applied Geosciences, Bishkek, Kyrgyzstan
[3] Institute of Water Problems, Hydro-Power Engineering and Ecology, Dushambe, Tajikistan
[4] UZHydromet, Tashkent, Uzbekistan
[5] Uzbek scientific investigation and design survey institute, UzGIP, Tashkent, Uzbekistan

Glaciers are a key component of the high-mountain environment in Central Asia. They are essential for water availability in the arid and intensely populated areas located downstream. Moreover, glacier retreat can trigger natural hazards, such as glacier lake outburst floods (GLOFs). However, in Central Asia, glacier mass balance observations, which are required for efficient water management and disaster risk reduction, are sparse and often discontinuous.

According to regional mass balance studies based on remote sensing data, glaciers in the Tien Shan are characterised by substantial mass loss during the last decades. As for glaciers located in the neighbouring Pamir Mountains, several geodetic mass balance studies suggest less negative mass balances or balanced conditions. However, changing processes cannot be fully understood based on remote sensing studies only. Such studies often rely on bulk estimates, provide only semi-decadal to decadal changes and are connected to uncertainties which are challenging to quantify. Therefore, a combination of approaches is necessary to reduce uncertainties. A promising approach, where observations of remotely sensed transient snowlines and geodetic mass balances are used to constrain a simple mass balance model, provides annual mass balance series for remote and inaccessible glaciers. Nevertheless, in-situ measurements of glacier mass balance are still a prerequisite for validation and calibration of any combined remote sensing/modelling approach.

On the one hand, extensive mass balance monitoring programmes are needed to overcome the data scarcity in Central Asia. On the other hand, capacity-building efforts in the research area of the fast changing cryosphere are necessary to ensure the sustainability of monitoring activities. Furthermore, from a societal perspective, capacity building needs to address related domains of Water Resource Management and Disaster Risk Reduction.

The project Cryospheric Climate Services for improved Adaption (CICADA) aims on a capacity building in the above-mentioned domains amongst stakeholders in Central Asia and the continuous monitoring and open access of in situ data from glaciers in this data sparse region. Here, we give an overview of the CICADA project and an insight into different mass balance studies of Central Asian Glaciers performed within CICADA and related projects.

P 13.7
Ice volume estimation in the Swiss Alps from helicopter-borne GPR and glaciological modeling

Melchior Grab [1,2], Lisbeth Langhammer [1], Andreas Bauder [2], Lasse Rabenstein [3], Lino Schmid [1,2] & Hansruedi Maurer [1]

[1] Institute for Geophysics, ETH Zurich, Sonneggstrasse 5, 8092 Zürich (melchior.grab@erdw.ethz.ch)
[2] Laboratory of Hydraulics, Hydrology and Glaciology, ETH Zurich, Hönggerbergring 26, 8092 Zürich
[3] Drift & Noise Polar Services GmbH, Hohenlohestr 8, 28209 Bremen

For overcoming future challenges arising from the ongoing melting of glaciers, an accurate prediction of the future river discharge and the topography of deglaciating regions is needed. A good knowledge of the current ice thickness distribution builds the basis for such predictions. To obtain this information for the glaciers in Switzerland, we have developed a helicopter-borne ground penetrating radar (GPR)-instrument from commercially available components (Langhammer et al., 2017) and a Matlab®-based data processing software package (Grab et al. 2018).
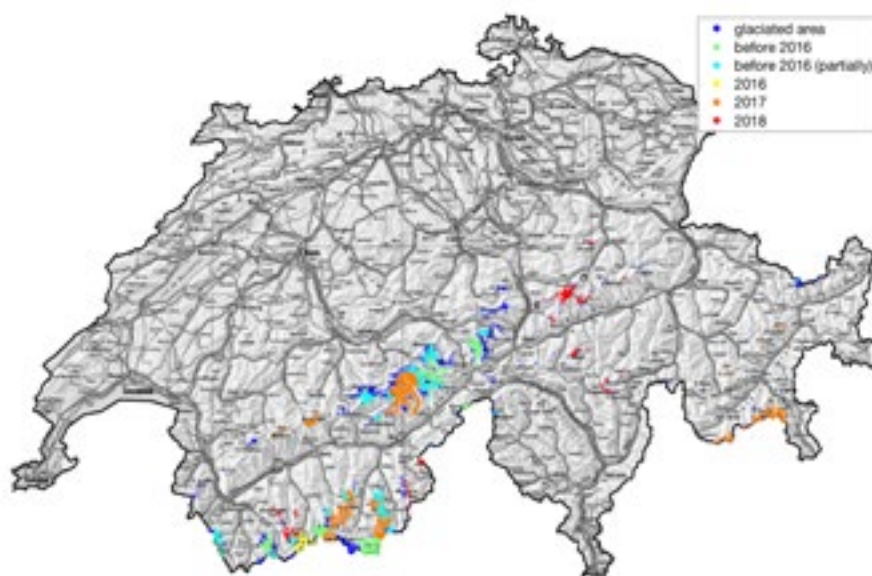
Figure 1: Current status (by August 2018) of the data acquisition. Glaciers are color-coded to show the year of data acquisition (green, yellow, orange, and red). Glaciers only partially surveyed are shown in light blue.

During the past years, the GPR-instrument has been used for recording data from numerous glaciers in the Swiss Alps. To date, a total of around 1'000 km of GPR-profiles has been recorded with the new instrument. Together with data recorded at earlier years (1999-2015, around 1'400 km), a large data base has been built, which includes data for most glaciated regions in Switzerland (Fig. 1).

The GPR data provide the ice thickness and the topography of the bedrock on a sparse grid across the glaciers. We combine these data with glaciological modeling techniques, in order to estimate the total ice volume and to provide continuous ice thickness maps and bedrock topography maps. Therefore, we have developed the **Gla**cier **T**hickness **E**stimation (**GlaTE**) algorithm. It allows to adequately invert for the three-dimensional ice thickness of Alpine glaciers based on glaciological modeling (after Clarke et al., 2013) and observable data constraints (glacier outlines, digital elevation model, and GPR data). An example result is shown in Fig. 2 for the Morteratsch glacier, computed by L. Langhammer (2018).
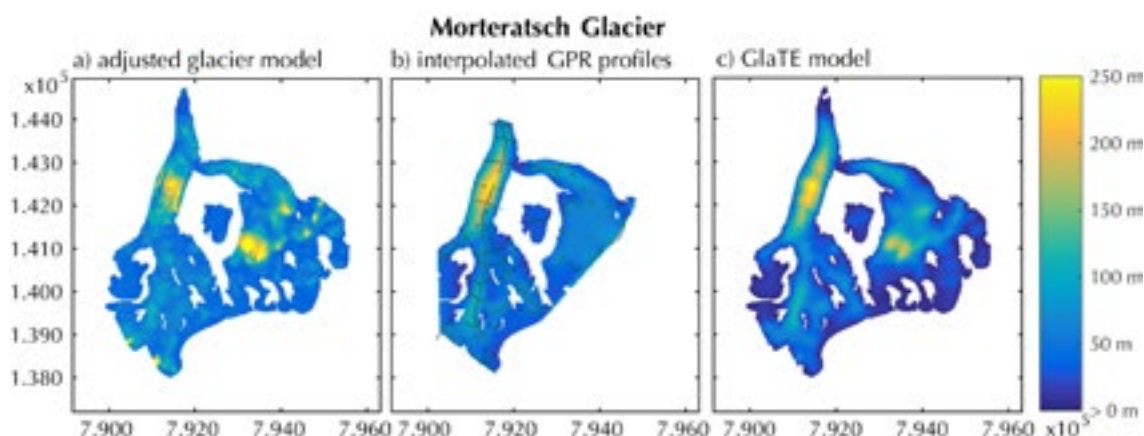
Figure 2: Ice thickness estimation of the Morteratsch Glacier: Computed by L. Langhammer (2018) using (a) the glaciological model after Clarke et al. (2013), (b) interpolation of GPR data, and (c) the GlaTE algorithm.

In the framework of the Swiss Competence Center for Energy Research – Supply of Electricity (SCCER-SoE), it is our aim to soon provide an update about the total ice volume in the Swiss Alps. The processing of the recorded GPR data is already finished and we currently work on the finalization of the interpretation of the numerous GPR profiles. Furthermore, some more measuring campaigns are planned to fill the data gabs (blue and light blue regions in Fig. 1) with the primary focus on the larger glaciers.

REFERENCES

Clarke, G. K., Anslow, F. S., Jarosch, A. H., Radić, V., Menounos, B., Bolch, T., & Berthier, E, Ice volume and subglacial topography for western Canadian glaciers from mass balance fields, thinning rates, and a bed stress model. Journal of Climate, 26(12), 4282-4303, 2013

Grab, M., A. Bauder, F. Ammann, L. Langhammer, S. Hellmann, G. J. Church, L. Schmid, L. Rabenstein, and H. R. Maurer. "Ice volume estimates of Swiss glaciers using helicopter-borne GPR—an example from the Glacier de la Plaine Morte." In 2018 17th International Conference on Ground Penetrating Radar (GPR), pp. 1-4. IEEE, 2018.

Langhammer, L., L. Rabenstein, A. Bauder, and H. Maurer, "Groundpenetrating radar antenna orientation effects on temperate mountain glaciers", in Geophysics, vol. 82, no. 3, pp. H15-H24, 2017

Langhammer, L., PhD Thesis "Helicopter-borne ground-penetrating radar surveying of temperate Alpine glaciers" (in preparation for final submission, defended in August 2018)

P 13.8

The potential of low-cost UAVs and open-source photogrammetry software for high-resolution glacier monitoring – A case study from the Kanderfirn (Swiss Alps)

Alexander Raphael Groos [1], Lukas Munz [1], Thalia Bertschinger [1]

[1] Institute of Geography, University of Bern, Hallerstrasse 12, CH-3012 Bern (alexander.groos@giub.unibe.ch)

Unmanned Aerial Vehicles (UAVs) represent a relatively new, but powerful, tool in the field of glaciology and are mainly used in combination with proprietary photogrammetry software to obtain high-resolution glacier surface information (e.g. Bhardwaj et al. 2016). As a free and low-cost alternative, self-developed fixed-wing UAVs equipped with optical instruments were tested for high-resolution monitoring of the Kanderfirn glacier in the Swiss Alps during summer 2017 and 2018. The taken aerial photographs were postprocessed in the open-source photogrammetry software OpenDroneMap to generate othophotos and digital surface models. Based on the comparison of the consecutive overflights, velocities, surface height changes, ablation, surface roughness etc. were calculated. The preliminery results demonstrate that low-cost UAVs in combination with open-source software are an affordable alternative to commercial remote sensing platforms and have the potential to deliver geo-data in high spatial and temporal resolution required for the investigation of glacier dynamics as well as the validation of model results and satellite products.
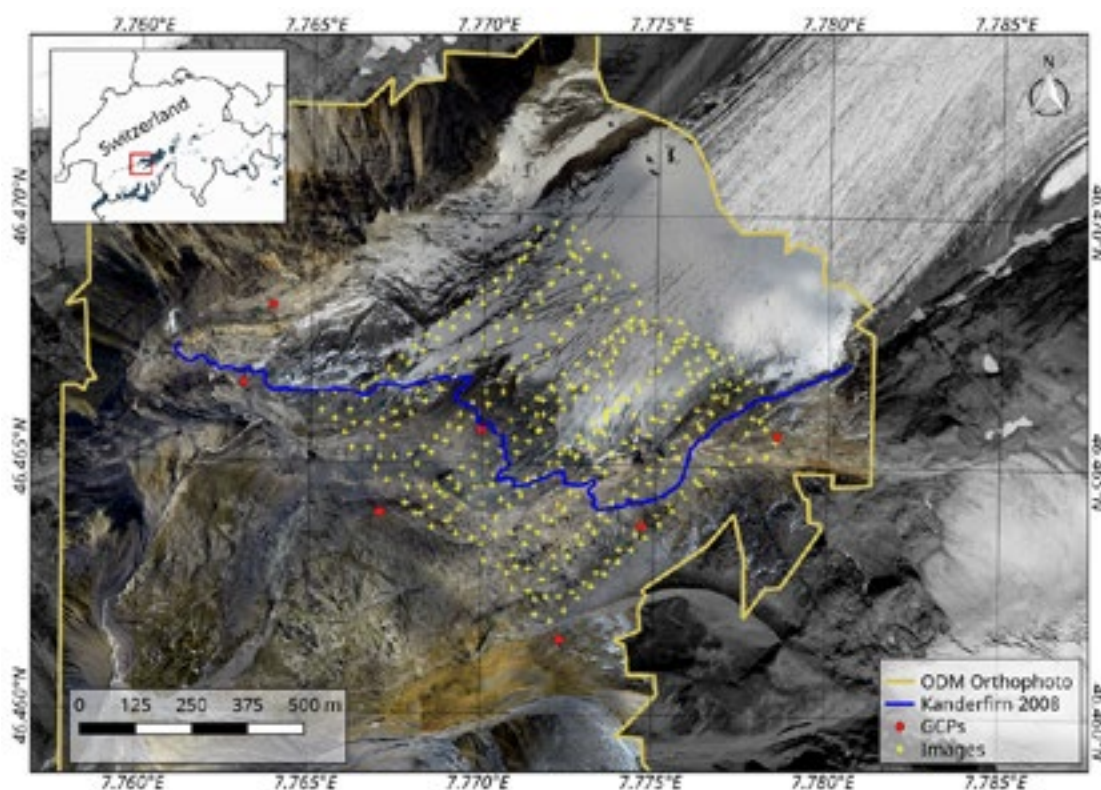
Figure 1. High-resolution orthophoto (pixel size: 5 x 5 cm) of the tongue of the Kanderfirn glacier (Swiss Alps) obtained from 393 UAV images using the photogrammetry software OpenDroneMap. An airborne orthophoto from the year 2008, provided by SwissTopo, is displayed in the background.
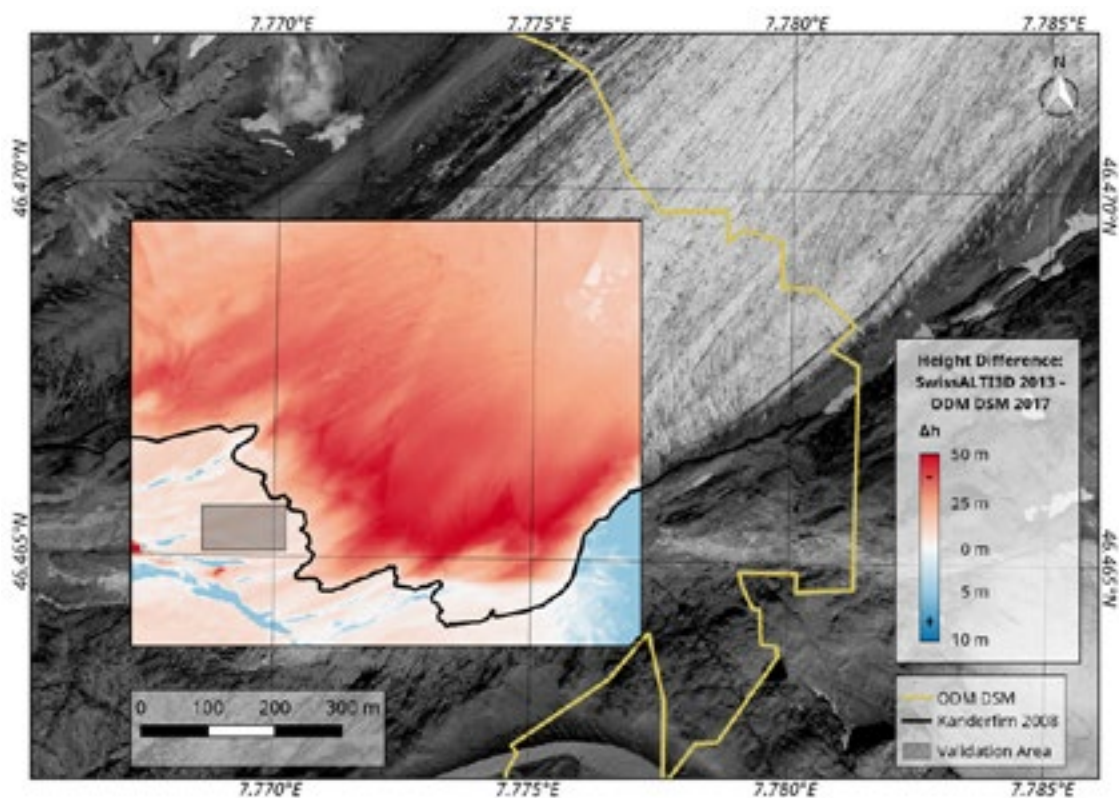
Figure 2. Elevation change at the tongue of the Kanderfirn glacier between summer 2011 and 2017 derived from the comparison of the SwissALTI3D Digital Surface Model (DSM), provided by SwissTopo, and the OpenDroneMap DSM obtained from UAV imagery.

REFERENCES

Bhardwaj, A., Sam, L., Akanksha, Martín-Torres, F.J. & Kumar, R. 2016: UAVs as remote sensing platform in glaciology: Present applications and future prospects. Remote Sensing of Environment, 175, 196–204.

P 13.9
Calorimetric determination of the unfrozen water content in glacier ice

Martin Lüthi [1]

[1] Geogrphical Institute, University of Zurich, Winterthurerstrasse 190, CH-8057 Zurich (martin.luethi@geo.uzh.ch)

Glacier ice at the melting temperature may contain up to 6% of unfrozen water, as was inferred with indirect methods such as ice-penetrating radar. This inter-grain water influences ice deformation, the thermal structure of ice sheets, and subglacial hydrology.

We determined by the content of free water in-situ in ice tunnels of serveral temperate glaciers. The calorimeter consists of an active cooling system in a central borehole and a set of thermistors which are placed in several distances from the center. We thus measure the velocity of the freezing front as well as the cooling rates. With help of a 3D finite element heat flow model synthetic freezing curves are obtained for various initial water contents. Matching these synthetic curves to the measurements yields in-situ water contents between 0 and about 3% in basal ice. These values confirm the indirectly derived free water contents.

P 13.10
Inverting debris thickness on glaciers from UAV thermal imagery

Martin Schulthess [1], Nico Mölg [1], Andreas Vieli [1]

[1] *Department of Geography, University of Zurich, Winterthurerstrasse 190, CH-8057 Zürich*
(martin.ch.schulthess@bluewin.ch)

The thickness of debris cover on glaciers is strongly affecting the rate of ablation and thereby changes the response in mass loss and flow dynamics of debris-covered glaciers in context of climate forcing. For example, only 6 cm of debris can reduce ablation by about a factor of two; thus, the debris thickness and its spatial distribution over the glacier tongue are crucial for estimating and predicting ablation, and consequently the mass balance and evolution of such glaciers.

On the example of the debris-covered tongue of Zmuttgletscher (Swiss Alps), we explore the capability of using thermal imagery from a UAV to derive high-resolution distribution maps of debris thickness on glaciers. Using aerial infra-red images from a fixed-wing UAV equipped with a thermal camera and Structure-from-Motion methods, we are able to derive a thermal orthophoto of surface temperatures for the debris-covered tongue of Zmuttgletscher. The surface-temperature image is corrected for calibration-offsets using melt-patches (0 ^{o}C) and in-situ surface measurements. Using the UAV-derived surface temperatures and DEM and additional data from an in-situ meteo-station and considering the energy fluxes within the debris under the simplification of assuming a linear average debris temperature gradient, we invert for the debris thickness. We then assess the produced debris thickness map with in-situ debris thickness measurements.

We find very high spatial variability in surface temperatures and hence debris thicknesses for thicknesses below about 12cm. Above this threshold debris-thickness variations are difficult to derive from thermal imagery, but they also do no longer substantially change the sub-debris melt rates, as they are already strongly reduced.

We further find that the time during the day of acquisition of the thermal images is affecting the debris-thickness inversion results and that a fully time-dependent consideration of energy fluxes would likely be beneficial.

P 13.11

Monitoring and modeling a recurrent calving event at Bowdoin Glacier, Greenland

Eef van Dongen [1], Andrea Walter [2], Guillaume Jouvet [1], Daniel Farinotti [1,3], Martin Funk [1]

[1] Laboratory of Hydraulics, Hydrology and Glaciology (VAW), ETH Zurich, CH-8093 Zürich (vandongen@vaw.baug.ethz.ch)
[2] Department of Geography, University of Zurich, CH-8057 Zürich
[3] Swiss Federal Institute for Forest, Snow and Landscape Research (WSL), CH-8903 Birmensdorf

The thinning and retreat of ocean-terminating, calving glaciers worldwide has contributed substantially to sea-level rise over the last decades. The size and the frequency of calving events may vary by several orders of magnitude. At Bowdoin Glacier, Northwest Greenland, most of the yearly mass loss by calving is due to a few large events (Jouvet 2017). Here, we analyse two relatively large-scale calving events in detail, which occurred nearly at the same location on Bowdoin Glacier and followed a very similar fracturing pattern. Our analysis relies on data obtained by interferometric radar and UAV photogrammetry during two summer fieldwork campaigns in July 2015 and July 2017.

As a result, our high temporal and spatial resolution data reveals the influence of tides on the opening of the crack. For both observed events, the cracks were likely water-filled and deepened by hydro-fracturing, and the tides may have caused fatigue crack growth. The ice flow model Elmer/Ice is used to analyse the observations further. In particular, we use observed surface ice flow velocities to infer the crevasse depth and water level in the crack prior to the calving events.

REFERENCES

Jouvet, G., Weidmann, Y., Seguinot, J., Funk, M., Abe, T., Sakakibara, D., Seddik, H., & Sugiyama, S. 2017: Initiation of a major calving event on the Bowdoin Glacier captured by UAV photogrammetry. The Cryosphere, 11(2):911–921

P 13.12
State and evolution of thermal conditions of a small ice cap on Disko Island, West Greenland

Andreas Vieli [1]

[1] *Department of Geography, University of Zurich, Winterthurerstrasse 190, CH-8057 Zürich (andreas.vieli@geo.uzh.ch)*

Independent marginal ice caps around the Greenland ice sheet often have relatively low-lying accumulation areas that experience summer melt and thus are expected to have relatively warm or even temperate conditions, but observations and our understanding of their thermal state are limited. Furthermore, with the recent rapid warming and related enhanced melt, the conditions at the surface boundary are currently rapidly changing.

In this study, the thermal state and evolution of Lyngmark ice cap on Disko Island is investigated by means of borehole-temperature observations and numerical modelling. A chain of thermistors is logging temperatures at the ice cap divide to a depth of 19m since March 2018. The measurements show ice temperatures of -3 $^{\circ}$C at the zero annual amplitude depth of 9m, which warm to -1.5 $^{\circ}$C at 19m depth. This data clearly indicates cold conditions in the upper third of the ice cap which is confirmed by the well visible internal layering in depth-radar profiles. But this result is also in contrast to the expected firn conditions in accumulation areas at similar elevations in West Greenland. Further, the rate of temperature increase is found to rapidly decrease with depth indicating a cooling from the surface.

In combination with numerical modelling, the observed temperature profile is explained by the disappearance of the accumulation area in the recent decade and hence the removal of the firn. The lack of a substantial firn-layer does no longer allow the retention of latent heat from refreezing of surface melt-water in the summer and further reduces the insulation of the ice body below from the cold winter temperatures at the surface. Thus, in summary, the atmospheric warming has for this ice cap the somewhat counterintuitive effect of cooling the ice cap which may also impact on it's flow dynamics.

P 13.13

Reconstructing century-long debris-covered glacier history from observation. How are changes in debris cover, surface topography, mass balance, and flow dynamics connected and interacting?

Nico Mölg [1], Tobias Bolch [1], Andrea Walter [1] & Andreas Vieli [1]

[1] Department of Geography, University of Zurich, Winterthurerstrasse 198, CH-8057 Zürich (nico.moelg@geo.uzh.ch)

Debris-covered glaciers often exhibited large, flat, down-wasting tongues at the end of the Little Ice Age (LIA). Many of these show high thinning rates today despite thick debris cover. Existing studies have not considered the dynamic interaction between debris cover and glacier evolution over longer time periods, mostly due to lack of longer-term data. The objective of this study was to investigate this interaction by reconstructing changes of debris cover, glacier geometry and dynamics, and down-wasting features of Zmuttgletscher (Valais, Switzerland), based on historic maps, satellite images, terrestrial and aerial photographs and field observations.

We show that since 1859 debris cover extent has increased from 13% to >30% of the total glacier surface and that the debris is sufficiently thick (commonly 15-20 cm) to reduce ablation compared to clean ice. At the same time, glacier mass balance has with -0.31 ±0.04 m w.e./yr from 1880-2017 been similarly negative as ice-free Swiss glaciers. Changes in length and area have been comparatively small, but velocities have strongly decreased since 2001 resulting in a stagnation of the lower areas of the glacier tongue. Years of positive mass balances in the 1970s and 1980s have led to an increase in flow velocities and a short-term decrease in debris-covered area; the effect of increased mass flux was visible at the terminus until 1995 and was followed by a strong reduction in surface elevation along the tongue, specifically in regions with ice cliffs.

We conclude that debris cover has strongly affected the geometric and dynamic – and less the volumetric – changes of Zmuttgletscher since the end of the LIA and that it is increasingly influencing its evolution.
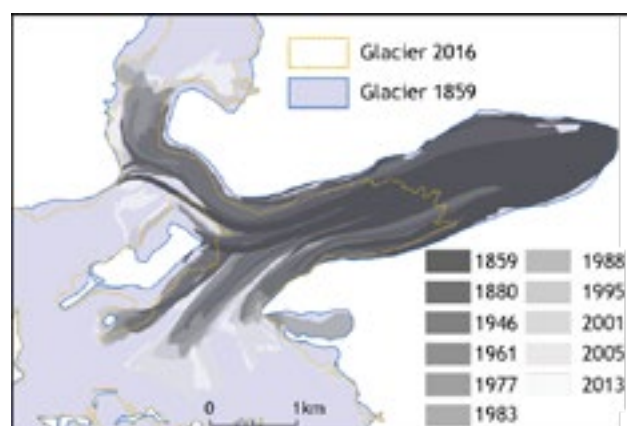

Figure 1. Extent of debris cover and its changes since the end of the LIA. Even though the glacier has retreated in the debris-covered region, debris covers more and more of the total glacier area.

P 13.14

The effect of volcanic eruptions on the long-term evolution of Alpine glaciers

Simon Förster [1], Matthias Huss [1], Martin Funk [1]

[1] Laboratory of Hydraulics, Hydrology and Glaciology (VAW), ETH Zürich, Hönggerbergring 26, CH-8093 Zürich
(foerster@vaw.baug.ethz.ch)

Large volcanic eruptions emit sulfur dioxide which can form aerosol particles in the stratosphere. These aerosol particles interact with and thus reduce incoming solar radiation, cooling the Earth's surface. Since less solar radiation reaches the glaciers' surface, this further reduces melt of ice. Volcanic eruptions may therefore have contributed to glacier advances in the Little Ice Age after several major eruptions around the year 1800. In this study, we quantify how the direct radiation effect on Alpine glaciers compares to the main drivers, air temperature and precipitation.

We developed a simple model for glacier volume change, which includes sensitivities of glacier mass balance to changes in temperature, precipitation, and solar radiation. Different reconstructions of temperature and precipitation are used (e.g. Casty et al. 2005, PAGES2K). In our framework, changes in the solar radiation are solely a function of volcanic aerosols. We use the Easy Volcanic Aerosol model (Toohey et al. 2016) and an extended version of the data set by Stenchikov et al. (1998) to estimate the effect of stratospheric aerosols on incoming radiation.

We present model results for the period 1700 to 2000 and different Alpine glaciers, e.g. Rhonegletscher and Unteraargletscher. The calculated volume changes are compared with available observations from the differencing of digital elevation models.

REFERENCES

Casty, C., Wanner, H., Luterbacher, J., Esper, J., & Böhm, R. 2005: Temperature and precipitation variability in the European Alps since 1500. International Journal of Climatology, 25, 1855-1880. doi:10.1002/joc.1216.

PAGES2k Consortium. 2017: A global multiproxy database for temperature reconstructions of the Common Era. Scientific Data, 4, 170088. doi:10.1038/sdata.2017.88.

Stenchikov, G. L., Kirchner, I., Robock, A., Graf, H.-F., Antuña, J. C., Grainger, R. G., Lambert, A., & Thomason, L. 1998: Radiative forcing from the 1991 Mount Pinatubo volcanic eruption. Journal of Geophysical Research: Atmospheres, 103, D12, 13837-13857. doi:10.1029/98JD00693.

Toohey, M., Stevens, B., Schmidt, H., & Timmreck, C. 2016: Easy Volcanic Aerosol (EVA v1.0): an idealized forcing generator for climate simulations. Geoscientific Model Development, 9, 4049-4070. doi:10.5194/gmd-9-4049-2016.

P 13.15
Development of a method for the measurement of $\delta^{15}NH_4$ in ice core samples

Prisca Lehmann [1,2], Barbara Seth [1,2], Jochen Schmitt [1,2], Hubertus Fischer [1,2]

*Climate and Environmental Physics, Physics Institute, University of Bern, Sidlerstrasse 5, CH-3012 Bern
 (lehmann@climate.unibe.ch)
[2] *Oeschger Centre for Climate Change Research, University of Bern, Falkenplatz 16, CH-3012 Bern*

Ammonium (NH_4^+) in Antarctic ice samples originates mainly from marine biogenic sources, where it is a key intermediate species in the metabolism of phytoplankton. After the release from the ocean, the formed ammonium-aerosol is transported to the ice sheet, where deposition takes place. In Greenland in addition to this process also ammonium from the nearby landmass, e.g. from biomass burning or soil and plant emissions, can be transported to the ice sheet and deposited on the snow surface.

At our division the Continuous Flow Analysis (CFA) system has a long history and the measurement of high-resolution aerosol chemistry records (e.g. NH_4^+ concentrations) is nowadays a routine application. With the coupling of "CFA" and "mass spectrometry" we want to extend our analytical capabilities and make also the nitrogen isotopic composition of ammonium measurable.

Thereby we envisage two different fields of applications:
1. Quantification of the nutrient cycling efficiency and the biological activity in the Southern Ocean.
2. Differentiation between terrestrial and marine sources of NH_4^+ found in ice cores from Greenland.

The low concentration of ammonium in ice and only small changes in the isotopic ratio make this analysis challenging. The basis of our new $\delta^{15}NH_4$ system is the well-established CFA system, which provides a continuous and contamination-free flow of meltwater containing ammonium. We are currently developing an interface that comprises four main steps: In a first step, the dissolved NH_4^+ is retained by an inorganic absorber (pre-concentration unit). First test, using the cation-exchange and molecular sieve properties of zeolites, are ongoing. The aim is the quantitative retention of ammonium from a larger ice sample in a small volume of zeolite material. After the collection is completed, the zeolite material will be dried under He-flow before ammonia will be desorbed thermally. Secondly, the released NH_3 is quantitatively oxidized to N_2 using Cu/CuO as redox agents (thermal conversion unit). In a third step, combustion side products (i.e. CO, CO_2, NO_x and H_2O) are separated using a series of cryotraps and a gas chromatography system. In the last step, the $\delta^{15}N$ of the purified N_2 is determined by isotopic ratio mass spectrometry (IRMS).

We already constructed and tested the lines for step 2-4 and the oxidative conversion works well for a NH_3-gas-standard. The construction of the pre-concentration unit and the coupling between the water phase (CFA) and gas phase (thermal conversion unit) will be our next step. In our poster we will present the current status of the analytical system.

P 13.16
Towards gas measurements in extremely thinned ice with sublimation extraction and mid-IR spectroscopy

Lars Maechler [1], Bernhard Bereiter [1,2], Phillip Scheidegger [2], Remo Walther [1], Béla Tuzson [2], Jochen Schmitt [1], Lukas Emmenegger [2], Hubertus Fischer [1]

[1] *University of Bern, Climate and Environmental Physics Division, Sidlerstrasse 5, 3012 Bern, Switzerland (maechler@climate.unibe.ch)*
[2] *Swiss Federal Laboratories for Materials Science and Technology, Empa, Überlandstrasse 129, 8600 Dübendorf, Switzerland.*

The European project Beyond EPICA – Oldest Ice Core (BE-OIC) plans to drill an ice core extending over 1.5 Ma, nearly doubling the time span of the existing greenhouse record and covering the time period of the Mid Pleistocene Transition. The oldest section from 1-1.5 Ma is expected to be close to the bedrock and, due to glacial flow, extremely thinned compacting a record of 10,000 yrs into a meter of ice. For a century-scale resolution, the sample vertical extent has to be reduced to cm-scales each containing only 1-2 ml air STP. Within the ERC Advanced Grant deepSlice project we aim to unlock such atmospheric archives by developing a novel coupled semi-continuous sublimation extraction/laser spectroscopy system.

Sublimation is the only dry method that extracts 100% of all gas species (Schmitt et al. 2011) avoiding potential issues with gas fractionation that showed to cause offsets between ice cores/different extraction methods (Bereiter et al. 2015). The development of the gas extraction method aims at vertically sublimating an ice sample with subsequent collecting the air via cryo trapping in a dip tube reducing sample loading and conditioning time and hence allowing a high sample throughput. However, there remain several challenges: the heat transport within the sample could induce subsurface melting or lateral sublimation, and inhomogeneity in the ice or of the radiation field, delivering the heat, could create a spatial inhomogeneous sublimation front.

The custom-made dual-laser spectrometer developed in this context measures simultaneously CO_2, CH_4 and N_2O concentrations and $\delta^{13}C(CO_2)$ isotope ratios in such small air samples without consuming the sample. The analytical approach is based on direct absorption using two Quantum Cascade Lasers emitting at 4.34 and 7.87 µm, respectively. The main challenge here stems from the small sample volume, which requires high precision and stability of the electronical and optical part of the system. For both systems (extraction and analysis) gas adsorption/desorption effects in the sample line add an additional complication.

REFERENCES
Bereiter, B. et al., 2015. Revision of the EPICA Dome C CO_2 record from 800 to 600 kyr before present. Geophysical Research Letters, 42(2), pp.542–549.
Schmitt, J., Schneider, R. & Fischer, H., 2011. A sublimation technique for high-precision measurements of $\delta^{13}CO_2$ and mixing ratios of CO_2 and N_2O from air trapped in ice cores. Atmospheric Measurement Techniques, 4(7), pp.1445–1461.

P 13.17

Calibration of the new wet-extraction system for CH$_4$ and N$_2$O, and plans for high-resolution measurements in the EPICA Dome C ice core (EDC)

Loïc Schmidely, Michael Bock, Christoph Nehrbass-Ahles, Jochen Schmitt, Hubertus Fischer and Thomas Stocker

Climate and Environmental Physics, Physics Institute, University of Bern
Oeschger Centre for Climate Change Research, University of Bern

Reconstructions of past CH$_4$, N$_2$O and CO$_2$ molar ratios from polar ice cores are extremely valuable to understand the coupling between greenhouse gases (GHG) and the climate system at decadal to orbital timescales. In the context of the ongoing climate change, a detailed understanding of past natural GHG variability and feedback mechanisms with global temperature is crucial to constrain the future evolution of the climate system.

To retrieve GHG molar ratios from ice core samples we employ a new extraction technique recently developed in our division coupled to a gas chromatograph. This extraction technique has already been successfully applied for isotope ratio measurements (Schmitt et al., 2014). It is characterized by a continuous vacuum extraction of the trapped gases and subsequent collection on an active coal adsorber. Apart from the high extraction efficiency, the main advantage is the low pressure in the sample vessel ensuring efficient extraction of soluble gases like N$_2$O.

Our efforts were recently devoted to precisely determine the blank of our instrument. For this purpose we built an injection system enabling the addition of standard gases over melting gas-free ice, reproducing the pressure and temperature conditions prevailing during gas extraction from an ice core sample. The offset in molar ratios between standard gases measured with a reference line and the standards injected over ice represents the blank of the device, integrating all sources modifying GHG abundances.

Our new instrument will be used to increase the temporal resolution of the EPICA Dome C (EDC) GHG record which consistently documented the natural variations of CH$_4$ and N$_2$O in the past 800'000 years (Loulergue, 2008, Schilt, 2010). Thanks to this knowledge and our capacity of measuring smaller amount of ice with augmented precision, we aim at zooming into selected abrupt climate fluctuations, for which our understanding of the dynamics of GHG and their interplay with temperature is still suffering from a lack of data. This will allow to better estimate the natural rate of change of GHG and to unveil unresolved fast GHG fluctuations (Bereiter, 2012, Nehrbass-Ahles, in prep.).

Our first measurements will focus on the last interglacial (LIG, 130 – 115 kyrs BP) with the goal of determining the timing of CO$_2$ changes with respect to CH$_4$ at the end of the penultimate deglaciation and during an abrupt antarctic warming episode at the end of the LIG. Because of the direct coupling of CH$_4$ and Northern-hemisphere temperature perturbations the combination of both GHG records will help pinpointing CO$_2$ sources during these abrupt release episodes.

REFERENCES

Loulergue L., et al. 2008: Orbital and millenial-scale features of atmospheric CH$_4$ over the past 800,000 years, Nature, 453, 383-386.

Schilt A., et al. 2010: Glacial–interglacial and millennial-scale variations in the atmospheric nitrous oxide concentration during the last 800,000 years, Quaternary Science Reviews, 29, 182-192.

Schmitt J., et al. 2014: Online technique for isotope and mixing ratios of CH$_4$, N$_2$O, Xe and mixing ratios of organic trace gases on a single ice core sample, Atmospheric Measurement Techniques, 7, 2645-2665.

Bereiter B., et al. 2012: Mode change of millenial CO$_2$ variability during the last glacial cycle associated with a bipolar marine carbon seesaw, Proceedings of the National Academy of Sciences (109), 25, 9755-9760.

P 13.18
Exploring centennial-scale CO$_2$ reconstruction in the last interglacial

Lucas Silva, Christoph Nehrbass-Ahles, Loïc Schmidely, Jochen Schmitt, Hubertus Fischer, Thomas F. Stocker

Climate and Environmental Physics, Physics Institute, University of Bern, Sidlerstrasse 5, CH-3012 Bern (silva@climate.unibe.ch)

Ice cores represent the only direct atmospheric archive to reconstruct past CO$_2$ atmospheric levels by analysing ancient air trapped in bubbles in the ice. While CO$_2$ concentrations have been documented over the last 800,000 years (800 kyr), insufficient resolution in many intervals precludes uncovering fine structure on the sub-millenial scale (Lüthi et al 2008). Restricted ice availability and difficulties with traditional CO$_2$ dry extraction techniques typically inhibit high-resolution data. In this paper we present a new (preliminary) CO$_2$ dataset for Marine Isotope Stage 5 from EPICA Dome C improving the available resolution by a factor of three. Discrete sampling with our Centrifugal Ice Microtome (CIM; Bereiter et al 2013) achieved ±1 ppm in precision and approximately 250 yr in resolution over the interval 104-135 kyr BP. The reconstruction shows a remarkably stable interglacial period between 127 and 115 kyr at 277 ppm and hints at potentially rapid CO$_2$ variations during Termination II. Future measurements will increase the resolution of the dataset to 100 yr, delivering a CO$_2$ record of significant value for our understanding of the last interglacial climate conditions and its relationship with the Holocene (Marcott et al 2014).

REFERENCES

Bereiter, B., Stocker, T. F., and Fischer, H. 2013: A centrifugal ice microtome for measurements of atmospheric CO$_2$ on air trapped in polar ice cores. Atmos. Meas. Tech., 6, 251-262

Lüthi, D. et al 2008: High-resolution carbon dioxide concentration record 650,000–800,000 years before present. Nature, 453, 379-382

Marcott, S. et al 2014: Centennial-scale changes in the global carbon cycle during the last deglaciation. Nature, 514, 616-619

P 13.19

Combining exposure dating, finite-element modelling, and feature tracking to decipher rockglacier evolution: A case study from the Bleis Marscha rockglacier (Val d'Err, Grisons)

Dominik Amschwand [1], Susan Ivy-Ochs [2], Marcel Frehner [1], Olivia Kronig [2], Marcus Christl [2]

[1] *Geological Institute, ETH Zürich, Sonneggstrasse 5, 8092 Zürich (adominik@student.ethz.ch)*
[2] *Laboratory of Ion Beam Physics, ETH Zürich, Otto-Stern-Weg 5, 8093 Zürich*

We attempt to reconstruct the formation of the *Bleis Marscha* rockglacier in the Val d'Err, Grisons (Switzerland). It is a one kilometer long, multi-unit talus rockglacier (Barsch 1996) with an active upper part that overrides a lower part. Lichen-covered boulders, vegetated, stabilized slopes, and signs of settling suggest that the parts below ~2500 m a.s.l. are relict. Internal front scarps separate the rockglacier into different units, each with its own activity phase. Morphological evidence suggests that the rockglacier started forming in the earliest Holocene.

Surface exposure dating with cosmogenic ^{10}Be and ^{36}Cl places a temporal framework (ka scale) on rockglacier movement periods (Ivy-Ochs et al. 2009). Furthermore, the present-day dynamics are numerically modelled using a two-dimensional finite-element approach to gain insights into the mechanical and material properties. Deformation above the shear zone is well captured by a linear viscous flow law (Frehner et al. 2015). The model is constrained with horizontal surface velocities obtained from feature-tracking analysis of multitemporal orthorectified aerial images (Messerli & Grinsted 2015).
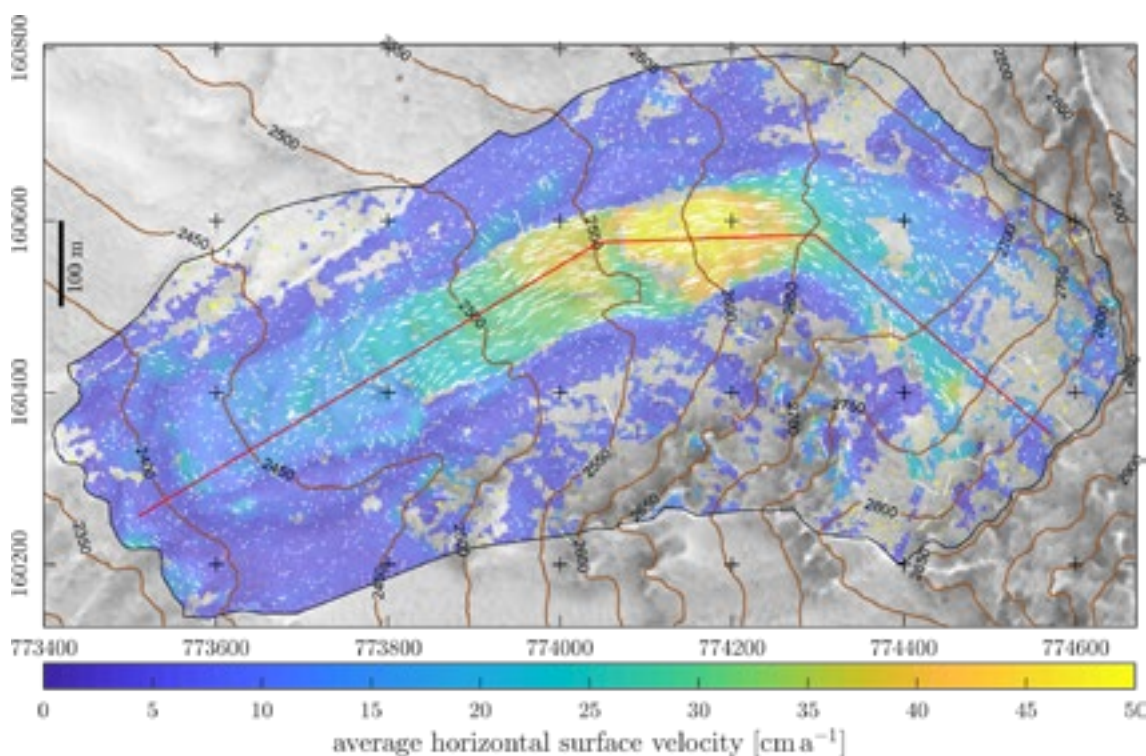
Figure 1. Noise-filtered horizontal surface velocity field 2003-2012 as obtained from feature-tracking analysis of orthorectified aerial images, draped over a sky-view map. Magnitude shown by colours, direction by white arrows. Significance level is 5 cm/a.
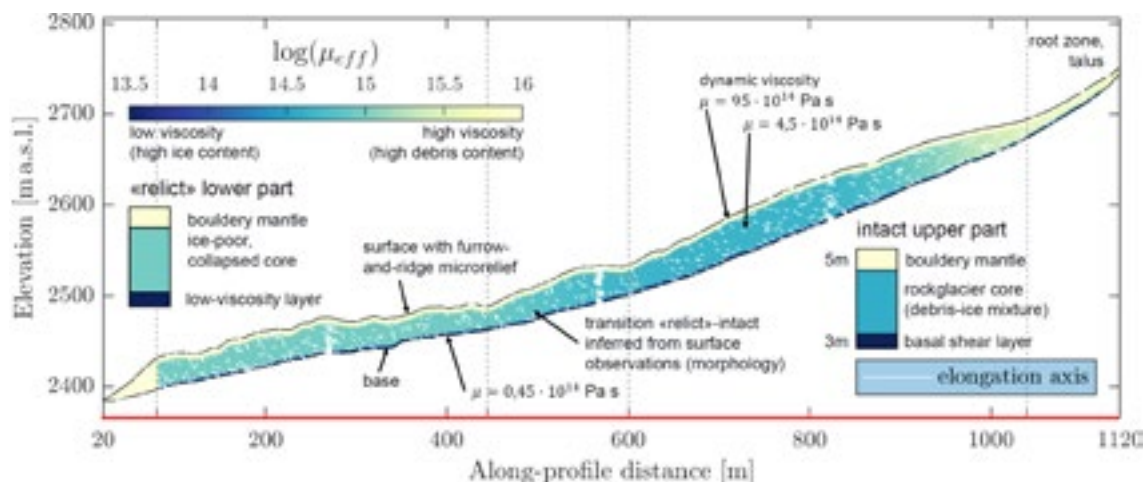
Figure 2. Inferred viscosity structure along a longitudinal section (trace in Fig. 1). Viscosity is interpreted as a proxy for ice and liquid water content.

An illumination-invariant method for correlating the orthophotos (Fitch 2002) yielded reliable displacements on the rugged rockglacier surface. The image correlation results (Fig. 1) support the subdivision of the *Bleis Marscha* rockglacer in an active upper part, characterised by moderate to high surface velocities controlled by the topography on a 100-m scale, and a relict, collapsing lower part, characterised by an irregular surface velocity field strongly coupled to the small-scale topography ("effet camembert"). However, surface velocities of up to 30 cm/a on the apparently relict part could only be numerically reproduced assuming a considerable fraction of ice and/or water that weakens the material (Fig. 2). The subsurface ice either has been preserved throughout the Holocene or has reformed more recently.

REFERENCES

Barsch, D. 1996: Rockglaciers. Indicators for the Present and Former Geoecology in High Mountain Environments. Springer, Berlin, Heidelberg.

Fitch, A. J., Kadyrov, A., Christmas, W. J. & Kittler, J. 2002: Orientation correlation. Proceedings of the 13th British Machine Vision Conference, Cardiff, England, 2-5 September, 133-142.

Frehner, M., Ling, A. H. M. & Gärtner-Roer, I. 2015: Furrow-and-ridge morphology on rockglaciers explained by gravity-driven buckle folding: A case study from the Murtèl rockglacier (Switzerland). Permafrost and Periglacial Processes 26, 57-66.

Ivy-Ochs, S., Kerschner, H., Maisch, M., Christl, M., Kubik, P. W. & Schlüchter, C. 2009: Latest Pleistocene and Holocene glacier variations in the European Alps. Quaternary Science Reviews 28, 2137-2149.

Messerli, A. & Grinsted, A. 2015. Image georectification and feature tracking toolbox: ImGRAFT. Geoscientific Instrumentation, Methods and Data Systems 4, 23-34.

P 13.20
Effects of ice cover and permafrost on groundwater flow during the last glacial cycle in the Swiss lowlands

Denis Cohen [1], Thomas Zwinger [2], Mark Person [1], Wilfried Haeberli [3], & Urs H. Fischer [4]

[1] Department of Earth and Environmental Science, New Mexico Tech, Socorro, NM, USA (denis.cohen@gmail.com)
[2] CSC – IT Center for Science Ltd, Espoo, Finland
[3] Department of Geography, University of Zurich, Zurich, Switzerland
[4] Nagra, Wettingen, Switzerland

There are compelling evidences that Pleistocene glaciations affected groundwater flow systems. Loading by ice sheets and glaciers and development of permafrost can affect the hydraulic and thermal properties of rocks and sediments beneath and along the margins of the ice, and thus can modify local groundwater flow patterns and discharge areas (e.g. Bense & Person 2008). Conditions at the bed of the ice mass, whether frozen or at the melting temperature, can also impact groundwater recharge into aquifers. Knowing and understanding modifications to groundwater flow systems during glaciation is important for the long-term safety of deep geological repositories for high-level radioactive wastes. Here, we couple a new groundwater flow and permafrost model (Hartikainen et al 2018) to a glacier evolution model implemented in Elmer/Ice (Gagliardini et al 2013). The system is applied to a two-dimensional cross-section of the Swiss Alps and lowlands that includes the main geological formations down to a depth of 15 km (Figure 1). Preliminary simulations of groundwater flow use a fixed LGM climate and glacier geometry. Groundwater flow simulations explore the effects of ice loading (Figure 2) and the connection between the autochtonous aquifer beneath the Alps and the Malm aquifer in the lowlands on the patterns and flux of groundwater in the lower Thur valley. Other simulations explore the effect of permafrost thickness on groundwater flow paths and discharge area near the repository siting region. Model results show that ice loading, aquifer connection, and values of substrate permeabilities have a significant effect on the groundwater flow patterns and fluxes in the Swiss lowlands.
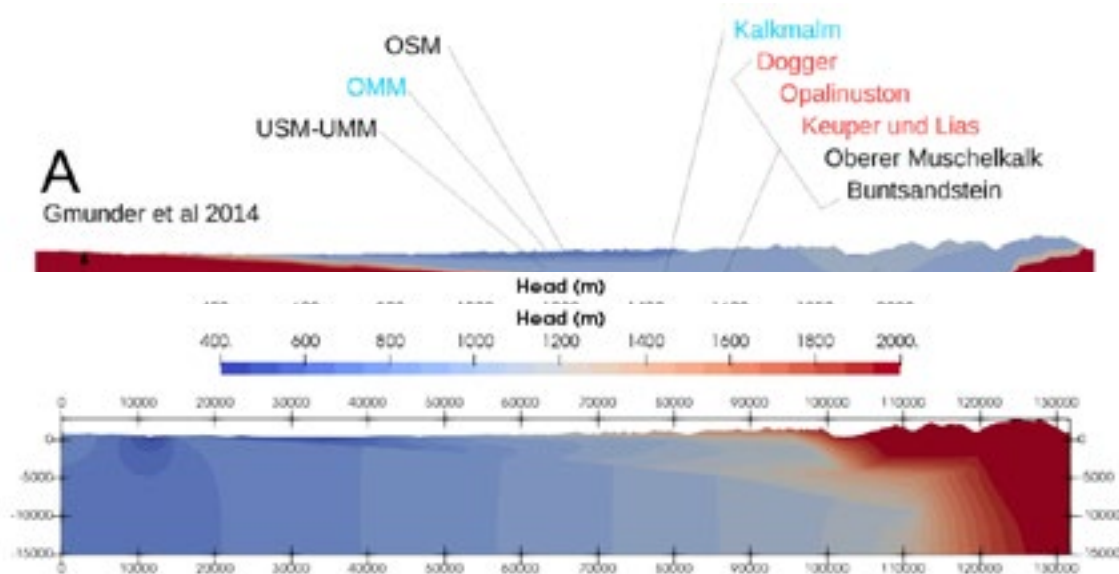

Figure 2. Calculated heads during interglacial (top) and at glacial maximum (bottom). Significant higher heads in the Alps are caused by ice loading.

REFERENCES

Bense, V. F. & Person, M. A. 2008: Transient hydrodynamics within intercratonic sedimentary basins during glacial cycles, Journal of Geophysical Research: Earth Surface113(F4).

Gagliardini, O., Zwinger, T., Gillet-Chaulet, F., Durand, G., Favier, L., de Fleurian, B., Greve, R., Malinen, M., Martín, C., Råback, P., Ruokolainen, J., Sacchettini, M., Schäfer, M., Seddik, H., & Thies, J. 2013: Capabilities and performance of Elmer/Ice, a new-generation ice sheet model, Geosci. Model Dev., 6, 1299-1318, https://doi.org/10.5194/gmd-6-1299-2013.

Gmünder, C., Malaguerra, F., Nusch, S. & Traber, D. 2014: Regional Hydrogeological Model of Northern Switzerland, Nagra Arbeitsbericht NAB 13-23.

Hartikainen J., Kolisoja, P. & Kouhia, R. 2018: Verifying the permafrost model and modelling of permafrost evolution, Interim evaluation report, Tampere University of Technology, p. 61.

P 13.21
Modeling permafrost occurrence, glacier-bed topography and possible future lakes for assessing changing hazard conditions in cold mountain regions

Wilfried Haeberli [1], Florence Magnin [2] [3] & Andreas Linsbauer [1] [4]

[1] *Geography Department, University of Zurich, Winterthurerstrasse 190, CH-8057 Zürich (wilfried.haeberli@geo.uzh.ch)*

[2] *Department of Geosciences, University of Oslo, Postbox 1047, Blindern, 0316 Oslo, Norway (florence.magnin@geo.uio.no)*

[3] *EDYTEM Lab, Université Savoie Mont Blanc, CNRS, 5 bd de la mer Caspienne, F-73376 Le Bourget du Lac, France*

[4] *Department of Geosciences, University of Fribourg, Chemin du Musée 4, CH-1700 Fribourg*

Under conditions of continued global warming in cold mountains, most glaciers tend to disappear within decades while the degradation of permafrost on exposed slopes can take centuries. Glacial landscapes are therefore rapidly but for extended future time periods transforming into periglacial landscapes with permafrost still existing but in strong thermal disequilibrium. Modeling such new landscapes is an important emerging research field. One key aspect thereby concerns changing hazard conditions related to decreasing slope stability due to permafrost degradation and glacial debuttressing, possibly causing impact/flood waves from rock/ice avalanchs into new lakes (Haeberli et al. 2017). Anticipation of critical future situations requires combined modeling of permafrost occurrence patterns (Magnin et al. 2017) and glacier-bed topographies (Linsbauer et al. 2016).

Figure 1 shows an example from an ongoing study in the Mont Blanc region, French Alps. It can be seen that possible future lakes will not only form at the immediate foot of large and steep permafrost slopes, for instance at Aiguille Verte and Les Droites, but also close to oversteepened, glacially de-buttressed lateral slopes that will be subject to seasonal frost and permafrost formation. Such new lakes exposed to potential rock/ice avalanches are multipliers of hazards and risks in the region. The probability of catastrophic events cannot be quantified but undoubtedly increases with continued ice vanishing. As a next step, rapid-simple flood/debris-flow modeling should help with defining priorities concerning damage potentials and risks and with early planning of corresponding measures to enable sustainable practical solutions.

REFERENCES

Haeberli, W., Schaub, Y. & Huggel, C. 2017: Increasing risks related to landslides from degrading permafrost into new lakes in de-glaciating mountain ranges, Geomorphology 293, 405-417.

Linsbauer, A., Frey, H., Haeberli, W., Machguth. H., Azam, M.F. & Allen, S. 2016: Modelling glacier-bed oberdeepenings and possible future lakes in the Himalaya-Karakoram region, Annals of Glaciology 57 (71), 119-130.

Magnin, F., Josnin, J.-Y., Ravanel, L., Pergaud, J., Pohl, B. & Deline, Ph. 2017: Modelling rock wall permafrost degradation in the Mont Blanc massif from LIA to the end of the 21st century, The Cryosphere 11, 1813-1834.
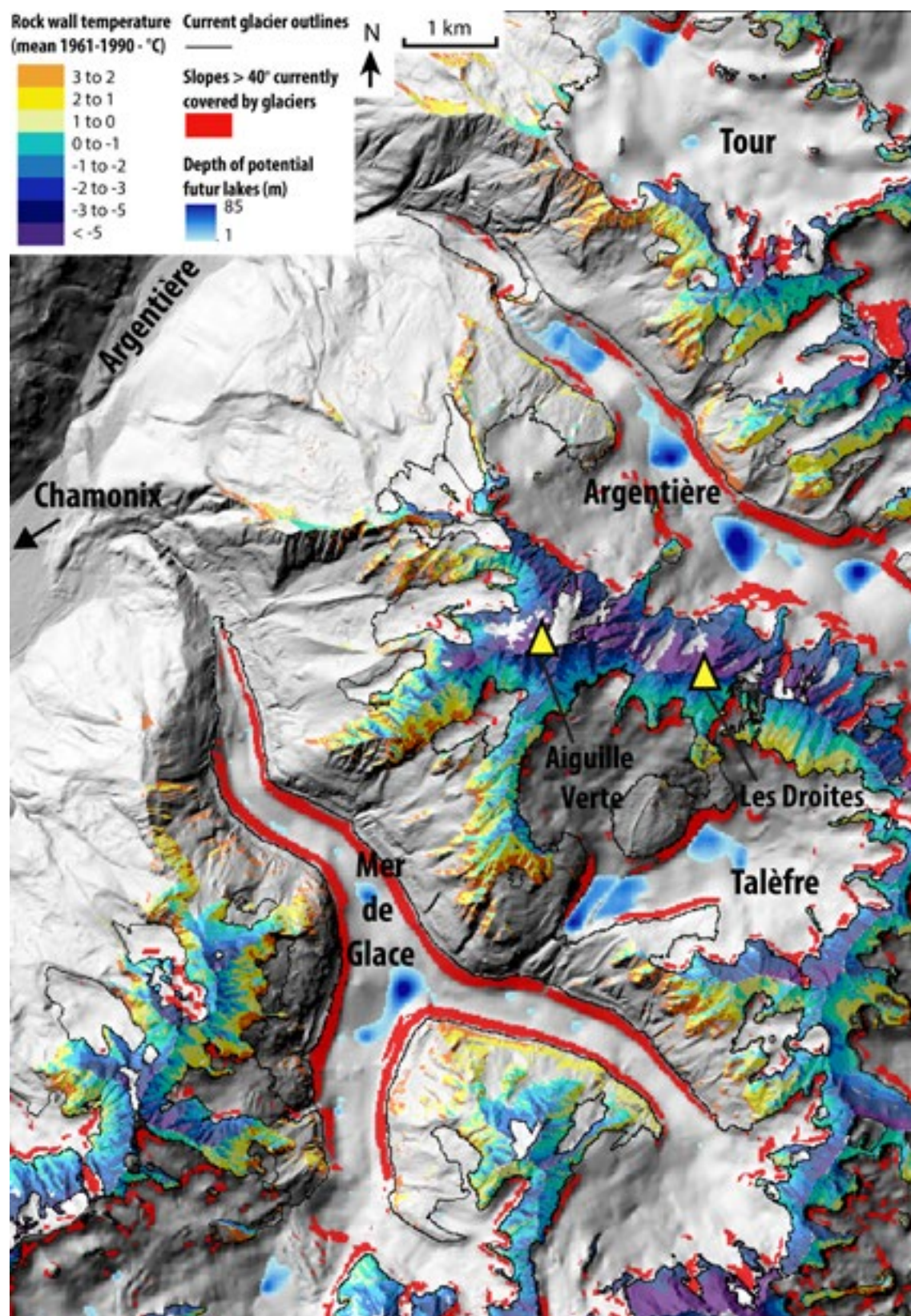
Figure 1. Mer de Glace, Glacier d'Argentière and surroundings with modeled present rock-wall temperatures, oversteepened and overdeepened parts of glacier beds. This information can be used for early anticipation of potential future risks related to a high-mountain environment in conditions beyond historical precedence and experience.

P 13.22

Towards a joint database and statistical analysis of electrical resistivity and refraction seismic tomography datasets in mountain permafrost

Coline Mollaret, Cécile Pellet, Christin Hilbich & Christian Hauck

Departement of geosciences, University of Fribourg, Chemin du Musée 4, CH-1700 Fribourg (coline.mollaret@unifr.ch)

Electrical Resistivity Tomography (ERT) and Refraction Seismic Tomography (RST) are commonly applied methods for the detection, mapping, characterisation and monitoring of permafrost occurrences around the world (Kneisel et al. 2008, Hauck 2013). The resulting datasets are either processed and interpreted individually or in a joint manner, including quantitative estimates of subsurface ice and water contents (e.g. Pellet et al. 2016) and joint inversion approaches (cf. Mollaret et al. 2018, this conference). However, ERT and RST datasets are up to now neither stored in joint databases, nor analysed in a comparative way with datasets from other permafrost occurrences worldwide.

In this contribution, we want to present a first step towards a joint database of ERT and RST datasets from coincident permafrost profiles over a wide range of countries, mountain ranges, locations, morphologies and subsurface ice contents. More than 100 profiles from the European Alps, the central European middle mountains, Scandinavia, the Andes and Antarctica were analysed regarding electrical resistivities and P-wave velocity distributions as well as common statistical parameters. As electrical and seismic data can be used as proxies for subsurface and ice and water contents in permafrost areas we believe that a joint database will make a useful contribution to the existing borehole temperature database of GTN-P (Biskaborn et al. 2015).

REFERENCES

Biskaborn, B.K., Lanckman, J.P., Lantuit, H., Elger, K., Dmitry, S., William, C. and Vladimir, R., 2015. The new database of the Global Terrestrial Network for Permafrost (GTN-P). Earth System Science Data, 7, 245-259

Hauck, C., Böttcher, M., & Maurer, H., 2011: A new model for estimating subsurface ice content based on combined electrical and seismic datasets. Cryosphere, 5, 453–468.

Hauck, C. (2013): New concepts in geophysical surveying and data interpretation for permafrost terrain. Permafrost and Periglac. Process. 24, 131–137, doi: 10.1002/ppp.1774.

Kneisel, C., Hauck, C., Fortier, R. & Moorman, B. (2008): Advances in geophysical methods for permafrost investigation. Permafrost and Periglacial Processes 19, 157-178.

Pellet C, Hilbich C, Marmy A and Hauck C (2016): Soil Moisture Data for the Validation of Permafrost Models Using Direct and Indirect Measurement Approaches at Three Alpine Sites. Front. Earth Sci. 3:91. doi: 10.3389/feart.2015.00091.

P 13.23

Establishing a permafrost monitoring network in the Bernese Alps: geophysical characterisation of potential monitoring sites and validation of permafrost distribution models

Christin Hilbich [1], Christian Hauck [1], Nils Hählen [2]

[1] *Department of Geosciences, University of Fribourg, Chemin du Musée 4, CH-1700 Fribourg (christin.hilbich@unifr.ch)*
[2] *Department of Natural Hazards, Canton of Bern, Schloss 2, CH-3800 Interlaken*

Permafrost monitoring has a long tradition in Switzerland and is operational since 2000 within the PERMOS network (www.permos.ch). Distribution of monitoring sites is however not homogeneous with an increased concentration of sites towards the Valais Alps in the West and the Grisons in the East, while the Bernese and Central Alps are underrepresented. The canton of Berne therefore recently initiated the establishment of a long-term permafrost monitoring network within the Bernese Alps, with the main goal to detect and map permafrost occurrences, monitor their long-term evolution and evaluate the probability of natural hazards related to degrading permafrost.

As a first step, potential monitoring sites are selected based on the modelled permafrost distribution (Alpine permafrost index map by Boeckli et al. 2012, and Map of potential permafrost distribution by BAFU 2005), and promising sites are investigated by means of geophysical measurements (Electrical Resistivity Tomography/Refraction Seismic Tomography), ground surface temperature measurements as well as geomorphological interpretation. From the joint analysis of all data, propositions for new boreholes are made.

In this contribution we will present a data set of more than 30 geophysical profiles from more than 14 new locations (without previous information). As many of the sites of interest are located close to the lower boundary of potential permafrost distribution (~2500 m asl), this extensive geophysical data set can further be used for the validation of existing permafrost distribution models for this region. We here present a comparative analysis of geophysical-based characterisation of the permafrost distribution and the modelled permafrost probability for the respective locations. The results confirm that geophysical surveying presents a cost-effective approach to detect permafrost over larger areas and evaluate permafrost distribution models with an independent data set.

REFERENCES

Boeckli, L. & S. Gruber 2011. Permafrostverbreitung in der Schweiz - Kurzbericht über den räumlichen Vergleich der „BAFU-Karte" und der vorläufigen „APMOD-Karte".

Boeckli, L., Brenning, A, Gruber, S. & Noetzli, J. 2012. Alpine permafrost index map. DOI:10.1594/PANGAEA.784450, Supplement to: Boeckli, L., Brenning, A., Gruber, S. & J. Noetzli 2012. Permafrost distribution in the European Alps: calculation and evaluation of an index map and summary statistics. The Cryosphere 6: 807-820, DOI:10.5194/tc-6-807-2012

Bundesamt für Umwelt (BAFU) 2005. Hinweiskarte der potentiellen Permafrostverbreitung in der Schweiz.

P 13.24
Interactive snow profile edition with niViz

Mathias Bavay [1], Thomas Egger [2], Charles Fierz [1]

[1] *WSL Institut für Schnee und Lawinenforschung SLF, Flüelastrasse 11, CH-7260 Davos Dorf (bavay@slf.ch)*
[2] *Egger Consulting, Postgasse 2, A-1010 Vienna, Austria*

The niViz software has been designed to visualize snow profiles and timeseries of profiles either online or offline, within a web browser. This applies to both measured and simulated data, based around the CAAML snow profile standard. A new module has been developed to create or edit snow profiles interactively. This module allows editing all properties present into the CAAML standard: metadata (including weather conditions, surface conditions or observer/station/profile ID); stratigraphy with all possible grain shapes subclasses, wetness or hardness and optional comments for each layer; multiple profiles of temperature, density, liquid water content, SSA, ram resistance or snow micropenetrometer profiles (that can be imported as CSV); stability information (as various stability tests, from classical compression test to propagation saw tests). Thanks to the standardized nature of CAAML, the generated profiles can then be exchanged between the many worldwide institutions supporting the standard.

This Javascript library and application is available under an Open Source license (GNU affero General Public License) thanks to the funding provided by an international consortium of more than ten institutions.
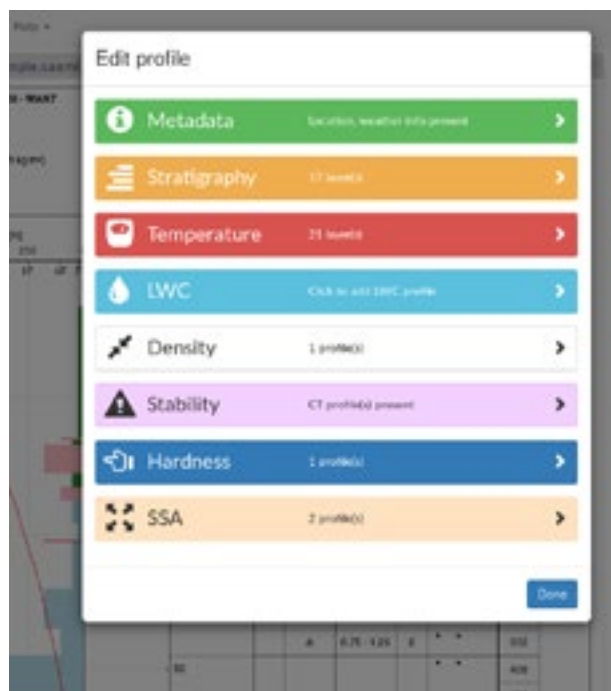
Figure 1. Modal dialogue to edit an existing profile (in the background).

REFERENCES
Fierz et al.: The International Classification for Seasonal Snow on the Ground, IHP-VII Technical Documents in Hydrology N°83, IACS Contribution N°1, UNESCO-IHP, Paris, 2009,

P 13.25
Prediction of snow failure: mission impossible?

Achille Capelli [1], Ingrid Reiweger [2], Jürg Schweizer [1]

[1] *WSL Institute for Snow and Avalanche Research SLF, Flüelastrasse 11, 7260 Davos Dorf, Switzerland,*
   (achille.capelli@slf.ch)
[2] *Institute of Mountain Risk Engineering, Department of Civil Engineering and Natural Hazards,*
   BOKU University of Natural Resources and Life Sciences, Peter-Jordan-Strasse 82, 1190 Wien, Austria

Slab avalanches are caused by a crack forming and propagating in a weak layer within the snow cover, which eventually causes the detachment of the overlying cohesive slab. It would be, therefore, useful to be able to predict the nucleation of the initial failure. Failure in heterogeneous materials, such as snow, is normally preceded by a progressive damage process. Therefore, monitoring this progressive damage should allow predicting the failure point. A possibility to monitor this damage process is to analyze the acoustic emissions (AE) generated by the damage (micro-cracking). We performed snow failure experiments in a cold laboratory and evaluated possible precursory features in the generated AE preceding failure. In addition, to the known differences in the deformational behavior as a function of the loading rate, also the AE characteristics clearly depended on the loading rate. Whereas, for experiments at high loading rates we identified some features that may be used to predict failure, for low loading rates these AE features were not or just partially present. In other words, at low loading rates failure seemed to occur abruptly, i.e. without obvious changes in the damage process. We then used a fiber bundle model to investigate the reasons of the observed differences in the AE signature. The ability of forming new bonds due to rapid sintering and viscous deformation causing load redistribution in the ice matrix, two particular properties of ice, were implemented in the FBM. Our FBM simulations revealed that both time dependent processes were necessary to reproduce the observed loading rate dependent differences in the mechanical deformation and AE signature of snow, and that at slow loading rates the failure can occur abruptly without precursors. Hence simulations as well as experimental results suggest that due to the rapid sintering and viscous deformation of the ice matrix the failure of snow cannot be predicted for low loading rates, at least not with the methods we employed. Hence applying AE techniques for snow avalanche prediction in the field seems not feasible. Still, the found AE characteristics may be useful to assess the mechanisms beyond the failure nucleation process that lead to the release of natural slab avalanches.

P 13.26
How meteorological input uncertainty affect modeled snow instability

Bettina Richter [1], Alec van Herwijnen [1], Mathias W. Rotach [2], Jürg Schweizer [1]

[1] *WSL Institute for Snow and Avalanche Research SLF, Flüelastrasse 11, CH-7260 Davos (bettina.richter@slf.ch)*
[2] *Department of Atmospheric and Cryospheric Sciences, ACINN, Innrain 52f, A-6020 Innsbruck*

Snow avalanches can endanger roads, villages and human lives. When assessing the avalanche danger in the context of avalanche forecasting, data on current snowpack and meteorological conditions are evaluated in combination with weather forecasts. Snowpack observations include data on snow stratigraphy and snow instability. The temporal and spatial resolution of snowpack data is, however, very limited. Detailed snow cover models, which simulate the full snowpack stratigraphy, can help fill this gap, in particular if they also provide snow instability information. Snow cover models are forced with meteorological data from either automatic weather stations or numerical weather models, and snow instability criteria can be derived from simulated stratigraphy. To perform spatial snow cover simulations for numerical avalanche forecasting, interpolation and downscaling of meteorological data is required, which can introduce uncertainties. The repercussions of these uncertainties on modeled snow instability remain mostly unknown.

We therefore investigated how meteorological input uncertainty influenced modeled snow instability using a global sensitivity analysis. We used the model SNOWPACK to simulate snow instability, i.e. the skier stability index and the critical crack length, for a field site equipped with an automatic weather station providing the necessary input for the model. We performed simulations for the winter season 2016-2017, when one weak layer persisted for the entire season and affected the avalanche activity within the region of Davos, Switzerland. Uncertainty ranges for precipitation, air temperature, relative humidity, wind, and short- and long-wave radiation covered typical differences observed within a distance of 2 km and an elevation change of 200 m. We selected the weak basal layer that formed between 16 November 2016 and 2 January 2017. Only simulated snow layers that were deposited between these two dates and consisted of either depth hoar, surface hoar, facets and rounded facets were considered as weak layer. We independently investigated the influence of meteorological input uncertainty in two scenarios covering distinct periods of a) weak layer formation and b) slab formation. For each scenario, 14,000 simulations were performed.

Results showed that during the weak layer formation period, the evolution of weak layer properties and subsequent snow instability were sensitive to all input parameters. In particular, increasing air temperature and increasing precipitation led to higher stability indices. Once a certain weak layer had formed, precipitation was the most prominent driver for snow instability during the slab formation period. While with increasing precipitation the skier stability index decreased, the critical crack length increased. While data from different winters are required to confirm these findings, such results will help with selecting model resolution and interpreting spatial snow simulations for numerical avalanche forecasting.

14. Hydrology, Limnology and Hydrogeology

Massimiliano Zappa, Michael Doering, Tobias Jonas, Michael Sinreich, Bettina Schaefli

Swiss Society for Hydrology and Limnology SGHL,
Swiss Hydrological Commission CHy,
Swiss Hydrogeological Society SGH

TALKS:

14.1   Andres N., Badoux A.: Normalization and trends of damage due to floods and landslides in Switzerland

14.2   Baracchini T., Bouffard D., Wüest A.: meteolakes.ch – An online platform for monitoring and forecasting the 3D bio-physical state of Swiss lakes

14.3   Benettin P., Queloz P., Bensimon M., McDonnell J.J., Rinaldo A.: A multitracer experiment on a vegetated lysimeter to measure water transit times in the subsurface

14.4   Bergami G., Molnar P., Burlando P.: Interactions between Surface Water and Groundwater in a regulated alpine gravel-bed River (Maggia)

14.5   Beria H., Larsen J., Schaefli B.: Development of a two-component linear mixing model to quantify the influence of rainfall and snowmelt in groundwater recharge

14.6   Brunner M.I., Zappa M., Stähli M.: Water shortages under current and future extreme streamflow conditions in Switzerland (Keynote)

14.7   Fiskal A., Deng L., Han X., Michel A., Eickenbusch P., Lagostina L., Rong Zhu, Bernasconi S.M., Dubois N. , Schroth M.H., Sander M., Lever M.A.: Effects of eutrophication on sedimentary organic carbon cycling in five Swiss lakes (Keynote)

14.8   Floriancic M., Berghuijs W.R., Molnar P.: Low flow seasonality across Switzerland – Climatic drivers and the influence of landscape

14.9   Kauzlaric M., Rössler O., Mosimann M., Zischg A.P.: A roadmap towards a short-term flood impact forecasting system

14.10   Moeck C., Grech-Cumbo N., Gurdak J., Schirmer M.: Global simulated distribution of periodic diffuse groundwater recharge response to climate variability

14.11   Sepúlveda Steiner O., Forrest A., McInerney J., Baracchini T., Lavanchy S., Bouffard D., Wüest A.: Basin-scale gyres: Rotationally-driven mixing in Lake Geneva

14.12   Thornton J.M., Mariethoz G., Brunner P.: Integrated hydrological modelling of a steep, geologically complex, snow-dominated Alpine catchment (Keynote)

POSTERS:

P 14.1 Battista G., Molnar P., Burlando P.: A spatially distributed numerical model for simulating sediment connectivity at the catchment scale

P 14.2 Brauchli T., Beria H., Michelon A., Larsen J., Schaefli B.: Estimating the precipitation in a high-alpine catchment combining local meteo stations and Swiss-wide meteo products

P 14.3 Bulgheroni M., Lepori F., Pozzoni M., Capelli C., Pera S., Scapozza C., Colombo L.: Reconstructing long-term trends in surface water summer temperature in a high-altitude lake: A modelling approach

P 14.4 Chun J., Sprenger M.: Investigation of Moisture Front Convection over Europe using Cloud-Resolving COSMO model: a Case Study

P 14.5 Doda T., Ulloa H., Ramón Casañas C., Wüest A., Bouffard D.: Buoyancy-driven cross-shore flows in lakes induced by night-time cooling: field observations

P 14.6 Falatkova K., Sobr M., Slavik M., Bruthans J., Jansky B.: Characteristics of meltwater passage through the proglacial area at Adygine complex, Northern Tien Shan

P 14.7 Horton P., Brönnimann S.: Sensitivity of statistical precipitation downscaling to the choice of an atmospheric reanalysis

P 14.8 Joss L., Prasuhn V.: Renewal of the high-resolution map of direct and indirect connectivity of erosion risk areas to surface waters in Switzerland

P 14.9 Kiewiet L., van Meerveld H.J., Seibert J.: Identification of pre-event water sources to streamflow and uncertainty associated with end-member characterization

P 14.10 Leonarduzzi E.: Resolution matters: numerical analysis of the effect of subgrid heterogeneities with a physically based hydrological model

P 14.11 Michel A., Brauchli T., Bavay M., Lehning M., Schaefli B., Huwald H.: Modelling Stream Temperature of Rivers in Switzerland

P 14.12 Pool S., Brunner M., Kiewiet L., Acheson E.: The other's perception of a streamflow sample: From a bottle of water to a data point

P 14.13 Sanchini A., Grosjean M.: New Approach to Quantify Organic Matter Freshness and Paleoproductivity In Lake Sediments Through Spectral Deconvolution of the UV-VIS Absorption Spectra

P 14.14 Wicki A., Stähli M.: Soil wetness data for landslide early warning

P 14.15 Zander P., Grosjean M., Tylmann W., Filipiak J.: Combining Hyperspectral Imaging and µXRF data to link varve-formation processes with meteorological data, Lake Zabinskie, Poland

14.1
Normalization and trends of damage due to floods and landslides in Switzerland

Norina Andres [1], Alexandre Badoux [1]

[1] Swiss Federal Research Institute WSL, Zürcherstrasse 111, CH-8903 Birmensdorf, Switzerland, norina.andres@wsl.ch

Natural hazards can cause considerable damage to infrastructure and settlements. Since 1972 damage due to floods, debris flows and landslides are collected in the Swiss flood and landslide damage database at the Swiss Federal Research Institute WSL (Hilker et al. 2009). We analysed this data and addressed questions about trends in the damage data and a potential connection to climate change. For the first time, the data set of the Swiss flood and landslide damage database was normalized with three different approaches and trend tests were applied for the yearly damage data of the period 1972-2016. In the normalization approaches, socio-economic developments like the development of the inflation, population and wealth were accounted for as suggested by Pielke & Landsea (1998). When applying normalization procedures, the question has to be asked how much a former event would cost nowadays under current societal conditions. Hence, we normalized the past loss data since 1972 for each year to 2016 values.

The normalization of the nominal damage data results in much higher values in the earlier years of the study period, especially for the high damage years (e.g. 1977, 1978, and 1987; see Figure 1). The total sum of damage as well as the mean is around twice as high after normalization. Around 71-75% of the total (nominal and normalized) damage occurs from June until August and spatial analysis shows highest damage in central Switzerland and along river reaches in the main Alpine valleys. The results reveal no statistically significant increase for the yearly nominal and normalized damage data (with all three normalization approaches). Potential effects of climate change on flood, debris flow and landslide damage data could therefore not be detected.
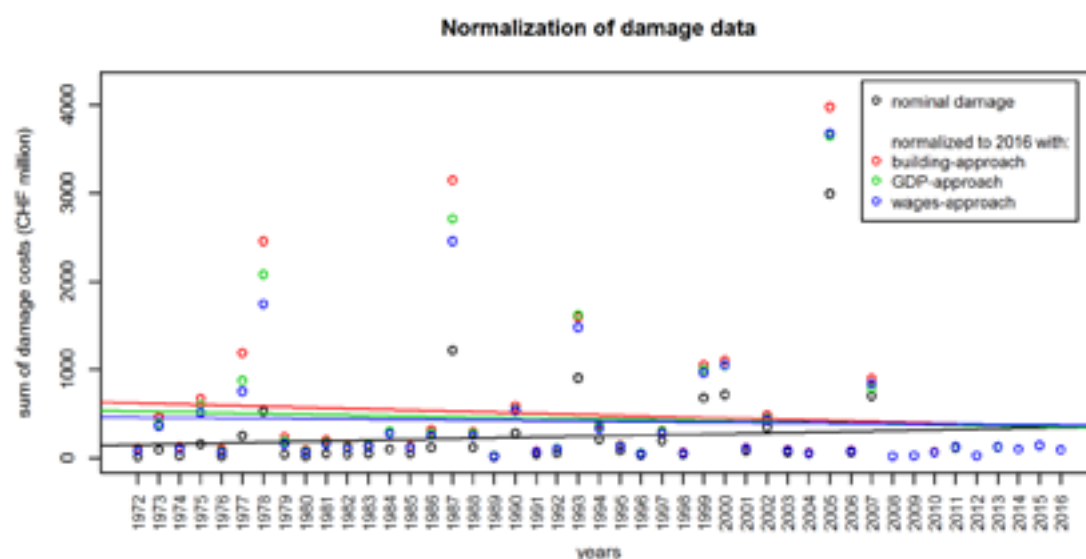

Figure 1. Normalization of yearly damage data (in CHF million) to 2016 with three different approaches: Building-approach, GDP-approach and wages-approach. The coloured lines represent the regression lines of nominal and normalized damage data. Note that none of the data sets show a statistically significant trend with the linear regression model (Figure 1 is part of a paper submitted to the Journal of Flood Risk Management in May 2018).

REFERENCES

Hilker, N., Badoux, A., Hegg, C. 2009: The Swiss flood and landslide damage database 1972-2007, Natural Hazards and Earth System Science, 9, 913-925.
Pielke Jr., R. A. & Landsea, C. W. 1998: Normalized hurricane damages in the United States: 1925-95, Weather and Forecasting, 13 (3), 621-631.

14.2

meteolakes.ch – An online platform for monitoring and forecasting the 3D bio-physical state of Swiss lakes

Theo Baracchini [1], Damien Bouffard [2], Alfred Wüest [1,2]

[1] *Physics of Aquatic Systems Laboratory Margaretha Kamprad Chair, ENAC, École Polytechnique Fédérale de Lausanne (EPFL), CH-1015 Lausanne (theo.baracchini@epfl.ch)*
[2] *Limnological Research Center, Swiss Federal Institute of Aquatic Science and Technology (Eawag), Seestrasse 79, CH-6047 Kastanienbaum*

The exceptional variability of lakes has been studied numerous times, yet no unique framework capable of reproducing the wide range of lake dynamics observed in various regions of the World (or within Switzerland itself) has been formulated. Increasingly facing external pressures, inland waters adaptation and change have to be understood and monitored efficiently to provide timely, scientifically credible, and policy-relevant environmental information.

Such monitoring capabilities and their importance for understanding the spatial and temporal heterogeneity in the distribution of all lake trophic levels is now largely recognized. Over the last decades, various research communities addressed this problem using different information sources, such as in-situ measurements, remote sensing observations and numerical simulations. The goal of this study is to couple those sources through adapted parameterization and data assimilation algorithms. This coupling approach implies mutual feedback mechanisms among those three information sources; model simulations are improved through the assimilation of in-situ measurements and remotely sensed products, remote sensing image processing is improved through parametrization with in-situ measurements and forecasts of hydrodynamic and biological models. Finally, in-situ measurements achieve a better representativeness when carried out along instantaneous gradients known from remotely sensed products and model simulations during the planning and sampling stages.

An online platform, *meteolakes.ch*, is developed with such aim for monitoring and forecasting the bio-physical state of Swiss lakes. Meteolakes is a web/Android-application that disseminates results of 3D coupled hydrodynamic-biological model forecasts out to 4.5 days for several Swiss lakes using real-time atmospheric, rivers and WWTPs data. With direct impacts at scientific and community level, this integrated data-model system also aims at assisting stakeholders in evidence-based decision-making and towards the sustainable management of our lakes.
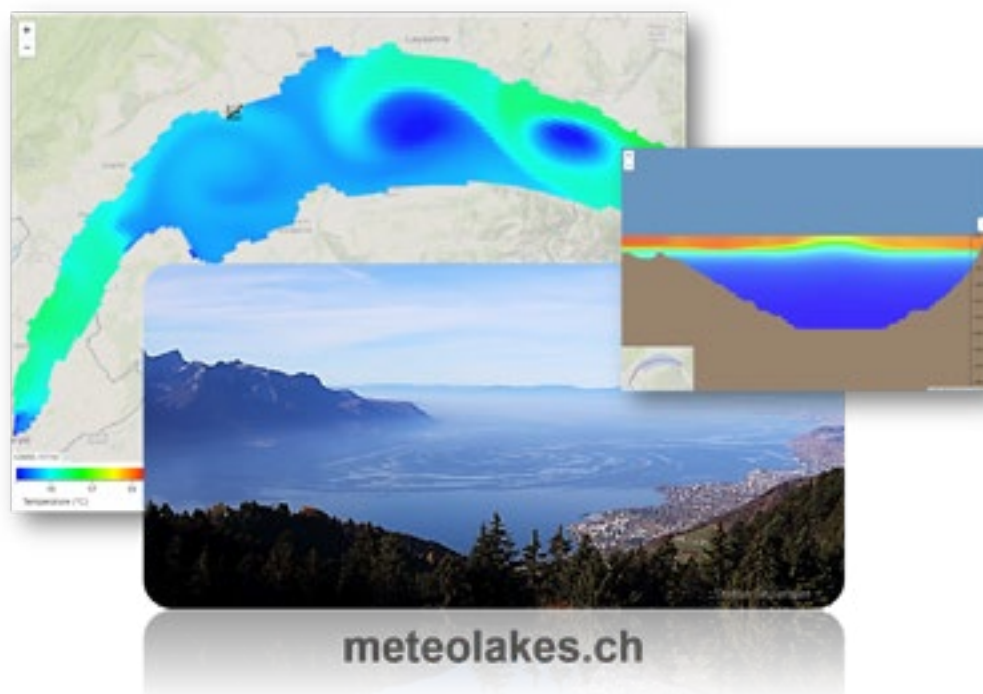

Figure 1. Surface temperature of Lake Geneva as displayed on meteolakes.ch (upper picture), transect of Lake Geneva temperature structure showing a thermocline uplift (mid picture), gyre observed over Lake Geneva (lower picture).

14.3
A multitracer experiment on a vegetated lysimeter to measure water transit times in the subsurface

Paolo Benettin [1], Pierre Queloz [2], Michaël Bensimon [3], Jeffrey J. McDonnell [4,5,6] Andrea Rinaldo [1,7]

[1] Laboratory of Ecohydrology ENAC/IIE/ECHO, École Polytechinque Fédérale de Lausanne (EPFL), Lausanne, Switzerland (paolo.benettin@epfl.ch)
[2] Institute of Territorial Engineering INSIT, School of Management and Engineering Vaud (HEIG-VD), Yverdon-les-Bains, Switzerland
[3] Central Environmental Laboratory ENAC/IIE/CEL, École Polytechinque Fédérale de Lausanne (EPFL), Lausanne, Switzerland.
[4] Global Institute for Water Security, School of Environment and Sustainability, University of Saskatchewan, Saskatoon, Canada.
[5] School of Resources and Environmental Engineering, Ludong University, Yantai, China
[6] School of Geography, Earth & Environmental Sciences, University of Birmingham, Birmingham, UK
[7] Dipartimento ICEA, Università degli studi di Padova, Padua, Italy.

Flow velocities, residence times and tracer breakthroughs in the subsurface are known to be affected by matrix properties and preferential flow. Despite their relevance to trasport processes, however, the relative timing of preferential flow, and its link to transit times through the soil block, is still poorly described. Here, we present and analyze tracer data from a large vegetated lysimeter experiment conducted within the EPFL campus. A solution of two fluorobenzoid acid (FBA) tracers added to 18 mm of isotopically labeled rain was injected as a pulse and then followed with a series of tracer-free controlled rainfall events for 5 months. Timeseries of soil water samples at three different depths and bottom drainage samples were collected and analyzed. Unlike past lysimeter experiments, a willow tree grown within the lysimeter exerted strong evapotranspiration fluxes. After the injection, all the tracers took around 35-40 days to be first recorded in soil water at 150 cm depth, while they only needed 15-20 days to be found in the bottom drainage at 250 cm depth (Figure 1). This implies that a solute could percolate and reach an aquifer twice as fast as observed through soil water samples, with implications for e.g. the propagation of pollutants spills. Tracer recovery indicates that roughly 30-40% of the labeled rainfall returned to the atmosphere via evapotranspiration, while the remaining 60-70% was released through the bottom outlet over roughly 5 months. Besides assessing the interplay between slow vertical percolation and fast recharge through macropores, our results highlight the effect of vegetation uptake on water and solute transport.
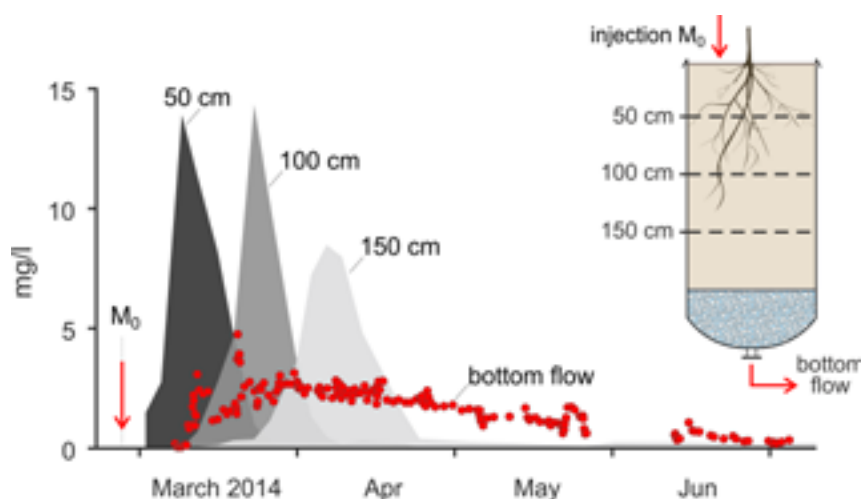

Figure 1. Concentration breakthrough curve for the FBA tracers obtained for the lysimeter base drainage (red dots) and for soil water samples (grey polygons) extracted at 50, 100 and 150 cm depths. The inset cartoon illustrates the general experimental setting.

14.4
Interactions between Surface Water and Groundwater in a regulated alpine gravel-bed River (Maggia)

Gianluca Bergami [1], Peter Molnar [1] & Paolo Burlando [1]

[1] Institute of Environmental Engineering, ETH Zürich, Stefano-Franscini-Platz 5, CH-8093 Zürich
(bergami@ifu.baug.ethz.ch)

While the importance of renewable energy sources is constantly rising and hydropower represents an increasingly fundamental means of energy production in Switzerland, the potential negative impact of hydropower production on downstream rivers remains an important issue. In many alpine basins, hydropower systems store water in headwater reservoirs and divert it to produce electricity, sometimes bypassing long reaches of downstream rivers. This potentially affects the hydrology, sedimentology and ecology of the impacted river reaches. The prediction of short- and long-term impacts of such changes on the river morphology, riparian vegetation, groundwater levels, and aquatic habitat requires the development of numerical tools which combine hydrodynamic simulations with riparian vegetation growth and aquatic habitat modules. Furthermore, these tools also have to be validated with ground measurements where possible.

Our goal in this research is to develop an integrated river simulator with which the response of river and groundwater systems to different environmental flow strategies, i.e. mandatory releases downstream of hydropower systems (e.g. constant releases, seasonal releases, artificial floods, etc.), as well as the evolution of riparian vegetation and aquatic habitat in such scenarios can be predicted. We achieved the first target through the design and combination of appropriate numerical tools for flow analysis, including a coupled model of river-aquifer interactions suitable for complex gravel-bed braided river floodplains (Ruf et al., 2008; Shaad, 2015). We illustrate here the river-aquifer coupling in the Maggia River, which is highly regulated by a hydropower system and intensively monitored by our group, as streamflow and groundwater levels, river bed morphology, riparian vegetation, etc. are kept under observation through sensors installed in the field.

The coupled model consists of a two-dimensional shallow water flow simulator (2dMb) iteratively coupled to a groundwater model (MODFLOW) on a high resolution regular grid (~10 m). The saturated hydraulic conductivity of the alluvial fill and the conductance of the river bed are key parameters to satisfactorily reproduce observed groundwater fluctuations in response to floods in boreholes close to the river (Fig. 1). The fluctuations occur with a very short response time, which requires high resolution monitoring and an accurate numerical coupling scheme. Surface roughness parameters in 2dMb were calibrated with water depth measurements. The surface flow model simulates flow depth, velocity and bed shear stress, which are crucial variables for sediment transport and erosion potential. Finally, the coupled river-aquifer model allows us to estimate the rates and areas of infiltration and/or exfiltration along the river system, and thereby to quantify river-aquifer connectivity, which is of great importance for aquatic ecosystems.

The next step is to integrate the river-aquifer flow simulator with long-term riparian vegetation modelling in the floodplain. To this end, the flow variables and groundwater levels will be used as drivers of vegetation growth, i.e. water stress by flood inundation and drought at low groundwater levels. Groundwater has been shown to have the potential to drive long-term changes in riparian vegetation succession (Bätz et al., 2016).

The modelling approach will allow us to examine and predict the effects of different environmental flow policies on riparian vegetation, and produce a model-based quantitative assessment of the response of surface water, groundwater and riparian vegetation to various flow releases. The ultimate goal is to develop a modelling framework with which we will be able to optimise flow releases in the least disruptive way with regards to the riparian system in the Maggia Valley, and possibly applicable in other alpine streams.

REFERENCES
Bätz, N., Colombini, P., Cherubini, P. & Lane, S. N. 2016: Groundwater controls on biogeomorphic succession and river channel morphodynamics, J. Geophys. Res. Earth Surf., 121, 1763–1785, doi:10.1002/2016JF004009.
Ruf, W., Foglia, L., Perona, P., Molnar, P., Fäh, R. & Burlando, P. 2008: Modelling the interaction between groundwater and river flow in an active alpine floodplain ecosystem, Peckiana, 5, 5–16.
Shaad, K. 2015: Development of a distributed surface-subsurface interaction model for river corridor hydrodynamics, doctoral thesis submitted to attain the degree of Doctor of Sciences of ETH Zürich.
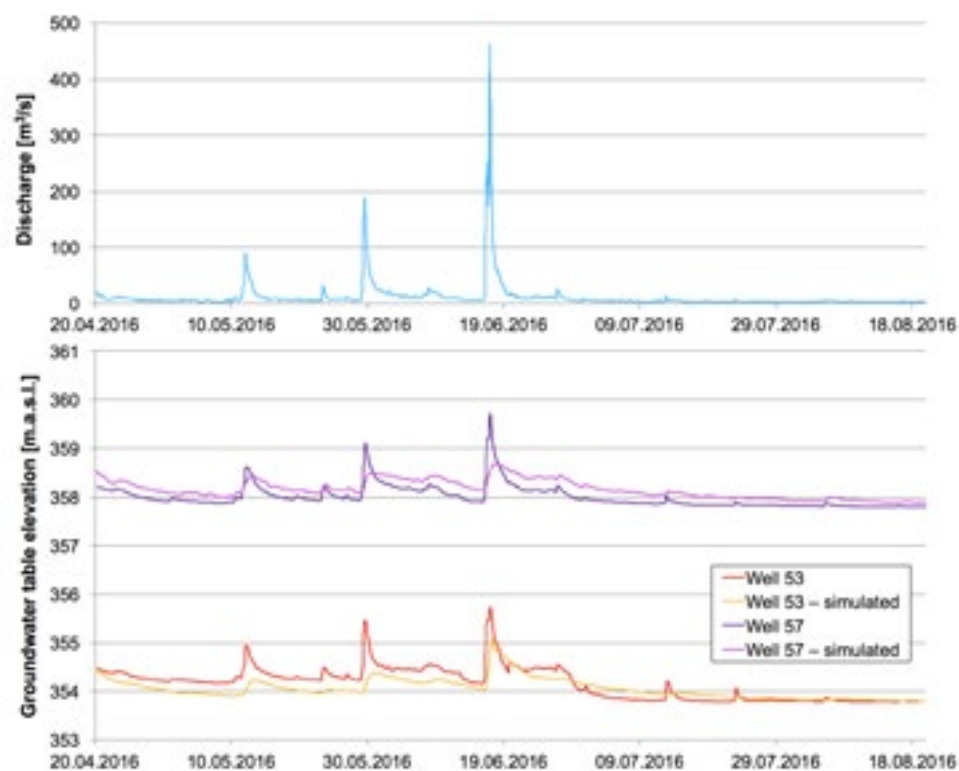
Figure 1. Discharge and corresponding groundwater level heads measured in the field and simulated by the coupled model for a 4-month period in 2016.

14.5
Development of a two-component linear mixing model to quantify the influence of rainfall and snowmelt in groundwater recharge

Harsh Beria [1], Josh Larsen[1,2], Bettina Schaefli [1]

[1] Institute of Earth Surface Dynamics (IDYST), University of Lausanne (UNIL), Switzerland (harsh.beria@unil.ch)
[2] School of Geography, Earth and Environmental Sciences, University of Birmingham

Stable isotopes of water have been used for over half a century to quantify the amount of groundwater recharge that comes from rainfall vs snowmelt. Classically, this has been done by solving a linear equation with one unknown variable, which in this case is snow fraction. In order to improve the reliability of the estimates of snow fraction, Bayesian mixing models have been proposed over the last decade. Such models assume a probability distribution function (pdf) for rainfall, snowmelt and groundwater and then by formal Bayesian inversion, obtain the coefficient of the snow fraction. A major caveat in this approach is the assumed pdf, which becomes hard to justify as the number of data points for the isotopic ratios are generally very low. We propose a frequentist alternative that does not assume any pdf function on the rainfall, snowmelt or groundwater, and also gives reliable uncertainty estimates for snow fraction. In this approach, each combination of rainfall and snowmelt isotopic ratios is mixed with each combination of groundwater isotopic ratio. We assume the error in the estimates to be normally distributed with zero mean and constant variance. By assuming a uniform prior distribution for snow fraction, we infer its value by applying a maximum likelihood procedure. As this is not formal Bayesian inference, the pseudo-posterior of snow fraction gives an estimate of its mean along with an uncertainty bound around it. Using a series of synthetic tests, we compare our estimates with those of the conventional Bayesian mixing model estimates. A key advantage of our method is that it uses the whole dataset instead of relying on the first few moments. Also in our method, it becomes much easier to account for other processes that may affect the amount of snow in groundwater. We demonstrate this by accounting for the spatial heterogeneity in a catchment induced by elevation gradient and homogenization induced by snow metamorphism.

14.6
Water shortages under current and future extreme streamflow conditions in Switzerland

Manuela I. Brunner [1], Massimiliano Zappa [1], and Manfred Stähli [1]

[1] Mountain Hydrology and Mass Movements, Swiss Federal Research Institute for Forest, Snow and Landscape Research (WSL), Zürcherstrasse 111, CH-8903 Birmensdorf (manuela.brunner@wsl.ch)

In Switzerland, water is currently abundant on a national scale but regional and local water shortages might occur in dry years when water demand exceeds natural water availability. The development of such shortages might be exacerbated by climate induced changes which lead to a shift in runoff regimes with relatively less runoff in summer when water demand is highest. These regime shifts are caused by both increasing temperatures which lead to glacier retreat, a reduction in snow cover, and earlier snowmelt and shifts in the seasonality of precipitation from summer to winter precipitation.

Water shortages have negative economic impacts related to a potential reduction in crop yields, hydropower, or artificial snow production and negative ecological impacts on e.g. fish populations or tree communities. To reduce such negative effects, water management plans have to be developed or adapted such that water demand can be reduced and/or water availability be increased e.g. by reservoir operation targeted at increasing water supply.

The development of such management plans requires reliable estimates on potential water shortages under extreme streamflow conditions. Such estimates are not yet available for Switzerland neither for current nor future conditions. Here, we therefore investigate which regions in Switzerland might be most affected by water shortages under current climate conditions and assess how water shortage situations caused by extremely low streamflow conditions might change under future climate conditions. To do so, we quantified both natural water availability and water demand for 22 large hydrological regions in Switzerland. Natural water availablity was simulated using the hydrological model PREVAH (Viviroli et al., 2009), on the one hand, driven with observed meteorological data and, on the other hand, with climate model simulations. Water demand was estimated for various water use categories including drinking water (domestic and tourism), industry (second and third sector), agriculture (irrigation and livestock), ecology, and hydropower production. Potential water shortages were then computed for mean and extreme streamflow conditions under current and future climate conditions as the difference between water availability and water demand.

Extreme streamflow conditions were defined in the form of annual design hydrographs for specified reoccurrence intervals of 10 and 100 years. To estimate such annual design hydrographs, we used three different techniques among which two account for the multivariate nature of the esimtation problem. The first approach involves a univariate frequency analysis of discharges of individual months (Coles, 2001). The second approach performs frequency analysis on the flow duration curve (Claps and Fiorentino, 1997) and uses a typical runoff regime for the reassignment of seasonality. The third approach performs frequency analysis on the annual hydrographs directly by using a functional data representation (Cuevas et al., 2007). The subsequent comparison of extreme annual hydrographs with regional water demand allowed for the identification of seasons and regions that are/will be affected by water shortages.

Our results show that water shortages can regionally and seasonall already occur under current extreme streamflow conditions (see Figure 1 for two example regions). Regions with rainfall dominated runoff regimes, such as northeastern Switzerland, are mostly affected by water shortages in summer while regions with snowmelt dominated regimes, such as the Valais, are mostly affected by winter water shortages. The results also show that these potential shortages are likely to get more severe under future extreme streamflow conditions. This knowledge about possible future regional and seasonal water shortages will help water managers to adapt water management and reservoir operation plans in order to ensure a save water supply.
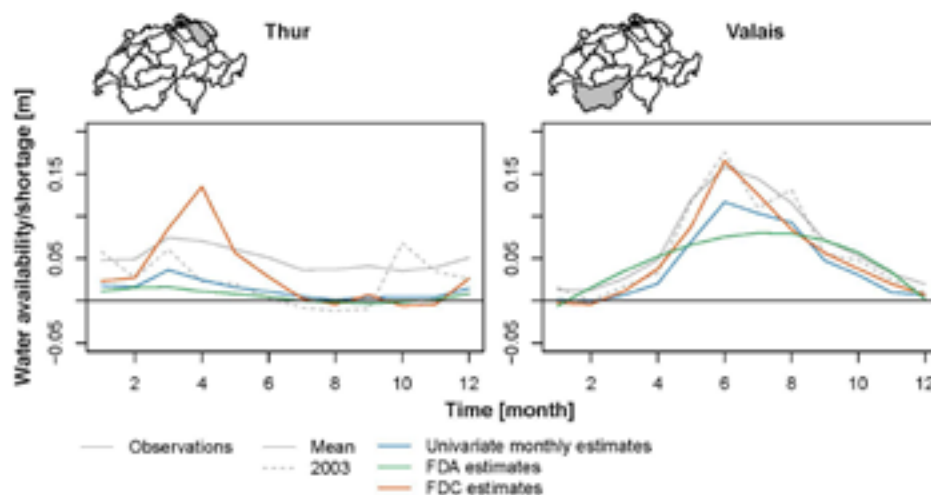
Figure 1. Water availability and shortages for two example regions (Thur and Valais) for the mean annual hydrograph, the hydrograph of the dry year 2003, and three extreme annual hydrographs derived using different estimation techniques under current climate conditions for a return period of 10 years. The extreme hydrographs include univariate monthly estimates, estimates derived by functional data analysis (FDA) and by flow duration curves (FDC).

REFERENCES

Claps, P. and Fiorentino, M.: Probabilistic Flow Duration Curve for Use in Environmental Planning and Management, Integr. Approach to Environ. Data Manag. Syst., (31), 255–266, doi:10.1007/978-94-011-5616-5, 1997.

Coles, S.: An introduction to statistical modeling of extreme values, Springer, London., 2001.

Cuevas, A., Febrero, M. and Fraiman, R.: Robust estimation and classification for functional data via projection-based depth notions, Comput. Stat., 22, 481–496, doi:10.1007/s00180-007-0053-0, 2007.

Viviroli, D., Zappa, M., Gurtz, J. and Weingartner, R.: An introduction to the hydrological modelling system PREVAH and its pre- and post-processing-tools, Environ. Model. Softw., 24, 1209–1222, doi:10.1016/j.envsoft.2009.04.001, 2009.

14.7

Effects of eutrophication on sedimentary organic carbon cycling in five Swiss lakes

Annika Fiskal [1], Longhui Deng [1], Xingguo Han [1], Anja Michel [1], Philip Eickenbusch [1], Lorenzo Lagostina [1], Rong Zhu [1], Stefano M. Bernasconi [3], Nathalie Dubois [3,2], Martin H. Schroth [1], Michael Sander [1], Mark A. Lever [1]

[1] Department of Environmental Systems Science, ETH Zurich, Universitätstrasse 16, 8092 Zurich, Switzerland
[2] Surface Waters Research – Management, Eawag, Swiss Federal Institute of Aquatic Science and Technology, Überlandstrasse 133, 8600 Dübendorf, Switzerland
[3] Department of Earth Sciences, ETH Zurich, Sonneggstrasse 5, 8092 Zurich, Switzerland

Eutrophication due to anthropogenic activities can have severe impacts on aquatic ecosystems. The increased nutrient load can lead to high primary production and thereby oxygen depletion due to increased organic matter (OM) degradation. Yet, the effects of eutrophication on total organic carbon (TOC) accumulation and degradation, are not well known. We study these effects using sedimentary records of five Swiss lakes covering the last 180 years. We investigate changes in content, stable isotopic composition of TOC, TOC accumulation rates and microbial OM remineralization in response to increased phosphorus (P) loadings due to eutrophication. Our results show elevated P concentration in the lake water column coincide with increased TOC and Chla content and TOC accumulation rates. In addition, the attempts to decrease eutrophication by reducing P loadings lead to decreased TOC accumulation rates. The sediments of eutrophic lakes show higher microbial respiration rates with a higher contribution of methanogenesis. Furthermore a clear redox zonation of dominant microbial respiration reactions is absent in all lakes. Our results suggest that in the studied lakes, anthropogenic P inputs have the potential to regulate TOC accumulation and methane production rates.
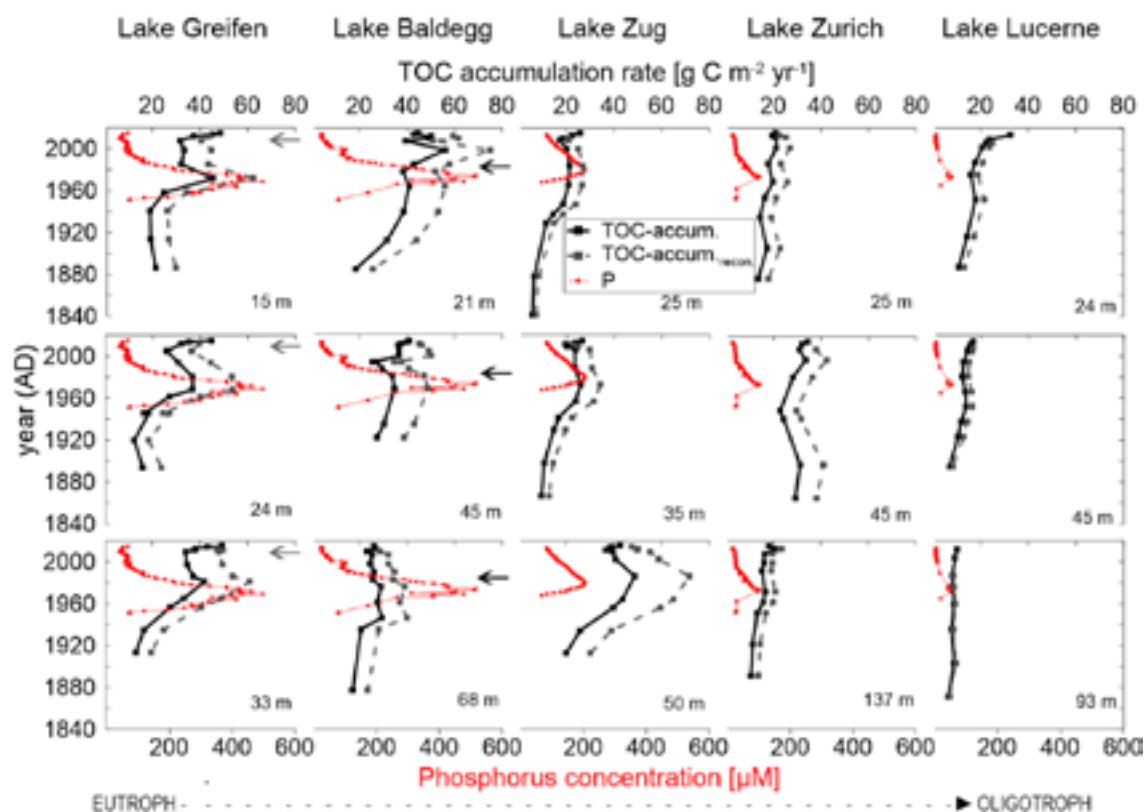

Figure 1. Carbon accumulation rates in black solid lines and reconstructed carbon accumulation rates [g C m^{-2} yr^{-1}] in dashed grey lines as well as water column phosphorus concentrations in red solid lines [µM] vs. age for each station of the five lakes, water depths of sampled stations are indicated at the bottom of each subplot. Grey and black arrows indicate onset of artificial mixing and aeration respectively.

REFERENCES

Anderson, N. J., Bennion, H., and Lotter, A. F.: Lake eutrophication and its implications for organic carbon sequestration in Europe, Global Change Biol, 20, 2741-2751, 2014.

Anderson, N. J., Dietz, R. D., and Engstrom, D. R.: Land-use change, not climate, controls organic carbon burial in lakes, P Roy Soc B-Biol Sci, 280, 2013.

Bastviken, D., Cole, J., Pace, M., and Tranvik, L.: Methane emissions from lakes: Dependence of lake characteristics, two regional assessments, and a global estimate, Global Biogeochem Cy, 18, 2004.

Canfield, D. E., Kristensen, E., and Thamdrup, B.: Aquatic Geomicrobiology, Aquatic Geomicrobiology, 48, 1-640, 2005.

Cole, J. J., Prairie, Y. T., Caraco, N. F., McDowell, W. H., Tranvik, L. J., Striegl, R. G., Duarte, C. M., Kortelainen, P., Downing, J. A., Middelburg, J. J., and Melack, J.: Plumbing the global carbon cycle: Integrating inland waters into the terrestrial carbon budget, Ecosystems, 10, 171-184, 2007.

Middelburg, J. J.: A Simple Rate Model for Organic-Matter Decomposition in Marine-Sediments, Geochim Cosmochim Ac, 53, 1577-1581, 1989.

14.8
Low flow seasonality across Switzerland –
Climatic drivers and the influence of landscape

Marius Floriancic [1], Wouter R. Berghuijs [2] & Peter Molnar [1]

[1] *Institute of Environmental Engineering, ETH Zurich, CH-8093 Zürich (floriancic@ifu.baug.ethz.ch)*
[2] *Department of Environmental Systems Science, ETH Zurich, CH-8092 Zürich*

Low flows impact society and the environment. Thus they are an important consideration when water is used for drinking, irrigation and agriculture, artificial snow, and hydropower purposes (Blanc & Schädler, 2013). In Switzerland, lowflow characteristics vary regionally (Wehren et al., 2010) and these variations are mostly caused by regional differences in climate and landscape properties (e.g. topography, morphology, geology, soils). In this work we provide a country-wide overview of the primary driving mechanisms of low flows that could support water management strategies during extended dry periods.

We collected discharge data of 380 gauges from BAFU and Cantons across Switzerland. We use seasonality statistics to identify and quantify lowflow (NM7Q) seasonality and its driving mechanisms in the studied catchments over the period 2000-2016. To infer what drives low flows, we compare the timing and magnitude of NM7Q to the timing and magnitude of several climatic characteristics derived from gridded precipitation and air temperature data (MeteoSwiss). To understand the role of the landscape, we relate the seasonality and magnitude of low flows to several physical catchment characteristics such as elevation, slopes, landuse, and geology.

Results show distinct regional patterns in the seasonality of low flows and their elevation dependency (Figure 1). Also the climatic drivers of low flows are regionally consistent and elevation-dependent. In low elevation regions of the Swiss Plateau low flows occur almost exclusively in late summer and early autumn, and are the result of high evapotranspiration and low precipitation. In the high-elevated Alpine catchments, low flows are mostly driven by below zero temperatures that result in no liquid water being released to the catchments.

The timescale over which a system changes from median flow (Q50) to low flow (NM7Q) is below two months in lower elevation areas, but this timescale increases with elevation. We found that occurrence and magnitude of low flows are primarily controlled by several weeks of specific weather conditions (e.g. low precipitation, high evapotranspiration) rather than showing log-term memory effects to climatic conditions of prior months and years.

We identified specific landscape features influencing the magnitude of low flows. There are distinct differences comparing low-flow contributions from different geologies, e.g. from Molasse layers along the Swiss Plateau or various quaternary sediment deposits in higher elevations. Also, elevation is an important control on low flows in Switzerland, mostly through its effect on climatic variables and associated hydrological processes of runoff generation. Therefore, elevation is a powerful indicator for when and why low flows are expected to occur across the mountainous landscape of Switzerland.

REFERENCES

Blanc P, Schädler B. 2013. Das Wasser in der Schweiz – ein Überblick. Schweizerische Hydrologische Kommission. Available at: ISBN: 978-3-9524235-0-9

Wehren B, Weingartner R, Schädler B, Viviroli D. 2010. General characteristics of Alpine waters. In Alpine Waters, Bundi U (ed.).Springer: Berlin; 17–58. DOI: info:doi/10.1007/978-3-540-88275-6_2
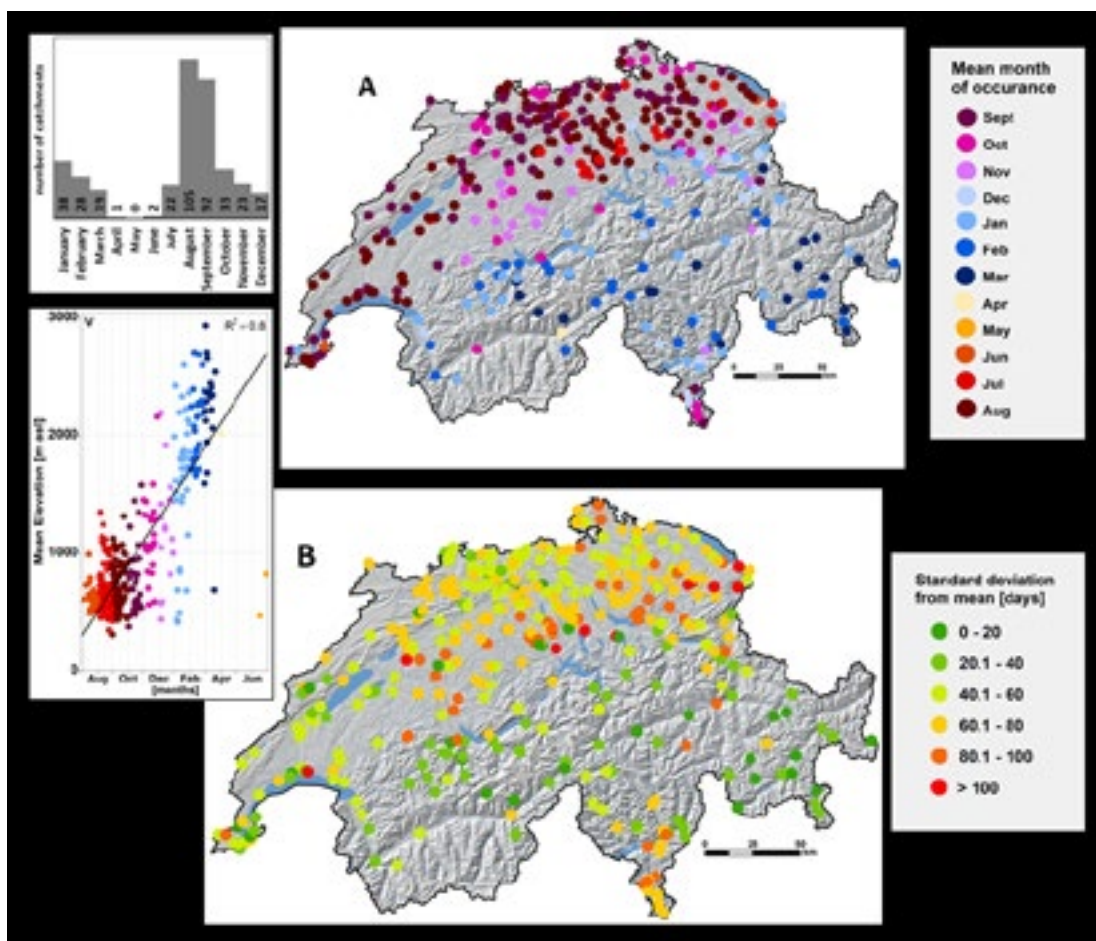
Figure 1: Low-flow seasonality across 380 gauges in Switzerland. The maps show (A) the mean date of occurrence of the lowest annual 7 consecutive day Q (NM7Q) and (B) the standard deviation from the mean date of occurrence in days for the years 2000–2016. The mean date of occurrence of NM7Q is related to elevation (inset figure)

14.9
A roadmap towards a short-term flood impact forecasting system

Martina Kauzlaric [1,2,3], Ole Rössler [2,3], Markus Mosimann [1,2,3] & Andreas Paul Zischg [1,2,3]

[1] Mobiliar Lab for Natural Risks, University of Bern, Hallerstrasse 12, CH-3012 Bern
[2] Oeschger Centre for Climate Change Research, University of Bern, Falkenplatz 16, CH-3012 Bern
[3] Hydrology Group, Institute of Geography, University of Bern, Hallerstrasse 12, CH-3012 Bern
  (martina.kauzlaric@giub.unibe.ch)

Recently, relevant progress has been made in river discharge forecasting. These forecasts support local crisis intervention forces in undertaking emergency measures, such as the temporary evacuation of people from hazard zones, the removal of movable goods (e.g. cars) from the potentially flooded areas, or the dislocation of movable household items from lower floors to upper floors in endangered houses. However, a reliable and precise forecast of an extreme precipitation's impact is fundamental for these interventions to be a valuable additional flood risk management option.

The prediction of the direct consequences of a forecasted rainfall event in the short-term (lead times of 6-24 h), and in particular the prediction of site-specific flood losses are poorly investigated topics. A translation of the discharge forecast to the potential impacts in terms of damage potential is therefore needed. Several models are used to research extreme events including numerical weather forecast models, hydrological models, hydrodynamic models, and damage and loss models. Although these model types are well established, and coupling two to three of these models has been successful, only recently an assessment of a full and comprehensive model chain from the atmospheric to local scale flood loss models has been conducted (Felder et al. 2018). The development of these model chains provides the basis for a spatially explicit prediction of local impacts of intense precipitation events.

Here we present a roadmap towards predicting flood impacts for short lead times. The concept bases on the experience gained from previous projects in elaborating full model chains from rainfall to flood losses at the single building scale. We will extend our investigations including a multi-model approach for the rainfall-runoff simulation, a routing system, and a fast-to-run surrogate model for predicting the flood losses (Zischg et al. 2018).
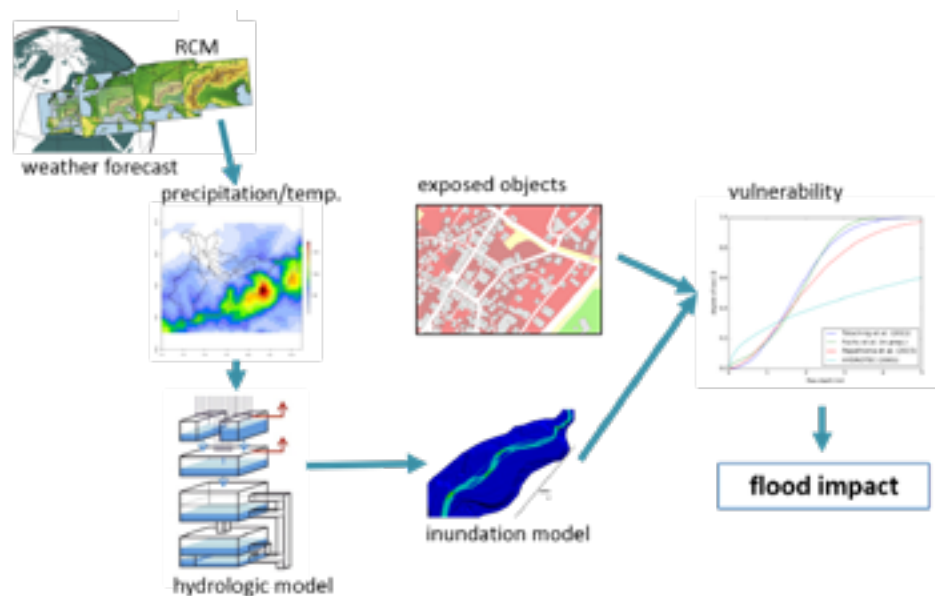

Figure 1. Schema of the flood impact forecasting system.

REFERENCES

Felder, G., Gómez-Navarro, J.J., Zischg, A.P., Raible, C.C., Röthlisberger, V., Bozhinova, D., Martius, O., Weingartner, R., 2018. From global circulation to local flood loss: Coupling models across the scales. Science of The Total Environment 635, 1225–1239. 10.1016/j.scitotenv.2018.04.170.

Zischg, A.P., Felder, G., Mosimann, M., Röthlisberger, V., Weingartner, R., 2018. Extending coupled hydrological-hydraulic model chains with a surrogate model for the estimation of flood losses. Environmental Modelling & Software 108, 174–185. 10.1016/j.envsoft.2018.08.009.

14.10

Global simulated distribution of periodic diffuse groundwater recharge response to climate variability

Christian Moeck [1], Nicolas Grech-Cumbo [1], Jason J. Gurdak [2] & Mario Schirmer [1,3]

[1] EAWAG, Swiss Federal Insitute of Aquatic Science and Technology, Ueberlandstrasse 133, CH-8600 Dübendorf
   (Christian.moeck@eawag.ch)
[2] Francisco State University, 1600 Holloway Avenue San Francisco 52, US-94132 San Francisco
[3] Centre d'hydrogéologie et de géothermie (CHYN), Université de Neuchâtel, Rue Emile-Argand 11, CH-2000 Neuchâtel

Groundwater depletion is a problem worldwide that requires groundwater management decisions using knowledge about spatiotemporal patterns in recharge. Global-scale climate variability can result in transient recharge rates, but under some circumstances dampen within the vadose zone, resulting in a constant rate. In this study, we show when and where steady-state and transient recharge is expected worldwide, and provide guidelines regarding damping depth of recharge fluxes on a global scale. We use the output of an analytical solution of the Richards equation to demonstrate how variability in fluxes at land surface dampen with depth in the vadose zone for monthly, seasonal and annual periods of flux variations. We also considered interannual and decadal periods of flux variations, which are generally consistent with global-scale climate variability of the Pacific-North American Oscillation (PNA), North Atlantic Oscillation (NAO), El Niño/Southern Oscillation (ENSO), and Pacific Decadal Oscillation (PDO). In addition, we use our newly compiled global dataset of site-specific recharge rates to validate the results.

We demonstrate that for vadose zone soils with large sand content and large recharge rates, it is likely to obtain transient recharge fluxes, especially from interannual to decadal climate variability. For the (semi-) arid regions with relatively small recharge fluxes, climate signals are preserved in the transient recharge flux when the depth to the water table is less than 10 m, which is rarely met for these regions. Only when focused or preferential recharge significantly increase the local recharge rates then transient recharge conditions might occur. The depth to the shallow water table is less than 70 m for the majority of the globe and therefore, transient recharge associated with teleconnection patterns such as the PNA, NAO, ENSO, and PDO are detectable at the water table depths in most aquifers worldwide.

Our global-scale assessment generally explains why some periodic infiltration fluxes associated with climate variability are absent in groundwater level fluctuations while others result in transient recharge rates and dynamic groundwater levels. These findings have important implications for climate change impact studies on recharge rates and mechanisms and global groundwater sustainability.

14.11
Basin-scale gyres: Rotationally-driven mixing in Lake Geneva

Oscar Sepúlveda Steiner [1], Alexander Forrest [2], Jasmin McInerney [2], Theo Baracchini [1], Sébastien Lavanchy [1], Damien Bouffard [3] & Alfred Wüest [1/3]

[1] Physics of Aquatic Systems Laboratory, Margaretha Kamprad Chair, EPFL-ENAC-IEE-APHYS, Lausanne, Switzerland
   (oscar.sepulvedasteiner@epfl.ch)
[2] Civil & Environmental Engineering, University of California – Davis, Davis, CA, USA
[3] Department of Surface Waters – Research and Management, Eawag, Kastanienbaum, Switzerland.

In large lakes, similar to oceans, the interaction between wind forcing and Earth's rotation can induce the formation of mesoscale rotational features known as gyres. These phenomena enhance horizontal transport throughout the water column and can persist for days to weeks. In this study, we explore the dynamics of gyres in Lake Geneva, using a buoyancy driven autonomous underwater vehicle (known as a glider; Slocum). The scientific payload includes sensors to sample water quality parameters (e.g. temperature, dissolved oxygen, etc.) but the focus of this work was a newly equipped sensor to measure mixing in the water column laterally over the entire lake. These observations offer high-resolution spatial measurement of temperature gradients, water quality parameters, and turbulence estimates, which are important for the understanding of lake-internal processes. The lateral temperature structure will be compared to hydrodynamic numerical model results from meteolakes.ch. Additionally, direct field measurements of currents were made in the eastern region of Lake Geneva's central basin (Figure 1) to further understand the dynamics of the gyres. From the two, quasi-stationary, basin-scale gyres that develop in Lake Geneva, we can use the solution of the geostrophic balance equation to estimate horizontal flow velocities using the observed doming structure measured with the glider. These gyres will also result in both vertical upwelling and downwelling of nutrients (depending on their cyclonic or anticyclonic nature) within the lake that have persistent influence on the ecosystem dynamics.
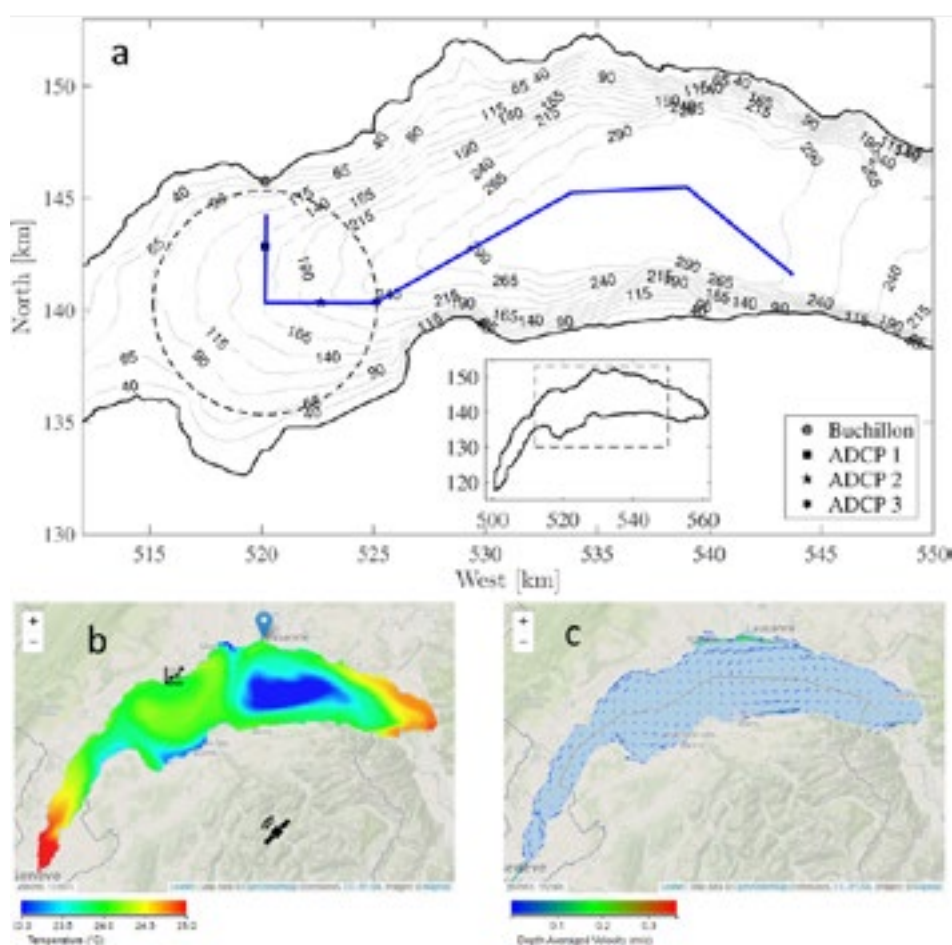

Figure 1. Inset of Lake Geneva with the geometry of one of the main gyres west of Morges (a), shown together with sur-face temperature of meteolakes.ch which strongly indicates a second gyre in the main basin (blue, b) and the depth-averaged currents (c).

14.12
Integrated hydrological modelling of a steep, geologically complex, snow-dominated Alpine catchment

James M. Thornton [1], Gregoire Mariethoz [2], and Philip Brunner [1]

[1] Centre for Hydrogeology and Geothermics, University of Neuchatel, Rue Emile-Argand 11, 2000 Neuchâtel, Switzerland
(james.thornton@unine.ch)
[2] Institute of Earth Surface Dynamics, University of Lausanne, UNIL-Mouline, Geopolis, 1015 Lausanne, Switzerland

The complex bedrock arrangements present in the European Alps can exert a strong influence on the broader hydrological cycle, especially in calcareous regions. At the same time, ongoing climate change is threatening the established function of the Alps as "water towers". Moreover, the responses of the various system components (snow, vegetation, groundwater, permafrost etc.), as well as their associated interactions and feedbacks, are likely to be complex. Despite this situation, conceptual, reservoir-based hydrological models, which employ highly simplified representations of groundwater and physical processes more generally, continue to form the basis of most predictions of climate change impacts upon Alpine water resources.

In this context, we are currently developing a physically-based, spatially-distributed, fully-integrated (i.e. snow, surface water, unsaturated zone, and saturated zone flows) hydrological model for the Vallon de Nant and Vallon de La Vare catchments (western Swiss Alps). A key benefit of such models to studies of mountain hydrology is their ability to account for the modulating influence of geology on subsurface water movement whilst simultaneously representing surface flows that can have high relevance for flood risk and sediment transport. More specifically, our model firstly enables the quantification of the water balance over recent years explicitly in time and space. Secondly, it represents a tool with which the sensitivity of predictions of interest (e.g. stream discharges, groundwater levels) to alternative representations of forcing data or model structure (e.g. daily vs. hourly and spatially-distributed vs. uniform meteorology, fine vs. course mesh discretisation etc.) can be assessed. Ultimately, it will be applied to explore the overall hydrological implications of combinations of expected future changes in climate, vegetation and permafrost.

This contribution will provide an update on progress to date (both field data collection and model development), and will conclude by outlining our future intentions.

P 14.1
A spatially distributed numerical model for simulating sediment connectivity at the catchment scale

Giulia Battista [1], Peter Molnar [1] and Paolo Burlando [1]

[1] Institute of Environmental Engineering, ETH Zurich, Stefano-Franschini-Platz 3, CH-8093 Zurich
  (battista@ifu.baug.ethz.ch)

In cultivated areas and populated river basins, excessively high rates of soil erosion and sediment production cause a number of problems, such as reduced crop productivity, decreased water quality, excessive sedimentation in rivers and streams, increased flood risk and reservoir siltation. A compelling understanding of these phenomena and their cause-effect relationship is necessary for water and land management, and can only be achieved with a catchment scale perspective on the sediment balance. Important elements are the sources and pathways of sediment in the catchment, their hydrological activation and connectivity to the fluvial network.

In this work, we develop a physically based numerical model for simulating sediment connectivity in time and space in river basins. The model is an extension of the spatially distributed TOPKAPI-ETH hydrological model (Fatichi et al., 2015) with new modules for overland flow erosion on hillslopes and for bedload and suspended sediment transport in the river network.

A first application of the model has been performed on the Kleine Emme river catchment (477 km^2, Canton Lucerne), by using a homogeneous parameterization of erodibility in the catchment. The model reproduces (a) erosional and depositional patterns that are coherent with the topographical features in the basin (Fig. 1); (b) bedload sediment yield that compares well with estimates reported in the literature (Heimann et al., 2015); and (c) a variable suspended sediment concentration to discharge (SSC-Q) relation that reflects the spatial variability of sediment production in the model (Fig. 2).

As a next step, the main sediment source areas and the dominant processes of sediment production will be identified throughout the catchment, based on geomorphological mapping in the basin (Schwab et al., 2008; Schlunegger and Schneider, 2005), field observations, and correlation between simulated overland flow and measured concentrations at the outlet. By parameterizing and calibrating the model based on potential sediment production rates in different areas of the catchment, we expect to be able to capture the main observed sediment sources and to better reproduce the scatter of the measured SSC-Q relationship at the basin outlet. This is a novel way to parameterize spatially distributed models with concurrent information on both hydrology (overland flow) and sediment transport.
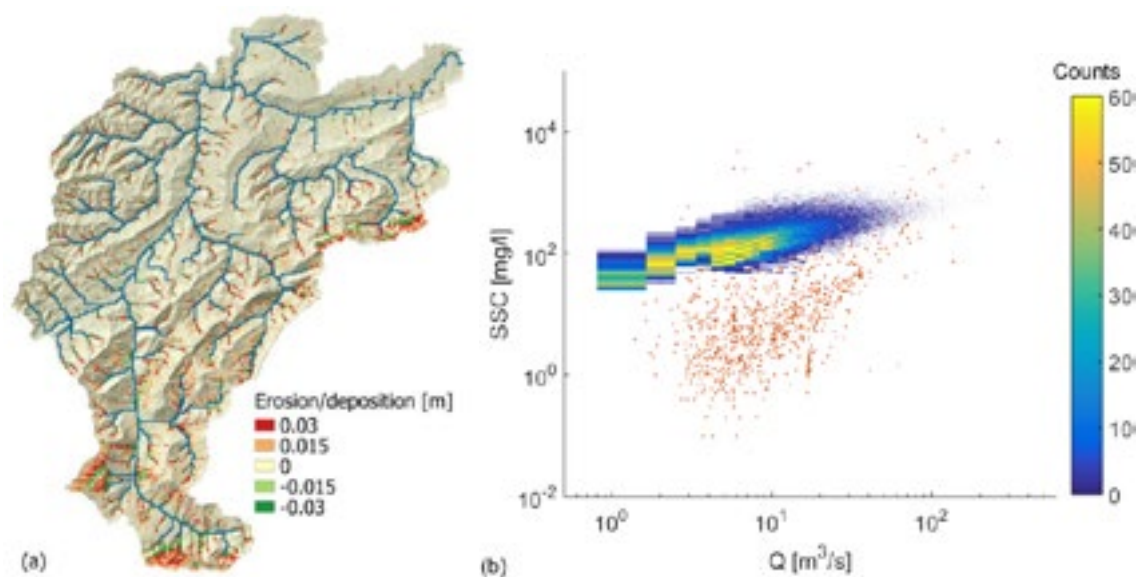

Figure 1. (a) Modelled erosion (red, >0) and deposition (green, <0) in the Kleine Emme catchment at the end of a 10 year simulation. (b) Modelled (histogram) and measured (red dots) suspended sediment concentration at the Kleine Emme River outlet for the period 2001-2009.

REFERENCES

Fatichi, S., Rimkus, S., Burlando, P., Bordoy, R. and Molnar, P., 2015. High-resolution distributed analysis of climate and anthropogenic changes on the hydrology of an Alpine catchment. Journal of Hydrology, 525, pp.362-382.

Schwab, M., Rieke-Zapp, D., Schneider, H., Liniger, M. and Schlunegger, F., 2008. Landsliding and sediment flux in the Central Swiss Alps: A photogrammetric study of the Schimbrig landslide, Entlebuch. Geomorphology, 97(3-4), pp.392-406.

Schlunegger, F. and Schneider, H., 2005. Relief-rejuvenation and topographic length scales in a fluvial drainage basin, Napf area, Central Switzerland. Geomorphology, 69(1-4), pp.102-117.

Heimann, F.U.M., Rickenmann, D., Böckli, M., Badoux, A., Turowski, J.M. and Kirchner, J.W., 2015. Calculation of bedload transport in Swiss mountain rivers using the model sedFlow: proof of concept. Earth Surface Dynamics, 3(1), p.35.

P 14.2

Estimating the precipitation in a high-alpine catchment combining local meteo stations and Swiss-wide meteo products

Tristan Brauchli [1] [2], Harsh Beria [1], Anthony Michelon [1], Josh Larsen [1] [3] & Bettina Schaefli [1]

[1] Institute of Earth Surface Dynamics, University of Lausanne, Switzerland
  (tristan.brauchli@unil.ch)

[2] School of Architecture, Civil and Environmental Engineering (ENAC), Ecole Polytechnique Fédérale de Lausanne
  (EPFL), Switzerland

[3] School of Geography, Earth and Environmental Sciences, University of Birmingham, Birmingham, United Kingdom

Mountainous regions are often considered as water towers with above average precipitation and seasonal storage under a solid form. This water is a paramount resource during spring and summer for natural ecosystems but also many human activities. Due to its high spatio-temporal variability, defining the precipitation over an entire catchment is still a challenge. This is especially true in mountainous terrain where precipitation measurement is biased by numerous processes including in particular wind undercatch, station representativity, precipitation phase. In this study, our aim is to define the precipitation over the Vallon de Nant, a small high-alpine catchment in the Swiss Alps. We are comparing different sources of data from classic instruments (tipping bucket rain gauge, radar precipitation sensor), grided products (CombiPrecip and RHIRES from MCH), model output (COSMO1) and indirect estimates derived from snow depth measurements. In a first step, we are comparing data at the point scale and then interpolate them over the entire catchment. We show the advantages of having different sources of data and the potential limitations of each of them.

P 14.3
Reconstructing long-term trends in surface water summer temperature in a high-altitude lake: A modelling approach

Monica Bulgheroni [1], Fabio Lepori [1], Maurizio Pozzoni [1], Camilla Capelli [1], Sébastian Pera [1], Cristian Scapozza [1], Luca Colombo [2]

[1] Institute of Earth Sciences, University of Applied Sciences and Arts of Southern Switzerland, Campus Trevano, CH-6952 Canobbio (fabio.lepori@supsi.ch)
[2] Department for Environment Constructions and Design, University of Applied Sciences and Arts of Southern Switzerland, Campus Trevano, CH-6952 Canobbio

During the last century, climate change has lad to the warming of lakes worldwide (Schneider & Hook 2010), with lakes in the Alpine region warming at particularly high rates. While temperature trends in large lowland lakes have been thoroughly studied thanks to the availability of historical data series of water temperature (either measured or reconstructed from infrared satellite data; Lepori & Roberts 2015; Pareeth et al. 2017), so far, the analysis of long-term temperature patterns in high-altitude lakes has been hampered by a dearth of data. In this study, we developed a mathematical model to reconstruct a long-term series of surface-water temperature of a high lake located in the North-western Alps where a monitoring program has been recently established (Lago Nero, Canton Ticino, 2385 m asl). The model, based on a simplified heat budget and spatially-interpolated meteorological conditions, was calibrated and validated using recent data (monthly and daily temperatures, Figure 1) and subsequently used to simulate summer surface-water temperatures from the early 1900s. Preliminary results indicate a warming trend, but also suggest that the warming has been irregular in time and affected different indicators of thermal conditions (minimum, maximum, mean) in different ways. These patterns, which will be analysed further, suggest probable increases of thermal stress to cold-water organisms and alterations of lake-ecosystem function.

Figure 1. Daily evolution of summer and autumn surface temperature of the lago Nero.

REFERENCES

Schneider, P. & Hook S.J. 2010: Space observations of inland water bodies show rapid surface warming since 1985. Geophysical Research Letters 37(22).
Lepori, F & Roberts J.J. 2015: Past and future warming of a deep European lake (Lake Lugano): What are the climatic drivers? Journal of Great Lakes Research 41(4), 973–81.
Pareeth, S., Bresciani, M., Buzzi, F., Leoni, B., Lepori, F., Ludovisi, A., Morabito, G., Adrian, R., Neteler, M. & Salmaso N. 2017: Warming trends of perialpine lakes from homogenised time series of historical satellite and in-situ data. Science of The Total Environment 578, 417–426.

P 14.4
Investigation of Moisture Front Convection over Europe using Cloud-Resolving COSMO model: a Case Study

Jeyun Chun [1], Michael Sprenger [1]

[1] Institute for Atmospheric and Climate Science, ETH Zurich, Universitaetstrasse 16, CH-8092 Zurich
 (chunj@student.ethz.ch)

This study investigated the impacts of moisture fronts, which have strong humidity contrast but weak thermal difference, on precipitation by implementing two case studies and climatological analysis over Europe. The two case studies revealed that two different mechanism can trigger the convection along the moisture fronts. The first case study showed that the large-scale pressure pattern leads to a strong confluence over France, Switzerland, and northern Italy (Figure 1a). The persistent flow induces an elongated line of a sharp moisture front. There was no precipitation over the front, but the convection was initiated by the large-scale upward motion in the vicinity of the moisture boundary. The precipitation was intensified on the moisture front, and continued for about 36 hours even though the large-scale forcing that initiated the convection was not available anymore. The moisture front obtained self-sustainability due to a cyclogenesis caused by the PV production at low and mid-tropospheric levels. The second case had the similar synoptic-scale condition but was initiated by a different mechanism (Figure 1b). The convection was initially suppressed by a thermodynamic energy barrier, but initiated over Mediterranean when the energy barrier moved away and conditional instability was generated near the moisture boundary. Its evolution was quite similar with the first case. It continued for about 36 hours with the support of the PV production by condensation. Climatological analysis revealed a clear temporal and spatial pattern in their occurrence (Figure 2). In general, more moisture fronts occur in summer than in winter. But the seasonality highly depends on geographical features (e.g., topography and climate features). Most of moisture fronts in flat terrains over western Europe are synoptic-scale. It is shown that they prevails in spring and autumn than in winter and summer. On the other hand, fronts over complex terrain such as Alps and Balkan Peninsula are determined by local-scale processes within the boundary layer. They are dominate in summer, because of the higher boundary layer and stronger radiative forcing. The local-scale moisture fronts also had a clear diurnal cycle as the boundary layer depth does: more frequent in afternoon than in night and early morning.
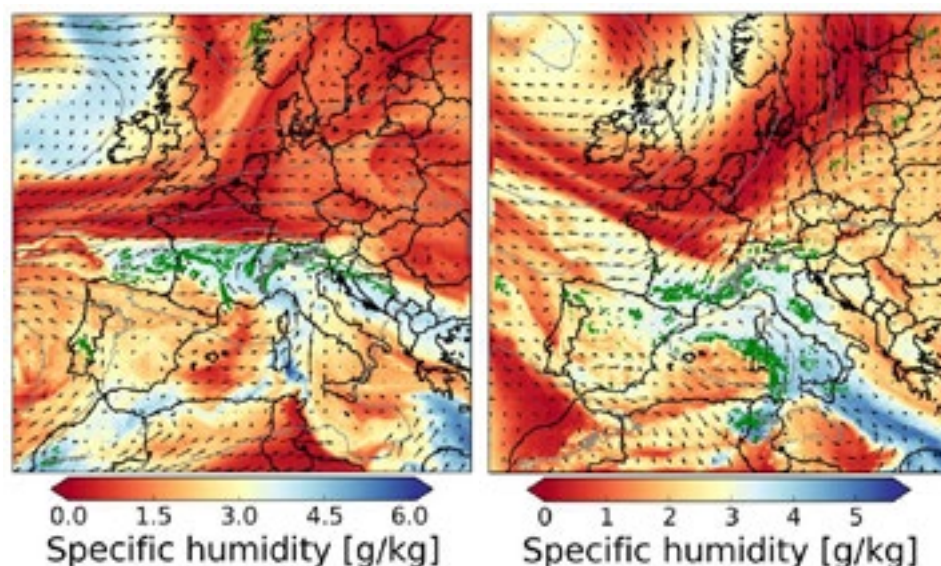

Figure 1. Specific humidity fields at 700 hPa over Europe on 0000 UTC 9 April 2002 (left) and 1800 UTC 3 April 2007 (right). Green contour represents precipitation greater than 1 mm/hr.
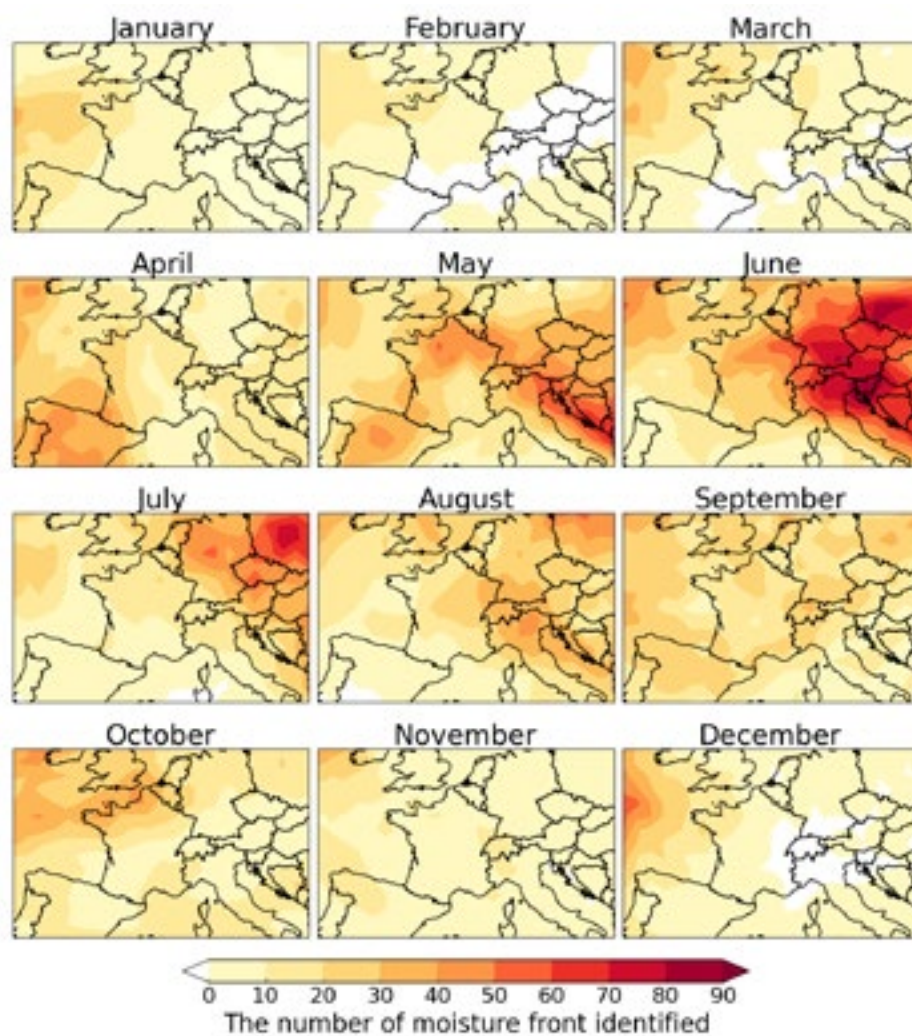
Figure 2. The numer of moisture fronts linked to precipitation which had taken place over Europe from 2000 to 2008.

P 14.5
Buoyancy-driven cross-shore flows in lakes induced by night-time cooling: field observations

Tomy Doda [1,2], Hugo Ulloa [2], Cintia Ramón Casañas [1], Alfred Wüest [1,2] & Damien Bouffard [1]

[1] *Eawag, Swiss Federal Institute of Aquatic Science and Technology, Surface Waters - Research and Management, Seestrasse 79, CH-6047 Kastanienbaum (tomy.doda@eawag.ch)*
[2] *Physics of Aquatic Systems Laboratory, École Polytechnique Fédérale de Lausanne, Station 2, CH-1015 Lausanne*

Cross-shore flows in lakes connect the littoral to the pelagic zones with major biogeochemical implications through the transport of nutrients, dissolved gases, particles and organisms (e.g., MacIntyre & Melack, 1995). One type of cross-shore exchange, referred to as "thermal siphon", is driven by horizontal temperature gradients associated with differential cooling/heating (Monismith et al., 1990). In this study, we investigate the cooling-driven thermal siphon. This occurs during night-time, in the nearshore region of lakes. For uniform heat flux conditions over the lake surface, shallower regions cool faster than deeper regions: nearshore waters become negatively buoyant and start to plunge creating a cold downslope density current that can reach the pelagic zone. This underflow differs from the density currents commonly studied in quiescent environments because it propagates into a turbulent environment, characterized by the presence of a convective mixed layer at the surface.

Although buoyancy-driven cross-shore flows have been the focus of several laboratory and modelling studies in the past (e.g., Sturman et al., 1999; Mao et al., 2010), field observations are limited (e.g., Monismith et al., 1990; Fer et al., 2002). In particular, little is known about (1) the temporal and spatial variabilities of the thermal siphon in lakes, (2) the turbulent mixing induced by the density current and its interactions with surface penetrative convection and (3) its effects on transport and biogeochemical cycles.

The present study aims at filling these three gaps by extensively monitoring both penetrative convection and buoyancy-driven cross-shore flows in Lake Cadagno, a small meromictic lake located in Ticino (Switzerland), at 1920 m above sea level (Fig. 1). Three vertical moorings M1, M2, M3 consisting of a chain of thermistors were deployed along a cross-shore transect from June to September 2018. They allowed to identify cross-shore temperature gradients driven by differential cooling. In addition, the evolution of the surface mixed layer could be examined. The vertical and horizontal temperature distributions were also obtained from CTD profiles collected along different transects. Two near-bed moorings were used to measure lake temperature 30 cm above the sediment and provided information on the thermal structure in the cross-shore (M4) and along-shore directions (M5). The flow velocity was recorded by three Acoustic Doppler Current Profilers (ADCP) located near each vertical mooring. Turbulence intensity in the surface mixed layer was estimated from temperature microstructure profiles collected from an offshore platform. Finally, surface heat fluxes, buoyancy flux and wind forcing were computed from meteorological data recorded by a weather station on the lake shore.

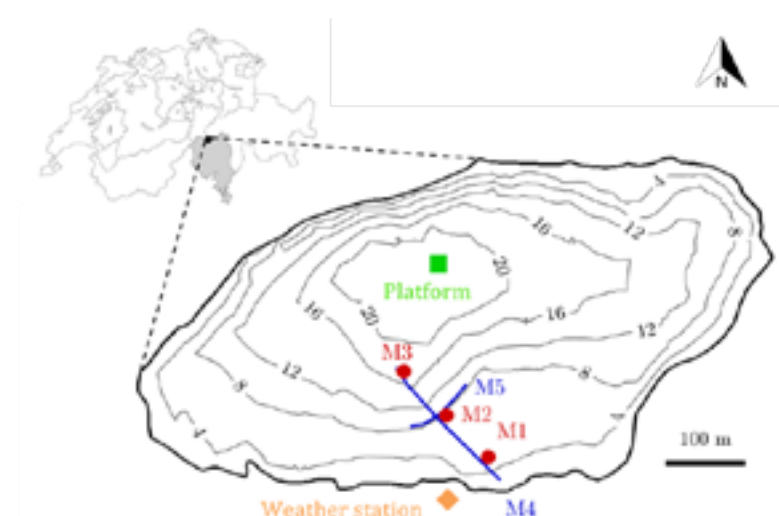Preliminary results from the 2018 experiments will be presented and discussed.

Figure 1. Location and bathymetric map of Lake Cadagno. The three vertical moorings are indicated in red and the two near-bed moorings in blue.

REFERENCES

Fer, I., Lemmin, U., & Thorpe, S. (2002). Winter cascading of cold water in Lake Geneva. Journal of Geophysical Research: Oceans, 107(C6).

MacIntyre, S., & Melack, J. M. (1995). Vertical and horizontal transport in lakes: linking littoral, benthic, and pelagic habitats. Journal of the North American Benthological Society, 14(4), 599–615.

Mao, Y., Lei, C., & Patterson, J. C. (2010). Unsteady near-shore natural convection induced by surface cooling. Journal of Fluid Mechanics, 642, 213–233.

Monismith, S. G., Imberger, J., & Morison, M. L. (1990). Convective motions in the sidearm of a small reservoir. Limnology and Oceanography, 35(8), 1676–1702.

Sturman, J., Oldham, C. E., & Ivey, G. N. (1999). Steady convective exchange flows down slopes. Aquatic Sciences, 61(3), 260–278.

P 14.6

Characteristics of meltwater passage through the proglacial area at Adygine complex, Northern Tien Shan

Kristyna Falatkova [1], Miroslav Sobr [1], Martin Slavik [2], Jiri Bruthans [2], Bohumir Jansky [1]

[1] Department of Physical Geography and Geoecology, Faculty of Science, Charles University, 12843 Prague, CZ
  (kristyna.falatkova@natur.cuni.cz)
[2] Institute of Hydrogeology, Engineering Geology and Applied Geophysics, Faculty of Science, Charles University, 12843
  Prague, CZ

The retreat of mountain glaciers has raised concern especially in those regions of the world, where the population is strongly dependent on glacier meltwater (Sorg et al., 2012). As the internal workings of glacier and proglacial systems have a significant influence on the overall hydrological regime of a glacierized basin (Moorman and Michel, 2000), mountain areas are the most important zones for water generation. That is particularly valid for dry Central Asia, where glacier meltwater contributes up to 40-70% to summer runoff (Aizen et al., 1996).

Groundwater sourced from periglacial landforms like rock glaciers or moraines has been shown to be important both in timing and quantity of alpine watershed discharge (Winkler et al., 2016). However, they represent a complicated system where layers of varying permeability occur (fine and coarse sediments, boulders, buried ice) and thus several drainage systems (delayed and fast water flow) may be present (Winkler et al., 2016). Although it is clear that proglacial lakes and landforms play an important role in transmitting and temporarily storing water, their internal hydrological processes and pathways are still not well understood.

In this study, we present research on meltwater passage through proglacial area, its influence on hydrological regime of lakes, and we test methods for revealing characteristics of subsurface drainage system. The used data include water level fluctuation of the main proglacial lakes forming the first part of the meltwater route, water samples from tarn lakes analysed to determine the isotopic composition, and a breakthrough curve based on a tracer experiment of the underground water passage.

Monitoring of lakes' water level fluctuation confirmed typical glacial regime in both seasonal and daily scale. The fluctuation characteristics of the individual lakes depend on amount of water inflow, position of a lake in terms of meltwater routing, and type and capacity of lake drainage channels. Isotopic composition of water in tarn lakes situated on the moraine complex revealed their linkage to meltwater and the influence of evaporation on their hydrological balance. Together with results of a tracer test this output enables us to outline the moraine's hydrological system. The relatively high water passage velocity suggests an efficient routing through highly permeable layer, however, there are likely multiple flow systems within the moraine complex.

REFERENCES

Aizen, V. B., Aizen, E. M., Melack, J. M. 1996: Precipitation, melt and runoff in the northern Tien Shan. J Hydrol, 186, 229-251.

Moorman, B. J., Michel, F. A. 2000: Glacial hydrological system characterization using ground-penetrating radar. Hydrol Process, 14(15), 2645-2667.

Sorg, A., Bolch, T., Stoffel, M., Solomina, O., Beniston, M. 2012: Climate change impacts on glaciers and runoff in Tien Shan (Central Asia). Nat Clim Change, 2(10), 725.

Winkler, G., Wagner, T., Pauritsch, M., Birk, S., Kellerer-Pirklbauer, A., Benischke, R., Leis, A., Morawetz, R., Schreilechner, M. G., Hergarten, S. 2016: Identification and assessment of groundwater flow and storage components of the relict Schöneben Rock Glacier, Niedere Tauern Range, Eastern Alps (Austria). Hydrogeol J, 24(4), 937-953.

P 14.7
Sensitivity of statistical precipitation downscaling to the choice of an atmospheric reanalysis

Pascal Horton [1], Stefan Brönnimann [1]

[1] Institute of Geography, University of Bern, Hallerstrasse 12, CH-3012 Bern (pascal.horton@giub.unibe.ch)

Hydrological climate impact assessment relies on climate variables that are dynamically and/or statistically downscaled to a relevant spatial scale. Some of these downscaling methods are based on perfect prognosis approaches (Maraun et al., 2010), which rely on statistical relationships between observed synoptic predictors and the local variable of interest, here daily precipitation. The synoptic predictors are often extracted from global atmospheric reanalyses, considered as pseudo-observations. Global atmospheric reanalyses are useful to fulfill this role, as they provide gridded large-scale variables that are available for any location in the world. Reanalyses are produced using a single version of a data assimilation system coupled with a forecast model constrained to follow observations over a long period. They provide multivariate outputs that are physically consistent, which contain information in locations where few or no observations are available, also for variables that are not directly observed (Gelaro et al., 2017). Their accuracy depends on both the quality of the model physics and that of the analysis process, and thus indirectly on the quantity and quality of the assimilated observations (Dee et al., 2011). Europe is a data-rich region, and the reanalyses are often considered as equivalent over the European domain. Thus, their impact on the downscaled variables is not often considered.

The present work focuses on the analogue method, which is a statistical downscaling technique that relies on the hypothesis that similar synoptic situations are likely to result in similar local effects, plus a certain variability that is not explained by the considered predictors (Lorenz, 1969). The local variable of interest, here, is daily precipitation. Different versions of AMs exist, relying on various predictors considered over domains of variable size. In order to take into account the unexplained variability, several analogue days are usually selected and their observed precipitation values are used to provide an empirical conditional distribution that is the statistical prediction for the considered target date.

The present work assessed the impact of ten reanalyses on the performance of seven variants of analogue methods for statistical precipitation downscaling at 301 stations in Switzerland. Significant differences were found between reanalyses and their impact on the performance of the method was found to be even higher than the choice of the predictor variables (Fig. 1).

Other properties of the reanalyses were analyzed, such as the spatial resolution. The use of datasets with a long period coverage, or providing multiple members, was also investigated, resulting in warnings about potential misuse.

REFERENCES

Dee, D. P., Uppala, S. M., Simmons, A. J., Berrisford, P., Poli, P., Kobayashi, S., … Vitart, F. 2011: The ERA-Interim reanalysis: Configuration and performance of the data assimilation system, Quarterly Journal of the Royal Meteorological Society, 137(656), 553–597. DOI:10.1002/qj.828

Gelaro, R., McCarty, W., Suárez, M. J., Todling, R., Molod, A., Takacs, L., … Zhao, B. 2017: The modern-era retrospective analysis for research and applications, version 2 (MERRA-2), Journal of Climate, 30(14), 5419–5454. DOI:10.1175/JCLI-D-16-0758.1

Lorenz, E. 1969: Atmospheric predictability as revealed by naturally occurring analogues, Journal of the Atmospheric Sciences, 26, 636–646. DOI:10.1175/1520-0469(1969)26<636:aparbn>2.0.co;2

Maraun, D., Wetterhall, F., Chandler, R. E., Kendon, E. J., Widmann, M., Brienen, S., … Thiele-Eich, I. 2010: Precipitation downscaling under climate change: Recent developements to bridge the gap between dynamical models and the end user, Reviews of Geophysics, 48(RG3003), 1–34. DOI:10.1029/2009RG000314
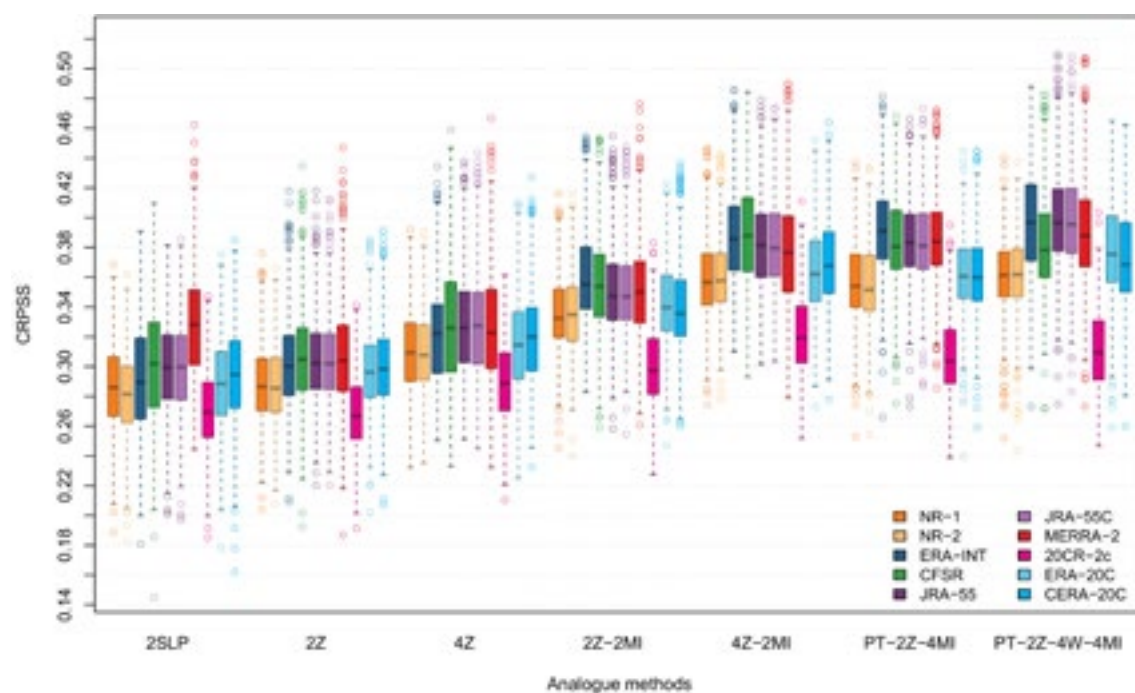
Figure 1. CRPSS (Continuous Ranked Probability Skill Score) for all stations, and for all considered analogue methods and reanalysis datasets on the validation period. A higher CRPSS means better performance. The parameters of the analogue methods were calibrated for every station, every dataset, and every method. The boxes show the 25th, 50th, and 75th percentiles. The whiskers extend to the most extreme data point which is no more than 1.5 times the interquartile range.

P 14.8
Renewal of the high-resolution map of direct and indirect connectivity of erosion risk areas to surface waters in Switzerland

Lorenz Joss [1], Volker Prasuhn [2]

[1] Agroscope, Water Protection and Substance Flows Research Group, Reckenholzstrasse 191, CH-8046 Zurich
(lorenz.joss@agroscope.admin.ch)
[2] Agroscope, Water Protection and Substance Flows Research Group, Reckenholzstrasse 191, CH-8046 Zurich
(volker.prasuhn@agroscope.admin.ch)

Nutrient and pesticide inputs from agriculture into waters through surface runoff and soil erosion is a current environmental problem in Switzerland. In recent years, especially the off-site effects of soil erosion have increasingly gained importance in research. As a result, the potential soil erosion map of Switzerland was created in 2010 (Gisler 2010 et al., Prasuhn 2013 et al.). Additionally, an associated high-resolution map of direct and indirect connectivity of agricultural erosion risk areas to surface waters was created in 2015. As a support tool, the map in many cases helped to develop environmentally efficient and cost effective soil erosion mitigation options (Alder et al. 2015). The results showed, that even areas that are far away from open water bodies can be indirectly connected and thus have to be taken into account as well when implementing mitigation measures. However, likewise the erosion risk map, the connectivity map only shows the potential risks of the agricultural areas. The actual risk can only be assessed by adding land cover information by using the map in the field. Despite this fact, the maps showed to be very practical for many applications.

As of today, both maps are outdated as they are based on the old Vector25 database and the DTM-AV topographic model from the Federal Office of Topography (Swisstopo). With the introduction of the updated high precision digital elevation model of Switzerland swissALTI[3D] new possibilities for mapping erosion risk have become available. Furthermore, with the topographic landscape model TLM fully being released in 2019, Swisstopo introduced an immense database for three-dimensional geodata. Based on up-to-date aerial images, information about buildings, roads, bodies of water and land cover information were selected, resulting in a never-seen before map of Switzerland with accurate data. Based on this newly available data, the high resolution connectivity map of the agricultural area is being renewed as of today. With GIS, runoff generation and flow pathways are calculated with multiple-flow accumulation algorithms. Furthermore, based on the TLM data and swissALTI[3D] an extended drainage system with drained roads, farm tracks and slope depressions indicating thalwegs are defined. With this, the probability and type of connection of today's agricultural area is calculated.

Figure 1 shows an extract of the old connectivity map by Alder et al. (2015). All agricultural areas can be divided into three types of connectivity. In blue colours, areas with low, moderate and high direct connectivity with a water body or a thalweg leading to a water body are represented. Orange to brown colours indicate an indirect connection through drained roads or thalweg that lead to drained roads. Finally, agricultural areas in white indicate no connection to surface waters, as these areas are too flat or too far away from the extended drainage system. The results of the older map showed, that most areas are indirectly connected through inlet shafts and drained roads. These results, however, are not entirely valid as of today due to the old data used. To reach the goals of the national action plan about pesticides passed in 2017, which include a reduction of the risk of pesticides by a half and promoting a sustainable usage of pesticides, a renewed map of direct and indirect connectivity of erosion risk areas to surface waters is inevitable (Bundesrat 2017).

REFERENCES
Alder, S., Prasuhn, V., Liniger, H., Herweg, K., Hurni, H., Candinas, A., & Gujer, H. U. (2015). A high-resolution map of direct and indirect connectivity of erosion risk areas to surface waters in Switzerland - A risk assessment tool for planning and policy-making. Land use policy, 48, 236-249.
Bundesrat (2017). Aktionsplan zur Risikoreduktion und nachhaltigen Anwendung von Pflanzenschutzmitteln. Bericht des Bundesrates vom 6. September 2017.
Gisler, S., Liniger, H. P., & Prasuhn, V. (2010). Technisch-wissenschaftlicher Bericht zur Erosionsrisikokarte der landwirtschaftlichen Nutzfläche der Schweiz im 2x2-Meter-Raster (ERK2). CDE Universität Bern und ART Zürich-Reckenholz.
Prasuhn, V., Liniger, H., Gisler, S., Herweg, K., Candinas, A., & Clément, J. P. (2013). A high-resolution soil erosion risk map of Switzerland as strategic policy support system. Land use policy, 32, 281-291.
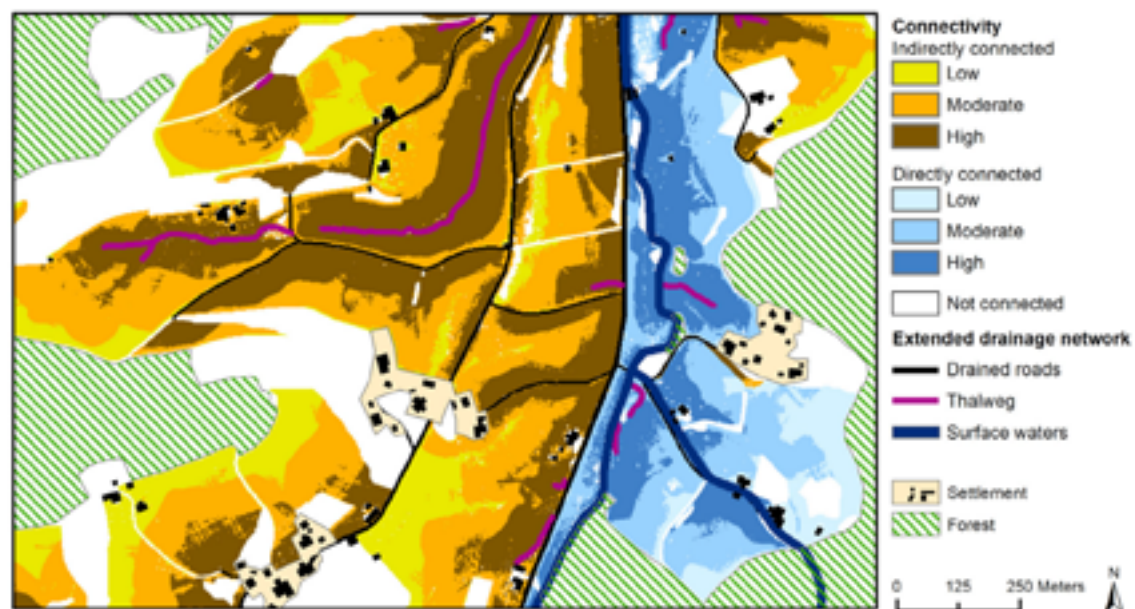
Figure 1. (Alder 2015 et al.) Extract of the connectivity map showing the probability of any area to be connected directly with a water body or a thalweg leading to a water body (a), or indirectly through drained roads or a thalweg leading onto a drained road (b), or not at all (c).

P 14.9

Identification of pre-event water sources to streamflow and uncertainty associated with end-member characterization

Leonie Kiewiet [1°], Ilja van Meerveld [1], Jan Seibert [1,2]

[1] Department of Geography, University of Zurich, Zürich, Switzerland
[2] Department of Earth Sciences, Uppsala University, Uppsala, Sweden
° Corresponding author: leonie.kiewiet@geo.uzh.ch

In End Member Mixing Analysis (EMMA), changes in streamwater chemistry and isotopic composition during rainfall or snowmelt events are used to determine the relative contributions of different source waters to streamflow. Usually only one (or a few) groundwater samples are used to characterize the groundwater component, although it is recognized that catchment groundwater storages are rarely well mixed and that not all parts of the catchment are continuously hydrologically connected to the stream. Similarly, for isotope based hydrograph analyses the pre-event streamflow sample is assumed to represent all pre-event water. However, the pre-event streamflow sample may reflect only a certain part of the groundwater storage if groundwater has a different chemical signature in different parts of the catchment and not all parts are connected to the stream during baseflow conditions. Therefore, in order to better understand which parts of the catchment contribute to streamflow during baseflow and rainfall events it is important to understand the spatial and temporal variations in groundwater chemistry.

We combined the results from nine baseflow sampling campaigns and detailed stream sampling for four events to identify the stream water sources in a 20-ha steep mountainous catchment in the Swiss pre-Alps. During the nine baseflow sampling campaigns, shallow groundwater was sampled from 34 to 47 wells, streamflow at seven locations and soil water at 13 to 18 sites. During the four stormflow campaigns, streamwater samples were taken at regular intervals at the catchment outlet, and for two of the campaigns also at an additional site half-way up the stream network. The samples were analyzed for major and trace ions and stable water isotopes (δ^2H and $\delta^{18}O$).

The results of the baseflow sampling campaigns indicated that the spatial variability in pre-event water chemistry is very large. For example, the Electrical Conductivity (EC) in groundwater ranged from 68 – 610 µS/cm during the campaign with the highest antecedent moisture conditions and from 194 – 780 µS/cm for the campaign during the driest conditions. The spatial variability in the isotopic composition of the groundwater was smallest in early summer and autumn (standard deviation: δ^2H 2.3 ‰ and 3.4 ‰, respectively) and largest during the dry conditions in late August (standard deviation: δ^2H 9.5 ‰). Based on the differences from the catchment average concentrations, we could distinguish four groundwater clusters, of which three corresponded to the main hydro-geomorphic units: riparian zone-like, hillslopes and areas with small upslope contributing areas, deeper groundwater. The fourth cluster was characterized by high magnesium and sulfate concentrations that likely reflect different bedrock material. The soil water was as variable as the groundwater: Electric Conductivity ranged from 10 – 668 µS/cm (standard deviation: 157 µS/cm) and the standard deviation of δ^2H per campaign ranged from 5.3 ‰ (May 2017) to 13.7 ‰ (August 2016).

Baseflow was not an equal mixture of the different groundwater clusters. During the majority of the baseflow campaigns streamflow chemistry at all but one site most strongly resembled groundwater from the riparian-like cluster, but the similarity to groundwater from the hillslope cluster was larger shortly after snowmelt, reflecting differences in hydrologic connectivity. Streamflow chemistry changed from the composition of shallow groundwater during the stormflow events, shifting in composition towards that of the incoming precipitation. However, there were marked differences in estimations of event water inputs when different tracers were used, or when the pre-event water component reflected the composition of a specific shallow groundwater cluster.

For instance, in two cases the isotope hydrograph separation results suggested that stormflow more strongly resembled pre-event water, while a mixing diagram with chloride and sodium concentrations of the same event indicated a much stronger influence of event water. Additionally, estimations of the pre-event water fraction changed up to 22% (using calcium as a tracer) when limiting the characterization of the pre-event water composition to samples from a single groundwater cluster rather than including all groundwater measurements. These results show how the spatial variability in different pre-event water compartments can be used to identify sources to streamflow and highlights the need of an adequate representation of the pre-event water component when analysing streamflow sources.

P 14.10

Resolution matters: numerical analysis of the effect of subgrid heterogeneities with a physically based hydrological model

Elena Leonarduzzi [1,2]

[1] *Institute of Environmental Engineering, ETH Zurich, Switzerland*
[2] *Swiss Federal Institute for Forest, Snow and Landscape Research WSL, Birmensdorf, Switzerland*

In Switzerland most of the natural hazards are triggered by precipitation, but the soil status prior to the rainfall event is an important factor. That is true, for example, for floods and landslides, which were responsible collectively for a loss of 7630 million Euros between 1972 and 2007 (Hilker et al., 2009). The water table height and soil saturation necessary to predict the occurrence of these natural hazards accurately are typically calculated employing hydrological models (e.g. Prevah, Viviroli et al., 2009). While in some cases high resolution small scale models are developed for specific case studies, there is also a need for regional scale warning system which provide a first order estimate of the vulnerability across the country (Staehli et al., 2015). These coarse scale models face problems of subgrid variability in topography and soil water dynamics and their effects on slope stability may be complex.

Here we use synthetic numerical experiments to address the effect of heterogeneities within a cell of the size typically used for regional hydrological applications. We chose the hydrological model ParFlow-CLM (Maxwell and Miller, 2009), which is an integrated, fully coupled, physically based model, which solves water and energy budgets, surface and subsurface flows. The reference simulation is represented by a domain of 400*400 m without any heterogeneities within. This setup corresponds to the information content of a cell of a regional scale model. Results are compared to those using similar domains, where heterogeneities in slope (creating a v-shape domain) or soil layering (permeability contrasts or soil thickness) are added (Fig 1a). These experiments aim to provide insights on what the under/over estimation of water pressure and soil saturation could be when using coarser resolutions which average out heterogeneities.

Different climates and soil properties are also investigated by comparing the results with the climatic forcing and soil properties for the site Napf in Switzerland (wet temperate) and Niwot in Colorado (semiarid). Forcing is found to be the main factor controlling dynamics and seasonalities of the snowpack and evapotranspiration, while soil properties influence greatly runoff generation mechanisms as well as the timing and intensity of runoff. All these conditions lead to very different scenarios in terms of calculated soil water pressure.

Finally, in order to quantify the effect of potential over/under estimation of soil water pressure and soil saturation for one possible application, the stability of the domains is calculated choosing the most critical point (where highest pressures are developed) following a simple infinite slope. The biggest differences are observed between flat domains and those that have any magnitude of side slope (first column in Fig 1a vs the other two columns). This can be observed for example comparing the different domains with forcing and soil properties from Colorado(Fig 2b). With a flat domain, soil water pressures and saturations in the central part of the domain are highly underestimated and the Factor of Safety remains approximately constant, always well above 1. When when some side slope is introduced which induces lateral flow, the FoS drops below 1 in May and June, when snowmelt has saturated the soil as well as in September, due to some intense rainfall events.

These results provide useful information on the potential errors when utilizing a regional hydrological model with such "coarse" resolution, which is particularly critical when the ultimate objective is predicting flooding and landsliding.

REFERENCES

Hilker, N., Badoux, A., and Hegg, C. 2009: The Swiss flood and landslide damage database 1972–2007, Nat. Hazards Earth Syst. Sci., 9, 913-925.

Maxwell, R.M., & Miller N.L. 2009: Development of a coupled land surface and groundwater model. Journal of Hydrometeorology, 6(3):233–247.

Stähli, M., Sättele, M., Huggel, C., McArdell, B.W., Lehmann, P., Van Herwijnen, A., Berne, A., Schleiss, M., Ferrari, A., Kos, A. and Or, D., 2015: Monitoring and prediction in early warning systems for rapid mass movements. Natural Hazards and Earth System Sciences, 15(4), pp.905-917.

Viviroli, D., Zappa, M., Gurtz, J. and Weingartner, R., 2009: An introduction to the hydrological modelling system PREVAH and its pre-and post-processing-tools. Environmental Modelling & Software, 24(10), pp.1209-1222.
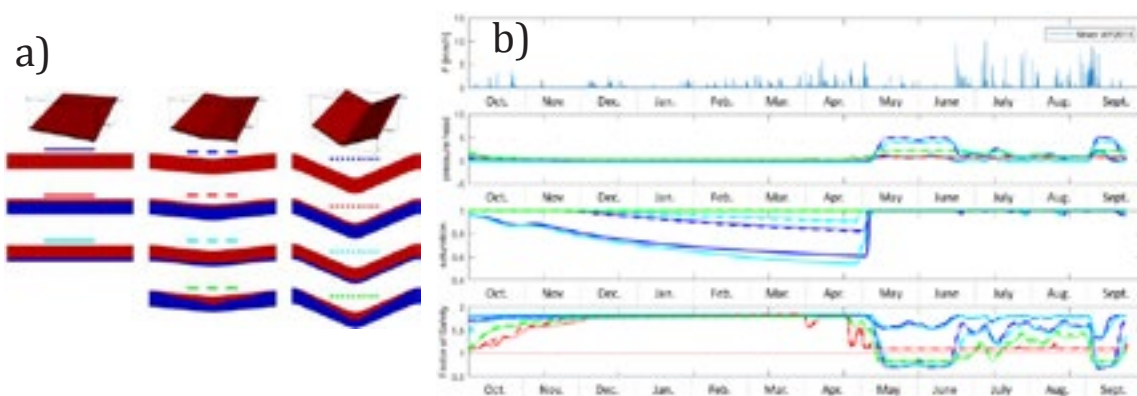
Figure 1. a) Synthetic domains used in the simulations, with increasing side slope (left to right) and changing soil layering: one soil layer, thin layer over bedrock, thick layer over bedrock and erosion soil layer over bedrock. Bedrock is represented in blue and soil in red. b) From top: timeseries of measured precipitation, simulated pressure head, saturation and factor of safety.

P 14.11
Modelling Stream Temperature of Rivers in Switzerland

Adrien Michel [1], Tristan Brauchli [2], Matthias Bavay [3], Michael Lehning [1,3], Bettina Schaefli [2] & Hendrik Huwald [1]

[1] Ecole Polytechnique Fédérale de Lausanne (EPFL), (adrien.michel@epfl.ch)
[2] Université de Lausanne, Lausanne, Switzerland
[3] WSL Institute for Snow and Avalanche Research SLF, Davos, Switzerland

While numerous past modelling efforts have attempted to accurately simulate stream discharge, water temperature of streams has obtained much less attention. This is recently changing as a result of potentially significant impact of climate change on stream temperature and therefore indirectly also on water quality, the aquatic fauna and fluvial ecosystem services. The current project addresses modelling of stream temperature in Swiss rivers, based on a chain of physical models, including MeteoIO, Alpine3D and StreamFlow. In a first step, selected watersheds (Dischma, Broye, Rietholzbach, Vallon de Nant) are simulated and results of discharge and water temperature are compared and validated against respective observational time series. This contribution presents results of simulations using the latest version of the mentioned model chain and the selected case studies, with particular focus on soil temperature, water percolation in snow and soil, and available input and forcing data. The ultimate objective is the development of a numerical model suitable for the simulation of thermodynamic response of rivers to climate forcing, climate change, and to develop projections of various scenarios, including adaptation and mitigation measures such as modified riparian vegetation, as well as consequences of potential river renaturation measures.

P 14.12
The other's perception of a streamflow sample: From a bottle of water to a data point

Sandra Pool [1], Manuela Brunner [1,2], Leonie Kiewiet [1] & Elise Acheson [1]

[1] Department of Geography, University of Zurich, Winterthurerstrasse 190, CH-8057 Zürich (sandra.pool@geo.uzh.ch)
[2] Swiss Federal Institute for Forest, Snow and Landscape Research WSL, Birmensdorf ZH, Switzerland

"Do you take runoff samples?" This seemingly simple question might lead to misunderstandings between two hydrologists if they don't share the same perception of a runoff sample. This study is motivated by such misunderstandings possibly occurring between different hydrological subcommunities, such as field hydrology, statistical hydrology, and hydrological modelling. More specifically, we analyzed the personal perceptions of hydrologists of the widely used terms sample, runoff, discharge, and streamflow. The analysis was based on qualitative and quantitative data from three sources of information: a drawing exercise with 15 hydrologists, a survey with 42 participants, and a literature corpus analysis including several thousand peer-reviewed journal articles. The multiple sources of information revealed distinct, deeply established, but sometimes diverging conceptualizations of these widely used terms. A thoughtful use of apparently common hydrological terms is therefore fundamental for an improved dialogue between hydrologists of different subdisciplines.

P 14.13

New Approach to Quantify Organic Matter Freshness and Paleoproductivity In Lake Sediments Through Spectral Deconvolution of the UV-VIS Absorption Spectra

Andrea Sanchini and Martin Grosjean

Institute of Geography & Oeschger Centre for Climate Change Research, University of Bern, Bern, Erlachstrasse 9a, 3012, Switzerland. (andrea.sanchini@giub.unibe.ch)

Assessments of paleoproductivity and organic matter freshness require accurate identification and quantification of sedimentary chloropigments. Chloropigments quantification by chromatography techniques is impracticable for long time-series at high-resolution because it is expensive, labor intensive, and time consuming. Here, we report on a new rapid and inexpensive approach to extract this information by mathematical analysis of the UV-VIS absorption spectra of untreated extracted sediment samples obtained from spectrophotometers measurements. The methodology consists in two steps, (i) the application of the iterative non-linear least squares fitting to deconvolute the chloropigment bulk absorption peak in two main components [1], Chloropigments-β and Chloropigments-α, (ii) the use of mono or dichroic equations on the deconvolute components. The methodology was developed and validated on standard solutions of known composition and tested on a short sediment core from a varved eutrophic lake, Ponte Tresa, southern Switzerland (1913–2015). Our approach is able to quantify Chlorophyll-β (=0.99; RMSEP~5.9%), Chlorophyll-α (=0.98; RMSEP~5.0%), and Pyropheorbide-α (=0.99; RMSEP~7.80%) in standard solutions and Chloropigments-α (=0.99; RMSEP~3.29%), Chlorophyll-α (=0.98; RMSEP~3.90%) and Chlorins-α (=0.98; RMSEP~5.96%) in lake sediment cores. Chlorophyll-β was not detected. In addition the methodology can be used to calculate the chlorin index and to quantify aquatic paleoproductivity and organic matter freshness. The chlorin index shows that circa the 55%-75% of the organic matter measured in sediment is already degraded on the water column. Chlorins-α reveal eutrophication peaks and paleoproductivity back in time. In conclusion chloropigments-α is an ideal proxy to reveal these processes because does not undertake post burial remineralization in anoxic sediment core (Chlorin index is linearly independent from Chlorins-α, $R^2= 0.13$).

REFERENCES
[1] O'Haver, T. (2018). Toolkit of functions, scripts and spreadsheet templates. https://terpconnect.umd.edu/~toh/spectrum/functions.html, 2018-02-27.

P 14.14
Soil wetness data for landslide early warning

Adrian Wicki [1], Manfred Stähli [1]

[1] Eidg. Forschungsanstalt WSL, Zürcherstrasse 111, CH-8903 Birmensdorf (adrian.wicki@wsl.ch)

In mountain areas, landslides triggered by heavy rain present a serious risk to people and infrastructure. Recent major events in Switzerland have demonstrated the numerousness, abruptness and seemingly unpredictability of shallow landslides using meteorological information only. Hence, several research projects have been initiated to advance fundamentals and to develop tools for the early warning of landslides at the regional scale. While most studies focus on the use of precipitation information to assess thresholds for the initiation of landslides (e.g. through intensity-duration-relationships), less work has been put into the utilization of soil wetness information. In this respect, most attempts were made to estimate soil saturation with hydrological models to assess the antecedent soil wetness as a measure for slope stability.

In our study, we assess the value of in-situ soil wetness measurements for its use in a regional landslide early warning system (LEWS). Soil moisture measurements from various research institutions and authorities in Switzerland are compiled for the first time in a comprehensive soil wetness data base. The data set comprises soil wetness time series of 34 measurement sites distributed all over Switzerland, with a total of 300 measurement sensors covering up to 10 years in time. Soil moisture has been measured at different depths using TDR, FDR and capacitance sensors with temporal resolution ranging from 10-minute to hourly time steps.

As the measurement set-ups, data quality and temporal resolution of the different data sets are very heterogeneous, the soil moisture time series had to be homogenized and normalized in a first step. Based on this, soil moisture dynamics were described by variability-mean relationships, by describing the antecedent soil wetness vs. short-term soil moisture changes and through water balance calculations at individual sensors, along specific depth profiles and for entire measurement sites. Finally, these dynamics were compared to a set of shallow landslide events derived from the Swiss flood and landslide damage database (WSL) covering 441 events from 2008 to 2017.

Here we present first results of this analysis showing characteristic patterns of soil moisture dynamics that can serve as a precursor for increased landslide activity and to separate events from non-events. The forecast goodness is assessed using Receiver Operating Characteristic (ROC) analysis. A concentration of landslide events is visible in pre-alpine areas and the Ticino as well as during the summer months (59% of the events happened in June, July and August). While most soil moisture measurements show the lowest seasonal mean soil moisture values during those months, increased soil moisture variability can be observed.
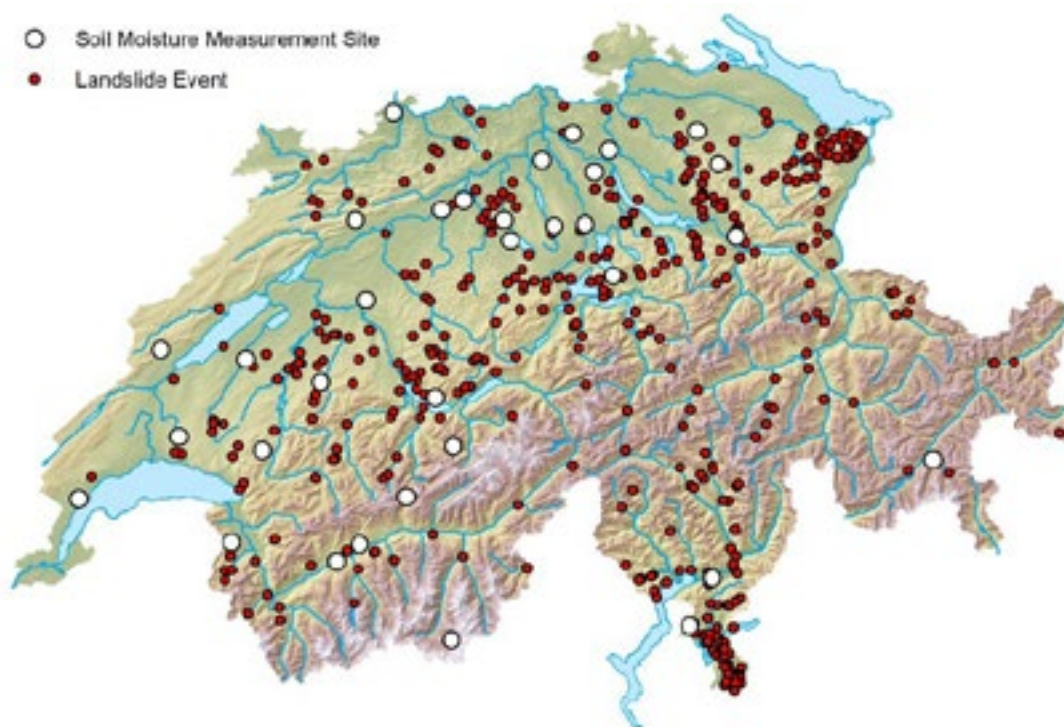
Figure 1. Location of the soil moisture measurement sites (white circles) and the shallow landslide events (period 2008 to 2017).

P 14.15

Combining Hyperspectral Imaging and µXRF data to link varve-formation processes with meteorological data, Lake Zabinskie, Poland

Paul Zander [1], Martin Grosjean [1], Wojciech Tylmann [2], Janusz Filipiak [2]

[1] *Oeschger Centre for Climate Change Research and Institute of Geography, University of Bern, Falkenplatz 16, 3012 Bern, Switzerland (paulzander@giub.unibe.ch)*

[2] *Faculty of Oceanography and Geography, University of Gdansk, Bażyńskiego 4, 80-952 Gdańsk, Poland*

Varved lake sediments are a valuable resource for paleoclimatological investigations due to the ability to produce proxy records at high-resolution with annually resolved chronologies. New advances in Hyperspectral Imaging (HSI) and Micro X-Ray Fluorescence (uXRF) provide opportunities to study the composition of varves at very high resolution (um scale), with the potential to yield new insights into sub-varve scale depositional processes, and relationships with limnological and meteorological phenomenon.

Hyperspectral Imaging has been demonstrated to be an effective method to measure the abundance of chloropigments in sediment at much higher resolution than would be possible with conventional pigment analysis using liquid chromatography (Butz et al., Journal of Paleolimnology, 2017). In this study we use HSI to determine the abundance of chloropigments (Chlorophyll-a and diagenetic products) in the sediments of Lake Zabinskie, Poland at a spatial resolution of 60 um (equivalent to approximately 70-80 data points per varve). The sediments of Lake Zabinskie contain well-preserved biogenic varves defined by the deposition of calcite and diatom remains in spring and summer, with clay and fine-grained organic matter deposited in winter. Previous work at Lake Zabinskie, Poland has demonstrated a relationship between chloropigments and instrumental measurements of spring (March to May) temperatures during the period 1907-2008 (Amann et al., Global and Planetary Change, 2014). In this study, we extend the calibration to the period 1779-2016 using higher resolution pigment data inferred from HSI. We find a significant positive relationship between green pigments and spring temperatures, however the correlation is much greater during the period 1900-2016. This result indicates that green pigments as measured by hyperspectral imaging may be useful as an indicator of temperature in the past, though caution is warranted due to weak correlation prior to 1900 CE. Additionally, the sub-annual resolution of the hyperspectral and uXRF datasets allow for the investigation of sub-seasonal scale depositional processes, which may be linked to limnological and meteorological conditions.

REFERENCES

Amann, B., Lobsiger, S., Fischer, D., Tylmann, W., Bonk, A., Filipiak, J., & Grosjean, M. 2014: Spring temperature variability and eutrophication history inferred from sedimentary pigments in the varved sediments of Lake Żabińskie, north-eastern Poland, AD 1907–2008. Global and Planetary Change 123, 86-96.

Butz, C., Grosjean, M., Goslar, T., & Tylmann, W. 2017: Hyperspectral imaging of sedimentary bacterial pigments: a 1700-year history of meromixis from varved Lake Jaczno, northeast Poland. *Journal of Paleolimnology 5*8(1), 57-72.

15. The new Climate Change Scenarios CH2018

Stefan Brönnimann, Andreas Fischer, Kuno Strassmann

Swiss Association of Geographers (ASG)
Commission for Atmospheric Chemistry and Physics (ACP)

TALKS:

15.1   Brönnimann S.: Climatic changes in Switzerland over the last 300 years

15.2   Casanueva A., Kotlarski S., Fischer A.M., Schwierz C., Liniger M.A.: The CH2018 scenarios: evaluation and projection of heat stress in Switzerland

15.3   Felber R., Calanca P.: Promoting the use of CH2018: interactive tools for exploring in a flexible way the implications of climate change

15.4   Frehner S., Berger M., Worlitschek J.: HVAC design based on Swiss Climate Scenarios CH2018

15.5   Holzkämper A., Rössler O., Cochand F., Brunner P, Hunkeler D.: Impacts of climate change and management adaptations on agriculture and water resources

15.6   Kotlarski S., Feigenwinter I., Casanueva A., Rajczak J., Fischer A.M., Schwierz C.: The localized CH2018 scenarios: Methods, products, limitations

15.7   Moraga J.S., Peleg N., Molnar P., Fatichi S., Burlando P.: Methodology to estimate future hydrological flows in Switzerland using the new CH2018 climate scenarios

15.8   Mülchi R., Rössler O., Schwanbeck J., Zekollari H., Huss M., Martius O., Weingartner R.: Hydro-CH2018 – new transient hydrological scenarios for Switzerland

15.9   Oliveira Hagen E., Sun Q., Liu Y., Wittwer R., Hartmann M., Keller T., van der Hejden M., Buchmann N.: Resilience of arable cropping systems against climate change – Drought Simulation – Part I Soil Physical parameters

15.10   Schirmer M., Peleg N.: Using the new gridded CH2018 climate scenarios for high resolution snowmelt modelling in small alpine catchments

15.11   Skelton M., Bresch D.N., Pohl C., Dessai S.: The CH2018 Stakeholder Dialogues on Urban Heat in Zurich and Schaffhausen: Discussing practitioners' challenges and science's support

15.12   Zappa M., Zekollari H., Farinotti D., Huss M., Brunner M., Bernhard L.: A hydrological perspective on the use of the CH2018 scenarios: first experiences

POSTER:

P 15.1   Fluixá-Sanmartín J., García Hernández J., Roquier B.: Effects of climate change on drought occurrence in the Valais region (Switzerland) under the new CH2018 scenarios

15.1
Climatic changes in Switzerland over the last 300 years

Brönnimann, S.

Institute of Geography, University of Bern, Hallerstrasse 12, CH-3012 Bern

Switzerland offers various types of information on past climates, including early instrumental data, documentary data, tree rings, and lake sediments. This talk presents climate reconstructions for Switzerland back to the late 17th century, the culmination of the Little Ice Age, against which recent climatic changes can be compared. The focus is on summer temperature, which is particularly well captured in reconstructions and for which confidence intervals referring to a 30-yr average can be constructed. While previous episodes of warming and cooling appear, they all dwarf against the recent warming signal. In particular, cold summers have been completely absent over the past more than 30 years. Precipitation is more difficult to reconstruct and summer precipitation shows no clear signal on multi-decadal time scales and no trends. Wind storms exhibit pronounced multi-decadal changes, but no long term trends. Together, the reconstructions show how climate in Switzerland transited from the Little Ice Age state to the anthropogenic climate of the present.

15.2
The CH2018 scenarios: evaluation and projection of heat stress in Switzerland

Ana Casanueva [1], Sven Kotlarski [1], Andreas M. Fischer [1], Cornelia Schwierz [1] & Mark A. Liniger [1]

[1] *Federal Office of Meteorology and Climatology MeteoSwiss, Operation Center 1, CH-8058 Zurich-Airport (ana.casanueva@meteoswiss.ch)*

Future climate change is likely to have important impacts in many socio-economic sectors. In particular, higher summer temperatures or more prolonged heat waves may be responsible for health problems and productivity losses related to heat stress. Under hot conditions the human body is able to regulate its core temperature via sweat evaporation, but this ability is reduced when air humidity is very high. These conditions of high temperature and humidity invoke heat stress, which is a major problem for vulnerable groups of the population and people exposed to such situations (e.g. working outside or without appropriate cooling systems).

In the present work we explore present and future heat stress over Switzerland in the context of the CH2018 Swiss climate scenarios (www.climate-scenarios.ch). Heat stress is expressed through the Wet Bulb Temperature (WBT), which is a relatively simple proxy for heat stress on the human body and depends non-linearly on temperature and humidity (Stull 2011). Since extreme heat stress conditions occur at sub-daily scale but only daily values are usually available from regional climate models (RCMs), we analyze the sensitivity of the WBT with respect to the use of different daily-aggregated values in its calculation, compared to the maximum WBT obtained from observed hourly data. A large ensemble of state-of-the-art RCM simulations from the EURO-CORDEX initiative (Jacob et al. 2013) is used to produce climate change projections of the WBT. Since RCMs cannot be directly used in impact studies due to their partly substantial biases, a standard bias correction method (empirical quantile mapping, Rajczak et al. 2016) is applied to correct the individual variables that are used to derive the heat stress index. The objectives of this study are twofold, 1) to test the ability of the separately bias-corrected variables to reproduce the main characteristics of the heat stress index in present climate conditions and 2) to explore climate change projections of heat stress considering different sources of uncertainty.

Our results show that the separate bias correction of temperature and humidity allows reproduction of the distribution of the daily maximum WBT. Climate change projections indicate increasing heat stress over Switzerland, which is accentuated towards the end of the century. Heat stress conditions are projected to become more frequent in the future (Fig.1) but the increase largely depends on the emission scenario. They might be about 3-5 times more frequent for the strong emission

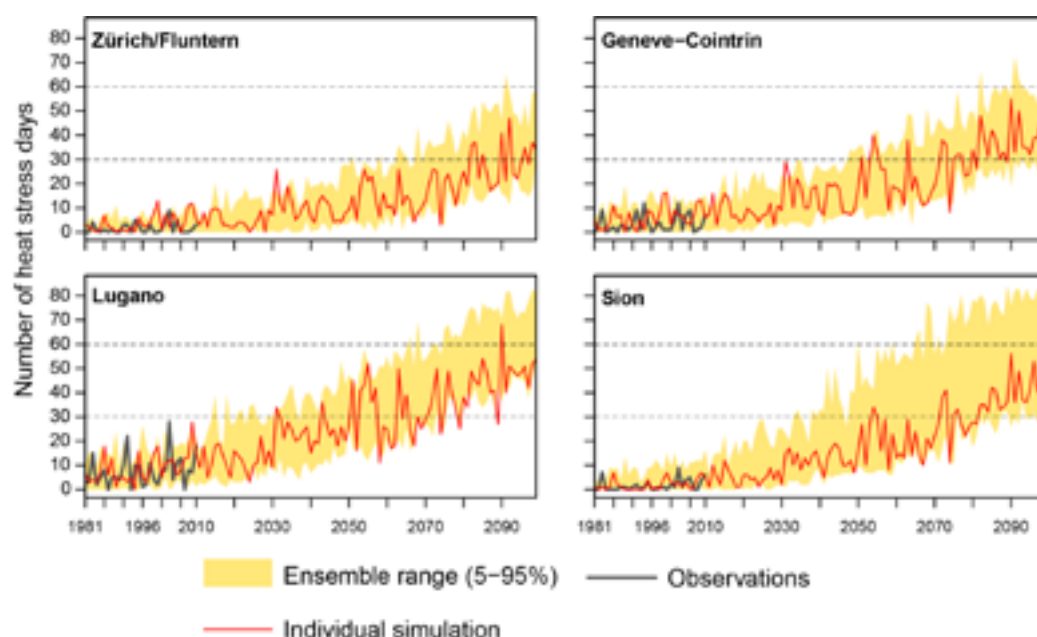scenario than for the mitigation scenario by the end of the 21st century.

Figure 1. Number of summer days with high heat stress (WBT above 22°C) at four Swiss stations for observations (black) and climate change projections (shadings: 90 % of the model range for the strong emission scenario). The red line shows an individual simulation as an example.

REFERENCES

Jacob D., Petersen J., Eggert B., Alias A., Christensen O. B., Bouwer L. M., Braun A., Colette A., Déqué M., Georgievski G., Georgopoulou E., Gobiet A., Menut L., Nikulin G., Haensler A., Hempelmann N., Jones C., Keuler K., Kovats S., Kröner N., Kotlarski S., Kriegsmann A., Martin E., Meijgaard E. v., Moseley C., Pfeifer S., Preuschmann S., Radermacher C., Radtke K., Rechid D., Rounsevell M., Samuelsson P., Somot S., Soussana J.-F., Teichmann C., Valentini R., Vautard R., Weber B. & Yiou P. 2014: EURO-CORDEX: new high-resolution climate change projections for European impact research, Reg. Environ Change. 14, 563-578.

Rajczak, J., Kotlarski, S., Salzmann, N. & Schär, C. 2016: Robust climate scenarios for sites with sparse observations: a two-step bias correction approach, Int. J. Climatology. 36, 1226–1243.

Stull R. 2011: Wet-Bulb Temperature from Relative Humidity and Air Temperature, Journal of Applied Meteorology and Climatology. 50, 2267–2269.

15.3
Promoting the use of CH2018: interactive tools for exploring in a flexible way the implications of climate change

Raphael Felber [1] & Pierluigi Calanca [1]

[1] Agroscope, Climate & Agriculture Group, Reckenholzstrasse 191, CH-8046 Zürich (raphael.felber@agroscope.admin.ch)

In Switzerland a National Centre for Climate Services (NCCS) has been established in 2015 (www.nccs.ch). It aims to deliver climate information for preparing society to climate change. NCCS targets in principle all economic sectors and covers a range of topics such as agriculture, water resources, natural hazards, energy, etc. As part of its activities, NCCS will soon publish the new climate change scenarios for Switzerland (CH2018). The latter will provide the most updated baseline for climate impact studies.

Impact studies are often implemented in a static way, which may limit their further use. For users interested in exploring in a more dynamic way the implications of CH2018 we propose to deliver interactive tools. As an example we present here an app called *FuturePheno*. The app was developed using Shiny, a programming environment that translates R code into interactive web apps. With *FuturePheno* users can investigate how the timing of phenological stages of plant or insect species will change under different climate scenarios. *FuturePheno* requires daily minimum and maximum temperature data provided by the user and applies in a first step an hourly temperature model. Thresholds defining phenological stages can also be specified by the users. Possibilities how interactive tools can be used to explore effects of climate change using CH2018 are discussed.

15.4
HVAC design based on Swiss Climate Scenarios CH2018

Stefan Frehner [1], Matthias Berger [1], Jörg Worlitschek [1]

[1] *Competence Center Thermal Energy Storage, Lucerne School of Engineering and Architecture*, Technikumstrasse 21, CH-6048 Horw (matthias.berger@hslu.ch)

Lucerne University of Applied Sciences and Arts' campus in Horw/ Switzerland will under scheduled retrofit and three-fold extension, to be finished by 2025 (Frehner 2018). The new heating, ventilation and air conditioning (HVAC) equipment has a lifetime of 40 years, serving until 2065. With current building construction norms by the *schweizerischer ingenieur- und architektenverein* (SIA) considering the climate normal period of 1981-2010, the related climate data is 70 years in the past. For dimensioning and design of the HVAC equipment, preliminary results from the Swiss Climate Scenarios CH2018 for RCPs 2.6, 4.5 and 8.5 have been used to determine future heating and cooling demand (Berger & Worlitschek 2018a, 2018b). Lake Lucerne will be tapped for feeding a low-temperature district heating & cooling network, and the campus is going to be one of the first clients. Since heating demand is expected to decrease, while cooling demand is increasing, this opportunity to use ambient energy would represent a testbed for a broader application, as many Swiss cities are located near the lakeshore. Depending on the scenario, heating and cooling degree days are a useful proxy for the HVAC energy demand. In the worst case (RCP8.5), the decrease in heating demand until 2065 is substantial (approximately 25 %), which influences both, necessary peak power and seasonal energy consumption. The opposite behaviour is observed for the cooling demand. Thermal energy storage technologies together with local solar photovoltaic production will enable a high level of self-sufficiency in terms of energy.

Due to the large thermal capacity and low temperature of the Lake Lucerne at the extraction point in a depth between 30 and 40 meters, cooling can be realized efficiently, carrying low operational costs. Furthermore, local microclimate conditions are not negatively impacted, neither in the Lake (Imboden & Wüest 1995) nor on shore. Overall, climate change has significant consequences for HVAC design, where a strong leverage for GHG reduction and energy efficiency are found.
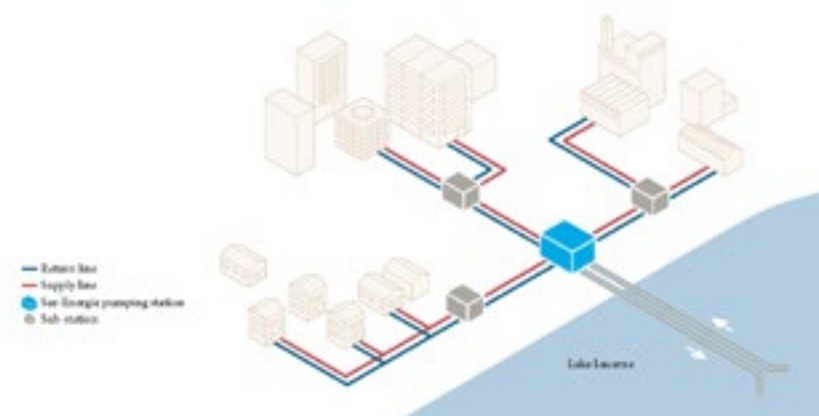
Figure 1. Concept of the district heating & cooling network using ambient energy from the Lake Lucerne. [Source: www.ewl-luzern.ch "See-Energie"]
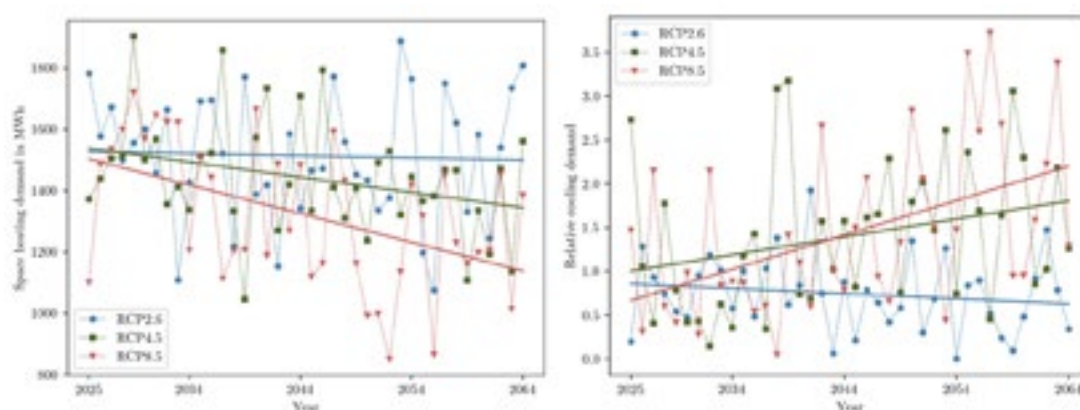

Figure 2. Future trends of the annual space heating & cooling demand of the Campus Horw for the three climate scenarios RCP2.6, RCP4.5 and RCP8.5.
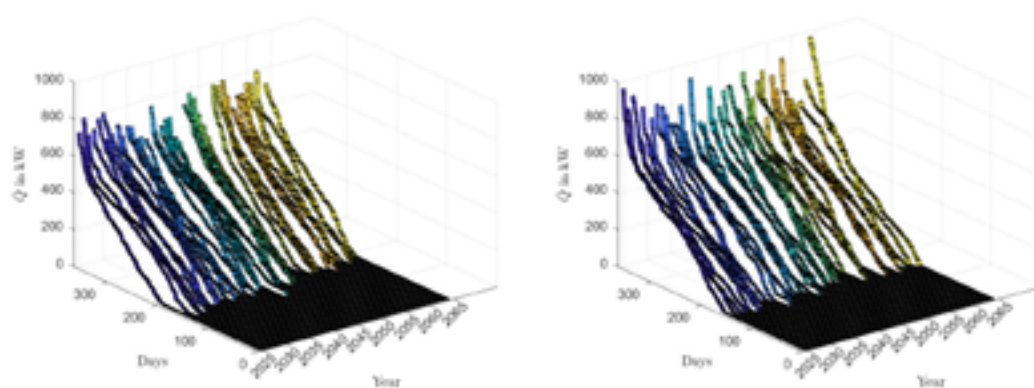

Figure 3. Annual accumulated heat load curves for the climate scenarios RCP2.6 (left) and RCP8.5 (right).

REFERENCES

Berger, M. & Worlitschek, J. 2018a: A novel approach for estimating residential space heating demand, Energy, 159, 294-301.

Berger, M. & Worlitschek, J. 2018b: The influence of climate trends on heating and cooling demand, [in preparation].

Frehner, S. 2018: The use of the lake lucerne as a thermal energy storage in combination with district heating in 2000W areas, Master Thesis.

Imboden D.M., Wüest A. 1995, Mixing Mechanisms in Lakes. In: Lerman A., Imboden D.M., Gat J.R. (eds), Physics and Chemistry of Lakes. Springer, Berlin, Heidelberg.

15.5
Impacts of climate change and management adaptations on agriculture and water resources

Annelie Holzkämper [1], Ole Rössler [2], Fabien Cochand [3], Philip Brunner [3], Daniel Hunkeler [3]

[1] Climate and Agriculture Group, Agroscope, Reckenholzstr. 191, CH-8046 Zurich
   (annelie.holzkaemper@agroscope.admin.ch)
[2] Institute of Geography, University of Bern, Hallerstr. 12, CH-3012 Bern
[3] Université de Neuchâtel, Centre d'hydrogéologie et de géothermie (CHYN), Emile-Argand 11, CH-2000 Neuchâtel

Climate change will profoundly alter production conditions for agriculture in Switzerland, making the need for adaptation unavoidable. Feedbacks of agricultural management adaptations on the hydrological system were not studied in Switzerland so far – leaving a potential risk of maladaptation unevaluated.

In this study, we apply a coupled modelling system (crop-hydrological-hydrogeorological) to an aquifer catchment in the Bernese Seeland (1) to evaluate impacts of climate change on future water demand for irrigation and on groundwater resources, (2) to evaluate combined effects of climate change and irrigation on groundwater resources, and (3) to explore which alternative adaptation strategies could reduce the risk of maladaptation in the long term (e.g. shifts in crop mixtures, allocation of cultivation zones).

For the most pessimistic emission pathway RCP8.5, the model results suggest that until 2099, crop productivity for most arable crops will be severely affected. Thereby, limitations through increasing temperatures are more severe than water limitations – making a shift in the varietal choice (towards varieties with higher temperature requirements) unavoidable. Considering that varieties will be adapted to increasing temperatures, net irrigation requirements will increase by up to 60% in annual mean until the end of the century. Expected impacts on agricultural production are accompanied by projected reductions in ground- and surface water resources. While annual streamflow into the aquifer catchment (Aare Hagneck) will remain on today's level until 2070, a decrease by 13 % in comparison to (1985-2009) is projected for the end of the century (2075-2099). Thereby, a strong decrease in summer and autumn streamflow (-46% and 30%, respectively) could not be compensated by the increases during winter (+39%) and spring (+13%). Regarding changes in groundwater resources, a decrease by about 50 cm in groundwater heads in summer is projected for the most pessimistic scenario (RCP8.5). Further investigations will show how sceanrios of agricultural intensification and extensification would influence ground- and surface water bodies as well as agricultural production.

15.6
The localized CH2018 scenarios: Methods, products, limitations

Sven Kotlarski [1], Iris Feigenwinter [1,2], Ana Casanueva [1], Jan Rajczak [1,3], Andreas M. Fischer [1] & Cornelia Schwierz [1]

[1] Federal Office of Meteorology and Climatology MeteoSwiss, Operation Center 1, CH-8058 Zurich-Airport
  (sven.kotlarski@meteoswiss.ch)
[2] Institute of Agricultural Sciences, ETH Zurich, Universitätstrasse 2, CH-8092 Zurich
[3] Institute for Atmospheric and Climate Science, ETH Zurich, Universitätstrasse 16, CH-8092 Zurich

In the context of the CH2018 Swiss climate scenarios (www.climate-scenarios.ch) empirical quantile mapping (QM) has been employed to bias-correct and downscale raw climate model output. The resulting data products are directly applicable in climate impact research. We here present the overall CH2018 QM approach as well as exemplary results. The approach consists of two different QM setups that target two different spatial scales: the local station scale and a high-resolution 2 km grid covering the whole of Switzerland (Fig. 1). All setups produce transient time series (1981-2099) of several meteorological variables at daily resolution and for all climate model chains considered in CH2018.

The evaluation of QM yields a satisfactory performance in the historical reference period. Systematic climate model biases of seasonally averaged quantities are largely removed, and spatial climate variability at climatological time scales is properly represented by the QM data. As a consequence of removing intensity-dependent climate model biases, QM can slightly modify the raw models' climate change signals. But the overall consistency with the raw model output and, hence, with further CH2018 products is maintained.

The QM-derived scenario-data products can ultimately be employed by climate impact studies over the Swiss terrain but, at the same time, are subject to a number of caveats and limitations. These need to be properly assessed by users for each specific application.
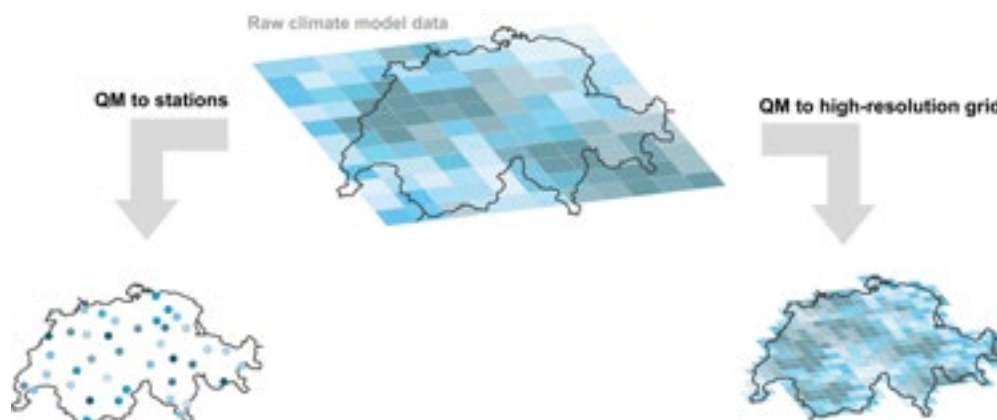

Figure 1. The two QM setups employed in the context of CH2018.

15.7
Methodology to estimate future hydrological flows in Switzerland using the new CH2018 climate scenarios

Jorge Sebastian Moraga, Nadav Peleg, Peter Molnar, Simone Fatichi, Paolo Burlando

Institute of Environmental Engineering, ETH Zurich, Switzerland (moraga@ifu.baug.ethz.ch)

The new CH2018 climate scenarios allow re-estimation of the impact climate change will have on the hydrological regime in Switzerland. With new tools and methods, the uncertainty derived from the natural variability of climate, and its propagation throughout the catchment response is studied. The methodology consists of a distributed weather generator, a physically-based hydrological model, and is set in a stochastic (simulation) framework.

First, using a two-dimensional stochastic weather generator model, AWE-GEN-2d [Peleg et al., 2017], an ensemble driven by the new CH2018 scenarios of future climate variables (e.g. precipitation, near-surface air temperature and incoming shortwave radiation) is generated for three Swiss catchments (Thur, Maggia and Kleine Emme). The model was calibrated with observations from weather stations, a weather radar system and satellite images to reproduce the current-climate on sub-kilometre and hourly resolutions (e.g. rainfall annual totals and monthly temperatures, Fig. 1 and 2 respectively) and was then re-parameterized to simulate climate variables for future periods (2020-2099) based on the new CH2018 scenarios using the factors of change method [Fatichi et al., 2011].

Second, the climate ensemble is used to feed the physically based distributed hydrological model Topkapi-ETH, in order to characterize the future hydrology of the catchments and to quantify the uncertainties in climate and hydrology under different emission scenarios and climate models. The modelling chain allows us to focus the analysis of impacts of climate change on a range of inter-related hydrological processes distributed in space (e.g. evapotranspiration, snow cover dynamics, high and low flows), providing information on elevation dependencies, catchment size effects, etc. A comparison is made between the impacts of the old and new Swiss climate scenarios on the hydrological regime and the changes that are of relevant for the policy makers are studies, with emphasize on extreme climatic and hydrological events.
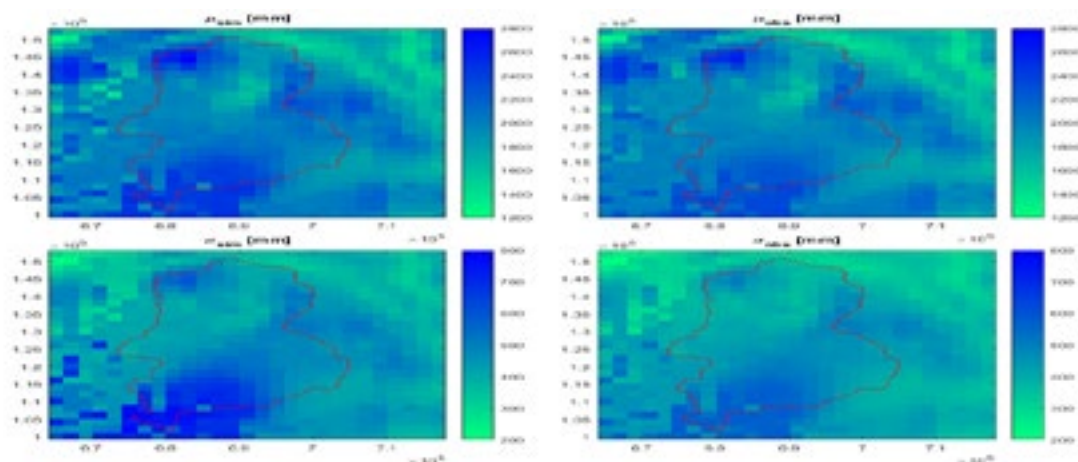

Figure 1. Simulated (μ_{sim}) and observed (μ_{obs}) mean annual rainfall (in mm) for the Maggia catchment.
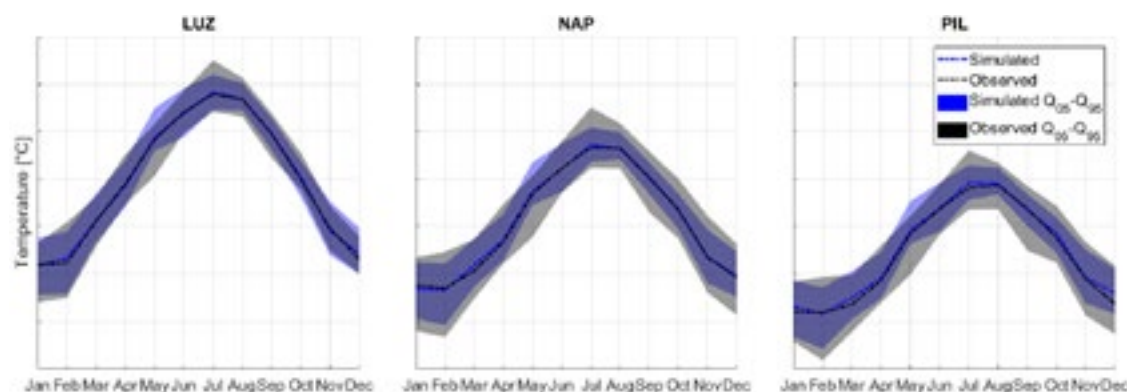

Figure 2: Monthly mean (dashed lines), and 5th-95th quantile range (transparent shade) of temperature for the simulated (blue) and observed (black) temperature in the Lucerne (LUZ, left), Napf (NAP, centre), and Pilatus (PIL, right) weather stations in the domain of the Kleine Emme catchment.

REFERENCES

Fatichi, S., Ivanov, V. Y., & Caporali, E. 2011. Simulation of future climate scenarios with a weather generator. Advances in Water Resources, 34(4), 448–467.

Fatichi, S., Ivanov, V. Y., Paschalis, A., Peleg, N., Molnar, P., Rimkus, S., Kim, J., & Caporali, E. 2016. Uncertainty partition challenges the predictability of vital details of climate change. Earth's Future, 4(5), 240–251.

Peleg, N., Fatichi, S., Paschalis, A., Molnar, P., & Burlando, P. (2017). An advanced stochastic weather generator for simulating 2-D high-resolution climate variables. Journal of Advances in Modeling Earth Systems, 9(3), 1595–1627.

15.8
Hydro-CH2018 – new transient hydrological scenarios for Switzerland

Regula Mülchi [1], Ole Rössler [1], Jan Schwanbeck [1], Harry Zekollari [2], Matthias Huss [2,3], Olivia Martius [1], Rolf Weingartner [1]

[1] Oeschger Centre for Climate Change Research and Institute of Geography, University of Bern, Hallerstrasse 12, CH-3012 Bern (regula.muelchi@giub.unibe.ch)
[2] Laboratory of Hydraulics, Hydrology and Glaciology, ETH Zurich, Hönggerbergring 26, CH-8093 Zurich
[3] Department of Geosciences, University of Fribourg, Chemin du Musée 4, CH-1700 Fribourg

Changes in runoff regimes have impacts on many different sectors such as agriculture, energy production, water management, etc. Thus, assessing future changes in runoff is very crucial for adaptation planners and decision-making authorities. Under the comprehensive framework Hydro-CH2018 (coordinated by the Swiss Federal Office for the Environment), we are simulating future runoff for the period 1980-2099 in Switzerland. The study uses the new transient Swiss climate change scenarios CH2018 (will be published by end of 2018) with different emission pathways (RCP2.6, RCP4.5 and RCP8.5) as input for the hydrological model. The hydrological simulations are based on the semi-distributed hydrological model PREVAH (Viviroli et al., 2009). Changes in the glacier extent are incorporated from external simulation of glacier development for the next century. Over 180 catchments distributed over Switzerland covering a wide range of different catchment characteristics are simulated and analyzed. The project determines potential runoff regime shifts under climate change. The transient property of the climate change scenarios enables the study to focus on the time of emergence of potential regime shifts. Further, analyzing trends in low flow (e.g. Q347) and high flow (e.g. flood frequency) indices provides a comprehensive perspective on the hydrological responses to climate change in Switzerland.

REFERENCES

Viviroli, D., Zappa, M., Gurtz, M., & Weingartner, R. 2009: An introduction to the hydrological modelling system PREVAH and its pre- and post-processing-tools, Environmental Modelling & Software, 24, 1209-1222.

15.9

Resilience of arable cropping systems against climate change – Drought Simulation - Part I Soil Physical parameters

Emily Oliveira Hagen [1,2], Qing Sun [2], Yujie Liu [2], Raphaël Wittwer [1,3], Martin Hartmann [4], Thomas Keller [1,5], Marcel van der Hejden [1, 6]and Nina Buchmann [2]

[1] Agroscope Reckenholz, Plant-soil Interaction Group
[2] ETH Zurich, Institute of Agricultural Sciences, Grassland Sciences
[3] University of Zürich
[4] ETH Zurich, Institute of Agricultural Sciences, Sustainable Agroecosystems
[5] Swedish University of Agricultural Sciences
[6] Utrecht University

Over the last 30 years, Swiss temperature has increased with an annual average warming rate of 0.35°C per decade. In addition, models project a higher frequency of extreme events and greater climate instability, with a mean reduction in Swiss summer precipitation by mid of the century of around 15% (CH2011).This, together with the increase in evapotranspiration associated with warming, will subject crops to more severe drought periods. Within the 3 years research project RELOAD (Resilience of Organic and Conventional Production Systems to Drought, Mercator Schweiz Stiftung) we investigate the resistance and resilience of important arable cropping systems to simulated summer drought. For this, we make use of the long-term Farming system and Tillage experiment (FAST) comparing since 2009 four main cropping systems: conventional cropping with intensive tillage and no tillage and organic cropping with intensive tillage and reduced tillage. Summer drought was simulated on field in two consecutive years with rainout shelters installed at the plot level. Our focus crop was Maize, since it is a crop particularly sensitive to drought (Daryanto et al. 2016) and therefore a good indicator to investigate the potential damages of the predicted increase in summer drought. Crop yield, nutrient uptake and grain quality are compared to a control, uncovered, part of the plots. These variables are coupled with other three research fronts; the plant water uptake dynamics, plant-soil microbial interaction and nitrogen related functions, by three PhD projects running in parallel at the field trial.

Precipitation balance and the amount of rain excluded were assessed, however, these are not directly translated to water accessibility, and could be influenced by soil properties and farming practices (Hatfield 2011). Therefore, as an initial step to better understand the potential occurrence of drought stress for crops, we investigate not only the spatial suitability and climatic conditions but also the interaction of soil properties and climate. In the FAST trial, we have the advantage of working on a long-term experiment, in which farming systems have been managed for 9 years under standardized conditions. Besides focusing on tillage effects on soil physical properties, we investigated the potential build-up of soil hydraulical properties due to different managements. To date, studies have shown the importance of soil management on root architecture and water accessibility (Moreno et al. 1997, Colombi et al. 2018) but it is not clear how different farming practices (i.e. Organic and Conventional with intensive and conservation tillage practices) respond to the eminent threat of summer droughts and related limitations in water accessibility. Therefore, coupling all the research fronts of this project, our results will contribute to i) a better understanding of important processes taking place at different cropping systems, and ii) formulating pro-active responses to climate change, allowing for gradual and informed adaptation to better meet agricultural goals. Here, we present the summary of the soil physical properties and plant water availability of the targeted cropping systems.

REFERENCES

CH2011 (2011). Swiss Climate Change Scenarios CH2011. Zürich, C2SM, MeteoSwiss, ETH, NCCR Climate, and OcCC.

Colombi, T., L. C. Torres, A. Walter and T. Keller (2018). "Feedbacks between soil penetration resistance, root architecture and water uptake limit water accessibility and crop growth – A vicious circle." Science of The Total Environment 626: 1026-1035.

Daryanto, S., L. Wang and P.-A. Jacinthe (2016). "Global Synthesis of Drought Effects on Maize and Wheat Production." PLoS ONE 11(5): e0156362.

Hatfield, J. L. (2011). Soil Management for Increasing Water Use Efficiency in Field Crops Under Changing Climates. UNL Faculty. U. S. D. o. A. A. R. Service. Lincoln, Nebraska: 1376.

Moreno, F., F. Pelegrín, J. E. Fernández and J. M. Murillo (1997). "Soil physical properties, water depletion and crop development under traditional and conservation tillage in southern Spain." Soil and Tillage Research 41(1): 25-42.
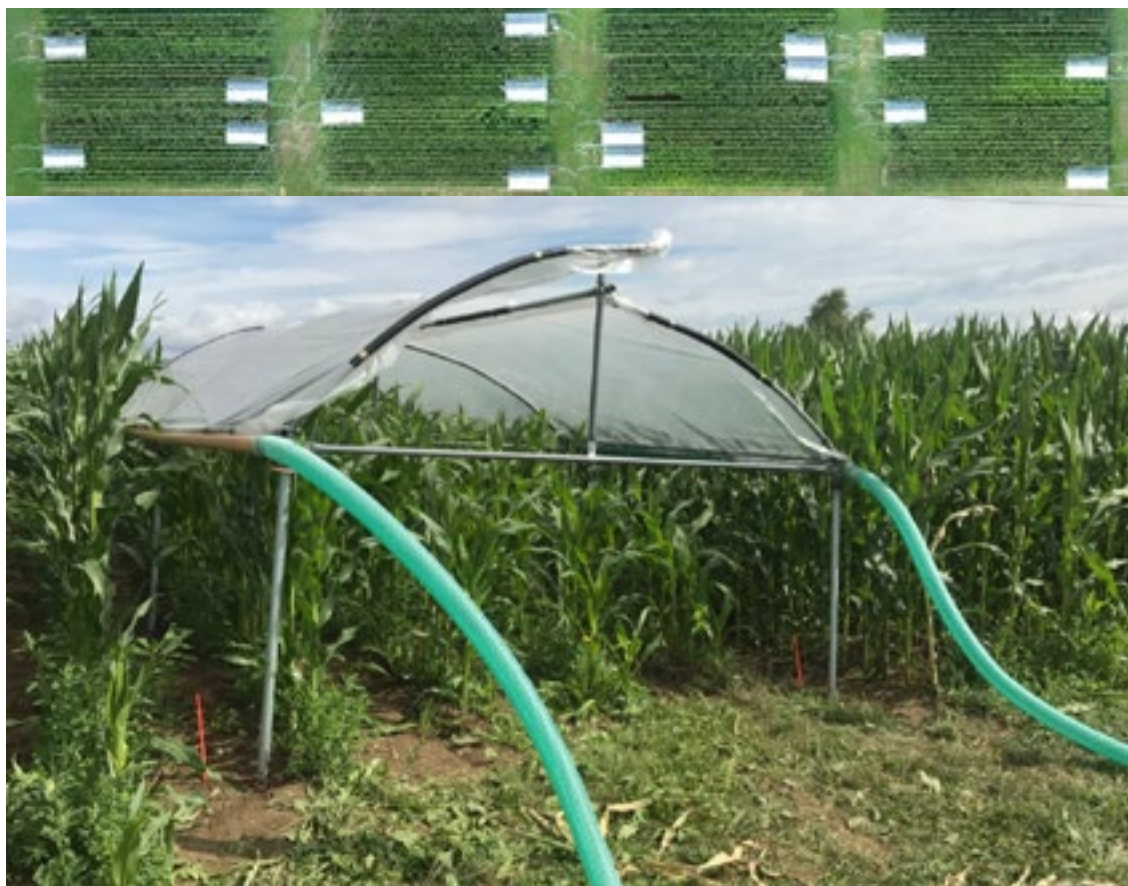
Figure 1. Up: Aerial photo of field trial with shelters installed in plots (Photo: Raphael Wittwer); and bottom picture, roof design at plot, with maize crop.

15.10

Using the new gridded CH2018 climate scenarios for high resolution snowmelt modelling in small alpine catchments

Michael Schirmer [1], Nadav Peleg [2]

[1] WSL Institute for Snow and Avalanche Research SLF, Flüelastrasse 11, 7260 Davos Dorf, (michael.schirmer@slf.ch)
[2] Hydrology and Water Resources Management, Institute of Environmental Engineering, ETH Zurich, Stefano-Franscini-Platz 5, 8093 Zurich

Snow in the Alps is affected by climate change with regard to duration, timing and amount. This has implications with respect to important societal issues as drinking water supply or hydropower generation. In Switzerland, the latter received a lot of attention following the political decision to phase out of nuclear electricity production. An increasing number of authorization requests for small hydropower plants located in small alpine catchments was observed in the recent years. This situation generates ecological conflicts, while the expected climate change poses a threat to water availability thus putting at risk investments in such hydropower plants. Reliable high-resolution climate scenarios are thus required, which account for small-scale processes to achieve realistic predictions of snowmelt runoff and its variability in small alpine catchments. We therefore used a novel model chain by coupling a stochastic 2-dimensional weather generator (AWE-GEN-2d) with a state-of-the-art energy balance snow cover model (JIM). AWE-GEN-2d was applied to generate ensembles of climate variables at high temporal and spatial resolution, thus providing all climatic input variables required for the energy balance modelling. The landsurface model JIM was used to describe spatially variable snow cover accumulation and melt processes. The JIM was refined to allow applications at very high spatial resolution by specifically accounting for small-scale processes, such as a subgrid-parametrization of snow covered area and snow redistribution. For the present study, simulations were shown for a small alpine mountain catchment. 40-year of monitoring data for snow water equivalent, snowmelt and snow-covered area for entire Switzerland was used to verify snow distribution patterns at coarser spatial and temporal scale. Subsequently, predictions of Snow Water Equivalent and snow melt were generated using CH2018 climate scenarios until the end of this century, addressing uncertainty sources associated with scenario uncertainty, climate model uncertainty and natural variability. The ability of the model chain to reproduce current climate conditions in small alpine catchments makes this model combination an outstanding candidate to produce high resolution climate scenarios of snowmelt in small alpine catchments.

15.11

The CH2018 Stakeholder Dialogues on Urban Heat in Zurich and Schaffhausen: Discussing practitioners' challenges and science's support

Maurice Skelton [1,2] David N. Bresch [1,2] Christian Pohl [1] & Suraje Dessai [3]

[1] Institute for Environmental Decisions, Swiss Federal Institute of Technology ETH Zurich, Universitätstrasse 16, CH-8092 Zürich (maurice.skelton@usys.ethz.ch)

[2] Federal Office of Meteorology and Climatology MeteoSwiss, Operation Center 1, P.O. Box 257, 8058 Zurich Airport, Switzerland

[3] Sustainability Research Institute and ESRC Centre for Climate Change Economics and Policy, School of Earth and Environment, University of Leeds, LS2 9JT, UK

Our previously undertaken qualitative research with sectoral experts in Swiss administration highlighted that the climate knowledge exchange between practitioners and scientists is, in Switzerland, not formally organised. This leads to a knowledge flow disruption, as people attend different events and discuss new knowledge products in different circles. As such, both practitioners and scientists remain too often unaware of new climate knowledge items. We conclude that not only the type of climate information itself can be a barrier for practitioners, but that also the *format of climate knowledge flow* is a barrier for climate information achieving its aim of supporting public and private decision-making. Which *type of information* the new CH2018 Swiss climate scenarios should contain has already been researched in MeteoSchweiz (2016). However, the question of the *format of climate knowledge flow* has not been addressed, both internationally nor nationally.

In order to address this issue in the new CH2018 Swiss climate scenarios, we have run various stakeholder engagement activities alongside the larger modelling efforts. Taking the specific challenge of urban heat, we ran two workshops in autumn 2018, one in the city of Schaffhausen and one in the city of Zurich. We invited experts from the sectors "urban greens", "building technology", "spatial planning" and "health" as well as CH2018 producers to discuss two questions: (i) what are the climate knowledge products used and climate events attended by all participants? And (ii) what are the sectoral challenges faced by practitioners, and what support can CH2018 scientists provide in meeting those adaptation challenges?

This presentation offers further insights into how the knowledge exchange between practitioners and scientists took place during these two workshops. We'll close by highlighting the final workshop discussion, on how the knowledge exchange flow could be improved, so that CH2018 and other climate information products achieve their aims of informing Swiss adaptation and mitigation decisions.

REFERENCES

MeteoSchweiz (2016) Analyse der Nutzerbedürfnisse zu nationalen Klimaszenarien, *Fachbericht MeteoSchweiz*, 258, 92 pp.

15.12
A hydrological perspective on the use of the CH2018 scenarios: first experiences

Massimiliano Zappa [1], Harry Zekollari [1], Daniel Farinotti [1], Matthias Huss [2], Manuela Brunner [1] & Luzi Bernhard [1]

[1] Swiss Federal Research Institute WSL, Zürcherstrasse 111, CH-8903 Birmensdorf (massimiliano.zappa@wsl.ch)
[2] University of Fribourg, Unit of Geography - Chemin du Musée 4 - 1700 Fribourg
[3] ETH Zurich Laboratory of Hydraulics Hydrology and Glaciology VAW, Hönggerbergring 26, 8093 Zürich

When climate scientits issue new scenarios on the future development of regional climate conditions, many other disciplines are interested in assessing the impacts of such projections on particular parts of the natural system such as rivers, forests, glaciers or agriculture. In the case of hydrology (Speich et al., 2015), such projections serve as the input for a hydrological model which is run to generate runoff time series representing future climate conditions. Such time series can be used to analyze different aspects related to the hydrological system such as sediment transport (Raymond Pralong et al. 2015), fish habitats (Junker et al., 2015) or hydropower generation (Schädler et al., 2011).

MeteoSwiss andC2SM are in in the last phase of preparing such climate scenarios for Switzerland (CH2018) and has provided selected users with access to these scenarios (via http://www.ch2018.ch/en/home-2/). In the framework of the Hydro-CH2018 program initiated by the Swiss Federal Office for Environment, we used these new scenarios to look at their impact on different parts of the hydrological system. The use of the new scenarios in hydrological impact studies, however, required some updates of the modeling system PREVAH used in previous studies (CCHYDRO, FOEN, 2012). First, the model had to be adjusted such that it can be used on transient simulations generated by 39 climate model chains consisting of different combinations of: a) global circulation model, b) regional circulation model and c) target of CO_2 emissions (RCP2.6, RCP4.5 and RCP8.5). Second, the glacier fields used for simulating glacier melt had to be adjusted in order to represent future glacier extents and volumes. This contribution presents highlights from generating the glacio-hydrological inputs needed to update the hydrological model PREVAH and presents a selection of preliminary technical and scientific findings from the application of these scenarios in Swiss catchments.

The general message of previous hydrological impact assessments might not change with respect to previous assessments (Figure 1), however, the use of transient simulations will allow for a more realistic representation of the variability in the hydrological system as compared to previous experiments relying on the "delta-change" methodology, which used observed temporal patterns for representing the variability of individual climate variables. A better representation of the variability in hydrological variables is expected to be of particular importance when interested in changes in drought indicators such as the frequency and duration of dry spells.
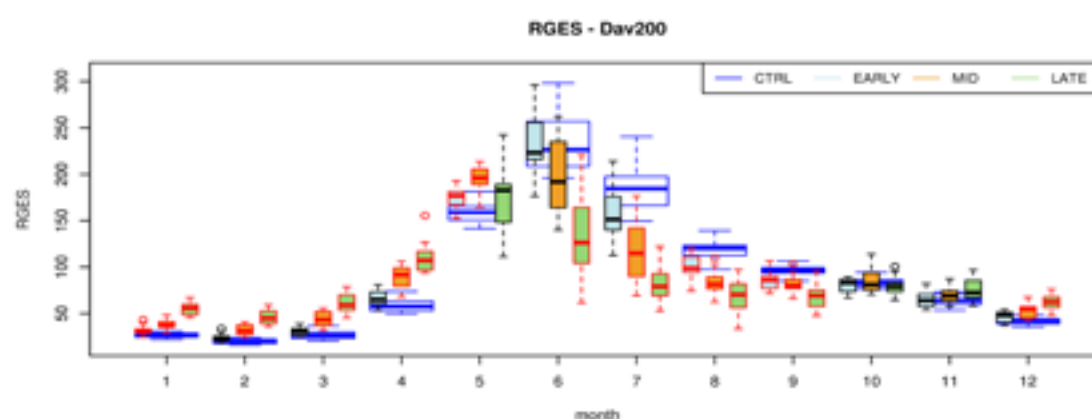

Figure 1. Landscape Davos: Preliminary visualization of simulated discharge (RGES, mm/month) obtained by using RCP8.5 forcing from the new CH2018 climate scenarios. Large blue boxes show the situation for 1981-2010 using bias corrected forcing. Lightblue boxes: situation 2005-2035. Orange boxes: situation 2035-2065. Green boxes: situation 2061-2099. Red-framed boxes are assigned in case of significant change. This figure is presented with the courtesy of and in aggreement with the providers of the CH2018 scenarios.

REFERENCES

Federal Office for the Environment FOEN. 2012: Effects of Climate Change on Water Resources and Waters. Synthesis report on "Climate Change and Hydrology in Switzerland" (CCHydro) project. Federal Office for the Environment, Bern. Umwelt-Wissen No 1217: 74

S. Junker, J., Heimann, F. U. M., Hauer, C., Turowski, J. M., Rickenmann, D., Zappa, M., & Peter, A. 2015: Assessing the impact of climate change on brown trout (Salmo trutta fario) recruitment. Hydrobiologia, 751(1), 1-21. https://doi.org/10.1007/s10750-014-2073-4

Raymond Pralong, M., Turowski, J. M., Rickenmann, D., & Zappa, M. 2015: Climate change impacts on bedload transport in alpine drainage basins with hydropower exploitation. Earth Surface Processes and Landforms, 40(12), 1587-1599. https://doi.org/10.1002/esp.3737

Schädler, B., Weingartner, R., & Zappa, M. 2011: Auswirkungen der Klimaänderung auf die Wasserkraftnutzung. Einleitung und Überblick über das Projekt. *Wasser, Energie, Luft*, *103*(4), 265-267.

Speich, M. J. R., Bernhard, L., Teuling, A. J., & Zappa, M. 2015: Application of bivariate mapping for hydrological classification and analysis of temporal change and scale effects in Switzerland. Journal of Hydrology, 523, 804-821. https://doi.org/10.1016/j.jhydrol.2015.01.086

P 15.1

Effects of climate change on drought occurrence in the Valais region (Switzerland) under the new CH2018 scenarios

Javier Fluixá-Sanmartín [1], Javier García Hernández [1] & Bastien Roquier [1]

[1] Centre de Rechercher sur l'Environnement Alpin, Rue de l'Industrie 45, CH-1951 Sion (javier.fluixa@crealp.vs.ch)

Drought is a phenomenon that results from persistent deficiency of precipitations over an extended period of time compared with long-term average condition. Morever, Climate change is susceptible to alter the rainfall deficiency patterns and thus impact on the occurrence of drought events and/or their intensity.

The use of drought indices is convenient for tracking droughts and for providing a quantitative assessment of the severity, location, timing and duration of such events (Hayes 2011). For instance, the widely used meteorological index Standardized Precipitation Index (SPI; McKee et al. 1993) employs historical precipitation records and can easily compute the occurrence and magnitude of droughts for various timescales. Lower SPI values indicate dryer conditions.

The impact of climate change on the drought occurrence based on the SPI values has been analyzed and applied to the Canton of Valais in Switzerland. The new Swiss scenarios CH2018 (Swiss Climate Scenarios CH2018, 2018) have been used to assess how climate change is expected to affect drought occurrence in the Valais. The CH2018 data employed are the daily precipitation projections at different stations of the Valais region, issued from different climate models and Representative Concentration Pathways (RCP2.6, RCP4.5, and RCP8.5). Data spans both the historical (1981-2010) and future horizons (2011-2099) of the simulation.

Based on this information, the SPI has been calculated for the complete 1981-2099 period to contrast the impact of climate change. The occurrence of drought events has been identified for the entire study region and contrasted with the conditions of the 1981-2010 period. In addition, a trend analysis using the Mann-Kendall test was performed to the SPI values, the duration of the events detected and the drought intensity[1]. It provided a general perception of how these values are expected to change until the end of the 21st century.

For each station, the SPI series have been computed for all the possible combinations of climate models and RCPs. Results show an important scattering and are sensible to the choice of the climate model, the RCP and the SPI timescale. No general trend can be confirmed towards lower or higher SPI values. Among the cases with a significant trend (about 30% of the total):
- Only 5% of the cases present decreasing SPI values while 95% present positive trend fro the RCP2.6.
- 35% present decreasing SPI values while 65% present positive trend fro the RCP4.5.
- 47% present decreasing SPI and 53% increasing values over the study period for the RCP8.5.

Regarding the duration and intensity of drought events obtained based on the criteria defined by McKee et al. (1993) no significant variations have been detected, except for some specific cases (in particular for the RCP8.5 scenario, cf. Figure 1).

Preliminary conclusions are thus not conclusive on the evolution of drought conditions in the future. Since temperatures are expected to increase with climate change, more reliable results have to been obtained using indices that rely on both precipitation and temperature variables, e.g. the Standardised Precipitation-Evapotranspiration Index (SPEI; Vicente-Serrano et al., 2010).

REFERENCES

Hayes, M.J., 2011: Comparison of Major Drought Indices: Introduction. National Drought Mitigation Center.

McKee, T.B., N.J. Doesken, & J. Kleist, 1993: The relationship of drought frequency and duration to time scales. Proceedings of the 8th Conference on Applied Climatology, 17–23 January 1993, Anaheim, CA. Boston, MA, American Meteorological Society.

Swiss Climate Scenarios CH2018, 2018 (www.climate-scenarios.ch).

Vicente-Serrano, S.M., Beguería, S. & López-Moreno, J.I., 2010: A Multi-scalar drought index sensitive to global warming: The Standardized Precipitation Evapotranspiration Index - SPEI. Journal of Climate 23: 1696-1718.

---

[1] The intensity of a drought is the positive sum of the SPI for each month during the drought event, divided by its duration.
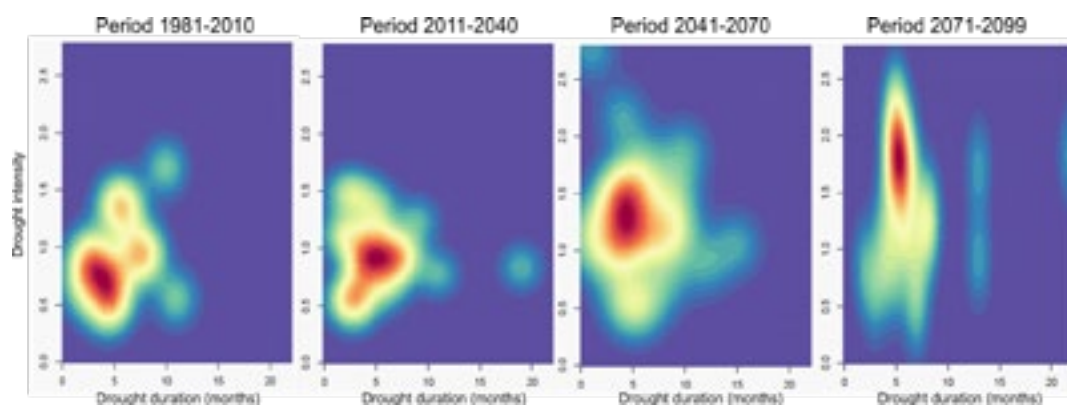
Figure 1. Example of evolution of the drought *Intensity vs Duration* relation of events according to the CLMCOM.CCLM4.HADGEM.EUR11 climate model under the RCP8.5 scenario (left to right: period 1981-2010, 2011-2040, 2041-2070, 2071-2099).

16. Climate Change Education and Outreach

Moritz Gubler, Marco Adamina, Matthias Probst, Sibylle Reinfried, Peter Stucki

Swiss Association of Geographers (ASG)
Swiss Association for Geographic Education (VGDch)

TALKS:

16.1   Colberg C.: Experiences of nature and environmental attitude of primary school children as a starting point for research-based Climate Change Education in teacher training

16.2   Gubler M., Brügger A., Brönnimann S., Eyer M.: Opportunities and limitations of local climate information in climate change education

16.3   Guckes K., Fischer S., Siegmund A.: Dem Klimawandel nachhaltig begegnen lernen – Förderung der Handlungskompetenz von Jugendlichen zur Anpassung an die regionalen Folgen von Klimaveränderungen in Baden-Württemberg

16.4   Linsbauer A., Chow N., Christen J.,Gattlen J., Gertschen M., Heeb N., Hoelzle M., Keller F., Lozza H., Meeus B., Millhäusler A., Scherler M., Spoerri R.: Expedition 2 degree: The 2°C target in the Alps – An Experience in Virtual Reality

16.5   Reinfried S., Adamina M., Probst M.: Education on climate change and climate policy: learning opportunities for all school levels.

POSTERS:

P 16.1   Eugster M.: Climate change education and projects in Swiss secondary schools

P 16.2   Hernández-Almeida I., Korpanty C., Boehnert S., Borges R., Cavaleiro C., Contreras A., Durán Toro V., Elyashiv H., Hohmann S., Kirillova V., Liu Y., Madaj L., Martínez Méndez G., Müller-Dum D., Neto dos Santos C., Paz Orfanoz-Cheuquelaf A., Costa Portilho-Ramos R., Rebotim A., Reyes Macaya D., Rossel P., Saavedra-Pellitero M., Schmidt C., Tamborrino L., Tangunan D., Wang H.: "Once Upon a Time…" – Using fictional stories to educate about climate, oceans and science

P 16.3   Subedi S., Hetényi G., Sauron A., Denton P.: Seismology-at-School in Nepal: Education and outreach

P 16.4   Winkler B., Cook J.: Using an interdisciplinary MOOC to teach climate science and science communication to a global classroom

P 16.5   Naegeli K., Habermann M., Kronenberg M., Hellmann L., Schwikowksi M.: Girls on Ice Switzerland – using immersion to inspire interest in science

16.1
Experiences of nature and environmental attitude of primary school children as a starting point for research-based Climate Change Education in teacher training

Christina Colberg

Pädagogische Hochschule Thurgau (PHTG) , Unterer Schulweg 3 , CH-8280 Kreuzlingen 2.
(christina.colberg@phtg.ch) UND
Departement für Umweltsystemwissenschaften, Didaktikzertifikat Umweltlehre, Universitätstrasse 16, CH-8006 Zürich.

Climate change is one of the challenges for the coming generations. Learners of all ages should be sensitized for this topic. The aim is to ensure that learners acquire skills that will enable them to actively and responsibly shape the future (éducation21, 2016).
In order to enable student teachers and in service teachers to implement climate change issues effectively in their classrooms different actions are taken at the Teacher Training University of Thurgau (PHTG):

1. *Research projects* on climate change education topics like e.g. the effectiveness of specific interventions in real school settings.
2. *Research studios* and thesis work at PHTG where the students are enabled to perform their own research projects within the field of climate change education.
3. *Pedagocical content knowledge (PCK) courses* at PHTG which address climate change and the methodology of teaching climate change related topics.

All three topics are addressed in this contribution.

Research projects:
How should learning situations be designed to acquire both knowledge and action competence in the field of climate change education? Teaching activities outside the classroom are generally considered as beneficial learning situations. However, the effectiveness of those has been insufficiently investigated (e.g. Messmer et al., 2011). In order to discuss the conditions of effective environmental outdoor education two aspects need to be taken into account: The value of experiences in nature in general and the learning effectiveness of a school-based interventions on the other hand. Therefore an intervention study with 5th and 6th graders in Swiss primary schools – which addressed climate change issues was performed by Imhof (2016): Applying a pre-post-follow-up-design two experimental groups (in- and outdoor) and one control group (to avoid testing effects) were tested concerning their environmental knowledge, environmental attitude and environmental action competence. Results show first, that two groups (in- and outdoor) significantly gain environmental knowledge. Second, the environmental attitude is not significantly affected in those groups. Third, the motivation to act environmentally responsible was increased in the two groups, whereas the increase of the outdoor students was significantly higher.

Research studios:
One objective of teacher training is that teachers are able to retrace the discussed questions and implement the results of such studies in their own teaching activities. This is addressed at the PHTG e.g. within the compulsory elective research studio "Environmental Awareness (3 ECTS)". A research studio is a research based educational course. The starting point is a quantitative study carried out by the students themselves, which invesitgates age-, gender-, and location-specific relationships between the experiences of nature and the environmental attitude of primary school children.

PCK-courses:
As a conclusion of the above mentioned study by Imhof (2016) teaching activities in nature are effective and advisable if general didactic considerations (e.g. structured planning, student-centered, action-orien-tation, implementation of problem solving) are taken into account (Colberg et al. 2014).
Furthermore didactic settings of climate change education, which promote action competence in the sense of Education for Sustainable Development (ESD) must be put up for discussion (Colberg, 2017). This is addressed at the PHTG e.g. within the compulsory elective study week "Weather Observation and Climate Change (2ECTS)". The starting point is an introduction into basic meteorology and climate change science. With that knowledge different aspects of the methodology of teaching climate change realted topics are being discussed. As a result a comprehensive study unit is designed and favourably implemented later on.

The interaction of these three aspects paired with in service training courses take up the challenge of enhancing climate change education with research based, interdisciplinary and multi-perspective problem solving approaches. This will be discussed in detail during the symposium.

REFERENCES

Colberg, C.A., Keller, F. & Imhof, A. 2014: Wirksamkeit von Umwelt-Unterricht in ausserschulischen Lernumgebungen. In Fischer, H.-J.; Giest, H. & Peschel, M. (Hrsg.). Lernsituationen und Aufgabenkultur im Sachunterricht. Bad-Heilbrunn. Klinkhardt.

Colberg, C.A. 2016: Naturwissenschaften in der Gesellschaft: Bildung für nachhaltige Entwicklung (BNE). In: Metzger, S., Colberg, C. und Kunz, P. (Hrsg.). SWiSE – Swiss Science Education. Band 1 Naturwissenschaftsdidaktische Perspektiven: Naturwissenschaftliche Grundbildung und didaktische Umsetzung im Rahmen von SWiSE. Bern: Haupt. S. 169-179.

éducation21. 2016: Understanding of education for sustainable development (ESD). Bern.

Imhof, A. 2016: Wirksamkeitsvergleich von Umweltunterricht innerhalb und ausserhalb des Schulzimmers am Beispiel des Themenkomplexes Klimawandel Dissertation an der ETH Zürich. Zürich.

Messmer, K.; Niederhäusern, R.v.; Rempfler, A. & Wilhelm, M. (Hrsg.). 2011: Außerschulische Lernorte – Positionen aus Geographie, Geschichte und Naturwissenschaften. Münster/ Berlin / Wien/ Zürich: LIT.

16.2
Opportunities and limitations of local climate information in climate change education

Moritz Gubler [1,3] , Adrian Brügger [2], Stefan Brönnimann [3] & Marc Eyer [4]

[1] Institut für Forschung, Entwicklung und Evaluation, Pädagogische Hochschule Bern, Fabrikstrasse 8, CH-3012 Bern (moritz.gubler@phbern.ch)
[2] Institut für Marketing und Unternehmensführung, Universität Bern, Engehaldestrasse 4, CH-3012 Bern
[3] Geographisches Institut, Universität Bern, Hallerstrasse 12, CH-3012 Bern
[4] Institut Sekundarstufe II, Pädagogische Hochschule Bern, Fabrikstrasse 8, CH-3012 Bern

The impacts of ongoing and future anthropogenic climate change impose one of the major societal and environmental challenges of the 21st century. In order to cope with these in a responsible and sustainable way, the individual perception of the related risks plays a crucial role in encouraging climate action. Several findings from social and behavioural sciences indicate that many people, at least in wealthy Western parts of the world, perceive climate change as an abstract phenomenon being distant in time, space.

Hence, a multitude of experimental studies has examined the relationship between variations of the so-called "psychological distance" of information about climate change impacts (i.e. global vs. local framing) and their effect on concerns about climate change as well as on sustainable behaviour intentions. Although some results suggest that highlighting proximal consequences may lead to an increase of individuals' willingness to take action, the majority of existing studies failed to prove a direct effect of spatially framed climate change information on their motivation to tackle cliamte change (Brügger et al., 2015).

However, most of these studies focused on adult people at all age levels and the above described approach regarding the perception of psychological distance has not yet been tested among adolescents. In view of the fact that it will be today's and future's youth that is primarily affected by climate change impacts, and that this group of the population comprises the future leaders of society, it is of high importance to shed light on their perception of and concerns about the (negative) consequences of climate change.

In this context, we conducted a written survey among 1st grade high-school students (n=172, 15-18 years old, June 2018) originating from different parts of the canton of Bern, Switzerland. Using a set of open and closed questions, we tried to reveal on one hand the perceived psychological distance towards climate change impacts, the level of concern about them, the students' self-efficacy expectation, as well as their intentions for climate action. On the other hand, we assessed the sources of knowledge about climate change, value orientations, travel habits, and different socio-economic factors.

Preliminary results indicate that the students' perceptions of climate change impacts are not restricted to a distant view, and that there exist differences regarding the perceived distance depending on the origin region of the students. After an in-depth analysis of the data, our results will form the basis for the development and evaluation of teaching materials dealing with local consequences of climate change in urban environments and its implications for the students' behaviour intentions. At this stage, the project will profit from the results of a high-resolution assessment of the summertime heat load within and around the city of Bern during the recent, very hot and dry summer 2018 (Bund, 08/03/2018).

REFERENCES
Brügger, A., Dessai, S., Devine-Wright, P., Morton, T.A., & Pidgeon N.F. 2015: Psychological responses to the proximity of climate change. Nature Climate Change, 5, 1031-1037.
Bund, 08/03/2018: https://www.derbund.ch/bern/nachrichten/Kies-statt-Asphalt-gegen-Hitzestress/story/30743895; last access: 08/20/2018.

16.3
Dem Klimawandel nachhaltig begegnen lernen - Förderung der Handlungskompetenz von Jugendlichen zur Anpassung an die regionalen Folgen von Klimaveränderungen in Baden-Württemberg

Kai Guckes [1], Simone Fischer [1], Alexander Siegmund [1,2]

[1] Abteilung Geographie - Research Group for Earth Observation (rgeo), Pädagogische Hochschule Heidelberg, Czernyring 22/11, 69115 Heidelberg, Deutschland
[2] Heidelberg Center for the Environment (HCE) & Geographisches Institut, Universität Heidelberg, Seminarstr. 2, 69117 Heidelberg, Deutschland

guckes@ph-heidelberg.de

Der Umgang mit den Herausforderungen des Klimawandels gehört zu den zentralen Aufgaben der Gesellschaft im 21. Jahrhundert. Sowohl auf globaler als auch auf regionaler Ebene sind die Auswirkungen der Veränderungen des Klimas bereits heute in vielfältiger Weise spürbar. Die damit verbundenen Prozesse laufen in komplexen Mensch-Umwelt-Systemen ab, die vielfältige Wechselwirkungen und Rückkopplungsprozesse aufweisen. Damit geht ein hoher Grad an Unsicherheiten einher (z.B. bei Klimaprognosen), die bei der Entwicklung nachhaltiger Anpassungsstrategien berücksichtigt werden müssen. Um diesen Herausforderungen zukünftig auf verschiedenen gesellschaftlichen Ebenen in angemessener Art und Weise begegnen zu können, ist die Förderung der Beurteilung der regionalen Folgen des Klimawandels und die Entwicklung nachhaltiger Anpassungsstrategien insbesondere bei Kindern und Jugendlichen als „Entscheidungsträgern von morgen", von zentraler Bedeutung. Dieser Anspruch an eine moderne Wissensvermittlung und Kommunikation im Kontext des Klimawandels steht jedoch oft in Divergenz zur gängigen Unterrichtspraxis. In vielen Fällen werden Lerneinheiten unterrichtet, die weder die Komplexität von Systemen adäquat vermitteln, noch auf die Unsicherheiten bei der Ableitung von regionalen Klimafolgen und Anpassungsstrategien eingehen. Meist wird im Unterricht eher auf globale Folgen des Klimawandels eingegangen und Anpassungsmaßnahmen an die Folgen des Klimawandels kaum beleuchtet.

Hier setzt das Projekt „Dem Klimawandel nachhaltig begegnen lernen (KliN!)" an: In einem interdisziplinären und multimethodischen Ansatz wird die Beurteilungs- und Handlungsfähigkeit von Jugendlichen in Baden-Württemberg im Themenkomplex des regionalen Klimawandels gefördert. Der Fokus auf regionale Klimaveränderungen erhöht dabei das Interesse und die Betroffenheit der Jugendlichen deutlich im Vergleich zu globalen Themenfeldern ohne direkten Alltagsbezug. Anhand von exemplarischen Phänomenen aus der Landwirtschaft, Forstwirtschaft und naturnahen Ökosystemen, sollen Jugendliche bisherige und zukünftige Auswirkungen des Klimawandels in ihrem unmittelbaren Lebensumfeld *erkennen*, *analysieren* und *beurteilen* lernen.

Grundlage der Vermittlung bildet dabei ein problemorientierter methodisch-didaktischer Dreiklang aus *Feld-*, *Labor-* und *Experiment-*/*Modellarbeit.* Dieser Dreiklang wurde im Geco-Lab, Kompetenzzentrum für geoökologische Raumerkundung der Abteilung Geographie der Pädagogischen Hochschule Heidelberg entwickelt.

Die Auswahl der Themen erfolgt dabei regional-spezifisch in enger Anlehnung an die deutsche Anpassungsstrategie an den Klimawandel sowie an den aktuellen Bildungsplan für das Bundesland Baden-Württemberg. Neben der Vermittlung und Erarbeitung fachlicher Zusammenhänge steht besonders die Entwicklung und Beurteilung von nachhaltigen Anpassungsmaßnahmen an den Klimawandel im Vordergrund des Projekts. Anhand ausgewählter Praxisbeispiele lernen die Jugendlichen komplexe Sachverhalte aus einer ökologischen, ökonomischen und sozialen Perspektive zu beurteilen. Durch die Verschneidung von Fachwissen und einer Beurteilung der Nachhaltigkeit von Anpassungsmaßnahmen, bettet sich das Projekt in eine Bildung für nachhaltige Entwicklung ein und steht somit in direktem Zusammenhang zu den globalen Entwicklungszielen im Rahmen der Agenda 2030.

Bei der Konzeptionierung der Lernmodule wird die Integration in den Regelunterricht berücksichtigt, um somit langfristig regionale Klimawandelthemen in die gängige Unterrichtspraxis einzubinden. Zur eigenständigen Fortführung der Lernmodule an den unterschiedlichen Kooperationsschulen, auch nach Projektende, werden für jedes Thema entsprechende Multiplikatorenschulungen mit Lehrkräften durchgeführt. Die Schulen werden dadurch langfristig befähigt Klimawandelkommunikation im Kontext der Bildung für nachhaltige Entwicklung umzusetzen.

16.4

Expedition 2 degree: The 2°C target in the Alps – An Experience in Virtual Reality

Andreas Linsbauer [1] [2], Noemi Chow [3], Jonas Christen [3], Janique Gattlen [4], Mario Gertschen [4], Niklaus Heeb [3], Martin Hoelzle [1], Felix Keller [5], Hans Lozza [6], Bruno Meeus [1], Andrea Millhäusler [6], Martin Scherler [1], Reto Spoerri [3]

[1] Département de Géosciences, Université de Fribourg, Chemin du Musée 4, 1700 Fribourg (andreas.linsbauer@unifr.ch)
[2] Geographisches Institut, Universität Zürich, Winterthurerstrasse 190, 8057 Zürich
[3] Knowledge Visualization, Zürcher Hochschule der Künste, Pfingstweidstr. 96, 8031 Zürich
[4] World Nature Forum, UNESCO-Welterbe Swiss Alps Jungfrau-Aletsch, Bahnhofstrasse 9a, 3904 Naters
[5] Abteilung Forschung und Entwicklung, Pädagogische Hochschule Graubünden,
   Scalärastrasse 17a, 7000 Chur
[6] Schweizerischer Nationalpark, Schloss Planta-Wildenberg, 7530 Zernez

Since the Industrial Revolution, anthropogenic emissions of greenhouse gases, has changed the climate drastically and global temperatures have risen sharply. At the climate conference COP21 in Paris, in December 2015, the United Nations agreed on the 2°C target, to limit the maximum temperature increase well below 2°C. The goal is easy to formulate, but what does it mean? For most people an average increase of 2°C in global temperature is hard to grasp.

This project (funded by SNF Agora: http://p3.snf.ch/project-178628) aims to make climate change tangible and produce an emotional involvement by means of Virtual Reality (VR). A VR-Experience will simulate the alpine environment around the Aletsch glacier to let the target audience, mainly young people – classes of secondary and gymnasium schools, experience scenarios of a future world at and beyond the 2°C target. With high-resolution geospatial data (Jouvet et al. 2011, Linsbauer et al. 2012) and a professional game environment, users can be transformed into a compelling reconstruction of the alpine environment (Figure 1). Glacier melt and related impacts on the entire Aletsch region can be experienced emotionally and realistically in time lapse. A partner playing a game at the tablet station will interactively control the experience of the user under VR (Figure 2).

The VR-Experience and the possibility of interaction will demonstrate that every individual can contribute by changing personal behavior and political activism. In addition, the audience will come to understand that a collective effort is required to control climate change. Users will learn that a social-ecological transformation is needed for a sustainable future with a more stable climate, a transformation that requires public debate and political consciousness.

The emotions triggered by the VR-experience and the tablet-game will not necessarily lead to sustainable behavioral changes. Therefore, the VR experience is combined with a space for dialogue (as a class) about causes and courses of action.

REFERENCES

Jouvet, G., Huss, M., Blatter, H. & Funk, M. 2011:Modelling the retreat of Grosser Aletschgletscher in a changing climate. Journal of Glaciology, 57(206).

Linsbauer, A., Paul, F., & Haeberli, W. 2012: Modeling glacier thickness distribution and bed topography over entire mountain ranges with GlabTop: Application of a fast and robust approach. Journal of Geophysical Research: Earth Surface 117(3). DOI:10.1029/2011JF002313.

Figure1: View from the VR-platform on the Eggishorn in direction of the accumulation area (upper picture) and ablation area (lower picture) of the Aletsch glacier. Screenshots through the VR-goggles.
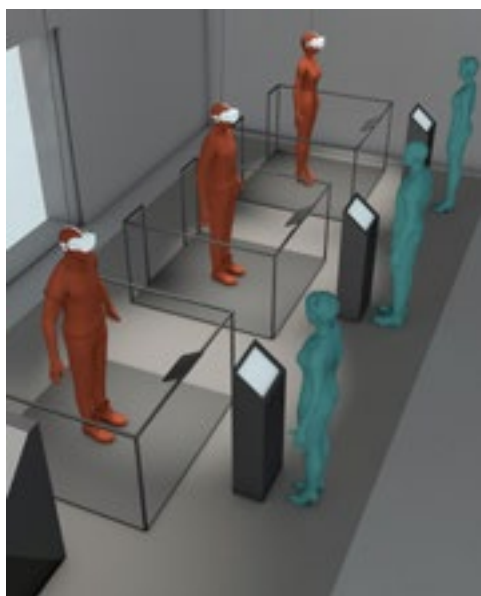

Figure 2: Set up of VR-experience for the museums. Three users experience a warming high mountain environment under VR, which will be interactively controlled by their partners playing at the tablet station.

16.5
Education on climate change and climate policy: learning opportunities for all school levels

Sibylle Reinfried [1], Marco Adamina [2] & Matthias Probst [3]

[1] Pädagogische Hochschule Luzern, Fachbereich Geographie, Pfistergasse 20, 6003 CH-Luzern (s.reinfried@bluewin.ch)
[2] Pädagogische Hochschule Bern, Institut Forschung, Entwicklung und Evaluation & Institut Vorschulstufe und Primarstufe
[3] Pädagogische Hochschule Bern, Institut Sekundarstufe II, Fachdidaktik Geographie

Within the framework of the project "Education on Climate Change and Climate Policy" (CCESO), learning opportunities for all levels of education in Switzerland are being developed on behalf of the Federal Office for the Environment. The development work is based on current scientific findings from climate research and on findings from subject specific edcational research and the findings from learning psychology. The aim of the project is a coherent and cumulative educational concept with learning opportunities that are similar in content orientation and structure. Based on the reports of the IPCC, a grid was developed to analyse the state of climate education in specialist journals for teaching and in textbooks for all school levels. In addition, interviews were conducted with teachers about their teaching on climate change and student preconceptions about the topic were researched. With this data collection, deficits and desiderata of climate education in Switzerland were identified and a cross-stage educational concept on climate change and climate policy was developed, which forms the basis for the development of learning opportunities (Adamina et al. 20128; Reinfried et al. 2018; Fig. 1).
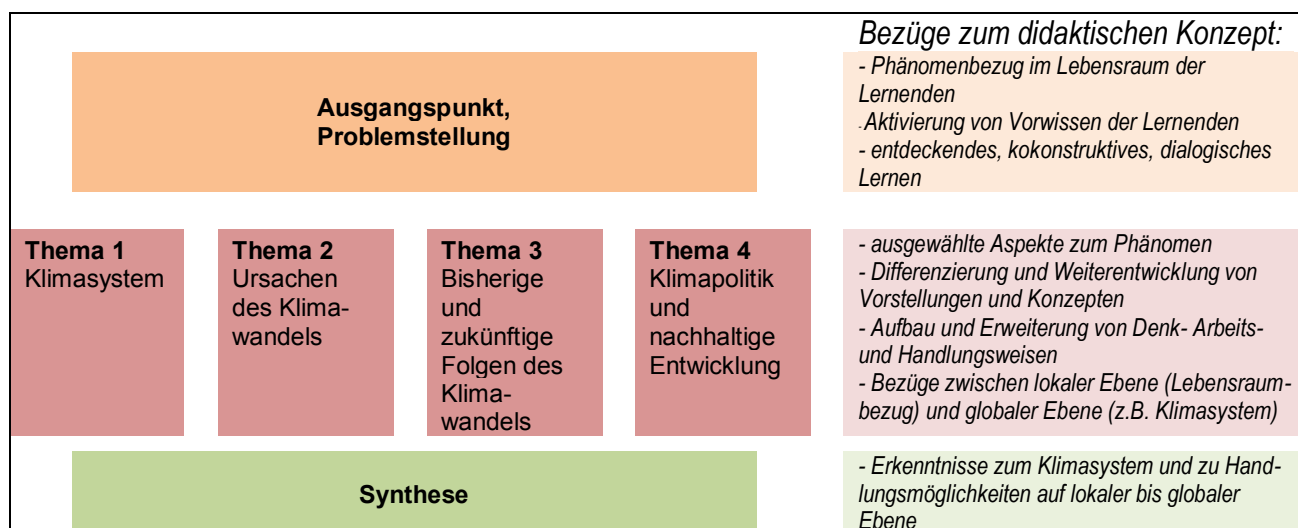

Figure 1: Structure of the learning opportunities

Learning opportunities developed as examples are currently being tested in class. An e-platform on which learning opportunities on climate change, climate policy and climate protection are made available to interested parties is being developed.
The results of the project to date will be presented at the symposium in three short presentations of 15' each (plus time for brief discussions).

Part 1: Project framework/output, analysis instrument
Part 2: Results of the data collection
Part 3: Educational concept, concept of the learning opportunities, examples of exemplary learning opportunities

REFERENCES

Adamina, M., Hertig, Ph., Probst, M., Reinfried, S. & Stucki, P., 2018: Klimabildung in allen Zyklen der Volksschule und in der Sekundarstufe II. Grundlagen und Erarbeitung eines Bildungskonzeptes. Schlussbericht Projektphase CCESO I 2016/2017 (vollständige Fassung). Bern: Globe Schweiz. https://www.globe-swiss.ch/files/Downloads/1568/Download/Schlussbericht_CCESO1_lang_2018.pdf

Reinfried, S., Probst, M., Adamina, M., Hertig, Ph. & Stucki, P. 2018: Klimabildung in allen Zyklen der Volksschule und in der Sekundarstufe II. Zusammenfassung der CCESO-Projektphase I 2016/2017 (Summary). Bern: Globe Schweiz. https://globe-swiss.ch/files/Downloads/1567/Download/Klimabildung_SummaryCCESO1.pdf

P 16.1
Climate change education and projects in Swiss secondary schools

Markus Eugster

*Sekundarschule, Schöntalstrasse 2, 9244 Niederuzwil
(*markus.eugster@schule-uzwil.ch*)*

In a nutshell
With the new curriculum (Lehrplan 21) climate change became an official topic in Swiss secondary schools. Several approaches to implement climate change education are presented and evaluated.

GLOBE
GLOBE (Global Learning and Observations to Benefit the Environment) offers many local scientific activities for students to better understand the earth as a system with all its interconnections by scientific exchange. Additionally it connects students and teachers worldwide and thus brings in an emotional component.

Excursions
Excursions face students with facts, help understand local processes and convey the message to the community.

Exhibitions...
...force students to summarize and to set priorities. The contact with visitors brings a precious learning effect.

Polar science
As climate change shows dramatically in polar regions, polar science is an impressive way to reveal the changes. Teachers and scientists collaborate as Polar Educators International and bring current science into the classroom.

Seasonal changes
Long term photo projects help detect slow local changes in climate.

Remote sensing
NASA runs several school programs to share scientific data and findings with students.

REFERENCES
https://www.globe.gov/de/do-globe/measurement-campaigns/past-projects/earth-as-a-system-projects/seasons-and-biomes
https://www.globe-swiss.ch/de/Zyklus3/
http://www.seasonsandbiomes.net/
https://polareducator.org/
https://pmm.nasa.gov/education/
https://www.pusch.ch/

P 16.2
"Once Upon a Time…" – Using fictional stories to educate about climate, oceans and science

Iván Hernández-Almeida [1], Chelsea Korpanty [2], Sandy Boehnert [2], Rebecca Borges [3], Catarina Cavaleiro [2], Ameris Contreras [4], Vicente Durán Toro [2], Hadar Elyashiv [2], Sabrina Hohmann [2] , Valeriia Kirillova [2], YangYang Liu [1], Lina Madaj [2], Gema Martínez Méndez [4], Denise Müller-Dum [5], Celia Neto dos Santos [2], Andrea Paz Orfanoz-Cheuquelaf [1], Rodrigo Costa Portilho-Ramos [2], Andrea Rebotim [2], Dharma Reyes Macaya [2], Pamela Rossel [1], Mariem Saavedra-Pellitero [2], Christiane Schmidt [2], Leonardo Tamborrino [2], Deborah Tangunan [2], Haozhuang Wang [2]
& the OUAT team of 2016-2017[1] and of 2018°

[1] Geological Institute, Department of Earth Science, ETH, 8092, Zürich, Switzerland (ivan.hernandez@erdw.ethz.ch)
[2] MARUM, University of Bremen, Bremen, 28359, Germany
[3] Zentrum für Marine Tropenforschung, Bremen, 28359, Bermany
[4] Alfred Wegener Institute for Polar and Marine Research, 27570 Bremerhaven, Germany
[5] Institute of Environmental Physics, University of Bremen, Otto-Hahn-Allee 1, 28359 Bremen, Germany
° contact first author for full names and affiliation list

Storytelling is a social act that involves sharing values and knowledge. It is a central part of human communities, taking place in every culture. Using storytelling as a form of dialogue between scientists and the general public can provide a tool for societal change by raising awareness and inspiring actions. "Once Upon a Time… a Scientific Fairy Tale" draws upon the versatility of storytelling to promote scientific knowledge to children and adults through illustrated short stories and poetry. The project was organized in 2016 by an international group of marine science PhD students and postdoctoral researchers at the University of Bremen. In 2017 the first "Once Upon a Time…" volume was published with funding from the "Show your Science" competition sponsored by the German science communication foundation "Science in Dialogue" (Wissenschaft im Dialog). The 12 stories and poems in this volume relate various marine science themes – from marine biology, ecology, and geology to human interactions with the oceans. The stories aim to convey, in a clear and engaging way, scientific content inspired by the authors' (the scientists') personal research and passions. The "Once Upon a Time…" volume was published as an illustrated and free to download e-book in English, German, and Spanish. In order to reach a wider readership, the e-book is also being translated to Italian, French, Chinese, Portuguese, Hebrew, Filipino, Korean, and Russian. To promote the volume and science communication, the "Once Upon a Time…" group does readings of the stories and poetry in schools and libraries and at science events. In addition to publishing a second volume (in progress), the group is seeking international collaboration with teachers, citizens, and scientists to expand the scope and readership of the "Once Upon a Time…" scientific storytelling network.

P 16.3
Seismology-at-School in Nepal: Education and outreach

Shiba Subedi [1], György Hetényi [1], Anne Sauron [2,3], Paul Denton [4]

[1] *Institute of Earth Sciences, University of Lausanne, Switzerland*
[2] *HES-SW Valais-Wallis, Sion, Switzerland*
[3] *Institute of Geophysics, ETH Zurich, Switzerland*
[4] *British Geological Survey, United Kingdom*

Nepal is located above the convergent plate boundary between the Indian and Eurasian plates. Therefore, it has experienced devastating earthquakes throughout history, claiming lives and causing significant damage. The most recent large Gorkha earthquake (M 7.8) in 2015 killed nearly 9,000 people and injured approximately 22,000. Still, these casualties and damage were far under the expectations. After the Gorkha earthquake, Nepali people are eager to know more about earthquakes and seek safety.

Schools play a vital role in the society and teach the essential elements of common values and culture. A proper education in a school not only teaches the children, but, also reaches deep across their families into the community. Earthquake education reaching a broad group of the population early in their life is strongly needed, but seismology is not part of the curriculum in Nepali schools. Our initiative aims to introduce seismology in Nepali schools with the specific focus on education and crowdsourcing.

We aim to develop several educational activities within this initiative. Beyond teaching adapted to various levels of classes, we strive for "learning-by-doing" and install low-cost seismometers in schools. We have started this scheme in the Western Nepal region, where seismologists expect a great (M>8) earthquake, by installing inexpensive seismometers and then seek that the example is spread to other areas. We tested several types of low-cost sensors in the lab. In the field, we have started installing Raspberry Shake 1D. The data will be available freely and used to make shake maps, so we hope that crowdsourcing will also be useful for scientific goals like as earthquake detection, shake map etc. Moreover, the seismometer in each school will allow students to check and see whether an earthquake has happened in the region, and what was the respective shaking.

We have installed the first low-cost seismometer in Nepal in western region, which is recording continuously in front of the student's eyes, and some local earthquakes have already been recorded. We also have conducted a survey to know the understanding level of local people where 500 responses are collected from 20 involved schools. This program will attract students towards seismology and will play a crucial role to make earthquake-safe communities.

P 16.4

Using an interdisciplinary MOOC to teach climate science and science communication to a global classroom

Bärbel Winkler [1], John Cook [2]

[1] Skeptical Science (baerbelw@skepticalscience.com)
[2] Center for Climate Change Communication, George Mason University, Fairfax, Virginia, United States of America (jcook20@gmu.edu)

MOOCs (Massive Open Online Courses) are a powerful tool, making educational content available to a large and diverse audience. The MOOC "Making Sense of Climate Science Denial" applies science communication principles derived from cognitive psychology and misconception-based learning in the design of video lectures covering many aspects of climate change. As well as teaching fundamental climate science, the course also presents psychological research into climate science denial, teaching students the most effective techniques for responding to misinformation. A number of the students enrolled up to now were secondary and tertiary educators, who adopted the course content in their own classes as well as adapted their teaching techniques based on the science communication principles presented in the lectures. The MOOC - developed by John Cook and the Skeptical Science team - integrates cognitive psychology, educational research and climate science in an interdisciplinary online course that has had over 35,000 enrolments from over 180 countries thus far.

REFERENCES

Cook, J., Schuennemann, K., Nuccitelli, D., Jacobs, P., Cowtan, K., Green, S., Way, R., Richardson, M., Cawley, G., Mandia, S., Skuce, A., & Bedford, D. (April 2015). Denial101x: Making Sense of Climate Science Denial. edX. https://www.edx.org/course/making-sense-of-climate-science-denial-0

Skeptical Science
https://skepticalscience.com/

P 16.5
Girls on Ice Switzerland – using immersion to inspire interest in science

Kathrin Naegeli [1,2,3], Marijke Habermann [1], Marlene Kronenberg [1,4], Lena Hellmann [1], Margit Schwikowksi [1,3]

[1] Laboratory of Environmental Chemistry, Paul Scherrer Institute, CH-5032 Villigen
(kathrin.naegeli@giub.unibe.ch, swiss@girlsonice.org)
[2] Department of Geography, Remote Sensing Research Group, University of Bern, Hallerstrasse 12, CH-3000 Bern
[3] Oeschger Centre for Climate Change Research, University of Bern, Falkenplatz 16, CH-3012 Bern
[4] Department of Geosciences, University of Fribourg, Chemin du Musée 4, CH-1700 Fribourg

Now more than ever, climate change warrants particular emphasis in education because of its potentially harmful effects on our society. The retreat of glaciers is one of the most visible and tangible results of climate change that is available to students (Carey, 2007). The alpine landscape, therefore, is an ideal classroom for studying the science of climate change. Citizens who are better informed about climate change also consider it a more pressing issue (EORG, 2008) and make better informed decisions.

Girls on Ice Switzerland provides a short course teaching format which combines the advantages of inquire-based teaching (e.g. Osborne and Dillon, 2007), experimental learning, and the tangibility of climate change science in the alpine environment. The glacier expeditions are tuition-free and target young women (15-17 years old) from diverse backgrounds, who are normally difficult to reach or to interest in scientific topics due to either their socioeconomic status, migration background, or similar challenging life situations. They are at a critical decision-making point in their education and career paths when a boost of confidence, encouraging role models, and new knowledge of what a science career offers can have a strong influence on their futures. The primary goals of Girls on Ice are i) increase young women's self-efficacy and interest in pursuing science (specifically STEM), ii) create lifelong advocates for the scientific process and its role in public policy, iii) teach critical thinking skills and iv) enhance leadership self-confidence.

Between 2017 and 2019, Girls on Ice Switzerland is funded by SNF Agora (http://p3.snf.ch/project-171620) and organises three to four glacier expeditions. During each expedition a team of 9 young women spends 11 days exploring and learning about the scientific process and the glacial landscape through authentic scientific field studies with professional glaciologists, ecologist, artist, and mountaineers. Inspired by these activities, there are growing efforts to establish a french-speaking Girls on Ice Switzerland as well as similar programs in other countries and regions (Austria, Central Asia).

REFERENCES

Carey, M. (2007). The history of ice: how glaciers became an endangered species. Environmental History, 12 (3), 497-527.
European Opinion Research Group (EORG) (2008). 'Europeans' attitudes towards climate change'. Special Eurobarometer 69.2 N°300 for Directorate-General Environment–survey managed and organised by Directorate-General Press and Communication "Public Opinion Analysis".
Osborne, J. and Dillon, J. (2007). Science Education in Europe: Critical Reflections, London: The Nuffield Foundation.

17. Aerosols and clouds in a changing world

Christopher Hoyle, Ulrich Krieger

ACP – Commission on Atmospheric Chemistry

TALKS:

17.1   Ammann M., Alpert P.A., Corral Arroyo P., Dou J., Luo B., Krieger U.K.: Feedbacks between indirect photochemical aerosol aging and microphysical properties

17.2   Brunamonti S., Jorge T., Wienhold F.G., Luo B.P., Peter T.: Balloon-borne measurements of cirrus clouds and aerosols in the Asian summer monsoon anticyclone during StratoClim 2016-2017

17.3   David R.O., Fahrni J., Marcolli C., Mahrt F., Brühwiler D., Lohmann U., Kanji Z.A.: The Role of Pores on Ice Nucleation

17.4   Eirund G., Possner A., Lohmann U.: Relaxation times of Arctic mixed-phase clouds to short-term aerosol perturbations

17.5   Friebel F., Mensah A.A.: From the lab to the atmosphere: Re-assessing the impact of Ozone and Temperature on the CCN-activity of soot particles.

17.6   Gilgen A., Wilkenskjeld S., Kaplan J., Raddatz T., Lohmann U.: Aerosols and land cover in the Roman Empire

17.7   Jorge T., Wienhold F.G., Cesbron G., Weers U., Vecellio M., Oelsner P., Meier S., Naebert T., Brossi S., Brossi T., Dirksen R., Peter T.: Peltier Cooled Frost point Hygrometer: PCFH Future instrument for balloon borne water vapor measurements in the UTLS

17.8   Kilchhofer K., Mahrt F., Kanji Z.A.: Pre-activation of soot particles and the effect on ice nucleation in subsequent cloud formation cycles

17.9   Mahrt F., Wieder J., Dietlicher R., Stopford C., Smith H., Kanji Z.A.: A new instrument for cloud particle phase determination

17.10   Molteni U., Sosedova Y., Dommen J., the NUCLACE collaboration: Free troposphere wintertime gas-phase composition using CI-APi-TOF

17.11   Sonwani S., Kulshrestha U.: Real-Time Wet Scavenging of Organic Carbon and Elemental Carbon during Monsoon and Non-Monsoon Seasons at Delhi

POSTER:

P 17.1   Mahrt F., Marcolli C., David R.O., Grönquist P., Barthazy Meier E.J., Lohmann U., Kanji Z.A.: Ice nucleation abilities of soot particles determined with the Horizontal Ice Nucleation Chamber

17.1
Feedbacks between indirect photochemical aerosol aging and microphysical properties

Markus Ammann [1], Peter A. Alpert [1], Pablo Corral Arroyo [1,2], Jing Dou [3], Beiping Luo [3], Ulrich K. Krieger [3]

[1] Laboratory of Environmental Chemistry, Paul Scherrer Institut, 5232 Villigen (markus. ammann@psi.ch)
[2] Department of Chemistry and Biochemistry, University of Bern, 3012 Bern
[3] Institute of Atmospheric and Climate Sciences, ETH Zürich, 8092 Zürich

Indirect photochemical processes are inititated by chromophores absorbing in the near UV and visible spectrum of the sunlight and lead to the oxidation of other non-absorbing compounds (Corral Arroyo et al., 2018). Iron carboxylate complexes are an important class of chromophores and represent an important sink of carboxylic acids in the condensed phase of atmospheric particles. Atmospheric particles dominated by organic components are known to exhibit substantial changes in viscosity in response to changes in relative humidity and temperature and may even attain semi-solid or glassy states under dry and / or cold conditions. It has been reasonably well established that increasing viscosity leads to increasing molecular diffusion and multiphase reaction kinetic limitations (Steimer et al., 2015; Berkemeier et al., 2016).

In the present project we have expanded these investigations to attempt at understanding viscosity and transport limitation effects on the degradation of organic aerosol initiated by iron carboxylate complexes. We specifically look at citric acid degradation due to iron citrate photochemistry. A multitude of chemical and microphysical tools are used to measure:

1) mass loss of single levitated particles in an electrodynamic balance (EDB, see Fig. 1, right),
2) cycling of radicals, formation of oxygenated volatile organic compounds and condensed phase products in organic films in a coated wall flow tube, and
3) spatially resolved analysis of the iron oxidation state within single micron sized particles using X-ray microspectroscopy (Steimer et al., 2014) (Figure 1, left).

We employ novel kinetic modelling tools to assist analysis of our experiments as opposed to more traditionally available steady-state analysis methods which are not applicable. The combined results indicate a strong limitation by diffusion of oxygen into the particles under high viscosity conditions. This leads to reduced reoxidation of iron in the oxidation state II (Fe(II)), which results from the initial photolysis of the Fe(III)-citrate complex. This reoxidation by Fenton type reactions with reactive oxygen intermediates is required to complete the photocatalytic cycle that leads to citric acid degradation and thus continued mass loss as observed in the EDB experiment. The absence of oxygen in the interior of the particles also leads to different condensed phase products at low relative humidity. Therefore, our results have direct implications for the degradation kinetics of carboxylic acids in aerosol particles, but may also more generally on the aging of viscous atmospheric aerosol particles and related effects on human health.
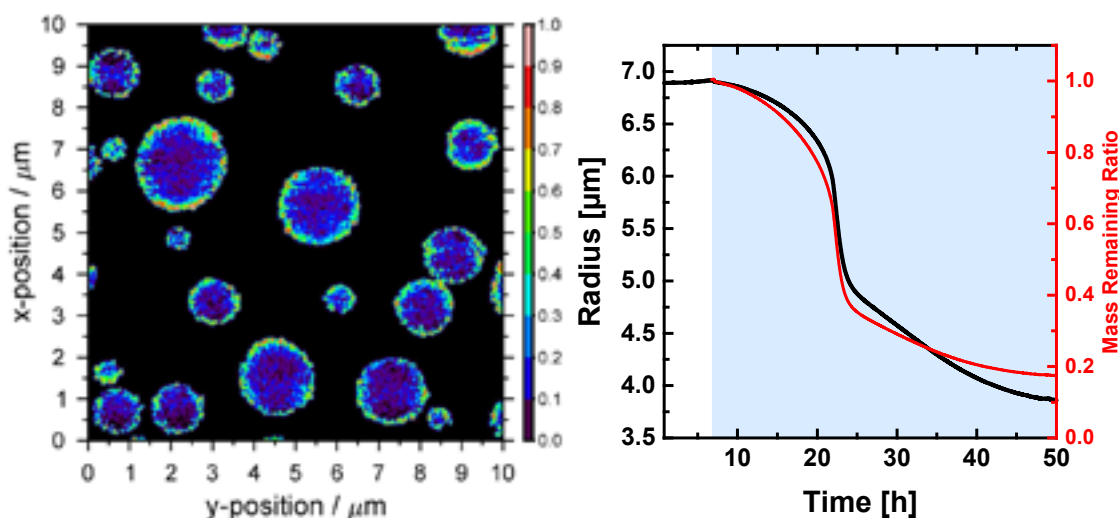

Figure 1. Left: Map of FeCit/CA particles (1:1 molar ratio) after illumination with UV light over 15 minutes in an atmosphere of 110 mbar of oxygen and 40 % RH. The color scale indicates Fe(iii)/(Fe(ii)+Fe(iii)). Right: Mass loss of a FeCit/CA particle (1:20 molar ratio) during illumination at 50 % RH; left axis: size , right axis: calculated mass remaining ratio.

REFERENCES

Berkemeier, T., Steimer, S. S., Krieger, U. K., Peter, T., Poschl, U., Ammann, M., & Shiraiwa, M. 2016: Ozone uptake on glassy, semi-solid and liquid organic matter and the role of reactive oxygen intermediates in atmospheric aerosol chemistry, Phys. Chem. Chem. Phys., 18, 12662-12674.

Corral Arroyo, P., Bartels-Rausch, T., Alpert, P. A., Dumas, S., Perrier, S., George, C., & Ammann, M. 2018: Particle-Phase Photosensitized Radical Production and Aerosol Aging, Environ. Sci. Technol., 52, 7680-7688.

Steimer, S. S., Lampimäki, M., Coz, E., Grzinic, G., and Ammann, M. 2014: The influence of physical state on shikimic acid ozonolysis: a case for in situ microspectroscopy, Atmos. Chem. Phys., 14, 10761-10772.

Steimer, S. S., Berkemeier, T., Gilgen, A., Krieger, U. K., Peter, T., Shiraiwa, M., and Ammann, M. 2015: Shikimic acid ozonolysis kinetics of the transition from liquid aqueous solution to highly viscous glass, Phys. Chem. Chem. Phys., 17, 31101-31109.

17.2
Balloon-borne measurements of cirrus clouds and aerosols in the Asian summer monsoon anticyclone during StratoClim 2016-2017

Simone Brunamonti [1], Teresa Jorge [1], Frank G. Wienhold [1], Bei Ping Luo [1] and Thomas Peter [1]

[1] Institute for Atmospheric and Climate science (IAC), Swiss Federal Institute of Technology (ETH), Zürich, Swittzerland

The Asian summer monsoon anticyclone (ASMA) is a major meteorological system of the upper troposphere-lower stratosphere (UTLS) during boreal summer. It is known to be enriched in water vapor and aerosols, forming the Asian tropopause aerosol layer (ATAL), due to rapid lifting of moist and polluted boundary layer air by deep convection and horizontal confinement in the UTLS. Given its dynamical structure, the ASMA provides an efficient pathway for the transport of water vapor and pollutants to the global stratosphere.

Within the StratoClim project, we performed balloon-borne measurements of temperature, water vapor, ozone and aerosol backscatter from two stations at the southern slopes of the Himalayas, near the center of the ASMA. In particular, we conducted two extensive monsoon-season campaigns, in 2016 in Nainital, India (29°N, 80°E) and 2017 in Dhulikhel, Nepal (28°N, 85°E), plus one post-monsoon campaign in 2016 in Nainital. These measurements provide unprecedented insights into the thermal structure, the distributions of water vapor, ozone and aerosols, cirrus cloud properties and interannual variability in ASMA.

Here we provide an overview of all the data collected during our three campaign periods, with focus on the aerosol backscatter measurements by the Compact Optical Backscatter Aerosol Detector (COBALD), developed at ETH Zürich. COBALD is able to detect both cirrus clouds and aerosols and is used here in tandem with cryogenic frost-point hygrometers (CFH) for accurate water vapor measurements, which allows to distinguish cirrus clouds from aerosol signal. Numerous thin cirrus clouds were detected near the cold-point tropopause (CPT) in ASMA. These clouds show remarkably low optical thickness, which indicates low ice crystal number densities, and suggests they are likely formed by heterogeneous freezing. This is consistent with preliminary results from the Zürich Optical and Microphysical Model (ZOMM), considering three types of INPs (mineral dust, meteoritic dust and glassy organics) in addition to sulfuric acid/water liquid droplets, showing that homogeneous freezing alone yields too high backscatter values (which are inconsistent with the COBALD measurements) whereas agreement is reached when INPs are included in the simulations.

Cloud filtering of the COBALD measurements also reveals the signature of ATAL, showing maximum backscatter at the CPT and extending up to 1.5 km above it. Cirrus clouds were often found embedded within the ATAL, suggesting that aerosol-cloud interactions may enhance cirrus cloud formation in ASMA. Future investigations will address this issue and the question of which INPs are most likely responsible for the formation of the observed cirrus clouds in ASMA.

17.3
The Role of Pores on Ice Nucleation

Robert O. David [1], Jonas Fahrni [2], Claudia Marcolli [1], Fabian Mahrt [1], Dominik Brühwiler [2], Ulrike Lohmann [1] and Zamin A. Kanji [1]

[1] Institute for Atmospheric and Climate Science, ETH Zürich, Zürich, Switzerland
[2] Institute of Chemistry and Biotechnology, Zürich University of Applied Sciences, Wädenswil, Switzerland

Deposition nucleation is conventionally described as the formation of ice directly from the vapor phase, without the prior formation of a bulk liquid water phase. However, water is capable of condensing in narrow pores and cavities well below water saturation as predicted by the Kelvin effect. Therefore, it is difficult to rule out the possibility that condensed water in pores is responsible for ice nucleation in conditions below water saturation (Marcolli, 2014)namely contact, condensation, immersion and deposition nucleation. Conceptually, deposition nucleation is the only pathway that does not involve liquid water, but occurs by direct water vapor deposition onto a surface. This study challenges this classical view by putting forward the hypothesis that what is called deposition nucleation is in fact pore condensation and freezing (PCF. In the atmosphere, porous particles make up the largest fraction of airborne dust and are associated with anthropogenic aerosols like soot. As such, understanding the role of pores on ice nucleation is critical for understanding and predicting ice formation globally.

To test the role of pores on ice nucleation, we exposed mesoporous silica with well-defined pore diameters ranging from 2.3 to 9 nm to varying temperatures and supersaturations with respect to ice in the Zurich Ice Nucleation Chamber (Stetzer et al., 2008). The porous samples have an enhanced freezing behavior relative to nonporous samples, which is not reconcilable with deposition nucleation occurring as a direct transition from water vapor to ice. Furthermore, particle batches were synthesized with different concentrations of hydroxyl and trimethylsilyl groups, effectively altering the contact angle of the particle surface with respect to water. When accounting for contact angle and pore diameter, the onset relative humidity required for ice nucleation was consistent with the humidity predicted for pore filling and subsequent freezing. Thus, the results indicate that pore condensation and freezing is likely the mechanism responsible for ice nucleation below water saturation. Ultimately, rendering deposition nucleation irrelevant for atmospherically relevant porous particles like dust and soot.

REFERENCES

Marcolli, C.: Deposition nucleation viewed as homogeneous or immersion freezing in pores and cavities, Atmos Chem Phys, 14(4), 2071–2104, doi:10.5194/acp-14-2071-2014, 2014.

Stetzer, O., Baschek, B., Lüönd, F. and Lohmann, U.: The Zurich Ice Nucleation Chamber (ZINC)-A New Instrument to Investigate Atmospheric Ice Formation, Aerosol Sci. Technol., 42(1), 64–74, doi:10.1080/02786820701787944, 2008.

17.4
Relaxation times of Arctic mixed-phase clouds to short-term aerosol perturbations

Gesa Eirund [1], Anna Possner [2], Ulrike Lohmann [1]

[1] Institute for Atmospheric and Climate Sciences, ETH Zurich, CH - 8092 Zurich (gesa.eirund@env.ethz.ch)
[2] Department of Global Ecology, Carnegie Institution for Science, US - 94305 Stanford CA

The formation and persistence of low lying mixed-phase clouds (MPCs) in the Arctic depends on a multitude of processes, such as surface conditions, the environmental state, air mass advection and the ambient aerosol concentration.

In this study, we focus on the relative importance of different aerosol perturbations (cloud condensation nuclei and ice nucleating particles; CCN and INP respectively) on MPC properties in the central Arctic. To address this topic, we performed high resolution large eddy simulations (LES) using the COSMO model and designed a case study for the Aerosol-Cloud Coupling and Climate Interactions in the Arctic (ACCACIA) campaign in March 2013. Motivated by current sea ice retreat, we additionally contrast the simulated MPC over open ocean versus sea ice surface.

We find that surface conditions highly impact cloud dynamics: over sea ice, a rather homogeneous, optically thin mixed-phase stratus cloud forms. In contrast, the MPC over the open ocean has a stratocumulus-like cloud structure. With cumuli feeding moisture into the stratus layer, the cloud features a higher liquid (LWC) and ice water content (IWC) and has a lifted cloud base compared to the cloud over sea ice.

Furthermore, we analyzed the aerosol impact on these two dynamically different regimes. Perturbations in the INP concentration increase the IWC and decrease the LWC, consistent between both regimes. The cloud microphysical response to CCN perturbations occurs faster in the stratocumulus regime over the ocean, where an increased moisture flux and strong updrafts lead to rapid cloud droplet activation and hence an increase in LWC following the CCN injection. In addition, the IWC increases through increased immersion freezing at cloud top. Over sea ice, the LWC increases followed by a distinct IWC increase. However, the response is delayed by a factor of 2 compared to the stratocumulus regime over open ocean.

However, independent of the cloud regime and the aerosol perturbation, the cloud organizes back to its unperturbed structure some hours after the perturbation was applied. The cloud microphysical properties return to the range of the control simulation and any aerosol impact is efficiently buffered. Additional CCN get transported out of the boundary layer into the capping inversion, thus constraining the ongoing droplet formation. Our results are robust across different temperature ranges and in addition insensitive to aerosol injection time. Hence, we postulate an efficient CCN processing and transport mechanism, preventing any long-term aerosol impact on Arctic MPC properties.

17.5

From the lab to the atmosphere: Re-assessing the impact of Ozone and Temperature on the CCN-activity of soot particles.

Franz Friebel, Amewu A. Mensah

Institute for Atmospheric and Climate Science, ETH Zürich (franz.friebel@env.ethz.ch)

Freshly emitted soot particles are known to be poor cloud condensation nuclei (CCN), but from atmospheric measurements it can be deduced that a significant fraction of soot particles act as CCNs. One process which might contribute to this discrepancy is the heterogeneous oxidation of soot particles. Soot particles have an average atmospheric lifetime of one week during which they are exposed to different aging processes (e.g. ozone oxidation).

The investigation of such processes is an experimentally challenging task due to the long time span which should be covered. Generally, studies are conducted in which soot is treated with high oxidant concentrations (up to 1000 x atmospheric average). This approach reduces the observation time needed but does not consider potential non-linear reaction kinetics (e.g. ozone with soot).

We investigated the reaction of ozone with soot particles under atmospheric conditions during a lab campaign at ETH Zurich. With the CSTR-approach we could observe 100 nm size selected soot particle up to 16 h. The particles were exposed to Ozone concentrations between 0 and 220 ppb at a temperature range of 5 to 35°C. We measured the CCN-activity at different super saturations between 0.3 % and 1.4 %.

We found that an increase of the ozone concentration by a factor of 10 (from 22 to 220ppb) almost halves the activation time at 1.0 % super saturation and 25 °C. In contrast, a temperature increase from 5°C to 35°C at a constant Ozone concentration (200 ppb) lead to a reduction of the activation time by a factor 5. Our results indicate, that the ambient temperature should be considered as much as the ozone concentration for a reasonable assessment of the cloud formation potential of soot particles.

According to literature, the initial reaction step is the adsorption of ozone (Langmuir-type reaction mechanism) which we confirm by analysis of auxiliary measurements of the physical properties of the particles. Our observations show the reaction speed being approximately proportional to concentration of ozone adsorbed on the soot surface but not to the concentration of ozone in the gas phase. (Lelièvre 2004) After exposure of soot particles to different Ozone concentrations the particle diameter increased by 3% and the particle mass by 20% within minutes but remained almost constant during further exposure.

Based on our temperature experiments we calculated an activation energy of 40 kJ/mol for the time limiting step causing CCN-activation. This value is in accordance with previous findings indicating that the conversion of physisorbed Ozone into reactive organic intermediates might be the limiting reaction step for CCN-activation of soot particles.(Berkemeier 2016) The combination of the concentration-dependence and the temperature-dependence creates a framework, which allows a fast estimation of the atmospheric relevance of laboratory soot aging experiments.

REFERENCES

Berkemeier, T. et.al.: Ozone uptake on glassy, semi-solid and liquid organic matter and the role of reactive oxygen intermediates in atmospheric aerosol chemistry, PCCP, (2016),18, 12662-12674

Lelièvre, S. et.al.: Heterogeneous reaction of ozone with hydrocarbon flame soot, PCCP, (2004),6, 1181-1191

17.6
Aerosols and land cover in the Roman Empire

Anina Gilgen [1], Stiig Wilkenskjeld [2], Jed Kaplan [3], Thomas Raddatz [2] & Ulrike Lohmann [1]

[1] *Institute for Atmospheric and Climate Science, ETH Zürich, CH-8092 Zürich (anina.gilgen@env.ethz.ch)*
[2] *Max-Planck-Institut for Meteorology, Bundesstrasse 53, D-20146 Hamburg*
[3] *University of Oxford, Oxford University Centre for the Environment, South Parks Road, Oxford, GB-OX1 3QY*

Around two thousand years ago, the Roman Empire was at its climax and spanned a considerable area of the globe. In this study, we assess the potential regional impact of humans, which influence land cover as well as aerosol emissions, on climate at the time. For this, we conduct several 20-year simulations using the global aerosol-climate model ECHAM-HAM-SALSA. When forest is converted to crop and pasture, surface properties such as the surface albedo change. These biogeophysical effects could lead to small regional changes in surface temperature. Two different reconstructions of anthropogenic land cover are used. Furthermore, we estimate anthropogenic aerosol emissions from crop residue and pasture burning as well as from fuel combustion. The impact of these emissions is assessed with ECHAM-HAM-SALSA.

17.7
Peltier Cooled Frost point Hygrometer: PCFH Future instrument for balloon borne water vapor measurements in the UTLS

Teresa Jorge [1], Frank G. Wienhold [1], Guillaume Cesbron [2], Uwe Weers [1], Marco Vecellio [1], Peter Oelsner [3], Susanne Meier [3], Tatjana Naebert [3], Steven Brossi [4], Thomas Brossi [4], Ruud Dirksen [3] & Thomas Peter [1]

[1] *Institute of Atmospheric and Climate Sciences, Swiss Federal Institute of Technology, Zürich Switzerland*
  (teresa.jorge@env.ethz.ch)
[2] *Institute des Sciences Appliquées Toulouse, France*
[3] *German Weather Service, GRUAN Lead Center, Lindenberg, Germany*
[4] *Mylab elektronik GmbH, Bubikon Switzerland*

For the past two years, an optimally controlled Peltier-cooled frost point hygrometer for balloon borne water vapor measurements in the upper troposphere and lower stratosphere (UTLS) has been under development at ETH Zürich. Considering what was accomplished so far in dew/frost point hygrometry, lessons learnt from SnowWhite (Vömel et al. 2003), CFH (Vömel et al. 2016) and FPH (Hall et al. 2016) and new approaches to the open problems are used to implement a more reliable water vapor measurements in the UTLS, hopefully suited as a long term solution. With the PCFH we address the long-standing problems with the cryogenically cooled frost point hygrometers, by replacing the inconvenient logistics of its handling and insecure perspective of future use by a plug-in solution. The Peltier element cooling range is maximized by a careful study of its limitations, behavior and response to its environment. A good development of SnowWhite was the replacement of the thermistor by thermocouples, more demanding but with better accuracy and versatility. These were characterized traceable to the national standard provided by METAS, the Swiss Federal Institute of Metrology. Further improvements are in the feedback control loop and the instrument housing, which is prone to self-pollution. In spite of the PID (proportional/ integral /derivative) control parameters tuned to different operating frost point temperatures and updated regularly during a flight, CFH and FPH still show instabilities that were only being addressed by a statistical treatment. Substantial progress is expected from introducing a Linear Quadratic Regulator scheme as state of the art optimal control method. Reduction of self-contamination interferences and improved data quality checks are also expected by designing a double instrument – with two independent sensor heads and inlets and optimization of the inlet tubes.

First flights were performed in July 2018. The results lead to fundamental changes of the instrument design, such as replacing the double stage Peltier element with a single stage to improve the performance under higher thermal load conditions on the cold side and to redesign the thermocouple for air temperature measurement. However, much was learn in term of instrument behaviour which allowed to further the instrument modelling efforts and derive a control scheme based on optimal control. The changes and further developments will be tested in second flights in November 2018 in Lindenberg Germany and the results first shown in the Swiss Geoscience meeting in Bern.

REFERENCES
Hall, E. G., Jordan, A. F., Hurst, D. F., Oltmans, S. J., Vömel, H., Kühnreich, B. & Ebert, V. 2016: Advancements, measurement uncertainties, and recent comparison of the NOAA frost point hygrometer, Atmospheric Measurement Techniques*, 9,* 4295-4310.
Vömel, H., Fujiwara, M., Shiotani, M., Hasebe, F., Oltmans, S. J., & Barnes, J. E., 2003: The Behavior of the Snow White Chilled-Mirror Hygrometer in Extremely Dry Conditions, Journal of Atmospheric and Oceanic Technology, 20, 1560-1567.
Vömel, H., Naebert, T., Dirksen, R. & Sommer, M., 2016: An update on the uncertainties of the vapor measurements using cryogenic frost point hygrometers, Atmospheric Measurement Techniques*, 9,* 3755-3768.
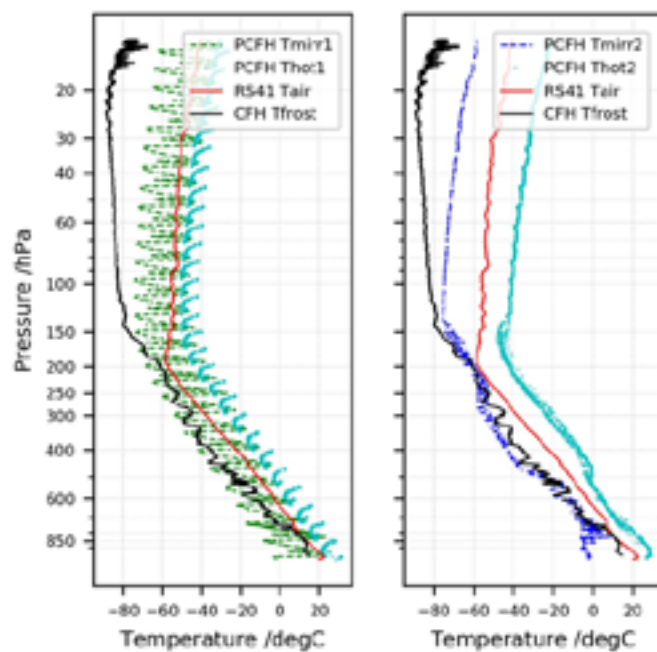
Figure 1. "2018-0725-02UT_LI_PCFH001" PCFH first flight in 25-07-2018 in Lindenberg Germany. Air temperature meausrement from RS41 in red and frost point temperature measurement from CFH in black. First panel: PCFH sub-unit 1 with "Peltier Identification" experiment, mirror temperature on the cold side of the peltier element in green and Peltier element hot side temperature in cyan. Second panel: PCFH sub-unit 2 with "Ice Reflectance to Frost point Temperature Difference" experiment, mirror temperature on the cold side of the peltier element in blue and Peltier element hot side temperature in cyan.

17.8

Pre-activation of soot particles and the effect on ice nucleation in subsequent cloud formation cycles

Kevin Kilchhofer [1], Fabian Mahrt [1] & Zamin A. Kanji [1]

[1] *Institute for Atmospheric and Climate Science, ETH Zurich, Zurich, 8092, Switzerland*

Soot influences the Earth's radiation budget by directly absorbing solar radiation. At the same time, soot particles can contribute to cloud formation by nucleating ice crystals or activating into cloud droplets, thus affecting climate through so-called aerosol-cloud interactions. A quantitative understanding of the aerosol-cloud interactions of soot particles, especially their potential to form cirrus clouds, remains a key factor to reduce the uncertainties in the estimates of the net radiative forcing (RF) of black carbon (Bond et al. 2013). The ability of soot particles to form ice crystals depends on the particle morphology and composition. Less emphasis has been placed on morphology in the past. Therefore, it is important to quantify the morphological properties of soot particles and understand processes that change this morphology.

Here we test the ice nucleation ability of soot generated from a propane flame Combustion Aerosol Standard Generator (miniCAST, JING AG), using the Horizontal Ice Nucleation Chamber (HINC, Lacher et al. (2017); Mahrt et al. (2018)), a Continuous Flow Diffusion Chamber. We tested the ice nucleation ability on mobility size-selected aerosol in the cirrus regime over a temperature range from 233 K to 218 K. The heterogeneous freezing ability of soot at low temperatures is especially important, as aircraft emissions are a direct source of combustion particles in the upper troposphere, where cirrus temperatures prevail. In parallel, we investigate soot particle morphology and how it changes as the soot particles form ice crystals, presenting a systematic investigation of the particle morphology derived from Transmission Electron Microscopy (TEM) images probed before and after the ice nucleation cycle within HINC. Finally, we demonstrate how the ice nucleation abilities of the soot particles change in subsequent cloud formation cycles. We attribute the change in ice nucleation ability to morphological changes of the soot particles upon ice crystal formation in an initial cloud cycle, a phenomenon known as pre-activation (D' Albe 1949; Marcolli 2016).

Our ice nucleation experiments reveal little heterogeneous freezing of the unprocessed propane soot particles. In the first cloud formation cycle we observe ice formation on 400 nm soot particles to take place close to homogeneous freezing conditions across all temperatures tested. However, our TEM results reveal a compaction of the soot particles upon ice nucleation. When the compacted soot particles are re-exposed to a second ice nucleation cycle within HINC, their ice formation ability is significantly altered. Ice processed soot particles show an enhanced ice formation ability with ice formation onset being lowered by as much as 10% relative humidity with respect to water (16% with respect to ice), depending on the temperature investigated in HINC. We discuss our results in context of cloud processing being responsible for the increased ice nucleation ability of the soot particles.

REFERENCES

Bond, T. C., et al. (2013), 'Bounding the role of black carbon in the climate system: A scientific assessment', *Journal of Geophysical Research-Atmospheres,* 118 (11), 5380-552.

D' Albe, E. M. F. (1949), 'Some experiments on the condensation of water vapour at temperatures below 0 °C', *Quarterly Journal of the Royal Meteorological Society,* 75 (323), 1-14.

Lacher, L., et al. (2017), 'The Horizontal Ice Nucleation Chamber (HINC): INP measurements at conditions relevant for mixed-phase clouds at the High Altitude Research Station Jungfraujoch', *Atmospheric Chemistry and Physics,* 17 (24), 15199-224.

Mahrt, F., et al. (2018), 'Ice nucleation abilities of soot particles determined with the Horizontal Ice Nucleation Chamber', *Atmos. Chem. Phys. Discuss.,* 2018, 1-41.

Marcolli, C. (2016), 'Pre-activation of aeosol particles by pore condensation and freezing', *Atmos. Chem. Phys. Discuss.,* 2016, 1-48.

17.9
A new instrument for cloud particle phase determination

Fabian Mahrt [1], Jörg Wieder [1], Remo Dietlicher [1], Chris Stopford [2], Helen Smith [2] & Zamin A. Kanji [1]

[1] *Institute for Atmospheric and Climate Science, ETH Zurich, Zurich, 8092, Switzerland*
[2] *Centre for Atmospheric and Instrumentation Research, University of Hertfordshire, Hatfield, Hertfordshire, United Kingdom*

Mixed-phase clouds (MPCs) are composed of both supercooled liquid droplets and ice crystals. They are thermodynamically instable as a result of the lower saturation vapor pressure over ice as compared to liquid water. A key reason to understand the complex microphysical processes in MPCs is to accurately represent different hydrometeor types and the corresponding phase partitioning of water. Phase discrimination, quantification of hydrometeor type and determination of their size distribution is essential for many processes including cloud lifetime and radiative properties as well as precipitation formation.

Precipitation formation in turn is mainly initiated through the ice phase (Mülmenstädt, Sourdeval et al. 2015, Tan, Storelvmo et al. 2016) highlighting the need for ice nucleation studies encompassing hydrometeor phase discrimination. Laboratory studies investigating formation of primary ice crystals under MPC conditions include the use of Continuous Flow Diffusion Chamber (CFDC) experiments. Many CFDC studies use conventional optical particle counters, where particle phase is solely inferred from optical particle size.

Here, we present a new instrument, the high-speed Particle Phase Discriminator (PPD-HS), developed at the University of Hertfordshire and designed to determine the phase of cloud particles. We present in-depth analysis of instrumental performance and verify its applicability to CFDC experiments when operated as a particle detector at thermodynamic conditions relevant for MPCs.

PPD-HS records near-forward spatial intensity distributions along two vertically oriented CMOS (Complementary Metal-Oxide-Semiconductor) arrays, aligned with the optical axis of light scattered by individual particles. The unique aspect of PPD-HS compared to its predecessors (Vochezer, Järvinen et al. 2016) is the reduction of the memory bandwidth by only recording one-dimensional slices of the scattered light pattern. This significantly improves its sampling rate, allowing for detection of more than 1200 particles per second, making it suitable for laboratory applications.

The intensity of scattered light is primarily a function of particle size and shape as well as polarization and wavelength of the light source (Hirst and Kaye 1996). We show that even the reduced intensity profiles encompass enough information on particle morphology to discriminate particles as either spherical cloud droplets or aspherical ice crystals. This is achieved through symmetry analysis of the recorded scattering pattern, which are based on formal measures, that have been carefully developed within the framework of this project. We quantify the phase discrimination capabilities of PPD-HS through a series of benchmark experiments. We therefore use a variety of monodisperse particle populations with well-controlled shape and size, ranging from 1 to 15 μm. This is a common size range of particles generated within CFDCs. Our results show that PPD-HS successfully discriminates particle phase with a maximum misclassification ratio below 11%. Initial experiments reveal that incorporating PPD-HS into a CFDC setup extends the thermodynamic range in which particle phase can be reliably determined as compared to using regular optical particle counters.

REFERENCES
Hirst, E. and P. H. Kaye (1996). "Experimental and theoretical light scattering profiles from spherical and nonspherical particles." Journal of Geophysical Research: Atmospheres **101**(D14): 19231-19235.
Mülmenstädt, J., O. Sourdeval, J. Delanoë and J. Quaas (2015). "Frequency of occurrence of rain from liquid-, mixed-, and ice-phase clouds derived from A-Train satellite retrievals." Geophysical Research Letters **42**(15): 6502-6509.
Tan, I., T. Storelvmo and M. D. Zelinka (2016). "Observational constraints on mixed-phase clouds imply higher climate sensitivity." Science **352**(6282): 224-227.
Vochezer, P., E. Järvinen, R. Wagner, P. Kupiszewski, T. Leisner and M. Schnaiter (2016). "In situ characterization of mixed phase clouds using the Small Ice Detector and the Particle Phase Discriminator." Atmos. Meas. Tech. **9**(1): 159-177.

17.10
Free troposphere wintertime gas-phase composition using CI-APi-TOF

Ugo Molteni [1], Yulia Sosedova [1], Josef Dommen [1] and the NUCLACE collaboration [1,2]

[1] Laboratory of Atmospheric Chemistry, Paul Scherrer Institute, PSI Ost, CH-5323 Villigen
 (ugo.molgeni@gmail.com)
[2] Department of Physics, University of Helsinki, FI-00014 Helsinki, Finland
[2] Goethe University Frankfurt, Institute for Atmospheric and Environmental **Sciences, 60438 Frankfurt am Main, Germany
[2] University of Eastern Finland, FI-70211 Kuopio, Finland
[2] Aerodyne Research Inc., Billerica, Massachusetts 01821, USA

Atmospheric aerosols influence radiative forcing through direct interaction with radiation and by acting as cloud condensation nuclei. Up to 45% of cloud condensation nuclei (CCN) are not directly emitted in the atmosphere but formed via new particle formation (NPF), with a large fraction formed in the free troposphere (FT). While in the planetary boundary layer (PBL), new particle formation events have been frequently observed in different scenarios: pristine, urban, rural and coastal areas, measurements at high altitude because of intrinsic technical difficulties are very scattered. Therefore NPF in free troposphere is often modelled only on sulphuric acid concentration, relative humidity and temperature.

The CLOUD (Cosmics Leaving Outdoor Droplets) experiment has already showed how ammonia, amines and oxidized organics interact in synergy with sulfuric acid in so called ternary nucleation processes (Almeida et al., 2013; Kirkby et al., 2011; Riccobono et al., 2014). Further CLOUD experiments observed NPF driven by highly oxygenated molecules (HOMs) from terpenes ozonolysis in absence of sulfuric acid (Kirkby et al., 2016). Pure biogenic NPF is expected to be important especially in the preindustrial atmosphere and in defining the climate sensitivity through albedo change (Gordon et al., 2016).

The high-altitude research station Jungfraujoch (JFJ), Switzerland (3580 m above sea level) is a research site in the Swiss Alps and is in the FT for a substantial fraction of the time (especially in winter). Compared to other high-altitude stations, it is easy to access, which makes it a unique site for atmospheric observations. NPF events often occurs at Jungfraujoch (Tröstl et al., 2016) and it has been shown that they involve either sulphuric acid-ammonia or HOMs (Bianchi et al., 2016). Nitrate chemical ionization atmospheric pressure interface time of flight mass spectrometer (CI-APi-TOF) has been shown to be very selective in detecting gas phase sulfuric acid and HOMs at extremely low concentration (ppq) (Ehn et al., 2014).

Here we present the results for 2 winter periods: January – March 2013 and February – March 2014 where the CI-APi-TOF was part of 2 intensive campaigns NUCLACE 2013 and NUCLACE 2014. We describe the chemistry and the oxidation processes linked to NPF episodes. A special focus is given to sulphur containing species, halogens and HOMs as well as their temporal variability. Positive Matrix Factorization is applied to reduce a complex mass spectrographic dataset in a few significant profiles that are changing in the time domain. This is resulting in a rich scenario where HOMs from biogenic and anthropogenic precursor are identified and produced via different oxidation paths and eventually participate in NPF. The result is that the FT is a highly dynamic environment where hundreds of organic species are transported and transformed.

REFERENCES

Almeida, J. et al. 2013: Molecular understanding of sulphuric acid-amine particle nucleation in the atmosphere., Nature, 502(7471), 359–63.
Bianchi, F. et al. 2016: New particle formation in the free troposphere: A question of chemistry and timing, Science (80)., 352(6289), 1109–1112.
Ehn, M. et al. 2014: A large source of low-volatility secondary organic aerosol, Nature, 506(7489), 476–479.
Gordon, H. et al. 2016: Reduced anthropogenic aerosol radiative forcing caused by biogenic new particle formation, Proc. Natl. Acad. Sci., 201602360.
Kirkby, J. et al. 2011: Role of sulphuric acid, ammonia and galactic cosmic rays in atmospheric aerosol nucleation., Nature, 476, 429–433.
Kirkby, J. et al. 2016: Ion-induced nucleation of pure biogenic particles, Nature, 533(7604), 521–526.
Riccobono, F. et al. 2014: Oxidation Products of Biogenic Emissions Contribute to Nucleation of Atmospheric Particles, 344(May), 717–721
Tröstl, J. et al. 2016: Contribution of new particle formation to the total aerosol concentration at the high-altitude site Jungfraujoch (3580 masl, Switzerland), J. Geophys. Res. Atmos., 121(19), 11,692-11,711.

17.11
Real-Time Wet Scavenging of Organic Carbon and Elemental Carbon during Monsoon and Non-Monsoon Seasons at Delhi

Saurabh Sonwani°, and Umesh Kulshrestha

School of Environmental Sciences, Jawaharlal Nehru University, New Delhi-110067 °(sonwani.s19@gmail.com)

Organic Carbon (OC) and Elemental Carbon (EC) measurements in PM10 and rainwater were carried out to study their wet scavenging from atmosphere over Delhi, India. The sampling procedure involved a simultaneous collection of PM10 and rainwater at Jawaharlal Nehru University (JNU) site during monsoon and Non-monsoon season during 2016-2017. The PM_{10} samples were collected Before Rain (BR), During Rain (DR) and After Rain (AR) events, while rainwater samples were collected on the event basis. The average level of OC was always found to be higher as compared to the average EC into the atmosphere. It was observed that the OC amount was significantly removed from the atmosphere as compared to EC. However, their removal percentage through rain was almost similar i.e. 29.9% for OC and 29.4% for EC aerosols. The Scavenging Ratios (SRs) for OC and EC were also determined to analyze their relationship with rain intensity. The SRs of EC were significantly higher during non-monsoon as compared to monsoon season. Such characteristics can be explained by on the particles size, source and the hygroscopicity of both types of carbonaceous aerosols.

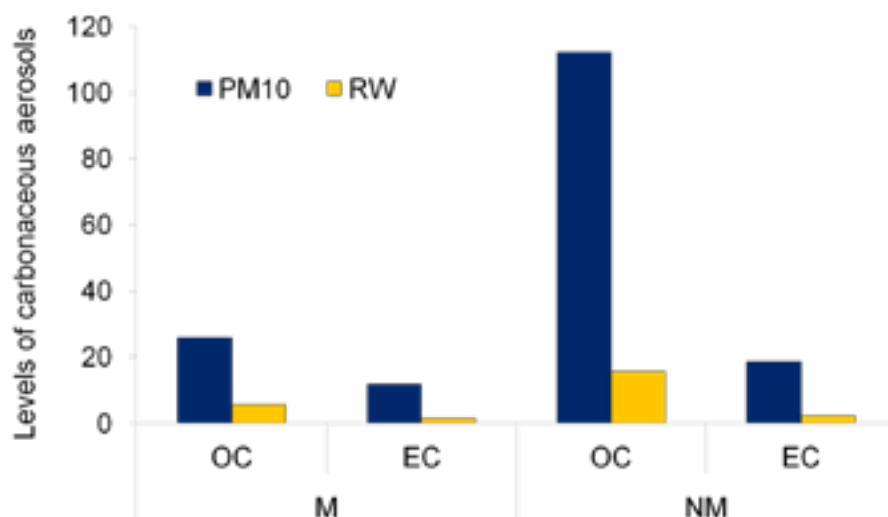Bullet lists: Organic Carbon, Elemental Carbon, Scavenging Ratio, Rain Intensity.

Figure 1. Mean of OC and EC levels during Monsoon (M) and Non-Monsoon (NM) season
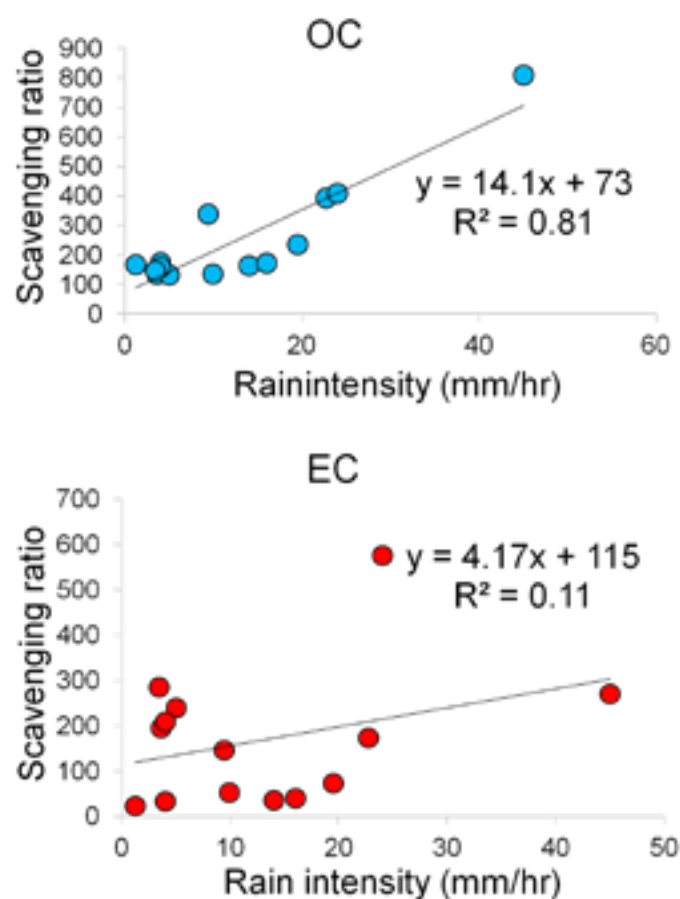
Fig. 2. Relationship between scavenging ratio of carbonaceous aerosols (OC and EC) and rain intensity

REFERENCES

Kulshrestha, U.C., Reddy, L.A.K., Satyanarayana, J. and Kulshrestha, M.J., 2009: Real-time wet scavenging of major chemical constituents of aerosols and role of rain intensity in Indian region. Atmospheric Environment, 43(32), pp.5123-5127.

Granat, L., Norman, M., Leck, C., Kulshrestha, U.C. and Rodhe, H., 2002: Wet scavenging of sulfur compounds and other constituents during the Indian Ocean Experiment (INDOEX). Journal of Geophysical Research: Atmospheres, 107(D19).

P 17.1
Ice nucleation abilities of soot particles determined with the Horizontal Ice Nucleation Chamber

Fabian Mahrt [1], C. Marcolli [1], Robert O. David [1], Philippe Grönquist [2], Eszter J. Barthazy Meier [3], Ulrike Lohmann [1] & Zamin A. Kanji [1]

[1] *Institute for Atmospheric and Climate Science, ETH Zurich, Zurich, 8092, Switzerland*
[2] *Institute for Building Materials, ETH Zurich, 8093 Zurich, Switzerland*
[3] *Scientific Center for Optical and Electron Microscopy, ETH Zurich, 8093 Zurich, Switzerland*

A quantitative understanding of the aerosol-cloud interactions of soot particles, especially their ability to form ice, remains a key factor to reduce the uncertainties in the estimates of the net radiative forcing of black carbon (Bond et al. 2013). However, previous studies have revealed significant spread, when reporting the ice nucleation ability of soot. This is partly caused by the diverse physico-chemical properties associated with morphologically complex soot aggregates.

 These varying results are the primary motivation of this study, which aims to better understand the ice nucleation behavior and mechanism of soot particles in relation to the particle properties. In this study, we present a systematic laboratory-based investigation of the ice nucleation behavior of different soot types. Various commercial soot samples are used, including an amorphous industrial black carbon, a fullerene soot, and Lamp Black carbon. In addition, soot generated from a propane flame Combustion Aerosol Standard Generator (miniCAST, JING AG), is investigated. Such soot has previously been used for ice nucleation studies and is frequently taken as proxy for atmospheric soot particles (e.g. Crawford et al. 2011).

We tested the ice nucleation ability of the above soot samples on DMA (Differential Mobility Analyzer) size-selected aerosol over a temperature range from 253 K to 218 K, covering both the mixed-phase and cirrus cloud regime. The heterogeneous freezing ability of soot at low temperatures is especially important, as aircraft emissions are a direct source of combustion particles in the upper troposphere, where cirrus temperatures prevail.

The ice nucleation ability of soot is probed using the Horizontal Ice Nucleation Chamber (HINC, Lacher et al. (2017)), a Continuous Flow Diffusion Chamber. A suite of auxiliary measurements complements ice nucleation observations to characterize the physio-chemical properties of the tested aerosol particles that ultimately aid in determining their ice nucleation behaviour: Thermogravimetric Analysis (TGA) was performed over a temperature range between 0 to 1000 °C to estimate the proportion of volatile components associated with the different soot types. Nitrogen adsorption following the BET-method (Brunauer et al. 1938) was conducted to obtain specific surface area. Water adsorption isotherms of the soot particles are also collected to allow assessment of the hydrophilicity and the porosity of the samples. Size and aggregate morphology are investigated by a dedicated set of coupled DMA – CPMA (Centrifugal Particle Mass Analyzer) experiments to determine fractal dimension of the soot particles. Finally, Transmission Electron Microscopy studies, performed on size selected particles, using the Zurich Electron Microscopy Impactor, complement our aerosol characterization.

Our results reveal droplet activation for all soot types at RH_w > 100% at temperatures above 233 K with absence of any heterogeneous freezing. However, in the cirrus cloud regime, some soot types show significant heterogeneous freezing, depending on the aerosol size. These soot types are associated with relatively high porosity and water affinity, whereas those soot types with poor ice nucleation ability show considerably reduced water adsorption characteristics. We discuss our result in context of a pore condensation and freezing type ice nucleation mechanism (Marcolli 2014) being responsible for the observed ice nucleation ability of the soot particles.

REFERENCES
Bond, T. C., et al. (2013), ‚Bounding the role of black carbon in the climate system: A scientific assessment', *Journal of Geophysical Research-Atmospheres,* 118 (11), 5380-552.
Brunauer, S., Emmett, P. H., and Teller, E. (1938), ‚Adsorption of gases in multimolecular layers', *Journal of the American Chemical Society,* 60, 309-19.
Crawford, I., et al. (2011), ‚Studies of propane flame soot acting as heterogeneous ice nuclei in conjunction with single particle soot photometer measurements', *Atmospheric Chemistry and Physics,* 11 (18), 9549-61.
Lacher, L., et al. (2017), ‚The Horizontal Ice Nucleation Chamber (HINC): INP measurements at conditions relevant for mixed-phase clouds at the High Altitude Research Station Jungfraujoch', *Atmospheric Chemistry and Physics,* 17 (24), 15199-224.
Marcolli, C. (2014), ‚Deposition nucleation viewed as homogeneous or immersion freezing in pores and cavities', *Atmos. Chem. Phys.,* 14 (4), 2071-104.

18. Atmospheric Processes and Interactions with the Biosphere

Christof Ammann, Stefan Brönnimann, Susanne Burri, Martin Steinbacher

ACP – Commission on Atmospheric Chemistry and Physics

TALKS:

18.1   Affolter S., Schibig M., Berhanu T., Leuenberger M.: Comparison of two high alpine CO_2 records from the Jungfraujoch area

18.2   Bernet L., Kämpfer N., Hocke K.: Stratospheric ozone recovery at mid-latitudes: improved ground-based time series and trend estimations

18.3   Brogli R., Kröner N., Sørland S.L., Lüthi D., Schär C.: The role of Hadley circulation and lapse-rate changes for the future European summer climate

18.4   Brönnimann S. and the OCCR-1868 team: 1868 – the flood that changed Switzerland

18.5   Jiskra M.: Effects of the vegetation mercury pump on seasonal variations in atmospheric mercury concentrations

18.6   Mazzotti G., Malle J., Barr S., Essery R., Jonas T.: Capturing spatial patterns of sub-canopy irradiance: mobile radiometer surveys and model results

18.7   Osterwalder S.: Upward, downward or neither: ecosystem scale mercury flux at forest and ocean ICOS sites

18.8   Paul S., Leifeld J., Alewell C., Ammann C.: Carbon budget response of an agriculturally used fen soil to a heavy precipitation event

18.9   Pieber S.M., Brunner D., Henne S., Steinbacher M., Tuzson B., Emmenegger L.: A decade of continuous atmospheric CO_2 isotope ratio measurements at Jungfraujoch

18.10   Vogt R., Schmutz M., Feigenwinter C., Parlow E.: Seasonal and inter-annual variability of CO_2 fluxes: 14 years of eddy covariance measurements in Basel

18.11   Volk M., Wahl A.-L., Giger R., Bassin S.: Subalpine grassland growth during five years of warming

18.12   Zamuriano M.: Atmospheric characteristics of a heavy snowfall event over the central Andes

POSTERS:

P 18.1   Feigenwinter I., Buchmann N.: Investigating N_2O fluxes over permanent grassland

P 18.2   Jensen C.M., Fischer H., Erhardt T.: First continous high-resolution record from the East Greenland Ice Core Project (EGRIP), covering the last 2800 years

P 18.3   Leuenberger M., Herrmann L.: First eddy covariance flux analysis at the tall tower site Beromünster, Switzerland

P 18.4   Li Y., Riedl A., Aemisegger F., Buchmann N., Eugster W.: Quantifying the effect of dew and fog water on Swiss grasslands with stable isotopes

P 18.5   Liu Y., Klaus V., Gilgen A.K., Buchmann N., Oliveira Hagen E., Wittwer R.,: Assessment of Ecosystem Services of Arable Land in Response to Farming Practice and Drought

P 18.6   Maier R., Buchmann N.: Assessing resilience against climate change from greenhouse gas flux measurements in Switzerland

P 18.7   Paul S., Ammann C., Alewell C., Leifeld J.: Do cover fills reduce peat oxidation and carbon emissions from managed organic soils?

P 18.8   Record S., Siegenthaler A.: Influence of the mangrove forest on the net emission of methane in water bodies of the Gandoca Lagoon (Costa Rica) and its managerial implications

P 18.9   Riedl A., Yafei Li, Eugster W.: The Importance of Dew and Fog for Swiss Grasslands

P 18.10   Saxena P., Ghosh C.: A Sustainable Tool for Assessment of Effect of Ozone on Delhi Ridge, India

P 18.11   Schibig M.F, Nyfeler P., Leuenberger M.C.: High precision CO_2 and O_2 measurements at the High Altitude Research Station Jungfraujoch, Switzerland

P 18.12   Qing Sun, Gilgen A.K., Klaus V., Signarbieux C., Buchmann N.: Plant water relations under drought in organic and conventional farming systems

P 18.13   Bühler M., Häni C., Kupper T., Ammann C., Brönnimann S..: Assesment of methane emissions from animal and waste processing operations using an inverse dispersion technique

18.1
# Comparison of two high alpine CO_2 records from the Jungfraujoch area

Stéphane Affolter[1], Michael Schibig[2,3], Tesfaye Berhanu[2,3] and Markus Leuenberger [2,3,1]

[1] *International Foundation High Altitude Research Stations Jungfraujoch and Gornergrat, Bern, Switzerland*
  (affolter@climate.unibe.ch)
[2] *Climate and Environmental Physics, Physics Institute, University of Bern, Switzerland*
[3] *Oeschger Centre for Climate Change Research, University of Bern, Switzerland*

The Sphinx observatory, part of the High Altitude Research Station located at the Jungfraujoch (Swiss Alps, 3570 m a.s.l.), has been hosting for decades several experiments of various research institutes worldwide and constitutes a key location for atmospheric measurements in Europe. Main features of the site are the remote setting and its exposure to pristine air masses with only sporadic pollution events originating from the lowlands. Since December 2014, we have an additional location available for research at the Jungfrau East Ridge (3690 m a.s.l.) around 1 km westward from the Sphinx observatory. It offers an alternative to the Sphinx location where space availability is limited. This new location is not accessible for tourists and thus well suited to compare air quality measurements to those recorded at the Sphinx observatory. A Picarro L2120-i laser based instrument has been installed in the East Ridge building which is continuously measuring the CO_2 mole fraction in the atmosphere that can be compared with the Sphinx data (i) to evaluate the suitability of the new site and (ii) to investigate the potential pollution inherent to anthropogenic activities at the Jungfraujoch. The two years long comparison of CO_2 records show a good agreement between both sites but exhibits annually averaged daily differences of less than 1 ppm whereas the corresponding nighttime values are within the measurement precision. Preliminary results indicate a potential influence of visitors at the Sphinx on CO_2 values, but other factors, i.e. different air mass movements, may also be involved in these diurnal variations. There is a distinct seasonal pattern with highest CO_2 excess values for mean summer midday values of maximal 1.5 ppm. Since spring 2017, tourists are informed about sensitive measurements being done at Jungfraujoch and are asked not to smoke on the tourist terrace, which helped to reduce the aerosol emissions. Yet, for CO_2 this had no effect. In summary and as expected, our preliminary results from CO_2 measurements show the suitability of the East Ridge as an additional new location to perform high quality atmospheric measurements.
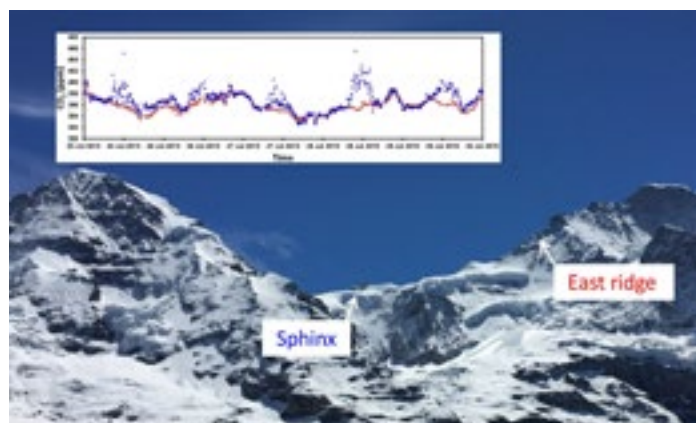
18.2

Stratospheric ozone recovery at mid-latitudes: improved ground-based time series and trend estimations

Leonie Bernet [1,2], Niklaus Kämpfer [1,2], Klemens Hocke [1,2]

[1] Institute of Applied Physics, University of Bern, Bern, Switzerland (leonie.bernet@iap.unibe.ch)
[2] Oeschger Centre for Climate Change Research, University of Bern, Bern, Switzerland

Monitoring the recovery of stratospheric ozone is essential to verify the effectiveness of the Montreal Protocol. After the protocol banned ozone depleting substances, first signs of an ozone recovery in the stratosphere were observed starting in 1997. Recent studies have confirmed that mid-latitudinal ozone is increasing in the middle stratosphere due to chemical and dynamical effects, whereas evidence is still missing for an increase in the lower stratosphere. To improve trend estimations of stratospheric ozone profiles, continuous and stable time series are crucial and trend uncertainties need to be addressed.

We present an updated and improved 23-years time series of stratospheric ozone from the GROMOS (GROund-based Millimeter-wave Ozone Spectrometer) microwave radiometer located at Bern, Switzerland, that provides ozone profiles from 20-50km. We compared the data with other ground-based instruments in central Europe from the Network for the Detection of Atmospheric Composition Change (NDACC). Based on the different data sets we estimated trends of stratospheric ozone volume mixing ratios (VMR) with a multilinear trend model that can handle uncertainties in a flexible way. The datasets show positive ozone VMR trends of 1-3% in the middle stratosphere (25-40km), and biased results in the lower stratosphere. Our study further elucidates how trend estimates of stratospheric ozone are influenced by factors such as uncertainties of the underlying ozone data, sampling rate and period length. The GROMOS data are well suited to investigate such factors thanks to the long and complete time series and the high temporal resolution.

18.3

The role of Hadley circulation and lapse-rate changes for the future European summer climate

Roman Brogli [1], Nico Kröner [1], Silje Lund Sørland [1], Daniel Lüthi [1] & Christoph Schär [1]

[1] Institute for Atmospheric and Climate Science, ETH Zürich, Universitätstrasse 16, CH-8092 Zürich (roman.brogli@env.ethz.ch)

By the end of the century, climate projections for Southern Europe exhibit an enhanced near-surface summer warming in response to greenhouse gas emissions, which is known as the Mediterranean Amplification. Possible causes for this amplified warming signal include a poleward Hadley cell expansion as well as tropospheric lapse-rate changes.
In this work, regional climate model (RCM) simulations driven by three different global climate models (GCMs) are performed. For every downscaled GCM, the climate change signal over Europe is separated into five contributions by modifying the lateral boundary conditions of the RCM. This simulation strategy is related to the pseudo-global-warming method, representing the RCP 8.5 emission scenario at the end of the century.

The results show that a poleward expansion of the Hadley cell is of minor importance for the Mediterranean Amplification. During summer, the simulated Hadley circulation is weak and projections show no distinct expansion in the European sector.

The north-south contrast in lapse-rate changes is suggested as the most important factor causing the Mediterranean Amplification. Lapse-rate changes are projected throughout Europe, but are weaker over the Mediterranean than over Northern Europe (around 0.15 K/km vs. 0.3 K/km by the end of the century). The weaker lapse-rate changes result in a strong near-surface summer warming over the Mediterranean since the upper-tropospheric warming is of similar magnitude throughout Europe. The differing lapse-rate changes can be understood as a thermodynamic response to lower-tropospheric humidity contrasts. Thus, the results suggest that the projected enhanced summer warming in Southern Europe can be linked to thermodynamic processes, which are thought to be relatively reliable in climate projections.

18.4
1868 - the flood that changed Switzerland

Brönnimann, S [1]. and the OCCR-1868 team

[1] *Institute of Geography. University of Bern. Hallerstrasse 12, CH-3012 Bern, Switzerland.*

In autumn 1868 — exactly 150 years ago — parts of Switzerland were affected by severe floods. Two phases of heavy rainfall on 27 and 28 September and from 1 to 5 October caused numerous rivers and lakes to overflow their banks. Coping with the enormous damage, managing the extensive donations, and finding a procedure of how to prevent such events in the future were a major challenge for the young nation. The discussions at that time set the course for the management of natural disasters during the 20th century, affecting today's landscape. Today, new methods allow the detailed reconstruction of precipitation events and floods, while, from a historical point of view, flood management and the socio-political effects can be evaluated. An interdisciplinary research project (of the Oeschger Centre for Climate Research at the University of Bern and the Mobiliar Lab for Natural Risks, in cooperation with MeteoSwiss, Meteotest and the Swiss Federal Institute for Forest, Snow and Landscape Research) has investigated these questions over the past two years. THe presentation focuses on the natural science aspects of the project. The meteorological background of the event is understood and can be reconstructed quite well on a large scale. The local weather situation can also be depicted using downscaling techniques. Hydrological modelling shows that due to the erosion that occurred during this event, such a high level of Lake Maggiore as in 1868 could no longer be reached today. Finally, hydraulic modelling is able to depict the flooded area and the endangered buildings, with and without river construction, for historical and present day building distributions.

18.5
Effects of the vegetation mercury pump on seasonal variations in atmospheric mercury concentrations

Martin Jiskra [1]

[1] *Umweltgeowissenschaften, University of Basel, Bernoullistrasse 30, CH-4056 Basel (martin.jiskra@unibas.ch)*

Mercury is a top priority global pollutant threatening human and ecosystem health. Anthropogenic mercury emissions are emitted and transported through the atmosphere as gaseous elemental mercury ($Hg0$) before being deposited on land and ocean. Strong seasonal variations in atmospheric $Hg0$ concentrations are observed in the Northern Hemisphere, with maxima in winter and minima in summer. The seasonality of atmospheric $Hg0$ has mainly been attributed to seasonal variations in anthropogenic $Hg0$ emissions peaking in winter due to high energy production for heating or seasonal variation in photochemically driven $Hg0$ oxidation with maximum rates in summer. Here, I present evidence that the seasonal variation of anthropogenic mercury emission can not fully explain atmospheric $Hg0$ seasonality and that the oxidation of atmospheric $Hg0$ is overestimated. I will discuss $Hg0$ drawdown by vegetation – the vegetation mercury pump – as alternative to explain variations in atmospheric $Hg0$ concentrations. Atmospheric $Hg0$ concentrations correlate with CO_2, known to exhibit a strong seasonal variation driven by vegetation assimilating CO_2 in summer. Both trace gases, $Hg0$ and CO_2, show a strong correlation with satelite-derived vegetation activity data. This suggests that the uptake of $Hg0$ by vegetation plays a dominant role in atmospheric $Hg0$ cycling. In this presentation I will also touch on how the vegetation mercury pump may have changed in the recent decades due to increases in net primary production and how $Hg0$ uptake by vegetation may be affected by climate change.

REFERENCES
Jiskra, M., Sonke, J. E., Obrist, D., Bieser, J., Ebinghaus, R., Myhre, C. L., Pfaffhuber, K. A., Wangberg, I., Kyllonen, K., Worthy, D., Martin, L. G., Labuschagne, C., Mkololo, T., Ramonet, M., Magand, O., Dommergue, A. 2018: A vegetation control on seasonal variations in global atmospheric mercury concentrations. Nat. Geosci. 11, (4), 244-250.

18.6
Capturing spatial patterns of sub-canopy irradiance: mobile radiometer surveys and model results

Giulia Mazzotti [1,2] Johanna Malle [1,3] Sarah Barr [1]   Richard Essery [4] Tobias Jonas [1]

[1] *WSL Institute for Snow and Avalanche Research SLF, Flüelastrasse 11, CH-7260 Davos Dorf (giulia.mazzotti@slf.ch)*
[2] *Laboratory of Hydraulics, Hydrology and Glaciology, ETHZ, CH-8093 Zürich*
[3] *Department of Geography, University of Northumbria, Newcastle, UK*
[4] *School of Geosciences, University of Edinburgh, Edinburgh, UK*

Incoming radiation to the forest floor impacts on a number of eco-hydrological processes; for example, it exerts a key control on forest snow melt dynamics. Small-scale variations in radiative transfer through forest canopies, which are closely linked to canopy structural heterogeneity, create complex spatial snow melt patterns and entail big challenges for snow cover modelling. To date however, upscaling of radiative transfer parametrizations developed at the point scale is hampered by i) a lack of approaches to represent canopy structure variability and ii) limited spatially explicit sub-canopy irradiance data to validate and assess the performance of radiative fluxes parametrizations at typical model resolutions.
This study presents a novel approach to in-situ characterization of canopy structure and sub-canopy irradiance over previously unprecedented spatial extents. The method involves two radiometers mounted to a motorized gimbal developed for continuous measurements of incoming shortwave and longwave radiation along forest transects. Coupling these to radiation and temperature data from a reference station, spatially-resolved estimates of canopy transmissivity, longwave enhancement and sky view fraction could be derived.

Validation of the new method against sky view fraction data from hemispherical photographs resulted in a RMSE of 0.03. Shortwave transmissivity and longwave enhancement along transects within forests of heterogeneous canopy cover revealed distinct spatial patterns, illustrating strong links between sub-canopy irradiance and the overlying canopy structure.

Concurrent modelling was conducted using the Flexible Snow Model FSM2, which includes coupled energy balances of the sub-canopy snow cover and a 1-layer canopy. Modelled sub-canopy radiative fluxes were compared to radiometer measurements to assess model performance. We show which modelling strategies within FSM2 best succeed in reproducing both average radiative transfer processes and their spatial variability. The application demonstrates that datasets from our mobile radiometer surveys yield a great potential to inform process model upscaling efforts, and to improve the representation of the sub-canopy radiation regime in snow cover models.

18.7

Upward, downward or neither: ecosystem scale mercury flux at forest and ocean ICOS sites

Stefan Osterwalder [1, 2]

[1] Department of Environmental Sciences, University of Basel, 4056 Basel, Switzerland
[2] Department of Forest Ecology and Management, Swedish University of Agricultural Sciences, 901 83 Umeå, Sweden
  (stefan.osterwalder@unibas.ch)

The toxic burden of anthropogenic mercury (Hg) pollution for human and ecosystem health is globally accepted by policy makers and has resulted in the signature of the UNEP Minamata Convention on mercury by over 100 countries. The 2013 convention aims to reduce Hg use and curb global anthropogenic Hg emissions to the atmosphere. However, since the middle ages over 1.5 Mio tons of anthropogenic Hg have been emitted to the environment forming large pools of legacy Hg in soils and the oceans. Re-emission of legacy Hg is now believed to account for about 60% of the Hg entering the atmosphere each year complicating the understanding of its biogeochemical cycle. But there is much uncertainty concerning re-emission, especially over forests and oceans. Current net Hg flux estimates range from -727 - 707 tons yr^{-1} for forests and 1900 - 4200 tons yr^{-1} for oceans. We use the infrastructure of ICOS stations in Sweden and Switzerland to investigate the sink-source characteristics of atmospheric Hg in forest and marine ecosystems. At the atmospheric ICOS station Svartberget, Sweden (64°15′N, 19°46′E) and CLASS 1 Ecosystem Monitoring Station in Davos Seehornwald, Switzerland (46°49′N, 9°51′E), we investigate the role of Hg atmosphere-canopy and near ground atmosphere-soil exchange in the Hg biogeochemical cycle. We will try to link our results to contemporaneous studies on the carbon balance there. At the marine ICOS station Östergarnsholm, Sweden (57°26′N, 18°59′E) we combine measurements of Hg isotope signatures with micrometeorological and bulk methods to assess processes of the ocean-atmosphere exchange of Hg and to determine its efflux. We aim to improve parameterization in ocean-air exchange models for Hg by applying micrometeorological methods, e.g. during periods of upwelling or high wind speeds. The ICOS infrastructure offers excellent conditions for long-term measurements of Hg surface-atmosphere exchange. Taking advantage of these infrastructures is a big asset for our ongoing Hg flux projects due to the free access to high precision, all-season meteorological and ecosystem flux data such as CO_2, CH_4 and H_2O and the possibilities for collaboration with long-term ecosystem research programs that have coalesced around the ICOS infrastructures.

18.8

Carbon budget response of an agriculturally used fen soil to a heavy precipitation event

Sonja Paul [1], Jens Leifeld [2], Christine Alewell [1] & Christof Ammann [2]

[1] Umweltgeowissenschaften, University of Basel, Bernoullistrasse 30, CH-4056 Basel, Switzerland (sonja.paul@unibas.ch)
[2] Climate and Agriculture Group, Agroscope, Reckenholzstrasse 191, 8046 Zürich, Switzerland

Peatlands have served as important carbon sinks in the past and currently they store globally more than 30% of the soil organic carbon, although they cover only 3% of the Earth's land surface. The agricultural use of peatlands usually requires drainage, thereby transforming these organic soils from a net carbon sink into a net source. These soils react sensitively to changes in temperature and water regimes and thus to several aspects related to the ongoing climate change. During the last century, increasing trends in heavy precipitation and heat waves events have been observed in Switzerland (Scherrer et al. 2016). Models project an intensification of heavy rain events as well (Rajczak et al. 2013). However, effects of heavy rain events on the carbon balance of these susceptible organic soils under agricultural have not yet been reported.

The Seeland region of Switzerland is characterised by fens that are intensively used for agriculture since 1900. Our study site was under crop rotation until 2009 when it was converted to extensively used grassland with the water regime still being regulated. However, an extreme rain event in May 2015 led to partial flooding of the grassland.

The carbon balance was determined for two full years (2015-2016) by accounting all relevant carbon fluxes entering and leaving the soil-vegetation system. Therefore net ecosystem exchange, CH_4 fluxes and carbon removal by harvest were measured. The gas exchange for CO_2 and CH_4 was determined using the eddy covariance method. Fast response gas concentrations were measured with open path devices (LI-COR LI7500A for CO_2 and H_2O; LI7700 for CH_4). The three-dimensional wind speed was measured with a sonic anemometer (Campbell CSAT-3). In addition, controlling parameters including global radiation, precipitation, soil temperature and humidity, and groundwater level were recorded.

For both years, the carbon balance indicates that the degraded fen site was a strong carbon source of approximately 450 g C m-2 a-1. As expected, highest methane fluxes were measured during the flooding event, while methane emissions were generally marginal throughout the two years. The year 2015, characterised by the heavy rain event in May followed by a dry and hot summer, showed a much lower net CO_2 uptake and lower carbon export by harvest compared to 2016. For a detailed analysis of the flooding effect on the carbon budget, the carbon fluxes were analysed separately for the western (non-flooded) and the eastern (flooded) part of the grassland field (see Fig. 1). The net CO_2 uptake of the flooded part was lower compared to the non-flooded part. In addition the yield of the first cut was also substantially smaller. For the net carbon balance, the reduced carbon uptake by the flooded area was largely offset by the reduced harvest. Thus, the flooding event altered the short-term carbon fluxes; however the total carbon source strength stayed rather constant on an annual basis.

Figure 1: Study site in the Seeland near Cressier, Neuchatel during a flooding event.

REFERENCES:
Rajczak, J., P. Pall, and C. Schaer (2013), Projections of extreme precipitation events in regional climate simulations for Europe and the Alpine Region, J. Geophys. Res. Atmos., 118, 3610–3626, doi:10.1002/jgrd.50297.
Scherrer, S. C., E. M. Fischer, R. Posselt, M. A. Liniger, M. Croci-Maspoli, and R. Knutti (2016), Emerging trends in heavy precipitation and hot temperature extremes in Switzerland, J. Geophys. Res. Atmos., 121, 2626–2637, doi:10.1002/2015JD024634.

18.9
A decade of continuous atmospheric CO$_2$ isotope ratio measurements at Jungfraujoch

Simone M. Pieber [1], Dominik Brunner [1], Stephan Henne [1], Martin Steinbacher [1], Béla Tuzson [1] & Lukas Emmenegger [1]

[1] Empa, Laboratory for Air Pollution and Environmental Technology, Ueberlandstrasse 129, CH-8600 Duebendorf
(simone.pieber@empa.ch)

Long-term observations of greenhouse gases such as carbon dioxide (CO$_2$) provide direct information about their variability and rate of change in the atmosphere. Coupled with atmospheric modelling, these measurements can also identify specific source and sink regions, especially when co-located continuous observations of the CO$_2$ isotope ratios are available. CO$_2$ isotope ratios provide unique information on the fluxes of CO$_2$ between the different environmental pools involved in the carbon cycle owing to isotopic fractionation during physical, chemical and biological processes.

The High Altitude Research Station Jungfraujoch (3580 m.a.s.l.), Switzerland, is a renowned monitoring site with a long-term history in atmospheric research. Continuous records of atmospheric CO$_2$ concentration and isotope ratios measured by online quantum cascade laser absorption spectroscopy (QCLAS) are available since December 2008 at this station (Tuzson et al., 2008 and 2011; Sturm et al. 2013). The time-series spanning one decade with 10 min resolution allow not only unprecedented insights into seasonal and long-term trends, but also capture variations on hourly and diurnal timescales. Thereby, isotopic signatures of specific anthropogenic pollution or biospheric depletion events become accessible.

Here we present a detailed analysis and interpretation of the CO$_2$, δ^{13}C-CO$_2$ and δ^{18}O-CO$_2$ time-series in the context of accompaning observations of other trace gases (including e.g., CO, NOy, aliphatic and aromatic hydrocarbons, and carbonyl sulfide), backward Lagrangian particle dispersion modelling (Stohl et al., 2005), and filtering techniques for free troposphere and statistical background conditions. The free troposphere conditions were determined using chemical tracers as well as the simulated residence time of air parcels within the planetary boundary layer (PBL) before arrival at the Jungfraujoch station, following the approach recently summarized by Herrmann et al., 2015. Background conditions, i.e. conditions not impacted by pollution or depletion events, are also calculated applying a statistical filtering technique directly to the observations (Ruckstuhl et al., 2012).

Our large scale synthesis reveals the potential of this unique continuous data set, showing the decadal trend in the parameters' background concentrations, as well as their annual patterns indicating a seasonal phase-shift between CO$_2$ concentration and the δ^{13}C and δ^{18}O signatures. Classification and clustering of the data based on atmospheric transport model simulations is ongoing with the aim to determine the isotopic signatures of individual and regional pollution and depletion events and associated implications for the sources and sinks of CO$_2$.

REFERENCES

Herrmann, E., Weingartner, E., Henne, S., Vuilleumier, L., Bukowiecki, N., Steinbacher, M., Conen, F., Coen, M. C., Hammer, E., Jurányi, Z., Baltensperger, U. & Gysel, M. 2015: Analysis of long-term aerosol size distribution data from Jungfraujoch with emphasis on free tropospheric conditions, cloud influence, and air mass transport, JGR, 120, 9459-9480.

Ruckstuhl, A. F., Henne, S., Reimann, S., Steinbacher, M., Vollmer, M. K., O'Doherty, S., Buchmann, B. & Hueglin, C. 2012: Robust extraction of baseline signal of atmospheric trace species using local regression, AMT, 5, 2613-2624.

Stohl, A., Forster, C., Frank, A., Seibert, P., & Wotawa, G. 2005: Technical note: The Lagrangian particle dispersion model FLEXPART version 6.2, ACP, 5, 2461-2474.

Sturm, P., Tuzson, B., Henne, S. & Emmenegger, L. 2013: Tracking isotopic signatures of CO$_2$ at the high altitude site Jungfraujoch with laser spectroscopy: Analytical improvements and representative results, AMT, 6, 1659-1671.

Tuzson, B., Henne, S., Brunner, D., Steinbacher, M., Mohn, J., Buchmann, B. & Emmenegger, L. 2011: Continuous isotopic composition measurements of tropospheric CO$_2$ at Jungfraujoch (3580 m a.s.l.), Switzerland: Real-time observation of regional pollution events, ACP, 11, 1685-1696.

Tuzson, B., Mohn, J., Zeeman, M. J., Werner, R. A., Eugster, W., Zahniser, M. S., Nelson, D. D., McManus, J. B. & Emmenegger, L. 2008: High precision and continuous field measurements of δ^{13}C and δ^{18}O in carbon dioxide with a cryogen-free QCLAS, Appl. Phys. B, 92, 451-458.

18.10
Seasonal and inter-annual variability of CO_2 fluxes:
14 years of eddy covariance measurements in Basel

Roland Vogt [1], Michael Schmutz [1], Christian Feigenwinter [1] & Eberhard Parlow [1]

[1] University of Basel, Klingelbergstrasse 27, CH-4057 Basel (roland.vogt@unibas.ch)

Urban micrometeorology has a long tradition in Basel. Measurements started as early as 1992 including flux towers focusing on turbulent exchange and energy balance at that time. During BUBBLE 2002 CO_2 fluxes (FC) were measured in Basel and in 2004 the long-term FC measurements started at Klingelbergstrasse (BKLI) in order to monitor cities as hot spots of anthropogenic activities with respect to CO_2 emissions. 2009 a second flux tower at Aeschenplatz (BAES) was added. Fluxes are determined using the eddy covariance method and data are processed with EddyPro®. There are ~30% data gaps due to rainfall events, maintenance work and post processing (quality flags). For the gap-filled FC time series horizontal averages were calculated. This improves the significance and comparability of measured fluxes and demonstrates the need of adequate weighting by horizontal averaging in such heterogeneous urban environments, especially for the derivation of cumulative quantities like the annual net ecosystem exchange. FC is presented with respect to diurnal and seasonal cycles as well as inter-annual variabilities. FC shows a large inter-annual variability in times of high source activity (e.g., during the day and in winter). In contrast, a relatively constant background flux of 5 µmol m^{-2} s^{-1} is found during periods of low source activity. The long-term trend of FC is mostly superimposed by the large temporal variability and is found to be around ±5% over 10 years.

18.11
Subalpine grassland growth during five years of warming

Volk Matthias [1], Anne-Lena Wahl [1], Robin Giger [1], Seraina Bassin [1]

[1] Agroscope, Climate & Agriculture, Zurich, Switzerland (matthias.volk@agroscope.admin.ch)

In a five year field experiment we quantified the response of subalpine pasture productivity to climate change factors temperature and precipitation in interaction with increased atmospheric N-deposition.

On six southerly exposed alps across the Canton Graubünden (all at c. 2150 m a.s.l., but six different plant communities) 0.25 × 0.40 m area turf monoliths were excavated. Some monoliths remained at the original sites to serve as controls, 216 monoliths were transported to the experimental Climate Change-scenario sites (CS) in Engiadina Bassa. Monoliths were reinstalled in the ground at six altitudinal levels (from 2360 to 1680 m a.s.l.) on the south slope of Piz Cotschen. Compared to the mean temperature at the original sites the altitudinal gradient of the CS represented a temperature contrast (April – October) of -1.4 to +3.0° C. Supplemental irrigation aimed at adding up to 50% of natural precipitation to compensate for increased evapotranspiration under higher temperatures. The N-deposition treatment was equivalent to +3 and +15 kg N ha^{-1} yr^{-1}, on top of a background deposition of c. 4 kg N ha^{-1} yr^{-1}. Grassland yield was assessed annually as aboveground plant dry matter (>2 cm) at canopy maturity.

Yield responses to experimental treatments and annually changing weather conditions showed the limits of beneficial temperature effects at different soil moisture availabilities in this warmth limited ecosystem. The 'comfort zone' for this ecosystem can now be clearly defined.

We found surprisingly high tolerance towards increasing water scarcity, making temperature related yield gains possible even at the +1.8° C site. Both warmth and water availability individually modulated the yield by about 30% of the maximum. Preliminary analysis has not yet revealed an N-deposition effect on plant productivity, even in the +15 kg N ha^{-1} yr^{-1} treatment.

18.12
Atmospheric characteristics of a heavy snowfall event over the central Andes

Marcelo Zamuriano [1]

[1] *Oeschger Centre for Climate Change Research and Institute of Geography. University of Bern. Hallerstrasse 12, CH-3012 Bern, Switzerland. (marcelo.zamuriano@giub.unibe.ch)*

Numerical studies are used to add new insights about the atmospheric characteristics of the historical snowfall event over the Bolivian Andes in August 2013; causing severe damage to people, infrastructure and livestock. This event was associated to a cold front passage following the eastern slope of the Andes-Amazon interface but little was known about the intensity and spatial distribution at a regional scale. Using the Weather Research and Forecasting (WRF-ARW) model, we conduct a series of high resolution numerical experiments that includes sensitivity studies to microphysics schemes and land surface model configuration. We compare our findings to MODIS snow cover estimates and local reports. Our results are consistent both with the satellite observations, damage reports and the known dynamics. We highlight the importance of orography and the Cold Front position and persistence for the snowfall spatial distribution, the microphysics schemes for the timing and intensity, and the land surface model for the snow depth simulated.

P 18.1
Investigating N_2O fluxes over permanent grassland

Iris Feigenwinter [1], Nina Buchmann [1]

[1] *Institute of Agricultural Sciences, ETH Zürich, Universitätstrasse 2, CH-8092 Zürich (iris.feigenwinter@usys.ethz.ch)*

A large fraction of anthropogenic nitrous oxide (N_2O) emissions is caused by agriculture. Since N_2O is a highly relevant greenhouse gas (GHG), it is critical to determine N_2O fluxes and to develop N_2O mitigation strategies for the agricultural sector.

The PhD thesis presented here will be conducted within a Horizon 2020 project called SUPER-G (Developing SUstainable PERmanent Grassland systems and policies). The main objective is to improve our understanding of C and N fluxes on the soil-atmosphere interface of intensively managed grassland systems. We will investigate GHG fluxes over permanent grassland and continue a N_2O mitigation experiment at one of our research sites (Chamau) in the pre-alpine area of Switzerland. Previous work showed that N_2O emissions at this site are significantly reduced by a change in management: Increasing the proportion of legumes (clover) and thus replacing N fertilization with biological N fixation, decreased N_2O fluxes at the experimental compared to the control parcel where N fertilizer still was applied, while yields stayed high at both parcels (Fuchs et al. 2018).

Hence, we will investigate in more detail the processes that are involved in the production of N_2O such as nitrification and denitrification. Moreover, long-term (>10 years) net ecosystem CO_2 fluxes will be examined and validated by changes in soil carbon stocks to address carbon sequestration at the site. Resistance and resilience of the net CO_2 fluxes will be analyzed to gain insight into the vulnerability of grassland to past and future climate change.

We will use eddy covariance to quantify GHG fluxes by correlating high frequency wind measurements with high frequency fluctuations in gas concentrations. Further meteorological data from the Chamau research station will be used in the study, as well as samples of biomass, soil and air, which will be analysed for carbon and nitrogen concentrations as well as stable isotopes ($\delta^{13}C$ and $\delta^{15}N$).

REFERENCES

Fuchs, K., Hörtnagl, L., Buchmann, N., Eugster, W., Snow, V. & Merbold, L. 2018: Management matters: Testing a mitigation strategy for nitrous oxide emissions on intensively managed grassland. Biogeosciences Discussions, 1–43. doi: 10.5194/bg-2018-192

P 18.2

First continous high-resolution record from the East Greenland Ice Core Project (EGRIP), covering the last 2800 years

Camilla Marie Jensen [1], Hubertus Fischer [1], Tobias Erhardt [1]

[1] *Climate and Environmental Physics, Physics Institute, Oeschger Centre for Climate Change Research, University of Bern*

Ice sheets are reliable archives of atmospheric impurities such as aerosols and gasses of both natural and anthropogenic origin. Impurity records from Greenland ice cores reveal much information about previous atmospheric conditions and long-range transport in the Northern hemisphere going back more than a hundred thousand years.The seasonal variability of impurities and stable water isotope ratios can be employed to count annual layers in ice cores going back several thousands of years.

Continuous analysis techniques, applied to soluble impurities and particles in ice cores, offer several benefits over discrete sampling approaches, including greater sampling resolution, simpler and more effective contamination control and greater sample throughput. Ions may be determined in ice cores by several techniques, of which Ion Chromatography (IC), Inductively-Coupled Plasma Mass Spectrometry (ICP-MS), absorption and florescence spectroscopy are the most common. ICP-MS systems typically use a nebuliser for introduction of a continuous liquid sample stream, and hence is coupled to CFA in a relatively straightforward manner. IC may also be coupled to continuous flow analysis (CFA) using the semi-cotinuous Fast Ion Chromatrography technique.

The CFA system used for ice cores has been developed and optimized at the University of Bern from the early 90s. The system consist of a melting unit, where the ice with a cross section of 3535 mm2 is melted continuously. Hereafter, only the sample stream from the inner uncontaminated part of the ice is continuously measured using mainly absorption and florescence spectroscopy. The current wet chemistry CFA system at the University of Bern is capable of measuring conductivity, dust, sodium (Na^+), calcium (Ca^{2+}), ammonium (NH_4^+), nitrate (NO_3^-) and hydrogen peroxide (H_2O_2). Clear annual cycles can be observed in most of the mentioned species. This can be used to date the ice cores by annual layer counting. Further, past wild fires and volcanic eruptions are visible as significant peaks in ammonium and conductivity, respectively.

One of the goals for the East Greenland Ice core Project (EGRIP) project is to obtain high resolution climate records of impurities continuously through the last 25.000 years covering the onset of the present interglacial, the climatic optimum 8,000 years ago and the industrial period of the past two hundred years and to cover the currently existing gab in the Greenland continuous impurity records during the middle part of the Holocene due to brittle ice.
Here we present the data from the upper 350 m from the EGRIP, revealing information about ocean sources, transport of terrestrial dust, soil and vegetation emissions as well as biomass burning, volcanic eruptions etc., covering the past 2800 years.

REFERENCES

Legrand M. & Meyewsk P. 1997: A Review, Reviews of Geophysics Glaciochemistry of Polar Ice Cores.

Winstrup M. et al 2012: An automated approach for annual layer counting in ice cores, Climate of the Past,

Sigg A. et al. 1994: A Continuous Analysis Technique for Trace Species in Ice Cores, Environmental Science and Technology.

Kaufmann P. R. et al. 2000: An Improved Continuous Flow Analysis System for High-Resolution Field Measurements on Ice Cores, Environmental Science and Technology, 21.

Röthlisberger R. et al. 2000: Technique for Continuous High-Resolution Analysis of Trace Substances in Firn and Ice Cores, Environmental Science and Technology .

Bigler M. et al 2011: On Optimization of High-Resolution Continuous Flow Analysis for Transient Climate Signals in Ice Cores, Environmental Science and Technology .

P 18.3
First eddy covariance flux analysis at the tall tower site Beromünster, Switzerland

Markus Leuenberger [1] and Lars Herrmann [1]

[1] Climate and Environmental Physics Division, Physics Institute and Oeschger Centre for Climate Change Research, University of Bern, Bern, Switzerland (leuenberger@climate.unibe.ch)

Trace gas measurements at the tall tower site Beromünster, Switzerland are being made since the year 2012. Attempts to calculate CO_2 and H_2O fluxes from the height dependent concentration measurements were limited by the fact that neither the advective nor the turbulent flux were available [Satar et al., 2016]. Here we present an update of flux estimates including Eddy covariance analysis at the top inlet of the tall tower. We show that the rather long transfer time from the inlet to the detector of roughly one minute has no obvious negative effects on the quality of the flux data. We also document that due to the height of 212 meters of Beromünster's uppermost tower inlet, the data sampling rate can safely be reduced to a few seconds with no loss of information compared to small eddy flux towers, where a significantly higher frequency is required. We will discuss variations of the CO_2 and H_2O fluxes as well as their annually integrated values and the water use efficency over the year. In the near future, a high precision oxygen analyzer will be placed at the site to investigate the interaction between the atmosphere and the biosphere further.

REFERENCES

Satar, E., T.A. Berhanu, D. Brunner, S. Henne, and M. Leuenberger, Continuous CO_2/CH_4/CO measurements (2012–2014) at Beromünster tall tower station in Switzerland, Biogeosciences, 13 (9), 2623, 2016.

P 18.4
Quantifying the effect of dew and fog water on Swiss grasslands with stable isotopes

Yafei Li [1], Andreas Riedl [1], Franziska Aemisegger [2], Nina Buchmann [1], Werner Eugster [1]

[1] Institute of Agricultural Sciences, ETH Zurich, Universitätstrasse 2, CH-8092 Zurich (yafei.li@usys.ethz.ch)
[2] Institute for Atmospheric and Climate Science, ETH Zurich, Universitätstrasse 16, CH-8092 Zurich

Dew and fog water have been essential moisture sources for plants in arid and semi-arid areas where rainfall rates are very low (Beysens, 2016). Research so far has only rarely focused on the dew or fog water used by plants in temperate ecosystems. Moreover, for grasses that are small compared to trees, a very tiny dew yield will have a stronger impact than for a tree where this amount is rather small compared to the internal water in the respective leaf canopy. Even temperate ecosystems can have relatively dry seasons (e.g. July 2018 in Europe), and this makes dew or fog droplets more important for grassland plants under water-limited seasons.

My proposed research aims at quantifying how fog and dew affect the performance of representative grassland species at different altitudes in Switzerland and how the relevance of fog and dew may increase in the future under climate change. We will test three working hypotheses: (1) during summer fair weather and drought periods, nocturnal dew formation and/or fog droplet has a measurable and nonnegligible quantitative effect on the plant water status of representative Swiss grass species; (2) this quantitative effect of fog and dew is more pronounced at higher elevations than at lower elevations; and (3) the role of fog and dew for temperate ecosystems will become more important with anticipated climatic conditions in Switzerland. Overall this research contributes to a better quantification of the moisture cycling in temperate grasslands and potential changes that can be expected with a warming climate.

Three Swiss FluxNet grasslands along an elevation gradient, where more than 10 years of half-hourly H_2O flux and meteorological data are available will be applied to conduct the measurements of gaseous and liquid water isotopes (^{18}O and ^2H) during intensive observation periods. The isotopes of water vapor in the atmospheric air will be measured every 1 to 2 seconds with cavity ring-down spectroscopy. Liquid isotopes of leaf, stem, soil and dew/fog water droplets on the leaf surface will be available through two-hourly destructive sampling during at least three expected dew or fog nights and analyzing with isotope ratio mass spectrometry. A water tracer with known stable isotope ratio will be manually applied to selected plants to quantify the share of fog or dew water taken up by typical grassland plants. Ecophysiological measurements (e.g., leaf water potential, relative water content, and stomatal conductivity) will be applied quantify the effect of fog and dew on grassland plant performance.
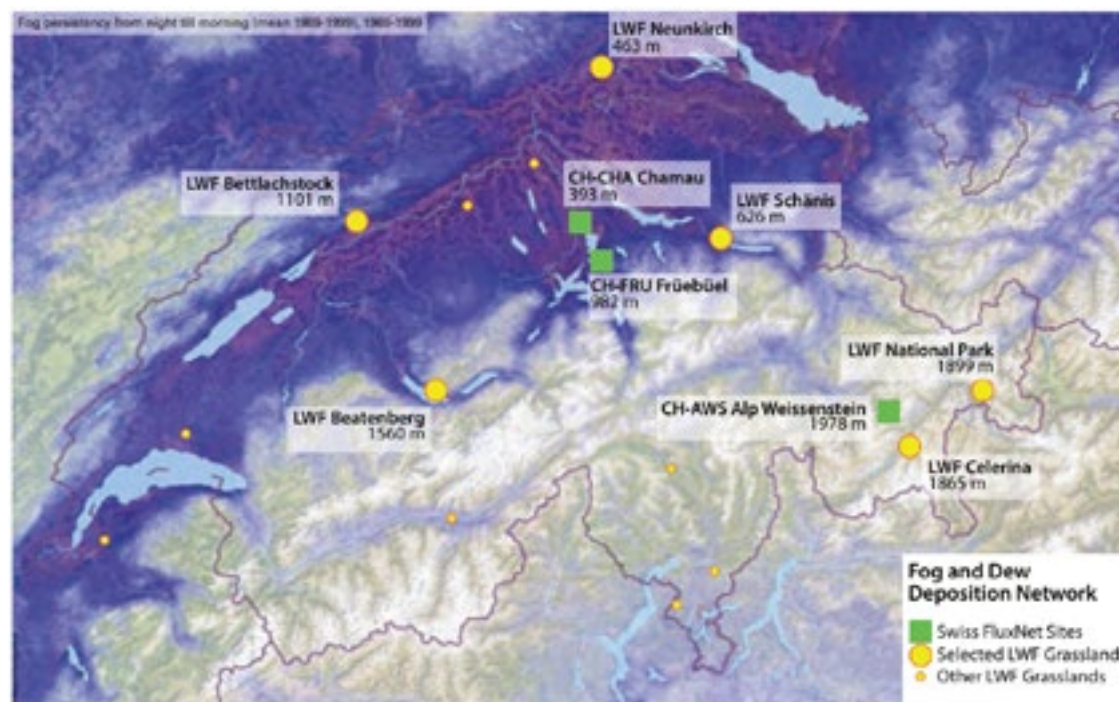

Figure 1. Three Swiss FluxNet sites (CH-CHA Chamau, CH-FRU Früebüel, CH-AWS Alp Weissenstein) which are long-term ETH research stations for eddy covariance CO_2 and H_2O flux measurements.

REFERENCES
Beysens, D.. 2016: Estimating dew yield worldwide from a few meteo data, Atmospheric Research, 167, 146-155.

P 18.5
Assessment of Ecosystem Services of Arable Land in Response to Farming Practice and Drought

Yujie Liu [1], Valentin Klaus [1], Anna Katarina Gilgen [1], Nina Buchmann [1], Emily Oliveira Hagen [2], Raphaël Wittwer [2],

[1] Institute of Agricultural Sciences, Department of Envionmental Systems Science, ETH Zürich, Universitätstrasse 2, CH-8006 Zürich (yujie.liu@usys.ethz.ch)
[2] Ecological Farming Group, Agroscope Reckenholz Tänikon, Reckenholzstrasse 191, CH-8046 Zürich

Ecosystem services are defined as the multiple benefits humans obtain from ecosystems. Agroecosystems are nowadays often confronted with ecosystem degradation due to unsustainable management intensification and climate change. One reason for intensification is that the projected demand for food and feed increases due to global population growth and dietary changes. Additionally, drought events are expected to increase in both frequency and severity in the future, with potentially strong effects on the ecosystem services provided by agroecosystems.

Organic farming has been proposed to better cope with the current agricultural challenges when compared to conventional farming. However, it is still unclear whether organic farming is able to solve the trade-off between production and non-production services and, thus, results in higher multifuctionaliy compared to conventional farming.

Intensive tillage gains relatively high crop yields but dries out the top soil and reduces the soil's ability to store water by decreasing the water infiltration rate. Conservative tillage systems are seen to overcome some of the negative effects of intensive tillage, but often show lower yields and potentially cause problems of crop nutrition and weed control. Nevertheless, agriculture is still interested in no-/conservation-tillage due to its ecological benefits and reduced energy costs. The performance of different tillage practices under drought stress, their contribution to the health and resilience of the crop, and their ability to sustain the provision of high quality ecosystems services still need further investigation.

The objective of this study is to assess the response of ecosystems services in organic and conventional cropping systems with different tillage methodsto simulated summer drought. The main hypotheses of this study are:
1) Organic farming exceeds conventional farming in terms of provision of ecosystem services when multiple (provisioning but also supporting and regulating) services are considered.
2) Conservation tillage exceeds conventional tillage in terms of provision of ecosystem service when multiple (provisioning but also supporting and regulating) services are considered for both conventional and organic farming systems.
3) Drought will decrease ecosystem service provision of both organic and conventional farming systems when compared to (non-drought) control conditions. This decrease will be more pronounced in conventional than in organic farming systems.

Several provisioning, supporting and regulating ecosystem services are being measured during the next three years. We collect data on aboveground biomass yield, crop quality, crop performance as provisioning services; litter decomposition, symbiotic nitrogen fixation, soil fertility, nitrogen availability as supporting services; and nitrate leaching risk, plant infection and soil erosion risk as regulating services.

The outcomes of this research will provide important information on the performance of various cropping system in response to summer drought and help to make recommendations for improved soil and crop management practices for farmers and policy makers.

P 18.6

Assessing resilience against climate change from greenhouse gas flux measurements in Switzerland

Regine Maier [1] and Nina Buchmann [1]

[1] *Institute of Agricultural Science, ETH Zurich, Universitätsstrasse 2, CH-8092 Zürich (regine.maier@usys.ethz.ch)*

Agriculture has major impacts on the Swiss environment: High amounts of fertilizer, biodiversity loss, nitrogen leaching and changing climatic conditions challenge the sustainability of future agricultural production. On the one hand, agricultural soils are a major source for greenhouse gases (GHG), mainly methane (CH_4) and nitrous oxide (N_2O); on the other hand, they can potentially also act as carbon sinks. Innovative technologies promote new farming practices such as climate-smart-agriculture or precision-farming aim at increasing agricultural production while reducing the ecological footprint. GHG flux measurements at a high temporal resolution reveal important information on how various agricultural practices can make an ecosystem a GHG source or GHG sink. An additional aspect of climate-smart agriculture is building up or increasing resilience against climate change impacts like heavy rain events, heatwaves or droughts.
Within the project InnoFarm (NRP 73, Sustainable Economy), we aim to quantify GHG fluxes from different Swiss agricultural production systems under varying production intensities. In addition, we measure several environmental variables such as soil variables, nitrate leaching, plant biomass and atmospheric variables to determine which agricultural production systems show highest resilience against climate change. As continuous GHG flux measurements at various sites are expensive, we will set up a mobile measurement system, which includes a CH_4/N_2O analyser providing high precision measurements at 10 Hz using the eddy covariance technique. Thus, we can measure GHG fluxes from varying management intensities covering relevant management events and production phases at selected cropland and grassland sites in our study region in the canton Solothurn. Finally, the short-term flux data from the measurement campaigns will be up-scaled to annual time series of GHG fluxes.

P 18.7

Do cover fills reduce peat oxidation and carbon emissions from managed organic soils?

Sonja Paul [1], Christof Ammann [2], Christine Alewell [1] & Jens Leifeld [2]

[1] *Umweltgeowissenschaften, University of Basel, Bernoullistrasse 30, CH-4056 Basel, Switzerland (sonja.paul@unibas.ch)*
[2] *Climate and Agriculture Group, Agroscope, Reckenholzstrasse 191, 8046 Zürich, Switzerland*

Peatlands have served as important carbon sinks in the past. The agricultural use of organic soils usually requires drainage thereby transforming these soils from a net carbon sink into a net source. Besides CO_2 emissions from peat oxidation, drainage also results in subsidence of organic soils. The drainage system requires a periodic renewal to sustain agricultural use. Finally, pumping systems are used after progressive subsidence. In Switzerland there is a high demand for maintaining agricultural use of organic soils while simultaneously reducing environmental impacts. One solution may be to cover the organic soils with excavated material in order to improve the productivity without the costly step to renew the draining system. Previous studies showed that the agricultural use seems do benefit from this measure; however, the impact on the greenhouse gas balance is unclear. Our newly established study site is situated in Rüthi, St. Gallen, Switzerland on the former flood plain of the Rhine River. In the 1970s, the land was drained, pastures established and intensively managed since then. Nowadays agriculture becomes problematic since the soil is water-saturated most of the season. Due to the high cost, drainage renewal was not an option to ensure the existence of the farm located at the study site. Instead, it is planned to cover 30 ha with excavated soil material. As a pilot project, 2 ha were covered with 30 to 50cm silty material already in 2006. The aim of the project is to evaluate the impact of soil coverings on the carbon balance. The carbon balance of the covered and an adjacent reference site is measured with an Eddy-Covariance system starting in March 2018. In addition, the ^{14}C signature of the emitted CO_2 will be measured occasionally to differentiate between carbon deriving from old peat and from newly formed soil organic matter. The first results of the carbon balance of the two sites will be presented.

P 18.8
Influence of the mangrove forest on the net emission of methane in water bodies of the Gandoca Lagoon (Costa Rica) and its managerial implications

Record S., Siegenthaler A.

This research was carried out in the Gandoca lagoon, a tropical and coastal ecosystem. The objective was to analyze with ecological modeling key variables that influence the net emission of CH_4 in the water bodies of a protected lagoon on the Caribbean sea, which surround mangrove communities, palm association and mangrove ferns, to improve the existing management strategy.

Different environmental variables were measured and the closed dynamic floating chambers were used in the sampling of diffusive and non-diffusing CH_4 in a continuous flow mode in 24 sites distributed evenly over the entire lagoon. The data was analyzed statistically with a GLMM model for net emissions, and two GLM models for organic matter volumetric mass in sediments as well as methane turnover. The results indicated that the net emissions are explained by the sum of influences of: tide, current, electrical conductivity of the sediments, PAR, distance to the forest, NDVI, plant communities and K in the sediments. The organic matter density was influenced by the oxido-reduction potentials in the sediments, NDVI and the temperature of the surface water. The turnover of methane was influenced by oxido-reduction potentials in the sediments and dissolved Cl in the water column. Furthermore, the results revealed that the sediments in the mangrove forest communities compensate for the higher emission of diffusive CH_4 compared to the other communities, by an increased sequestration of C based on differences in absolute volumetric mass.

This study is a useful tool to help managers and researchers to establish measures to prevent, control and / or mitigate impacts that increase net CH_4 emissions or reduce the carbon storage capacity of the system through a potential proliferation of the palm forest association. Some of these measures will be presented.

P 18.9
The Importance of Dew and Fog for Swiss Grasslands

Andreas Riedl [1], Yafei Li [1], Werner Eugster [1]

[1] Grassland Sciences Group, Institute of Agricultural Sciences, ETH Zurich, Universitätsstrasse 2, CH-8092 Zürich (andreas.riedl@usys.ethz.ch)

Dew and fog occur rather frequently in ecosystems all over the world. Yet, little is known about their role and influence on plant performance and plant water relations in temperate climate ecosystems.
Dew forms when the plant temperature drops below the dew-point temperature. As a consequence, gaseous water vapor from the air condenses on the leaves. This occurs predominantly on nights with clear skies, where thermal energy from the surface is easily lost to the atmosphere. Under the same conditions, it is also likely that radiation fog forms close to the Earth surface. Fog droplets form on condensation nuclei in the air and are then deposited to plants.
These two phenomena both provide water to ecosystems, we thus hypothesize that during summer fair weather and drought periods, nocturnal dew and fog have a measurable and nonneglible quantitative effect on the water status of plants in Swiss grasslands. This is due to the fact that plants cannot only take up water via their roots, but also directly via the leaves, referred to as foliar water uptake. Overnight dew and fog formation lead to notable leaf wetness duration, which, in turn, leaves enough time for foliar water uptake. Furthermore, there may be other physiological effects, such as enhanced cooling through leaf-wetting during the early morning hours of hot summer days.
Within the framework of this project, we plan to quantify how much dew and fog water is provided to grassland leaves under today's climate conditions in Switzerland. For that purpose, existing long-term meteorological field sites will be supplemented by microlysimeters, visibility and leaf moisture sensors at 9 locations with different climatic conditions and altitudes throughout Switzerland.
The goal is to establish a functional relationship with the meteorological data measured that allows for explicit spatial estimations of dew and fog deposition. In a further step, this functional relationship will be used in combination with very latest climate scenarios for Switzerland in pursuit of estimating the effect in the future, where prolonged drought periods during summer fair weather tend to increase. Overall, we expect that the outcome of the project will be useful for grassland management decisions, with impacts on grassland productivity and resilience today and in future.

P 18.10
A Sustainable Tool for Assessment of Effect of Ozone on Delhi Ridge, India

Pallavi Saxena [1] & Chirashree Ghosh [2]

[1] Department of Environmental Sciences, Hindu College, University of Delhi, New Delhi-110007
  (pallavienvironment@gmail.com)
[2] Department of Environmental Studies, University of Delhi, New Delhi-110007

Tropospheric ozone high concentrations posing an alarming threat in the atmosphere. In developing countries like India, this is one of the major significant problem particularly in a city like Delhi. Though, there are various methods for evaluating the impact of ozone on plant species but, there is only one sustainable tool which is used to examine the potential of effect of ozone on plant species. AOT40 is an evaluation index which is used to quantify the ozone exposure on plant species. In the present study, a detailed analysis of ozone in relation to its phytotoxic potential over Delhi Ridge Forest area during the period 2012-2013. The phytotoxic potential is determined by exposure index AOT40 for forests calculated from hourly based monitoring data at 2 sites in Delhi Ridge forest area. The results indicate that high phytotoxic potential for most of Delhi Ridge with significant inter-annual and spatial variability. The highest AOT40 values were found to be 25-30 ppm/h. The critical range for forest protection was generally high during the month of May. In high temperatures condition in Delhi during the year 2013, the critical level of forests was crossed the threshold limit of about 25% of the Delhi ridge region. Much more research is required to explain these exceedances into forest injury in Delhi Ridge area.
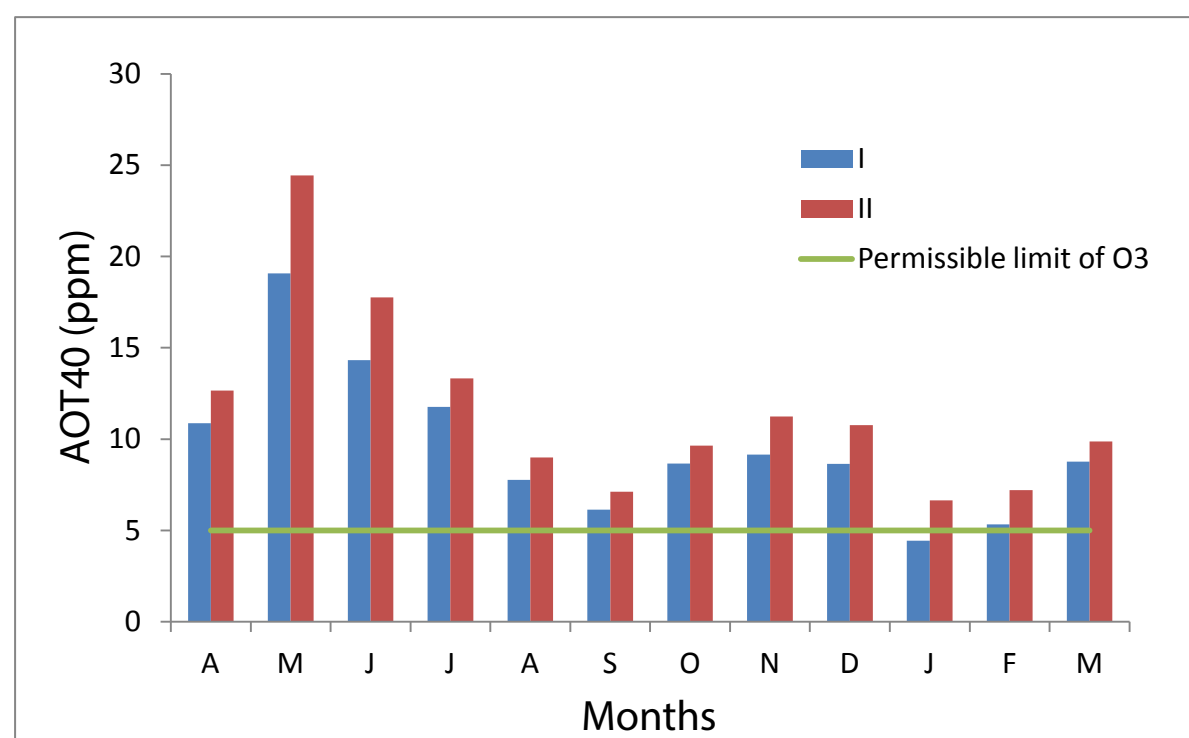Keywords: Tropospheric ozone, AOT40, Forests, Delhi.

Figure 1: AOT40 Monthly Average Variation (2012-13) at selected sites in Delhi Ridge, India

REFERENCES

Baumgarten M, Huber C, Buker P, Emberson L, Dietrich H-P, Nunn AJ, Heerdt C, Beudert B, Matyssek R (2009). Are Bavarian forests (southern Germany) at risk from ground-level ozone? Assessment using exposure and flux based ozone indices. Environmental Pollution 157: 2091-2107. - doi: 10.1016/j.envpol.2009.02.012

Hůnova I, Novotny R, Uhlirova H, Vrablik T, Horalek J, Lomsky B, Sramek V (2010). The impact of ambient ozone on mountain spruce forests in the Czech Republic as indicated by malondialdehyde. Environmental Pollution 158: 2393-2401. - doi: 10.1016/j.envpol.2010.04.006

P 18.11

High precision CO_2 and O_2 measurements at the High Altitude Research Station Jungfraujoch, Switzerland

Michael F. Schibig [1], Peter Nyfeler [1], Markus C. Leuenberger [1]

[1] Climate and Environmental Physics, Physics Institute, and Oeschger Centre for Climate Change Research, University of Bern, Sidlerstrasse 5, CH-3012 Bern (schibig@climate.unibe.ch)

The atmospheric CO_2 (carbon dioxide) mole fraction is increasing because of human activities such as fossil fuel combustion or land use change. However, the observed CO_2 increase corresponds only to about half of the carbon emitted. The other half is taken up partly by the ocean and partly by the terrestrial biosphere. It is crucial to know the partitioning between the ocean and the biosphere because of the different nature of the two reservoirs. Carbon stored in the ocean is bound for longer time scales, whereas carbon stored in the biosphere will re-enter the atmosphere relatively soon.

To estimate the partitioning of the carbon between the two reservoirs combined measurements of atmospheric CO_2 and O_2 (oxygen) can be used. The CO_2 and O_2 exchange between the biosphere and the atmosphere by photosynthesis and respiration is inversely coupled and has a rather constant stoichiometric ratio of about -1.1 mol O_2 / mol CO_2. Similarly, the anthropogenic combustion of CO_2 requires O_2 resulting in an average stoichiometric ratio of about -1.4 mol O_2 / mol CO_2. In contrast, the air-sea exchange of CO_2 and O_2 is decoupled because CO_2 is chemically bound while O_2 remains unaffected, except temperature induced solubility changes. Therefore, one can separate the total CO_2 uptake into land and ocean components.

The University of Bern monitors ambient CO_2 and O_2 (oxygen) at the High Altitude Research Station Jungfraujoch (JFJ) by means of flask sampling since 2000 and with a continuous measurement system since 2005. JFJ was chosen due to the high altitude, the station lies most of the time above the planetary boundary layer and receives therefore mostly background air originating from a large footprint covering most of the European continent and a significant part of the North Atlantic. Since CO_2 and O_2 are well mixed in the free troposphere, it is possible to use these measurements to give an estimate about the partitioning of the anthropogenic carbon into the different reservoirs in the northern hemisphere.

P 18.12

Plant water relations under drought in organic and conventional farming systems

Qing Sun [1], Anna K. Gilgen [1], Valentin Klaus [1], Constant Signarbieux [2] & Nina Buchmann [1]

[1] Institute of Agricultural Sciences, ETH Zurich, Universitatstrasse 2, 8092 Zurich (qing.sun@usys.ethz.ch)
[2] Laboratory of Ecological Systems, EPF Lausanne, GR B2 387 - Station 2, 1015 Lausanne

Due to the changing climate, agricultural production systems will be progressively subjected to more frequent severe weather events such as prolonged summer droughts. Thus, there is an increasing need for a better understanding of water use of crop plants in agricultural systems during water shortage. Adaptations of farming practices to climate change require assessing and improving the resilience of agricultural systems to ensure food security.

In Switzerland, the main farming systems are organic and conventional farming, with different tillage strategies i.e., intensive and conservation tillage (reduced tillage in organic farming and no-tillage in conventional farming). In order to understand the responses of different farming systems to drought, this work assesses (1) if crop plant water relations differ significantly in different farming systems under different soil water availabilities, and (2) if crop drought resistance is higher under organic farming compared to conventional farming, and conservation tillage compared to intensive tillage. Drought periods are simulated with portable shelters. Water stress was estimated using measurements of plant vulnerability to xylem embolism with the cavitron technique of different crop species under different farming systems. Preliminary results indicate that: (1) pea was more resistant to drought than barley showing less degree of xylem embolism under drought; (2) barley was more resistant to drought under intensive tillage compared to conservation tillage, and organic farming compared to conventional farming; drought resistance of pea was highest in the conventional intensive tillage system and lowest in the conventional no-tillage system; (3) the relative yield loss of pea-barley mixture was lowest in the organic intensive system, whilst highest in the conventional no-tillage system. The outcome of this work will help to inform farmes and other stakeholders about necessary adaptations of soil and crop management to future drought conditions.

P 18.13

Assesment of methane emissions from animal and waste processing operations using an inverse dispersion technique

Bühler Marcel [1,3], Häni Christoph [1], Kupper Thomas [1], Ammann Christof [2], Brönnimann Stefan [3]

[1] School of Agricultural, Forest and Food Sciences HAFL, Bern University of Applied Sciences, Länggasse 85, CH-3052 Zollikofen (marcel.buehler@bfh.ch)
[2] Climate and Agriculture Group, Agroscope, Reckenholzstrasse 191, CH-8046 Zürich
[3] Institute of Geography, University of Bern, Hallerstrasse 12, CH-3012 Bern

Inverse dispersion techniques are becoming more important in dertermining gas emissions from animal and waste processing operations (AWPO). The application of this method requires for a horizontal, flat and homogeneous surrounding without any nearby sources of the gas. However, these criteria are rarely met in countries like Switzerland. The present PhD aims to evaluate and establish inverse dispersion technique using a backward Lagrangian stochastic (bLS) model with up and downwind concentration measurements for the determination of methane emissions from AWPO at an environmental scale under non-ideal model conditions. This poster presents the applied method and the planned measurements which contribute to tackle the related challenges.

REFERENCES

Flesch, T., Wilson, J.D., Harper, L.A., Crenna, B.P. 2005: Estimating gas emissions from a farm with an inverse-dispersion technique, Atmospheric Environment, 39, 4863-4874.

19. Environmental Biogeochemistry of Trace Elements

Moritz Bigalke, Montserrat Filella, Adrien Mestrot, Andreas Voegelin, Lenny Winkel

TALKS:

19.1   Bagnoud A., Chourey K., Hettich R.L., de Bruijn I., Andersson A.F., Diomidis N., Leupin O.X., Schwyn B., Bernier-Latmani R.: A microbial ecosystem in Opalinus Clay rock fueled by hydrogen gas

19.2   Bernier-Latmani R., Loreggian L., Bretagne S., Novotny A.: Oxidation of non-crystalline U(IV): role of reduced sulfur

19.3   Caplette J., Mestrot A.: Trapping of volatile antimony (Sb): method validation and first in-situ measurements

19.4   Catrouillet C., Hirosue S., Manetti N., Peña J.: Arsenic removal in manganese-containing groundwater

19.5   Cheolyong Kim, Inseong Hwang: Transformation of Nano Zero-Valent Iron during Oxidation Process using Persulfate

19.6   de Meyer C., Rodriguez J., Wahnfried I. , Kipfer R., Berg M.: Geogenic contaminants in groundwater resources of Amazonian riverine communities: results of a vast exploratory field-study

19.7   Etique M., Bouchet S., Byrne J., Thomas Arrigo L., Kaegi R., Kretzschmar R.: Mercury reduction by vivianite

19.8   Feinberg A., Maliki M., Stenke A., Sudret B., Gysin S., Peter T., Winkel L.H.E.: Using global sensitivity analysis to establish priorities in atmospheric selenium research

19.9   Filella M., Turner A.: Should plastics be considered in the biogeochemical cycles of trace elements?

19.10   Gogos A., Wielinski J., Voegelin A., Kaegi R.: Transformation of cerium dioxide nanoparticles during incineration of sewage sludge

19.11   Hitzfeld B.,: Challenges of trace elements in the Swiss environment

19.12   Liu Y., Schäffer A., Lenz M.: Studying Bacterial Selenium Methylation at Environmental Relevant Concentrations

19.13   Marafatto F.F., Ferreira-Sanchez D., Grolimund D., Göttlicher J., Voegelin A.: X-ray spectroscopic characterization of As(V)-rich Tl(III)-particles in a weathered Tl-As-Fe-sulfide mineralization

19.14   Van Groeningen N., Christl I., Kretzschmar R.: Competitive sorption of Mn(II) and Cd(II) to clay minerals

19.15   Viacava K., Dyer S., Leberdalle Meibom K., Mestrot A., Bernier-Latmani R.: Arsenic methylation across microbial phyla

19.16   Wanner C., Pöthig R., Carrero S., Fernandez-Martinez A., Jäger C., Furrer G.: Uptake of As by nanocrystalline Al-hydroxysulfates naturally forming along a mountainous stream in the Engadin area

19.17   Wick S., Peña J., Voegelin A.: Thallium Sorption onto Birnessite

POSTERS:

P 19.1   Gfeller L., Mestrot A.: Methylmercury distribution and formation in polluted agricultural floodplain soils

P 19.2   Hausladen D., Keiluweit M., Peña J.: Transformation of Manganese Oxides by Organic Constituents in Natural and Laboratory Systems

P 19.3   Imseng M., Wiggenhauser M., Frossard E., Müller M., Keller A., Wilcke W., Bigalke M.: Copper mass balances and stable isotopes as analytical tool to tace sources and processes in agricultural systems

P 19.4   Jiranek G., Filella M., Loizeau J.-L., Cobelo-García A.: Evolution of Technology-Critical Element contents in sediments of a contaminated bay of Lake Geneva (Switzerland) over the past century

P 19.5   Manetti N., Catrouillet C., Peña J.: Arsenic removal from lake water, river water and groundwater using an electrocoagulation system

P 19.6   Müller E., Bouchet S., von Gunten U., Winkel L.: Reactions between hypobromous acid, organic sulfur species and dissolved organic matter in marine waters

P 19.7   Roethlin R.L., Dubois N.: Paleo-ecotoxicology: Shining a light on the true impacts of pollution

P 19.8   Segovia Campos I., Martignier A., Jaquet J.-M., Barja F., Filella M. , Ariztegui D.: Investigating the potential of intracellular mineral inclusions in microalgae as a novel bioremediation method for radioactive ^{90}Sr water pollution

P 19.9   Wielinski J., Gogos A., Marafatto F., Voegelin A., Morgenroth E., Kaegi R.: Transformation of Cu (nanoparticles) during sewage sludge incineration studied by bulk- and micro-XAS

19.1
A microbial ecosystem in Opalinus Clay rock fueled by hydrogen gas

Alexandre Bagnoud [1,2], Karuna Chourey [3], Robert L. Hettich [3], Ino de Buijn [4], Anders F. Andersson [5], Nikitas Diomidis [6], Olivier X. Leupin [6], Bernhard Schwyn [6], Rizlan Bernier-Latmani [1]

[1] *Ecole Polytechnique Federale de Lausanne, EPFL, Lausanne, Switzerland*
   (alexandre.bagnoud@gmail.com; rizlan.bernier-latmani@epfl.ch)
[2] *Haute Ecole d'Ingénierie et de Gestion du Canton de Vaud, 1401 Yverdon-les-Bains, Switzerland*
[3] *Oak Ridge National Laboratory, Oak Ridge, USA*
[4] *Bioinformatics Infrastructure for Life Sciences, Stockholm, Sweden*
[5] *Science for Life Laboratory, Stockholm, Sweden*
[6] *National Cooperative for the Disposal of Radioactive Waste, Wettingen, Switzerland*

A significant part of microbial biomass is found in the deep subsurface and little is known about metabolisms in these environments (McMahon and Parnell 2014). This remote biosphere is decoupled from sunlight-derived organic carbon and rely exclusively on geogenic gases, such as methane or hydrogen (Lovley and Chapelle 1995)

Opalinus Clay is a low-porosity clay rock, which is supposed to host nuclear repositories in Switzerland. In this regard and thanks to the underground rock laboratory of Mont-Terri in St-Ursanne, it has been extensively characterized (Bossart and Thury 2008). It is well established that pristine rock, because of its small pore size distribution, is not suitable for hosting microbial activity. But as soon as space is provided, because of the presence of organic matter (i.e., acetate) and electron donor (i.e., sulfate) in Opalinus Clay rock, microbial activity can take place (Stroes-Gascoyne *et al.* 2007). Thus, this project aimed at characterizing the biological response to H_2, which will be produced by the anoxic corrosion of steel canisters, in repository-relevant conditions. An *in-situ* experiment was carried out where H_2 was amended to borehole water for more than 500 days.

H_2 was rapidly consumed concomitantly with a production of hydrogen sulphide, an increase in planktonic cell density, and a decrease in CO_2 concentration, suggesting that autotrophic sulfate reduction was the dominating process in this system. A metagenomic sequencing allowed the assembly of 15 high-quality genomes, together representing 75% of the microbial community. Metaproteomic analysis highlighted the presence of a complete carbon cycle. Two organisms oxidize hydrogen: a sulfate-reducing bacterium (Desulfobulbaceae) representing 42% of the community, and a Rhodospirillaceae reducing sulfite. Biomass produced by autotrophs is then oxidized to acetate by a *Hyphomonas* species. Fermentation products are finally oxidized to CO_2 by several species of heterotrophic sulphate-reducing bacteria (Figure 1).

This work provides the first insight into a complete carbon cycle in the deep subsurface and significantly expands our knowledge of microbial metabolisms in the deep biosphere. It also suggests that allowing microbial activity in nuclear waste repositories is beneficial, by buffering the pressure increase due to *in-situ* H_2 production.

REFERENCES
Bossart P, Thury M. Mont Terri Rock Laboratory. Project, Programme 1996 to 2007 and Results. Bern: Federal office of topography swisstopo, 2008.
Lovley DR, Chapelle FH. Deep subsurface microbial processes. Rev Geophys 1995;33:365–81.
McMahon S, Parnell J. Weighing the deep continental biosphere. FEMS Microbiol Ecol 2014;87:113–20.
Stroes-Gascoyne S, Schippers A, Schwyn B et al. Microbial community analysis of Opalinus Clay drill core samples from the Mont Terri underground research laboratory, Switzerland. Geomicrobiol J 2007;24:1–17.
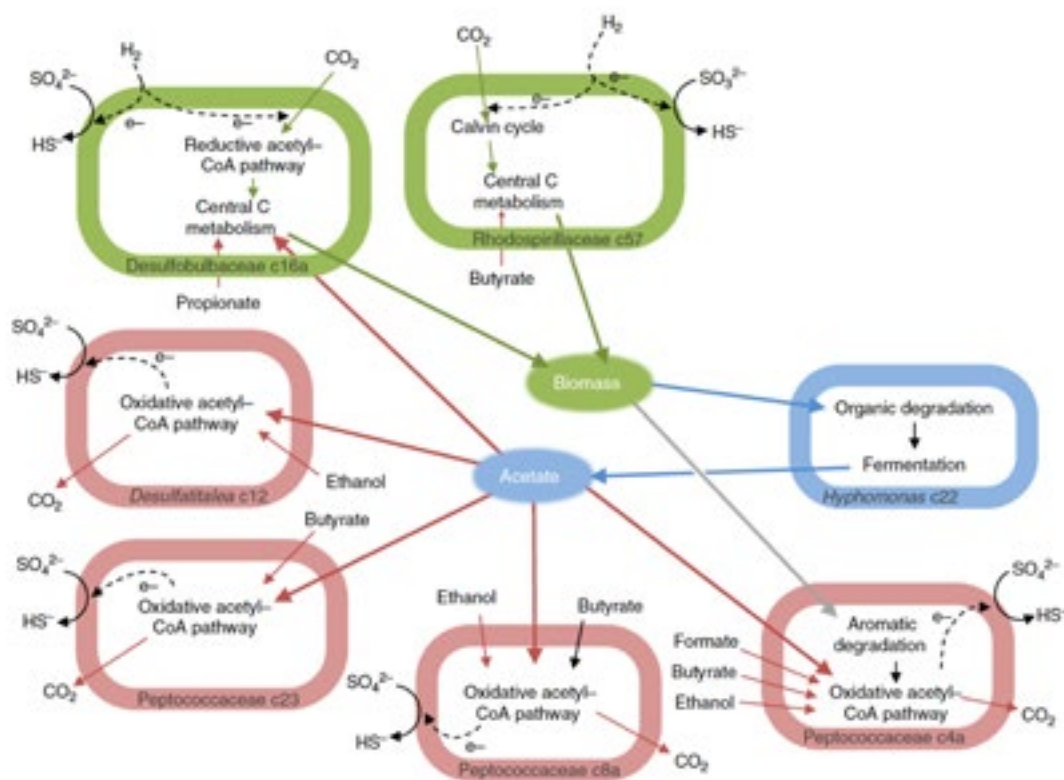
Figure 1. Microbial ecosystem fueled by hydrogen in Opalinus Clay rock.

19.2
Oxidation of non-crystalline U(IV): role of reduced sulfur

Rizlan Bernier-Latmani°, Luca Loreggian, Sophie Bretagne, Agens Novotny

Environmental Microbiology Laboratory, IIE, Ecole Polytechnique Federale de Lausanne (EPFL)
(°rizlan.bernier-latmani@epfl.ch)

Uranium is a contaminant of concern in subsurface environments impacted by mining or ore processing or in areas of naturally occurring uranium-bearing rocks. Hexavalent uranium is soluble and highly mobile, and represents a threat to water quality. Remediation approaches aim at immobilizing uranium, preferably *in situ*. Reductive precipitation is one such strategy and relies on microbial processes to reduce hexavalent uranium to its tetravalent state, which is largely insoluble. Two major types of U(IV) precipitates have been identified: crystalline U(IV) such as uraninite (UO_2) and non-crystalline forms in which U(IV) is associated with a solid phase but coordinated with functional groups such as carboxylic or phosphato groups [1,2]. The latter, referred to as non-crystalline U(IV) (NCU4), is not well characterized, its reactivity is not well constrained and the role of iron sulfide precipitates in its stability poorly understood [3]. In this work, we seek to compare NCU4 stability under oxic conditions in the presence and absence of iron sulfide species. Non-crystalline U(IV) was produced through the reduction of U(VI) in a flow-through column packed with sediment from the Old Rifle CO (USA), experimental site and receiving a cocktail of electon donors in the presence and absence of sulfate (and thus, iron sulfide precipitates). After accumulation of U(IV) in the sediment, it was characterized and found to harbor approximately ~85-95% NCU4. Each sediment type (with or without sulfate) was then placed in continuously stirred tank reactors through which oxic or anoxic water was flowing. The water contained either 1 or 10 mM sodium bicarbonate. The leaching of uranium was monitored and the speciation of the sediment post-leaching characterized. We observed that, under oxic conditions, about ~90% of the NCU4 was oxidized both both conditions (sulfate and no sulfate) while UO_2 largely remained constant. In contrast, batch experiments revealed that, surprisingly, the presence of reduced sulfur in the sediment enhanced the rate of oxidation of NCU4. Further investigation showed that reactive oxygen species play an important role in NCU4 oxidation under fully oxic conditions. The work presented offers a more definitive view of the fate of NCU4 under environmentally relevant conditions.

REFERENCES
1. D. S. Alessi, J. S. Lezama-Pacheco, J. E. Stubbs, M. Janousch and J. R. Bargar et al. The product of microbial uranium reduction includes multiple species with U(IV)-phosphate coordination, in Geochimica et Cosmochimica Acta, vol. 131, p. 115-127, 2014.
2. R. Bernier-Latmani, H. Veeramani, E. Dalla Vecchia, P. Junier and J. Lezama-Pacheco et al. Non-uraninite products of microbial U(VI) reduction, in Environmental Science and Technology, vol. 44, num. 24, p. 9456-9462, 2010.
3. Y. Bi, M. Stylo, R. Bernier-Latmani and K. F. Hayes. Rapid mobilization of noncrystalline U(IV) coupled with FeS oxidation, in Environmental Science and Technology, vol. 50, num. 3, p. 1403-1411, 2016.

19.3
Trapping of volatile antimony (Sb): method validation and first in-situ measurements

Jaime Caplette [1] and Adrien Mestrot [1]

[1] Trace Element Speciation Group, Geographisches Institut, Universitat Bern, Hallerstrasse 12, CH-3012 Bern
(jaime.caplette@giub.unibe.ch)

Antimony (Sb) is a naturally occurring element, ranging from 0.3 – 8.4 mg kg^{-1} in the soil environment. Sb concentrations can be elevated in the vicinity of mining and smelting, industrial, and shooting range activities. The United States Environmental Protection Agency and European Union consider Sb a priority pollutant of interest and potentially carcinogenic.

Volatile Sb, stibine (SbH_3), monomethylstibine (MeSb), dimethylstibine (Me_2Sb), and trimethylstibine (Me_3Sb), can be produced at low temperatures under aerobic and anaerobic conditions and represent an understudied portion of the biogeochemical cycling of Sb. Very few studies have investigated volatile Sb production in natural media with a majority of the works focussed on sewage sludge fermentation and hydrothermal vents, landfills, and production in headspace gases from fungi (e.g., *S. brevicaulis*) and methanogenic Archaea. However, the current knowledge of volatile Sb production from the soil environment is poorly understood.

In this work, we validated a method for SbH_3 and Me_3Sb trapping using activated carbon sorbent tubes. The volatile species were formed by hydride generation from dissolved solutions of Sb(III) and trimethylstibine oxide, respectively. Activated carbon traps were digested using an aqua regia closed vessel digestion. Recoveries of trapped SbH_3 and Me_3Sb were 93.7% ± 7.95 and 95.5% ± 1.34, respectively. This method was used to capture volatile Sb produced from manure amended (5%) flooded shooting range soils (Laupen, Switzerland) during an incubation period of 36 days. After 12 days of incubation, 37.9 - 155 ng of total Sb was detected on the traps, with a maximum flux of 31.2 µg $kg^{-1} \cdot yr^{-1}$.

Furthermore, we investigated the in-situ production of volatile Sb in two rice paddy fields in the vicinity of the worlds largest Sb deposit (Xikuangshan mine, Lengshuijiang, China) using the newly validated trapping method for SbH_3 and Me_3Sb. We used six gas collection chambers equipped with filter cassettes and activated carbon adsorbent traps on the inlet and outlet ports, respectively at each field site for 4 days and preliminary results will be discussed.

Sb biovolatilisation in soils can be quantitatively assessed using the aforementioned method in-situ as well as in incubation experiments. This method can yield information on the importance of volatilisation with regards to the biogeochemical cycling of Sb.

19.4
Arsenic removal in manganese-containing groundwater

Charlotte Catrouillet [1], Sachiko Hirosue [1], Nathalie Manetti [1] & Jasquelin Peña [1,1]

[1] University of Lausanne IDYST, Geopolis, CH-1015 Lausanne (charlotte.catrouillet@unil.ch)

Arsenic (As) can occur naturally in groundwaters worldwide (e.g., Bengladesh, India, Amazon region, etc.). Because of this large-scale contamination and its high toxicity and carconegicity, exposure to As leads to millions of deaths worldwide. Therefore, strategies to remove As from water using efficient and cheap treatement system are critically needed. Iron(0) electrocoagulation (EC) has gained attention as a low-cost method for As removal because it has short supply chain and low energy requirements and, importantly, is easy to operate. In EC, a current is passed through an Fe(0) electrode, such that Fe(0) is oxidized to Fe(II). The production of Fe(II) generates reactive oxidants that oxidize As(III) to form As(V) – a less dangerous form of As, and Fe(II) to Fe(III), which forms nanoscale iron precipitates that remove arsenic from solution (van Genuchten et al. 2012, Nidheesh et al. 2017). However, the mechanism and efficiency of As removaldepend strongly on the chemical composition of the groundwater. Thus, successful implementation of EC requires systematic chemical and mineralogical studies under varying operating conditions and groundwater chemistry.

In some waters, As and Mn co-occur at high concentrations (Gillipsie et al. 2016, de Meyer et al. 2017). Recent work shows that Mn(II) can also be removed from water using an EC system. Moreover different oxidants are responsible of the oxidation of Fe and Mn at different pH and the greatest Mn removal occurs at pH 8.5 (van Genuchten et al. 2017). Combined, these studies suggest that As and Mn compete for the same pool of oxidants in an EC system and therefore that the efficiency of As removal may be influenced by the presence of Mn. The main goal of this work is thus to understand the extent to which As and Mn are removed during EC when aqueous As(III) and Mn(II) are initially present in the groundwater. In addition, knowledge of the speciation of As and Mn in the solid phase is needed in order to understand the mechanism of contaminant removal (oxidation and sorption) under varying conditions (concentrations of Mn, As, pH, and presence or absence of H_2O_2).

Analysis of aqueous and solid phase samples showed that the kinetics of As and Mn oxidation and mechanism of removal to the solid phase vary strongly according to the type of oxidant present in the system (e.g., $^.$OH and Fe(IV), respectively). At acidic pH, As concentrations were less than the 10 μg L^{-1} (WHO recomendation) in the presence of H_2O_2 after 30 min, but at basic pH the concentrations of As were higher than the WHO recomendation. In the O_2 system, As concentrations decreased over time, but did not attain the 10 μg L^{-1} target. Solution pH, the initial oxidant (O_2 vs. H_2O_2) and Mn concentration influenced significantly the extent of As and Mn removal. The speciation of As and Mn in the solid phase, as determined by X-ray absorption spectroscopy (Stanford Synchrotron Radiation Lightsource, BL 4-1), showed greater As oxidation at pH 4.5 than at pH 8.5 and in the presence of Mn. On the contrary, greater Mn oxidation was observed at pH 8.5 than at pH 4.5. Moreover, in the O_2 system, Mn and As were mainly present in reduced form in the solid phase. Then, the acidic pH are the most favorable pH to remove As from water because of favorable oxidation of As(III) and sorption of As(V), but this pH is not practical for water treatment. The other best pH to remove As depends on Mn concentrations in waters. Determine water matrice is then a very critical point to improve the performances of the system.

REFERENCES

Gillipsie, E.C., Andujar, E., Polizzotto, M., 2016. Chemical controls on aiotic and biotic release of geogenic arsenic from Pleistocene aquifer sediments to groundwater. Environmental Science Processes & Impacts, 18, 1090-1103.

de Meyer, C. M. C., Rodríguez, J. M., Carpio, E. A., García, P. A., Stengel, C. & Berg, M. 2017: Arsenic, manganese and aluminum contamination in groundwater resources of Western Amazonia (Peru). Science of The Total Environment, 607-608, 1437-1450.

Nidheesh, P. V. & Singh, T. S. A. 2017: Arsenic removal by electrocoagulation process: Recent trends and removal mechanism. Chemosphere, 181, 418-432.

van Genuchten, C. M., Addy S.E.A., Peña, J., Gadgil, A.J. 2012: Removal Arsenic from Synthetic Groundwater with Iron Electrocoagulation: An Fe and As K-edge EXAFS Study. Environmental Science & Technology, 51, 2982-2991.

van Genuchten, C. M. & Peña, J. 2017: Mn(II) Oxidation in Fenton and Fenton Type Systems: Identification of Reaction Efficiency and Reaction Products. Environmental Science & Technology, 46, 986-994.

19.5
Transformation of Nano Zero-Valent Iron during Oxidation Process using Persulfate

Cheolyong Kim [1,2] & Inseong Hwang [1]

[1] Department of Civil and Environmental Engineering, Pusan National University, 2 Busandaehak-ro 63 beon-gil, Busan, 46241, Korea (cheolyong.kim@eawag.ch)
[2] Department Water Resources & Drinking Water, Eawag - Swiss Federal Institute of Aquatic Science and Technology, Überlandstrasse 133, 8600 Dübendorf, Switzerland

The sulfate radical ($SO_4^{\bullet-}$), which can be generated by activating persulfate, is an emerging oxidant for treating groundwater contaminants. Recently, nano zero-valent iron (NZVI) has attracted interest as a persulfate activator because it is more efficient than conventional activators such as aqueous Fe^{2+} (Li et al., 2014). NZVI transformation products such as Fe-(oxyhydr)oxide minerals substantially affect the persulfate activation by NZVI. Therefore, the transformation of NZVI during the oxidation process needs to be elucidated in order to predict the efficiency of sulfate radical formation. This study aimed to identify the transformation products of NZVI and to predict the evolution of the NZVI core-shell structure during the reaction of persulfate with NZVI.

The X-ray diffraction pattern of the Fe solid after 1 h reaction time contained a peak characteristic for poorly ordered crystals of schwertmannite. Scanning electron microscopy coupled with energy dispersive spectroscopy indicated that the surface of the reacted NZVI was composed of 56% Fe, 33% O, 7% S, and traces of other elements, matching closely to the ideal formula of schwertmannite, $Fe_8O_8(OH)_6SO_4$ (Bigham et al., 1996).
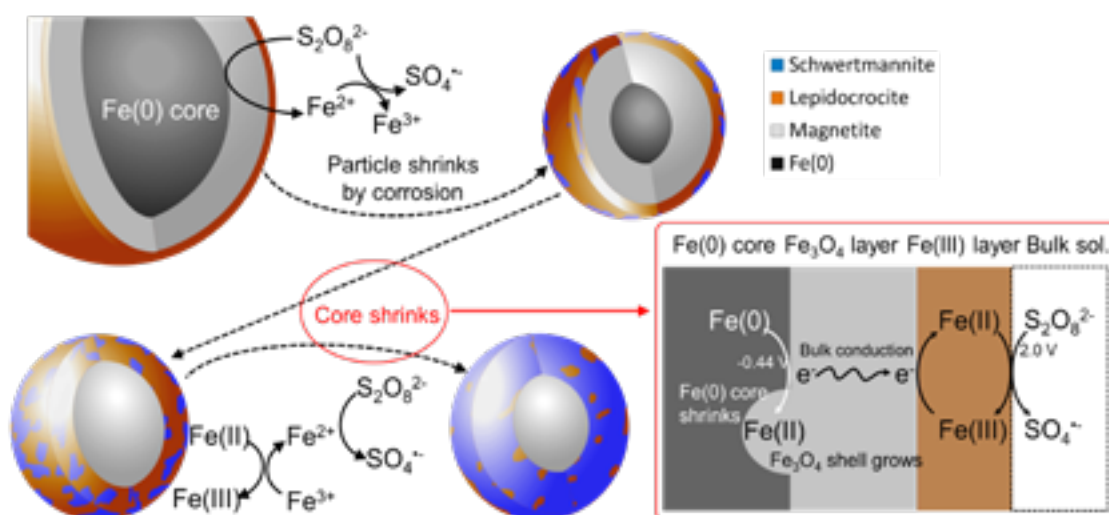

Figure 1. Scheme of nano zero-valent iron transformation in the presence of persulfate (Kim et al., 2018).

Extended X-ray absorption fine stucture (EXAFS) spectroscopy at the Fe K-edge showed that Fe^0 in the NZVI particles was completely consumed after a reaction time with persulfate of only 10 min. The Fe^0 reacted with persulfate rapidly to form aqueous Fe^{2+} and Fe^{3+}, and Fe-(oxyhydr)oxide minerals. Magnetite, lepidocrocite and schwertmannite were major NZVI transformation products according to the EXAFS analysis. In a first stage, Fe^0 was oxidized to form magnetite, schwertmannite then formed through further oxidation of the magnetite and reaction of the Fe(III) with sulfate ions.

The magnetite content of the reacted NZVI was intially 26%, then increased to 74% after 10 min reaction time. The increase in magnetite content implied that the reacted NZVI became coated with multiple shells during reaction with persulfate, because magnetite at the later stage could only form directly on the surface because of the very low steady state aqueous Fe^{2+} concentration. The bulk conduction of electrons through the Fe-(oxyhydr)oxide shell presumably played an important role in the evolution of a multi-layered shell of NZVI (Handler et al., 2009). Bulk conduction would not only allow the growth of the magnetite shell by electron transfer from Fe^0 to magnetite shell but also the continuing activation of persulfate by electron transfer from the Fe^0 core to the solution.

The NZVI transformation processes elucidated in the current study impact on the extent of sulfate radical formation during oxidation processes using persulfate and NZVI. The impact of the the different Fe minerals on sulfate radical formation and the activation mechanism require further study.

REFERENCES

Li, H., Wan, J., Ma, Y., Wang, Y., & Huang, M. 2014: Influence of particle size of zero-valent iron and dissolved silica on the reactivity of activated persulfate for degradation of acid orange 7. Chem. Eng. J., 237, 487-496.

Bigham, J.M., Schwertmann, U., Traina, S.J., Winland, R.L., & Wolf, M. 1996: Schwertmannite and the chemical modeling of iron in acid sulfate waters. Geochim. Cosmochim. Acta, 60 (12), 2111-2121.

Kim, C., Ahn, J. Y., Kim, T. Y., Shin, W. S., & Hwang, I. 2018: Activation of Persulfate by Nanosized Zero-Valent Iron (NZVI): Mechanisms and Transformation Products of NZVI. Environmental science & technology, 52(6), 3625-3633.

Handler, R.M., Beard, B.L., Johnson, C.M. & Scherer, M.M. 2009: Atom exchange between aqueous Fe (II) and goethite: an Fe isotope tracer study. Environ. Sci. Technol., 43 (4), 1102-1107.

19.6

Geogenic contaminants in groundwater resources of Amazonian riverine communities: results of a vast exploratory field-study

Caroline de Meyer [1], Juan Rodriguez [2], Ingo Wahnfried [3] , Rolf Kipfer [1] & Michael Berg [1]

[1] Eawag, Swiss Federal Institute of Aquatic Science & Technology, Ueberlandstrasse 133, CH- 8600 Dübendorf (caroline.demeyer@eawag.ch)
[2] Facultad de Ciencias, Universidad Nacional de Ingeniería, Av. Tupac Amaru 210, Lima, Peru
[3] Geosciences Department, Universidade Federal do Amazonas, Av. Gal. Rodrigo Otávio Jordão Ramos, 3000, Manaus, Brazil

World-wide, river basins and deltas with arsenic (As) and manganese (Mn) contaminated groundwater are characterized by a locally high spatial variability of contaminant concentrations. Since As and Mn are of concern for human health, it is important to understand where and under which environmental conditions these elements are mobilized from aquifer sediments and accumulated in groundwater. Unraveling the regional geochemical mechanisms triggering the enrichment of toxic elements in groundwater forms therefore a particularly important step to raise awareness and implement mitigation where needed.

Here, we discuss the results of a large-scale field study, exploring geogenic contaminants in shallow groundwater resources throughout the vast Amazon Basin. We sampled groundwater from household tube-wells from riverine communities along the main Amazon River and some of its major tributaries, covering large parts of the Peruvian and Brazilian Amazon region. We compare the main and trace element hydrochemistry of groundwater pumped by wells located on the older terraces, with those located in the actual river plain, characterized by young, reactive deposits. The latter are most prone to reach aquifers in which strongly reducing conditions prevail, leading to mobilization of redox sensitive trace elements, such as arsenic, manganese and iron. We further link patterns of measured groundwater arsenic concentrations with available remote sensing data for different geological settings along the Amazon River and its tributaries, with the aim to gain insights on the factors inducing spatial variability in contaminant groundwater chemistry.

Our study highlights the importance of the geological history of this dynamic river basin on the presence and distribution of trace elements in groundwater resources of Amazonian riverine communities.

19.7
Mercury reduction by vivianite

Marjorie Etique [1], Sylvain Bouchet [1], James Byrne [2], Laurel Thomas Arrigo [1], Ralf Kaegi [3], Ruben Kretzschmar [1]

[1] *Soil Chemistry Group, IBP, ETH Zürich, Universitaetstrasse 16, CH-8092 Zürich (marjorie.etique@usys.ethz.ch)*
[2] *Geomicrobiology, Center for Applied Geosciences, University of Tuebingen, Sigwartsrasse 10, D-72076 Tuebingen*
[3] *Eawag, Swiss Federal Institute of Aquatic Science and Technology, Ueberlandstrasse 133, CH-8600 Duebendorf*

Mercury (Hg) is a toxic element of global environmental concern, released into the environment by human activities since the late 1700s. In aquatic/terrestrial systems, Hg can be converted by anaerobic microorganisms to mono-methylmercury (MeHg), a potent neurotoxin accumulated in the food web [1]. In iron-rich sediments where Hg is methylated, vivianite, a ferrous phosphate mineral, commonly occurs in immediate vicinity of organic remains. However, Fe^{II}-bearing minerals are recognized as Hg^{II} reducers such as magnetite [2] or green rusts [3]. The reduction of Hg^{II} to Hg^0 by vivianite ($Fe^{II}_3(PO_4)_2 \cdot 8H_2O$) was investigated by fluctuating Hg/Fe ratios (0.1, 1, 100) at circumneutral pH under anoxic conditions to illuminate kinetic parameters and the nature Fe^{III}-bearing minerals formed. The ability of vivianite to reduce inorganic divalent Hg is of high importance to (i) unravel the interplay of Hg and Fe biogeochemical cycles, and to (ii) limit the production of MeHg in anoxic sediments by the formation of elemental Hg.
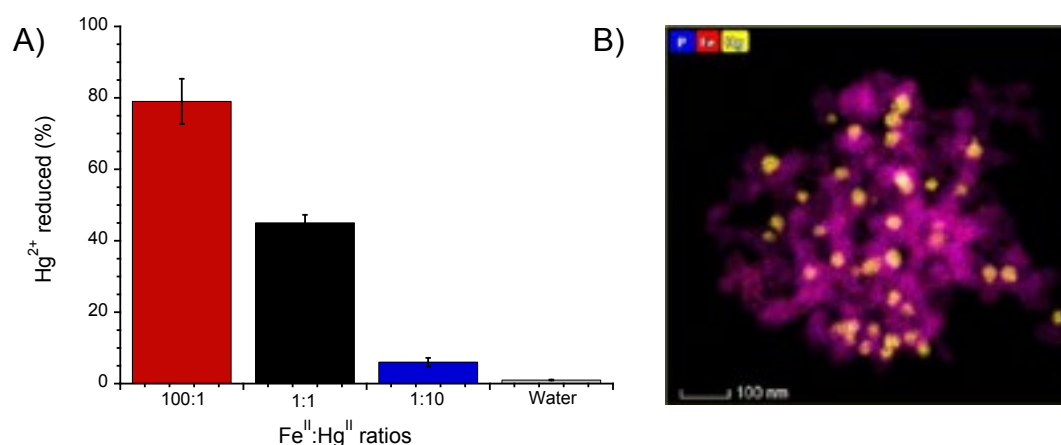

Figure 1. Percentage of inorganic divalent mercury (Hg^{2+}) reduced by vivianite with various Fe/Hg ratios (100:1, 1:1, 1:10); a control was done with water (A). Elemental distribution map of vivianite nanoparticles after mercury reduction (B).

REFERENCES

[1] Syversen T., Kaur P. (**2012**) The toxicology of mercury and its compounds. *Journal of Trace Elements in Medicine and Biology*, 26:215-226.
[2] Wiatrowski H.A., et al. (**2009**) Reduction of Hg(II) to Hg(0) by magnetite. *Environmental Science & Technology*, 43:5307-5313.
[3] Remy P.-Ph., et al. (**2015**) Pseudo-first-order reaction of chemically and biologically formed green rusts with Hg^{II} and $C_{15}H_{15}N_3O_2$: Effects of pH and stabilizing agents (phosphate, silicate, polyacrylic acid, and bacterial cells). *Water Research*, 70:266-278.

19.8
Using global sensitivity analysis to establish priorities in atmospheric selenium research

Aryeh Feinberg [1,2], Moustapha Maliki [3], Andrea Stenke [1], Bruno Sudret [3], Severin Gysin [1], Thomas Peter [1] & Lenny H. E. Winkel [1,2]

[1] Department of Environmental Systems Science, ETH Zürich, Universitätstrasse 16, CH-8092 Zürich
  (aryeh.feinberg@env.ethz.ch)
[2] Eawag, Swiss Federal Institute of Aquatic Science and Technology, Überlandstrasse 133, CH-8600 Dübendorf
[3] Chair of Risk, Safety and Uncertainty Quantification, Department of Civil Engineering, ETH Zürich, Stefano-Franscini-
  Platz 5, 8093 Zürich, Switzerland

Selenium is an essential trace element for humans and animals, as it is included in several proteins which have anti-oxidative functions. Although selenium toxicity has affected people in specific regions in the past, there is a more widespread risk for selenium deficiency. Selenium deficiency is a concern for people and animals that eat food grown in soils with low levels of bioavailable selenium. In addition to geological sources, selenium deposition from the atmosphere is one of the sources of selenium to soil. Selenium levels in soil have been linked to the local amount of precipitation for several regions worldwide. Atmospheric selenium cycling may therefore play an important role in determining the distribution of selenium in soils worldwide, as well as the prevalence of selenium deficiency.

To investigate the atmospheric selenium cycle further, we have implemented selenium chemistry in a global chemistry-climate model, SOCOL-AER. The modelled selenium cycle is based on the existing sulfur cycle in SOCOL-AER, because these two elements are expected to behave in a similar way. Gas phase selenium species (DMSe, H_2Se, CSSe, CSe_2, OCSe, and SeO_2) are emitted in the model through natural (e.g. volcanoes, biogenic sources) and anthropogenic (e.g. coal combustion, metal smelting) activities. These species are oxidized in the atmosphere, forming condensable compounds that can be taken up by aerosols. With SOCOL-AER we can track the transport and speciation of atmospheric selenium, from emission to deposition.

However, since the atmospheric selenium cycle has not been thoroughly investigated in the past, the input parameters for our model related to selenium are very uncertain. Parametric uncertainties include the magnitude and speciation of emissions, the atmospheric reaction rates of selenium species, and the amount and size of particulate matter not calculated online by SOCOL-AER, which only includes sulfate aerosols. We can apportion the uncertainties in the model output into contributions from 34 model input parameters, using techniques from the field of global sensitivity analysis (Saltelli et al., 2008). Since our model is computationally expensive (simulating one year of SOCOL-AER requires ~25 CPU days; on a parallel architecture with 48 CPU it requires 12 hours), we replaced it with a surrogate model using the MATLAB-based UQLAB software (Marelli & Sudret, 2014). The surrogate model, in the form of polynomial chaos expansions (PCE, Ghanem & Spanos (2003)), is constructed from a series of SOCOL-AER training simulations conducted throughout the parametric uncertainty space. This surrogate model is analyzed using the variance-based Sobol› method, which yields the contribution of each input parameter to the overall variance of the model output (Sudret, 2008). We focus on identifying which input parameters are most important in determining the atmospheric lifetime of selenium, and therefore would most affect the long-range transport of selenium. This sensitivity analysis study can help prioritize research into the atmospheric selenium cycle. Input parameters that are found to play a major role in determining the atmospheric selenium lifetime are the most important to be constrained by future studies. We can also identify parameters that can be neglected, for example reaction rates that are not important for the atmospheric selenium lifetime and therefore further research into these reaction rates would not be necessary to understand the global selenium cycle. The application of global sensitivity analysis to our atmospheric selenium model is the first step towards more accurate predictions of selenium deposition to agricultural soils.

REFERENCES

Ghanem, R. & Spanos, P. (2003) Stochastic Finite Elements: A Spectral Approach, Courier Dover Publications, Mineola.
Marelli, S., & Sudret B. 2014: UQLab: A framework for uncertainty quantification in Matlab, Vulnerability, Uncertainty, and
    Risk: Quantification, Mitigation, and Management, 2554-2563.
Saltelli, A., Ratto, M., Andres, T., Campolongo, F., Cariboni, J., Gatelli, D., Saisana, M. & Tarantola, S. (2008) Global
    sensitivity analysis -- the primer, Wiley.
Sudret, B. (2008) Global sensitivity analysis using polynomial chaos expansions Reliab. Eng. Sys. Safety, 93, 964-979.

19.9

Should plastics be considered in the biogeochemical cycles of trace elements?

Montserrat Filella [1] & Andrew Turner [2]

[1] Department F.-A. Forel, University of Geneva, Boulevard Carl-Vogt 66, CH-1205 Geneva, Switzerland, (montserrat.filella@unige.ch)
[2] School of Geography, Earth and Environmental Sciences, Plymouth University, Drake Circus, Plymouth PL4 8AA, UK

Plastic debris hase emerged as a global environmental problem and a potential marker of the anthropocene. It is generally acknowledged that the ubiquitous presence of plastics of different sizes in all environmental compartments raises important health problems. Some studies have recently mentioned the plastic cycling itself (Lecher, 2018) or the role of the plastics in the elemental cycle of elements such C, P, S, directly involved in the degrading, transporting and burial of microbial organic matter (Posth et al., 2017). However, plastics also contain a number of trace elements like Pb, Cd, Sb, sometimes at very high concentrations (Turner, 2016; Filella and Turner, 2018). Thus, it is probably timely to consider whether they should be included as active actors in the biogeochemical cycles of these elements. In an initial step, this would require the evaluation of their presence (i.e., how much) and the study of their behaviour (e.g., leaching, sorption, etc.). A first evaluation will be presented and discussed.

REFERENCES

Filella, M., & Turner, A. 2018. Observational study unveils the extensive presence of hazardous elements in beached plastics from Lake Geneva. Frontiers in Environmental Science, 6, doi: 10.3389/fenvs.2018.00001

Lecher, A.L. 2018: Piecing together the plastic cycle. Nature Geoscience, 11, 153.

Posth, N.R., Chiriaev, S., Gorokhova, E., Neu, T., & Strand, J. 2017. Biogeochemical cycling in the Plastisphere. Goldschmidt2017 Abstract.

Turner, A. 2016. Hazardous metals, metalloids and other elements in marine litter. Marine Pollution Bulletin, 111, 136–142

19.10
Transformation of cerium dioxide nanoparticles during incineration of sewage sludge

Alexander Gogos [1], Jonas Wielinski [1,2], Andreas Voegelin [1] and Ralf Kaegi [1]

[1] Eawag, Swiss Federal Institute of Aquatic Science and Technology, 8600 Dübendorf / Switzerland
  (alexander.gogos@eawag.ch)
[2] ETH Zürich, Institute of Environmental Engineering, 8093 Zürich / Switzerland

Wastewater treatment plants (WWTP) show high removal efficiencies for different types of (engineered) nanomaterials ((E) NM), resulting in their accumulation within sewage sludge, which is incinerated at an increasing share in many countries including Germany (~30%) and Switzerland (~70%). Given the predicted increase of cerium dioxide nanoparticle (CeO_2 NP) production and related release to WWTP and the growing importance of sewage sludge incineration, knowledge on the physical-chemical transformations of CeO_2 NP during these treatments is required for understanding the fate of CeO_2 NP and assessing the (eco-)toxicological effects related to their increased use. Previous studies indicate that the complexity of the experimental system (e.g. type of incineration, matrix in which the CeO_2 NP are dispersed) influences the speciation of Ce in the ashes.

We therefore incinerated municipal sewage sludge spiked with CeO_2 NP in a pilot fluidized bed reactor (FBR) to investigate physical- chemical changes of the CeO_2 NP caused by the incineration process. We used Ce K-edge X-ray absorption spectroscopy (XAS) to assess the chemical speciation of the CeO_2 NP in both sludge and corresponding ash. Linear combination fit analysis (LCF) conducted on extended X-ray absorption fine structure (EXAFS) spectra suggests that ~20% of the total Ce was reduced to a Ce(III)-phase in the sewage sludge after one week of anaerobic incubation. After incineration, a nearly complete reduction (86%) of the remaining $Ce(IV)O_2$ to a Ce(III)-phase was observed. Enrichment factors (Ce concentration ash:sludge) obtained from different analytical techniques (ICP-MS, XRF, XAS) ranged between 1.2 and 1.5. Ashes from pristine sludges obtained using the same FBR, however, revealed enrichment factors of ~3-4, which is expected for non-volatile components. These results therefore suggest significant losses of Ce during incineration of nanoparticulate CeO_2 and thus a significant difference in the incineration behaviour between spiked nanoparticulate and other Ce-phases present in the sewage sludge.

19.11
Challenges of trace elements in the Swiss environment

Bettina Hitzfeld

Federal Office for the Environment, Berne, Switzerland; Bettina.Hitzfeld@bafu.admin.ch

Trace elements of geogenic and anthropogenic origin still pose many challenges in the Swiss environment. Especially metals and heavy metals such as lead, arsenic and mercury but also fluor are present in soils and other environmental media and are a danger to human health and the environment. Arsenic of geogenic origin seems to pose a risk in certain regions in Switzerland when it is present in agricultural areas. The concentrations and the extent of the putative pollution are however as yet unknown. Mercury pollution in Switzerland is of anthropogenic origin and concentrated in regions where industrial activity led to contamination of extended areas of land. Effects on the human population, agricultural land and studies that inform risk assessment will be presented. Lead pollution is known in soils in the proximity of shooting ranges and in city centres as a legacy of industrial activities. This pollution may have effects on wildlife, cattle and humans, esp. children. It is therefore essential to develop knowledge on toxicological and ecotoxicological effects and environmental processes in order to keep legislation up to date, so that human health and the environment may be protected. The challenges of the Swiss Federal Administration when dealing with the pollution of legacy and emerging trace elements will be discussed in the context of European and international activities.

19.12
Studying Bacterial Selenium Methylation at Environmental Relevant Concentrations

Ying Liu [1,2], Andreas Schäffer [2], Markus Lenz [1]

[1] Institute for Ecopreneurship, School of Life Sciences, University of Applied Sciences and Arts Northwestern Switzerland, Hofackerstrasse 30, 4132 Muttenz, Switzerland (ying.liu@fhnw.ch)
[2] Institute for Environmental Research (Biology V), RWTH Aachen University, 52074 Aachen, Germany

The trace element selenium (Se) which acts as a component of major metabolic pathways is essential for animals and humans health. However there are abundant Se deficiencies worldwide and millions of people may be affected by the accompanying endemic diseases (Fairweather-Tait et al., 2011). Methylation and subsequent volatilization is an important Se cycle process in natural environments which may lessen available Se in soils, ultimately limiting its entry into the food chain (Winkel et al., 2012). Se methylation is mostly regarded as a detoxification process for organisms since volatilization decreases the intracellular Se content. Previous studies of Se volatilization were performed using Se concentrations 10^3 - 10^6 fold higher (sub-ppm / ppm) than those commonly found in the environment (Luxem et al., 2017; Vriens et al., 2016). Se volatilization fluxes based on those experiments using high concentrations may have limited relevance for most environments which only contain trace amounts of Se.

Here, we developed a method to study Se methylation using a *Pseudomonas* strain with treatment of different concentrations of SeIV in sub-ppb to ppb range. The substrate ^{74}Se-selenite were synthesized from elemental ^{74}Se through a nitric acid oxidation reaction. Headspace SPME-GC-MS was used to quantify methylated ^{74}Se compounds while ^{80}Se methylated from the background Se in the culture medium was measured. Using Se stable isotope allowed distinguishing external from endogenous Se methylation and for the first time studying microbial selenium methylation at environmental relevant concentrations.

REFERENCES

Fairweather-Tait, S. J., Bao, Y., Broadley, M. R., Collings, R., Ford, D., Hesketh, J. E. & Hurst, R., 2011: Selenium in Human Health and Disease, Antioxidants & Redox Signaling 14(7), 1337-1383.

Luxem, K. E., Vriens, B., Behra, R. & Winkel, L. H. E., 2017: Studying selenium and sulfur volatilisation by marine algae Emiliania huxleyi and Thalassiosira oceanica in culture, Environmental Chemistry 14(4), 199-206.

Vriens, B., Behra, R., Voegelin, A., Zupanic, A. & Winkel, L. H. E., 2016: Selenium Uptake and Methylation by the Microalga Chlamydomonas reinhardtii, Environmental Science & Technology 50(2), 711-720.

Winkel, L. H. E., Johnson, C. A., Lenz, M., Grundl, T., Leupin, O. X., Amini, M. & Charlet, L., 2012: Environmental Selenium Research: From Microscopic Processes to Global Understanding, Environmental Science & Technology 46(2), 571-579.

19.13

X-ray spectroscopic characterization of As(V)-rich Tl(III)-particles in a weathered Tl-As-Fe-sulfide mineralization

Francesco Femi Marafatto [1,2], Dario Ferreira-Sanchez [1], Daniel Grolimund [1], Jörg Göttlicher [3], Andreas Voegelin [2]

[1] Paul Scherrer Institut, CH-5232 Villigen PSI (francesco.marafatto@psi.ch)
[2] Eawag, CH-8600 Dübendorf
[3] Karlsruhe Institute of Technology, D-76344 Eggenstein-Leopoldshafen

Thallium is a highly toxic trace metal of growing environmental concern. In Erzmatt (Swiss Jura mountains) soils were found to contain high levels of Tl and As due to their formation from carbonate rock hosting a weathered hydrothermal Tl-As-Fe mineralization. Although Tl in this site was constrained to a limited area, it is ideally suited to study the long-term transformation of Tl at contaminated sites and its speciation in soils.

In a previous study, the Erzmatt soils were found to contain Tl^I-substituted jarosite and avicennite ($Tl^{III}_2O_3$) as important secondary Tl-bearing minerals [1]. The dominant soil-formed Tl species was Tl^I associated with illite. Elevated levels of Tl^{III} were associated with soil Mn concretions, but accounted for only a minor fraction of total soil Tl. Circumstantial evidence suggested that another unidentified Tl^{III}-rich phase is present in the Erzmatt soils.

In continuing work, we identified and characterized the unknown Tl^{III}-rich phase by examining soil and rock thin sections as well as individual particles isolated from soil and rock combining laboratory X-ray fluorescence spectrometry (XRF) and X-ray diffraction (XRD) with synchrotron-based bulk X-ray absorption spectroscopy (XAS) and micro-resolved XRF/XRD tomography.

Our results suggest that the composition of the Tl-rich particles corresponds to Tl_2O_3 with up to 0.25 As(V)/Tl. Extended X-ray absorption fine structure (EXAFS) spectra in combination with XRD data suggest that the As^V-rich $Tl^{III}_2O_3$ grains are amorphous or nanocrystalline precursors of crystalline avicennite. We speculate that these particles form by the oxidation of Tl-As sulfide minerals such as lorandite ($TlAsS_2$) or ellisite (Tl_3AsS_4) and that the As^V inhibits the crystallization of Tl_2O_3 into avicennite.

Avicennite and As^V-rich Tl_2O_3 particles in the Erzmatt soils are coated with Mn-oxides that we identified as layered MnO_2, possibly in association with a tectomanganate. The MnO_2-crusts contain up to 0.2 Tl/Mn as Tl(I) and may have formed via a redox reaction between dissolved Mn^{2+} and Tl^{III}.

The results from this work provide new insights into the processes that control the release of Tl from Tl-bearing sulfide minerals and the sequestration of Tl in soils, and are relevant with respect to the assessment of risks arising from geogenically and anthropogenically Tl-contaminated sites.

REFERENCES

1. Voegelin, A.; Pfenninger, N.; Petrikis, J.; Majzlan, J.; Plotze, M.; Senn, A. C.; Mangold, S.; Steininger, R.; Gottlicher, J., Thallium speciation and extractability in a thallium- and arsenic-rich soil developed from mineralized carbonate rock. Environ Sci Technol 2015, 49, 5390-5398.

19.14
Competitive sorption of Mn(II) and Cd(II) to clay minerals

Natacha Van Groeningen [1], Iso Christl [1] & Ruben Kretzschmar [1]

[1] Soil Chemistry Group, Institute of Biogeochemistry and Pollutant Dynamics, Department of Environmental Systems Science, CHN, ETH Zurich, Universitätstrasse 16, CH-8092 Zurich, Switzerland

Redox variable environments such as riparian floodplain soils, wetlands, and rice paddies are of great importance for the mobilization of trace elements from terrestrial environments into aquatic systems. Elevated dissolved concentrations of trace elements in terrestrial and aquatic systems are of concern since they can cause detrimental effects on biota due to toxic responses in plants (e.g. Mn, Zn, Cu) as well as in animals and humans (e.g. Cd, Pb). Both natural and anthropogenic sources can lead to local enrichments of trace elements in the environment. During periods of water-saturation, high concentrations of dissolved Mn^{2+} are observed in redox variable environments as a result of the reductive dissolution of Mn(IV,III)-(oxyhydr)oxides. The high concentrations of Mn^{2+} are expected to influence fate of trace elements cations (e.g. Zn^{2+}, Cd^{2+}) as Mn^{2+} competes for cation adsorption to mineral surfaces. Herein, clay minerals are considered key sorbent phases for trace element cations due to their large specific surface area, the presence of permanently negatively charged surfaces and reactive surface hydroxyl groups, and due to their chemical stability under anoxic conditions.

To date, it is not well known how and to which extent the sorption of Mn^{2+} to clay minerals surfaces influences the retention of others trace elements under reducing conditions. To investigate this, we studied Cd(II) and Mn(II) sorption to smectite (Syn-1) separately under anoxic conditions (O_2 < 0.1 ppm). The experiment were carried out to cover a wide range with respect to pH, total metal concentration and $CaCl_2$ background electrolyte concentration in order to obtain a large database for modelling single metal sorption to smectite. Based on model parameter optimization of single metal sorption data, the competitive effect of Mn^{2+} on Cd^{2+} sorption was predicted.

Two types of binding sites were assumed for the sorption of metal onto the smectite: edge sites ($Y^{-0.5}$) which have a pH-dependent charge and face sites (Ex^-) with a permanently negative charge. The mineral-water interface at the edge sites was described with a 1-pK three plane model (TPM). Interactions at the face sites were modelled with a three plane model and a conventional cation exchange model (Gaines-Thomas) for comparison. To obtain site densities and protonation constants for edge and face sites, acid-base titration data of Syn-1 were fitted. To describe acid-base titration data, the charge of Ca^{2+} had to be placed partially inner sphere at the edge sites (Dz_0=+1.2). The use of the three plane model for the face sites yielded a better description of the acid-base titration data and was thus selected for modelling metal sorption to smectite.

The results for Mn^{2+} and Cd^{2+} sorption to Syn-1 as a function of pH and ionic strength are shown in Figure 1. Both Mn^{2+} and Cd^{2+} sorption was increased with increasing pH due to proton-metal cation competition for binding sites. A pronounced ionic strength effect was observed for both Mn^{2+} and Cd^{2+} sorption at pH below 6.5 indicating the predominance of sorption to face sites under acidic conditions. The comparison of Cd^{2+} and Mn^{2+} sorption revealed that Mn^{2+} was more strongly influenced by the presence of Ca^{2+} indicating a weaker sorption of Mn^{2+}. Accordingly, very high concentrations of dissolved Mn^{2+} as typically found in water-saturated soils are required to affect Cd^{2+} sorption to clays. Environmental impacts of the presence of Mn^{2+} on trace element sorption to clays will be discussed.
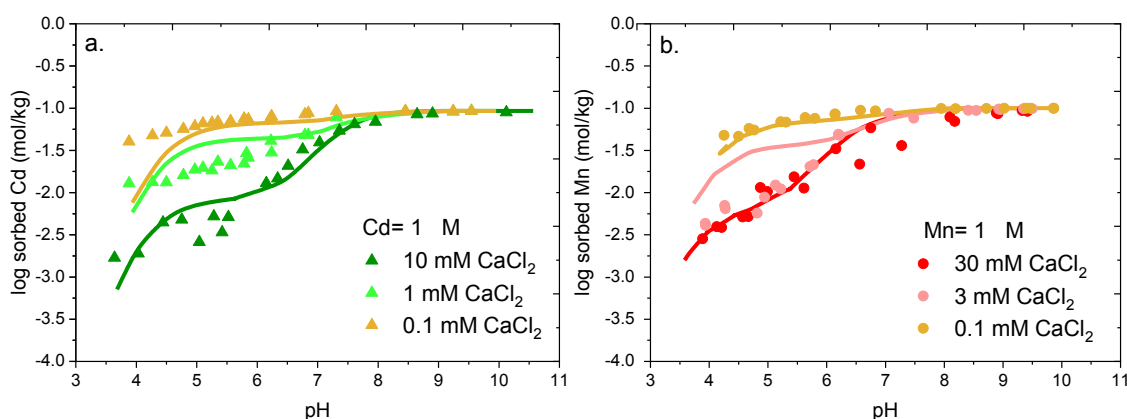

Figure 1. Sorption of Cd^{2+} (a) and Mn^{2+} (b) on Syn-1 (~1 g/L) as function of pH at $CaCl_2$ concentration. Total metal concentrations of 1 μM were used for both Cd^{2+} and Mn^{2+}, respectively. All samples were equilibrated for 1 day. Lines represent best-fit description with the TPM/TPM-model.

19.15
Arsenic methylation across microbial phyla

Karen Viacava [1], Shannon Dyer [1], Karin Lederballe Meibom [1], Adrien Mestrot [2] & Rizlan Bernier-Latmani [1]

[1] *École Polytechniqeu Fédéral de Lausanne (EPFL), ENAC - IIE -EML Station 6, CH-1015 Lausanne*
 (karen.viacava@epfl.ch)
[2] *TrES group, Institute of Geography, University of Bern, Hallerstrasse 12, CH-3012 Bern*

Arsenic (As) undergoes extensive microbial cycling in the environment, and, because of the toxicity of this metalloid, many bacteria and archaea harbour genes that confer resistance to it [1]. As methylation is one of the many microbially-mediated process, it consists in the addition of one or several methyl groups to inorganic arsenic generating volatile and non-volatile arsenicals. The reaction is catalysed by the enzyme arsenite methyltransferase (ArsM). It has been proposed as a detoxification mechanism but also as an activation pathway or a precursor reaction for the synthesis of more complex arseno-organic molecules. As methylation has been subject of study due to the presence of methylarsenicals in rice, a major source of arsenic in the human diet. The methylarsenicals are derived from microorganisms in paddy soils given that rice plants lack the ability to catalyse the reaction [2].

In paddy soils, *arsM*-harbouring microorganisms are phylogetically diverse and abundant [3] but it is still unclear whether all synthesize functional proteins and active methylate As once present in the soil. Previous studies have identified a few active As methylators, most of them aerobic microbial species, including the Bacteroidete *Arsenicibacter rosenii* SM-1 [4]. In contrast, only two anaerobic species were identified: the Firmicute *Clostridium* sp. BXM [5] and the archaeon *Methanorsarcina acetivorans* C2A [6]. Thus, the goal of this study is twofold: first, to test the As-methylation activity of *arsM*-harbouring microbial species belonging to various phyla and representing diverse metabolisms present in paddy soils and, second, to systematically probe the functionality and the *in vivo* activity of the enzymes encoded in their *arsM* genes.

As(III) methylation and volatilization was tested across five anaerobic microbial strains: two archaea (*Methanosarcina mazei* Gö1, *Methanosarcina acetivorans* C2A); two Firmicutes (*Anaeromusa acidaminophila* DSM 3853, *Clostridium pasteurianum* DSM 525); a Deltaproteobacterium (*Geobacter metallireducens* GS-15); and two aerobic strains: a Streptomycete (*Streptomyces vietnamensis* DSM 41927); and a Bacteroidete (*Arsenicibacter rosenii* SM-1). All *arsM* genes were cloned into the arsenic-sensitive *Escherichia coli* AW3110(DE3) and As methylation quantified.

The results show that most of the strains were not able to methylate As despite harbouring *arsM* genes that encode functional ArsM proteins. Our first conclusion is that the presence of *arsM* does not equate As methylation even in the presence of the metalloid. Further, we hypothesize that more efficient As detoxification pathways might be prevalent, precluding methylation, therefore more work is warranted to deconvolute *arsM* regulation.

REFERENCES
[1] Andres *et al.* 2016: The microbial genomics of arsenic, FEMS Microbiol. Rev., 40, 299-322.
[2] Zhao et al. 2013: Methylated arsenic species in rice: Geographical variation, origin, and uptake mechanisms, Environ. Sci. Technol., 47, 3957-3966.
[3] Reid *et al.* 2017: Arsenic methylation in a rice paddy soil anaerobic enrichment culture, Environ. Sci. Technol., 51, 10546-10554.
[4] Huang *et al.* 2016: Efficient Arsenic Methylation and Volatilization mediated by a novel bacterium from an arsenic-contaminated paddy soil, Environ. Sci. Technol., 50, 6389-6396.
[5] Wang *et al.* 2015: Identification and catalytic residues of the arsenite methyltransferase from a sulfate-reducing bacterium, *Clostridium* sp. BXM, FEMS Microbiol. Lett., 362, 1-8.
[6] Wang *et al.* 2014: Identification and characterization of arsenite methyltransferase from an archaeon *Methanorsarcina acetivorans* C2A, Environ. Sci. Technol., 48, 12706-12713.

19.16
Uptake of As by nanocrystalline Al-hydroxysulfates naturally forming along a mountainous stream in the Engadin area

Christoph Wanner [1], Rosemarie Pöthig [2], Sergio Carrero [3], Alejandro Fernandez-Martinez [4], Christian Jäger [5] & Gerhard Furrer [6]

[1] Rock-Water Interaction Group, Institute of Geological Sciences, University of Bern, Baltzerstrasse 3, CH-3012 Bern, Switzerland (wanner@geo.unibe.ch)
[2] Leibniz-Institute of Freshwater Ecology and Inland Fisheries, Berlin, Germany
[3] Department of Earth and Planetary Science, University of California Berkeley, USA [4] Univ. Grenoble Alpes, Univ. Savoie Mont Blanc, CNRS, IRD, IFSTTAR, ISTerre, Grenoble, France
[5] BAM-Federal Institute for Materials Research and Testing, Division I.3, Working Group NMR Spectroscopy, D-12489 Berlin, Germany
[6] Institute of Biogeochemistry and Pollutant Dynamics (IBP), Department of Environmental Systems Science, ETH Zurich, CH-8092 Zurich, Switzerland

Nanocrystalline basaluminite $[Al_4OH_{10}(SO_4) \cdot (H_2O)_{3-5}]$ and aggregation of the ε-Keggin polyoxocation $[Al_{12}(AlO_4)(OH)_{24}(H_2O)_{12}]^{7+}$, referred to as Al_{13}, have both been described to form in acid mine drainage environments. Although the chemical composition is quite similar, their crystalline varieties significantly differ, demonstrating that various types of precipitates can form under very similar conditions and that their respective formation is not fully understood yet.

Here we report the occurrence of large amounts of nanocrystalline Al-hydroxysulfates that form naturally in a small alpine catchment in the Engadin area where an acidic mountainous stream (pH~4) is neutralized successively after mixing with several neutral tributaries (Fig. 1).

Synchrotron-based high-energy X-ray diffraction (HEXD) and subsequent pair distribution function (PDF) analyses demonstrate that these precipitates are structurally the same as basaluminite samples obtained from acid mine drainage sites (Wanner et al., 2018). In contrast, only minor amounts of tetrahedrally coordinated Al, as present in Al_{13}, were identified by nuclear magnetic resonance (NMR) spectroscopy.

We hypothesize that in our field system, high sulfate and fluoride concentrations on the order of 1-2 and 100 mg/L, respectively, as well as low water temperatures (<8°C) favor the formation of basaluminite instead of Al_{13}-bearing sulfate precipitates.

Interestingly, the basaluminite precipitates are characterized by elevated As concentrations up to 600 µg/g, whereas other heavy metals are at background concentrations only. Given the low As concentrations in the stream from which precipitation occurs (<0.03 mg/L), high As concentrations confirm that basaluminite serves as a highly efficient As sink.

We conclude that the high affinity for As results from the high sorption capacity of basaluminite and hence from the uptake of arsenate anions under the prevailing oxidizing conditions.

REFERENCE
Wanner, C., Pöthig, R., Carrero, S., Fernandez-Martinez, A., Jäger, C. & Furrer, G. 2018: Natural occurrence of nanocrystalline Al-hydroxysulfates: Insights on formation, Al solubility control and As retention, Geochimica et Cosmochimica Acta, 238, 252-269.
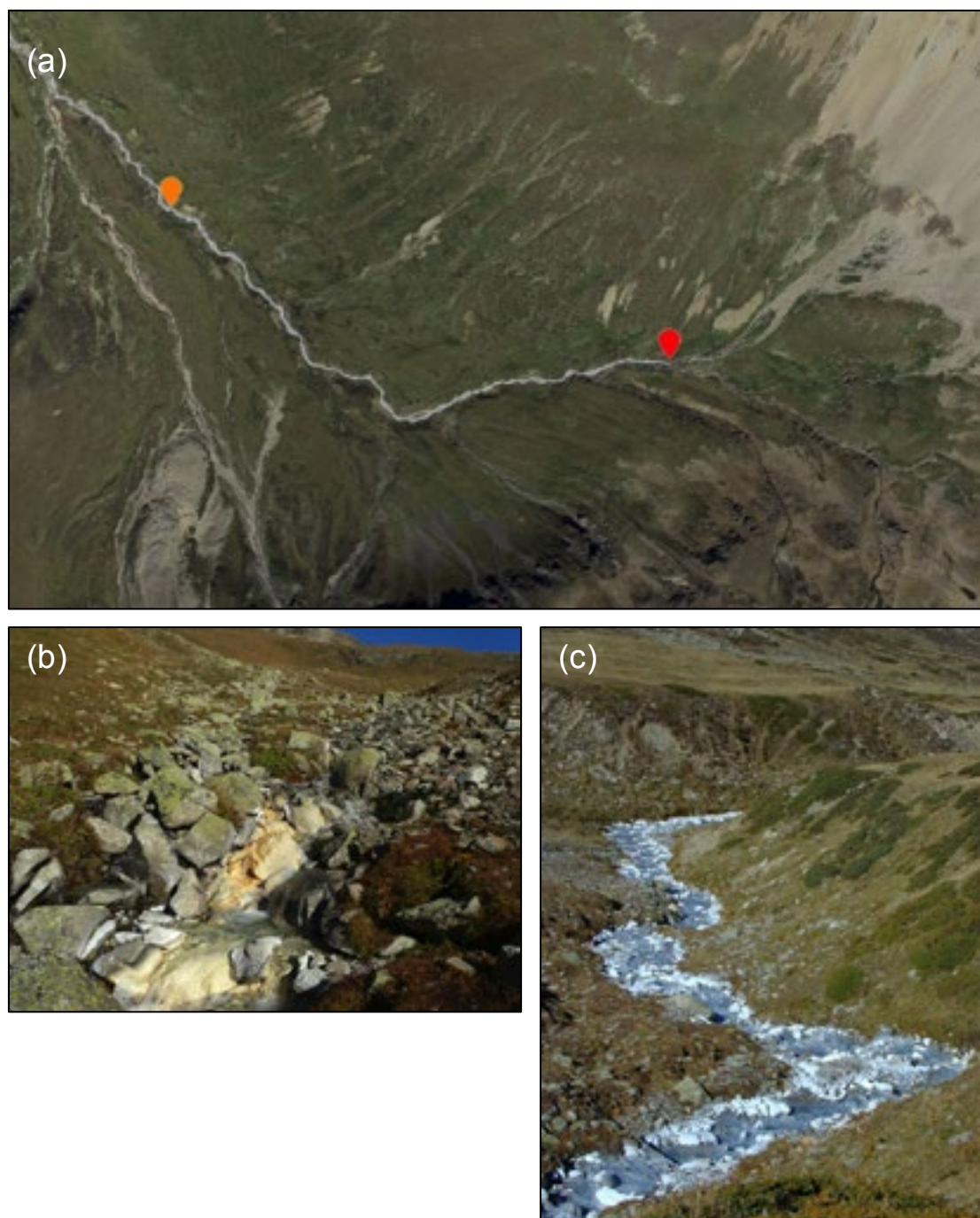
Figure 1. Photographs of basaluminite precipitation occurring along "Ova Lavirun", a mountainous stream in the Engadin area. (a): Aerial photograph of the Ova Lavirun watershed, clearly illustrating the white bedload coating originating from basaluminite precipitation. (b) Photograph of the first basaluminite occurrence near the red marker shown in (a). (c) Photograph of the widespread basaluminite occurrence along a section near the yellow marker shown in (a).

19.17
Thallium Sorption onto Birnessite

Silvan Wick [1], Jasquelin Peña [2] & Andreas Voegelin [1]

[1] *Eawag, Swiss Federal Institute of Aquatic Science and Technology, Überlandstrasse 133, CH-8600 Dübendorf (silvan.wick@eawag.ch)*
[2] *Institute of Earth Surface Dynamics, Faculty of Geosciences and Environment, University of Lausanne, CH-1015 Lausanne*

Thallium (Tl) is a highly toxic trace element and may pose a serious threat to human health when present in soil or water resources. Tl commonly occurs in the environment as monovalent Tl^I and, to a lesser extent, as trivalent Tl^{III}. Micaceous clay minerals and Mn-oxides are key sorbents for Tl in soils [1]. With respect to Mn-oxides, it has been shown that hexagonal birnessite can oxidatively sequester Tl^{III}, whereas triclinic birnessite binds Tl^I without oxidation [2]. However, the sorption capacity and affinity of these different uptake mechanisms on Mn-oxides and their impact on Tl speciation and solubility in soils has not been studied to date.

We combined batch sorption experiments with X-ray absorption spectroscopy to elucidate the extent and mechanisms of Tl sorption onto synthetic $d-MnO_2$ and triclinic birnessite. Our results confirm that the uptake mechanism depends on the oxide structure, especially the vacancy and Mn^{III} content. In contact with $d-MnO_2$ with a high vacancy content and an average Mn oxidation state close to IV, dissolved Tl is oxidized to Tl^{III} during sorption. Only at Tl-loadings >30'000 mg/kg (molar Tl/Mn ~ 0.025), the maximum capacity for oxidative Tl uptake is approached. That is evidenced by increasing fractions of sorbed Tl^I at these or higher Tl loadings. In contact with triclinic birnessite, whose structure consists of $Mn^{III,IV}$-sheets without vacancies, no Tl oxidation is observed and the dominant sorption process appears to be cation exchange. The distribution coefficients (log K_d-values; for K_d in L/kg) of $d-MnO_2$ range from ~9 at low loadings (~3'000 mg/kg) to ~5 at the highest loadings (~300'000 mg/kg), whereas log K_d-values for Tl sorption onto triclinic birnessite varied only between 4.5 and 5.0 over the tested concentration range.

Our results yield information on the affinity and capacity of non-oxidative and oxidative Tl uptake by different birnessites. The importance of these uptake mechanisms in soils will depend on the abundance of birnessite minerals relative to other sorbent phases as well as on the competition of other (trace) metal cations for reactive surface sites on birnessites.

REFERENCES
[1] Voegelin, A.; Pfenninger, N.; Petrikis, J.; Majzlan, J.; Plötze, M.; Senn, A. C.; Mangold, S.; Steininger, R.; Gottlicher, J. 2015: Thallium speciation and extractability in a thallium- and arsenic-rich soil developed from mineralized carbonate rock, Environmental Science and Technology, 49, 5390-5398.
[2] Peacock, C. L.; Moon, E. M. 2012: Oxidative scavenging of thallium by birnessite: Explanation for thallium enrichment and stable isotope fractionation in marine ferromanganese precipitates. Geochimica et Cosmochimica Acta, 84, 297-313.

P 19.1

Methylmercury distribution and formation in polluted agricultural floodplain soils.

Lorenz Gfeller*, Adrien Mestrot*

[1] *Institute of Geography, University of Bern, Hallerstrasse 12, CH-3012 Bern (lorenz.gfeller@giub.unibe.ch)*

The biomethylation of mercury (Hg) is well studied in the marine environment. However, there is still a lack of knowledge concerning monomethyl-mercury (MMHg) formation in soils. Our main aim with this study was to characterize soil parameters potentially driving MMHg formation in agricultural soils. To do so, we investgated a Hg polluted agricultural floodplain situated between Visp and Raron, in the Canton of Valais.

There, an acetaldehyde producing plant released an estimated 50 t of Hg into a discharge canal between the 1930s and the 1970s. On several occasions, the Hg-rich canal sediments were used to fertilize agricultural fields and private gardens. In this area, we chose five agricultural sites (1 gradient, 2 hotspot and 2 background). The soil was sampled in a rectangular grid to a depth of 50 cm in 10 cm intervals. 300 Samples were analysed for Hg, MMHg, other relevant metals and a range of soil parameters such as pH, N, S and organic carbon (OC).

In the top soil, concentrations ranged from 0.05 - 107 mg kg^{-1} and 0.3 - 11.2 µg kg^{-1} for Hg and MMHg respectively. MMHg/Hg$_{tot}$ ranged from 0.004 - 3.785 % . In background sites the soil Hg methylation potential MMHg/Hg$_{tot}$ was negativly correlated with pH and Fe concentration and positively correlated with OC. We also found that MMHg/Hg$_{tot}$ varies with land-use types (cornfiled vs. pasture field).

According to our results, Hg methylation in soil is influenced by pH and OC, which is similar to Hg methylation in sediments. Furthermore, the type of fertilizer application in an agricultural soil may change OC and pH drastically. To what extend fertilisation (e.g. manure application) is governing Hg methylation is still an open question.

P 19.2
Transformation of Manganese Oxides by Organic Constituents in Natural and Laboratory Systems

Debra Hausladen [1], Marco Keiluweit [2], & Jasquelin Peña [1]

[1] *Institute of Earth Surface Dynamics, University of Lausanne, CH-1015 Lausanne, Switzerland. (debra.hausladen@unil.ch)*
[2] *Stockbridge School of Agriculture, University of Massachusetts Amherst, Amherst, MA, USA.*

Biological processes are the predominant driver of manganese oxide precipitation in the environment. The formation of Mn biooxides, one of nature's most potent solid-phase oxidants and an important scavenger of metals in the environment, depends on organic carbon compounds to fuel microbial catalysis. Additionally, the precipitation of these Mn oxides within biofilm matrices can contribute to either the retention or oxidation of carbon. This study investigates the reaction of both chemogenic and biogenic manganese oxides with a range of organic compounds. First, we look at how three commonly used Good's buffers transform Mn oxide reactivity. Our results show that the differences in chemical structure, initially designed to allow the buffers to function over their respective pH ranges, influence the capacity for electron transfer from redox-active amine moieties to Mn oxides, with TRIS buffer showing the most reduction followed by HEPES and then MES buffers. Biogenic Mn oxides were precipitated in the absence of C compounds (e.g., growth media, organic buffers) and initial reduction by HEPES followed the same trend as predicted by abiotic oxides, although continued reduction does not occur between 1 and 24 h as with abiotic oxides. Next, biogenic and abiotic Mn oxides were reacted with phenolic model compounds in order to better understand the role of Mn biominerals on lignin biodegradation in soil systems. The results of this study assess to what extent the use of chemically synthesized versus biogenically precipitated Mn oxides may impact predictions of natural organic matter degradation. In addition, this study provides insight into the control of organic carbon species on Mn oxide structure and oxidation state within the environment.

P 19.3

Copper mass balances and stable isotopes as analytical tool to trace sources and processes in agricultural systems

Martin Imseng [1], Matthias Wiggenhauser [2/3], E. Frossard [3], Michael Müller [4], Armin Keller [4], Wolfgang Wilcke [5] and Moritz Bigalke [1]

[1] *Geographic Institute, University of Bern, Hallerstrasse 12, CH-3012 Bern*
[2] *Institute of Agricultural Sciences, ETH Zürich, Eischikon 33, CH-8315 Lindau*
[3] *Institut des Sciences de la terre, Université Grenoble Alpes – CNRS, F-38058 Grenoble Cedex 9*
[4] *Swiss Soil Monitoring Network (NABO), Agroscope, Reckenholzstrasse 191, CH-8046 Zürich*
[5] *Institute of Geography and Geoecology, Karlsruhe Institute of Technology (KIT), Reinhard-Baumeister-Platz 1, D-76131 Karlsruhe*

In animal husbandary, copper (Cu) is used as feed additive and pharmaceutical. The Cu is tranferred into manure and distributed on agricultural land. Finally, the Cu from the manure can accumulate in agricultural soils. Although being a micronutrient, high Cu concentrations are toxic for microorganisms and invertebrates and endanger the soil fertility. Former studies revealed Cu accumulations in Swiss agricultural soils in the past decades. However, these studies were not completely based on in-situ measured data. The aim of this study was to fill this gap and measure Cu fluxes at selected Swiss agricultural sites. Specifically, the aim was to trace Cu in the soil and to differentiate between anthropogenic and geogenic sources. Additionally, the metal distribution in Swiss agricultural systems was further elucidated, based on stable isotope ratios of system fluxes and soil pools.

For that purpose, Cu balances of three grassland sites were determined by measuring the soil metal concentrations and all inputs (atmospheric bulk deposition, manure & parent material) and outputs (seepage water and grass harvest) during one hydrological year (May 2014 – May 2015). Furthermore, stable Cu isotope compositions of the soil and all inputs will be measured.

Cu mass balances showed net accumulations at all three sites (25-209 g ha^{-1} yr^{-1}) and manure application was the most important flux (146-340 g ha^{-1} yr^{-1}). Inputs with bulk deposition and through parent material weathering were by 1-2 orders of magnitude smaller. Beside the Cu budgets, stable isotope data (not yet analysed) will be presented and discussed to assess the biogeochemical processes and redistribution of (anthropogenic) Cu in agricultural systems.

REFERENCES

Keller, A., Rosser, N. & Desaules A. 2005: Agroscope FAL.
Schultheiß, U., Döhler, H., Roth, U., Eckel, H., Goldbach, H., Kühnen, V., Wilcke, W., Uihlein, A., Früchtenicht, K. & Steffens, G. 2004: VDLUFA-Schriftenreihe, 59, 232-243.
Sheppard, S. C. & Sanipelli, B. 2012: Journal of Environmental Quality, 41, 1846-1856.

P 19.4

Evolution of Technology-Critical Element contents in sediments of a contaminated bay of Lake Geneva (Switzerland) over the past century

Guillaume Jiranek [1], Montserrat Filella [1], Jean-Luc Loizeau [1], Antonio Cobelo-García [2]

[1] Department F.-A. Forel, University of Geneva, Boulevard Carl-Vogt 66, CH-1205 Geneva, Switzerland, (Guillaume.Jiranek@etu.unige.ch)
[2] IIM-CSIC. Eduardo Cabello 6, E-36208 Vigo, Spain

Research on environmental concentrations and processes of technology-critical elements (TCE) is gaining relevance in the recent years due to their increasing use in a variety of emerging technological applications (e.g. Cobelo-García et al. 2015). However, knowledge on their temporal evolution in anthropogenically impacted areas during the past century has not been well documented. To this aim, TCE (e.g. Ta, Te, Nb, Ga, Ge, In, Tl, Rare Earth Elements, platinum group elements) have been analyzed in a dated sediment core collected from a contaminated bay of Lake Geneva, Switzerland in which a high degree of enrichment for 'common' (e.g. Pb, Cu, Hg, Ni) metals has already been reported (Gascón Díez et al. 2017). We observed a significant degree of contamination for several TCE (e.g. In, Te; Figure 1) following a trend similar to other common metals, and linked to the implementation of the Lausanne city wastewater treatment plant discharging its treated and untreated effluent in the bay. For other TCE like Tl or Ge, low or null contamination was found.
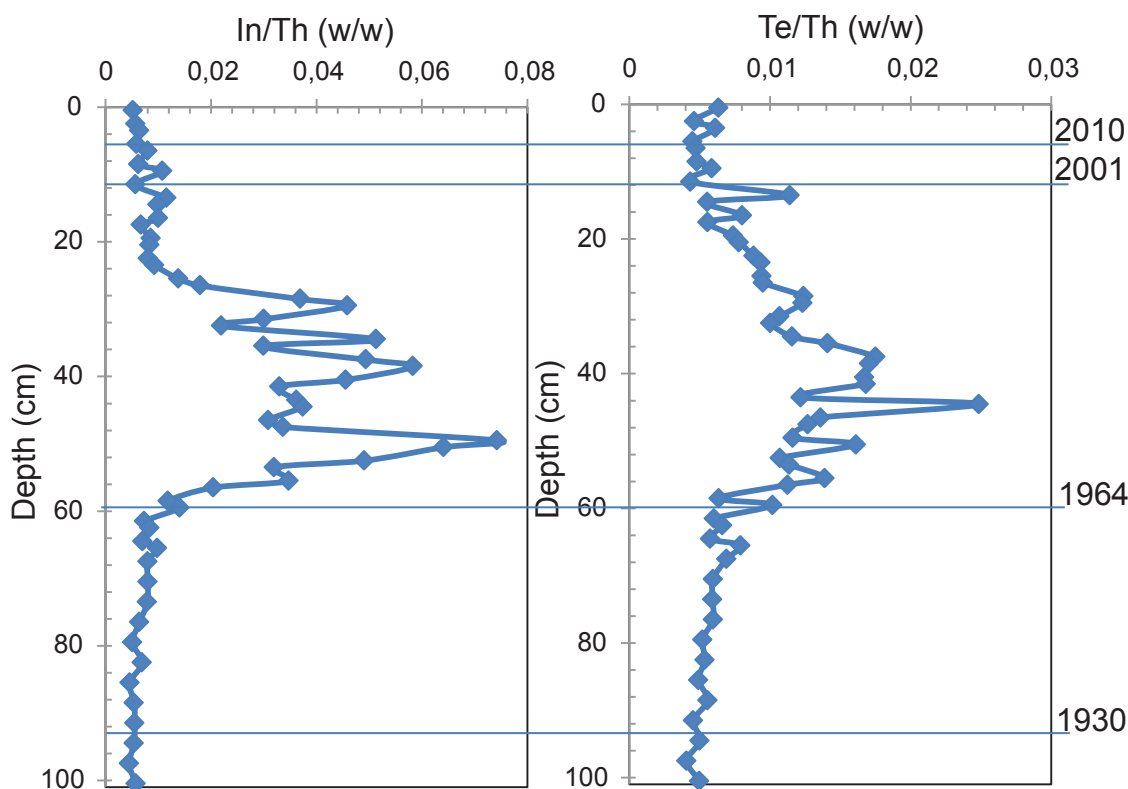

Figure 1. Temporal trend of Th-normalized concentrations of In (left) and Te (right) in a sediment core collected in the Vidy Bay (Lake Geneva, Switzerland).

REFERENCES

Cobelo-García, A., Filella, M,. Croot, P., Frazzoli, C., Du Laing, G., Ospina-Álvarez, N., Rauch, S., Salaun, P., Schäfer, J., & Zimermann, S., 2015: COST Action TD1407 network of technology critical elements – from environmental processes to human health threats, Environmental Science and Pollution Research, 22, 15188-15194.

Gascón Díez, E., Corella, J.P., Adatte, Th., Thevenon, F., & Loizeau, J.-L., 2017: High-resolution reconstruction of the 20th century history of trace metals, major elements, and organic matter in sediments in a contaminated area of Lake Geneva, Switzerland, Applied Geochemistry, 78, 1-11.

P 19.5
Arsenic removal from lake water, river water and groundwater using an electrocoagulation system

Nathalie Manetti [1], Charlotte Catrouillet [1] & Jasquelin Peña [1]

[1] *University of Lausanne IDYST, Geopolis, CH-1015 Lausanne*

Arsenic (As) is a toxic element that occurs naturally in the environment. The contamination of groundwater by arsenic is a worldwide concern, affecting the health of thousands of people, especially in South-East of Asia (West Bengal, Bangladesh, etc.). The consumption of drinking water represents a major source of human exposure to arsenic, which can lead to the development of different types of cancer, skin lesions, cardiovascular diseases, etc.

A number of studies have investigated the potential to use iron electrocoagulation (EC) as a method to remove arsenic from water. This system is a low-cost water treatment method with low energy requirements, both of which are important requirements for water treatment in decentralized communities. In this system, a current is passed through an Fe(0) electrode which is oxidized and dissolved to Fe(II). Successive reactions including Fe(II) oxidation to Fe(III) generate oxidants (Fenton reactions) able to oxidize either Fe(II) and As(III) to As(V), the less dangerous form of As. Furthermore, Fe(III) forms nanoscale Fe precipitates that efficiently sorb (according to the pH) As(III) and As(V). Subsequently, As-rich iron precipitates can be removed from water by filtration and/or settling (Ratna Kumar, Chaudhari, Khilar, & Mahajan, 2004).

Ions and substances present in the raw groundwater can compete with As for sorption sites of Fe oxides (e.g., phosphates, transition metals, organic matter) and/or oxidation (redox sensitive elements such as Mn) (van Genuchten & Peña, 2017). To test the performance of the system for different water chemistries, lake water, river water and groundwater were sampled from the University of Lausanne campus and spiked with As(III) or As(V).

The different waters were first filtered using a 0.2 µm filter and spiked with 10 µM As(III) or As(V). The experiments were conducted in the presence of natural O_2 (from air) and with the addition of 250 µM of H_2O_2, an oxidant naturally produced in the system. As(III), As(V) and Fe aqueous concentrations (after filtration at 0.2 µM) and Fe and As concentrations in the total phase were measured over time (0, 6, 13, 23 and 32 minutes). Total organic carbon and the major cations and anions were also determined at the beginning and at the end of the experiment to determine which elements are in competition with As.

River water and groundwater generally contained higher concentrations of ions such as Ca, Mg, K and Na compared to lake water. However, the As removal was faster for the lake water than for the other waters. The total organic carbon (TOC) concentrations were similar for the three waters (less than 5 mg L^{-1}). These results provide insight into the control of co-occuring elements on the reactions and the As removal efficiency in EC systems.

REFERENCES

Kumar, P. R., Chaudhari, S., Khilar, K. C., & Mahajan, S. P. 2004: Removal of arsenic from water by electrocoagulation. Chemosphere, 55, 1245-1252.

van Genuchten, C. M. & Peña, J. 2017: Mn(II) Oxidation in Fenton and Fenton Type Systems: Identification of Reaction Efficiency and Reaction Products. Environmental Science & Technology, 51, 2982-2991.

P 19.6
Reactions between hypobromous acid, organic sulfur species and dissolved organic matter in marine waters

Emanuel Müller [1], Sylvain Bouchet [2], Urs von Gunten [1,2,3], Lenny H.E. Winkel [1,2]

[1] Eawag, Swiss Federal Institute of Aquatic Science and Technology, Department of Water Resources and Drinking Water (W+T), Überlandstrasse 133, CH-8600 Dübendorf
[2] ETH Zurich, Swiss Federal Institute of Technology, Institute of Biogeochemistry and Pollutant Dynamics (IBP), Department of Environment Systems (D-USYS), Universitätstrasse 16, 8092 Zürich
[3] EPFL, École polytechnique fédérale de Lausanne, Route Cantonale, 1015 Lausanne

Volatile organic bromine (e.g. bromoform, $CHBr_3$) and sulfur (dimethylsulfide, DMS) compounds produced in marine waters are important constituents in atmospheric chemistry and climatic processes.[1,2] In the atmosphere, volatile organic bromine species photolyze to Br atoms which are known for their ozone destruction potential.[3] Dimethylsulfide triggers the formation of aerosols and clouds via its oxidation to sulfuric acid.[2] A key compound in the production of volatile bromine species in marine waters is enzymatically produced hypobromous acid ($HOBr/OBr^-$) which reacts with dissolved organic matter (DOM).[1,4] However, apart from its reaction with DOM, we hypothesize that HOBr might also react with marine organic sulfur compounds (i.e. dimethylsulfide, DMS; dimethylsulfoxide, DMSO and dimethylsulfoniopropionate, DMSP), potentially implying a competition between reactions of DOM and organic sulfur species with HOBr. Therefore, reactions between HOBr and marine organic sulfur compounds may affect the production of volatile organic Br species and also represent an additional sink for marine S compounds. We studied the reactivity between HOBr and marine organic S species and determined the second order rate constants of these reactions. The reaction between HOBr and DMS was found to have a very high second order rate constant ($k=2\cdot10^9$ M^{-1} s^{-1}), which is around 10 orders of magnitude higher than for the corresponding HOBr reactions with DMSO (0.4 M^{-1} s^{-1}) and DMSP (< 0.1 M^{-1} s^{-1}). To identify and quantify the S products of these reactions we developed a HPLC-ICP-MS/MS method, with which we could show that DMS and DMSO oxidation by HOBr results in DMSO and $DMSO_2$ formation, respectively. In combination with estimated marine HOBr concentrations via reported HOBr production and sink fluxes, our results indicate that the reaction between DMS and HOBr respresents an additional, so far ignored, major sink for marine DMS.

However, as DOM is a well-known sink of HOBr in marine waters (leading to production of bromoform among other products), the reactions between HOBr and DMS will compete with the reaction between HOBr and DOM. Therefore, we further studied the reactivity of HOBr and DMS in the presence of representative DOM. In these experiments we found that increasing DMS concentrations lowered the production of brominated volatile organic compounds (i.e., $CHBr_3$ and $CHBr_2Cl$) indicating that DMS can indeed play a role in diminishing the production of volatile organic Br species. Furthermore, we could show that for DMS and DOM concentrations reflecting marine concentration ratios, a major fraction of DMS was consumed by HOBr and that the reacted DMS was found as DMSO (100% yield). These results confirm the high reactivity between DMS and HOBr for relevant ratios of DMS, HOBr and DOM and the corresponding reactions thus need to be considered in marine-atmosphere systems.

References

[1] Wever, R., & van der Horst M.A. 2013: The role of vanadium haloperoxidases in the formation of volatile brominated compounds and their impact on the environment. Dalton Transactions 42, 11778-11786.
[2] Stefels et al. 2007: Environmental constraints on the production and removal of the climatically active gas dimethylsulphide (DMS) and implications for ecosystem modelling. Biogeochemistry 83, 245-275.
[3] Salawitch, R. 2006: Atmospheric chemistry: Biogenic bromine. Nature 439, 275-277.
[4] Rehder D. 2014: Vanadate-Dependent Peroxidases in Macroalgae: Function, Applications, and Environmental Impact. Oceanography 2, 121.

P 19.7
Paleo-ecotoxicology: Shining a light on the true impacts of pollution

Remo L. Roethlin [1,2], Nathalie Dubois [1,2]

[1] Eawag, Department of Surface Waters Research + Management, Überlandstrasse 133, CH-8600 Dübendorf
  (remo.roethlin@eawag.ch)
[2] ETH Zürich, Department of Earth Sciences, Soneggstrasse 5, CH-8092 Zürich

Traditional ecotoxicology is focused on short-term toxicological effects of pollution on biota. Paleo-ecotoxicology is an emerging discipline using sediment archives to extend the scope of ecotoxicology by looking at changes of biological proxies over long timespans (Korosi, Thienpont, Smol, & Blais, 2017). It allows assessing the long-term dynamics of aquatic ecosystems exposed to pollutants.

Here we present the outline of a new project, where we will retrieve data on past changes in aquatic ecosystems induced by the introduction of anthropogenic pollutants through a multi-proxy analysis of lacustrine sediment cores. We warmly welcome suggestions and discussions that could provide useful inputs for the project's progress.

We will especially focus on the connection of bioassays and other means commonly used in ecotoxicology with sediment records to overcome limitations of short-term effect models. We then will use the remains of indicator organisms found in sediment archives, such as Diatoms, Chironomids, Cladocera and others to assess the impact of pollutants on the bioindicators.

This approach will be validated using different target organisms and different lakes with varying pollutants. Finally, we will extend this paleo-ecotoxicological approach to include meta-genomic surveys of aquatic ecosystems in sediment records. By extracting ancient DNA from sediment samples (sedDNA), it will be possible to assess the long-term impact of pollution on an ecosystem without the bias of morphological identification and including those species that leave no identifiable subfossil remains in sediment cores.

REFERENCES
Korosi, J. B., Thienpont, J. R., Smol, J. P., & Blais, J. M. (2017). Paleo-ecotoxicology: What Can Lake Sediments Tell Us about Ecosystem Responses to Environmental Pollutants? *Environmental Science & Technology*, *51*, 9446–9457. https://doi.org/10.1021/acs.est.7b02375

P 19.8

Investigating the potential of intracellular mineral inclusions in microalgae as a novel bioremediation method for radioactive ^{90}Sr water pollution

Inés Segovia Campos [1], Agathe Martignier [1], Jean-Michel Jaquet [1], François Barja [2], Montserrat Filella [3] & Daniel Ariztegui [1]

[1] Département des Sciences de la Terre, Université de Genève, Rue de Maraîchers 13, CH-1205 Genève, Suisse
  (ines.segoviacampos@unige.ch)
[2] Unité de Microbiologie, Université de Genève, Quai Ernest-Ansermet 30, CH-1205 Genève, Suisse
[3] Département F.-A. Forel, Université de Genève, Boulevard Carl-Vogt 66, CH-1205 Genève, Suisse

It has been recently discovered that numerous microalgae species of the genus *Tetraselmis* (Chlorophyta) form intracellular carbonates called *micropearls*. These mineral inclusions are composed of hydrated amorphous calcium carbonate (ACC) in which other elements such as strontium can also accumulate. Under both laboratory and natural conditions, the Sr/Ca ratio of the micropearls can be more than 200 times higher than in the growing medium, indicating that these *Tetraselmis* species have a strong capacity to concentrate strontium (Martignier et al., 2018). Ongoing experiments with cultures of *Tetraselmis* under controlled laboratory conditions will provide missing information about the uptake mechanism of this element. Because these algae are widely spread in the aquatic environment (brackish water, seawater and freshwater), they may have a larger impact on the geochemical cycle of this alkaline-earth metal than previously thought. Hence, they should be considered as potential candidates for new bioremediation solutions regarding radioactive ^{90}Sr water pollution.

REFERENCES
Martignier, A., Filella, M., Pollok, K., Melkonian, M., Bensimon, M., Barja, F., Langenhorst, F., Jaquet, J.M. & Ariztegui, D. 2018: Marine and freshwater micropearls: Biomineralization producing strontium-rich amorphous calcium carbonate inclusions is widespread in the genus Tetraselmis (Chlorophyta). Biogeosciences Discuss. 2018, 1-22.

P 19.9
Transformation of Cu (nanoparticles) during sewage sludge incineration studied by bulk- and micro-XAS

Jonas Wielinski [1,2], Alexander Gogos [1], Francesco Marafatto [1,3], Andreas Voegelin [1], Eberhard Morgenroth [1,2] & Ralf Kaegi [1]

[1] *Eawag, Swiss Federal Institute of Aquatic Science and Technology, Überlandstrasse 133, CH-8600 Dübendorf*
[2] *Institute of Environmental Engineering, ETH Zürich, Stefano-Franscini-Platz 5, CH-8093 Zürich*
[3] *MicroXAS-X05LA beamline, Swiss Light Source, Paul Scherrer Institute, Forschungsstrasse 111, CH-5235 Villigen*
    Contact: jonas.wielinski@eawag.ch

Engineered nanoparticles (NP) are well retained during wastewater treatment (WWT) and accumulate in the sewage sludge. In Switzerland sewage sludge is mostly digested and incinerated preferably in mono-combustion facilities for volume reduction and energy recovery. The resulting ash is landfilled for potential phosphate recovery in the future. Previous studies suggested that CuO-NP transform into Cu-sulfides during the WWT and in environments with comparable redox conditions (Donner et al., 2011; Gogos et al., 2017; Ma et al., 2014) but did not address further Cu transformation during sludge incineration.

We spiked CuO-NP or dissolved Cu to digested sewage sludge and reacted the sludge under mesophilic, anaerobic conditions for 24 h. Sludge aliquots were collected and freeze dried for solid-phase analysis. The remaining sludge was dried at 105 °C overnight and incinerated in a pilot- bubbling bed type fluidized bed incinerator. To determine the speciation of Cu in the spiked sludges and ashes, the homogenized sludge and ash samples were prepared as 7-mm diameter pellets for bulk EXAFS analysis at the SuperXAS beamline at the Swiss Light Source (SLS, Paul Scherrer Institute, Villigen). To assess the distribution and speciation of Cu at the micrometer-scale, the undisturbed samples were embedded in resin and cut into thin sections (30 µm) on Si-wafers. These sections were investigated at the microXAS beamline at the SLS. One 500×500 µm^2 area was mapped by X-ray fluorescence (XRF) with a 3×3 µm^2 spatial resolution at an incident photon energy of 18 keV to assess the spatial distribution of Cu and other elements (Fe, Ce, etc.). On the same area, 7 XRF maps were recorded at incident photon energies around the Cu K-edge to obtain spatially-resolved information on Cu speciation.

Linear combination fit (LCF) analysis of the bulk-EXAFS spectra indicated complete sulfidation of Cu spiked in dissolved form to digested sludge after 24 h reaction time, whereas a minor fraction (8%) of the spiked CuO-NP were still present in the digested CuO-NP-spiked sludge (Fig. 1). LCF analysis of the ash samples indicated that incineration lead to a significant change in Cu speciation which was independent of the initially spiked form of Cu. The respective EXAFS spectra were described as a combination of about 33% amorphous CuS, 33% tenorite (CuO), 17% copper sulphate (CuSO$_4$) and 17% cupro spinel (CuFe$_2$O$_4$) (Fig. 1). A preliminary analysis of the spatially-resolved measurements revealed an uneven distribution of individual Cu species in the sludge and ash samples. Whether CuO-NP spiked to digested sludge and the corresponding ashes resulted in distinct distribution patterns in terms of Cu concentration or bonding environment is currently under investigation.

REFERENCES

Donner, E., Howard, D. L., Jonge, M. D. d., Paterson, D., Cheah, M. H., Naidu, R., & Lombi, E. (2011). X-ray Absorption and Micro X-ray Fluorescence Spectroscopy Investigation of Copper and Zinc Speciation in Biosolids. *Environmental Science & Technology, 45*(17), 7249-7257. doi:10.1021/es201710z

Gogos, A., Thalmann, B., Voegelin, A., & Kaegi, R. (2017). Sulfidation kinetics of copper oxide nanoparticles. *Environmental Science: Nano, 4*(8), 1733-1741. doi:10.1039/C7EN00309A

Ma, R., Stegemeier, J., Levard, C., Dale, J. G., Noack, C. W., Yang, T., Lowry, G. V. (2014). Sulfidation of copper oxide nanoparticles and properties of resulting copper sulfide. *Environmental Science: Nano, 1*(4), 347-357. doi:10.1039/C4EN00018H
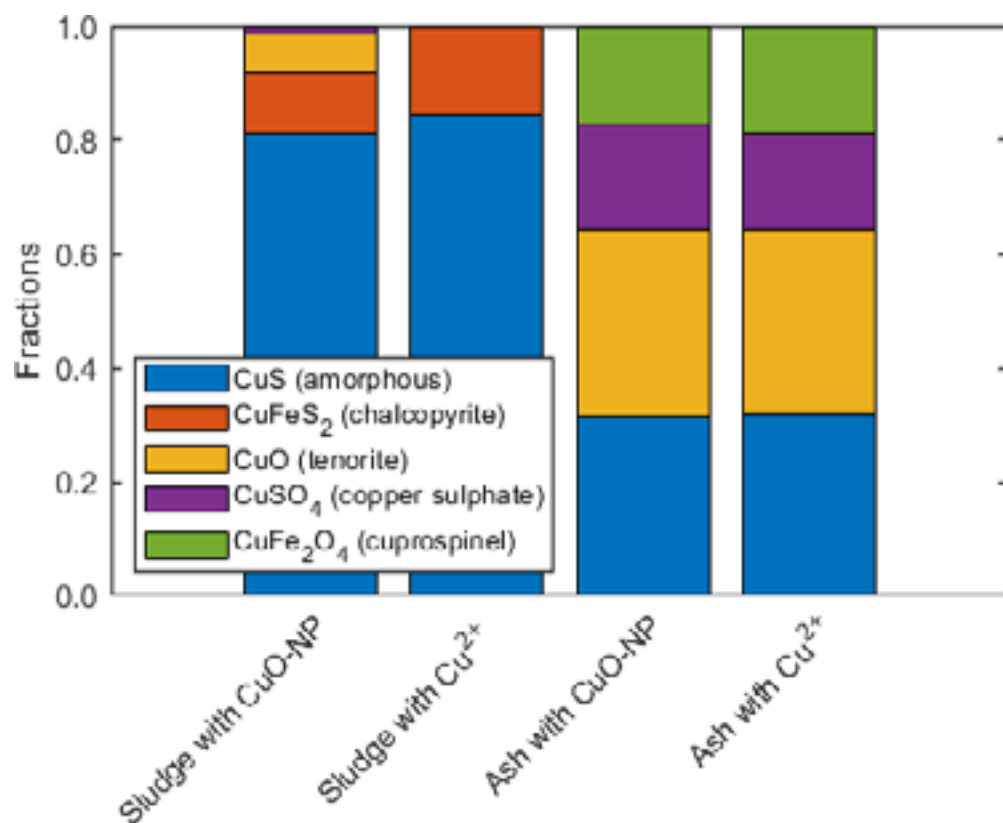
Figure 1. Results of LCF to sludge and ash samples. Digested sludge was spiked with either CuO-NP or dissolved Cu, reacted for 24 h and incinerated in a pilot reactor.

20. Remote Sensing of the Spheres

Stefan Wunderle, Mathias Kneubühler, Dominik Brunner, Alain Geiger

Swiss Commission for Remote Sensing,
Swiss Geodetic Commission

TALKS:

20.1 Baffelli S., Frey O., Hajnsek I.: Polarimetric Analysis of Natural Terrain Observed With A Ku-Band Terrestrial Radar

20.2 Giuliani G., Chatenoux B., Poussin C., Richard J.-P., Dao H., Allenbach K., Rodila D., De Bono A., Peduzzi P., Schaepman M.E., Small D., Steinmeier C.: Swiss Data Cube: Big Earth Observation Data for Sustainable Development

20.3 Manconi A., Casu F., Zinno I., De Luca C., Manunta M., Manzo M., Bonano M., Lanari R.: Monitoring Surface Deformation with Radar Interferometry at the Country-scale in Alpine Regions? First Results obtained With Sentinel-1 over Switzerland

20.4 Rietze N., Dizerens C.: Snow Classification of Webcam Images in Switzerland

20.5 Rodriguez A.C., Wegner J.D.: Counting the Uncountable: Deep Semantic Density Estimation from Space

20.6 Röösli C., de Jong R., Schaepman M.E.: From Space to Earth: Observing Land Surface Phenology Processes using Dense Time-Series of Landsat 8, Sentinel-2 and Phenocams

20.7 Rothenbühler E., Wunderle S., Dizerens C.: Comparison of Cloud Base Retrieval from Satellites with Ceilometer and Observer Data

20.8 Wilgan K., Siddique M.A., Strozzi T., Geiger A., Frey O.: Tropospheric Path Delays derived from Global Navigation Satellite Systems Data and Spaceborne SAR Interferometry: A Case Study in Swiss Alps

20.9 Zweifel L., Meusburger K., Alewell C.: Spatio-Temporal Pattern of Soil Degradation in Swiss Alpine Grasslands Revealed by Object-Based Image Analysis

POSTERS:

P 20.1 Lainer M., Hocke K., Kämpfer N.   Long-term measurements of middle atmospheric water vapor at the Zimmerwald observatory

P 20.2 Leuenberger M. Quality check of water isotope distribution from space to ground by vertical profiling and altitude dependent in-situ records

P 20.3 Leuenberger M. Glider-AirCore analyses linking ground-based and column integrated trace gas measurements with satellite retrievals

P 20.4 Leuenberger M. Horizontal open-path FTS measurements for bridging the gap between high accurate point measurements and spatially averaging atmospheric models using vertical greenhouse gas retrievals from satellite (H-OP-FTS)

P 20.5 Rossi C., Risch A.C., Kneubühler M., Schütz M., Haller R.M., Schaepman M.E. Assessing plant traits and diversity from local to regional scales in differently managed alpine grasslands

P 20.6 Schranz F., Tschanz B., Rüfenacht R., Kämpfer N.   Middle-atmospheric H_2O and O_3 measurements by ground-based microwave radiometry in the Arctic.

20.1
Polarimetric Analysis of Natural Terrain Observed With A Ku-Band Terrestrial Radar

Simone Baffelli [1], Othmar Frey [1,2] & Irena Hajnsek [1,3]

[1] Institut f. Umweltingenieurwiss, ETH Zurich, Stefano-Franscini-Platz 3 , CH-8093 Zürich (baffelli@ifu.baug.ethz.ch)
[2] Gamma Remote Sensing AG, Worbstrasse 225, CH-3073 Gümligen (frey@ifu.baug.ethz.ch)
[3] Microwaves and Radar Institute, German Aerospace Centre, DE-82234 Oberpfaffenhofen-Wessling

Terrestrial radar interferometers (TRI) are used to monitor changes in the natural and built environment. The sensitivity of the phase of electromagnetic waves to the location of the scatterers they interact with permits to estimate displacements using the technique of differential interferometry. The signal diversity given by polarimetric measurements permits to discriminate different scattering types within a resolution cell and enables the estimation of several environmental parameters thanks to the sensitivity of polarized microwaves to the dielectric and geometrical properties of the objects they are scattered from.

The polarimetric scattering behaviour of natural surfaces in the wavelength range between 1 m and 3 cm -especially at L and X band at 30 and 3 cm- is well characterized thanks to the availability of space- and airborne polarimetric SAR sensors. However, the polarimetric response of natural target at the shorter wavelengths -especially Ku-Band- that are often employed by terrestrial radar systems is less studied because polarimetric devices operating in this band are still relatively rare.

In this work, a polarimetric analysis of two datasets acquired using a quad-polarimetric Ku-Band (wavelength 1.7 cm) terrestrial radar is presented, aiming to characterize the polarimetric signature of natural surfaces at these frequencies. The data was acquired using KAPRI[2], a modified, polarimetric Ku-Band terrestrial radar based on the GPRI[3]. Two scenes, acquired in the Bisgletscher region, Mattertal and in the vicinity of Bern are used.

Several standard polarimetric parameters are computed, among them the Cloude-Pottier scattering entropy H[1] that serves as indicator of the scattering randomness within resolution cells.

An high entropy is observed for most terrain types, accompanied by predominantly crosspolarized backscatter. Low values of H – indicating deterministic scatterers – are only seen in correspondence of individual buildings or objects with a large radar scattering coefficient dominating in their resolution cell.

These observations suggest the presence of depolarizing scattering mechanisms, typical of natural targets, that are normally modelled as random volumes of "elementary" point-like or spheroidal scatterers with stochastic distributions of particle ellipticity and orientations[4].

The hypothesis of depolarizing scattering is compatible with the land cover types prevalent in both scenes, mostly comprising of short vegetation, forests, rough soils and ice.

Another factor contributing to the high entropy is the ratio of the resolution cell size to the wavelength: the main scattering contribution is expected to come from objects of sizes comparable to the wavelength such as grass tufts, gravel, ice crystals etc so that a large number of "elementary" scatterers per resolution cell is observed, increasing the scattering randomness and hence the entropy and the crosspolarized power.

REFERENCES
[1] S. R. Cloude and E. Pottier, "An entropy based classification scheme for land applications of polarimetric SAR," IEEE Transactions on Geoscience and Remote Sensing, vol. 35, no. 1, pp. 68–78, 1997.
[2] S. Baffelli, O. Frey, C. Werner, and I. Hajnsek, "Polarimetric Calibration of the Ku-Band Advanced Polarimetric Radar Interferometer," IEEE Transactions on Geoscience and Remote Sensing, vol. 56, no. 4, pp. 2295–2311, Apr. 2018.
[3] Charles L. Werner, Andreas Wiesmann, Tazio Strozzi, Andrew Kos, Rafael Caduff, and Urs Wegmuller. The GPRI multi-mode differential interferometric radar for ground-based observations. In Proc. EUSAR 2012 - 9th European Conference on Synthetic Aperture Radar, pages 304-307, April 2012
[4] S. Cloude, Polarisation: Applications in Remote Sensing. Oxford: Oxford University Press, 2009.
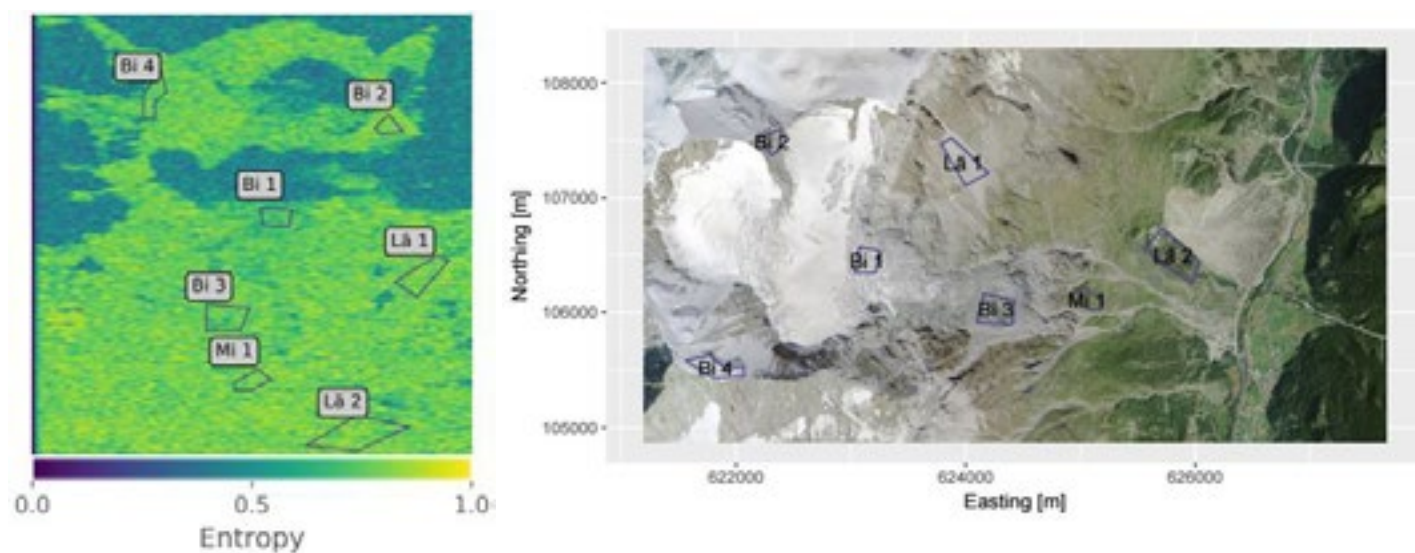
Figure 1: Example of Cloude-Pottier Entropy map in radar coordinates (x axis is azimuth angle, y axis is slant range distance) for the "Bisgletscher" dataset. To the right an orthophoto of the scene is shown, with the locations of the ROIs drawn in dark blue: they correspond to the polygons shown in the entropy map on the left. A high entropy indicates a larger scattering randomness.

20.2
Swiss Data Cube: Big Earth Observation Data for Sustainable Development

Gregory Giuliani [1,2], Bruno Chatenoux [1,2], Charlotte Poussin [1,2], Jean-Philippe Richard [1,2], Hy Dao [1,2], Karin Allenbach [1,2], Denisa Rodila [1,2], Andrea De Bono [1,2], Pascal Peduzzi [2], Michael E. Schaepman [3], David Small [3], Charlotte Steinmeier [4]

[1] Institute for Environmental Sciences, University of Geneva, Boulevard Carl-Vogt 66, CH-1205 Geneva
   (gregory.giuliani@unige.ch)
[2] UN Environment/GRID-Geneva, Chemin des Anémones 11, CH-1219 Châtelaine
[3] Remote Sensing Laboratories, Department of Geography, University of Zurich, Winterthurstrasse 190, CH-8057 Zürich
[4] Swiss Federal Institute for Forest, Snow and Landscape Research WSL, Zürcherstrasse 111, CH-8903 Birmensdorf

Pressures on natural resources are increasing and a number of challenges need to be overcome to meet the needs of a growing population in a period of environmental variability. The key to sustainable development is achieving a balance between the exploitation of natural resources for socioeconomic development, and maintaining ecosystem services that are critical to human's wellbeing and livelihoods. Some of these environmental issues can be monitored using remotely-sensed Earth Observations (EO) data that are increasingly available from freely and openly accessible repositories. However, the full information potential of EO data has not been yet realized. They remain still underutilized mainly because of their complexity, increasing volume, and the lack of efficient processing capabilities (Giuliani, Dao, et al. 2017)»container-title»:»Remote Sensing of Environment»,»source»:»ScienceDirect»,»abstract»:»Global environmental changes are mostly induced by human activities (e.g., food and energy production, urbanization, mining activities.

Following the work done by Geoscience Australia, the Swiss Data Cube (SDC) is a new paradigm revolutionizing the way users can interact with EO data. It lowers the barrier caused by Big Data challenges (e.g., Volume, Velocity, Variety) and provides access to large spatiotemporal data in an analysis ready format. It significantly reduces the time and scientific knowledge required to access and prepare EO data having consistent and spatially aligned calibrated surface reflectance observations (Giuliani, Chatenoux, et al. 2017).

Switzerland is the second country in the world to have a national-scale Data Cube. The SDC is supported by the Federal Office for the Environment and developed, implemented and operated by the UN Environment /GRID-Geneva in partnership with the University of Geneva, the University of Zurich and the Swiss Federal Institute for Forest, Snow and Landscape Research. Currently, the SDC holds 34 years of Landsat 5,7,8 (1984-2018) and 3 years of Sentinel-2 (2015-2018) Analysis Ready Data (ARD) over Switzerland.

The SDC is aiming at delivering a unique capability to track environmental changes in unprecedented detail using EO data, enabling more effective responses to problems of national significance. This near real-time information can be readily used as an evidence base for the design, implementation, and evaluation of policies, programs, and regulation, and for developing policy advices. Indeed, the Swiss government has national and international reporting commitments and obligations as well as national environmental programs. They all need information that is synoptic, consistent, spatially-explicit, sufficiently detailed to capture anthropogenic impacts, and national in scope. For example, 44 of the 169 Sustainable Development Goals (SDGs) targets defined by the United Nations focus directly on improving the environment and human well-being. The SDC can provide the long baseline required to determine trends, define present, and inform future. It will also enable scientific institutions to facilitate research and new insights on Switzerland's environment.

We will present various examples on how the SDC can help monitoring SDG related to water. Switzerland is acknowledged as the water reservoir of Europe. While its territory represents four thousandths of the continent's total area, 6% of Europe's freshwater reserves are stored in Switzerland. In particular, snow is one of the most relevant natural water resources present in nature. It stores water in winter and releases it in spring during the melting season. Monitoring snow cover and its variability is an indicator of climate change and identification of snowmelt processes is essential for effective water-resource management.

Recently, we have developed a new algorithm using the SDC to map snow cover extension (Frau et al. 2018)"container-title":"IGARSS 2018","publisher":"IEEE","publisher-place":"Valencia, Spain","event":"International Geoscience and Remote Sensing Symposium (IGARSS. Preliminary results have shown a clear decrease of snow cover extension over the Alps in the last 30 years (Figure 1). This can be complemented by Synthetic-Aperture Radar (SAR) images that are effective and robust measures to identify melting snow (Small 2011)"page":"3081-3093","volume":"49","issue":"8","source":"IEEE Xplore","abstract":"Enabling intercomparison of synthetic aperture radar (SAR.
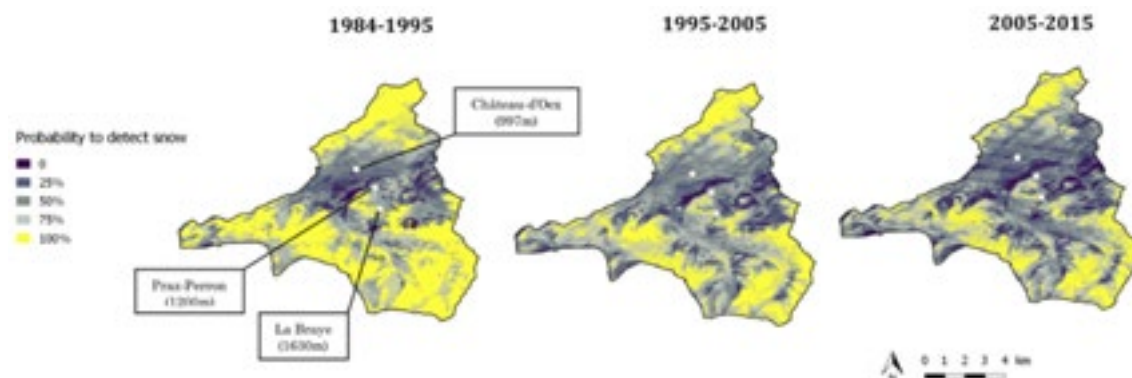
Figure 1. Snow cover evolution for the ski season (December-April) in Châteaux-d'Oex using the Snow Observations from Space (SOfS) algorithm.

REFERENCES

Frau, Lorenzo, Syed R. Rizvi, Chatenoux, Bruno, Charlotte Poussin, Jean-Philippe Richard, and Giuliani, Gregory. 2018. "Snow Observations from Space: An Approach to Map Snow Cover from Three Decades of Landat Imagery across Switzerland." In *IGARSS 2018*. Valencia, Spain: IEEE.

Giuliani, Gregory, Bruno Chatenoux, Andrea De Bono, Denisa Rodila, Jean-Philippe Richard, Karin Allenbach, Hy Dao, and Pascal Peduzzi. 2017. "Building an Earth Observations Data Cube: Lessons Learned from the Swiss Data Cube (SDC) on Generating Analysis Ready Data (ARD)." *Big Earth Data* 1 (1): 1–18. https://doi.org/10.1080/20964471.2017.1398903.

Giuliani, Gregory, Hy Dao, Andrea De Bono, Bruno Chatenoux, Karin Allenbach, Pierric De Laborie, Denisa Rodila, Nikos Alexandris, and Pascal Peduzzi. 2017. "Live Monitoring of Earth Surface (LiMES): A Framework for Monitoring Environmental Changes from Earth Observations." *Remote Sensing of Environment*. https://doi.org/10.1016/j.rse.2017.05.040.

Small, D. 2011. "Flattening Gamma: Radiometric Terrain Correction for SAR Imagery." *IEEE Transactions on Geoscience and Remote Sensing* 49 (8): 3081–93. https://doi.org/10.1109/TGRS.2011.2120616.

20.3
Monitoring Surface Deformation with Radar Interferometry at the Country-scale in Alpine Regions? First Results obtained With Sentinel-1 over Switzerland

Andrea Manconi [1], Francesco Casu [2], Ivana Zinno [2], Claudio De Luca [2], Michele Manunta [2], Mariarosaria Manzo [2], Manuela Bonano [3], Riccardo Lanari [2]

[1] Department of Earth Sciences, Engineering Geology, ETH Zurich, Zurich, Switzerland (andrea.manconi@erdw.ethz.ch)
[2] CNR IREA, Italy
[3] CNR IMAA, Italy

Studying surface deformation may help understanding processes, detecting indicators of potential failure events, and planning countermeasures. Among Earth Observation methods, spaceborne radar interferometry has demonstrated great advantages to perform these tasks. Moreover, the recent advent of the Copernicus Sentinel-1 (S1) constellation has increased our capability to observe surface deformation over wide regions with higher revisit times. Here we present the results obtained by processing images acquired from S1 constellation between October, 2015 and June, 2018. Differential interferograms were computed and combined taking advantage of the P-SBAS algorithm to obtain ground velocities and displacement time series at the country scale. We discuss the potential of such datasets in alpine countries such as Switzerland, as well the challenges for their thoughtful utilization.
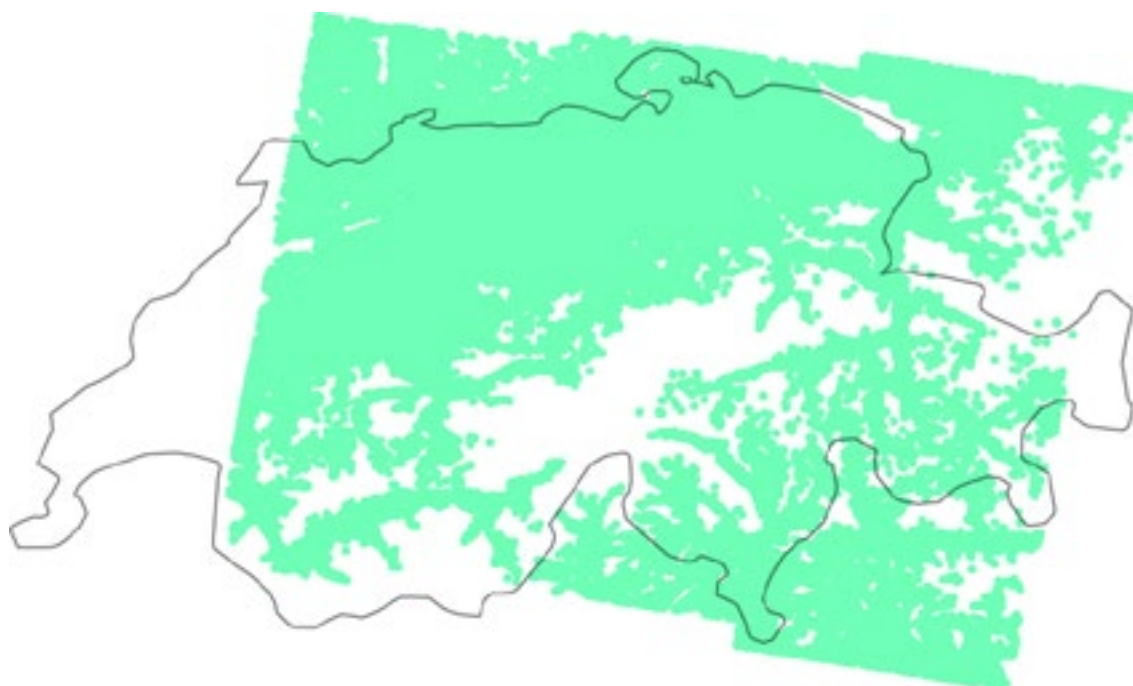
Figure 1. Coverage of surface deformation measurements obtained with the P-SBAS method applied to Sentinel-1 data, track 66, descending orbit.

20.4
Snow classification of webcam images in Switzerland

Nils Rietze [1], Céline Dizerens [1]

[1] Geographisches Institut, Remote Sensing Research Group, University of Bern, Hallerstrasse 12, CH-3000 Bern
 (nils.rietze@students.unibe.ch; celine.dizerens@giub.unibe.ch)

Snow cover is an important climate variable and can be regarded as a climate indicator. Monitoring and measuring local snow cover extent (SCE) has since been mostly achieved by observations at meteorological as point data. Accurate areal extents can be collected by using the vast public camera network, for this thesis understandably in Switzerland. Such data sets can provide a new source of small-scale areal snow cover data. Two existing and empirically tested snow classification algorithms have been applied to a sample of five Swiss webcams. The first method for classifying RGB images is based on blue band histogram analysis, while the second performs a principal component analysis (PCA) of the red and green component. Images in the morning, noon and evening are processed for further comparison of influence of shade and sunlight on the algorithms. Both algorithms performed during well-illuminated images with clear snow cover extent. The blue band classification shows significant misclassifications occurring in shaded areas and the skies. On the other hand, the PCA algorithm has fewer false classifications in the shade but shows false positives in the summer on pastures. Further comparison to a manually tagged snow cover data set, as a ground truth, shows these tendencies confirmed. Altogether, pixelwise classification of webcam images by the used algorithms is viable but needs fine-tuning in several areas. A combination of both however, would be an effective solution to start creating a large-scale SCE dataset.

REFERENCES

Härer, S., Bernhardt, M., & Schulz, K. (2016). PRACTISE - Photo Rectification and ClassificaTIon SoftwarE (V.2.1). *Geoscientific Model Development*, *9*(1), 307–321.

Salvatori, R., Plini, P., Giusto, M., Valt, M., Salzano, R., Montagnoli, M., . . . Sigismondi, D. (2011). Snow cover monitoring with images from digital camera systems. *Italian Journal of Remote Sensing*(March 2015), 137–145.

20.5
Counting the uncountable: deep semantic density estimation from Space

Andres C. Rodriguez [1] & Jan D. Wegner [1]

[1] *EcoVision Lab, Photogrammetry and Remote Sensing, ETH Zurich, Stefano-Franscini-Platz 5, CH-8093 Zurich*
(andres.rodriguez@geod.baug.ethz.ch)

We propose a new method to count objects of specific categories that are significantly smaller than the ground sampling distance of a satellite image. This task is hard due to the cluttered nature of scenes where different object categories occur. Target objects can be partially occluded, vary in appearance within the same class and look alike to different categories. Sentinel-2 satellite configuration provides since 2015 multi-spectral images of up to 10 meters ground sampling distance (GSD). For such dataset, traditional object detection with tools like Faster R-CNN (Ren et al., 2017) is infeasible due to the small size of objects with respect to the pixel size, we cast object counting as a density estimation problem.

To distinguish objects of different classes, our approach combines density estimation with semantic segmentation in an end-to-end learnable convolutional neural network (CNN) to count objects of 1/3 the size of the GSD. We compare our proposed architecture with state-of-the-art semantic segmentation methods for terrestrial images that use among other ideas atrous convolutions to prevent lowering the resolution of the learned features keeping a large receptive field (Chen et al. 2017).

Experiments on four different objects show that deep semantic density estimation can robustly count objects of various classes in cluttered scenes. For the semantic segmentation task of Olive Trees we obtained Intersection over Union of 0.86 and precision of 0.90 in our test set. See Figure 1 for a visualization. Experiments with our Tree objects (Olives, Coconuts and Palms) show the importance of infrared bands in the prediction. In contrast, Cars benefited mostly from the high spatial resolution of the RGB bands. Our Experiments also suggest that we need specific CNN architectures in remote sensing instead of blindly applying existing ones from computer vision.
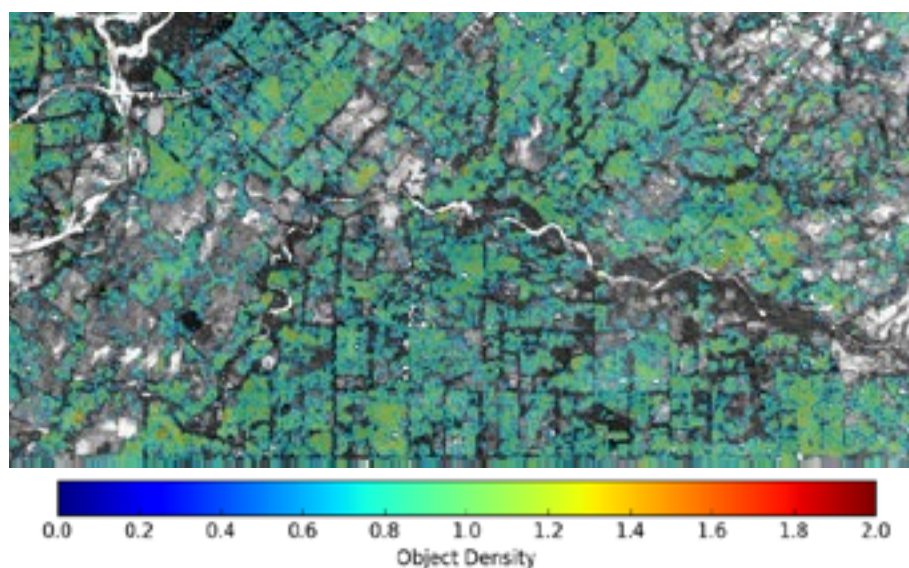

Figure 1. Predicted density estimation of coconuts overlaid to a greyscale version of the aerial image. Densities below 0.5 were trimmed for visualization.

REFERENCES

Chen, L., Papandreou, G., Kokkinos, I., Murphy, K., Yuille, A.L.: Deeplab: Semantic image segmentation with deep convolutional nets, atrous convolution, and fully connected crfs. IEEE Transactions on Pattern Analysis & Machine Intelligence 40(4), 834-848 (April 2018)

Ren, S., He, K., Girshick, R., Sun, J.: Faster r-cnn: Towards real-time object detection with region proposal networks. IEEE Transactions on Pattern Analysis and Machine Intelligence 39(6), 1137-1149 (June 2017)

20.6
From Space to Earth: observing land surface phenology processes using dense time-series of landsat 8, sentinel-2 and phenocams

Claudia Röösli [1], Rogier de Jong [1], Michael E. Schaepman [1]

[1] *Dept. of Geography, University of Zurich, Zurich, Switzerland*

Land surface phenology (LSP) characterises recurrent biological events in the annual profile of vegetated land surface at ecosystem scale as observed from remote sensing. LSP is a widely used indicator for terrestrial ecosystems' responses to changes of environmental conditions or for characterising species composition and biodiversity of an ecosystem.
We developed a new approach to observe LSP within the frame of a project of the European Space Agency ESA with the aim to contribute to the development of Essential Biodiversity Variables EBVs. Within the EBV-framework, biodiversity shall be observed and monitored in high-resolution and on a global scale, similar to the Essential Climate Variables ECVs. Monitoring LSP requires a dense time series of vegetation activity in the region of interest in order to study the yearly vegetation profile. This data is available from space and in high-resolution and sufficient dense time series since ESA's Sentinel-fleet has been launched. In our study we combine Landsat 8 and Sentinel-2 observations to extract LSP from the visual and near visual bands at three test sites located in temperate forest, arctic tundra and Mediterranean wetlands. We then compare the results to phenocams installed on ground to link the satellite observations to terrestrial observations. In the analysis, we focus on ecological processes and how these can be used for biodiversity assessment. This method is a crucial step for narrowing the scale gap between plant phenology and land-surface phenology and shows the potential for application at large – even global – spatial extent.
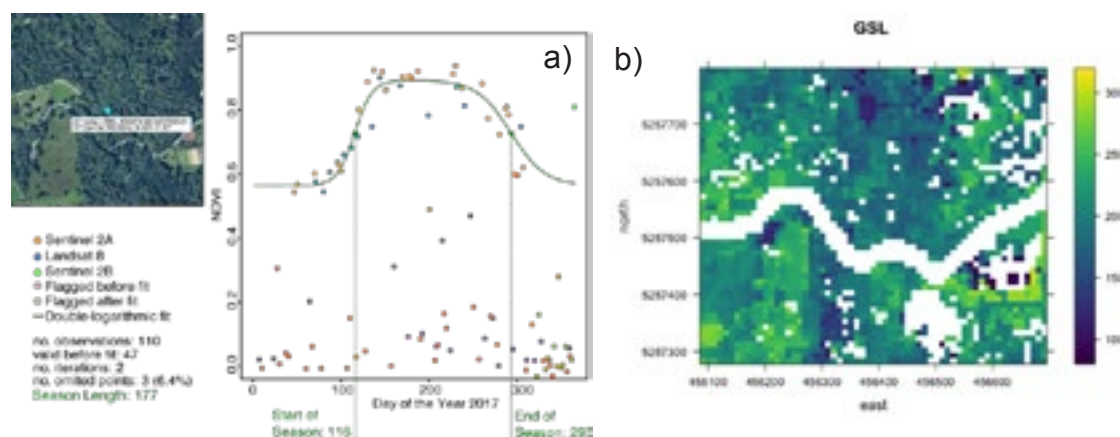
Figure 1. a) Yearly vegetation profile for one pixel extracted from Sentinel-2 and Landsat 8 images based on the Normalized Difference Vegetation Index (NDVI), fitted with a double logarithmic model. Outliers were flagged before (e.g. due to cloud cover) and after the fit (iterative fitting procedure). b) Growing Season Length (GSL=end - start of season) from the same area as shown in a). White pixels are invalid pixels due to for instance the road or a house.

20.7
Comparison of cloud base retrieval from satellites with ceilometer and observer data

Evi Rothenbühler [1], Stefan Wunderle [1,2] Céline Dizerens [1,2]

[1] Geographisches Institut, University of Bern, Hallerstrasse 12, CH-3012 Bern (evi.rothenbuehler@students.unibe.ch)
[2] Oeschger Center for Climate Change Research, University of Bern, Falkenplatz 16, CH-3012 Bern

Cloud and other weather related measurements have been done manually for many decades but their number decreases due to economic reasons. They are replaced by a network of measurement stations that collect point measurements at specific locations. For applications such as flight planning and weather forecast spatial information is needed. Satellite data provide information over large areas but in fact measure a different aspect of the atmosphere in question than the ground based instrument (e.g. observer or ceilometer). Therefore a comparison between satellite based and ground based measurements has been conducted. Data for one year at Payerne (CH) has been analysed using ceilometer and observer data (MeteoSchweiz) and Climate Satellite Application Facility (CSAF) satellite data (Deutscher Wetterdienst).

Results show that first, the two data sets measure different properties of the cloud layer. The ceilometer data gives the cloud base height (CBH) up to 7500m whereas the satellite data gives the cloud top height (CTH) (Figure 1). Second, comparing the two datasets with observer data shows restrictions related to spatial resolution (Figure 2), resulting from measuring conventions (observer), point measurements (ceilometer) and cloud detection algorithms (satellite). Third, in situations with multiple cloud layers the ceilometer measures low and middle clouds whereas the satellite data measures the topmost cloud layer. Fourth, no significant differences between day and night measurements has been found (Median height day: 2620.1m; median height night: 2363.3m). Fifth, the analysis shows that deriving information of CBH from satellite data is difficult as they measure CTH. Finding a relation to calculate CBH from CTH is difficult as many other factors of cloud properties such as cloud type, temperature profile and cloud water path play a significant role. Some of these findings will be presented and discussed during the talk.
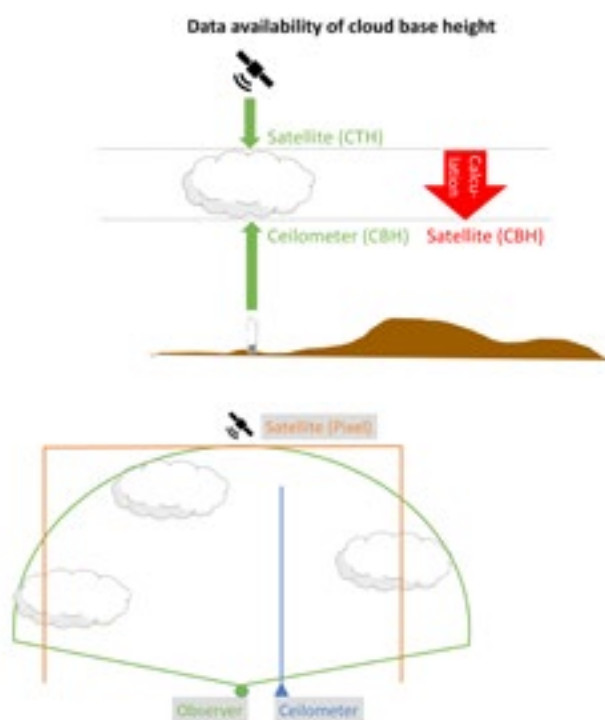
Figure 1. Different properties of the cloud layer measured by ground based and satellite based instruments. Satellites reliably measure the cloud top height, ceilometers in comparison offer detailed information about cloud base heights.

Figure 2. Different spatial resolution of the three analysed datasets. Ceilometer are very point specific measurements whereas satellite and observer are more spatial.

REFERENCES
Meerkötter R, & Bugliaro L. 2009: Diurnal evolution of cloud base heights in convective cloud fields from MSG/SEVIRI data, Atmos. Chem. Phys., 9, 1767-1778.

20.8

Tropospheric path delays derived from Global Navigation Satellite Systems data and spaceborne SAR interferometry: A case study in Swiss Alps

Karina Wilgan[1], Muhammad Adnan Siddique[2], Tazio Strozzi[1], Alain Geiger[1], Othmar Frey[2,3]

[1] *Chair of Mathematical and Physical Geodesy, Institute of Geodesy and Photogrammetry, ETH Zürich, Robert-Gnehm-Weg 15, CH-8093 Zürich (kwilgan@ethz.ch)*
[2] *Chair of Earth Observation and Remote Sensing, Institute of Environmental Engineering, ETH Zürich, Stefano-Franscini-Platz 3, CH-8093 Zürich*
[3] *Gamma Remote Sensing, Worbstrasse 225, CH-3073 Gümligen*

The Alps constitute about 60% of the Swiss total area. To assess the risk of geohazards in these areas, such as landslides and rockfall, it is important to regularly monitor land surface deformation. It has been demonstrated that both the spaceborne Synthetic Aperture Radar Interferometry (InSAR) and Global Navigation Satellite Systems (GNSS) are useful technologies for deformation monitoring. However, their use in this context requires that signal delays accumulated over the wave propagation path through the atmosphere are removed or mitigated. The troposphere is a non-dispersive medium at frequencies investigated in this study, thus, the delays estimated by one technique may be useful for mutual corrections.

For SAR images at high frequencies, such as X-band, the ionospheric effects can often be ignored, although the tropospheric delays remain relevant. The SAR interferometry is essentially exploiting the phase differences among two or more SAR images, and strives to estimate the deformation by extracting the deformation-related phases among other phase contributions (residual topography, atmosphere-induced phases). The phase information is meaningful only for those scatterers in the terrain that exhibit temporal phase coherence. These are the so-called "persistent" scatterers (PS).

However, the natural terrain in alpine regions generally limits PS behavior. It has been shown in earlier works that the atmospheric phases can be effectively isolated at PS locations [Strozzi et al. (2015), Siddique et al. (2018)]. Since interferometric phases are relative in nature, they can only be expressed as double-differenced tropospheric slant delays (dSTD), i.e. relative to the reference point as well as the reference (master) SAR acquisition. For GNSS, the tropospheric zenith delays are usually estimated along with the coordinates in the processing and can be converted into delays in slant range with an appropriate choice of the mapping function (based on the incidence angle for the SAR acquisitions).

In this study, we compare the dSTD retrieved from GNSS against the dSTD estimated with a PSI processing chain for alpine regions in Switzerland. The GNSS-based models are interpolated to PS locations using the in-house developed software package COMEDIE (Collocation of Meteorological Data for Interpretation and Estimation of Tropospheric Pathdelays). The models are calculated for 32 acquisitions of COSMO-SkyMed satellite in a period between 2008 and 2013. The acquisitions were taken from the snow-free period from June to October, always around similar time, some minutes before 6 pm. The chosen research area of around 20 km x 25 km is located in Zermatt and Matter Valley in the Swiss Alps. The GNSS-based models are calculated from 5 to 8 stations located within or close to the area of the study for the years 2008 – 2011 and from 11 stations for years 2012 – 2013.

The preliminary results show a good agreement between InSAR and GNSS estimates for some of the interferometric layers. The correlation coefficient averaged from all of the interferograms is equal to 0.64. The average bias of the residuals between InSAR and GNSS equals -6 mm with a standard deviation of 4 mm. For the period of only 2012 – 2013, with more GNSS data, the bias is reduced to -2 mm. Figure 1 shows the example of a comparison between InSAR and GNSS for one date with a good agreement between these two techniques. We are currently working on adding also the information from the low-cost L-1 only GPS stations located within the area of the study. In the next steps, the GNSS delays will be introduced as a priori models at the interferogram level and the reasons for the poor agreement between InSAR and GNSS estimates for some of the layers will be further investigated.
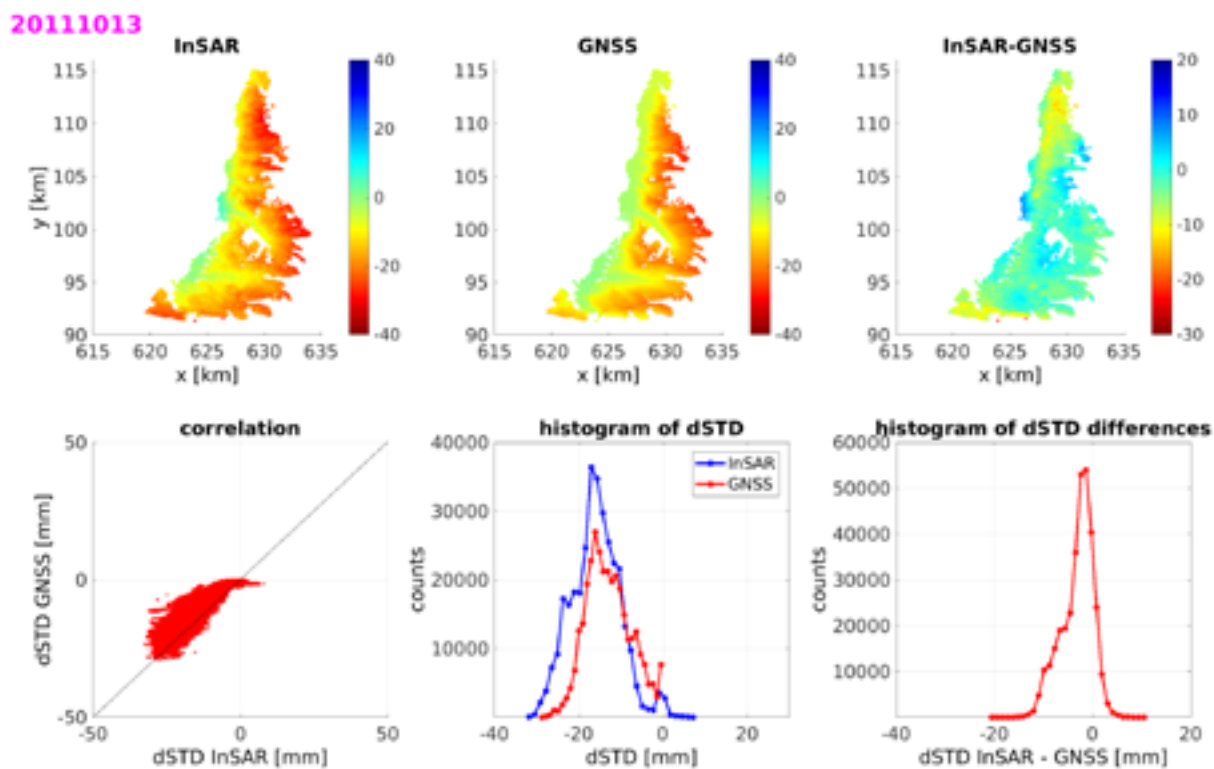
Figure 1. The comparison between dSTDs from InSAR and GNSS for one sample date (2011-10-13, 17:42:42) with a good agreement between the two techniques.

REFERENCES

Siddique, M. A., Strozzi, T., Hajnsek, I., & Frey O. 2018: A Case Study on the Correction of Atmospheric Phases for SAR Tomography in Mountainous Regions, IEEE Transactions on Geoscience and Remote Sensing, 99, 1-16

Strozzi, T., Raetzo, H., Wegmüller, U., Papke, J., Caduff, R., Werner, C., & Wiesmann, A. 2015: Satellite and terrestrial radar interferometry for the measurement of slope deformation, Engineering Geology for Society and Territory, 5, 161–165

20.9

Spatio-temporal pattern of soil degradation in Swiss alpine grasslands revealed by Object-Based Image Analysis

Lauren Zweifel [1], Katrin Meusburger [2] & Christine Alewell [1]

[1] Environmental Geosciences, Department of Environmental Sciences, University of Basel, Switzerland
  (lauren.zweifel@unibas.ch)
[2] Swiss Federal Research Institute WSL, Birmensdorf, Switzerland

Many grassland areas in the Swiss Alps are strongly affected by soil degradation due to various processes of soil erosion, intensified by the extreme prevailing topographic and climatic conditions. The changes in our climate are predicted to have a pronounced impact on the alpine regions causing not only higher temperatures but also a change in frequency and intensity of precipitation events as well as strongly altered snow dynamics (CH2011, 2011; Frei et al. 2018). In combination with changing land-use practices, an increase in soil degradation is expected (Meusburger & Alewell, 2014).

Past scientific studies mostly focus on one or two types of soil erosion processes (e.g. landslides, rill or sheet erosion). In this study we present a holistic approach to identify and map all erosion processes occurring in alpine grasslands over space and time on catchment scale (Urseren Valley, Canton of Uri). For the mapping of the degraded soil areas we apply object-based image analysis (OBIA) to orthophotos *SwissImage* taken between 2000 and 2016. The semi-automated workflow profits from the high spatial resolution of the orthophotos (0.5 - 0.25m) and takes into account spectral, spatial, contextual and textural image properties as well as accompanying information gained from digital elevation models. Additionally, the mapped areas are classified according to their predominating erosion process (landslides, sheet erosion, livestock-trails and management degradation).

The temporal analysis of the mapped sites shows an overall increase in degraded areas for all erosion types for the Urseren Valley. Since we analyse a time series consisting of several images, it becomes possible to distinguish between fast and gradually evolving processes. Spatial analysis reveals a high dynamic within the catchment, highlighting areas especially prone to newly emerging erosion, such as lower areas on south facing slopes intensely used for pasturing. An increasing amount of livestock trails can lead to larger areas affected by sheet erosion over time through trampling and grazing.
The dynamic aspect of single erosion features can be monitored and classified according to their temporal behaviour as increasing, decreasing, fluctuating and permanent degradation. The results provide an extensive understanding of the ongoing degradation processes over time as well as their spatial distribution and as such may improve our comprehension of the status and trends of alpine grassland soil degradation.

REFERENCES

CH2011, Swiss Climate Change Scenarios CH2011, published by C2SM, MeteoSwiss, ETH, NCCR Climate, and OcCC, Zurich, Switzerland, 88 (2011).

Frei, P., Kotlarski, S., Liniger, M. A. & Schär, C. Future snowfall in the Alps: Projections based on the EURO-CORDEX regional climate models. *Cryosphere* 12, 1–24 (2018).

Meusburger, K. & Alewell, C. Soil Erosion in the Alps. *Fed. Off. Environ. FOEN* 118 (2014).

P 20.1
Long-term measurements of middle atmospheric water vapor at the Zimmerwald observatory

Martin Lainer [1], Klemens Hocke [1], Niklaus Kämpfer [1]

[1] *Institut für Angewandte Physik und Oeschger-Zentrum für Klimaforschung, Universität Bern, Sidlerstr. 5, CH-3012 Bern (klemens.hocke@iap.unibe.ch)*

Atmospheric water vapor is a major field of research at the Institute of Applied Physics (IAP) at the University of Bern. Water vapor plays a key role in the earth's radiative budget and is the most important greenhouse gas in the atmosphere. In the middle atmosphere (30-80 km) water vapor is the major source of the OH (hydroxyl) radical which is involved in the destruction of the ozone layer. Mechanisms that control the long term variability of stratospheric and mesospheric water vapor are not well understood. Therefore, long-term high quality measurements of middle atmospheric water vapor are very important. With the MIAWARA radiometer more than a decade of continuous observations are achieved now.

Figure 1. The observatory for water vapor at Zimmerwald and the Middle Atmospheric Water Vapor Radiometer (MIAWARA).

P 20.2

Quality check of water isotope distribution from space to ground by vertical profiling and altitude dependent in-situ records

Markus Leuenberger [1]

[1] Climate and Environmental Physics Division, Physics Institute and Oeschger Centre for Climate Change Research, University of Bern, Bern, Switzerland (leuenberger@climate.unibe.ch)

There is only limited information available on water stable isotope ratios from satellites. Among which the shortwave infrared spectrometer SCIAMACHY onboard ENVISAT resulted in a total column measurement of HDO, the thermal infrared spectrometer on Aura, sensitive to mid-troposphere HDO as well as retrievals from high-resolution GOSAT shortwave infrared spectra are the most valuable ones. Yet, they experience substantial uncertainties as these techniques are relatively new and require proper comparisons. In this respect high resolution models combined with ground-based in-situ and column integrated measurements are inevitable. Until recently water vapor measurements even at the ground was rather challenging. Nowadays a couple of commercial instruments are available to perform high precision measurements. We will investigate variations of water isotopes along vertical profiles taken by the Glider-AirCore proposal. This will yield a direct comparison of the vertical distribution obtained by sophisticated models on the one hand and satellite products on the other hand. Water stable isotopes have a tremendous potential to tackle important questions of the Earth's water cycle, in this respect the new expected HDO data from the TROPOMI instrument onboard Sentinel-5 Precursor mission will be extremely interesting.

P 20.3

Glider-AirCore analyses linking ground-based and column integrated trace gas measurements with satellite retrievals

Markus Leuenberger [1] and Andreas Kräuchi [2]

[1] Climate and Environmental Physics Division, Physics Institute and Oeschger Centre for Climate Change Research, University of Bern, Bern, Switzerland (leuenberger@climate.unibe.ch)
[2] Meteolabor AG, Wetzikon, Switzerland

The ESA Sentinel satellite family missions are dedicated to the needs of the Copernicus programme. The proposed Glider-AirCore proposal results – once established – in high resolution vertical profiles of trace gases and auxiliary data and is therefore naturally linked to the ESA Sentinel 5P as well as the Sentinel 4 missions focusing on column integrated trace gas retrievals and weather observation data with high spatial resolution. The Glider-AirCore consists of a robust light-weighted glider carrying a long (> 100 meters) surface coated metal tube to sample air during autonomous descending in a spiral after its lift up to stratospheric heights by a balloon. Onboard instrumentations includes GPS tracker for navigation and wind retrievals, conventional humidity, temperature, pressure sensors, pyranometer (short-waves sun radiation) and pyrgeometer (long-wave thermal radiation) both up- and downward oriented. A CRDS spectrometer will be hooked up after landing of the Glider-AirCore to determine trace gas concentrations of CO_2, CO, CH_4 and H_2O with highest precision in the sub-ppm or sub-ppb range.

P 20.4

Horizontal open-path FTS measurements for bridging the gap between high accurate point measurements and spatially averaging atmospheric models using vertical greenhouse gas retrievals from satellite (H-OP-FTS)

Markus Leuenberger [1]

[1] Climate and Environmental Physics Division, Physics Institute and Oeschger Centre for Climate Change Research, University of Bern, Bern, Switzerland (leuenberger@climate.unibe.ch)

ESA Sentinel satellite family has already and will increasingly contribute to our understanding of the Earth's climate focusing on the major biogeochemical cycles by measurements of greenhouse gases. Thereby, a good spatial coverage of column integrated measures will be combined with spatially high resolution state-of-the-art atmospheric models – also often used as weather prediction models. H-OP-FTS proposes to add regional-scale horizontal column retrievals over kilometer-scale in order to fill the gap between high precision in-situ measurements and rapidly growing high resolution atmospheric modelling on kilometer scale. A suggested pilot study will focus on a high altitude site which comprises a complex topography – ideally suited for high resolution model studies – and highly variable dynamic situations combined with strongly variable distributions of greenhouse gas concentrations. We anticipate that H-OP-FTS naturally complement present applications of satellite data with ground-based measurements.

P 20.5
Assessing plant traits and diversity from local to regional scales in differently managed alpine grasslands

Christian Rossi [1,2,3°], Anita C. Risch [2], Mathias Kneubühler [1], Martin Schütz [2], Rudolf M. Haller [3] and Michael E. Schaepman [1]

° Correspondence: christian.rossi@nationalpark.ch
[1] Remote Sensing Laboratories, University of Zurich, Winterthurerstrasse 190, CH-8057 Zurich, Switzerland.
[2] Research Unit Community Ecology, Swiss Federal Institute for Forest, Snow and Landscape Research WSL,
 Zürcherstrasse 111, 8903 Birmensdorf, Switzerland.
[3] Department of Research and Geoinformation, Swiss National Park, Chastè Planta-Wildenberg, 7530 Zernez, Switzerland.

Ecosystem functions in grasslands are essential for the survival of plant and animal species and vital in sustaining human life. Such functions are locally strongly linked to different plant traits, like leaf dry matter content or specific leaf area (SLA), and to their diversity (Díaz et al. 2007). This relationship between trait diversity, called plant functional diversity, and ecosystem functions is likely to be scale dependent and functions operate across a range of scales (Thompson et al., 2018). Generally, to transfer relationships between plant functional diversity and ecosystem functions from local to regional scales it is necessary to know the rarely studied direct relation between regional and local plant functional diversity. However, capturing the trait variations at distinct spatial scales and in differently managed grassland remains challenging, mainly because only a limited number of trait measurements are available and field measurements of plant traits are time consuming.

Modern remote sensing systems bear the potential to close this gap (Homolová et al., 2013). Satellite images provide a complete landscape picture, benefiting from the unique light reflectance properties of plant traits. Based on reflected sunlight, we quantified plant traits in grasslands of the Swiss National Park and the agricultural landscape in its surroundings (Figure 1a). For trait quantification we took advantage of a physical model that describes reflectance of the aboveground portion of plant communities. Applied to our study area, it was possible to distinguish the impact of different fertilization and grazing intensities on plant traits and functional diversity on different spatial scales (Figure 1b,c). The plant trait assessment produces evidence for the evaluation of protective and agricultural measurements. Further, due to high temporal resolution of the Sentinel-2 satellite data acquisition scheme, the proposed method is suitable for incorporation into monitoring schemes.
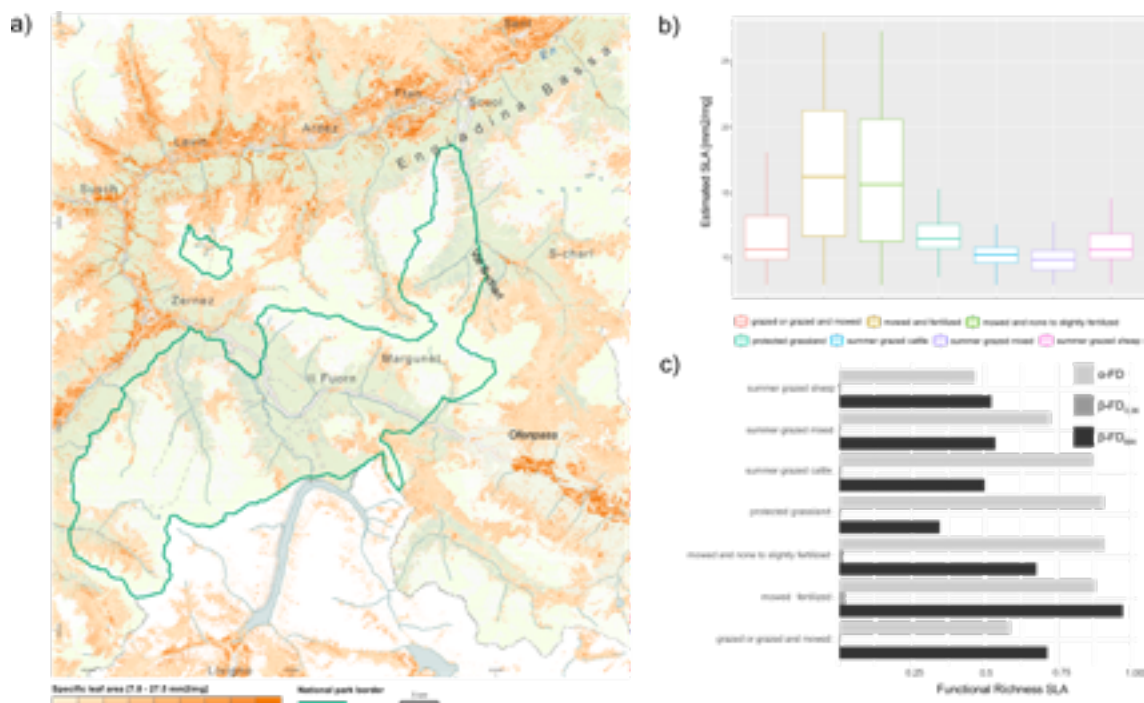

Figure 1. a) Specific leaf area (SLA) mapped for the study area through a physical model from a Sentinel-2 dataset of 06 June 2017. SLA ranges from 7.87 to 27.37 mm²/mg (12.24 ± 3.87 mm²/mg ; mean ± standard deviation);
b) Boxplots showing the differences in SLA estimated for the whole dataset among the different management practices (significant differences, Welch's ANOVA, $p < .05$); c) One aspect of SLA functional diversity (FD) in dependency of grassland management for three different spatial scales: α-FD calculated from trait measurements in reference plots (400 m²); β-FD derived from remotely sensed SLA calculated on two different scales, i.e., neighborhood (0.36 ha) β-FD$_{0.36}$ and landscape (600 ha) β-FD$_{600}$.

REFERENCES

Díaz, S., Lavorel, S., Stuart Chapin III, F., Tecco, PA., Gurvich, DE., Grigulis, K. 2007: Functional diversity—at the crossroads between ecosystem functioning and environmental filters. In Terrestrial ecosystems in a changing world, pages 81–91. Springer.

Homolová, L., Malenovský, Z., Clevers, JGPW., García-Santos, G., Schaepman, ME. 2013: Review of optical-based remote sensing for plant trait mapping. Ecological Complexity, 15:1–16.

Thompson, PL., Isbell, F., Loreau, M., O'Connor, MI., Gonzalez, A. 2018: The strength of the biodiversity–ecosystem function relationship depends on spatial scale. Proc. R. Soc. B 285: 20180038.

P 20.6

Middle-atmospheric H$_2$O and O$_3$ measurements by ground-based microwave radiometry in the Arctic

Franziska Schranz [1], Brigitte Tschanz [1], Rolf Rüfenacht [1] & Niklaus Kämpfer [1]

[1] Institute of Applied Physics, University of Bern, Sidlerstrasse 5, CH-3012 Bern (franziska.schranz@iap.unibe.ch)

Water vapour and ozone profiles in the Arctic middle atmosphere have been measured with the two ground-based microwave radiometers MIAWARA-C and GROMOS-C for 3 years. The instruments have been located at the AWIPEV research base at Ny-Ålesund, Svalbard (79° N, 12° E) since September 2015 and the measurements are ongoing. We present the 3-year long and almost continuous datasets of water vapour and ozone which are characterised by a high time resolution. A thorough intercomparison of these datasets with models and with satellite, ground-based and in-situ measurements was performed. During these first three years of the measurement campaign we observed dynamical events which are typical for the Arctic middle atmosphere. The descent rate of mesospheric water vapour inside the polar vortex in fall was found to be 435 m/day on average. In early 2017 distinct increases in mesospheric water vapour of about 2 ppm were observed when the polar vortex was displaced and midlatitude air was brought to Ny-Ålesund. Two major sudden stratospheric warmings took place in March 2016 and February 2018 where stratospheric ozone enhancements of up to 4 ppm were observed. The zonal wind reversals accompanying a major SSW were captured in the GROMOS-C wind profiles which are retrieved from the ozone spectra. After the SSW in 2018 the polar vortex reestablished and the water vapour descent rate in the mesosphere was 355 m/day.

21. Geoscience and Geoinformation – From data acquisition to modelling and visualisation

Nils Oesterling, Adrian Wiget, Massimiliano Cannata, Michael Sinreich

Georesources Switzerland Group,
Swiss Geodetic Commission,
Swiss Geophysical Commission,
Swiss Hydrogeological Society

TALKS:

21.1   Antonovic M., Brodhag S., Cannata M., Hoffmann M., Oesterling N.: Open source web-application for acquisition and exchange of borehole data

21.2   Brockmann E., Ineichen D., Lutz S., Schaer S.: Stability of the Swiss National Reference frame derived from GNSS analysis in Switzerland and Europe

21.3   Fulda D., Grünig A., Heuberger S.: The Resource Information System (RIS) – the digital memory of mineral resource occurrences in Switzerland

21.4   Garrard R., Landgraf A., Limpach F., Brockmann P., Spillmann T., Madritsch H., Schnellmann M., Müller R. M.: A permanent GNSS network for recording geodynamic movements in northern Switzerland

21.5   Gechter D., Allenbach R., Baumberger R.: Development of a Geophysics Management System: Aims and first results with 2D deep seismic reflection data

21.6   Grünig A., Fulda D.: Harmonizing and aggregating datasets of different periods of time – the process explained by means of Swiss quarries

21.7   Heuberger S.: 120 years of institutional research on Swiss georesources

21.8   Huber E., Ginsbourger D., Caers J., Huggenberger P.: A marked Strauss process model for uncertainty quantification in geophysical stereology

21.9   Makhloufi Y., Le Cotonnec A., Moscariello A., Samankassou E.: Constraining architecture and geometry of sedimentary bodies in a reef complex using high-resolution 3D digital outcrop model from UAV photogrammetry (Saint-Germain-de-Joux, Eastern France).

21.10   Perego R., Pera S., Galgaro A., Dalla Santa G., Cultrera M., De Carli M., Emmi G., Bertermann D., Müller J., Mendrinos D., Karytsas K., Vercruysse J, Pasquali R., O'Neill N., Bernardi A,: Mapping the techno-economic potential of closed-loop geothermal systems: a Europe-tested method

21.11   Röthlisberger V., Zischg A., Keiler M.: Data mining for (flood) exposure analyses

21.12   Vivero S., Lambiel C.: Monitoring the crisis of a rock glacier in the Western Swiss Alps with UAV surveys

POSTERS:

P 21.1   Alcanié M., Collignon M., Carrier A., Møyner O., Lupi M.: Numerical modeling of the Geneva Basin : Various scale geological model building for groundwater flow simulations

P 21.2   Cierpka A., Mettier R., Corbe S.: Simulating surface runoff in urban areas on a budget: How efficient is model refinement through terrain mapping with a consumer drone?

P 21.3   Fulda D., Grünig A.: The Resource Information System (RIS): A web application for mineral resource data of Switzerland

P 21.4   Guignard F., Lovallo M., Laib M., Golay J., Kanevski M., Helbig N., Telesca L.: Application of the Fisher-Shannon plane to high frequency wind speed in Switzerland

P 21.5   Hunziker J., Greenwood A., Minato S., Barbosa N., Caspari N., Holliger K.: Estimating fracture apertures and related parameters using tube-wave data

P 21.6   Laib M., Guignard F., Kanevski M., Telesca L.: Mutual information-based complex network for wind speed in Switzerland

P 21.7   Milani A. S., Pouladi G., Mohammadi Z.: Hazard and Risk Mapping During a Flood Event in Bangladesh

P 21.8   Tonini M., Cama M.E., Kanevski K.: Spatio-temporal kernel density analysis and 3D visualisation of landslides causing damage in Switzerland

21.1
Open source web-application for acquisition and exchange of borehole data

Milan Antonovic [1], Sabine Brodhag [2], Massimiliano Cannata [1], Marcus Hoffmann [1], Nils Oesterling [2]

[1] Institute of Earth Sciences, University of Applied Sciences and Arts of Southern Switzerland, Cannobio, Switzerland
[2] Swiss Geological Survey, Federal Office of Topography swisstopo, Bern, Switzerland

During the last years, the Swiss Geological Survey (SGS) developed a *Borehole Data Management System* (BDMS). One of its main purposes is the management of a large amount of borehole data stored in the IT infrastructure of the Confederation. Since the BDMS applies the SGS standards for describing borehole data it helps to harmonize and standardize the huge variation of available data from various public and private entities. Currently swisstopo is using a commercial desktop application, which is continuously being enhanced to meet the requirements of the SGS and its partners. The application is connected to a centralized database, different other internal databases and applications.

So far, data import into the database can be done via the application itself or – for external users - via a standalone light-version of the application. As a connection to the internet is not yet established, this project was initiated to fill this gap. The goal is to develop a dynamic *open source* web-based interface to facilitate data acquisition and exchange not only for external users and the SGS but also for external users and their own databases (e.g. cantonal databases). Furthermore, the web-interface allows harmonized data management using the SGS standards and an exchange and synchronisation between single database instances of different users and the central database.
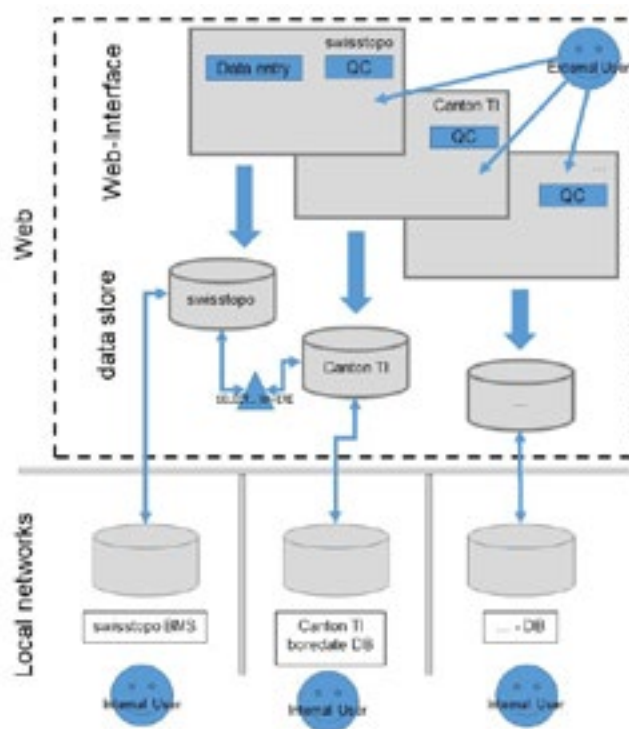

Figure 1. Model of the architecture for the *open source* web-based BDMS.

REFERENCES

Nils Oesterling, Sabine Brodhag : Datenmodell Bohrdaten – Module, Bundesamt für Landestopografie swisstopo, Bern, in preparation

Sabine Brodhag, Nils Oesterling 2014: Datenmodell Bohrdaten, Version 2.0. Bundesamt für Landestopografie swisstopo, Bern

Sabine Brodhag 2018: geologie-news N°2 – Neuer Standard für Bohrdaten. Bundesamt für Landestopografie swisstopo, Bern

21.2
Stability of the Swiss National Reference frame derived from GNSS analysis in Switzerland and Europe

E. Brockmann, D. Ineichen, S. Lutz, S. Schaer

Swiss Federal Office of Topography swisstopo

Between 1988 and 1995, the Federal Office of Topography swisstopo installed the Swiss Reference Network LV95 (Landesvermessung 95) as the national first order network. LV95 consists of about 200 reference stations and is based on the Global Positioning System GPS. Together with the 30 permanent GPS stations of the Automatic GNSS Network for Switzerland (AGNES), initiated in 1998, the LV95 stations represent the backbone of the geodetic reference frame and the national geodata infrastructure, the Swiss Terrestrial Reference Frame (CHTRF).

For validation purposes and for studying the stability of the reference frame, swisstopo re-observed the whole network four times: 1998, 2004, 2010 and 2016. The 2016 campaign measurement data of about 44 hours for each of the reference points, as well as the data of the further developed permanent network AGNES, include the four satellite systems GPS, GLONASS, Galileo and BeiDou. The paper emphasizes some challenges of the enhancement towards Multi-GNSS.

The permanent networks in Switzerland and Europe are analyzed on a daily processing scheme. Timeseries of up to 20 years are available today. Also densified networks in Switzerland, like the 11 station network NaGNet (owned by Nagra), are included. To ensure best possible consistency, data were re-processed using the most up-to date models.

A newly established project "EU Dense Velocities" under the umbrella auf EUREF (European Reference Frame in Europe) enables the generation of an European-wide determination of regional movements.

The detection of potential tectonic movements at a level of clearly below 1 mm/year is achievable with the existing data sets. The analysis of the horizontal and vertical velocities is a further step towards the determination of a kinematic model for the recent crustal deformations in Switzerland and a well-suited dataset to exchange knowledge with geologists, seismologist and geophysicist.

21.3

The Resource Information System (RIS) – the digital memory of mineral resource occurrences in Switzerland

Donat Fulda [1], Arsin Grünig [1], Stefan Heuberger [1]

[1] Georesources Switzerland Group, Department of Earth Sciences, ETH Zürich, Sonneggstrasse 5, 8092 Zürich
(donat.fulda@erdw.ethz.ch)

In the late 19th century, the importance of systematical investigations of distribution, occurrence and application of mineral resources in Switzerland was recognized. A huge amount of georesources data were collected by different organisations and compiled by the Swiss Geotechnical Commission (SGTK) during the last 120 years (Heuberger *this volume*). Today, the Georesources Switzerland Group maintains and extends this outstanding data archive.

Only parts of the data are digitized and available to the public at the moment. Furthermore, the datasets are heterogeneous in terms of structure, documentation, quality and data format. Therefore, assessing, analysing or evaluating the data is not straightforward. There is increasing need to 1) structure, harmonize and verify these data, 2) migrate them to a uniform, data model-based platform and 3) make them all available to the public.

These needs are addressed with the development of a comprehensive, web-based management system containing these mineral resource occurences, the so-called Resource Information System (RIS). It succeeds and builds on SGTK's innovative digital databases like the "Rohstoffinventar" (Vogler 1995) and the "Geotechnischer Umwelt-Atlas (GUA)" (Baumeler et al. 2005). But in contrast to these former inventories, the RIS is built upon data models, i.e. the Georesources Switzerland Group's raw materials data model as well as swisstopo's «Geology» data model (swisstopo 2017a). Using data models leads to higher data quality and reduces data errors. Furthermore, modelled data can be accessed, compared and analysed more easily. However, data models increase the complexity of a system. Therefore, migration and integration of data remains a time-consuming task. Although some data can be imported automatically, lots of datasets still need manual editing or research (Grünig & Fulda *this volume*).

Since the RIS data management platform was put into operation in 2015, nearly 2000 datasets on ores, energy resources and industrial minerals were harmonized and migrated from the "Rohstoffinventar" to the RIS. Today, datasets of most resource groups currently mined in Switzerland are processed and migrated into the system and updated on a yearly basis. However, the huge amount of already digitized data on historical mining sites and products (produced before 1980) containing more than 20'000 datasets, is still waiting to be harmonized and integrated into the platform. The RIS represents an important data basis for the future implementation of the measures defined in swisstopo's report on mineral resources in Switzerland (swisstopo 2017b). Mainly measure A1 "Acquisition and characterisation of geological raw material occurences" is heavily depending on such data.

REFERENCES

Baumeler, A., Kündig, R. & Rütti, R. 2005: «Geotechnischer Umwelt-Atlas» – Verwaltung und Visualisierung von Geodaten für geopolitische und -wirtschaftliche Fragen, Schweizerische Geotechnische Kommission SGTK. Abstract Swiss Geoscience Meeting, Zürich, 19. November 2005.

Grünig, A. & Fulda, D. *this volume*: Harmonizing and aggregating datasets of different periods of time – the process explained by means of Swiss quarries

Heuberger, S. *this volume*: 120 years of institutional research on Swiss georesources.

swisstopo 2017a: Datenmodell Geologie – Beschreibung im UML-Format und Objektkatalog, Version 3.0.

swisstopo 2017b: Bericht über die Versorgung der Schweiz mit nichtenergetischen mineralischen Rohstoffen (Bericht mineralische Rohstoffe). – Ber. Landesgeol. 11 DE (nur als pdf).

Vogler, R. 1995: Inventar und Karte der Vorkommen mineralischer Rohstoffe der Schweiz 1:200'000, Bulletin der Schweiz. Vereinigung von Petroleum-Geologen und Ingenieuren, 62/141, 37-42.
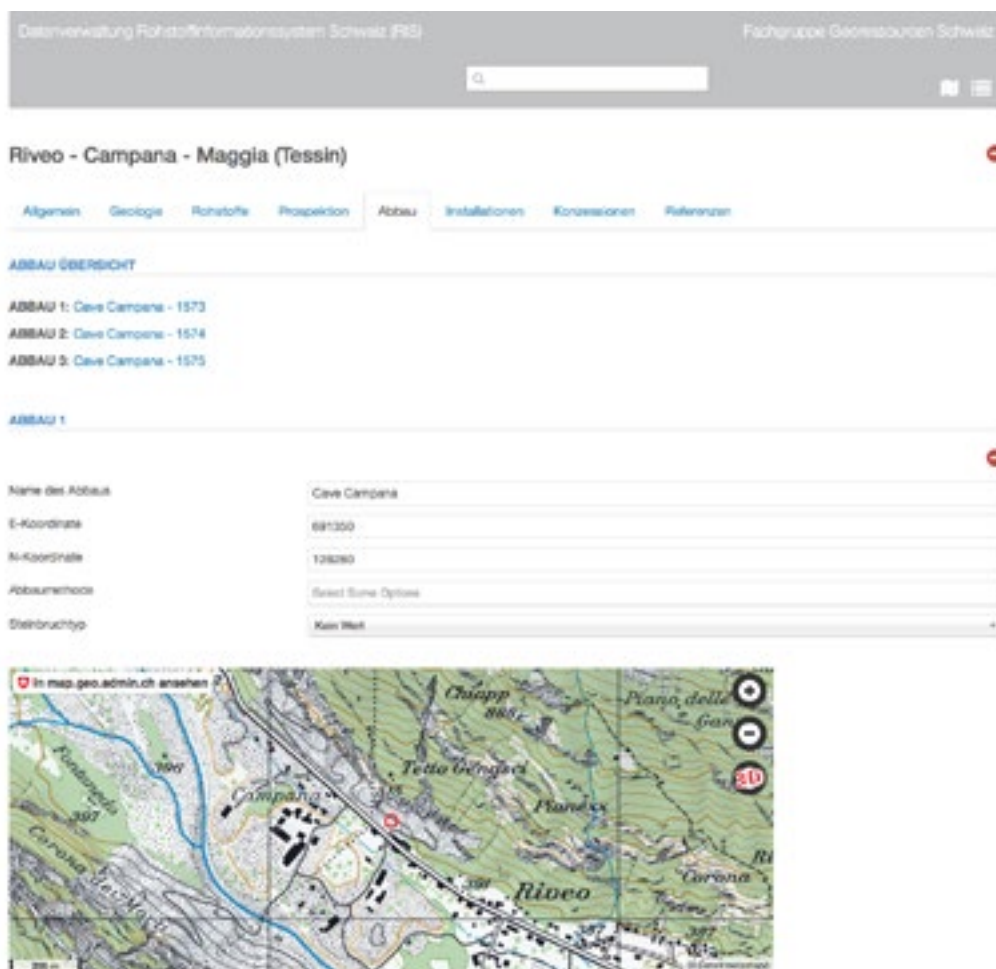
Figure 1: data management platform of the RIS showing exploitation data of a dimension stone quarry in the Canton of Ticino.

21.4
A permanent GNSS network for recording geodynamic movements in northern Switzerland

Rodney Garrard[1°], Angela Landgraf[1], Philippe Limpach[2], Elmar Brockmann[3], Thomas Spillmann[1], Herfried Madritsch[1], Michael Schnellmann[1], Herwig R. Müller[1]

[1] Nagra, Hardstrasse 73, CH-5430 Wettingen
[2] BSF Swissphoto AG, Dorfstrasse 53, 8105 Regensdorf-Watt
[3] Swisstopo; Seftigenstrasse 264, 3084 Wabern
[°] corresponding author (rodney.garrard@nagra.ch)

The pattern of large-scale neo-tectonic movements and shift rates in Switzerland is determined on precision levelling (Schlatter 2007), GNSS campaign measurements (Schlatter & Brockmann 2010) and long-term GNSS permanent network data (Brockmann et al., 2006). However, the low deformation rates present some technical challenges to these measurements. The National Cooperative for the Disposal of Radioactive Waste (NAGRA) therefore initiated NaGNet (Nagra's permanent GNSS network) to refine the existing GNSS permanent network, the automated GNSS Network for Switzerland (AGNES) by Swisstopo.

The designed measuring network has a station distance of approx. 12 - 32 km (Fig. 1), which seeks the most uniform mesh geometry possible. The stations cover an area of approximately 75 by 135 km in north-central Switzerland and were placed on the main tectonic blocks away from known regional fault zones. Important factors in the choice of measurement location were the quality of the locally receivable GNSS signals (e.g., signal-to-noise ratio, multipath) as well as the free horizon (maximisation of visible satellites). Importantly, the choice of measurement location was influenced by the best possible avoidance of near surface effects such as mass movements, ground water level fluctuations or subsidence by connecting the station foundation wherever possible to the bed rock. In addition, the suitability of potential sites for the reception of GNSS signals were pre-tested with a minimum measurement duration of at least 72 hours. After obtaining the required consent of the owners and the granting of permits from the competent authorities, 11 stations were installed between 2010 and 2012 by BSF Swissphoto AG, whom are responsible for the operation of the stations.

For an analysis of geodynamic interpretation, the quality of the foundation is of crucial importance. For example, some stations a direct foundation on bed rock was achieved. Where a direct foundation was not possible, the stations were anchored with three up to 15 m deep self-drilling cement injected rock bolts. In addition, to record any local movement, a surveying control of the position and height of the stations is carried out biannually. The data generation performance of each station is checked once a month to determine data completeness, delivery, cycle slips, signal-to-noise ratio, code multipath and coordinates repeatability. Considering the very low rates of surface deformation in northern Switzerland, the discrimination of potential station bias from the actual signal is crucial.

Now with eight years of continuous measurements, it is possible to derive reliable velocity parameters for the NaGNet-stations. As expected for northern Switzerland, the observed horizontal and vertical velocities are submillimetre and below the level of uncertainty. These rates are the lowest for Switzerland. To better integrate these results into a regional tectonic framework, we have thus recently started a collaboration with colleagues at Karlsruhe Institute of Technology (KIT), who combine precise levelling, GNSS, and InSAR to investigate the vertical deformation of the Upper Rhinegraben. The collaboration allows to extend the GNSS network data set across the bordering regions into southern Germany and will support observations by providing a tectonic reference frame.

REFERENCES

Brockmann, E., Grünig, S., Ineichen, D. & Schaer, S. (2006): Monitoring the Automated GPS Network of Switzerland AGNES. In: Torres, J.A. & Hornik, H. (Eds.): Rep. on the Symp. of the IAG Sub-commission for Europe (EUREF) in Riga, 14-17 Juni 2006, EUREF Publication No 16, pp. 176-83.

Schlatter, A. & Brockmann, E. (2010): Dritte Wiederholungsmessung im GNSS-Landesnetz LV95, Messkampagne und erste Resultate. Swisstopo Kolloquium 1. April 2011.

Schlatter, A. (2007): Neotektonische Untersuchungen in der Nordschweiz und Süddeutschland. Kinematische Ausgleichung der Landesnivellementlinien CH/D. Nagra Arb. Ber. NAB 07-13.

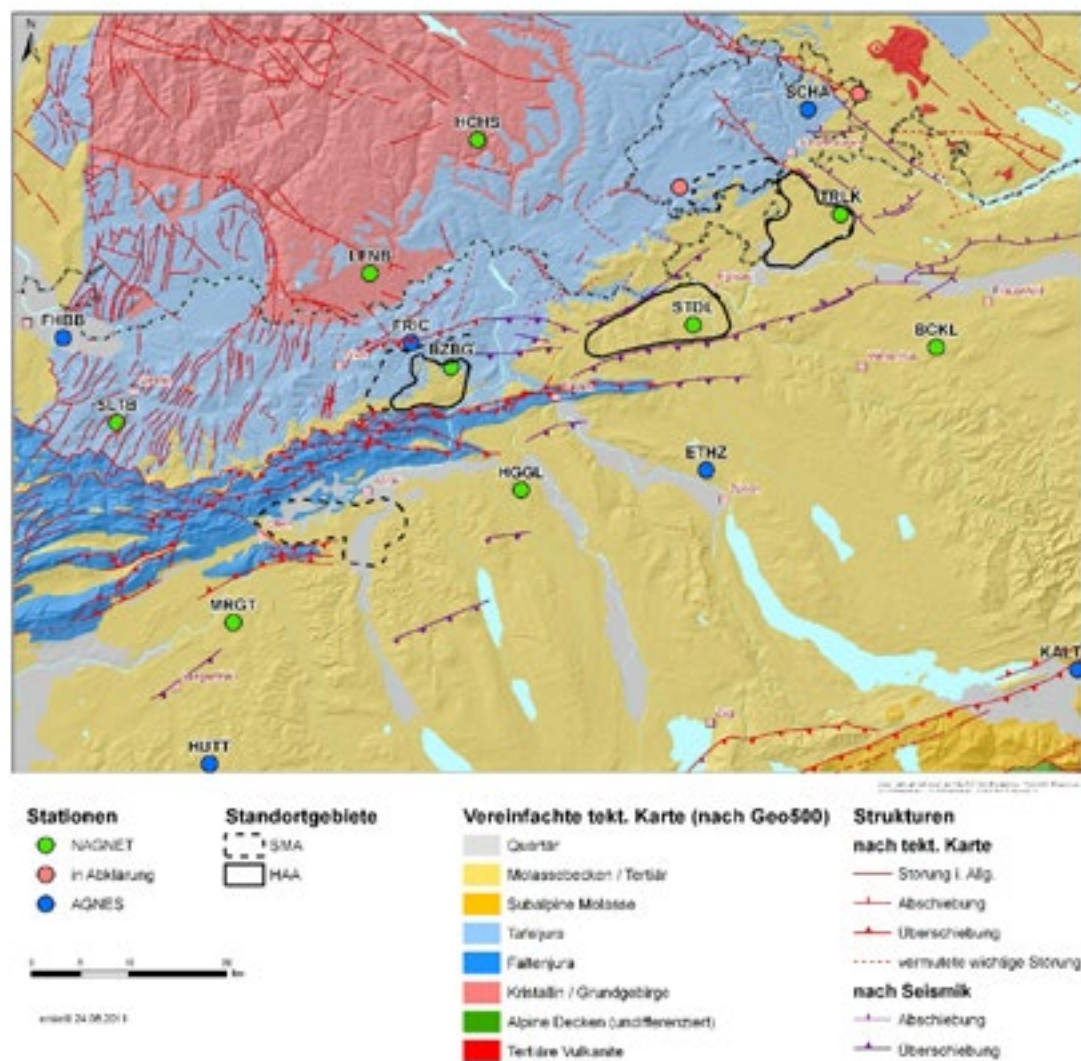Studer, M and Zanini, M. (2013): Aufbau und Betrieb eines eigenständigen CORS-GNSS Netzes. Nagra Arb. Ber. NAB 10-14.

Figure 1: Simplified tectonic map and distribution of NaGNet (green) and AGNES stations (blue). Red: NaGNet locations under investigation.

21.5

Development of a Geophysics Management System: Aims and first results with 2D deep seismic reflection data

Daniel Gechter [1], Robin Allenbach [1] & Roland Baumberger [1]

[1] Federal Office of Topography swisstopo, Swiss Geological Survey, Seftigenstrasse 264, CH-3084 Wabern
(daniel.gechter@swisstopo.ch)

The Swiss Geological Survey is developing a geophysical data management system (GDMS) based on ESRI's ArcGIS suite. The GDMS will contain geophysical measurements and evaluations primarily from Switzerland. Currently, the GDMS focuses on the management of 2D reflection seismic and gravimetric data. A modular expansion of the system is foreseen as additional geophysical data becomes available. It will also form the foundation for a centralised, digital access to the various geophysical data collections of swisstopo and third parties via the federal geoportal (https://map.geo.admin.ch) and via the 3D viewer of the Swiss Geological Survey (https://viewer.geomol.ch) in the future.

Deep 2D seismic reflection data are of national interest and are an important basis for existing and future projects in the deep subsurface (e.g., geothermal energy exploration, use of deep groundwater, use of deep geological repositories). In Switzerland, approx. 1'400 such 2D reflection seismic lines exist. Most of these data have their origin in the hydrocarbon exploration of the 1960s to 1990s. However, due to legal aspects, these data are currently not stored in a structured form in a geodatabase and are not readily available to third party users. In other words, there is no sustainable accessibility.

The prototype developed by swisstopo includes a tool, which automatically reads the header and trace information of the standard SEG-Y format (digital format of a seismic section) and imports the information directly into the GDMS. The procedure is also applicable to 3D SEG-Ys. Another toolbox directly links a seismic section with its corresponding line geometry in map view in ArcMap. This allows the user to identify a specific marked position simultaneously in map view and on the seismic section.

The GDMS of swisstopo will be open for use and further development by third parties. All legal rights and obligations remain with the data owner.

21.6
Harmonizing and aggregating datasets of different periods of time – the process explained by means of Swiss quarries

Arsin Grünig [1], Donat Fulda [1]

[1] Georesources Switzerland Group, Department of Earth Sciences, ETH Zürich, Sonneggstrasse 5, 8092 Zürich
 (arsin.gruenig@erdw.ethz.ch)

The Resource Information System (RIS) of the Georesources Switzerland Group (Heuberger *this volume*) contains operational and geological data of mineral resources in Switzerland (Fulda et al. *this volume*, Fulda & Grünig *this volume*). One major mineral resource group of the RIS covers quarries. The data has been collected over a long period of time and ranges from the Roman Empire to this day. Our dataset contains a separate geodatabase for each acquisition period (Roman Empire to 1910, 1915, 1935, 1965, 1980, 1995, and 2015). The type and amount of data in each geodatabase varies highly. For example, the 1915 dataset consists of many historical sites but only with sparse details for each entry (3564 data entries with 9 attributes). In contrast, the data entries for 2015 are more detailed but far less numerous because the dataset contains only the active sites and many quarries are not in operation anymore (141 data entries with 17 attributes).

One task of the Georesources Switzerland Group's RIS project was the harmonization and aggregation of the datasets for the years 1980, 1995, and 2015 into one single combined dataset. Due to economical restrictions, the datasets from 1965 and before were not included in the aggregation; if necessary, these datasets can be processed at a later date. The advantages of such an aggregation are 1) quarries can be viewed on a single layer instead of multiple layers (one for each period of time), 2) data is stored in a central database, 3) data can be managed continuously instead of periodically, and 4) geological terms such as lithology and stratigraphy are updated to today's terminology. The main challenges of the aggregation are that 1) some quarries can occur in one, two or all three periods of time, 2) a quarry can consist of one or multiple exploitation sites which all should be represented by a single object, and 3) some source data is inconsistent, which makes manual research inevitable and thus is time consuming.

Figure 1. Screenshot of FileMaker application for harmonizing and aggregating data. Aggregated data on the left, data of different points in time (1980, 1995, and 2015) on the right.

In order to support the harmonization and aggregation of the datasets, a utility FileMaker database solution has been developed. The solution allows to import the source data and establish relations for quarries and its exploitation sites between datasets. Subsequently, all the data for a single quarry is arranged on a single screen (cf. Figure 1). This kind of arrangement allows the editor to decide for each data attribute whether to transfer it from one of the datasets into the aggregated data record, or to enter it manually.

The aggregated data from the utility database was migrated into the relational data structure of the RIS by means of a technique called Selector Connector (Young 2015). This FileMaker technique allows to connect different data sources and transfer data easily between them. Source tables and destination tables are connected by a central transistor table which is then used for script-controlled copying of the field data, one by one. The data from the seven source tables of the utility database were successfully migrated and distributed into 15 PostgreSQL tables of the RIS, cf. Figure 2.

The migrated data has been published at map.georessourcen.ethz.ch and map.geo.admin.ch (layers «Natural stone: mining» and «Broken rock: mining»).
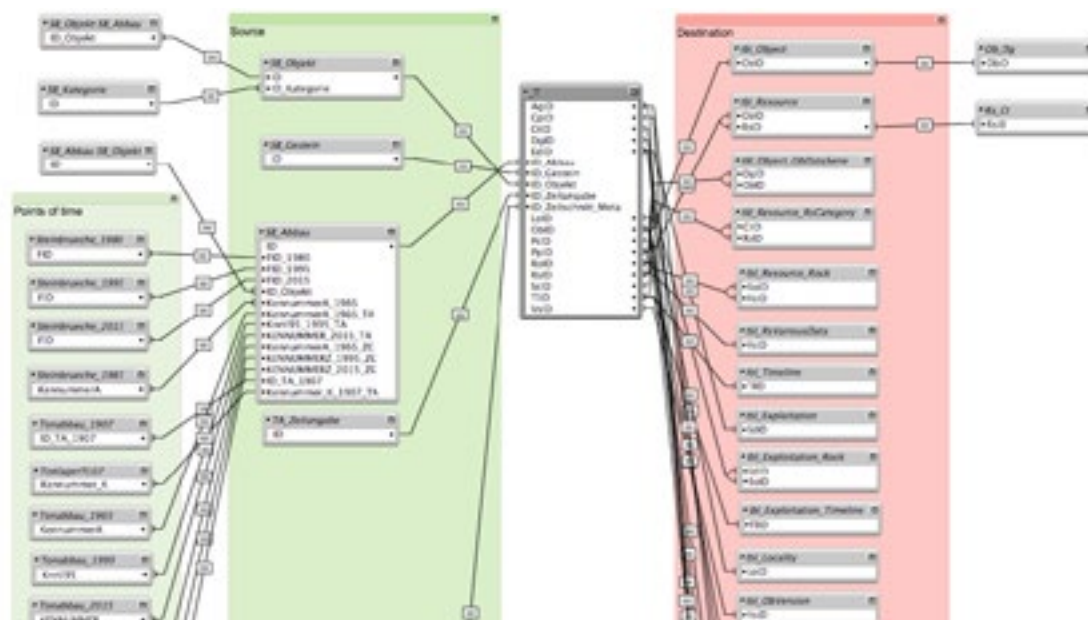
Figure 2. Data schema of the utility FileMaker database with the Selector Connector technique for transfering data. Harmonized and aggregated data of quarries in green on the left (source tables), PostgreSQL tables of RIS in red on the right (destination tables), connecting transistor table with ID fields in the centre.

REFERENCES

Fulda, D., Grünig, A. & Heuberger, S. *this volume*: The Resource Information System – the digital memory of mineral resource occurrences in Switzerland

Heuberger, S. *this volume*: 120 years of institutional research on Swiss Georesources.

Fulda, D. & Grünig, A. *this volume*: The Resource Information System (RIS): A web application for mineral resource data of Switzerland.

Heuberger, S. *this volume*: 120 years of institutional research on Swiss Georesources.

Young, J. 2015: FileMaker Data Modeling with Selector Connector, Seedcode, www.seedcode.com/filemaker-data-modeling-with-selector-connector.

21.7
120 years of institutional research on Swiss georesources

Stefan Heuberger [1]

[1] Georesources Switzerland Group, Department of Earth Sciences, ETH Zürich, Sonneggstrasse 5, 8092 Zürich
 (stefan.heuberger@erdw.ethz.ch)

The Georesources Switzerland Group (Fachgruppe Georessourcen Schweiz) was founded in July 2018 at ETH Zürich and succeeds the office of the Swiss Geotechnical Commission (SGTK). It forms an associated group in the Department of Earth Sciences. The staff and the premises are equivalent to ones of the former SGTK office which already was located at ETH Zürich. The group conducts applied research in close collaboration with the Swiss Geological Survey (Federal Office of Topography swisstopo) as well as with different partners from industry and administration. This includes collecting and compiling fundamental geological data and data related to the use of the geological resources of Switzerland. Focus areas are the mineral resources of Switzerland, energy resources from the deep underground (geothermal energy and hydrocarbons), secondary raw materials as well as geological questions related to the use of georesources and the underground in general.

This presentation will take you through the history of evaluation and documentation of Switzerland's geological resources from the late 19th century until today. Swiss georesources were firstly documented as becoming a major national issue during the national exhibitions (Landesausstellungen) 1883 in Zürich and 1896 in Geneva. In the mid 19th century, many European countries founded geological surveys in order to provide base data for the exploitation of geological resources. Research and data compilations were coordinated by the Swiss Geological Commission (SGC), founded in 1860 by the Schweizerische Naturforschende Gesellschaft (e.g. Nabholz & Spicher 1973), today the Swiss Academy of Sciences (SCNAT). In the framework of the exhibitions, a mineral resources map of Switzerland (Weber & Brosi 1883, Fig. 1), a comprehensive monograph on construction material (Meister et al. 1884) and several other fundamental datasets on Swiss geology and georesources were published. These activities, among others, led to the establishment of several organisations looking after georesources. Swiss industrialists founded the Swiss Coal Drilling Society in 1874. This private organisation was succeeded by the Swiss Coal Commission in 1892 as subcommission of the SGC. This subcommission was then replaced by the SGTK in 1899, which was turned into a self-contained commission in 1909 (e.g. Grubenmann 1915). Since then, the commission's president was always a professor of an earth science institute of ETH Zürich. SGTK's office was located first at EMPA Dübendorf until 1927 when it was moved to ETH Zürich.

From 1899 to 2012, SGTK published more than 100 technical reports of Swiss georesources in the series "Beiträge zur Geologie der Schweiz – Geotechnische Serie". Until 1925, main research focus was on hydrocarbons, 1925 it switched to mainly metallic raw materials with a short interlude of hydrocarbon studies during and after world war II. Around 1975, the study focus significantly diversified also including construction materials (aggregates, clay), unconsolidated rocks and Nagra's deep drilling program. Today, the Georesources Switzerland Group continues this institutional, applied research and maintains the different archives and online data portals (e.g. Fulda et al. *this volume*, Fig. 1, Grünig & Fulda *this volume*) in close collaboration with the Swiss Geological Survey.

This compilation of SGTK's history thus nicely illustrates how the demands for georesources in Switzerland have changed through time.

Figure 1. Left: exemplary extract of the georesources map by Weber & Brosi (1883). Right: Extract of today's online portal map. georessourcen.ethz.ch.

REFERENCES

Fulda, D., Grünig, A. & Heuberger, S. *this volume*: The Resource Information System (RIS) – the digital memory of mineral resource occurrences in Switzerland.

Grubenmann 1915: Die Schweizerische Geotechnische Kommission. Verhandlungen der Schweizerischen Naturforschenden Gesellschaft 97, 185-188.

Grünig, A. & Fulda, D. *this volume*: Harmonizing and aggregating datasets of different periods of time – the process explained by means of Swiss quarries.

Meister, U., Locher, F., Koch, A. & Tetmajer, L. 1884: Die Baumaterialien der Schweiz an der Landesausstellung 1883. Verlag von Cäsar Schmidt. 296 p.

Nabholz, W. & Spicher, A. 1973: Die Reorganisation der geologischen Landesuntersuchung in der Schweiz: Orientierung über den gegenwärtigen Stand. Eclogae Geologicae Helvetiae 66, 245-253.

Weber, J. & Brosi, A. 1883: Karte der Fundorte von Rohproducten in der Schweiz: Reproduction der von den Experten der Gruppe XVI für die schweizerische Landesausstellung 1883 hergestellten Originalkarte. J. Wurster & Cie.

21.8
A marked Strauss process model for uncertainty quantification in geophysical stereology

Emanuel Huber [1], David Ginsbourger [2,3], Jef Caers [4], Peter Huggenberger [1]

[1] *Applied and environmental Geology, University of Basel, Bernoullistrasse 32, CH-4056 Basel (emanuel.huber@unibas.ch)*
[2] *Idiap research institute, Martigny, Switzerland*
[3] *Department of Mathematics and Statistics, University of Bern, Switzerland*
[4] *Department of Geological Sciences, Stanford University, USA*

We present a new stochastic object-based model (OBM), relying on the formalism of marked point processes (MPP), that mimics the formation of the dominant structures of coarse, braided river deposits. This grid-free three-dimensional MPP is a compound marked Strauss process introduced in the challenging context of stereology in which the three-dimensional subsurface structure is inferred from two-dimensional data. Although it is straightforward to simulate unconditional realisations of the MPP, conditional simulation as well as parameter inference are hindered by the normalisation constant of the prior probability distribution that is analytically intractable and is a function of the model parameters.

We therefore propose an original Bayesian framework to solve the stereological problem. First, we quantify the maximum a posteriori estimate of the model parameters with Monte Carlo sampling followed by a local Bayesian regression between data statistics and parameters in the canonical correlation space. This method is compared to the Approximate Bayesian Computation (ABC) with post-sampling regression adjustment. Then, we detail how to condition correctly the MPP to interpreted GPR data with a Bayesian Monte Carlo Markov Chain (MCMC) approach based on the extended Metropolis update.

We test our framework with the new MPP by quantifying subsurface uncertainty given an interpreted two-dimensional ground-penetrating radar (GPR) profile. The local Bayesian regression in the canonical correlation space slightly outperforms ABC regression and is more robust.
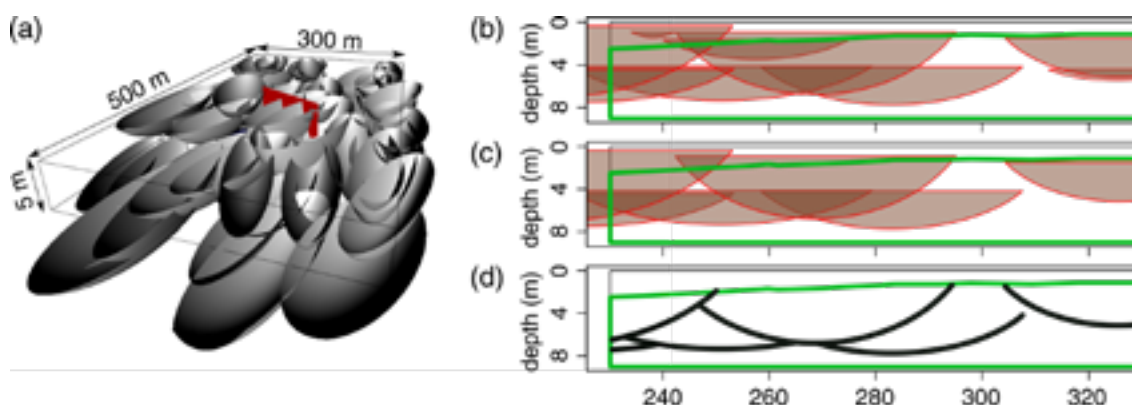
Figure 1. (a) Three-dimensional visualisation of an unconditional realisation.
The red plane corresponds to the section planes shown in (b)-(d). (b) Section of (a), the green boundary indicates the observation window.
(c) Section (b) after removal of the small remnants. (d) Ellipse arcs remaining after erosion process applied to (c).

20.9

Constraining architecture and geometry of sedimentary bodies in a reef complex using high-resolution 3D digital outcrop model from UAV photogrammetry (Saint-Germain-de-Joux, Eastern France).

Yasin Makhloufi [1], Aymeric Le Cotonnec [1], Andrea Moscariello [1] & Elias Samankassou [1]

[1] Department of Earth Sciences, University of Geneva, Rue des Maraîchers 13, CH-1205 Geneva
 (yasin.makhloufi@unige.ch)

The Canton of Geneva (Switzerland) is currently exploring the opportunities for geothermal energy exploitation in the Geneva Basin (GB) sub-surface.

To better characterize the geometry, architecture, distribution and lateral variations of the different sedimentary units present in the GB sub-surface, it is necessary to produce high-fidelity 3D depositional models. Photogrammetry using Unmanned Aerial Vehicles (UAV) has become an efficient, low-cost method capable of producing high-resolution, photo-realistic 3D models of rock outcrops. These models, once interpreted and imported into a 3D geologic modelling software (e.g. Petrel©), can help understanding spatial relationships between geological objects and identifying geological structures as well as sedimentary bodies (Blistan et al., 2016). The aim of this study is to produce a high-resolution 3D digital model of the Upper Jurassic Reef Complex cropping out in the Saint-Germain-de-Joux area, Eastern France. This outcrop has proven to be a good analog to the Upper Jurassic limestones present in the GB sub-surface (Fookes, 1995). Furthermore, these limestones are considered as a potential target for geothermal energy production.

The outcrop model was obtained using Agisoft Photoscan©. The acquired model was then interpreted in terms of depositional environments using Virtual Reality Geological Studio©. This interpreted model is further used to constrain dimensions and orientations of the different sedimentary bodies with great accuracy. Once imported in Petrel©, these data are used to produce a high-fidelity depositional model which can be propagated into the whole basin.

The study presented here will help to improve the current 3D model of the Geneva Basin. Moreover, this project is of added value for the Electrical Resistivity Tomography study of this outcrop currently being developed at the University of Geneva. Additionally, the data produced in this study will provide key inputs for reservoir modelling which is crucial for further potential exploitation of geothermal energy in the Canton of Geneva.

REFERENCES
Blistan, Peter & Kovanič, Ľudovít & Zelizňaková, Vladislava & Palková, Jana. (2016). Using UAV photogrammetry to document rock outcrops. Acta Montanistica Slovaca, 21, 154-161.
Fookes, E. (1995). Development and eustatic control of an Upper Jurassic reef complex (Saint Germain-de-Joux, Eastern France). Facies, 33(1), 129-150.

20.10
Mapping the techno-economic potential of closed-loop geothermal systems: a Europe-tested method

Rodolfo Perego [1], Sebastian Pera [1], Antonio Galgaro [2], Giorgia dalla Santa [2], Matteo Cultrera [2], Michele De Carli [3], Giuseppe Emmi [3], David Bertermann [4], Johannes Müller [4], Dimitrios Mendrinos [5], Kostas Karytsas [5], Jacques Vercruysse [6], Riccardo Pasquali [7], Nick O'Neill [7], Adriana Bernardi [8]

[1] *Institute of Earth Science, SUPSI, Campus Trevano, CH-6952 Canobbio, Switzerland (rodolfo.perego@supsi.ch)*
[2] *Department of Geosciences, Università degli Studi di Padova, Italy*
[3] *Department of Industrial Engineering, Università degli Studi di Padova, Italy*
[4] *GeoZentrum Nordbayern, Friedrich-Alexander-University Erlangen-Nuremberg, Schlossgarten 5, 91054, Erlangen, Germany*
[5] *CRES (Centre for Renewable Energy Sources and Saving), Pikérmi, Greece*
[6] *GEO-GREEN sprl - Rue de Priesmont, 63 - B-1495 Marbais, Belgium*
[7] *SLR Environmental Consulting Ireland Ltd. 7, Dundrum Business Park, Windy Arbour, D14, Ireland*
[8] *CNR-ISAC (Institute of Atmospheric Sciences and Climate), Padova, Italy*

In order to promote the deployment of low temperature geothermal closed-loop systems at European scale, the definition and quantification of the feasibility and potential for different locations is fundamental. In particular, spatial information presented as thematic maps allow optimization of the decision process, identifying more suitable or unsuitable zones and even quantifying technologic potential. The mapping work described hereafter is related to the HORIZON2020 project Cheap-GSHPs, which aims to reduce the total cost of ownership, composed out of investment and operating costs, increase the safety of shallow geothermal systems during installation and operation and increase the awareness of this technology throughout Europe. The project is in its 4th year: within this timeframe, a huge amount of geological [1], climatic [2] and technological data have been produced.

The work presented here had the aim of merging all of these data into a method to map the techno-economic potential of closed-loop shallow geothermal systems (expressed as €/kW) that could be robust and consistent at European scale. The method started with the collection of geological, climatic, energetic, technological and economic data produced within the project.

These data were the basis for the execution of a large amount of numerical simulations, which allowed us to extrapolate empirical correlations between mappable parameters such as ground surface temperature (GST), thermal conductivity (λ) and required BHE length for given energy demands, in form of different referential building types.

Seven case studies across Europe were considered for the application of the method, in order to test its reliability for different geologies, climates and data availability.

GST maps and λ maps were produced for each of the analyzed case study starting respectively from air temperature climatic normals and from large scale geological maps (from 1:25000 to 1:100000). To estimate a weighted λ, stratigraphic and hydrogeological information were also integrated in the mapping procedure. The identified regression algorithms were then applied on GST and λ maps in order to produce required BHE length maps, which allowed the creation of €/kW maps by using a previously produced costs database. GST, λ and required BHE length maps were compared against real data (usually thermal response tests), where available.

The estimated specific capital cost €/kW index greatly varies from country to country, ranging from approximately 1100 €/kW in Belgium to 2600 €/kW in Switzerland. The cartographic products were also developed with the integration of political constraints, such as the presence of groundwater protection areas where the installation of closed-loop systems is not allowed or allowed after a case-by-case analysis. The method seems reliable, not only to create €/kW maps, but also semi-quantitative ones related to other techno-economic indexes for different European countries.

REFERENCES
[1] Müller, J., Galgaro, A., Dalla Santa, G., Cultrera, M., Karytsas, C., Mendrinos, D., Pera, S., Perego, R., O'Neill, N., and Pasquali, R., 2018, Generalized Pan-European Geological Database for Shallow Geothermal Installations: Geosciences, v. 8, no. 1, p. 32.
[2] Carli, M. de, Bernardi, A., Cultrera, M., Dalla Santa, G., Di Bella, A., Emmi, G., Galgaro, A., Graci, S., Mendrinos, D., Mezzasalma, G., Pasquali, R., Pera, S., Perego, R., and Zarrella, A., 2018, A Database for Climatic Conditions around Europe for Promoting GSHP Solutions: Geosciences, v. 8, no. 2, p. 71.
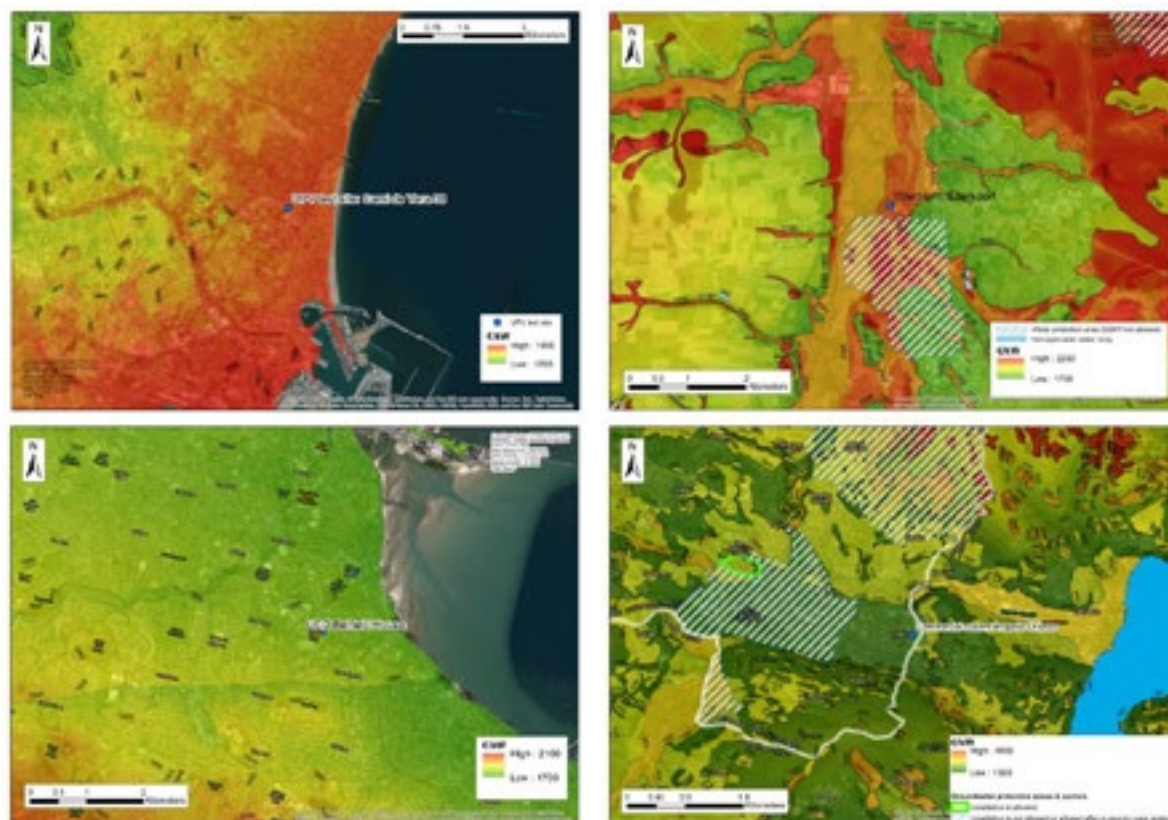
Figure 1. €/kW maps produced for 4 different case studies across Europe: [up-left] Valencia (Spain); [up-right] Erlangen (Germany); [down-left] Dublin (Ireland); [down-right] Chiasso (Switzerland)

21.11
Data mining for (flood) exposure analyses

Veronika Röthlisberger [1,2,3], Andreas Zischg [1,2,3] & Margreth Keiler [1,2]

[1] *Institute of Geography, University of Bern, Hallerstrasse 12, CH-3012 Bern (veronika.roethlisberger@unibe.giub.ch)*
[2] *Mobiliar Lab for Natural Risks, University of Bern, Hallerstrasse 12, CH-3012 Bern*
[3] *Oeschger Centre for Climate Change Research, University of Bern, Falkenplatz 16, CH-3012 Bern*

We present challenges and opportunities of data mining approaches for exposure analyses at the regional to national scale. For the value estimation of potentially flood exposed buildings we combine countrywide available data on buildings and land use with points of insurance contracts provided by eleven Cantonal insurance companies for buildings. We compare two different types of value estimations models, 1) based on individual buildings and 2) based on area. The results suggest that models based on individual buildings perform better and that the buildings' volumes are key for reliable value estimations; which in turn are crucial for the optimal allocation of resources for protection measures in decision-making processes based on cost-efficiency. Yet, at the national scale, no harmonized data on building volumes are available. We derive them from buildings polygons, intersected with data on elevation (DEM) and surface (DOM). A pre-process, which is computationally intensive and time demanding. However, with regard to the spatial distribution of flood exposed buildings values, all applied value estimation models produce results that are very similar (Figure 1). Therefore, for spatial prioritizations, simpler models based on less pre-processed data are preferable.

Figure 1. Spatial distribution of Switzerland's most flood exposed building values, estimated by (left) a straight forward model based on flooded area and land use and (right) a sophisticated model based on individual building parameters including volume. Blue indicates for both models the upper 35% of flood exposed building values.

REFERENCES
Röthlisberger, V., Zischg, A. P., and Keiler, M. 2018 (accepted): A comparison of building value models for flood risk analysis, Nat. Hazards Earth Syst. Sci., https://doi.org/10.5194/nhess-2017-442.

21.12
Monitoring the crisis of a rock glacier in the Western Swiss Alps with UAV surveys

Sebastián Vivero [1] & Christophe Lambiel [1]

[1] Institute of Earth Surface Dynamics (IDYST), University of Lausanne, Bâtiment Géopolis UNIL Mouline, CH-1015 Lausanne

Rock glacier movement represents the expression of creeping mountain permafrost, which has received substantial attention about their current dynamical changes, particularly in the European Alps. La Roussette rock glacier (0.02 km^2) is located in the Arolla valley (Valais Alps) and occupies a very small cirque at 3100 m a.s.l with a south-westerly aspect. It was recently discovered in April 2016 due to the appearance of crevasses in the snow cover. Moreover, results of a statistical model of permafrost occurrence at a very high spatial resolution, based on machine learning algorithms, informed us that the area shows high probabilities of discontinuous permafrost presence.

High creeping rates and rapid topographic changes caused by the destabilisation of this rock glacier in a steep mountain flank between June 2016 and September 2017 were investigated in detail with five Unmanned Aerial Vehicle (UAV) surveys. State-of-the-art photogrammetric techniques were employed to derived very-high resolution orthophoto mosaics and point clouds from the rock glacier and its environs. The accuracy of the co-registration of subsequent point clouds was carefully examined and adjusted based on comparing stable areas outside the rock glacier, which minimised 3-D alignment errors to a mean of 0.12 m. Elevation and volumetric changes of the destabilised rock glacier were quantified over the study period. Surface kinematics were computed from recurrent orthophoto mosaics and with the aid of image correlation algorithms. Between June 2016 and September 2017, the destabilised part of the rock glacier mobilised a volume of around 27,000 m^3 of material and dispersed it over the lower talus slope. We demonstrate with this study that repeated UAV surveys and photogrammetric techniques can be very useful to improve our understanding of rock glacier dynamics in a context of permafrost warming.

P 21.1

Numerical modeling of the Geneva Basin : Various scale geological model building for groundwater flow simulations

Marion Alcanié [1], Marine Collignon [1], Aurore Carrier [1], Olav Møyner [2], Matteo Lupi [1]

[1] Crustal Deformation and Fluid Flow group, Earth and Environmental Sciences section, University of Geneva, Rue des Maraîchers 13, CH-1205 Geneva. (marion.alcanie@unige.ch)

[2] SINTEF Digital, Department of Mathematics & Cybernetics, Computational Geosciences group, SINTEF Byggforsk Oslo, Forskningsveien 3b, Pb 124 Blindern, 0314 Oslo.

Switzerland promotes the energetic transition by sustaining the development of geothermal energy (among other resources). In particular, the Canton of Geneva is currently exploring geothermal assets in the Geneva Basin producing a large amount of data. Previous and ongoing projects have shown the geothermal potential of the Geneva Basin but a consistent basin-scale fluid flow model of the region is yet to be defined.Numerical fluid flow models can hence be constrained by a wealth of well-data, active seismic and gravity surveys.

We built a 3D basin-scale dynamic model using MRST (Matlab Reservoir Simulation Toolbox). MRST was originally designed for the simulation of oil and gas problems as well as carbon capture storage. However, a geothermal module was still missing and it is currently being developed in the framework of this study. The goal of the numerical experiments is to investigate large-scale fluid flow processes and how fault systems and lithological hetherogeneities may focus or hinder fluid flow in the Geneva Basin.

We present a basin-scale static model derived from active seismic data and gravity inversion integrating available data. Preliminary results are based on simulations lasting for about thousand years, after which fluid flow becomes steady state. Petrophysical data and fault locations are derived from available data and allow us to identify preferential fluid flow pathways. The numerical models point out regions where high-resolution geophysical exploration may focus in the future.

REFERENCES

Lie K.-A., 2016: An introduction to reservoir simulation using MATLAB: User guide for the Matlab Reservoir Simulation Toolbox (MRST), SINTEF ICT, http://www.sintef.no/projectweb/mrst/.

GeoMol Team, 2015: GeoMol – Assessing subsurface potentials of the Alpine Foreland Basins for sustainable planning and use of natural resources – Project Report, 188 pp., Bayerisches Landesamt für Umwelt (LfU).

P 21.2

Simulating surface runoff in urban areas on a budget: How efficient is model refinement through terrain mapping with a consumer drone?

Alexander Cierpka [1], Ralph Mettier [1], Steffen Corbe [2]

[1] Bereich Elementarschadenprävention, Basellandschaftliche Gebäudeversicherung, Gräubernstrasse 18, CH-4410 Liestal
  (alexander.cierpka@bgv.ch)
[2] TK – Consult AG, Neugasse 136, CH-8005 Zürich

Insurance claims due to damage from pluvial flooding in urban areas have become increasingly important in recent years. If the hazard potential can be determined early, relatively cheap measures can be implemented to prevent or at least reduce potential damage.

2D numerical runoff simulations based on current terrain surveys are proven tools for identification of hazard potential. However, high quality, high resolution and up-to-date digital terrain data is often unavailable and detailed aerial surveys are time consuming and often not economically feasible for small areas.

Using a consumer grade drone and commonly available software, it was tested how quickly suitable data can be acquired, and how well they are suited for the task. The mapping results show that an accuracy similar to LIDAR surveys can be achieved fairly easily. Automated point cloud classification and meshing – followed by a limited manual processing effort – allow us to produce a suitably stable mesh for numerical modelling.

In the municipality of Frenkendorf (BL) a storm event was modelled with the program BASEMENT, once based on LIDAR alone and once based on LIDAR refined with the terrain mapping from a consumer grade drone. Images and video from a comparable event were used for model verification. Compared with the observation data, the results of the refined model show a noticeable improvement over the LIDAR only model.

Even without detailed geodetic field data, the terrain mapping with a consumer drone can be used for runoff simulations, efficiently identifying buildings which have an elevated risk potential.
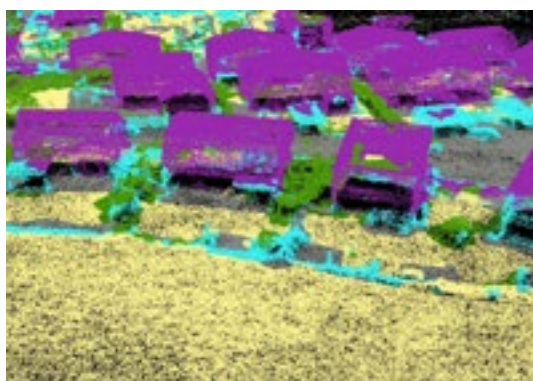
Figure 1 Clipping digital surface model (categorized point cloud)

Figure 2 Clipping simulation result (difference plot depth between LIDAR mapping and terrain mapping by a drone)

P 21.3
The Resource Information System (RIS): A web application for mineral resource data of Switzerland

Donat Fulda [1], Arsin Grünig [1]

[1] *Georesources Switzerland Group, Department of Earth Sciences, ETH Zürich, Sonneggstrasse 5, 8092 Zürich*
(donat.fulda@erdw.ethz.ch)

The Resource Information System (RIS) is a freely accessible web-based information system providing data on occurrences and extraction sites of mineral resources in Switzerland (Fulda et al. *this volume*). It includes data on gravel, sand, cement raw materials, brickyard raw materials, crushed rocks, natural stone, gypsum and salt, all of which are currently extracted in Switzerland. Furthermore, the RIS also contains data on currently not produced mineral resources like energy resources, industrial minerals (except salt and gypsum) and metals (cf. Fig. 1).
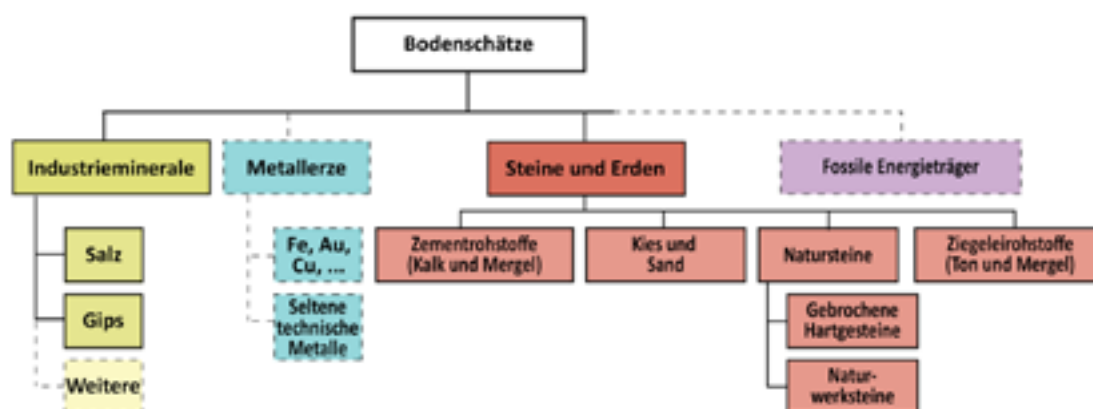

Figure 1. The RIS includes data on all mineral resource groups while the main focus is on raw materials which are currently extracted in Switzerland (boxes with solid lines). Figure by swisstopo (swisstopo 2017a).

Map viewer application
The data of the RIS is published on two platforms. Firstly, on the RIS map viewer application (map.georessourcen.ethz.ch), where all available data can be accessed, and secondly – for overview purposes – as a condensed version on the federal geodata portal map.geo.admin.ch (cf. Fulda et al. *this volume*). The objects on the two platforms are two-way linked, i. e. the object information of a quarry on map.geo.admin.ch links to the same object on map.georessourcen.ethz.ch, and vice versa. Complementary to map.geo.admin.ch, the RIS map viewer provides the following functionalities: 1) by clicking on a point of interest a data window is shown which contains data on the exploited resources, geology, operational information and literature references as well as photos of sites and rock samples (cf. screenshot in Fig. 2), and 2) advanced filtering, i. e. objects can be shown/hidden depending on the exploitation status (both, current and past periods of time), the importance of sites, or the material (rock group, lithology, minerals and elements).

Data management
The data of RIS is managed with a custom web application that has been developed by the Georesources Switzerland Group. Besides functionality for searching and editing data entries, the application features a simple method for tracking changes.

Technical architecture and interfaces
The RIS is based on a model-view-controller pattern, a commonly used architecture to build web applications. This architecture separates the data layer (data storage and retrieval) from the presentation layer (e. g. user interface for back- and frontend) and the application logic, a controller that processes in- and outputs. The data structure is based on the data model for raw materials developed by our group and the data model «Geology» published by swisstopo (swisstopo 2017b). The controller serves data to both, a backend view where editors can manage the data and to a frontend view where mineral resource data is published on a map interface (map.georessources.ethz.ch). A JSON module pushes the data to map.geo.admin.ch and other web applications for synchronization. Front- and backend views of the RIS are built upon different open source web services and libraries (e.g. the swisstopo GeoAdmin API, Leaflet, and Bootstrap). The business logic is written in PHP; the data is stored in a PostgreSQL database with the PostGIS extension for storage of spatial data. QGIS applications can directly be connected to the PostgreSQL database with read/write access.
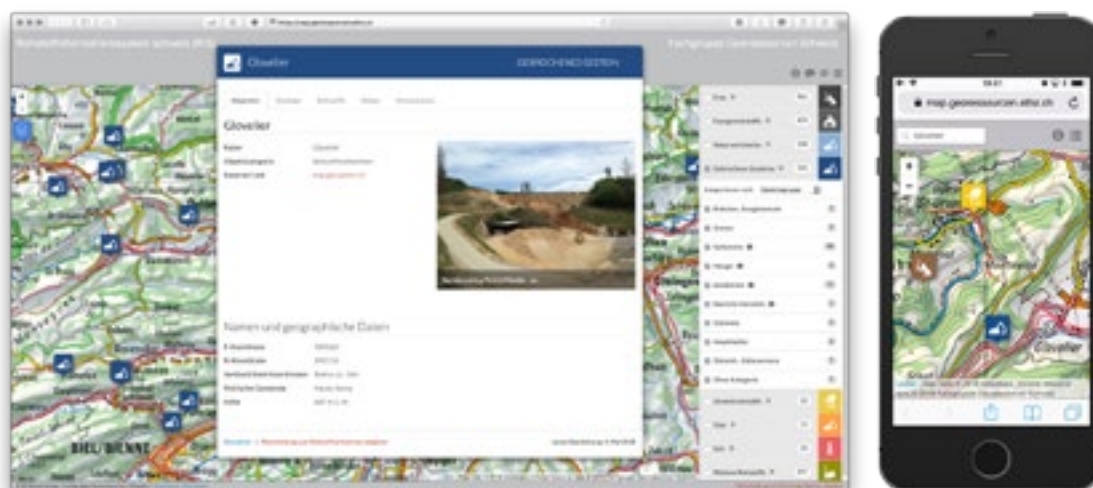
Figure 2. Desktop and mobile version of map.georessourcen.ethz.ch. Here in focus: Glovelier, an active quarry for crushed rocks in the canton of Jura.

REFERENCES

Baumeler, A., Kündig, R. & Rütti, R. 2005: «Geotechnischer Umwelt-Atlas» – Verwaltung und Visualisierung von Geodaten für geopolitische und -wirtschaftliche Fragen, Schweizerische Geotechnische Kommission SGTK, Abstract Swiss Geoscience Meeting, Zürich, 19. November 2005.

Fulda, D., Grünig, A., Heuberger, S. *this volume*: The Resource Information System (RIS) – the digital memory of mineral resource occurrences in Switzerland.

swisstopo 2017a: Bericht über die Versorgung der Schweiz mit nichtenergetischen mineralischen Rohstoffen (Bericht mineralische Rohstoffe). – Ber. Landesgeol. 11 DE (only available as PDF document).

swisstopo 2017b: Datenmodell Geologie – Beschreibung im UML-Format und Objektkatalog, Version 3.0.

P 21.4
Application of the Fisher-Shannon plane to high frequency wind speed in Switzerland

Fabian Guignard [1], Michele Lovallo [2], Mohamed Laib [1], Jean Golay [1], Mikhail Kanevski [1], Nora Helbig [3] Luciano Telesca [4]

[1] IDYST, Faculty of Geosciences and Environment, University of Lausanne, Switzerland. (fabian.guignard@unil.ch)
[2] Agenzia Regionale per la Protezione dell' Ambiente di Basilicata, Potenza, Italy.
[3] WSL Institute for Snow and Avalanche Research SLF, Davos, Switzerland.
[4] CNR, Istituto di Metodologie per l'Analisi Ambientale, Tito (PZ), Italy.

Among the environmental variables, wind speed is very important as a renewable and sustainable energy source. Several investigations on wind speed measured over the Swiss territory have been carried out, including machine learning algorithms, time series forecasting, fractal analysis, multifractal analysis, visibility graph, and complex network.

This research studies time series recorded from 2012 to 2016 by 293 measuring stations of two monitoring networks:
IMIS: managed by the WSL Institute for Snow and Avalanche Research SLF.
SwissMetNet: managed by the Federal Office of Meteorology and Climatology.

In this work, the Fisher-Shannon (FS) method is used to investigate the time dynamics of high frequency wind speed in Switzerland. FS method has been shown to be very efficient to analyze the complexity of the time evolution of signals.

The results show that both the elevation and slope play an important role in determining the time dynamics of wind speed, which seems to be characterized by more disorder as soon as the elevation as well as the slope increases. In fact, the Fisher information measure of wind speed decreases with elevation and slope, while the Shannon entropy power increases with them.

Overall, our results could contribute to a better understanding of the time dynamics of wind speed over mountainous terrain.

REFERENCES
R. A. Fisher, Theory of statistical estimation, Mathematical Proceedings of the Cambridge philosophical Society 22 (5) (1925) 700–725. doi:10.1017/S0305004100009580.
C. E. Shannon, A mathematical theory of communication, Bell System Technical Journal 27 (3) (1948) 379–423. doi:10.1002/j.1538-7305.1948.tb01338.x.

P 21.5
Estimating fracture apertures and related parameters using tube-wave data

Jürg Hunziker [1], Andrew Greenwood [1], Shohei Minato [2], Nicolas Barbosa [1], Eva Caspari [1] & Klaus Holliger [1]

[1] *University of Lausanne, Applied and Environmental Geophysics Group, Institute of Earth Sciences, Lausanne, Switzerland (jurg.hunziker@unil.ch)*
[2] *Delft University of Technology, Faculty of Civil Engineering and Geosciences, Delft, The Netherlands*

Fracture characterization is crucial for a number of applications, such as hydrocarbon exploration, geothermal energy production, carbon dioxide sequestration, and nuclear waste storage. We aim to use tube-waves to obtain pertinent information about fractures, notably the effective hydraulic aperture, the fracture compliance or the dip angle. Tube-waves propagate along borehole walls. They are generated when a seismic body-wave encounters a fracture that is intersecting a borehole or if another tube-wave encounters a fracture in the borehole (Figure 1).

We invert full-waveform tube-wave recordings from vertical seismic profiling (VSP) experiments with a stochastic inversion approach to infer the fracture parameters. As a forward solver we use the semi-analytical model derived by Minato and Ghose (2017). To sample the solution-space efficiently, we use the DREAM(ZS) algorithm (ter Braak and Vrugt, 2008; Laloy and Vrugt, 2012), which is a Markov chain Monte Carlo (MCMC) algorithm exploiting an archive of past states using differential evolution to determine the next step of the Markov chain. Besides the fracture parameters mentioned above, we invert also for the bulk and shear moduli of the formation. The standard deviation of the data error and the shape of the source-wavelet are retrieved as well. The algorithm exploits the amplitude ratio between the incident P-wave and the generated tube-wave. As the complete preprocessed VSP recording serves as input, no picking of events is required.

The algorithm assumes zero-offset VSP data, which places the seismic source at the wellhead. Furthermore, it is assumed that the background medium is homogeneous. In the presence of an inhomogeneous background, we subsequently invert for sections along the borehole, which can be considered as being approximately homogeneous.

Figure 2 shows some results of an experiment with synthetic data featuring two fractures and contamination with measured noise. This experiment demonstrates that the algorithm is capable of retrieving the fracture aperture, compliance and the elastic formation moduli, even in the presence of multiple fractures with different apertures and inclinations. Thereby, the standard deviation of the data error and the shape of the wavelet are adequately estimated. Conversely, the inclinations of the fractures can only be constrained with significant uncertainties. For real data, the forward solver needs to be extended to accommodate additional effects like transmission losses across fractures. These extensions are currently under development.
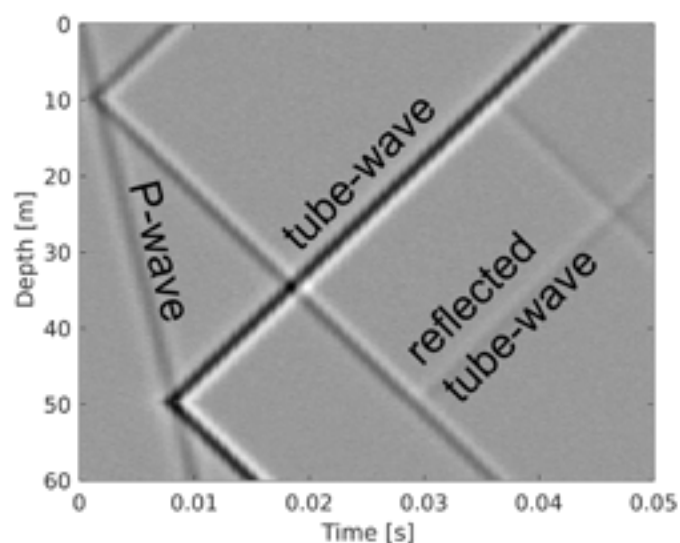

Figure 1. Synthetic VSP data showing the downgoing P-wave and the tube-waves which are generated and reflected at fractures at 10 m and 50 m depth.
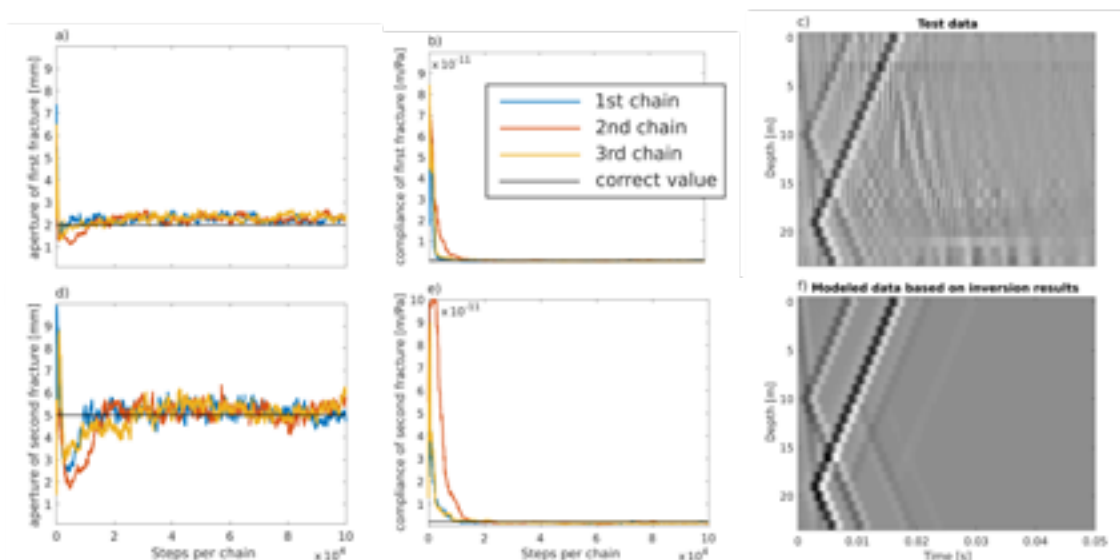
Figure 2. Inversion results of synthetic data containing two fractures and measured noise: a), d) fracture aperture, b), e) fracture compliance, c) synthetic input data, f) forward modeled data based on the inferred model.

REFERENCES

Laloy, E., & Vrugt, J. A., 2012: High-dimensional posterior exploration of hydrologic models using multiple-try DREAM(ZS) and high-performance

computing, Water Resources Research, 48, WO1526.

Minato, S. & Ghose, R., 2017: Low-frequency guided waves in a fluid-filled borehole: Simultaneous effects of generation and scattering due to multiple fractures, Journal of Applied Physics, 121, 104902.

ter Braak, C. J. F., & Vrugt, J. A., 2008: Differential evolution Markov Chain with snooker updater and fewer chains, Statistics and Computing, 18, 435–446.

P 21.6
Mutual information-based complex network for wind speed in Switzerland

Mohamed Laib [1], Fabian Guignard [1], Mikhail Kanevski [1], & Luciano Telesca [2]

[1] IDYST, Faculty of Geosciences and Environment, University of Lausanne [1015], Switzerland. (Mohamed.Laib@unil.ch)
[2] CNR, Istituto di Metodologie per l'Analisi Ambientale, 85050 Tito (PZ), Italy.

Networks are gaining popularity in describing the cooperative behaviour within a complex system involving relationships among its constituent units. A network can easily present a wind speed-monitoring system, by considering the measuring stations as nodes and the links by a linear or non-linear metric. The links in this work are weighted by the mutual information between the wind time series recorded at each station, which quantifies the dependence between them.

The data are collected from 119 measuring stations (see Fig. 1) from 2012 to 2016 by SwissMetNet, which is managed by the Federal Office of Meteorology and Climatology (MeteoSwiss).

The first step of this work consists of building two different networks, one on the original data (Fig. 2.a) and the other on their residuals (Fig. 2.b) after applying the seasonal decomposition of time series by loess (STL).

Then, the multilevel community detection method is applied on these networks separately. The results show two communities well separated for the second network (constructed on the residuals). These two communities situated respectively on the Alps and on the Jura-Plateau region. This work proposes a new approach, using mutual information-based network, to find non-linear interactions among wind time series recorded in different topographic regions.
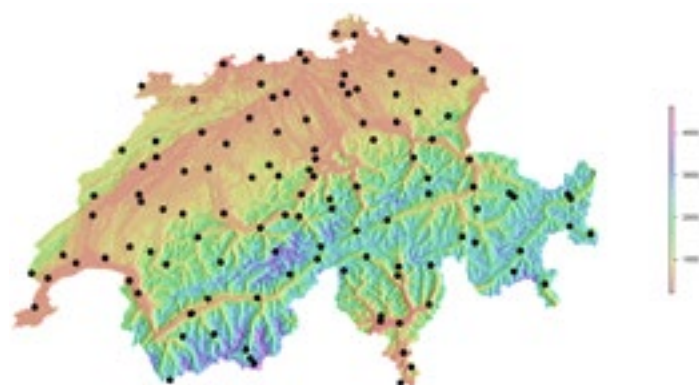

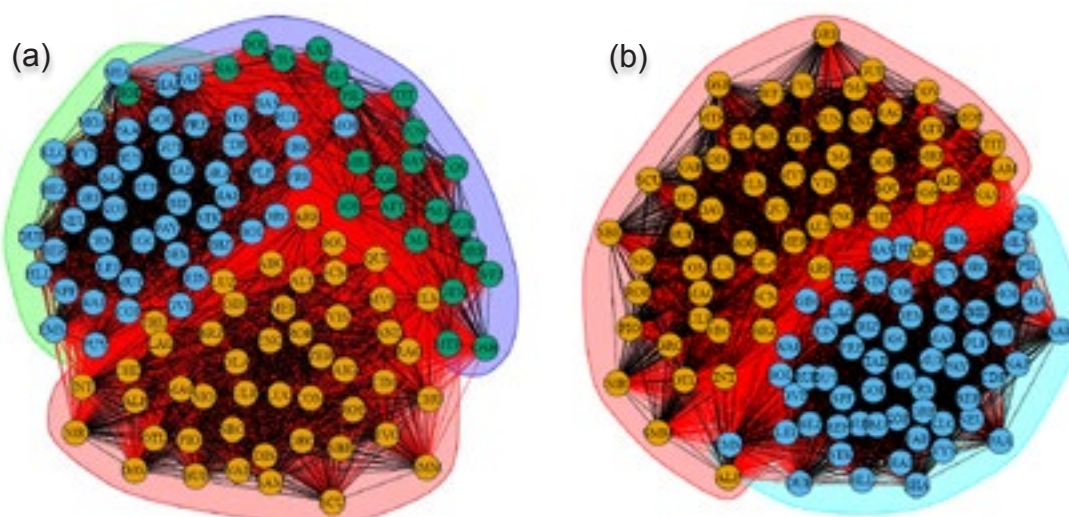Fig. 1. Study area and location of measuring stations

Fig. 2. Two constructed networks. Network constructed before applying STL (a). Network constructed after applying STL (b).

REFERENCES

Blondel, V. D., Guillaume, J.-L., Lambiotte, R., and Lefebvre, E., Fast unfolding of communities in large networks, Journal of Statistical Mechanics: Theory and Experiment, P10008 (2008).

Csardi G, Nepusz T: The igraph software package for complex network Research, InterJournal, Complex Systems 1695. 2006. http://igraph.org

P 21.7
Hazard and Risk Mapping During a Flood Event in Bangladesh

Alireza Salehipour Milani [1], Ghazaleh Pouladi [1],Zahra Mohammadi [1]

[1] Department of Physical Geography,Faculty of Earth Science,University of Shahid Beheshti, Velenjak,Tehran ,Iran
 (ar.salehipour@gmail.com)

River/Sea flooding, also known as monsoon flooding (June to September), is the most common type of flooding in Bangladesh. It refers to, both, "normal" inundation of up to 25% of the country as well as extreme flooding which can inundate up to 70% of the country (WMO 2003). The most affected areas are in the Haor Basin of the northern belt of Bangladesh, which is made up of Sylhet, Sunamganj, Moulvibazar, Habiganj, and Netrakona Districts, as well as the southeast in Chittagong, Cox's Bazar and Bandarban Districts (BWDB 2014; WMO 2003). Rise of water levels in the various rivers in the northern part of the country due to heavy rainfalls as well as water flow from the upstream hills in India have led to the inundation of the river basin areas in the northern parts of Bangladesh in April, July and august of 2017. Severe floods in 2017 have affected at least 8 million people, causing deaths and injuries, loss of livestock and food supplies, and damage to housing and infrastructure. The severe effects of floods can only be minimized by suitable land use planning in any region, which needs precise knowledge of flood extent for locating flood prone areas, is a key tool to develop flood management and to mitigate its disastrous effects (Atif,2015). In this current study we have used the Operational Land Imager (OLI) 30 m resolution to delineate the flood extents 2017 flood. The suitable images (without clouds) that shows flooded region in study area belong to 1 November 2017 and used for this area. The study area for this research is the Sylhet and Dhaka province of Bangladesh located between 23°51'54.89"N to 24°55'30.77"N and 90°47'57.03"E to 92°22'15.56 as shown in Figure The modified NDWI (MNDWI) can enhance open water features while efficiently suppressing and even removing built-up land noise as well as vegetation and soil noise. Take advantage of the high reflectance of NIR by vegetation and soil features (McFeeters,1996). Using the proposed technique, predictions of inundation were evaluated. The results demonstrate that incorporation of multiple sources of data can aid extract of flood extents using the proposed methodology. in study area more than 467905 hectare of land area inundate in flood spatially in Dhaka providence.

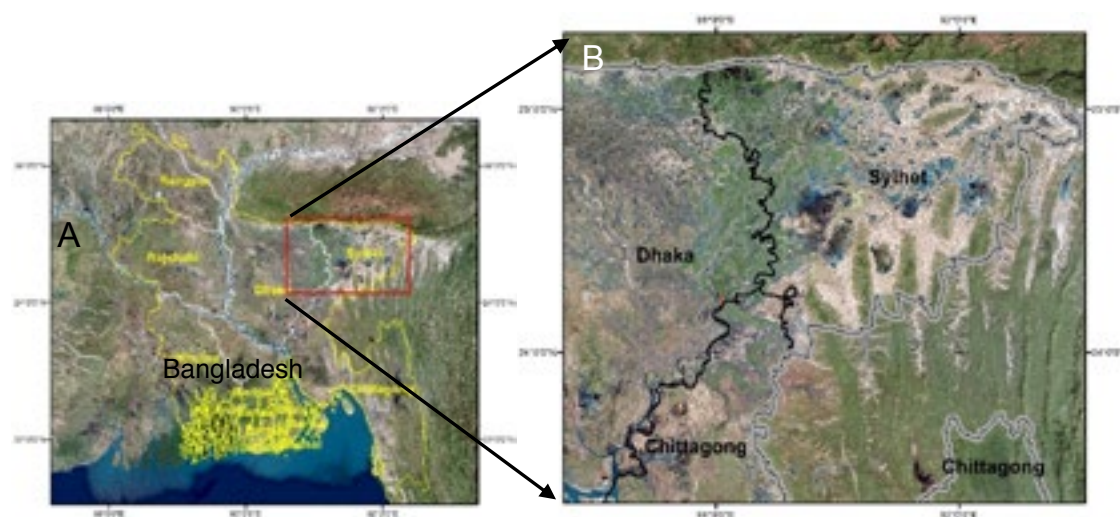Keyword: Flood Hazard Zoning, MNDWI, Remote Sensing, Bangladesh

Fig1. A: Study area in the Bangladesh (red rectangle), B: Study Area Before the floods of the summer of 2017
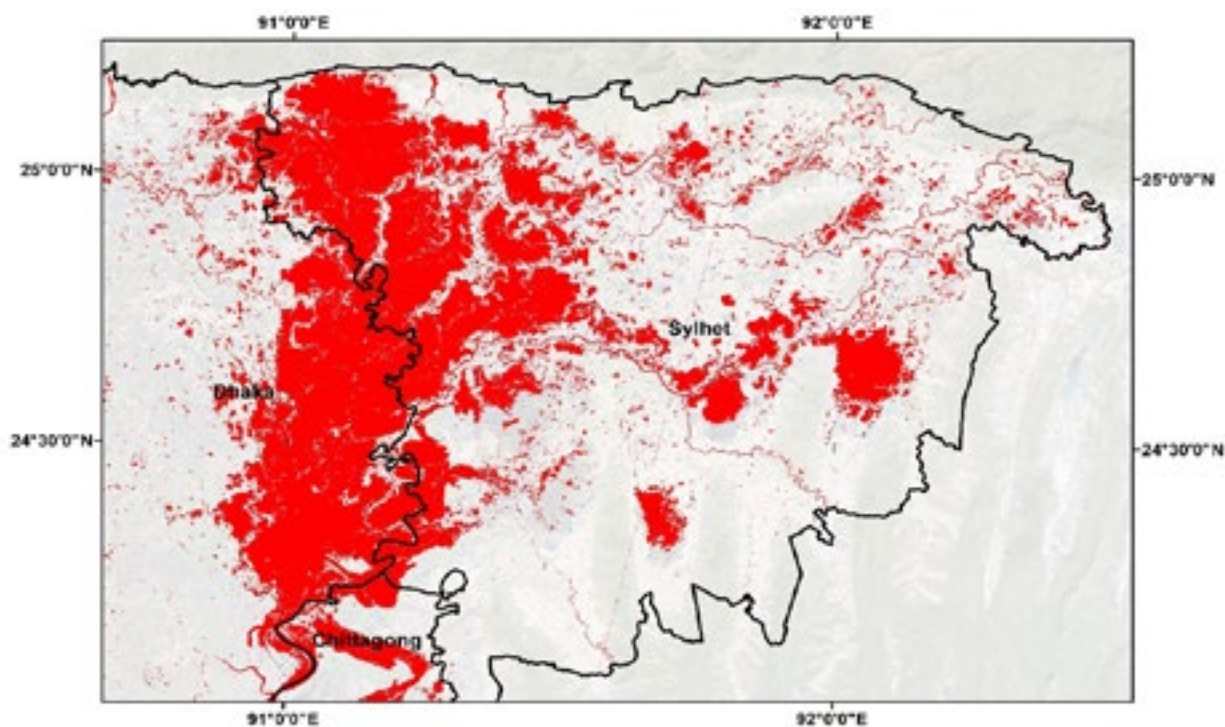
Fig2: extraction of flood area using MNDWI induce in study area

REFERENCES

Atif, Iqra., Mahboob, Muhammad Ahsan & Waheed Abdul. 2015: Spatio-Temporal Mapping and Multi-Sector Damage Assessment of 2014 Flood in Pakistan using Remote Sensing and GIS, Indian Journal of Science and Technology, *Vol 8(35)*

Bangladesh Water Development Board (BWDB) .2014: Annual Flood Report. Flood Forecasting and Warning Centre, Dhaka.

McFeeters, S. K. 1996: The use of normalized difference water index (NDWI) in the delineation of open water features. *International Journal of Remote Sensing*, 17: 1425–1432.

World Meteorological Organization.2003: WMO Statement on the Status of the global climate change in 2003, WMO-No. 966

P 21.8
Spatio-temporal kernel density analysis and 3D visualisation of landslides causing damage in Switzerland

Marj Tonini [1], Maria Elena Cama [2], Mikhail Kanevski [1]

[1] *Institute of Earth Surface Dynamics, Faculty of Geosciences and Environment, University of Lausanne, Switzerland (marj.tonini@unil.ch; mikhail.kanevski@unil.ch)*
[2] *Indipendent researcher, Tübingen, Germany (mariaelenacama@gmail.com)*

Nowadays the availability of massive digital geo-referenced databases led GISscientists to search for new tools able to make sense of such complexity. In this context, the spatial and temporal distribution of hazardous events is an example of complex pattern, which strongly influences the landscape and the surrounding anthropogenic space. Statistical methods developed for spatio-temporal stochastic point processes can be employed to detect over-densities and address towards prevention and forecasting measures.

The present research analyses the spatio-temporal pattern distribution of landslides causing damage in Switzerland in the last twenty years (1995-2015). Data came from the multi-temporal landslide damage database implemented by the Swiss Federal Institute for Forest, Snow and Landscape Research (WSL) on the base of historical information. Both global and local cluster indicators were applied to detect 3D-over densities, both in space and time dimensions. Specifically, the Ripley's K-function was applied to detect the degree of clustering at different scales. These metrics were retained to define the bandwidth of the 3D-Kernel density estimator, which allowed assessing and geo-visualizing landslides' over densities. The volume rendering technique was therefore used to combine the yearly smoothed kernel densities into a unique image that displays the entire internal structure of the volumetric dataset, consisting in the space-time dimensions plus a scalar indicating the estimated kernel density values. Analyses were performed under "R" software (by R Core Team), and specifically the Ripley's K-functions and the space–time Kernel were estimated using the package splancs.

More detailed analyses are required for the determination of cause-effect relationships among landslides and other environmental variables. Nevertheless, some influences of meteorological conditions can already be argued, indicating a possible path dependency effect among detected clusters and extreme rainfall. Ultimately, the application of spatio-temporal cluster analysis allowed detecting frame-periods with greater landslide activity concentrates in certain area and, more in general, to find a structure in data, allowing highlighting local over-densities and geo-visualize them.
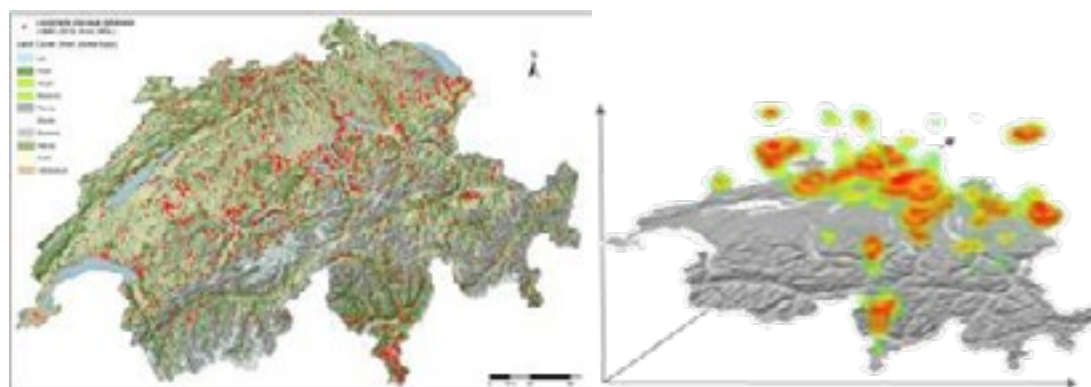

Figure 1. Spatial distribution (left) and space-time kernel density 3D-map (right) of landslides causing damage in the Swiss territory (data from WSL)

REFERENCES

Tonini, M., Pereira, M. G., Parente, J., Vega Orozco C. 2017: Evolution of forest fires in Portugal: from spatio-temporal point events to smoothed density maps, Nat Hazards, 85, 1489-1510
Tonini, M., Pedrazzini A., Penna I., Jaboyedoff M. (2013): Spatial pattern of landslides in Swiss Rhone Valley, Nat Hazards, 73, 97-110
Hilker, N., Badoux, A., & Hegg, C. 2009: The Swiss flood and landslide damage database 1972-2007. Natural Hazards and Earth System Science, 9(3), 913-925.

22. Human Geographies

Martin Müller, Jevgeniy Bluwstein, Karine Duplan, Olivier Graefe, Francisco Klauser, Christian Kull, Rafael Matos-Wasem, Elisabeth Militz, Patrick Rérat

Swiss Association for Geography (ASG)

TALKS:

22.1   Andriamahefazafy M., Sinan H.: The paradox of tuna fisheries in the Indian Ocean: between visions of sustainable management and realities of access

22.2   Backhaus N.: The (im)possibility of creating a national park with a bottom-up process

22.3   Bétrisey F., Boisvert V.: Amaranth: Superweed, Superfood or Decolonising Agent? Exploring powerful 'promising' discourses

22.4   Chossiere F.: Spaces and scales of queer refugees' intimate: global sexualized geographies of power

22.5   Fall J.J.: When and where is nature natural? Invasive alien species, colonisation, and scientific denialism

22.6   Florin I.: Exploring the political natures of large-scale conservation in Northern Europe : underlying values and strategic uses

22.7   Hergon F.: French State Of Emergency, Police Searches & Islamophobia: A Coercive Rupture Of Intimate Spaces, Bodies and Subjectivities

22.8   Hug M.: Planned Improvisation. The Rail Redevelopment Neugasse Zürich

22.9   Ishitsuka A.M.: When Business Interests Meet Racialized Desires: Young Professionals' Bodies in Global Shanghai

22.10   Laketa S.: The atmospheric (geo)politics of love and vigilance: Affect and urban security in Brussels

22.11   Oldfield S.; discussants: Barella J., Narayanan N.: Keynote: The Urban as Political Terrain: Building Collaborative Urban Geography in Everyday Southern City Life

22.12   Paulos J.: Governing the 'multiple city': From planning logics to normative objects

22.13   Sanchez J.: The depoliticization of urban governance in Myanmar: insights from sanitation planning in Mandalay

22.14   Söderström O.: What travelling architecture types and urban development models do

22.15   Weber H.: The role of sheep in the political dynamics within sheep farming in Switzerland

22.1
The paradox of tuna fisheries in the Indian Ocean:
between visions of sustainable management and realities of access

Mialy Andriamahefazafy [1], Hussain Sinan [2]

[1] *Institute of Geography and Sustainability, University of Lausanne, Géopolis CH -1015 Lausanne*
  (mialyzanah.andriamahefazafy@unil.ch)
[2] *Marine Affairs Program, Dalhousie University, B3H 4R2, Halifax, Canada*

For many coastal nations in Indian Ocean (IO), tuna fishery is considered one of the main pillars of economic development, providing large foreign revenues and jobs whilst ensuring food security. The Indian Ocean is a productive marine space for tuna and has long been considered one of the last frontiers for tuna fisheries. In the IO region, tuna is harvested by fishers of the coastal nations but also by foreign countries, including European and Asian.

In a global context where a blue economy is promoted and where economic growth and sustainable use of resources are fostered as jointly achievable (Llewellyn et al. 2016), tuna fisheries in the IO are an illustration of the paradox that blue economy presents for renewable resources. As propelled by Winder and Le Heron (2015), we attempt to pinpoint "the political challenges of dealing with ocean space" (p.5) by unravelling the politics of accumulation and access to tuna resources in the IO.

Using insights from political ecology through concepts of co-production (Jasanoff 2006, Robbins 2012) and geopolitical ecology (Bigger and Neimark 2017), we produced narratives that constitute the paradox of sustainable tuna fisheries and highlight the power relations that make this paradox persistent in the IO region. To this end, we analysed policy documents, countries' fisheries reports and fishing data from the Indian Ocean Tuna Commission, in the past five years. We coupled those with semi-structured interviews with key actors.

We present a sustainability narrative within which the idea of fishing within ecological limits is embraced by governments in their public policy and by industrial fishers in their public discourse. This, however, co-exists with a second narrative of accumulation and growth within which the realities of access struggles and capital accumulation prevail. We showed that, while stakeholders have co-produced a strong discourse of sustainable tuna fisheries, when measures towards ecological preservation are to be taken, geopolitics of access to the sea and tuna enter the stage and change the position and discourse of the same actors. We emphasise the difficult and nearly impossible path of practicing sustainability in the current growth-driven tuna fisheries. We support the idea of repoliticizing the practice of sustainability (Asara et al. 2015) especially in tuna fisheries, through the questioning of what we see in tuna fisheries: a soon-to-be hegemonic narrative of sustainability without socio-ecological transformations.

REFERENCES

Asara, V., Otero, I., Demaria, F. & Crobera, E. 2015: Socially sustainable degrowth as a social–ecological transformation: repoliticizing sustainability. Sustainable Science 10:375-384.

Bigger, P., & Neimark, B.D. 2017: Weaponizing nature: The geopolitical ecology of the US Navy's biofuel program. Political Geography 60:13-22.

Jasanoff, S. 2006: Ordering knowledge, ordering-society. In States of knowledge, the co-production of science and social order, edited by Sheila Jasanoff, 13045. New York: Routledge.

Llewellyn, L. E., English, S. & Barnwell S. 2016: A roadmap to a sustainable Indian Ocean blue economy. Journal of the Indian Ocean Region 12 (1):52-66.

Robbins, P. 2012: Challenges in social construction. In Political Ecology, A Critical Introduction, Second Edition. Sussex. Wiley-Blackwell.

Winder, G. M. & Le Heron, R. 2017: Assembling a Blue Economy moment?Geographic engagement with globalizing biological-economic relations in multi-use marine environments. Dialogues in Human Geography 7 (1):3-26.

22.2
The (im)possibility of creating a national park with a bottom-up process

Backhaus, N.

Human Geography Unit, Department of Geography, University of Zurich, Winterthurerstr. 190, CH-8057 Zurich, Switzerland

Although Switzerland has the oldest national park of the Alps (founded 1914), two recent attempts to create a second national park failed. Both Parc Adula and Parco Locarnese were voted against in municipal referenda in 2016 and 2018. Although in total yes and no votes were in both cases almost equal (with a small majority of no-votes), the result was clear since each municipality was counted separately. Swiss legislation asks for a bottom-up process for creating a new (national) park, a process that has no equivalent at least in Europe even though the principle of local support has been identified as key prerequisite in conservation theory (cf Brockington 2004). Is it then generally impossible to create a national park in a bottom-up process and should we therefore question or even abolish this prerequisite in favor of nature conservation as Holmes (2013) suggests? Based on a recent study (Backhaus et al. forthcoming), in which we analyzed the reasons for the no-vote in Parc Adula, we try to answer these questions. Our results indicate that there is no simple answer and that the problem starts with different notions of what nature conservation is for. We, moreover, identified the following conflict areas, through which the conservation discourse was shaped: nature/biodiversity protection vs. regional development, lowland/outside vs. highland/inside, and people's identification with a new region. We will conclude the presentation with recommendations and a discussion of the feasibility of creating national parks in a bottom-up process.

REFERENCES

Backhaus N., Pleger L., von Atzigen A., Bosello O., Graefe O., Hunziker M., Sager S. & Siegrist D. (forthcoming): Parc Adula: Gründe und Hintergründe der Ablehnung in den Gemeindeabstimmungen. Geographisches Institut der Universität Zürich, Zürich.

Brockington, D. (2004): Community conservation, inequality and injustice: myths of power in protected area management. Conservation and society 2(2): 411–432

Holmes, G. (2013): Exploring the Relationship Between Local Support and the Success of Protected Areas, Conservation and Society, 11(1): 72-82.

22.3
Amaranth: Superweed, Superfood or Decolonising Agent? Exploring powerful 'promising' discourses.

Florence Bétrisey [1] & Valérie Boisvert [1]

[1] Institut de Géographie et Durabilité, Université de Lausanne, 1015 Lausanne

Amaranth is a nutritious pseudo-cereal whose cultivation dates back to 5000 BC in Mexico (Russell, 2015). Since the 2000s it has gained worldwide attention as a "superfood" and a "superweed". Today, farmers in 37 states of the USA as well as in Brazil, and Argentina[1] are « fighting » to eradicate *superweed* amaranth, with the help of weed scientists and agro-chemical industry, whereas farmers in Mexico are planting and "safeguarding" *superfood* amaranth with the help of agronomists and non-profit organisations.

Following a *political agronomy* approach (Sumberg et al., 2014), we posit that understanding such different representations of the plant and the associated institutional arrangements and practices requires to examine the discourses that legitimate them. We define "discourse" as "a way of construing aspects of the world associated with particular social perspective" (Fairclough, 2013, p. 179) that is to be analysed critically. This first implies highlighting "framing" processes that "set the stage" (Sumberg et al., 2013, p. 77) for the production of discourses. Framing consist in the "selecting, emphasizing and organising aspects of complex issues" (Daviter, 2007, p. 654) according to specific frames, i.e. "overriding evaluative or analytical criterion" (Daviter, 2007, p. 654). The latter are not neutral but embedded in social norms (Butler, 2007) and performative. Indeed, when frames are used within discourses, they become "obligatory passage points" (Callon, 1985).

Although not focusing especially on amaranth, scholars have critically assessed framing processes in superweed discourse and showed how framings varied according to ideological positions on GMO (Bain et al., 2017). Superfood discourse is based on series of problem framings in various fields ranging from nutrition to agro-biodiversity conservation that have yet been assessed separately (Breeze, 2017; McDonell, 2015).

Here we propose to examine framing processes in both superweed and superfood discourses on amaranth and expand the analysis to the language and rhetoric choices within those discourses. We first focus on the use of narratives also known as storytelling techniques (Salmon, 2007) whose effect of creating sense of authenticity for the reader (Boltanski and Chiapello, 2005) is well known. Secondly, we consider the discursive construction of promises. The latter are based on social imaginaries and former framings of consensual global problems that are to be solved. STS scholars have shown how promises of brighter futures or impeding disasters have been used to legitimize and gain acceptance for technological innovation (Audétat, 2015; Joly, 2013). Finally we examine the use of metaphorical language whose effect of "raising the emotional temperature"(Breeze, 2017, p. 71) and is also documented.
We also posit that the choice of amaranth makes it possible to jointly analyze the discourses on super foods and super weeds, and thus to depict thoroughly the discursive construction of underlying categories and their political nature beyond scientific evidence.

We therefore collected scientific reports and papers, policy briefs, press-releases, professional and non-professional magazines' and newspapers' articles, as well as websites and blog articles related to pre-identified superweed and superfood amaranth discourses. Following a purposive sampling approach, we used keywords in general web engine and then referred to our own judgement to select relevant contributions. We then manually coded the collected 'texts' based on a grounded theory approach.

As a result, we show that *superweed* discourse is filled with metaphors denigrating amaranth belonging to six registers (aggressivity, wickedness, evil, monstrosity, unsightly character and contamination), that are used by scientists and medias indifferently from their ideological position on GMO. Stories of American farmers "fighting" amaranth are also told. Negative promises, such as unmanageable contamination or economic collapse shape a future that no one would wish for, thus legitimizing immediate action. **Superfood** discourse uses metaphors from registers that almost perfectly mirror those on superweeds, i.e. tolerance, gift, cure/panacea and aesthetics. In terms of narratives, stories are built on the ancient Inca/Maya uses of amaranth and the rediscovery by contemporary farmers of their cultural heritage. Promises to overcome health problems, hunger, food insecurity, biodiversity erosion, and the loss of cultural heritage are drawing normative visions of future that no one wants to oppose.

Finally, two alternative discourses emerge that we called "decolonising superweed" and "decolonising superfood based on set of metaphors partly common with those of the superweed and superfood discourses, but which draw on different framings of "the problem", and consequently give rise to different narratives and promises.

---

1 http://weedscience.org/Summary/Species.aspx, consulted on the 01.08.2018

Metaphors, narratives and promises empower the discourses and the framing and priorities that underlie them, as well as the legitimate solutions they lead to, and the policy instruments and institutional arrangements through which they are implemented at different scales. Our purpose here is to explore the performative power of these rhetoric devices applies to amaranth discourses.

REFERENCES

Audétat, M., 2015. Sciences et technologies émergentes: Pourquoi tant de promesses ? Hermann, Paris.

Bain, C., Selfa, T., Dandachi, T., Velardi, S., 2017. 'Superweeds' or 'survivors'? Framing the problem of glyphosate resistant weeds and genetically engineered crops. Journal of Rural Studies 51, 211–221.

Boltanski, L., Chiapello, E., 2005. The New Spirit of Capitalism. Verso, New York, NY, US.

Breeze, R., 2017. Explaining superfoods: exploring metaphor scenarios in media science reports. Ibérica: Revista de la Asociación Europea de Lenguas para Fines Específicos (AELFE) 67–88.

Butler, J., 2007. Le récit de soi. Presses Universitaires de France - PUF, Paris.

Callon, M. 1985. Some Elements of a Sociology of Translation: Domestication of the Scallops and the Fishermen of St. Brieuc Bay. In John Law (ed.), Power, Action and Belief, Sociological Review Monograph No. 32. London: Routledge & Kegan Paul, 196-230.

Daviter, F., 2007. Policy Framing in the European Union. Journal of European Public Policy 14, 654–666.

Fairclough, N., 2013. Critical discourse analysis and critical policy studies. Critical Policy Studies 7, 177–197.

Joly, P.-B., 2013. On the economics of techno-scientific promises, in: Akrich, M., Barthe, Y., Muniesa, F., Mustar, P. (Eds.), Débordements : Mélanges Offerts à Michel Callon, Sciences Sociales. Presses des Mines, Paris, pp. 203–221.

McDonell, E., 2015. Miracle Foods: Quinoa, Curative Metaphors, and the Depoliticization of Global Hunger Politics. Gastronomica: The Journal of Critical Food Studies 15, 70–85.

Russell, P., 2015. The Essential History of Mexico: From Pre-Conquest to Present. Routledge.

Salmon, C., 2007. Storytelling: La machine à fabriquer des histoires et à formater les esprits. LA DECOUVERTE, Paris.

Sumberg, J., Thompson, J., Woodhouse, P., 2014. Political Agronomy, in: Encyclopedia of Food and Agricultural Ethics. Springer, Dordrecht, pp. 1–8.

Sumberg, J., Thompson, J., Woodhouse, P., 2013. Why agronomy in the developing world has become contentious. Agric Hum Values 30, 71–83.

Turnhout, E., 2018. The Politics of Environmental Knowledge. Conservation and Society 16, 363.

22.4
Spaces and scales of queer refugees' intimate:
global sexualized geographies of power

Florent Chossière [1]

[1] *Laboratoire Analyse Comparée des Pouvoirs, Université Paris-Est Marne-la-Vallée, Bois de l'Etang, 5, rue Galilée, 77454 Champs-sur-Marne (florent.chossiere@gmail.com)*

Fleeing their country because of their homosexuality or bisexuality, some migrants apply for asylum in France on the grounds of their sexual orientation. These migrations, motivated and shaped by sexuality, illustrate how the intimate and the global can be linked. Following feminist geographies framework, inviting to pay attention to multiple spaces and scales in the understanding of a gendered geography of power (Pessar & Mahler 2003), this intervention aims to analyse sexualized geographies of power in queer refugees lives. It relies on a one-year-long ethnographic work, based on a participant observation within an association that supports queer asylum seekers and refugees, combined with semi-structured interviews. First, focus is put on the scale of the State and how it establishes sexual borders. In a context of suspicion, asylum seekers have to prove their sexuality, revealing borders as "confrontational moment in which we must declare ourselves and in which others exercise power to identify" (Mountz & Hyndman 2006). The paradoxical expectation of a constructed authenticity (Giametta 2017) and the impacts of this asylum procedure on migrants' subjectivities and everyday lives need to be emphasized. Secondly, relations across transnational spaces may lead these migrants to face forms of transnational heteronormativity, thus echoing the works showing that there is nothing inherently emancipatory in transnationalism (Pratt & Yeoh 2003). However, their agency allows us to think migrations as tensions (Schmoll 2017) rather than with binaries categories. Sexuality becomes a category regulating border crossing but also a dimension of social location (Pessar & Mahler 2003) of individuals they have to negotiate with transnationnally, thus illustrating the key role it plays in the stretching of intimacy in a global context.

REFERENCES

Giametta, C. 2017: The Sexual Politics of Asylum – Sexual Orientation and Gender Identity in the UK Asylum System. Abingdon: Routledge.

Mountz A., & Hyndman J. 2006: Feminist Approaches to the Global Intimate, Women's Studies Quarterly, 34, 446-463.

Pessar P. R., & Mahler S. J. 2003: Transnational Migration: Bringing Gender In, International Migration Review, 37, 812-846.

Pratt G., & Yeoh B. 2003: Transnational (Counter) Topographies, Gender, Place & Culture, 10, 159-166.

Schmoll C. 2017: Spatialités de la migration féminine en Europe du Sud. Une approche par le genre. Habilitation à des diriger des recherches, Université de Poitiers.

22.5

When and where is nature natural? Invasive alien species, colonisation, and scientific denialism

Juliet J. Fall

Département de géographie et environnement, Université de Genève

Invasive exotic species (IES), or invasive alien species, are called many things, be they animals, plants, or fungi. For most natural scientists, what distinguishes them from other species is that that they are identified with a distant location from the place where their thriving, and apparently creating substantial environmental damage. This is not an everyday, well-known category that has widespread vernacular recognition: it needs explaining, and relies on a belief that species belong is particular places. Defining the category of 'invasive species' relies on rhetorical acts of category-building, part of what has been called the classifying imagination (Ritvo 1997), born from a wide range of classificatory practices that emerged in the 18th and 19th century, and narrowed down further in the 20th century, relying on a precise sets of arguments to justify their singularity as a collective. It is rooted in a belief that the effects of human agency in moving living species around are unique, have consequences that are distinct from other causes of such movement, creating a *metataxonomic* category that transcends the classificatory grid of biological nomenclature. By analysing recent scientific debates published within scientific journals that mobilise terms such as *colonisation* and *denialism* that have long histories, I discuss how scientific claims are grounded in unacknowledged but contentious ontologies of nature, strongly connected to individual professional identities and fields of expertise. Unlike debates between social and natural scientists, such debates between experts rooted in the life scientists have received less attention from social scientists. As anthropogenic climate change threatens how we understand what changes might be considered as outside of human influence, i.e. what can still be considered 'natural' in the everyday use of the term, debating what is or is not 'natural' in exotic invasive species is particularly poignant.

Key words: Invasive alien species; categories; scientific identities; colonisation.

22.6
Exploring the political natures of large-scale conservation in Northern Europe : underlying values and strategic uses

Ian Florin [1]

[1] Institut des Sciences de l'Environnement – Pôle de Gouvernance de l'Environnement et de Développement Territorial, Université de Genève, Boulevard Carl Vogt 66, CH-1205 Genève

Following works on the intersection of neoliberalism and nature conservation, social scientists – notably political ecologists – have recently explored ways in which the contemporary upscaling of biodiversity governance in Europe is "lapsing" with de-politicization processes (Apostolopoulou et al., 2014). Using a large-scale protected area network project in Scandinavia as a case study, this paper shows that if the de-politicization of conservation in Europe is indeed related to governance arrangements, it is also conditioned and defined by particular conceptions of nature.

Drawing on earlier theoretical efforts (*e.g.* Büscher, Dressler & Fletcher, 2014), I propose a typology that allows to critically address the variety and complexity of nature conceptions and their political implications in protected areas. In using *spectacular*, *liquid* and *derivative* frames to examine stakeholder claims about the identification of environmental problems and the way to solve them, I explore *what* political natures inform protected area networks and *how* they (de-)politicize, shape and territorialize conservation discourses and practices.

First, I look at underlying values and beliefs that characterizes different conceptions of nature in my case study, such as the contemporary faith in connections and megaprojects. Second, I analyze how these conceptions facilitate different strategic uses, aiming at attracting extra funds or obtaining (sometimes undue) credit for particular actions.

I conclude that the combination of *spectacular*, *liquid* and *derivative* natures in large-scale protected area networks corresponds to a form of *fictitious conservation* (Büscher, 2012) that contributes to de-politicization processes through an inclusive and consensus-driven rhetoric.

REFERENCES

Apostolopoulou, E., Bornmpoudakis, D., Paloniemi, R., Cent, J., Grodzińska-Jurczak, M., Pietrzyk-Kaszyńska, A., & Pantis, J. 2014: Governance rescaling and the neoliberalization of nature: the case of biodiversity conservation in four EU countries, International Journal of Sustainable Development & World Ecology, 21(6), 481-494.

Büscher, B. 2012: Nature on the move: the value and circulation of liquid nature and the emergence of fictitious conservation, New Proposals: Journal of Marxism and Interdisciplinary Inquiry, 6 (1-2), 20-36

Büscher, B., Dressler, W.H., & Fletcher, R. 2014: Nature inc.: environmental conservation in the neoliberal age. University of Arizona Press, Tuscon.

22.7

French State Of Emergency, Police Searches & Islamophobia: A Coercive Rupture Of Intimate Spaces, Bodies and Subjectivities

Flora Hergon

Ecole des Hautes Etudes en Sciences Sociales (EHESS), 54 boulevard Raspail 75006 Paris, France (flora.hergon1@gmail.com)

According to the Ministry of the Interior, French authorities decreed 4469 police searches and 754 house arrests to counter terrorism in France after Paris attacks between November 2015 and October 2017. Only 23 of these measures ended up in the opening of formal investigations related to terrorism. While these procedures allowed the French State to perform its reactivity against global terrorism, it impacted thousands of intimate spaces, mainly those of Muslim citizens. My work is based on an analysis of interviews I conducted with Muslim subjects who have been searched or under house arrest because they constituted "a threat for public order" while it turned out they had no relations with any terrorist group.

In the French context of *laïcité*, domestic space can constitute an intimate sanctuary for pious subjects who are not allowed to visibly express their religion in secular public spaces (Asad 2006, Fernando 2013, Scott 2010). Through a violent control of religious practices within domestic spaces, police searches actually disrupt the artificial secular separation between private and public spheres. Searches not only materially devastate the intimate space but also the intimate subjectivity of the families I interviewed. Their bodies, including children ones, keep experiencing the trauma of the search, which makes them question their way of being as (too) visible non-White Muslim subjects. This work allows us to focus on a very local and intimate scale that embodies and unveils some global power relations (Massey 1994). It can reveal how state islamophobia and gendered racism against postcolonial subjects operate locally (Mohammed and Hajjat 2013).

REFERENCES

Asad, T., 2006: "Trying To Understand French Secularism" in Hent de Vries and Lawrence E. Sullivan. Political Theologies: Public Religions in a Post-Secular World. Fordham: Fordham University Press.

Fernando, M. 2014: The Republic Unsettled. Muslim French and the Contradiction of Secularism. Durham: Duke University Press.

Hajjat A., Mohammed, M. 2013: Islamophobie. Comment Les Élites Françaises Fabriquent Le « Problème Musulman ». Paris: Editions La Découverte.

Massey, Doreen. 1994: "A Global Sense of Place" in Space, Place and Gender, Minnesota: University of Minnesota Press, 146-156.

Scott, Joan Wallach. 2010: The Politics of the Veil. Princeton: Princeton University Press.

22.8
Planned Improvisation. The Rail Redevelopment Project Neugasse Zürich

Miriam Hug [1]

[1] Miriam Hug, (miriamhug@bluewin.ch)

Brownfields, including former rail areas, are a central pillar of inner-city redevelopment and densification. Yet brownfield redevelopment creates conflicts of interest. Private investors and city governments are tempted to realise large urban developments, positioning themselves within an environment of increasing competition. Opposed to this are claims for liveable cities and affordable housing. Redeveloping brownfields is a complex task full of uncertainty, where social factors entangle with the materialty of urban space. In this presentation I examine how planners in the *Neugasse Zürich* rail redevelopment project approach the complexity of an inner-city rail redevelopment. I structure my argument around two main questions: *first* I am going to explore how planners deal with complexity in practice and *second* I provide a conceptualisation of these practices. I adopt an analytical frame which joins a complexity perspective with the concept of improvisation. Drawing on interviews, participant observation and document analysis, I show that the *Neugasse* project embraces moments of improvisation; it is planned improvisation. Practically dealing with complexity requires planning for improvisation. Planned improvisation is characterised by multidisciplinarity, dialogue and consensus-oriented planning, attempts at bottom-up planning, and planning step-by-step. I identify two forms of improvisation, *collaborative improvisation* at the level of the planning context and *individual improvisation* at the level of individuals. *Neugasse* shows that there is a need to find new ways of planning which incorporate complexity and uncertainty. I propose that planning for improvisation is one way of doing so.

22.9
When Business Interests Meet Racialized Desires: Young Professionals' Bodies in Global Shanghai

Aurélia M. Ishitsuka [1]

[1] Institute of Gender Studies, University of Geneva, Centre Maurice Halbwachs, École des hautes études en sciences sociales, 48 boulevard Jourdan 75014 Paris, aurelia.ishitsuka@etu.unige.ch

Research has shown how global capitalism promotes modes of intimacy linked to specific labour flows, thereby producing some bodies that 'belong' and others that are 'out of place'. The predominance of white male bodies and heteronormative expatriate family forms in corporate mobilities has long been a subject of exploration, but there has been less scrutiny of the intimate configurations and bodies of highly skilled migrants who autonomously decide to relocate internationally at the start of their careers. My ethnographic study aims to fill this gap by exploring two transnational sites patronized by mobile young professionals in Shanghai: a coworking space and a nightlife zone. This paper focuses on the everyday bodily encounters and affective ties that occur in the former. Drawing on six months of participant observation, it shows how entrepreneurs' bodies are worked upon to fit the management and dating ideal of a healthy, active and flexible body. It further examines how, as bodies are read along racial and gendered histories, more or less desirable figures of business and sexual partners emerge. By examining how racialized erotic desires align with desires of capitalist expansion, this paper provides new insights on the politics of difference at play in the reproduction of capital on a global scale.

22.10

The atmospheric (geo)politics of love and vigilance: Affect and urban security in Brussels

Sunčana Laketa [1]

[1] *Center for Governance and Culture in Europe, University of St Gallen, Unterer Graben 21, CH-9000 St Gallen (suncana.laketa@unisg.ch)*

This paper offers a spatio-emotional account of responses to terrorism in the city of Brussels following the attacks in 2016, introducing the concept of affective urban atmosphere as a crucial level of experience through which terrorism and security discourses operate, as well as through which they are transformed, negotiated and contested. Bridging a conceptual and methodological gap between urban security studies, geographies of affect and emotions, and feminist geopolitics, I seek to take account of the experiential mechanisms as relevant for questions of urban governance and affective life in situations of violence, terrorism and geopolitical conflict. Specifically, I draw on my empirical work on the emerging practice of lockdown and other more long-term security and governance technologies in Brussels in the context of an upsurge of more or less coordinated acts of terrorism in Western European cities. The paper analyses how embodiment and affective life are targeted through different urban governance and security practices in the city and how managing affective atmospheres becomes the matter of politics. In particular, I analyse the way atmospheres of love and vigilance turn into regulatory spheres within the militarization of cities in face of security challenges, uncovering the increasingly elusive ways terrorism and security seep into people's everyday lives.

22.11

The Urban as Political Terrain: Building Collaborative Urban Geography in Everyday Southern City Life

Sophie Oldfield [1]

[1] *African Centre for Cities, University of Cape Town, Rondebosch 7701, Cape Town, South Africa (sophie.oldfield@uct.ac.za);*
  Urban Studies, University of Basel, Spalenvorstadt 2, CH-4051 Basel (sophie.oldfield@unibas.ch)

This paper explores collaborative forms of urban geography, immersed in the registers, inspirations and meanings of everyday struggles and learning across the southern city. This approach brings together multiple voices, registers and accounts, shaping urban theory in shared spaces across the city. In contexts of extreme urban inequality, this approach to theory building and critique infuses the personal, political, and public struggles through which urban theory is generated, expertise opened up, and solidarity and commitment built. Rooted in the political and physical realities of everyday southern city life, the approach engages the urban as a political terrain.

22.12
Governing the 'multiple city': From planning logics to normative objects

Julio Paulos

ETH Wohnforum – ETH CASE, ETH Zürich, Departement Architektur, HIT H13, Wolfgang-Pauli-Strasse 27, CH-8093 Zürich (julio.paulos@arch.ehtz.ch)

During the last two decades, a series of 'western cities' have adopted integrative and prospective urban agendas. This paper explores the multiple ways in which 'the city' is enacted through devices. Empirically, it engages with the recent emergence of three administrative programmes that inscribe the futurity of cities in contemporary instruments: *Lisboa 2020*, *SteP 2025* and *Zurich Strategies 2035*. These documents are not legally binding and complement traditionally existing devices like public policies or land-use plans. They do, however, display a typical way of prescribing the city into an epistemic object. The object-oriented methodology draws on ANT's *empirical ontology* (Law and Lien 2013) to question the changing dimensions, forums and formats of contemporary urban politics. To do so, this paper investigates how 'urban knowledge' is not only generated within certain administrative confinements and/or professional circuits, but also explores how non-human dispositions allow certain knowledge archetypes to locally *configure* urban professions and regimes. In short, the respective agendas consolidate superlative strategies into open devices by actively influencing current government logics to operate according to verified international paradigms. The paper then takes the notion of *material politics* (Barry 2001, 2013) by advancing the inadequacy of material inscriptions if those are not aligned with democratic issues claiming that the only versions of the city that matter need to align local concerns with international issues.

To conclude, a theoretical engagement with recent paradigmatic perspectives in urban research is made, mostly engaging cities by exposing (material, affective) conditions, and argues to trace urban change via the lens of socio-technical assemblages.

REFERENCES

Barry, Andrew. 2001. *Political Machines: Governing a Technological Society*. A&C Black.2013. *Material Politics: Disputes Along the Pipeline*. John Wiley & Sons.

Law, John, and Marianne Elisabeth Lien. 2013. 'Slippery: Field Notes in Empirical Ontology'. *Social Studies of Science* 43 (3): 363–78. https://doi.org/10.1177/0306312712456947.

22.13
The depoliticization of urban governance in Myanmar: insights from sanitation planning in Mandalay

Jérémie Sanchez [1]

[1] Institut de Géographie et Durabilité, Université de Lausanne, Géopolis CH -1015 Lausanne (Jeremie.Sanchez@unil.ch)

Urban governance, and particularly the delivery of basic services, is still conceptualized and approached in mostly technocratic terms by municipalities, multilateral donors and transnational development companies in the global South. Sanitation, for instance, remains the realm of engineers and urban planners despite decades of evidence that conventional, top-down, civil engineering approaches focusing on infrastructure have failed to deliver on their promise to provide safe and equitable access to sanitation and to reduce environmental pollution. Against this background, this paper explores urban sanitation planning in Mandalay, the second largest city of Myanmar. Here, the municipality, the Asian Development Bank and a transnational consulting firm have embarked on a multi-million dollar sanitation improvement project following the country's recent political and economic opening. Drawing upon insights from Urban Political Ecology and the literatures on sanitation planning in the Global South and on development cooperation in Myanmar, the paper first provides a politicized reading of past and current socio-ecological injustices associated with sanitation in Mandalay. It further shows how the project de-politicized these challenges and framed them in mere infrastructural terms, resulting in disillusionment and implementation failures. The paper finally suggests that the Mandalay case hints at how urban governance is being jeopardized by international cooperation projects in contemporary Myanmar.

22.14
What travelling architecture types and urban development models do

Ola Söderström [1]

[1] Institut de Géographie, Université de Neuchâtel, Espace Louis-Agassiz, 2000 Neuchâtel (ola.soderstrom@unine.ch)

The materiality of cities is shaped by local socio-natural processes and also increasingly by translocal relations and flows. My talk will discuss the latter. It will draw on previous work on how cities in the Global South are relationally constructed (Söderström 2014) and on on-going comparative work studying the 'smart city effect' in India and South Africa. I will first show how travelling architecture types shape the materiality of cities and provide affordances for new forms of urban practices. I will then show how the smart city narrative has ben 'rolled out' in India and South Africa since 2000, how it changes municipal agendas and affects the materiality (and immateriality) of cities in those two contexts. The general argument running through my presentation will be that we need to provincialise our analysis of cities' material dynamics if we want to approach it with a truly global approach.

REFERENCES
Söderström, O. *Cities in Relations. Trajectories of Urban Development in Hanoi and Ouagadougou*, Oxford, Wiley-Blackwell.
   https://provincialsmartcities.wordpress.com/

22.15
The role of sheep in the political dynamics within sheep farming in Switzerland

Hélène Weber [1]

[1] Institute of geography and sustainability, University of Lausanne, UNIL-Geopolis, Quartier Mouline, CH-1015 Lausanne
(helene.weber@unil.ch)

In Switzerland there is two types of sheep flocks: small flocks composed of a unique breed whose sheep are pure-bred and tall, with consistent fleeces, and larger flocks gathering a variety of sheep breeds, diverse fleeces, and fleshy sheep. Sheep in Switzerland are largely bred in a dispersed manner by individual farmers. Knowledge practices associated with breeding sheep, as it has developed in Switzerland, have tended to be associated with experiential knowledge of the animal qualities, developed over many years of working with sheep within specific farming conditions, sheep shows and through the activities of breed societies. In that respect, both types of flock reflect specific knowledge regarding the qualities of a "good" sheep.

There is a culturally and commercially significant set of knowledge-practices associated in particular with breeding pedigree sheep, based around breed societies and sheep shows. Pedigree breeding involves breeding 'pure-bred' sheep of a particular breed, with the aim of 'improving' the breed and, in many cases, winning prizes at agricultural shows. But it is also a commercial activity with pedigree animals being sold; prizewinning animals often achieve higher financial values (Morris and Holloway 2009). Pedigree and breeds of sheep are based on the material and relational qualities of the animals: a combination of appearance, performance, and maternal behaviour. They are certified by breed societies, which are organizations promoting their particular breeds of sheep and attempting to guide the development of the breed in particular directions. These societies record the genealogy of particular sheep, and work on the assumption that the mating of animals of similar qualities will produce another similar animal. Visual assessment of pedigree sheep has become ritualized in sheep scoring and shows, where animals are assessed according to formalized breed standards which tend to focus on their phenotypic features, such as the fertility, the conformation and wool quality.

In breed standards, the materiality of sheep is at stake. Materiality refers to the stuff of the world, both animate and inanimate, including the bodies, and is central to various forms of human experience and action (Castree *et al.* 2013). Entangled in political economies, it is historically, culturally and socially constructed and transformed, and constitutes a condition of the use of a resource (Bakker and Bridge 2006, Robbins 2012). When the materiality and its qualities play a role in the social world and human struggles, they acquire a political dimension (Robbins 2012).

Indeed, the materiality of a "good" sheep is a contested field. Showing and judging animals acts to reproduce particular institutionalized understandings of sheep qualities, and to have the effect, then, of encouraging the production of particular features of animal body among breeders of specific breeds (Morris and Holloway 2009). But selecting animals is also selecting breeders. In this context, knowledge regarding sheep materiality is being challenged by professional sheep farmers, a term used to refer to breeding with the objective of supplying animals to the meat market. Sheep corresponding to breed standards do not meet the requirements of the market, *i.e.* new consumers and retailers demand, which is centred around the qualities of the prime cuts (legs, fillets, and chops). These sheep farmers thus develop their own selective breeding to meet the expectations of their buyers and to assert their social identities as professional sheep farmers. Moreover, the state is now promoting new ways of "knowing" the bodies of sheep. Through dedicated subsidies allocated to breed societies, the state supports the development of new breeding values based on the carcasses' qualities, and develops the use of genetic markers to control rams' pedigrees. These also represent distinctive ways of knowing and evaluating sheep materiality.

Sheep breeding knowledge-practices are thus being reconfigured in relation to these various modes of knowing, evaluating and transforming sheep materiality. These new knowledge-practices are negotiated by individual sheep farmers, breed societies and the state, resulting in new knowledge communities and a shift in the location of power over decision-making about breeding.

This presentation aims at exploring the role of sheep in the reconfiguration of power relations within the sheep farming sector. Methods used are composed of: 1) a survey questionnaire of breeding, husbandry and marketing practices distributed to sheep farmers, 2) interviews of actors involved in sheep farming and value chains, 3) and my experience working as a shepherd during 2017 and 2018. By examining the materiality of sheep and sheep flocks through a political ecology lens, I will present how sheep materiality imposes specific relations between sheep, sheep farmers, sheep breed societies, processors, retailers, consumers and the state. These relations in turn reflect differing visions of what can stand for an animal, for livestock farming and meat production sustainability.

REFERENCES

Bakker, K. and G. Bridge. 2006. Material worlds? Resource geographies and the 'matter of nature'. *Progress in human geography*, 30(1), 5–27.

Castree, N., R. Kitchin, and A. Rogers. 2013. Materiality. *In*: *A Dictionary of Human Geography*. Oxford: Oxford University Press.

Morris, C. and L. Holloway. 2009. Genetic technologies and the transformation of the geographies of UK livestock agriculture: a research agenda. *Progress in Human Geography*, 33(3), 313–33.

Robbins, P. 2012. Political objects and actors. *In*: *Political Ecology. Second edition*. Chichester, pp. 231–43.

23. Sustainable social-ecological systems: from local to global challenges

Chinwe Ifejika Speranza, Sébastien Boillat, MD Sarwar Hossain Sohel

TALKS:

23.1   Adams T.: The effects of Large-scale land investments, institutional change and gender relations: Case studies of sugarcane outgrower contract farming in Malawi.

23.2   Adenle A.A., Ifejika Speranza C., Daniel D.: Characterising Land Degradation in the Guinea Savannah Region of Nigeria

23.3   Ellison D.: The Forest-Water Divide – Is More Debate Really Necessary?

23.4   Garrard R., Carey M.: Beyond Images of Melting Ice: Hidden Histories of People, Place, and Time in Repeat Photography of Glaciers

23.5   Jendoubi D., Liniger H., Karbout N., Ifejika Speranza C., Critchley W.: Effects of land use management, landscape forms and soil types on soil organic carbon in the watershed of Wadi Beja in Northwest of Tunisia

23.6   Llopis J.C., Diebold C., Zaehringer J.G.: Sustainable development and human well-being under telecoupling: insights from the biodiversity hotspot of northeast Madagascar

23.7   Payne D., Snethlage M., Spehn E.M., Fischer M.: Towards biodiversity-related opportunities for sustainable livelihoods in mountains

23.8   Ramirez J.A., Hossain S., Haisch T., Martius O., Ifejika Speranza C., Mayer H., Keiler M.: A coupled human and landscape conceptual model of risk and resilience in Alpine mountain communities

23.9   Rodrigues L., Sprafke T., Comptour M., Bokatola C., McKey C.: Wetland raised-field agriculture and its potential role in adapting to climate change in floodplains of the Congo Basin's cuvette centrale

23.10   Skelton M., Porter J., Dessai S., Bresch D.N., Knutti R.: A new north-south divide for climate knowledge? A case study of climate projections in UNFCCC's National Communications

23.11   Sobecka K., Allen J.: Cycles of Discussion, Circulation of Images

23.1
The effects of Large-scale land investments, institutional change and gender relations: Case studies of sugarcane outgrower contract farming in Malawi.

Timothy Adams

University of Bern, Institute of geography and Center for Regional Economic Development

Contract Farming (CF) is considered a more gender sensitive approach to rural development and a positive alternative to 'land grabbing'. CF arrangements can bring in investment while allowing smallholders to remain on their land, promote inclusiveness through guaranteed gendered participation, while increasing gains to smallholders for 'win-win' outcomes. Against this backdrop, this thesis assesses the complexity of institutional change and gendered transition in outgrower contract farming. It highlights these complex relationships in two thematic areas to ascertain: [1] the extent of institutional changes and the implications of that on the local communities engaged in CF arrangements; [2] the extent of change to gender relations in households engaged in CF and the implications of that on the existing gendered ideologies as well as the empowerment or disempowerment of women.

Through the analysis of four different cases of CF we show that the institutional changes associated with CF creates dependencies in outgrower communities with consequences on local production, consumption and exchange relations as well as control of land. The mechanisms of institutionalised dependencies are twofold: dependencies are created through the redefinition of use rights to customary land and through the redefinition of cash flows into outgrower communities. Through this two-dimensional process, corporations can secure access to land, exert control over local communities and transform the local social relations of reciprocity serving as the pillars of resistance and resilience.

In relations to change in gender relations, CF has a complex gendered impact on households. At the individual level, some can benefit from it; especially women who manage to engage in cane farming are able to attain financial independence and increase their bargaining power within their households. However, such benefits are reserved for households with access to land. Nevertheless, women engagement in cane farming coupled with increased gender awareness through NGOs sensitization is contributing to a change in gendered social perceptions and increased valuation of women abilities in commercial farming, their needs and contributions and may be modifying the gender balance at the community level. This result indicates that empowering women by making them cane farmers alone is not enough to change women position within their communities, unless community members accompany such empowerment with the recognition and acknowledgement of the women's contribution. The finding suggests that combining active women participation in outgrower CF with authority enhancing programs through community education whilst creating the possibilities for women to take independent action may be a good way to improve the gender relations between men and women. Our results indicate that, not only does contract farming change rural agrarian relations, it also transforms local family institutions through its strategy of divide and rule, by carefully selecting few household members with influence into the scheme and leaving most of poor local community members out. This CF system makes it difficult for the positive gendered outcomes to be sustained because it reinforces existing inequalities in local communities.

23.2
Characterising Land Degradation in the Guinea Savannah Region of Nigeria

Ademola A. ADENLE, Chinwe IFEJIKA SPERANZA, Desiree DANIEL

Institute of Geography, University of Bern, Switzerland (ademola.adenle@giub.unibe.ch)

In Nigeria, the severe reliance of people on the agro-ecological resources as a means of livelihood and sustenance has taken a toll on the composition and preservation of the natural ecosystems. The country's 92 million hectares of land are subjected to the negative effects of degradation. The agro-ecological zone of the Guinea Savannah region has been impaired by severe erosion, loss of agricultural soil, and the conversion of primary vegetation. However, the vegetation loss in the Nigerian Guinea Savanah has received less attention and there is a need to understand the drivers of land degradation in order to arrest the depletion of the natural vegetation.

Thus, the objective of this study is to characterise the drivers of land degradation and its impacts on the sustainability of the Guinea Savannah as an agro-ecological system. We apply the DPSIR (Driver, Pressure, State, Impact, and Response) framework to a critical literature review of empirical cases of degradation in the Guinea Savannah region. Through this analysis, we make explicit the causal linkages that result in long-term loss of ecosystem services in this region. The outcome from the DPSIR analysis showed that the depletion of the guinea savannah is the greatest form of land degradation in the region. The state and trajectory of vegetation indicates the emergence of Sudan vegetation in the Guinea Savannah belt due to the southern extension of Sahelian grassland. Human interaction such as intensive grazing underlined by social economic needs and survival quest, which places demands on the natural resource, plays a more crucial role than climate variation in altering the vegetation composition in the zone.
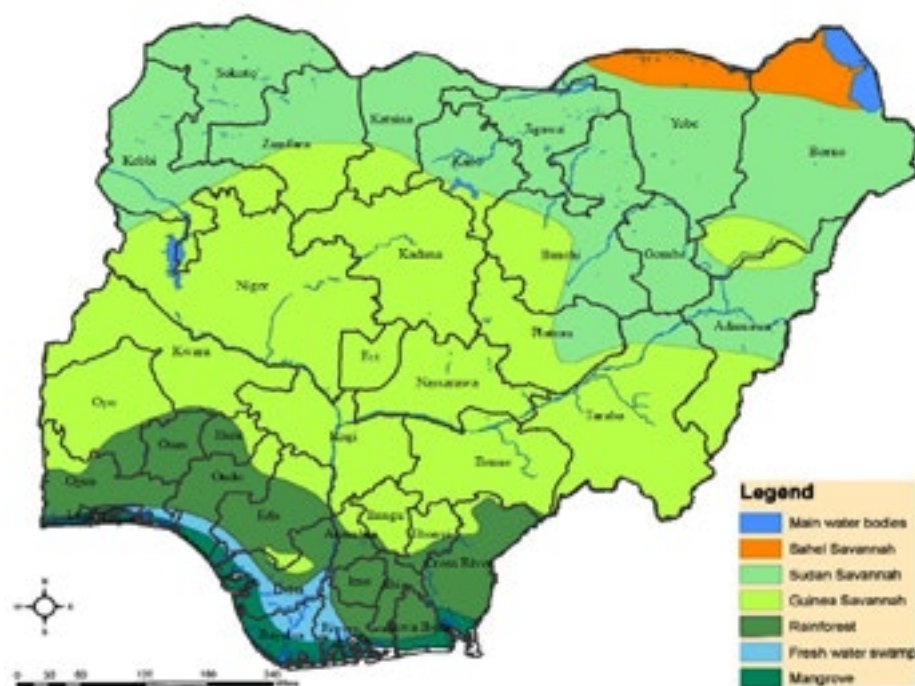
Agro-ecological zones in Nigeria and their overlap with administrative divisions (Source Adapted from Iloeje, 2001)

23.3
The Forest-Water Divide – Is More Debate Really Necessary?

David Ellison

External Consultant, Swedish University of Agricultural Sciences (SLU), Umea, SE
Ellison Consulting, Baar, Switzerland

Rapid population growth, increasing agricultural production, mushrooming urban (and suburban) settlements and the continuous decline of forest cover bode ill for the delicate balance between carbon, water, energy and climate. Climate change further exacerbates the already fundamental imbalances created by the anthropogenic modification of terrestrial landscapes, creating complex and interactive feedbacks across these two phenomena. Globally warming temperatures and declining rainfall (at least in the tropical and temperate regions), both compound and further aggravate an increasingly grim misuse of the available planetary resources. Most concerning of all, conventional forest management strategies based on the predominant view of forests and water interactions could result in additional reductions of the existing continental atmospheric moisture budget, further endangering the livelihoods and lives of those at most risk.

The policy realm's response to this twofold onslaught and challenge is either woefully inadequate or, at least in the forest-water case, entirely absent. Where the forest-water debate is concerned, however, the scientific world remains divided into easily politicized camps, seemingly unable to observe and adequately understand what the other camp is up to. The reasons for this, however, are unclear. Many or most of the tools necessary for repairing at least a part of that delicate balance between the major ecosystem components are increasingly well understood and documented. Moreover, an optimized ecosystem strategy could effectively use these tools to at least partially address the rapid advance of climate change and its increasingly threatening impacts on the availability of at-risk water resources, and on the millions to billions of people and livelihoods that depend on them.

Given this state of affairs, how are we to proceed? What is the key to resolving the decades, even centuries, old forest-water debate? Is the Science – Policy interface broken? And if so, how can we embark on trying to fix it?

23.4
Beyond Images of Melting Ice: Hidden Histories of People, Place, and Time in Repeat Photography of Glaciers

Rodney Garrard[11] and Mark Carey[2]

[1]*Institute of Geography, University of Bern, Hallerstrasse 12, 3012 Bern, Switzerland*
[2]*History and Environmental Studies, Robert D. Clark College, 1293 University of Oregon, Eugene, USA.*

The popular documentary film Chasing Ice (2012) captures the way glaciers—presented in time-lapse photography and a gripping narrative—are vanishing before our eyes, thereby offering a prime example of global climate change impacts. The film's main protagonist, photographer James Balog, provides compelling images of vanishing ice around the world. His photographs and movies allow the ice to speak for itself: it is disappearing everywhere as a result of climate change (Balog 2012). From Alaska and the Alps to Greenland, repeat photography shows without question that glaciers are shrinking, that ice is disappearing, and that climate change is irrevocably transforming the natural world. In consequence, ice has become one of the world's principal symbols of global warming (Carey 2010; Orlove, Wiegandt, and Luckman 2008). Balog is not alone: news stories, media accounts, scientific research, NGO reports, and government policies worldwide increasingly highlight glacier recession and ice loss to focus attention on climate change impacts.

Yet, while repeat photography of glaciers is ideal for showing glacier change over time and publicizing climate change (Webb et al. 2010), its use can also create problems because it fails to explore why and for whom glacier retreat is a problem, or how to fix it. To be sure, repeat photography reveals the specific extent of glacier retreat and landscape change (Cerney 2010), and some scientists are able to use it to analyze and document important cryospheric dynamics, which have implications for climatology and climate history (e.g. Byers 2007). Repeat photography - evolving over time from ground-level photographs to aerial photography to satellite images - can help to provide insight into how glaciers move and calve, to identify key aspects of ice dynamics for further investigation, to corroborate results from other glacier studies, to allow a greater historical reach in present-day analyses, and to vividly display these changes for diverse audiences worldwide.

But repeat photography can also obscure historical processes. It can oversimplify conditions, focus solely on loss and apocalyptic perspectives, mislead the public about the roots of glacier- and climaterelated hazards, fail to explain how knowledge and cultural values of glaciers have changed over time, implicitly promote techno-scientific solutions to climate change and glacier recession, and neglect possible impacts on local societies because of the imagery's emphasis on glaciers as scenery and mountaineering terrain. The underlying aim of most repeat photography of glaciers is to trigger alarm about vanishing ice, thus generating awareness of and action on climate change. But there is generally no portrayal or even recognition of human vulnerability to glacier hazards or climate change. This sharp divide in the connectedness of humans and ice—between culture and nature—contrasts with decades of scholarship seeking to blur nature-culture binaries (e.g., Tadaki et al. 2012). Most repeat photography analyses of glaciers leave society invisible, thereby concealing all the factors that create differential vulnerability to climate change and natural hazards, such as wealth, education, class, race, gender, infrastructure, building codes and protection policies (or lack thereof), access to government aid, and many other variables that affect risk to glacier loss (IPCC 2012).

Repeat photography of glaciers creates its own discourse and narratives about ice, which in turn influence scientific assessments, public perceptions, and government policies. In essence, this presentation contends that, while repeat photography plays a vital role in scientific observation and public perception of glaciers (Fagre and McKeon 2010) it can simultaneously yield misinformation by steering viewers toward false conclusions about changes over time, the drivers of those changes, and the production of the images.

Our presentation analyzes four iconic glaciated regions, all of which are within UNESCO World Natural Heritage (WNH) sites, to examine how repeat photography at these sites neglects the hidden histories of people, places, knowledge, vulnerability, and the ever-evolving politics of glacier representation. The four case studies are: the Aletsch Glacier in Switzerland, the Lewis Glacier in Mount Kenya National Park, Glacial Lake Palcacocha in Peru's Cordillera Blanca, and Nepal's Khumbu (Mt. Everest) region.

All these glaciers are powerful symbols of global climate change. Each case exposes how repeat photography presents different narratives about climate change, thus demonstrating how this method is not simply an unbiased «seeing is believing» approach, but rather presents an implied or overt argument—yet, one that misses many relevant underlying variables influencing causality related to both effects of and solutions to glacier retreat and climate change.
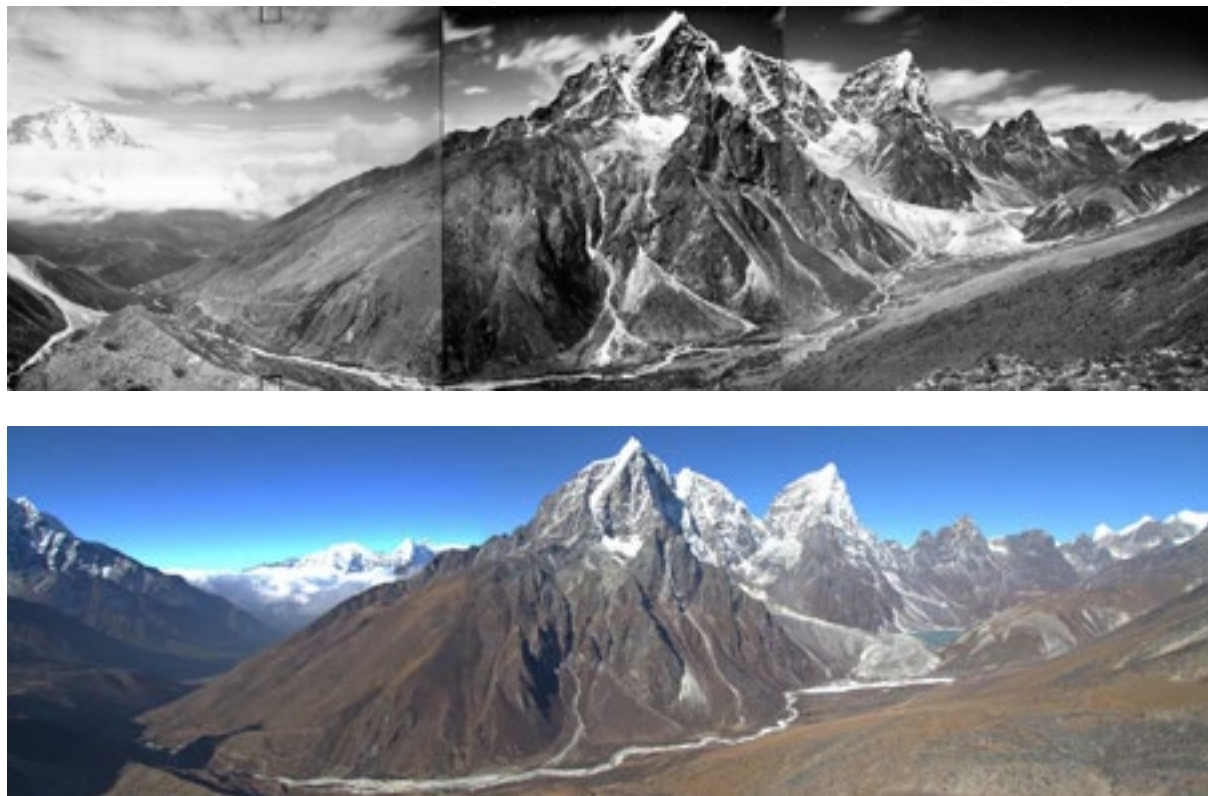
Fig: 1. Taboche, Khumbu Valley, Everest region, Nepal. Top: E.Schneider, 1950s; below R.Garrard, 2012.

REFERENCES

Balog, James. 2012. Ice: Portraits of Vanishing Glaciers. New York: Rizzoli.

Byers, A.C. 2007. «An assessment of contemporary glacier fluctuations in Nepal's Khumbu Himal using repeat photography.» Himalayan Journal of Sciences no. 4 (6):21-26.

Carey, Mark. 2010. In the Shadow of Melting Glaciers: Climate Change and Andean Society. New York: Oxford University Press.

Cerney, L.D. 2010. The Use of Repeat Photography in Contemporary Geomorphic Studies: An Evolving Approach to Understanding Landscape Change. Geography Compass 4 (9): 1339–1357.

Garrard, R., T. Kohler, U. Wiesmann, F.M. Price, A.C. Byers & A.R. Sherpa (2012). An Ever-Changing Place: Interpreting landscape change in Sagarmatha (Mt Everest) National Park, Nepal: rephotographic survey and encounter. ecomont 4 (2) pp 49-55.

16th Swiss Geoscience Meeting, Bern 2018

IPCC, Intergovernmental Panel on Climate Change. 2012. Managing the Risks of Extreme Events and Disasters to Advance Climate Change Adaptation. A Special Report of Working Groups I and II of the Intergovernmental Panel on Climate Change. New York: Cambridge University Press.

Orlove, Ben, Ellen Wiegandt, and Brian H. Luckman. 2008. «The Place of Glaciers in Natural and Cultural Landscapes.» In Darkening Peaks: Glacial Retreat, Science, and Society, edited by Ben

Orlove, Ellen Wiegandt and Brian H. Luckman, 3-19. Berkeley: University of California Press.

Tadaki, Marc, Jennifer Salmond, Richard Le Heron, and Gary Brierley. 2012. «Nature, Culture, and the Work of Physical Geography.» Transactions of the Institute of British Geographers:DOI: 10.1111/j.1475-5661.2011.00495.x.

23.5

Effects of land use management, landscape forms and soil types on soil organic carbon in the watershed of Wadi Beja in Northwest of Tunisia.

Donia Jendoubi [1], Hanpeter Liniger [1], Nissaf Karbout [2], Chinwe Ifejika Speranza [3], William Critchley

[1] Centre for Development and Environment (CDE). University of Bern, Switzerland
[2] Arid Regions Institute Medenine, Tunisia
[3] Institute of Geography. University of Bern, Switzerland

Understanding changes in soil quality resulting from land management changes, landscape forms and soil types is crucial to design sustainable land management plans and interventions. This study evaluated the influence of land use/ management, landscape forms (slope/aspect) and soil types on soil organic carbon (SOC) which is a key soil quality indicator within a watershed of Wadi Beja in the northwest of Tunisia. Factor analysis based on Multiple Correspondence analysis (MCA) was used to visualize relativities between the selected factors. Surface (0–20 cm) soil samples were collected from four main LU/management types in the watershed (i.e., field crops, Permanent crops, plantation forest, grazing land) and at two aspects classes (north and south), 3 slope classes (flat, moderate and steep) and 7 different type of soils (Vertisols, Pedosols, brown calcareous, Isohumic, regosols and rendzinas). A soil spectral library was developed and used to assess the variation of the SOC across all the selected variables. A factorial analysis of variance ANOVA showed that all the variables significantly affected the soil organic carbon (SOC) levels. Under the grazing land use, the aspect, slope and soil types together affected significantly the SOC levels. Under the permanent crops land use, only the slope and the soil type affected significantly the SOC levels. Under the field crops, only the slope has a significant effect as well. However, in the forest, there is no significant effects of any of the selected variables on the SOC. The afforestation of the field crops with olive trees can significantly increase the SOC at different levels of slopes especially in vertisols and brown calcareous soils. Since 71 % of the area is field crops land use system includes 64 % of steep terrain under intensive monoculture, SOC level appear better in flat area compared to others. Regarding grazing lands, level of SOC was increased significantly in the flat and north facing areas particularly in brown calcareous soils.
Soil fertility decline on sloping agricultural land poses a serious problem for the environment as well as for soil quality and productivity. In areas with highly erodible soils, such as those in steep slopes and south facing zones, application of soil and water conservation measures is crucial to sustain agricultural fields and to prevent or reduce soil degradation. There is strong indications that agroforestry have been successful in retaining soil fertility.
**Keywords:** SOC, landscape, land use management, ANOVA, MCA

23.6
Sustainable development and human well-being under telecoupling: insights from the biodiversity hotspot of northeast Madagascar

Jorge C. Llopis [1,2], Clara Diebold [1] & Julie G. Zaehringer [1].

[1] Centre for Development and Environment, University of Bern, Mittlestrasse 43, CH-3012 Bern (jorge.llopis@cde.unibe.ch)
[2] Institute of Geography, University of Bern, Hallerstrasse 12, CH-3012 Bern

Land-use change in the humid tropics plays a pivotal role across geographical scales and distant stakeholders, prominently visible in forest-frontier contexts. These regions are in the midst of a triple pressure: mounting demand to produce commodities for the international market, meeting the well-being needs and development aspirations of local populations, and serving global objectives of biodiversity conservation and carbon sequestration. These interlinked dynamics are giving rise to *telecoupled* situations, where external factors outpace local determinants of land-use change (Eakin *et al.* 2014). Some of these emerging processes hold the potential to constitute stepping stones towards sustainable development pathways, but at the same time might have unforeseen implications for human well-being.
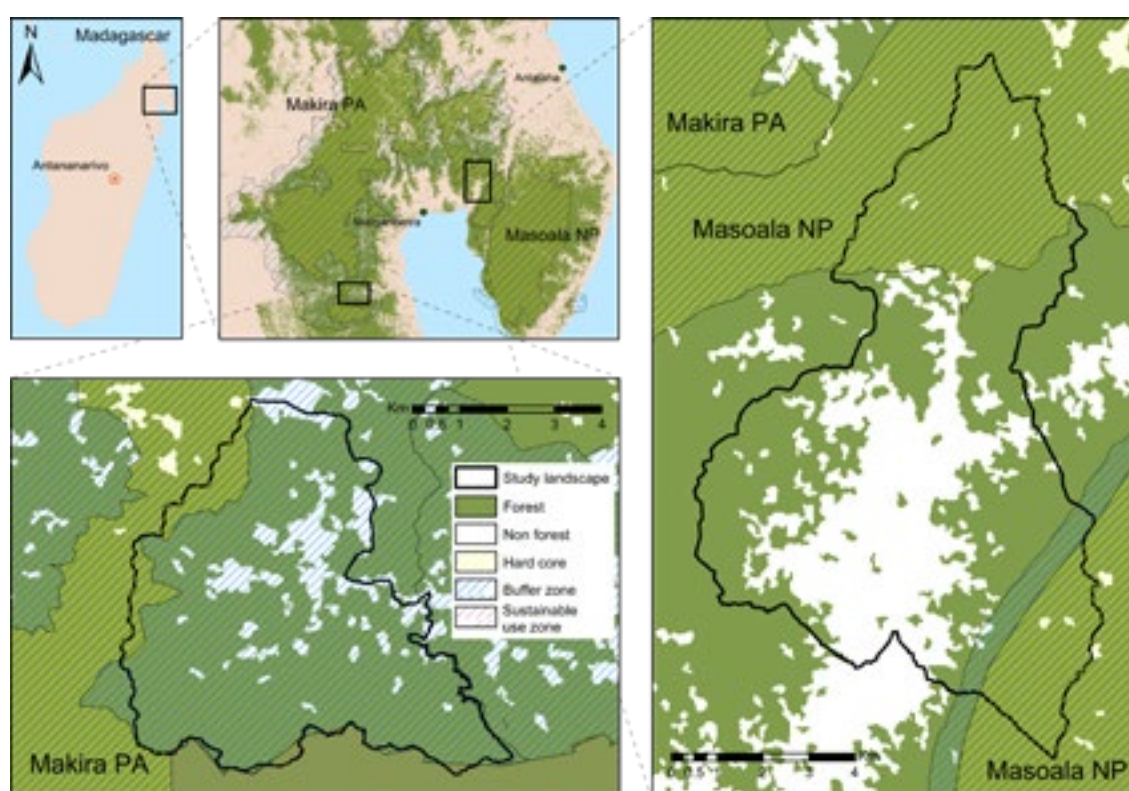
Sources: forest: MEEF et al. 2013; PA boundaries: MNP and WCS 2017;

Figure 1. Location of the study landscapes in northeast Madagascar.

In this paper, we present results from research conducted in two highly dynamics landscapes in northeast Madagascar, a region that prominently illustrates the implications of telecoupled situations. On the one hand, several protected areas were implemented here in recent decades, meaning the closure of the forest frontier in an until recently shifting cultivation-dominated area. In the other hand, vanilla and clove, the main cash crops produced in the region and linking the local economy to global markets, are experiencing acute price fluctuations, which have unclear implications for local well-being and ecological systems.

For this research, we developed an integrative methodology combining participatory land-use change mapping based on very high resolution satellite imagery (Zaehringer *et al.* 2018), with a mixed methods toolbox operationalising the capabilities approach (Nussbaum 2000) to explore local well-being. This methodology allow us to reconstruct and quantify spatially explicit landscape dynamics over the last three decades, and crucially, to relate these trends with parallel changes in the well-being of local communities. Key findings relevant for supporting sustainable development endeavours include the following. First, that externally-led processes got deeply reflected in the local landscapes, with unexpected outcomes for environmental dynamics. And second, the realisation that these landscape dynamics relate to local populations' well-

being in a non-linear manner, leading to increases in some capabilities but triggering decreases in others. While these trade-offs currently challenge efforts to sustainably manage these landscapes, better understanding on them possibilitate extracting important lessons from which to inform initiatives to steer socio-ecological systems in forest-frontier contexts towards sustainable development.

REFERENCES

Eakin, H., R. DeFries, S. Kerr, E. F. Lambin, J. Liu, P. J. Marcotullio, P. Messerli, A. Reenberg, X. Rueda, S. R. Swaffield, B. Wicke and K. Zimmerer (2014). *Significance of Telecoupling for Exploration of Land-Use Change.* Rethinking Global land Use in an Urban Era. K. C. Seto and A. Reenberg. Cambridge, Massachusetts and London, England, The MIT Press**:** 141-162.

Nussbaum, M. (2000). *Women and Human Development: The Capabilities Approach.* New York, Cambridge University Press.

Zaehringer, J. G., Llopis, J. C., Latthachack, P., Thein T. T. & Heinimann A. 2018. A novel participatory and remote-sensing-based approach to mapping annual land use change on forest frontiers in Laos, Myanmar, and Madagascar. *Journal of Land Use Science*: 1-16.

23.7
Towards biodiversity-related opportunities for sustainable livelihoods in mountains

Davnah Payne [1], Mark Snethlage [1], Eva M. Spehn [1] & Markus Fischer [1]

[1] Global Mountain Biodiversity Assessment, University of Bern, Institute of Plant Sciences, Altenbergrain 21, CH-3013 Bern (davnah.payne@ips.unibe.ch)

Mountains are of immense ecological, cultural, and socio-economic importance. They cover about 12% of all terrestrial land area outside Antarctica (Körner et al., 2011); are home to about 10% of the world's total human population (Körner et al., 2017), including some of the poorest and most politically, socially, and economically marginalized people (Wymann von Dach et al. 2016); host an immense biological, ecological, and cultural diversity (Körner 2004; Hassan et al., 2005; Wymann von Dach et al. 2016); and support vital ecosystem goods and services, including the supply of freshwater as well as timber and non-timber products and the protection against natural hazards (Palomo 2017). However, the combination of increasing global demographic and economic pressure with high biodiversity and ecosystems service value makes mountains particularly vulnerable. The formulation and implementation of effective policies and management approaches to safeguard the natural assets underpinning human well-being in mountains requires a thorough understanding of the interactions between nature and people particular to mountain social-ecological systems. Yet, we are currently missing the mountain-specific assessments necessary to improve our understanding of these interactions, of the geogaphic, cultural, social, economic, and biological factors underlying them, and of the biodiversity-related opportunities that exist for sustainable development in mountains.

Ongoing efforts at the Global Mountain Biodiversity Assessment (GMBA) aim at addressing this gap with a comparative assessment of the status of, trends in, and relations between biodiversity, ecosystem services, and human well-being across mountains worldwide. Data acquisition in the >1000 mountain ranges of the GMBA mountain inventory (Körner et al., 2017) broadly followed the conceptual framework of the Intergovernmental Platform on Biodiversity and Ecosystem Services (IPBES, Diaz et al., 2015), and combined an online questionnaire to the mountain research community at large with a literature review. The online survey in English, Spanish, and French included questions on (i) the mountain area assessed by each respondent, (ii) the status of and trends in mountain ecosystems (including their condition, coverage and biodiversity), the ecosystem services they deliver, and the well-being of their populations; (iii) the status of and trends in the direct factors driving the observed changes in these key components; (iv) the contribution of biodiversity and ecosystem services to human well-being; and (v) the governance of natural resources. Mountain ecosystems were grouped into five natural systems – above the treeline, forest, below the treeline, freshwater, and highly modified – and human well-being was assessed along five dimensions, namely material and social well-being, health, security, and freedom of choice. Direct drivers consisted of climate change, land use change, invasive species, overexploitation, and pollution, and the IPBES list of Nature's Contribution to People, NCP) was used as a selection of ecosystem services. The literature review was perfromed on a subset of review papers selected from Scopus based on a combination of keywords including (variants of) the word "mountain" and the various elements of the IPBES conceptual framework. This literature review was primarily performed to provide contextual information in view of data analysis and interpretation.

The 141 survey received cover all continents, yet with a very low response rate in North America. Despite the numerous challenges associated with these survey data, including that the areas covered by individual responses ranged from watersheds to entire mountain massifs, preliminary analyses indicate interesting patterns across mountain areas, ecosystems, dimensions of human well-being, and drivers of global changes. Indications of a comparatively higher importance of land use than climate change in driving observed patterns across mountain ecosystems, for instance, are of particular interest in view of ongoing sustainable mountain development debates.

By systematically examining the relationships between nature and people in mountains worldwide, these efforts contribute to a better understanding of the specific challenges associated with the sustainable management and conservation of mountain biodiversity (Sustainable Development Goal 15.4) and to identifying economically and ecologically efficient, socially acceptable, and politically feasible pathways towards sustainable development.

REFERENCES

Díaz, S., Demissew, S., et al. 2015:The IPBES Conceptual Framework — Connecting nature. Current Opinion in Environmental Sustainability 14: 1-16.

Körner, C. 2004: Mountain biodiversity, its causes and function. Ambio 13:11-17.

Körner, C., Paulsen, J. & Spehn, E.M. 2011: A definition of mountains and their bioclimatic belts for global comparisons of biodiversity data. Alpine Botany 121, 73-78.

Körner, C., Jetz, W., Paulsen, J., Payne, D., Rudmann-Maurer, K. & Sephn, E.M. 2017: A global inventory of the worlds mountains for bio-geographic applications. Alpine Botany, 127, 1-15.

Hassan, R., Scholes, R., Ash, N. (eds) 2005: Millenium Ecosystem Assessment — Ecosystems and human wellbeing: current state and trends.

Palomo, I. 2017. Climate change impacts on ecosystem services in high mountain areas: a literature review. Mountain Research and Development 37: 179-187.

Wymann von Dach, S., Bachmann, F., Borsdorf, A., Kohler, T., Jurek, M., & Sharma, E. 2016: Investing in sustainable mountain development; opportunities, resources and benefit.

23.8

A coupled human and landscape conceptual model of risk and resilience in Alpine mountain communities

Jorge Alberto Ramirez [1], Md Sarwar Hossain [1], Tina Haisch [2], Olivia Martius [1,3], Chinwe Ifejika Speranza [1], Heike Mayer [1], Margreth Keiler [1]

[1] *Institute of Geography, University of Bern, Hallerstrasse 12, 3012 Bern, CH (jorge.ramirez@giub.unibe.ch)*
[2] *School of Business, Institute for Nonprofit and Public Management, University of Applied Sciences and Arts Northwestern Switzerland, Peter Merian-Strasse 86, 4002 Basel*
[3] *Oeschger Centre for Climate Change Research, University of Bern, Bern, Switzerland*

Recent extreme natural disasters have focused the attention of the global community to society's vulnerability to these events. In the brief period between 1980 and 2014 the number of natural disasters due to climatological, hydrological, and geophysical processes have increased by approximately 150%, and caused annual economic loses near US$150 billion. Simultaneously these natural disasters occur within a broader social and physical context that is interconnected and may include economic crises and climate change that can further exacerbate loses and fatalities. These social and physical conditions are also apparent in Alpine mountain communities that differ regarding their ability to cope with these risks and build resilience.

A major challenge in natural hazard risk reduction in Alpine communities is estimating how risk and resilience will change in the future. Despite the growing research emphasis on dynamic relationships between human and natural systems, assessments of future risk and resilience for Alpine communties rarely consider the interaction between biophysical and socioeconomic components. Here, we make a first attempt to develop a conceptual model of a coupled human landscape system considering the dynamic relationships between human and natural systems for European Alpine communities. We accomplish this by identifying system boundaries, structures, components, and processes required to describe interlinked human and landscape systems and determining interactions and feedbacks within and between both systems. Using this approach, we develop a conceptual model considering three mountain communities in Switzerland. This conceptual model can later be used as a "blueprint" for a computer model that can: 1) provide information on future trajectories of mountain community risk and resilience, 2) investigate how mountain communities buffer socio-economic (e.g. economic downturn) and biophysical (e.g. floods) "shocks", 3) determine which shocks have a greater effect on mountain communities, and (4) serve as a basis for transdisciplinary deliberative resilience building processes.

23.10

Wetland raised-field agriculture and its potential role in adapting to climate change in floodplains of the Congo Basin's cuvette centrale

Leonor Rodrigues [1,2]; Tobias Sprafke [2]; Marion Comptour [3]; Carine Bokatola [4]; Doyle McKey [1]

[1] Centre d'Écologie Fonctionnelle et Évolutive, CNRS, 1919, route de Mende, 34293 Montpellier, Frankreich
   (leonor.rodrigues@gmx.ch)
[2] Geographisches Institut, Universität Bern,Hallerstarsse 12, CH-3012 Bern
[3] Laboratoire Ecologie, Environnement, Interactions des systèmes amazoniens (LEEISA, UMR 3456), CNRS, University
   of Guyane, Ifremer, Centre de recherche de Montabo, 97334 Cayenne, French Guiana
[4] Université Marien Ngouabi, Laboratoire de Botanique et Ecologie, Faculté des Sciences, B.P. 69, Brazzaville,
   République du Congo.

In today's context of climate change, population growth and rising demands of society, increasing human pressure is leading to widespread degradation of ecosystems, loss of their biodiversity and reduction of services provided to humans. Wetlands are an important example of fragile ecosystems, which in many regions are severely endangered due to drainage and intensive agriculture. An important example of agriculture in wetlands without their destruction is farming on agricultural raised fields, elevated earthworks of variable height and extent that can be found worldwide. Raised fields create a microrelief in a previously more uniform landscape.

We studied raised fields in Mossaka, Republic of the Congo, a small but fast-growing city located in the heart of a seasonally inundated wetland of the Congo basin. We used a multi-methodological approach including sedimentology, geochemistry and micromorphology, to evaluate the properties and functioning of raised fields, to quantify how farmers concentrate soil resources in raised fields and to show how practices of raised-field farmers positively affect soil organisms, microbial activity and plant-available nutrients. This resource concentration permits the persistence of organisms that would not survive in a uniform landscape and, together with topographical and habitat heterogeneity, make ecosystems more resilient to climatic fluctuations. Raised-field agriculture is very labor demanding and is therefore currently declining in Mossaka, in favor of a less labor-intensive kind of agriculture, i.e., flood-recessional agriculture on islands in the Congo River. These islands are normally only flooded during the annual long rainy season, and crops are grown in the interval between successive long rainy seasons.

For two of the past three years, however, unexpected high-water levels during the short rainy season, which occurs in the middle of this interval, resulted in major crop loss. During these events, raised fields were never flooded. According to the IPCC reports, such extreme events are expected to increase in frequency in central Africa under climate change. Recognition of the value of raised fields as a flood-mitigation technology and a reliable storehouse of agricultural biodiversity could focus attention on their role in strategies to adapt to climate change.

Figure 1. Left: Mossaka—Study are in the Congo Basin. Right: Raised field in the dry season.

23.11

A new north-south divide for climate knowledge? A case study of climate projections in UNFCCC's National Communications

Maurice Skelton [1,2,3] James Porter [4], Suraje Dessai [5], David N. Bresch [1,3] Reto Knutti [2]

[1] Institute for Environmental Decisions, Swiss Federal Institute of Technology ETH Zurich, Universitätstrasse 16, CH-8092 Zürich (maurice.skelton@usys.ethz.ch)

[2] Institute for Atmospheric and Climate Science, Swiss Federal Institute of Technology ETH Zurich, Switzerland

[3] Federal Office of Meteorology and Climatology MeteoSwiss, Operation Center 1, P.O. Box 257, 8058 Zurich Airport, Switzerland

[4] Department of Geography, King's College London, London, WC2R 2LS, UK

[5] Sustainability Research Institute and ESRC Centre for Climate Change Economics and Policy, School of Earth and Environment, University of Leeds, LS2 9JT, UK.

A north-south divide in the production of climate knowledge exists. While the north enjoys a wide variety of climate models, data infrastructures and climate knowledge expertise, the south often lacks these same attributes. Such a clear-cut dichotomy can be misleading, however. We use a unique global dataset, the UNFCCC National Communications, to perform a global documentary analysis of scientific submissions from individual countries (n=189). Focusing on the production and use of climate projections, our research both supports, and importantly, challenges a north-south divide. For instance, the global north in general uses more complex climate modelling techniques yet numerous countries in the global south have a higher scientific capacity than some northern ones. Beyond scientific capacities, the north has a preference for long-term time horizons (2090s) and is more optimistic of global mitigation efforts, when selecting a single emission scenario often using a middle-of-the-road scenario. The south reports more often more mid-term timeframes (2050s) and uses the worst-case emission scenario more often than the north. While the use of GCM ensembles is widespread in the global north and south, the south's access to climate models is restricted to mobile climate projection tools. Modelling software such as PRECIS, although crucial in enabling countries with little scientific capacity to produce robust and reliable climate risk assessments, may hide a new divide between the global north and global south. Unable to customise inputs, such as country-specific observations or modelling information, the global south might become dependent upon the climate modelling tools circulated by the global north. Our research calls for a more nuanced and critical use of the north-south divide, and highlights that well-intended modelling and training efforts may unwittingly restrict, rather than foster, scientific capacities in the global south.

23.12
Cycles of Discussion, Circulation of Images

Karolina Sobecka [1], Jamie Allen [2]

[1] *Institute for Aesthetic Practice and Theory, Basel Academy of Art and Design FHNW, Freilager-Platz 1, Basel (Karolina.Sobecka@fhnw.ch)*
[2] *Institute of Experimental Design and Media Cultures / Critical Media Lab, Basel Academy of Art and Design, FHNW, Freilager-Platz 1, Basel (Jamie.Allen@fhnw.ch)*

Karolina Sobecka (karolinasobecka.com) and Jamie Allen (jamieallen.com) are collaborating researchers, part of a research group interested in environmental humanities, art, design and science at the Hochschule für Gestaltung und Kunst FHNW in Basel, and associated with the media arts production facilities at the Critical Media Lab Basel. We are artist-researchers who often manifest our work as artworks, events and through mediums other than text-based publications, while writing and publications focus on the relationships between aesthetics, knowledge and environment (Allen 2017).

Methodologically this work and research often encounters interdisciplinary collectives as a means of evoking, reflecting and understanding communities of practice (Allen et. al 2011) and attempts to devise alternative representations of these. Our current project and focus is on exploring the ways that climate science and planetary magnitude technologies are represented, deliberated and thought about in science, engineering on through policy, governance, technology and popular media.

The use of different languages, linguistic metaphors and canonical examples in discussions relating to our common environment of planet earth greatly influence the ways in which we imagine solutions, design decisions, create policy and enact governance. Geoengineers use hopeful, domestic and clarifying phrasings like "resetting the global thermostat", to describe the necessity and effectiveness of, for example, aerosol injection into Earth's atmosphere. The term "greenhouse effect", for example, coined in 1907, forms part of a rhetorical trajectory begun by geologist Thomas Sterry Hunt in 1867 when he wrote of climatological conditions "producing an effect precisely as if we had covered the whole earth with an immense dome of glass, had transformed it into a great Orchid-house" (Hunt 1867). What would be different about our technological and geoengineering landscape were modelled on a somewhat or completely different "as if"?

Research into the ways that discourse can change behaviour is a central part of behavioural research around dilemma of the commons, and how the mobilisation of nomenclature and information is best transferred to embodied or actionable knowledge (Nerlich 2010). Just as with language, but further to and along with it, choice made regarding the formats and contexts of events and discussions, the visualisation of data, the distribution of images and iconography and the rendering of time based media (audio and video), impacts the ways in which we treat ecosystems and imagine their modulation and adjustment. How we imagine the future is predicated on the means and mediums we use to plan for and project into this future (Fløttum, et. al 2014). For the 16th Swiss Geoscience Meeting in Bern, we propose a brief textual and image based interview and study for three of the workshops that are taking place at the event in Bern on November 30th and December 1st, 2018.

We would like to discuss with groups prior to the sessions, via a quick questionaire and gathering of materials, the ways in which they imagine the 16th Swiss Geoscience Meeting, Bern 2018 work they are doing and the presentations they will make in Bern. From these resources, collected over the weeks following the abstract submission deadline of August 31st, 2018 and prior to the event itself, we would develop short reflections for the participating groups, to be presented as part of workshops.

These would take the form of a re-narativisation of the thematics, common examples, linguistic tropes, visual concurrences and aesthetics and information design styles emergent in the discussions and materials presented in Bern. (We have made contact with the "Geomorphology for a habitable planet at the Swiss Geoscience Meeting" and the "Sustainable social-ecological systems: from local to global challenges at the Swiss Geoscience Meeting" who have expressed interest in the research)

We would hope that such perspective, as arts and design researchers exploring the way that climate engineering is deliberated and communicated, would be of use to the community of researchers participating in Bern and these materials would for us form the basis for further research outputs to be shared with the groups in attendance.
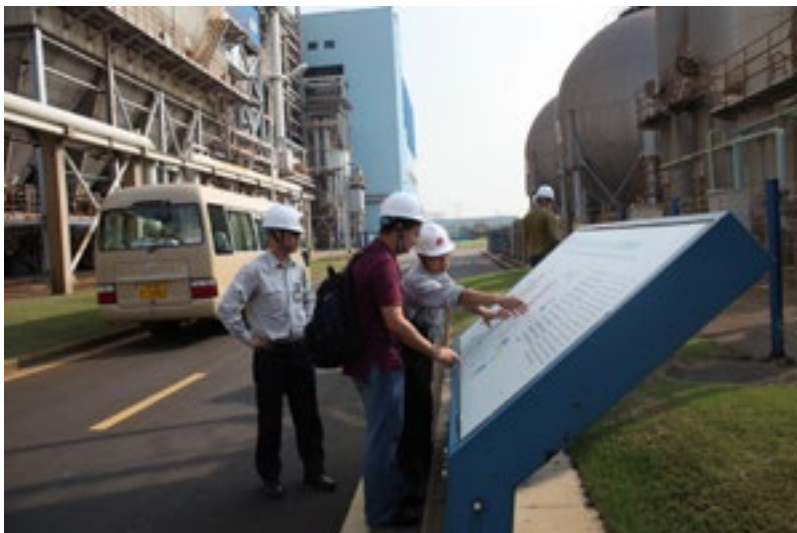
Figure 1. Recent fieldwork in China, visiting the coal fired power plant carbon capture facilities and discussing with plant engineers.

REFERENCES

Allen, J., 2018. The Overgrounds and Undergrounds of Pure and Applied Science: Cosmic Collisions and Industrial Collusion. Media Theory, 2(1), pp.352-392.

Allen, J., Clarke, R., Galani, A. and Wajda, K., 2011, November. Creative Ecologies in Action: Technology and the Workshop-as-artwork. In Proceedings of the 8th ACM conference on Creativity and cognition (pp. 309-310). ACM.

Fløttum, K., Gjesdal, A.M., Gjerstad, Ø., Koteyko, N. and Salway, A., 2014. Representations of the future in English language blogs on climate change. Global Environmental Change, 29, pp.213-222.

Hunt, T.S., 1867. The chemistry of the primeval Earth. Geological Magazine, 4(40), pp.477-478.

Nerlich, B., Koteyko, N. and Brown, B., 2010. Theory and language of climate change communication. Wiley Interdisciplinary Reviews: Climate Change, 1(1), pp.97-110.